WtE Center
CHANGWON NATIONAL UNIVERSITY

PerkinElmer
For the Better

ESRC
Environmental Science Research Center
Faculty of Science, Chiang Mai University

The 5th *EnvironmentAsia*
International Conference

Website: www.environmentasia-2019.science.cmu.ac.th
Email: environmentasia2019@gmail.com
Facebook: The 5th EnvironmentAsia International Conference 2019

The 5th *EnvironmentAsia* International Conference on Transboundary Environmental Nexus: From Local To Regional Perspectives

Chiang Mai University
CHIANG MAI UNIVERSITY 1964

สอสก
TSHE

The 5th *EnvironmentAsia*
International Conference on
Transboundary Environmental Nexus: From Local To Regional Perspectives

CONFERENCE PROCEEDINGS

June 13-15, 2019

at Convention Center, The Empress Hotel,
Chiang Mai, Thailand

CONTENTS

CONTENTS

CONTENTS

Session I Environmental Science and Technology

CONTENTS

CONTENTS

Parichat Muensita, Suwimol Asavapisit, Rungroj Piyaphanuwat

CONTENTS

CONTENTS

CONTENTS

WELCOME MESSAGE

The Thai Society for Higher Education on Environment (TSHE) founded in 2005. Originally, TSHE was collaborated among universities and institutes in Thailand that concern solving environmental problems. We aim to enhance the quality and reference of educational and training in Environmental inter-discipline programs to apply in policy and leadership development in the area of natural resources and environment. TSHE has continuously organized the international conference every two year since 2011.

This year 2019, welcome to Chiang Mai, where TSHE is holding our 5th EnvironmentAsia International Conference "**Trans boundary Environment Nexus from Local to Regional Perspectives**". This event is an extremely valuable opportunity to connect and share information with those in government, industry, consulting, environmental professionals and academia. I am proud to be part of this esteemed regional conference, providing a neutral forum for the discussion and debate on important environment issues. Everyone is encouraged to attend the meetings to participate or just observe. Check the program schedule for meeting date and times.

I would like to especially thank our Chair conference, Assistant Professor Dr. Somporn Chantra, Chiang Mai University, local host committee team, our dedicated TSHE staff, as well as our generous sponsors and exhibitors. Without their support and hard work this conference would not be possible.

On behalf of the Thai Society of Higher Education Institutes on Environment (TSHE), I am delighted to welcome all participants to learn, to meet and have fun exploring Chiang Mai. Thank you for joining us, and hope you enjoy your time at our conference.

Professor Dr. Wanida Jinsart
TSHE President

MESSAGE FROM CHIANG MAI UNIVERSITY

It is an honor for Chiang Mai University to co-organize this 5th Environment Asia International Conference together with the Thai Society of Higher Education Institute. The current Chiang Mai University Educational Development Plan considers "Environment and Energy" as one of its key strategies and is fully supportive of education and research relating to the environment including renewable energy, sustainable environment, and a green campus.

Even though Northern Thailand is blessed with magnificent natural surroundings, it is not without its environmental problems. However, there is cause for optimism. Various global movements are addressing these problems and this conference is a good example of one of them. I truly believe that events such as this in which new research findings are shared can lead to solutions to the ongoing problems. The conference's main theme of "Transboundary Environmental Nexus, from Local to Regional Perspectives" is very timely since many environmental issues are borderless. The recurring air pollution problem in Northern Thailand is an example of how local actions are needed to create regional impacts.

We therefore hope that this conference will highlight research results findings from both local and international researchers to tackle this and other environmental issues. It is also an opportunity to hear about exciting new areas of technology and innovations in the environmental field. In closing, I wish you all a fruitful and rewarding conference and I hope you can take the time to visit our campus and enjoy the many cultural attractions on offer in Chiang Mai.

Thank you.

N. Nantachit

Clinical Professor Niwes NANTACHIT, M.D.
President of Chiang Mai University, Chiang Mai, Thailand

MESSAGE FROM CONFERENCE CHAIR

It is a great honor for the Environmental Science Research Center (ESRC), Chiang Mai University to co-organize this important international conference in conjunction with the Thai Society of Higher Education Institutes of Environment (TSHE) here in the city of Chiang Mai.

This conference brings together scientists and environmentalists to address environmental issues and provide a forum for international cooperation for an environmentally sustainable world. The search for a global policy to cope with current and projected environmental dynamics requires international collaboration. There are 5 conference sessions covering all aspects of environmental sciences: 1) Environmental Science and Technology, 2) Natural Resources Management and Sustainability, 3) Environmental Engineering, 4) Environmental Management, and 5) Environmental Pollution and Health Impacts.

We are delighted to welcome guests from the US Consulate here in Chiang Mai and the Ministry of Natural Resources and the Environment. There are also numerous invited speakers from universities and organizations in Europe, North America, and Asia, including Thailand. Conference sessions will be chaired by experts in their respective fields.

The ESRC is particularly excited as a new international Bachelor's degree in Environmental Science (ES) will be offered for the first time starting this August. The new program has already attracted much interest both at home and abroad. The Faculty of Science has been offering international graduate degrees in Environmental Science for many years. This year is also an auspicious year for the Faculty as it is its 55th anniversary which is being celebrated with a series of events. Co-organizing this conference is one of the highlights. It should also be mentioned that Chiang Mai University has supported the ESRC in establishing a Center of Excellence in Environmental Science to conduct innovative research.

I would therefore like to thank most sincerely the Thai Society of Higher Education Institute on Environment for trusting us to co-organize this important conference. The various contributions of the national and international co-organizers as well as the financial support of the corporate sponsors are greatly appreciated.

On behalf of the ESRC, I hope that you will find the conference both informative and very rewarding and I wish you an enjoyable stay here in Chiang Mai.

Thank you.
Best wishes,

Assistant Prof. Dr. Somporn CHANTARA
Head of Environmental Science Research Center (ESRC)
Faculty of Science, Chiang Mai University, Chiang Mai, Thailand

OPENNING REMARK

On behalf of the Ministry of Natural Resources and Environment, the Royal Thai Government, I would like to express our sincere appreciation to the Thai Society of Higher Education Institutes on Environment (TSHE) and the Faculty of Science, Chiang Mai University, the organizer of the 5th EnvironmentAsia International Conference for inviting us to join the conference. It is timely and important event as we just celebrated the World Environment day last week under the theme of "Beat Air Pollution."

The World Environment Day takes place every year on June 5 . Since the first celebration in 1974 where the topic was "only one Earth," it has become the largest annual celebration of the environment, with millions of people joining in to leave a lasting legacy for the planet. The theme of this year is formulated by China as the host country, aiming to spur governments, industry and individuals to come together to explore renewable energy and green technologies and improve air quality across the world. According to the World Health Organization, every year, around 7 million people die prematurely from diseased caused by air pollution and approximately, 4 million of these deaths occur in the Asia Pacific region. It is apparently that this complex challenge demands immediate attention and action. We, thus, need to act now.

However, not only air pollution but also other environmental problems such as marine debris and wildlife trafficking are transboundary issues.

Ladies and Gentlemen, You may know very well that Thailand, as the Chair of ASEAN, is going to host the ASEAN SUMMIT during June 22-23. We highly anticipate that the outcomes of the SUMMIT will include the declarations and frameworks of action on the transboundary environmental issues, particularly on the issues of marine debris and wildlife trafficking. This will significantly advance our partnership for sustainability.

Thailand faces the same challenges on air pollution and other environmental problems as the other countries in the Region. Cities in the country including Bangkok and Chiang Mai were choked by high level of air pollution and have been struggling with tons of trash. In this regard, I am very please to inform you that we have already started a new pathway to deal with the environmental issues both at the national and international level under our long term national strategy or so call "20 years National Strategy," in which I will further elaborate during the panel discussion.

Having said that, I would like to conclude that the theme of our conference on "Transboundary Environmental Nexus, from Local to Regional Perspectives," is fully concurred with the current trend and situation.

I wish that all of us will have the productive deliberation during the conference and come up with the fruitful outcomes.

Last but not least, I hope that apart from heavy discussion in the conference room, you will have time to explore and enjoy the beautiful city of Chiang Mai.

With this, I would like to declare this 5th EnvironmentAsia International Conference open.

Thank you.

A. Krairapanond

Dr. Asdaporn KRAIRAPANOND
Inspector General, Ministry of Natural Resources and Environment, Thailand

COMMITTEE

Chair
Assistant Professor Dr. Somporn Chantara
Chiang Mai University

Advisory Committee
Assistant Professor Dr. Sittipong Dilokwanich
Mahidol University

International Committee
Professor Dr. Mark Morgan
Missouri University, USA
Professor Steven W. Edwards
University of Liverpool, UK
Dr. Sarah Clement
University of Liverpool, UK
Dr. Mike le Duc
University of Liverpool, UK
Professor Dr. Tamao Kasahara
Kyushu University
Professor Dr. Shin'ichi Okamoto
Tokyo University of Information Sciences, Japan
Professor Wangyun Won
Changwon National University, Republic of Korea
Dr. Stephen D.Elliott
Chiang Mai University
Professor Dr. Akihiko Terada
Tokyo University of Agriculture and Technology, Japan
Professor Dr. Kunio Kawamura
Hiroshima Shudo University
Professor Dr. Eiji Yano MD
Teikyo University, Japan
Senior Assistant Professor Dr. Yoko Tsuda
Teikyo University, Japan
Professor Dae-Woon Jeong
Changwon National University, Republic of Korea
Professor Won-Jun Jang
Kyungnam University, Republic of Korea

Local Committee
Professor Dr. Wanida Jinsart
Chulalongkorn University
Associate Professor Dr. Alice Sharp
Chiang Mai University
Assistant Professor Dr. Charanai Panichajakul
Kasetsart University
Assistant Professor Dr. Deacha Tapunya
Chiang Mai University
Dr. Dia Shannon
Chiang Mai University
Associate Professor Dr. Jaroon Jakmunee
Chiang Mai University
Assistant Professor Dr. Jeeraporn Pekkoh
Chiang Mai University
Lieutenant Colonel Dr. Kittiphop Promdee
Chulachomklao Royal Military Academy
Assistant Professor Dr. Panwadee Suwattiga
King Mongkut's University of Technology North Bangkok
Associate Professor Dr. Patana Anurakpongsatorn
Kasetsart University
Assistant Professor Dr. Pitchaya Mungkornasawakul
Chiang Mai University
Associate Professor Dr. Pongsak Noophan
Kasetsart University
Lieutenant Colonel Pongsakorn Keawkornmeung
Chulachomklao Royal Military Academy
Associate Professor Dr. Prasit Wangpakapattanawong
Chiang Mai University
Dr. Pumis Thuptimdang
Chiang Mai University
Assistant Professor Dr. Ratcha Chaichana
Kasetsart University
Assistant Professor Dr. Siranee Sreesai
Mahidol University
Assistant Professor Dr. Sitthichok Puangthongtub
Chulalongkorn University
Assistant Professor Dr. Soontree Khuntong
Kasetsart University
Assistant Professor Dr. Sutthathorn Chairuangsri
Chiang Mai University
Assistant Professor Dr. Thipsuree Kornboonraksa
Thammasat University
Assistant Professor Turenjai Doolgindachbaporn
Khon Kaen University
Assistant Professor Dr. Uma Langkulsen
Thammasat University
Dr. Wan Wiriya
Chiang Mai University

PM10 and PM2.5 and PAHs exposures in urban parks of Bangkok

Panjamaporn Suwannapun[1] and Wanida Jinsart[2*]

[1*] International Program in Hazardous Substance and Environmental Management, Graduate School, Chulalongkorn University, Bangkok 10330, Thailand
[2] Department of Environmental Science, Faculty of Science, Chulalongkorn University, Bangkok 10330, Thailand
e-mail: pjmpswnp@gmail.com

ABSTRACT

Polycyclic aromatic hydrocarbons (PAHs) are group of chemicals that were produced during incomplete combustion of coal, oil, and gasoline. In congested traffic areas of Bangkok, PAHs emitted from vehicles were considered a serious problem of urban air quality. These compounds can cause serious health problems in human such as respiratory symptoms and lung cancer. In this study, PAHs bound PM_{10} and $PM_{2.5}$ were determined at three urban parks in Bangkok from January 2018 - March 2018 and January 2019 - March 2019 (dry season). Moreover, air samples were also collected at the roadside area (Victory Monument) to be compared as a reference site. Particulate matter samples were collected using personal modular impactor with filters pack attached and air pump sampler flowrate 3 L/min for 24 hours on both weekend and weekdays. PAHs were extracted from PM_{10} and $PM_{2.5}$ filters by ultrasonic extraction method and were analysed by HPLC. The PM_{10} concentration in urban parks was ranged from 26.33 $\mu g/m^3$ to 109.14 $\mu g/m^3$. The $PM_{2.5}$ concentration in urban parks was ranged from 14.83 $\mu g/m^3$ to 84.03 $\mu g/m^3$. The highest concentration of PM_{10} and $PM_{2.5}$ were found in Chatuchak Park and Santiphap Park, respectively. The PM_{10} concentration in the roadside area (Victory Monument) was ranged from 77.60 $\mu g/m^3$ to 113.41 $\mu g/m^3$. The

$PM_{2.5}$ concentration in the roadside area (Victory Monument) was ranged from 51.36 µg/m^3 to 82.33 µg/m^3. The results show that the concentration of PM_{10} and $PM_{2.5}$ in the reference area is much higher than in the urban parks and exceed the pollution control standard for 24-hour average.

Keywords: PAHs, PM_{10} and $PM_{2.5}$, Urban parks

INTRODUCTION

The growth of Thailand's economic and industrial development has resulted in regions of overpopulation as people from rural area move to urban area or major cities such as Bangkok which is the capital city of Thailand with an obstinate traffic problem to have new careers so that they may improve their living conditions and have better lives [1][2]. Owning to these developments, there are many problems occur if urban planning is not efficient enough to deal with the problems. Major concerned problems are severe traffic congestion since the number of vehicles in urban area has increased. Severe vehicular congestion causes areas where air quality is being concerned. Pollutants that are mostly emitted from the fuel burning of vehicles and traffic congestion are particulate matter as well as PAHs which are occurred by combustion and bound to particulate matters. Moreover, Particulate matter contains microscopic pollutants which cause adverse health effects such as PAHs found in a many area especially in urban areas [1]. Particulate matter is also known as particle pollution with a complex mixture of extremely small particles and liquid droplets that get into the air and once inhaled, these particles can affect the heart and lungs and cause serious health effects [3]. $PM_{2.5}$ produced from industrial activities and engine exhausts is now globally concerned [4]. PM_{10} with PAHs suspended in the air and has a large amount in urban area particularly in high traffic area. Population in the urban area may exposed to these particles in high levels especially when they are near the roadside [5]. People who expose to these

pollutants for short-time period (hours or days) and long-time period may have risk on respiratory and cardiovascular diseases and lung cancer. PAHs are organic pollutants found widely in the environment. They were emitted by combustion of fossil fuels process such as gasoline and coal, natural resources such as volcanic eruptions and forest fires and especially vehicles emission [6]. Moreover, PAHs are interested in environmental science field because of their persistence, bioaccumulation, carcinogenic, and mutagenic effects [7]. On the other hand, exposure of dust bound to PAHs in human has not been studied much [8]. In addition, the major path way of these pollutants is inhalation. Human may expose to them easily by inhalation; therefore, Toxic compounds get into body and affect to their system. The ambient guideline levels are set by the World Health Organization (WHO). The standard of PM_{10}, $PM_{2.5}$ as a 24-hour mean are 50 $\mu g/m^3$ and 25 $\mu g/m^3$ respectively. Many researchers reported that exposure levels always exceed the World Health Organization standard; therefore, the organization which related to this problem should concern and find the way to protect people from the pollutions. However, Urban planning department manages to prevent the problems by providing park in many areas in Bangkok. The park has become an important place for people's daily leisure. People can exercise or do any other activities every day in the park. However, there were few researches about Particulate matter in urban park in Thailand. This is the reason why researcher decide to investigate the exposure of particulate matter and PAHs in urban park in Bangkok. Public Parks are the place that encourage biodiversity, variety of vegetation and provide important ecosystem services. Greenery in urban parks has been noted as an efficient tool to improve air quality and noise pollution [9]. Parks are effective sink for air pollution since vegetation can captures gases, particulate matters and aerosols in the atmosphere [10]. Plants were noted to be practical scheme to alleviate ambient air pollution [11]. Therefore, urban greenery can be sustainable filter for

particulate matter in urban area [12]. Due to rapid growth of economic and urbanization, most urban parks are located near main roads or industrial areas [13]. Large number of population and human activities in urban parks which involved in human's daily life and health [14]. Over 90,000 people average per day participated exercising and doing aerobic dance in the parks especially on weekends [15]. Many people spend their leisure time in urban parks for doing a various kind of activities such as exercising and taking a rest [16]. Most of them go the park with their family consist of different life span included children, elder, pregnant woman who would be at the greatest risk [17]. These people recognize that the park has benefits for their health, but few people know the concentrations of toxin in public parks since there are little studies about PAHs and particulate matter in public parks [18]. Vegetation in public park are important for an air quality in the way of quality improving, but the effect of urban parks on levels of air pollution was hardly been experimentally determined [16].

METHODOLOGY

Site location and Sampling point

Chulalongkorn Centenary Park (CCP), Chatuchak Park (CP) and Santiphap Park (SP) are urban parks which located in the center of Bangkok, Thailand. There are abundant of the greenery of the trees and shrubs. Moreover, variety of activities and facilities are provided in the area so that people can have their leisure time relaxing in the parks. Moreover, the parks located near many main road, public transportation route such as Bangkok mass transit system and public bus. The location of the parks is in the area where has a serious traffic congestion and located near residential area. Figure (1-2) shows the site area of three parks and the location of reference site which is around the Victory Monument (VM). Each site consists of three sampling point which can be categorized into three types which are traffic transboundary, inside and recreation area. Total 12 sampling points are

established, and 73 samples are collected in this study.

Figure 1 Sampling sites location

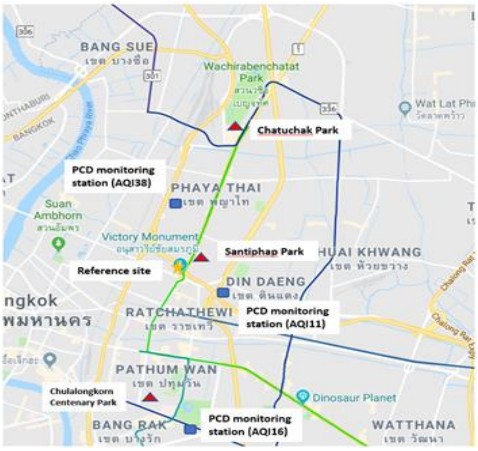

Figure 2 Sampling sites (red triangles), PCD monitoring stations and reference site

Sampling collecting and Sample preparation

PM_{10} and $PM_{2.5}$ collecting was conducted by a personal modular impactor using air sampler pump with a flow rate of 3 L/min installed at the breathing zone approximately 4-6 feet above ground according to ASHRAE at four sites. PM_{10} and $PM_{2.5}$ samples were collected on PVC membrane disc filter (Ø 25mm, 5 µm) and PTFE filter (Ø 37 mm, 1.0 µm), respectively. The duration time of sampling is 24 hours on 2 weekdays and a weekend from March to November. After sample collection, each filter was weighed using microbalance with 7 decimals and kept in desiccator.

PAHs extraction and Chemical analysis

PAHs were extracted from the filters by ultrasonic method. First, the filters were cut into small pieces and put in the flask or test tube. Next, pipet acetonitrile (HPLC Grade) 5 ml into the flask. After that, the flask was put into ultrasonic bath for 30 minutes at controlled temperature 75 degree Celsius to extract PAHs from the filters. Extracts were injected through PTFE syringe filter size 0.45 µm to filtrate the solution. Next, sample solutions were evaporated by air dry to get 0.15 ml solution and kept it in sample vial with volume mark.

Sample solutions were analyzed

by HPLCs using UV detector (λ=254 nm) and fluorescence detector (λ=240 nm, EM 425 nm) The concentration of PAHs was determined between area and standard solution concentration from standard graphs.

Data analysis

PM_{10} and $PM_{2.5}$ concentration

Each filter was weighed using microbalance with 7 decimals and the concentration of PM were calculated by equation (1) and (2)

$$C\ (\mu g/m^3) = \frac{(Wf - Wi)}{V} \times 10^3 \qquad (1)$$

$$V(m^3) = Q \times T \times 10^{-3} \qquad (2)$$

where, C is the concentration of particulate matter. Wf and Wi is the weight of filter after and before measurement, respectively. V is the volume of air. Q is the flowrate and T is the time of collecting.

PAHs calculation

PAHs standard graph was established from six exact PAHs concentration which are 0.1, 0.5, 1, 5 and 10 ppb. PAHs from samples could be calculated by equation (3)

$$PAHs\ (ng/m^3) = \frac{C \times V}{V\ air} \qquad (3)$$

where, C (ng/ml) is the PAHs concentration from standard curve. V (ml) is the sample solution volume which is 0.15 ml and Vair (m^3) is the air volume flowing through filter.

RESULTS AND DISCUSSION

$PM_{2.5}$ and PM_{10} concentration

The results of the PM_{10} and $PM_{2.5}$ average concentration in urban parks are shown in Table1 compared to PCD value. The concentration of PM_{10} ranged from 26.33 to 109.14 µg/m^3 and the concentration of $PM_{2.5}$ ranged from 14.83 to 84.03 µg/m^3 in urban parks, with means of 54.35, 90.05 and 71.21 µg/m^3 for PM_{10} and 39.03, 59.71 and 50.66 µg/m^3 for $PM_{2.5}$ in CCP, CP and SP, respectively The concentration of PM is compared with the concentration of PM in reference site as a background value which means of 97.91 µg/m^3 for PM_{10} and 69.23 µg/m^3 for $PM_{2.5}$. The results show that the PM mean concentrations in urban parks are much lower than the reference site (VC). According to the standard of PM_{10} and $PM_{2.5}$ set by WHO which is

50 and 20 µg/m^3, the concentrations at sampling sites exceed the standard about 2-3 times. The source of these particles is associated with transportation, industrial and human activities. The means concentration of PM_{10} and $PM_{2.5}$ is lower, indicating that plants and vegetation in urban park has potential of reducing since there is wax on the leaves. The concentration in a background sites which located in high traffic area, indicating that most particles are emitted from vehicles and human activities.

PAHs concentration

shows that the major PAHs bound $PM_{2.5}$ in the atmosphere is BaP (benzo(a)pyrene) which is categorized as a carcinogen by EPA. Next two species which obviously

The PAHs concentration of 16 species in urban parks are shown in Figure (4) and Figure (5). The concentration of total PAHs bound $PM_{2.5}$ in CCP, CP and SP are 9.16, 10.08 and 11.79 ng/m^3, respectively. The concentration of total PAHs bound PM_{10} in CCP, CP and SP are 17.66, 11.55 and 33.97 ng/m^3, respectively. The concentration of total PAHs bound $PM_{2.5}$ and PM_{10} is compared with a background value from VC which is 56.52 and 17.41 ng/m^3. The results show that the concentration of total PAHs in urban parks is much lower than in the reference site. Moreover, the result found are dibenzo(a,h)anthracene and benzo (g,h,i) perylene. For $PM_{10-2.5}$, the major PAH species found are acenaphthylene, Benzo(a)pyrene and dibenzo(a,h)anthracene.

Table 1 PM_{10} and $PM_{2.5}$ and PCD daily average measured and monitored data at 4 studied sites.

Sampling site	Measured $PM_{10-2.5}$(µg/m^3)	Measured PM_{10}(µg/m^3)	Measured $PM_{2.5}$(µg/m^3)	PCD PM_{10}(µg/m^3)	PCD $PM_{2.5}$(µg/m^3)	Measured $PM_{2.5}$: PM_{10}	PCD $PM_{2.5}$: PM_{10}
CCP	7.60±2.89	54.35±22.68	39.03±19.39	57.33±21.78	38.17±18.57	0.72	0.67
CP	16.04±1.80	90.05±15.34	59.71±10.81	62.86±27.30	39.15±11.15	0.66	0.62
SP	20.52±5.15	71.21±22.78	50.66±20.19	88.17±25.74	60.00±25.96	0.71	0.68
VC	28.67±4.67	97.91±15.95	69.23±12.52	92.17±20.76	56.50±20.72	0.71	0.61

Where, CCP is Chulalongkorn Centenary Park, CP is Chatuchak Park, SP is Santiphap Park and VC is Victory Monument.

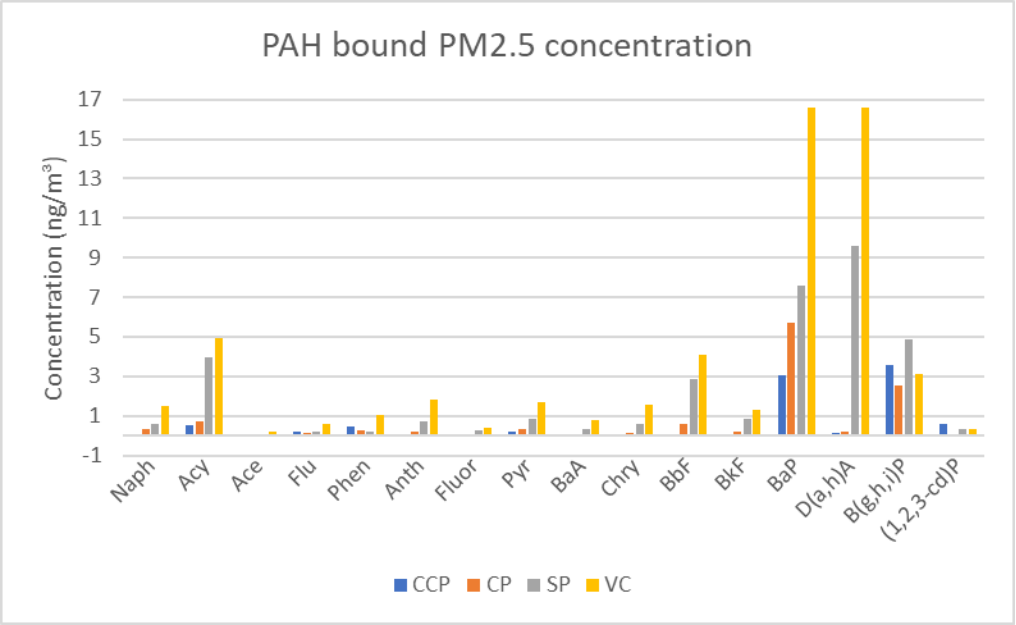

Figure 3 PAHs bound PM2.5 concentration at 4 studied sites (ng/m^3)

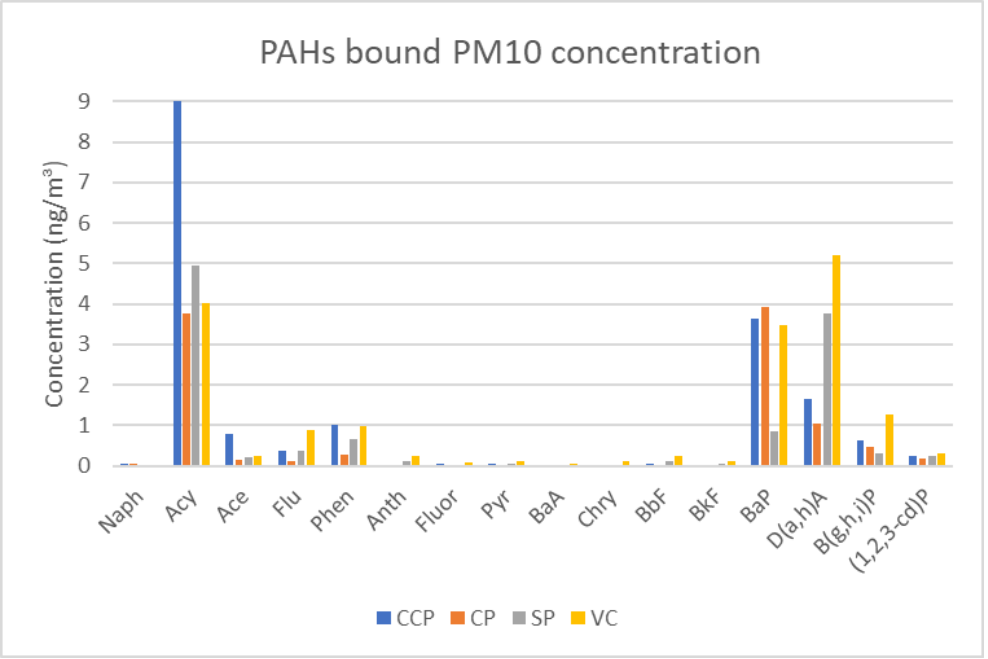

Figure 4 PAHs bound $PM_{10-2.5}$ concentration at 4 studied sites (ng/m^3).

CONCLUSIONS

The PAHs bound PM_{10} and $PM_{2.5}$ concentrations in urban parks in Bangkok were investigated in this study. The average concentration of PM_{10} in CCP, CP, SP and VC were 54.35, 90.05, 71.21 and 97.91 μg/m^3 and $PM_{2.5}$ are 39.03, 59.71, 50.66 and 69.23 μg/m^3, respectively. The PAHs concentrations in urban parks ranged from 0.02 to 210 ng/m^3. The concentration of both PM and PAHs in three parks is much lower than the reference site which located in the high traffic area. This result indicates that vegetation in parks may reduce particulate matter which comes from variety sources. The major PAH compound which is benzo(a)pyrene should be paid more attention due to its large amount in the atmosphere compared to other species and cancer potential. In conclusion, this study will be quite useful for residents and urban planning department in case of increasing more plants to prevent particulate matters.

ACKNOWLEDGEMENTS

This research was supported by Center of Excellence on Hazardous

Substance Management (HSM), The S&T Postgraduate Education and Research Development Office (PERDO), Scientific and Technological Research Equipment Centre m(STREC) and Department of Environmental Science, Faculty of Science, Chulalongkorn University.

REFERENCES

[1] Sahavin N., Tantrakarnapa K., Preuksasit T. Ambient PM10 and PM2.5 concentrations at different high traffic-related street configurations in Bangkok, Thailand. Southeast Asian Trop Med Public Health. 2016; 47: 528-535.

[2] Vanderzalm J., Hooper M., Maenhaut W., Tapper N. Particulate Air Quality and Polycyclic Aromatic Hydrocarbons in regional Northwest Australia and Southeast Asia. Clean Air and Environmental Quality. 2000; 34: 29-30.

[3] United States Environmental Protection Agency. Particulate matter (PM) pollution. 2017; (online): https://www.epa.gov/pm-pollution

[4] Liu J., Man R., Ma S., Li J., Wu Q., Peng J. Atmospheric levels and health risk of polycyclic aromatic hydrocarbons (PAHs) bound to PM2.5¬ in Guangzhou, China. Marine Pollution Bulletin. 2015; 100: 134-143.

[5] Jinsart W., Tamura K., Loetkamonwit S., Thepanondh S., Karita K., Yano E. Roadside Particulate Air Pollution in Bangkok. Journal of the Air & Waste Management Association. 2011; 52:9, 1102-1110.

[6] Franco C., Resende M., Furtado L., Brasil T., Eberlin M., Netto A. Polycyclic aromatic hydrocarbons (PAHs) in street dust of Rio de Janeiro and Niteroi, Brazil: Particle size distribution, sources and cancer risk assessment. Science of the Total Environment. 2017; 599-699: 305-313.

[7] Hu y., Bai Z., Zhang L., Wang X., Zhang L., Yu Q., Zhu T. Health risk assessment for traffic policeman exposed to polycyclic aromatic hydrocarbons (PAHs) in Tianjin, China. Science of the Total Environment. 2007; 382: 240-250.

[8] Kamal A., Malik R., Martellini T., Cincinelli A. Cancer risk evaluation of brick kiln workers exposed to dust bound PAHs in Punjab province (Pakistan). Science of the Total Environment. (2014); 493: 562-570.

[9] Cohen P., Potchter O., Schnell I. The impact of an urban park on air pollution and noise levels in the Mediterranean city of Tel-Aviv,Israel. Environmental Pollution. 2014; 195: 73-83.

[10] Chen L., Liu C., Zou R., Yang M., Zhang Z. Experimental examination of effectiveness of vegetation as bio-filter of particulate matters in the urban

environment. Environmental Pollution. (2016); 208: 198-208.

[11] Leonard R., McArthur C., Hochuli D. Particulate matter deposition in roadside plants and the importance of leaf trait combinations. Urban Forestry & Urban Greening. (2016); 20: 249-253.

[12] Chaudhary., Rathore D. Suspended particulate matter deposition and its impact on urban trees. Atmospheric Pollution Research. (2018); 9: 1072-1082.

[13] Qiang L., Yang W., Jingshuang L., Quanying W., Mingying Z. Grain-size distribution and heavy metals contamination of road dusts in urban parks and squares in Changchun, China. Environ Geochem health. (2015); 37: 71-82.

[14] Wang J., Li S., Cui X., Li H., Qian X., Wang C., Sun Y. Bioaccessibility, sources and health risk assessment of trace metals in urban park dust in Nanjing, Southeast China. Ecotoxicology and Environmental Safety. (2016); 128: 161-170.

[15] BMA Data Center. สวนสาธารณะกทม.ปลอดภัย คนใช้วันละแสน. 2018; (online): https://siamrath.co.th/n/49324

[16] Yin S., Shen Z., Zhou P., Zou X., Che S., Wang W. Quantifying air pollution attenuation within urban parks: an experimental approach in Shanghai, China. Environmental Pollution. 2011; 159: 2155-2163.

[17] United States Environmental Protection Agency. Human Health Risk Assessment. 2016; (online): https://www.epa.gov/risk/human-health-risk-assessment

[18] Du Y,. Gao B., Zhou H., Ju X., Hao H., Yin s. Heath risk assessment of heavy metals in road dust in urban parks of Beijing, China. Procedia Environmental Sciences. 2013; 18: 299-309.Sellers, RM. Spectrophotometric determination of hydrogen peroxide using potassium titanium (IV) oxalate. The Analyst 1980; 105(1255): 950-954.

Long-Term Satellite Assessment of Particulate Matter in Thailand

Sakonwach Mongkolphew[1] and Pichnaree Lalitaporn[1*]

[1*]Department of Environmental Engineering, Faculty of Engineering,
Kasetsart University, Bangkok 10900, Thailand;
Corresponding author: e-mail: fengprla@ku.ac.th

ABSTRACT

Satellite data of AOD were retrieved from MODIS-Terra and -Aqua satellites from 2000-2019 in the northern and central parts of Thailand. Long-term time series of AOD plotted with ground PM_{10} and $PM_{2.5}$ concentrations showed good consistency in seasonal pattern, especially in the northern region. Both satellite and ground data presented high levels during March in the North. In the central region, AOD presented similar pattern as the northern region whereas PM_{10} and $PM_{2.5}$ concentrations presented higher levels during November-March. The model results showed that the discrepancy was due to the dust aloft traveling from neighboring countries. The relationship of AOD and $PM_{10}/PM_{2.5}$ were also investigated during air pollution episode in Bangkok during January 2019. The results presented well correlated between the data when the AOD data were retrieved from Aqua. The levels of AOD, PM_{10} and $PM_{2.5}$ in January revealed increasing trends from 2016-2019. Moreover, the relationship of satellite and ground based data were analyzed with cloud fraction (CF). Overall, the analysis with CF=0.2 provided slightly better correlation than CF=1. The regression models of AOD-$PM_{2.5}$ under CF=0.2 were developed with meteorological variables using the data from 2000-2016 for based data to estimate $PM_{2.5}$ concentrations in 2017 and 2018

in the North. The correlation coefficients (R) of modeled and observed data range from 0.72-0.82.

Keywords: AOD, MODIS, $PM_{2.5}$, PM_{10}, Thailand

INTRODUCTION

Nowadays, technology has played an important role in society making the environment changing due to the rapid growth of communities and industries. Air pollution has become a serious problem. One indicator is particulate matter (PM) in the atmosphere of Thailand that has increased significantly over the years, especially in the central and northern regions.

Thailand is one of the countries that have experienced air pollution problems. The problems generally occur during the dry season from December to April of every year. In 2015, the amount of particulate matter exceeds the standard criteria up to 42 days (Pollution Control Department, 2015). During January-April 2019, has reported that Chiang Mai has the highest air quality index in the world at AQI=271, with $PM_{2.5}$ being around 170 micrograms per cubic meter (μg/m3) while, Bangkok has the top 5 highest air quality index in the world at AQI=164, with $PM_{2.5}$ concentration exceeds the standard for all ground measurement stations. Smog conditions cover a large area in the north caused by biomass open burning was mainly related to the collection and harvest of forest products (41%), while agricultural area (crop and paddy fields) was accounted for 31% (Punsompong and Chantrara, 2015). This problem affects the well-being of people buildings, economic, tourism and transportation especially the health effects of respiratory system. In addition, the monitoring methods for particulate matter with an aerodynamic diameter smaller than 10 microns (PM_{10}) and 2.5 microns ($PM_{2.5}$) in the atmosphere that is currently used are ground-

based measurements which are not covering some areas. Most of them are installed in urban areas and in densely populated areas, while rural areas and remote areas, air quality measurements are not yet reached. Therefore, in order to effectively monitor the air quality in accordance with the increasing air quality problems, the study of the ability to use satellite data in conjunction with ground measurement data is necessary. Meanwhile, Satellite-derived AOD data are generated by two algorithms depending on the surface: over-land and over-ocean. These algorithms allow cloud pixel rejection while maintaining other cloud free pixels. In MODIS procedures, algorithms are applied to individual boxes of 20x20 pixels at 500 m resolution to produce 1 pixel at 10 km resolution of AOD. At least 10 pixels must be computed by the over-ocean algorithm and 12 by the over-land algorithm. Otherwise, no AOD data were reported (Levy et al., 2009). Most of the studies have developed correlations between AOD and PM variables in US and Europe (Engel-Cox et al; 2006; Gupta et al. 2006; Pelletier et al. 2007; Wang et al., 2010) while, many recent studies also derived the long-term trends of AOD over East Asia using MODIS data. Tsai et al. (2009) used ground-based measurements to assess AOD in Taiwan, showing that high correlations between AOD and $PM_{2.5}$ range from 0.88-0.93 in autumn, while 0.76-0.87 in winter and 0.77-0.80 in spring. The objective of this study was to determine the relationship between ground $PM_{10/2.5}$ concentrations and satellite Aerosol Optical Depth (AOD) in the northern and central parts of Thailand over 20 years from 2000-2019. Daily ground $PM_{10/2.5}$ data were collected from the Pollution Control Department (PCD). Satellite AOD data were retrieved from MODIS-Terra and -Aqua satellites.

METHODOLOGY

Data Collection

Ground monitoring data of hourly PM_{10} and $PM_{2.5}$ concentrations were collected from

PCD at 39 air quality monitoring stations covering the areas of northern part and central part of Thailand. The northern part is the secondary largest part in the country with a population around 6 millions. Its terrain mostly consists of forested mountains which are accounted to be around 64.37% of total area, following by agricultural area (12%) and urban land (23.33%). Yearly average temperature ranged 25.5-28.5˚C and yearly average relative humidity ranged 68-79% (National Statistical Office, 2018). Though like most of Thailand, it has a tropical savanna climate, its relatively high elevation and latitude contribute to more pronounced seasonal temperature variation, with cooler winters than the other regions. The hottest month is April while the coolest month is January. The ground monitoring stations used for data collection are located at Chiangmai, Mae hong son, Chiangrai, Phayao, Lamphun, Lampang, Nan and Phrae. $PM_{2.5}$ data were available only at Chiangmai and Lampang. The central part has a total population around 20 millions, representing the population of Bangkok about 6 millions (Bureau of Registration Administration, 2018). Additionally, it consists of agricultural area which are accounted to be around 49.11% of total area, following by forested area (33.60%) and urban land (10.06%) (Land Development Department, 2016). The stations used for data collection are located at Nakhon Sawan, Ayutthaya, Saraburi, Samut-Prakan, Samut Sakhon, Nonthaburi, Pathum Thani and Bangkok. $PM_{2.5}$ data were available only at Saraburi, Samut Prakan and Bangkok as shown in Figure 1 during January 2000-June 2018 and January 2019 due to availability of the data. Also, meteorological variables play an important role in the AOD-PM relationship (Khoshsima et al., 2014; Wu et al., 2016) Temperature T, relative humidity (RH) and wind speed (WS) were gathered from PCD for the same period.

This study focuses on the detection of PM_{10} and $PM_{2.5}$ using the daily average particulate matter at the time of 9:00-12:00 LST (UTC+7)

and 12:00-15:00 LST (UTC+7) from the air quality monitoring station of PCD. Satellite data which are AOD and CF were obtained from the Moderate Resolution Imaging Spectroradiometer (MODIS) on the Terra satellite product MOD04_L2 and MOD06_L2 at 10:30 LST and on the Aqua satellite product MYD04_L2 and MYD06_L2 at 13:30 LST. The Satellite data reported at 50 km spatial resolution

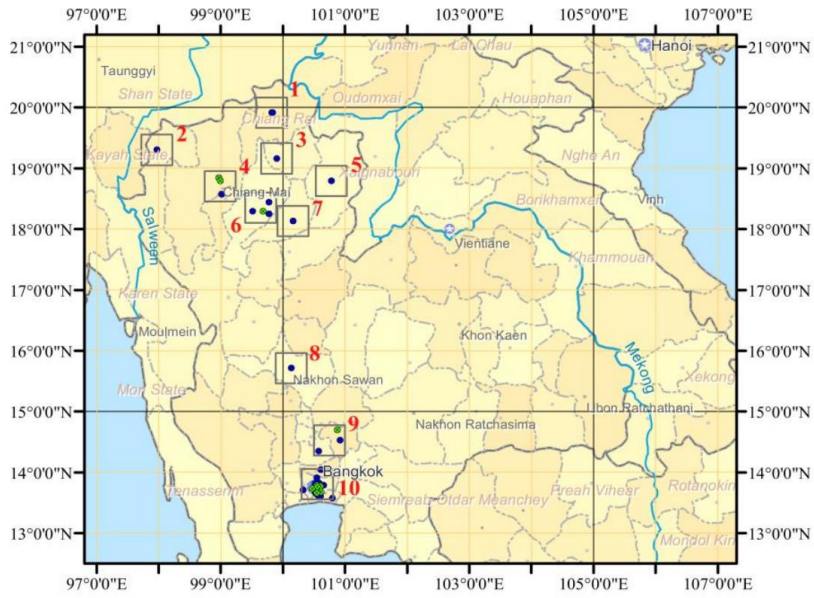

Figure 1 Study Area.

Data Analysis

Correlation Analysis is used to study the relationship between PM_{10} and $PM_{2.5}$ with AOD data in the study area using daily analysis to see trends in the correlation coefficient (R). If the coefficient between that variables is close to -1 or 1, there is a high level of relevance. On the other hand, if the coefficients of the relationship between the variables are close to 0, there is little or no relationship (Pimonsree, 2010).

Correlation between MODIS Terra/ Aqua AOD data and PM_{10}/ $PM_{2.5}$ concentrations were investigated to assess applicability to air quality monitoring. Hourly PM were averaged as 3-hour average during 09: 00-12: 00 LST and 12: 00-

15: 00 LST cover MODIS Terra and Aqua overpasses respectively. MODIS- Terra/ Aqua AOD and PM data were averaged within a 50 x 50 km2 around sampling sites (PCD station). In this study, cloud screening process was adopted at CF=0.2 and CF=1 in order to investigate the variations of the correlations between PM mass measurements and retrieved AOD values, with the different classes of cloudiness.

Finally, regression analysis was applied for identifying a relationship between PM concentrations and AOD. Multiple linear regressions was conducted considering the meteorological parameter effects on the relationship between AOD and hourly average PM.

The development of multiple linear regression models to estimate surface PM mass concentrations used 17-year database of AOD, PM_{10}, $PM_{2.5}$, RH, T and WS during 2000-2016. To evaluate the validity of the regression model, estimated surface PM_{10} and $PM_{2.5}$ mass concentrations over Thailand for year 2017 and 2018 (January- June) were compared with those collected from PCD, Thailand during the same periods.

RESULTS AND DISCUSSION

Preliminary Analysis

Based on the collected data, to analyze the preliminary trends as shown in Figure 2, it is found that either Terra or Aqua AOD and PM are consistent. In the northern region, there is a very similar increase around dry season and decrease of AOD, PM_{10} and $PM_{2.5}$ at the same date and time. However, in the central region, the trend is quite similar but not as much as the north; Increasing and decreasing in the same period, but not the same date and time which may be caused by weather factors and the particulate matter moving or being detained due to weather conditions. The monthly average trend analysis as shown in Figure 3 showed that in the north, AOD and PM increased at the highest level during March every year since biomass open burning in

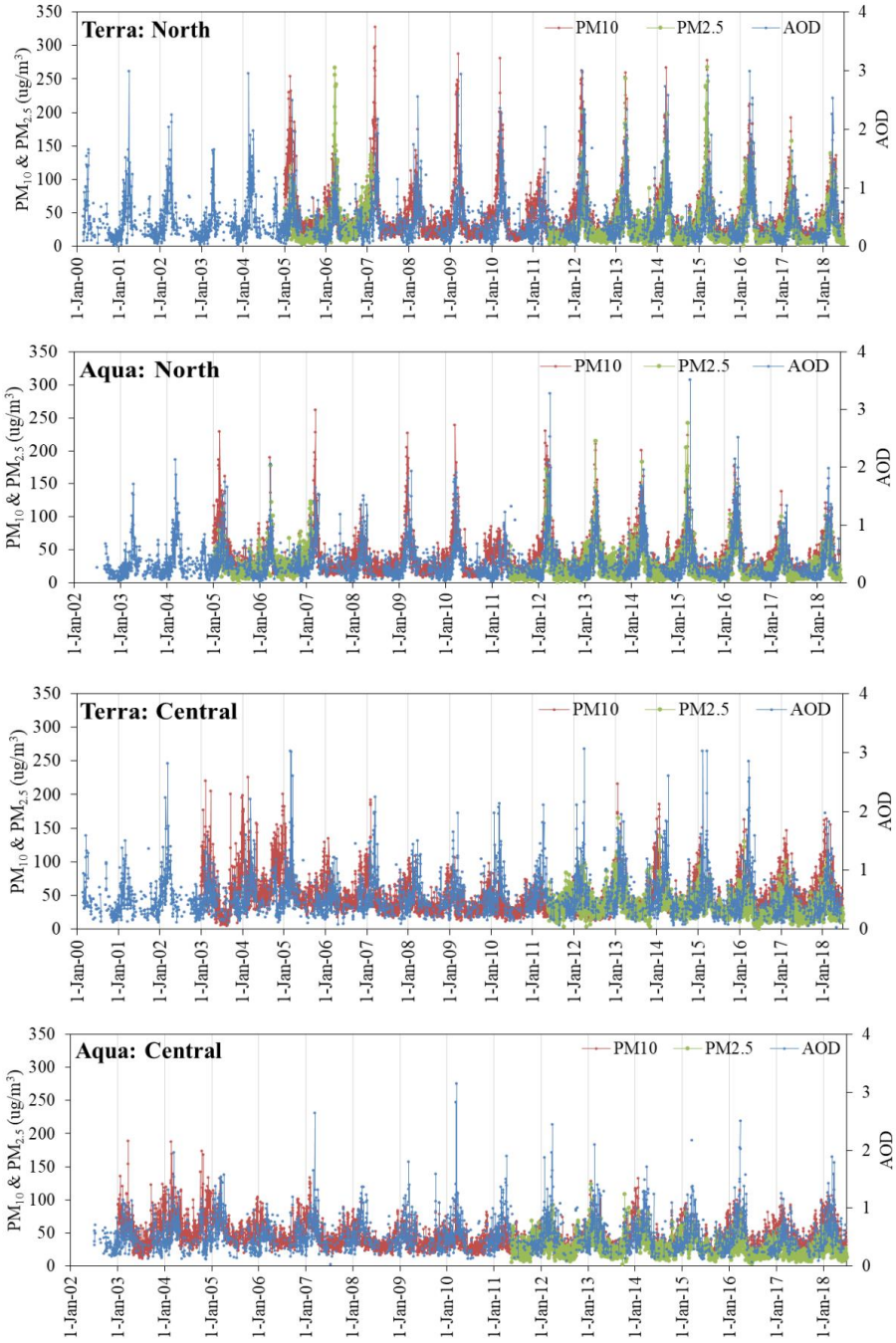

Figure 2 AOD-PM trends from 2000-2018 in North and Central of Thailand.

Northern Thailand, including forest fires, crop residue burning and solid waste burning, had been found to be the major cause of haze episodes for

more than two decades in the north of Thailand (Tiyapairat and Sajor 2012) and are recognized as the important sources of high PM concentrations in the area, particularly during the dry season between November to April (Kim Oanh and Leelasakultum, 2011).

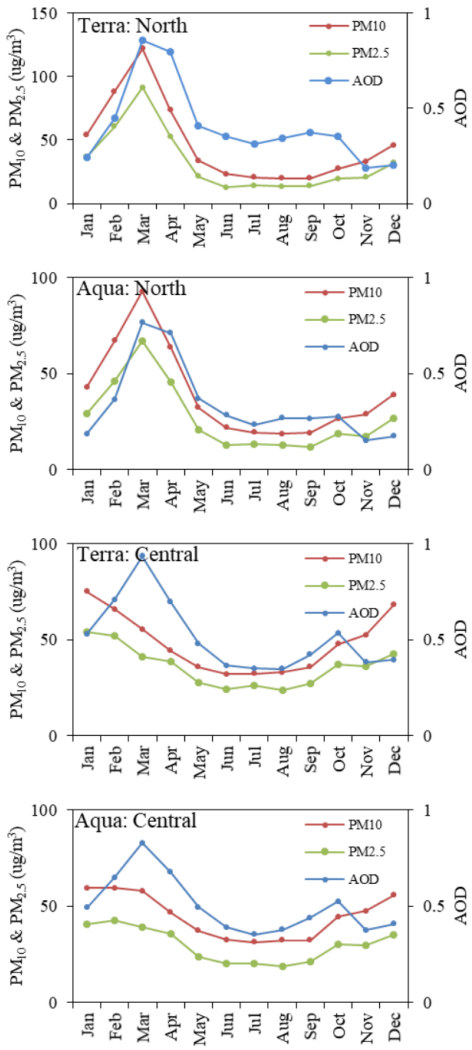

Figure 3 AOD-PM monthly trends from 2000-2018.

In the central region, AOD levels were significantly higher in March while PM concentrations were higher during November to March. The Hybrid Single Particle Lagrangian Integrated Trajectory (HYSPLIT) Model was used to compute 3-day air mass transporting and plotted with fire hotspots from Visible Infrared Imaging Radiometer Suite (VIIRS) sensor as shown in Figure 4. It was found that the air mass transport into the central region from the east and south at various altitudes, both from neighboring countries and the Gulf of Thailand, as well as the air mass transport from the north of Thailand, which passed the area that has high burning activities during March causing high dust aloft in the atmosphere. However, PM ground measurement is normally restricted to the surface layer or planetary boundary layer (PBL). Therefore, satellites that can detect AOD values at entire vertical altitude provide higher AOD values during March, but the ground monitoring stations cannot detect PM values at a high altitude.

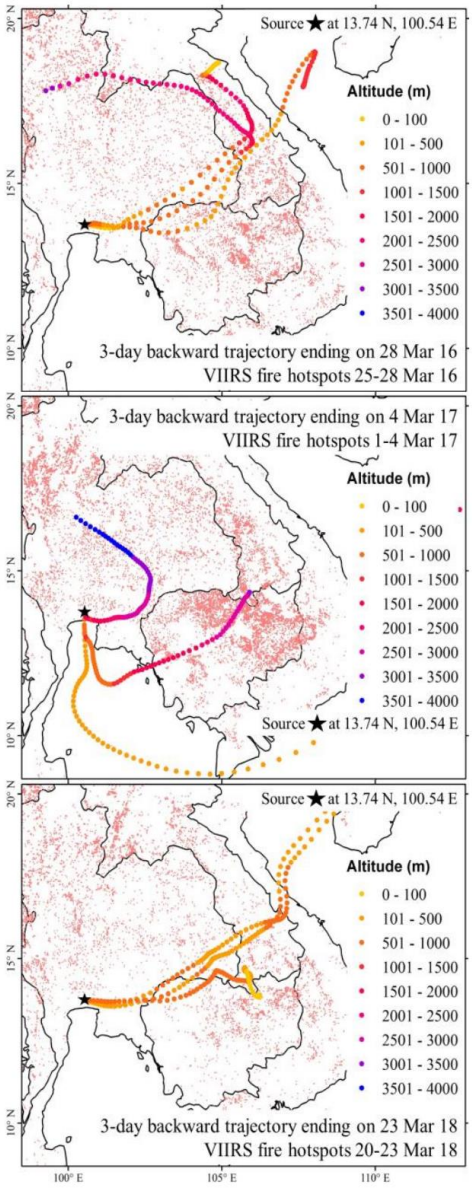

Figure 4 VIIRS 3-day backward trajectory in March in Bangkok since 2016-2018.

In Bangkok, the expansion of urban land use due to unplanned and rapid growth in terms of population and economic took place in horizontal manner to the provinces surrounding Bangkok causing the crisis of $PM_{2.5}$ exceeding the standard in Bangkok Metropolitan Region in January 2019. This study applied satellite data to analyze the relationship between AOD and PM. It was found that the data from Aqua satellites have R = 0.78 for AOD-PM_{10} and R = 0.76 for AOD-$PM_{2.5}$ which shows higher correlation than the data from Terra satellites with R = 0.50, for both AOD-PM_{10} and AOD-$PM_{2.5}$ as shown in Figure 5. The results showed AOD data derived from Aqua provided better assessment results than the data from Terra. Furthermore, this study showed better results of AOD-PM_{10} in Bangkok than previous study; during January-December 2006, the R value from 0.18-0.51 and during January-May 2007, the R value from 0.31-0.51 (Juntarakumtorn, 2012).

Moreover, considering the maximum and average values of AOD and PM in January in Bangkok for the past 4 years, they have been continuously increasing since 2016-2019 as shown in Figure 6.

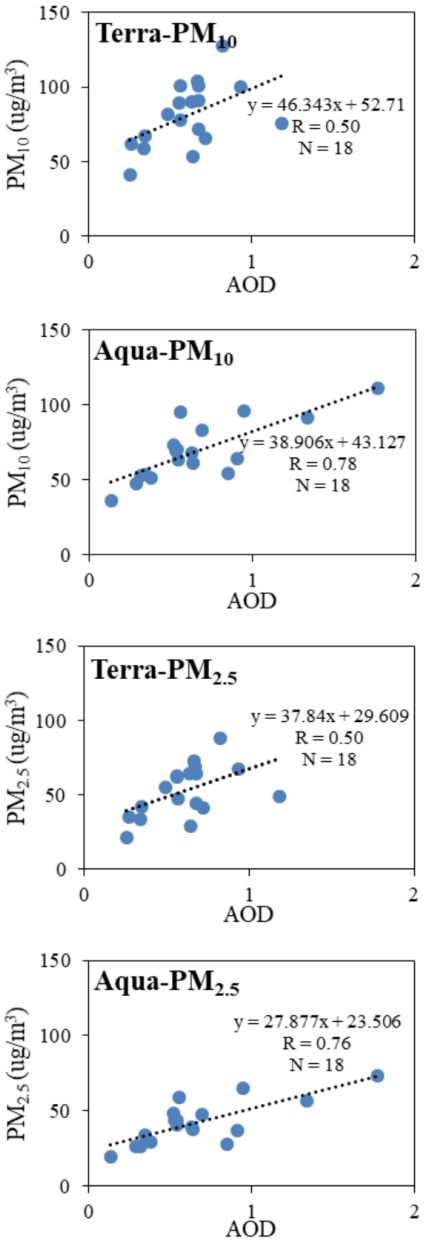

Figure 5 AOD-PM relationships in Bangkok in January 2019.

Correlation with cloud screening

This section, cloud screening was applied to the analysis of the relationship of AOD-PM_{10} and AOD-$PM_{2.5}$ in 2000-2016 in cases of full cloud (CF=1) and almost clear sky (CF=0.2).

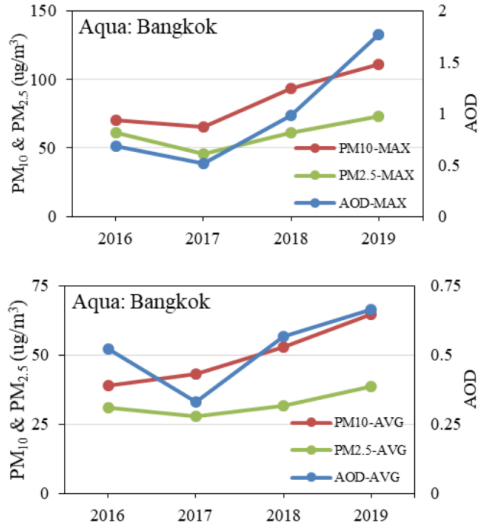

Figure 6 AOD, PM Maximum & Average in January in Bangkok since 2016-2019.

In Figure 7, in the northern part, the relationship between AOD-PM_{10} showed R values of CF=0.2 was 0.70 and 0.82 for Terra and Aqua, respectively, and R of CF= 1 was 0.59 and 0.70 for Terra and Aqua, respectively, while AOD-$PM_{2.5}$ showed R of CF=0.2 was 0.61 and 0.70 for Terra and Aqua, respectively, and R of CF=1 was 0.54 and 0.68 for Terra and Aqua, respectively. Meanwhile, in central

part, the relationship between AOD-PM_{10} showed R of CF=0.2 was 0.16 and 0.35 for Terra and Aqua, respectively, and R of CF=1 was 0.16 and 0.30 for Terra and Aqua, respectively, while AOD-$PM_{2.5}$ showed R of CF=0.2 was around 0.27 and 0.38 for Terra and Aqua, respectively, and R of CF=1 was and 0.36 for Terra and A respectively. The results indicat the R values of the relationsh AOD-PM increase when analyz clear sky conditions. Howeve number of the data reduces ar 75%.

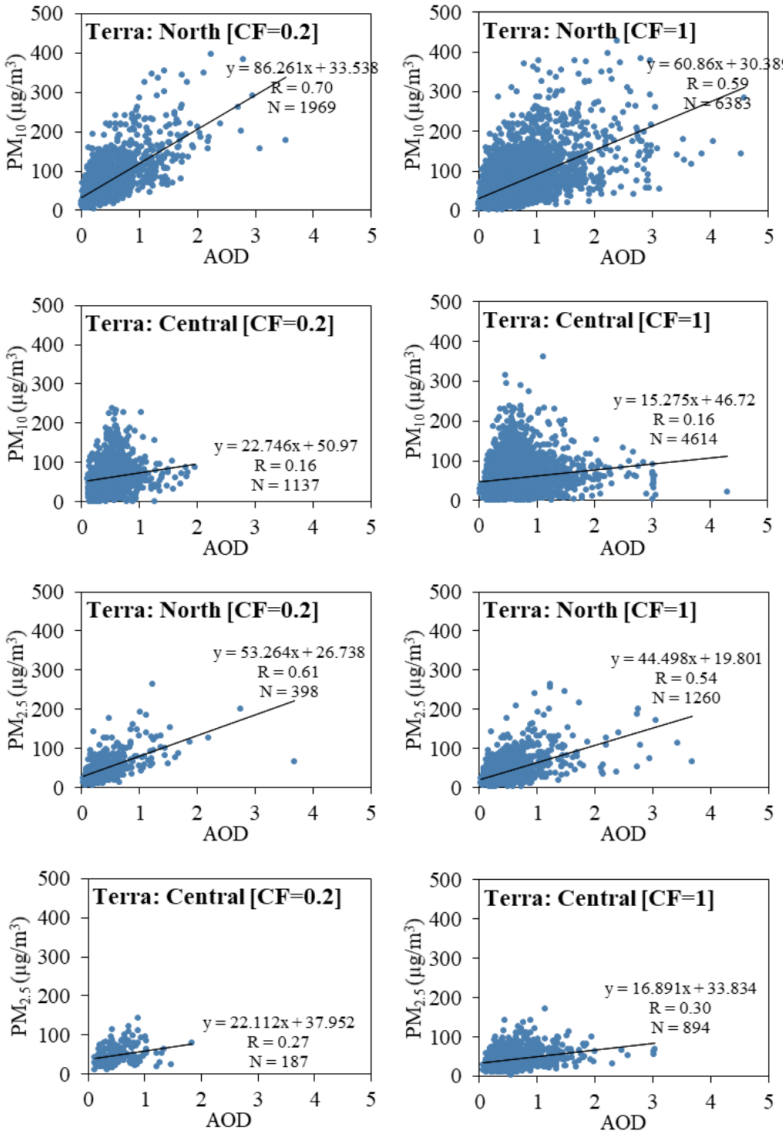

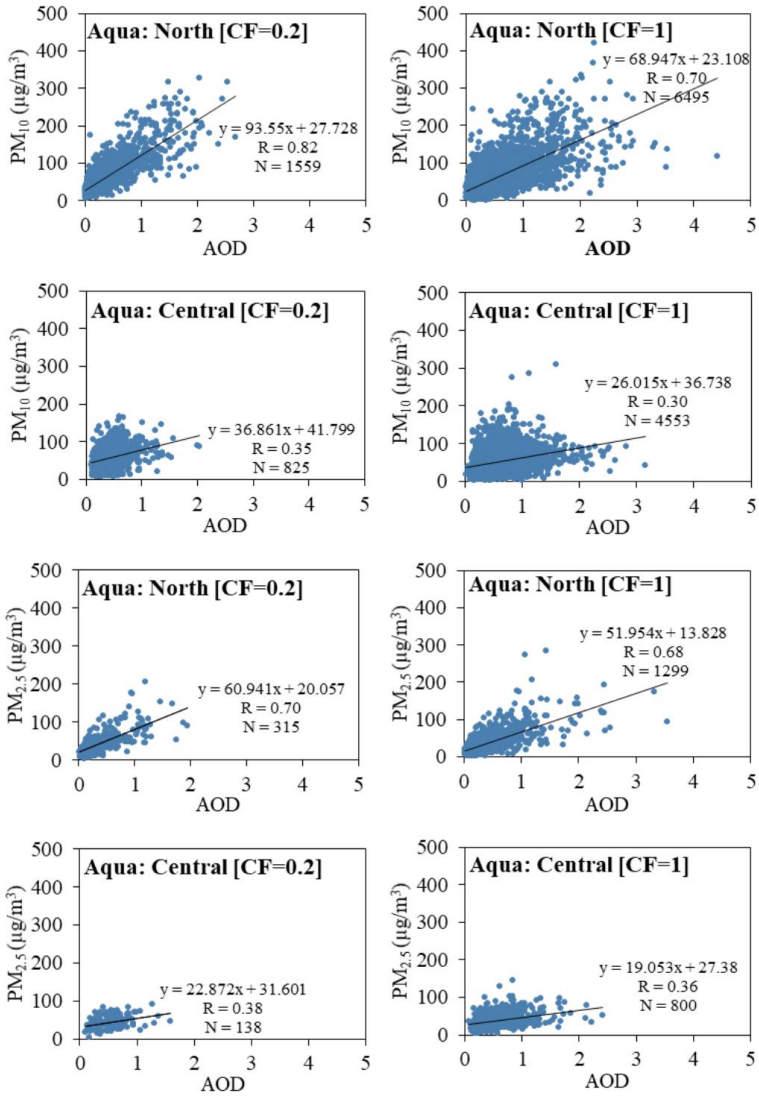

Figure 7 AOD-$PM_{10/2.5}$ in Northern and Central of Thailand at CF=0.2 and CF=1 from 2000-2016.

Equation development & Evaluation

The relationship between PM concentrations and AOD is expected to depend on meteorological condition (Dinoi et al. 2010). Thus, multiple linear regression was conducted considering the meteorological parameter (T and RH) that can effects on the relationship between AOD and hourly average PM at CF=0.2. Northern part data from 2000-2016 were used to

develop equations by SPSS due to the highest correlation of Thailand. The analysis in Figure 8 shows that WS has no significance on AOD seasonal trend. The results show that when RH decreases and T increases, AOD increases. Therefore, WS will not include in the equation. The equations was fitted using the dataset (PM, AOD, T and RH) to estimate the model coefficients. Overall, the equations result performed a considerably significance ($p<0.01$) and the equations gave R values between AOD-$PM_{2.5}$ of 0.69 and 0.71 for Terra and Aqua, respectively as shown in Table 1.

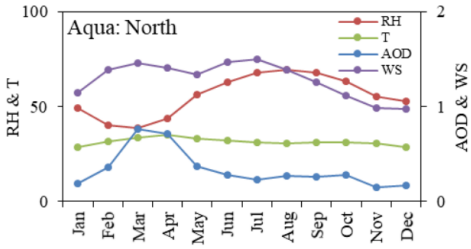

Figure 8 AOD, RH, T and WS Relationships from 2000-2018.

The regression models were validated with observed hourly average $PM_{2.5}$ in Northern during 2017 and 2018 (January-June). The results in Figure 9 showed good consistency in seasonal pattern. Both satellite and ground data presented high levels during February-April with the peak in March same as the previous results. In case of Terra Model, the R values of modeled and observed data in the northern part is 0.75. For station 4 and 6, the R values range from 0.75-0.77. In case of Aqua model, the R values for the northern part is 0.77 and for the station 4 and 6, the R values range from 0.77-0.82. Moreover, Models were often overestimate when $PM_{2.5}$ is less than 100 $\mu g/m^3$. On the Other hand, the models underestimate when $PM_{2.5}$ is more than 100 $\mu g/m^3$. Overall, Aqua Model is more accurate than Terra.

Table 1 Multiple linear regression model of AOD and $PM_{2.5}$ included meteorological factors.

Platform	Regression Model	R	P-Value
MODIS-Terra	$PM_{2.5}$ = 173.526 + 52.270 (AOD) - 1.218 (RH) - 2.814 (T)	0.69	< 0.01
MODIS-Aqua	$PM_{2.5}$ = 103.797 + 65.209 (AOD) - 0.922 (RH) - 1.509 (T)	0.71	< 0.01

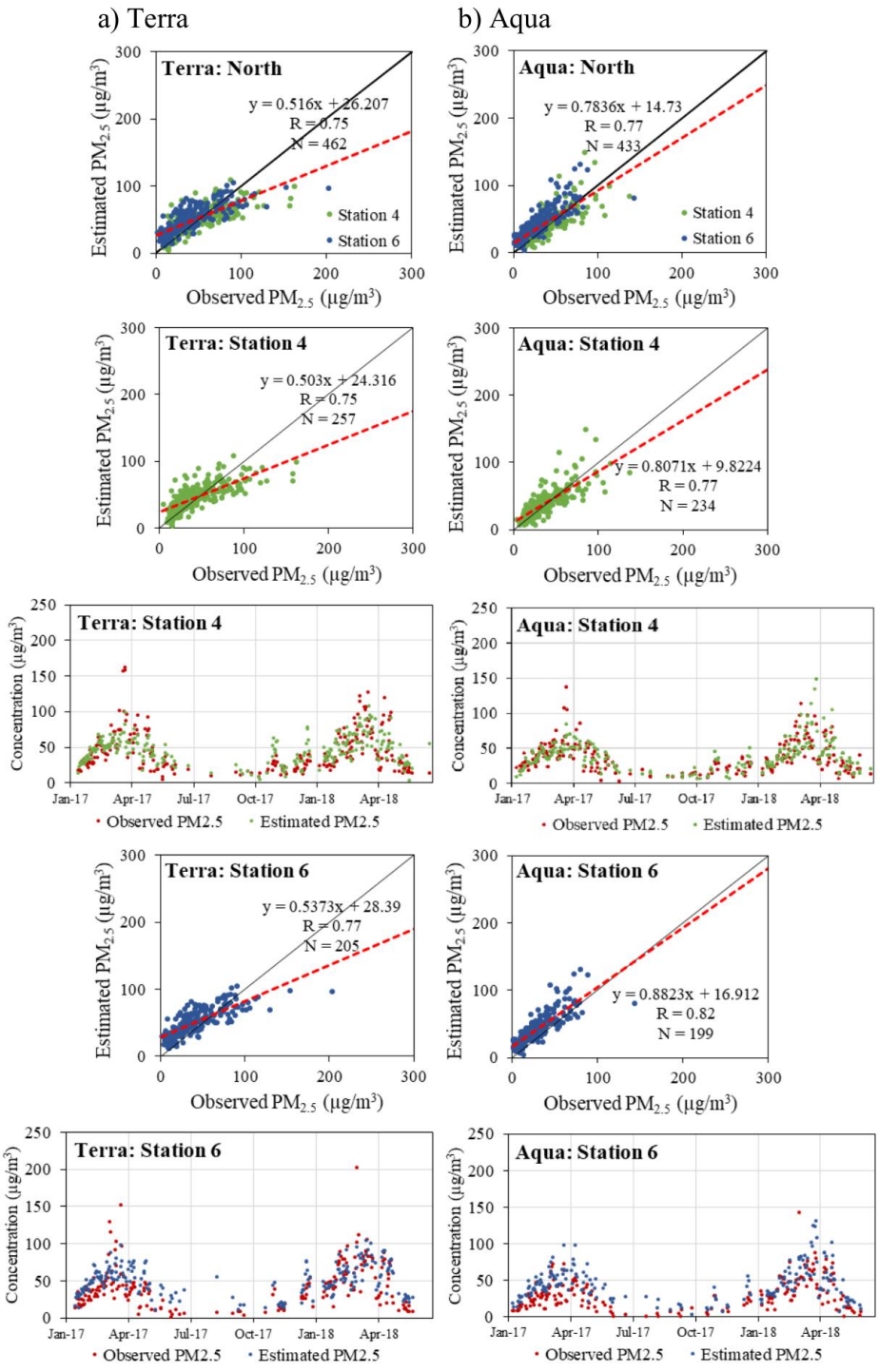

Figure 9 Observed and Estimated $PM_{2.5}$ in Northern Thailand from 2017-2018 (January-June) using AOD data sets from a) Terra b) Aqua.

CONCLUSIONS

The results showed positive correlations between AOD-$PM_{2.5}$. The R values were 0.75 for Terra and 0.77 for Aqua. Incorporation of temperature and relative humidity improved the relationship between AOD and PM. The R values obtained from multiple linear regression AOD-$PM_{2.5}$ were 0.69 for Terra and 0.71 for Aqua. The model validity for 2017-2018 confirmed possibility to apply the regression correlation between AOD-PM in Northern Thailand. This study focuses on the North because the Central region or other areas are involve with many factors such as wind direction, planetary boundary layer, pollution source, topography including the availability of the measurement station. For further study, the validity should be investigated to ensure the applicability for other areas.

ACKNOWLEDGEMENTS

The authors would like to thank NASA for providing the satellite data in LAADS DAAC, also Pollution Control Department (PCD) for air quality data. Extended thanks Department of Environmental Engineering, Kasetsart University and the Kasetsart University Research and Development Institute (KURDI) for research fund which is necessary to develop the model. Without their participation, this study would not have been successfully.

REFERENCES

Pollution Control Department. Thailand State of Pollution Report 2015; 3-26.

Department of Provincial Administration. Announcement of the Bureau of Registration Administration 2018; http://stat.bora.dopa.go.th/stat/y_stat61.html: Retrieved on April 2019.

Dinoi, A., Perrone. 2010. Application of MODIS products for air quality studies over Southeastern Italy. Remote Sensing of Environment, 2, 1767-1796.

Engel-Cox, J. A., Hoff. 2006. Integrating lidar and satellite optical depth with ambient monitoring for 3-dimension particulate characterization, Atmos. Environ., 40, 8056-8067.

Gupta, P., Wang, J. 2006. Satellite remote sensing of particulate matter and air quality over global cities. Atmospheric Environment 40 (30), 5880-5892.

Kim Oanh, N. T., & Leelasakultum, K. 2011. Analysis of meteorology and emission

in haze episode prevalence over mountain-bounded region for early warning. Science of the Total Environment, 409(11), 2261-2271.

Khoshsima, M., Ahmadi-Givi, F. 2014. Impact of meteorological parameters on relation between aerosol optical indices and air pollution in a suburban area. J. Aerosol Sci. 68, 46–57.

Land Development Department. Summary of land use categories, Thailand. 2017 http://www1.ldd.go.th/WEB_OLP/result/luse_result58-59.html: Retrieved on April 2019

Levy RC, Remer LA, Kaufman YJ. Algorithm for Remote Sensing of Tropospheric Aerosol over Dark Targets from MODIS, National Aeronautics and Space Administration 2009; https://modis-atmosphere.gsfc-.nasa.gov/: Retrieved on April 2018

National Statistical Office. 2018. Statistical Yearbook Thailand; http://www.nso-.go.th: Retrieved on October 2018.

Pelletier, B., Santer, R. & Vidot, J. 2007. Retrieving of particulate matter from optical measurements: a semi-parametric approach. Journal of Geophysical Research 112 (D06208)

Pimonsree, S. 2010. Status of Particulate problems in Northern Thailand. Phayao University; 2(15)

Punsompong, P. and Chantrara, S.2015. Pattern of Biomass Burning in Chiang Mai, Thailand and Transportation of Air Pollutants in Dry Season. Thai Society of Higher Education Institutes on Environment. Retrieved July 2018

Tian J, Chen D. A Semi-Empirical Model for Predicting Hourly Ground-Level Fine Particulate Matter ($PM_{2.5}$) in Southern Ontario. Remote Sensing of Environment 2010; 114: 221-29.

Tiyapairat Y, Sajor EE. State Simplifcation, Heterogeneous Causes of Vegetation Fires and Implications on Local Haze Management:Case Study in Thailand. Environment, Development and Sustainability 2012; 14: 1047-64.

Tsai, T.-C., Jeng, Y.-J., Chu, D.A. 2009. Analysis of the relationship between MODIS aerosol optical depth and particulate matter from 2006 to 2008. Atmos. Environ; 107, 1-12

Juntarakumtorn K. Mapping of Particulate Matters Less Than 10 Microns (PM_{10}) Surface Concentrations Derived from Terra/Aqua-MODIS in Upper Northern Thailand 2012. Chiangmai University; 1(27)

Wang Z, Chen L, Tao J, Zhang Y, Su L. Satellite-Based Estimation of Regional Particulate Matter (PM) in Beijing Using Vertical-and-RH Correcting Method. Remote Sensing of Environment 2010; 114: 50-63

Wu, J.S., Yao, F., Li, W.F., Si, M.L. 2016. VIIRS-based remote sensing estimation of ground-level $PM_{2.5}$ concentrations in Beijing-Tianjin-He bei: a spatiotemporal statistical model. Remote Sens. Environ. 184, 316-328.

Environmental Analysis of Coal-Fired Power Plants in Ultra Supercritical Technology Versus Integrated Gasification Combined Cycle

Dwi Ratna Mustafida[1*], Abdul Wahid [2], and Yuli Amalia Husnil[3]

[1*,2] Chemical Engineering Department, Faculty of Engineering, Universitas Indonesia, Depok 16424, Indonesia

[3]Chemical Engineering Department, Institut Teknologi Indonesia, Serpong 15314, Indonesia.

*E-mail: mustafida25@gmail.com

ABSTRACT

This study evaluates and compared the performance of coal-fired power plants in ultra-supercritical (USC) versus integrated gasification combined cycle (IGCC). System performance in terms of environmental analysis. Base on the exhaust emissions than IGCC and USC in terms of SO_2, CO_2, CO, and H_2S. The IGCC system is modeled and simulated with post-combustion capture and both of them used sub-bituminous coal from the Indramayu PLTU. The result display that with the same amount of raw materials (20 ton/h coal) the IGCC produce lower exhaust emissions than USC. IGCC produced 7.80 ton CO_2-eq. / MWh and USC of 27.93 ton CO_2-eq. / MWh. IGCC technology for the long term will be better than USC because it has produced greater electrical power with the amount of material the same coal standard and produces lower exhaust emissions.

Keywords: Clean Coal Technology, USC, IGCC, environmental analysis, sub-bituminous

INTRODUCTION

(Coal contributed the largest share of global electricity generation in 2015 by 39%, followed by 23% for natural gas, 16% for hydro and 11% for nuclear (Figure 1) Until 2050, the share of coal, although declining, will remain the largest, with coal continuing to function as a basic electricity source ((IEEJ), 2017).

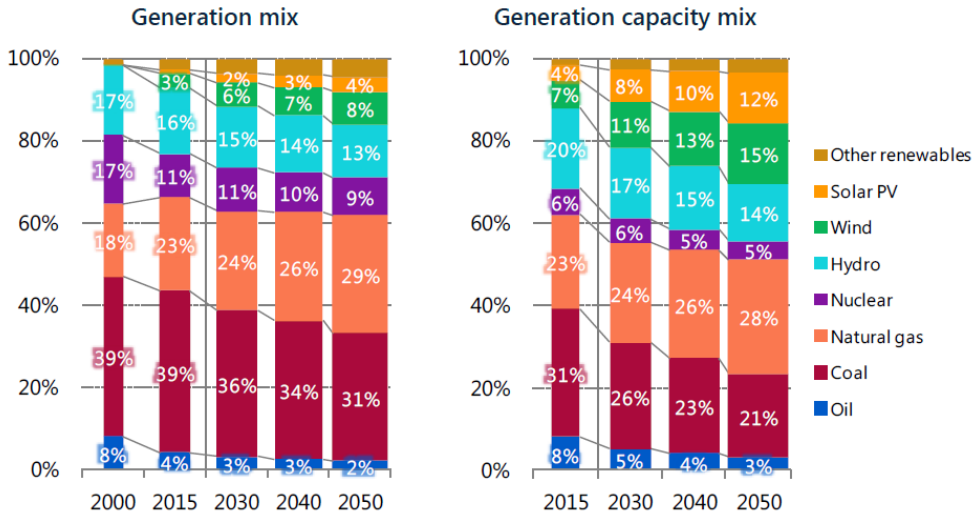

Figure. 1 Global Power Plant Energy Sources [Reference Scenario]((IEEJ), 2017)

Combustion of fuel produced high exhaust emission especially CO_2 gases which increased pollutant concentration in air. Coal contributed 44% of total global CO_2 emissions and became the largest source of GHG (greenhouse gas) emissions, which trigger the acceleration of climate change. In 2017 the composition of Indonesia's electricity production was projected to be 55.6% using coal, and in 2026 coal use would still 50.4% ((persero), 2017). In addition, Indonesia had signed a Paris Agreement in 2015 where Indonesia should reduce CO_2 emissions by 29% in 2030.

The existing technology in the electricity sector was Ultra Supercritical (USC) and Integrated Gasification Combined Cycle (IGCC). The study of this research is to compare the efficiency of both of these technologies to environmental analysis aspect using Unisim and

Promax Simulation Program. The coal data was obtained from Indramayu PLTU. The data of this research were compared to the *Intergovernmental Panel on Climate Change Guidelines* to obtain the calculation. From report Huaneng Greengen Co the result shows that USC has higher exhaust emissions than IGCC in terms of SO_2, CO_2, NO_x, CO and slag (Co., 2008).

Much research has been done to improve equipment efficiency and optimization in the (CCT) power plants by analyzing processes from various aspects such as energy (first law of thermodynamics), exergy (second law of thermodynamics), economy and environmental (4-E). The main purpose of this paper is to analyze the previous work done by researchers related to CCT power plant 4-E analysis. If anyone extracts the ideas for the development of the concept of using the article, we will achieve our goal. This review also indicates the scope of future research in the clean coal technology power plants

METHODOLOGY

Process description

The flowsheet of the IGCC process used in the analysis is shown in Figure 2. The process is composed of the following five integrated blocks: coal sizing and slurry preparation, gasification, syngas cooling, and cleaning, acid gas removal (AGR), CO_2 gas Removal and combined cycle power section. However, Figure 2, directly shows the flow diagram of the process of separating H_2S until the process of generating electricity from the syngas of the gasifier reactor output and Figure 3 shown the cryogenic CO_2 separation. Figure 4. Shown the flowsheet of the process of USC. The process is composed of the following two integrated blocks: boiler subsystem and the steam turbine system.

Modeling, simulation, and calculation

An IGCC post-combustion and USC plant integrated with CO_2 capture are modeled and simulated using UniSim Design® R450 and Promax® 4.0 simulation software. The composition of syngas products and IGCC process

model based on experimental data (Asif, Bak, Saleem, & Kim, 2015; Wang, 2017). The USC proses model is based on the validated model of Yang, et al. and Zhou, et al. (Yang et al., 2013; Zhao et al., 2017). The Cryogenic is based on a reference model (Air Liquide Indonesia. PT). The model is based on a steady-state operation. In the heat exchanger, there is a pressure drop of 5 psi. Pump efficiency of 65%, Turbine efficiency, and compressor of 75 %. Coal specification was obtained from the Indramayu PLTU and mass was 20000 kg/h shown in Table 1.

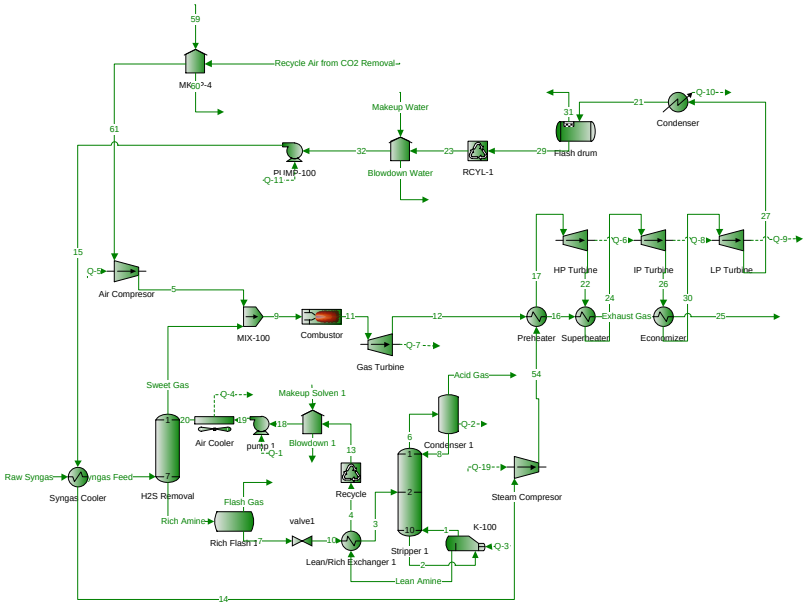

Figure 2. Schematic of the IGCC system with *Promax® 4.0*

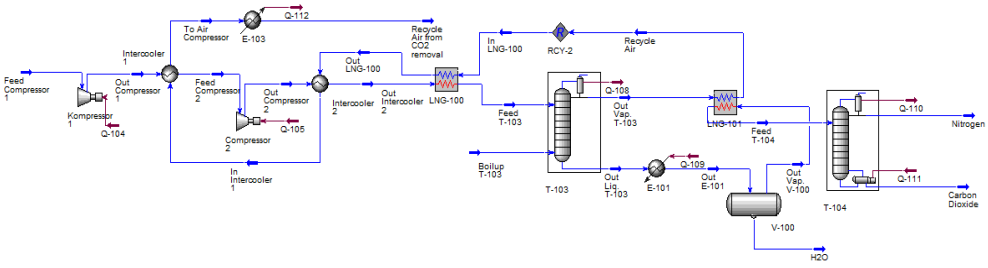

Figure 3. Schematic of the cryogenic CO_2 separation system

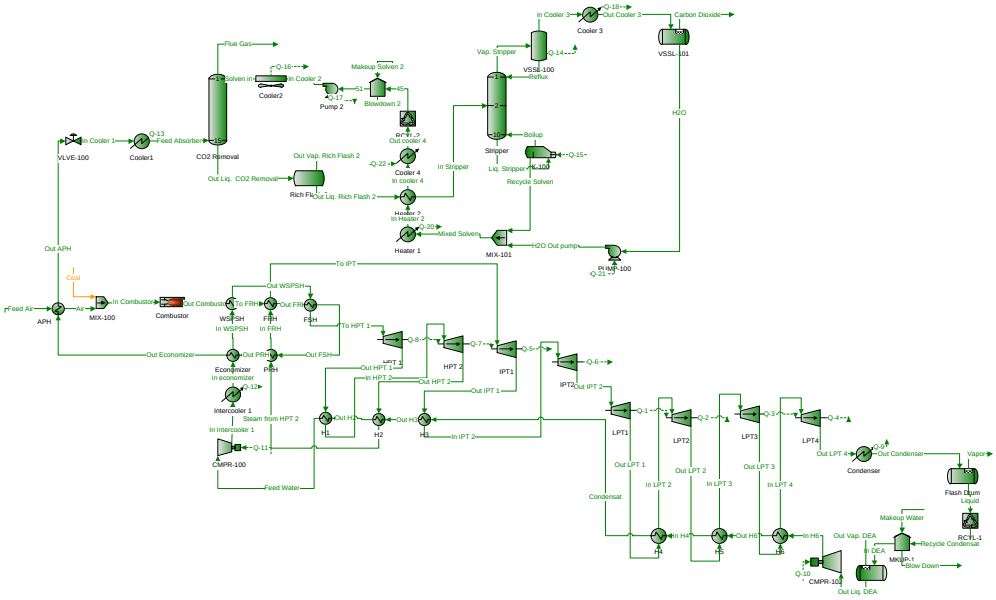

Figure 4. Schematic of the USC system with *Promax® 4.0*

Table 1. Composition analysis of coal

Composition	Value (% wt)
Proximate analysis	
Moisture	14.34
Fixed carbon	37.63
Volatile matter	43.47
Ash	4.56
Ultimate analysis	
C	55.42
H	4.20
N	0.71
S	0.1
O	20.67
Ash	4.56
Calorific value, HHV (kcal/kg)	4236

Environmental analysis is carried out based on the calculation of GHG emissions (CO_2) in the energy sector in the power plant sub-sector. The methodology used in calculating this emission is the method established by the Intergovernmental Panel on Climate Change Guidelines in the

2006 IPCC Guidelines. The application of this method has been stipulated in LHK Ministerial Regulation Number P.73 / Men LHK / Setjen / Kum.1 / 12/2017 dated 29 December 2017 concerning the Implementation and Reporting Guidelines for Greenhouse Gas Inventories. Broadly speaking, the calculation of GHG emissions/ removals is obtained through multiplying data on activities with emission factors, the Global Warming Potential (GWP) index was used to evaluate the climate change impact. The GWP index allows all of the GHG flows during the operation period, $\dot{m}_{GHG}^{op}$, to be expressed on a CO_2_eq basis as shown in the simple equation:

$$\dot{m}_{GHG}^{op} = \sum_{j=1}^{N} \dot{m}_j^{GHG} \times GWP_j \quad (1)$$

According to the Intergovernmental Panel on Climate Change (IPCC 2007), the GWP index evaluated over 100 years was considered to be 1 for CO_2, 28 for CH_4 and 265 for N_2O (Restrepo, Miyake, Kleveston, & Bazzo, 2012)

RESULTS AND DISCUSSION

Environmental analysis

The environmental model predicted an emission from the process of 7.249 ton CO_2-eq./MWh to IGCC and 25.97 ton CO_2-eq./MWh to USC. The power plant emissions correspond to 87.7%, followed by the pre-burning process (belt conveyors, fans, mills, and others) with 7.3%. The mining and transport stages account for 5% (Restrepo et al., 2012). Figure 5. Shown GHG emissions for IGCC and USC. Table 2 shown the gas emission produce from IGCC and USC.

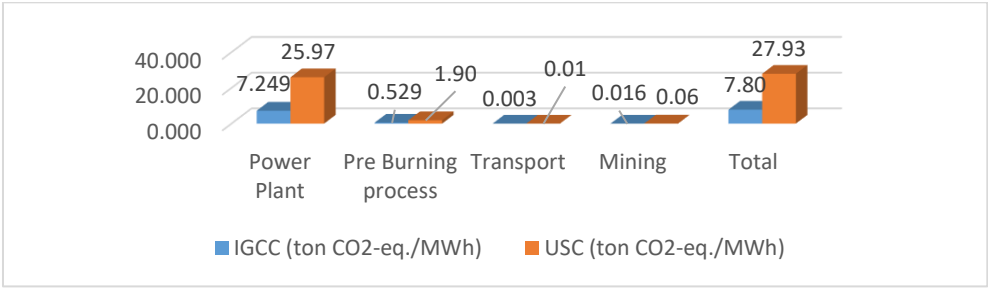

Figure 5. GHG emissions for IGCC and USC

Table 2. Gas emission produce from IGCC and USC

Emission	IGCC (kg/h)	USC (kg/h)
CO	0.005	12.493
CO_2	37351.860	43936.008
Methane	165.744	-
H_2S	23.293	-
SO_2	0.088	39.959
Ammonia	0.457	-

Gas emission produces on IGCC technology shown in Table. 2 in kg/h and then convert to tons/year and N_2O emission obtained from CO_2 emissions produced are multiplied by the mass of coal and the emission factor N_2O. CO_2 emissions produced amounted to 295826.73 tons/year, of CH_4 emissions 1312.70 tons/year and N_2O emissions of 7864.594 tons/year and then multiplying with Global Warming Potential (GWP) index to obtain CH_4 emissions of 36755.49 tons of CO_2-eq/year and emissions of N_2O 2084117.36 tons of CO_2-eq/year and total GHG emissions of 2416699.58 tons of CO_2-eq/year.

These emissions are the emissions generated in the power plant process and it is assumed that the pre-burning process (belt conveyors, fans, mills, and others) emissions are 7.3% and the mining and transport stages account for 5%. The total GHG emissions produced are divided by the total net power produced which is 42 MWh or 333373.91 MWh/year. after being divided by total electricity production, the following emissions were obtained: 7.249 tons of CO_2-eq./MWh in the power plant process, 0.529 tons of CO_2-eq./MWh on the Pre Burning process, 0.003 tons of CO_2-eq./MWh in Transport and 0.016 tons of CO_2 -eq./MWh on Mining so that total GHG emissions

amounted to 7.80 tons of CO_2-eq./MWh

In USC technology the emissions calculation would equal with IGCC, The CO_2 produced is 347973.18 tons/year, of CH_4 emissions 61672.762 tons/year and N_2O emissions are 9250.914 tons/year and then after multiplying with Global Warming Potential (GWP) index to obtain emissions of CH_4 1726837.34 tons CO_2-eq/year and N_2O emissions 2451492.295 tons CO_2-eq/year and total GHG emissions of 5083038.062 tons CO_2-eq/year. The total GHG emissions produced are divided by the total net power produced which is 22 MWh or 174266.70 MWh/year. After being divided by the total electricity production, the following emissions are obtained 25.97 tons CO_2-eq./MWh in the power plant process, 1.90 tons CO_2-eq./MWh on the Pre Burning process, 0.01 tons CO_2-eq./MWh at Transport and 0.06 tons CO_2-eq./MWh on Mining so that the total GHG emissions are 27.93 tons of CO_2-eq./MWh.

Another gas emission produced is IGCC, producing CO emission of 0.005 kg/h, H_2S 23.293 kg/h, SO_2 0.088 Kg/h and Ammonia 0.457 kg/h while USC produces CO emissions of 12.493 kg/h and SO_2 of 39.959 kg/h.

CONCLUSIONS

This paper conducted a comprehensive study to evaluate and compare the performance of coal fire power plants between ultra-supercritical (USC) and integrated gasification combined cycle (IGCC). Both processes are modeled and simulated, and environmental analysis is used to evaluate the results. The following conclusions can be derivate:

- Total GHG emissions for IGCC was 7.80 tons of CO_2-eq./MWh and USC of 27.93 tons of CO_2-eq./MWh.
- Another gas emission produced is IGCC, producing CO emission of 0.005 kg/h, H_2S 23.293 kg/h, SO_2 0.088 kg/h and Ammonia 0.457 kg/h while USC produces CO

emissions of 12.493 kg/h and SO_2 of 39.959 kg/h.

IGCC technology requires a greater investment because there are several additional tools such as gasifiers gas turbines and H_2S removal, but when compared to USC, this technology for the long term will be better because it has produced greater electrical power with the amount of material the same coal standard and produces lower exhaust emissions.

ACKNOWLEDGEMENTS

The author would like to thank for the support provided by all parties involved in writing this paper especially the mentors, Universitas Indonesia which has funded this research through the scheme of Hibah Publikasi Internasional Terindeks Untuk Tugas Akhir Mahasiswa (PITTA B) No. NKB-0691/UN2.R3.1/HKP.05.00/2019 and Institut Teknologi Indonesia

REFERENCES

(IEEJ), T. I. o. E. E. (2017). Outlook 2018, Prospects and challenges until 2050, Energy, Environment and Economy. Retrieved from

(persero), P. P. (2017). Rancangan Usaha Penyediaan Tenaga Listrik (RUPTL) PLN 2017-2026. Retrieved from

Asif, M., Bak, C.-u., Saleem, M. W., & Kim, W.-S. (2015). Performance evaluation of integrated gasification combined cycle (IGCC) utilizing a blended solution of ammonia and 2-amino-2-methyl-1-propanol (AMP) for CO2 capture. Fuel, 160, 513-524. doi:10.1016/j.fuel.2015.08.008

Co., H. G. (2008). People's Republic of China: Tianjin Integrated Gasification Combined Cycle Power Plant Project (42117). Retrieved from

Restrepo, Á., Miyake, R., Kleveston, F., & Bazzo, E. (2012). Exergetic and environmental analysis of a pulverized coal power plant. Energy, 45(1), 195-202. doi:https://doi.org/10.1016/j.energy.2012.01.080

Wang, T. (2017). An overview of IGCC systems. In Integrated Gasification Combined Cycle (IGCC) Technologies (pp. 1-80).

Yang, Y., Wang, L., Dong, C., Xu, G., Morosuk, T., & Tsatsaronis, G. (2013). Comprehensive exergy-based evaluation and parametric study of a coal-fired ultra-supercritical power plant. Applied Energy, 112, 1087-1099. doi:10.1016/j.apenergy.2012.12.063

Zhao, Z., Su, S., Si, N., Hu, S., Wang, Y., Xu, J., . . . Xiang, J. (2017). Exergy

analysis of the turbine system in a 1000 MW double reheat ultra-supercritical power plant. Energy, 119, 540-548. doi:https://doi.org/10.1016/j.energy.2016.12.07

Optimization of $Ca(OH)_2$ pretreatment to enhance methane production of rice straw using response surface methodology

Witthayaporn Kongyoo[1], Muhammad Zaeem Zubair Bin Sazali[2], Nopawan Ratasuk[1], Daoroong Sungthong[1]*

[1]Department of Environmental Science, Faculty of Science, Silpakorn University, Nakhon Pathom, Thailand
[2]Environmental and Water Technology, School of Life Sciences and Chemical Technology, Ngee Ann Polytechnic, Singapore
*Corresponding author: dao_roong@hotmail.com

ABSTRACT

In this study, an alkaline pretreatment process with $Ca(OH)_2$ for rice straw at different conditions to enhance methane production was investigated through biochemical methane potential (BMP) tests. The pretreatment process factors including $Ca(OH)_2$ concentrations of 5 – 15% (by weight) and temperatures of 70 – 90°C with pretreatment time of 2 h were studied. A response surface methodology (RSM) combined with a face-centered composite design (FCCD) was employed in obtaining the optimized pretreatment conditions for the highest methane yield of rice straw. The BMP experimental results show that the methane yield for all pretreated rice straws was increased by 55.44 – 78.59%, compared to the untreated rice straw. The statistical analyses show that the maximum methane yield of 304.31 NmL/g VS was obtained at the desirable pretreatment conditions of 5% $Ca(OH)_2$ and 87.34°C with pretreatment time of 2 h. The ANOVA test also revealed that the model was considered statistically significant with a determination coefficient (R^2) of 81.65%. The model could be efficiently used to predict the methane yield from the anaerobic digestion process of the pretreated rice straw. Furthermore, $Ca(OH)_2$ concentration was a more significant factor affecting methane production than temperature.

Keywords: Rice straw, Alkaline pretreatment, Biochemical methane potential (BMP), Methane production, Response surface methodology (RSM)

INTRODUCTION

Globally, agricultural crop residues are significant contributors of biomass resources and can be transformed into different types of bioenergy which can then be utilized as a promising source of alternative energy to fossil fuels. As one of the appropriate conversion methods of agricultural crop residues for bioenergy synthesis, the anaerobic digestion process is being used extensively to produce biogas, mainly containing methane (Cheng, 2010).

As one of the world's major producer and exporter of rice, Thailand consequently has an abundance of agricultural crop residues comprising a large amount of abandoned rice straw (Department of Alternative Energy Development and Efficiency, 2014). As a primary agricultural crop residue, rice straw is considered to have the potential for bioenergy synthesis by being transformed into biogas through the anaerobic digestion process. However, rice straw is a lignocellulosic material that predominantly contains cellulose, hemicellulose, and lignin. Rice straw, therefore, becomes recalcitrant to biological degradation. Consequently, the anaerobic digestion of rice straw for methane production is then hindered because water-soluble low molecular weight compounds are less available for anaerobic microorganisms (Song et al., 2014; Taherzadeh & Karimi, 2008). Thus, the pretreatment of rice straw prior to the anaerobic digestion process is quite essential and it is used to destroy the complex structure of lignin and decrease the crystallinity of cellulose and hemicellulose resulting in increasing the degradability and the potential of methane yield and accelerating the digestion process (Ferreira et al., 2013; Teghammar et al., 2010).

Several approaches for the pretreatment of rice straw have been investigated including physical, chemical, biological or a combination of these (Gu et al., 2015; Kim et al., 2012; Chen, 2014). As one of the pretreatment methods, the alkaline pretreatment with calcium hydroxide or lime ($Ca(OH)_2$) has

been extensively used due to its low cost, safe handling, and minor environmental impacts (Montgomery & Bochmann, 2014). For instance, Song et al. (2013) showed that the main compositions of rice straw pretreated with $Ca(OH)_2$ such as lignin, cellulose, and hemicellulose, were significantly degraded with increasing $Ca(OH)_2$ concentration. The modeling and optimization using response surface methodology (RSM) combined with Box-Behnken experimental design confirmed that the optimum conditions for the pretreated rice straw in an anaerobic digestion were 9.81% $Ca(OH)_2$ (w/w TS), 5.89 days treatment time, and 45.12% inoculum content, which resulted in a methane yield of 225.3 mL/g VS. Gu et al. (2015) reported that the rice straw pretreated with $Ca(OH)_2$ at the concentrations of 8% and 10% (w/w TS) under ambient temperature for 72 h gave the highest methane yield of 564.7 mL/g VS and 574.5 mL/g VS, respectively, which were 34.3% and 36.7% higher than the untreated.

Even though, there have been many studies reported about the effects of $Ca(OH)_2$ as a pretreatment chemical in terms of chemical concentration, pretreatment time, and inoculum amount on the digestibility of rice straw, however, there has been very little research reported about the effects of $Ca(OH)_2$ as a pretreatment chemical in terms of temperature. Also, in the last few years, RSM has been applied in optimizing and evaluating the interactive effects of independent factors of numerous chemicals and biochemical processes involved in anaerobic digestion (Song et al., 2013; Zou et al., 2016).

Therefore, this work has been made to find out the effectiveness of two operating parameters, including the concentration of calcium hydroxide and the temperature as pretreatment methods of rice straw on methane yield under batch conditions. Additionally, a response surface methodology (RSM) combined with a face-centered composite design (FCCD) was applied to determine the optimum pretreatment conditions of the two operating pretreatment

parameters on methane yield. The information from this study will not only make use of rice straw in the form of renewable energy, i.e., methane, but also to reduce the pollutants from rice straw open-field burning.

METHODOLOGY

Rice straw preparation

Rice straw was obtained from a rice planting area located in Ratchaburi, Thailand. At first, the collected rice straw was oven dried at 60℃ for about 24 h, then ground into fine particles by a cutting mill. The ground particles of rice straw were later screened to have an average particle size between 0.5 and 2.0 mm and stored in a polyethylene zipper bag at room temperature before being subjected to the pretreatment. Some physical and chemical characteristics of the rice straw sample are shown in Table 1. This prepared rice straw sample was defined as untreated rice straw.

Pretreatment process

$Ca(OH)_2$ solution at concentrations of 5%, 10%, and 15% (by weight) combined with temperature levels of 70℃, 80℃, and 90℃ was used for the pretreatments. The conditions of

Table 1 The physical and chemical characteristics of untreated rice straw.

Parameter	Values
Total solids (%)	92.01 ± 0.05
Volatile solids (%TS)	86.67 ± 0.10
Fixed solids (%TS)	13.33 ± 0.10
Organic carbon (%TS)	54.69 ± 0.66
Total nitrogen (%TS)	0.5056 ± 0.0127
Carbon to nitrogen (C/N) ratio	108
Extractives (%TS)	1.21 ± 0.11
Cellulose (%TS)	25.15
Hemicellulose (%TS)	47.79 ± 0.55
Lignin (%TS)	12.51 ± 0.15

Result = mean ± standard deviation (SD).

the pretreatment used in this study are shown in Table 2.

For each experiment (Table 2), a sample of 50 g prepared rice straw was mixed with 1 kg of $Ca(OH)_2$ solution in a 1-L laboratory bottle resulting in the ratio of rice straw to $Ca(OH)_2$ solution loading of 1:20 (by weight). The bottle was then heated on a hot plate to a specific temperature and was later kept in a hot air oven at that temperature for 2 h. Afterwards, the bottle was removed from the oven, and the pretreated rice straw sample was washed with tap water until neutral pH and then oven-dried at 60℃ for about 24 h. The pretreated rice straw sample was homogenized and kept in a polyethylene zipper bag at room temperature for being further investigated the effects of the pretreatments on methane yield using biochemical methane potential test.

Table 2 The pretreatment conditions.

Experiment	Concentration (%)	Temperature (℃)	Time (h)
1	5	70	2
2	5	80	2
3	5	90	2
4	10	70	2
5	10	80	2
6	10	90	2
7	15	70	2
8	15	80	2
9	15	90	2

Inoculum preparation

The inoculum used in this study being characterized as granular sludge, was taken from an anaerobic wastewater treatment reactor operated by Choheng Rice Vermicelli Factory Company Limited, located in Nakhon Pathom, Thailand. The collected inoculum was washed with anaerobic mineral

salt medium, then transferred into a 10-L stainless steel bioreactor and incubated at 35 ℃ under the anaerobic condition for approximately 5 days in order to deplete the residual biodegradable organic material (degasification), according to the recommendation of Angelidaki et al. (2009).

Biochemical methane potential tests

The biochemical methane potential (BMP) tests of the untreated and pretreated rice straws were evaluated according to the method described by Angelidaki et al. (2009) and Hansen et al. (2004) with some modifications. Batch experiments were carried out in 500-mL laboratory bottles (Schott Duran, Germany). Firstly, a sample of 5 g volatile solids (VS) from the untreated and pretreated rice straws was weighed and added into the bottle. Secondly, a certain amount of incubated inoculum was fed into the bottle with a substrate-to-inoculum ratio of 1:2 on a VS basis. Dry forms of ammonium chloride (NH_4Cl) and potassium phosphate (KH_2PO_4) were added to adjust a COD:N:P ratio of the substrate to 100:5:1 (by weight) (Eskicioglu & Ghorbani, 2011). Sodium bicarbonate ($NaHCO_3$) powder was also added in order for the mixture to achieve alkalinity of 5,000 mg/L (as $CaCO_3$) (McCarty, 1964). Thirdly, distilled water was added to the bottle for reaching the working volume of 400 mL. Finally, the headspace was filled with nitrogen gas for 1 min to remove oxygen traces and to ensure anaerobic condition in the bottle. The bottle was then sealed with two pieces of 3-mm thick silicone discs which were held tightly to the bottle head by a plastic screw cap punched in the middle (Schott Duran, Germany). To enable biogas transfer from the bottle to the methane content measurement device, a 27-gauge needle equipped with 3-way stopcock was pierced through the silicone discs. After that, the bottle was placed in the incubator at 35℃ for 30 days. During the BMP experiment, the bottle was occasionally shaken. In the first week, methane content was daily measured due to very high biogas production, after that occasionally measured. The methane

content in the produced biogas in the bottle was directly obtained through an alkaline, and water displacement method (Wellinger et al., 2013) with 12% NaOH used as a barrier solution to entrap CO_2 and H_2S that had been produced and the residual methane volume to be measured by water displacement. A blank control without substrate added was also conducted under the same conditions to remove endogenous methane production from the inoculum. All tests were performed in triplicate. The methane yield over a period of 30 days was calculated at standard temperature and pressure (273 K and 1 atm) and expressed as the methane content (NmL) per gram of VS from the substrate introduced to the bottle.

Statistical analysis, and optimization of the experimental data

Design Expert software version 11, a statistical program, was used for data analysis and model building. RSM coupled with FCCD was applied to optimize the pretreatment condition variables and was also used to determine the optimum conditions and the effects of two independent variables, including $Ca(OH)_2$ concentration (X_1) and temperature (X_2) on methane yield (Y) which was a response variable or a dependent variable. The range of the independent variables and their levels are presented in Table 3. All experimental data with a total of 27 runs, as shown in Table 4, were performed according to the FCCD configuration. The functional relationships between the response variable (methane yield) and the two independent variables (concentration and temperature) were obtained by estimating the coefficients of the following polynomial model:

$$Y = \beta + \sum_{i=1}^{2} \beta_i X_i + \sum_{i=1}^{2} \sum_{j=1}^{2} \beta_{ij} X_i X_j + \sum_{i=1}^{2} \sum_{j=1}^{2} \sum_{k=1}^{2} \beta_{ijk} X_i X_j X_k \quad (1)$$

where Y is the predicted response, β is the intercept, β_i is the linear constant coefficient, and β_{ij} and β_{ijk} are the interaction constant coefficients. The independent variables are denoted by X.

The model was then validated by analysis of variance (ANOVA). Response surface plots were also generated to examine the effects of $Ca(OH)_2$ concentration and temperature on methane yield. The optimum values of $Ca(OH)_2$ concentration and temperature were obtained by the numerical optimization feature in the Design Expert software.

Table 3 Independent variables and corresponding levels.

Variables	Actual values of coded levels		
	-1	0	1
Concentration, X_1 (%)	5	10	15
Temperature, X_2 (°C)	70	80	90

RESULTS AND DISCUSSION

Effectiveness of the pretreatments on methane yields

According to the BMP experimental results, the cumulative methane yields for the untreated and all pretreated rice straws are depicted in Figure 1. Results show that the methane yield for all pretreated rice straw samples was higher than the untreated rice straw, and it was increased by 55.44 – 78.59% compared to the untreated rice straw. These results are consistent with other studies (Gu et al., 2015; Song et al., 2012), which verified the effectiveness of $Ca(OH)_2$ as an alkaline pretreatment in improving the biodegradability and enhancing the bioenergy production. This phenomenon can be explained by the fact that $Ca(OH)_2$ pretreatment is capable of removing amorphous substances (e.g., lignin and hemicellulose), which increases the crystallinity index (Kim et al., 2016). However, the methane yield was not increased as the $Ca(OH)_2$ concentration, and the temperature increased. The reason may be due to the fact that calcium hydroxide is relatively insoluble in water, and its solubility also decreases as temperature increases (Athanassiadis et al., 2017). Therefore, it is possible that increasing $Ca(OH)_2$ loading and

Table 4 Coded and actual values of experimental data and corresponding methane yield with different combinations of two independent variables for FCCD.

Run	Space type	Coded values		Actual values		Response methane yield (NmL/g VS)	
		X_1	X_2	Concentration (%)	Temperature (°C)	Experimental	Predicted
1	Factorial	-1	-1	5	70	278.74	282.52
2	Factorial	-1	-1	5	70	289.34	282.52
3	Factorial	-1	-1	5	70	282.56	282.52
4	Axial	0	-1	10	70	291.99	296.14
5	Axial	0	-1	10	70	295.16	296.14
6	Axial	0	-1	10	70	295.69	296.14
7	Factorial	1	-1	15	70	290.54	288.08
8	Factorial	1	-1	15	70	285.68	288.08
9	Factorial	1	-1	15	70	291.40	288.08
10	Axial	-1	0	5	80	296.88	300.35
11	Axial	-1	0	5	80	304.92	300.35
12	Axial	-1	0	5	80	293.56	300.35
13	Center	0	0	10	80	289.33	284.99
14	Center	0	0	10	80	288.27	284.99
15	Center	0	0	10	80	289.50	284.99
16	Axial	1	0	15	80	261.62	267.00
17	Axial	1	0	15	80	259.75	267.00
18	Axial	1	0	15	80	274.36	267.00
19	Factorial	-1	1	5	90	303.82	303.72
20	Factorial	-1	1	5	90	304.71	303.72
21	Factorial	-1	1	5	90	305.79	303.72
22	Axial	0	1	10	90	279.88	294.08
23	Axial	0	1	10	90	304.02	294.08
24	Axial	0	1	10	90	292.98	294.08
25	Factorial	1	1	15	90	297.83	300.83
26	Factorial	1	1	15	90	307.22	300.83
27	Factorial	1	1	15	90	301.13	300.83

temperature level for the pretreatment of rice straw did not affect the methane yield.

Model building

Based on the two independent variables, including $Ca(OH)_2$ concentration and temperature, and

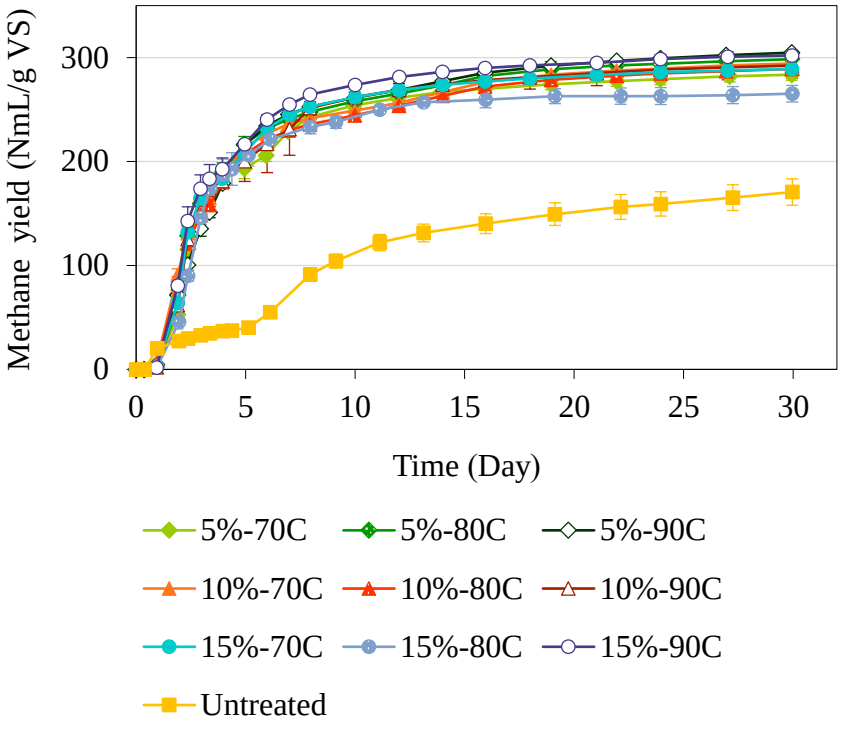

(a) Variations of the cumulative methane yields over a period of 30 days.

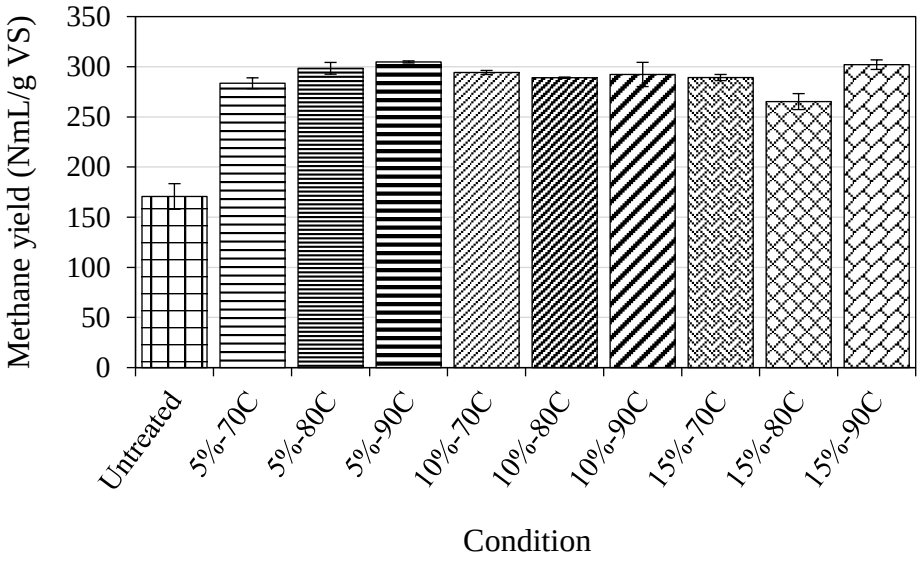

(b) Cumulative methane yields over a period of 30 days.

Figure 1 Cumulative methane yield of the untreated and $Ca(OH)_2$ pretreated rice straws.

the response variable that is the experimental methane yield, along with FCCD (Table 4), the significance of the cubic model as shown in Eq. (1) was evaluated by ANOVA. However, the insignificant terms were eliminated from the model, with the exception of those required to maintain the model hierarchy. Consequently, the final model obtained for methane yield of pretreated rice straw in terms of $Ca(OH)_2$ concentration and temperature is given as follow:

$$Y = -1589.21 + 283.949X_1 + 43.4312X_2 - 6.35224X_1X_2 - 3.09763X_1^2 - 0.24566X_2^2 + 0.03806X_1^2X_2 + 0.03468X_1X_2^2 \quad (2)$$

where Y represents the methane yield (NmL/g VS), X_1 and X_2 represent $Ca(OH)_2$ concentration (% by weight) and temperature (°C), respectively.

The results of the ANOVA for the developed model are tabulated in Table 5. As noted in the Table, the model F-value of 12.08 with a p-value of <0.0001 ($p<0.05$) implies that this model was statistically significant at 95% confidence level, indicating the suitability of the model to predict the methane yield in terms of $Ca(OH)_2$ concentration and temperature. The lack of fit with a p-value of 0.10007 ($p > 0.05$) was not significant, meaning that the model exhibits fitness for the prediction. The R^2 value of 81.65% and the adjusted R^2 value of 74.89% were quite high, suggesting the model adequacy. As shown in Figure 2, the predicted methane yield values were found in close agreement with the experimental methane yield results (R^2 = 77.59%), suggesting a good relationship between the experimental and predicted values of the methane yield. The ANOVA results also imply that $Ca(OH)_2$ concentration was the most significant factor, with an F-value of 43.50, and signify that the other important factors were the second-order polynomial of temperature and the interactive effects.

Analysis of response surfaces

A three-dimensional plot and a contour plot, as shown in Figure 3,

were drawn to visualize the interaction between the two pretreatment variables ($Ca(OH)_2$ concentration and temperature) and the methane yield. An increase in the temperature allowed for an increase

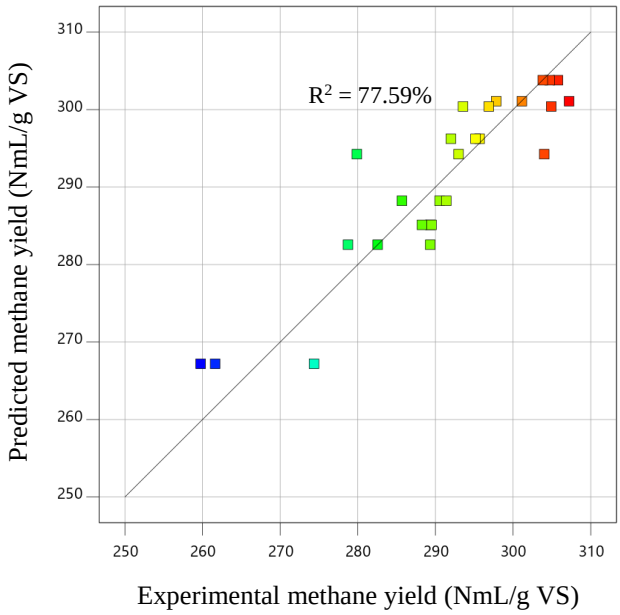

Figure 2 Plot of the experimental and predicted methane yield.

Table 5 ANOVA for response surface methodology.

Source	Sum of squares	df	Mean square	F-value	p-value	
Model	3214.73	7	459.25	12.08	< 0.0001	Significant
X_1-Concentration	1653.97	1	1653.97	43.50	< 0.0001	
X_2-Temperature	5.93	1	5.93	0.1560	0.6973	
X_1X_2	52.59	1	52.59	1.38	0.2541	
X_1^2	10.50	1	10.50	0.2761	0.6053	
X_2^2	614.02	1	614.02	16.15	0.0007	
$X_1^2X_2$	362.12	1	362.12	9.52	0.0061	
$X_1X_2^2$	1202.87	1	1202.87	31.63	< 0.0001	
Residual	722.50	19	38.03			
Lack of Fit	103.03	1	103.03	2.99	0.1007	Not significant
Pure Error	619.47	18	34.42			
Cor Total	3937.24	26				

R^2 = 81.65%.
Adjusted R^2 = 74.89%.

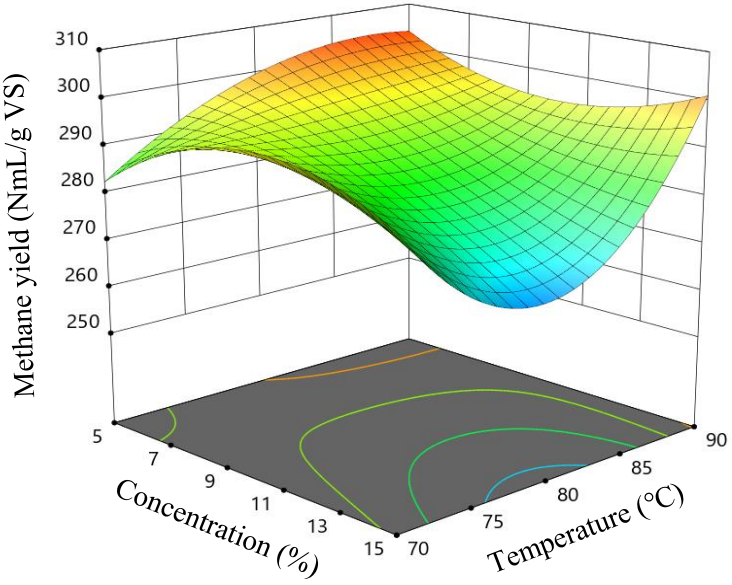

(a) A three dimensional plot.

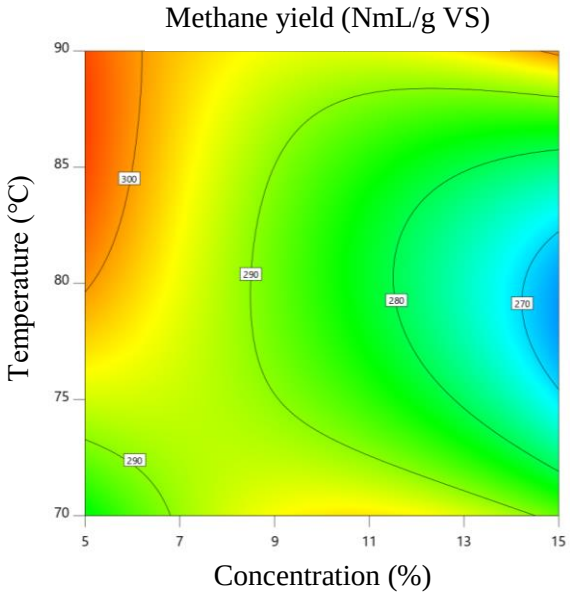

(b) A contour plot.

Figure 3 Response surface plots for the interactions of $Ca(OH)_2$ concentration and temperature on the methane yield.

in the methane yield, however hitting a maximum at 87℃, and thereafter, a slow decrease in the methane yield was found. Increasing $Ca(OH)_2$ concentrations above 10% may cause a decrease in the methane yield, and increasing the $Ca(OH)_2$ concentrations from 5% to 10% will increase the methane yield at a lower temperature, however, at a higher temperature the results are inverted. This can be compared to the results in Song et al. (2014), where increasing $Ca(OH)_2$ concentrations from 8% to 10% led to a decrease in methane yield. Therefore, in this study, the optimum methane yield has led to a point where the temperature is near 87℃ and where the concentration is low.

According to the optimization process of the developed model, the optimum conditions for maximizing the methane yield were found to be at 5% of $Ca(OH)_2$ concentration and 87.34℃ of temperature, resulting in the predicted methane yield of 304.31 Nml/g VS. Under the optimum conditions, the methane yield was 1.78-fold greater than the methane yield of the untreated rice straw (170.65 Nml/g VS).

CONCLUSIONS

This study examined the effectiveness of $Ca(OH)_2$ loading and reaction temperature as the pretreatment methods of rice straw on methane production in an anaerobic digestion process. From the BMP experiment results, it was found that the pretreated rice straws had significantly increased in methane yields by 55.44 – 78.59%, compared to the untreated rice straw. From the statistical analyses, it was revealed that $Ca(OH)_2$ concentration was a more significant factor affecting methane production than reaction temperature. The optimum conditions for maximizing the methane yield were $Ca(OH)_2$ concentration of 5% (by weight), and temperature of 87.34℃ with pretreatment time of 2 h in which maximum methane yield of 304.31 NmL/g VS was obtained.

ACKNOWLEDGMENTS

This work was partially funded by the National Research Council of Thailand (NRCT) under the program of Research Scholarships for Graduate Students 2017. We would like to thank the Department of Environmental Science, Faculty of Science, Silpakorn University, Nakhon Pathom, Thailand, for providing the laboratory facilities. We would like to extend our gratitude to our undergraduate students for their contribution to some laboratory works. Thanks are also due to the Choheng Rice Vermicelli Factory Company Limited, Nakhon Pathom, Thailand for their kindness providing the granular sludge.

REFERENCES

Angelidaki I, Alves M, Bolzonella D, Borzacconi L, Campos JL, Guwy AJ, et al. Defining the biomethane potential (BMP) of solid organic wastes and energy crops: A proposed protocol for batch assays. Water Science and Technology. 2009;59(5):927-34.

Athanassiadis B, Walsh LJ. Aspects of Solvent Chemistry for Calcium Hydroxide Medicaments. Materials. 2017;10(10):1-8.

Chen X, Zhang Y, Gu Y, Liu Z, Shen Z, Chu H, et al. Enhancing methane production from rice straw by extrusion pretreatment. Applied Energy. 2014;122:34-41.

Cheng JJ. Biomass to renewable energy process. United States of America: CRC Press; 2010.

Department of Alternative Energy Development and Efficiency. The potential of biomass in Thailand 2014 [Available from: http://biomass.dede.go.th/biomass_web/index.html.

Eskicioglu C, Ghorbani M. Effect of inoculum/substrate ratio on mesophilic anaerobic digestion of bioethanol plant whole stillage in batch mode. Process Biochemistry. 2011;46(8):1682-7.

Ferreira LC, Donoso-Bravo A, Nilsen PJ, Fdz-Polanco F, Pérez-Elvira SI. Influence of thermal pretreatment on the biochemical methane potential of wheat straw. Bioresource Technology. 2013;143:251-7.

Gu Y, Zhang Y, Zhou X. Effect of $Ca(OH)_2$ pretreatment on extruded rice straw anaerobic digestion. Bioresource Technology. 2015;196:116-22.

Hansen TL, Schmidt JE, Angelidaki I, Marca E, Jansen JlC, Mosbæk H, et al. Method for determination of methane potentials of solid organic waste. Waste Management. 2004;24(4):393-400.

Kim I, Han J-I. Optimization of alkaline pretreatment conditions for enhancing glucose yield of rice straw by response surface methodology. Biomass and Bioenergy. 2012;46:210-7.

Kim JS, Lee YY, Kim TH. A review on alkaline pretreatment technology for bioconversion of lignocellulosic biomass. Bioresource Technology. 2016;199:42-8.

McCarty PL. Anaerobic waste treatment fundamentals. Public Work. 1964;95(9):107-12.

Montgomery LFR, Bochmann G. Pretreatment of feedstock for enhanced biogas production. United Kingdom: IEA Bioenergy; 2014.

Song Z, Gaihe Y, Liu X, Yan Z, Yuan Y, Liao Y. Comparison of seven chemical pretreatments of corn straw for improving methane yield by anaerobic digestion. PloS one. 2014;9(4):1-8.

Song Z, Yang G, Han X, Feng Y, Ren G. Optimization of the alkaline pretreatment of rice straw for enhanced methane yield. BioMed Research International. 2013;2013:1-9.

Song Z, Yang G, Zhang T, Feng Y, Ren G, Han X. Effect of $Ca(OH)_2$ pretreatment on biogas production of rice straw fermentation. Transactions of the Chinese Society of Agricultural Engineering. 2012;28(19):207-13.

Taherzadeh MJ, Karimi K. Pretreatment of lignocellulosic wastes to improve ethanol and biogas production: A review. International Journal of Molecular Sciences. 2008;9(9):1621-51.

Teghammar A, Yngvesson J, Lundin M, Taherzadeh MJ, Horváth IS. Pretreatment of paper tube residuals for improved biogas production. Bioresource Technology. 2010;101(4):1206-12.

Wellinger A, Murphy J, Baxter D. The biogas handbook: science, production and applications. United States of America: Woodhead; 2013.

Zou S, Wang H, Wang X, Zhou S, Li X, Feng Y. Application of experimental design techniques in the optimization of the ultrasonic pretreatment time and enhancement of methane production in anaerobic co-digestion. Applied Energy. 2016;179:191-202.

Electrospun Poly(lactic acid)/Polyvinylpyrrolidone Composite for Biodegradable Face Mask

Pattama Madaeng[1], Chariya Kaewsaneha[2], Alice Sharp[3],

and Pakorn Opaprakasit[2*]

[1]Sustainable Energy and Resources Engineering, Sirindhorn International Institute of Technology (SIIT), Thammasat University, Pathum Thani, 12121, Thailand

[2]School of Bio-Chemical Engineering and Technology, Sirindhorn International Institute of Technology (SIIT), Thammasat University, Pathum Thani, 12121, Thailand

[3]Department of Biology, Faculty of Science, Chiang Mai University,

Chiang Mai, 50200, Thailand.

*E-mail: pakorn@siit.tu.ac.th

ABSTRACT

Recently, PM2.5 (particulate matter with a diameter of 2.5 microns or less) in polluted air has become a major health hazard in Thailand, especially in the northern region. Regular face masks are used to prevent inhaling of hazardous particles. However, these are not able to filter out PM2.5 because of their larger pore size. In addition, the majority of these commercial masks are produced from petroleum-based plastics, e.g., polypropylene, which becomes non-degradable wastes after use. Rising environment concerns have forced many industries to seek more environmentally-friendly processing and safer materials alternatives. Poly(lactic acid) (PLA), a biodegradable polyester derived from renewable resources, e.g., corn, cassava, and sugarcane has been widely used in various applications. Herein, biodegradable face mask based on PLA nanofibers has been developed by an electrospinning technique. To

further improve the mask efficiency, polyvinylpyrrolidone and negatively-charged graphene oxide (GO) nanoparticles were introduced to the PLA nanofibers. The obtained composite nanofibers were characterized by scanning electron microscope (SEM), air permeability tests, and PM2.5 trapping experiments. The results showed that the composite nanofibers can effectively filter out 98% of PM2.5 particles, while that of regular commercial face mask is 70%, and simultaneously preserve a good breathability. We attribute such improvements to the nano-scaled inter-fiber space and the presence of negative charges on the fiber surface.

Keywords: Degradable polymer, PLA, electrospinning, dust capturing, face mask, filter

INTRODUCTION

Recently, air pollution caused by particular matters, especially those with diameters of ≤ 2.5 μm (PM2.5), has become a major health hazard in Thailand, especially in the northern region. In attempts to prevent inhaling of PM2.5 in haze, people wear regular masks. Most of these masks are made of non-woven fabric, or cotton which has fiber diameter of several micrometers. However, these have significant shortcomings of poor PM2.5 filtration and low air permeability (Li, 2015). Rengasamy S et al. reported filtration efficiency of general fabric products, e.g., sweatshirts, T-shirts, towels, scarves, and cloth masks, in comparison with commercial N95 as control media (Rengasamy, 2010). The results on aerosol penetration showed that N95 filter media had 0.12% penetration at 5.5 cm/s face velocity while other fabric products: cloth mask, sweatshirts, T-shirts, towels, scarves, and cloth masks had 60-82 % penetration at both 5.5 and 16.5 cm/s face velocity. Although N95 showed high filtration efficiency, the

majority of this mask are produced from petroleum-based plastics, e.g., polypropylene, which becomes non-degradable wastes after use.

Rising environment concerns have forced many industries to seek more environmentally-friendly processing and safer materials alternatives. Poly(lactide) or PLA, a biodegradable polymer obtained from natural resources e.g., corn, cassava, and sugarcane has been widely used in various applications, such as plastic bag, plastic film, food packaging (Jamshidian, 2010), and medical device (Noh, 2010). In practical use, compounding PLA with fillers, especially nano-scale fillers, could help improving the composite's mechanical properties (Xing, 2016) and provides functionality for specific applications. Dias et al. (Dias, 2017) successfully prepared PLA/multi-layer graphene oxide (MLG) via an electrospinning technique, and the result showed that the incorporation of MLG leaded to a decrease in fiber size distribution. This resulted in enhancements of surface area to volume ratio of the materials for potential use as filter products.

Polyvinylpyrrolidone (PVP) is conductive and hydrophilic polymer that is widely used in industry, especially in biomedical applications, because of its low toxicity, high biocompatibility, and excellent solubility in almost all organic solvents. To further optimize its property, mixing with other polymers have been practiced. PVP was blended with polyacrylamide to form a thin film, and the results showed that increasing amount of PVP leaded to an increase in conductivity of the thin film (Rawat, 2014). Moreover, PVP can also form fibers via an electrospinning process. By using dimethylformamide (DMF) solvent, uniform, and bead-free electrospun PVP fibers were obtained (Huang, 2016).

In this study, biodegradable face masks, based on PLA nanofibers, are developed by using an electrospinning technique. To further improve the mask's efficiency, PVP and various amounts of graphene oxide nanoparticles were introduced.

The obtained composite nanofibers are then characterized by scanning electron microscopy, transmission electron microscope and PM2.5 filtration efficiency.

METHODOLOGY

Materials

PLA (Mw = 1.5×10^5 g/mol, film grade, NatureWork®), PVP (Mw = 5.8 x 10^4 g/mol, Acros), graphite powder (Acros), Potassium permanganate (ACS, Carlo Erba), *N*,*N*-dimethylformamide (DMF, ACS, Carlo Erba), Chloroform (CHL, ACS, Carlo Erba), Sodium nitrate (Extrs pure, Loba Chmie), Sulfuric acid (AR, QREC), Hydrochloric acid (HCl, ACS, Carlo Erba). Hydrogen Peroxide (GPO). Deionized (DI) water was used throughout the work.

Preparation of Graphene Oxide

Graphene oxide (GO) was synthesized by using the Hummers' method, as previously described (Marcano, 2010). Briefly, graphite powder (3.0 g) and sodium nitrate (1.5 g) were added into sulfuric acid (69 ml) at 0 °C. Potassium permanganate (9.0 g) was gradually added to maintain the reaction temperature below 20˚C. After stirring for 30 min, DI water (138.0 ml) was dropped into the solution and the temperature was raised to 98 °C for 15 min. The mixture was then cooled down using an ice bath for 10 min. Subsequently, DI water (420 mL) and 30% hydrogen peroxide (3 mL) were added. The mixture was purified by adding HCl (5%), and centrifuged at 4,000 rpm for 5 min, alternating with DI water for twice. Finally, the mixture was dried at 60 ºC in a vacuum oven for two weeks.

The obtained GO (3.0 g) was dissolved in DMF (150.0 ml) before passing through Microfluidizer (M-110P Microfluidizer®) at 30,000 PSI, 20 °C to reduce the particle size for 20 cycles. The particle size and zeta potential of GO were determined by using a Zetasizer (Zetasizer Ver. 7.11 Malvern Instruments Ltd.).

Preparation of nanofibers by electrospinning process

PLA and PVP (5:1) were dissolved in a mixture of CHL and DMF (7:1)

to obtain polymer solution having concentration of 10 %w/v. Briefly, PLA was dissolved in CHL until homogeneous then PVP was added and the mixture was stirred at room temperature for overnight. After that, DMF was added, with further stirring for 4 hours. GO dispersed in DMF with a concentration of 2 %w/v was added into the PLA/PVP solution and stirred at room temperature for overnight.

The electrospinning system consists of a high voltage supply (Gamma High Voltage Research, 0–40 kV, Cleveland, Ohio), an aluminum foil collector and a feed system consisting of a syringe pump (KDS100, KD Scientific, Holliston, MA, USA) and a needle injector. A feeding rate of the polymer mixture was 1 ml/h. The needle tip to collector distance was kept at 20 cm, and the applied voltage was 15 kV. The total amount of polymer solution used was 2 ml per mat.

Characterization of nanofibers

Scanning electron microscopy (SEM, JEOL, JSM-7800F) and transmission electron microscopy (TEM, JEOL, JEM 2100 Plus) were used to determine morphology of the nanofibers. For TEM sample preparation, the sample was dispersed in ethanol and a few drops of fibers dispersion solution was dropped on grid and dried at room temperature overnight before characterization.

Filtration Efficiency Tests

The filtration efficiency tests were conducted on fiber mats of neat PLA and the composite material, using commercial non-woven face mask as a supporting layer. The experiments were conducted at 60% relative humidity, 1 atm, and at 30˚C. An atomizer aerosol generator (model 3076, TSI company) was employed to generate monodisperse aerosol in a range of 0.01 – 1.00 μm, and flow through the sample which was held by a filter holder, with a flow rate of 0.6 L/min for 1 hour. A condensation particle counter (model of CPC 3788, TSI company) was employed to measure concentrations of particles (diameter between 2.5 nm – 3.0 μm).

The filtration efficiency (η) was calculated from the equation below;

$$\eta = \frac{c_{inlet} - c_{outlet}}{c_{inlet}}$$

Where c_{inlet} is a concentration of particles before the filter. c_{outlet} is concentration of particle after filtration by the sample.

RESULTS AND DISCUSSION

GO nanoparticles

To effectively incorporate GO particles into the nano-fibers, particle size, size distribution and surface charge of the particles must be optimized. The particles size and size distribution of GO after size reduction was determined and data is shown in **Figure 1**

The initial size of GO before size reduction operation was around 13 μm in diameter. After the size reduction by using a microfluidizer for 20 passes, the size of GO was reduced to 450 nm in diameter, with monodispersion in DMF solution.

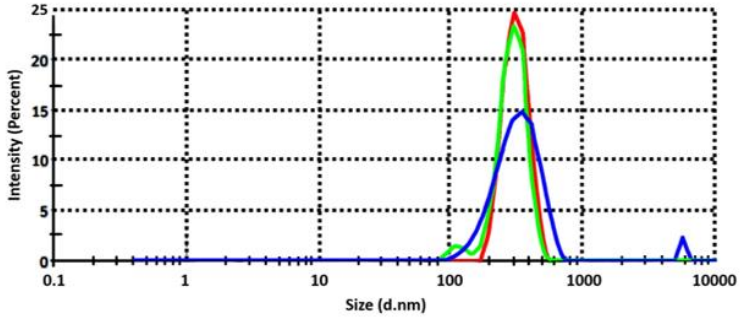

Figure 1 Particle size and size distribution of GO particles after size reduction

Moreover, the GO nanoparticles showed a zeta potential value of -25.1 mV, due to the residual oxygen groups on the particle's surface (Shao, 2014).

PLA nanofibers

Morphology

Appearance of the fiber mat products and morphology of the fibers are examined. The thickness of the nanofiber mats was ranging from 10 - 40 µm, measured by a Mitutoyo 2046S Dial Indicator Gage. All fiber mats are white in color, including those containing GO, which is black in nature. To confirm the presence of GO in the composite nanofibers, TEM was employed in morphology examination.

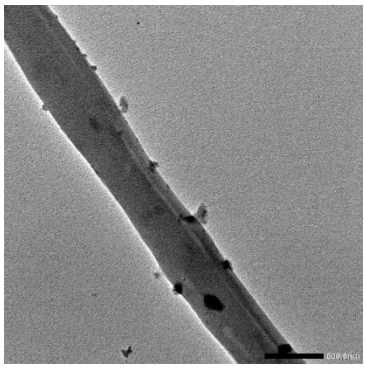

Figure 2 TEM image of PLA/PVP/GO nanofiber filaments

A TEM picture, as shown in **Figure 3**, clearly depicts the presence of GO as black particles, with sizes of ~ 200 nm, randomly embedded on the interface of the filaments. It is noted that during the sample preparation for TEM measurement, the fiber mat was dispersed in ethanol for a few hours to separate each filaments. The results indicated that the GO nanoparticles were strongly attached on the fiber surface by physical interaction.

According to SEM images (**Figure 3**), the nanofibers of both PLA and PLA/PVP/GO were significantly similar at 1.0 – 1.2 µm in diameter, with random orientation and high inter-fiber porosity.

Filtration Efficiency

The filtration efficiency of the prepared nanofibers compared with that of a regular face mask is shown in **Figure 4A.**

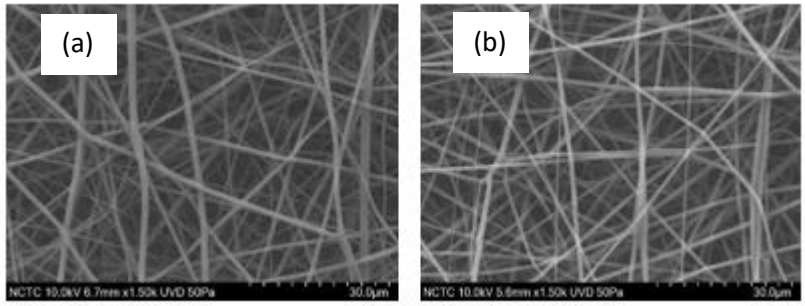

Figure 3 SEM images of (a) PLA, (b) PLA/PVP/GO nanofibers

The results show that the filtration efficiency of PLA and PLA/PVP/GO nanofiber mats are > 98%, while that of a regular commercial mask is 70%. This implies that the prepared nanofiber mats can effectively prevent the flow of small particles or PM2.5. Although PLA and PLA/PVP/GO nanofiber mats show similar filtration efficiency, the effectiveness in filtration of smaller particles (in a range of 10 – 100 nm) is significant different, as shown in **Figure 4B**. When considering the amount of small particles passing through both nanofibers (right column, b and c), it was clearly seen that by using PLA/PVP/GO nanofiber as a filter, these small particles cannot penetrate. Typically, the particle-capturing efficiency of filter may be depending on its fibrous

(A)

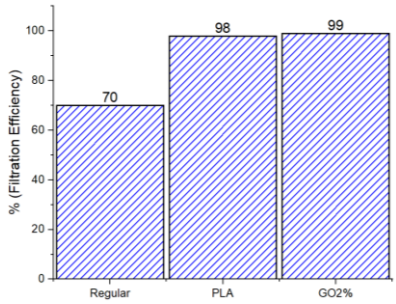

(B)

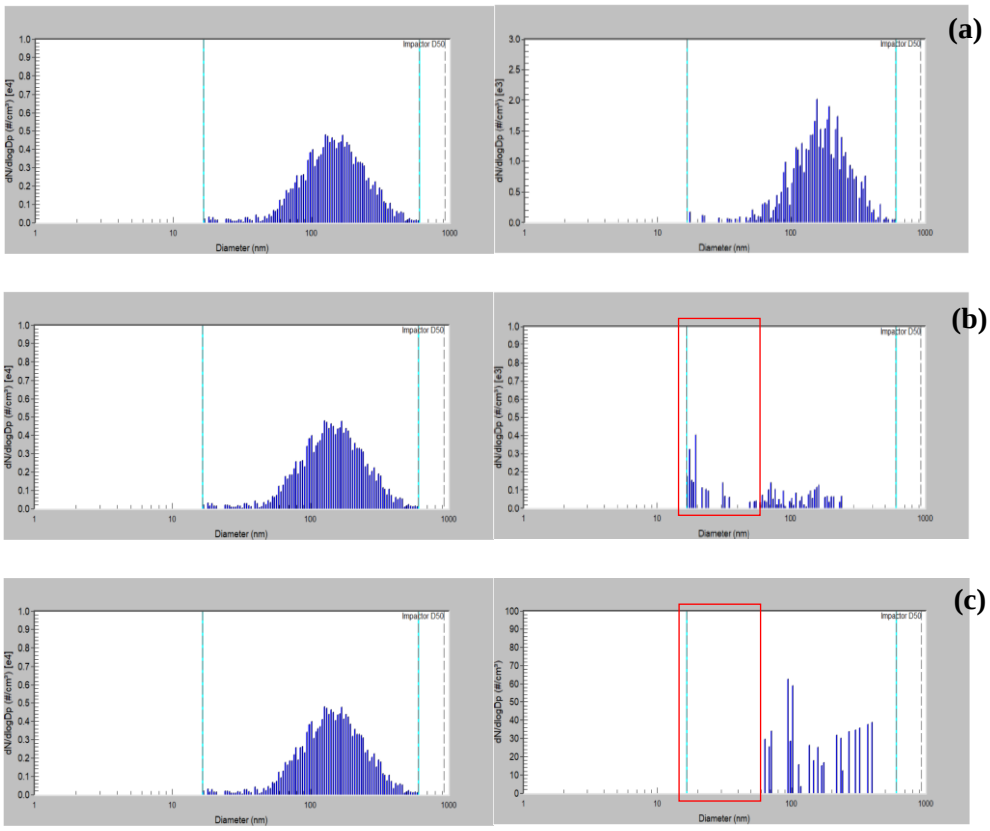

Figure 4 (A) filtration efficiency and (B) particle size distribution of generated particles before (left) and after passing through the filter products (right) of: (a) regular face mask, (b) PLA fiber mat and (c) PLA/PVP/GO nanofiber mat

structure, void size between fibers, and size of fibers, in which particles or dust with bigger size may stick on the fibers or being trapped in inter-fiber voids. However, the presence of negatively-charged GO particles on the composite fiber's surface may enhance attraction interaction with dust particle, leading to higher trapping efficiency, especially for particles with smaller sizes. It was reported that filtration efficiency of masks which use only physical mechanism revealed higher percentage of aerosol penetration than the masks containing both physical and electrical mechanisms (Brown, 1995).

CONCLUSIONS

Nanofibers derived from degradable PLA with uniform fibers and high porosity are successfully prepared by an electrospinning technique. The PLA nanofibers can effectively filter out PM2.5 particles, with 98% efficiency, compared to that of regular commercial face mask of 70%. Although, the filtration efficiency of PM2.5 for both nanofiber mat samples are almost similar, the presence of proper PVP and negatively-charged GO contents on PLA provides improved filtration efficiency toward smaller dust particles, in the range of 10 – 100 nm. SEM images show high porosity of composited PLA nanofibers, implying that the nanofibers would simultaneously preserve a good breathability. Although it is well-known that PLA is biodegradable polymer, experiments on durability and degradability tests of the face masks after use are undergoing.

ACKNOWLEDGEMENTS

Financial supports from the National Research Council of Thailand (NRCT) through a Research University Network (RUN), Center of Excellence in Materials and Plasma Technology (CoE M@P Tech), and Center of Scientific Equipment for Advanced Research, Thammasat University, are gratefully acknowledged. P.M.

thanks support from the TAIST-Tokyo Tech scholarship program and SIIT.

REFERENCES

Brown RC. Protection Against Dust by Respirators. International journal of Occupational safety and ergonomics 1995; 1(1): 14-28.

Chen BK, Shen CH, Chen SC and Chen AF. Ductile PLA modified with methacryloyloxyalkylisocyanate improves mechanical properties. Polymer 2010; 51(21): 4667-4672.

Dias ML, Dip RMM, Souza DHS, Nascimento JP, Santos AP and Furtado CA. Electrospun Nanofibers of Poly(lactic acid)/Graphene Nanocomposites. Journal of Nanoscience and Nanotechnology 2017; 17(4): 2531- 2540.

Huang S, Zhou L, Li MC, Wu Q, Kojima Y and Zhou D. Preparation and Properties of Electrospun Poly (Vinyl Pyrrolidone)/Cellulose Nanocrystal/Silver Nanoparticle Composite Fibers. Materials 2016; 9(7): 523.

Jamshidian M, Tehrany EA, Imran M, Jacquot M and Desobry S. Poly-Lactic Acid: Production, Applications, Nanocomposites, and Release Studies 2010. Comprehensive Reviews in Food Science and Food Safety; 9(5): 552-571.

Li X, Gong Y. Design of Polymeric Nanofiber Gauze Mask to Prevent Inhaling PM2.5 Particles from Haze Pollution. Journal of Chemistry 2015; 2015: 5.

Marcano DC, Kosynkin DV, Berlin JM, Sinitskii A, Sun Z, Slesarev A, Alemany LB, Lu W and Tour JM. Improved Synthesis of Graphene Oxide. ACS Nano 2010; 4 (8): 4806–4814.

Noh KT, Lee HY, Shin US and Kim HW. Composite nanofiber of bioactive glass nanofiller incorporated poly(lactic acid) for bone regeneration. Materials Letters 2010; 64(7): 802-805.

Rawat A, Mahavar HK, Tanwar A and Singh PJ. Study of electrical properties of polyvinylpyrrolidone/polyacrylamide blend thin films. Bulletin of Materials Science 2014; 37(2): 273-279.

Rengasamy S, Eimer B and Shaffer RE. Simple Respiratory Protection-Evaluation of the Filtration Performance of Cloth Masks and Common Fabric Materials Against 20–1000 nm Size Particles.

Ann Occup Hyg 2010; 54(7): 789-798.

Shao JJ, Lv W and Yang QH. Self-Assembly of Graphene Oxide at Interfaces. Advanced Materials 2014; 26: 5586 - 5612.

Sun B, Duan B and Yuan X. Preparation of Core/Shell PVP/PLA Ultrafine Fibers by Coaxial Electrospinning. Journal of Applied Polymer Science 2006; 102(1): 39-45.

Xing YF, Xu YH, Shi MH and Lian YX. The impact of PM2.5 on the human respiratory system. Journal of Thoracic Disease 2016; 8(1): 69-74.

Optimization of microwave-assisted extraction for enhancing reducing sugar of water hyacinth pretreatment at Klong Yong community in Phutthamonthon, Nakhon Pathom, Thailand

Hendri Rantau Silalahi[1], Nuttawan Yoswathana[2*]

[1*]Department of Chemical Engineering, Faculty of Engineering, Mahidol University
[2]Department of Chemical Engineering, Faculty of Engineering, Mahidol University
Corresponding author: e-mail: nuttawan.yos@mahidol.ac.th

ABSTRACT

Water hyacinth is an aquatic plant that has emerged as a major invasive weed and high reproduction rate at Soi Bon canal in Klong Yong, Phutthamonthon, Thailand. As a lignocellulosic plant material, it can be made into an organic fertilizer at 60-90 days. Microwave-assisted extraction technique was investigated to optimize hydrolysis of cellulose and hemicellulose and disrupt lignin structure using Calcium hydroxide solution, Sodium bicarbonate solution and Distilled water and also various size of raw material (0.1-0.5 cm and 3-5 cm). The result showed that calcium hydroxide solution was the best solvent for total reducing sugar extraction from water hyacinth with size of 3-5 cm. Box-Behnken design was conducted for microwave-assisted pretreatment at 450 watts using three parameters; the solid to liquid ratios as 1:10, 1:15, and 1:20 with volume of liquid at 30 ml, extraction times of 20, 30, and 40 minutes, and calcium hydroxide solution at various concentrations as 0.1, 0.55, and 1 %wt. The optimum conditions of total reducing sugar from water hyacinth solution were 54 mg/g at the solid to liquid ratio as 1:10, concentration of calcium hydroxide at 0.55 %wt, 30 minutes of extraction

time, and %brix was 5.74. Microwave-assisted pretreatment using calcium hydroxide solution was an alternative to hydrolyze cellulose and hemicellulose and disrupt lignin structure.

Keywords: Water hyacinth, Total reducing sugar, Lignocellulosic, Microwave-assisted extraction, Box-Behnken**.**

INTRODUCTION

The water hyacinth (*Eichhornia crassipes*) is an aquatic plant that originated from South America (Keawmanee, 2015) (Bolenz *et al*, 1990). Water hyacinth lives in tropical and sub-tropical regions such as in Indonesia and Thailand. In Thailand, water hyacinth can be found such as in lakes, dams, and rivers. Water hyacinth is known for their rapid growth rates, extensive dispersal capabilities, large and rapid reproductive output and broad environmental tolerance (Bolenz *et al*, 1990). These makes water hyacinth become water pollution that cause major problem in the area, such as block water flow in the river, reduce oxygen content in the water thus reducing of fishes in the water, increase sedimentation, and also provoke health problem (Bolenz *et al*, 1990) (Lee B, 1979) (Carina et al, 2007). Current solution, especially in Thailand, for this problem is dispose water hyacinth manually someplace else. This solution is temporary solution and requires high cost.

Despite of disadvantages, as one of the biomass material, water hyacinth has many advantages. Water hyacinth can be made into organic fertilizer (Polprasert *et al*, 1994), craft (Keawmanee, 2015), bio adsorbent (Kasem *et al*, 2012), bioethanol (Yang *et al*, 2016), animal feed (Abdel *et al*, 1991), and biogas (Chanakya *et al*, 1993) also can be produced from water hyacinth. Those benefits of water hyacinth can have good impacts to the community. For example, water hyacinth craft can be done by local community and can increase their income. But this has limitation due to only small amount

of water hyacinth is used. The other benefit is water hyacinth organic fertilizer. The organic fertilizer also can be done by local community, can increase community income, and can reduce dependence on the use of chemical fertilizers. Muoma John (2016) and Polpraset *et al* (1994) had done research of making water hyacinth organic fertilizer. In addition, the use of chemical fertilizers continuously raises environmental and health problem and also can reduce soil quality and crop productivity. On the other hand, organic fertilizer can improve fertility of the soil and production of the crop such as paddy production in Indonesia.

Water hyacinth is one of the lignocellulosic material. As a lignocellulosic material, it has lignin, cellulose, and hemicellulose. And these are the primary building block of plant cell material. Table 1 shows the components of each material in water hyacinth from many researchers.

Table 1. Components of lignocellulosic material in water hyacinth

Components (%dry matter basis)			**References**
Lignin	**Cellulose**	**Hemicellulose**	
9.27	19.5	33.4	Gunnarsson and Petersen (2007)
7	31	22	Bolenz et al (1991)
7.8	17.8	43.4	Patel et al (1993)

Pretreatment of water hyacinth need to be carried out to extract cellulose and hemicellulose, and to degrade lignin. Among these materials, lignin is the most difficult material to be degraded due to rigid structure compare to cellulose and hemicellulose. Lignin appears in

forms of crystalline and amorphous. The efficiency of pretreatment can be evaluated through the material dissolved, increase of anaerobic biodegradation and operational costs. In lignocellulosic biomass, the effect of heat occurs at a temperature of 150 – 180 ^{o}C where hemicellulose and lignin first began to dissolve (Hendriks and Zeeman, 2009).

Many researchers had done many experiment to extract cellulose and hemicellulose and degrade lignin more efficient, such as using mechanical, thermal, acid hydrolysis, alkaline hydrolysis, or combination of these methods. One of the pretreatment is microwave pretreatment. This pretreatment is using radiation of electromagnetic energy that is converted into heat energy. The Advantage of microwave pretreatment method is energy efficient due to short time for process and no temperature gradient. In conventional heating, the heat transfer from heat source to material through convection, conduction, and radiation processes and produce temperature gradient. This process also require longer time compare to microwave treatment.

Microwave irradiation can alter the structure of cellulosic biomass, including increasing the specific surface area, decreasing the polymerization and crystalline cellulose, the hydrolysis of hemicellulose and lignin depolymerization (Berglund *et al*, 2012). Thermal pretreatment with microwaves can destroy complex structure of lignocellulosic material. Eskicioglu *et al* (2007) had studied using microwave pretreatment method, the production of methane 16 + 4% higher compared to conventional heating on waste activated sludge after 15 days. Budiyono *et al* (2015) had studied the effects of microwave pretreatment of fresh water hyacinth for biogas production and the optimum condition for this was obtained at 560W for 7 minutes, producing 75.12 mililiter biogas per gram of total solids. Ethaib *et al* (2016) evaluated the effect of acid and alkali on dragon

fruit foliage using microwave at power 800 W for 5 minutes using microwave pretreatment and 0.1 N NaOH which gave highest result of monomeric sugar at 15.56 mg/g. Therefore, microwave pretreatment can be used as an approach over conventional heating for pretreatment of biomass in biogas production. Optimization of bioethanol production using water hyacinth had been studied by Zhang *et al* (2016) using microwave pretreatment at power 150 W, H_2SO_4 concentration at 1 wt% for 20 minutes treatment time and the optimum bioethanol production was 1.291 g/L. Zhu *et al* (2006) reported that microwave pretreatment on rice straw was an effective pretreatment method for increasing the rate of hydrolysis.

For optimization of the process, Box-Behnken design method was being used for this experiment. Yang *et al* (2006) had studied the optimization using Box-Behnken design for maximizing biofuel content of water hyacinth using microwave pretreatment method at power 1110 W and 3.5 minutes treatment time. The experimental are microwave power, amount of absorbent, and treatment time.

Previous researchers have studied production of water hyacinth organic fertilizer using subcritical pre-treatment and without pretreatment and the result was the fertilizer can be produced in 10 days (subcritical method) and 30 days–58 days (conventional method). Also, previous researchers had studied the effect of microwave pretreatment on lignocellulosic biomass using strong base (NaOH) and strong acid (H_2SO_4). However, there is no researcher investigating the influence of the microwave pretreatment method on water hyacinth for organic fertilizer production using calcium hydroxide solution. The objective of this research was to study the effect of microwave pretreatment at various microwave levels of power, various solvents concentration and times on improving the digestion of water hyacinth.

METHODOLOGY

Material

The water hyacinth was collected from Klong Yong district in Nakhon Pathom Province, Thailand. The water hyacinth was then sun dried for 14 days and cut 3-5 cm long.

Microwave-assisted pretreatment

Microwave-assisted pretreatment were performed using Microwave digestion system (Anton Paar Multiwave PRO). The pretreatment was conducted using microwave power 450 W, various type of solvents (Distilled water, Sodium bicarbonate, and Calcium hydroxide), different size of raw material (size 3-5 cm long and size 0.1-0.5 cm long), various treatment time (5, 10, 20, 30 minutes), at solid to solvent ratio 1:10, and at 1.2%wt solvent concentration. After cooling, the content was filtered using filter paper and %Brix of the filtrate was measured using digital refractometer. The filtrate contain of sugar solution due to of the hydrolysis of cellulose and hemicellulose produce sugar (Joseph and Ronald, 2010).

Box-Behnken Design

The Box-Behnken design method used for optimization. Factors and levels for Box-Behnken design was:

Table 2 Variables and codes for Box-Behnken Design

Variables	Codes	Ranges and level		
		-1	**0**	**1**
Ratio	x1	1:10	1:15	1:20
Concentration	x2	0.1 %wt	0.55 %wt	1 %wt
Time	x3	20 min	30 min	40 min

Reducing sugar analysis

The reducing sugar analysis were performed using 3.5 - Dinitrosalicylic acid (DNS) (Miller, 1959). The reagent is a solution formed by the following compounds: 3.5 - Dinitrosalicylic acid which acts as an oxidant, Rochelle salt (sodium-potassium tartrate), which prevents the dissolution of oxygen in the reagent and sodium hydroxide to provide the medium required for the redox reaction to occur. The analysis was conducted using UV VIS Spectrophotometer at wavelength 540 nm.

Figure 1a Before pretreatment

Figure 1b After pretreatment

RESULTS AND DISCUSSION

Effect of microwave pretreatment on water hyacinth

Figure 1a showed dried water hyacinth before microwave pretreatment. Figure 1b showed water hyacinth after pretreatment method. After pretreatment, color of water hyacinth turned into dark brown and has soft texture.

From table 3, range of experimental temperature start from 175 ^{o}C to 222 ^{o}C and pressure was 20 bar.

Microwave heating heats polar substances. Water is a strongly polar substance. It can absorb microwave irradiation, generate heat, and rapidly vaporize during microwave irradiation. The rapid vibration of the water molecules leads to a rapid increase of the osmotic pressure, which disrupts the cell wall of water hyacinth. This process will change structural composition and appearance of water hyacinth.

From table 3, the result showed %brix of microwave pretreatment of water hyacinth using different types of solvent and various treatment times. It showed that, using calcium hydroxide solution and big size of raw material (3- 5 cm cutting) optimum result was obtained compare to others.

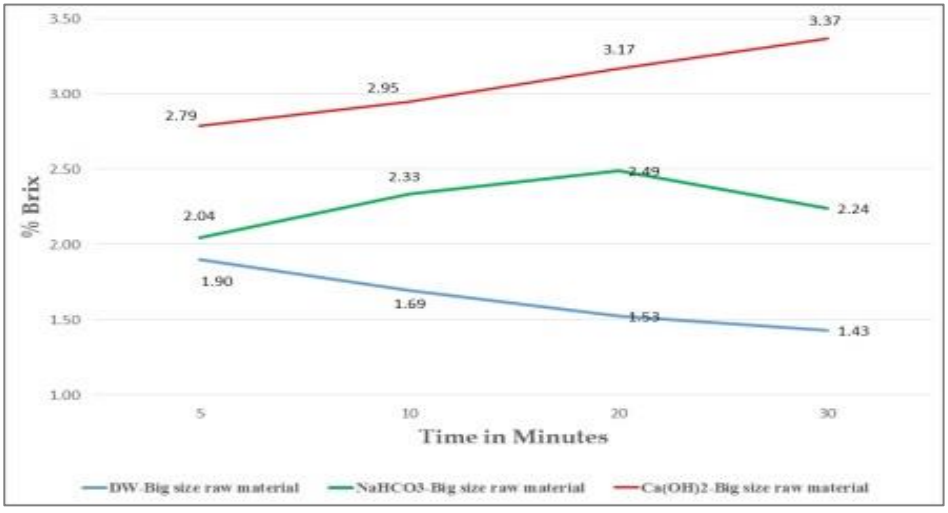

Figure 2 Effect of microwave pretreatment on water hyacinth using calcium hydroxide, sodium bicarbonate solution and distilled water

From figure 2, for big size raw material, when using calcium hydroxide (red line) , the result increase from 5 minutes treatment time to 30 minutes treatment time. When using sodium bicarbonate (green line), the figure showed that result increase from 5 minutes treatment time to 20 minutes treatment time, then decrease when treatment time at 30 minutes. When using distilled water (blue line), the result decrease from 5 minutes treatment time to 30 minutes treatment time.

From this result, using calcium hydroxide gave the optimum result compare to other solvents (distilled water and sodium bicarbonate). And using big size raw material (3-5 cm cutting) also gave optimum result compare to small size raw material (0.1-0.5 cm).

Box-Behnken Design

From table 3 below, experimental value obtained of % brix for Box-Behnken design range from 1.8-5.4 %brix.

By using Microsoft Excel® 2013, regression analysis model as shown in Eq.1 below

$$Y = 5.27 - 1.11X_1 + 0.11X_2 - 0.13X_3 - 0.76X_1^2 - 1.66X_2^2 - 1.88X_3^2 - 0.25X_1X_2 + 0.48X_1X_3 - 0.08X_2X_3$$

Where Y is Experimental yield, X_1 is solid to solvent ratio, X_2 is concentration of calcium hydroxide solution. And X_3 is experimental time. From regression analysis, value of Multiple R is 0.987 found to be statistically significant when performing a hyphothesis testing with significance level of 5%. The value of R square (R^2) is 0.975 indicates that 97.50% of variation in %brix (y) can be explained by variation of concentration of solution, solid to solvent ratio, and experimental time.

The 3D- response surface graphs showed the interaction effect of variables (concentration of solution, solid to solvent ratio, and experimental time) on % brix were plotted and shown in figures 3-5.

Table 3 Box-Behnken design of microwave-assisted extraction

No	x1 = Solid to solvent ratio	x2 = Concentration	x3 = Time	Y = Yield (%Brix)	Temp (°C)
1	-1(1:10)	-1(0.1%wt)	0(30)	3.4	196
2	1(1:20)	-1(0.1%wt)	0(30)	1.9	184
3	-1(1:10)	1(1%wt)	0(30)	4.3	200
4	1(1:20)	1(1%wt)	0(30)	1.8	198
5	-1(1:10)	0(0.55%wt)	-1(20)	5.4	196
6	1(1:20)	0(0.55%wt)	-1(20)	2	175
7	-1(1:10)	0(0.55%wt)	1(40)	3.7	222
8	1 (1:20)	0(0.55%wt)	1(40)	2.2	211
9	0 (1:15)	-1(0.1%wt)	-1(20)	2.2	184
10	0 (1:15)	1(1%wt)	-1(20)	2.4	187
11	0 (1:15)	-1(0.1%wt)	1(40)	2.6	209
12	0 (1:15)	1(1%wt)	1(40)	2.5	212
13	0 (1:15)	0(0.55%wt)	0 (30)	5.2	209
14	0 (1:15)	0(0.55%wt)	0 (30)	5.3	210
15	0 (1:15)	0(0.55%wt)	0 (30)	5.3	209

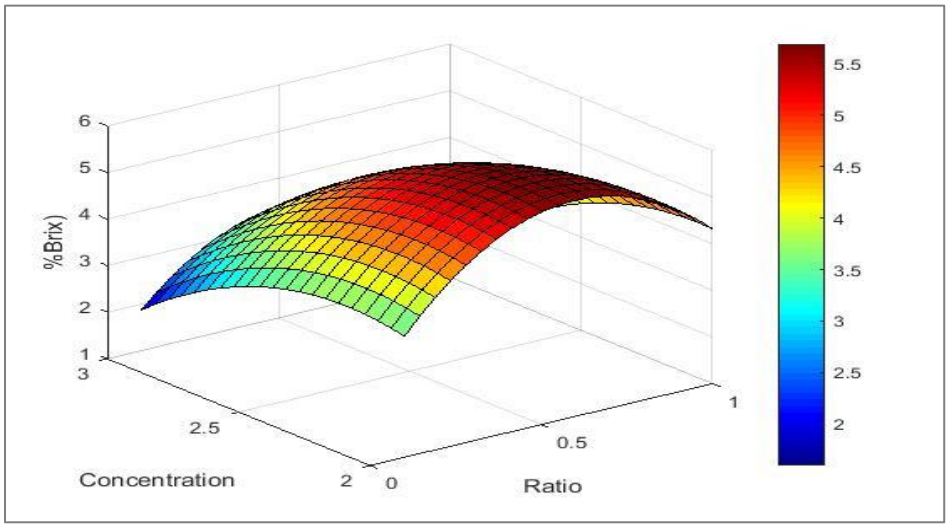

Figure 3 The 3D-graph showing the effect of concentration of solvent and solid to solvent ratio on %brix at 30 minutes treatment time.

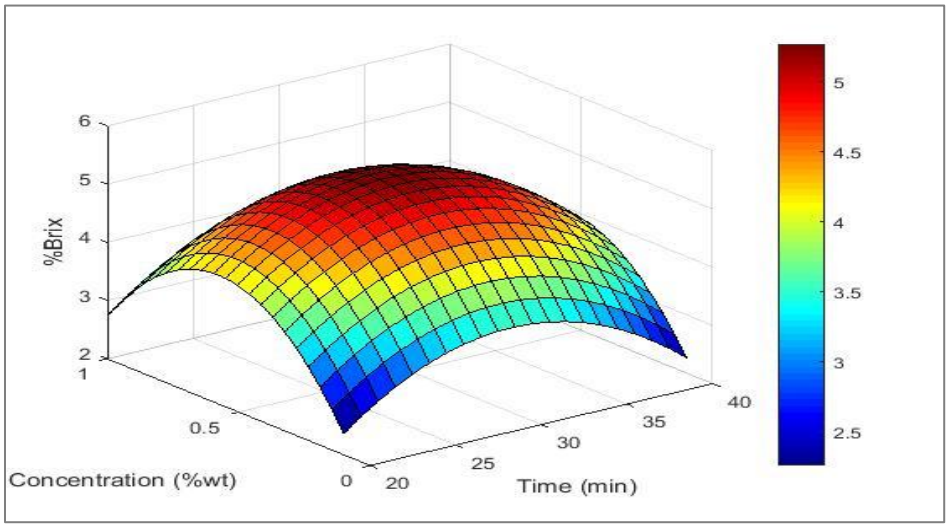

Figure 4 The 3D-graph showing the effect of concentration of solvent and treatment time on %brix at 1:15 solid to solvent ratio.

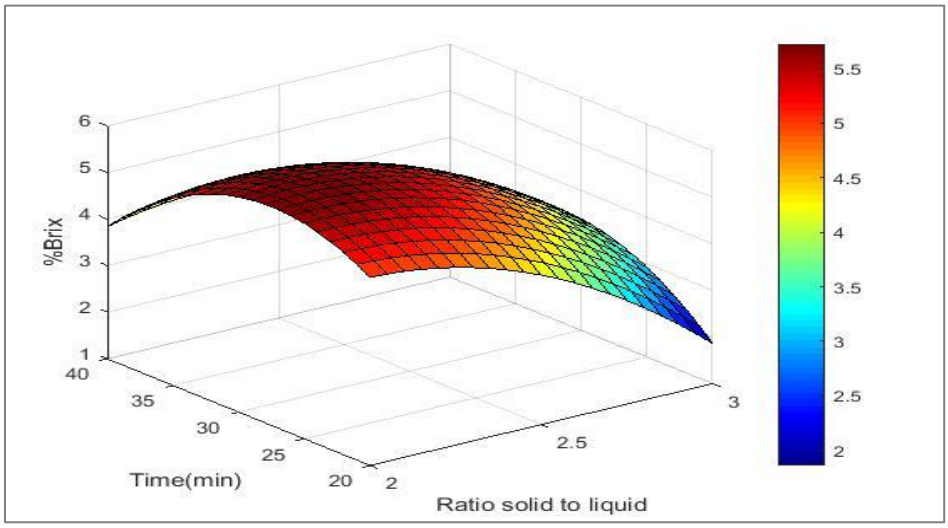

Figure 5 The 3D-graph showing the effect of treatment time and 1:15 solid to solvent ratio on %brix at 0.55%wt concentration of solution

The optimum condition for microwave pretreatment using calcium hydroxide solution was observed at the solid to liquid ratio as 1: 10, concentration of calcium hydroxide at 0. 55 % wt, and 30 minutes of extraction time, and %brix was 5.74.

From figure, higher solvent concentration and higher treatment time at certain solid to solvent ratio, the yield becoming lower. Also at lower solvent concentration and shorter treatment time, the yield was also lower. This means important factors for hydrolysis was the concentration of solvent and treatment time.

Reducing sugar analysis

The method showed linearity range from 0.15-1.4 mg/ml with linearity curve as in figure 5 below.

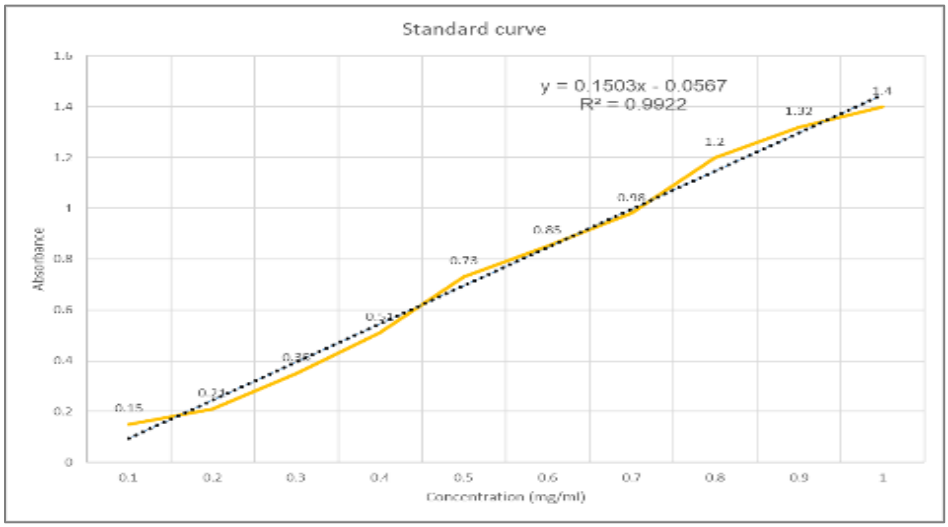

Figure 6 Calibration curve for determination of reducing sugar in extract of water hyacinth by MAE method using UV-Visible spectrophotometer

From the figure 6, value of Multiple R is 0.996 found to be statistically significant when performing a hyphothesis testing with significance level of 5%. The value of R square (R^2) is 0.9922 indicates that 99.22% of variation in absorbance (y) can be explained by variation of concentration (x) and the calibration curve is represented as y = 0.1503x - 0.0567.

The amount of total reducing sugars released from the substrate equated to the effectiveness of the pretreatment method (Das *et al*, 2015). Experimental amount of total reducing sugar of water hyacinth before and after microwave pretreatment was 27 mg/g WH and 54 mg/ g WH. The amount of reducing sugar after microwave pretreatment was obtained from optimum condition.

Rezania *et al* (2019) number of reducing sugar obtained was 25+1.5 mg/ g in untreated WH. Similarly, Harun *et al* (2011) obtained 24.7 mg sugar/ g dry matter of sugars in untreated WH. Ethaib *et al* (2016) number of reducing sugar obtained was 15.56 mg/g and 6.45 mg/g of dragon fruit foliage for microwave-

pretreatment method using sodium hydroxide and sodium bicarbonate solution. Jongmeesuk *et al* (2014) obtained reducing sugar from water hyacinth $2.35 + 0.34$ g/ L using sodium hydroxide solution. Rezania *et al* (2019) obtained reducing sugar from water hyacinth was 95 ± 3.1 mg/ g of Water Hyacinth using microwave-pretreatment and sodium hydroxide solution.

CONCLUSIONS

Water hyacinth can be utilized for many organic material, such as organic fertilizer, bioethanol, and many more. Water hyacinth can be hydrolyzed using many pretreatment methods and many solvent, one of the method is microwave method using calcium hydroxide solution.

Water hyacinth was hydrolyzed using various concentration of calcium hydroxide solution, different treatment time, and various solid to solvent ratio. And the optimum condition obtained at solid to liquid ratio as 1: 10, concentration of calcium hydroxide at 0.55 % wt, and 30 minutes of extraction time with total reducing sugar was 54 mg/ g WH. The reducing sugar using calcium hydroxide solution was less comparing to sodium hydroxide (95 mg/ g WH) (Rezania *et al*, 2019) compare to sodium hydroxide, calcium hydroxide is better for making organic fertilizer due to sodium hydroxide is toxic, corrosive and irritating to the skin, eyes and mucous membranes, and also it will endanger environment (USEPA, 1992).

Microwave pretreatment using calcium hydroxide solution can be one of the method to hydrolysis lignocellulosic material from water hyacinth.

ACKNOWLEDGEMENTS

The authors acknowledge the support from Department of Chemical Engineering, Faculty of Engineering, Mahidol University, Thailand.

REFERENCES

Keawmanee, Ratchanon. Water Hyacinth - The Green Potential. Tesis. Rochester Institute of Technology. 2015.

Accessed from http://scholarworks.rit.edu/theses.

Bolenz, S. , Omran, H. , Gierschner, K. Treatments of water hyacinth tissue to obtain useful products. Biological Wastes 33 (4), 1990, pages 263–274.

Lee B. Insects for controlling water weeds. Rural-Research (105), 1979, 25–29.

Carina C. Gunnarsson, Cecilia Mattsson Petersen. Water hyacinths as a resource in agriculture and energy production: A literature review. Waste Management 27, 2007, pages 117–129.

Kasem Chunkao, Chatri Nimpee, Kittichai Duangmal. The King's initiatives using water hyacinth to remove heavy metals and plant nutrients from wastewater through Bueng Makkasan in Bangkok, Thailand. Ecological Engineering, Volume 39, 2012, Pages 40-52, ISSN 0925-8574.

T.Yang, G. Wei Zhang, W. Zhe Zhu, J. Bin Su, Y. Zhao. Microwave Pyrolysis Parameter Design of Water Hyacinth after Optimization based on Box-Behnken. 2016 International Conference on Power Engineering & Energy, Environment (PEEE 2016). ISBN: 978-1-60595-376-2.

Bolenz, S., Omran, H., Gierschner, K., 1990. Treatments of water hyacinth tissue to obtain useful products. Biological Wastes 33 (4), 263–274.

Abdelhamid, A.M., Gabr, A.A. Evaluation of water hyacinth as feed for ruminants. Archives of Animal Nutrition (Archiv fuer Tierernaïhrung) 41 (7/8), 1991. 745–756.

Chanakya, H.N., Borgaonkar, S., Meena, G., Jagadish, K. S. Solid phase biogas production with garbage or water hyacinth. Bioresource Technology 46, 1993, 227–231.

Gunnarsson, C, Petersen, C. Water hyacinths as a resource in agriculture and energy production: a literature review. Waste Manage. 27, 2007, 117–129.

Patel, V., Desai, M., Madamwar, D. A Thermochemical pretreatment of water hyacinth for improved biomethanation. Applied Biochemistry and Biotechnology, 42, 1993, 67–74.

Patel, V. B., Patel, A. R., Patel, M. C., Madamwar, D. B., 1993b. Effect of metals on anaerobic digestion of water hyacinth- cattle dung. Applied Biochemistry and Biotechnology 43, 45–50.

Hendriks, A. and Zeeman, G. Pretreatments to enhance the digestibility of lignocellulosic biomass. Bioresource Technology, Vol. 100, No. 1, 2009, 10-18.

Kumar, P., Barrett, D.M., Delwiche, M.J., and Stroeve, P. A. Methods for Pretreatment of Lignocellulosic Biomass for Efficient Hydrolysis and Biofuel Production. Industrial &

Engineering Chemistry Research, 2009.

Polprasert C, N. Kongsricharoern and W. Kanjanaprapin. Production of feed and fertilizer from water hyacinth plants in the tropics. Waste management & research, 1994, 12. 3-11.

Muoma John. Production of Organic Compost from Water Hyacinth (Eichhornia crassipes [Mart.] Solms) in the Lake Victoria Basin: A Lake Victoria Research Initiative (VicRes). Journal of Agriculture and Allied Sciences, 2016, ISSN: 2319-9857.

Budiyono, S. Sumardiono, D. Tri Mardiani. Microwave Pretreatment of Fresh Water Hyacinth (Eichhornia crassipes) in Batch Anaerobic Digestion Tank. International Journal of Engineering, IJE TRANSACTIONS C: Aspects Vol. 28, No. 6, 2015, 832-840.

Berglund Odhner, P., Sárvári Horváth, I., Kabir, M. M. and Shabbauer,A. , "Biogas from lignocellulosic biomass, Rapport SGC, sgc.camero.se, 2012.

Cigdem Eskicioglu, Nicolas Terzian, Kevin J. Kennedy, Ronald L. Droste, Mohamed Hamoda, “Athermal microwave effects for enhancing digestibility of waste activated sludge”, Water Research, Volume 41, Issue 11, 2007.

Zhu, S., Wu, Y., Yu, Z., Wang, C., Yu, F., Jin, S., Ding, Y., Chi,R.a., Liao, J. and Zhang, Y. , Comparison of three microwave/ chemical pretreatment processes for enzymatic hydrolysis of rice straw. Biosystems Engineering, Vol. 93, No. 3, 2006, 279-283.

Jackowiak, D., Bassard, D., Pauss, A. and Ribeiro, T. Optimisation of a microwave pretreatment of wheat straw for methane production. Bioresource Technology, Vol. 102, No. 12, 2011, 6750-6756.

Sapci, Z., Morken, J. and Linjordet, R. An investigation of the enhancement of biogas yields from lignocellulosic material using two pretreatment methods: Microwave irradiation and steam explosion. BioResources, Vol. 8, No. 2, 2013, 1976-1985.

Banik, S., Bandyopadhyay, S., Ganguly, S. and Dan, D., "Effect of microwave irradiated ethanosarcina barkeri dsm-804 on biomethanation", Bioresource Technology, Vol. 97, No. 6, 2006, 819-823.

Eskicioglu, C., Prorot, A., Marin, J., Droste, R. L. and Kennedy, K. J. Synergetic pretreatment of sewage sludge by microwave irradiation in presence of h 2 o 2 for enhanced anaerobic digestion. Water Research, Vol. 42, No. 18, 2008, 4674-4682.

Marin, J., Kennedy, K.J. and Eskicioglu, C. Effect of microwave irradiation on anaerobic degradability of model kitchen waste. Waste Management, Vol. 30, No. 10, 2010, 1772-1779.

Mudhoo, A., Moorateeah, P.R. and Mohee, R. Effects of microwave heating on biogas production, chemical oxygen demand and volatile solids solubilization of food residue. Citeseer, 2012.

Shahriari, H., Warith, M., Hamoda, M. and Kennedy, K.J. Anaerobic digestion of organic fraction of municipal solid waste combining two pretreatment modalities, high temperature microwave and hydrogen peroxide. Waste Management, Vol. 32, No. 1, 2012, 41-52.

Mehdizadeh, S. N. , Eskicioglu, C. , Bobowski, J. and Johnson, T. Conductive heating and microwave hydrolysis under identical heating profiles for advanced anaerobic digestion of municipal sludge. Water Research, Vol.47, No. 14, 2013, 5040-5051.

Saifuddin, N. and Fazlili, S. Effect of microwave and ultrasonic pretreatments on biogas production from anaerobic digestion of palm oil mill effluent. American Journal of Engineering and Applied Sciences, Vol. 2, No. 1, 2009, 23-34.

Qiuzhuo Zhang, Chen Weng, Huiqin Huang, Varenyam Achal, and Duanchao Wang. Optimization of bioethanol production using whole plant of water hyacinth as substrate in simultaneous saccharification and fermentation process. Frontiers in Microbiology. January 2016. Volume 6. Article 1411.

Ethaib, S., Omar, R.,Mazlina, M.,Radiah, A.,Syafiie, S. and Harun, M. Y. Effect of microwave-assisted acid or alkali pretreatment on sugar release from Dragon fruit foliage. International Food Research Journal 23(Suppl) : S149-S154 December 2016.

G. L. Miller. Use of Dinitrosalicylic Acid Reagent for Determination of Reducing Sugar. Anal. Chem., 1959, 31 (3) , pp 426– 428. DOI: 10. 1021/ ac60147a030. Publication Date: March 1959.

Marisa Garriga, Melisa Almaraz, Alicia Marchiaro. Determination of reducing sugars in extracts of Undaria pinnatifida (harvey) algae by UV-visible spectrophotometry (DNS method) . Actas de Ingeniería. Volumen 3, pp. 173-179, 2017.

Bai-Hang Zhao, Jie Chen, Han-Qing Yu, Zhen-Hu Hu, Zheng-Bo Yue, and Jun Li. Optimization of microwave pretreatment of lignocellulosic waste for enhancing methane production: Hyacinth as an example. Front. Environ. Sci. Eng. 2017, 11(6): 17. DOI 10.1007/s11783-017-0965-z.

A. Shitu, S. Izhar, T. M. Tahir. Sub-critical water as a green solvent for production of valuable materials from agricultural waste biomass: A review of recent work. Global J. Environ. Sci. Manage., 1(3): 255-264, Summer 2015, ISSN

2383 – 3572.

Shahabaldin Rezania, Hossein Alizadeh, Junboum Park, Mohd Fadhil Md Din, Negisa Darajeh,Shirin Shafiei Ebrahimi, Bidyut Baran Saha, and Hesam Kamyab. Effect of Various Pretreatment Methods on Sugar and Ethanol Production from Cellulosic Water Hyacinth. BioResources Vol 14, No. 1, 01.02.2019, p. 592-606.

Harun, M. Y., Radiah, A. D., Abidin, Z. Z., and Yunus, R. (2011). Effect of physical pretreatment on dilute acid hydrolysis of water hyacinth (Eichhornia crassipes). Bioresource Technology 102(8), 5193-5199. DOI: 10.1016/j.biortech.2011.02.001.

Atcharaporn Jongmeesuk, Vorapat Sanguanchaipaiwong, and Duangjai Ochaikul. Pretreatment and Enzymatic Hydrolysis from Water Hyacinth (Eichhornia crassipes). KMITL Sci. Tech. J. Vol. 14 No. 2 Jul.-Dec. 2014.

R.E.D. FACTS. Sodium Hydroxide. United States Environmental Protection Agency. EPA- 738- F- 92- 008 September 1992.

Zhang Q, Weng C, Huang H, Achal V, Wang D. Optimization of Bioethanol Production Using Whole Plant of Water Hyacinth as Substrate in Simultaneous Saccharification and Fermentation Process. Front Microbiol. 2016; 6: 1411. Published 2016 Jan 7.

Fiorella P. Cardenas-Toro, Sylvia C. Alcazar-Alay, Tânia Forster-Carneiro, M. Angela A. Meireles. Obtaining Oligo- and Monosaccharides from Agroindustrial and Agricultural Residues Using Hydrothermal Treatments. Food and Public Health 2014, 4(3): 123-139. DOI: 10.5923/j.fph.20140403.08.

Joseph B. Binder and Ronald T. Raines. Fermentable sugars by chemical hydrolysis of biomass. Proceedings of the National Academy of Sciences Mar 2010, 107 (10) 4516-4521; DOI: 10.1073/pnas.0912073107

S.Das, A. Bhattacharya, S. Haldar, A. Ganguly, Sai Gu, Y.P. Ting, P.K. Chatterjee. Optimization of enzymatic saccharification of water hyacinth biomass for bio-ethanol: Comparison between artificial neural network and response surface methodology. Sustainable Materials and Technologies. Volume 3. 2015. Pages 17-28. ISSN 2214-99

Discrimination of Seismic Events in Lampang Province: A Complexity Approach

Santawat Sukrungsri, Chutimon Promsuk, Chirawat Kamjudpai, and Sukrit Kirtsaeng*

Earthquake Observation Division, Thai Meteorological Department, Bangkok 10260, Thailand; *Corresponding author: e-mail: Sukritk@hotmail.com

ABSTRACT

This study aimed to distinguish microearthquakes from quarry blasts in order to clarify seismic hazard situation in Lampang province. Complexity (C) technique is regarded as an effective statistical approach for seismic discrimination that quarry blasts generate larger P-wave energy than that of earthquakes in specific time window. This technique was carried out utilizing 30 short period seismograms with local magnitudes of 1.0-1.9, recorded in February 2019 by Thai Meteorological Department (TMD). The events posed in vicinity of both the quarry and the fault rupture zone which associated with the M4.9 earthquake in Lampang province. The suitable Complexity parameters obtained from successive retrospective tests indicating the time windows of t_1 = 3s and t_2 = 6s were appropriate in classifying seismic events in the region. The seismic events in the mining area had C-value lower than 1.0 (in the range of 0.23-0.95) while the events with C-value higher than 1.0 (varies from 1.12 to 4.31) were located only within the aftershock zone of M4.9 earthquake. The proposed criteria in this study were the seismic events with C-value lower than 1.0 and higher than 1.0 be identified as quarry blast and earthquake, respectively. The above criteria will be useful for seismic discrimination, decontamination of earthquake catalogue, as well as seismic hazard investigations, particularly for Lampang province.

Keywords: Discrimination, Microearthquake, Quarry blast, Lampang province, Complexity

INTRODUCTION

The Indian-Eurasian plate collision causes the tectonic activity, the intraplate seismic sources, and the seismogenic fault zones along the intermountain basin of the northern Thailand, such as Mae-Chan, Mae-Tha, Phayao, Pua, and Thoen fault zones. Thoen active fault has been recognized as the significant seismic source in Lampang province (Charusiri et al. 1998). The tectonic geomorphology in the region (i.e. triangular facet and shutter ridge) illustrate obviously the Thoen fault strikes mainly NE-SW direction that aligns 120 km cross the area between the Phrae basin to east and the Lampang, Mae Moh, and Thoen basins to west (Charoenprawat et al. 1994). The rate of the last fault movement in the region was 0.18 mm/year with a recurrence interval for the large earthquakes of 1,700 years (Pailoplee et al. 2009). Tectonically, Lampang province is situated in the seismically active zone with the accumulated seismotectonic stress as expressed in Fig. 1. As a result, a large number of shallow crustal earthquakes have been detected in Lampang province over the last four decades. The latest event was a M4.9 strike-slip faulting earthquake in February 2019. Although the event is small in sense of the earthquake magnitude, the shallow of focal depth adjacent to the densely populated zones cause the shaking intensity is noticeable within the areas covering approximately 50 km from the earthquake epicenter with no significant damage or casualties. However, the clusters of microearthquakes were generated, the more than 100 aftershocks have been observed around the main shock source that many people can be felt and were panic. The historical earthquake information, instrumental seismic records including paleoseismological evidence realized that the Lampang province is an earthquake-prone area. However, there is the large quarry in the

Lampang province, known as the Mae Moh Mine. The observe seismic waves could be originated from both the quarry blast and active faults in the region, referred as man-made activity and earthquake hazard, respectively. Therefore, in order to clarify the seismic hazard situation, this study aimed to discriminate the seismic events in the region with respect to suitable technique for Lampang Province.

METHODOLOGY

The seismic events occurred in Lampang province with the local magnitude of 1.0-1.9 in February 2019 were employed in this study. The magnitudes and locations of the seismic events are provided from Earthquake Observation Division of TMD. We investigated
vertical components of velocity seismograms
from 30 seismic events that were recorded by the OMKO short period station with a 148-km radius of the Mae Moh mining area. The seismicity and waveform data of 30 events are shown in Table 1 and Fig. 2, respectively. Complexity (C) is the ratio of integrated powers of the seismogram in the selected time windows (Yoshida, 2016) as illustrated in Eq. (1).

Generally, the P-wave energy of a quarry blast is greater than that of the S-wave. C-value becomes larger for earthquakes than for probable mining blasts, since the P-wave amplitude on the seismogram is larger than the S-wave amplitude for mining blasts (Horasan et al. 2009; Ogutcu et al. 2010). Based on the locations of the events, we analyzed 15 probable mining blast waveforms and 15 earthquake waveforms. The parameters of t_1 and t_2 were tested retrospectively with 30 seismic events as mentioned above. A long-time window length of about 18 sec depending on the distance to the seismic source from the OMKO seismic station.

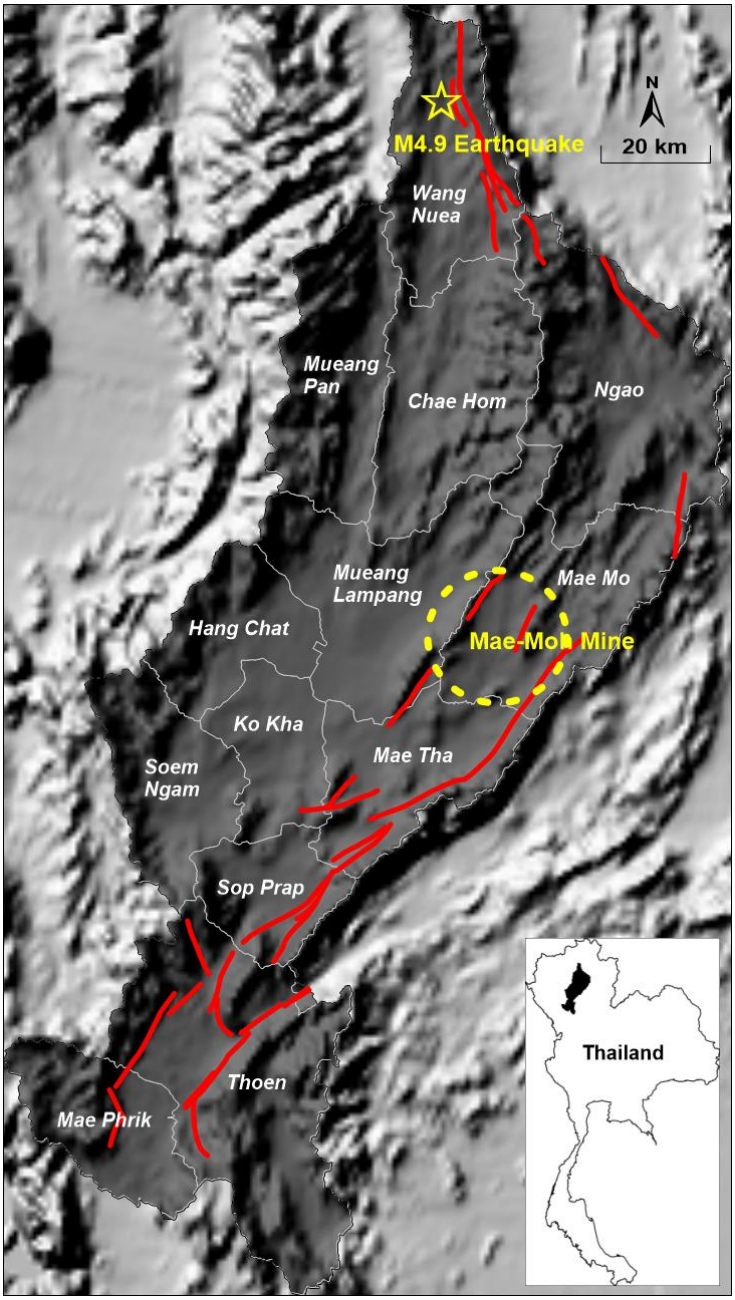

Fig. 1. Map of Lampang province showing the Mae-Moh mining area (dashed circle) and epicenter of M4.9 (yellow star) along the active fault zones (red lines).

$$C = \frac{\int_{t_1}^{t_2} S^2(t)dt}{\int_{t_0}^{t_1} S^2(t)dt}, \qquad (1)$$

where S(t) denotes the signal amplitude as a function of time (t). The t_0, t_1, and t_2 are limits of the integrals of C-value indicating the time window parameters of Complexity.

In this study, the parameters of t_1 and t_2 were varied from 1 to 8 s with a second stepping time window to determine the best representative C-values for discrimination of blasts and earthquakes. The suitable parameters were used to calculate the C-values for the 30 seismic events. The plot of C-value versus the focal depth of the probable mining events and earthquake revealing a discrimination line that can distinguish obviously the independent seismic events into two clusters.

Table 1. List of seismic events that were used in this study

Event no	Date	Origin time	Latitude (N)	Longitude (E)	Mag
1	03-02-2019	04:23:56	18.33	99.72	1.5
2	03-02-2019	06:33:12	18.32	99.72	1.6
3	03-02-2019	07:20:59	18.32	99.73	1.5
4	04-02-2019	04:29:13	18.35	99.73	1.6
5	04-02-2019	09:45:24	18.35	99.72	1.8
6	12-02-2019	04:24:17	18.30	99.77	1.6
7	12-02-2019	04:41:58	18.35	99.73	1.5
8	13-02-2019	09:39:42	18.32	99.76	1.4
9	15-02-2019	07:47:10	18.33	99.72	1.6
10	17-02-2019	04:47:09	18.34	99.71	1.6
11	18-02-2019	04:37:20	18.35	99.73	1.7
12	22-02-2019	04:40:19	18.32	99.76	1.6
13	23-02-2019	05:19:19	18.35	99.72	1.3
14	25-02-2019	04:08:21	18.34	99.68	1.7

Table 1. (Continued)

Event no	Date	Origin time	Latitude (N)	Longitude (E)	Mag
15	26-02-2019	03:56:26	18.31	99.72	1.6
16	20-02-2019	05:01:55	19.26	99.58	1.0
17	20-02-2019	19:36:34	19.28	99.62	1.7
18	20-02-2019	21:02:43	19.29	99.63	1.5
19	20-02-2019	21:05:35	19.27	99.66	1.5
20	21-02-2019	19:02:36	19.26	99.62	1.9
21	21-02-2019	21:24:32	19.28	99.62	1.7
22	22-02-2019	15:02:18	19.25	99.61	1.5
23	22-02-2019	18:23:21	19.29	99.62	1.8
24	22-02-2019	18:59:00	19.29	99.64	1.7
25	22-02-2019	20:15:10	19.28	99.65	1.3
26	24-02-2019	00:24:20	19.24	99.62	1.6
27	25-02-2019	20:17:39	19.28	99.60	1.0
28	27-02-2019	04:13:45	19.26	99.57	1.9
29	27-02-2019	17:07:23	19.25	99.63	1.5
30	28-02-2019	21:08:57	19.25	99.62	1.9

RESULTS AND DISCUSSION

In this study, we analyzed 30 seismic events with magnitude of 1.0-1.9 occurred in Lampang province in February 2019. Complexity was utilized to discriminate between quarry blasts and earthquakes. The suitable parameters for the discrimination obtained from successive retrospective tests and were applied to determine the C-values of 30 seismic events indicating the criteria for classifying the seismic events in the region. The results illustrate 30 seismic events could reasonably be classified into two clusters with the time window parameters of t_1 = 3s and t_2 = 6s. The events located within Mae Moh mining zone, C-values would be only lower than 1.0 in the range of 0.23-0.95 while the events with C-values be higher than 1.0 (varies from 1.12 to 4.31) generated only within the aftershock zone of M4.9 earthquake in Lampang province. The plot of C-value versus the focal depth of the probable mining events and earthquake reveal a discrimination line of C-values = 1.0 was

appropriate for discrimination of the seismic events, which all of quarry blast are placed below the discrimination line while most of earthquake located above the line as illustrated in Fig. 3. However, some earthquakes remained below the line of discrimination indicating the events were not completely discriminated by a Complexity approach in the region.

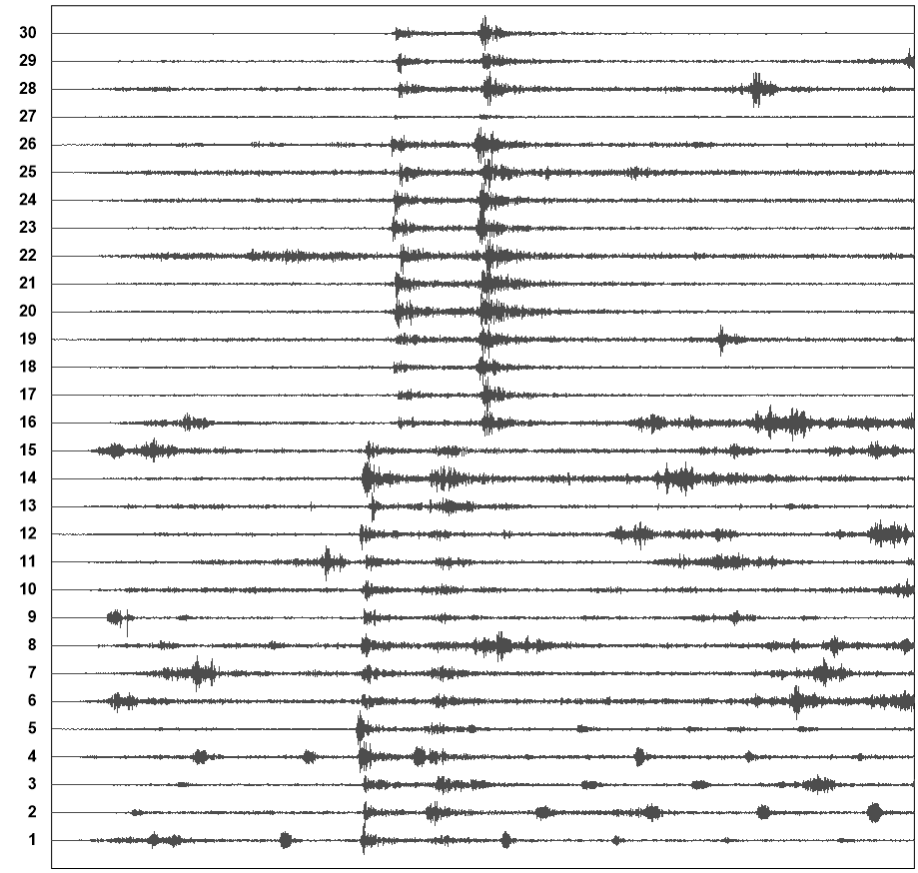

Fig. 2. The seismograms of 30 seismic events that were used in this study.

This is a limitation of Complexity for classifying the seismic events (Ogutcu et al. 2010; Yilmaz et al. 2012). The limitation should be clarified using the increasing seismic data in further study. According to the seismic events in Lampang province, discrimination of quarry blasts from earthquakes using satellite images may not be accurate since the quarries are situated along active fault zones in Lampang region

as well as the seismic events with magnitude less than 2.0 were not precisely reported by TMD network. Additionally, the discrimination by using the occurrence times is difficult since the information regarding the location and blasting time from quarries have not been reported to TMD on a regular basis.

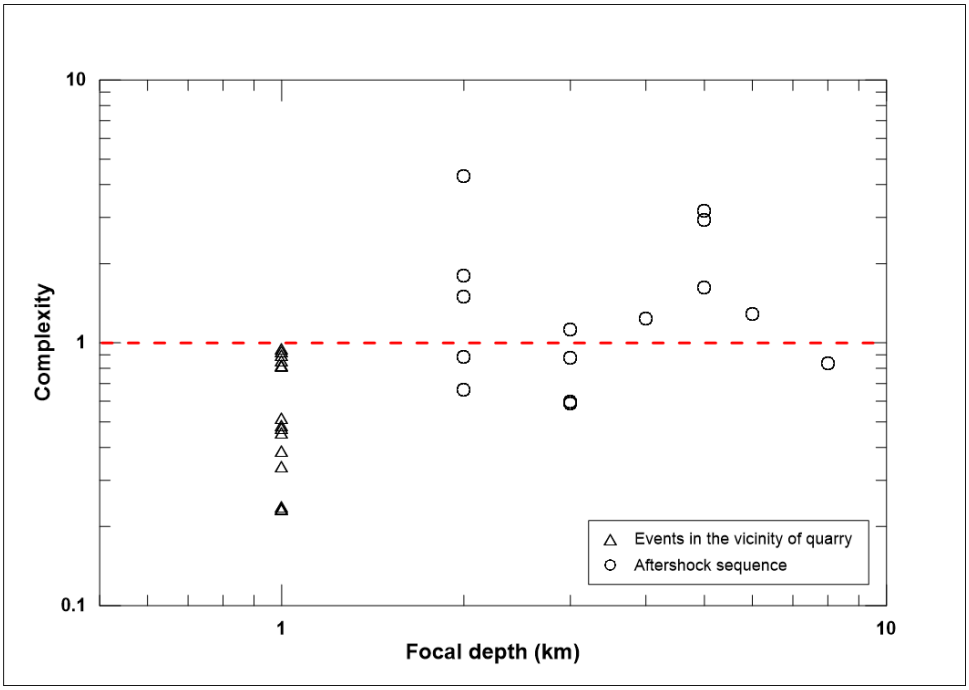

Fig. 3. Distribution of Complexity for the seismic events in Lampang province with the discrimination line (dashed line) obtained from this study.

CONCLUSIONS

The presence of the quarries along the active fault zones in Lampang province caused the significant contamination of the earthquake catalogue by blasts as well as misinterpretation of the present-day seismotectonic activities. In order to clarify the earthquake hazard situation in Lampang province, Complexity approach with the suitable parameters was employed to discriminate the seismic events in the region. The obtained results lead to the conclusion as follows:

i) Suitable Complexity Parameters for Lampang province were derived in order to discriminate

the seismic events in the region. The time window parameters of t_1 = 3s and t_2 = 6s can reasonably distinguish seismic events within mining zone and the earthquake within aftershock zone of M4.9 main shock.

ii) The C-value of 1.0 is appropriate sufficiently to distinguish seismic events in the mining area (C < 1.0) while the events with C-value higher than 1.0 were located within the aftershock zone of M4.9 earthquake.

iii) The plot of C-value versus focal depth indicates some earthquakes are placed below a discrimination line of C-value of 1.0 representing the limitation of Complexity that the events were not completely discriminated in the region.

iv) Discrimination of earthquakes from quarry blasts in Lampang province using simple criteria, i.e., satellite images, occurrence times, may not be accurate since quarries are located along the active fault zone as well as the insufficiency of information regarding the location and blasting time from quarries in the region.

ACKNOWLEDGMENTS

This research was supported by Thai Meteorological Department (TMD). The authors appreciate the thoughtful comments and suggestions by the anonymous reviewers. We are grateful to the staff of Earthquake Observation Division for recording the seismic data that were used in this study. Thanks are also extended to Parwapath Phunthirawuthi for a critical review and improved English.

REFERENCES

Charoenprawat, A., Chuaviroj, S., Hintong, C., and Chonglakmani, C., 1994. Geological map of Changwat Lampang quadrangle. Geological Survey Division, Department of Mineral Resources, Bangkok, Thailand, scale 1:250,000.

Charusiri, P., Kosuwan, S., Lumjuan, A., and Wechbunthung, B., 1998. Review of active fault and seismicity in Thailand. Geological Society of Malaysia Bulletin, 653-665.

Horasan, G., Boztepe-Guney, A., Kusmezer, A., Bekler, F., Ogutcu, Z., Musaoglu, N., 2009. Contamination of

seismicity catalogs by quarry blasts: an example from Istanbul and its vicinity, northwestern Turkey. Journal of Asian Earth Sciences, 34: 90-99.

Ogutcu, Z., Horasan, G., Kalafat, D., 2010. Investigation of microseismic activity source in Konya and its vicinity, Central Turkey. Natural Hazards, 58: 497-509.

Pailoplee, S., Takashima, I., Kosuwan, S., and Charusiri, P., 2009. Earthquake activities along the Lampang-Thoen fault zone, northern Thailand: evidence from paleoseismological and seismicity data. Journal of Applied Sciences Research, 5(2): 168-180.

Yilmaz, S., Bayrak, Y., and Cinar, H., 2012. Discrimination of earthquake and quarry blasts in the eastern Black Sea region of Turkey. Journal of Seismology, 17: 721-734.

Yoshida, Y., 2016. Discrimination by short-period seismograms. International Institute of Seismology and Earthquake Engineering, Building Research Institute, Lecture Notes, Global Course, Tsukuba, Japan, 19 pp.

Effect of silver nanoparticles on *Pseudomonas putida* and *Bacillus subtilis* biofilm formation

Rungnapa Takam[1], Kritchaya Issakul[1], Pumis Thuptimdang[2,3,*]

[1]Department of Environmental Science, School of Energy and Environment, University of Phayao, Phayao 56000, Thailand

[2]Department of Chemistry, Faculty of Science, Chiang Mai University, Chiang Mai 50200, Thailand

[3]Environmental Science Research Center, Faculty of Science, Chiang Mai University, Chiang Mai 50200, Thailand; Corresponding author: e-mail: pumis.th@gmail.com

ABSTRACT

Wide applications of silver nanoparticles (AgNPs) could possibly lead to the release into the environment. Environmental bacteria are normally living together in a protective layer of extracellular polymeric substances (EPS) called biofilms. The toxicity of AgNPs probably results in the unfavorable conditions for biofilm formation, causing the reduction of biofilm biomass and consequently the activities beneficial to the ecosystem. The objective of this research is to study the effect of various concentrations of AgNPs on the formation of gram-negative and gram-positive bacteria. By using soil bacteria, *Pseudomonas putida* KT2440 and *Bacillus subtilis*, as the representatives of environmental bacteria. The experiments were conducted in a 96-well plate with the presence of AgNPs (average size of 5-20 nm) at the concentrations of 0, 0.1, 0.5, 1, 10, 50, 100, 500 and 1000 mg/L. The plate was incubated at room temperature for 48 h, and biofilm formation was measured by crystal violet staining throughout the incubation period. The growth curve of biofilm formation under different AgNP concentrations was conducted. The results showed that AgNPs at 10 and 50 mg/L resulted in the formation of *P. putida* KT2440 biofilms similar to the control (0 mg/L) while the formation was

inhibited completely at the AgNP concentrations of 100, 500 and 1,000 mg/L. Interestingly, AgNPs at low concentrations of 0.1, 0.5 and 1 mg/L could increase *P. putida* KT2440 biofilm formation compared with the control. Differently, AgNPs at the studied concentrations only inhibited *B. subtilis* biofilm formation, and no increased formation of biofilms was observed. The findings from this study can be used in the determination of AgNP impacts on environmental biofilms of both gram negative and positive bacteria.

Keywords: Silver nanoparticles, Biofilms, Extracellular polymeric substances

INTRODUCTION

Silver nanoparticles (AgNPs) are widely used as antimicrobial agents in various consumer products for environmental, medical, and industrial applications (Dorobantu et al., 2015; Duran et al., 2016). Since AgNPs possess antimicrobial properties (Garuglieri et al., 2017), the widespread uses can possibly release high loads of AgNPs into wastewater and natural water environment (Angel et al., 2013). AgNPs in the environment could suppress the growth and activity of various microorganisms including bacteria, yeast, and algae (Gutierrez et al., 2013; Dorobantu et al., 2015).

Bacteria in nature often live in the form of biofilms, which are clusters of bacteria forming on surface by assembling the cells within the extracellular polymeric substance (EPS). In both natural water and wastewater systems, bacteria form biofilms to promote nutrient diffusion and uptake for growth, to survive in diverse conditions, or to protect themselves from harmful substances (Flemming et al., 2007; Jamal et al., 2015; Donlan, 2002).

AgNPs with strong activity are capable of eradicating the wastewater biofilms, changing the biofilm structure, and reducing the wastewater treatment ability. Also, AgNPs that accumulate in the soil

will reduce the activity and diversity of bacteria (Morones et al., 2005; Nadell, 2009; Samarajeewa et al., 2017).

The concentrations of AgNPs found in wastewater or natural water might be possibly low and did not completely eradicate the biofilms (Melissa et al., 2013). However, these low or sub-lethal concentrations of AgNPs could still have an impact on the process of biofilm formation, and research in this area is still limited. Therefore, the objective of this research is to study the effect of various concentrations of AgNPs on the process of biofilm formation of gram-negative and gram-positive bacteria. Firstly, the sub-lethal concentrations of AgNPs that did not inhibit biofilm formation were chosen. After that, the impact of AgNPs on the alteration of biofilms was determined from biomass production.

METHODOLOGY

Bacterial culture preparation

P. putida KT2440 (ATCC 47054), a gram-negative bacterial strain, was cultivated in Luria-Bertani (LB) medium at 30°C. *Bacillus subtilis* (TISTR1248 and TISTR1451), gram-positive bacterial strains, were cultivated in Nutrient Broth (NB) medium at 37 °C. Before each experiment, all strains were shaken overnight corresponding to their media and temperature at 100 rpm of shaking speed. The cell suspension was centrifuged at 7000 rpm for 1 min and the cell pellet was washed twice with 0.85% NaCl solution. The cell suspension was prepared by adding 0.85% NaCl to the pellet and adjust the optical density at 600 nm (OD_{600}) of the suspension to 0.4. This is to ensure the same starting number of cells (10^7 CFU/ml) in each biofilm experiment.

AgNP preparation

The commercial AgNPs was obtained from Prime Nano Technology (Bangkok, Thailand). According to the manufacturer, the

AgNPs are rounded-shape with the size range between 5–20 nm and the concentration of 10,000 mg/L. Before use, the AgNP suspension was diluted to the desired concentrations using sterile de-ionized (DI) water.

Biofilm experiment

Biofilm formation was conducted in a polystyrene, flat-bottom, 96-well plate. Each well (200 µl) contained the cell suspension, LB (0.5X) or NB (0.5X) medium, DI water, and with or without the AgNP suspension. DI water was used to adjust the volume and dilute AgNPs to the required concentrations (0, 0.1, 0.5, 1, 10, 50, 100, 500 and 1000 mg/L). The plate was incubated at room temperature for 48 h. Every experiment was conducted with three wells representing three replicates.

At each sampling time, after the biofilms formed, the media was carefully removed before the biofilms were slowly rinsed twice with 0.85% NaCl. The biomass amount was determined by crystal violet (CV) staining, which was then measured at the absorbance of 600 nm (A_{600}) according to Thuptimdang et al. (2015). The appearance of biofilms before and after CV staining is shown in Figure 1.

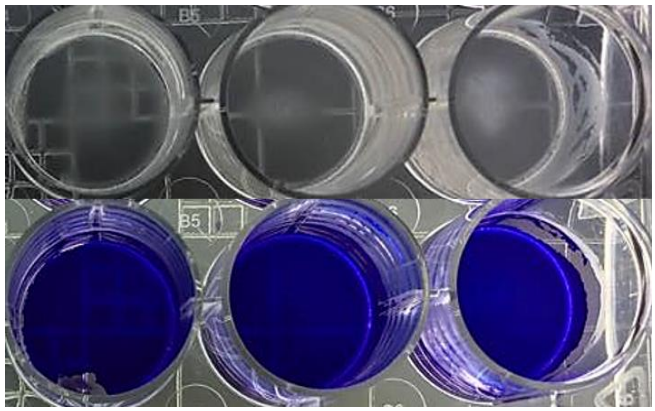

Figure 1 Biofilms before (upper row) and after (lower row) CV staining.

RESULTS AND DISCUSSION

Determination of Minimum Biofilm Inhibitory Concentration (MBIC) of AgNPs

that range, a preliminary experiment was conducted to determine the minimum biofilm inhibitory concentrations (MBIC) of AgNPs. *Pseudomonas putida* KT2440 were exposed to different concentrations (a series of half-dilutions) of AgNPs in the 96-well plate for 12 h to allow biofilm formation. The results showed that the MBIC of AgNPs was 62.5 mg/L, and the concentrations below 62.5 to 0.12 mg/L were sub-lethal to biofilms, showing similar biofilm formation compared with the control (0 mg/L) (Figure 2). The MBIC from this study is higher compared to the study of another gram-negative bacteria, *E. coli* AB1157 (Radzig et al., 2013), which showed the sub-lethal concentrations of AgNPs between 0.10 to 0.15 mg/L. This might

The objective of this study was to determine the effect of AgNPs in the range of sub-lethal concentrations. In order to find

suggest higher AgNP tolerance in *P. putida* KT2440 biofilms. According to the data from this experiment, the concentrations below MBIC (0.1, 0.5, 1, 10, and 50 mg/L) and above MBIC (100, 500, and 1,000 mg/L) were selected for further experiments.

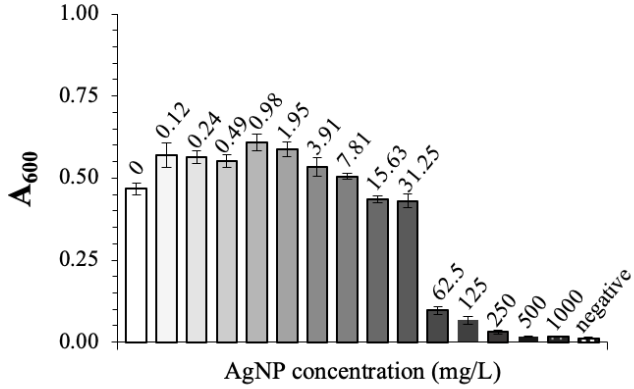

Figure 2 Effect of different AgNP concentrations on *Pseudomonas putida* KT2440 biofilm formation at 12 h.

Effect of AgNPs on P. putida KT 2440 biofilm formation

The 48-h growth curve of biofilm formation was conducted under different AgNP concentrations (below or above the MBIC). The results showed that the effect of AgNPs can be divided into three groups (Figure 3): inhibition of biofilm formation, no effect on biofilm formation, and increased biofilm formation. Above the MBIC level (100, 500, and 1,000 mg/L), *P. putida* KT2440 biofilm formation was inhibited, resulting in no biomass or less biomass compared with the control (0 mg/L). For the concentrations below the MBIC, AgNPs at 10 and 50 mg/L showed no effect on the formation of *P. putida* KT2440 biofilms, resulting in similar formation compared with the control. Interestingly, AgNPs at sub-lethal concentrations of 0.1, 0.5 and 1 mg/L could increase *P. putida* KT2440 biofilm formation. This finding has previously been observed in the study by Yang and Alvarez (2015), which showed the increased formation of *Pseudomonas aeruginosa* PAO1 biofilms when exposed to AgNPs at low concentrations. This study is the very first report on the promotion of *P. putida* biofilms by AgNPs. The finding from this study will be useful in the determination of AgNP effect

on environmental biofilms. Small concentrations of AgNPs might not be harmful to environmental biofilms since the promotion of biomass can be expected. However, the activities in the promoted biofilms need to be studied further to confirm whether there is no adverse effect of sub-lethal AgNPs on biofilms.

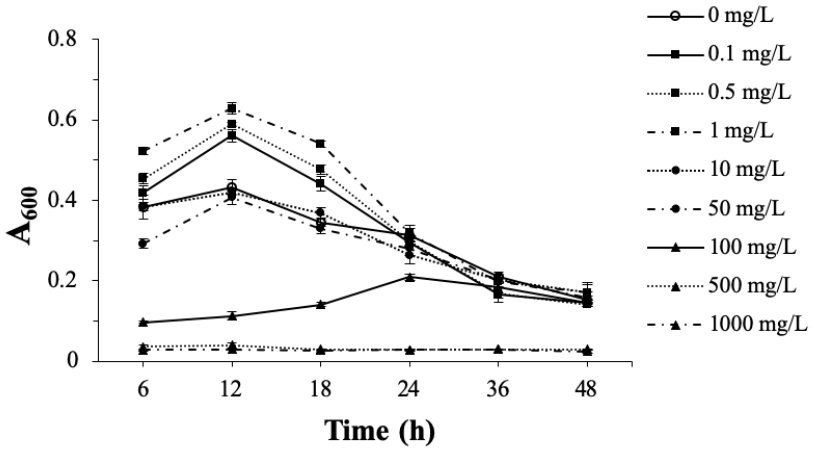

Figure 3 Effect of AgNPs on *Pseudomonas putida* KT2440 biofilm formation.

Effect of AgNPs on B. subtilis biofilm formation

This part of the study was to determine whether the sub-lethal concentrations of AgNPs could increase the biofilm formation of the gram-positive bacteria: *B. subtilis* TISTR1248 and *B. subtilis* TISTR1451. The experiments were conducted in a 96-well plate in the similar manner as *P. putida* KT2440 with different temperature and growth media as described in the method section. The growth curve of *B. subtilis* biofilm formation under different AgNP concentrations was conducted (Figure 4). The results showed that AgNPs at the studied concentrations only showed no effect (concentrations below MBIC: 0.1, 0.5, 1, 10, 50 mg/L) or slightly inhibited *B. subtilis* biofilm formation (concentrations above MBIC: 100, 500, 1,000 mg/L), and no increased formation of biofilms was observed as in *P. putida* KT2440 biofilms. The results also showed that the impact of AgNPs on bacterial biofilms depend on the strain type (gram-positive or gram-negative). On

the other hand, Gambino et al. (2015) found more polysaccharide production in the biofilms of *B. subtilis* wild type strain Cu1065 after exposed to 1 and 10 mg/L of AgNPs, which was not observed in this study. This difference might be due to the low amount of *B. subtilis* biofilm formation (Branda et al., 2001); therefore, the small increase or decrease in biofilm formation that might be affected by AgNPs could not be measured by the crude method like CV staining used in this study.

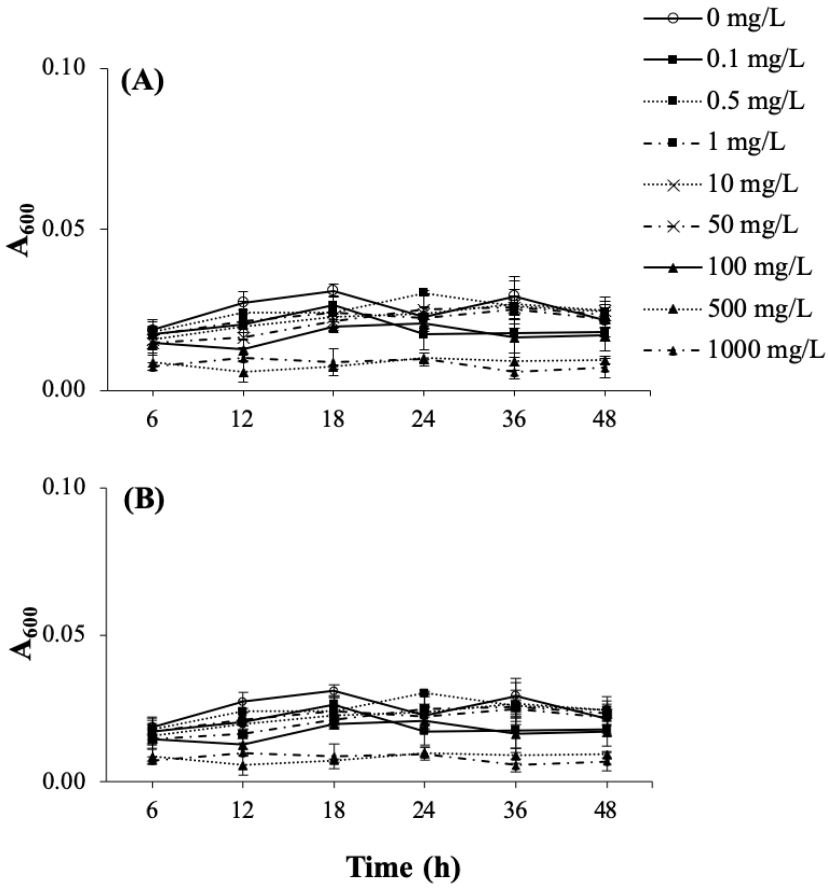

Figure 4 Effect of AgNPs on *B. subtilis* biofilm formation: (A) *B. subtilis* TISTR1248 and (B) *B. subtilis* TISTR1451.

CONCLUSIONS

Effects of AgNPs on *P. putida* and *B. subtilis* biofilm formation were observed in this research. The data showed that biofilms from gram-negative bacteria were more resistant to AgNPs than gram-positive bacteria, which was proved by the increased biomass of biofilm formation at low AgNPs concentrations of 0.1, 0.5 and 1 mg/L. The findings from this research will help elucidating the impact of AgNPs on wastewater and environmental biofilms. In wastewater systems, more biomass production of biofilms caused by AgNPs could lead to more biofouling. However, bacteria effective in producing EPS might be an important indicator to detect the contamination of AgNPs in environment since they will be able to withstand AgNPs and produce more biomass.

ACKNOWLEDGEMENTS

This research was partly granted by TRF Research Grant for New Scholar (Grant number MRG6080156). The authors would like to thank School of Energy and Environment, University of Phayao, for providing laboratorial space and equipment.

REFERENCES

Angel BM, Batley GE, Jarolimek CV, Rogers NJ. The impact of size on the fate and toxicity of nanoparticulate silver in aquatic systems. Chemosphere 2013; 93: 359-365.

Donlan RM. Biofilms: microbial life on surfaces. Emerging Infectious Diseases 2002; 8(9): 881-890.

Dorobantu LS, Fallone C, Noble AJ, Veinot J, Ma G, Goss GG, Burrell, R.E. Toxicity of silver nanoparticles against bacteria, yeast, and algae. Journal of Nanoparticle Research 2015; 17: 1-13.

Duran N, Duran M, de Jesus MB, Seabra AB, Favaro WJ, Nakazato G, Silver nanoparticles: a new view on mechanistic aspects on antimicrobial activity. Nanomedicine 2016; 12: 789-799.

Flemming HC, Neu TR, Wozniak DJ. The EPS matrix: The “House of Biofilm Cells”. Journal of Bacteriology 2007; 189(22): 7945–7947.

Gambino M, Marzano V, Villa F, Vitali A, Vannini C, Landini P, Cappitelli F. Effects of sublethal doses of silver nanoparticles on *Bacillus subtilis* planktonic and sessile cells. Journal of

Applied Microbiology 2015; 118: 1103-1115.

Garuglieri E, Meroni E, Cattò C, Villa F, Cappitelli F, Erba D. Effects of Sub-lethal concentrations of silver nanoparticles on a simulated intestinal prokaryotic–eukaryotic interface. Frontiers in microbiology 2017; 8: 1-13.

Jamal M, Hussain T, Das CR, Andleeb S. Characterization of Siphoviridae phage Z and studying its efficacy against multidrug-resistant *Klebsiella pneumoniae* planktonic cells and biofilm. Journal of Medical Microbiology 2015; 64: 454–462.

Martinez-Gutierrez F, Boegli L, Agostinho A, Sanchez EM, Bach H, Ruiz F, James G. Anti-biofilm activity of silver nanoparticles against different microorganisms. Biofouling 2013; 29: 651-660.

Melissa A, Jones M, Gunsolus IL, Murphy CJ, Haynes CL. Toxicity of Engineered Nanoparticles in the Environment. Analytical Chemistry 2013; 85(6): 3036–3049.

Morones JR. The bactericidal effect of silver nanoparticles. Journal of Nano-technology 2005; 16(10): 2346-2353.

Nadell CD, Xavier JB, Foster KR. The sociobiology of biofilms. FEMS Microbiology Reviews 2009; 33(1): 206-24.

Radzig MA, Nadtochenko VA, Koksharova OA, Kiwi J, Lipasova VA,.Khmel IA. Antibacterial effects of silver nanoparticles on gram-negative bacteria: Influence on the growth and biofilms formation, mechanisms of action. Colloids and Surfaces B: Biointerfaces 2013; 102(1): 300-306.

Samarajeewa AD. Effect of silver nano-particles on soil microbial growth, activity and community diversity in a sandy loam soil. Journal of Environmental Pollution 2017; 504-513.

Branda SS, Pastor JEG, Yehuda SB, Losick R, Kolter R. Fruiting body formation by *Bacillus subtilis*. Department of Molecular and Cellular Biology 2001; 98(20): 11621–11626.

Yang Y, Alvarez PJJ. Sublethal concentrations of silver nanoparticles stimulate biofilm development. Environmental Science and Technology Letters 2015; 2(8): 221-226.

Comparison of water quality and caddisfly (Trichoptera) communities between old and new reservoirs in Chiang Mai university

Miatta Kiawu[1], Terdthai Phutthanurak[2], Pornpimon Buntha[2], Decha Thapanya[2*]

[1]Master's Degree Program in Environmental Science, Environmental Science Research Center, Faculty of Science, Chiang Mai University, Chiang Mai, 50200, Thailand

[2]Department of Biology, Faculty of Science, Chiang Mai University, Chiang Mai,50200, Thailand

[*]Corresponding author: e-mail: thapanya2@hotmail.com

ABSTRACT

Some physicochemical parameters and adult caddisfly specimens were sampled using portable black light traps at Angkaew (approximately 50 years old) and Tart Chompoo (3 years old) reservoirs, during October 2018 to February 2019. Air and water temperature, pH, total dissolved solids, electrical conductivity, biological oxygen demand, dissolved oxygen, and wind speed were measured for 3 replications per site. Both reservoirs had the significant difference ($p < 0.05$) of air and water temperature, pH, electrical conductivity, total dissolved solids, orthophosphate, and wind speed. For example, the mean values of electrical conductivity at Angkaew and Tart Chompoo reservoirs were 116.4 and 226.0 µS cm^{-1} respectively. Angkaew was significantly lower of pH than Tart Chompoo, which was 6.94 and 7.61 respectively. A total of 487 adult male caddisflies were collected from the sampling sites representing 2 species, *Dipseudopsis robustior* and *Amphipsyche meridiana*. *D. robustior* contained the highest number of species at Angkaew reservoir (217 individuals, 44.6%); while Tart Chompoo consisted of (143 individuals, 29.4%). On the other hand, *A. meridiana*

contained (72 individuals, 14.7%) at Angkaew; and (55 individuals, 11.3%) at Tart Chompoo reservoir. Results from correlation showed that air temperature, is the physicochemical factor to affect the abundance of both caddisfly species.

Keywords: water quality, Trichoptera, newly created reservoir

INTRODUCTION

Reservoirs, or dams, are man-made bodies of open water serving as public water supply sources, as winter storage for crop irrigation or as flood storage facilities. Reservoirs are among the more useful means of controlling the natural character of water flows, instead of depending on nature (Votruba, and Broža, 1989). Aquatic habitats are greatly altered by construction of reservoirs from running rivers, to deep standing waters which are not suitable for original organisms (Thapanya *et al.*, 2013).

Trichoptera, or caddisfly are holometabolous insects with aquatic larvae, pupae, and terrestrial adults. The order is the largest diverse insect order presenting the aquatic ecosystems. They include three suborders: spicipalpia, annulipalpia and intergripalpia each one containing 4, 8, and 33 families, respectively (Makekei-Ravasa et al., 2013). *A. meridiana* belongs to the family Hydropsychidae and is widely distributed in the Oriental region including Thailand. It is an aquatic species that inhabits lake outlets; is light brown to yellowish in color, and can be distinguished under the microscope by a black spot on the wings. *D. robustior* is a species of Trichoptera in the family Dipseudopsidae which can also be found in the Oriental area. It has a chestnut brown color and the genitalia of all species are totally alike. Another distinguishing feature is a tusk like organ in the mouth part when viewing under the microscope. The known caddisfly fauna of Thailand includes, 1,004 species belonging to 28 families

(Chantaramongkol *et al.,* 2010, Malicky, 2010). Adults have been studied widely because they are easily collected by light traps. Genus and species level identifications of adult caddisflies are possible and clearly produce more accurate results than the family level identification, thereby giving better ability to assess the change of water quality (Prommi *et al.,* 2014). Previous studies on the use of adult caddisflies as bioindicator of water quality in Thailand have been reported by Chiabu, Laudee, Cheunbarn, and Prommi and Thamsenanupap (Prommi *et al.,* 2014). Caddisflies were chosen for this study because they are usually more diverse than other aquatic insect orders, and are academically recognized as a good indicator in aquatic ecosystem. The objective of this study is to compare the physicochemical parameters and caddisfly communities between the old and new reservoirs, in order to provide knowledge on the properties of water in the newly created reservoir.

MATERIALS AND METHODS

2.1. Study site

The study was conducted at Angkaew (18º48′24″N, 98º56′59″E) and Tart Chompoo reservoir (18º48′13″N, 98º56′53″E) Chiang Mai University campus. A total of 5 study sites were located at both reservoirs, 3 at Angkaew and 2 at Tart Chompoo. Angkaew, the main reservoir which is approximately more than 50 years old can hold 300,000 cubic meters of water and usually dries up during the dry season; while Tart Chompoo, the new reservoir is about 3 years old and can hold up to 100,000 cubic meters of water. The main source of water of both reservoirs is Doi Suthep. Angkaew reservoir receives water from Huai Kaew and Kookaew streams, whereas Tart Chompoo receives water from Mae Ra Npong stream and a household waste water pipe that empties into the reservoir. The substrate at Tart Chompoo is rocky and consists mainly of stones and sand, while on the other hand, substrate at Angkaew is rather muddy consisting of clay and silt. Both reservoirs are characterized by

human activities which has potential for input of waste water run-off. At each site, samples were collected once every month from October 2018 to February 2019.

2.2. Physicochemical analysis

Some physicochemical parameters such as air and water temperature, pH, electrical conductivity, total dissolved solids, dissolved oxygen, biological oxygen demand, and wind speed each had 3 replicates; while other physicochemical parameters of water quality at both reservoirs were recorded at sampling sites. These parameters include: pH, total dissolved solids (TDS), and electrical conductivity (EC), were measured using the multi parameter analyzer. Water and air temperature was measured by means of a glass thermometer, percentage humidity was calculated using a wet and dry thermometer; dissolved oxygen (DO) and biological oxygen demand (BOD) was measured using APHA 4500-O C Azide modification method in laboratory. Ammonia-nitrogen was determined by means of Nessler method with powder pillows using Hach DR 2000 Direct Spectrophotometer, nitrate-nitrogen by cadmium reaction method with powder pillows using Hach DR Direct Spectrophotometer; while ortho-phosphate was measured by PhosVer 3 (Ascorbic Acid) method with powder pillows using Hach DR 2000 Direct Spectrophotometer. Turbidity was also measured by the Hach DR 2000 Direct spectrophotometer using absorptometric method, while wind speed was determined using an anemometer.

2.3. Adult Trichoptera collection

Adults were collected using portable black light traps (12 volts DC motorcycle batteries), and 10 watts fluorescent tube suspended across a pan containing water and detergent solution. Light traps were set up before sunset and collected the next morning. Insects that were attracted to the black light were collected in the detergent solution and transferred into 95% ethyl alcohol until sorting, and later preserved in 80% ethyl alcohol. Specimens were examined

under a stereomicroscope, and adult caddisfly males were used for making species determinations. Identification of species was carried out at the species level using Malicky, 2010. Species counts from collections were later summed and recorded.

2.4. Data analysis

Paleontological Statistics (Past3version 2.22) was used to determine statistical differences between the means of the five sampling sites at both old and new reservoirs.

RESULTS AND DISCUSSION

3.1. Physicochemical variables

Results of physicochemical variables at Angkaew and Tart Chompoo reservoirs are provided in Table 1. Air and water temperature, pH, electrical conductivity, total dissolved solids, and orthophosphate; with a physical parameter wind speed were significantly different ($p<0.05$) during the period of sampling; whereas biological oxygen demand, dissolved oxygen, percentage humidity, ammonia- nitrate, nitrate-nitrogen, orthophosphate, and turbidity were not of significant difference ($p>0.05$)

Table 1 Mean ± SD physicochemical water quality parameters at Angkaew and Tart Chompoo reservoirs from October 2018 to February 2019

Phtsico-chemical	Angkaew					Tart Chompoo					Avg ± SD	
Parameter	Oct	Nov	Dec	Jan	Feb	Oct	Nov	Dec	Jan	Feb	Ang	Tart
Air temperature (ºC)	33.0 ±0.0	30.0 ±1.9	25.1 ±8.8	29.3 ±0.5	34.0 ±0.1	27.0 ±3.5	26.5 ±0.0	24.7 ±0.7	27.4 ±0.3	33.2 ±0.1	30.3 ±3.51	27.7 ±3.22*
Water temperature (ºC)	31.7 ±0.6	26.4 ±1.9	24.7 ±2.0	23.9 ±1.4	25.3 ±1.8	32.0 ±0.0	26.0 ±1.1	26.6 ±1.1	25.7 ±1.6	26.7 ±0.3	26.4 ±3.09	27.4 ±2.61*
pH	9.05 ±0.09	5.71 ±3.52	6.36 ±3.27	6.16 ±3.12	7.40 ±0.21	9.08 ±0.10	6.21 ±3.87	7.06 ±3.14	7.04 ±3.12	8.64 ±0.06	6.94 ±1.34	7.61 ±1.20*
Electrical Conductivity (µS/cm)	87.0 ±3.2	123.9 ±75.9	115.9 ±72.2	113.7 ±65.4	141.4 ±100.5	175.7 ±1.5	162.8 ±22.1	174.0 ±15.7	297.8 ±115.6	319. ±136.0	116.4 ±19.72	226 ±76.04*
Total Dissolved Solids (mg/l)	46.9 ±3.5	67.0 ±41.7	61.5 ±38.6	61.4 ±35.2	73.0 ±51.0	92.7 ±0.6	88.0 ±11.3	93.5 ±9.0	158.7 ±61.7	172.5 ±76.4	62.0 ±9.66	121.1 ±40.98*

Dissolved Oxygen (mg/l)	11.7 ±0.3	5.5 ±3.6	7.5 ±4.8	7.5 ±5.6	8.3 ±2.2	10.6 ±0.4	5.6 ±3.5	6.9 ±3.1	6.9 ±3.1	9.6 ±1.7	8.1 ±2.2	7.9 ±2.1
Biological Oxygen Demand (mg/l)	2.5 ±0.1	3.2 ±2.0	4.46 ±2.8	2.9 ±2.2	6.1 ±1.3	2.7 ±0.4	2.7 ±1.7	2.9 1.3)	3.0 ±1.4	5.4 ±1.2	3.8 ±1.5	3.3 ±1.1
Percentage Humidity	"-"	75.0 ±4.2	70.0 ±0.0	48.2± 39.5	40.7± 10.8	"-"	81.5± 3.5	91 ±0.0	61.2± 12.5	39.1± 8.5	58.5± 16.6	68.2 ±23.0
Ammonia Nitrate (mg/l) N NH_3 Ness	0.05	0.12	0.11	0.42	0.57	0.07	0.09	0.09	0.38	0.41	0.25 ±0.23	0.21 ±0.17
Nitrate Nitrogen (mg/l) N NO_3- H	1.6	1.9	2.1	3.5	3.2	2.4	1.9	2.6	1.9	2.7	2.5 ±0.8	2.3 ±0.4
Ortho Phosphate (mg/l) PO_4^{3-} PV	0.22	0.20	0.25	0.30	0.32	0.15	0.24	0.16	0.24	0.27	0.26 ±0.05	0.21 ±0.05*
Turbidity (FTU)	16.67 ±1.53	2.50 ±4.28	3.44 ±5.46	3.56 ±5.81	7.67 ±3.79	20 ±1.00	7.50 ±3.54	9.50 ±2.12	10.50 ±0.71	4.50 ±2.12	6.77 ±5.88	10.40 ±5.84
Wind speed (m/s)	"-"	"-"	1.48 ±0.40	1.91 ±1.00	2.65 ±0.54	"-"	"-"	0.66 ±0.39	0.90 ±0.40	1.98 ±0.24	2.01 ±0.59	1.18 ±0.70*

*: Indicates significant difference ($p<0.05$), PAST

Ang: Angkaew and Tart: Tart chompoo

The average air temperature at both study areas were significantly different ($p<0.05$). Angkaew reservoir had an average temperature of 30.3 ºC. The highest average temperature was 34.0 ºC in February 2019, while the lowest was 25.1 ºC in December 2018. Tart Chompoo reservoir had an average temperature of 27.7 ºC. The highest average air temperature in February 2019 was 33.2 ºC, and lowest of 24.7 ºC in December 2018.

Average water temperature at all sites were significantly different ($p<0.05$). The average temperature at Angkaew reservoir was 26.4 ºC. The highest temperature was observed in October which was 31.7 ºC; while the lowest was 23.9 ºC in January 2019. On the other hand, the average water temperature at Tart Chompoo was 27.4 ºC. The month of October 2018 had the highest temperature which was 32.0 ºC, while a lower temperature of 25.7 ºC was observed in January 2019.

pH was significantly different at both study areas ($p<0.05$). The average pH at Angkaew reservoir was 6.94; with highest average of 9.05 in October 2018, and lowest of 5.71 in

November 2018. At the same time, the average pH at Tart Chompoo was 7.61. the highest average was 9.08 in October 2018, while the lowest was 6.21 in November 2018.

The average electrical conductivity at both reservoirs was significantly different ($p<0.05$). Angkaew reservoir showed average value of 116.4 µS/cm. February 2019 had the highest value of 141.4µS/cm, and a low value of 87.0 µS/cm in October. Tart Chompoo had an average electrical conductivity of 226.0 µS/cm; with highest average of 319.5 µS/cm in February 2019, and lowest of 162.8 µS/cm in November 2018.

The phenomenon of higher electrical conductivity was observed at Tart Chompoo because sediment at this reservoir is made of stone, which might have basic properties that can cause higher conductivity. Moreover, there was some contamination from dissolved ions.

Orthophosphate was significantly different at both sites ($p<0.05$). Angkaew reservoir had an average of 0.26 mg/l, whereas Tart Chompoo had an average value of 0.21 mg/l.

The average total dissolved solids at both study areas was significantly different ($p<0.05$). Angkaew reservoir had an average total dissolved solids of 62.0 mg/l. The highest value was 73.0 mg/l in February 2019, while the lowest was 46.9 mg/l in October 2018. Tart Chompoo reservoir's average total dissolved solids was 121.1 mg/l; with the highest value of 172.5 mg/l in February 2019, and lowest of 88.0 mg/l in November 2018.

The average physical parameter of wind speed was significantly different ($p<0.05$). The average at Angkaew reservoir was 2.01 m/s; with the highest of 2.65 m/s in February 2019, and the lowest of 1.48 m/s in December 2018.

On the overall, Tart Chompoo reservoir showed higher average mean values for water temperature, pH, electrical conductivity, and total dissolved solids than Angkaew, indicating that Tart Chompoo is hotter than Angkaew reservoir. This

can be due to the lack of vegetation, native trees and shrubs around the reservoir, which provide shade and help reduce extreme temperature. High electrical conductivity was observed at Tart Chompoo due to elevated temperatures owing to the fact that electrical conductivity is dependent on temperature. Even though in the case of this study it is expected that Angkaew which is the older reservoir, should be more stable than Tart Chompoo the new reservoir in terms of water quality and biodiversity. Environmental factors such as clearing of vegetation, waste water run-off, and eutrophication which leads to algae bloom are among the main factors affecting the biodiversity and water quality of both reservoirs regardless of their ages.

The number of caddisfly diversity found in this study were far less than that of previous studies. For example, Prommi and Thani, 2014. This is because most caddisfly species are known to proliferate in lotic than lentic ecosystems.

3.2. Adult caddisflies survey

A total of 487 adult Trichoptera representing 2 species; *Dipseudopsis robustior* ULMER 1929 and *Amphipsyche meridian* ULMER 1909 were collected by light traps (Fig. 1). *D. robustior* showed the greatest number of individuals (73.9%, 360 individuals) at both reservoirs; whereas *A. meridian* showed a lower amount of individuals (26.1%, 127 individuals), therefore making *D. robustior* a high abundance species and Angkaew reservoir the site with higher abundance. During the course of the study October and November were months of high abundance for both species; while on the other hand, December- February were months of low abundance which can be associated with seasonal changes. Another reason for low abundance at Tart Chompoo reservoir is the construction of street lights which

attracted more caddisflies than the light trap.

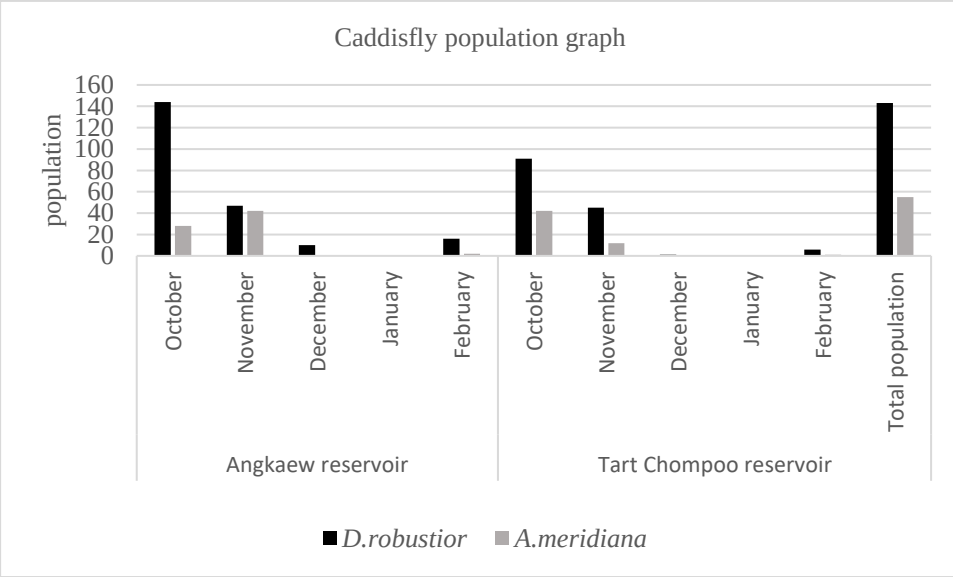

Figure 1 Overall number of individual caddisfly species collected at Angkaew and Tart Chompoo reservoirs during October 2018 to February 2019.

3.3. The correlation between Trichoptera species and physicochemical variables

Pearson's correlation coefficient (r) relationship between Trichoptera and physicochemical variables are shown in Table 2.

Correlation values between the range of 0.000- 0.299 are considered weak, 0.300-0.499 moderate, and 0.500-1.000 strong (Bootdee *et al.*, 2016). Both *Amphipsyche meridiana* and *Dipseudopsis robustior* exhibited a positive correlation with all parameters. There was a weak correlation with *A. meridian* and water temperature, biological oxygen demand, ammonia-nitrate, nitrate-nitrogen, orthophosphate, turbidity, and wind speed. This finding corresponds with results from (Prommi and Thani, 2014) which proposed *A. meridiana* as a taxon intolerant to ammonia-nitrogen, nitrate-nitrogen, orthophosphate, and

turbidity of water as seen in this study. There was a strong correlation between air temperature, and *A. meridian*. Other parameters such as: pH, electrical conductivity, total dissolved solids, dissolved oxygen, and percentage humidity had a moderate correlation. On the other hand, *D. robustior* had a weak correlation with water temperature, pH, electrical conductivity, total dissolved solids, dissolved oxygen, biological oxygen demand, ammonia-nitrate, nitrate-nitrogen, turbidity, and wind speed. Air temperature, percentage humidity, and orthophosphate had a moderate correlation. There was no strong correlation found to exist between *D. robustior* and any parameter.

The present study shows that higher air was the suitable condition for the flight of A. *meridian*, while orthophosphate appears to moderately affect the population of *D. robustior.* The high orthophosphate levels were found during October 2018, December 2018, and February 2019 at Angkaew reservoir which was concurrent to the high population of emerging adult caddisfly especially in October 2018. The concentrations of phosphate in Angkaew reservoir were higher than that of Tart Chompoo. Orthophosphate concentrations at Tart Chompoo were close to the concentration of orthophosphate in natural stream such as headwater stream of Mae Ngat Dam, Chiang Mai (Thapanya *et al.*, 2013). Therefore, phosphate concentrations should be monitored on a long-term basis in order to keep the water quality of both reservoirs in the good condition

Table 2 Pearson's correlation between parameters of water quality and Trichoptera species during sampling interval at Angkaew and Tart Chompoo reservoirs.

Parameters	Amphipsyche Meridian	Dipseudopsis robustior
Air temperature	0.79636*	0.47081
Water temperature	0.034341	0.0018
pH	0.4941	0.093957
Electrical conductivity	0.34622	0.21558
Total dissolved solids	0.34898	0.21774
Dissolved oxygen	0.43939	0.037601
Biological oxygen demand	0.172	0.077712
Percentage humidity	0.43681	0.37992
Ammonia nitrogen	0.089397	0.085645
Nitrate nitrogen	0.18841	0.11357
Orthophosphate	0.072772	0.31767
Turbidity	0.077837	0.019921
Wind speed	0.053121	0.11437

*: Indicates strong correlation, PAST

CONCLUSION

The physicochemical parameters that were of significant difference ($p<0.05$) are: air and water temperature, pH of water, electrical conductivity, orthophosphate, and wind speed; while dissolved oxygen, biological oxygen demand speed; percentage humidity, ammonia nitrogen, nitrate nitrogen, orthophosphate, and turbidity were not significantly different ($p>0.05$). From results gathered throughout the study, there was a total of 487 caddisflies representing 2 species

that were collected at Angkaew and Tart Chompoo reservoirs from October 2018 to February 2019. *A. meridian* increased when the air temperature increased. Other physicochemical factors such as pH, electrical conductivity, total dissolved solids, dissolved oxygen, and percentage humidity also affect the above mentioned species. On the other hand, *D. robustior* was affected by air temperature, percentage humidity and orthophosphate; and intolerant to water temperature, pH, electrical conductivity, total dissolved solids, dissolved oxygen, biological oxygen demand, ammonia-nitrate, nitrate-nitrogen, turbidity, and wind speed. It may be preferable to use a single insect order for adult bio monitoring. Caddisfly (Trichoptera) are an ideal taxon since they can be found in many types of aquatic ecosystems, and can be sampled without much effort and difficulty.

ACKNOWLEDGEMENT

We thank Thailand International Cooperative Agency (TICA) for financial support, Aquatic Insect Research Lab, Faculty of Science, Department of Biology, Chiang Mai University, and Environmental Science Research

Center, Faculty of Science, Chiang Mai University, Chiang Mai.

REFERENCES

American Public Health Association, and American Water Works Association. (1989). Standard methods for the examination of water and wastewater. American public health association.

Bootdee, S., Chantara, S., and Prapamontol, T. (2016). Determination of PM2. 5 and polycyclic aromatic hydrocarbons from emission burning for health risk assessment. Atmospheric Pollution Research, 7 (4), 680-689.

Chantaramongkol, P., Thapanya, D., and Bunlue, P. (2010). The Aquatic Insect Research Unit (AIRU) of Chiang Mai University, Thailand, with an updated list of the Trichoptera species of Thailand. Denisia, 29, 55-79.

Malekei-Ravasan, N., Bahrami, A., Shayeghi, M., Oshaghi, M. A., Malek, M., Mansoorian,. A. B., and Vatandoost, H. (2013). Notes on the Iran Caddisflies and role of

Annulipalpian hydropsychid Caddisflies as a bio-monitoring agent. Journal of arthropod-borne diseases, 7(1), 71.

Malicky, H. (2010). Atlas of Southeast Asian Trichoptera, Biology Department, Science Faculty, Chiang Mai University

Prommi, T. O., Laudee, P., and Chareonviriyaphap, T. (2014). Biodiversity of adult Trichoptera and water quality variables in streams, northern Thailand. APCBEE procedia, 10, 292-298.

Prommi, T. O., and Thani, I. (2014). Diversity of trichoptera fauna and its correlation with water quality parameters at Pasak Cholasit reservoir, Central Thailand. Environment and Natural Resources Journal, 12(2), 35-41.

Thapanya, D., Bunlue, P., and Chantaramongkol, P. (2013). Adult caddisfly assemblages from upstream and downstream of the Mae Ngat Dam, Chiang Mai, northern Thailand. In Proceedings of the 1st Symposium of Benthological Society of Asia. Scientific Research Society of Inland Water Biology, Sakai, Osaka, Japan. Biology of Inland Waters (Vol. 2, pp. 151-156).

Votruba, L., and Broža, V. (1989). Water management in reservoirs (Vol. 33). Elsevier.

Determination of profenofos and cypermethrin in Chinese kale using a modified quick, easy, cheap, effective, rugged and safe method with Fe_3O_4 magnetic nanoparticles

Nipawan Phosri[1] and Thitiya Pung[2*]

[1]Graduate student in Chemistry Department, Faculty of Liberal Arts and Science, Kasetsart University, Kamphaeng Saen Campus, Nakhon Pathom, 73140 Thailand

[2]Chemistry Department, Faculty of Liberal Arts and Science, Kasetsart University, Kamphaeng Saen Campus, Nakhon Pathom, 73140 Thailand

Correspondig author: e-mail: faasthp@ku.ac.th

ABSTRACT

A modified quick, easy, cheap, effective, rugged and safe (QuEChERS) sample preparation with Fe_3O_4 magnetic nanoparticles (MNPs) was established to determine profenofos and cypermethrin in Chinese kale. The magnetic nanoparticles have excellent function as adsorbents and fast separated from the extract. Fe_3O_4 MNPs were synthesized by co-precipitation of $FeCl_3.6H_2O$ and $FeCl_2.4H_2O$. Sample extracts were analyzed by HPLC-UV with C18 column (25 mm× 4.6 mm, 5.0 μm) at 219 nm. The extractions of profenofos and cypermethrin with MNPs 40 mg and without MPNs gave similar recoveries and RSDs. The amounts of Fe_3O_4 MNPs were investigated and found that the optimum amount of Fe_3O_4 MNPs was 20 mg. Moreover, the recoveries and precisions of profenofos and cypermethrin were evaluated by spiking with the concentrations of 0.5, 1.0 and 2.0 mg/kg and they were in the range 100.37-102.58% and 98.86-102.04%, respectively, with relative standard deviations

less than 2.55 and 2.77, respectively. LOD and LOQ of profenofos were 0.04 and 0.12 mg/kg. LOD and LOQ of cypermethrin were 0.08 and 0.28 mg/kg. The matrix effects of profenofos and cypermethrin were not significant. This method was applied to the analysis of raw Chinese kale from local markets. Chinese kales were purchased from 5 markets in Suphan Buri and Nakhon Pathom(Thailand) , profenofos and cypermethrin in each sample were determined in triplicates. The concentrations of profenofos of 2 samples were higher than 0.5 mg/kg (EU maximum residue limit, MRL) but concentrations of cypermethrin were less than 1 mg/kg (EUMRL). Therefore, using Fe_3O_4 MNPs as adsorbent in QuEChERS to analyze these insecticides provides similar efficiency as QuEChERS without Fe_3O_4 MNPs, but it is faster and more convenient.

Keyword: Fe_3O_4 magnetic nanoparticles, QuEChERS, Profenofos, Cypermethr

INTRODUCTION

Profenofos (O-4-bromo-2-chlorophenyl O-ethyl S-propylphos phorothioate and cypermethrin cyano-(3-phenoxyphenyl) methyl)3-(2,2-dichloroethenyl) -2,2- dimethyl cyclopro pane-1-carboxylate**)** are insecticides.

They are mainly used to control economical pests in vegetables and crops. Profenofos and cypermethrin residues were found in vegetables such as Chinese kale in Thailand. Their residues were reported exceed the maximum residue limits (MRLs) and even washing could not remove all of them (Wanwimolruk *et al*., 2015). Recently, a variety of sample preparation techniques have been reported for determination of pesticides in samples. Traditional and commonly used pesticide sample preparation technologies include solid-phase extraction (Juan-Garcia *et al*., 2005), dispersive liquid–liquid microextraction (Cunha *et al*., 2009; Melo *et al*., 2012), solid

phase microextraction (Rodrigues *et al.*, 2011; Song *et al.*, 2013) and matrix solid-phase dispersion (Silva *et al*., 2008) have been used to extract pesticide residues. However, these methods have some drawback such as time consuming and/ or labor intensive, expensive and consume a large volume of solvent.

QuEChERS method was first reported in 2003 (Anastassiades *et al.*, 2003). The method involves an initial extraction with solvent followed by cleanup steps: using dispersive adsorbents such as anhydrous magnesium sulphate, primary secondary amine (PSA), graphitised carbon black (GCB). Currently, QuEChERS is a popular sample preparation technique for determination of pesticide (Heidari *et al.*, 2012; Lehotay *et al.*, 2010; Fernandes *et al.*, 2018). Due to QuEChERS has several advantages and easy for modification.

Magnetic nanoparticles (MNPs) are applied as adsorbents and can easily be separated out from sample extract by magnetic field. Wu *et al.* (2011) used a graphene-based magnetic nanocomposite as an effective adsorbent for the pre-concentration of five carbamate pesticides in environmental water samples. Heidari and Razmi (2012) used carbon coated Fe_3O_4 nanoparticles for the determination of some organophosphorus pesticides in aquatic samples. Deng *et al.* (2014) used multi-walled carbon-nanotube MNPs to analyze eight pesticide residues in tea samples. Moreover, bare MNPs were modified with QuEChERS method for determination of multiple pesticides in fruits and vegetables and analyzed by GC-tandom-MS (Li *et al.*, 2014). In this study, bare Fe_3O_4 MNPs were synthesized by co-precipitation and used as co-adsorbent in QuEChERS for the determination profenofos and cypermethrin in Chinese kale and analysis by HPLC-UV (Harshit *et al.*, 2017). We modified HPLC-UV to determine profenofos and cypermethrin because HPLC – UV is common use in laboratory.

METHODOLOGY

2.1 Material

Standard solutions of profenofos (99.7%) and cypermethrin (99%) were purchased from Sigma-Aldrich Supelco (Sigma-Aldrich Corp., USA). Primary secondary amine (PSA, particle size 40 μm) and graphitised carbon black (GCB) was purchased from Agilent Technologies. Ferric chloride($FeCl_3 \cdot 6H_2O$, ferrous chloride($FeCl_2 \cdot 4H_2O$, sodium chloride(NaCl) and anhydrous magnesium sulphate($MgSO_4$) were purchased from QRëc. Fe_3O_4 magnetic nanoparticle powders (MNPs) (size 50-100 nm (by SEM) 97% were purchased from Sigma-Aldrich Supelco (Sigma-Aldrich Corp., USA). Acetonitrile and methanol were HPLC grade and obtained from Daejung Chemicals&Metals Co. LTD.

Working standards of pesticides were prepared with acetonitrile at a concentration of 100 μg/mL.

A centrifuge (Hitachi, high-speed refrigerated centrifuge) from Hitachi Centrifuge Instrument Co., Ltd. (China) was used for precipitation. Vortex Mixer (VM-10) was obtained from Witeg Co., Ltd. The grinder (SJ303-250) was obtained from Supor Co., Ltd.

2.2 Preparation of Fe_3O_4 magnetic nanoparticles

MNPs were synthesized by co-precipitation method. Briefly, $FeCl_3 \cdot 6H_2O$ and $FeCl_2 \cdot 4H_2O$ (Li *et al.*, 2014). were dissolved in deionized water (100 mL) in a 250-mL erlenmayer flask. After that, 110 mL of ammonia were added and stirred in an oil bath at 80 ˚C for 3 h. The MNPs were magnetically collected and washed with 100 mL of deionized water for three times, and then washed with ethanol. Finally, they were dried in oven at 55 °C for 12 h.

2.3 Sample preparation

A schematic of developed sample preparation based on the proposed QuEChERS method is shown in

Figure 1. Chinese kales were cut into small pieces and comminuted with an electric grinder to achieve good sample homogeneity.

The homogenized sample (10.0 g) was weighed into a centrifuge tube (50 mL) and appropriate volumes of pesticide standards were added. The sample was extracted with 10 mL acetonitrile and the centrifuge tube was shaken vigorously for 30 s. Then, 4.0 g anhydrous $MgSO_4$ and 1.0 g NaCl were added and shaken vigorously for 30 s. After that, the extract was centrifuged for 5 min at 6000 rpm, the supernatant (1.0 mL) was transferred to an Eppendorf vial (1.5 mL) that containing 150 mg anhydrous $MgSO_4$, 7.5 mg GCB, 50 mg PSA and 40 mg MNPs (optimized condition). The mixture was shaken vigorously for 60 s and the supernatant was collected with the aid of an external magnet. The final sample extract was injected to HPLC-UV.

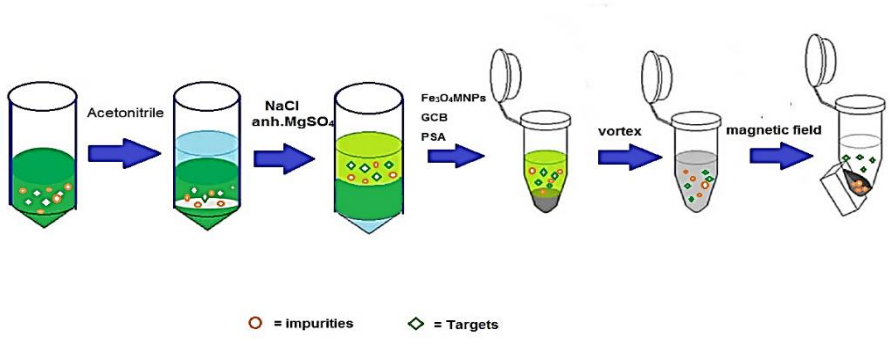

Figure 1 Schematic of developed sample preparation. Fe_3O_4 magnetic nanoparticles (Fe_3O_4 MNPs); graphitised carbon black (GCB); primary secondary amine (PSA)

2.4 Instrumentation and analytical conditions

PSA, GCB, MNPs were examined by a Field Emission Transmission Electron Microscope (FE-SEM) for their morphology characterization.

Analysis of pesticides was performed by high-performance liquid chromatography (HPLC) Hitachi CM 5000 connected to UV detector. ACE Generix 5 C-18 column (250 mm, 4.6 mm, 5μ) was used and column temperature was maintained at 25˚C. The injected sample volume was 20 μL. The isocratic mobile phase consisted of acetonitrile: water (74: 26, v/v). Flow rate of mobile phase was 1 mL/min. The eluent was monitored using UV detector at a wavelength of 219 nm.

RESULTS AND DISCUSSION

3.1 Characterization of materials

Micro-morphologies of PSA, GCB, MNPs were investigated by FE-SEM (Figure 2a–c). PSA had nearly irregular shape and its size is about 40-50 μm. GCB and MNPs have smaller sizes about 20-50 nm.

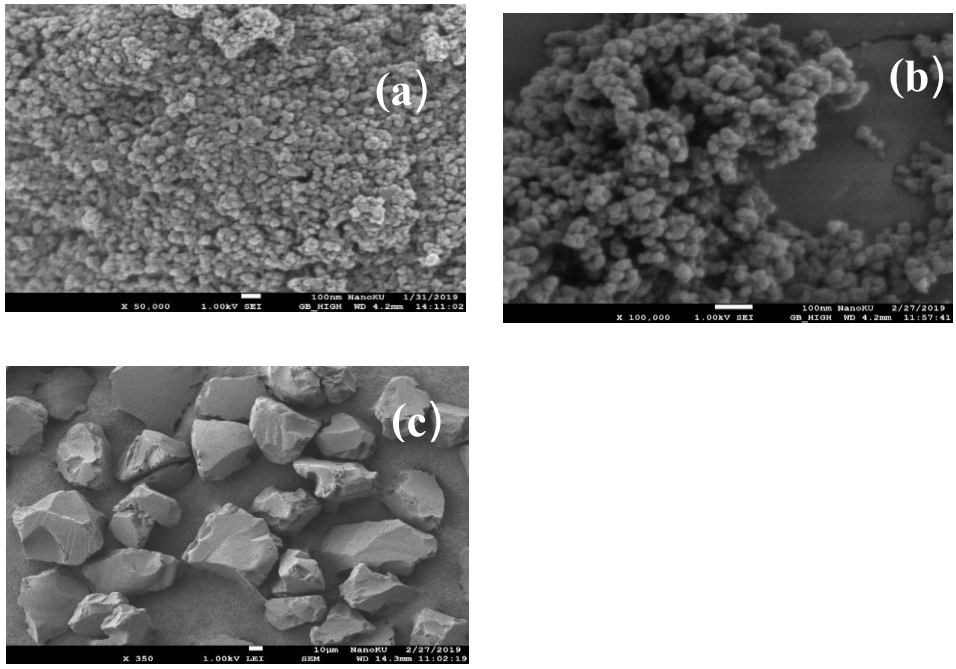

Figure 2 The FE-SEM of the adsorbents. The scale bar represents 100 nm, (a) Fe_3O_4 magnetite nanoparticles (MNPs); (b) GCB; (c) PSA

3.2 Comparison of QuEChERS extractions with and without MNPs

To verify the developed MNP- QuEChERS method, it was compared with traditional QuEChERS method. The traditional QuEChERS, PSA/ GCB/ anh.$MgSO_4$ were used as adsorbents but the developed QuEChERS method, Fe_3O_4 MNPs/ PSA/ GCB/ anh. $MgSO_4$ were used. The final Chinese kale extracts purified by traditional QuEChERS and Fe_3O_4 MNPs/PSA/ GCB/ anh.$MgSO_4$ were more transparent than the extract without purified (Figure 3). PSA could remove various polar organic acids, polar pigments, some sugar and fatty acids (Wilkowska and Biziuk, 2011). GCB used to remove pigments and steroids (Wilkowska and Biziuk, 2011). GCB absorbed molecules with planar structures including pigments, steroids and pesticides. Therefore, increasing amount of GCB may lower recovery of structurally planar pesticides (Zhang *et al.*, 2013). QuEChERS extractions with and without MNPs (40 mg) gave similar percent recoveries and percentages of RSD (Table 1)

Table 1 Effects of QuEChERS extraction with and without MNPs on recovery and percent of RSD

Compound		**Fe_3O_4MNPs**	**Concentration (mg/kg)**	**Percent of recovery (n=5) Mean ± SE**	**Percent of RSD**
Profenofos	-	Without	5.19±0.15[a]	105.26 ± 2.65[a]	2.52
	synthesis	MNPs 40 mg	5.08±0.06[a]	101.78 ± 1.14[a]	2.51
Cypermetrin	-	Without	5.17±0.14[a]	101.74 ± 1.93[a]	1.90
	synthesis	MNPs 40 mg	5.19±0.04[a]	103.90 ± 0.84[a]	1.73

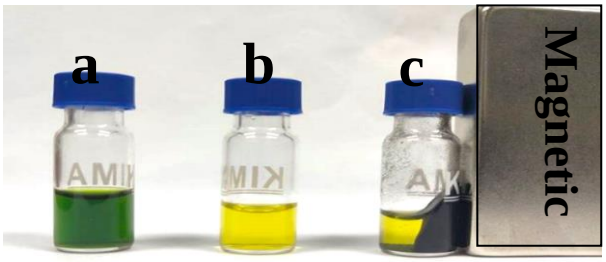

Figure 3 Photography of clean- up performance by different DSPE adsorbents: (a) 1 mL Chinese kale extracts without DSPE clean-up; (b) 1 mL Chinese kale extracts with DSPE clean-up by 150 mg anh.$MgSO_4$, 7.5 mg GCB 50 mg PSA and without Fe_3O_4 MNPs; (c) 1 mL Chinese kale extracts with DSPE clean-up by 150 mg anh.$MgSO_4$, 7.5 mg GCB and 50 mg PSA and 40 mg Fe_3O_4 MNPs.

3.3 Optimization of the amount of Fe_3O_4 MNPs adsorbents

The amount of Fe_3O_4 MNPs was optimized by using 1 mL of the Chinese kale sample extract at the spiked profenofos and cypermethrin of 5 mg/kg. The adsorbents were 50 mg PSA, 7.5 mg GCB and different amounts of Fe_3O_4 MNPs (20, 30, 40 and 50 mg). As shown in Figure 4 when the amount of Fe_3O_4 MNPs increased between 20– 50 mg, the recoveries of both pesticides have no obvious difference. Therefore, the amount of MNPs would be set at 20 mg.

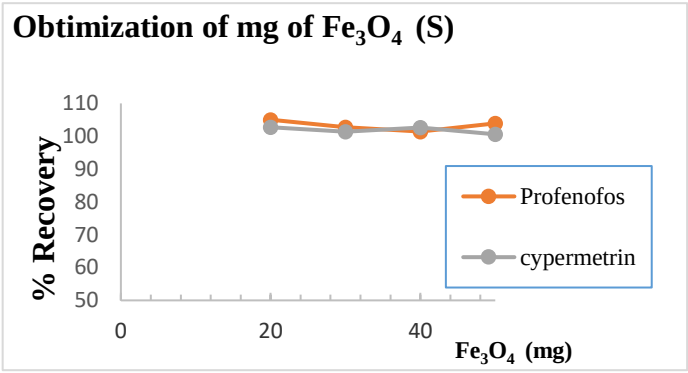

Figure 4 Effect of mass of Fe_3O_4 on the extraction efficiency of profenofos and cypermethrin (5 mg/ kg).

4. Method validation

4.1 Accuracy and precision

We spiked profenofos and cypermethrin into Chinese kale at 0. 5, 1. 0 and 2. 0 mg/ kg, and each concentration was tested in five replicates. Recoveries of profenofos and cypermethrin were obtained by comparing the amount calculated from the calibration curves with the corresponding spiked amount.

The recoveries of profenofos and cypermethrin were in the range 100. 37- 102. 58% and 98. 86- 102. 04%, respectively, with relative standard deviations less than 2.55 and 2. 77, respectively (Table 2). The recoveries were in the range of 80- 120 %, their accuracies could be accepted (AOAC, 2002. The relative standard deviations were less than 10% indicated that their precision were accepted (AOAC, 2002)

Table 2 Recoveries and repeatability (RSD) obtained from profenofos and cypermetrin spiked in Chinese kale.

Insecticide	**0.5 (mg/kg)**		**1.0 (mg/kg)**		**2.0 (mg/kg)**	
	% recovery	**%RSD**	**% recovery**	**%RSD**	**% recovery**	**%RSD**
Profenofos	102.58	2.55	101.18	2.46	100.37	1.24
Cypermetrin	102.04	2.77	101.16	1.92	98.86	1.37

Table 3 LOD and LOQ obtained from profenofos and cypermetrin

Compound	**LOD (mg/kg)**	**LOQ (mg/kg)**	**MRLs (mg/kg)**
Profenofos	0.04	0.12	0.5
Cypermetrin	0.08	0.26	1

spiked in Chinese kale.

4.2 LOD and LOQ

The sensitivity of method was estimated by examining the LOD and LOQ. LOD was defined as the lowest detectable concentration with a signal-to-noise ratio of at least 3. LOQ was defined as the lowest quantifiable concentration with a signal-to-noise ratio of at least 10. LOD and LOQ of profenofos were 0.04 and 0.12 mg/kg. LOD and LOQ of cypermethrin were 0.08 and 0.28 mg/kg (Table 3). LOQs of profenofos and cypermethrin were less than MRLs (0.5 ppm and 1. 0 ppm, respectively) . The developed method had sufficient sensitivity.

4.2 Matrix effect

Chinese kale has high amounts of pigments such as chlorophyll, carotenoids, and lycopene.

Matrix components can interact with active sites in the column or they can reduce signals, given by analytes when they reach the detector. Therefore, matrix effects were analyzed. A comparison between the calibration equations obtained from standards dissolved in solvent and matrix- matched standards was performed (Zhao *et al.*, 2012). Percent of matrix effects of prophenofos and cypermethrin were -0.81and 6.87 (Figure 5). The clean- up step was efficiency because of matrix effect were within ±10%. Therefore, the matrix effects of profenofos and cypermethrin were not significant.

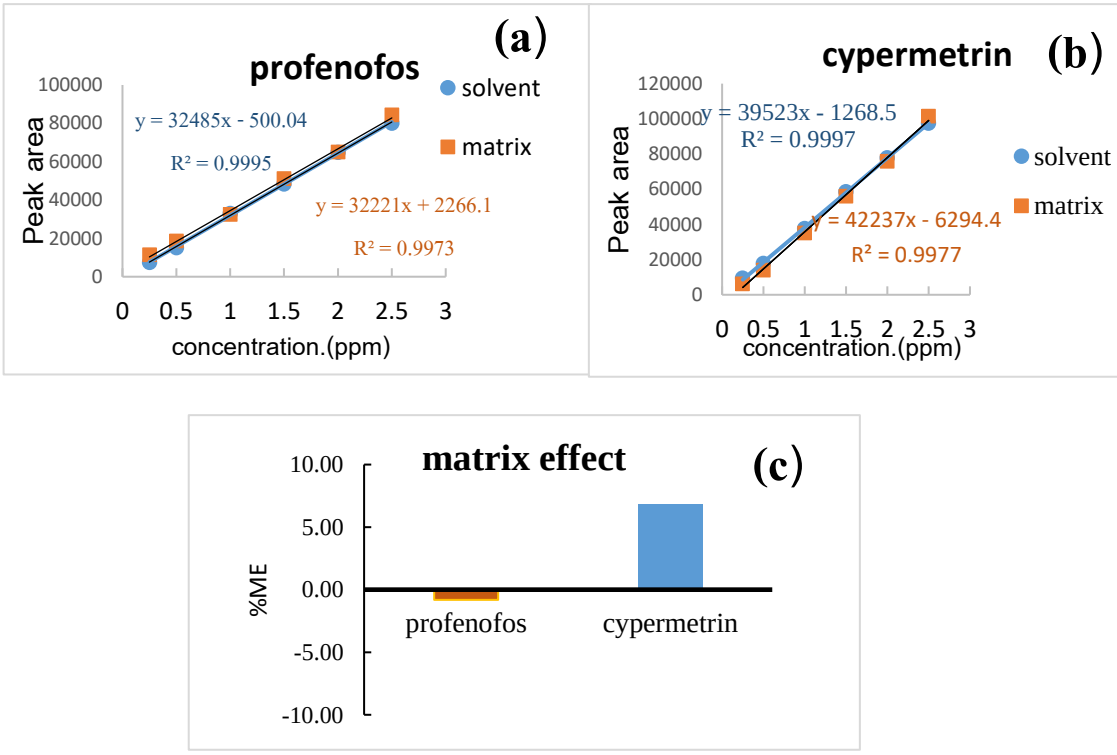

Figure 5 Matrix effect (ME) in Chinese kale : superposition of solvent and matrix curves of profenofos(a) and cypermetrin (b). Distribution of percent of ME for profenofos and cypermetrin in Chinese kale (c)

4.3 Application to commercial Chinese kale samples

This method was applied to the analysis of raw Chinese kale from local markets. Chinese kales were purchased from 5 markets in Suphan Buri and Nakhon Pathom (Thailand) and profenofos and cypermethrin in each sample were determined in triplicates. The concentrations of profenofos of 2 samples in Nakhon Pathom were higher than 0.5 mg/kg (EU MRL) but concentrations of cypermethrin in all samples were less than 1 mg/kg (Figure 6) which is EU MRL.

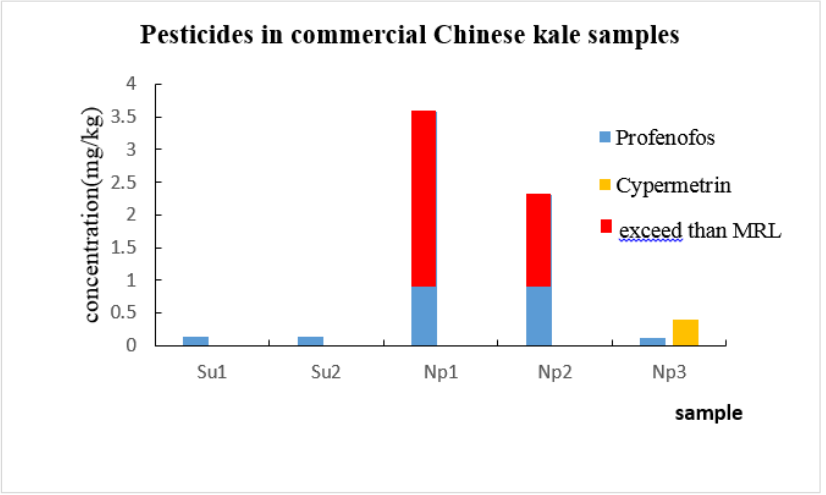

Figure 6 Concentrations of profenofos and cypermetrin in raw Chinese kale samples from local markets. (Su1= Suphan Buri(1), Su2= Suphan Buri(2), Np1=Nakhon Pathom(1), Np2=Nakhon Pathom(2), Np3=Nakhon Pathom(3

CONCLUSIONS

In this study, bare Fe_3O_4 MNPs were synthesized by co-precipitation method and used with QuEChERS method for determination of profenofos and cypermethrin in Chinese kale, coupled with HPLC-UV. When compared with Li *et al*. (2014), this method using amounts of Fe_3O_4 MNPs and GCB less than Li's

group. While Li's group used 50 mg PSA, 10 mg GCB and 50 mg Fe_3O_4 MNPs, We used 50 mg PSA, 7.5 mg GCB and Fe_3O_4 MNPs 20 mg. Our modified method gave high recovery, low percent RSD and reducing extraction time.

Moreover, LODs of profenofos and cypermethrin 0.04 and 0.08 mg/kg. LOQ of profenofos and cypermethrin were 0.12 and 0.28 mg/kg, which were above MRL values (profenofos is 0.5mg/kg, cypermethrin is 1 mg/kg, EU). Therefore, using Fe_3O_4 MNPs as adsorbent in QuEChERS method to analyze these insecticides provides similar efficiency as QuEChERS without Fe_3O_4 MNPs, but it is faster and more convenient.

ACKNOWLEDGEMENTS

Authours and thankful to Department of Chemistry, Faculty of Liberal Arts and Science Kasetsart University for providing the facility to carry out this research.

REFERENCES

Anastassiades M, Lehotay SJ, Stajnbaher D and Schenck F. Fast and easy multiresiduemethodemploying acetonitrile extraction/ partitioning and "dispersive solid- phase extraction" for the determination of pesticide residues in produce . J. AOAC 2003; 86: 412–431.

AOAC (2002) Official Method of Analysis. 16th Edition, Association of Official Analytical, Washington DC.

Cunha SC, Fernandes JO, Oliveira MBPP. Fast analysis of multiple pesticide residues in apple juice using dispersive liquid– liquid microextraction and multidimensional gas chromatography– mass spectrometry Journal of Chromatography A 2009; 1216: 8835–8844.

Deng XJ, Guo QJ, Chen XP, Xue T, Wang H, Yao P. Rapid and effective sample clean- up based on magnetic multiwalled carbon nanotubes for the determination of pesticide residues in tea by gas chromatography– mass spectrometry. Food Chemistry 2014; 145:853–858.

Harshit D, Charmy D, Nrupesh P. Organophosphorus pesticides determination by novel HPLC and spectrophotometric method. Food Chemistry 2017; 230: 448-453.

Heidari H, Razmi H. Multi- response optimization of magnetic solid phase extraction based on carbon coated Fe_3O_4 nanoparticles using desirability function approach for the determination of the organophosphorus pesticides in aquatic samples by HPLC– UV. Talanta 2012; 99: 13–21.

Fernandes VC, Freitas M, Pacheco JPG, Oliveira JM, Domingues VF, Matos CD. Magnetic dispersive micro solid-phase extraction and gas chromatography determination of organophosphorus pesticides instrawberries Journal of Chromatography A 2018; 1566: 1–12.

Juan- Garcia A, Pico Y, Font G, Capillary electrophoresis for analyzing pesticides in fruits and vegetables using solid- phase extraction and stir-bar sorptiveextractionJ. Journal of Chromatography A 2005; 1073 229- 236.

Li YF, Qiao YQ, Li FW, Ding Y, Yang ZJ, Wang ML. Determination of multiple pesticides in fruits and vegetables using a modified quick, easy, cheap, effective, rugged and safe method with magnetic nanoparticles and gas chromatography tandem massspectrometry. Journal of Chromatography A 2014; 1300: 127-133.

Lehotay SJ, Son AK, Kwon H, Koesukwiwat U, Fu W, MastovskaK. Comparison of QuEChERS sample preparation methods for the analysis of pesticide residues in fruits and vegetable. Journal of Chromatography A 2010; 1217: 2548-2560.

Melo A, Cunha SC, Mansilha C, Aguiar A, Pinho O, Ferreira IMPLVO. Monitoring pesticide residues in greenhouse tomato by combining acetonitrile- based extraction with dispersive liquid– liquid microextraction followed by gas-chromatography-mass spectrometry Food Chemistry 2012; 135: 1071-1077.

Rodrigues FDM, Mesquita PRR, Oliveira LSD, Oliveira FSD, Filho AM, Pereira PADP, Andrade JBD. Development of a headspace solid-phase microextraction/ gas chromatography– mass spectrometry method for determination of organophosphorus pesticide residues in cow milk. Microchemical Journal 2011; 98: 56–61.

Silva MGD, Aquino A, Dórea HS, Navickiene S, Simultaneous determination of eight pesticide residues in coconut using MSPD and GC/ MS. Talanta 2008; 76: 680–684.

Song XY, Shi YP, Chen J, Carbon nanotubes- reinforced hollow fibre solid- phase microextraction coupled

with high performance liquid chromatography for the determination of carbamate pesticides in apples. Food Chem. 2013; 139: 246–252.

Wanwimolruk S, Kanchanamayoon O, Phopin K, Prachayasittikul V. Food safety in Thailand 2: Pesticide residues found in Chinese kale (Brassica oleracea) , a commonly consumed vegetable in Asian countries. Science of the Total Environment 2015;532: 447– 455.

Wilkowska A, BiziekM. Determination of pesticide residues in food matrices using QuEChERS methodology**.** Food Chemistry.2011; 125: 803-812.

Wu QH, Zhao GY, Feng C, Wang C, Wang Z. Preparation of a graphene-based magnetic nanocomposite for the extraction of carbamate pesticides from environmental water samples. Journal of Chromatography A. 2011; 1218: 7936 -7942.

Zhao P, Wang L, Zhou L, Zhang F, Kang S, Pan C. Multi- walled carbon nanotubes as alternative reversed-dispersive solid phase extraction materials in pesticide multi- residue analysis with QuEChERSmethod. Journal of Chromatography A 2012; 1225: 17-25.

Zheng HB, Zhao Q, Mo JZ, Huang YQ, Luo YB, Yu QW, Feng YQ. Quick, easy, cheap, effective, rugged and safe method with magnetic graphitized carbon black and primary secondary amine as adsorbent and its application in pesticide residue analysis. Journal of Chromatography A 2013; 1300: 127-133.

Chlorpyrifos tolerance of *Pseudomonas pseudoalcaligenes* biofilms under water-limiting conditions

Suthi Rattanaprapha[1], Kritchaya Issakul[1], Pumis Thuptimdang[2,3,*]

[1]Department of Environmental Science, School of Energy and Environment, University of Phayao, Phayao 56000, Thailand
[2]Department of Chemistry, Faculty of Science, Chiang Mai University, Chiang Mai 50200, Thailand
[3]Environmental Science Research Center, Faculty of Science, Chiang Mai University, Chiang Mai 50200, Thailand; Corresponding author: e-mail: pumis.th@gmail.com

ABSTRACT

Chlorpyrifos (CP) is an insecticide widely used in agricultural area in northern Thailand. Due to its high toxicity, CP may have an adverse effect on the beneficial bacteria in soil. Bacteria normally develop biofilms to protect the cells from toxic substances. However, during a dry season, drought may induce more stress to the biofilms in soil by creating water-limiting conditions, which could affect the biofilm tolerance to CP, leading to a decrease in soil fertility. The objective of this study is to determine the CP tolerance of the biofilms of an indigenous bacterium from agricultural soil under water-limiting conditions. *Pseudomonas pseudoalcaligenes*, a biofilm-forming bacterium able to tolerate CP, was isolated from the tangerine-field soil in Nan province that had received continuous application of CP. The biofilm experiments were conducted in a 96-well plate at room temperature in media added with different CP concentrations. Water-limiting conditions were simulated using NaCl and polyethylene glycol (PEG) at various concentrations of NaCl (0, 20 and 40 mg/L) and PEG (0, 5 and 10%). Reduction in biofilm biomass after the exposure was determined by crystal

violet staining. The results showed that *P. pseudoalcaligenes* biofilms showed high tolerance to CP up to 300 mg/L. Biofilms formed with highest biomass at 12 and 24 h at the CP concentrations of 5 to 300 mg/L. The biofilms at 24-h formation time was then selected for further experiments. When forming under water-limiting conditions (20 mg/L of NaCl and 5 and 10% of PEG), biofilms produced more biomass than those in the regular conditions. Our findings suggest that during drought season, soil bacteria could produce higher biomass as a stress response to provide the protection from CP residue in the field.

Keywords: Chlorpyrifos, Biofilms, Water-limiting conditions

INTRODUCTION

Thailand has been commercially developing agricultural products to meet the needs of exporters and consumers. In order to meet the specific criteria and the cost-effectiveness in production, the use of fertilizers and pesticides is unavoidable, and the trend is increasing. From the amount of pesticide imports in 2017, it was found that imports were more than 198 million kilograms/year, which accounted of active ingredient for more than 102 million kilograms/year (Thailand Pesticide Alert Networks, 2017). According to formulas, structures and actions, pesticides can be categorized into classes such as organophosphate, carbamates, organochlorine and other groups. The most imported substance is organophosphate group followed by the carbamates group (Putkham, 2007).

Chlorpyrifos (CP) is a common organophosphate pesticide used in agricultural areas. Based on the import data in 2017 from The Office of Agriculture Regulation, Department of Agriculture, the amount was found to be as high as 375,291 kilograms per year (Thailand Pesticide Alert Networks, 2017). Even though banning this

chemical had been proposed, it did not yet pass to be prohibited by law. This high use creates a risk of being contaminated in agricultural products and residues in the environment. CP is harmful to humans and other organisms at moderate to high levels depending on the amount and time of the exposure, and it may accumulate in the environment for more than a year (Putkham, 2007)

In agricultural areas, the environmental effect of residual pesticides after using is an important concern. Although CP is toxic to microorganisms (Mahmood et al., 2016), there are some species of environmental bacteria that have the ability to tolerate or degrade CP. Bacteria in the environment generally form biofilms, which are bacterial cells adhering on surface such as soil particles within the secreted mucus-substance called extracellular polymeric substances (EPS). EPS acts as a barrier, making biofilms highly resistant to toxic substances in the environment (Thuptimdang et al., 2015). However, drought during the dry season can cause water-limiting conditions to soil biofilms. This may result in changes in cell membrane and protein structure or the EPS production process, leading to the reduction on the biofilm formation and resistance to chlorpyrifos (Ngumbi and Kloepper, 2016).

The objective of this research is to study the effect of chlorpyrifos on *Pseudomonas pseudoalcaligenes* biofilm formation under water-limiting conditions. This bacterial strain was isolated from a local agricultural area that has a CP usage history, and it showed CP tolerance and pollutant degrading abilities (Nishino and Spin, 1993). CP tolerance was determined by measuring the change in biomass of biofilms forming under normal and water-limiting conditions. The knowledge from this study will be useful for assessing the impact of CP on bacteria in the environment.

METHODOLOGY

Soil sample for bacterial isolation

A tangerine-field in Ban Pha Khwang, Moo 4, Bo Subdistrict, Mueang District, Nan Province, with the history of CP usage was chosen for soil sampling. A sampling site was divided into 15 sub-plots. Soil was randomly collected through a 5-inch depth from each sub-plot. Soil samples from all sub-plots were entirely mixed in a container before dividing into 4 piles. One pile of soil was then used for isolation of bacteria that have the ability to tolerate CP.

Isolation and identification of chlorpyrifos-tolerate bacteria

Ten grams of soil sample was added to a flask containing 100 mL of minimal salt medium (MSM) and CP as a sole carbon source. Flasks were replicated with different CP concentrations of 30, 60 and 100 mg/L. MSM contains 5.8 g/L of Na_2HPO_4, 3 g/L of KH_2PO_4, 0.5 g/L of NaCl, 1 g/L of NH_4Cl, and 0.25 g/L of $MgSO_4$. The flasks were incubated at 30°C on a rotary shaker at 120 rpm. After 2 weeks, 1 mL of enrichment culture was sub-cultured into a flask containing fresh MSM spiked with CP according to previous concentrations. After three successive transfers, the culture was pipetted, serially diluted, and spread on MSM agar plate containing 50 mg/L of CP. The plates were incubated at 30°C for 3 days. Bacterial colonies grown on the plate were purified by repeatedly streaking on MSM agar plate containing 50 and 100 mg/L of CP to confirm the tolerance of bacteria. The purified culture was grown in Luria-Bertani (LB) medium and preserved at -80°C by mixing with glycerol at a ratio of 60:40 (culture:glycerol). Pure colonies were sent for DNA extraction, purification, and sequencing for identification of bacterial species (Macrogen, Republic of Korea). Among all identified species, *P. pseudoalcaligenes* was selected for this study as it was able to form colonies in CP up to 100 mg/L.

Culture preparation

Culture was prepared before each biofilm experiment. One colony of *P. pseudoalcaligenes* grown on an NB agar plate was taken to a 50-mL bottle containing 20 mL of NB medium. The flask was incubated at 30°C on a rotary shaker at 120 rpm for 18 hours. Then, 1 mL was taken to a 250-mL Erlenmeyer flask containing 100 mL of NB medium and incubated at the same condition. After shaking overnight, the cells were in stationary phase according to the preliminary experiment conducted (data not shown). Cells were harvested by centrifuging at 5,000 ×g for 5 min at room temperature, washed with autoclaved saline solution (0.85% NaCl) twice, and adjusted with 0.85% NaCl to obtain the optical density at 600 nm (OD_{600}) of 0.3-0.4 (10^8 CFU/ mL). The culture was then used for further experiments for biofilm formation.

Effect of CP on the formation of P. pseudoalcaligenes biofilms

The experiments for studying the CP tolerance of biofilms were conducted in a polystyrene, flat-bottom, 96-well plate. Each well (200 µL) contained 5 µL of the prepared culture, 100 µL of NB medium, and 95 µL of CP diluted in de-ionized (DI) water. The commercial grade CP (40% v/v) purchased from a local market was used. By using the density value (1.398 g/cm^3) for calculation, CP concentrations were adjusted with DI water to 0, 5, 10, 25, 50, 100, and 300 mg/L. After pipetting the mixed solution into the wells, the plate was incubated at room temperature to allow biofilm formation. At each sampling time, media was removed from the well, and biofilms were carefully rinsed twice with 0.85% NaCl. The biofilms were air-dried and measured for their biomass using crystal violet (CV) staining according to the method by Thuptimdang et al. (2017). The data were represented as the absorbance at 600 nm (A_{600}). Three wells were used as three replicates for each sample to create standard deviation values represented in error bars.

CP tolerance of P. pseudoalcaligenes biofilms under water-limiting conditions

The biofilm experiments were conducted similar to previous section. Water-limiting conditions were simulated by adding NaCl solution at the concentrations of 0, 20 and 40 g/L and poly-ethylene glycol 6000 (PEG-6000) solution at the concentrations of 0, 5 and 10% (w/v). CP concentrations were at 0, 5, 10, 25, 50, 100, and 300 mg/L. After biofilms formed at 24 h, CV staining was conducted to measure the biomass of the biofilms. CP tolerance was determined by comparing the amount of biomass, implying higher CP tolerance in biofilms forming with higher biomass (higher A_{600} value). Three wells were used as three replicates for each sample to create standard deviation values represented in error bars.

Biodegradation of CP by P. pseudoalcaligenes

To determine whether the CP tolerance of biofilms was contributed by the ability to degrade CP by the bacterial cells, biodegradation experiments were conducted. One milliliter of *P. pseudoalcaligenes* culture (prepared as described before) was added into a flask containing 100 mL of MSM medium amended with 0 and 50 mg/L of commercial grade CP. The flask was shaken at 120 rpm and 30ºC for 5 days. At day 1, 3, and 5, 1 mL of sample was taken and mixed vigorously with 2 mL of HPLC-grade methanol (RCI Labscan) using a vortex mixer. The sample was then centrifuged at 7,200 ×g for 10 min. Two milliliters of the supernatant were then filtered through a 0.45 µm filter membrane. Twenty microliters of sample was then analyzed for CP by HPLC (Shimadzu LC-20A) using a mixture of methanol and DI water as a mobile phase and the reagent grade (99.8%) CP (Dr.Ehrenstorfer GmbH, Germany) as a standard. The biodegradation results were represented as C_t/C_0, where C_t is the CP concentration at time t (day) and C_0 is the CP concentration at day 0.

RESULTS AND DISCUSSION

Effect of CP on the formation of P. pseudoalcaligenes biofilms

In environment, biofilms are the form of bacteria able to tolerate toxic substances including pesticides through EPS production (Lundqvist et al., 2010). In this study, *P. pseudoalcaligenes* was isolated from agricultural soil with the history of CP application. This strain was able to tolerate CP by forming colonies on CP agar plate; therefore, it was chosen for the study determining the effect of CP on biofilm formation.

The results show that, during 48 h of formation, the biomass of biofilms increased with time with the highest biomass at 24 h (Figure 1). Interestingly, when CP was added, biofilms were able to form with higher biomass compared to the control (0 mg/L), which proves that this strain and its biofilms could tolerate CP. The highest amount of biomass was still at 24 h except the biofilms forming under 300 mg/L of CP, in which the highest biomass was at 12 h.

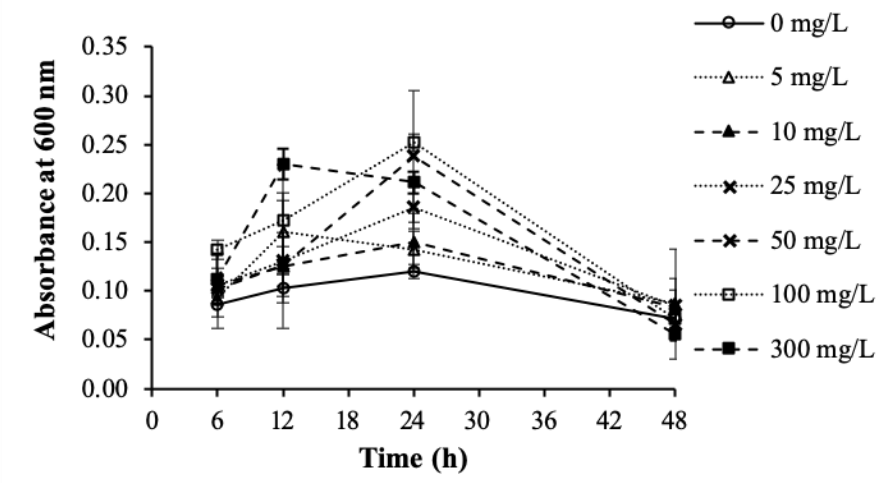

Figure 1 *P. pseudoalcaligenes* biofilm formation under different CP concentrations.

There are two reasons contributing to higher biofilm formation when CP was added: the bacterial stress response mechanism and the ability to use CP as a carbon source for growth promotion.

For the first reason on the stress response mechanism, there are reports on more biofilm formation after exposed to antimicrobial agents (Gambino et al., 2015; Yang and Alvarez, 2015). EPS production was governed by various genes responsible for producing EPS molecules such as alginate or other polysaccharides (Thuptimdang et al., 2015), and bacterial cells use the expression of those genes to produce more EPS after the exposure to toxic substances, resulting in more biofilm amount compared to the unexposed biofilms.

For the second reason that cells might be able to use CP as a carbon source to promote cell growth and biofilm formation, further experiment has been conducted and the results are reported in the last subsection.

Tolerance of P. pseudoalcaligenes biofilms to CP under water-limiting conditions

Since *P. pseudoalcaligenes* biofilms showed CP tolerance by forming with higher biomass with the presence of CP, further experiment was conducted to observe the CP tolerance under water-limiting conditions.

Water-limiting conditions was created by adding NaCl and PEG at different concentrations. When forming under 20 g/L of NaCl, biofilms showed higher biomass at the CP concentrations of 100 and 300 mg/L compared with the control (0 mg/L) (Figure 2(a) and (b)). This proves that with the presence of water-limiting condition, biofilms exhibited higher CP tolerance. The reason for this phenomenon could also be explained by the stress response mechanism. In this case, two kinds of stress might contribute to each other, which results in more promotion of biofilm formation than the normal condition or the condition with CP only.

However, when the water-limiting condition was increased to 40 g/L of NaCl (Figure 2(c)), biofilm formation was reduced to the comparable amount to the control.

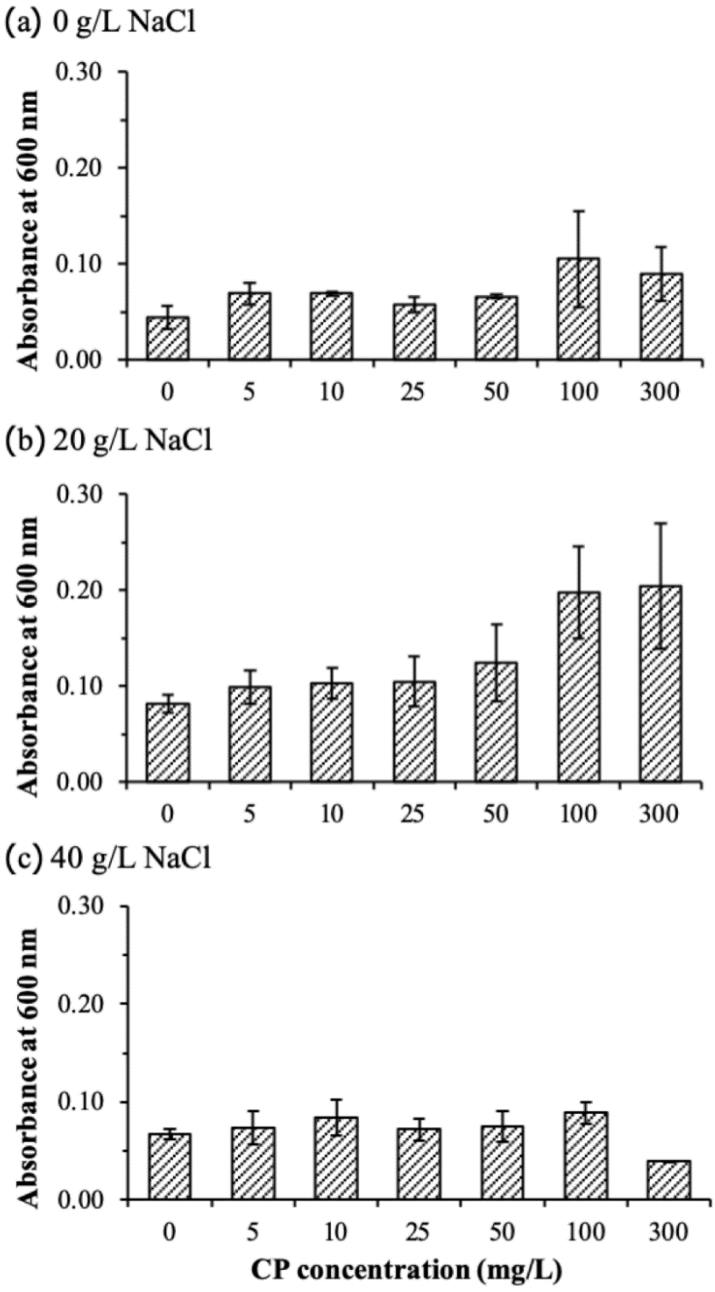

Figure 2 CP tolerance of *P. pseudoalcaligenes* 24-h biofilms under different NaCl concentrations: (a) 0 g/L, (b) 20 g/L, and (c) 40 g/L.

When forming under 5% of PEG, biofilms showed higher biomass compared with the control at the CP concentrations of 50, 100, and 300 mg/L (Figure 3(a) and (b)). After increasing the water-limiting condition to 10% of PEG, higher formation of biofilms was only observed at 100 mg/L of CP, showing the sign of too much water limitation.

High concentrations of NaCl (40 g/L) and PEG (10%) could result in strong osmotic pressure toward the outside of bacterial cell, resulting in cell shrink or excessive stress for biofilm formation process (Ngumbi and Kloepper, 2016).

It should be noted that the addition of CP, NaCl, or PEG alone did not result in more CV staining (data not shown); therefore, higher A_{600} observed under the presence of CP, NaCl, and PEG in this study was from biofilm formation. The molecular aspects of biofilm formation processes should be observed in future study to explain the phenomenon discovered in this study.

Biodegradation of CP by P. pseudoalcaligenes

As stated earlier, CP tolerance of the biofilms could be from the ability to biodegrade CP and use it as a carbon source. So, the biodegradation experiment was conducted with the planktonic cells of *P. pseudoalcaligenes* and 50 mg/L of CP. Two types of growth media were used to understand the mechanism of degradation: minimal medium (MSM) and rich medium (NB). The results show that *P. pseudoalcaligenes* could not use CP as a sole carbon source as observed by no degradation in MSM medium after 5 days (Figure 4(a)). On the other hand, some biodegradation (around 30%) was observed at day 5 in NB medium (Figure 4(b)).

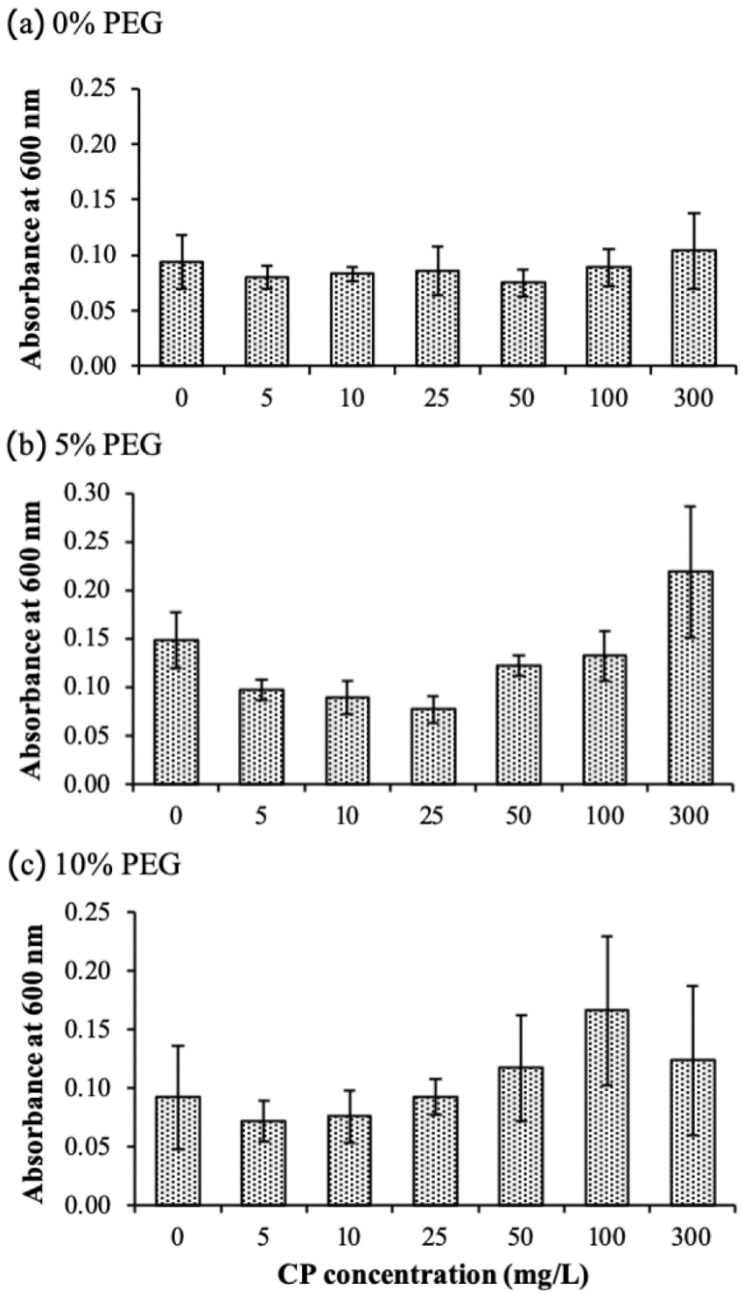

Figure 3 CP tolerance of *P. pseudoalcaligenes* 24-h biofilms under different PEG concentrations: (a) 0%, (b) 5%, and (c) 10%.

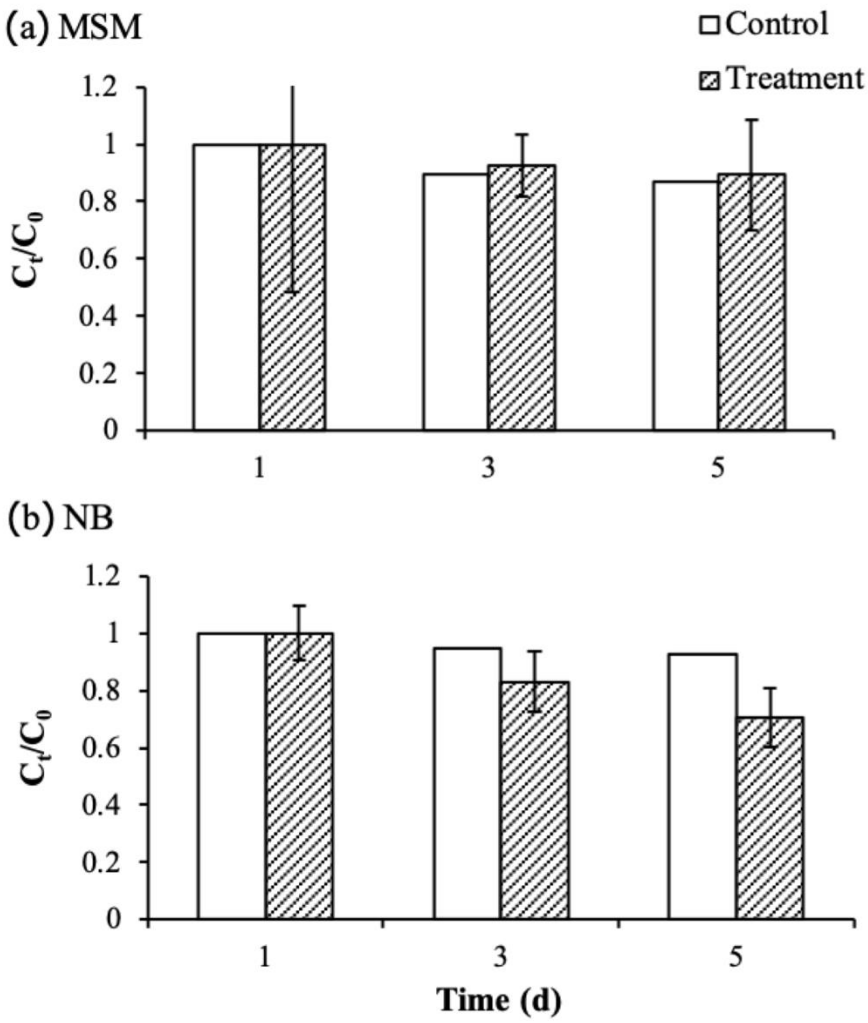

Figure 4 CP degradation by *P. pseudoalcaligenes* in different growth media: (a) MSM and (b) NB.

According to the manufacturer, NB contains peptone and yeast extract, which consists of various amino acids. Therefore, biodegradation of CP by *P. pseudoalcaligenes* in NB medium suggested that the process could be co-metabolism where the responsible enzymes were secreted in order to degrade other amino acids while able to degrade CP at the same time. This proves to be the reason for the biofilm tolerance to CP observed earlier where the biofilm experiment was conducted using NB medium. The results could be implied that, in environment where there are some

specific carbon sources available, *P. pseudoalcaligenes* biofilms would show high tolerance to CP since it can degrade the pesticide at that condition.

CONCLUSIONS

This study aims to determine *P. pseudoalcaligenes* biofilm tolerance to CP under water-limiting conditions, which were created by adding NaCl and PE) at the concentrations of 0, 20 and 40 mg/L and 0, 5 and 10%, respectively. The results from CV staining showed high tolerance of biofilms to CP up to 300 mg/L with the highest biomass at 12 and 24 h at the CP concentrations of 5 to 300 mg/L, respectively. When forming under water-limiting conditions (20 mg/L of NaCl and 5 and 10% of PEG), biofilms produced more biomass than those in the regular conditions. Also, *P. pseudoalcaligenes* showed the ability to degrade CP under the presence of other carbon sources, leading to the CP tolerance of biofilms. The data obtained from this study suggest that this soil bacterium is capable of producing higher biomass as a stress response to drought during the dry season, which can provide protection from CP residue in the field.

ACKNOWLEDGEMENTS

This research was partially supported by Kurita Water and Environment Foundation (KWEF) through KWEF-AIT Research Grant 2016.

REFERENCES

Gambino M, Marzano V, Villa F, Vitali A, Vannini C, Landini P, Cappitelli F. Effects of sublethal doses of silver nanoparticles on *Bacillus subtilis* planktonic and sessile cells. Journal of Applied Microbiology 2015; 118: 1103-1115.

Lundqvist A, Bertilsson S, Goedkoop W. Effects of extracellular polymeric and humic substances on chlorpyrifos bioavailability to *Chironomus riparius*. Ecotoxicology 2010; 19: 614-622.

Mahmood I, Imadi SR, Shazadi K, Gul A, Hakeem KR. Effects of Pesticides on Environment. Springer International Publishing Switzerland 2016; 2 5 3 - 268.

Ngumbi E, Kloepper J. Bacterial-mediated drought tolerance: Current and future

prospects. Applied Soil Ecology 2016; 105: 109-125.

Nishino SF, Spain JC. Degradation of nitrobenzene by a *Pseudomonas pseudoalcaligenes*. Applied and Environmental Microbiology 1993; 59(8): 2520-2525.

Putkham S. Acetylcholinesterase inhibition in golden apple snail (*pomacea canaliculata lamarck*) exposed to chlorpyrifos dichlorvos and carbaryl. Master of Science thesis 2007. Burapha University.

Thailand Pesticide Alert Networks. 2017. Report on the import of agricultural hazardous substances. Online source: https://thaipan.org/wp-content/uploads/2018/10/pesticide_doc54.pdf. Access on February 22, 2019.

Thuptimdang P, Limpiyakorn T, McEvoy J, Prüß BM, Khan E. Effect of silver nanoparticles on *Pseudomonas putida* biofilms atdifferent stages of maturity. Journal of Hazardous Materials 2015; 290: 127-133.

Thuptimdang P, Limpiyakorn T, Khan E. Dependence of toxicity of silver nanoparticles on *Pseudomonas putida* biofilm structure. Chemosphere 2017; 188: 199-207.

Yang Y, Alvarez PJJ. Sublethal concentrations of silver nanoparticles stimulate biofilm development. Environmental Science and Technology Letters 2015; 2(8): 221-226.

Photocatalytic Degradation and Mechanism of Glyphosate Herbicide Contaminated in Water by TiO_2 Pellet Photocatalyst

Kanokwan Yamsomphong[1], Chonlada Pokhum[2], Eden G Mariqui[3], Hirofumi Hinode[3], Paiboon Sreearunothai[1], Chamorn Chawengkijwanich[2*,]

[1]Sustainable Energy and Resources Engineering, Sirindhorn International Institute of Technology, Thammasat University, Thailand

[2*] National Nanotechnology Center, National Science and Technology Development Agency, Thailand

[3]Hinode Laboratory, Department of Transdisciplinary Science and Engineering, School of Environment and Society, Tokyo Institute of Technology, Japan; Corresponding author: e-mail: chamorn@nanotec.or.th

ABSTRACT

In Thailand, glyphosate has been used intensively to prevent food crops from weeds and grass, contributing to the contamination of water resources. In this paper, two types of TiO_2 pellets—clay TiO_2 pellets and Polyethylene (PE)-TiO_2 pellets— have been studied for photocatalytic degradation of glyphosate in water. The clay TiO_2 pellets were prepared in the laboratory by using TiO_2 powder (Degussa P-25) as raw material, whereas the PE-TiO_2 pellets were purchased from Shandong Longsheng Masterbatch Co., Ltd, China. Such TiO_2 pellets were characterized by X-ray diffraction (XRD), Brunauer-Emmett-Teller (BET) and scanning electron microscopy with energy dispersive X-ray spectroscopy (SEM/EDX). Meanwhile, the photocatalytic degradation of glyphosate as well as its possible mechanisms have been investigated. Results showed that 99.08% of glyphosate degradation was reached by using clay TiO_2 pellets within 240 mins under UV_A illumination, while the photocatalytic degradation of glyphosate by using PE-TiO_2 pellets was lower, with 74.02%.

Keywords: Glyphosate, TiO_2, Photocatalysis, Contamination

INTRODUCTION

Glyphosate (N-(phosphono-methyl) glycine) is an organophosphate herbicide extensively used to prevent food crops in agriculture, especially in Thailand. It is a common substance used to control broadleaf weeds and grass prior to planting or after the crops are harvested. However, it has been reported that glyphosate was found in water resources such as drinking water and tap water in Thailand (Patsiriwong, 2015). It is an organic pollutant, which is classified as "probably carcinogenic" to humans reported by the International Agency for Research on Cancer (IARC) in March 2015. It can cause serious harmful effects on people who use water which surrounds these agricultural areas.

During recent decades, the titanium dioxide (TiO_2) photocatalysis has been an effective process to degrade organic pesticide including glyphosate in water (Chen et al., 2012; Echavia et al., 2009; Muneer and Boxall, 2008). Once TiO_2 photocatalyst is used to absorb light, with light having energy equal or higher than 3.2 eV, generating reactive oxygen species (ROS) to degrade or transform the organic compounds into carbon dioxide (CO_2), water and mineral byproducts (Umar and Aziz, 2013; Carp et al., 2004). Although TiO_2 has been widely applied in the photocatalytic degradation of pesticides, using the commercial TiO_2 powder as a catalyst causes difficulties during separation of photocatalyst from water for the real-life applications. Consequently, the development of TiO_2 photocatalyst has been attracting a lot of recent attention from researches in this field.

Transforming TiO_2 powder into larger pellets is an interesting way to solve the problem. Recently, TiO_2 companies i.e. Shandong Longsheng Masterbatch Co., Ltd and Soltex Petro Products, Ltd has lunched TiO_2

Pellets for commercial and research applications. Moreover, many researchers have used clay to exhibit larger specific surface areas with TiO_2 (Bouna et al., 2011; Kutláková et al., 2011; Wang et al., 2011). Previous studies have shown that using clay with TiO_2 as photocatalyst offers several advantages: They can be easily separated and recovered from decontaminated water; increase adsorption ability and enhance photocatalytic activity for removing organic pollutants. Nevertheless, few studies relating to the degradation of TiO_2 pellet have been presented (Shimizu et al., 2007; Yamazaki et al., 2001) and the photocatalytic degradation of glyphosate in water has rarely been investigated.

Hence, the aim of this research is to prepare two types of TiO_2 pellets: clay TiO_2 pellets and PE-TiO_2 pellets to investigate the applicability of the TiO_2 pellets under UVA light to degrade glyphosate herbicide in water, specifically, the extent of its products formed during the degradation process. Based on the above goals, X-ray diffraction (XRD), Brunauer-Emmett-Teller (BET) and scanning electron microscopy with energy dispersive X-ray spectroscopy (SEM/EDX) are employed to investigate the composition, and surface charge of the pellets.

METHODOLOGY

Materials

All the chemical reagents used were of analytical grade and the water used was deionized water purified by Barnstead Lab Tower EDI Water Purification Systems, Thermo Scientific, U.S. Glyphosate (N-(Phosphonomethyl)glycine, 96% purity) was purchased from Sigma–Aldrich Chemical Co., UK. Aminomethyl phosphonic acid (AMPA, 98% purity) was purchased from Alfa Chemicals Ltd, UK. Phosphate (PO_4^{3-}) Standard (1000 mgL^{-1}) was purchased from Environmental Express, USA. TiO_2 powder (80% anatase and 20 % rutile, Degussa P-25, Evonik Industries, Germany) and White clay (Wako Pure Chemical Ind., Ltd, Japan) were

used as raw materials. PE-TiO_2 pellets (70% anatase) were purchased from Shandong Longsheng Masterbatch Co., Ltd, China and used directly.

Preparation of chemical solutions

A stock solution of 1000 mgL^{-1} of glyphosate was prepared by dissolving approximately 100 mg of glyphosate in 100 mL of deionized water. The experimental solutions were carried out by diluting the stock solution until concentration of 1 mgL^{-1} was reached. Also, AMPA stock solution (1000 mgL^{-1}) was prepared by dissolving approximately 100 mg of AMPA in 100 mL of deionized water. The working phosphate solution was prepared by further diluting of the concentrated phosphate (1000 mgL^{-1}). These prepared stock solutions were needed for further use and so were stored at 4 °C for 1 month. To prepare an appropriate series of calibration curves, these stock solutions were diluted with deionized water until the desired concentrations were reached.

Clay TiO_2 pellet preparation

White clay and TiO_2 powder (Degussa P-25) were manually mixed with 50-60% distilled water at room temperature. Subsequently, these mixtures were heated up to 110 °C for 5 h and then distilled water was added until the mixture became soft. After that, the product was formed into 4-7 mm clay TiO_2 pellets. The prepared samples were finally calcined at 600 °C for 2 h in a L 3/12 Burnout furnace, Nabertherm GmbH, Germany (modified from (DĚDKOVÁ et al., 2013; Kutláková et al., 2011). The pellets were prepared with different ratios of white clay and TiO_2 powder as shown in 1.

Characterization methods

XRD analysis

The crystalline structures of TiO_2 pellets were determined by x-ray diffraction at room temperature by using Bruker D8 Venture diffractometer with CuKα radiation. The diffractograms were recorded in the range of 2θ from 15˚ to 80˚.

Table 1 Weight ratios of white clay and TiO_2 powder in clay TiO_2 pellets

Clay TiO_2 pellets	TiO_2 powder (%wt)	White clay (%wt)
CT0 pellet	0	100
CT5 pellet	5	95
CT10 pellet	10	90
CT20 pellet	20	80
CT30 pellet	30	70
CT40 pellet	40	60
CT50 pellet	50	50

SEM/EDX analysis

The morphology and the elemental distribution of Titanium (Ti) in the pellets were evaluated by a scanning electron microscope (SEM, HITACHI SU-5000, Japan) that was equipped with an energy dispersive X-ray spectroscopy (EDX, Horiba, Hitachi High-Technologies, Japan)

BET analysis

The specific surface areas and total pore volumes of TiO_2 pellets were analyzed from the nitrogen isotherms in BELSORP-max (BEL Japan Inc., Japan) after the samples were degassed at 110 ^oC for 1.5 h.

Photocatalytic activity tests

TiO_2 photocatalysts were added to 400 mL of a 1 mgL^{-1} glyphosate solution in a beaker and stirred to obtain a dispersion inside a UV enclosure box. The UV enclosure box consisted of six blacklight (UV_A) lamps with a UV_A intensity of 2500 $\mu W/cm^2$. The mixture was stirred in a dark condition until well-mixed. After that, the mixture continued to be stirring throughout the photocatalytic process. The 10 mL sample was collected using a syringe at certain time intervals and was separated into the TiO_2 particles using a 0.22 μm filter paper. In all experiments, TiO_2 powders and pellets were studied in the absence of light to determine the degradation efficiency compared to the presence of UV_A light.

Glyphosate analysis

The amount of glyphosate in water was directly measured by ion chromatography (Dionex ICS-5000+, Dionex Corp., USA) equipped with a variable wavelength detector (VWD), Ion Pac AG11 (4 x 50 mm), AS11 (4 x 250 mm) guard, an ASRS-300 (4 mm) self-regenerating suppressor, EG eluent generator, and an AS-HV auto sampler. The removal efficiency for each sample was calculated using the following equation:

$$\eta = \frac{(C_0 - C_t)}{C_0} \times 100$$

where η% is the removal efficiency of glyphosate; C_t is the concentration of glyphosate in the solution after t illumination and C_0 is the initial concentration of glyphosate before illumination.

Mechanisms of the photocatalytic degradation of glyphosate

Through the possible degradation pathways, the products monitored were aminomethyl- phosphonic acid (AMPA) and phosphate ion (PO_4^{3-}). PO_4^{3-}which could be identified under the same operation of glyphosate. Meanwhile, AMPA was examined by using 6495 Triple Quadrupole Liquid chromatography–mass spectrometry (LC–MS, Agilent Technologies, USA) equipped with a Agilent *Poroshell 120 HILIC-Z*, (2.7 μm, 2.1 mm × 100 mm) and a *HILIC guard column (2.7* μm, 2.1 mm × 5 mm)

RESULTS AND DISCUSSION

TiO_2 samples characterization

In the experiment, 2 types of TiO_2 pellets used were investigated. The clay TiO_2 pellets comprising of 0, 5, 10, 20, 30, 40 and 50 wt% of TiO_2 (CT0, CT5, CT910, CT20, CT30, CT40 and CT50 pellets, respectively) with a diameter of 4-7 mm were prepared for this experiment, whereas the PE-TiO_2 pellets that were 2.5-3 mm in diameter were purchased commercially. All clay TiO_2 pellets had a similar external appearance (Figure 1A). However, the stability of the clay TiO_2 pellets in water decreases with the increasing clay content. After immersion in water, the stability of CT0, CT5 and CT10 pellets proved to be in effective because they broke down

immediately (Figure 1B(b-d)). Clay-TiO_2 particles on CT0 pellets *spread out more quickly than* CT5 and CT10 pellets, respectively. The calcination temperature at 600 °C does not enough to produce strong clay TiO_2 pellets. Generally, calcination temperature should be over 1000 °C

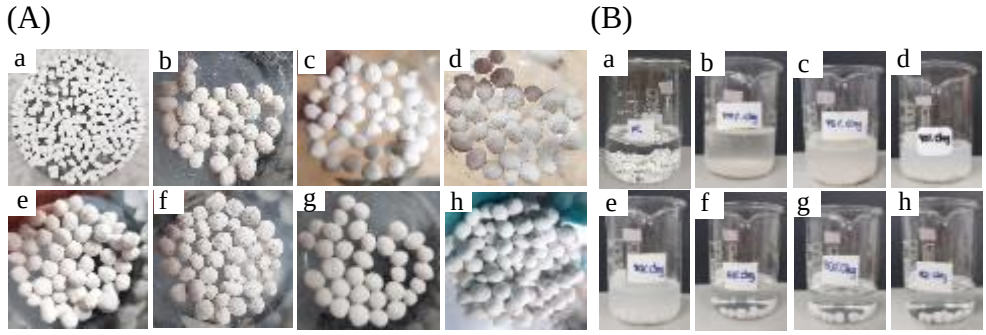

Figure 1 (A) The appearance and (B) the stability of TiO_2 pellets in water by observed the turbidity (a) PE-TiO_2 pellets, (b) CT0 pellets, (c) CT5 pellets, (d) CT10 pellets, (e) CT20 pellets, (f) CT30 pellets, (g) CT40 pellets and (h) CT50 pellets

to produce strong clay TiO_2 pellets. All water molecules are removed from clay particles. Neighboring clay particles become connecting to each other, with strong oxygen bridge (Breuer, 2012). Also, clay- TiO_2 particles of CT20 pellets gradually broke down after immersion (Figure 1B(e)). However, the CT30, CT40 and CT50 pellets were stable in water at least 240 mins, and the loss of clay-TiO_2 particles was minimal (Figure 1B(f-h)). As calcination at 600 °C, new chemical bonds are generated between clay and TiO_2. TiO_2 connects to clay via Si–O–Ti and Al–O–Ti bonds, resulting in improved the stability of the pellets in water (Zhang et al., 2013; Wang et al., 2010). Thereby, CT30, CT40 and CT50 pellets will be applied for the photocatalytic degradation process.

XRD analysis

XRD patterns of non-calcined and calcined TiO_2 powders are shown in Figure 2a. The obtained XRD pattern of calcined and non-calcined TiO_2 powders were not different. It can be seen that both rutile and

anatase phases obviously appeared in both TiO_2 powder samples. The percentage of crystalline phases of the calcined TiO_2 powder is quite similar to non-calcined TiO_2 powder (Table 2). Also, as previously reported by; Bayan et al., (2017) Bowering et al., (2007); Raj and Viswanathan (2009) investigated that the phase transformation from anatase to rutile in TiO_2 appeared at temperatures above 700 °C. For XRD patterns of the white clay, quartz and pyrophyllite represented as typical mineral mixtures of white clay (Figure 2a). No phase transformation of calcined clay was observed at 600 °C for 2 h. These mineral clays started transforming after being heated to over 1000 ^oC (Sanchez-Soto and Perez-Rodriguez, 1989; Zheng et al., 2018). The overall result indicated calcination at 600 ^oC for 2 h does not have significant in transforming the composition of TiO_2 and the white clay.

Figure 2b confirms that in the PE-TiO_2 pellets, only anatase phase obviously appeared, as claimed by the manufacturer. Meanwhile, the presence of quartz, pyrophyllite, rutile and anatase TiO_2 was also detected in all the clay TiO_2 pellets. These mineral mixtures of white clay had no obvious effect on any composition change in TiO_2. The phase contents of TiO_2 in clay TiO_2 pellets are also shown in Table 2. The percentage of anatase and rutile contents in CT30, CT40 and CT50 pellets were similar. The result was also similar to the non-calcined TiO_2 powder. Evidently, the decrease of the TiO_2 weight ratios in clay TiO_2 pellet is related to a decrease in the peak intensity of anatase and rutile.

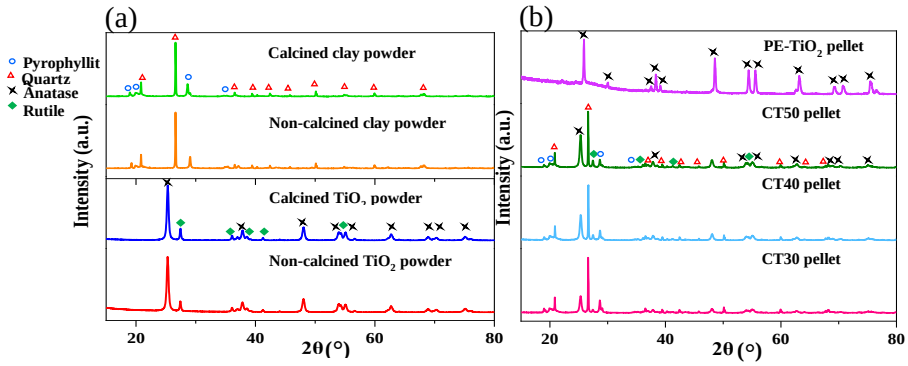

Figure 2 XRD diffraction patterns of the TiO_2 samples (a) TiO_2 powder and white clay and (b) PE-TiO_2 pellets and clay TiO_2 pellets

Table 2 The percentage of anatase and rutile phases of TiO_2 samples

Sample	TiO_2 phase (wt%)	
	Anatase	**Rutile**
Non-calcined TiO_2 powder	79.5	20.5
Calcined TiO_2 powder	76.6	23.4
PE-TiO_2 Pellet	100.0	0.0
CT30 pellet	77.3	22.7
CT40 pellet	80.2	19.8
CT50 pellet	77.2	22.8

BET analysis

The surface areas, pore volumes and pore sizes of PE-TiO_2 and clay TiO_2 pellets were investigated (as shown in Table 3). In the manufacturers specifications, TiO_2 powder showed a large surface area, and its value reaches 50 ± 15 m^2/g (Evonik Industries, Thailand). Also, Raj and Viswanathan (2009) invastigated that TiO_2 powder has pore volume 0.177 cm^3/g and *pore size* 17.5 nm. As a result, the surface area and pore volume of the clay TiO_2 pellets decreased, compared with TiO_2 powder.

Moreover, the CT30, CT40 and CT50 pellets had quite similar surface areas, pore volumes and pore sizes, whereas the surface area, pore volume and pore size of the PE-TiO_2 pellets were considerably less than clay TiO_2 pellets. This result indicates that such large surface areas, pore volume and pore size of clay TiO_2 pellets were presumably better candidate material for photocatalytic activity than PE-TiO_2 pellets.

Table 3 BET surface area, pore volume and pore size of TiO_2 samples

Sample	Surface area (m^2/g)	Pore volume (cm^3 /g)	Pore size (nm)
TiO_2 powder	50 ± 15	0.250*	17.500*
PE-TiO_2 Pellet	2.160	0.005	7.541
CT30 pellet	30.710	0.145	20.465
CT40 pellet	36.989	0.203	24.493
CT50 pellet	33.124	0.153	18.836

***** Raj and Viswanathan, (2009)

SEM/EDX analysis

SEM images and results of EDX analysis of PE-TiO_2 and clay TiO_2 pellets are shown in Figure 3. Clay TiO_2 pellets appeared to have a less smooth and homogeneous surface than PE-TiO_2 pellets. CT50 pellets exhibited a smoother surface than other composites (Figure 3b). Obviously, as the amount of the TiO_2 increased, surface of the clay TiO_2 pellets became smooth. Also, EDX mapping analysis revealed that the Titanium (Ti), Silica (Si) and Aluminum (Al) were uniformly distributed either throughout the entire external or internal surface of clay TiO_2 pellets. Furthermore, EDX results showed that Ti was found in both external and internal surfaces of CT30, CT40 and CT50 pellets in the range from 15.5 to 15.9 %wt, 21.1 to 25.4%wt and 25.3 to 35.4 %wt, respectively (Table 4).

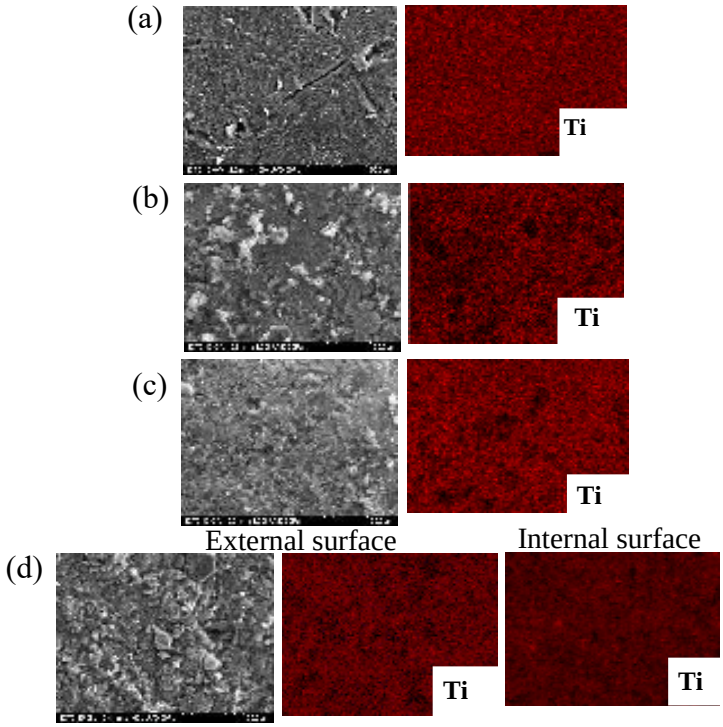

Figure 3 SEM and EDX mapping images of TiO_2 samples (a) External surface of PE-TiO_2 pellets, (b) External surface of CT 50 pellets, (c) External surface of CT40 pellets and (d) External and internal surface of CT30 pellets.

Table 4 EDX analysis of clay TiO_2 pellets

Sample	Al (%wt)	Si (%wt)	Ti (%wt)
CT30 pellet	5.4-5.9	15.4-15.6	15.5-15.9
CT40 pellet	4.3-4.9	13.1-14.2	21.1-25.4
CT50 pellet	3.6-4.0	11.5-13.4	25.3-35.4

Photocatalytic activity tests

Preliminary, the photocataly- tic activities of CT50, CT40 and CT30 pellets UV_A light were studied by using methylene blue (MB) as a model organic pollutant. As a result, CT30 pellets showed the highest photocatalytic activity for MB.

Consequently, CT30 pellets will be used for the photodegradation of glyphosate.

Figure 4 illustrates the removal efficiency of the glyphosate over the course of the experiment. When the TiO_2 powder was employed under dark condition, glyphosate was adsorbed on the TiO_2 surface. The concentration of glyphosate decreased from 1 to 0.6 mgL^{-1} (approximately 39.82% removal efficiency) within 30 min and then the concentration became stable until the end of experiment. Upon UV irradiation, glyphosate rapidly decreased and completely disappeared by TiO_2 powder within 30 min (Figure 4a). In the absence of TiO_2, however, the concentration of glyphosate slightly decreased under UV irradiation at 240 min, approximately 9% removal efficiency.

Apart from TiO_2 powder, PE-TiO_2 and CT30 pellets also can remove glyphosate effectively (Figure 4b). The removal efficiency of glyphosate using both PE-TiO_2 and CT30 pellets under UV irradiation represented a considerable increase with time. For CT30 pellets, the concentration of glyphosate was reduced from 1 to 0.01 mgL^{-1}, with 99.08% removal efficiency, whereas the removal efficiency of glyphosate reached 74.02% by using PE-TiO_2 pellets after 240 mins. Although both PE-TiO_2 and CT30 pellets showed a lower performance than TiO_2 powder, they were much easier to separate from water than TiO_2 powder. As mentioned previously, clay TiO_2 pellets showed a higher performance for the photocatalytic degradation of glyphosate, compared with PE-TiO_2 pellets. Also, clay TiO_2 pellets had a mixture of anatase-rutile phase, while the PE-TiO_2 pellets only have anatase phase (Figure 2b). The mixture of rutile and anatase phases enhance photocatalytic activity, leading to improve electron–hole separation (Ohtani et al., 2010). Also, clay TiO_2 pellets had a larger surface area than the PE-TiO_2 pellets. The high surface area relates to the greater number of active sites for reactive

oxygen species (ROS) production to degrade glyphosate (Dârjan et al., 2013; Kumar and Pandey, 2017; Hurum et al., 2003).

Apart from the photocatalytic degradation of glyphosate, glyphosate can be adsorbed by PE-TiO_2 and CT30 pellets. The results showed that 6.77% of glyphosate was adsorbed by PE-TiO_2 pellets, while about 41.72% of glyphosate was adsorbed by using CT30 pellets within 240 mins (Figure 4b). Obviously, CT30 pellets showed dual functions with adsorption and photocatalytic degradation of glyphosate, while the decrease of glyphosate by using PE- TiO_2 pellets was mainly due to the influence of photocatalytic degradation. Considering the removal efficiency of glyphosate, CT30 pellet showed the higher performance with convenient separation from the water.

Mechanisms of the photocatalytic degradation of glyphosate

A possible photocatalytic degradation pathway of glyphosate was supposed to occur due to the strongly oxidizing species (i.e. hydroxyl radicals and/or superoxide anion radicals). It is presumed that decomposition of glyphosate released AMPA, glycolic acid, sarcosine ,phosphoric acid (H_3PO_4), carbon dioxide (CO_2) and, inorganic anions i.e. phosphate (PO_4^{3-}) and nitrate (NO_3^-) (Echavia et al., 2009; Muneer and Boxall, 2008; Chen and Liu, 2007) . Among these byproducts, AMPA is initially produced and frequently occurs within glyphosate decomposition, while PO_4^{3-} is stable major byproduct. In relation to glyphosate decomposition pathway, this study investigated AMPA and PO_4^{3-} formation.

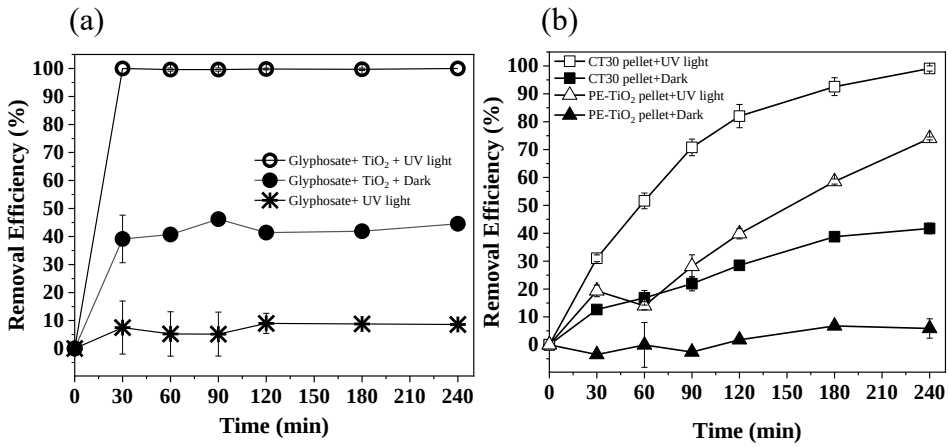

Figure 4 Degradation of glyphosate under dark and UV conditions (a) TiO_2 powder and (b) clay TiO_2 pellets and PE-TiO_2 pellets

The concentrations of AMPA and PO_4^{3-} during photocatalytic degradation of glyphosate by using TiO_2 powder are shown in Figure 5a. The complete removal of glyphosate at concentration of 1 mgL^{-1} was achieved, and PO_4^{3-} formation was observed at 30 mins and stable until 240 mins. It can be seen that the formation of PO_4^{3-} was related to the disappearance of glyphosate.

Compared to CT30 pellets, the photocatalytic degradation of glyphosate by using CT30 pellets showed a different result in the formation of PO_4^{3-} (Figure 5b). The concentration of glyphosate was gradually decreased and PO_4^{3-} concentration increased gradually, reaching its highest level at 120 mins. Then, PO_4^{3-} concentration decreased until 240 mins (Figure 5b).

Also, the formation of AMPA is related to the decrease of glyphosate (Figure 5b). When the concentration of glyphosate was gradually decreased, AMPA concentration increased gradually, reaching its highest level at 90 mins. Thereafter, AMPA decreased until 240 mins.

From previous studies, glyphosate can be directly oxidized to AMPA. The generated AMPA can be also directly changed into PO_4^{3-} (Echavia

et al., 2009; Muneer and Boxall, 2008). Thereby, it is presumed that the gradual decrease of AMPA is resulted from the decrease of *glyphosate and increase of* PO_4^{3-} in water. Interestingly, AMPA was no observed in the photocatalytic degradation of glyphosate by using TiO_2 powder. This is possibly due to high performance photocatalytic activity of TiO_2 powder for degradation of the AMPA and glyphosate.

Overall, formation of by products during the photocatalytic degradation of glyphosate by using TiO_2 powder showed different result from CT30 pellets. Photocatalytic degradation of glyphosate by using TiO_2 powder found only PO_4^{3-}, while photocatalytic degradation of the glyphosate by using CT30 pellets found both AMPA and PO_4^{3-}. This difference is might be due to the lower photocatalytic activity of CT30 pellets than TiO_2 powder, resulting in AMPA is not rapidly decomposed. However, there was a trend in decreasing of AMPA after 90 mins (Fig. 5b). Due to AMPA are more toxic and longer *half-life* than glyphosate (Grandcoin et al., 2017), complete degradation of AMPA is essential. Therefore, increase photocatalytic activity of CT30, e.g. increasing reaction time, light intensity and amount of clay TiO_2 pellets, can lead to complete degradation of AMPA as well as degradation of glyphosate.

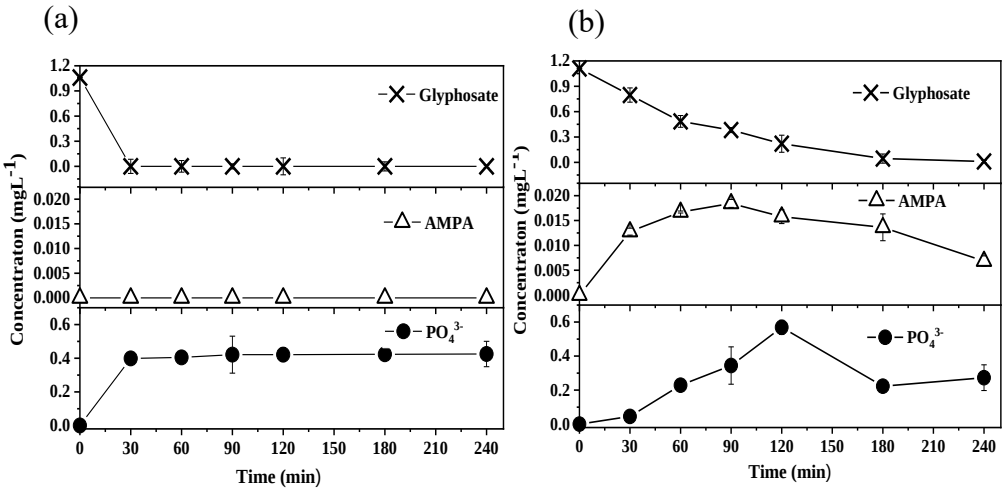

Figure 5 Concentration of glyphosate and its byproducts during photocatalytic degradation (a) TiO_2 powder and (b) CT30 pellets

CONCLUSIONS

As shown in this work, CT30 pellets were simply prepared, easily removed from water and resulted in highly photocatalytic activity. The removal efficiency of glyphosate by the CT30 pellets reached 99.08%. Also, AMPA and PO_4^{3-} has been observed in the photocatalytic degradation pathway of glyphosate by CT30 pellets.

ACKNOWLEDGEMENTS

The authors are grateful to National Nanotechnology Center (NANOTEC) (No. P1751698), Thailand Graduate Institute of Science and Technology (TGIST) and Thailand Advanced Institute of Science and Technology-Tokyo Institute of Technology (TAIST-Tokyo Tech), National Science and Technology Development Agency, Thailand for their financial support as well as Miss Duangkamon Viboonratanasri, senior assistant research for technical help in using IC.

The study was also made possible through the support provided by Hinode Laboratory, School of Environment and Society, Tokyo Institute of Technology, Japan and

Sirindhorn International Institute of Technology (SIIT), Thailand.

REFERENCES

Bayan EM, Lupeiko TG, Kolupaeva EV, Pustovaya LE, Fedorenko AG. Fluorine-Doped Titanium Dioxide: Synthesis, Structure, Morphology, Size and Photocatalytic Activity. In: Advanced Materials: Springer; 2017. 17-24.

Bouna L, Rhouta B, Amjoud M, Maury F, Lafont M-C, Jada A, et al. Synthesis, characterization and photocatalytic activity of TiO2 supported natural palygorskite microfibers. Applied Clay Science 2011; 52(3): 301-311.

Bowering N, Croston D, Harrison PG, Walker GS. Silver modified Degussa P25 for the photocatalytic removal of nitric oxide. International Journal of Photoenergy 2007;2007.

Breuer S. The chemistry of pottery. chemistry 2012.

Carp O, Huisman CL, Reller A. Photoinduced reactivity of titanium dioxide. Progress in solid state chemistry 2004; 32(1-2): 33-177.

Chen JQ, Hu ZJ, Wang NX. Photocatalytic mineralization of glyphosate in a small-scale plug flow simulation reactor by UV/TiO2. Journal of Environmental Science and Health, Part B 2012; 47(6): 579-588.

Dârjan A, Drăghici C, Perniu D, Duţă A. Degradation of Pesticides by TiO 2 Photocatalysis. In: Environmental Security Assessment and Management of Obsolete Pesticides in Southeast Europe: Springer; 2013. 155-163.

Dědková K, Peikertová P, Matějová K, Lang J, Kukutschová K. Study of the antibacterial activity of composites kaolinite/Tio2. nanocon 2012.

Echavia GRM, Matzusawa F, Negishi N. Photocatalytic degradation of organophosphate and phosphonoglycine pesticides using TiO2 immobilized on silica gel. Chemosphere 2009; 76(5): 595-600.

Edzwald JK, Toensing DC, Leung MC-Y. Phosphate adsorption reactions with clay minerals. Environmental Science & Technology 1976; 10(5): 485-490.

Grandcoin A, Piel S, Baures E. AminoMethylPhosphonic acid (AMPA) in natural waters: Its sources, behavior and environmental fate. Water research 2017; 117: 187-197.

Hurum DC, Agrios AG, Gray KA, Rajh T, Thurnauer MC. Explaining the enhanced photocatalytic activity of Degussa P25 mixed-phase TiO2 using EPR. The Journal of Physical Chemistry B 2003; 107(19): 4545-4549.

Kumar A, Pandey G. A review on the factors affecting the photocatalytic degradation of hazardous materials.

Material Sci & Eng Int J 2017; 1(3): 106-114.

Kutláková KM, Tokarský J, Kovář P, Vojtěšková S, Kovářová A, Smetana B, et al. Preparation and characterization of photoactive composite kaolinite/TiO2. Journal of Hazardous Materials 2011; 188(1-3): 212-220.

Muneer M, Boxall C. Photocatalyzed degradation of a pesticide derivative glyphosate in aqueous suspensions of titanium dioxide. International Journal of Photoenergy 2008; 2008.

Pattarasiriwong WW, P; Sittisorn, T; Yindee, T; Kerdnoi, T; Hongsibsong, S. Research on Organophosphate Pesticide Risk Management in the Upper Northern Part of Thailand phayamengrai, Chaingrai Provinces 2016; 3.

Raj K, Viswanathan B. Effect of surface area, pore volume and particle size of P25 titania on the phase transformation of anatase to rutile. 2009.

Sanchez-Soto P, Perez-Rodriguez J. Thermal analysis of pyrophyllite transformations. Thermochimica Acta 1989; 138(2): 267-276.

Shimizu N, Ogino C, Dadjour MF, Murata T. Sonocatalytic degradation of methylene blue with TiO2 pellets in water. Ultrasonics sonochemistry 2007; 14(2): 184-190.

Umar M, Aziz HA. Photocatalytic degradation of organic pollutants in water. In: Organic Pollutants-Monitoring, Risk and Treatment: InTech; 2013.

Wang B, Ding H, Deng Y. Characterization of calcined kaolin/TiO 2 composite particle material prepared by mechano-chemical method. Journal of Wuhan University of Technology-Mater. Sci. Ed. 2010;25(5): 765-769.

Wang C, Shi H, Zhang P, Li Y. Synthesis and characterization of kaolinite/TiO2 nano-photocatalysts. Applied Clay Science 2011; 53(4): 646-649.

Wang G, Xu L, Zhang J, Yin T, Han D. Enhanced Photocatalytic Activity of TiO_2 Powders (P25) via Calcination Treatment; 2012.

Yamazaki S, Matsunaga S, Hori K. Photocatalytic degradation of trichloroethylene in water using TiO2 pellets. Water Research 2001; 35(4): 1022-1028.

Zhang Q, Shan A, Wang D, Jian L, Cheng L, Ma H, et al. A new acidic Ti sol impregnated kaolin photocatalyst: synthesis, characterization and visible light photocatalytic performance. Journal of sol-gel science and technology 2013; 65(2): 204-211.

Zheng R, Ren Z, Gao H, Zhang A, Bian Z. Effects of calcination on silica phase transition in diatomite. Journal of Alloys and Compounds 2018; 757: 364-371.

Treatment of Highly Colored Wastewater from Commercial Biogas Reactor Discharge using Fenton Oxidation Process

Hatairut Samakkarn[1], Paiboon Sreearunothai[2], Maythee Saisriyoot[3], Korakot Sombatmankhong[4*]

[1]Thailand Advanced Institute of Science and Technology-Tokyo Institute of Technology (TAIST-Tokyo Tech), Sirindhorn International Institute of Technology, Thammasat University, Thailand

[2]School of Bio-Chemical Engineering and Technology, Sirindhorn International Institute of Technology, Thammasat University, Thailand

[3]The Department of Chemical Engineering, Faculty of Engineering, Kasetsart University, Thailand

[4]National Metal and Materials Technology Center, 114 Thailand Science Park, Thanon Phahonyothin, Tambon Khlong Nueng, Amphoe Khlong Luang, Pathum Thani, 12120, Thailand; Corresponding author: e-mail: korakots@mtec.or.th

ABSTRACT

Biogas generation utilizes vinasse, a by-product of ethanol distillation, as one of its ingredients is gaining more interests in recent years. However, discharge from biogas reactors utilizing vinasse is highly colored and is difficult to be further degraded by conventional biological treatment. In this work, the Fenton oxidation process has been employed to test for the color reduction of the discharge from a commercial biogas reactor using vinasse as its feedstock. The operating factors, such as the pH and the amount of the Fenton reagents have been explored to determine their effects on the efficiency of the Fenton oxidation process. The operating ranges tested, using 2^k full factorial design of experiment (DOE), are the Fe^{2+} concentrations between 1.7-8.9 mM, the

H_2O_2 concentrations between 6.5-13.1 M, and the pH between 3-6. The Fenton treatment of this wastewater showed a very high color removal efficiency of up to 90% color removal from the initial value of over 200,000 ADMI (American Dye Manufacturers Institute) standard.

Keywords: Vinasse, Decolorization, Fenton oxidation process, DOE

INTRODUCTION

Biogas production from wastewater has gained increasing interest as a viable way for energy production especially in wastewater from the bio-industries which are rich in organic compounds. One of the feedstock that has been used for biogas reactor comes from the by-product of the ethanol distillation known as vinasse [1, 2]. Vinasse is the dark-brown liquid remained after the ethanol distillation. It is generated in a large amount normally by about 9-14 liters for every liter of the ethanol produced. Vinasse has been characterized to be rich in phenolic compounds and melanoidin [2-4]. Melanoidin is a by-product from the Maillard reaction between sugars and amino groups [5, 6] and has a dark brown to black color similar to that of molasses. Although anaerobic digestion taking place in the biogas reactor is very efficient in treating the vinasse with BOD removal efficiency of over 80% and also produces energy in the form of biogas [7]. The color of the final effluent from the biogas reactor utilized vinasse still remains very dark.

Recently, new regulation in Thailand set the color value of water discharge of not more than 300 ADMI [8]. This has made decolorization of industrial wastewater to become one of the important priorities. Unfortunately, decolorization of the effluent from the biogas generation utilizing vinasse as its feedstock has been a difficult task. Physical or biological wastewater treatment have been employed for the color removal,

however these techniques are rather not effective and the use of chemical oxidation may help degrading these biologically recalcitrant compounds. Advanced oxidation processes (AOPs) has been in high demand for treatment of organic pollutants that are difficult to be degraded biologically [9] [10]. Choosing the optimum dosage of chemicals and also conditions of treatment in order to minimize the cost associated with AOPs can be challenging. The application of standard statistical design of experiment (DOE) approach can help to reduce number of tests necessary to find optimum conditions [11]. DOE investigates the effects of the input variables (factors) on the output variables (responses) yielding the optimum conditions.

The aim of this study is to decrease color of the effluent discharged from a commercial biogas reactor utilizing vinasse as its main feedstock and to investigate on the efficiency of Fenton's processes and optimum conditions for the color removal using DOE method.

METHODOLOGY

Chemicals and materials

The biogas wastewater sample was received from a biogas plant utilizing vinasse from an ethanol distillery as its major influent. The wastewater sample was kept in a dark container at temperature of 4°C prior to use. sulfuric acid, $FeSO_4 \cdot 7H_2O$, H_2O_2 30% w/w and were purchased from Dajung Co., Ltd.

Procedure

The experiment was performed at ambient temperature and pressure. The Fenton oxidation process was conducted in a 250 ml glass bottle containing 20 ml sample. The pH of the sample was adjusted in the range between 3-6 using sulfuric acid. $FeSO_4 \cdot 7H_2O$ and H_2O_2 were then added into the sample and the sample was left under continuous stirring for 24 hours.

Color Measurement

The color measurement standard is the APHA 2120F ADMI Weighted-Ordinate Spectrometer. For color standard method, the sample was first

filtered to remove turbidity using a cellulose acetate syringe filter with a nominal pore of 0.45 μm. The color according to the ADMI color standard was then carried out using a 10mm disposable cuvette using Spectroquant model Pharo 300.

COD Measurement

COD measurement was carried out by standard method APHA 5220 D. closed reflux, colorimetric method. The sample was added to vials and digested for 2 hours at 150 °C in a Spectroquant TR 420 and cooled down to room temperature for 30 min. The COD concentration was then measured photometrically using the Spectroquant model Pharo 300.

RESULTS AND DISCUSSION

ANOVA results

In order to study and optimize Fenton's process on the color reduction, the 2^k full factorial DOE was analyzed using Minitab. The experiment investigated on the 3 factors (pH, Fe^{2+} and H_2O_2 concentrations) resulting in possible combinations of 8 runs for the low and high in each factor. The operating factors on color reduction were adopted by varying pH of wastewater between 3-6, Fe^{2+} concentrations between 1.7- 8.9 mM, and H_2O_2 concentrations between 6.5- 13.1 M. The goal of this type of experiment is usually focused on developing a full predictive model (Y = f(X)) describing how the process inputs jointly affect the process output and determining the optimal settings of the inputs.

Based on the ANOVA analysis conducted (table not shown), the P-values of the main effects, the two-way interactions and the three-way interactions among the factors are almost 0 (less than 0.05). This implies that the linear assumption between the factors and the responses are statistically significant and that the pH range between 3-6, the Fe^{2+} concentration between 1.7- 8.9 mM, and the H_2O_2 concentration between 6.5-13.1 M are statistically significant.

Regression equation

The estimated coefficients generated

from the 2^k full factorial DOE were then used to obtain the regression model (Y=f(X)) which is displayed in Table 1.

Table 1 Regression equation for the predicted color value of the treated wastewater as a function of the pH, Fe^{2+} and H_2O_2 concentrations.

Color (ADMI)	=	525 + 19362 pH + 2354 Fe (mM) + 1280 H_2O_2 (M)
		- 2318.0 pH*Fe (mM) - 1179.1 pH*H_2O_2 (M)
		- 288.1 Fe (mM)*H_2O_2 (M) + 144.30 pH*Fe (mM)*H_2O_2 (M)

Effects plot

The Pareto chart in Fig.1 shows the absolute values of the standardized effects from the largest effect to the smallest effect. The chart also plots a reference line to indicate which effects are statistically significant. This chart determines the magnitude and the importance of the effects.

Model of color response to input factors

To determine if the model in Table 1 can fit our data, one examines the goodness-of-fit statistics. The standard deviation between the color data values and the fitted color values is approximately 602.4 ADMI. R^2 is a statistical measure of how close the data are to the fitted regression line. The high R^2 value of 99.94% means all the variability of the response data center around its mean and the model fits the data well. The predicted-R^2 determine, given new observation, how well the model can predict the response. In this work, the model has also a quite good predicted-R^2 value of 99.86% and hence the model should have a good predictive ability.This work illustrates that main effects, two-way interactions and three-way interactions among factors cross the reference line at 2.1 so these factors are statistically significant with the current model terms. The Fe concentration is a major factor that affects the color response.

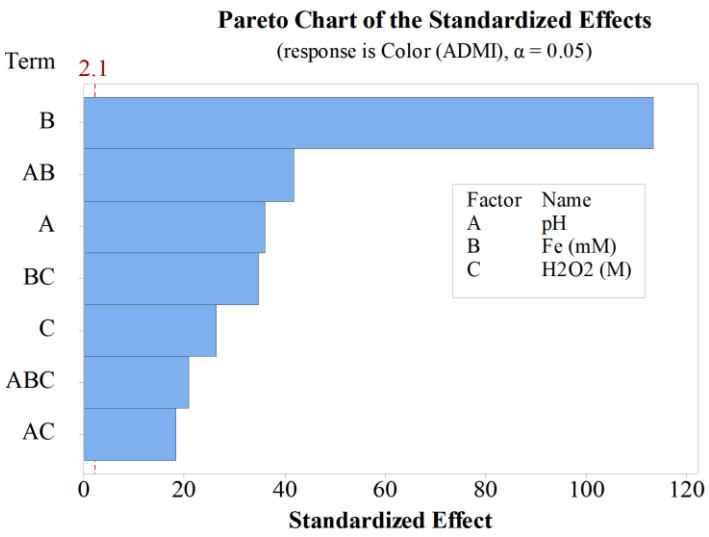

Figure 1 The Pareto graph of all factors on color response

Residual analysis

The normal probability plot verifies assumption of normality of error terms that the residuals approximately follow a straight line. The histogram shown in Fig. 2 indicates the normal distribution of the residuals for all observations. Moreover, the versus fits plot shows the error term against the fitted value to verify the assumption that the residuals are randomly distributed. They should fall randomly half above and half below the 0 line, with no recognizable patterns in the points so that indicate our assumption of error terms having mean 0 is valid

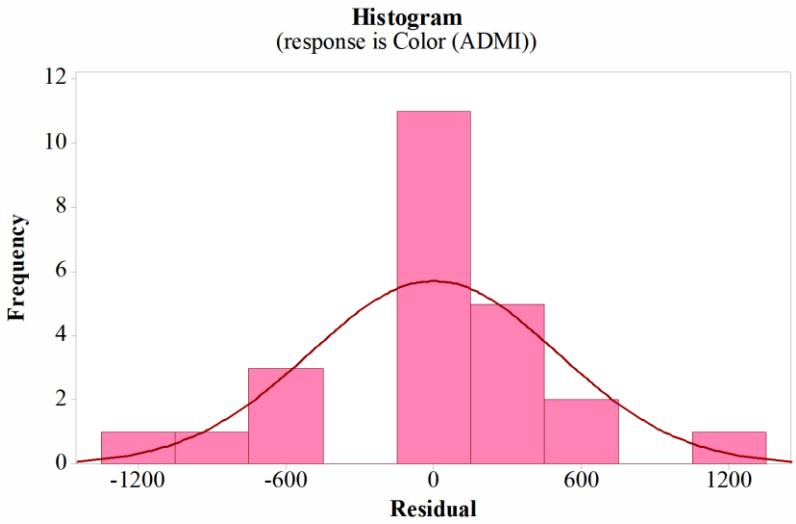

Figure 2 The normal distribution of histogram of the color response around the mean value

Optimization

The optimization plot shows how the factor variables affects the predicted responses. According to the calculation, the color value of Fenton oxidation process can be minimized at the operating temperature of 25 °C, the reaction time of 24 hours, pH of 3, the Fe^{2+} concentration of 8.9 mM, and the H_2O_2 concentration of 13.1 M. The highest color removal efficiency using Fenton oxidation process of 97.5% is then obtained. This prediction is also verified in an experiment and obtained a color value of 4,983 ADMI. The COD removal efficiency is about 30% from the initial COD concentration of 68,000 mg/L to about 47,709 mg/L after treatment.

Validation of the minimum condition

After investigation of the minimum color condition (pH of wastewater 3, Fe^{2+} concentrations of 8.9 mM, and H_2O_2 concentrations 13.1 M), we validate response. The experimental measured color is 4,912 ADMI and is very close to that of the predicted value of 4,983 ADMI. The result shows that the percentage difference between the actual experimental value and that of the predicted value

from the model is only 1.4%. Thus, it is possible to predict for the color results using the model in Table 1.

Figure 3

Original wastewater vs the Fenton's treated wastewater at optimized conditions obtained from the full 2^k factorial DOE

Contour plot

Contour plot displays the three-dimensional relationship, with the factors or variables on the x- and y-axes, and the response on the z-axis. The plots can help visualization of how the factors relates to the response. The contour plot is the cross-section of the surface plot at various constant response value projected onto the x-y plane.

Figure 4 shows the contour plot of the color response to the Fe^{2+} and pH used in the Fenton process holding H_2O_2 concentration constant at 9.8 M. It can be seen that in this case the higher the Fe^{2+} concentration the lower the color value, or the better the color removal efficiency. pH also affects at low Fe^{2+} concentration where the low value is needed in order to achieve low color value. However, at high Fe^{2+} concentration, the pH does not affect the color reduction much. Hence, using high Fe^{2+} concentrations, is more effective in lowering the color value of the treated wastewater than using low Fe^{2+} concentration.

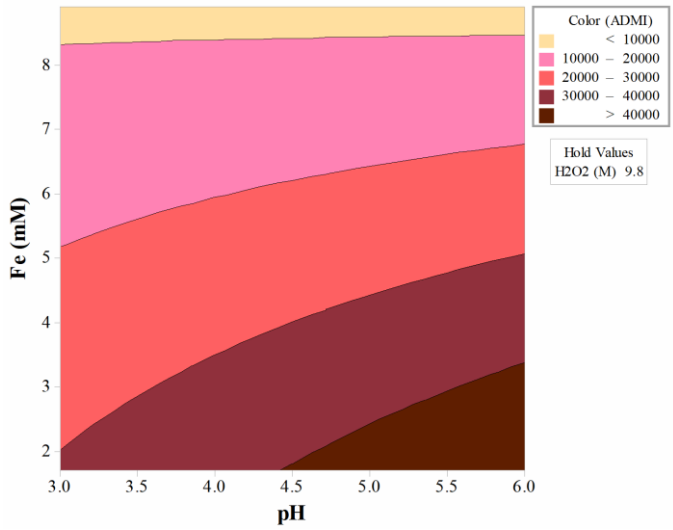

Figure 4 Contour plot of color (ADMI) vs Fe^{2+}, pH

Figure 5 shows the contour plot of the color response from the model to the H_2O_2 concentrations and the pH used to hold the Fe^{2+} concentration constant in the mid-range at 5.3 mM. The response is classified by the color shade. It can be seen that the low color value is obtained when the low color value is achieved at sufficiently high concentration of H_2O_2 and low pH value. Thus, the higher H_2O_2 concentrations and lower pH are prefer at moderate level of Fe^{2+}.

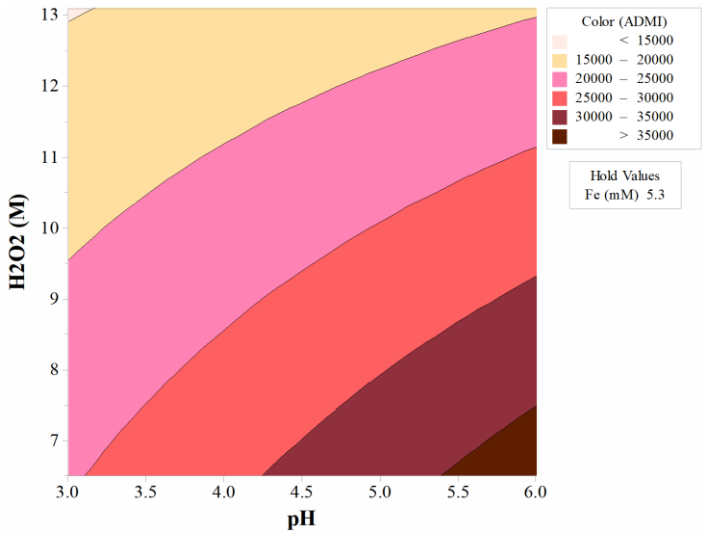

Figure 5 Contour plot of color (ADMI) vs H_2O_2, pH

Figure 6 shows the contour plot of the color response to the H_2O_2 and Fe^{2+} concentrations used to react in Fenton process holding pH constant in the mid-range at 4.5. It can be seen that in order to achieve low color value, the Fe^{2+} has to be sufficiently high in the range of about 8mM, and at this level, the low amount of H_2O_2 can also be used leading to the lower process cost.

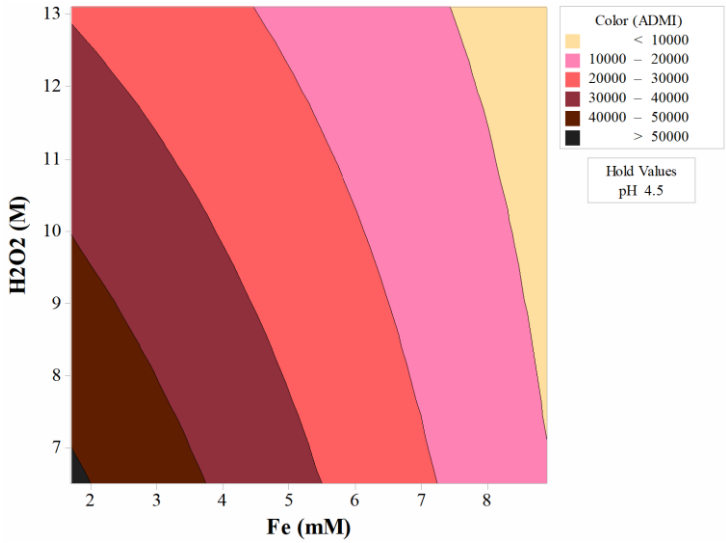

Figure 6 Contour plot of color (ADMI) vs H_2O_2, Fe^{2+}

CONCLUSIONS

In this work, Fenton's oxidation process has been shown to be very effective in reducing the color of the biogas reactor discharge from the color value of over 200,000 ADMI to the color value of about 4,983 ADMI.

The optimized Fenton's conditions were found to be at the pH value of 3, Fe^{2+} concentration of 8.9 mM, and the H_2O_2 concentration of 13.1 M with color removal efficiency 97.5% at the optimized condition. The 2^k full factorial DOE helps to also obtain a model that can predict the final color value of the treated effluent given the Fenton's parameters of pH, Fe^{2+} and H_2O_2 concentrations used and show that the Fe^{2+} concentrations to be a major factor affecting the color, and that operating in the high Fe^{2+} concentration range is preferred in

order to minimize the use of H_2O_2 and to operate in the near neutral pH.

ACKNOWLEDGEMENTS

The authors gratefully acknowledge the TAIST-Tokyo Tech scholarship, the National Science and Technology Development Agency (NSTDA), and Sirindhorn International Institute of Technology (SIIT), Thammasat University.

REFERENCES

Cristiano E. R. Reis, H.B.S.B., Thiago M. Alves, Ana K. F. Carvalho and Heizir F. De Castro, *Vinasse Treatment within the Sugarcane-Ethanol Industry Using Ozone Combined with Anaerobic and Aerobic Microbial Processes.*

Hu, C.E.R.R.a.B., *Vinasse from Sugarcane Ethanol Production: Better Treatment or Better Utilization.*

V. Parnaudeau, N.C., R. Oliver, P. Cazevieille, S. Recous, *Vinasse Organic Matter Quality and Mineralization Potential, as Influenced by Raw Material, Fermentation and Concentration Processes.*

Elda España-Gamboa, T.V., Xavier Font, Jorge Dominguez-Maldonado, Blondy Canto-Canché and Liliana Alzate-Gaviria, *Pretreatment of vinasse from* the sugar refinery industry under non-sterile conditions by Trametes versicolor in a fluidized bed bioreactor and its effect when coupled to an UASB reactor.

Sara I.F.S. Martins*, W.M.F.J.a.M.A.J.S.v.B., A review of Maillard reaction in food and implications to kinetic modelling.

Surasak Bunrung, S.P., Poonsuk Prasertsan, Decolourisation of Biogas Effluent of Palm Oil Mill using Palm Ash.

Y. Satyawali, M.B., Wastewater treatment in molasses-based alcohol distilleries for COD and color removal: a review.

Thailand, M.o.I., Notification of Ministry of Industry Industrial Effluent Standards B.E. 2560. 2560.

STASINAKIS, A.S., USE OF SELECTED ADVANCED OXIDATION PROCESSES (AOPs) FOR WASTEWATER TREATMENT – A MINI REVIEW

Adina Elena Segneanu, C.O., Carmen Lazau, Paula Sfirloaga, Paulina Vlazan, Cornelia Bandas and Ioan Grozescu, Waste Water Treatment Methods.

Is'haq A. Mohammed*, M.T.B., Ambali S. Abdulkareem, Stephen S. Ochigbo, Ayo S. Afolabi, Oladiran K. Abubakre Full factorial design approach to carbon nanotubes synthesis by CVD method in argon environment.

Effect of Yeast Volatile Organic Compounds Produced by Yeast Strains on Growth and Ochratoxin A Production by *Aspergillus carbonarius*

Pichamon Soma[1], Supat Chareonpornwattana[1], Cheewanun Dachoupakan Sirisomboon[1*]

[1] Department of Microbiology, Faculty of Science, Chulalongkorn University, Bangkok 10330, Thailand
*E-mail: cheewanun.d@chula.ac.th

ABSTRACT

The objective of this study was to evaluate inhibitory activities of *Wickerharmomyces anomalus* MSCU 0652 and *Kluyveromyces marxianus* MSCU 0655 on growth and ochratoxin A (OTA) production of *Aspergillus carbonarius* TK4.2. We found that *W. anomalus* MSCU 0652 and *K. marxianus* MSCU 0655 showed the inhibitory effect of 83.81% and 66.04%, respectively, on growth of *A. carbonarius* TK4.2. OTA production was also inhibited 99.77% by both antagonistic yeasts. GC-MS analysis showed that the major component of volatile organic compound (VOCs) was ethyl acetate and other minor VOCs compounds were also produced by *W. anomalus* MSCU 0652 and *K. marxianus* MSCU 0655 and found to be 1-butanol, 3-methyl, acetic acid, phenylethyl alcohol, 1-propanol, 2-methyl etc.

Keywords: Ochratoxin A, *Aspergillus carbonarius*, *Wickerharmomyces anomalus*, *Kluyveromyces marxianus*, Volatile Organic Compounds

INTRODUCTION

Ochartoxin A (OTA) is a mycotoxin, a toxic secondary metabolite of filamentous fungi. OTA is one of the most common naturally occurring mycotoxin produced by genera *Aspergillus* and *Penicillium* particularly *A. carbonarius*, *A. ochraceus* and *P. verrucosum* (Gupta, 2007). This mycotoxin has well recognized nephrotoxic, teratotoxic and immunotoxic properties and was classified as a possible human carcinogen (group 2B) (IARC, 1993). The contamination of OTA was detected in a wide range of agricultural products. These include cereals, coffee beans, cocoa, nuts, spices, dried fruit, beer and wine (Wolff et al., 2000).

Several methods were developed and used in pre- and postharvesting for controlling fungi and mycotoxin contamination. Among the strategies, an alternative method such as biological control has increasingly draun attention as agent for fungal growth inhibition and mycotoxin reduction for example, biological control agents (BCAs) using bacteria, fungi and yeasts (Janisiewicz and Korsten, 2002). Yeasts are high of potential as BCAs since they have several attributes that make them suitable for use as BCAs including genetics stability, non-allergenic and non-toxic effects, growth in various conditions and requirement of basic nutrients (Droby and Chalutz, 1994; Wilsons and Wisniewski, 1998). To date, several studies have reported the capability of antagonistic yeasts for inhibiting fungal growth and mycotoxin reduction with different mechanism of action such as competition for nutrients and space (Janisiewicz et al., 2000; Zhu et al., 2015), the release of hydrolytic enzymes (Gil-Serna et al., 2011; Parafati et al., 2015) volatile organic compounds (VOCs) (Spadaro and Droby, 2016) and mycotoxin adsorption or degradation (Bejaoui et al., 2004; Péteri et al., 2006)

VOCs produced by yeasts have been as part of biological control strategies to prevent the growth of plant pathogen (Arrebola et al., 2010).

Several strains of antagonistic yeasts showed the effect to inhibit *A. carbonarius* growth and reduce OTA production. Farbo et al. (2018) reported that antagonistic yeast strains produced the VOCs as the one of antagonistic activities that reduced the fungal mycelial growth, sporulation and OTA production of *A. carbonarius* MPVA566 and *A. ochraceus* MPVA703. *Wickerharmomyces anomalus* is one of antagonictic yeast that produce various VOCs component, used as BCA on sweet cherries and strawberry (Oro et al., 2014) to inhibit fungal growth that cause of postharveast decay such as *B. cinerea, Moilinia fructicola* and *A. carbonarius* (Oro et al., 2018). Geng et al., 2011 reported that *Kluyveromyces marxianus* could produce several VOCs inhibiting spore germination of *Penicillium digitatum* in citrus fruit. The aim of this study was to evaluate the effect of VOCs produced by *W. anomalus* MSCU0652 and *K. marxianus* MSCU 0655 isolated from corn silage on growth and OTA production of *A. carbonarius* TK4.2

METHODOLOGY

Microorganisms

All microorganisms in this study were provided from the Culture Collection Center at the Department of Microbiology, Faculty of Science, Chulalongkorn University, Thailand. Antagonistics yeasts (*W. anomalus* MSCU 0652 and *K. marxianus* MSCU 0655) grown on YPD (Yeast extract-Peptone-Dextrose, Himedia, India) agar at 30 °C for 48 h. were cultivated in YM (Yeast extract-Malt extract, Himedia, India) broth at 37 °C for 9.5 h. to obtain mid-log culture. Yeast cells were havested by centrifugation (5000 rpm, 10 mins), washed twice with PBS (Phosphate Buffer Solution) pH 7.2 and counted by using hemacytometer then adjusted to 10^6 cell/mL. *A. carbonarius* TK4.2 was grown on PDA (Potato dextrose Agar, Difco, USA) at 25°C for 7 days. The fungal spore were collected in sterile normal saline solution with 0.01% Tween 80

then adjusted to final concentration of 10^6 spore/mL.

Effect of VOCs on fungal growth

A face to face double petri dish technique (Fiori et al., 2014) was used to evaluate the inhibitory efficacy of VOCs produced by antagonistic yeast strains on growth of *A. carbonarius* TK4.2. YPD agar plate was spreaded with 100 μL of each yeast suspension. Then, the lid of the plate was replaced by another PDA Petri dish that was point inoculated with 10 μL of fungal spore suspension. These plates were double sealed with Parafilm® and incubated at 25°C for 7 days. The control plate of *A. carbonarius* was sealed with YPD plate without yeast cell. The fungal colony was measured and examined the morphology and microscopic detail. The percentage of inhibition was calculated by using the following formula: [(fungal growth diameter of control – fungal growth diameter with antagonistic yeasts)/fungal growth diameter of control] × 100

Effect of VOCs on mycotoxins production

After calculated the percentage of inhibition, 6 agar plugs were removed from the center area of the fungal colony and introduced into a small vial. OTA extraction was carried out by adding 2.5 mL of methanol: formic acid (25: 1) under sonication for 15 min. (Dachoupakan et al., 2009). Extracts were passed though filter paper WhattmanTM No.1 and evaporated under a nitrogen stream at 40°C. The dried extracts were re-suspended in the mobile phase of HPLC (High Performance Liquid Chromatography). The decontamination of OTA was performed by HPLC system (Scientific and Technological Research Equipment Centre, Chulalongkorn University, Thailand) with C18 column (250 x 4.60 mm; 5 μm) and fluorescence detector by using the method of Dachoupakan et al., 2009. OTA contents were expressed as ng/g medium.

VOCs analysis

Each antagonistic yeast was inoculated in 20 mL clear vial and a screw cap containing 10 mL of YPD, incubated at 25°C for 2 days. VOCs components were analyzed by Solid Head-Space analysis (SHS) following Gas Chromatography Mass Spectrometry (GC/MS) (Scientific and Technological Research Equipment Centre, Chulalongkorn University, Thailand). For sampling, the 7697A Headspace Sampler (Agilent Technologies, Palo Alto, CA, USA) was used, 1 mL of loop size was inserted into headspace at 80°C for 60 min and GC/MS system was used to determine the VOCs by using Agilent 7890B GC system equipped with Agilent 7633 ALS autosampler and Agilent 7000C GC/MS Triplr Quad MSD model. Separation was performed on HP-INNOWAX column (30 m x 0.25 mm, 0.25 μm) with following temperature program: initial 40°C hold for 5 min, ramped to 230°C hold of 5 min at 5°C/min. The split injection port was held 180°C with a split ratio of 50:1. Helium was used as a carrier with constant flow rate set to 1 mL/min. MS system following by scanning range at 33-500 m/z. the ionic source temperature was 230°C with ionizing energy 70 eV and mass transfer line temperature of 250°C.

Statistical analysis

All data were analyzed by using SPSS 16.0 (SPSS Inc., Chicago, IL, USA). One-way ANOVA and Tukey's multiple-range test were used to verify significant differences between means ($p < 0.05$) of each experiment.

RESULTS

Effect of VOCs on fungal growth and OTA production

From face to face double petri dish assay, VOCs production of 2 yeast strains significantly inhibited *A.carbonarius* TK4.2 growth. VOCs of *W. anomalus* MSCU 0652 showed the highest efficacy against *A. carbonarius* TK4.2 growth with 83.18% inhibition. While *K. marxianus* MSCU 0655 was less efficient (66.04%) (Table 1). Fungal

colony development that combination with antagonistic yeasts showed marked difference compared with the control. *A. carbonarius* The VOCs produced by *W. anomalus* MSCU 0652 and *K. marxianus* MSCU 0655 were analyzed by GC-MS (Fig. 2, 3). The major VOC emitted by *W. anomalus* MSCU 0652 was ethyl acetate and the presence of 1-butanol, 3-methyl, acetic acid and phenylethyl alcohol was exposed to *W. anomalus* MSCU 0652 showed a small colony size with white mycelium, non-sporulation and short hyphae elongation compared to the control (Fig. 1A, 1B). After 7 days, fungal plates were extracted and analyzed the OTA production. OTA production of *A. carbonarius* TK4.2 was showed in Table 1. Both *W. anomalus* MSCU 0652 and *K. marxianus* MSCU 0655 were able to reduce OTA production more than 99%. The amount of mycotoxin generated by *A. carbonarius* TK4.2 extremely reduced compared with control (Table 1).

SHS-GC/MS analysis of yeasts VOCs

Alcohol was observed (Fig. 2). *K. marxianus* MSCU 0655 also mainly produced ethyl acetate. 1-butanol, 3-methyl, 1-propanol, 2-methyl, acetic acid and acetic acid, 2-phenyl were also detected (Fig. 3)

Table 1 Growth inhibition and OTA reduction of *A. carbonarius* TK4.2at day 7 of exposure to yeast VOCs. Results are expressed means of colony diameter (cm) and OTA production (ng/g) ± standard error. Values in each column following by different letters are significant difference as per Turkey's test ($p < 0.05$).

Treatment	Colony diameter (cm) (%inhibition)	OTA production (ng/g) (%reduction)
Control	$5.35^{a} \pm 0.64$	$526.61^{a} \pm 149.78$
W. anomalus MSCU 0652	$0.9^{b} \pm 0.0$ (83.18%)	$1.20^{b} \pm 0.44$ (99.77%)
K. marxianus MSCU 0655	$1.82^{c} \pm 0.68$ (66.04%)	$1.21^{b} \pm 0.85$ (99.77%)

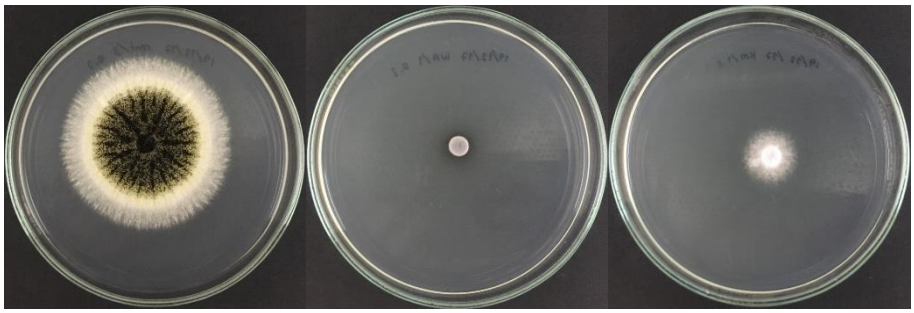

Fig. 1 Colony morphology of *A.carbonarius* TK4.2 incubated by face to face double petri dish assay with *W. anomalus* MSCU 0652 (B) and *K. marxianus* MSCU 0655 (C) compared with control (A) after 7 days at 25°

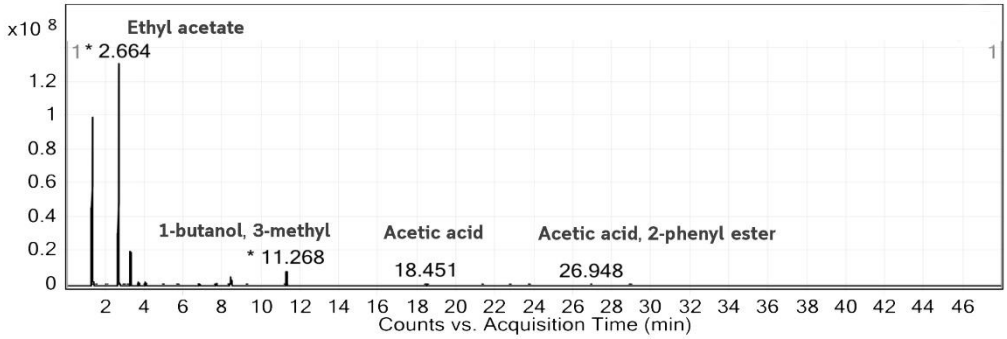

Fig. 2 GC-MS chromatogram corresponding to VOCs produce by *W. anomalus* MSCU 0652 grown on YPD agar at 25°C for 2 days.

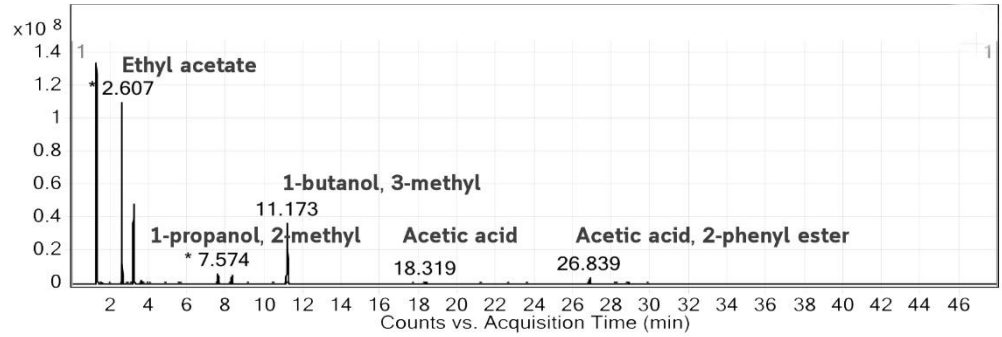

Fig. 3 GC-MS chromatogram corresponding to VOCs produce by *K. marxianus* MSCU 0655 grown on YPD agar at 25°C for 2 days.

DISCUSSION

Various strains of antagonistic yeasts were used in currently fields such as agricultural food and feed stuffs, medical and pharmaceutical fields (Golubev, 2006) so they were not pathogenic to human, animals and environment. Yeast VOCs were well-known to use as biocontrol agent in biotechnology for food and agricultural industries. (Morath et al., 2012; Francesco et al., 2015). From our study, VOCs produced by *W. anomalus* MSCU 0652 and *K. marxianus* MSCU 0655 affected to *A. carbonarius* TK4.2 by inhibiting mycelium growth and sporulation leading to reduce OTA-production. Recently, Oro et al. (2018) reported that VOCs from *W. anomalus* decreased mycelial growth of decay causing fungi in strawberries including *A.carbonarius.*

VOCs from several antagonistic yeasts play key as biocontrol agets (BCAS). They are superior over oter BCAs including, VOCs act like biofumigants so do not require direct contact and do not remain on products (Parafati et al., 2017). Presently, VOCs compounds produced by fungi are approximately 250 different components and they can be produced more than one compound such as group of alcohols, aldehydes, ketones, ketones, phenols, heterocyclics hydrocarbons and derivatives (Morath et al., 2012; Oro et al., 2018). VOCs compounds that analyze from headspace of studying yeast cultures were identified in several components such as alcohols, aldehydes and esters. Ethyl acetate was a dominant VOC compound of *W. anomalus* MSCU 0652 and *K. marxianus* MSCU 0655. According to Fredlund et al. (2004), ethyl acetate production of *W. anomalus* was a major compound of anti-mould activity against *Penicillium roqueforti*. Moreover, Leclercq-Perlat et al. (2004) confirmed that ethyl acetate is a main compound produced by *K. marxianus* producing other derivatives of esters and alcohol.

The mechanism of fungal inhibition by ethyl acetate is to bind to the fungal membrane sterol which leads

to membrane leakage and loss of intracellular components (Campoy and Adrio, 2017) or inhibiton of ergosterol synthesis which is the fungal membrane component (Ahmad et al., 2015). Alcohols especially aliphatic alcohols like 1-butanol, 3-methyl have high potential to disrupt the plasma membrane arrangement and the stability of lipid bilayer (Rezende et al., 2015; Toffano et al., 2017).

According to Farbo et al. (2018) found the VOCs of *C. jadinii*, *C. friedrichii*, *C. intermedia* and *L. thermotolerant* reduced the OTA production of *A. carbonarius* and *A. ochraceus* by produced 2-phenylethanol that play important role to inhibit mycelial growth and reduce the amount of OTA. The downregulation of OTA biosynthetic genes (*Ac*OTA*pks*, *Ac*OTA*nrps* and *acpks*) and regulatory genes *veA* and *laeA* of *A. carbonarius* were suppressed by antagonistic yeasts VOCs as a key to reduce OTA biosynthesis.

The present study can be concluded that VOCs released by *W. anomalus* MSCU 0652 and *K. marxianus* MSCU 0655 can inhibit *A. carbonarius* TK4.2 growth and reduce OTA production. These antagonistic yeasts may be efficiently developed as biocontrol agent appied for food, feed and agricultural sectors.

ACKNOWLEDGEMENTS

This study is supported by Department of Microbiology, Faculty of Science, Chulalongkorn University, Thailand.

REFERENCES

Ahmad A, Wani MY, Khan A, Manzoor N and Molepo J. Synergistic interactions of eugenol- tosylate and its congeners with fluconazole against *Candida albicans*. PLoS One 2015; 10: e0145053.

Arrebola E, Sivakumar D and Korsten L. Effect of volatile compounds produced by *Bacillus* strains on postharvest decay in citrus. Biological Control 2010; 53: 122–128.

Bejaoui H, Mathieu F, Taillandier P, and Lebrihi A. Ochratoxin A removal in synthetic and natural grape juices by selected oenological *Saccharomyces*

strains. Journal of Applied Microbiology 2004; 9: 1038–1044.

Campoy S and Adrio JL. Antifungals. Biochemical Pharmacology 2017; 133: 86-96.

Dachoupakan C, Ratomahenina R, Martinez V, Guiraud JP, Baccou JC and Schorr-Galindo. Study of the phenotypic and genotypic biodiversity of potentially ochratoxigenicblack aspergilla isolated from grapes. International Journal of Food Microbiology 2009; 132; 14-23.

Di Francesco A, Ugolini L, Lazzeri L and Mari M. Production of volatile organic compounds by *Aureobasidium pullulans* as a potential mechanism of action against postharvest fruit pathogens. Biological Control 2015; 81: 8-14.

Droby S and Chalutz E. Mode of action of biocontrol agents of postharvest disease. The Polish Phytopathological Society 1994; 39: 63–75.

de Souza JRB, Kupper KC and Augusto F. In vivo investigation of the volatile metabolome of antiphytopathogenic T yeast strains active against *Penicillium digitatum* using comprehensive two-dimensional gas chromatography and multivariate data analysis. Microchemical Journal 2018; 141: 362-368.

Farbo MG, Urgeghe PP, Fiori S, Marcello A, Oggiano S,Balmas V, Hassan ZU, Jaoua S and Migheli Q. Effect of yeast volatile organic compounds on ochratoxin A-producing *Aspergillus carbonarius* and *A. ochraceus*. International Journal of Food Microbiology 2018; 284: 1-10.

Fialho MB, Toffano L, Pozzobo PM, Augusto F and Florentino PS. Volatile organic compounds produced by *Saccharomyces cerevisiae* inhibit the in vitro development of *Guignardia citricarpa*, the causal agent of citrus black spot. World Journal of Microbiological Biotechnology 2010; 26: 925-932.

Fiori S, Urgeghe PP, Hammami W, Razzu S, Jaoua S and Migheli Q. Biocontrol activity of four non- and low-fermenting yeast strains against *Aspergillus carbonarius* and their ability to remove ochratoxin A from grape juice. International Journal of Food Microbiology 2014; 189: 45–50.

Fredlund E, Druvefors UA, Olstorpe MN, Possoth V and Schürer J. Influence of ethyl acetate production and ploidy on the anti-mould activity of *Pichia anomala*. FEMS Microbiology Letters 2004; 238: 133-137.

Geng P, Chen S, Hu M, Haq MR, Lai K, Qu F and Zhang Y. Combination of *Kluyveromyces marxianus* and sodium bicarbonate for controlling green mold of citrus fruit. International Journal of Food Microbiology 2011; 151: 190-194.

Gil-Sernaa J, Patiñoa B, Cortésc L, González-Jaénb MT and Vázquez C.

Mechanisms involved in reduction of ochratoxin A produced by *Aspergillus westerdijkiae* using *Debaryomyces hansenii* CYC 1244. International Journal of Food Microbiology 2011; 151: 113-118.

Golubev WI. Antagonistic Interactions Among Yeasts. Biodiversity ana Ecophysiology of Yeasts 2010; 197-219 pp.

Gupta RC. Ochratoxins and citrinin. Veterinary Toxicology 2012; 997-1003.

Hua SST, Beck JJ, Sarreal SBL and Gee W. The major volatile compound 2 – phenylethanol from the biocontrol yeast, Pichia anamala, inhibits growth and expression of aflatoxin biosynthetic genes of *Aspergillus flavus*. Mycotoxin Research 2014; 30: 71-78.

IARC. Some naturally occurring substances: Food item and constituents, heterocyclic aromatic amines, and mycotoxins. IARC. Science Public 1993; 56: 489 pp.

Janisiewicz WJ, Tworkoski TJ and Sharer C. Characterizing the Mechanism of Biological Control of Postharvest Diseases on Fruits with a Simple Method to Study Competition for Nutrients. Phytopathology 2000; 90: 1196-1200.

Janisiewicz WJ and Korsten L. Biological control of postharvest diseases of fruits. Phytopathol 2002; 40: 411–441.

Leclercq-Perlat MN, Corrieu G and Spinnler HE. Comparison of Volatile Compounds Produced in Model Cheese Medium Deacidified by *Debaryomyces hansenii* or *Kluyveromyces marxianus*. Journal of Dairy Science 2004; 87: 1545-1550.

Mari M, Bautista-Baños S and Sivakumar D. Decay control in the postharvest system: Role of microbial and plant volatile organic compounds. Postharvest Biological Technology 2016; 122: 70-81.

Morath SU, Hung R and Bennett JW. Fungal volatile organic compounds: A review with emphasis on their biotechnological potential. Fungal Biological Review 2016; 26: 73-83.

Oro L, Feliziani E, Ciani M, Romanazzi G and Comitini F. Biocontrol of post-harvest brown rot of sweet cherries by *Saccharomyces cerevisiae* Disva 599, *Metschnikowia pulcherrima* Disva 267 and *Wickerhamomyces anomalus* Disva 2 strains. Postharvest Biological Technology 2014; 96: 64–68.

Oro L, Feliziani E, Ciani M, Rommanazzi G and Comitini F. 2018. Volatile organic compounds from *Wickerhamomyces anomalus, Metschnikowia pulcherrima* and *Saccharomyces cerevisiae* inhibit growth. International Journal of Food Microbiology 2018; 265: 18-22.

Parafati L, Vitale A, Restuccia C and Cirvilleri G. Biocontrol ability and action mechanism of food-isolated yeast strains against *Botrytis cinerea* causing post-harvest bunch rot of table grape. Food Microbiology 2015; 47: 85-92.

Péteri Z, Téren J, Vagvölgyi C and Varga J. Ochratoxin degradation and adsorption caused by astaxanthin-producing yeasts. Food Microbiology 2007; 24: 205–210.

Rezende DC, Fialho MB, Brand SC, Blumer S and Pascholati SF. Antimicrobial activity of volatile organic compounds and their effect on lipid peroxidation and electrolyte loss in *Colletotrichum gloeosporioides* and *Colletotrichum acutatum* mycelia. African Journal of Microbiology Research 2015; 9: 1527-1535.

Spadara D and Droby S. Development of biocontrol products for postharvest diseases of fruit: The importance of elucidating the mechanisms of action of yeast antagonists. Trends in Food Science and Technology 2016; 47: 39-49.

Toffana L, Fialho MB and Pascholati F. Potential of fumigation of orange fruits with volatile organic compounds produced by *Saccharomyces cerevisiae* to control citrus black spot disease at postharvest. Biological Control 2017; 108: 77-82.

Wilson C and Wisniewski M. 1989. Biological control of postharvest diseases of fruits and vegetables: an emerging technology. Annual Review Phytopathology 1989; 27: 425–441.

Wolff J, Bresch H, Cholmakov-Bodechtel C, Engel G, Garais M, Majerus P, Rosner H and Scheuer R. Ochratoxin A: Contamination of foods and consumer exposure final evaluation. Archiv für Lebensmittelhygiene 2000; 51: 115-117.

Zhu C, Shi J, Jiang C and Liu Y. Inhibition of

the growth and ochratoxinA production by *Aspergillus carbonarius* and *Aspergillus ochraceus in vitro* and *in vivo* through antagonistic yeasts. Food Control 2015; 50: 125-132.

Comparison of anaerobic sequencing batch reactor (ASBR) and anaerobic baffled reactor (ABR) configuration for biogas production of co-digestion process as a treatment option of concentrated latex wastewater

Thongchai Wongsuvan [1], Sumate Chaiprapat [2], Jarupat Kanjanarong[3] and Piyarat Boonsawang[1]*

[1]Biotechnology for Bioresource Utilization Laboratory, Department of Industrial Biotechnology, Faculty of Agro-Industry, Prince of Songkla University, Hat Yai, Songkhla, 90112, Thailand

[2]Department of Civil Engineering, Faculty of Engineering, Prince of Songkla University, Hat Yai Campus, Hat Yai, Songkhla 90112, Thailand

[3]Divison of Environmental Science, Faculty of Science and Technology, Rajamangala University of Technology Rattanakosin, Nakhon Pathom, 73170, Thailand; Corresponding author: e-mail: piyarat.b@psu.ac.th

ABSTRACT

This study focused on the improvement of the anaerobic digestion of concentrated latex wastewater (CW) via co-digestion process. In general, the low methane content in biogas production from CW was obtained due to low chemical oxygen demand/ sulfate (COD/SO_4^{2-}) ratio. In this study, the effect of co-digestion was investigated by the palm oil decanter cake (PDC) addition of 0.3, 0.6 and 0.9% TS with organic loading rate (OLR) of 0.89, 1.12 and 1.44 kg·COD/m^3·day. In addition, the performance of three different reactors; anaerobic sequencing batch reactor (ASBR) by propeller mixing (pASBR), ASBR with liquid recirculation (lASBR) and anaerobic baffled reactor (ABR) were compared. All experiments were operated at hydraulic retention time (HRT) of 10 day with semi-continuous mode at 28 ± 2 ºC. The result showed that pASBR gave the highest biogas production of 3,611 ml/day with the methane yield of 0.28 m^3 CH_4/$kgCOD_{added}$ at OLR of 1.44 kgCOD/m^3·day. Biogas production from the co-digestion process was 2.65-fold higher than

that from the mono digestion with only CW as substrate. The performance of lASBR and ABR systems was not stable. After 17 days, the biogas production gradually decreased probably due to the foaming on top of lASBR and the accumulation of solid in the bottom of ABR system. It should be noted that the pASBR system was the suitable reactor for the biogas production of co-digestion with PDC addition.

Keywords: Co-digestion, Palm oil decanter cake, Concentrated latex Wastewater, Biogas production

INTRODUCTION

The production of concentrated latex is increasing every year due to supply of exportation for worldwide which leads to the increasing amount of concentrated latex wastewater (CW). The concentrated latex processing generated 2.43 m^3 of wastewater per ton of product (Pollution Control Department, 2015) which caused of water and air pollution. The compositions of CW contained the high COD and sulfate contents with low pH. The high sulfate content was generated from recovering rubber particles in a waste stream by using sulfuric acid (H_2SO_4) (Saritpongteeraka and Chaiprapat, 2008). Presently, wastewater treatment systems in the concentrated latex industry use activated sludge, aerated lagoon, oxidation pond and anaerobic lagoon (Jawjit *et al.,* 2010). In the case of open system, a malodorous hydrogen sulfide gas caused by an anaerobic digestion of sulfate-rich wastewater was produced and caused complaint from nearby communities. Therefore, anaerobic close system becomes an attractive choice because it can prevent gas emission, requires low energy input for operation, and the organic pollutant converted to methane gas can be used readily as fuel. Suitable anaerobic technology for

this wastewater is needed (Saritpongteeraka and Chaiprapat., 2008; Kongjan *et al.*, 2014). However, the anaerobic reactor was not popular in latex industrial wastewater treatment due to low biogas production. A high content of sulfate in CW can inhibit the anaerobic process by two mechanisms; the substrate competition between sulfate reducing bacteria (SRB) and methane producing bacteria (MPB) and the direct inhibition of cell functions by soluble sulfides (Jeong *et al.*, 2008). One approach to increase the biogas production in the CW is the use the co-digestion process. Co-digestion is a methodology to apply for simultaneous treatment of several liquid and solid organic wastes. The addition of co-substrates is a solution to adjust nutrient content in waste composition and balance COD/sulfate ratio for microbial growth. The anaerobic process at COD/SO_4 ratio of 1.7 to 2.7 is the resulted in the high competition between SRB and MPB (Vossoughi *et al.*, 2003). Palm oil decanter cake (PDC) is a waste residue of palm oil mill, which was normally disposed by dumping in areas adjacent to the mill, or letting composted in the palm oil plantation (Chavalpalit *et al.*,2006). Therefore, PDC containing high total organic carbon with low sulfate content could be used to balance COD/SO_4^{2-} ratio for the anaerobic digestion of CW.

Several types of anaerobic digesters have been evaluated for treatment of CW in lab scale (Saritpongteeraka and Chaiprapat, 2008; Chaiprapat and Laklam, 2011; Kongjan *et al.*, 2014). The anaerobic baffled reactor (ABR) is a single reactor configuration with separated compartments. The concept of compartmentalization could employ the benefits of a stage separation (hydrolysis and methanogenesis), which protected shock load from high substrate loading in the first part of the reactor. Moreover, it is able to protect the biomass in the reactor from wash out (Barber and Stucky, 1999). Meanwhile, the anaerobic sequencing batch reactor (ASBR) is able to provide high organic removal. The concept of ASBR employs the

cyclic operation with feeding, reacting, settling and decanting, respectively. The settling phase is an important step for protection wash out. The potential of using ASBR system for treating CW has previously been compared with up-flow anaerobic sludge blanket (UASB). It was found that ASBR system showed the efficiency on sulfate removal higher than UASB system (Chaiprapat et *al.,* 2011).

Although, the biogas production improved by co-digestion process gave the effectiveness in batch assay. There has been no report for performance of ASBR and ABR system to improve biogas production from co-digestion of CW with PDC. This study aimed to investigate the comparison of ASBR and ABR for the production of biogas from the co-digestion of CW and PDC. Moreover, the suitable amount of PDC addition in CW was also examined.

METHODOLOGY

Waste material collection and preparation

The PDC was obtained from the palm oil mil industry located in Surathani province, Thailand. The CW was collected from the equalization pond of rubber latex industry in Songkhla province, Thailand. Both materials were kept at -20 ^{o}C until use. The anaerobic sludge used as inoculum was taken from an anaerobic digester at rubber latex industry, Songkhla province. The characterization of the wastewater and decanter cake is showed in Table 1

Reactors configuration

-Anaerobic baffled reactor (ABR)

Four laboratory-scales of ABR system was fabricated using stainless steel standard 304. The ABR consisted of 3 chambers (CH_1 - CH_3) of equal size, shape and volume, connected in series. They were arranged in 3 parallel sets as showed in Figure1a.

Table 1 The characterization of the wastewater and decanter cake

Parameters	CW	Parameters	PDC
pH	3.98	Moisture (%)	79.18
BOD_5 (mg/L)	2,970	Total solid (%)	20.82
TCOD (mg/L)	4,557	Total organic carbon (% dry basis)	46.35
SCOD (mg/L)	3,050	Volatile solid (% dry basis)	83.65
TS (mg/L)	8,045	Carbohydrate (% dry basis)	3.65
SS (mg/L)	635	Protein (% dry basis)	3.13
VS (mg/L)	5,665	Crude Fiber (% dry basis)	2.33
TKN (mg/L)	700	Oil & Grease (% dry basis)	10.67
NH_4^+-N (mg/L)	1,378	Total phosphorus (% dry basis)	0.41
SO_4^{2-} (mg/L)	3,326	Total potassium (% dry basis)	2.64
S^{2-} ion (mg/L)	29		

Note: CW; concentrated latex wastewater, PDC; palm oil decanter cake

The whole unit appeared square in shape with length to width ratio (l/w) of 1.0 and length × wide × high dimensions of 10 cm × 10 cm × 60 cm. To collect the biogas production, three separate gas manifolds was provided with the separate biogas. The individual chamber contained a hanging baffle to allow liquid connecting with the sludge at the bottom. The each side of bottom portion in each chamber was inclined at 45 °C. The total volume of the anaerobic baffled reactor (ABR) was 22.5 L with the working volume of 16.5 L. The volume of each chamber (CH_1-CH_3) was 5.5 L.

-Anaerobic sequencing batch reactor with liquid recirculates mixing (lASBR)

Four bench-scale lASBRs used in this study were constructed from stainless steel standard 304. The fermenter appeared square in shape with length to width ratio (l/w) of 1.0 and length × wide × high dimensions

of 10 cm × 10 cm × 60 cm. The total volume of lASBR was 6.5 L with the working volume of 5.5 L. A schematic representation of the reactor is given in Figure 1b. The lASBR was operated in the up flow mode and mixing was operated by ascending liquid recirculation (60 l/h) using a peristaltic pump. The outlet biogas tube from the headspace was connected to gas bag.

-Anaerobic sequencing batch reactor with propeller mixing (pASBR)

A schematic of the experimental apparatus is illustrated in Figure 1c. Four pASBR reactors were constructed from 15 cm internal diameter PVC tube with total volume of pASBR was 6.5 L (working volume of 5.5 L). The reactor was provided with three set of four-vertical-blade turbine impeller with 110 rpm.

Experimental setup

Three systems with twelve reactors were conducted by feeding the CW with the addition of 20,000 mg VSS/L of fresh sludge. The initial pH of CW was adjusted to 6.8 ± 0.3 by $NaHCO_3$. The systems were operated at room temperature 28 ± 2 ^oC under HRT of 10 day. CW was fed continuously one week before feeding PDC at varying concentration PDC of 0, 0.3, 0.6 and 0.9% (total solid). The ABRs were performed with a continuous mode with flow rate of wastewater of 1.65 L whereas ASBRs were performed with a sequencing batch mode (24 h per cycle). At the beginning of each cycle the reactor was fed with 0.55 L wastewater for 5 min with the recirculation pump turned off. The reaction step was 20 h with the recirculation pump turned on every 2 h for 5 min. The sedimentation step was 4 h and at the end of the cycle the 0.55 L of effluent was discharged in 5 min with the recirculation pump and motor turned off. All steps were performed by an automation system using on-off programmed timers. The systems reached a steady state condition when biogas production rate was 10% variation. Biogas production from each reactor was measured daily and a methane (CH_4)

content was analyzed only at steady-state condition.

Analytical methods

Routine analyses such as pH, volatile fatty acid (VFA), alkalinity and COD were determined according to Standard Methods (APHA, 2008). The CH_4 content and hydrogen sulfide in the head space of the reactor was measured using gas chromatography (GC-8A, Shimazu) with Porapak-Q column connected with a thermal conductivity detector (TCD), using helium as a carrier gas under isothermal conditions at 40/100 ^oC of oven and detector . The foam tendency was determined as percentage of foam remaining in the reactor at 1 h after mixing compared with the total volume of reactor. The solid accumulation was estimated as percentage of biogas production loss.

RESULTS AND DISCUSSION

The system performance for biogas production

The biogas production by the mono digestions of CW and the co-digestion of PDC with CW is showed in Figure 2. The biogas production profiles from only CW alone in all systems was similar (220-240 ml/L reactor·d) (Fig. 2a). The PDC addition enhanced the biogas production in the beginning of operation. However, the ABR efficiency continuously decreased with PDC addition after 5 days (Fig. 2b) Moreover, the biogas production was gradually decreased with increasing of PDC concentration to 0.6 and 0.9% respectively. The efficiency of lASBR and ABR system was showed that the system cannot operate continuously to digest organic matter of co-digestion process (Figure. 2c and 2d). However, the steady state condition achieved in pASBR system at PDC addition of 0.3-0.9%.

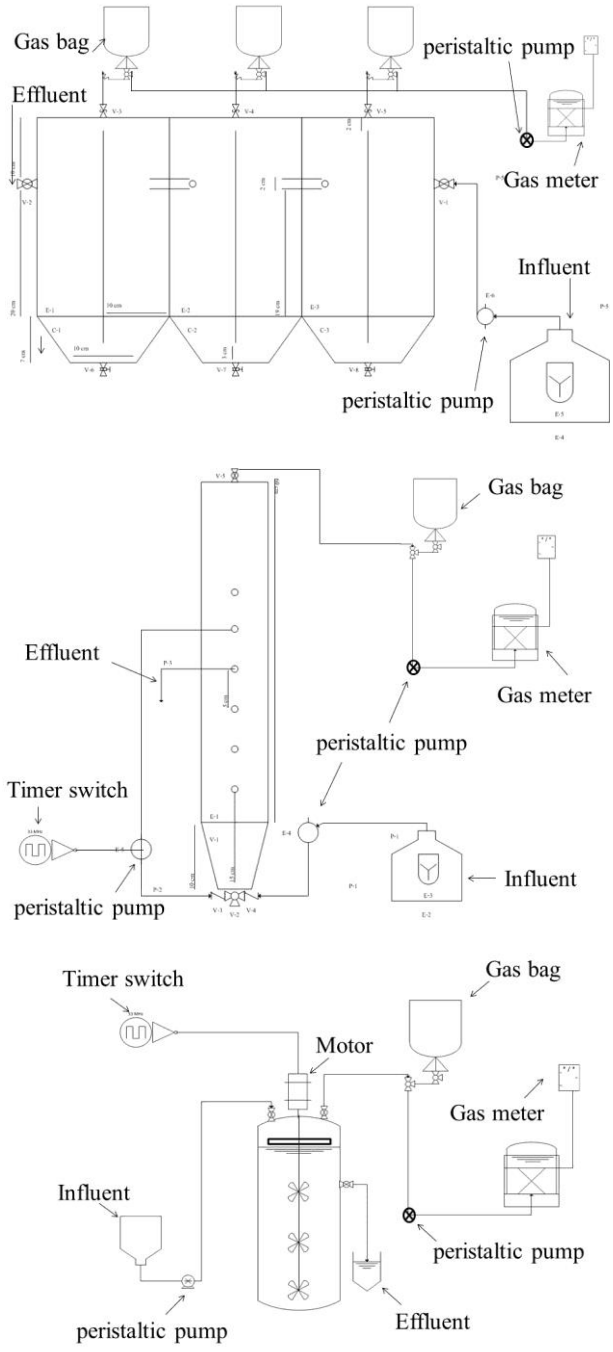

Figure 1 Schematic representation of the ABR (a), lASBR (b) and pASBR reactor (c) used in this study

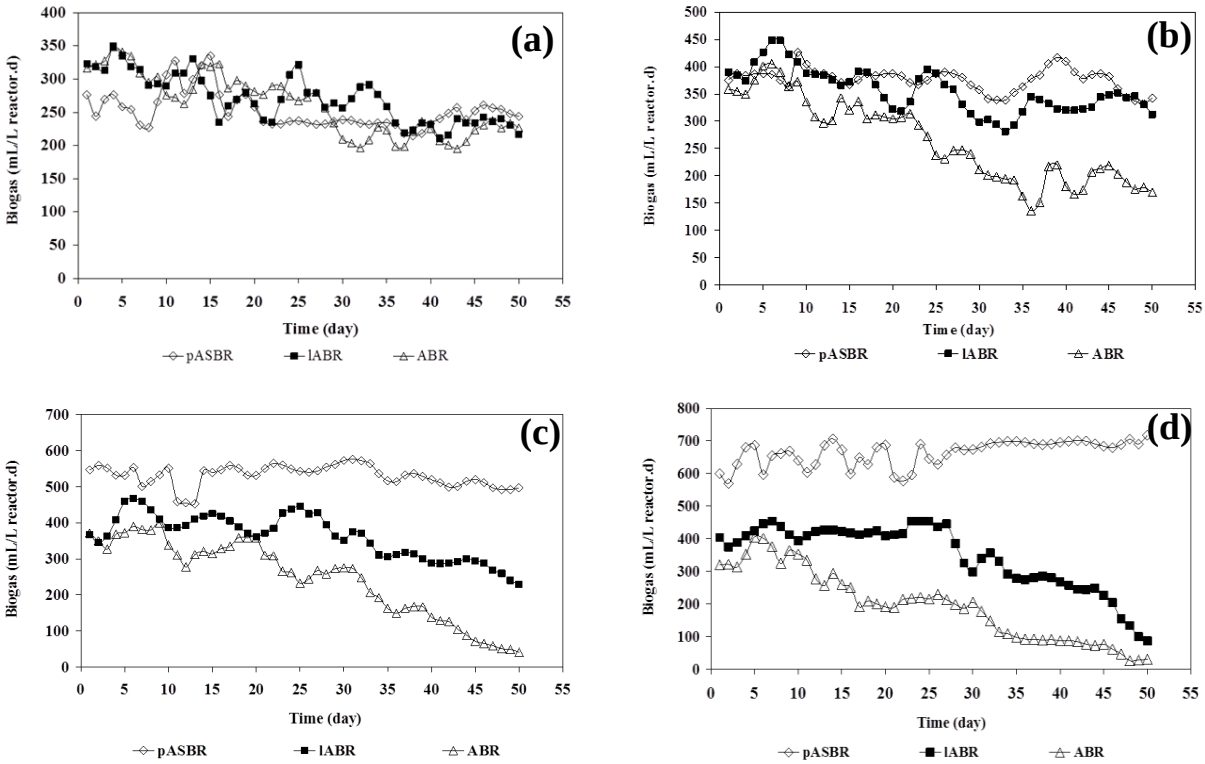

Figure 2 Biogas production rate from anaerobic digestion of different reactor configuration and variation percentage total solid (TS) of co-substrate; (a) CW alone, (b) CW+0.3% PDC, (c) CW+0.6% PDC and (d) CW+0.9% PDC

It indicated that the co-substrate digestion gave a better biogas production than those obtained from the digestion of mono-substrate (CW alone). The average biogas production varies between 385, 529 and 656 ml/L·reactor·day, after co-substrate concentration was increased to 0.3, 0.6 and 0.9 % TS, respectively using pASBR. The efficiency of pASBR was respond to specific production rate and composition of biogas showed in Table 3-2. Although the co-digestion process improved biogas production, hydrogen sulfide was still high due to more organic matter for SRB. These results indicated that the reactor configurations affected the substrate digestion of CW and PDC.

The system performance for COD removal and methane yield

The performance of reactors fed with CW and co-substrate of CW+PDC is summarized in Table 2. pASBR gave the higher COD removal than lASBR and ABR. The COD removal of 78.9-92.4% was obtained from pSBR whereas the COD removal of 62.3-72.0% was obtained from lABR and ABR. In pASBR, it was found that the increases of PCD addition resulted in the decreases of COD removal. According to methane yield, it was found that pASBR gave the highest methane yield of 0.24-0.28 $m^3 \cdot CH4_{.}$ $/KgCOD_{added}$ which was slightly lower theoretical value. The failure performance of lASBR and ABR system with low COD removal and methane yield was found. Therefore, it was necessary to consider other factors such as pH change and alkalinity of system. From Figure 3, the pH in both systems was 7.55-7.70 and alkalinity was about 3,100-5,000 mg $CaCO_3$/L. Moreover, it was found that the VFA/Alk ratio had a value in the range of 0.1 - 0.25 which ensures that no have acid accumulation. The optimum VFA/Alk ratio for anaerobic digestion must be less than 0.4 (Panpong *et al*., 2014)

For this reason, It can be noted that the substrate did not converted to fatty acid due to degradation of organic matter was not appeared. It results to biogas production will gradually decline. In other words, the configuration of lASBR and ABR obstructed the digestion of PDC and were not suitable for application of co-digestion process

Foaming and solid accumulation in reactors

Figure 4 presents the solid accumulation in ABR (Figure 4A) and foam generation in lASBR (Figure 4B). Forming was visible found in lASBR after feeding with co-substrate about two week but not in ABR and pASBR. The foam was forming in lASBR increased with the increasing PDC addition. This might affect the mass transfer between substrate and microorganism and resulted in low biogas production.

Table 2. Summary of pASBR, lASBR and ABR performance on co-digestion process.

	PDC addition (%)	OLR (kgCOD /m^3·day)	COD Removal (%)	Biogas Production rate (mL/l·reactor.d)	CH_4 yield (m^3·CH_4 /$KgCOD_{added}$)	CH_4 (%)	H_2S (ppm)
pASBR							
1	0	0.59	91.4	260	0.24	61.81	22,499
2	0.3	0.86	92.4	367	0.26	63.22	35,223
3	0.6	1.10	87.4	505	0.27	58.57	32,805
4	0.9	1.33	78.9	694	0.28	58.27	31,836
lASBR							
1	0	0.59	61.7	233	0.11	52.20	30,500
2	0.3	0.86	66.9	330	0.12	54.94	9,179
3	0.6	1.10	69.2	306	0.08	49.06	19,486
4	0.9	1.33	72.0	277	0.05	41.58	7,729
ABR							
1	0	0.59	64.7	218	0.31	61.31	8,090
2	0.3	0.86	70.9	180	0.13	48.51	15,873
3	0.6	1.10	69.7	167	0.07	38.41	11,698
4	0.9	1.33	62.3	95	0.03	29.42	19,017

The composition in PDC showed considerable potential to create foaming such as oil, grease, protein and fiber (suspended solid) (Boe *et al.*, 2012). Although foaming did not appearein ABR system but the solid was accumulated at the bottom of reactor. The increasing PDC resulted in the higher solid content in the effluent and at the bottom of reactor. It implied that the low digestion of substrate with the PDC addition. This corresponded to the low methane content and methane yield. We also found that the microbial sludge was changed from black to brown which results from the accumulation of PDC (Fig. 4A). This indicated the lower methane producing bacteria with the PDC addition.

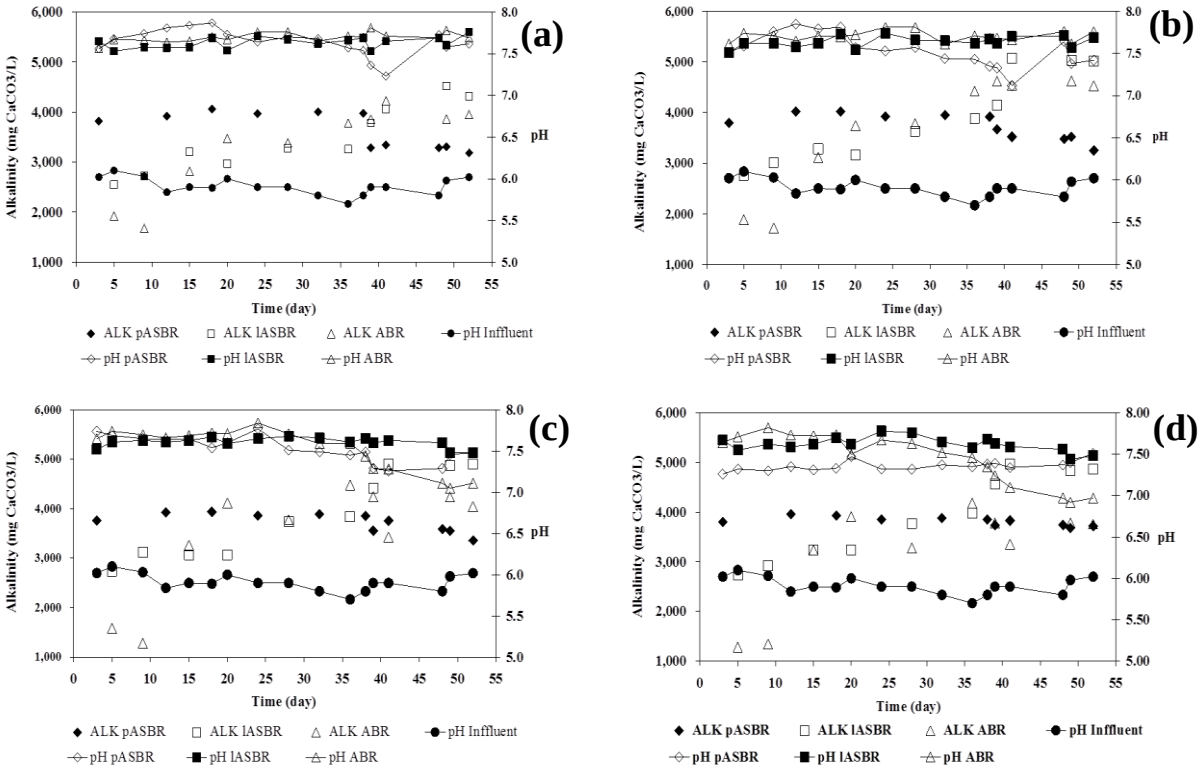

Figure 3 pH and Alkalinity profile of effluent from anaerobic digestion of different reactor configuration and variation percentage total solid (TS) of co-substrate; (a) CW alone, (b) CW+0.3% PDC, (c) CW+0.6% PDC and (d) CW+0.9% PDC

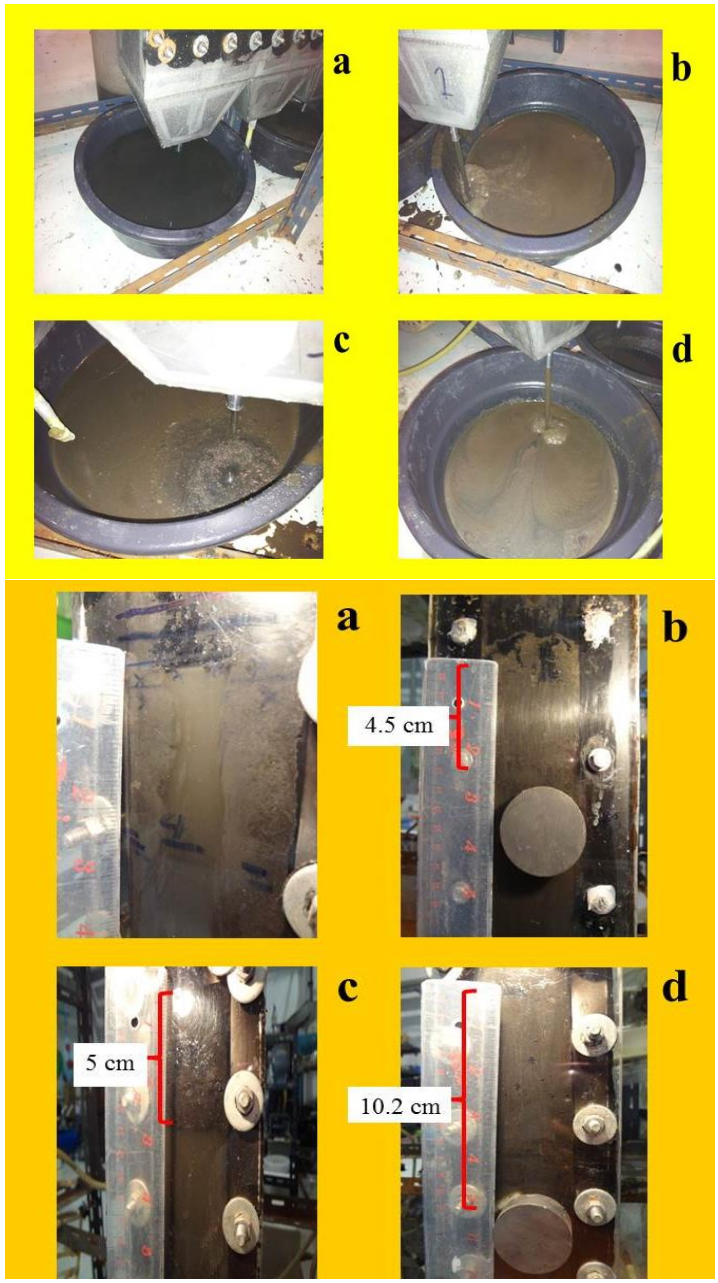

Figure 4 The appearance of solid accumulation in ABR system (A) and foaming in lASBR system (B) with the PDC addition of a) 0%, b) 0.3%, c) 0.6%, d) 0.9%.

CONCLUSIONS

pASBR with the propeller mixing was the good configuration of bioreactor for the biogas production from CW. Mixing system is important on contacting of microbial with substrate and reduced dead zone by break foam and complete mix. Moreover, the co-digestion of PDC and CW enhanced biogas production and methane yield. The configuration of lASBR and ABR were unsuitable for application of co-digestion process. The foaming and solid accumulation obstructed the microbial growth.

ACKNOWLEDGEMENTS

The authors wish to thank the graduate school, Prince of Songkla University and the Higher Education Research Promotion and National Research University Project of Thailand (ENG540559S), Office of the Higher Education Commission for providing financial support in this study and Dr. Jarupat Kanjanarong from Rajamangala University of Technology Rattanakosin for helpful discussion.

REFERENCES

APHA Standard methods for the examination of water and wastewater. 20th ed. Washington (DC), USA American Public Health Association; 1998.

Barber, W.P. and Stucky D.C. The use of anaerobic baffled reactor (ABR) for wastewater treatment: A review. Water Research 1999; 7: 1559-1578.

Boe, K., Kougias, P. G., Pacheco, F., O-Thong, S. and Angelidaki, I. Effect of substrates and intermediate compounds on foaming in manure digestion systems. Water Science and Technology 2012; 66: 2146-2154.

Chaiprapat, S., Preechalertmit, P., Boonsawang, P. and Karnchanawong, S. Sulfidogenesis in Pretreatment of High-Sulfate Acidic Wastewater Using Anaerobic Sequencing Batch Reactor and Upflow Anaerobic Sludge Blanket Reactor. Environmental Engineering Science 2011. 28(8): 597-604.

Chaiprapat, S. and Laklam, T. Enhancing digestion efficiency of POME in anaerobic sequencing batch reactor with ozonation pretreatment and cycle time reduction. Bioresource technology 2011; 102(5): 4061-4068.

Chavalparit O., Rulkens WH., Mol A.P.J. and Khaodhair S. Options for environmental sustainability of the crude palmoil industry in Thailand through enhancement of industrial ecosystems. Environment Development and Sustainability 2006; 8: 271–287.

Huajun, F., Lifang, H., Dan, S., Chengran, F., Yonghua, H. and Dongsheng, S. Effects of operational factors on soluble microbial products in a carrier anaerobic baffled reactor treating dilute wastewater. Journal of Environmental Sciences. 2008; 20: 690-695.

Jawjit S. and Liengchareonsit W. Anaerobic treatment of concentrated latex processing wastewater in two-stage upflow anaerobic sludge blanket. Canadian Journal of Civil Engineering 2010; 37: 805-813.

Jeong, T.Y., Cha, G.C., Seo, Y.C., Jeon, C. and Choi, S.S. Effect of COD/sulfate ratios on batch anaerobic digestion using waste activated sludge. Journal of Industrial and Engineering Chemistry 2008; 14: 693–697.

Katemanee, A. Appropriate technology evaluation for oil palm by-products utilization in Krabi province. Faculty of graduate study, Mahidol University. 2006; 1-89.

Kongjan. P., Jariyaboon. R. and O-Thong. S. Anaerobic digestion of skim latex serum (SLS) for hydrogen and methane production using a twostage process in a series of up-flow anaerobic sludge blanket (UASB) reactor. International journal of hydrogen energy 2014; 39: 19343-19348

Panpong, K., Srisuwan, G., O-Thong, S. and Kongjan, P. Anaerobic Co-digestion of canned seafood wastewater with glycerol waste for enhanced biogas production. Energy Procedia 2014; 52: 328–336.

Pollution Control Department. Ministry of Natural Resources and Environment. Good practices in the prevention and reduction of pollution in industrial latex. http://www.pcd.go.th/count/waterdl.cfm?FileName=rubbertree.pdf. (Accessed on 27 April 2018).

Saritpongteeraka, K. and Chaiprapat, S. Effects of pH djustment by parawood ash and effluent recycle ratio on the performance of anaerobic baffled reactors treating high sulfate wastewater. Bioresource Technology 2008; 99: 8987-8994.

Vossoughi, M., Shakeri, M. and Alemzadeh, I. Performance of anaerobic baffled reactor treating synthetic wastewater influenced by decreasing COD/SO_4 ratios. Chemical Engineering and Processing: Process Intensification 2003; 42: 811 – 816.

Relationship between habitat characteristics and immature mosquitoes and their natural predators in Chiang mai city

Panipak Saetan[1], Decha Tapanya[2], and Chitchol Phalaraksh[2*]

[1]Master's Degree Program in Environmental Science, Environmental Science Research Center (ESRC), Faculty of Science, Chiang Mai University, Chiang Mai, 50200, Thailand

[2]Department of Biology, Faculty of Science, Chiang Mai University, Chiang Mai, 50200, Thailand

[*]Corresponding author's E-mail: chitcholp@gmail.com

ABSTRACT

The study of mosquito's habitat is very important in order to predict risk associated to humans and to reduce the mosquito population by biological means. Biological control can be potentially applied at the larval stage of mosquito. This study was aimed to investigate the relationship between habitat types, immature mosquitoes and their predators. Eleven (11) sampling sites were selected in Chiang mai city considering permanent habitats of immature mosquitoes and their predators. Mosquito larvae were collected using standard dipping method. The D-frame net was used to collect mosquito predators. Physico-chemical parameters were measured *in situ* and in laboratory. For biological data, 9,354 mosquito larvae were collected from 11 study sites belonging to 3 genera of *Culex*, *Lutzia*, and *Mimomyia*. The damselfly nymph (Odonata) was the most abundant macro-invertebrate predator (Protoneuridae, 71.7% and Coenagrionidae, 13.3%). Whilst, the mosquito fish, *Gambusia* spp. (15%) was one of abundant vertebrate predator in some habitats. The result showed that the mosquito larvae and their predators have high tolerance to survive in highly polluted water. It is expected that, the findings from this research will help to predict the oviposition sites and accordingly design mosquito larval control programs.

Keywords: mosquito larvae, predators, water quality, habitat characteristic, biocontrol

INTRODUCTION

Approximately 3,400 mosquito species have been recorded worldwide (Manguin and Boëte, 2011). One of the major concerns related to mosquitoes that responsible for the transmission of numerous serious pathogens to human and animals (Wilke *et al.*, 2017) such as dengue fever, malaria, and chikungunya. South and South-east Asian countries have experienced large outbreaks of mosquito-borne infectious diseases mainly due to impact of climate change affecting temperature and precipitation. Therefore, it is important to understand the impact of climate change on mosquito population. Human activities have major impact on environment. The growth of economic activity, tourism, and human migration is leading to ever more cases of the movement of both disease vectors and the pathogens (Tatem *et al.*, 2006; Servadioab *et al.*, 2018). Biodiversity of mosquitos is on the rise around the world (Manguin and Boëte, 2011). Members of the Aedes and Culex genera, which includes many important vectors of mosquito-borne diseases, are highly invasive and adaptive to man-made environments (Wilke *et al.*, 2017). Water quality is one of the important factors that directly influences the health of human and all other organisms. The impact of urban area with high organic and nutrient are positive loading for mosquito abundance. With increase in salinity and conductivity there is corresponding increase in density of *Anopheles* mosquito (Ma *et al.*, 2016; Emidi *et al.*, 2017). Light and vegetation is one habitat characteristics appropriate with *An. Culicifacies* (Piyaratne *et al.*, 2005). The biological control is a technique to control mosquitoes

using another organism to feed on them. The abundance of such predators is influenced by dissolved oxygen, temperature and turbidity of water (Dida *et al.*, 2015). Poecillidae (vertebrate), damselfly nymph (Odonata) and Hemiptera are some of the known mosquito predators (Wongsiri, 1982). The purpose of this research is to study the impacts of environmental factors on distribution of immature mosquitoes and their aquatic predators in its permanent habitat around Chaing mai city. The objective of this study is to find relationship between habitat, immature mosquitoes, and its predators.

METHODOLOGY

Study area

The study was conducted in Chiang Mai City (18°48′37″E 98°58′4″N), 320 m above sea level located at northern part of Thailand. It has an average annual precipitation of 1,157.21 mm (2003-2015). The extreme high temperature was 42.4°C and extreme minimum temperature 9.8°C (Meteorological department, Thailand). The sampling was surveyed permanent habitat with different types of habitats in 11 sites around Chiang Mai city in area 36 km^2 (Figure 1).

Figure 1 Study site location (Chiang Mai City)

Mosquito and predator collection

Immature mosquitoes and their predator were collected in February 2019. Mosquitoes samples were collected using standard dipping method (500 mL) (6 dips per site). Immature mosquitoes were brought to laboratory and identified using Rattanrithikul *et al.* (2005) keys. Aquatic predators were collected using D-frame dip net (4 dips per site) and preserved in 95% alcohol and brought to laboratory and identified to family level using stereomicroscope.

Water quality study of immature mosquito and predator

Water samples were collected from all sites where immature mosquitoes and predators were found. Physico-chemical parameters like dissolved oxygen, air temperature, water temperature, pH, electrical conductivity, light intensity, salinity and turbidity were measured at site, using multiparameter. Whereas, nitrate-nitrogen, ammonia-nitrogen, *ortho*-phosphate, and 5-day biochemical oxygen demand were analyzed in laboratory.

Data analysis

The mean of difference among various physico-chemical parameters in eleven sampling sites were determined using ANOVA (analysis of variance). Chi-square test was used to analyze between the number of mosquito and predator and to find correlation between mosquito and predator with habitat types (standing water or running water, wall of habitat, vegetation, and shading). Pearson correlation coefficient was used to find correlation between physico-chemical with mosquito and predator.

RESULTS AND DISCUSSION

Mosquito and predator collection

A total of 9,354 immature mosquito samples belonging to three genera were identified. 59 predators were collected (51 belonging to Protoneuridae, Coenagrionidae of order Odonata) and 8 mosquito eating fishes were identified from all 11 sampling sites. *Culex* was found in all 11 sites, while *Lutzia* and *Mimomyia*

were found only in 1 site (9.10%). Predator, Odonata (Protoneuridae) was found only in one site (9.10%) and Coenagrionidae in two sites (18.18%), while *Gambusia* was found in two sampling sites (18.18%) as shown in Table 1.

The population of immature mosquitos and predators were significantly different (Chi-square test, $p < 0.0001$). Habitat types (running and standing water, concrete wall, vegetation, shade) were not significantly different with *Culex*, *Lutzia*, and *Mimomyoia* mosquitoes as same as the case of Protoneuridae, Coenagrionidae, and Gambusia ($p > 0.05$)

Table 1 The number of immature mosquitoes and predators found in 11 sites

	Mosquito			**Predator**		
Site*	*Culex*	*Lutzia*	*Mimomyia*	Protoneuridae	Coenagrionidae	*Gambusia*
Cp1	153	0	0	0	0	0
Sp1	745	0	0	0	0	0
Pt1	1086	0	0	7	0	0
Cm1	576	0	0	0	0	0
Su1	5	0	0	0	43	0
Ck1	577	0	0	0	0	0
Ck2	333	0	0	0	0	7
Ck3	32	0	0	0	0	0
Ck4	964	0	0	0	0	2
Pd1	3200	0	0	0	0	0
Nh1	1683	2	1	0	1	0

*Cp=Change phueak, Sp=Sri phum, Pt=Pa tan, Cm=Chiang moi, Suthep, Chang khland, Pd=Pa daet, Nh=Nong hoi sub-district.

Physicochemical characteristics

The physico-chemical parameters of all 11 sites were measured. The water temperature ranged from 23℃ to 30 ℃. The water pH was 7.0 to 7.5. The highest dissolved oxygen recorded in Cm1 (4.60 ± 0 mg/L) and Su1 (1.63 ± 0.02 mg/L). A significant different in mean DO was determined among the 11 sites types (ANOVA, d.f.= 10, 22, $p < 0.001$). Turbidity with highest level found in sites Sp1 (337 ± 5 NTU) and found less in Nh1 (27 ± 0.29). ANOVA test a significant different in turbidity among 11 sites (ANOVA, d.f. = 10, 22, $p < 0.001$). The range of conductivity recorded between 703 μS/cm to 349 μS/cm. There was significant difference in mean of NO3-N, NH3-N, and O-PO43- with different sampling sites (ANOVA, d.f. = 10, 22, $p < 0.001$). The highest of NO3-N value measured in Cp1 in 28.82 ± 0.16 mg/L and Ck2 (22.00 ± 0.93 mg/ L). Ranging among 11 sites of measured in NH3-N record between 6.30 ± 1.00 mg/L, to 0.20 ± 0.40 mg/L. Ortho-phosphate highest in Cp1 with 10.45 ± 2.11 mg/L follow by Nh1 (8.59 ± 0.94 mg/L), and Pd1 (6.86 ± 1.82 mg/L). A significant different between mean of BOD5 among sampling sites was found, the values ranged between 89.72 ± 1.40 mg/L, to 23.60 ± 0.40 mg/L (ANOVA, d.f. = 10, 22, $p < 0.001$) as shown in Table 2.

Pearson correlation of the physico-chemical parameters with number of mosquito and predator in aquatic habitat

In the study, Pearson correlation was used to analyze the relationship between number of mosquitoes and predator with environmental parameters in aquatic habitat. We found that *Culex* mosquito had positive significant relationship with ortho-phosphate ($r = .357$, $p = .041$) but it was negative significant relationship with turbidity ($r = -.681$, $p = .0001$) and dissolved oxygen ($r = -.352$, $p = .044$), while *Lutzia* and *Mimomyia* mosquito were significant positive with ortho-phosphate ($r = .399$, $p = .022$), pH ($r = .434$, $p = .012$),

Table 2 Mean and standard deviation of physicochemical characteristics of immature mosquito and predator aquatic habitats

	Parameter**											
Site (n=11)	**AT** (°C)	**WT** (°C)	**pH** (-)	**LI** (LUX)	**Turbidity** (NTU)	**EC** (µS/cm)	**TDS** (mg/L)	**DO** (mg/L)	**Salinity** (ppt)	**NO_3-N** (mg/L)	**NH_3-N** (mg/L)	**PO_4^{3-}** (mg/L)	**BOD_5** (mg/L)
Cp1	32 ± 0	27.70 ±0	7.05 ±0	119053 ±6796.30	151 ±1	686 ±0	439 ±0	1.04 ±0	0.30 ± 0	5.80 ± 0.80	28.82 ±0.16	10.45 ± 2.11	89.72 ± 1.40
Sp1	33 ±0	26.10 ±0	7.23 ±0	72712 ±7063.00	337 ±5	591 ±1	377 ±0	0.68 ±0	0.30 ± 0	6.30 ± 1	21.89 ±0	6.51 ±0	54.80 ±1.00
Pt1	33 ±0	30.00 ±0	7.28 ±0	57753 ±6573.00	81 ±0	694 ±1	445 ±0	0.63 ±0	0.03 ±0	4.90 ±1	16.40 ±0	7.14 ±0	28.87 ±1.00
Cm1	32 ±0	28.15 ±0	7.46 ±0	54597 ±4022.60	75 ±0.55	349 ±0	227 ±0	4.60 ±0	0.20 ±0	4.20 ±0	6.42 ±0.14	1.66 ±0.08	23.60 ±0.40
Su1	25 ±0	23.00 ±0	7.05 ±0	40533 ±351.19	131 ±1.53	683 ±0	436 ±0	1.63 ±0.02	0.30 ±0	2.33 ±0.40	11.92 ±0.15	5.20 ±0.18	28.04 ±0.80
Ck1	32 ±0	27.90 ±0	7.36 ±0	40979 ±1497.50	82 ±0.10	730 ±0	467 ±0.60	0.50 ±0	0.40 ±0	0.20 ±0.4	21.80 ±0.20	5.80 ±0.70	49.70 ±6.70

Table 2 Mean and standard deviation of physicochemical characteristics of immature mosquito and predator aquatic habitats (continue)

	Parameter*											
Site (n=11)	**AT** (°C)	**WT** (°C)	**pH** (-)	**LI** (LUX)	**Turbidity** (NTU)	**EC** (µS/cm)	**TDS** (mg/L)	**DO** (mg/L)	**Salinity** (ppt)	**NO_3-N** (mg/L)	**NH_3-N** (mg/L)	**PO_4^{3-}** (mg/L)	**BOD_5** (mg/L)
Ck2	32 ±0	26.00 ±0	7.54 ±0	24780.67 ±1407.15	94 ±0.58	666 ±0	425 ±0	0.62 ±0	0.30 ±0	5.83 ±0.40	22.00 ±0.93	6.58 ±0.28	51.87 ±0.46
Ck3	32 ±0	28.00 ±0	7.41 ±0	20989 ±617.25	91 ±0.57	514 ±0	329 ±0	1.29 ±0.15	0.20 ±0	0.70 ±0	16.38 ±1.21	3.87 ±0.40	60.67 ±2.34
Ck4	23 ±0	26.00 ±0	7.17 ±0	29800 ±173.20	75 ±0.05	613 ±0	393 ±0	1.48 ±0	0.30 ±0	0.26 ±0.38	13.93 ±0.25	5.06 ±0.22	52.69 ±0.56
Pd1	23 ±0	26.50 ±0	7.16 ±0	18312 ±173.79	52 ±0.64	598 ±0	382 ±0	0.81 ±0.02	0.30 ±0	0.47 ±0.4	19.88 ±0.12	6.86 ±1.82	35.33 ±2.31
Nh1	24 ±0	23.67 ±0	7.46 ±0	79186 ±0	27 ±0.29	563 ±0	361 ±0	0.98 ±0	0.30 ±0	0.47 ±0.40	22.19 ±1.64	8.59 ±0.94	39.40 ±1.21

* AT=air temperature, WT=water temperature, LI=light intensity, EC=electrical conductivity, TDS=total dissolved solids, DO= dissolved oxygen, NO_3-N=nitrate-nitrogen NH_3-N=ammonia-nitrogen, PO_4^{3-}=*ortho*-phosphate, $BOD_{5=}$5-day biochemical oxygen demand

Table 3 ***Pearson correlation of the physico-chemical parameters***

		Mosquito			Predator		
Parameter*		*Culex*	*Lutzia*	*Mimomyia*	Protoneuridae	Coenagrionidae	*Gambusia*
AT	r	-.244	-.316	-.316	.474	-.384	.156
	p	.171	.073	.073	.005	.027	.385
WT	r	.036	-.401	-.401	.501	-.676	.365
	p	.840	.021	.021	.003	0.000	.037
pH	r	.114	.434	.434	-.033	-.072	.261
	p	.529	.012	.012	.854	.691	.143
LI	r	.031	.382	.382	.166	.204	-.296
	p	.865	.028	.028	.355	.255	.095
Turbidity	r	-.681	-.499	-.499	-.100	-.094	.067
	p	.000	.003	.003	.580	.602	.710
EC	r	-.064	-.300	-.300	.400	-.404	.135
	p	.725	.090	.090	.021	.823	.455
TDS	r	-.064	-.300	-.300	.400	-.040	.135
	p	.725	.090	.090	.021	.823	.454
DO	r	-.352	.000	.000	-.316	.323	-.269
	p	.044	1.000	1.000	.073	.067	.130
Salinity	r	.290	.064	.064	.064	.095	.129
	P	.101	.724	.724	.724	.600	.474
NO_3-N	r	-.309	-.292	-.292	.219	-.197	-.455
	p	.080	.099	.099	.221	.272	.009
NH_3-N	r	.094	.222	.222	-.166	-.173	.099
	p	.604	.215	.215	.355	.335	.585
O-PO_4^{3-}	r	.357	.399	.399	.260	.094	-.305
	p	.041	.022	.022	.143	.602	.085
BOD_5	r	-.238	-.100	-.100	-.321	-.372	.381
	p	.183	.581	.581	.068	.033	.029

*AT=air temperature, WT=water temperature, LI=light intensity, EC=electrical conductivity, TDS=total dissolved solids, DO= dissolved oxygen, NO_3-N=nitrate-nitrogen NH_3-N=ammonia-nitrogen, PO_4^{3-}=ortho-phosphate, BOD_5=5-day biochemical oxygen demand

and light intensity (r = .382, p =.028) but negative significant with water temperature (r = -.401, p =.021) and turbidity (r = -.499, p =.003). In part of aquatic predator, we found that Protoneuridae had positive significant with air temperature (r = .474, p = .005), water temperature (r = .501, p = .003), electrical conductivity (r = .400, p = .021), turbidity (r = .400, p = .021), while Coenagrionidae had negative significant relationship with air temperature (r = -.384, p = .027) and water temperature (r = -.676, p = .000) and 5-day biochemical oxygen demand (r = -.372, p = .033). *Gambusia* fish had positive significant with water temperature (r = .365, p = .037) and 5-day biochemical oxygen demand (r = .381, p = .029) but negative significant with nitrate nitrogen (r = -.455, p = .009) as shown in Table 3.

Discussion

Culex mosquito can transmit Japanese encephalitis, Lymphatic filariasis, West Nile fever (WHO, 2017). In this study we found that, *Culex* had highest distribution, while *Lutzia* and *Mimomyia* were least found in all sites. *Culex* immature mosquitoes were found both in standing and running water but *Lutzia* and *Mimomyia* were captured in standing water. *Luzia fuscana* can find in habitat including swamps, marshes, rice fields, ditches, rock and flood pools. Larval stages of the mosquito *Lutzia fuscana* can act like as a biological control of mosquitoes that can feed in *Culex quinquefasciatus* larvae (Singh *et al.*, 2014). *Culex* mosquito was found permanent habitat, which was similarly reported by Vanlalruia *et al*. (2014). Abiotic factors (wall of habitat, shade, and vegetation) had no impact on number of mosquitoes and predators. However, Bashar *et al*. (2016) found *Culex* mosquitoes preferred areas which were exposed, partial shady, and shady but *Aedes* were not found in habitat that were exposed. In this study we found predators both macro- invertebrate and vertebrate. Dameselflies of suborder Zygoptera Coenagrionidae and Protoneuridae were captured in

this study. The habitat of Coenagrionidae were found in ponds and flowing water with vegetation at the margins because it has high tolerance and lives in polluted water (Bouchard, 2004). Similarly, we found Coenagrionidae in standing water with vegetation cover of habitat. Small fish were found in habitat with running water with open area. The 3 families of mosquito predatory fish were found by Wongsiri (1982) including Poecilidae, Anabantidae, and Cyprinodantidae. Ammonia nitrogen level in water can have an impact on aquatic life. However, in this study, we did not find any relationship between NH_3-N with neither mosquito nor predator. In similar studies in past, Bashar *et al*. (2016) reported no association of NH_3-N with *Culex* spp., *Aedes* spp., and *Anopheles* spp.; while, Ma *et a*l. (2016) found positive relationship between NH_3-N with larvae density. Ortho-phosphate showed positive relationship with density of immature mosquitoes and predators. We found negative relationship for dissolved oxygen and Culex mosquitoes which was also similarly reported by Bashar *et al*. (2016) and Ma *et al*. (2016). This shows that, mosquito larvae can live in habitats with low level of oxygen. Because of mosquito have a structure call “siphon” that it can absorb oxygen from air. Water temperature and BOD_5 showed positive relationship with small fish. Thailand Standards for waste water from urban area must contain less than 20 mg/L of NH_3-N but in this study, we found that, NH_3-N level ranging from 23 mg/L to 89.72 mg/L. We found that, in places with huge number of predators had lower number of mosquitoes. However, other factors like habitat characteristics also may have determine the mosquito population.

CONCLUSION

Culex mosquitoes was most abundant in and around Chiang Mai city. It was found that both mosquitoes and predators share similar habitats, which shows that applicability of biological control in areas with high risk of vector borne diseases.

ACKNOWLEDGEMENTS

This research has been supported by Center of excellence on Biodiversity (BDC), Office of higher Education Commission (BDC-PG2-160010). Special thanks to the staffs of Environmental Science Research Center (ESRC) and Freshwater Biomonitoring Research Laboratory (FBRL) for their kind support at field.

REFERENCES

Bashar, M. S. Rahman, Md. S. Nodi, I. J., & Howlader, A. J. (2016). Species composition and habitat characterization of mosquito (Diptera: Culicidae) larvae in semi-urban areas of Dhaka, Bangladesh. Pathogens and Global Health, 48-61.

Bouchard RW. (2014). Guide to aquatic macroinvertebrated of the upper Midwest. St. paul, MN: water Resources Center, university of Minnosota.

Dida, G. O., Gelder, F. B., Anyona, D. N., Abuom, P. O., Onyuka, J. O., Matano, A., Adoka, S. O., kanangire, C. K., Owuor, P. O., Ouma, C. & Ofulla A. V.(2015). Presence and distribution of mosquito larvae predators and factors influencing their abundance along the Mara River, Kenya and Tanzania. Springerplus, 1-14.

Emidi, B., Kisinza, W. N., Mmbando, B. Malima, R., & Mosha, F. W. (2017). Effect of physicochemical parameters on Anopheles and Culex mosquito larvae abundance in different breeding sites in a rural setting of Muherza, Tanzania. Parasites & vectors, 1-12.

Ma, M., Huang, M., & Leng, P. (2016). Abundance and distribution of immature mosquitoes in urban rivers proximate to their larval habitats. Acta Tropica, 121-129.

Manguin, S., & Boëte, C. (2011). Global Impact of Mosquito Biodiversity, Human Vector- Borne Diseases and Environmental Change. In J.LÃ³pez-Pujol, The Importance of Biological Interactions in the Study o Biodiversity, 27-49.

Rattanarithikul, R., Harrison, BA., Panthusiri P., & Coleman, RE. (2005). Illustrated keys to the mosquitoes of Thailand I. Southeast Asian J Trop Med Public Health, 1-80.

Servadio, J. L., Rosenthal, S. R., Carlson, L., & Bauer, C. (2018). Climate patterns and mosquito-borne disease outbreaks in South and Southeast Asia. Journal of Infection and Public Health, 566-571.

Tatem, A. J., Rogers, D., & Hay, S. I. (2006). Global Transport Networks and

Infectious Disease Spread. Advances in Parasitology, 293-343. doi: 10.1016/S0065-308X(05)62009-X

Vanlalruia, K. Senthilkumar, N., & Gurusubramanian, G. (2014). Diversity and abundane of mosquito species in ralation to their larval habitats in Mizoram, North Eastern Himalayan region. Acta Tropica, 1-18.

Wilke, A. B. B., Medeiros-Sousa, A. R., Ceretti-Junior, W., Marrelli, M. T. (2017). Mosquito populations dynamics associated with climate variations. Acta Tropical, 343-350., https://doi.org/10.1016/j.actatropica. 2016.10.025

Wongsiri, S., (1982). Preliminary survey of the natural enemies of mosquitoes in Thailand. Journal of the Science Society of Thailand, 205-213.

World Health Organization. (2017). Retrieved from world health organization: [Website]. From URL http://www.who.int/en/news-room/fact-sheets/detail/vector-borne-diseases

Isolation of crude oil-degrading bacteria and bioremediation of crude oil-contaminated soil microcosms

Wannarak Nopcharoenkul[1*]

[1*]Division of Environmental Technology Department of Agro-Industrial, Food, and Environmental Technology, Faculty of Applied Science, King Mongkut's University of Technology North Bangkok, Thailand;
Corresponding author: e-mail: wannarak.n@sci.kmutnb.ac.th

ABSTRACT

The problem of crude oil contaminated environment is originated from the accidental release of crude oil from production unit and distribution processes. Crude oil contains many toxic compounds, which impact all living organisms. Bioremediation is one option to clean up the environment by using microorganism. In this study, five mixed bacterial consortiums were isolated from five petroleum-contaminated sites by enrichment technique with crude oil. The results of crude oil degrading capability were obtained from five consortiums around 96, 70, 46, 79 and 76%, respectively, of 4,500 mg/L crude oil in liquid cultures was degraded within 9 days. The consortiums #1 was the most effective in degrading crude oil. In addition, the consortiums #1 can produce biosurfactant, which emulsifying activity index with crude oil was 39%. Moreover, the mixed bacterial consortiums #1 was applied in soil microcosms. The consortiums could also degrade crude oil about 87% of the initial concentrations at 20,000 mg/kg soil within 4 weeks. The results showed that these consortiums could be used for environmental bioremediation.

Keywords: Crude oil-degrading bacteria, Bioremediation, Soil microcosms

INTRODUCTION

Growth of the economy means increased demand for crude oil and petroleum products. This rises in chance for crude oil contamination in the environment (Onwurah et al., 2007). Crude oil contains many different kinds of organic compounds, of which some components are persistent toxic substances. They can accumulate in food chains, potentially causing health problems (Briggs and Briggs, 2018). Bioremediation is one of the effective petroleum hydrocarbon remediation methods. This process uses living microbes to break down or transform harmful substances into less toxic or nontoxic compounds. Microorganisms are essential key factor to clean up the environment (Endeshaw et al., 2017). However, the single bacterial strain usually had low efficiency. Due to the combined activities of different bacteria, bacterial consortia can enhance degradation activity and increase resistance on environmental stress factors. Moreover, a variety of enzymatic system can aggregate for biodegradation of various petroleum components (Olajire and Essien, 2014). Enhanced bioremediation involves the addition of activated carbon to increase hydrocarbon biodegradation rate. Activated carbon have been shown to reduce toxicity and improve aeration which stimulated an increase in microbial growth rate and activities(Agarry et al., 2015). Therefore, the objective of this study was to isolate crude oil degrading bacteria from petroleum contaminated soil, select the efficient strains for development of mixed bacterial inoculum, and apply them to clean up soil contaminated with crude oil in microcosm.

METHODOLOGY

Sampling

Petroleum contaminated soil samples were collected from five garages, 1 site in Nonthaburi, 1 site in Chonburi and 3 sites in Bangkok, Thailand. At each sampling point, the soil was collected at depths of 0-10 cm using a sterile hand auger and put in a

plastic bottle and then kept in the refrigerator at 4°C prior to use.

Isolation of crude oil-degrading bacteria

Crude oil degrading bacteria were isolated from samples by the enrichment culture technique, 5 g of each soil sample was transferred into Erlenmeyer flask containing 50 mL of carbon free mineral medium (CFMM) (Habe et al., 2004) contain with 1 mL crude oil as carbon source. Light crude oil was obtained from Bongkot fields *in the Gulf of Thailand.* The culture medium was cultivated at room temperature with shaking at 150 rpm for 7 days. Then, 5 mL of supernatant was transferred into fresh CFMM with crude oil, incubated under similar condition. After cultivation for 7 days, 1 mL of supernatant was spreaded on CFMM with crude oil on surface agar plate and incubated at room temperature for 7 days. The bacterial colonies of different morphologies were selected and purified by cross-streak techniques on nutrient agar.

Screening of crude oil degrading bacteria

Isolated bacteria were inoculated in 5 mL of CFMM broth contain with 1.0% (v/v) crude oil and incubated 7 days at 150 rpm and room temperature. Growth efficiency in crude oil as carbon source in CFMM broth was monitored by culture turbidity and compared to non-inoculated control. The crude oil-degrading bacteria show high turbidity and were selected for the next experiment.

Crude oil degradation efficiency of mixed bacterial consortium

The mixed bacterial consortium was a mixture of all isolates from one sample site. It was prepared as follow; each bacteria were grown separately in nutrient broth at room temperature and 150 rpm for 24 hours. After that, the bacteria were harvested, washed and resuspended in 0.85% NaCl. Approx. 10^8 CFU/mL of each bacterial suspension was mixed in equal proportion before inoculating in 50 of CFMM broth containing crude oil at 4500 mg/L,

incubated for 10 days at 150 rpm and room temperature. A medium no inoculant served as abiotic control. After that, the remaining crude oil was assessed by gravimetric method after extracted twice with an equal volume of n-hexane and the solvent phase was dried (Rajakovic et al., 2007; Parthipan et al., 2017). Crude oil degrading bacteria were enumerated on CFMM agar containing crude oil. The crude oil removal efficiency was calculated according to the following equation: % crude oil removal efficiency = [(the oil weight of abiotic control - the residual oil weight of the treatments)/the oil weight of abiotic control] ×100.

Biosurfactant producing test of mixed bacterial consortium

Biosurfactant production was assessed in liquid culture conditions. The mixed bacterial consortium was cultivated in CFMM with 4500 mg/L of crude oil incubated for 7 days at 150 rpm and room temperature. After that, the culture broth was centrifuged at 8000 rpm at 4^{o}C for 10 min and the supernatant was carried out for evaluation of the biosurfactant activity. The emulsification of biosurfactant was determined by measuring the emulsification index (E24). Two mL of crude oil was added to 2 mL of the supernatant in a flat bottom tube and vortexed vigorously for 2 min and incubated at room temperature for 24 hours (Cooper and Goldenberg, 1987). The E24 was calculated according to the equation: E24 = the height of the emulsified layer /total height of liquid × 100.

Application of the mixed bacterial consortium for crude oil degradation in soil microcosms

The efficient consortium was selected for remediation of crude oil contaminated soil in microcosms. The soil sample used was collected from a garden in Nonthaburi, Thailand. The sample had a clay texture (35% sand: 20% silt: 45% clay), pH 6.79 and ratio of C: N: P = 100: 4.7: 4.2. The soil was air-dried and sieved through a 2 mm sieve size prior to removing large debris. A microcosm was prepared by

transferring 50 g of soil to each 500 mL-glass bottle supplemented with crude oil at a final concentration of 20,000 mg/kg. Microcosms were set up into four groups of treatments consisting of biostimulation (BS) by adding 1 g of granular activated carbon, bioaugmentation (BA) by adding the bacteria consortium (at 10^7CFU/g of the final concentration), biostimulation and bioaugmentation (BSBA) by adding 1 g of granular activated carbon with the bacteria consortium (at the final concentration of 10^7 CFU/g) and natural attenuation control (NAC) without the additives. Microcosms were incubated in the dark at room temperature for 4 weeks. Each microcosm was mixed weekly and added deionized water to maintain approximately 60% of the soil's water holding capacity. After 4 weeks, crude oil degrading bacteria were enumerated on CFMM agar containing crude oil. Total heterotrophic bacteria were determined by viable plate count on nutrient agar. The remaining crude oil was assessed by gravimetric method.

For crude oil extraction was performed following a slight *modification* of the method *described* by Li et al., (2012). Ten g of soil was extracted with 10 mL of mixtures of hexane and acetone at the *ratio* of 4:1 v/v, mixed with 1 mL of 15% TritonX-100 and dehydrated by adding anhydrous Na_2SO_4. After shaking at 150 rpm for 30 min and the solvent phase was dried. The remaining crude oil was assessed by gravimetric method. The crude oil degradation percentage was calculated according to the following equation: % Crude oil degradation = [(the initial oil weight - the residual oil weight of the treatments)/the initial oil weight] ×100.

RESULTS AND DISCUSSION

Isolation and screening of crude oil degrading bacteria

The enrichment culture technique, cultivation, a total of 32 bacterial isolates were obtained from the petroleum-contaminated soil sample of five garages. After screening, 15 isolates that showed high turbidity (high growth) (Table 1). The

enrichment culture technique gave rise to isolates that had increasing specific metabolic capability and toxic resistance. Bacteria isolates have significant ability to *utilize crude oil* as *carbon and energy sources* (*Howland and Garfield, 1993;* Obi et al., 2016). *The* advantage of consortium is a variety of enzymatic activities and more

Table 1 The isolate of crude oil degrading bacteria from petroleum hydrocarbon-contaminated soil.

Sample	Number of isolate		Name of mixed bacterial culture
	enrichment technique	screening test	
Nonthaburi,	7	3	consortium#1
Chonburi	6	3	consortium#2
Bangkok #1	7	4	consortium#3
Bangkok #2	7	2	consortium#4
Bangkok #3	5	3	consortium#5

effective in bioremediation (Olajire and Essien, 2014). Therefore, the isolates of each sample site were mixed bacterial culture as inoculum for crude oil degradation efficiency study.

Crude oil degradation efficiency of mixed bacterial consortium

This experiment compared the crude oil-degrading efficiency of the mixed bacterial consortium. The five consortiums degraded crude oil at 4500 mg/L, 96.38, 70.17, 46.47, 78.91 and 76.03% after 10 days incubation, respectively (Figure 1). After 10 days, the number of crude oil degrading bacteria in CFMM both increased from 10^8 up to 10^9 CFU/mL (Figure 2). The results indicated that all consortiums could *grow by using*

crude oil as sole *carbon and energy sources*.

The liquid culture from crude oil degradation experiment was evaluated for biosurfactant production of bacteria consortium. The biosurfactant property was analyzed by determining the emulsification index (E24). The results found that five bacterial consortia produce biosurfactants, which E24 was 39.28, 38. 09, 6. 72, 37. 77, and 35. 55%, respectively (Figure 3). While, the E24 of control (CFMM) was zero. The results from this study are in accordance with several reports (Hashemi et al., 2016; Muthukamalam et al., 2017; Parthipan et al., 2017). It demonstrated that petroleum hydrocarbons degraders produce biosurfactants by utilizing hydrocarbons as their carbon source. Moreover, biosurfactants can enhance the bioavailability of petroleum hydrocarbons and increase petroleum degradation efficiency (Bustamante et al., 2012)

The results indicated that the consortium#1 performed the best cooperative action and was the highest crude oil biodegradation. Therefore, the consortium#1 was chosen for bioremediation of crude oil contaminated soil microcosm experiments.

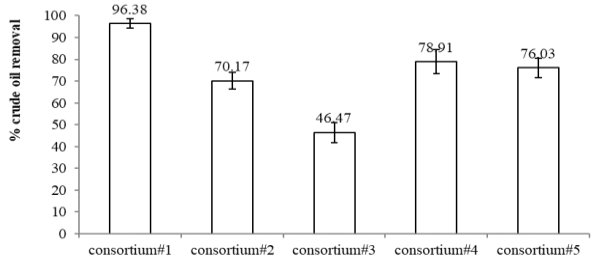

Figure 1 The crude oil removal of the mixed bacterial consortium in CFMM broth containing crude oil at 4500 mg/L, after 10 days.

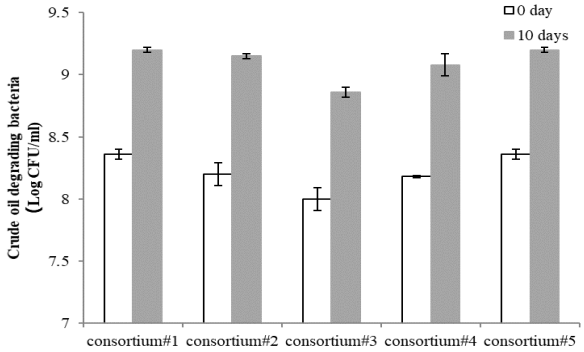

Figure 2 The crude oil degrading bacteria of the mixed bacterial consortium in. CFMM broth containing crude oil at 4500 mg/L, after 10 days

Crude oil degradation in soil microcosms

Bioremediation of crude oil contaminated soil in microcosm was performed by four treatments including biostimulation (BS) by adding activated carbon, bioaugmentation (BA) by adding the consortium#1, biostimulation and bioaugmentation (BSBA) by adding activated carbon and the consortium #1 and natural attenuation control (NAC) without the additives. The results shown in Figure 4, the highest remediation was obtained at BSBA treatment, crude oil removal was 87% of the initial amount 20,000 mg/kg, and crude oil degrader number was up to 10^9 CFU/g soil (Figure 5). Meanwhile, 52.35 % of crude oil removal was low degradation activity in BS treatment. Applying activated carbon improved physical-chemical properties of soil, maintain moisture content, and aeration in soil structure, which are significant factor of microbial activity. Thus activated carbon enhances microbial growth in soil (Ibrahim et al., 2016). This corresponds to the study by Semenyuk et al., in 2014 which indicated that activated carbon decrease bio-toxicity of petroleum-contaminants and increase petroleum-degraders, which thereby activated carbon can be used to

enhance the biodegradation rate of petroleum hydrocarbon in the soil. Whereas, natural attenuation control had 18%of the crude oil removal. This result indicated that the indigenous bacteria in soil were able to degrade crude oil. In addition, the compositions of light crude oil are typically high in saturated and aromatic hydrocarbons. These components were easily biodegradable in naturally environment (Hassanshahian and Cappello, 2013).

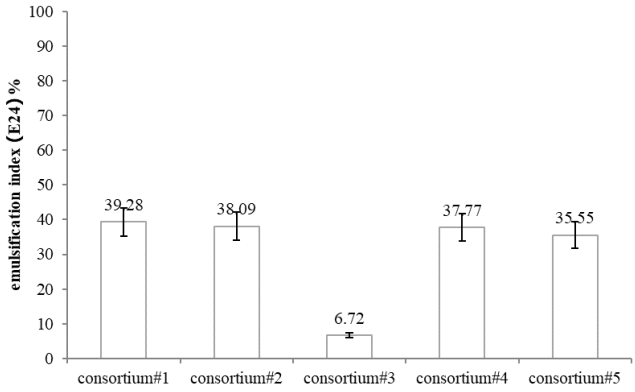

Figure 3 The emulsification index (E24) of the mixed bacterial consortium.

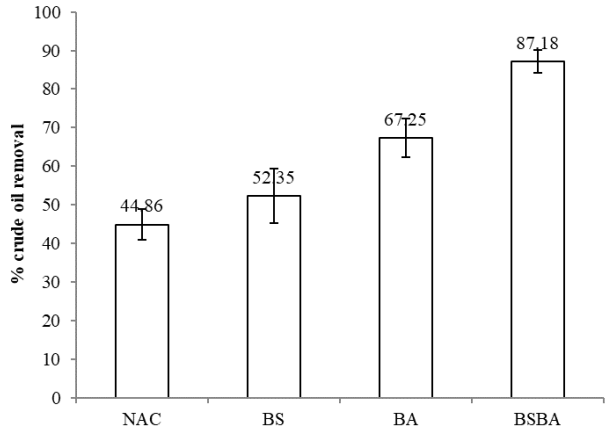

Figure 4 Degradation of crude oil contaminated soil in microcosms by biostimulation (BS) using granular activated carbon, bioaugmentation (BA)

using the bacteria consortium, biostimulation and bioaugmentation (BSBA) using granular activated carbon and the consortium#1 and natural attenuation control (NAC) without the additives.

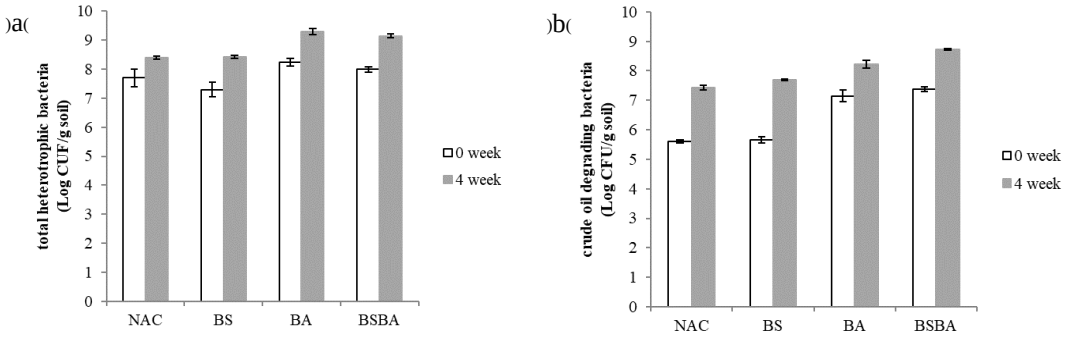

Figure 5 The quantity of total heterotrophic bacteria (a) and crude oil degrading bacteria (b) in crude oil contaminated soil in microcosms.

CONCLUSIONS

The crude oil degrading bacteria were isolated from petroleum hydrocarbon contaminated soil. The consortium#1 was combined from three crude oil degrading isolates and had the highest ability to degrade 4500 mg/kg crude oil. Consequently, this bacteria consortium could be used for bioremediation of crude oil contaminated sites. From the results of crude oil degradation in soil microcosms demonstrated that the addition of activated carbon in soil treatment could enhance the biodegradation rate and reduce the period of the bioremediation process. To increase the crude oil removal efficiency for bioremediation of petroleum-contaminated soil, the combination between consortium inoculant and granular activated carbon should be considered.

ACKNOWLEDGEMENTS

The work was supported by Faculty of Applied Science, King Mongkut's University of Technology North Bangkok.

REFERENCES

Agarry SE, Oghenejoboh KM, Solomon BO. Kinetic modelling and half life study of adsorptive bioremediation of soil artificially contaminated with bonny light crude oil. Journal of Ecological Engineering. 2015;16(3):1-13.

Briggs IL, Briggs BC. Petroleum industry activities and human health. In: Ndimele PE. The political ecology of oil and gas activities in the nigerian aquatic ecosystem. Academic Press; 2018 p.143-147.

Bustamante M, Durán N, Diez MC. Biosurfactants are useful tools for the bioremediation of contaminated soil: a review. Journal of Soil Science and Plant Nutrition 2012;12 (4): 667- 687.

Cooper DG, Goldenberg BG. Surface-active agents from two *Bacilllus* species. Applied and Environmental Microbiology 1987; 53:224-229.

Endeshaw A. The role of microorganisms in bioremediation- a review. Open Journal of Environmental Biology 2017; 038–046.

Habe H, Kanemitsu M, Nomura M, Takemura T, Iwata K, Nojiri H, Yamane H, Omori T. Isolation and characterization of an alkaliphilic bacterium utilizing pyrene as a carbon source. Journal of Bioscience and Bioengineering 2004; 98:306-308.

Hashemi SZ, Fooladi J, Ebrahimipour G, Khodayari S. Isolation and identification of crude oil degrading and biosurfactant producing bacteria from the oil-contaminated soils of Gachsaran. Applied Food Biotechnology 2016; 3(2): 83-89.

Hassanshahian M, Cappello S. Crude oil biodegradation in the marine environments. In: Chamy R, Rosenkranz F. Biodegradation - engineering and technology. Intechopen. 2013 p. 101- 135.

Howland JL, Garfield A. Enrichment culture technique can be used to introduce variety into a biochemical laboratory course. Biochemical education 1993. 21:218

Li X, Du Y, Wu G, Li Z, Li H, Sui H. Solvent extraction for heavy crude oil removal from contaminated soils. Chemosphere 2012; 88(2):245-249

Obi LU, Atagana HI, Adeleke RA. Isolation and characterisation of crude oil sludge degrading bacteria. Springerplus. 2016; 5(1):1946.

Olajire AA, Essien JP. Aerobic degradation of petroleum components by microbial consortia. Journal of Petroleum & Environmental Biotechnology 2014; 5:195.

Onwurah I NE, Ogugua V N, Onyike NB, Ochonogor AE, Otitoju O F. Crude oil

spills in the environment, effects and some innovative clean-up biotechnologies. International Journal of Environmental Research 2007; 1(4):307-320

Parthipan P, Preetham E, Machuca LL, Rahman PK, Murugan K, Rajasekar A. Biosurfactant and degradative enzymes mediated crude oil degradation by bacterium *Bacillus subtilis* A1. Frontiers in Microbiology 2017; 8:193.

Rajakovic V, Aleksic G, Radetic M, Rajakovic L. Efficiency of oil removal from real wastewater with different sorbent materials. Journal of Hazardous Materials 2007; 143:494–499.

Co-digestion of rice straw with pig manure improves biogas production - effects of pretreatment

Nam Tran Sy[1]*, Thao Huynh Van[1], Ngan Nguyen Vo Chau[1], Viet Le Hoang[1], Chiem Nguyen Huu[1] & Kjeld Ingvorsen[2]

[1]Department of Environmental Sciences, College of Environment and Natural resources, Can Tho University, Vietnam

[2]Department of Bioscience, Section for Microbiology, Aarhus University, Denmark

*Corresponding author e-mail: tsnam@ctu.edu.vn

ABSTRACT

In the Mekong Delta of Vietnam, many household biogas digesters are temporarily limited on pig manure which constitutes the main substrate. Abundantly available waste biomass such as rice straw have not been thoroughly investigated as a supplementary feedstock for small household digesters to secure a more steady production of biogas. In this study, the anaerobic co-digestion of pig manure (PM) with rice straw (RS) was evaluated in 21 L batch digesters loaded with mixtures of PM/RS in a 1:1 ratio as based on volatile solid (VS) at a total loading of 45 g VS/L. The experiments were conducted for investigating the effect of different types of environmentally friendly pretreatments of RS on biogas production. This study demonstrates that anaerobic co-digestion of RS with PM could enhance total biogas production by 79 - 85% as compared to control reactors digesting pure pig manure during 60 days of digestion. The use of simple pretreatment methods such as soaking the RS biomass in suspensions of anoxic river sediment or digester effluent also enhanced biogas production from RS slightly more as compared to pretreatment in tap water.

Keywords: *anaerobic co-digestion, biogas yield, pig manure, pretreatment, rice straw*

1. INTRODUCTION

An increase in the standard of living is usually accompanied by increased consumption of fossil fuels and undesirable CO_2 emission. Biogas, a renewable and eco-friendly energy source producible from agricultural residues, animal manure or other types of organic waste may substitute for conventional sources of energy (petrol, natural gas, LPG, coal, firewood, etc.) and provide the basis for economic growth and development in a sustainable way (Yadvika et al., 2004). Biogas production by anaerobic digestion is considered a competitive process for the production of renewable energy compared to bioethanol production in terms of efficiency, cost and simplicity (Chandra et al., 2012). A further advantage of biogas compared with other renewable energies is that it can easily be applied by the consumers using existing technologies (Schnurer and Jarvis, 2009; Taherdanak and Zilouei, 2013).

In recent years, anaerobic digestion has been increasingly applied in Vietnam and is considered an attractive solution to environmental problems caused by traditional manure management in rural farming communities (Thu et al., 2012). On farm scale, biogas can be used for cooking and heating (pig lamps), which saves the use of LPG and firewood, resulted in reducing of deforestation. The use of biogas not only provides cheap CO_2-neutral energy but also improves the working environment for women, reduces odor, pathogens, and flies and decreases the workload for farmers, who would otherwise have to spend time to collect firewood (Xiaohua et al., 2007). Despite these socioeconomic advantages, the main constraints for installing a biogas digester are initial investment costs, farmer's lack of knowledge and periodic shortage of pig manure for biogas production. Thus in rural areas of the Mekong Delta, small households encounter high

fluctuations in manure production due to diseases and variable market situation (Thong et al., 2013).

Rice straw (RS) is one of the most abundant agricultural waste materials in the world (Demirbas et al., 2011). Based on global rice production, approximately 650–975 million tons of waste RS are estimated to be produced annually (Binod et al., 2010). In the Mekong Delta, the annual production of RS is nearly 26 million tons.year^{-1} (Nam et al., 2014). Field burning is the main practice for disposing of RS, but it causes air pollution and consequently affects public health (Gadde et al., 2009; Binod et al., 2010). Furthermore, it is a waste of fixed and CO_2-neutral organic carbon.

Co-digestion of RS with pig manure could allow for a more flexible process in small household digesters and potentially enhance biogas production by changing the C/N ratio to a more favorable range (Yadvika et al., 2004). Relatively few systematic studies have addressed the use of RS as supplementary feedstock for biogas production. This study was carried out to investigate the effects of various pretreatments of RS in co-digestion with pig manure (50 % VS/VS) on biogas production in lab-scale batch reactors. Such studies are necessary to establish the potential of RS for production of clean and sustainable biogas in household biogas digesters.

2. METHODOLOGY

2.1 Origin and preparation of biogas substrates

Rice straw (RS) used in this study was collected from a rural area in Binhthuy – Cantho City, Vietnam. RS (rice variety: IR50404) was sundried and then chopped into smaller particles around 1.39±0.14cm in size (mean±Sd, n=100). Pig manure (PM) was collected from a pig farm near Cantho City. The pig manure was dried in a cool place and then grinded into fine particles (approximately <1mm). The characteristics of the three substrates, the four-pretreatment media and inoculum are listed in Table 1.

Table 1 Main characteristic of the substrates, pretreatment media and inoculum

Characteristic	Unit	Rice straw	Pig Manure	Tap Water	Digester effluent	Ditch water	Anoxic sediment	Inoculum
Moisture content	%	12.3	7.1	na	99.58	99.95	98.33	99.60
Total solids (TS)	%(w)	87.7	92.9	na	0.42	0.05	1.67	0.40
Volatile solids (VS)	%(w)	73.6	66.1	na	0.23	0.02	0.36	0.21
VS/TS	%	83.9	71.2	na	54.2	41.8	21.4	53.6
TN	%TS	0.92	1.99	<0.1mg/L	250mg/L	15mg/L	52mg/L	236mg/L
TC	%TS	48.7	41.3	na	na	na	na	na
C/N	-	53.2	20.8	na	na	na	na	na
pH	-	na	na	7.28	7.96	7.22	7.37	7.96
Alkalinity	$mgCaCO_3L^{-1}$	na	na	65	938	138	350	1093

2.2 Experimental design

The reactors used in this study were 21L plastic containers with a working volume of 17L. Each reactor was fitted with a sampling pipe and a gas sampling outlet. The lid was sealed with a 3 mm thick rubber disc pierced by a gas outlet pipe which was connected to an aluminum foil gas bag (Fig. 1). Once a day just prior to sampling of gas, the content of each digester was manually mixed by vigorous shaking and the produced biogas volume measured and analyzed as described below. All experimental treatments were simultaneously performed in 5 replicates and run for 60 days at ambient temperature (25 – 30°C). The batch digesters were covered with thick black plastic to avoid oxygen production from cyanobacteria photosynthesis during incubation.

RS was subjected to different pretreatments for five days in separated plastic containers before anaerobic digestion. The pretreatments consisted of soaking the biomass (0.455 Kg DW of RS) in different media: 10L of de-chlorinated tap water, 10 L of digester effluent, 10 L of ditch water and anoxic ditch sediment (1kg anoxic sediment in 9.2 L of tap water). Pre-incubated biomass was mixed thoroughly by shaking each day. On day 5, dried pig manure (0.537 Kg DW) was added to all containers with pre-incubated biomass, and the mixtures were subsequently transferred to the reactors, and the volume made up to 17 L with tap water and then 200 ml

of fresh biogas digester effluent was added to all reactors to initiate methane fermentation. All batch digesters were started at an initial concentration of 45 g VS.L^{-1}. Each digester contained a total of 765 g of VS. The mixing ratio of RS : PM was 50:50 as based on VS. The experimental design are summarized in Table 2.

Table 2: Experimental design

Pretreatment	RS:PM	C/N	VS (g)		Volume (L)				Inoculum	Total Volume (L)
			RS	PM	Tap water	Digester effluent	Ditch water	Anoxic sediment		
Tap water	50 : 50	37.0	382.5	382.5	17.0	0	0	0	0.2	17.2
Digester effluent	50 : 50	37.0	382.5	382.5	7.0	10.0	0	0	0.2	17.2
Ditch water	50 : 50	37.0	382.5	382.5	7.0	0	10.0	0	0.2	17.2
Anoxic sediment	50 : 50	37.0	382.5	382.5	7.0	0	0	10.0	0.2	17.2
Pig manure	0 : 100	20.8	0	765.0	17.0	0	0	0	0.2	17.2

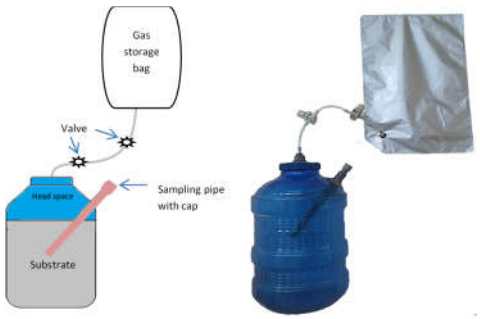

Figure 1 Schematic drawing of the experimental digester with aluminum film gas storage bag

2.3 Analytical methods

The daily biogas was collected in aluminum foil bags and measured by a gas flow meter (TG 02, Ritter, Germany). The methane content of the biogas was measured daily using a Biogas 5000 gas analyzer (Geotechnology, UK) and checked weekly using a Shimadzu GC 2014AT (Shimadzu, Japan) gas chromatograph with a thermal conductivity detector (TCD) and a 60/80 Carboxen-1000 column (L x O.D x I.D : 4.57m x 3.1 mm x 2.1 mm). The operational temperatures of the injection port, column oven, and detector were 240, 180, and 240 °C, respectively. Nitrogen was used as the carrier gas at a flow rate of 10 mL/min. A standard gas mixture (Air Liquids Ltd., Singapore) composed of 49.95% methane, 30.05% carbon dioxide in nitrogen was used for calibration. A 2.5 mL gas-tight Samplelock® syringe (Hamilton, USA) was used for gas sampling.

Total solids (TS), volatile solids (VS), total carbon, total phosphorus, total nitrogen and alkalinity of rice straw, pig manure, digester effluent, anoxic sediment, waters, and their mixtures, were determined according

to the standard methods (APHA, 1998). The temperature and pH of digester liquids were measured directly in the reactors through the sampling pipe using a digital pH meter (pH 6+, EUTECH Instrument, Singapore).

2.4 Data analysis

All the data were checked and transformed as appropriate to meet the normality and variance homogeneity requirements prior to statistical analysis and then used one-way ANOVA and Duncan post-hoc test for multiple comparisons. An alpha (α) level of 0.05 was used to determine the statistical significance of all analyses.

The analysis was performed by using the statistical software SPSS (version 13.0 for Windows). Graphs were plotted using SigmaPlot software version 10.0.

3 RESULTS AND DISCUSSION

3.1 Biogas production

Figure 2a. illustrates the daily and cumulative biogas production in reactors containing 100% untreated pig manure and RS pretreated with tap water, digester effluent, ditch water, anoxic sediment. The results strongly indicate that RS pretreated with biogas effluent and anoxic sediment (Fig. 2a) produced biogas faster than other pretreatments. These treatments produced biogas on the first day of the fermentation process while biogas production in reactors containing RS pretreated with tap water and ditch water started on the 4th day (Fig. 2b, 2d). The control reactors containing 100% untreated pig manure did not produce measurable amounts of biogas until the 7th day (Fig. 2a). These findings indicate that pretreatment of biomass using biogas effluent and anoxic sediment can reduce the lag phase of biogas production by several days (Fig. 2c, 2e). The initial enhanced biogas production observed by pretreatment with digester effluent and anoxic sediment is most likely due to higher microbial cell numbers and it also resulted in lower initial redox potentials in these reactors. It is well established that low redox potentials are conducive to methane production (Kazunori and Naoki, 2005, 2006; Chandra et al., 2012;

Fetzer and Conrad, 1993). Furthermore, digester effluent and anoxic sediment are likely to contain high numbers of polysaccharide hydrolyzing microorganisms effecting rapid initial hydrolysis and fermentation of the biomass.

Soaking of dried biomass prior to digestion may pose other advantages when up-scaling to semi-continuous digestion in farm-scale biogas reactors by reducing absorption of water from the digester liquid and introducing water into air-filled intercellular spaces of the plant material thereby possibly reducing flotation problems often associated with usage of biomass feedstock (Polprasert et al. ,1986).

At the end of the incubation period (at day 60), the cumulative biogas production in reactors containing RS pretreated with digester effluent, anoxic sediment, ditch water, tap water were 283, 273, 267, 259 liters/ kg VS_{added}, respectively, all of which were significantly higher (Duncan post-hoc test, $\alpha = 0.05$) than that of the control reactors (153 liters/kg VS_{added}) containing 100 % non-pretreated PM (Fig. 2). The cumulative biogas production of RS pretreated with digester effluent was not significantly different from that using anoxic sediment ($p>0.05$) but significantly higher than those using ditch water and tap water pretreatments.

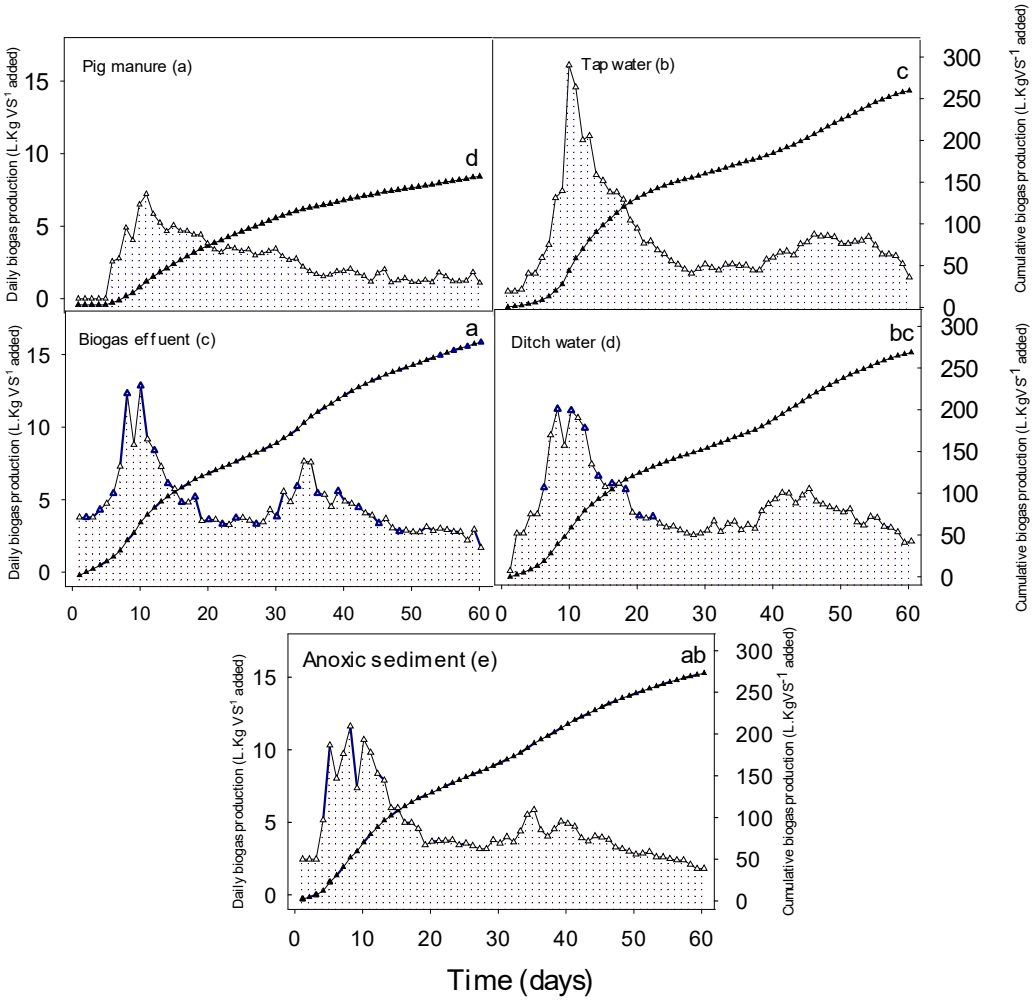

Figure 2 Daily and cumulative biogas production in the reactors

In summary, all types of pretreatment of RS in combination with 50 % PM produced approximately 100 % more biogas as compared to reactors digesting 100% untreated PM. In the Mekong delta of Vietnam, PM is currently the dominant substrate used for biogas fermentation in rural households. The results in this study shows that RS are promising supplementary substrates for existing biogas digesters – when mixed with PM in a 1:1 ratio based on VS.

3.2 Specific methane yield

Fig. 3 depicts total methane yields for all four pretreatments of RS expressed as methane produced per kg VS degraded (hereinafter referred to as specific biogas yield) after 60 days of digestion. These yields have been corrected for the number of volatile compounds present in the liquid samples/suspensions used in the different pretreatment processes (Table 2). The specific methane yield of untreated 100% PM was 234 liters/kg $VS_{degraded}$. The maximum specific methane yields obtained were 354 and 370 liters/Kg VS for co-digested RS ($p<0.05$) (digester effluent and anoxic sediment pretreatment, Fig 3). Co-digestion of RS resulted in 49% higher specific methane yields than that of pure PM. Other types of pretreatment of RS resulted in slightly lower specific methane production values. It can be seen that all reactors performing co-digestion of pig manure and plant biomass (RS) yielded significantly higher specific biogas yields ($p<0.05$) than reactors containing 100 % pig manure, irrespective of the type of pre-treatment used.

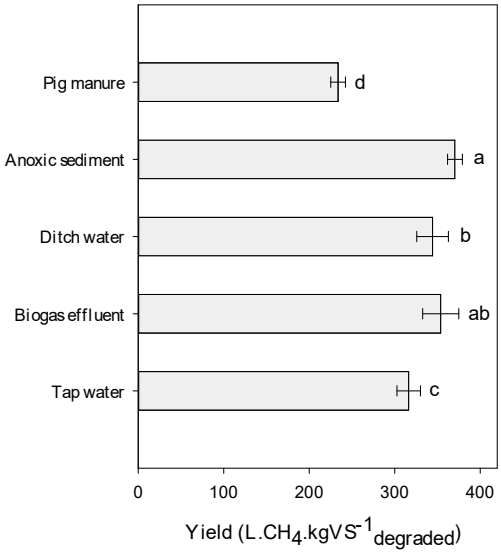

Fig. 3. Methane yields in reactors

Many researchers have reported that biogas yields obtained from anaerobic digestion of various kinds of lignocellulose wastes although results are generally, expressed in units of liters of CH_4/VS_{added}

(Chandra et al., 2012, Zhang et al., 2014) and may vary considerably due to differences in digestion time. Dinuccio et al. (2010) and Lei et al. (2010) reported yields of rice straw biomass ranging from 195 – 290 L CH_4/Kg VS (/Kg VS_{added}, in co-digestion with PM/dewater sewage). By comparison, the average biogas yield of the reactors in this study ranged between 394 and 654 liters biogas/kg $VS_{degraded}$ (Fig. 3) with an average methane content of 50-60% (Fig. 4).

3.3 Methane concentration

The average methane concentrations in biogas produced during the fermentation of rice straw using different pretreatments are shown in Fig. 4. During the first seven days of fermentation, methane concentrations were low and varied significantly among the different reactors. The lowest methane concentrations were detected in reactors receiving pretreatment with tap and ditch water. During the second period (day 8 – 21) differences in methane concentration almost equalized and in the period from day 22 to day 60 methane concentrations were fairly constant at 50 – 60 %. Also, the final methane concentration of the biogas showed little dependence on the type of pretreatment used indicating that Any type of organic materials containing carbohydrates, proteins, and fats as main components can be used as a substrate for the biomethanation process (Chandra et al., 2012). However, different types of VS exhibit different rates and of biodegradation during anaerobic digestion (Raposo et al., 2011). Xie et al. (2012) reported that degradation of lipids resulted in the highest methane contents of 67–74%, compared to 50–58% for proteins and about 50% for carbohydrates. RS used as substrates for anaerobic digestion in this study contained high proportions of carbohydrates (> 50 %) (Chandra et al., 2012; Gunnarson and Petersen 2007; Saha 2003). In the present study the methane content was quite constant at 50 – 60 % and similar to values reported in other studies (Risberg et al., 2013, Dinuccio et al., 2010).

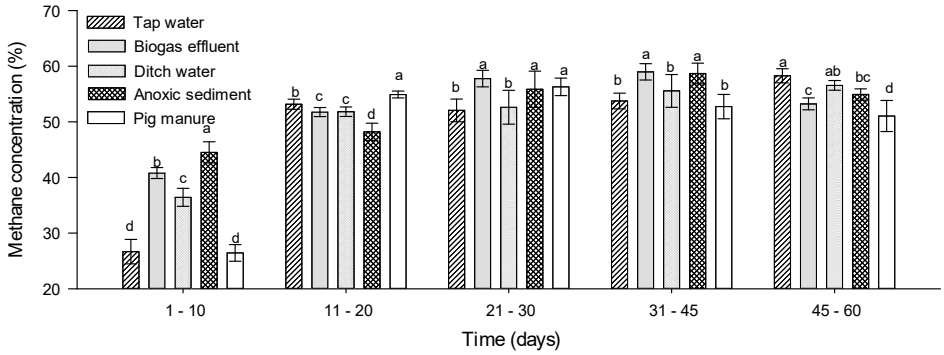

Figure 4 Methane concentration in biogas reactors

3.4 pH

Figure 5 shows the time courses of pH in the different reactors during the 60 days of operation. As a common feature, the pH in all reactors initially decreased to about 5.9 – 6.2 due to VFA production, followed by a rise then stabilized at values around 6.8 – 7.0. Reactors containing 100% PM showed a less pronounced initial drop in pH.

The chemical composition of RS changed during the anaerobic digestion process. One of the most useful parameters for evaluating the efficiency of anaerobic digestion is the reduction in volatile solids (VS). The lowest reduction (36%) was found for untreated pig manure for 60 days. In this study, PM had a C:N ratio of 20.8 as compared to average C/N ratios of 37 for co-digestion of RS (Table 2). The data show that efficient VS removal (coupled to high methane production) is possible also when using feedstock with C/N ratios higher than 20 - 30 that is generally considered to be the optimal range for biogas production (Chandra et al. 2012; Puyuelo et al., 2011; Li et al, 2011).

From Figs. 2 and 3 it is clear that biogas production was still ongoing after 60 days of digestion when the experiments were terminated and therefore VS removal efficiencies higher than those mentioned above would be obtained at fermentation times > 60 days.

Table 3 Volatile solids removal efficiency after 60 days of digestion

Reactors	Pretreatment	Initial VS concentration (%)	Final VS concentration (%)	VS removal efficiency (%)
1	None (tap water)	4.5	2.67	40.7
2	Digester effluent	4.5	2.76	38.7
3	Ditch water	4.5	2.44	45.8
4	Anoxic sediment	4.5	2.67	40.7
5	None (100 % PM)	4.5	2.88	36.0

Lei et al., (2010) studied methane production from co-digestion of RS and acclimated anaerobic sludge and reported that VS removal varied from 63.5 – 66. the VS removed rate of PM and dewatered sewage sludge in batch anaerobic was ranged from 34.7 – 62.6% for the period of 85 days

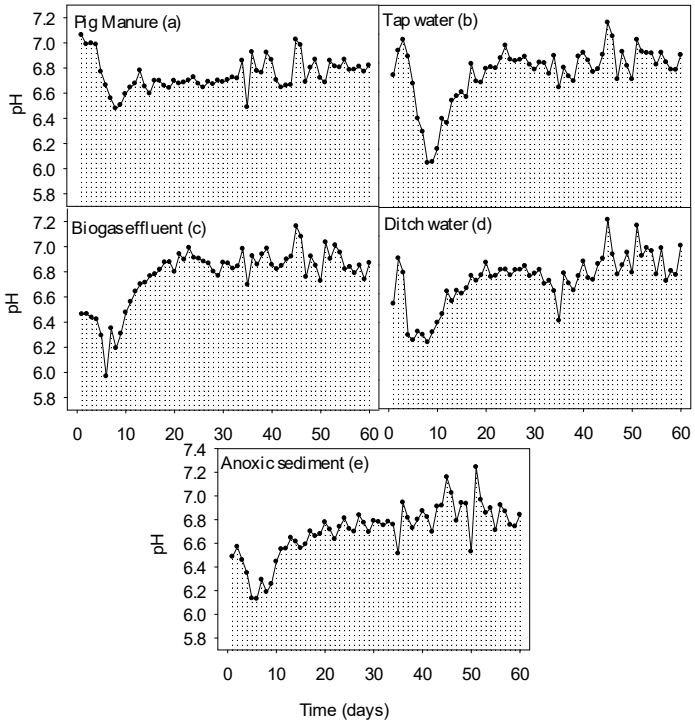

Figure. 6 Variations of pH in reactors.

Zhong et al (2011) reported VS reductions of corn straw of 40% to 56%. Zhang et al (2014) reported that co-digestion of PM with dewatered sewage sludge (DSS) resulted in 48.– 53.% VS reduction as compared with 38 % when digesting DSS as the sole substrate. Many studies conducted in batch experiments reported VS removal of 21-55% (Meyer and

Edwards, 2014). He et al., (2008) obtained VS reductions of about 66 % for mixtures of RS and acclimated anaerobic sludge incubated for 200 days.

The data in Table 4 indicate a general trend that reactors containing RS produced final digestates containing significantly higher concentrations of total N, total P, and COD than those reactors digesting 100 % PM. – thereby in all likelihood increasing their utility as cheap organic fertilizer.

Table 4 Total nitrogen, total phosphorus and COD of final digestate in batch experiments

Pretreatment	Total Nitrogen (mgN/L)	Total Phosphorus (mgP/L)	COD (g/L)
Tap water	819 ± 16	972 ± 84	18.4 ± 2.4
Digester effluent	776 ± 91	1067 ± 66	15.7 ± 1.8
Ditch water	654 ± 46	1082 ± 82	16.6 ± 3.3
Anoxic sediment	715 ± 6	1052 ± 93	17.4 ± 4.2
None (100 % PM)	809 ± 11	690 ± 50	5.3 ± 0.6

4 CONCLUSION

The results obtained in this study demonstrate that rice straw (RS) is a superior substrate for biogas production as compared to pig manure calculated based on VS_{added} or $VS_{degraded}$. This scenario was valid for all types of pretreatments tested (and all mixtures of RS and PM tested) and most certainly is due to the overall chemical composition of RS which has a higher biogas potential than PM.

RS has a comparatively low lignin content at 7 -12 % (Saha, 2003, He et al.,2008; Jin and Chen, 2007; Lee, 1997) as compared with other lignocellulose waste materials such as wheat straw at 15-20 % (Saha, 2003; Lee, 1997) and wood at 18-35 % (Lee, 1997 and Sung and Chen, 2002) on a DW basis. The low lignin content of RS may greatly facilitate pretreatment, enzymatic hydrolysis and biogas production from this cheap and abundant waste material as a sole substrate or in co-digestion with animal manure. Apparently, the high silica content of RS is less an obstacle to biodegradation than lignin.

Chandra et al., (2012) demonstrated

that NaOH (4%) pretreatment enhanced biogas production by 87.5% as compared to untreated RS whereas hydrothermal pretreatment alone increased the biogas yield by only 9.2%. He et al., (2008) obtained biogas yield improvements of 27 – 65 % using 6 % NaOH pretreatment of RS at about 20 °C for three weeks. Other studies (Sapci, 2013; Risberg et al., 2013; Zhong et al., 2011; Jing et al., 2013) have likewise shown that harsh and energy-intensive pretreatment methods are necessary to increase biogas or ethanol yields from plant biomass substantially. Such methods are not likely to gain widespread practice for small household biogas digesters in rural areas – for safety and economic reasons.

This study demonstrates that simple co-digestion and ecologically acceptable pretreatment methods of RS by soaking in anoxic sediment or digester effluent may enhance biogas production by 79 - 85 %, respectively as compared to digestion of pure pig manure. Considering that rice straw is an abundant and cheap waste material which often disposed by burning in many countries.

Increased production of biogas from the abundant supply of RS would facilitate the use of cheap and sustainable energy for additional activities such as lightning, sanitation. The results strongly indicate that effluents from biogas reactors preforming co-digestion of rice straw with pig manure are significantly enriched with respect to total N, total P and COD as compared to effluents derived from reactors digesting 100 % pig manure (Ngan, 2012). Therefore, increased usage of digester effluents as a substitute or supplement for commercial inorganic fertilizers would further lead to improve the economics of rural biogas households which so far are heavily dependent on imported inorganic fertilizers.

ACKNOWLEDGMENTS

We gratefully acknowledge the support of the Danish International Development Agency (DANIDA), who funded this research through the SubProM project (Ref. No. 11-016AU).

REFERENCES

Binod P, Sindhu R, Singhania RR, Vikram S, Devi L, Nagalakshmi S, et al., 2010. Bioethanol production from rice straw. Bioresour Technol 2010;101:4767–74.

Chandra R., Takeuchi H., Hasegawa T., 2012. Methane production from lignocellulosic agricultural crop wastes: A review in context to the second generation of biofuel production. Renewable and Sustainable Energy Reviews 16 (2012) 1462– 1476

Demirbas M. F., Balat M., Balat H., 2011. Biowastes-to-biofuels. Energy Conversion and Management 52 (2011) 1815–1828.

Dinuccio E., Balsari P., Gioelli F., Menardo S., 2010. Evaluation of the biogas productivity potential of some Italian agro-industrial biomasses. Bioresource Technology 2010; 101(10):3780–3.

Fetzer, S., Conrad R. 1993. Effect of redox potential on methanogenesis by Methanosarcina barkeri. Arch. Microbiol. 160:108-113.

Gadde B, Menke C, Wassmann R. Rice straw as a renewable energy source in India, Thailand, and the Philippines: overall potential and limitations for energy contribution and greenhouse gas mitigation. Biomass Bioenergy 2009;33:1532–46.

He Y, Pang Y., Liu Y., Li X. and Wang K., 2008. Physicochemical characterization of Rice straw pretreated with sodium hydroxide in the solid state for enhancing biogas production. Energy and Fuels 22:2775-2781.

Jin S, Chen H., 2007. Near-infrared analysis of the chemical composition of rice straw. Ind Crops Prod 2007; 26:207-11.

Jing Gao, Li Chen, Ke Yuan, Hemao Huang, Zongcheng Yan. 2013. Ionic liquid pretreatment to enhance the anaerobic digestion of lignocellulosic biomass. Bioresource Technology 150 (2013) 352–358

Kazunori M., Naoki S., 2005. The effect of water management based on soil redox potential on methane emission from two kinds of paddy soils in Japan. Agriculture, Ecosystems and Environment 107 (2005) 397–407.

Kazunori M., Naoki S., 2006. The practical use of water management based on soil redox potential for decreasing methane emission from a paddy field in Japan. Agriculture, Ecosystems and Environment 116 (2006) 181–188

Lee J., 1997. Biological conversion of lignocellulosic biomass to ethanol. J. Biotechnol. 56:1-24.

Lei Z., Chen J., Zhang Z., Sugiura N., 2010. Methane production from rice straw with acclimated anaerobic sludge: effect of phosphate supplementation. Bioresource Technology 2010;101(12):4343–8.

Li Y, Park SY, Zhu J, 2011. Solid-state anaerobic digestion for methane

production from organic waste. Re new Sustain Energy Rev 2011; 15:821–6.

Li Y., Zhang R., Liu G., Chen C., He Y., Liu X., 2013. Biogas production from wheat straw and manure – Impact of pretreatment and process operating parameters. Bioresource Technology 149 (2013) 232–237

Meyer Torsten, Edwards A. Elizabeth, 2014. Anaerobic digestion of pulp and paper mill wastewater and sludge. Water research 65 (2014) 321 - 349

Ngan N. V. C, 2012. Promotion of biogas plant application in the Mekong Delta of Viet Nam. Dissertation of PhD, Braunschweig University of Technology.

Nam T.S., Nhu N.T.H., Chiem N.H., Ngan N.V., Viet L.H., Ingvorsen K., 2014. To quantify the seasonal rice straw and its use in different provinces in the Vietnamese Mekong Delta. Scientific Journal of CanTho University 32 (2014):

Paepatung N., Nopharatana A., Warinthorn S., 2009. Bio-methane potential of biological solid materials and agricultural wastes. Asian Journal on Energy and Environment 2009;10(1):19–27.

Polpraesert C., Edwards P., Rajput V. S., Pacharaprakiti C. 1986. Integrated biogas technology in the tropics 1. Performance of small-scale digesters. Waste Management and Research 4:197-213.

Puyuelo B, Ponsá S, Gea T, Sánchez A, 2011. Determining C/N ratios for typical organic wastes using biodegradable fractions.Chemosphere 2011; 85:653–9.

Raposo F., M.A. De la Rubia, V. Fernández-Cegrí, R Borja, 2011. Anaerobic of solid organic substraté in bath mode: An overview relating to methane yields and experimental procedures. Renewable and sustainable energy Reviews 16 (2011) 861-877.

Risberg K., Sun L., Levén L., Horn S. J., Schnürer A., 2013. Biogas production from wheat straw and manure – Impact of pretreatment and process operating parameters. Bioresource Technology 149 (2013) 232–237

Saha, B.C., 2003. Hemicellulose bioconversion. Ind. Microbiol. Biotechnol. 30, 279–291.

Schnurer A., Jarvis A., 2009. Microbiological Handbook for Biogas Plants. AVFALL SVERIGE utveckling; 2009.

Sun Y., Chen J., 2002. Hydrolysis of lignocellulosic materials for ethanol production: a review. Bioresource Technology 83:1-11.

Taherdanak M., Zilouei H. , 2014. Improving biogas production from wheat plant using alkaline pretreatment. Fuel 115 (2014) 714–719

Thong N.M., 2013. Pig production status in Soctrang province. Scientific journal of Cantho University – Part B:

Agriculture, aquaculture and Biotechnology 26 (2013): 213-218

Thu C.T.T., Cuong P.H., Hang L.T., Chao N.V., Anh L.X, Trach N.X., Sommer S.G. Manure management practices on biogas and non-biogas pig farms in developing countries e using livestock farms in Vietnam as an example. Journal of Cleaner Production 27 (2012) 64-71

Zhong Weizhang, Zhongzhi Zhang, Yijing Luo, Shanshan Sun, Wei Qiao, Meng Xiao. 2011. Effect of biological pretreatments in enhancing corn straw biogas production. Bioresource Technology 102 (2011) 11177–11182.

Xiaohua, W., Chonglan, D., Xiaoyan, H., Weiming, W., Xiaoping, J., Sangyun, J., 2007. The influence of using biogas digesters on family energy consumption and its economic benefit in rural areas-comparative study between Lianshui and Guichi in China. Renewable Sustainable Energy Reviews. 11: 1018-1024.

Xie, S., Wu, G., Lawlor, P.G., Frost, J.P., Zhan, X., 2012. Methane production from anaerobic co-digestion of the separated solid fraction of pig manure with dried grass silage. Bioresource Technology 104, 289–297.

Yadvika, S. Santosh, T.R. Sreekrishnan, S. Kohli & V. Rana, 2004. Enhancement of biogas production from solid substrates using different techniques – a review. Journal of Bioresource Technology 95:1–10.

Zhang C., Su H., Baeyens J., Tan T., 2014. Reviewing the anaerobic digestion of food waste for biogas production. Renewable and Sustainable Energy Reviews 38 (2014) 383–392

Zhang W., Wei Q., Wub S., Qi D., Li W., Zuo Z., Dong R., 2014. Batch anaerobic co-digestion of pig manure with dewatered sewage sludge under mesophilic conditions. Applied Energy 128 (2014) 175–183

Zhong W., Zhang Z., Luo Y., Sun S., Qiao W., Xiao M., 2011. Effect of biological pretreatments in enhancing corn straw biogas production. Bioresource Technology 102 (2011) 11177–11182.

Bioethanol from Cassava Starch Using *Amylomyces rouxii* TISTR 3182 and Immobilized *Saccharomyces cerevisiae* TISTR 5088

Wachiraya Janthachot[1], Cherdsak Maneeruttanarungroj[1] and Duangjai Ochaikul[1*]

[1]Department of biology, Faculty of science, Bioenergy research unit, King Mongkut's Institute of Technology Ladkrabang, Bangkok, Thailand;
Corresponding author: e-mail: daungjai.oc@kmitl.ac.th

ABSTRACT

The objective of this research is to produce ethanol using cassava starch saccharification by *Amylomyces rouxii* TISTR 3182 and with following fermentation by *Saccharomyces cerevisiae* TISTR 5088. The separate hydrolysis and fermentation (SHF) and simultaneous saccharification and fermentation (SSF) process were compared. The SHF process showed the higher ethanol yield (22.84 ± 0.82 g/L) than the SSF process (14.46 ± 3.90 g/L) at 96 hr. Further study on ethanol production was carried out using the SHF process. The immobilization of *S. cerevisiae* TISTR 5088 by calcium alginate with concentrations of 2.0%, 3.0% and 4.0% (w/v) were prepared. The result revealed that the free cell of *S. cerevisiae* TISTR 5088 resulted in the highest ethanol yield (19.65 ± 1.97 g/L, Q_p 0.20 ± 0.02 g/L/h) whereas the highest yield was observed in the immobilized cells with 4.0% of calcium alginate (11.73 ± 1.06 g/L, Q_p 0.09 ± 0.02 g/L/h). The production yield from cell in alginate bead diameter in a range of at 0.4-1.2 mm. were obtained in a range of 15.78-16.41 g/L, which didn't show statistically significant difference.

Keywords: Immobilization, Bioethanol, Cassava starch, *Amylomyces rouxii*, *Saccharomyces cerevisiae*

INTRODUCTION

Energy consumption is increasing in a form of commerce energy such as fossil fuel which is limited and negative affect to the environment. Therefore, alternative energy source such as biofuel or bioethanol become interesting choice. Bioethanol can be produced from lignocellulose, sugar or starch materials. Cassava has starch as the main compound approximately 63% (Ray et al., 2004) and was produced approximately 31 million tons per year (Office of Agricultural Economic, 2016) which make over demand in Thailand. Bioethanol from cassava starch can be produced in two steps comprising hydrolysis starch to sugar form and following fermentation of sugar to ethanol. The process can be performed by two common processes are including the separate hydrolysis fermentation and the simultaneous saccharification and fermentation. However, the production can be inhibited by the high substrate concentration used in the system. Thus, to develop and enhance the production efficiency of the fermentation, cell immobilization techniques is another valuable option. The matrix of stationary phase can reduce from the cells exposure to the substrate or product, reducing in feedback inhibition. Immobilized cells can be easy to transfer out from the medium, has less cell growth (lag phase) and reusable. (Orrego et al., 2018) Calcium alginate is the most commonly polysaccharide material used for immobilized cells because of lower price, simple to carry out, non-toxic, mild condition, (Ciesarova et al., 1998) and more mechanical resistant than other matrix such as chitosan (Duarte et al., 2013). The objective of this research is to investigate bioethanol yield from cassava starch using *A. rouxii* TISTR 3182 and *S. cerevisiae* TISTR 5088. The yield from SHF and SSF process will be compared. Then the influence factor of immobilized *S. cerevisiae* TISTR 5088 such as sodium alginate concentration and bead diameter will be studied.

METHODOLOGY

2.1 Preparation of culture medium and inoculum

Amylomyces rouxii TISTR 3182 (Thailand Institute of Scientific and Technological Research, TISTR) was cultured on potato dextrose agar (PDA) slants and incubated at 30℃ for 10 days. Spore suspension was diluted to 10^7 spore/mL (Mercial et al., 2006) by using sterile 0.1% Tween 80 solution. *Saccharomyces cerevisiae* TISTR 5088 (TISTR) was cultured on YPD agar (glucose 20 g/L, peptone 20 g/L, yeast extract 10 g/L and agar 20 g/L) slants incubated at 30 ℃ for 72 hr. One loop was subcultured in YPD broth and incubated at 30℃ for 24 hr. The optical density (OD_{660}) was adjusted to 0.5 (Petrea, 2008) for inoculum.

2.2 Preparation of immobilization

The inoculum of *S. cerevisiae* TISTR 5088 was poured into various sodium alginate concentrations (2%, 3%, and 4% w/v) in the ratio 1:1 (v/v). Then the mixture was dropped into 0.1 M $CaCl_2$ using sterilized syringe The bead was left to be harden for 1 hr. and later washed with 0.9% (w/v) sterile sodium chloride to remove the $CaCl_2$ and cell residue. (Idris and Suzana, 2006). Furthermore, the bead diameter of 0.4, 0.8 and 1.2 mm. were excluded for specific experiments.

2.3 Preparation of fermentation medium

Cassava was obtained from local market in Bangkok. Cassava were cleaned, cut into pieces and dried out in an oven at 70℃ for 48 hr. Then the pieces were milled to powder and sieved through 50 mesh to obtain a powder size of 300 µm. The 6% w/v cassava was used as a fermentation medium. Cassava powder was weighed and gelatinized in water at 90℃ for 30 min until liquefied followed by autoclave at 121℃ for 15 min.

2.4 Batch fermentation

2.4.1 SHF process

Batch fermentation was carried in 150 ml liquefied cassava starch. 15 ml of *A. rouxii* TISTR 3182 spore suspension was added prior to incubate the mixture at 30℃ agitating

at 150 rpm for 48 hr. Another 15 ml of *S. cerevisiae* TISTR 5088 culture was added. The mixture was continuously incubated at the same condition for 120 hr. The *S. cerevisiae* TISTR 5088 cells were replaced by immobilized cells for a comparison purpose.

2.4.2 SSF process

Batch fermentation was carried in 150 ml of liquefied cassava starch. 15 ml of *A. rouxii* TISTR 3182 spore suspension and 15 ml of *S. cerevisiae* TISTR 5088 culture were added. The mixture was incubated at the same condition as in SHF process for 120 hr.

2.5 Analytical method

Samples were collected on every 24 hr. during the fermentation process. The samples were centrifuged at 4,000 rpm 4℃ for 10 min to remove cells and debris. The supernatant was further analyzed for reducing sugars using 3,5-dinitrosalicylic acid (DNS) technique (Miller, 1959). Sugar concentration was calculated against a glucose standard curve. The ethanol concentrations were determined by gas chromatography (Shimadzu model, GC-2014, Japan) with a DB-1 column using helium as a carrier gas with a flow rate of 244.2 mL/min, equipped with flame ionization detection (FID), maintained the temperature at 180℃. The column temperature was maintained at 60℃. The N-propanol 10% (v/v) was used as internal standard. The experiments were studied in triplicate. Statistical analysis was done by completely randomized design (CRD). The significant level was set to 0.05.

RESULTS AND DISCUSSION

3.1 Efficiency of SHF and SSF processes on ethanol production

The processes of SHF and SSF had effect to bioethanol yield from cassava starch. The ethanol product from two processes were compared. As shown in Figure 1, The SHF process showed the significant improvement in ethanol production than SSF process within 96 hr. of fermentation time, yielding 22.84 ± 0.82 g/L and 14.46 ± 3.90 g/L, respectively. Our results suggested

that the SHF process was suitable for ethanol production. The explanation could be form the fact that the cassava starch was hydrolyzed by *A. rouxii* TISTR 3182 to produce reducing sugars between 24-48 hr. As a consequence, the reducing sugars could be utilized by *S. cerevisiae* TISTR 5088 in order to establish fermentation process. Our results were similar to Wirawan et al. (2012) found that the ethanol production from cellulosic using SHF and SSF approaches by immobilized cells showed a higher ethanol yield in SHF process. Duangwan and Sangwichien (2015) was also investigated ethanol production from oil palm using SHF process from baker's yeast. The yield was obtained at 8.49 g/L of ethanol. Soderstrom et al. (2003) studied bioethanol production using two-step process comprising of stream pretreatment of softwood followed by SHF process and the result revealed a higher ethanol yield than SSF process. Ask et al. (2012) achieved the highest ethanol yield with SHF process (0.27 g/g) when compared with SSF process (0.24 g/g).

3.2 Effect of alginate concentration on immobilized cells to ethanol production

Immobilized cells of various alginate concentrations had effective on the bioethanol fermentation. The rate of reducing sugar consumption was relevant to ethanol productivity rate. As shown in Figure 2A, free cell yielded in the higher ethanol (19.54 ± 0.47 g/L) than immobilized cells at 120 hr. The reducing sugar in a free cell system was rapidly consumed approximately 48-72 hr. whereas the immobilized cells were gradually consumed (figure 2B). At 120 hr., free cell consumed reducing sugars as 25.90 ± 0.93 g/L while immobilized cells in 2%, 3% and 4% (w/v) alginate consumed 6.97 ± 1.49, 11.30 ± 6.07 and 14.65 ± 10.02 g/L, respectively. The higher sugar consumption found in free cell system could be explained that has no obstacle between the cell and the culture, thus the substrate transfer in free cell is more available than in immobilized cells. Similar to other

reports, Orrego et al. (2018) showed that free cell yield in higher ethanol and higher rate of sugar consumption than immobilized cells (2-4% (w/v) alginate) and Nikolic et al. (2010) studied bioethanol from corn meal. The result showed that free cell had more efficient than the immobilized cells. Mariam et al. (2009) also showed that free cell produced higher ethanol from cane molasses than immobilized cells. Even the free cell system could produce the bioethanol in lower portion, the advantage of immobilized cells is cell recycling (Duarte et al., 2013). In addition, our studies showed immobilized cells in 4% (w/v) alginate resulted in the highest ethanol yield (11.73 ± 1.06 g/L) than other concentrations. Similar to, Swain et al. (2007), they were studied ethanol fermentation using 4% alginate concentration, the result showed that immobilized cells gave higher ethanol than free cell. The 4% calcium alginate bead form had mild conditions as compared with agar agar. (Behera et al., 2010) and Bandaru et al. (2006) obtained the maximum ethanol yield by using 4% sodium alginate solution from sago starch. Finally, our results proved that 3% and 4% of immobilized beads were stable and harder than 2% bead which was broken after 5 days of fermentation. This finding was coherent with Najapour et al. (2004) results. They reported that high alginate concentrations exhibits more rigidity and stable bead. Maswanna et al. (2018) noted that the alginate bead above 4% (w/v) was harder and had tail. However, observation was different from Ercan et al. (2013) that 2% alginate was the optimum conditions for the bioethanol fermentation and high concentrations had limit diffusion substrate to cell (Lee et al., 2011).

3.3 Effect of bead diameter on immobilized cells on ethanol production

From the above result, 4% calcium alginate concentration had showed the suitable application in bioethanol fermentation. Then immobilized cells were studied with various bead diameters at 0.4, 0.8 and 1.2 mm. The

result showed in Figure 3A and 3B that ethanol production and reducing sugar consumption from bead diameters of 0.4, 0.8 and 1.2 mm. were 15.78 ± 2.46, 16.69 ± 1.60, 16.41 ± 2.51 g/L, respectively and 26.89 ± 4.31, 29.18 ± 3.13 and 29.76 ± 1.93 g/L, respectively, which didn't shown the statistically significant difference. Our results were similar to Gilson and Thomas (1995) that increasing bead diameter (> 2.00 mm.) effect to the reduction of glucose consumption and reducing the product yield because smaller bead diameter had larger surface areas. Idris and Suzana (2006) proved the use of 1 mm. diameter bead resulted in the higher productivity than the use of 5 mm. Goksungur and Guvenc (1999) obtained the highest production when used 1.3-1.7 mm. and 2.0-2.4 mm. bead diameter whereas bead diameter above 3 mm. that showed low productivity (Abdel-Naby et al., 1992) Rakin et al. (2009) studied bioethanol fermentation with 0.8 mm. diameter bead of immobilized *S. cerevisiae*, the result showed the maximum ethanol concentration was 10.05 % (w/w). Small bead diameter was appropriate for substrate transfer to immobilized cells (Margaritis and Kilonzo, 2005).

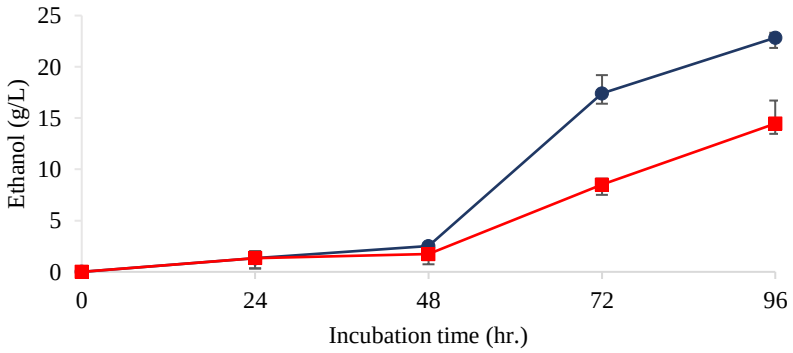

Figure 1 Comparison of SHF and SSF process for bioethanol fermentation. Separate hydrolysis fermentation; SHF (●), Simultaneous saccharification and fermentation; SSF (■)

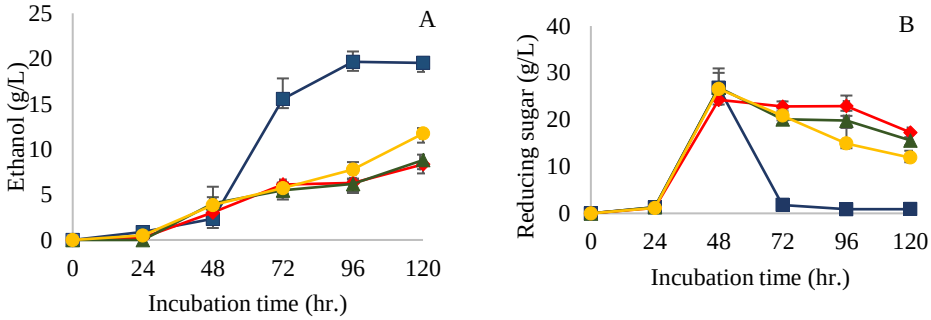

Figure 2 Ethanol production on the effect of Ca-alginate concentration (A) and reducing sugar consumption on the effect of Ca-alginate concentration (B). Free cell of *S. cerevisiae* TISTR 5088 **(■),** Immobilized cells with 2% calcium alginate (◆), Immobilized cells with 3% calcium alginate (▲) and Immobilized cells with 4% calcium alginate. (●)

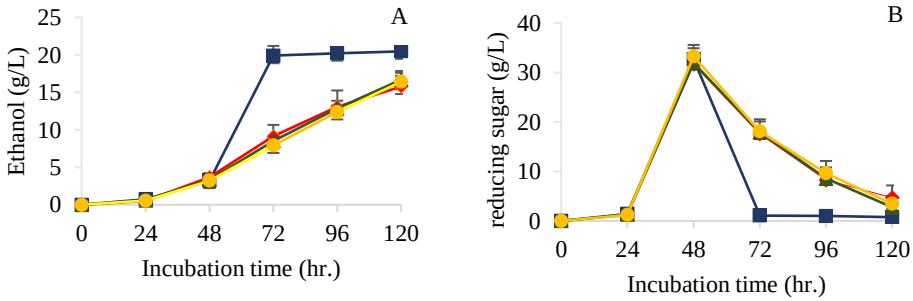

Figure 3 Ethanol production on the effect of bead diameter of *S. cerevisiae* TISTR 5088 immobilized cells (A) and reducing sugar consumption on the effect of bead diameter of *S. cerevisiae* TISTR 5088 immobilized cells (B). Free cell of *S. cerevisiae* TISTR 5088 (■), Immobilized cells with 0.4 mm. bead diameter (◆), Immobilized cells with 0.8 mm. bead diameter (▲) and immobilized cells with 1.2 mm. bead diameter (●).

CONCLUSIONS

The studied proved that separate hydrolysis and fermentation (SHF) process showed the improvement ethanol fermentation from cassava starch using cultured of *A. rouxii* TISTR 3182 and *S. cerevisiae* TISTR 5088. Moreover, to improve the bioethanol process, the immobilized cells of *S. cerevisiae* TISTR 5088 shows the promising capability in the process. The 4% calcium alginate concentration gave the highest ethanol production yielding 11.73 ± 1.06 g/L. Cell in bead diameters at 0.4, 0.8 and 1.2 showed the suitable production yield which didn't significant difference rate. However, the immobilized cells were useful in cell recycling process.

ACKNOWLEDGEMENTS

This work was supported by the research grant by the Faculty of Science, King Mongkut's Institute of technology Ladkrabang.

REFERENCES

Adel-Naby M, Mok C, Lee C. Production of organic acid from enzymatic hydrolysate of starch by immobilized lactic acid bacteria. UNIDO Proceedings 1992; 227-243.

Ask M, Olofsson K, Felice TD, Ruohonen L, Penttila M, Liden G, Olsson L. Challenges in enzymatic hydrolysis and fermentation of pretreated *Arundo donax* revealed by comparison between SHF and SSF. Process Biochemistry 2012; 47: 1452-1459.

Bandaru VVR, Somalanka SR, Mendu DR, Madicherla NR, Chityala A. Optimization of fermentation condition for the production of ethanol from sago starch by co-immobilized amylo-glucosidase and cells of *Zymomonas mobilis* using response surface methodology. Enzyme and Microbial Technology 2006; 38: 209-214.

Behera S, Kar S, Mohanty RC, Ray RC. Comparative study of bio-ethanol production from mahula (*Madhuca latifolia L.*) flowers by *Saccharomyces cerevisiae* cells immobilized in agar agar and Ca-alginate matrices. Applied energy 2010; 87: 96-100.

Ciesarova Z, Domeny Z, Smogrovicova D, Patkova J, Sturdik E. Comparison of ethanol tolerance of free and immobilized *Saccharomyces uvarum* yeast. Folia Microbiol 1998; 43: 55-58.

Duangwang S, Sangwichien C. Utiilization of oil palm empty fruit bund hydrolysate for ethanol production by baker's yeast and loog-pang. Energy Procedia 2015; 79: 157-162.

Duart JC, Rodrigues JAR, Moran PJS,

Valenca GP, Nunhez JR. Effect of immobilized cell in calcium alginate beads in alcohol fermentation. AMB Express 2013; 3: 31.

Ercan Y, Irfan T, Mustafa K. Optimization of ethanol production from carob pod extract using immobilized *S. cerevisiae* cells in a stirred tank bioreactor. Bioresource Technology 2013; 135: 365-371.

Gilson C, Thomas A. Ethanol production by alginate immobilized yeast in a fluidized bed bioreactor. Journal of Chemical Technology and Bio-technology 1995; 62: 38-45.

Goksungur Y, Guvenc U. Production of lactic acid from beet molasses by calcium alginate immobilized *Lactobacillus delbrueckii* IFO 3202. Journal of chemical technology and biotechnology 1999; 74: 131-136.

Idris A, Suzana W. Effect of sodium alginate concentration, bead diameter, initial pH and temperature on lactic acid production from pineapple waste using immobilize *Lactobacillus delbrueckii*. Process Biochemistry 2006; 41: 1117-1123.

Lee KH, Choi IS, Kim YG, Yang DJ, Bae HJ. Enhanced production of bioethanol and ultrastructural characteristic of reused *Saccharomyces cerevisiae* immobilized calcium alginate beads. Bioresource Technology 2011; 102: 8191-8198.

Margaritis A, Kilonzo PM. Production of ethanol using immobilized cell bioreactor system. Application of cell immobilization biotechnology 2005; 375-405.

Mariam I, Manzoor K, Ali S, Haq I. Enhance production of ethanol from free and immobilized *S.cerevisiae* under stationary culture. Pakistan Journal of Botany 2009; 41: 821-833.

Maswanna T, Phunpruch S, Lindblad P, Maneeruttanarungroj C. Enhanced hydrogen production by optimization of immobilized cells of the green alga *Tetraspora* sp. CU2551 grown under anaerobic condition. Biomass and Bioenergy 2018; 111: 88-95.

Mercial J, Barrios GJ, Tomasini A. Effect of medium composition on pentachloro-phenol removal by *Amylomyces rouxii* in solid-state culture. Process Bio -chemistry 2006; 41: 496-500.

Miller GL. Use of dinitrosalicylic acid reagent for determination of reducing sugar. Analytical chemistry 1959; 31(3): 426-428.

Najafpour G, Younesi H, Ismail KSK. Ethanol fermentation in an immobilized cell reactor using *Saccharomyces cerevisiae*. Bio-resource Technology 2004; 92: 251-260.

Nikolic S, Mojovic L, Pejin D, Rakin M, Vukasinovic M. Production of bioethanol from corn meal hydrolyzates by free and immobilized cells of *Saccharomycrs cerevisiae*

var. *ellipsoideus.* Biomass Bioenergy 2010; 34: 1449-1456.

Office of Agricultural Economics. Cassava starch. Agricultural statistics 2016. Retrieved from http://oldwed.oae .go,th/production.html.

Orrego D, Zapata ADZ, Kim D. Ethanol production from coffee mucilage fermentation by *S.cerevisiae* immobilized in calcium-alginate beads. Bioresource Technology reports 2018; 3: 200-204.

Petrea L. Characterization of two *Saccharo -myces cerevisiae* strain obtained by UV mutagenesis. Innovative Romanian Food Biotechnology 2008; 2: 40-47.

Rakin M, Mojovic L, Nikolic S, Vukasinovic M, Nedovic V. Bioethanol production by immobilized *Saccharomyces cerevisiae* var. *ellipsoideus* cells. African journal of Biotechnology 2009; 8: 464-471.

Ray RC. Extracellular amylase(s) production by fungi botryodiplodia theobromae and *Rhizopus oryzae* grown on cassava starch residue. Journal Environment Biology 2004; 25: 489-495.

Soderstrom J, Pilcher L, Galbe M, Zacchi G. Two-step steam pretreatment of softwood by dilute H_2SO_4 impregnation for ethanol production. Biomass and Bioenergy 2003; 24: 475-486.

Swain MR, Kar S, Sahoo AK, Ray RC. Ethanol fermentation of mahula (*Madhuca latifolia* L.) flowers using free and immobilized yeast *Saccharomyces cerevisiae.* Microbiological Research 2007; 162: 93-98.

Wirawan F, Cheng CL, Kao WC, Lee DJ, Chang JS. Cellulosic ethanol production performance with SSF and SHF process using immobilized *Zymomonas mobilis*. Applied energy 2012; 100: 19-26.

Correlation between $PM_{2.5}$ concentrations and VIIRS hotspot counts during intensive biomass burning period in Nakhon Pathom

Siraphop Pinitkarn[1], Rattapon Onchang[2], Danutawat Tipayarom[3], Aungsiri Tipayarom[4*]

[1*]Department of Environmental Science, Faculty of Science, Silpakorn University

[2]Department of Environmental Science, Faculty of Science, Silpakorn University

[3]Division of Research and Innovation, Electricity Generating Authority of Thailand

[4]Department of Environmental Science, Faculty of Science, Silpakorn University; Corresponding author: e-mail: aungsiri@gmail.com

ABSTRACT

In Thailand, an agro-residue burning starts after harvesting. Burning of agricultural wastes, however, results in ambient $PM_{2.5}$. In this study, the ambient and indoor $PM_{2.5}$ and hotspot counts in Nakhon Pathom, Thailand, and neighboring countries including China were monitored for correlation analysis. The biomass burnings were monitored by the VIIRS aboard the Suomi-NPP satellite. The back trajectories of air masses were determined by the HYSPLIT model. The results from HYSPLIT showed that the air masses were originated from the Northeast of Thailand and subsequently entered Nakhon Pathom. The average concentrations of ambient and indoor $PM_{2.5}$ were 31 and 56 μg m^{-3}, respectively. The concentrations of $PM_{2.5}$ were somewhat higher than Thailand's air quality standard and guideline. Additionally, due to poor ventilation of the building, indoor concentrations

were approximately 2.2 times higher than ambient concentrations. The ambient and indoor concentrations were strongly correlated (r=0.8). During 3 months, the ambient $PM_{2.5}$ concentrations in Nakhon Pathom were moderately correlated with hotspot counts per area of Cambodia (r=0.56) which corresponds to the air mass direction acquired from HYSPLIT. The degrees of correlation, however, were not high since the hotspot counts obtained from VIIRS reflect counts of burning rather than the sizes of burning area.

Keywords: $PM_{2.5}$, Biomass burning, Air quality monitoring, Hotspots

INTRODUCTION

Biomass burning is the burning of living and dead vegetation for various purposes, mainly for land clearing. In various agricultural countries, especially in Southeast Asia, crop residue burning is a widespread practice. An open burning is particularly intensive during dry season like harvesting season. Crucially, the burning of agricultural wastes such as rice straw, corn stalks, and sugarcane stubbles has critically impacted on the local and regional haze particle problems during the harvesting season. In addition, it is the largest source of air pollution in many rural areas of the developed and developing countries.

In addition to $PM_{2.5}$ source, burning of biomass causes significant local and regional environmental effects. The emissions from agro-residue burning including CO_2, CH_4, CO, NO_X, SO_2, PM_{10}, black carbon (BC), organic carbon (OC), volatile organic compounds (VOCs), and polycyclic aromatic hydrocarbons (PAHs) (Tipayarom and Kim Oanh, 2007; Kim Oanh et al., 2015; Kim Oanh et al., 2016, Kim Oanh et al., 2018; Junpen et al., 2018; Phairuang et al., 2019).

The health effects of biomass burning are well-established. Epidemiological evidence of $PM_{2.5}$ damage on human respiratory system has been mentioned in Xing et al.

(2016). A considerable correlation between $PM_{2.5}$ and respiratory morbidity and mortality was also observed. In European Union countries, a decrease of the average life span by 8.6 months was triggered by $PM_{2.5}$. The outstanding symptoms of exposure to biomass burning are chronic obstructive lung disease (COLD), acute respiratory infection (ARI), adverse pregnancy outcomes, interstitial lung disease, tuberculosis, eye problem, asthma and cardiovascular disease (FAO, 2000).

The Visible Infrared Imaging Radiometer Suite (VIIRS) sensor aboard the joint NASA/NOAA Suomi National Polar-orbiting Partnership (Suomi-NPP) satellite monitors fire activity over the world. VIIRS data expand upon the Moderate Resolution Imaging Spectroradiometer – so called MODIS – application to fire monitoring (NASA, 2016). MODIS and VIIRS show good agreement in hotspot detection. However, VIIRS has been improved for spatial resolution of the 375 m data. It not only provides a greater response over fires of relatively small areas but also provides improved mapping of large fire boundaries. The 375 m data also has improved nighttime performance (NASA, 2018).

In Thailand open burning is illegal. Farmers therefore habitually burn their crop residues at night. For this reason the hotspot data obtained from VIIRS is more appropriate than MODIS.

This study aims to investigate the correlation between $PM_{2.5}$ concentrations and VIIRS hotspot counts during intensive biomass burning period in Nakhon Pathom and adjacent provinces. The relationship between indoor and ambient $PM_{2.5}$ is explored since - the ambient $PM_{2.5}$ level in Nakhon Pathom is so high that it exceeds the Thailand air quality standard. The building users begin to have eyes and nose irritation as well as respiratory symptoms such as coughing, throat irritation and recurrent dust allergies. The elevated level of $PM_{2.5}$ is

possibly resulted from to the influence of high-pressure systems that bring stable air masses from the northeast of Thailand.

METHODOLOGY

Study areas

Nakhon Pathom is one of the central provinces of Thailand (Figure 1). Located west of Bangkok, it is a perimeter of the Bangkok Metropolitan Region. Nakhon Pathom is located in the flat river plain of the Tha Chin River valley, which makes it one of the agricultural areas. The region is relatively dominated by agricultural lands which are used for rice, sugarcane, corn, fruit and vegetable growing. The total area of Nakhon Pathom is 2,168 km^2 (Office of Nakhon Pathom Province, 2016).

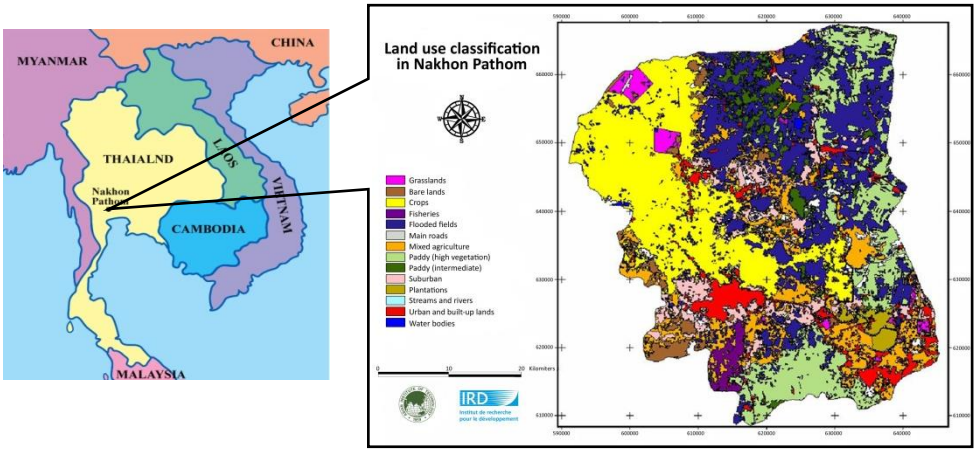

Figure 1 Map of study areas.

Source: Herbreteau (2001)

Ambient and indoor $PM_{2.5}$ sampling equipment were located in Silpakorn University, Sanam Chandra Palace Campus. This university was selected as a sampling site since it was located moderately far (3 km) from downtown and also the traffic in the university was considered light. Ambient sampler (AQM 65 Ambient Air Monitoring Station, AEROQUAL, Auckland, New Zealand) was located 3 meters away from university main road. Two Personal Environment Monitor

Model 2000 (PEM) (SKC Inc., Eighty Four, PA, USA) equipped with personal air pump (Sensidyne, LP, St. Petersburg, FL, USA) were placed in the middle of the 5th floor of Science Building 4, Faculty of Science.

$PM_{2.5}$ sampling and analysis

The AQM 65 Ambient Air Monitoring Station was continuously measured for $PM_{2.5}$ 24 hours a day at a flow rate of 2 L m^{-1}. The equipment sensor is a laser nephelometer with a measurement range 0-2,000 μg m^{-3}. The hourly $PM_{2.5}$ data were remotely retrieved through direct internet connection. Afterwards, the daily amount was calculated by averaging all hourly data.

For indoor $PM_{2.5}$ measurement, the PEM with glass fiber filters (GFF) GC-50 (Advantec MFS, Inc., Dublin, CA, USA) loaded were used. The PEM operates on the airborne particles using an impactor. $PM_{2.5}$ was collected using a PEM connected with a personal air pump, which was adjusted at 2 L m^{-1}. Before sampling, filter was desiccated at constant relative humidity and temperature for at least 24 hours and weighed by a seven-digit balance (Mettler Toledo, Greifensee, Switzerland). After sampling, the filter was desiccated and weighed again to measure the $PM_{2.5}$ weight on the sample filters for mass analysis. Proper flow calibration of the personal air pump (2 L m^{-1}) was done for the correct fractionation of the particles below 2.5 μm (US EPA, 1990).

All measurements were performed for 27 days covering 3 months, from December 2018 to February 2019. The results from two monitoring means were subsequently analyzed for Pearson's correlation (r).

VIIRS active fire data

The archived hotspots data in Nakhon Pathom, Thailand, and neighboring countries including Cambodia, Laos, Myanmar, and Vietnam as well as China were extracted daily from NASA's Fire Information for Resource Management System (FIRM). The

active fires were shown appeared as hotspots on the fire map (Figure 2). This study acquired the fires information (hotspots) for three months on the same day of $PM_{2.5}$ measurements.

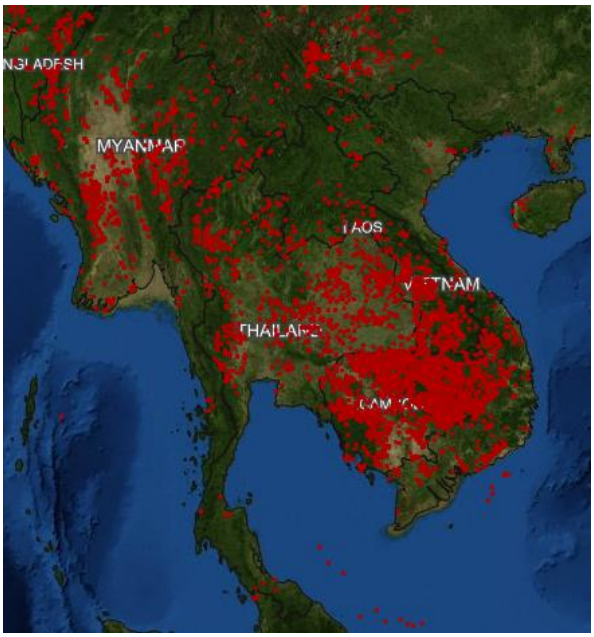

Figure 2 Hotspots appeared on the fire map on February 13, 2019.

HYSPLIT model

The 24-hr air parcel back trajectories (Figure 3) were obtained from The Hybrid Single Particle Lagrangian Integrated Trajectory Model (HYSPLIT) developed by NOAA and Australia's Bureau of Meteorology. This model was widely used in numerous air and atmospheric pollution studies (Tipayarom and Kim Oanh, 2007; Xu et al., 2008; Tipayarom, 2012; Wang et al., 2017). The model is useful for investigation the regional transport of air pollutants.

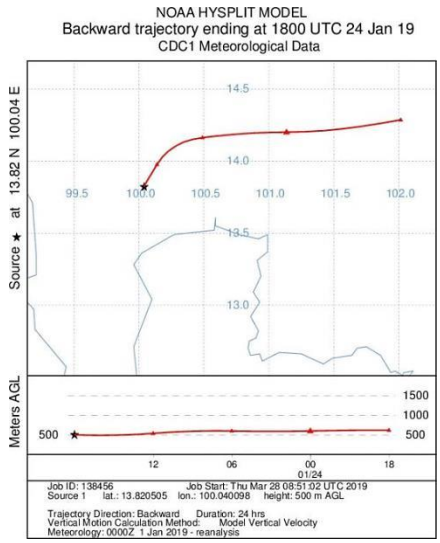

Figure 3 Air parcel trajectories on January 24, 2019 from HYSPLIT Model.

RESULTS AND DISCUSSION

In this study, to capture understand the effect of biomass open burning, both the ambient and indoor $PM_{2.5}$ concentrations were investigated along with the number of hotspots counted over the study area.

The correlation between ambient and indoor $PM_{2.5}$

The ambient and indoor $PM_{2.5}$ concentrations during the studying period were found to be strongly correlated (r=0.8). The linear relationship between the ambient and indoor $PM_{2.5}$ concentrations was found (Figure 4) as a result of air exchange between indoor and ambient air, which could possibly due to the fact that windows and doors of the studied building were kept opened during daytime.

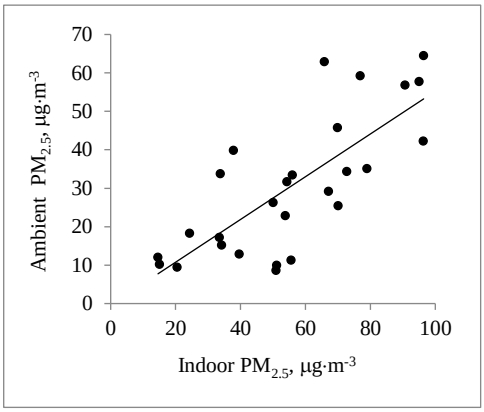

Figure 4 Correlation between ambient and indoor $PM_{2.5}$ concentrations.

However, indoor concentrations were in the order of 2.2 times higher than ambient concentrations (Figure 5) owing to poor ventilation of the building. The samplers were placed on the 5^{th} floor (highest floor) of the building. During daytime, the warm air contaminated with $PM_{2.5}$ elevated due to buoyancy which caused the accumulation of $PM_{2.5}$ on the sampling location. The results were

reliable since outdoor PM2.5 concentrations acquired from the equipment used in this study were robustly correlated with the data obtained from US EPA's reference method conducted by Thailand's Pollution Control Department (r=0.9 and r^2=0.8). Moreover, indoor air sampling and analysis method are US EPA Federal Reference Method (FRM). This finding corresponded to Challoner and Gill (2014) in term of the indoor/outdoor ratio of $PM_{2.5}$ being greater than 1 in several types of building.

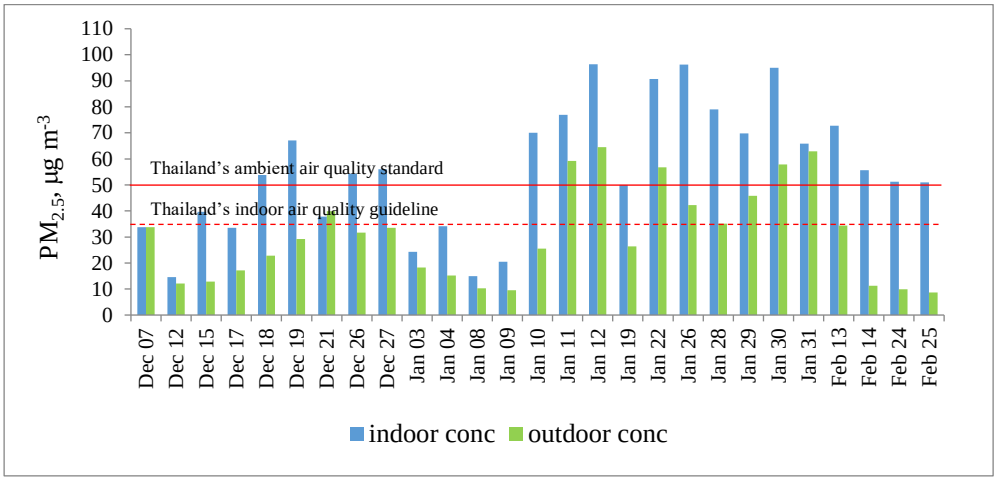

Figure 5 Concentrations of $PM_{2.5}$.

It was evident in Figure 5 that the daily concentration of ambient and indoor $PM_{2.5}$ was extremely high and frequently exceeded the Thailand's ambient and indoor air quality standard. The average concentrations of ambient and indoor $PM_{2.5}$ were 30.6$\pm$18.0 and 55.7$\pm$24.5 µg m^{-3}, respectively while the corresponding air quality standard and guideline were 50 and 35 µg m^{-3}, respectively (Thailand's Pollution Control Department, 2019; Thailand's Department of Health, 2017). The high concentration leads to human health risks especially among elderly people, children and people with asthma (Khalili et al., 2018; US EPA, 2018; WHO, 2019).

The high concentrations of $PM_{2.5}$ possibly came from the forest fires, agricultural wastes burned in Nakhon Pathom, upwind provinces, and upwind countries. Furthermore, the atmospheric conditions of Nakhon Pathom during the measurement period was somewhat stagnant air which was influenced by the following factors; (1) high pressure expanding from China to Southeast Asia, (2) less wet removal from intensive rain, and (3) very high photochemical reaction in the atmosphere.

Hotspot count data

The total number of hotspot counts per area (Hotspot km^{-2}) in Nakhon Pathom, Thailand, Cambodia, Laos, Myanmar, Vietnam, and China during study period was indicated in Figure 6.

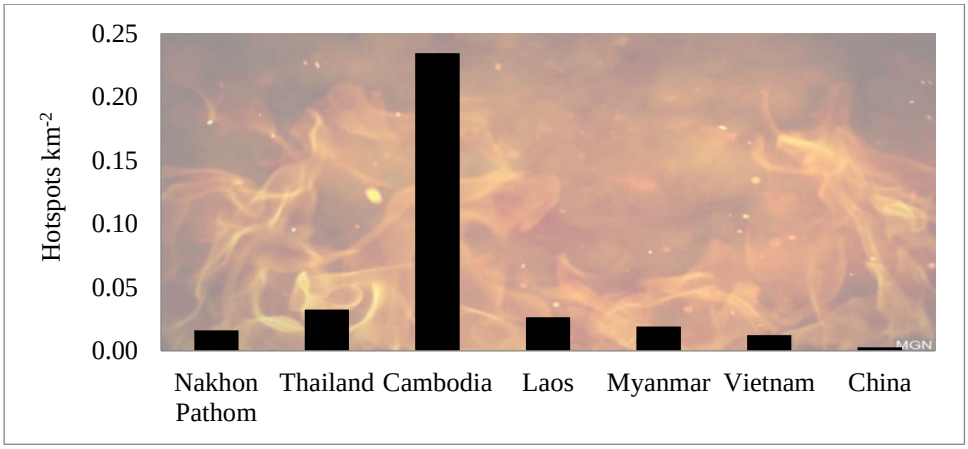

Figure 6 The number of hotspot counts per area during 3-month $PM_{2.5}$ measurement.

It was evident that among the 6 countries, the highest number of hotspot counts per area was found in Cambodia followed by Thailand, Laos, Myanmar, Vietnam, and China, respectively. Although Nakhon Pathom is the only province, the ratio was as high as Myanmar.

The HYSPLIT model results illustrated that the air mass coming to Nakhon Pathom during the three months of sampling was originated from the northeast direction (Figure

7). Hence, the high $PM_{2.5}$ concentrations were probably influenced by the biomass burning in the provinces and countries located in the northeast of Nakhon Pathom.

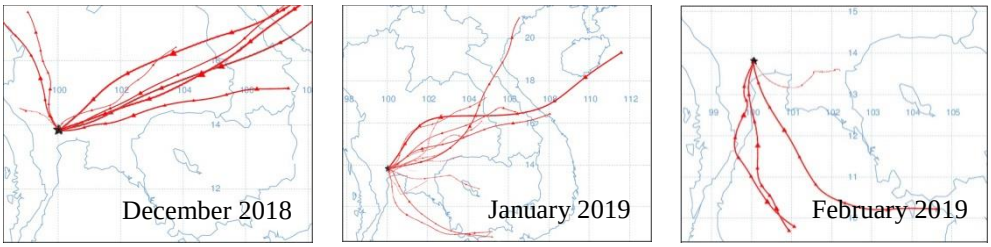

Figure 7 Air parcel back trajectories

However, to prove this assumption the correlation between daily ambient $PM_{2.5}$ concentrations and the number of hotspot counts per area should be further investigated.

Correlation between ambient $PM_{2.5}$ and hotspot counts per area

The correlations between daily average ambient $PM_{2.5}$ and the daily hotspot counts per area were highest for Cambodia followed by Nakhon Pathom, Thailand, Vietnam, Laos, and China with corresponding values of 0.56, 0.26, 0.19, 0.12, 0.11, and -0.09, respectively. There was a moderate correlation between ambient $PM_{2.5}$ concentration and the number of hotspot counts per area in Cambodia (r=0.56). The correlations were not very strong since the hotspot counts obtained from VIIRS display counts of burning rather than the sizes of burning area. Even in Nakhon Pathom and other countries, the correlation is obviously weaker comparing to Cambodia. As a result of the noticeably highest hotspot counts per area of Cambodia, the regional air quality in the Southeast Asia was highly affected. It is possible that the strong sources of $PM_{2.5}$ in Cambodia contribute $PM_{2.5}$ transboundary to Nakhon Pathom area, as shown in the HYPLIST model results (Figure 4). The

presumption was consistent with findings in Hou et al. (2019)'s study. Choi et al. (2019) found transboundary of $PM_{2.5}$ from China to South Korea. The contribution accounts for almost 68% while the local sources contribute only 57%. Zhang et al. (2017) mentioned that $PM_{2.5}$ originated in China in 2007 was related to more than 64,800 premature deaths in other regions, including more than 3,100 premature deaths in Western Europe and the USA. Trends of ambient $PM_{2.5}$ concentrations and hotspot counts per area were illustrated in Figure 8.

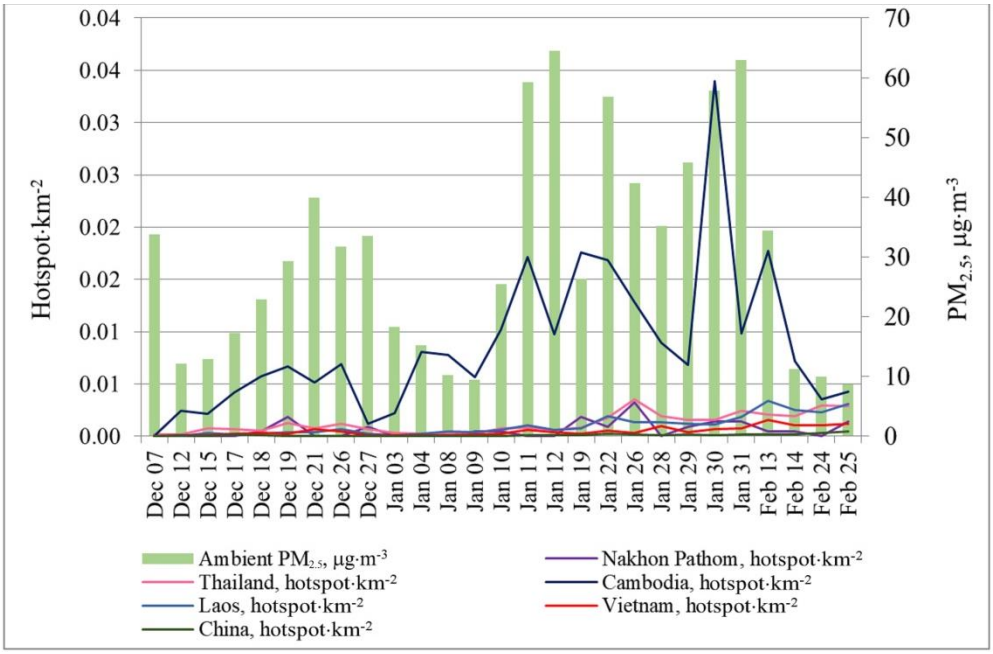

Figure 8 Trends of ambient $PM_{2.5}$ concentrations and hotspot counts per area

CONCLUSIONS

$PM_{2.5}$ concentrations were monitored in ambient and indoor air during intensive biomass burning period in Nakhon Pathom and other provinces as well as other countries. The results showed that the concentrations exceeded the air quality standards and put - people in the areas at risk for their health.

Moreover, correlations between the ambient and indoor $PM_{2.5}$ concentration as well as between

ambient $PM_{2.5}$ concentration and hotspot counts per area were also analyzed. The results showed that $PM_{2.5}$ concentrations in the ambient and indoor air were strongly correlated. However, the indoor concentrations were significantly higher than ambient concentrations due to the accumulation caused by the poor ventilation inside the building.

The highest hotspot counts per area in Cambodia implied that biomass burning in Cambodia is a strong source of $PM_{2.5}$ in Southeast Asia region. That means local air quality can also be affected by atmospheric transport of pollution from distant sources.

The findings from this research suggested that agro-residue burning contribute to high $PM_{2.5}$ concentration. Nowadays, although open burning is prohibited in Thailand, agricultural wastes are still illegally burned, particularly in the rural areas. Consequently, further strict and applicable strategies should be implemented not only in Thailand but also in other agricultural countries.

ACKNOWLEDGEMENTS

We thank Department of Environmental Science, Faculty of Science, Silpakorn University for assistance with sampling equipment, Dr. Prapat Pongkiatkul, Assist. Prof. for data compilation, and Dr. Boonjeera Chiravate, Assist. Prof., Silpakorn University for comments that greatly improved the manuscript. We would also like to thank reviewers for their so-called insights.

REFERENCES

Challoner A, and Gill L. Indoor/outdoor air pollution ships in ten commercial buildings: $PM_{2.5}$ and NO_2. Building and Environment 2014; 80: 159-173.

Choi J, Park RJ, Lee HM, Lee S, Jo DS, Jeong JI, et al. Impacts of local vs trans-boundary emissions from different sectors on 2.5 exposure in South Korea during the KORUS-AQ campaign. Atmospheric Environment 2019; 203: 196-205.

FAO Wood Energy, Climate and Health – International Expert Consultation,

Regional Wood Energy Development Programme in Asia, Field Document no. 58. Bangkok: Food and Agriculture Organization of the United Nations; 2000. 55 p.

Herbreteau, V. Remote sensing and GIS in risk zonation of human exposure to Hantavirus related diseases. Case of Nakhon Pathom province, Thailand. Master of Engineering Thesis 2001. Asian Institute of Technology.

Hou X, Chan CK, Dong GH, and Yim SHL. Impact of transboundary air pollution and local emissions on PM2.5 pollution in the Pearl River Delta region of China and the public health, and the policy implications. Environmental Research Letters 2019; 14(3): 1-11.

Junpen A, Pansuk J, Kamnoet O, Cheewaphongphan P, and Garivait S. Emission of air pollutants from rice residue open burning in Thailand, 2018. Atmosphere 2018; 9(11): 499.

Kalili R, Bartell SM, Hu X, Liu Y, Chang HH, Belanoff C, Strickland MJ, and Viera VM. Early-life exposure to $PM_{2.5}$ and risk of acute asthma clinical encounters among children in Massachusetts: a case-crossover analysis. Environmental Health 2018; 17: 20. Available from: 10.1186/s12940-018-0361-6.

Kim Oanh NT, Permadi DA, Hopke PK, Smith KR, Phan Dong N, Nguyet Dang A. Annual emissions of air toxics emitted from crop residue open burning in Southeast Asia over the period of 2010-2015. Atmospheric Environment 2018; 187: 163-173.

Kim Oanh NT, Thanh Hang N, Tipayarom A, Thiansathit W, Tipayarom D. Characterization of particulate matter measured at remote forest site in relation to local and distant contributing sources. Aerosol and Air Quality Research 2016; 16: 2671-2684.

Kim Oanh NT, Tipayarom A, Bich TL, Tipayarom D, Simpson CD, Hardie D, Liu AJS. Characterization of gaseous and semi-volatile organic compounds emitted from field burning of rice straw. Atmospheric Environment 2015; 119: 182-191.

NASA. Joint polar satellite system. USA: NAZA; 2016. [Updated 2016 June 9; cited 2019 Apr 16]. Available from https://jointmission.gsfc.nasa.gov/viirs.html

NASA. VIIRS I-Band 375 m Active Fire Data. USA: NAZA; 2018. [Updated 2018 July 19; cited 2019 Apr 16]. Available from https://earthdata.nasa.gov/earth-observation-data/near-real-time/firms/viirs-i-band-active-fire-data

Office of Nakhon Pathom Province. General Information of Province. Nakhon Pathom: Office of Nakhon Pathom Province. General Information of Province; 2016. [Updated 2016 May

11; cited 2019 Apr 16]. Available from http://www.nakhonpathom.go.th/content/information

Phairuang W, Suwattiga P, Chetiyanukornkul T, Hongtieab S, Limpaseni W, Ikemori F, Hata M, Furuuchi M. The influence of the open burning of agricultural biomass and forest fires in Thailand on the carbonaceous components in size-fractionated particles. Environmental Pollution 2019; 247: 238-247.

Thailand's Department of Health. Indoor air quality assessment manual. Bangkok: Bureau of Environmental Health, Department of Health, Ministry of Public Health; 2017. 95 p.

Thailand's Pollution Control Department [Internet]. Bangkok: Thailand's Pollution Control Department; 2019. Air and noise quality standards [2019 Apr 17]; [about 5 screens]. Available from http://www.pcd.go.th/info_serv/reg_std_airsnd01.html

Tipayarom A. PM10 concentrations and hotspots in Western Thailand in agro-residue burning season. Silpakorn University Science and Technology Journal 2012; 6(2): 30-36.

Tipayarom D, Kim Oanh NT. Effects from open rice straw burning emission on air quality in the Bangkok Metropolitan Region. ScienceAsia 2007; 33: 339-345.

US EPA [Internet]. Washington DC: US EAP; 2018. Health and environmental effects of Particulate matter (PM); 2018 June 20 [cited 2019 Apr 17]; [about 3 screens]. Available from https://www.epa.gov/ pm-pollution/health-and-environmental-effects-particulate-matter-pm

US EPA. Compendium of methods for the determination of air pollution in indoor air. Springfield: U.S. Department of Commerce National Technical Information Service; 1990. 403 p.

Wang J, Zhang M, Bai X, Tan H, Li S, Liu J, et al. Large-scale transport of PM2.5 in the lower troposphere during winter cold surges in China. Scientific Report 2017; 7: Available from: 10.1038/s41598-017-13217-2

WHO [Internet]. Geneva: WHO; 2019. More than 90% of the world's children breathe toxic air every day; 2018 Oct 29 [cited 2019 Apr 19]. Available from https://www.who. int/news-room/detail/29-10-2018-more-than-90-of-the-world%E2% 80%99s-children-breathe-toxic-air-every-day

Xing Y-F, Xu Y-H, Shi M-H, and Lian Y-X. The impact o2f $PM_{2.5}$ on the human respiratory system. Journal of Thoracic Disease 2016; 8(1): E69-E74.

Xu X, Barsha NAF, and Li J. Analyzing regional influence of particulate matter on the city of Beijing, China. Aerosol and Air Quality Research 2008; 8(1): 78-93.

Zhang Q, Jiang X, Tong D, Davis SJ, Zhao H, Geng G. et al. Transboundary health impacts of transported global air pollution and international trade. Nature 2017; 543: 705-709.

Arsenic in rice and paddy soil samples

Wannee Srinuttrakul[1*], Vorapot Permnamtip[2], Wiranee Sriweing[1], Satoshi Yoshida[3]

[1]Research and Development Division, Thailand Institute of Nuclear Technology (Public Organization, Ongkharak, Nakhon Nayok, 26120, Thailand

[2]Nuclear Technology Service Center, Thailand Institute of Nuclear Technology (Public Organization, Ongkharak, Nakhon Nayok, 26120, Thailand

[3]Department of Management and Planning, National Institutes for Quantum and Radiological Science and Technology, Chiba, 263-8555, Japan

Corresponding author: E-mail: neesrinut@yahoo.com

ABSTRACT

Arsenic (As) is a toxic element that is widely found naturally in the environment. In this study, the concentration of As in rice and paddy soil samples collected from the northeastern region of Thailand was determined by inductively coupled plasma mass spectrometry. The mean concentration of As in rice and soil samples were 0.140±0.059 and 1.82±1.37 mg kg^{-1}, respectively. All rice samples showed inorganic As lower than the limit data of Codex (0.2 mg kg^{-1}). As in paddy soil samples was less than the US EPA cancer soil screening level (22 mg kg^{-1}). The estimated daily intake (EDI) of inorganic As from rice consumption was 0.023 ± 0.010 mg day^{-1}. The percentage contribution to Provisional Tolerable Weekly Intake (PTWI) value of As for Thai male (body weight of 69 kg) was 15.5% and for Thai female (body weight of 57 kg) was 18.7%. The findings indicated that all studied rice samples are safe for consumption.

Keywords: Arsenic, Rice, Soil, Estimated daily intake, ICP-MS

INTRODUCTION

Rice is a staple food for a large part of the world's population including Thailand. It is an important source of carbohydrates, proteins, fats, fiber, vitamins, mineral elements, and other nutrients (Houston and Kohler, 1970). The increasing of toxic element levels in the environment has been a great concern worldwide because of its toxicity. Toxic element such as arsenic (As) has been widely found in the environment including soil, water and air, because it is a naturally occurring substance and contamination from human activity (Hang et al, 2009; Nadimi-Goki et al, 2014; Ma et al, 2016; Shrivastava, 2017). Arsenic in the environment can enter to agricultural crops via root uptake or aerial contamination. The intake of As can cause cancer in several internal organs (such as liver, kidney, lung, bladder), and can increase the risk for skin cancer (US EPA, 1993). Therefore, it is important to control the levels of As in agricultural crops or foodstuffs in order to protect human health.

Thailand is one of the world's biggest rice producers and exporters. Rice is the most important economic crop of Thailand. Thai Hom Mali rice is famous rice of Thailand and well known in the world. It is considered as premium rice in the world market. The data of arsenic in Thai Hom Mali rice would be useful for Thai rice database not only for commerce but also for health risk assessment. Furthermore, the obtained information also provides the accumulation of As in the agricultural ecosystem and serves as a baseline data of Thai rice for future environmental monitoring. The determination of As in rice samples is important to evaluate its exposure to population.

The objective of this study was to determine the level of As in polished Thai Hom Mali rice samples and paddy soil samples collected from the northeastern region of Thailand by inductively coupled plasma mass spectrometry (ICP-MS). The concentration of As in rice was compared with the maximum limit of

inorganic arsenic for polished rice set by Codex value of 0.2 mg kg^{-1} (FAO, 2014). The estimated daily intake (EDI) and Provisional Tolerable Weekly Intake (PTWI) of As resulting from rice consumption were also carried out.

MATERIALS AND METHODS

Reagents and standards

All the chemical reagents used were supra-pure analytical grade. Ultrapure water was produced by a Milli-Q water purification system (Millipore Corporation; Billerica, MA, USA). The standard solution was purchased from Agilent Technologies (New Haven, CT, USA).The standard reference materials were rice flour (NIST 1568a) from National Institute of Standards and Technology (NIST; MD, USA) and soil (NCS ZC 73007) from China National Analysis Center for Iron and Steel (Beijing, China)

Sample collection and preparation

Fifty Thai Hom Mali rice and associated soil samples were collected from the paddy fields in Maha Sarakham (5), Roi Et (20), Si Sa Ket (10), Surin (5) and Yasothon (10) in the northeast of Thailand in November 2014.

Rice grains (2-3 kg) harvested from the paddy field were dehulled and polished to be the polished rice or white rice samples. All polished rice samples were dried in an electric oven at 60 ± 2°C and ground to a fine powder by the high speed blender (1093 Cyclotec Sample Mill, Hoganas, Sweden). The rice powders were dried again in an oven at 60 ± 2°C untill constant weight, kept in polyethylene containers and stored in a desiccator until chemical analysis.

All dried rice powder samples (0.5 g) were digested in PTFE vessels on a hot plate with 10 mL of 65% HNO_3 and 4 mL of 48% HF at 120 °C for 5 h. After digestion, the samples were evaporated to dryness and the residues were dissolved in 1 mL of 65% HNO_3 and 0.5 mL of 30% H_2O_2. After drying, the residues were dissolved and diluted to 10 mL with 2% HNO_3. Sample digestions were done in triplicate. The standard

reference material of rice flour (NIST 1568a) was used to validate the analytical method.

Soil samples were collected at 0 - 10 cm depth, passed through a 2 mm stainless steel sieve, dried in an oven at 110 °C and ground to powder. All dried soil samples (0.1 g) were digested in PTFE vessels on a hot plate with 7.5 mL of 65% HNO_3, 7.5 mL of 70% $HClO_4$ and 1 mL of 48% HF at 140 °C for 5 h. After digestion, the samples were evaporated to dryness and the residues were dissolved in 1 mL of 65% HNO_3 and 0.5 mL of 30% H_2O_2. After drying, the residues were dissolved and diluted to 10 mL with 2% HNO_3. Sample digestions were done in triplicate. The standard reference material of soil (NCS ZC 73007) was used to validate the analytical procedure.

Determination of As by ICP-MS

The concentrations of As in rice and soil samples were analyzed by ICP-MS (Agilent 7900, Agilent Technologies, USA). The instrumental operating conditions for the determination of the elements are presented by Srinuttrakul et al (2018). Indium (In) was used for internal standard to compensate for changes in analytical signals during the operation. Standard solutions were prepared from Agilent multi-element solution and used to create a calibration standard curve with minimum of 5 points.

Transfer factor of As from soil to rice

The transfer factor (TF) of As from soil to rice was calculated from the As concentration in rice (mg kg^{-1} dry weight) divided by the As concentration in a soil (mg kg^{-1} dry weight).

Estimated daily intake of Arsenic

The Estimated Daily Intake (EDI) of As resulting from rice consumption was calculated from the following formula:

$$EDI = C_{As} \times DC_{rice}$$

where C_{As} is the mean value of arsenic in rice and DC_{rice} is the daily average rice consumption assumed to be 233 g/person/day for Thai which is

equivalent to yearly amount of about 85 kg per person (National Statistical Office and Office of Agricultural Economics of the Kingdom of Thailand, 2012).

Provisional tolerable weekly intake

The Provisional Tolerable Weekly Intake (PTWI) of arsenic resulting from rice consumption was calculated from the following formula:

$$PTWI = C_{As} \times WC_{rice}/bw$$

where WC_{rice} is the average per capita weekly consumption of rice (1,631g) and bw is the individual's body weight assumed to be 69 kg for male and 57 kg for female of Thai (NECTEC, NSTDA, 2017).

Statistical analysis

The statistical analysis of Microsoft Office Excel 2016 was used to calculate the mean, and standard deviation (SD). The difference between the means of two data sets was evaluated using the Student's *t*-test at the 95% confidence interval (*t*-test; $p < 0.05$).

Results and Discussion

Quality control

The standard reference materials of rice flour (NIST 1568a) and of soil (NCS ZC 73007) were used to validate the analytical procedure. The result of analyzed value presented in Table 1 showed good agreement with the certified value. Error of observed values for As was less than 6% of the certified value.

Table 1. Analyzed value of reference materials by ICP-MS.

Reference material	Certified value (mg kg^{-1})	Analyzed value (mg kg^{-1})	% Error
NIST 1568a	0.29±0.03	0.29 ±0.01	5
NCS ZC 73007	18 ± 2	18.6 ±0.9	3

Concentrations of As in rice samples

The mean concentration of As in fifty polished rice samples determined by ICP-MS were 0.140±0.059 mg kg^{-1}. The As level in rice samples according to the cultivation province was presented in Table 2. The highest mean concentration of As (0.215± 0.063 mg kg^{-1}) was found for rice samples from Maha Sarakham. Whereas Rice samples from

Yasothon had the lowest mean content of As (0.094±0.033 mg kg^{-1}). The mean As content of rice samples from Maha Sarakham was different from the other area except Si Sa Ket (*t* test; $p < 0.05$).

Table 2. Concentration of As in rice samples (mg kg^{-1}).

Cultivation province	Mean	SD	Min.	Max.
Maha Sarakham (*n* = 5)	0.215	0.063	0.114	0.272
Roi Et (*n* = 20)	0.112	0.050	0.032	0.215
Si Sa Ket (*n* = 10)	0.145	0.056	0.041	0.227
Surin (*n* = 5)	0.107	0.010	0.094	0.120
Yasothon (*n* = 10)	0.094	0.033	0.054	0.166

As is a toxic heavy metal that is occurred naturally and contaminated in the environment by human activities (Hang et al., 2009). The maximum limit of inorganic arsenic for polished rice set by Codex (FAO, 2014) was 0.2 mg kg^{-1}. The concentration of As observed from this study (0.032-0.272 mg kg^{-1}) was the total arsenic. EFSA (EFSA, 2014) reported that inorganic arsenic represents approximately 70% of the total arsenic. Therefore, the inorganic As concentration of the studied rice samples calculated based on EFSA report was 0.022-0.190 mg kg^{-1}. All studied rice samples had the inorganic arsenic was lower than the maximum limit.

The concentrations of As in Thai Hom Mali rice samples from this study were compared with the data of Sangyod rice reported by Srinuttrakul et al (2018). The concentration range of As was found to be similar level for both works (0.032-0.272 vs. 0.022 - 0.248 mg kg^{-1}). Two rice samples from the present study showed the higher content of As than that of the previous report.

In comparison to the results of Thai rice with those of Japanese rice, the mean content of As from this study (0.140 ± 0.059 mg kg^{-1}) was significantly higher than those from the literatures reported by Tsukada et al (2007) (0.085±0.020 mg kg^{-1}) and Uchida et al (2007) (0.057 mg kg^{-1}). Kelly et al (2002) reported that topography, soil property, fertilizer and pesticide used were influence on the elemental concentration in rice.

Concentrations of As in soil samples

The As level in fifty paddy soil samples collected from the same area of rice samples was 1.82±1.37 mg kg^{-1}. The As content in soil samples according to the cultivation province was given in Table 3. Surin showed the greatest As with the mean of 3.49 ± 1.92 mg kg^{-1}. Maha Sarakham had the lowest As of 0.732 ± 0.103 mg kg^{-1}. As concentration in all paddy soil samples was in the range of As in the natural soils (0.1 to 40 mg kg^{-1}) (Mandal and Suzuki, 2002; WHO, 2001). All studied soil samples had As content less than the EPA soil screening level to protect against non-cancer effects (22 mg kg^{-1}) (U.S. EPA, 2011).

In comparison with the As level of soil collected around the monazite processing facility in Phathum Thani, Thailand, most of soil samples from the present work (0.440 - 6.703 mg kg^{-1}) had As lower than from the previous reported (3.85 - 36.01 mg kg^{-1}) (Srinuttrakul and Yoshida, 2012).

Table 3. Concentration of As in paddy soil samples (mg kg^{-1}).

Cultivation province	Mean	SD	Min.	Max.
Maha Sarakham (*n* = 5)	0.732	0.103	0.634	0.905
Roi Et (*n* = 20)	1.83	0.946	0.440	3.66
Si Sa Ket (*n* = 10)	1.56	0.743	0.866	3.33
Surin (*n* = 5)	3.49	1.92	1.67	6.70
Yasothon (*n* = 10)	1.71	0.683	1.00	3.033

Transfer factor of As from soil to polished rice

The transfer factor (TF) of As from soil to polished rice is the uptake of As by polished rice from the soil. The TF of As ranged from 0.015 to 0.489. The highest mean TF was observed for sample from Maha Sarakham, followed by Si Sa Ket, Roi Et, Yasothon and Surin, shown in Table 3. Uchida et al (2007) reported that the water management practices and amounts of elements in plant available fractions in soil affect the TFs. As is a toxic element, therefore the rice and soil samples from Maha Sarakham should be studied more to monitor the accumulation of As in the environment.

Table 4. Transfer factor of As from paddy soil to polished rice.

Cultivation province	Mean	SD	Min.	Max.
Maha Sarakham (n = 5)	0.295	0.092	0.179	0.388
Roi Et (n = 20)	0.097	0.112	0.019	0.489
Si Sa Ket (n = 10)	0.111	0.067	0.035	0.251
Surin (n = 5)	0.038	0.019	0.015	0.068
Yasothon (n = 10)	0.059	0.018	0.027	0.086

Estimated daily intake of Arsenic

The Estimated Daily Intake (EDI) of As resulting from rice consumption was evaluated. The EDIs of total As and inorganic As were 0.033±0.014 and 0.023 ± 0.010 mg day^{-1}, respectively.

Provisional tolerable weekly intake

The Provisional Tolerable Weekly Intakes (PTWIs) of As from rice consumption for Thai was evaluated. The obtained PTWI values were compared with the PTWI value established by the Joint FAO/WHO Committee on Contaminants in Foods (0.015 mg kg^{-1} bw) (JECFA, 2011), displayed in Table 5.

The estimated contribution from As ranged from 14.9-40.9% of PTWI. The daily intake of As was highest in rice samples from Maha Sarakham with 33.8% and 40.9% of the PTWI for males and females, respectively. The daily intake of As from this study (Table 5) was calculated from the total arsenic. Thus the daily intake of inorganic As from rice samples of Maha Sarakham was 23.7% and 28.7% of the PTWI for males and females, respectively. The percentage contribution to PTWI value of inorganic As for all studied samples was 15.5% for males and 18.7% for females. All rice samples from this study had the dietary intake of As lower than the PTWI.

Table 5. Provisional Tolerable Weekly Intake (PTWI) of total As by Thai consumer.

Cultivation province	Daily Intake (mg day^{-1})	% of the established PTWI	
		Male	Female
Maha Sarakham (n = 5)	0.050 ± 0.015	33.8	40.9
Roi Et (n = 20)	0.026 ± 0.012	17.7	21.4
Si Sa Ket (n = 10)	0.034 ± 0.013	22.8	27.7
Surin (n = 5)	0.025 ± 0.002	16.8	20.3
Yasothon (n = 10)	0.022 ± 0.008	14.9	18.0

CONCLUSIONS

ICP-MS is a suitable technique for determination of As concentrations in rice and soil sample. The concentrations of As in polished rice samples was 0.116±0.050 mg kg^{-1}. The highest concentration of As was found in rice samples from Maha Sarakham and in paddy soil sample from Surin. The studied samples of Thai Hom Mali rice are safe for consumption. However, As in rice and associated soil samples should be continuously determined to ensure the safety of rice consumption.

ACKNOWLEDGEMENTS

We would like to thank the staff of Agricultural Extension Office for their assistance in cooperation with the farmers. We thank the farmers for providing their rice samples.

REFERENCES

1. EFSA. Dietary exposure to inorganic arsenic in the European population. EFSA Journal 2014; 12(3): 3597.
2. FAO-Food and Agriculture Organization of the United Nations. 2014. Report of the Eight Session of the Codex Committee on Contaminants in Foods.
3. Hang X, Wang H, Zhou J, Ma C, Du C, Chen X. Risk assessment of potentially toxic element pollution in soils and rice (*Oryza sativa*) in a typical area of the Yangtze River Delta. Environmental Pollution 2009; 157: 2542-2549.
4. Houston DF, Kohler GO. Nutritional properties of rice. Washington DC: The National Academies Press; 1970.
5. JECFA. Joint FAO/WHO food standards programme Codex Committee on contaminants in foods: Working document for information and use in discussions related to contaminants and toxins in the GSCTFF 2011.
6. Kelly S, Baxter M, Chapman S, Rhodes C, Dennis J, Brereton P. The application of isotopic and elemental analysis to determine the geographical origin of premium long grain rice. European Food Research and Technology 2002; 214: 72-78.
7. Mandal BK, Suzuki KT. Arsenic round the world: a review. Talanta 2002; 58: 201-235.
8. Ma L, Wang L, Jia Y, Yang Z. Arsenic speciation in locally grown rice grains from Hunan Province, China: Spatial distribution and potential health risk. Science Total Environment 2016; 557-558: 438-444.
9. Nadimi-Goki M, Wahsha M, Bini C, Kato T, Vianello G, Antisari LV. Assessment of total soil and plant

elements in rice-based production systems in NE Italy. Journal of Geochemical Exploration 2014; 147: 200-214.

10. NECTEC, NSTDA. SizeThai (Online). Avaiable: http://www.sizethailand.org/region_all.html.
11. National Statistical Office and Office of Agricultural Economics of the Kingdom of Thailand. Food insecurity assessment at national and subnational levels in Thailand, 2011, Bangkok, Thailand. 2012.
12. Regional Screening Level (RSL) Resident Soil Table. U.S. Environmental Protection Agency 2011.
13. Shrivastava A, Barla A, Singh S, Mandraha S, Bose S. Arsenic contamination in agricultural soils of Bengal deltaic region of West Bengal and its higher assimilation in monsoon rice. Journal of Hazardous Materials 2017; 324: 526-534.
14. Srinuttrakul W, Yoshida S. Concentration of arsenic in soil samples collected around the monazite processing facility, Thailand. Journal of Radioanalytical and Nuclear Chemistry 2012; DOI 10.1007/s10967-012-2347-0.
15. Srinuttrakul W, Permnamtip V, Yoshida S. Heavy Metals in Sangyod Rice Samples Cultivated in Phatthalung, Thailand. Food and Applied Bioscience Journal 2018; 6(Special Issue on Food and Applied Bioscience): 45-54.
16. Tsukada H, Hasegawa H, Takeda A, Hisamatsu S. Concentrations of major and trace elements in polished rice and paddy soils collected in Aomori, Japan. Journal of Radioanalytical and Nuclear Chemistry 2007; 273(1): 199-203.
17. Uchida S, Tagami K, Hirai I. Soil-to-plant transfer factors of stable elements and occurring radionuclides: (2) Rice collected in Japan. Journal of Nuclear Science and Technology 2007; 44: 779-790.
18. United States Environmental Protection Agency (US EPA). Arsenic, Inorganic; Environmental Protection Agency, Integrated Risk Information System: Washington, DC, USA, 1993; CASRN 7440-38-2.
19. WHO. Environmental health criteria 224, arsenic and arsenic compound. Inter-organization programme for the sound management of chemicals, Geneva 2001.

Isotopic mass balance approach for verification of shallow groundwater recharge, Phitsanulok

Wutthikrai Kulsawat[1*] and Phatchada Nochit[1]

[1] *Thailand Institute of Nuclear Technology (Public Organization),
Head Office 9/9 Moo7 Ongkharak, Nakhon-Nayok
Corresponding author; e-mail: wutthikrai@tint.or.th

ABSTRACT

This study employs a mass balance approach on stable isotopes to verify shallow groundwater recharge in Chumsaeng Songkhram district, Phitsanulok during 2016-2017. Precipitation, shallow groundwater, and surface water samples were collected and analyzed for stable hydrogen and oxygen isotopic compositions. The study area had low humidity and high ambient temperature causing the observed Local Meteoric Water Line (LWML) shown smaller slope and intercept than in the Global Meteoric Water Line. The surface water was enriched in heavier stable isotopes of oxygen and hydrogen and offset from the LMWL indicating an evaporation of surface water. Overall, hydrogen and oxygen isotopic compositions of shallow groundwater were distributed along the LMWL implying that local rainfall was the main source of recharge for shallow groundwater. Using isotopic mass balance approach, the percentage recharge contribution of surface water and rainwater to groundwater was calculated. This study found that groundwater recharge during the monsoon season was consisted of approximately 90.17% rainwater. Similarly, the average contribution of surface water during the high flow period was about 9.83%.

Keywords: Mass balance, Stable isotopes, Shallow groundwater

INTRODUCTION

Stable isotopes of hydrogen and oxygen are part of the water molecule. They are not affected by environment and degradation of water quality (Kendall and McDonnel, 2012). Hydrological processes and different stages in the water cycle including the movement of water bodies control the hydrogen and oxygen isotopic signatures or compositions with a low temporal variation. Therefore, stable isotopes of hydrogen and oxygen are particularly useful as natural tracers in studies of groundwater recharge sources (Liu, et al., 2016; Ma, et al., 2017; Krishan, et al., 2017; Shamsuddin, et al., 2018; Yeh and Lee, 2018).

The economy of Chumsaeng Songkram sub-district, Phitsanulok is agriculture-based which peasant rain-fed agriculture is the main employment. However, recent erratic patterns of rainfall in the area coupled with rising populations in the province, have increased interests in assessing the potentials of developing the groundwater in the area. Chumsaeng Songkram has frequently suffered from flooding during the rainy/monsoon season, droughts in summer and even both in some particular areas. The highest demand for water in the area during summer arise from a municipal water supply, industries, and agriculture. Therefore, the lack of national capacity to supply irrigating water coupled with low precipitation has led to the heightened use of groundwater. Groundwater is non-renewable resource because of their extremely slow rate of recharge (Shamsuddin, et al., 2018; Yeh and Lee, 2018). It often takes hundreds to thousands of years to accumulate significant water in them. That is, groundwater should be rendered the same protective status as precious resources. The information on the recharge sources of groundwater in the area is crucial to sustainable groundwater exploitation. In order to investigate the water sources of groundwater recharge, conventional methods are rather time consuming, expensive and yield information only

on the absolute groundwater. The stable isotope mass balance method can be applied satisfactorily to analyze groundwater inflow and outflow contributions separately.

In this study, isotopic signatures of hydrogen (δ^2H) and oxygen ($\delta^{18}O$) of precipitation, surface water and groundwater in the Chumsaeng Songkram sub-district, Phitsanulok province have been used to estimate the contribution of precipitation, river water to groundwater recharge.

METHODOLOGY

Study area

Chumsaeng Songkhram (16°50′00″ N and 100°04′00″ E) is a sub-district situated in the Bang Rakam District of Phitsanulok Province (Fig. 1).

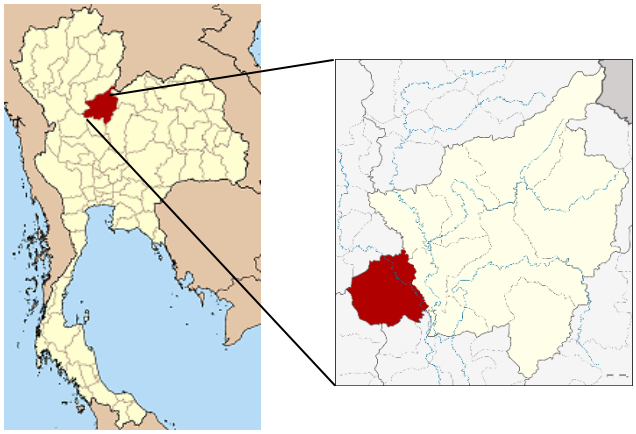

Figure 1 The study area in Bang Rakam district, Phitsanulok, Thailand

Three seasons have been identified which consists of summer or dry, rainy or wet, and cold or dry. The rainy season starts in May to October with an average annual rainfall of 1,375 mm. The rest of the year is relatively dry with occasional rains. However, due to the current fluctuation in weather patterns, attending the effects of climate change/ variability, the rainy season is highly erratic and unpredictable.

Total area of Chumsaeng Songkhram is 120.39 km^2, arable land covers 97.39 km^2 which equal to 81.87 % of total area. Economic crops are rice,

sugar canes maize and the standing timbers which mostly grow in the northern part area. Chumsaeng Songkhram is facing the water shortage for agriculture as all of the water resources in the area cannot store water throughout the whole year long. Local farmers built the artesian wells for additional supply because rain-fed agriculture cannot be sustained in the long run.

Sampling and analytical method

Samples of precipitation (daily event), shallow groundwater and surface water were collected for the analyses of $\delta^{2}H$ and $\delta^{18}O$ isotopic from the period of 2016-2017 during both dry and wet periods. Sampling of daily event precipitation was carried out not more than one day passed between the precipitation event and sample collection. Therefore, it excluded a measureable effect of the sampling procedure on the stable isotopic compositions of the samples. Rain sample was taken with a collector composed of a polyethylene tank and a funnel, fitted a ping-pong ball to prevent evaporation of the sample once collected. All rainwater samples were measured and collected unfiltered in 100 mL high-density polyethylene bottles. Air temperature and relative humidity were measured on site every day. During a sampling period, River water was collected monthly approximately 0.2 m in below the river surface and stored in 100 mL high-density polyethylene bottles. The shallow groundwater (pumping well) sample was collected monthly from two wells in 100 mL high-density polyethylene bottles after rinsing the bottle by the groundwater that was to be sampled. Prior to collection, groundwater was flushed adequately until pH and EC was achieved. All samples of precipitation, groundwater, and surface water were stored in a cool dry container and transported to the laboratory for analyses (IAEA, 2014).

The stable isotopes of precipitation, groundwater and surface water (Yom River) were analyzed using a Picarro L2130-i water isotope analyzer

(Picarro, Santa Clara, California, USA), in the Radiochemistry laboratory, Thailand Institute of Nuclear Technology (Public Organization). The isotope values were reported using the standard δ notation relative to the Vienna Standard Mean Ocean (V-SMOW). Each sample analyzed 6 times; the precision (one standard deviation) was determined as ± 0.7‰ for δ^2H and ± 0.08‰ for $\delta^{18}O$.

RESULTS AND DISCUSSION

Isotopic signatures of precipitation

Individual rain events were sampled from 2016 to 2017 with the total rainfall was observed to be 1140.0 and 1109.3 mm, during the years 2016 and 2017, respectively. Analysis of 97 rainwater samples revealed that δ^2H and $\delta^{18}O$ values were distributed between -100.74 to 19.43‰ and -14.35 to 2.58‰, respectively. The δ^2H and $\delta^{18}O$ values of precipitation enriched gradually in dry season and depleted in wet season which were highly comparable to air temperature trends, with high temperature in the dry season and low in wet season, indicating that temperature effects controlled the δ^2H and $\delta^{18}O$ values present in precipitation. In addition, the depletion of δ^2H and $\delta^{18}O$ in rainfall during August, September and October (monsoon) is because of the 'amount effect' of isotopes in precipitation (Yeh and Lee, 2018; Shamsuddin, et al., 2018; Yidana, 2013). The Local Meteoric Water Line, LMWL of Chumsaeng Songkram was found to be $\delta^2H = 7.289\delta^{18}O + 2.063$. The lower slope and intercept of LMWL relative to the Global Meteoric Water Line (GMWL $\delta^2H = 8.13\delta^{18}O + 10.8$; Craig, 1961) indicating that rainfall formation occurs under isotopic equilibrium conditions with similar rates of condensation and vaporization (Govender et al., 2013; Yidana, 2013; Cui and Li, 2015). Relative humidity in Chumsaeng Songkram fall in the range of 60% to 94% during the rainy season and therefore can lead to significant kinetic fractionation attending the evaporation of raindrops. Amount of rainfall, temperature, and relative

humidity all have important roles in affecting isotopic signatures of precipitation. The observation in this study whereas both the slope and intercept of the LMWL are lower than those of the GMWL is consistent with the literatures (Yidana, 2013, Govender, 2013).

Isotopic signatures of river water

Stable isotopes of surface water range from -43.92 to -21.67‰ for δ^2H and from -7.64 to -1.57‰ for $\delta^{18}O$. The δ^2H-$\delta^{18}O$ plot of the surface water (Yom River) appears more enriched than those of rainwater samples. The data fall on a Local Evaporation Line (LEL) defined by $\delta^2H = 3.543\delta^{18}O - 19.227$ ($R^2 = 0.978$) whose slope is lower than that of the LMWL and even lower than that of the GMWL. This observation is attributed to evaporative enrichment of the heavier isotopes of both elements. Evaporation of surface water bodies causes an enrichment in the heavier isotopes of the residual water, resulting in slopes of the δ^2H-$\delta^{18}O$ diagram in the range of 4 and 5.5 (Yidana, 2013). The slope of the regression equation for δ^2H-$\delta^{18}O$ plot depends on the atmospheric conditions prevailing during the period of the evaporation. The slope increases with increasing humidity and decreases when the humidity drops. Kinetic fractionation is an important factor responsible for isotopic enrichment arising from evaporation processes in open surface water (Shamsuddin, et al., 2018). The average deuterium excess of the surface water was 12.4‰, which is larger than the GMWL (10‰), indicating a faster evaporation process.

Characteristics of groundwater

The δ^2H values of the shallow groundwater samples ranged from -61.31 to -33.04‰ and the $\delta^{18}O$ values ranged from -8.81 to -3.82‰. The regression line equation for the groundwater is $\delta^2H = 5.009\delta^{18}O - 16.629$. The slope of the Local Groundwater Line is comparatively lower than those observed for the LMWL. This suggests that infiltrating rainwater underwent some enrichment of the heavier

isotopes prior to recharge during the processes of infiltration and percolation through the unsaturated zone to the saturated zone.

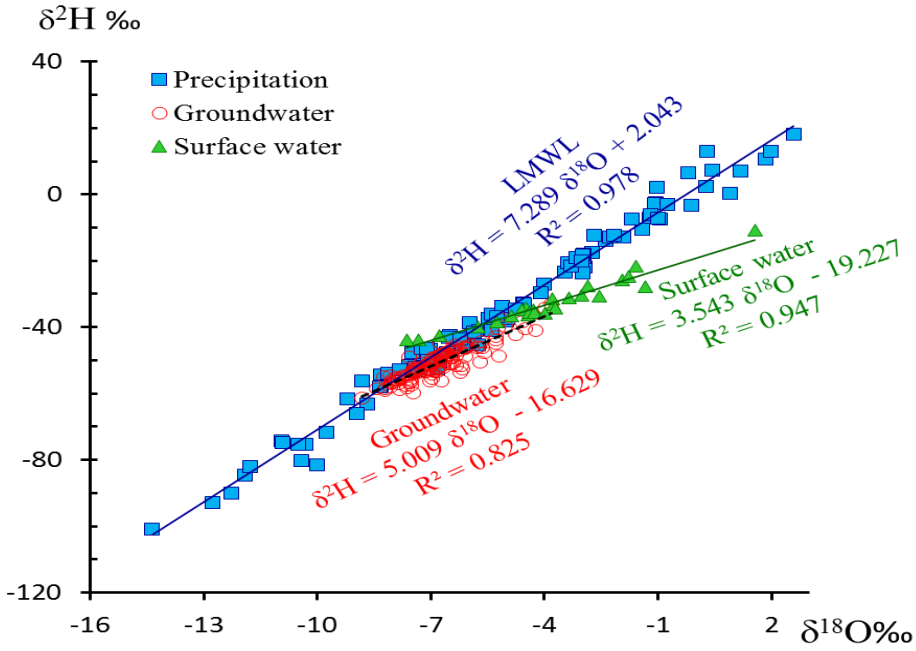

Figure 2 δ^2H and $\delta^{18}O$ plot of precipitation, surface water and groundwater

The isotopic characteristics of precipitation, surface waters from Yom River and shallow groundwater in the study area were compared using δ^2H-$\delta^{18}O$ plot (Fig. 2). The δ – diagram of rainwater, surface waters and groundwater revealed isotopic compositions of groundwater were closely distributed along the LMWL, indicating that local rainfall is the main source of recharge for groundwater in the study area.

Groundwater recharge estimation using mass balance analysis

The groundwater recharge in Chumsaeng Songkram is contributed by two constituent components, precipitation and surface water. A two component mixing model was performed in this study to verify the rainwater and surface water fraction in groundwater recharge. The results of isotopic compositions of δ^2H and $\delta^{18}O$ indicated a distinct difference

among precipitation, surface water and groundwater samples (Fig. 2).

The fraction of precipitation and surface water in groundwater was quantitatively verified from isotopic mass balance equation (Hameed et al., 2015; Yeh et al., 2014; Yidana, 2013) which were resulting 90.17% of precipitation and 9.83% of surface water recharged into the shallow groundwater in the study area.

CONCLUSIONS

Temporal variations in the hydrogen and oxygen isotopic signatures (δ^2H and $\delta^{18}O$) of precipitation, surface water and shallow groundwater were determined to estimate groundwater recharge sources from rainwater and Yom river water in the Chumsaeng Songkram sub-district, Bang Rakam district, Phitsanulok province, Thailand during 2016-2017. The isotopes of δ^2H and $\delta^{18}O$ in precipitation revealed that variations in the rainfall amount were resulted in the enrichment of δ^2H and $\delta^{18}O$ isotopes for precipitation in wet seasons compared to precipitation in dry seasons. River water had more enriched water isotopes of δ^2H and $\delta^{18}O$ compared to precipitation, signifying that the river water evaporated due to high temperature and low humidity. Based on the isotopic mass balance method, the results show that 90.17% of the shallow groundwater in the plain area of Chumsaeng Songkram is derived from meteoric water and 9.83% is from river water. The results provide useful information on the interaction of precipitation, river water, and groundwater including verifying the isotopic mass balance approach for estimating shallow groundwater recharge in the study area. The suggestion is that efficient use of available water resources should be given more emphasis than the provision of more water and responsibilities which would ensure the sustainability exploitation should be imposed on the public

ACKNOWLEDGEMENTS

This research was financially supported by the National Research Council of Thailand. The authors would like to thank anonymous

reviewers and the editorial staff of the EnvironAsia2019 for assistance in the revision and production of this manuscript.

REFERENCES

Craig, H. Isotopic variations in meteoric waters. Science 1961; 133, 1702–1703.

Cui, BL, Li XY.. Stable isotopes reveal sources of precipitation in the Quinghai lake basin of the northeastern Tibetan Plateau. Science of the Total Environment 2015; 527-528:26-37.

Hameed, AS, Resmi, TR, Suraj, S, Unnikrishnan Warrier, C, Sudheesh, M, Despande, RD. Isotopic characterization and mass balance reveals groundwater recharge pattern in Chaliyar river basin, Kerala, India. Journal of Hydrology: Regional Studies 2015; 4: 48-58.

International Atomic Energy Agency, IAEA/GNIP Precipitation Sampling Guide; IAEA, Vienna, Austria, 2014.

Kendall C., McDonnell J.J. Isotope Tracers in Catchment Hydrology. 2nd Ed. Elsevier, 2012.

Krishan, G, Singh, S, Sharma, A, Sandhu, C, Kumar, S, Gurja, S. Assessment of river Yamuna and groundwater interaction using isotopes in Agra and Muthura area of Uttar Pradesh, India. International Journal of Hydrology 2017; 3:86-89.

Liu, J, Chen, Z, Zhang, Y, Li, Z, Zhang, L, Liu, F. Stable isotope evidences on sources and mechanisms of groundwater recharge in Hohhot basin, China. Environ. Earth Sci. 2016; 75, 1–10.

Ma, B, Liang, X., Liu, S, Jin, M, Nimmo, JR, Li, J. Evaluation of diffuse and preferential flow pathways of infiltrated precipitation and irrigation using oxygen and hydrogen isotopes. Hydrogeol. J. 2017; 25, 675–688.

Shamsuddin, MKN, Sulaiman, WNA, Ramli, MF, Kusin, FM, Samuding, K. Applied Water Science 2018; 8:120-132.

Yeh, HF, Lin, HI, Lee, CH, Hsu, KC, Wu, CH. Identifying seasonal groundwater recharge using environmental stable isotopes. Water 2014; 6:2849-2861.

Yeh, HF, Lee, JW. Stable hydrogen and oxygen isotopes for groundwater sources of Penghu islands, Taiwan. Geosciences 2018; 8: 84-92.

Yidana, SM. The stable isotope characteristics of groundwater in the Voltaian basin- An evaluation of the role of meteoric recharge in the basin. Journal of hydrogeology & hydrologic engineering 2018; 2(2):1-10

Kinetic Study and Adsorption Isotherm of Lead Adsorption from Aqueous Solution onto Polyvinyl Alcohol - Alginate Beads Immobilized with Spent Yeast

Mongkol Phensaijai[1*] and Muanmai Apintanapong[2]

[1*]Department of Biology, Faculty of Science, King Mongkut's Institute of Technology Ladkrabang, Chalongkrung Rd., Ladkrabang, Bangkok, Thailand; Corresponding author: e-mail: mongkol.ph@kmitl.ac.th

[2] School of Science and Technology, University of the Thai Chamber of Commerce, 126/1 Vibhavadee-Rangsit Rd., Dindaeng, Bangkok, Thailand

ABSTRACT

Spent yeast was immobilized with polyvinyl alcohol and sodium alginate and used in the study on adsorption of lead to determine the effect of initial lead concentration. A kinetic model has been developed using pseudo-first and pseudo-second order equations. The sorption capacity was evaluated using four equilibrium isotherm models. The results showed that the sorption of lead can be described by a pseudo-second order model as shown from higher correlation coefficients (R^2). The values of the rate constants (k_2) and initial sorption rate (h) were calculated and tended to decrease with an increase in the initial concentration of lead. Langmuir, Freundlich, Temkin and Dubinin-Radushkevich (D-R) isotherms were used to fit the equilibrium sorption data. The results showed that the R^2 value of Freundlich isotherm was the highest. The sorption intensity was 2.40 indicating a favorable sorption process. Langmuir isotherm is also favorable, the maximum monolayer coverage was 12.29 mg/g and the separation factor was 0.006-0.024. The heat of sorption process was estimated to be 791.86 J/mol from Temkin isotherm model and the mean free energy was 2.93 kJ/mol calculated from D-R isotherm model.

Keywords: Sorption isotherm, Spent yeast, Polyvinyl alcohol, Sodium alginate, Lead

INTRODUCTION

Discharge wastes from various industries, agricultural and domestic use contain with different types of heavy metals and become one of the most important environmental problems nowadays (Macek and Mackova, 2011). Lead is classified in the group of toxic metals (Wang and Chen, 2006) that may cause human health risks. Contamination of lead still has significant amounts and impact on human health and environment, although use of lead in many industries tends to reduce in recent years (Tchounwou et al., 2012). Removal of heavy metal ions from wastewater can be done by conventional methods, such as chemical precipitation, ion exchange, electrochemical treatment, membrane technologies, and adsorption on activated carbon (Wang and Chen, 2006). According to expensive adsorption processes by using ion exchange, membrane technologies and activated carbon, biosorption process using biological materials is new cost-effective technologies (Das et al., 2008).

Yeast, *Saccharomyces cerevisiae*, is one of biomaterials with high metal-binding capacity and can be produced in high quantity by using fermentation (Wang and Chen, 2006). El-Gendy and Nassar (2015) studied on application of spent waste biomass yeast *S. cerevisiae* from bioethanol production process for removal of phenol from aqueous solution showed good affinity towards phenol (17.96 mg/g). Farhan and Khadom (2015) evaluated the potential of *S. cerevisiae* to remove heavy metals, they found that metal removal occurred rapidly at pH values 5.0–6.0, and the order of accumulated metal ions is Pb>Zn>Cr>Co>Cd>Cu.

Various types of adsorbents have been used for heavy metals adsorption such as polyvinyl alcohol

(PVA), sodium alginate, chitosan, polyvinyl chloride, and halloysite nanotubes (Lee et al., 2018). Khuathan and Pongjanyakul (2014) explained that sodium alginate is a negatively charged polysaccharide that is composed of β-D-mannuronic acid and α-L-guluronic acid. Cadmium and zinc biosorption were studied using sodium alginate immobilized *Chlorella homosphaera* cells, the metal removal achieved values near 100% (da Costa and Leite, 1991). Polyvinyl alcohol (PVA) is a highly soluble, biodegradable with mechanical stability, high diffusivity, and chemical stability of a synthetic polymer. It can be dissolved in water easily according to the existence of hydroxyl groups in its chemical structure (Kadaiji, 2011). PVA also has excellent adsorption abilities similar to sodium alginate and it is a synthetic polymer suitable for blending with other natural polymers due to its high polarity and water solubility (Majidnia and Fulazzaky, 2017; Majidnia and Idris, 2015).

Many publications reported on the application of PVA, as reported by Hsu et al. (2010), PVA immobilized with sulfate-reducing bacteria (SRB) was studied. PVA-immobilized SRB could enhance heavy metal removal and the resistance of SRB to heavy metal toxicity. PVA-immobilized SRB had heavy metal removal efficiencies of 76.3%, 95.6%, 100%, and 91.2% for Cu, Zn, Pb, and Cd, respectively (Li et al., 2017). The PVA-alginate beads showed high potential in Cr (VI) removal from wastewater and gave high adsorption efficiency (Lee et al., 2018). Ting and Sun (2000) demonstrated that copper biosorption by PVA matrix showed very favourable performance and negligible effect on the uptake capacity of the inactivated yeast used as the biosorbent. Biosorption equilibrium showed that the specific copper uptake of the biomass tended to increase with an increase in the initial copper concentration while the uptake decreased with an increase in biomass loading. Moreover, Chuan et al. (2018) revealed that the Cr (VI) adsorption rates increased

remarkably with dosages of PVA and sodium alginate according to the increasing number of the active sites for adsorption.

Therefore, this research aimed to study the possibility of using immobilized spent yeast entrapped with polyvinyl alcohol and sodium alginate as sorbent for the sorption of lead from aqueous solutions. The influence of initial concentration of metal ion on the uptake of lead from the solution were evaluated. Two simplified kinetic models including the pseudo-first order and the pseudo-second order equations were used to discuss the biosorption mechanism. The sorption constants for the Langmuir, Freundlich, Temkin and D-R isotherms were determined.

METHODOLOGY

Chemicals and adsorbent

All reagents used in this study were of analytical grade. Separate metal stock solutions containing lead (Merck) with a concentration of 1000 mg/L were prepared using deionized distilled water. Spent yeast was obtained from Thai Amarit Brewery Ltd. (Thailand). It was dried at 80°C for 24 hours and stored in sealed bags at room temperature until use.

Immobilization method

Immobilized spent yeast in polyvinyl chloride - alginate beads were prepared by mixing 5 g of dried spent yeast in 100 mL of 1% w/v sodium alginate (Sigma-Aldrich) and 6.5% w/v of polyvinyl alcohol (Sigma-Aldrich). The mixture was stirred thoroughly to ensure complete mixing before dropping into 0.1 M $CaCl_2$ solution (Merck), to form polyvinyl chloride - alginate beads. The beads were hardened for 30 min and then collected and washed with deionized water.

Adsorption experiment

In batch adsorption tests, the effects of initial lead concentration (20, 40, 60 and 80 mg/L) were studied. The experiments were carried out in triplicate in 500 mL Erlenmeyer flask containing 150 mL of heavy metal solution. The immobilized spent

yeast in polyvinyl chloride - alginate beads was added into solution. All flasks were shaken at 200 rpm for 8 hours at 35°C. The concentration of metal ions was monitored before and after the sorption period.

Analysis of heavy metal

The polyvinyl chloride - alginate beads was separated from lead solution before heavy metal analysis by using filtration through filter paper Whatman No. 1. The residual concentration of the metal ion was analyzed by an atomic absorption spectrophotometer (GBC, Model Avanta 1.33) calibrated with standard solutions prepared from 1000 mg/L certified reference solutions (Merck).

Kinetic studies

(1) The pseudo-first order equation

Lagergren's kinetic equation was applied to explain the adsorption of ocalic acid and malonic acid onto charcoal (Lagergren, 1898; Ho, 2004). This kinetic analysis of adsorption that was used to investigate the mechanism of sorption is called pseudo - first order equation of Lagergren (Ho and McKay, 1999b). The equation is shown as (1):

$$dq_t / dt = k_1 (q_e - q_t) \quad \ldots(1)$$

where k_1 is the rate constant of pseudo-first order adsorption, q_t is the amount of adsorbate adsorbed on the surface of the adsorbent at any time t (mg/g) and q_e is the amount of adsorption at equilibrium (mg/g). Applying integration by using the initial conditions $q_t = 0$ at $t = 0$ and $q_t = q_t$ at $t = t$, Eq. (1) can be expressed as (2),

$$\log (q_e - q_t) = \log q_e - (k_1 / 2.303)t \quad \ldots(2)$$

where q_e must be beforehand obtained from the equilibrium experiments.

(2) The pseudo-second order equation

Based on adsorption capacity, a pseudo - second order equation may be expressed in the form (Ho and McKay, 1999a and 1999b),

$$dq_t / dt = k_2 (q_e - q_t)^2 \quad \ldots(3)$$

where k_2 is the rate constant of pseudo- second- order adsorption and q_e is the amount of adsorption at equilibrium. Integration of Eq (3) and

applying the initial conditions we have

$t/ q_t = (1/ k_2 q_e^2) + (1/q_e) t$ …(4)

The k_2 and q_e in Eq (4) can be calculated from the intercept and slope of the plot of (t/q_t) against. t and there is no need to know any parameter beforehand. In Eq (4), the initial rate of adsorption, h (mg/g min), is given by:

$h = k_2 q_e^2$ …(5)

Isotherm Modeling

(1) Langmuir isotherm

The Langmuir isotherm suggests that metal uptake occurs by monolayer adsorption on a homogeneous surface (Langmuir, 1916). This model assumes that the adsorption energy is constant, and in the plane of the surface, there is no transmigration of adsorbate (Özer et al., 2009). The Langmuir equation is presented as (6),

$$q_e = \frac{q_m K_L C_e}{1+K_L C_e} \quad \ldots(6)$$

where C_e is the equilibrium concentration (mg/L); q_e is the amount of metal ions adsorbed (mg/g); q_m is the monolayer sorption capacity (mg/g); K_L is the Langmuir constant (L/mg). One of the linear forms of the equation was as follows (as cited in Foo and Hameed, 2010):

$$\frac{1}{q_e} = \frac{1}{q_m} + \frac{1}{K_L q_m C_e} \quad \ldots(7)$$

Parameters such as q_m, and K_L are obtained by making the appropriate plots using the equations (7). A dimensionless constant (R_L) or separation factor can be calculated as (8) (Weber and Chakravorti, 1974),

$$R_L = \frac{1}{1+K_L C_0} \quad \ldots(8)$$

where C_0 is the initial concentration of adsorbate. The nature of adsorption can be explained by the value of R_L as either unfavorable ($R_L>1$), linear ($R_L=1$), favorable ($0<R_L<1$) or irreversible ($R_L = 0$).

(2) Freundlich isotherm

Freundlich isotherm (Freundlich, 1906) is an empirical model which applies to multilayer adsorption which the adsorbent surface is heterogeneous and the adsorption is a non-uniform distribution of adsorption heat (as cited in Foo and Hameed, 2010). The equation is expressed as (9),

$$q_e = K_F C_e^{\,1/n} \quad \ldots(9)$$

The equation can be expressed in its linear form as:

$$log\, q_e = log\, K_F + {}^1/_n\, log\, C_e \ldots(10)$$

K_F is the Freundlich constant that indicated the adsorption capacity while ${}^1/_n$ is a function of the adsorption strength. From a plot of $logq_e$ against $logC_e$, the slope and the intercept are ${}^1/_n$ and $logK_F$, respectively. Haghseresht and Lu explained that ${}^1/_n$ value between 0 and 1 is an evaluation of adsorption intensity or surface heterogeneity when a value above one indicates cooperative adsorption (as cited in Foo and Hameed, 2010). Also, ${}^1/_n$ is a heterogeneity parameter. The smaller the ${}^1/_n$ value, the greater the heterogeneity of the adsorption process. Moreover, the adsorption process is favorable when the value n lies between one and ten (Goldberg, 2005).

(3) Temkin isotherm

The assumption of Temkin adsorption isotherm is the heat of adsorption decreases with the sorption coverage as a linear relationship according to adsorbent-adsorbate interactions (as cited in Sampranpiboon *et al.*, 2014). The model is given as,

$$q_e = \frac{RT}{b_T} lnA_T C_e \quad \ldots(11)$$

The linear form is expressed as,

$$q_e = \left(\frac{RT}{b_T}\right) lnA_T + \left(\frac{RT}{b_T}\right) C_e \quad \ldots(12)$$

where A_T is Temkin isotherm equilibrium binding constant (L/g), b_T is Temkin isotherm constant (J/mol), R is Universal gas constant (8.314 J/mol K) and T is Temperature at 298 K.

(4) D-R isotherm

D - R isotherm (Dubinin and Radushkevich, 1947) is a fundamental equation for adsorption from the gas phase by microporous solids (as cited in Dabrowski, 2001). The model is expressed as,

$$q_e = (q_s) exp(-K_{ad})\varepsilon^2 \quad \ldots(13)$$

where q_e is the amount of adsorbate in the adsorbent at equilibrium (mg/g) , q_s is theoretical isotherm saturation capacity (mg/g), K_{ad} is D–R isotherm constant (mol^2/kJ^2) and ε can be correlated as,

$$\varepsilon = RTln\left[1 + \frac{1}{C_e}\right] \quad \ldots(14)$$

where R, T and C_e are the gas constant (8.314 J/mol K), absolute

temperature (K) and adsorbate equilibrium concentration (mg/L) , respectively. The linear relationship of the D–R isotherm is obtained from the following equation.

$$ln\,(q_e) = ln(q_s) - K_{ad}\varepsilon^2 \quad \ldots(15)$$

K_{ad} is related to the free energy of sorption / mole of the sorbate as it migrates to the surface of the adsorbent from infinite distance in the solution (Horsfall and Spiff, 2004) . The apparent energy of adsorption (E, kJ/mol) from D– R model can be computed using the equation (Igwe and Abia, 2006):

$$E = \frac{1}{\sqrt{2k_{ad}}} \quad \ldots(16)$$

Error Analysis

The residual root mean square error (RMSE) and the chi-square test were used to evaluate the fit of isotherm equations to the experimental data. RMSE can be defined as (Vijayaraghavan *et al*., 2006):

$$RMSE = \sqrt{\frac{1}{n-2}\sum_{i=1}^{n}\left(q_{e,exp} - q_{e,calc}\right)^2} \quad \ldots(17)$$

The experimental and calculated values are shown using subscripts "exp" and 'calc" and n is the number of observations in the experimental isotherm. The small the RMSE value, the better the curve fitting. The chi-square test (Ho *et al.*, 2005) is given as,

$$\chi^2 = \sum_{i=1}^{n}\frac{\left(q_{e,exp} - q_{e,calc}\right)^2}{q_{e,exp}} \quad \ldots(18)$$

If data from the model are similar to the experimental data, χ^2 will be a small number; if they are different, χ^2 will be a large number.

RESULTS AND DISCUSSION

The rate of lead sorption by immobilized spent yeast in polyvinyl chloride - alginate beads was determined as a function of the initial lead concentration as shown in Figure 1. The sorption rate was rapid at the beginning of the period. It was observed that the equilibrium uptake of lead by immobilized spent yeast was occurred after 1 hours for 20 and 40 mg/L of lead and 1.5 hours for 60 and 80 mg/L of lead.

Kinetic studies of adsorption

The results from Table 1 show that the correlation coefficients obtained

from pseudo- first order were significantly lower than the equivalent pseudo- second order correlation coefficients. Moreover, pseudo- first order equation is only applicable for the first 1- 2 hours of biosorption. This strongly suggests that the sorption of divalent metal ions on to immobilized spent yeast in polyvinyl chloride - alginate beads is most appropriately represented by a pseudo- second order rate process. Quek et al. (1998) and Ho and McKay (1999b) also suggested using the pseudo- second order model in adsorption.

The gradients, k_1, have been determined from pseudo- first order adsorption and are listed in Table 1. Calculation from the intercept and slope of the straight line of pseudo- second order equation (Figure 2), the initial rate of adsorption (h, mg/g min) was obtained (Table 1) . The highest initial sorption rate (1.881 mg/g min) was obtained from lead sorption at 20 mg/L initial lead concentration. From Table 1, the initial sorption rate tended to decrease from 1.881 to 1.490 mg/g min and rate constant decreased from 0. 121 to 0. 007 g/mg min with an increase in the initial concentration of lead from 20 to 80 mg/L. While the amount of adsorption at equilibrium were found to increase from 3. 950 to 14.947 mg/g with an increase in the initial concentration of lead from 20 to 80 mg/L. This data is in agreement with the results obtained in removal of lead by *S. cerevisiae* that a rise in lead concentration from 25 to 100 mg/L resulted in an increase in its uptake by *S. cerevisiae* from 0.75 to 2.34 mg/g (Parvathi et al., 2007). Increasing the initial concentration of lead in this study (Figure 1) resulted in decreasing percentage of lead removal according to its saturation uptake capacity (Pandey et al., 2007).

Figure 2 shows the extremely linear variation of t/q_t with time, t, for a large initial fraction of the sorption period. The pseudo- second order model gave the best correlation of these data, this supported that the adsorption's mechanism is

chemically rate controlling or chemisorption (Ho and McKay, 1999b) . The pseudo- second order rate expression has also been applied successfully in many studies on heavy metal biosorption. Buranaboripan et al. (2009) used dead chitosan- immobilized and grown fungal beads for Pb(II) biosorption. The kinetic biosorption model of pseudo- second order fitted better than pseudo- first order and modified pseudo- first order models. In contrast, chitosan beads encapsulated with dead biomass of Rhizopus arrhizus were used to study the biosorption of nonylphenol, the authors found that pseudo first- order kinetics gave the best fit with the experimental data (Lang et al.,2009).

Adsorption Isotherm

The sorption isotherms of lead were studied by fitting the obtained data to Langmuir, Freundlich, Temkin and D-R Isotherm models. The results showed that the R^2 value (0.953) of Freundlich isotherm was the highest (Table 2).

It can be seen from Figure 3 that the isotherm data fits the Langmuir equation well (R^2=0.929). The value of q_m and K_L from lead adsorption were 12.296 mg/g and 2.027 L/mg. The values of R_L were 0.006-0.024 indicated that the nature of lead adsorption on polyvinyl alcohol - alginate immobilized with spent yeast is favorable.

For Freundlich isotherm, a plot of $logq_e$ against $logC_e$ gave $1/n$ and $logK_F$ as the slope and the intercept, respectively (Figure 4). The values of $1/n$ for lead adsorption was 0.417. This shows that lead adsorption implies chemisorptions. Sorption of lead onto polyvinyl chloride-alginate immobilized with spent yeast is favorable as the values of n in both cases lie between one and ten as described by Goldberg (2005).

From Temkin plot shown in Figure 5, the Temkin constant (b_T) that related to heat of sorption for lead was 791.856 J/mol. A weak interaction between sorbate and sorbent was indicated from this low value (Shahmohammadi- Kalalagh *et al.*, 2011).

D–R isotherm constant was obtained from the plot as shown on Figure 6 and reported in Table 2. The estimated constant, K_{ad}, related to adsorption energy was presented as $0.058\ mol^2/kJ^2$ for lead. The mean free energy (E) that is a parameter used in the type of adsorption prediction was 2.935 kJ/mol. An E value was less than 8 kJ/mol and was an indication of physisorption (Monika *et al.*, 2009).

By comparing the values of the error functions, it was found that Freundlich models best fit the lead adsorption onto polyvinyl alcohol-alginate immobilized with spent yeast. The models show high correlation coefficients and low RMSE and chi-square values (Table 2).

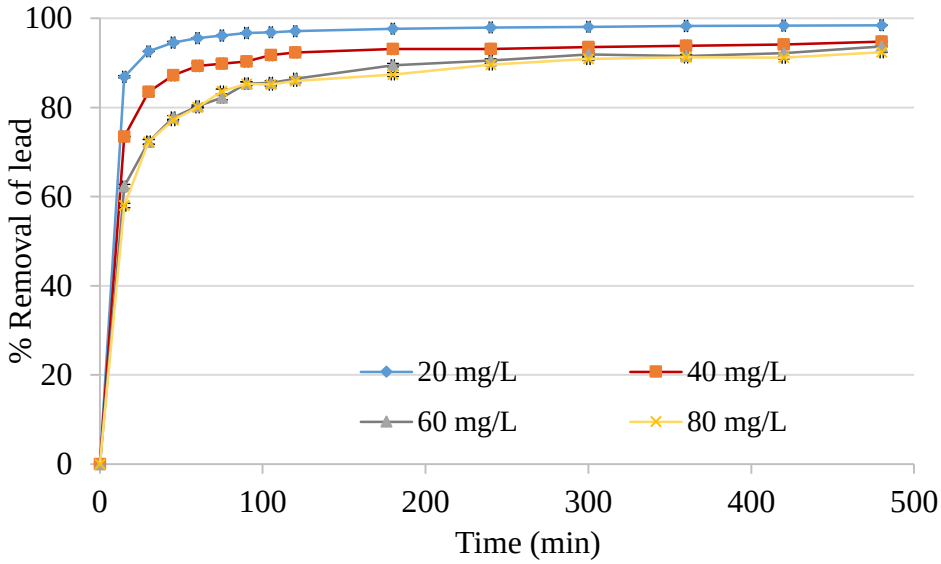

Figure 1 Lead uptake capacity by immobilized spent yeast at different initial lead concentration. Error bars indicate the standard deviation.

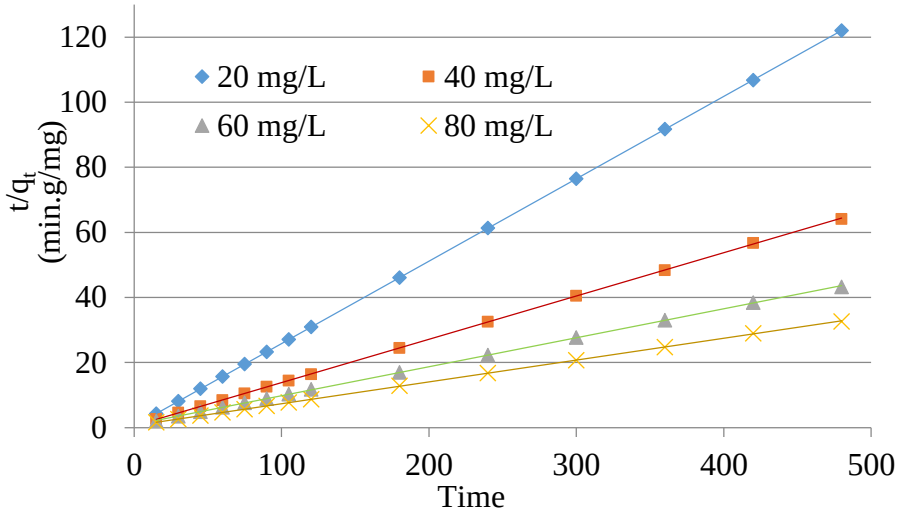

Figure 2 Pseudo- second- order reaction for lead adsorbed onto polyvinyl alcohol - alginate beads immobilized with spent yeast at different initial lead concentration.

Table 1 Comparison between the adsorption rate constants, q_e, estimated and correlation coefficients associated with pseudo-first-order and to the pseudo-second-order rate equations.

Treatment	First-order*		
	q_e (mg/g)	k_1 (min^{-1})	*Coefficient of Determination,* R^2
20 mg/L	3.935±0.003	0.029±0.003	0.957 ± 0.004
40 mg/L	7.469±0.037	0.022±0.005	0.900 ± 0.056
60 mg/L	11.104±0.046	0.016±0.001	0.962 ± 0.020
80 mg/L	14.739±0.081	0.021±0.000	0.971 ± 0.009

Treatment	Second-order*			
	q_e (mg/g)	k_2 (g/mg.min)	h (mg/g.min)	*Coefficient of Determination,* R^2
20 mg/L	3.950±0.000	0.121±0.001	1.881±0.020	1.000 ± 0.000
40 mg/L	7.520±0.025	0.030±0.002	1.713±0.103	0.999 ± 0.000
60 mg/L	11.238±0.013	0.008±0.000	1.073±0.004	0.999 ± 0.000
80 mg/L	14.947±0.018	0.007±0.000	1.490±0.029	0.999 ± 0.000

* Values are mean ± SD.

Table 2 Models constants, correlation coefficients, RMSE and χ^2 for adsorption of lead from aqueous solution.

Isotherm model	Constants	Values	Isotherm model	Constants	Values
Langmuir	q_m	12.296 mg/g	Temkin	b_T	791.856 J/mol
	K_L	2.027 L/mg		A_T	11.485 L/g
	R_L	0.006-0.024			
	R^2	0.929		R^2	0.851
	RMSE	2.421		RMSE	1.738
	χ^2	4.931		χ^2	3.554
Freundlich	K_F	6.909 mg/g	D-R	q_s	11.291 mol/g
	1/n	0.417		K_{ad}	0.058 mol^2/kJ^2
	n	2.400		E	2.935 kJ/mol
	R^2	0.953		R^2	0.799
	RMSE	1.160		RMSE	2.662
	χ^2	1.371		χ^2	6.553

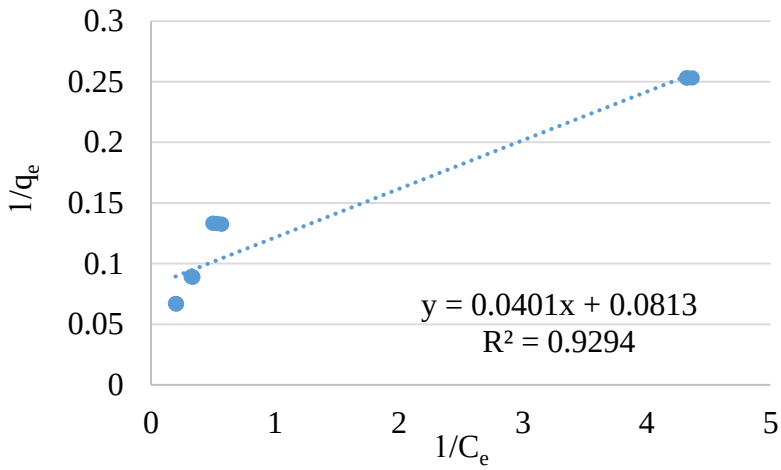

Figure 3 Langmuir isotherm plot for lead.

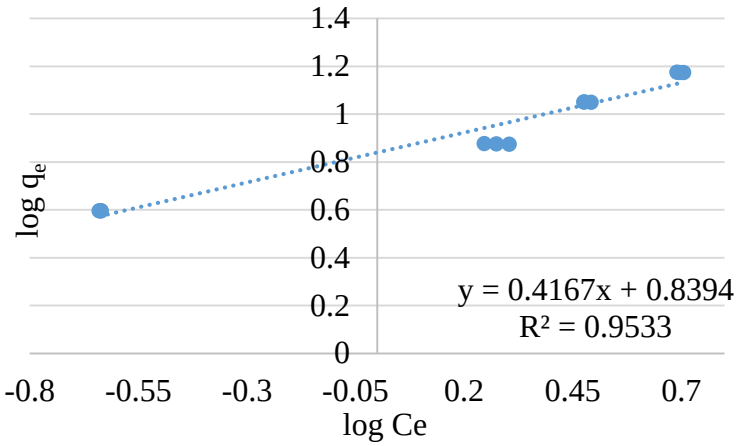

Figure 4 Freundlich isotherm plot for lead.

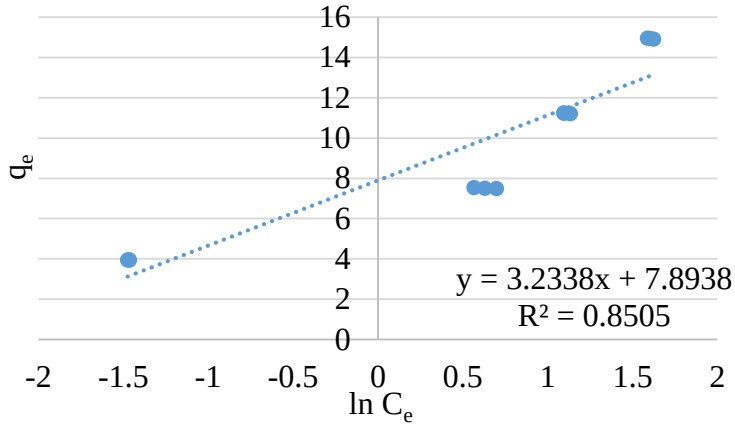

Figure 5 Temkin isotherm plot for lead.

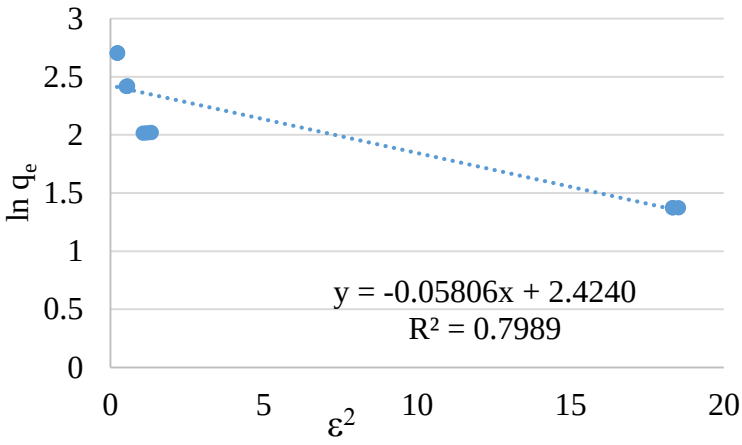

Figure 6 D-R isotherm plot for lead.

CONCLUSIONS

The initial lead concentration affected on lead adsorption onto polyvinyl alcohol-alginate beads immobilized with spent yeast. The sorption of lead can be described by a pseudo- second order model. From fitting the equilibrium sorption data, Freundlich isotherm was a favorable sorption process and the R^2 value was the highest with the lowest RMSE and χ^2. Langmuir isotherm is also favorable from R_L value was between 0 and 1. From Temkin plot, the low value of Temkin constant showed a weak interaction between sorbate and sorbent. Indication of physisorption was obtained from D– R isotherm from mean free energy that was lower than 8 kJ/mol.

ACKNOWLEDGEMENTS

The authors are grateful to Ms. Monrudee Kitpaiboonwattana for providing them with original experimental data for the adsorption of lead on immobilized spent yeast in polyvinyl chloride-alginate beads.

REFERENCES

Buranaboripan W, Sirisansaneeyakul S, Parakulsuksatid P, Vanichsriratana W, Sakairi N, Lang W. Adsorption modeling of lead biosorption by dead chitosan immobilized fungal beads. Proceedings of Thailand Research Symposium 2009; Bangkok, Thailand.

Chuan LT, Manap N, Abdullah HZ, Idris MI. Polyvinyl Alcohol-Alginate Adsorbent Beads for Chromium (VI) Removal. International Journal of Engineering & Technology 2018; 7: 95-99.

da Costa ACA, Leite SGF. Metals biosorption by sodium alginate immobilized *Chlorella homosphaera* cells. Biotechnology Letter 1991; 13(8): 559-562.

Dabrowski A. Adsorption – from theory to practice. Advance Colloid Interface Science 2001; 93: 135-224.

Das N, Vimala R, Karthika P. Biosorption of heavy metals-an overview. Indian Journal of Biotechnology 2008; 7: 159-169.

Dubinin MM, Radushkevich LV. The equation of the characteristic curve of activated charcoal. Proceedings of the Academy of Sciences of the USSR. Physical chemistry section 1947; 55: 331-337.

El-Gendy NSh, Nassar HN. A comparative study for batch process of phenol biosorption onto different spent waste biomass: kinetics and equilibrium.

Energy Sources, Part A: Recovery, Utilization, and Environmental Effects 2015; 37(10): 1098-1109.

Farhan SN, Khadom AA. Biosorption of heavy metals from aqueous solutions by *Saccharomyces cerevisiae*. International Journal of Indian Chemistry 2015; 6: 119–130.

Foo KY, Hammed BH. Review: Insight into the modeling of adsorption isotherms systems. Chemical Engineering Journal 2010; 156: 2-10.

Freundlich HMF. Over the adsorption in solution. Journal of Physical Chemistry 1906; 57: 385-471.

Goldberg S. Equation and models describing adsorption processes in soils. In: Tabatabai MA, Sparks DL (eds), Chemical Processes in Soils. Soil Science Society of America, Madison, Wisconsin, 2005; pp. 489-517.

Ho YS, Chiu WT, Wang CC. Regression analysis for the sorption isotherms of basic dyes on sugarcane dust. Bioresource Technology 2005; 96: 1285–1291.

Ho YS, McKay G. Comparative sorption kinetic studies of dye and aromatic compounds onto fly ash. Journal of Environmental Science and Health, Part A: Toxic/Hazardous Substances & Environmental Engineering 1999a; 34(5): 1179-1204.

Ho YS, McKay G. Pseudo-second order model for sorption processes. Process Biochemistry 1999b; 34(5): 451-465.

Ho YS. Citation review of Lagergren kinetic rate equation on adsorption reactions. Scientometrics 2004; 59(1): 171-177.

Horsfall MJ, Spiff AI. Studies on the effect of pH on the sorption of Pb^{2+} and Cd^{2+} ions from aqueous solutions by *Caladium bicolor* (wild cocoyam) biomass. Electronic Journal of Biotechnology 2004; 7(3): 313-323.

Hsu HF, Jhuo YS, Kumar M, Ma YS, Lin JG. Simultaneous sulfate reduction and copper removal by a PVA-immobilized sulfate reducing bacterial culture. Bioresource Technology 2010; 101: 4354.

Igwe JC, Abia AA. Review: A biosorption process for removing heavy metals from wastewater using biosorbents. African Journal of Biotechnology 2006; 5(12):1167-1179.

Kadajji VG, Betageri GV. Water soluble polymers for pharmaceutical applications. Polymers 2011; 3(4): 1972-2009.

Khuathan N, Pongjanyakul T. Modification of quaternary polymethacrylate films using sodium alginate: Film characterization and drug permeability. International Journal of Pharmaceutical 2014; 460(1): 63–72.

Lagergren S. About the theory of so-called adsorption of soluble substances, der Sogenanntenadsorption geloster stoffe Kungliga Svenska Vetenska psalka de Miens Handlingar 1898; 24: 1–39.

Lang W, Chomawan D, Sirisansaneeyakul S, Sakairi N. Biosorption of nonylphenol on dead biomass of *Rhizopus arrhizus* encapsulated in chitosan beads. Bioresource Technology 2009; 100(23): 5616 – 5623.

Langmuir I. The constitution and fundamental properties of solids and liquids. Journal of the American Chemical Society 1916; 38(11): 2221-2295.

Lee TC, Aizat Ahmad AN, Mohd Pu'ad NAS, Manap N, Abdullah HZ, Idris MI. Adsorption Efficiency of Polyvinyl Alcohol -Alginate Beads on Cr (VI): Effect of pH and Temperature. International Journal of Integrated Engineering: Special Issue 2018: Innovations in Civil Engineering 2018; 10(9): 43-47.

Li X, Dai L, Zhang C, Zeng G, Liu Y, Zhou C, Xu W, Wu Y, Tang X, Liu W, Lan S. Enhanced biological stabilization of heavy metals in sediment using immobilized sulfate reducing bacteria beads with inner cohesive nutrient. Journal of Hazardous Materials 2017; 324(Pt B):340-347.

Macek T, Mackova M. Potential of biosorption technology. In: Kotrba P, Mackova M, Macek T (eds), Microbial Biosorption of Metals. New York, Springer, 2011; pp. 7-17.

Majidnia Z, Fulazzaky MA. Photocatalytic reduction of Cs(I) ions removed by combined maghemite-titania PVAalginate beads from aqueous solution. Journal of Environmental Management 2017; 191: 219-227.

Majidnia Z, Idris A. Evaluation of cesium removal from radioactive waste water using maghemite PVA-alginate beads. Chemical Engineering Journal 2015; 262: 372-382.

Monika J, Garg V, Kadirvelu K. Chromium (VI) removal from aqueous solution, using sunflower stem waste. J Hazardous Materials 2009; 162: 365 – 372.

Özer A, Gürbüz G, Çalimli A, Körbahti BK. Biosorption of copper(II) ions on Enteromorpha prolifera: application of response surface methodology (RSM). Chemical Engineering Journal. 2009; 146(3): 377–387.

Pandey PK, Choubey S, Verma Y, Pandey M, Kamal SSK, Chandrashekhar K. Biosorptive removal of Ni(II) from wastewater and industrial effluent. International Journal of Environmental Research and Public Health 2007; 4(4): 332-339.

Parvathi K, Nagendran R, Nareshkumar R. Lead biosorption onto waste beer yeast by-product, a means to decontaminate effluent generated from battery manufacturing industry. Electronic Journal of Biotechnology, Environmental Biotechnology 2007; 10(1). DOI: 10.2225/vol10-issue1-fulltext-13

Quek SY, Wase DAJ, Forster CF. The use of sago waste for the sorption of lead and copper. Water SA 1998; 24: 251-256.

Sampranpiboon P, Charnkeitkong P, Feng X. Equilibrium isotherm models for adsorption of zinc (II) ion from aqueous solution on pulp waste. WSEAS Transactions on Environment and Development 2014; 10: 35-47.

Shahmohammadi-Kalalagh S, Babazadeh H, Nazemi A, Manshouri M. Isotherm and kinetic studies on adsorption of Pb, Zn and Cu by kaolinite. Caspian Journal of Environmental Sciences 2011; 9: 243-255.

Tchounwou PB, Yedjou CG, Patlolla AK, Sutton DJ. Heavy metals toxicity and the environment. Berlin, Springer, 2012; pp. 133-164

Ting YP, Sun G. Use of polyvinyl alcohol as a cell immobilization matrix for copper biosorption by yeast cells. Journal of Chemical Technology & Biotechnology 2000; 75(7): 541 – 546.

Vijayaraghavan K, Padmesh TVN, Palanivelu K, Velan M. Biosorption of nickel(II) ions onto *Sargassum wightii*: Application of two parameter and three-parameter isotherm models. Journal of Hazardous Materials 2006; B133: 304- 308.

Wang JL, Chen C. Biosorption of heavy metals by Saccharomyces cerevisiae: a review. Biotechnology Advance 2006; 24: 427–451.

Weber TW, Chakravorti RK. Pore and solid diffusion models for fixed- bed adsorbers. AIChE Journal 1974; 20: 787-794.

Evaluation of using a cost-effective open tubular capillary ion chromatograph for some ions determination in environmental samples

Kanlayarat Tianrungarun[1,2,4], Chanida Puangpila[1,3], Jaroon Jakmunee[1,2,3], and Tinakorn Kanyanee[1,2,3*]

[1]Department of Chemistry, Faculty of Science, Chiang Mai University, Chiang Mai, 50200, Thailand

[2]Center of Excellence for Innovation in Chemistry, Faculty of Science, Chiang Mai University, Chiang Mai, 50200, Thailand

[3]Center of Excellence in Materials Science and Technology, Chiang Mai University, 50200, Thailand

[4]Graduate School, Chiang Mai University, Chiang Mai, 50200, Thailand

[*]Corresponding author: e-mail: tkanyanee@gmail.com

ABSTRACT

A cost-effective lab-built open tubular capillary ion chromatography (OTIC) has been fabricated for the determination of some cations in environmental samples. The analytical column was prepared in-house by coating inner wall of a 50 μm ID fused silica capillary 130 cm-length with 13 layers of poly (butadiene-maleic acid) for used as a cation exchange column. The in-house column is able to separate four alkaline/alkaline earth cations within 14 min using 1 mM pyridine-2,6-dicarboxylic acid as eluent without using a suppressor. The proposed system can be operated with low pressure of 15 psi, and the flow rate of eluent was less than 1 μL/min. It was successfully applied for the determination of alkaline/ alkaline earth cations in hot spring water samples with the LOD of Na^+, K^+, Ca^{2+}, and Mg^{2+} were 18 μM, 13 μM, 29 μM, and 53 μM, respectively.

Keywords: Cations determination in water, Open tubular capillary ion chromatography, Cost-effective device

INTRODUCTION

Ion chromatography (IC) is well established as a routine method for the determination of ionic analytes in environmental samples. IC has been incorporated into environmental regulatory methods, worldwide, for quantifying contaminants in drinking water, wastewater, surface water, and groundwater (Michalski, 2009). The IC plays a predominant role in ion determinations and offers several advantages over the conventional ion sensor, such as simultaneous determinations of inorganic cations (Michalski, 2006). Currently, analytical chemistry has been developed towards miniaturization (Ohno *et al*., 2008), green chemical analysis (Sheldon *et al*., 2007), and cost-effective instrumentation. However, the conventional commercial packed column IC requires a high-pressure pump to propel the mobile phase solution to flow through the separation column, which is a large and expensive instrument. It is interesting to perform IC by using an open tubular capillary column due to the advantages of lower operating pressure requirement, smaller and lower cost instrument, and less chemical consumption (Kuban *et al*., 2004). The open tubular ion chromatography (OTIC) was performed by coating various ion exchanged materials on the surface of fused silica capillary and applying for some inorganic ions separation. Maller *et al.* (1989 and 1991) reported the preparation of 4.6 μm ID capillary column coated with (3-sulfopropyltrihydroxysilane) or (3-(2-aminoethyl amino)-propyl silane) for both cations and anions separation and they used an ion selective micro-electrode as a detector. However, the sensitivity is poor due to the logarithmic response of the ion selective electrode detection. Moreover, the low reproducibility of detection was resulted because of the improper position of the electrodes. In last ten years with the coming of a capacitively coupled contactless conductivity detector (C4D), it is a good choice of detector for the capillary scale separation technique such as CE/CEC (Kuban *et al*., 2008). With the convenience of using C4D detector and the low-pressure requirement for OTIC operation, a low-pressure gravity flow was exploited to perform OTIC with C4D detection (Kuban *et al*., 2008; Kiplagat *et al*., 2010). Kuban *et al*. (2008 and 2007) developed the multi-layered stationary phase on a 75 μm ID fused silica capillary tube with less than 1 μm thick porous layer for anions separation.

The number of theoretical plate (N) was more than 30000 for anions separation. In addition, capillary IC system was demonstrated for cations separation using a gravity-flow and provided the number of theoretical plate of 1308 to 10400. Kiplagat *et al*. (2010) demonstrated the fabrication of a portable capillary IC as a light-weight setup (<1 kg without a notebook computer) with low power consumption and inexpensive capacitance detector. They had successfully developed the OTIC system with various prepared columns and detectors in various size of the inner capillary tube of 75-250 µm bore. In addition, the system can separate the inorganic cations in river water, mineral water and snow samples. The OTIC with coating of ion exchanged latex on acrylic tube had been demonstrated and described (Zhang *et al*., 2013). The OTIC approach was introduced for extraterrestrial exploration for ion determination in soil from Mars exploration (Yang *et al*., 2014).

In Thailand and some developing countries where modern equipment is limited by budget constrain, the cost-effective instrumentation is of interest. Therefore, this work aims to fabricate a lower cost OTIC system and evaluate for application in environmental analysis. Although the OTIC with poly(butadiene-maleic acid) (PBMA) coated on 75-µm bore capillary was successfully fabricated as reported previously (Kiplagat *et al*., 2010), this research investigated the use of a smaller size of inner bore capillary (50 µm bore) to increase the separation efficiency per length of the PBMA-OTIC column. However, the lower sensitivity of ion detection using a smaller size of the proposed system is a crucial point to be evaluated for the real sample analysis.

METHODOLOGY

Open tubular ion chromatography system

The chromatographic components were set up as described by Kiplagat *et al*. (2010). The OTIC set up is depicted in Figure 1. The chromatographic injection was driven by using nitrogen gas as a hydrodynamic injection procedure as described in a previous literature (Kiplagat *et al*., 2010). Flow rate of eluent depends on the applied pressure, capillary tube inner diameter, and capillary length as governed by the Hagen-Poiseuille equation (Christian *et al*., 2014). In this experiment, the flow rate of eluent was adjusted by using a pressure regulator at the nitrogen gas

cylinder. The desired pressure of nitrogen gas (10 or 15 psi) was applied to the 50-mL glass eluent container (Duran, Germany). The outlet tube (1/16" OD Peek tube, Upchurch Scientific, USA) of the eluent container was connected to the position #2 of a 6-port injection valve (VICI, Valco Instrument Co. Inc., USA). The capacitance sensor circuit (AD7746EB evaluation board, Analog device, USA) was modified to be a simple C4D detector. This device is a high resolution capacitance-to-digital converter with 21-bit effective resolution and provides 32 kHz pulse with an operating voltage of 5V supplied by the USB port of the computer. The data from the capacitance sensor were collected through the same USB connector. The capacitance sensor was connected to two tubular stainless steel electrodes of 400-µm ID, placing on the capillary with 0.3 mm gap between the electrodes forming a detection cell as described in the previous document (Takeuchi *et al*., 2008). In some experiments, a commercial C4D (Tracedec, Austria) was also used and evaluated the detection ability.

Chemical and sample preparation

All solutions were prepared with deionized (DI) water. Poly (butadiene-maleic acid) prepolymer (PBMA, 42% solids in aq. solution, Polysciences, Taiwan), pyridine-2,6-dicarboxylic acid (99%, Sigma Aldrich), tartaric acid (Carlo Erba) and oxalic acid (99.5%, Loba Chemie) were used as received. The chemical structure of substances for the stationary phase and eluents are depicted in Figure 2. All other stock solutions for eluent preparation and those of standard solution of cations were prepared from analytical grade reagents. The prepared eluent was then filtered with a 0.2 µm pore size polytetrafluoroethylene (PTFE) syringe filter and degassed by using the ultrasonic bath for 15 minutes. The hot spring water samples were filtered and diluted with DI water prior to analysis.

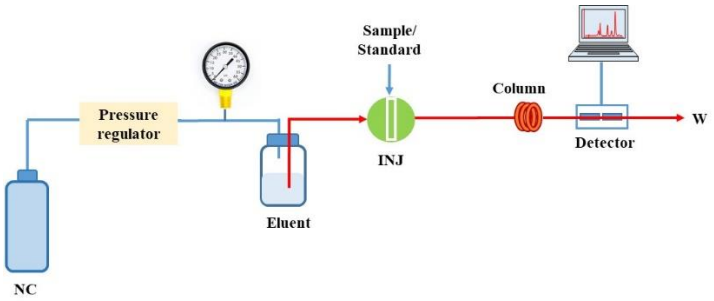

Figure 1 Schematic diagram of the OTIC system; NC=nitrogen gas cylinder, INJ= 2-position-6-ports-injection valve, W=waste.

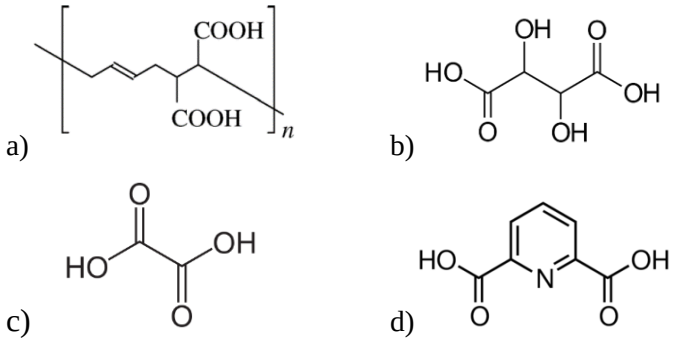

Figure 2 The structure of a) poly (butadiene-maleic acid) (PBMA), b) Tartaric acid, c) Oxalic acid, and d) Pyridine-2,6-dicarboxylic acid (PDCA) (Kolla *et al*., 1987; Kolb *el at*., 2001).

RESULTS AND DISCUSSION ***The PBMA OTIC for alkali /alkaline earth metal ions separation***

In the preliminary study, the OTIC system using the modified capacitance sensor as a C4D detector was employed. The basis of using this sensor board was explained by Kuban *et al*. (2008). They used a suppressor system to decrease the high background conductivity of an eluent. In our experiment, the weak organic acid, and mineral acid can also be used as eluent without using a suppressor. However, the conductivity of the eluent is higher than that of analyte ions. Therefore, the obtained chromatogram is the negative peak shape. Although the sensitivity is not as high as using suppressor IC, the non-suppressor system provides simplicity,

convenience, and inexpensive device. In our work, a PBMA coated open tubular cation exchange column was prepared from a monomer containing two carboxyl groups as cation exchanger as shown the structure of the polymer in the Figure 2a (Kolla *et al*., 1987). The separation of alkali/ alkaline earth metal and transition metal cations is possible on this stationary phase using various types of eluents such as tartaric acid, oxalic acid and PDCA as shown the molecular structure of the eluents in Figure 2b-d. A prediction of the affinity order is based on the properties of the solute and the ion exchanger including: a) the charge on the solute ion, b) the solvated size of the solute ion, and c) the polarizability of the solute ion (Kolb *et al*., 2001). The cation exchanged polymer of PBMA copolymer was coated on 1.3 m length of 50 µm bore fused silica capillary. This OTIC system was performed by using a computerized control as explained previously in the instrumentation section. The selected main eluents for this experiment is PDCA. By using 1 mM PDCA as an eluent, the alkali and alkaline earth metal cations can be separated within 14 minutes with the retention order as Na^+, K^+, Ca^{2+}, and Mg^{2+} as shown the chromatogram in Figure 3. The performance of the prepared column was characterized with important factors such as the number of theoretical plates (N), capacity factor (k') and resolution (Rs). The separation efficiency, N can be calculated from peak width at half height as expressed in equations (1) (Christian *et al*., 2014):

$$N = 5.54\,(t_R/W_{1/2})^2 \qquad (1)$$

Where t_R is the retention time and $W_{1/2}$ is the peak width at half-height.

The k´ is the product of the phase ratio between stationary and mobile phases in the separation column, as calculated from the equation (2) (Weiss, 2009):

$$k' = \frac{t_R - t_m}{t_m} \qquad (2)$$

Where k´ is the capacity factor, t_R is the solute retention time, and t_m is the retention time of system peak. The low values of k´ imply that the respective component elutes near the void volume resulting in poor

separation. High values of k´ indicate the longer analysis time and peak broadening. The Rs between two peaks in a chromatogram is given by equation (3) (Christian *et al*., 2014):

$$Rs = \frac{2(t_{R2} - t_{R1})}{(W_{b1} + W_{b2})} \qquad (3)$$

Where t_{R1} and t_{R2} are the retention time, W_{b1} and W_{b2} are the peak width measured by the baseline intercept. The Rs value indicates the quality of separation between two adjacent peaks. The separation efficiencies of capillary column coated with 13 layers of PBMA were 4549, 3861, 674, 402 for Na^+, K^+, Ca^{2+}, and Mg^{2+}, respectively. However, the retention of cations is controlled by the concentration of the eluent. Therefore, various eluent concentrations of PDCA for alkali and alkaline earth metal cations separation were investigated. The choice of eluent concentration can be considered from k' and Rs. It was found that k' and Rs of all cations decrease with increasing of PDCA concentration as shown in Figure 4 and Figure 5. Therefore, the appropriate eluent concentrations of PDCA of ≤ 1 mM should be selected.

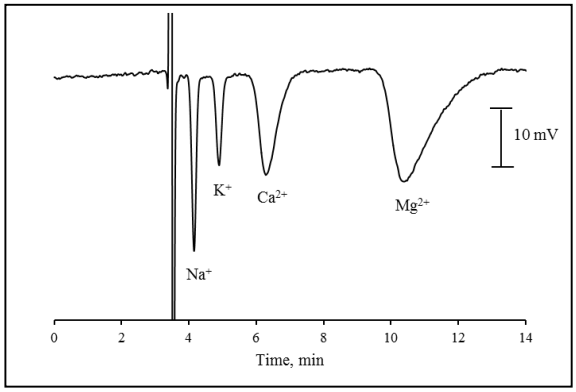

Figure 3 Chromatograms of alkali and alkaline earth metal with 1 mM PDCA as an eluent for mixed cation (111 µM Na^+, 78 µM K^+, 117 µM Ca^{2+}, and 316 µM Mg^{2+}) with 25 nL injected. Column 1.3 m x 50 µm, 13 layers of PBMA polymer, eluent 1 mM PDCA, flow rate 0.7 µL/min, using a commercial C4D detector.

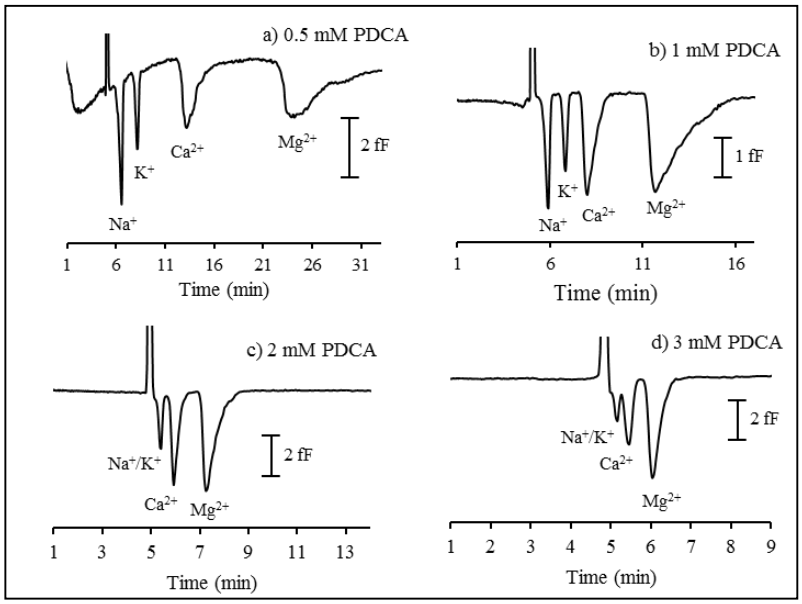

Figure 4 The chromatogram of using various concentration of PDCA: a) 0.5 mM PDCA, b) 1 mM PDCA, c) 2 mM PDCA, and d) 3 mM PDCA using a column 1.5 m x 50 µm, 13 layers of PBMA polymer, flow rate 0.6 µL/min, AD7746 capacitance board as detector, injection volume 20 nL, mixed standards cations solution of 739 µM Na^+, 517 µM K^+, 1178 µM Ca^{2+}, and 2110 µM Mg^{2+}). The unit of capacitance value is femtofarad (fF).

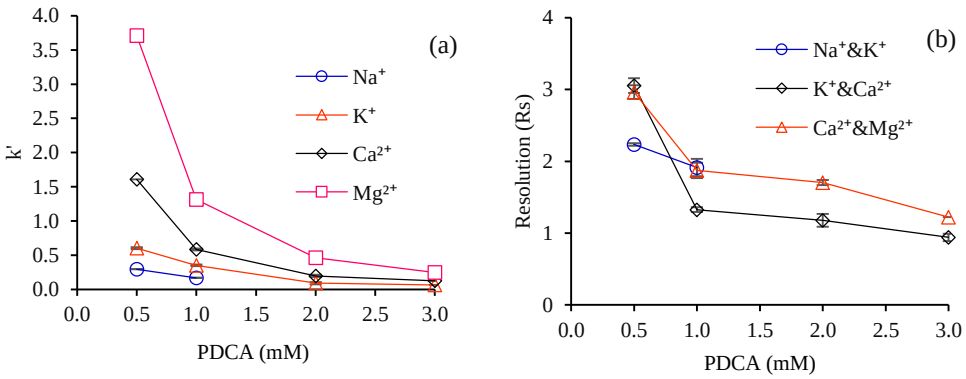

Figure 5 The performance of metal ion separation using different concentrations of PDCA. The data represent: a) k´ and (b) resolution (Rs). The experimental condition is the same as described in Figure 4.

The detection ability for the cations determination

The detection abilities of four cations (Na^+, K^+, Ca^{2+}, and Mg^{2+}) using AD7746 capacitance sensor and commercial C4D detector were also compared. In this experiment, 1.3 m capillary length of 50 µm bore with 13 layers of PBMA and 1 mM PDCA of eluent were selected with the experimental condition of 20 nL injection volume and the flow rate of 0.6 µL/min for AD7746 (25 nL injection volume, and 0.7 µL/min flow rate for the commercial C4D). The linear calibration graph equation and limit of detection (LOD) of both detectors are shown in Table 1. The AD7746 detection provides the linear relationship of Na^+, K^+, Ca^{2+}, and Mg^{2+} were in the range of 111-1848 µM, 78-1293 µM, 177-2946 µM, and 316-5275 µM, respectively. The LOD of Na^+, K^+, Ca^{2+}, and Mg^{2+} were 111 µM, 78 µM, 177 µM, and 316 µM respectively, (which the LOD was estimated from the lowest concentration in the calibration range). With using the commercial C4D, the concentration ranges were from 18-1109 µM, 13-776 µM, 29-1768 µM, and 53-2110 µM of Na^+, K^+, Ca^{2+} and Mg^{2+}, respectively. The LOD of Na^+, K^+, Ca^{2+}, and Mg^{2+} detection were 18 µM, 13 µM, 29 µM, and 53 µM, respectively. Both detectors provide a good precision with relative standard deviations (RSD) of $\leq$ 5%. Although the LOD of using AD7746 capacitance board is not as sensitive as using the commercial C4D, it is an extremely low cost detector (about 150 USD), and the performance would be enough for ions determination in some tap water (Zlotorzynska *et al*., 1993), river water (Rong *et a*l., 2012), mineral water (Fa *et al*., 2018), underground water (Dawood e*t al*., 2014), and wastewater (Thomas *et al*., 2002). The LOD levels were adequate for alkali and alkaline earth metal in hot spring water samples.

Table 1 The detection ability of using 50-µm bore fused silica capillary with capacitance board (AD7746) and the commercial C4D as a detector for the proposed OTIC system

Cation	Range (µM)	Linear equation	r^2	LOD	
				(µM)*	(mg/L)
a) OTIC system using capacitance board (AD7746) as a detector					
Na^+	111-1848	y** = 0.0005x + 0.0442	0.9956	111	2.6
K^+	78-1293	y = 0.0005x + 0.0176	0.9964	78	3.0
Ca^{2+}	177-2946	y = 0.0008x + 0.1193	0.9957	177	7.1
Mg^{2+}	316-5275	y = 0.0011x + 0.2380	0.9934	316	7.7
b) OTIC system using commercial C4D as a detector					
Na^+	18-1109	y*** = 0.0276x + 1.2307	0.9903	18	0.4
K^+	13-776	y = 0.0305x + 0.3151	0.9984	13	0.5
Ca^{2+}	29-1768	y =0.0462x + 1.4130	0.9950	29	1.2
Mg^{2+}	53-2110	y = 0.0733x + 1.6073	0.9983	53	1.3

* Limit of detection (LOD) was estimated from the lowest concentration of a calibration range, ** = the peak area of using capacitance board and present as fF*min, *** = the peak area of using commercial C4D and present as mV*min.

The application of OTIC system for cations determination in hot spring water

The proposed OTIC system with non-suppressor was applied for analysis of the alkaline and alkaline earth metal cations in hot spring water samples. The separation of cations was achieved on a 1.3 m capillary column length of 50 µm bore and 13-layer of PBMA coated, and using a 1 mM PDCA as an eluent. Hot spring water samples were collected from San Kamphang hot spring, in Chiang Mai province. There is no water samples treatment step except filtration and dilution. The hot spring water samples were diluted 100 folds (sample 1,2) and 50 folds (sample 3,4) with DI water for analysis of Na^+. The mixed standard of all the studies cations was spiked into all samples at a concentration of 185 µM, 129 µM, 295 µM, and 527 µM of Na^+, K^+, Ca^{2+}, and Mg^{2+}, respectively. Each sample solution was

analysed in triplicated, and standard deviation of triplicate analysis for each sample was ≤ 5%. The recoveries of the analysis were in the range of 87-112%. The quantitative results are summarized in Table 2. The results suggest that the proposed OTIC method can be applied for environmental samples.

Table 2 The %recovery of alkali and alkaline earth metal cations determination in hot spring water samples

Sample	Add (µM)	Na^+ Found[a] (µM)	Na^+ Recovery (%)	Add (µM)	K^+ Found (µM)	K^+ Recovery (%)
1	0	45.3±3.6		0	370.9±8.9	
(pH=8.9)	185	246.4±8.8	109	129	485.6±5.0	89
2	0	39.7±4.3		0	381.8±2.6	
(pH=8.9)	185	243.8±8.5	110	129	518.1±5.5	106
3	0	146.2±7.6		0	374.5±7.7	
(pH=9.0)	185	343.9±11.5	107	129	512.1±1.9	107
4	0	131.4±6.1		0	404.2±9.4	
(pH=9.0)	185	339.3±11.4	112	129	533.9±6.1	101

Sample	Add (µM)	Ca^{2+} Found (µM)	Ca^{2+} Recovery (%)	Add (µM)	Mg^{2+} Found (µM)	Mg^{2+} Recovery (%)
1	0	9.4±0.4		0	ND[b]	
(pH=8.9)	295	266.1±8.8	87	527	516.9±21.9	98
2	0	ND		0	ND	
(pH=8.9)	295	291.0±8.4	99	527	566.5±3.8	107
3	0	29.5±3.1		0	ND	
(pH=9.0)	295	294.5±6.1	90	527	561.9±0.8	107
4	0	17.9±1.8		0	ND	
(pH=9.0)	295	274.0±12.6	87	527	535.9±23.0	102

[a]Average value ± standard deviation of triplicate results, [b]ND= not detected (the analyte signal is less than the LOD). The condition was the same as described in Table 1b. (OTIC system using a commercial C4D as a detector)

Some preliminary result for transition metal ions separation

The OTIC column was also reported to separate some transition metal ions. In this experiment, the eluent was modified as described in the previous section by adding oxalic acid in 2 mM tartaric acid as an eluent to separate the mixed solution of Fe^{2+}, Zn^{2+}, and Pb^{2+}. The performance using a mixture of 2 mM tartaric acid/1 mM oxalic acid was obtained as shown the chromatogram in Figure 6. The transition metals (e.g. Fe^{2+}, Zn^{2+}, and Pb^{2+}) could be separated using a 1.3 m length of 50-µm bore capillary, 13-layer PBMA column. The commercial C4D detector which provides better sensitivity was used. The linear relationship of peak area and concentration of transition metal ions can be obtained in the range of 62-2083 µM of Zn^{2+}, 82-1360 µM for Fe^{2+} and 128-1599 µM for Pb^{2+} with correlation coefficients > 0.9908. The repeatability of the peak area from the triplicate injection of the standard mixed transition metal cations was less than 5% RSD. The detection ability is summarized in Table 3. The limit of detection of Fe^{2+} and Zn^{2+} detection using 50-µm bore capillary is about 4.1 ppm and 4.6 ppm, respectively, which is sensitive enough for determination of some transition metal ions in sewage treatment plant stream as report by Cardelhcchto *et al*. (1997), e.g., Zn^{2+} was found at 23.8 mg/L in an inlet stream.

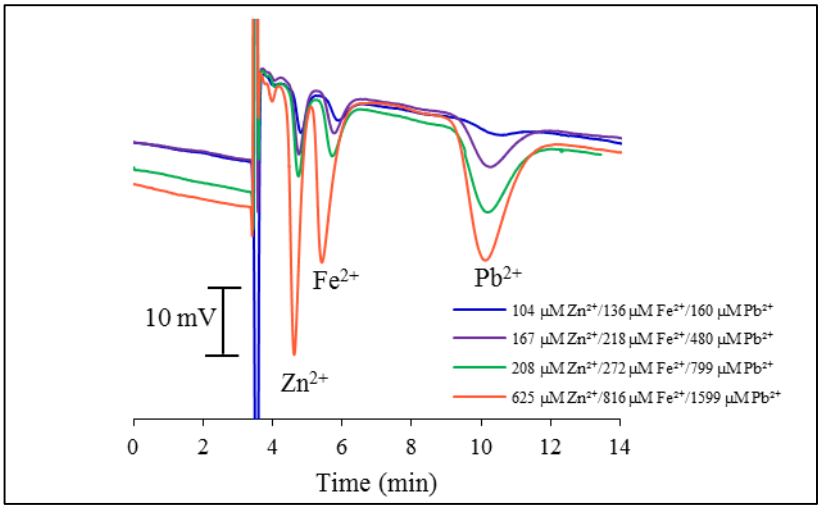

Figure 6 Chromatogram of standard transition metal. Column 1.3 m x 50 µm, 13 layers of PBMA, eluent 2 mM tartaric acid/1 mM oxalic acid, flow rate 0.7 µL/min, commercial C4D detector, injection volume 24 nL.

Table 3 The detection ability of transition metal cations using commercial C4D detector

Ion	Range (µM)	Linear equation	r^2	LOD	
				(µM)*	(mg/L)
Zn^{2+}	62-2083	y = 0.0146x + 1.1376	0.9908	62	4.1
Fe^{2+}	82-1360	y = 0.0129x + 0.0271	0.9984	82	4.6
Pb^{2+}	128-1599	y = 0.0153x + 0.2024	0.9929	128	26.5

* Limit of detection (LOD) was estimated from the lowest concentration of a calibration range. The experimental condition was the same as described in Figure 6.

CONCLUSIONS

The cost-effective open tubular ion chromatography using PBMA as a stationary phase coated on the inner wall of a 50-µm bore capillary tube for alkali/ alkaline earth cation separation has been successfully developed. The cost of this system is about 6,000 USD (including commercial contactless conductivity detector), while the typical cost of a commercial ion chromatograph is about 17,000 USD. The system provides a low-pressure propelling device for eluent delivery and as a result, the extremely low flow rate of the proposed system in the level of < 1 µL/min, with the injection volume of ≤ 25 nL was achieved. Due to the lower chemical and energy consumption, less waste generation, and small size, the developed system can be classified as a versatile green analytical device. The proposed system was applied for the determination of Na^+, K^+, Ca^{2+}, Mg^{2+} in hot spring water samples. Moreover, this system has been investigated for some transition metal ions separation. It has high potential to be applied for ion determination in various water samples such as tap water, river water, mineral water, underground water, and wastewater. The proposed system will be developed further to be a compact instrumental setup for filed analysis of alkaline earth and transition metal cations in various environmental samples.

ACKNOWLEDGEMENTS

The authors thank Center of Excellence for Innovation in Chemistry (PERCH-CIC), Center of excellence in Material Science Research center (MSRC), Chiang Mai University, and International Foundation for Science (IFS)(W-5094-1).

REFERENCES

Michalski R. Applications of Ion Chromatography for the Determination of Inorganic Cations. Critical Reviews in Analytical Chemistry 2009; 39: 230-250.

Michalski R. Ion Chromatography as a Reference Method for Determination of Inorganic Ions in Water and Wastewater. Critical Reviews in Analytical Chemistry 2006; 36: 107-127.

Ohno K, Tachikawa K, Manz A. Microfluidics: Applications for analytical purposes in chemistry and biochemistry. Electrophoresis 2008; 29: 4443-4453.

Sheldon RA. The E Factor: fifteen years on. Green Chemistry 2007; 9: 1273-1283.

Kuban P, Dasgupta PK. Capillary ion chromatography. Journal of Separation Science 2004; 27: 1441-1457.

Muller SR, Simon W, Widmer HM, Grolimund K, Schomburd G, Kolla P. Separation of cations by open-tubular column liquid chromatography. Analytical Chemistry 1989; 61(24): 2747-2750.

Muller SR, Sheidegger D, Haber C, Simon W. Fast separations with open tubular ion exchange capillary columns. Journal of High Resolution Chromatography 1991; 14: 174-177.

Kuban P, Hauser PC. A review of the recent achievements in capacitively coupled contactless conductivity detection. Analytica Chimica Acta 2008; 607(1): 15-29.

Kuban P, Pelcova P, Kuban V, Klakurkova L, Dasgupta PK. Gravity-flow open tubular cation chromatography. Journal of Separation Science 2008; 31: 2745-2753.

Kiplagat IK, Kuban P, Pelcov P, Kuban V. Portable, lightweight, low power. ion chromatographic system with open tubular capillary columns. Journal of Chromatography A 2010; 1217: 5116-5123.

Kuban P, Dasgupta PK, Pohl CA. Open Tubular Anion Exchange Chromatography Controlled Layered Architecture of Stationary Phase by Successive Condensation Polymerization. Analytical Chemistry 2007; 79: 5462-5467.

Zhang M, Yang B, Dasgupta PK. Polymethylmethacrylate open tubular ion exchange columns: nondestructive measurement of very small ion exchange capacities. Analytical Chemistry 2013; 85: 7994-8000.

Yang B, Zhang M, Kanyanee T, Stamos BN, Dasgupta PK. An open tubular ion chromatograph. Analytical Chemistry 2014; 86: 11554-11561.

Christian GD, Dasgupta PK, Schug K. Analytical chemistry. 7th ed. John Wiley & Sons, USA. 2014; 607-615, 676.

Takeuchi M, Li Q, Yang B, Dasgupta PK, Wilde VE. Use of a capacitance measurement device for surrogate noncontact conductance measurement. Talanta 2008; 76: 617-620.

Kolla P, Kohler J, Schomburg G. Polymer-coated cation-exchange stationary phases on the basis of silica. Chromatographia 1987; 23(7): 465-472.

Kolb M, Seubert A, Viehweger KH. Practical ion chromatography. Metrohm, Switzerland. 2001; 17-18, 44-45.

Weiss J. Handbook of ion chromatography. 4th ed., Wiley-

VCH, New York, USA. 2009; 18-19, 453-455.

Cardelhcchto N, Ragone P, Cavalli S, Riviello J. Use of ion chromatography for the determination of transition metals in the control of sewage-treatment-plant and related waters. Journal of Chromatography A 1997; 770: 185-193.

Zlotorzynska ED, Dlouhy JF. Simultaneous determination of alkali, alkaline-earth metal cations and ammonium in environmental samples by gradient ion chromatography. Journal of Chromatography 1993; 638: 35-41.

Rong L, Liu Z, Ma M, Liu J, Xu Z, Lim LW, Takeuchi T. Simultaneous Determination of Inorganic Cations by Capillary Ion Chromatography with a Non-suppressed Contactless Conductivity Detector. Analytical Sciences 2012; 28: 367-371.

Fa Y, Yu Y, Li F, Du F, Liang X, Liu H. Simultaneous detection of anions and cations in mineral water by two dimensional ion chromatography. Journal of Chromatography A 2018; 1554: 123-127.

Dawood DH, Sanad MI. Determination Of Ions (Anion And Cation) By Ion Chromatography In Drinking Water From Talkha Territory And Some Its Villages, Dakahlia, Egypt. Journal of Agricultural Chemistry and Biotechnology 2014; 5 (9): 215-226.

Thomas DH, Rey M, Jackson PE. Determination of inorganic cations and ammonium in environmental waters by ion chromatography with a high-capacity cation-exchange column. Journal of Chromatography A 2002; 956: 181-186.

Appropriate scenarios for mercury emission control from coal-fired power plant using iPOG and CALPUFF model

Vasita Tunlathorntham[1,2], Piyapat Saenpao[1,2], Krisda Chidsanit[1,2], Kanisorn Jindamanee[1,2] and Sarawut Thepanondh[1,2*]

[1]Department of Sanitary Engineering, Faculty of Public Health, Mahidol University, Bangkok, 10400, Thailand
[2]Center of Excellence on Environmental Health and Toxicology (EHT), Bangkok, 10400, Thailand
[*]Corresponding author: e-mail: sarawut.the@mahidol.ac.th

ABSTRACT

Combustion of coal in a power plant is one of the major anthropogenic sources that release mercury into the atmosphere. However, its emission is expected to be decreased by implementing several emission control strategies. This research evaluates the success of mitigation scenarios in controlling mercury emissions from coal-fired power plant. These measures include gas cleaning systems, coal properties, furnace conditions, specific mercury control technologies as well as the co-benefit of mercury reduction from existing air pollution control devices installed at the power plant. Emissions are estimated using an actual characteristic of the power plant as an input for the iPOG model. As for the best practice in controlling of mercury emission, it is found that the appropriate scenario in this study can be achieved by adding the brominated activated carbon injection to the air pollution control devices (electrostatic precipitator and wet flue gas desulfurization) currently be installed at the power plant which can reduce the amount of mercury emission by 9.15 times of the baseline emission and causes the change of mercury concentration in the atmosphere from the current situation up to 92.8%. These results revealed the co-benefit of air pollution control technologies used in

controlling conventional air pollutants (dust, SO_2 and NOx) towards controlling of mercury emission.

Keywords: Co-benefit, Mercury emission, Coal combustion, iPOG

INTRODUCTION

Mercury and mercury compounds can accumulate in the human body and the environment. Mercury is often transferred by water and air. In addition, mercury has a long atmospheric lifetime of about 6-18 months that means mercury can be transported around the world. Mercury occurs both from natural sources such as soil erosion, forest fires, rock erosion and human sources such as fuel combustion, metal smelting can release mercury into the environment (UNEP, 2008; Hu and Cheng, 2016). Mercury is released into the environment in three forms: vapor-phase elemental mercury (Hg^0), vapor-phase oxidized mercury (Hg^{2+}) and particle-bound mercury (Hg_p). Hg^0 is a form of mercury found in the atmosphere due to the high volatility, low water solubility species and inert chemical reactive by being able to stay in the atmosphere for up to 0.5-2 years, causing it to spread around the world. Hg^{2+} and Hg_p are water-soluble and sensitive to chemical reactions, so they have shorter lives (1-2 weeks) (Hu and Cheng, 2016; Lopez-Anton, 2010; UNEP, 2002; Zhang *et al*., 2008). Based on human activities, it was found that fossil fuel burning such as coal base activities is the main source of mercury emissions form anthropogenic sources, which accounts for about 45% of all mercury emissions in the atmosphere (UNEP, 2008; Dziok *et al*., 2015).

To control the mercury emission from coal combustion can be divided into 3 main methods: pre-combustion (coal washing and fuel change) (Hu and Cheng, 2016) combustion control and post-combustion (air pollution control devices installation and mercury-specific control technologies installation) (Hu and Cheng, 2016; Dziok *et al*., 2015).

Methods for controlling mercury released from coal-fired power plants in many situations have different mercury removal efficiency due to different mercury species such as Hg^{2+} can be dissolved in water and can be removed in a wet scrubber such as wet flue gas desulfurization systems (WFGD) or Hg_p is almost completely capture in the PM control device such as ESP. Therefore, the form of mercury has an effect on choosing the appropriate scenarios to reduce mercury emission (UNEP, 2008). iPOG is a model that predicts the rate of Hg emissions from a full gas cleaning system that can predict the mercury emission by changing parameters in a specially designed interactive computer model such as coal properties, gas cleaning configuration, furnace conditions and air pollution control devices installation (UNEP, 2012). This makes iPOG useful for those who are new to the techniques of Hg control problems by playing with various parameters in iPOG and factory design options and discovering that how much simple changes in coal characteristics or plant operation may affect emissions (Krishnakumar *et al*., 2012). Therefore, this model will help select the appropriate scenarios for mercury control. The main objective of this research is to find an appropriate situation to reduce mercury emissions from coal-fired power plants from the existing data using the iPOG model and using the CALPUFF model to assess mercury concentrations in the atmosphere to compare the concentration and dispersion of mercury in the current situation.

METHODOLOGY

The proportion of coal use in Thailand during January to November 2018 shows that the supply of coal / lignite has increased from the previous year, which is an increase in imports of coal according to increased demand, which increased by 36,984 thousand tons or up 4.6%, imported coal accounted for 23,437 thousand tons or 63% and produced in Thailand equal to 13,547 thousand tons or 37% divided by divided into Mae Moh mine 13,226

thousand tons or 36% and other 321 thousand tons or 1%.

The use of coal / lignite increases as a result of the use of coal in both the power generation and industrial sectors, while using lignite in electricity generation decreased as the domestic lignite production capacity decreased, divided into 52% of coal for industrial use and 48% for electricity production (EPPO, 2018).

Site Description

The coal power plant used in the study is the Mae Moh coal-fired power plant, Thailand. Mae Moh Power Plant is a thermal power plant that uses lignite as fuel approximately 16 million tons per year by converting the accumulated energy of lignite into electricity using water as an intermediary. Lignite that is used as fuel is taken from coal mines near the power plant. The total generating capacity of 10 stacks in coal-fired power plant is 2,400 MW including unit 4-7 installed capacity is 150 MWs and unit 8-13 installed capacity is 300 MWs, along with the installation of pollution control equipment are electrostatic precipitator (ESP) and flue gas desulfurization (FGD).

Air Model

iPOG model (The Interactive Process Optimization Guidance) is a software program was developed by Niksa Energy Associates LLC (NEA) for the United Nations Environment Program that was developed using the "decision tree" concept in iPOG model to estimates the mercury emission rate and mercury species from the gas cleaning system under the parameters in the model by user can input coal characteristics in the area, gas cleaning conditions such as halogen injection, co-benefit from pollution control device and Hg-specific control technologies. iPOG is a tool that designed as a model for which is in the form "What if…" questions regarding variations in parameters (Krishnakumar *et al.*, 2012). Although iPOG model does not estimated the cost for each options but iPOG can be a tool for

determining the appropriate alternatives to reduce the release of mercury from the power plant, which is a good result as supplementary information for worthwhile study. Estimated mercury emissions depend on the engineering correlations of the mercury field test database from the US utilities, supported by the NEA detailed using the principle of chemical mass balance.

CALPUFF model was developed by Sigma Research Corporation for the mathematical estimation of the impact of the source, which is related to the transport of pollutants in the atmosphere, meteorological conditions, emissions characteristics and surrounding terrain. CALPUFF is called a puff model that can calculated in hours per hour and wind variation (Scire *et al*., 2000) CALPUFF is a form of gas and particle diffusion using spatial data, time and meteorological data, in addition CALPUFF model is a mathematical estimate of the effects of pollution from emissions sources within the study area (Holmes and Morawska, 2006). This model consists of three components are CALMET, CALPUFF and CALPOST, in which the CALMET model is a meteorological simulation in the area, together with the simulation of the dispersion by CALPUFF model and then expressed as images with CALPOST model.

Data Collection and Data Treatment

Data collection is an important to emission data from coal-fired power plant in this study by the data is derived from the actual input of the power plant, comparing with the parameter changes to obtain data using as a representation of various situations in order to compare as much as increasing or decreasing. The information that has been changed is within the scope of the study within the iPOG model.

iPOG model was used to predict mercury emissions from coal-fired power plant. Mercury emission was calculated from 10-point source in gram per hour (g/hr) by evaluating in two forms, Furnace unit 4-7 rating

150 MWe, Furnace unit 8-13 rating 300 MWe. It also contains O_2 economizer 3.5%, LOI 1%, ESP efficiency 98%, Limestone wet FGD efficiency 90% and lignite was used to as fuel in this study.

The CALMET and CALPUFF models use the EPA approved version (version 5.8.5) and the CALPOST model uses the EPA approved version (version 6.221) to determine the mercury concentration in the environment. The creation of the CALPUFF model system consists of three main parts: CALMET, CALPUFF, and the post-processing and graphical display format.The study domain was designed for grid center coordinate at Latitude 18°29"N Longitude 99°75"E, grid spacing 1x1 km, cover an area of 30 x 30 km^2 And use the WRF model to predict meteorological data in 2017. The dispersion coefficient of mercury was calculated in nanogram per cubic meter (ng/m^3) as an average of 1 year.

RESULTS AND DISCUSSION

Mercury emission analysis

Under the current air pollution control of the power plant (ESP+WFGD), emission of mercury was estimated as 41 g/hr. Without these current control devices, it was estimated that about 374 g/hr of mercury will be emitted from this power plant. Therefore, the co-benefit of installing current equipment which primarily aimed to control emissions of particulate matter and SO_2 towards reduction of mercury was about 89%. This result clearly revealed the co-benefit of common air pollution control devices on the reduction of airborne mercury released from the power plant.

We further analyze mercury emission under several scenarios such as adding additional control technologies to the current situation, coal washing as well as changing of existing control technology. Results are as summarized in figure 1, 2, 3, 4. It was estimated that mercury emission can be reduced up to 9.15 times from its current emission by employing the brominated activated

carbon injection (ACI) before the ESP/APH and WFGD. This high removal efficiency is obtained as a result of the fine porosity which leads to high specific surface area of the adsorbent. The results of the analysis are divided into 4 cases.

Case 1 for Fig. 1 shows a change in the mercury emission that is increasing and decreasing from the baseline situation of pollution control equipment installation and mercury control options, which are shown in red and blue graphs. In this case, most of the situations are equipped with specific dust treatment equipment, such as the installation of fabric filter (FF), which causes the release of 7.02 times from the baseline scenario or the installation of electrostatic precipitator (ESP), which drains mercury up to 368 g/hr or increase mercury emissions from current emission 8.98 times with only 1.5% mercury removal efficiency. Although these dust removal devices are effective in removal of mercury dust (Hg_P) in the form of co-benefits up to 99.55% - 99.97% (Zhao *et al*., 2017) but have a low elimination of mercury in other forms ($Hg^{2+,}$ Hg^0). Therefore, the installation of the dust removal device alone cannot reduce the overall mercury.

In addition, if observing the installation of pollution control equipment of the current situation is the installation of electrostatic precipitator and wet flue gas desulfurization (ESP+WFGD installation) that reduces mercury emission due to installation WFGD, in addition to being able to eliminate SO_2, there is also the ability to convert mercury in various forms into Hg^{2+}, which causes pollution control devices to trap more mercury. However, in this case there is a way to reduce mercury emission from the current situation shown in the blue graph, such as adding the untreated activated carbon injection or brominated activated carbon injection to electrostatic precipitator (untreated ACI+ESPc or brominated ACI+ESPc) reduces the emission of mercury 1.22 times and 2.20 times

from current emission, respectively, because ACI technology is a device specifically for mercury removal and also has a high mercury removal rate (Ancora *et al*., 2015).

Fig. 2 shows the second case by increasing the installation of existing pollution control equipment or cleaning coal. For most cases, mercury emission decreased from the current situation, for example, increasing coal washing before air pollution control devices (ESPc+WFGD) that reduced mercury up to 1.67 times from the baseline emission due to cleaning coal as a mercury reduction method before combustion, which can reduce the average concentration of mercury in coal by about 30%, resulting in lower ash content, heat value and increased efficiency of coal combustion process. In addition, coal washing is the least cost-effective method for reducing mercury emission before burning (Ancora *et al*., 2015, Streets *et al*., 2005) or in the case of adding halogen compounds in coal or furnace together with current air pollution control equipment (ESPc+WFGD) which has a common benefit of reducing mercury emission to 1.05 times. For halogen injections, such as adding chlorine or bromine from other research, it is found that if the amount of chlorine in the coal increases, the pollution control device will be able to absorb more mercury. In addition, the addition of halogen in coal shows that it is effective in reducing mercury drainage for coal-fired power plants by increasing the cost by only 6% from installing dust control equipment (Hu and Cheng, 2016).

Fig. 3 shows the increase in the installation of pollution control equipment (SCR, ESP, ACI) from baseline air pollution control devices and in the case of the absence of pollution control technology, which increases mercury emissions to 9.12 times from the current emission. As for the addition of brominated activated carbon injection (ACI) to the air pollution control equipment (ESP and WFGD) will reduces the

mercury emission to 9.15 from baseline emission, which is the least mercury emission situation because ACI technology can reduce mercury in the form of Hg^0 affects 80% reduction in mercury in the form of Hg^{2+} (UNEP, 2018) and is a technology that specifically uses mercury removal. In addition, coal-fired power plants have a replacement coal power plant development project, which increases the installation selective catalytic reduction (SCR), which is used as a control device NO_x to the current air pollution control equipment. However, in this research, the installation of SCR does not cause changes in mercury emission.

Fig. 4 shows the current air pollution control equipment installation together with the changing conditions of the furnace (LOI, bottom ash, coal blend properties). It was found that the loss of combustion (LOI) from 1 to 0.9 and 0.8 caused mercury emissions to decrease by 1.01 times and 1.03 times from the original, because the loss of ignation (LOI) value was directly related to the carbon surface area, unburned carbon and fly ash, which affects mercury trapping because mercury can be absorbed by fly ash but the blending of coal causes more mercury due to the lignite coal in Mae Moh mine being high quality coal and high chlorine peroxide resulting in increased mercury capture which the amount of chloride will determine the amount of mercury emissions (Hu and Cheng, 2016; Burmistrz *et al*., 2016).

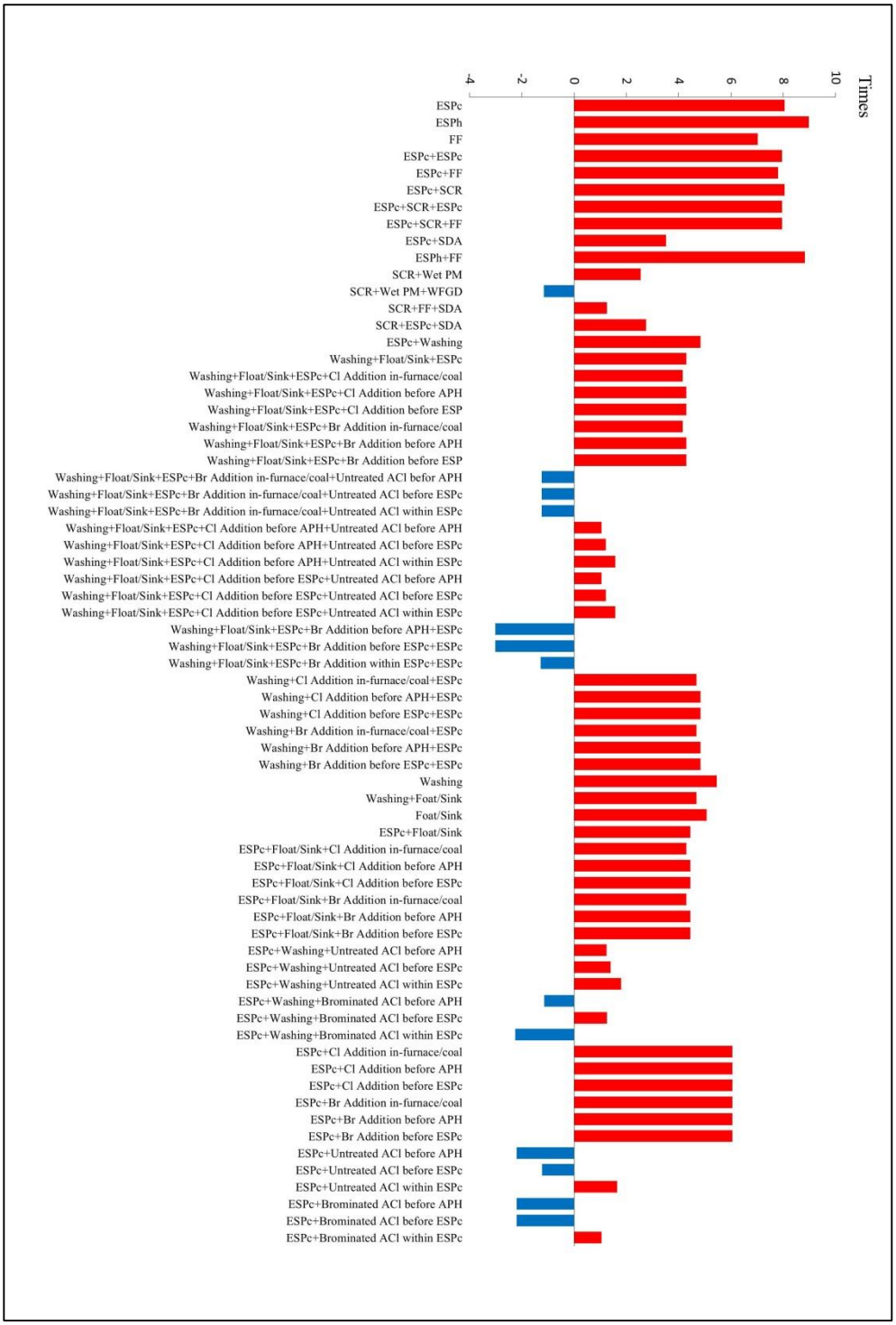

Figure 1 Pollution control devices installation and options to reduce mercury

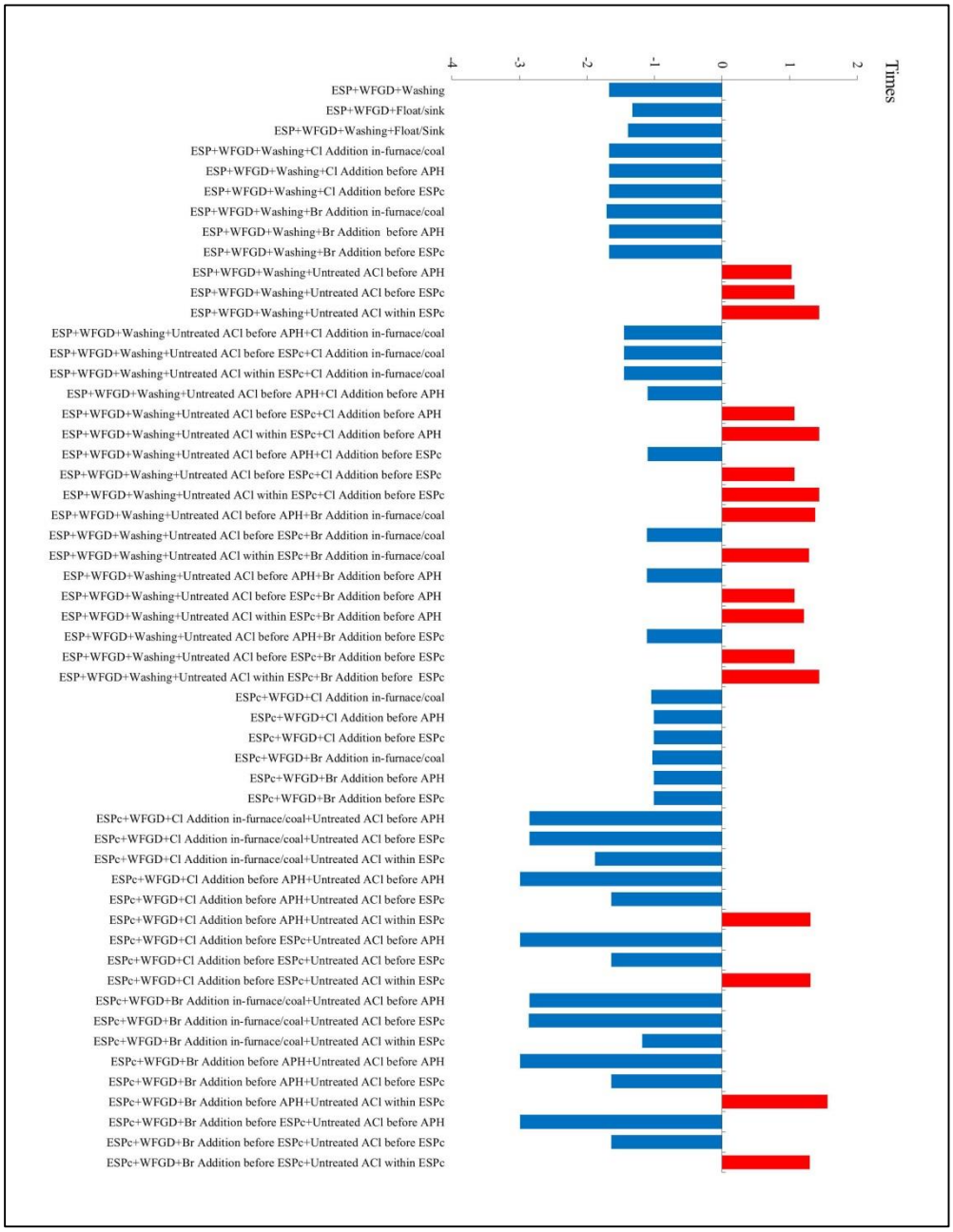

Figure 2 Existing (ESP+WFGD installation) + adding pollution control devices or coal cleaning

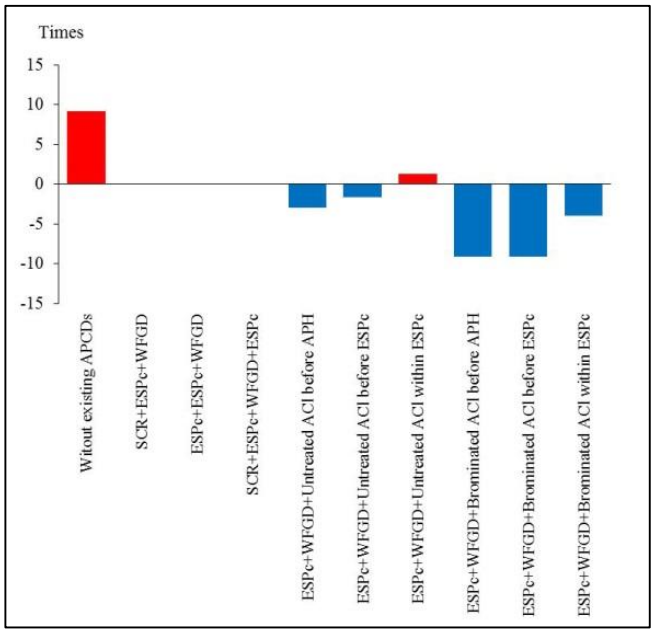

Figure 3 Existing (ESP+WFGD installation) + air pollution control devices (SCR, ESP, ACI installation) and without existing air pollution control devices

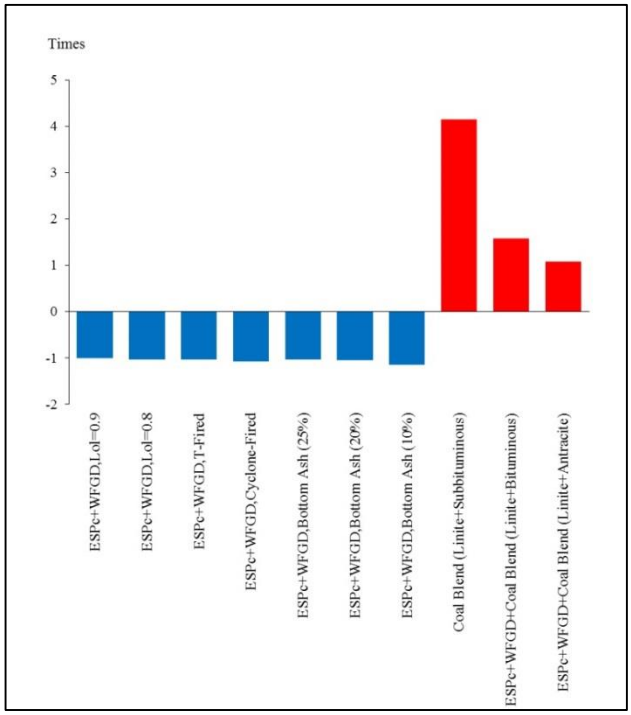

Figure 4 Existing (ESP+WFGD installation) + Furnace condition (LOI, bottom ash, coal blend properties)

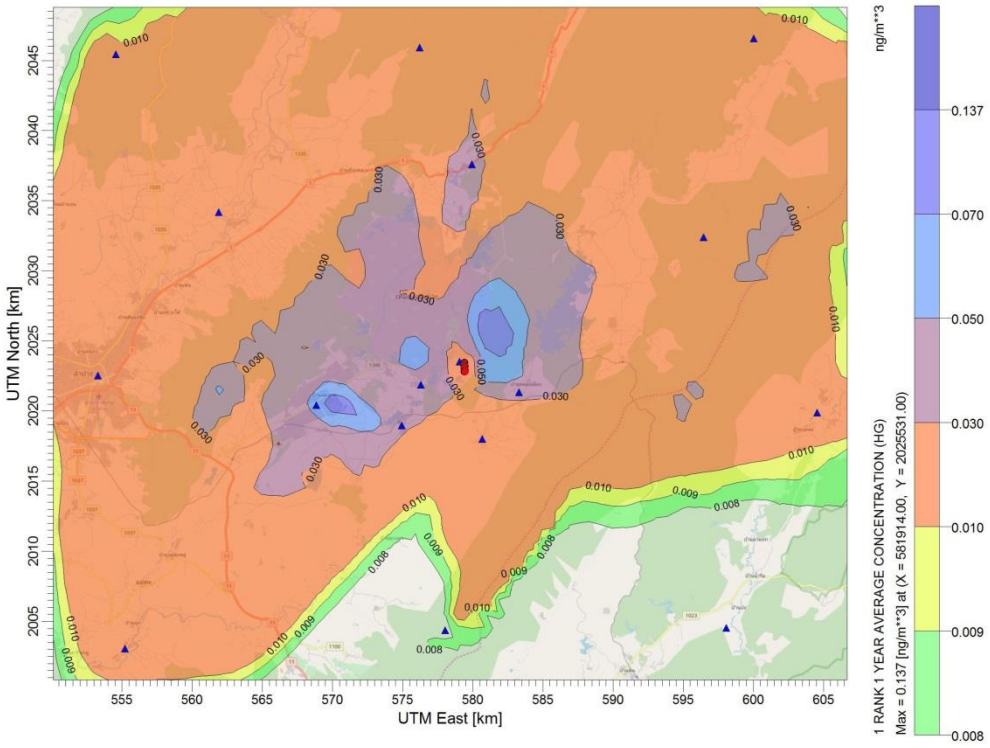

Figure 5 Annual average mercury concentration (ng/m^3) of ESPc+WFGD case (baseline scenarios)

Distribution of mercury concentration

In addition, the results showed In addition that the comparison of the average diffusion and mercury concentration between the current situation and adding the brominated activated carbon injection to the air pollution control devices (electrostatic precipitator and wet flue gas desulfurization could reduce the concentration of mercury to 92.8% as shown in Figure 5 and 6.

Coal is increasingly used as a fuel to respond to human life, but development often occurs with pollution. Coal-fired power plants are one source that emits pollutants into the atmosphere as an anthropogenic source. One of those pollutants is the mercury that comes out of the power plant. Therefore, it must be controlled to emission. Mercury emission can be reduced by controlling both pre-combustion

CONCLUSIONS

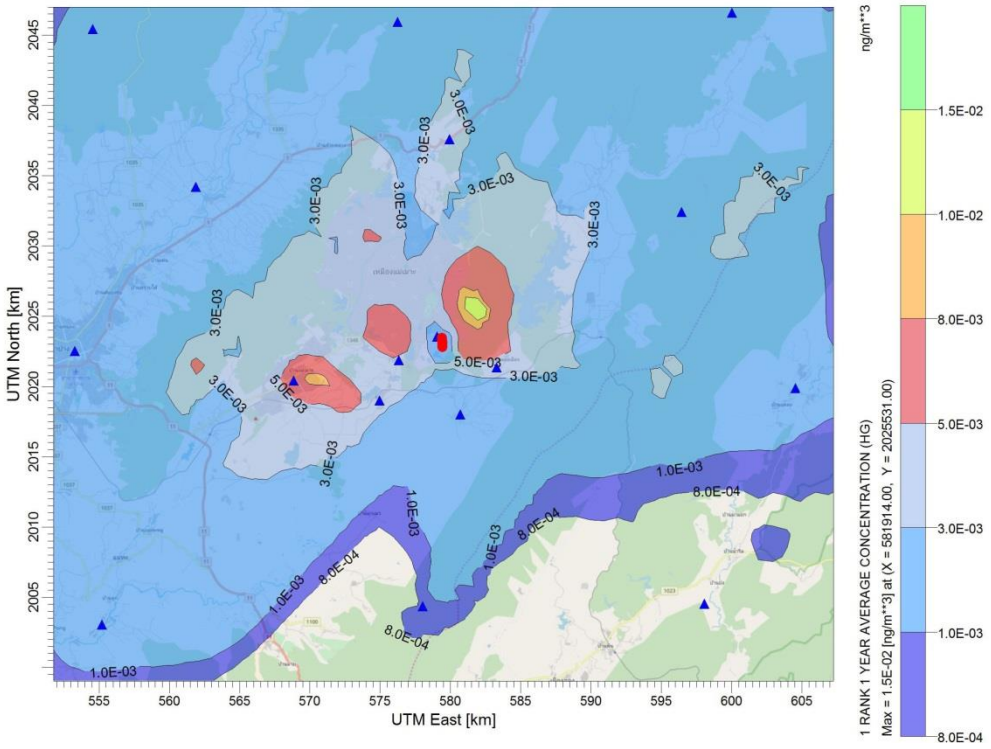

Figure 6 Annual average mercury concentration (ng/m^3) (ESPc+WFGD+ Brominated ACI before ESP scenario)

(washing, changing fuel, coal blending), during combustion (LOI, Bottom ash adjustment) and post-combustion (installation of air pollution control device, installation of specific mercury removal equipment, halogen injection in flue gas). The case that causes the most reduction of mercury for this research is to increase the brominated ACI technology to air pollution control devices (ESPc and WFGD), which can reduce mercury emission to 9.15 times from the baseline emission.

ACKNOWLEDGEMENTS

The authors would like to thanks the Faculty of Public Health and Faculty of Graduate studies, Mahidol University, Thailand for supporting this study.

REFERENCES

Balaji K, Stephen N, Lesley S, Wojciech J Gunner F. Process Optimization Guidance (POG and iPOG) for Mercury Emission Control. Energy Fuel 2012; 26: 4624-4634.

David GS, Jiming H, Ye W, Jingkun J, Melissa C, Hezhong T, Xinbin F. Anthropogenic mercury emissions in China. Atmospheric Environment 2005; 39(40): 7789-7806.

EPPO. Energy Overview. 2018. http://www.eppo.go.th/images/Energy-Statistics/energyinformation/Energy_Statistics/00All.pdf.

Liang Z, Yuqun Z, Lei C, Xuchang X, Changhe C. Mercury emissions from six coal-fired power plants in China. Fuel Processing Technology 2008; 89: 1033-1040.

Maria P. A, Lei Z, Shuxiao W, Jeremy S, Jiming H. Economic analysis of atmospheric mercury emission control for coal-fired power plants in China. Environmental Sciences 2015; 33: 125-134.

M. Antonia L. A, Yang Y, Ron P, M. Mercedes M. Analysis of mercury species present during coal combustion by thermal desorption. Fuel 2010; 89: 629-34.

Nicholas S. H, Lidia M. A review of dispersion modeling and its application to the dispersion of particles: An overview of different dispersion models available. Atmospheric environmental 2006; 40(30): 5902-5928.

Piotr B, Krzysztof K, Marta M and Jerzy Z. Lignites and subbituminous coals combustion in Polish power plants as a source of anthropogenic mercury emission. Fuel Processing Technology 2016; 152: 250-258.

Joseph S. S, David G. S, Robert J. Y. A User's Guide for CALPUFF Dispersion Model (ver. 5). Earth Tech Inc. 2000. http://www.src.com/calpuff/download/CALPUFF_Users Guide. pdf.

Shilin Z, Yufeng D, Lei C, Yaning L, Ting Y, Shuai L, Meng L, Jianhong L. Study on emission of hazardous trace elements in a 350 MW coal-fired power plant. Part 1. Mercury. Environmental Pollution 2017; 229: 863-870.

Tadeusz D, Andrzej S, Andrzej R, Mariusz M. Studies of the correlation between mercury content and the content of various forms of sulfur in Polish hard coals. Fuel 2015; 159: 206-213.

U.N. Environment Programme (UNEP). Global Mercury Assessment. 2002. https://wedocs.unep.org/handle/20.500.11822/11718.

U. N. Environment Programme (UNEP). The Global Atmospheric Mercury Assessment Sources. 2008. https://wedocs.unep.org/bitstream/ha

ndle/20.500.11822/11517/UNEP_GlobalAtmosphericMercuryAssessment_May2009.pdf.

U.N. Environment Programme (UNEP), .iPOG™ User-guide. Division of Technology, Industry and Economics (DTIE). 2012. https://wedocs.unep.org /Handle/20.500.11822/11885.

U.N. Environment Programme (UNEP). iPOG™ Reducing mercury emission from coal combustion in the energy sector in Thailand. 2018. http://infofile.pcd.go.th/haz/Final_edit_06_2018.pdf?CFID=1180107&CFTOKEN=65780703.

Yuanan H, Hefe C. Control of mercury emissions from stationary coal combustion sources in China: Current status and recommendations. Environmental Pollution; 2016: 218, 1209-1221.

Assessment of hydrogen sulfide concentration and dispersion in ambient air using AERMOD model from Saen Saeb canal in Bangkok, Thailand

Piyapat Saenpao[1,2], Krisda Chidsanit[1,2], Vasita Tunlathorntham[1,2] , Kanisorn Jindamanee[1,2], and Sarawut Thepanondh[1,2*]

[1] Department of Sanitary Engineering, Faculty of Public Health, Mahidol University, Bangkok, 10400, Thailand

[2] Center of Excellence on Environmental Health and Toxicology (EHT), Bangkok, 10400, Thailand;

[*]Corresponding author: e-mail: sarawut.the@mahidol.ac.th

ABSTRACT

Hydrogen sulfide (H_2S) released as by product of anaerobic process from the Saen Saeb canal in Bangkok is evaluated for its potential impact on odour nuisance to nearby residents and businesses. Emissions of H_2S were estimated by the U.S.EPA WATER 9 model by using actual concentrations of H_2S in the canal obtained from the direct measurements as one of the input data along with the physical characteristics of the canal. Calculated emission rates under 2 scenarios (with and without operations of the public-transportation boat) were further evaluated for spatial distribution of ambient H_2S concentrations using the AERMOD model. Predicted results revealed that with an operation of the public-transportation boat in the canal, H_2S concentrations were about 67% higher than those without canal-boat operation. Seventeen sensitive receptors in the study area were evaluated for their potential threat on odour nuisance problem. It was found that there were 9 and 4 receptors predicted to have H_2S concentrations greater than its odour annoyance threshold of 7 $\mu g/m^3$ under with and without the canal-boat operation scenarios, respectively. Predicted concentrations under the scenario with the canal-boat operation

were ranging from 2.57 to 38.31 μg/m^3. On the other hand, without canal-boat operation, it was predicted that H_2S ambient air concentrations at those receptors will be varied from 0.83 to 12.35 μg/m^3. The study clearly indicated that the effort in controlling H_2S concentration in the canal taking into consideration the water quality standard is not enough to minimize the potential impact on an odour nuisance from this compound particularly when the canal is aerated from the operation of the public-transportation boat. Therefore, a concern on an odour impact should also be given when setting up a river water quality standard for those rivers which serve as a public transportation route in an urban area.

Keywords: Hydrogen sulfide, AERMOD model, Saen Saeb canal, Odour

INTRODUCTION

The number of households living, population and economic growth in urban areas increased continuously. People increasingly consume water from rivers and canals for activities, tourism, transportation and consumption (Prasartkul *et al.*, 2016). In many developing countries, waste and domestic wastewater are directly and indirectly discharge to the water sources (Yu *et al*., 2014). These problems affect the quality of water sources, resulting in lack of oxygen in water, emission of hydrogen sulfide from water, health effect of odour and decrease of air quality in areas (Nguyen *et al*., 2012).

Hydrogen sulfide (H_2S) is a colourless, flammable gas with a characteristic odour of rotten eggs. It is produced from natural sources and human activities. Generally, hydrogen sulfide in wastewater occurs when wastewater contains organic matter (BOD and COD), sulfate and under anaerobic conditions (zero DO in wastewater) (Cheowchan, n.d.). In addition, hydrogen sulfide may easily evaporate into the atmosphere, depending on pH and temperature

(U.S.EPA, 1993; WHO, 2003). Therefore, the odour of hydrogen sulfide that is released from the wastewater into the atmosphere causes nuisance and affects human health (Latos *et al*, 2011).

The main effect of the odour of hydrogen sulfide emitted from water causes nuisance to humans. The odour may also affect damage to economy, life quality of residents and surrounding air quality (U.S.EPA, 1993; Godoi *et al*, 2018). Humans detect it at levels of concentrations 0.2-2.0 μg/m^3, depending on its purity. In order to avoid complaint about odour exposure of population, the concentration of hydrogen sulfide should not exceed 7 μg/m^3 (1-hour average) (The Ministry for the Environment, 2002). Therefore, air dispersion models are used as one of a tool to tackle this problem taking into consideration the objectives to manage air quality, effectively (Baawain *et al*, 2017; Gulia *et al*, 2017).

Atmospheric dispersion modeling has been applied as a reliable tool to determine the impact of odour emissions in several cases using mainly Gaussian models such as the AERMOD model (Latos *et al*, 2011; Yu *et al*, 2009; O'Shaughnessy and Altmaier, 2009). Dispersion modeling can effectively be used in order to estimate the dispersion of odours using available emission data and to correlate with complaints (Latos *et al*, 2011). The AERMOD dispersion modeling is the one of the current best available tool for dispersion studies in different areas (Baawain *et al*, 2017). In addition, the AERMOD model has also been considered to predict ambient hydrogen sulfide concentrations produced by swine CAFOs (Nguyen *et al*., 2012), wastewater treatment plants (Latos *et al*, 2011; Godoi *et al*, 2018; Baawain *et al*, 2017) and rivers (Yu *et al*., 2014) that affect nearby residences.

In this study, Saen Saeb canal located in Bangkok, Thailand is selected as the study area. The canal is one of

important canals for transportation and shipment, which flows through communities in commercial and industrial areas. This canal plays a role in drainage of the area to prevent and correct floods including support communities wastewater (Somsook, 2013; Suwandee, 2013). Saen Saeb canal was affected from change of urbanization in Bangkok, resulting in very degrade of water quality with high organic content (black water) and air quality with unpleasant odour. Although water quality in the canal has improved, it is not good enough. This study is aimed to determine emission of H_2S released to the air from the canal and to assess concentrations and dispersions of H_2S in the ambient air using AERMOD model. This information can be used as a guide to study of air quality and its link to the potential odour and health impacts in the future.

METHODOLOGY

Study area

The study area was Saen Saeb canal located in Bangkok, Thailand. Saen Saeb canal is one of the longest canals in Thailand. The total length of Saen Saeb canal is about 72 kilometers (km). The length of the canal in Bangkok is 45.5 kilometers and the width of the canal in Bangkok is about 20-30 meters (m). This study covers the central business district (CBD) area of Bangkok covering an area of 6x6 km^2 or 3-km centered from Pratunam.

Data collection

Emissions of H_2S were estimated by the U.S.EPA WATER 9 model using actual concentrations of H_2S in the canal obtained from the direct measurements as one of the input data along with the physical characteristics of the canal. Calculated emission rates were performed under 2 scenarios (with and without operations of the public-transportation boat) and were further evaluated for spatial distribution of ambient H_2S concentrations using the AERMOD model.

The data used in the study included water quality data, emission data, meteorological data and receptors.

Results of water quality analyze of Saen Saeb canal were obtained from the Water Quality Management Office of Bangkok Metropolitan Administration. The concentration of H_2S in the worst case of the analyzed water (4 mg/l) was chosen. Estimated emission values are in grams per second (g/s). Meteorological data were achieved from Donmuang international airport meteorological radar station in 2017. These data were wind speed, temperature, cloud cover, ceiling height, surface pressure and relative humidity. Most of the wind directions blow to the Northeast with an average wind speed was 2.55 m/s and calm winds of 3.48% were detected. In addition, the locations of sensitive receptors in the area of study were determined to predict ground level concentrations of H_2S for 17 receptors covering the study domain and populated areas.

WATER 9 model configurations

In this study, U.S.EPA WATER9 Version 3.0 was used to assess emission of H_2S. Unit type options are defined in different scenarios, open sump unit was selected as a representative of Saen Saeb canal (Scenario 2 without operation of public boat-transportation in the canal) and aerated bio treatment unit was chosen to represent scenario 1 (with operation of public boat-transportation).

AERMOD model configurations

AERMOD was designed to support the EPA's regulatory modeling program. In this study, Lakes Environmental Software's AERMOD Version 9.5.0 model was used to assess concentrations and dispersion of H_2S. Study domain is centered at latitude 13.749346 deg, longitude 100.540875 deg and zone 47 (north). The modeling domain covers an area of 6×6 km with a horizontal and vertical grid spacing of 100 m. H_2S emissions from line source located within urban. Meteorological data were obtained from the Donmuang meteorological radar station in 2017. Meteorological data file was read from 1st hour of January 1, 2017 to 24th hour of December 31, 2017. Topographical characteristic of the

study area is derived from the Shuttle Radar Topography Mission (SRTM3). These data are used as input data for analysis. H_2S concentrations were defined as output data in microgram per cubic meter ($\mu g/m^3$). The concentrations of H_2S are calculated as annual average, 1-hour maximum, and percentiles 99^{th}, 97.5^{th}, 95^{th} and 90^{th}.

RESULTS AND DISCUSSION

Determination of H_2S emission

Emissions of H_2S from Saen Saeb canal using WATER9 model were determined under 2 different scenarios (with and without canal-boat operation in Saen Saeb canal). Highest concentration of H_2S water quality measured in the canal was used to represent the water quality along with other water quality parameter such as suspended solid, water temperature, etc. Results indicated that H_2S emission to ambient air from the operation of canal-boat in Saen Saeb canal was about 3.74×10^{-3} g/s. As for the 2^{nd} scenario (without canal boat operation), predicted H_2S emission was 1.21×10^{-3} g/s. These emissions were further used to assess H_2S concentration and dispersion by AERMOD dispersion model.

Assessment of H_2S concentration and dispersion

H_2S emission data obtained from WATER9 model and meteorological data from Donmuang meteorological radar station in 2017 were used as input data to predict concentration and dispersion of H_2S from Saen Saeb Canal using AERMOD model. The recommended concentration of H_2S in atmosphere is not excess 7 $\mu g/m^3$ (1-hour average) to avoid annoyance odour complaints (The Ministry for the Environment, 2002) was used for comparison purpose in this evaluation.

The concentration of H_2S was calculated for 1-hour maximum concentration, together with its level at percentile of 99, 97.5, 95, 90 and annual average concentrations. H_2S concentrations were assessed for both 24 and 14 hours with canal boat operation. The results of

concentration and dispersion of the H_2S as illustrated in Fig. 1, presents the predicted concentration and dispersion of H_2S under scenario with canal-boat operation in Saen Saeb Canal in 24 hours. The study revealed that the maximum 1-hour concentration of H_2S could reach the level of 351.74 µg/m^3. High concentrations of H_2S were found in the area of Asok Bridge, Pratunam and Hua Chang Bridge of Saen Saeb canal. High concentrations predicted in these areas could be an effect of high-rise buildings influenced to the dispersion and atmospheric dilution ability of H_2S. However, the dispersion of the highest concentration was not far from line source and was not affect receptors. The annual average concentration of H_2S was 25 µg/m^3. The 1-hour average concentrations at 17 receptors were predicted in the range of 2.58 to 38.31 µg/m^3. It was found that H_2S concentration at receptor 9 points were above the annoyance odour threshold.

Fig. 2 shows H_2S concentration and dispersion under scenario with 14 hours (06:00-20:00 p.m.) canal-boat operation in Saen Saeb Canal. It revealed that the 1-hour maximum concentration of H_2S was 351.20 µg/m^3. The annual average concentration of H_2S was 22.09 µg/m^3. H_2S concentrations at receptors ranging from 2.57 to 38.17 µg/m^3. Highest concentration under scenario without canal-boat operation (Fig. 3) was 113.62 µg/m^3 which receptor 4 points exceeded the odour threshold.

Comparison of predicted concentrations for 14 hours, 24 hours with canal-boat operation and without canal-boat operation in Saen Saeb Canal is presented in Fig 4. It should be noted that the profile of concentrations as depicted in Fig. 4 were derived from modeled 1-hour concentrations. Therefore, there were only slightly difference

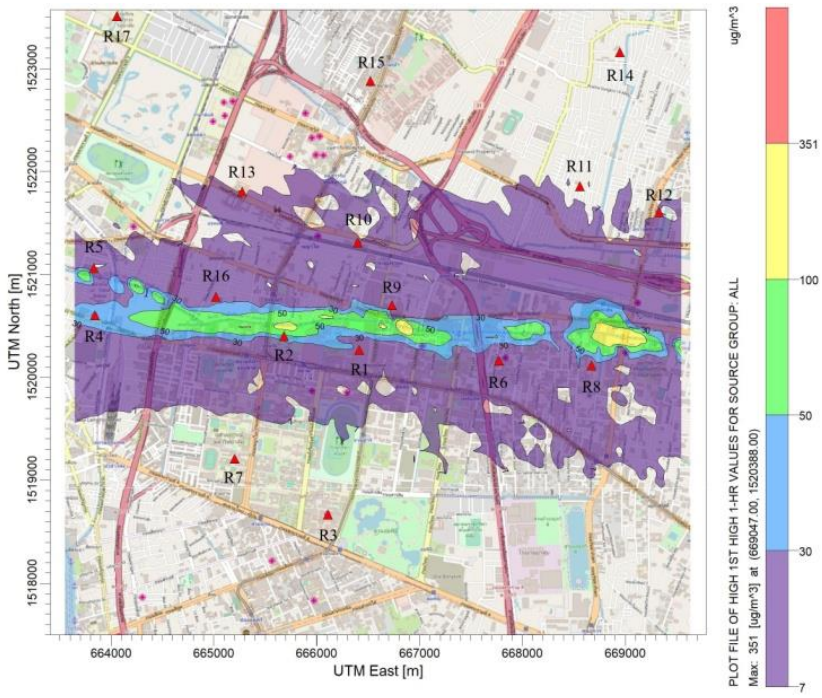

Figure 1 H_2S concentrations and dispersion under scenario with 24 hours canal-boat operation

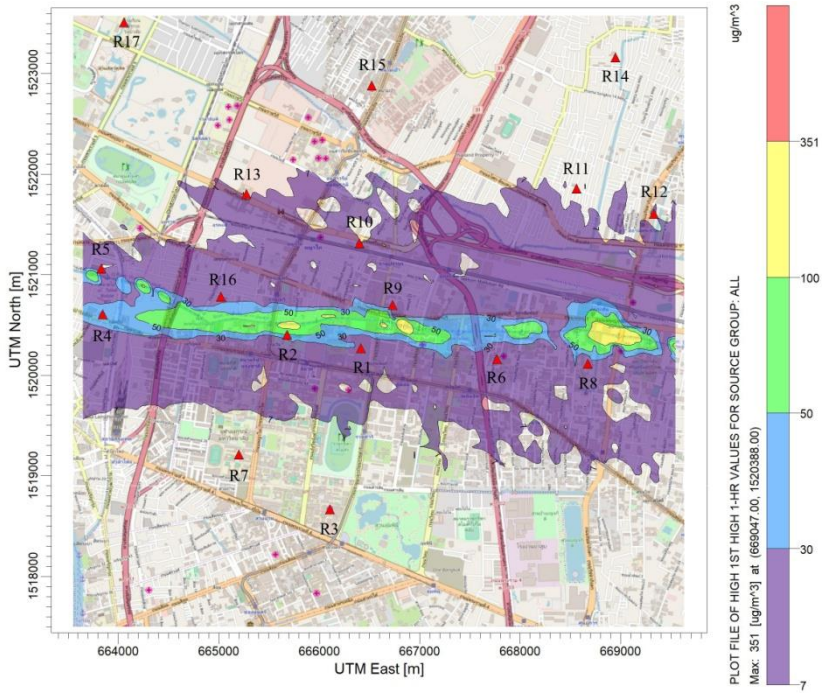

Figure 2 H_2S concentrations and dispersion under scenario with 14 hours canal-boat operation

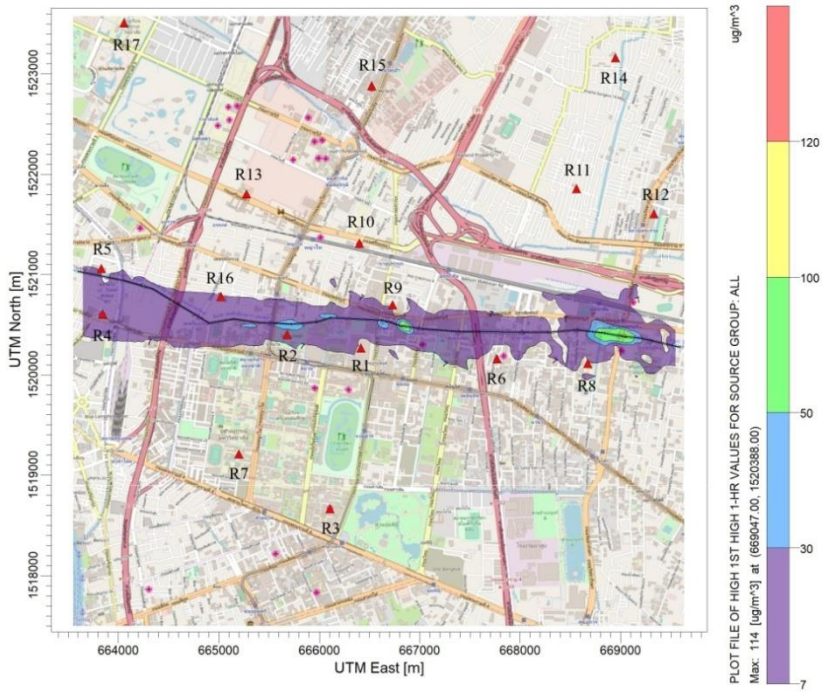

Figure 3 H_2S concentrations and dispersion under scenario without canal-boat operation

Between predicted date from the model simulation under 24-hour and 14-hour canal-boat operations. However, It was found that these concentrations were significantly higher than the predicted concentration under the scenario of no operation of canal- boat (about 67.6% and 67.5% lower than the scenarios of 24 hours and

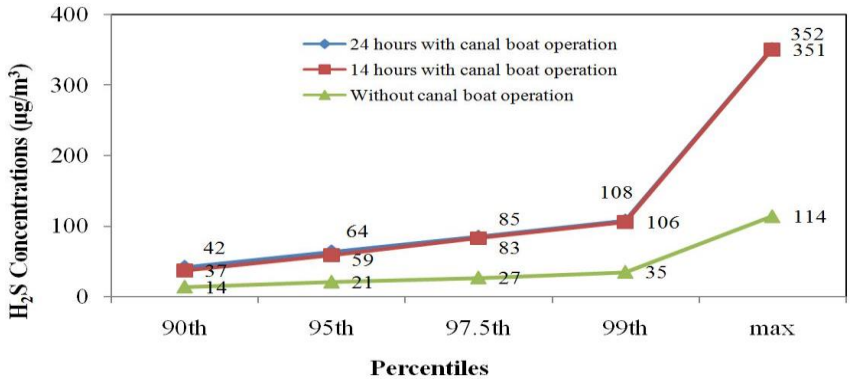

Figure 4 Comparison of H_2S concentrations between with and without canal-boat operation in Saen Saeb canal

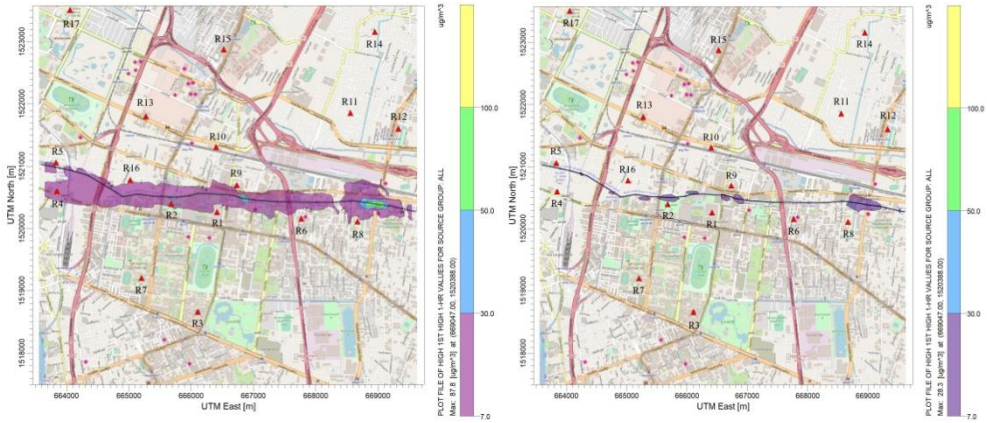

(a) (b)

Figure 5 H_2S concentrations and dispersion that has been evaluated according to the water quality standards under 2 scenarios: (a) with canal-boat operation and (b) without canal-boat operation

14 hours canal-boat operations, respectively. Previously, H_2S concentration in water of Saen Saeb canal used in the determination of emission value using WATER9 model was determined to use the highest H_2S concentration from the water quality analysis results in all scenarios and throughout line source with the value of 4 mg/l. We further evaluated the extent of H_2S ambient air concentration using the Thai's water quality control standards from buildings into public water sources which recommended for H_2S concentrations in water not exceeding 1 mg/l (Pollution Control Department, 2005). H_2S emission and concentrations were assessed according to the recommended water quality standards under both scenarios (with and without canal-boat operations). It was found that there was still a problem with the odour causing nuisance to people in the vicinity of the canal under the scenario with canal-boat operation. However, in scenario without canal-boat operation, it is found that effort to control water quality to meet it environmental standard could significantly minimize the potential odor nuisance problem as shown in Fig 5.

CONCLUSIONS

In this study, WATER9 model was used to estimate air emissions of H_2S from Saen Saeb canal in 2 scenarios. It was found that the emissions of H_2S in scenario under the canal-boat operation was higher than those under without the canal-boat operation in Saen Saeb canal. The concentrations and dispersion of H_2S in scenario with canal-boat operation were assessed at 24 hours and 14 hours using the AERMOD dispersion model. Predicted results showed that there were no different in the operations of the boat canal under different operating time. Some receptors were predicted to have their H_2S concentrations greater than the recommended level of odour causing nuisance to population. Without canal-boat operation, it was estimated that the 1-hour maximum concentration will be about 67% lower than the level under with the canal-boat operation. Under the scenario without canal-boat operation, the concentration of H_2S exceeded the guideline values of odour nuisance at 4 points all of 17 receptors. In addition, the results of the assessment of the concentration of H_2S were high in the area of Asok Bridge, Pratunam and Hua Chang Bridge, which is mainly affected by the high-rise building with minimize the atmospheric dilution ability of H_2S released from the canal.

ACKNOWLEDGEMENTS

The authors would like to thank the Water Quality Management Office (WQMO) in providing water quality data used in this study. This study was partially supported for publication by Faculty of Public Health, Mahidol University, Graduate Studies of Mahidol University Alumni Association and National Research Council of Thailand (NRCT).

REFERENCES

Baawain M, Al-Mamun A, Omidvarborna, H, Al-Jabri A. Assessment of hydrogen sulfide emission from a sewage treatment plant using AERMOD. Environ. Monit. Assess. 2017; 189(6).

Cheowchan P. Hydrogen sulfide in wastewater. Journal of safety and health. http://www.xn--22cd2clarkbdm

ea1adsd9bk3c7crjcdn1mxj.com/Journal.html.

Godoi AFL, Grasel AM, Polezer G, Brown A, Potgieter-Vermaak S, Scremim DC, Yamamoto CI, Godoi RHM. Human exposure to hydrogen sulphide concentrations near wastewater treatment plants. Sci Total Environ 2018; 610-611: 583-590.

Gulia S, Shrivastava A, Nema AK, Khare M. Assessment of Urban Air Quality around a Heritage Site Using AERMOD: A Case Study of Amritsar City, India. Environ. Model. Assess. 2017; 20: 599-608.

Kourtidis K, Kelesis A, Petrakakis M. Hydrogen sulfide (H_2S) in urban ambient air. Atmospheric Environment 2008; 42(32): 7476-7482. doi:10.1016/j.atmosenv.2008.05.066.

Latos M, Karageorgos P, Kalogerakis N, Lazaridis M. Dispersion of Odorous Gaseous Compounds Emitted from Wastewater Treatment Plants. Water Air Soil Pollut 2011; 215(1-4): 667-677.

Marine Department. Saen Saeb canal-boat passenger density survey report. https://www.md.go.th/stat/images/pdf_report_stat/ 2560/Saen_Saep_60.pdf, 2017.

Nguyen HH, Nguyen HX, Tran Y, Nguyen TN. METI-LIS model to estimate H2S emission rates from to Lich river, Vietnam. ARPN Journal of Engineering and Applied Sciences 2012; 7.

O'Shaughnessy PT, Altmaier R. Use of AERMOD to determine a hydrogen sulfide emission factor for swine operations by inverse modeling. Atmospheric Environment 2011; 45(27): 4617-4625.

Pollution Control Department. Water Quality Standard. 2005. http://www.pcd.go.th/info_serv/reg_std_water04.html.

Prasartkul P, Rittirong J, Kaikeaw S. Household projection of the Thai population during 2010-2020. Thai Population Journal 2016; 2: 45-60.

Somsook K. The Study of Khlong Saen Saep Water Quality and Improvement Guideline with Use of MIKE 11 Model. Kasetsart University. Department of Water Resources Engineering 2013.

Suwandee S, Anupunpisit V, Ratanamaneichat C, Sukcharoen N, Boonpen P. Quality of Life and Environment of Communities Along Saen Saeb Canal: A Survey Foundation of the Physical and the Current Situation (Phase I). Procedia - Social and Behavioral Sciences 2013; 88: 205-211. doi:10.1016/j.sbspro.2013.08.497.

The Ministry for the Environment. Ambient Air Quality Guidelines 2002 Update. Air Quality Report No 32.

U.S.EPA. Report to Congress on Hydrogen Sulfide Air Emissions Associated with the Extraction of Oil and Natural Gas

1993. https://nepis.epa.gov/Exe/ZyPDF.cgi/00002WG3.PDF?Dockey=00002WG3.PDF.

Wan Y, Ruan X, Wang X, Ma Q, Lu X. Odour emission characteristics of 22 recreational rivers in Nanjing. Environmental Monitoring and Assessment 2014; 186(10): 6061-6081.

WHO. Hydrogen sulfide. 2003. http://www.who.int/ipcs/publications/cicad/en/cicad53.pdf.

Yu Z, Guo H, Xing Y, Lague C. Setting acceptable odour criteria using steady-state and annual hourly weather data. Biosystems Engineering 2009; 103: 329-337.

Enhancing the predictive performance of colorimetric sensors using multivariate calibration models

Nutthatida Phuangsaijai[1], Jaroon jakmunee[1,2], Sila kittiwachana[1,3]*

[1] Department of Chemistry, Faculty of Science, Chiang Mai University, Chiang Mai, Thailand, 50200

[2] Center of Excellence for Innovation in Chemistry, Faculty of Science, Chiang Mai University, Chiang Mai, Thailand, 50200

[3] Environmental Science Research Center (ESRC), Faculty of Science, Chiang Mai University, Chiang Mai, Thailand, 50200

* Corresponding author e-mail: silacmu@gmail.com

ABSTRACT

This research investigated the predictive performance of various calibration models when applied to the digital coded color values obtained from colorimetric strip tests. Commercially available test strips (colorimetric sensors and sensor arrays) used for detection of some water quality parameters including nitrate (NO_3^-), phosphate (PO_4^{3-}), total hardness and pH, were used in the demonstration. After reacting with analyte, the sensor images were converted into the digital coded RGB (Red, Green, Blue) values by an office scanner and calibration models including univariate linear regression (ULR), multivariate linear regression (MLR) principal component regression (PCR) and partial least squares (PLS) were established. The comparison of the predictive performance was assessed in terms of root mean square error of calibration (RMSEC) and prediction (RMSEP), coefficients of determination for calibration (R^2) and prediction (Q^2). In most cases, PCR and PLS provided satisfactory predictive results especially when they were applied for the test strips having more than one sensing chemicals. ULR resulted in the minimum predictive error when it was used to capture the color change which was

directly related to the color of the chemical sensing. The developed models were also tested with the surface water samples collected in Chiang Mai areas.

Keywords: Colorimetric sensor, Chemometrics, Multivariate calibration, Water quality monitoring

INTRODUCTION

Colorimetric strip sensors have been becoming a more popular analytical technique because they enable chemical detection without or less complicated analytical instruments (Bordbar *et al*., 2018; Petruci *et al*., 2015). This analytical detection gadget is based on observation of changing color when a sensing chemical reacts with analyte. The colorimetric strip sensor can be operated using a single reagent which specifically responds to a sample compound. In addition, multiple reagents can be used to construct a sensor array. As a result, multiple analytes can be probed in a single test or the colorimetric pattern of the array color combination can be used to confirm the unique substance identification enhancing the prediction ability of the detection (Huo *et al.*, 2010).

In general, the color change could be observed using naked eye; however, the accuracy and precision of the measurement could be enhanced by converting the changing color into digital coded values using a digital camera or an ordinary scanner. After that, these digital coded values can be mathematically interpreted with an aid of various univariate and multivariate calibration methods (Choodum *et al*., 2015; Lin *et al*., 2017; Xiao-wei *et al.*, 2015). RGB is among the most common digital coded formats (Moonrungsee *et al.*, 2015; Tahir *et al*., 2016). It is an additive color model characterized by three primary colors of red (R), green (G) and blue (B). For example, white is a full combination between R G and B or [255 255 255]. Using the digital coded value format results in data structure with multivariate nature. For example, a pH test strip

composing four pH indicators generates in a total of 12 variables comprising of three digital coded RGB parameters from four different chemical sensing (3 [RGB values] x 4 sensing chemicals). In this circumstance, the analytical decision should be made based on the use of all available data in multivariate manner instead of the use only a single parameter (Theanjumpol *et al*., 2019).

Chemometrics is a set of multivariate data analysis that can be categorized into groups according to the purposes of the analyses such as data exploratory analysis, design of experiment, classification, and calibration (Brereton, 2003). Calibration is among the important applications of chemometrics which normally involves using some predictive measurements to predict the value of an underlying property or response. In general, calibration establishes the relationship between predictive (***X***) and response (***y***) parameters and this relationship information can be used for predicting the response of unknown or test sample. Univariate linear regression (ULR) could be the simplest calibration model where only one predictive parameter is used for the prediction of response assuming they have a linear association (Brereton, 2007). Multiple linear regression (MLR) is an extended version of ULR where more than one predictive parameters are employed for the estimation at the same time (Ghasemi *et al.*, 2007). Partial least square (PLS) regression could be regarded as the most widespread multivariate calibration technique (Wongsaipun *et al*., 2018). PLS captures and utilizes both variations from the predictive (***X***) and response (***y***) data for the modelling. In contrast to principal component regression (PCR), the multivariate calibration model correlates with the variation of the predictive data directly to the response (Brereton, 2009).

This research aimed to enhance the predictive performance of colorimetric sensors by adopting

some chemometric models. A set of commercially available colorimetric sensors and sensor arrays were used. The developed models were tested with synthetic solutions as well as some surface water samples collected in Chiang Mai areas. This research emphasized that the choice of calibration model was important to the quantitative analysis using colorimetric sensors as the selection could have much influence on the predictive performance of the colorimetric sensor test.

METHODLOGY

Colorimetric sensors and chemical standard solutions

A total of four commercially available chemical sensors and sensor arrays were used in this research. These chemical test strips were used for testing the concentrations of some ions relating to surface water quality including pH, nitrate (NO_3^-), phosphate (PO_4^{3-}) and total hardness ($CaCO_3$). The NO_3^- (REF 913 13), PO_4^{3-} (REF 913 20) and total hardness (REF 912 902) test strips were purchased from Macherey-Nagel (Germany). The pH test strip (REF 1.09535.0001) was from Merck (Germany). Chemicals, such as sodium nitrate ($NaNO_3$), sodium phosphate (Na_2HPO_4), calcium carbonate ($CaCO_3$), potassium dihydrogen phosphate (KH_2PO_4), disodium hydrogen phosphate (Na_2HPO_4) and potassium hydrogen phthalate (KHP) were prepared using analytical grade chemicals (Merck, Germany). A series of chemical solutions was prepared where the concentration range was varied from minimum to maximum values stated on the product manual of each chemical test strip. The samples were divided into two sets; training and test data, for establishing calibration models and evaluating the model performance, respectively. The detail of training and test samples for each of the colorimetric sensors was summarized in Table 1.

Real samples

Water samples collected in Chiang Mai, Thailand, representing three water types including sewage canal

(W1), water reservoirs (W2 and W3) and wastewater treatment pond (W4), were used in this research. The water samples were collected in December of 2018. The concentration of NO_3^- was determined following the Brucine colorimetric method (AOAC, 2012). The pH values were measured using a pH meter (SevenCompact pH/Ion meter S220, Mettler-Toledo, Switzerland) which was routinely

Table 1 Detail of colorimetric sensors used in the investigation

Analyte	No. of sensors	Manufacture	Concentration range	Concentrations of training samples	Concentrations of validation samples
Nitrate (NO_3^-)	1	MACHEREY-NAGEL, Germany	10-500 (ppm)	0.00, 10.00, 20.00, 30.00, 50.00, 100.00, 200.00, 350.00 and 500.00 (ppm)	5.00, 15.00, 25.00, 40.00, 75.00, 150.00, 250.00 and 450.00 (ppm)
Phosphate (PO_4^{3-})	1	MACHEREY-NAGEL, Germany	3-100 (ppm)	0.00, 2.00, 5.00, 10.00, 20.00, 30.00, 50.00, 70.00, 90.00 and 100.00 (ppm)	1.00, 3.00, 7.00, 15.00, 25.00, 40.00, 60.00 and 80.00 (ppm)
Total hardness ($CaCO_3$)	5	MACHEREY-NAGEL, Germany	<55, >90, >180, >270 >360, >450 (ppm)	0.00, 59.00, 75.00, 100.00, 137.00, 250.00 and 450.00 (ppm)	50.00, 62.00, 87.00, 106.00, 150.00, 200.00 and 375.00 (ppm)
pH	4	Merck, Germany	1-14	0.934, 2.855, 4.702, 6.656, 9.101, 10.973 and 12.656	1.831, 3.853, 5.831, 7.201, 9.639 and 11.760

calibrated. The total hardness was evaluated following the method (APHA, 2017). An ascorbic acid method was used to quantify the concentration of PO_4^{3-} (APHA, 2017).

Image processing

The images of the colorimetric sensors or sensor arrays after exposing to the sample solution were acquired using a flatbed scanner (L220, Epson, Philippines). They

were recorded in a TIFF format to avoid loss of information due to compression with a resolution of 300 dots per inch (dpi). The images were then decoded in the RGB values using a homemade Matlab script. With 8-bit color depth, each pixel was characterized by the digital values of RGB ranking from 0 to 255. For example, a completely red was represented by [255 0 0] of [R G B]. For each sensing chemical, all of the digital coded RGB values were averaged to provide a mean value. For instance, each of the total hardness strip resulted in 15 digital values comprising of three digitals coded RGB values from five different chemical sensing (3 [RGB values] x 5 sensing chemicals). The NO_3^- which was a representative of colorimetric strip sensor resulted in 3 RGB parameters from a single chemical sensing (3 [RGB values] x 1 sensing chemical).

Chemometric analysis

In this research, the color profiles (RGB intensities) of the test strips (defined as $\boldsymbol{X}$) were used as predictive parameters and the concentrations of analyte were use as predictor or response ($\boldsymbol{y}$). Linear calibration models including univariate calibration such as univariate linear regression (ULR); and multivariate calibrations such as multivariate linear regression (MLR), principal component regression (PCR) and partial least squares (PLS), were used to calibrate the prediction models of the colorimetric sensors.

ULR describes relationship between only one predictive (independent) and response (dependent) variables. The simplest linear function of ULR is:

$$y = ax + c$$

Where y is an estimation of the response variable or, in this research, a concentration of analyte. The a and c parameters are slope and intercept of the univariate linear regression line, respectively. MLR is similar to ULR in that the prediction of the response is based on the simple linear regression. But, the influence of more than one independent variable are

contributed into the estimation of the response with the use of a matrix operation:

$$y = X.b$$

Where $\boldsymbol{y}$ is a vector containing the response values estimated by the predictive data ($\boldsymbol{X}$). $\boldsymbol{b}$ is a vector containing coefficient of each predictive variable indicating the relationship between the predictive variables in estimation of the $\boldsymbol{y}$ response. PCR is an extension of MLR. Using PCR, principal component analysis (PCA) is used to capture the main variation in the predictive data matrix ($\boldsymbol{X}$). The prediction of PCR is then based on the relationship between the data scores ($\boldsymbol{T}$) and the response values ($\boldsymbol{y}$) using the same equation as used for MLR.

PLS is different from PCR in that the model captures variations from both the predictive ($\boldsymbol{X}$) and response ($\boldsymbol{y}$) parameters and simultaneously uses them for constructing the regression model. Using PLS, the covariance between the variation of $\boldsymbol{X}$ and $\boldsymbol{y}$ is maximized; therefore, in most case, PLS is a linear multivariate calibration method that offers satisfactory predictive results. In this research, the PLS1 algorithm reported in (Brereton, 2003). The PLS modelling can be represented using two equations:

$$\boldsymbol{X = T.P + E}$$

$$\boldsymbol{y = T.q + f}$$

Here, $\boldsymbol{X}$ is decomposed into $\boldsymbol{X}$-scores ($\boldsymbol{T}$) and $\boldsymbol{X}$-loadings ($\boldsymbol{P}$). As the same time, $\boldsymbol{y}$ is the product approximation of $\boldsymbol{T}$ and $\boldsymbol{y}$-loadings ($\boldsymbol{q}$) where the algorithm aims to minimize the norm of $\boldsymbol{f}$. To predict the response of unknown sample $\boldsymbol{X}_{test}$, the following equation is used:

$$\hat{\boldsymbol{y}} = \boldsymbol{X_{test} W q}$$

Where $\boldsymbol{W}$ refers to normalized PLS weights. In this research, the optimum number of PLS latent variable was identified using leave one out-cross validation (LOO-CV) method (Brereton, 2009).

Model statistics

In order to compare the accuracy and robustness of the developed models, root mean square error of calibration (RMSEC) and prediction (RMSEP), coefficients of determination for

calibration (R^2) and prediction (Q^2), and ratio between RMSEP and RMSEC (R_x) were calculated (Wongsaipun *et al.*, 2018). RMSEC is the average difference between predicted ($\hat{y}_i$) and expected (y_i) response values of training samples as:

$$\text{RMSEC}=\sqrt{\frac{\sum_{i=1}^{I}(y_{trian,i}-\hat{y}_i)^2}{I}}$$

Where I is the number of samples. The values of R^2 can be calculated by:

$$R^2=1-\frac{\sum_{i=1}^{I}(y_{\text{train},i}-\hat{y}_i)^2}{\sum_{i=1}^{I}(y_{\text{train},i}-\bar{y})^2}$$

The RMSEP and Q^2 can be calculated by the same equations as for RMSEC and R^2, respectively, but using the predictive results of test or validation samples. Ideally, it is expected an accurate model should have high R^2 and Q^2 and low RMSEC and RMSEP. However, a marginal difference between RMSEC and RMSEP indicates the stability of the model and this can be evaluated using the ratio of RMSEP and RMSEC (R_x). The value of R_x as close as possible to 1.00 implies the consistency of the model when it is used to predict new or unknown samples which are not included in the model training.

RESULTS AND DISCUSSION

Acquisition of the RGB color data

Figure 1(a) shows images of the colorimetric sensors and sensor arrays after reacted to the standard solutions with different concentrations. The detection of PO_4^{3-} ion resulted in the change of color from gray to blue-green. On the other hand, the NO_3^- strip test resulted in the change from background (gray) to a reddish-purple or magenta. For example, the higher concentration of NO_3^- in the solution resulted in the more intense color of magenta. It is noted here that magenta is a *secondary color* which is the mixture between two primary colors (red and blue). The detection of NO_3^- and PO_4^{3-} ions were based on the uses of colorimetric sensor having a single sensing chemical whereas the detection of pH and total hardness were based on colorimetric sensor array composing of several sensing chemicals which were

simultaneously used for the interpretation**.** Figure 1(b) visualizes the RGB coded values on the PCA score plots. The linearity trends can be observed in the data acquired from the detections of NO_3^-, PO_4^{3-} and pH implying the sensible utilization of the linear calibration methods. However, the scattering trend in the total hardness detection could be due to that the strip was originally created for scanning purpose. Since, each of the sensors was designed to specifically respond to the different concentration of analytes. The color intensity was not monotonically changed to increased concentration of the analyte.

Calibration models

Table 2 summarizes the predictive performance of the calibration models using ULR, MLR, PCR and PLS. The corresponding correlation graphs are presented in Figure 2. These results demonstrated that different calibration models possessed different predictive abilities.

Figure 1 (a) The colorimetric sensors and sensor arrays after immersed in the standard solutions and (b) PCA score plots of the RGB digital coded data

Table 2 Predictive results of the calibration models using ULR, MLR, PCR and PLS

Analyte	**Calibration models**	**Model statistics**					**$RMSEP_{eye}$**
		R^2	**Q^2**	**RMSEC**	**RMSEP**	**R_X**	
NO_3^-	ULR (R)	0.381	-0.709	131.15	189.48	1.44	33
	R (G)	0.960	0.916	33.56	42.10	1.25	
	(B)	0.940	0.862	40.89	53.82	1.32	
	MLR	0.960	0.927	33.43	39.26	1.17	
	PCR	0.956	0.940	35.00	35.52	1.01	

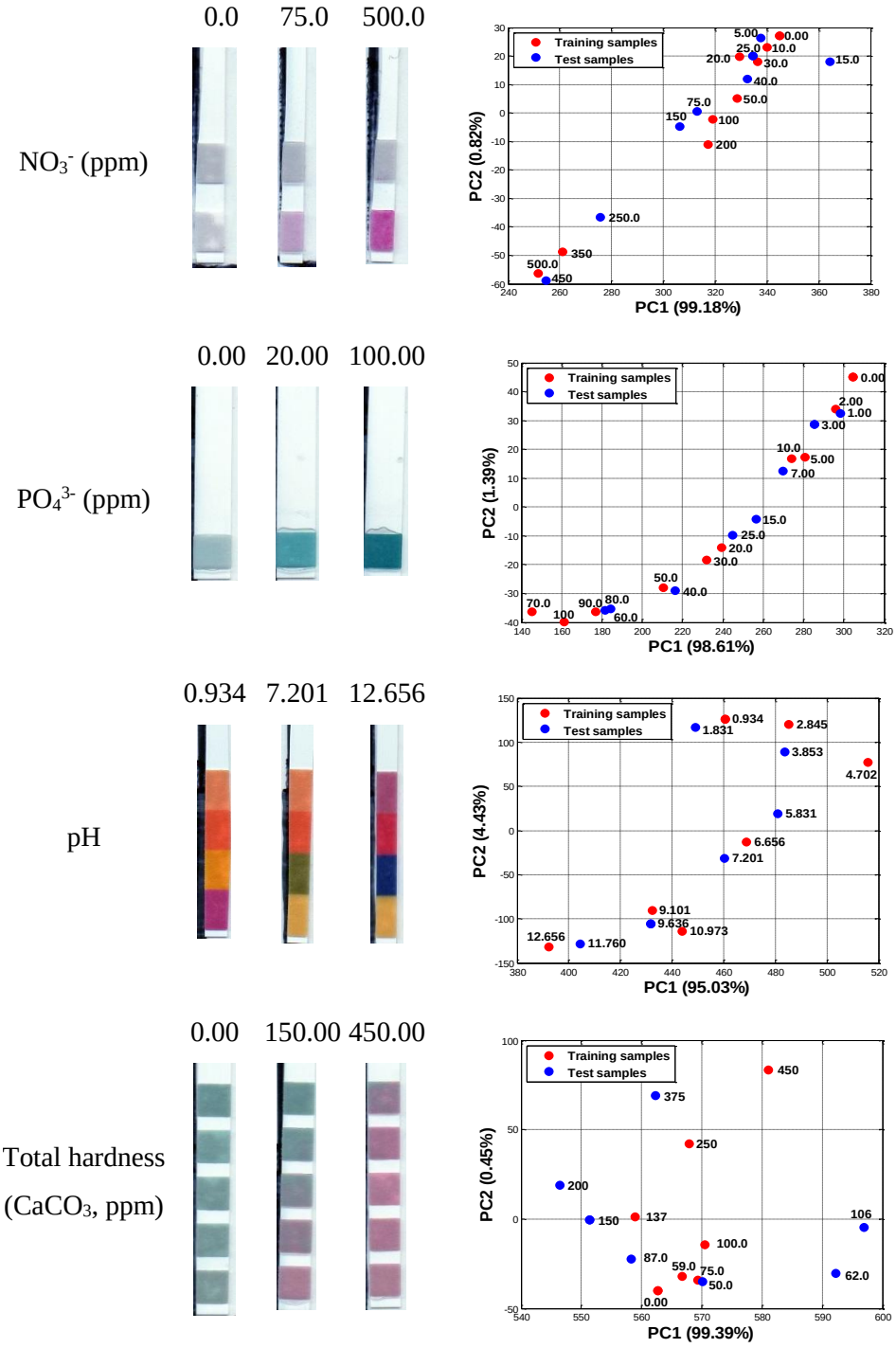

(a) (b)

	PLS		0.956	0.940	34.99	35.51	1.01	
PO_4^{3-}	UL	R	0.846	0.830	14.00	11.15	0.80	9.7
	R	G	0.890	0.942	11.83	6.50	0.55	

	B	0.881	0.932	12.32	7.05	0.57	
	MLR	0.892	0.900	11.73	8.56	0.73	
	PCR	0.892	0.900	11.73	8.56	0.73	
	PLS	0.892	0.900	11.73	8.56	0.73	
pH	MLR	-38.8	-69.7	25.18	28.10	1.12	0.7
	PCR	1.00	0.993	0.040	0.270	7.78	
	PLS	1.00	0.993	0.020	0.270	12.4	
Total hardness	MLR	-15.7	-24.6	575.59	529.92	0.921	49
	PCR	0.968	0.980	25.16	14.97	0.595	
	PLS	1.00	0.954	2.86	22.51	7.88	

Prediction of colorimetric sensors

For the detection of NO_3^-, PCR and PLS provided the comparable predictive results. Both of the models gave the comparatively the best predictive result having high R^2 and Q^2 with low RMSEC and RMSEP. The worst prediction was obtained from the ULR model using the R component. Although magenta is the combination of red and blue, in this case, the change in the red intensity was not much related to the concentration of the NO_3^- as revealed in Figure 3(a). In contrast, PO_4^{3-} colorimetric strip sensor, the best prediction was obtained from the ULR model using the G component. In fact, relatively good predictive results also obtained from the prediction of PO_4^{3-} using both univariate and multivariate models. In Figure 3(b), all RGB values could be used for the prediction having R^2 close to 1. The green color resulted in the minimum error could be due to that it represented closely to the change in the chemical sensing.

Prediction of colorimetric sensor arrays

In order to utilize all of the sensing chemicals, ULR could not be

practical since it can only model one independent variable each time for the prediction of response. In all cases, MLR resulted in high predictive errors. This was due to the number of modeling samples was lower than the number of predictive variables, therefore, the pseudo-inverse was mathematically inappropriate (Saxena and Prathipati, 2003). For the pH modeling, PCR and PLS showed

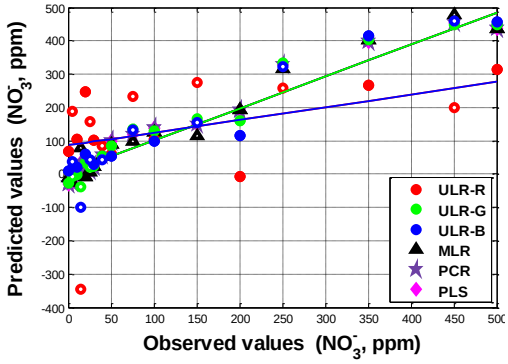

(a)

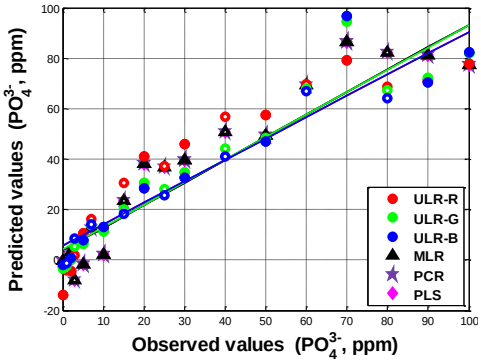

(b)

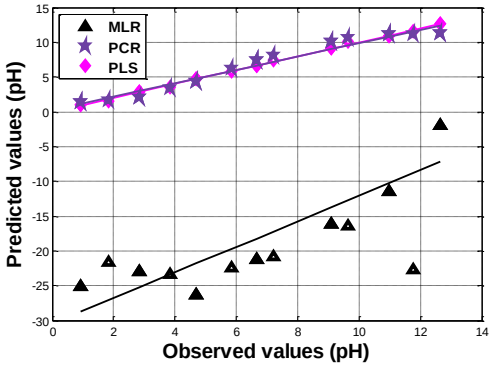

(c)

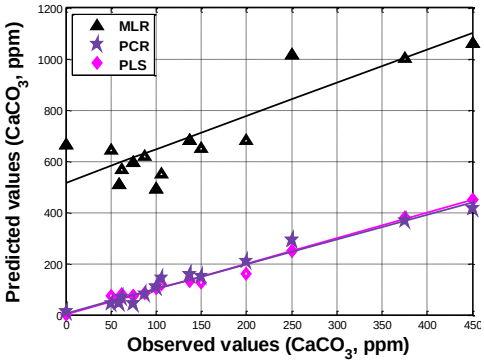

(d)

Figure 2 Correlation graphs between expected and predicted of (a) NO_3^-, (b) PO_4^{3-}, (c) pH and (d) total hardness. Training and test samples were labeled using opened and closed face symbols, respectively.

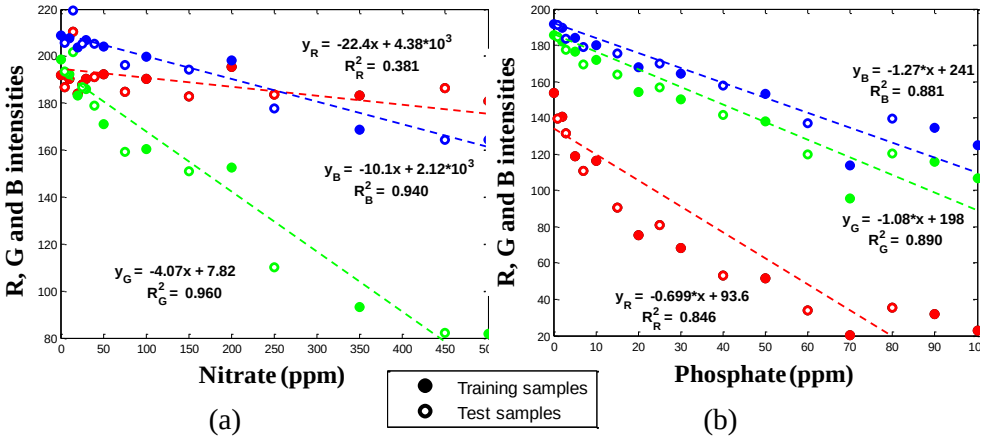

Figure 3 Relationship between the concentrations of (a) NO_3^- and (b) PO_4^{3-} and the RGB intensities where the red, green and blue circle symbols represent each of the corresponding color intensities.

promising results with low predictive errors. Both of the models have nearly identical regression lines in the correlation graph in Figure 2(c). The high value of Q^2 with low R_x (Table 2) implied that the developed model could be practically used for the prediction of unknown or test samples.

For the prediction of total hardness, although PLS provided very low RMSEC, it felt to minimize the RMSEP. In this case, the model was prone to have an overfitting problem **since it resembled the variation of training very well. However, the** variation of unknown samples could not be fit in the prediction space. PCR, on the other hand, results in lower RMSEP. In Figure 2(d), the test samples were not much deviated from the regression for both PCR and PLS confirming the practical use of the developed models for quantitative analysis purpose.

In this research, only the NO_3^- strip offered slightly lower RMSEP with an aided eye than those from the chemometric-calibration models. However, it should be noted that not

any data-preprocessing was applied to the digital RGB coded data prior to the prediction of the calibration models. The data-preprocessing can certainly affect to the predictive characteristics of the calibration models which will be investigated in the further study.

Table 3 Comparison between the predictive values from the standard methods and those from the colorimetric sensors and sensor arrays

Sample No.	NO_3^- (ppm)		Naked eye*	PO_4^{3-} (ppm)		Naked eye
	Standard method	Test strip*		Standard method	Test strip	
W1	<1.77	67.15±8.05	50	0.00	10.53±3.28	7
W2	ND	30.28±10.29	25	0.00	0.86±1.84	3
W3	ND	19.15±10.25	25	11.34	40.40±7.61	50
W4	<1.77	241.64±14.55	250	ND	3.65±2.13	3
Sample No.	**pH**		**Naked eye**	**Total hardness**		**Naked eye**
	Standard method	**Test strip**		**Standard method**	**Test strip**	
W1	7.43	7.14±0.11	6	93.3	67.41±6.89	110
W2	7.32	6.15±0.14	5	24.0	76.94±15.17	54
W3	7.96	7.90±0.80	8	189	226.50±22.71	280
W4	7.32	6.76±0.32	6	85.3	125.49±5.50	130

ND = Not detect, * = the samples were spiked with 22.13 ppm of standard NO_3^-.

Monitoring of real water samples

The four sensor strips were tested with the four surface water samples using the developed calibration models. The results were compared with those obtaining from the standard methods and summarized in Table 3. The comparable results could be seen in the measurements of the pH and total hardness values. Variation of errors can be observed, and this could be due to the complex matrices in the water samples.

CONCLUSION

Multivariate analysis can be a useful tool for analyzing the digital color-coded data. In this research, ULR could result in the best predictive results in the case that the color changing was characterized by the primary color such as green color. Both PCR and PLS successfully provided good predictive performance especially for the test strips based on the use of several sensing chemicals . The meaningfu interpretation to which variables could be important can be revealed using PLS coefficients, in contrast, PCR coefficients could be only related to the sizes of the variation in the principal components used for the prediction model.

ACKNOWLEDGEMENTS

S. Kittiwachana would like to acknowledge the Chiang Mai University (CMU) Junior Research Fellowship Program. N. Phuangsaijai would like to thank the Science Achievement Scholarship of Thailand (SAST).

REFERENCES

AOAC. Official methods of analysis of AOAC. AOAC international. 2012.

APHA. Standard methods for examination of water and wastewater. American Public Health Association. 2017.

Bordbar MM, Tashkhourian J, Hemmateenejad B. Qualitative and quantitative analysis of toxic materials in adulterated fruit pickle samples by a colorimetric sensor array. Sensors and Actuators B: Chemical 2018; 257: 783-791.

Brereton RG. Chemometrics: data analysis for the laboratory and chemical plant. John Wiley & Sons. 2003.

Brereton RG. Applied chemometrics for scientists. John Wiley & Sons. 2007.

Brereton RG. Chemometrics for pattern recognition. John Wiley & Sons. 2009.

Choodum A, Kanatharana P, Wongniramaikul W, NicDaeid N. A sol–gel colorimetric sensor for methamphetamine detection. Sensors and Actuators B: Chemical 2015; 21: 553-560.

Ghasemi J, Saaidpour S, Brown SD. QSPR study for estimation of acidity constants of some aromatic acids derivatives using multiple linear regression (MLR) analysis. Journal of Molecular Structure: THEOCHEM 2007; 805(1): 27-32.

Huang X-w, Zou X-b, Shi J-y, Guo Y, Zhao J-w, Zhang J, Hao-L. Determination of pork spoilage by colorimetric gas sensor array based on natural pigments. Food Chemistry 2014; 145: 549-554.

Huo D-Q, Zhang G-P, Hou C-J, Dong J-L, Zhang Y-C, Liu Z, Luo X-G, Fa H-B, Zhang S-Y. A colorimetric sensor array for identification of natural amino acids. Chinese Journal of Analytical Chemistry 2010; 38(8): 1115-1120.

Lin H, Man Z-x, Guan B-b, Chen Q-s, Jin H-j, Xue Z-l. In situ quantification of volatile ethanol in complex components based on colorimetric sensor array. Analytical Methods 2017; 9(40): 5873-5879.

Moonrungsee N, Pencharee S, Jakmunee J. Colorimetric analyzer based on mobile phone camera for determination of available phosphorus in soil. Talanta 2015; 136: 204-209.

Musto CJ, Lim SH, Suslick KS. Colorimetric detection and identification of natural and artificial sweeteners. Analytical Chemistry 2009; 81: 6526-6533.

Petruci JFdS, Cardoso AA. Sensitive luminescent paper-based sensor for the determination of gaseous hydrogen sulfide. Analytical Methods 2015; 7(6): 2687-2692.

Salinas Y, Ros-Lis JV, Vivancos J-L, Martínez-Máñez R, Marcos M D, Aucejo S, Herranz N, Lorente I. A novel colorimetric sensor array for monitoring fresh pork sausages spoilage. Food Control 2014; 35(1): 166-176.

Saxena AK, Prathipati P. Comparison of MLR, PLS and GA-MLR in QSAR analysis. SAR and QSAR in Environmental Research 2003; 14(5-6): 433-445.

Tahir HE, Xiaobo Z, Xiao-wei H, Jiyong S, Mariod AA. (2016). Discrimination of honeys using colorimetric sensor arrays, sensory analysis and gas chromatography

techniques. Food Chemistry 2016; 206: 37-43.

Theanjumpol P, Wongzeewasakun K, Muenmanee N, Wongsaipun S, Krongchai C, Changrue V, Boonyakiat D, Kitiwachana S. Non-destructive identification and estimation of granulation in 'Sai Num Pung'tangerine fruit using near infrared spectroscopy and chemometrics. Postharvest Biology and Technology 2019; 153: 13-

Prediction of MP10 Concentrations over Upper Northern Thailand using Statistical Approach

Ammar Gaber[1*], Somporn Chantara[12]

[1]* Master Degree Program in Environmental Science, Environmental Science Research Center, Faculty of Science, Chiang Mai University, Chiang Mai, 50200, Thailand

[2] Environmental Chemistry Research Laboratory, Chemistry Department, Faculty of Science, Chiang Mai University, Chiang Mai 50200, Thailand

Corresponding author: e-mail: ammar_gaber@cmu.ac.th

ABSTRACT

This study aims to predict daily PM10 concentration and to investigate the effects of extreme meteorological variables and air pollutants over six provinces in Upper Northern Thailand (UNT) region. To this end, two models; Multiple Linear Regression (MLR) and Quantile Regression (QR) models with ten predictors each have been developed. Five meteorological variables (maximum temperature, rainfall, relative humidity, air pressure, and wind speed) and five air pollutants (CO, PM10, O3, NOx and SO2) observations from 2003 to 2015 were used to construct and verify the MLR model. The coefficient of determination and adjusted R^2 ($p < 0.01$) were 0.71 and 0.70, respectively. The model performance has been assessed over the period from 2012 to 2015 over UNT using three statistical performance indicators including Root Mean Square Error (RMSE), Mean Absolute Error (MAE), and Index of Agreement (IOA). Their value ranges were 20.35-40.00, 12.00-30.00, and 0.65-0.93, respectively. QR model reflected the sensitivity of predicted PM_{10} concentrations to the extreme covariate values (5 % and 95 % quantiles) over this region. The effects of extreme meteorological variables are found to be mixed. CO is found to be the most significant contributor to

PM_{10} concentrations compared with the other air pollutants. In terms of air quality management in UNT, these models can be used effectively to aid air quality regulations and policies formulation to improve the air quality during the dry seasons, as they showed high performance in predicting PM_{10} concentrations and investigating the effect of extreme values on its concentrations.

Keywords: Air quality, Monitoring, Aerosol formation, Transport, Climate

INTRODUCTION

Prediction of air pollutants concentrations provides invaluable information for air quality management purposes. Environmental impact studies, source emission regulation policies and human health problems, such as airborne diseases due to air pollution, are heavily depending on accurate and timely air pollution prediction models' outputs. Statistical models have been developed and employed intensively to predict air pollutants concentrations to provide accurate estimations to decision support processes and air pollution management. Multiple Liner Regression (MLR) model is one of the predictive models that used to predict air pollutants concentrations levels worldwide. In a recent study, MLR model exhibited optimal performance in term of Normalized Absolute Error (NAE= 0.2762), Index of Agreement (IOA=0.9211) and coefficient of determination (R^2 =0.7354), when it applied by Awang et al. (2015) to predict the ground ozone level during daytime in urban areas. Azid et al. (2015) obtained high values of coefficient of determination (R^2 >0.85) for low, moderate and slightly high pollution sources, when they applied MLR to identify the source variation on regional impact of air quality patterns in Peninsular Malaysia.

PM_{10} that originated from dust storm also modeled by Munir et al. (2013) over Makkah, Saudi Arabia. The model found to be able to explain about 50% of the variations in PM_{10}

concentrations during the dust storm episodes. MLR can be coupled by meteorology to assess the temporal and spatial variations of air pollutants. Liu et al. (2015) used this approach to evaluate NO_2 and PM_{10} temporal and spatial variations over Changsha, China. Their results showed that the model explained 51% and 62% of the variation in NO_2 and PM_{10}, respectively. Considerable efforts have been exerted to predict and characterized PM_{10} concentrations seasonal variations over Upper Northern Thailand (UNT) region. Pengchai et al. (2009) applied Principle Component Analysis (PCA), Absolute Principle Component Analysis (APCA) and Multiple Linear Regression Model (MLR) to characterize the seasonal variations of PM_{10} and its constituents in Chiang Mai and Lamphun provinces. Kim Oanh and Leelasakultum (2011) developed a lag regression model to predict PM10 concentration over Chiang Mai, Thailand, using the previous day PM_{10} concentration, horizontal visibility and Sea Level Pressure observations. PM_{10} emissions are originally generated from the open biomass burning in UNT and neighboring countries as showed by backtrack trajectories studies that aimed to identify the emission sources over this region, e.g., (Wiriya et al., 2013).

Since the weather conditions have strong influence on air pollutants transport and dispersion, their presence in air quality models play a vital role in forecasting pollutants fate and transport. Low pressure conditions associated with high temperature and low wind speed are favorable for air pollutants dispersion. On the contrary, high-pressure systems are likely to prevent pollutants dispersion and transport. Relative humidity is the most important meteorological variables for PM_{10} concentrations prediction, as it affects the presence of PM_{10} constituents in the atmosphere, while they mixed with water vapor, grown and decent (Munir et al., 2013).

In addition to meteorology effects, the topography plays an important

role in air pollutants dispersion and deposition. The rough terrain is likely to influence pollutants presence for long time. Upper Northern Thailand has mountain topography with highest peaks in the country, which likely to enhance the air pollutants presence over the valleys for long periods. During the dry season, from February through April, the effect of the meteorological variables (i.e. temperature, wind speed, relative humidity, rainfall and surface pressure) combined with the topography effect, are likely to capitalize the level of pollutants' concentrations during the biomass burning episodes. Low wind speeds and high temperature are prevailing during the dry season over this region, which enhance the pollution concentration levels. So, the aim of this work is to construct a multiple linear regression (MLR) and quantile regression (QR) models to predict PM10 concentrations and to investigate the effects of the extreme meteorological variables and air pollutants on its concentrations over Upper Northern Thailand, respectively.

The combined results from the two models will support the decision-making process by providing a good picture about the influences of extreme meteorological variables and air pollutants on PM_{10} concentrations over UNT. This will help to understand the effects of meteorological variables and the air pollutants concentrations on the average and extreme values (lowest and highest) of predicted PM_{10} concentrations in the region.

This work organized as follows: Section 2 describes the models' construction approach, verification methods and the data set used to construct and to verify the multiple linear regression model. Section 3 presents the results of the two models over the six provinces in UNT and discusses the models' performance and the effects of extreme values on PM_{10} concentrations. Section 4 concludes the study findings and shows the potential applications of the two models.

Study Area

Upper Northern Thailand (UNT) is located in the most northern side of Thailand, it borders Myanmar and Laos from west, north and northeast sides, respectively. UNT contains eight provinces; Mae Hong Son, Chiang Mai, Lamphun, Lampang, Chiang Rai, Nan, Phrae and Phayao. It extends from latitude 17°N to 20.5°N and from longitude 97°E to 101°E. The topography of this rejoin is featured by the high mountains and the major cities are in the valleys. The weather conditions are influence by onset and locations of Indian Monsson and Inter-Tropical Conversion Zone (ITCZ) over Thailand. Fig. 1 shows the location of the study area, administrative, elevation and hills maps and the distribution of the meteorological and air quality monitoring stations in UNT.

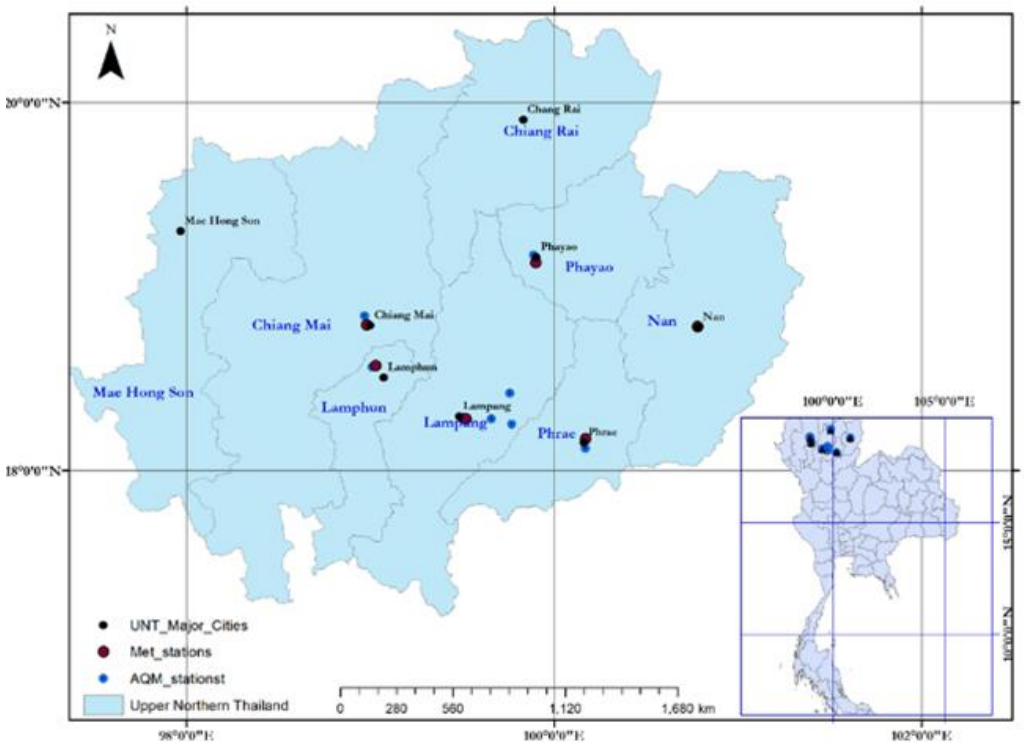

Figure 1 Title of the figure should be capitalized only the first word.

Table 1: Locations, altitudes, station type, and station name of meteorological stations (6) and air quality monitoring stations (6), and the names of the provinces that they represent in UNT.

Province	Station Name	Station type	Latitude (°N)	Longitude (°E)	Altitude (m)
Phayao	Phayao	Meteorology	19.13	99.90	396.89
	Phayao	Air Quality	19.17	99.89	494.52
Chiang Mai	Chiang Mai	Meteorology	18.07	98.98	313.20
	City Hall	Air Quality	18.84	98.97	318.43
	Yupparaj Wittayalai School		18.79	98.99	313.81
Lamphun	Lamphun	Meteorology	18.02	99.52	242.00
	Lamphun	Air Quality	18.56	99.01	292.32
Lampang	Lampang	Meteorology	18.05	99.03	296.42
	Lampang	Air Quality	18.29	99.51	241.59
Phrae	Phrae	Meteorology	18.02	100.17	161.79
	Phrae	Air Quality	18.12	100.17	164.81
Nan	Nan	Meteorology	18.08	100.78	200.00
	Nan	Air Quality	18.79	100.77	205.81

MODELS AND DATA

Multiple Linear Regression and Quantile Regression Models

Multiple liner regression (MLR) and quantile regressions (QR) models are used to investigate the variations in the explanatory variables. The main differences between these models are the way that they are handling the explanatory variables and prediction methods. MLR model predicts the average values of the dependent variable given the independent variables values, while QR predicts the level of change in the dependent variable given extreme values of the

independent variables, usually quantiles. The equation of MLR model is as follows:

$$\hat{Y} = \hat{\beta}_0 + \sum_{i=1}^{N} \hat{\beta}_i V_i + \varepsilon_i \quad (1)$$

Where:

$\hat{Y}$: Predicted value

$\hat{\beta}_0$: Estimated coefficient.

$\hat{\beta}_i$: Coefficients of the covariates from1 to *i*.

V_i : Model covariates.

ϵ_i: Error term.

The main advantage of quantile regression method is that it allows understanding the relationships between variables outside of the mean range of the data, making it useful in understanding outcomes that are non-normal distributed and that have nonlinear relationships with predictor variables (Cook and Manning, 2013). The general form of the quantile regression function is specified as:

$$y_i = x_i'\beta_\tau + \varepsilon_\tau \ ,$$
$$Quant_\tau(y_i|x_i) = x_i'\beta_\tau \quad (2)$$

Where:

$Quant_\tau(y_i|x_i) = x_i'\beta_\tau$ represents the τ^{th} conditional quantile (for this study it is: 0.05 and 0.95) of PM10 concentrations and x_i' is the independents variables (meteorological variables and air pollutants).

Model Selection and Verification

Model Selection

The coefficient of determination (R^2) and Adjusted-R^2 are used as model selection metrics. R^2 is the quotient of the variance of the fitted values and observed values of the dependent variable; it describes the proportion of the total variance in the observed data that can be explained by the model. It ranges from 0.0 to 1.0 with higher values indicating better agreement (Legates and McCabe Jr., 1999). R^2 is calculated using the following equation:

$$R^2 = \frac{\sum(\hat{y}_i - \bar{y})^2}{\sum(y_i - \bar{y})^2} \quad (3)$$

Adjusted-R^2 is spatial form of R^2 and it describes the explanatory power of the model. The following equations shows calculation of Adjusted-R^2:

$$R_{adj}{}^2 = 1 - (1 - R^2)\frac{n-1}{n-p-1} \quad (4)$$

Where; n is the number of observations in the data set, and p is the number of independent variables. Adding a variable to a model can only decrease the Residual Sum of Squares (RSS). Therefore, R^2 by itself is not a good criterion because it would always choose the largest possible model. Both R^2 and Adjusted-R^2 will be used to select the variable with significant contribution to the model.

Model Verification

The model performance is assessed using the following three statistical performance indicators:

Root Mean Square Error (RMSE), it makes an excellent general-purpose error metric for numerical predictions as recommended by (Chai and Draxler, 2014):

$$RMSE = \sqrt{\frac{1}{n}\sum_{i=1}^{n}(y_i - \hat{y}_i)^2} \qquad (5)$$

Mean Absolute Error (MAE), describes how close model simulations are to the observations, it given by:

$$MAE = \frac{1}{n}\sum_{i=1}^{N}|(y_i - \hat{y}_i)| \qquad (6)$$

Index of Agreement (IOA) or (d) is first introduced by Willmott (1981) in order to overcome the insensitivity of coefficient of determination R^2 to differences in the observed and model simulated means and variances. IOA is given by the following formula:

$$d = 1.0 - \frac{\sum_{i=1}^{N}(O_i+P_i)^2}{\sum_{i=1}^{N}(|P_i+\bar{O}|+|O_i+\bar{O}|)^2} \qquad (7)$$

Where; O_i and P_i are, the observed and predicted values, respectively. $\bar{O}$ and $\bar{P}$ the averages of observed and predicted values, respectively. N is the total number of observations.

Model Construction

Two statistical models, (MLR) and Quantile Regression (QR), were developed to predict PM_{10} concentrations and to investigate the effect of extreme covariates on its concentration levels over UNT using meteorological and air quality data, respectively. The models have the same number of independent variables (10 variables) including five air pollutants (i.e., NO_x, CO, PM_{10}, O_3, and SO_2) and five meteorological variables, i.e., Maximum Temperature (T_{max}),

Rainfall (Rain), Relative Humidity (RH), Wind Speed (WS), and Air Pressure (Press).

24-hr average air pollution data from City Hall air quality monitoring station (18.84°N, 98.97°E) spans from 2003 to 2014 and daily meteorological data from Chiang Mai Meteorological station (18.07°N, 98.97°E) spans over the same period, are used to develop and to verify the models. The data is divided into two sets randomly, i.e., training dataset (75% of the data) and verification dataset (25% of the data) including the dependent and independent variables.

MLR Model

Eq. (8) shows the constructed MLR model for PM_{10} concentrations prediction:

$$PM_{10} = \beta_0 + \beta_1 T_{max} + \beta_2 Rain - \beta_3 RH - \beta_4 Pressure - \beta_5 WS + \beta_6 CO + \beta_7 O_3 + \beta_8 NO_x + \beta_9 SO_2 \quad (8)$$

Where: β_i (i=0,1, ... ,10) are the model estimated coefficients presented in Table 2., as well as, standard errors and p-values.

Concerning multicollinearity problems, Variance Inflation Factors (VIFs) are calculated for each predictor in the regression model using car package (Fox and Weisberg, 2011), as well as Tolerance value (TOL) and covariance matrix. Moreover, Bridge Regression in MASS package (Venables and Ripley, 2002) is used to test the model coefficients stability.

QR Model

Investigation the effects of extreme independent variables values on the PM_{10} concentration is performed by utilizing QR model. The mode is built with the same structure of MLR model. Two quartiles (τ=0.05 and 0.95) that represent the lowest and highest extreme limits were used. Eq. (9) shows the mathematical formula of the model.

$$PM_{10} = \beta_{0\tau} T_{max} + \beta_{1\tau} Rain + \beta_{2\tau} RH + \beta_{3\tau} Pressure + \beta_{4\tau} WS + \beta_{5\tau} CO + \beta_{6\tau} O_3 + \beta_{7\tau} NO_x + \beta_{8\tau} SO_2 \quad (9)$$

Where: τ = 0.05, 0.10, 0.50, 0.75, and 0.95 presented in Table 5., along with

the estimated model coefficients (β_i) correspondent to each quantile (τ) value.

R software environment for statistical computing and graphics (https://cran.**r**-project.org) is used to construct and test the models. Metrics (Hamner, 2012), quantreg (Roger, 2015) and ggplot2 (H. Wickham, 2009) packages are used to assess MLR model performance, construct QR model and to produce the plots.

Data

Air pollutants

Air Quality Monitoring (AQM) data obtained from Pollution Control Department (PCD), Thailand. It consists of five pollutants that collected from ten AQM stations in the UNT. These pollutants are: Particulate Matter less than 10 µm in diameter (PM_{10}, µg/m^3), Ozone (O_3, ppb), Nitrogen Oxides (NO_x, ppb), Carbon Monoxide (CO, ppm), and Sulfur dioxide (SO_2, ppb). The air quality data covered the period from 1st January 2012 through 30th April 2015. For Quality Control (QC) purposes, this study excluded each station that has number of missing values that exceeded 25% of its total data available since 1st January 2012. Three stations violated this condition and have been excluded from this study as they lack O_3 and SO_2 observations for the entire analysis period. These stations are, two stations in Chiang Rai province, Mae Sai (19.90°N, 99.82°E) and Natural Resources and Environment Office (19.90°N, 99.82°E), and one station in Mae Hong Son province, Mae Hong Son (19.30°N, 97.97°E). The other seven stations are satisfied the missing values condition and are used in the study, i.e., City Hall, Yupparaj Wittayalai School, Lamphun, Lampang, Phayao, Phrae and Nan. Table 1 shows the locations, elevation, station type, station name and the provinces that the air quality stations (AQ) represent.

Meteorological Variables

Thailand Meteorological Department (TMD) is the competent entity that collecting and managing the metrological data through its synoptic network that spread all over

the country. Daily data from six meteorological stations (represents six provinces) were used in this study, i.e., Chiang Mai, Lamphun, Lampang, Phrae, Phayao and Nan. The data spans over the period from 1st January 2012 through 30th April 2015. The data comprised of five meteorological variables (i.e., Maximum Temperature (T_{max}), Relative Humidity (RH), Wind Speed (WS), Rainfall (Rain), Air Pressure (Press)). Table 1. shows the locations, elevation, station type, station name and the provinces that the meteorological stations (Met.) represent.

According to the current TMD's climatological normal (1981-2010) of the Upper Northern Thailand region, the dry season (February-April) is characterized by maximum temperature ranges from 32°C to 38°C, wind directions are from south and southwest with average speed ranges from 0.4 to 3.5 knots, average rainfall is about 100 mm, relative humidity varies from 70 to 58% and the air pressure is the lowest during this period, it is well known as pre-monsoon season.

Table 2: Descriptive statistics of Meteorological variables and air pollutants from 2003 to 2014. Meteorological variables and air pollutants are from Chiang Mai meteorological station and City Hall air quality monitoring station in Chiang Mai province, Thailand. Number of missing values represented by number (dashes show data is complete)

	Meteorological Variables					Air Pollutants				
	Pressure	Tmax	RH	Rainfall	WS	PM_{10}	O_3	NO_x	CO	SO_2
Min	999.20	19.00	38.13	0.00	0.00	3.80	1.52	0.20	0.00	0.00
Max	1023.70	42.40	99.00	144.40	27.78	317.00	59.74	43.04	3.00	11.91
Median	1008.90	32.40	73.88	0.00	5.28	33.75	20.04	10.57	0.46	0.65
Mean	1009.20	32.46	72.52	3.26	5.74	44.60	21.93	12.07	0.51	0.82
1st Qu	1006.10	30.60	66.13	0.00	4.17	22.09	14.04	7.52	0.29	0.13
3rd Qu	1012.20	34.40	80.63	1.20	7.22	55.39	27.95	15.35	0.66	1.17
Missing Values	-	-		7	-	116	117	165	137	154

Min	999.20	19.00	38.13	0.00	0.00	3.80	1.52	0.20	0.00	0.00

- Units of meteorological variables are as followed; T_{max} (°C), RH (%), Rain (mm), Press (hPa), and WS (ms^{-1}).
- Units of air pollutants are as followed; PM_{10} ($\mu g/m^3$), O_3 (°C), NO_x (%), CO (mm), SO_2 (hPa).

Results and Discussion

MLR Model

MLR model was built using daily data from Chiang Mai meteorological station and City Hall air quality monitoring station in Chiang Mai province, UNT. Descriptive statistics of meteorological variables and air pollutants from both stations for the period from 2003 to 2014 are presented in Table 2. MLR model estimated coefficients and coefficient of determination (R^2) and Adjusted-R^2 are presented in Table 3. These results show that the model succeeded to explain 71% of the variations in PM_{10} concentrations with the power of explanation about 70% as reflected by Adjusted-R^2 value and the significant p-value of covariates coefficients ($p < 0.01$). The model is found to be more explanatory compared with that obtained by Munir et al. (2013) where $R^2 = 0.52$ and (Liu, et al. 2015) where $R^2 = 0.62$, but less than that values obtained by Awang et al. (2015) and Azid et al. (2015) which are $R^2 = 0.735$ and $R^2 > 0.85$, respectively.

Table 3: Estimated coefficients, Standard Errors (SE) and p-values of the multiple linear regression model (Eq. 5). The P-values are for two-sided t-test against the hypothesis that the coefficient is zero (df=3047), data from City Hall AQM station, Chiang Mai province.

	Estimated Parameters	Standard Error	Pr(>|t|)
Intercept	355.51254	123.0504	0.00389**
Maximum Temperature	0.50477	0.18616	0.00674**
Relative Humidity	- 0.6644	0.05523	< 2.00E-16***
Rainfall	0.04429	0.03797	0.24346
Wind Speed	- 0.78395	0.14132	3.15E-8***
Air Pressure	- 0.32435	0.11734	0.00574**

Ozone	0.67687	0.04722	< 2.00E-16***
Carbon Monoxide	39.40836	1.36542	< 2.00E-16***
Nitrogen Oxides	1.28383	0.074	< 2.00E-16***
Sulfur Dioxides	4.64896	0.42188	< 2.00E-16***

- Significance code: '***' 0.001 '**' 0.01 '*' 0.05 '.' 0.1
- Residual standard error: 18.28 on 3047 degrees of freedom
- Multiple R-squared: 0.7052, Adjusted R-squared: 0.7043
- F-statistic: 809.8 on 9 and 3047 DF, p-value: < 2.2e-16

Eq. (8) shows PM_{10} concentration increases as T_{max}, rain, O_3, NO_x, CO, and SO_2 increase. While it decreases with the increase in RH, Press and WS. The air quality data shows a pronounced decrease in PM_{10} concentrations during the rainy season as the emissions from the open biomass burning decreased and also due to the increase in WS and RH. Therefore, the increase in the number of rainy days has a direct effect on PM_{10} concentrations reduction. Rainfall occasions during the dry period (January-April), have no much effect on PM_{10} concentration levels, as they are rare, few and short duration. During the dry season, PM_{10} showed its highest concentration levels throughout the analysis period that exceeded Thai 24-hr PM_{10} standard (120 $\mu g/m^3$). While it showed a considerable decrease towards the rainy and winter seasons. The increased open biomass burning practices that toke place during the dry season, caused CO emissions, which contributed to the increased levels of PM_{10} concentration in this region. In the other hand, the complex topography of this region also contributed to the air pollutants presence over the cities for long duration especially during the dry season.

The model is checked for multicollinearity problems using VIF, TOL, and covariance matrix. The diagnostic tests revealed that there is no parameter with VIF or TOL greater than 10 and 2.05, respectively. Although, the covariance matrix showed strong correlations among some covariates

(i.e., RH and T_{max} (r= -0.59), RH and O_3 (r= -0.68), and between NO_x and CO(r=0.55)).

Further multicollinearity diagnostics that performed using ridge regression showed that the model's estimated coefficients are robust and they did not undergo any changes in their magnitudes or signs. Therefore, no need to eliminate any of these variables from the model or use the central procedure technique to reduce the autocorrelation effects.

Figs. 2-3 show MLR model daily PM_{10} concentration predictions over six provinces, the observed values and Thai 24-hr PM_{10} standard from 2012 to 2015.

The model performance was assessed by three statistical performance indicators (i.e., RMSE, MAE and IOA). MLR model performance results are presented in Table 4. The values of these indicators are varied from province to another during the analysis period, according to their differences in air pollutants and meteorological data quality and completeness. RMSE evaluates the model prediction effectiveness, small values indicate high effectiveness. Over these provinces, RMSE values ranged from 14.14 to 40.00 during the analysis period. The highest RMSE value registered at Phayao in 2015. This indicates that the model performance was poor over this province as shown in Table 4 and Fig. 2(c), where the model underestimated PM_{10} concentrations in many occasions.

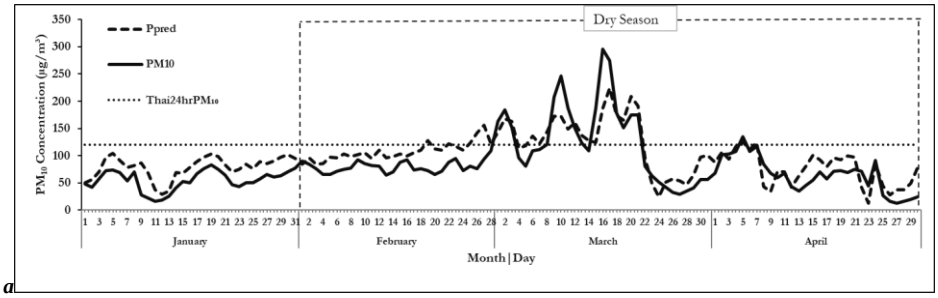

a

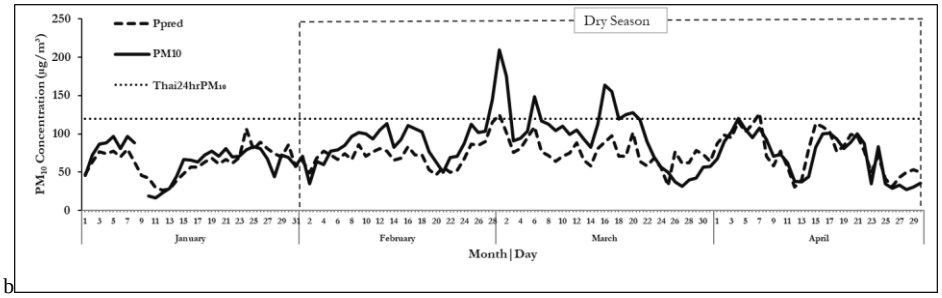

b

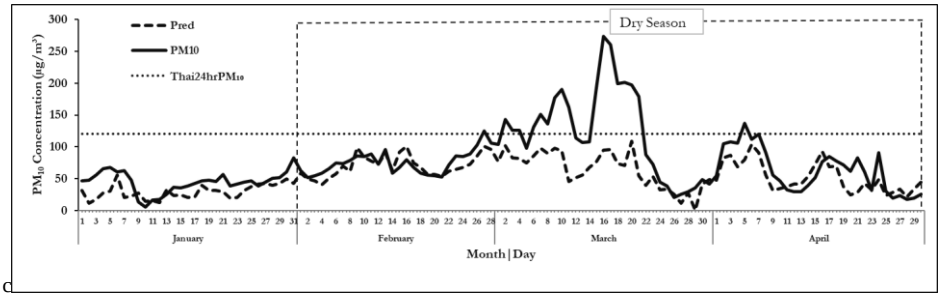

c

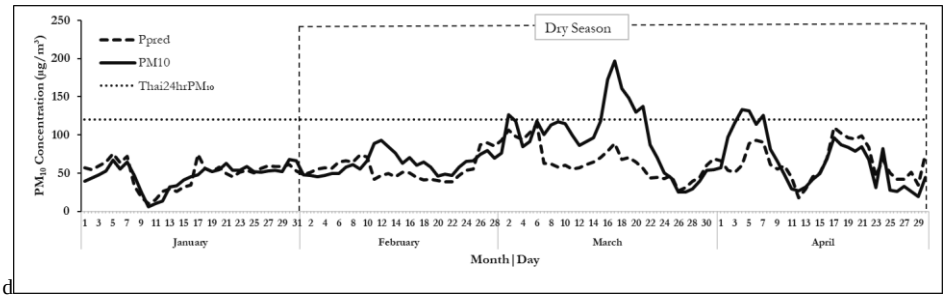

d

Figure 2: Daily predicted (dashed line), observed (solid line), and Thai 24hr PM_{10} standard (gray dashed line) PM_{10} concentrations over: a) Chiang Mai, b) Phrae, c) Phayao, and d) Nan provinces during January – April 2015.

Huge discrepancies between the model predictions and the observations are observed during February and March. On the other hand, the lowest RMSE value registered at Lamphun in 2014, as shown in Table 3 and Fig. 3(c).

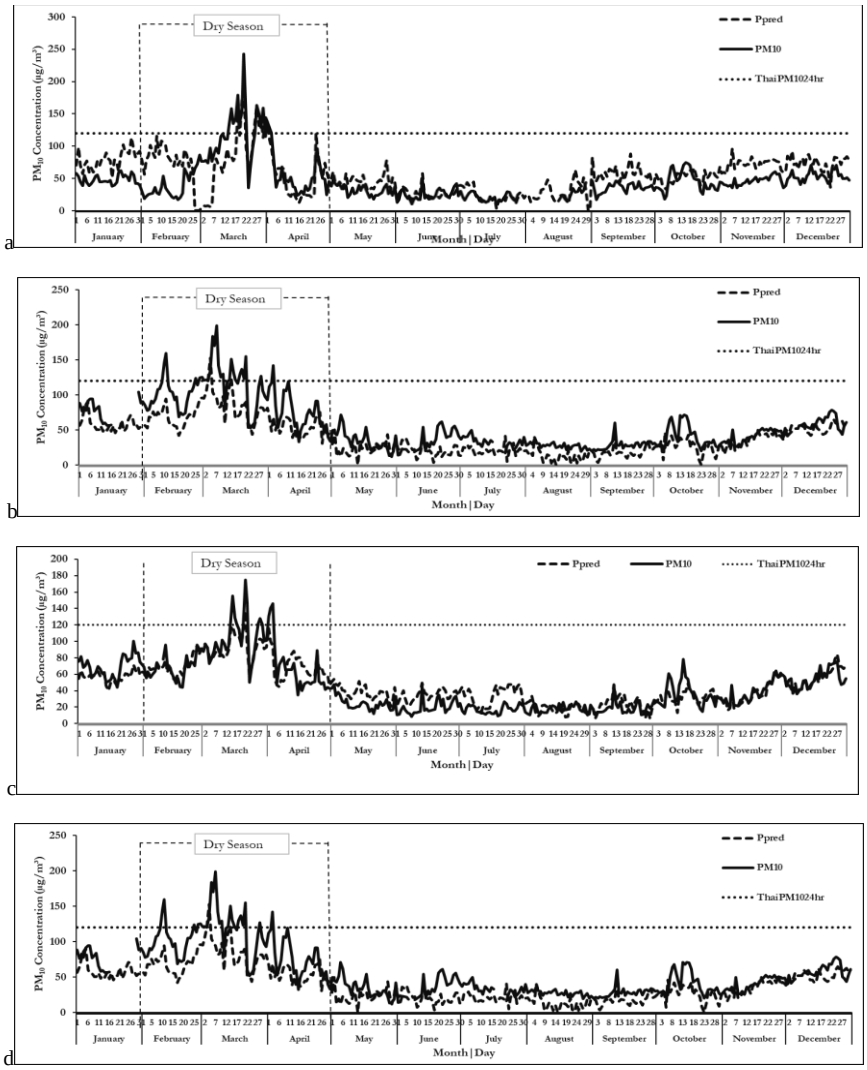

Figure 3: Daily predicted (dashed line), observed (solid line), and Thai 24hr PM_{10} standard (gray dashed line) PM_{10} concentrations over: a) Chiang Mai, b) Phrae, c) Lamphun, and d) Nan provinces during January – December 2014.

It is clear that, the model performed well over this station and its predicted PM_{10} concentrations were very close to the observed concentrations. Also, there are very small discrepancies observed between the model predictions and the observed concentrations during March and early April (Fig. 3(c)). The model performance over the other provinces as measured by RMSE is varied between these two values (14.14 and 40.00). In the most cases, these discrepancies between the predicted

and observed concentrations can be related to the presence of missing values and outliers in the air pollutants data.

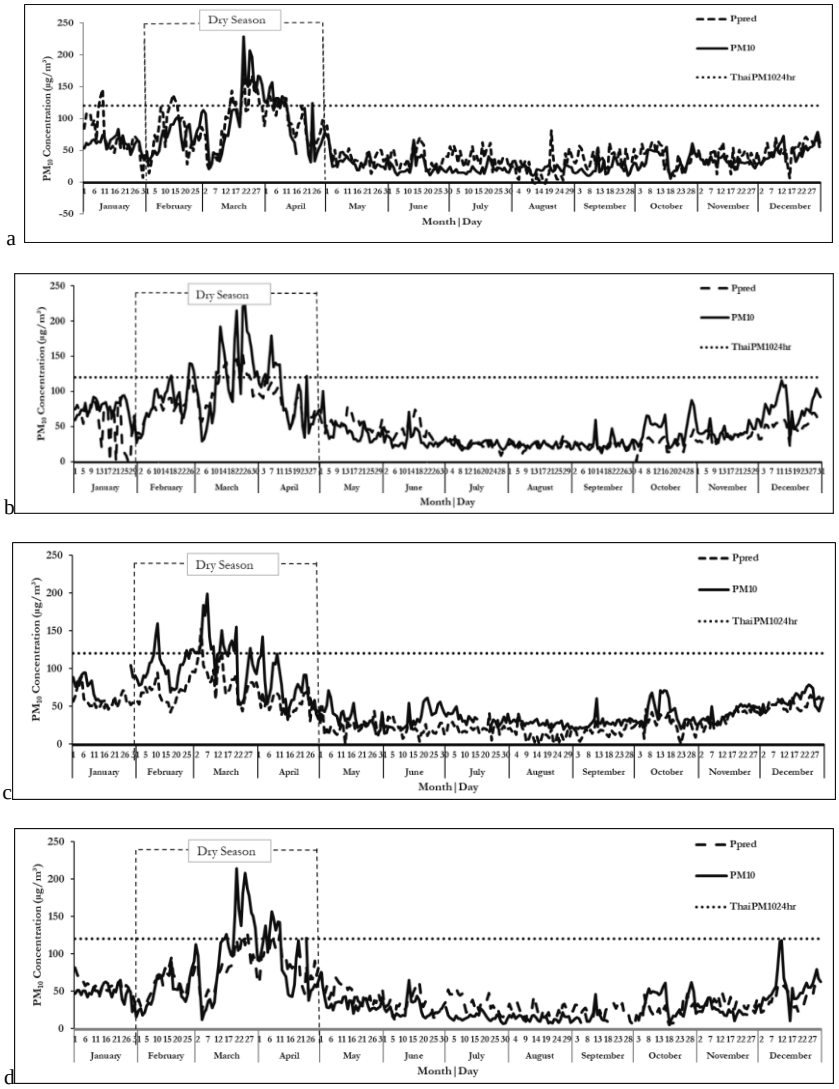

Figure 4: Daily predicted (dashed line), observed (solid line), and Thai 24hr PM_{10} standard (gray dashed line) PM_{10} concentrations over: a) Chiang Mai, b) Phrae, c) Nan, and d) Phayao provinces during January - December 2013.

MAE is also applied to measures the variations between the model predictions and observed PM_{10} concentrations over each province. MAE ranged from 12.74 to 34.18. The lowest and highest values are recorded in Nan and Chiang Mai provinces in 2012 and 2015,

respectively. Fig. 5 (d) shows that, the model predictions over Nan province were very close to the observed concentrations, although, it underestimated its concentrations during February and March, where the peaks occurred. It is also shown that, it underestimated PM_{10} concentrations during January, but this is mainly due to the missing values.

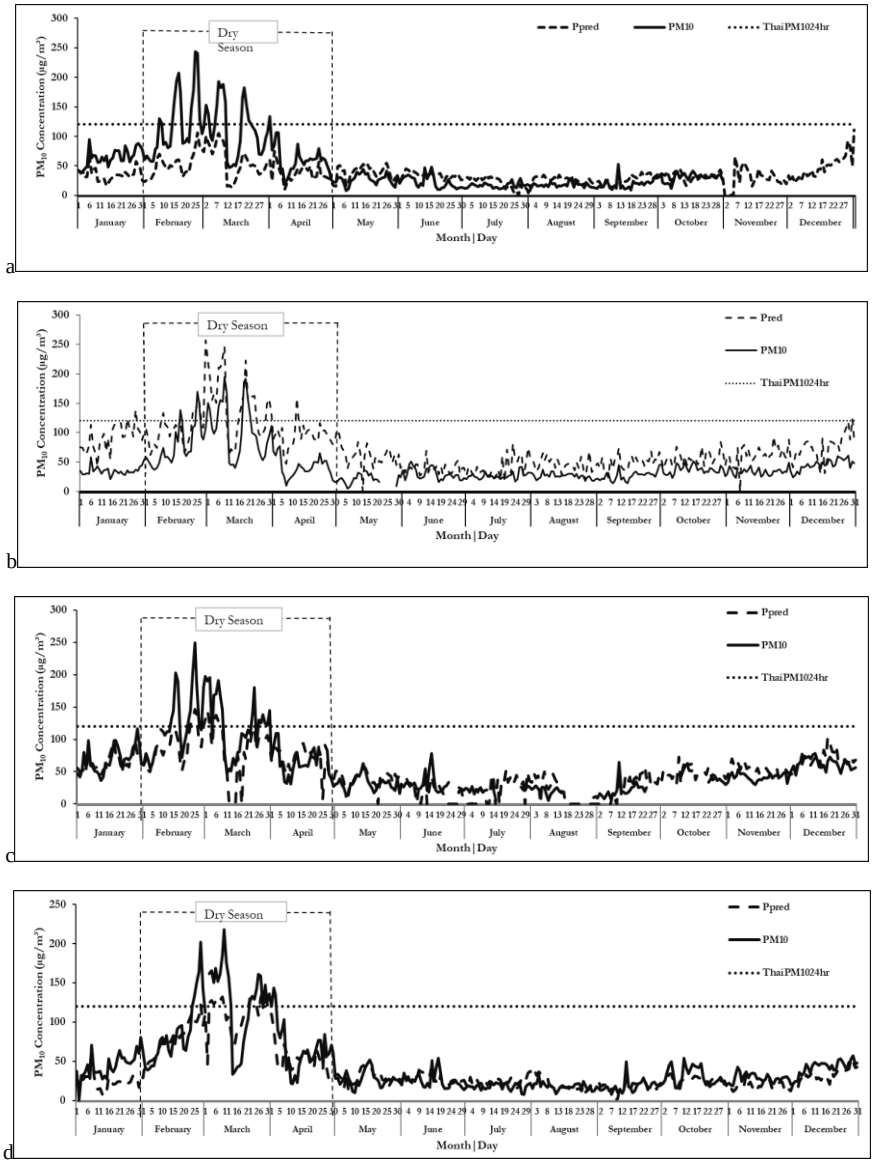

Figure 5: Daily predicted (dashed line), observed (solid line), Thai 24hr PM_{10} standard (gray dashed line) PM_{10} concentrations over: a) Lamphun, b) Chiang Mai, c) Phrae, and d) Nan provinces during January – December 2012.

Fig. 2(a) shows that, the model predictions at Chiang Mai province are far from the observed concentrations, especially during March, where the PM_{10} peaks occurred. Elsewhere, the model predictions were so close to the observed concentrations. In general, the PM_{10} concentration fluctuations during this period were well captured by the model and the main source of discrepancies is the missing values in air pollutants data set.

The third statistical performance indicator is IOA, which measures the variations between model predictions and the observed concentrations as a percentage. IOA ranged from 65% to 93% over the six provinces during the analysis period, with lowest and highest values registered at Lamphun province in 2012 and 2014, respectively. Fig. 5 (a) shows how the model predictions are disagreed with the observed values at Lamphun province (IOA=0.65). Also, the model underestimated PM_{10} concentrations over the first four months of 2012 in this province. This reflected the effect of missing and extreme values on the model prediction accuracy. The highest observed concentration in this year was 240 $\mu g/m^3$, which was above the Thai 24-hr PM_{10} standard (120 $\mu g/m^3$). In contrast, Fig. 3(c) shows a good agreement between the model predictions and the observed concentrations (IOA=93%) at Lamphun province during 2014. The model succeeded to predict PM_{10} concentrations with high accuracy as compared with observed values, even during the dry season in this year.

In general, the model successfully captured PM_{10} concentration trends over these provinces reasonably accurately. However, it tended to underestimate and overestimate its concentration levels in some occasions as shown in Figs. 2-5. The overestimation and underestimation performance are mainly due to the missing values that inherited in the air pollutants data and the presence of outliers, especially during the dry season where PM_{10} concentrations exceeded Thai 24-hr PM_{10} standard. Moreover, the model estimated the missing values of PM_{10}

concentrations with good accuracy depend on the observed air pollutants and meteorological variables. It is observed that, when there are one or more missing values in AQM data, the model tended to misbehave, and this resulted in over or underestimation of PM_{10} concentration for that day. When the five air pollutants values are missed in one day, the model estimated zero PM_{10} concentration for that day as shown in Fig. 3(b) and Fig .5(c). The effect of missing values on the predicted values of PM_{10} is obvious in Nan station (Fig. 3(d)), where the model predicted very low concentrations as there was no data from day 21 to 34 in 2014. Thus, it is very crucial to feed the model with complete air quality observations in order to produce continuous PM_{10} concentrations over the entire analysis period.

QR Model

Table 4 shows the estimated coefficients of the QR model and their correspondents quantile values of meteorological variables and air pollutants by using Eq. (9). Although, five quantiles were estimated (i.e., 5%, 10%, 50%, 75% and 95%) shown in Table 4, but only two quantiles (0.05 and 0.95) were used to predict the effects of extreme meteorological variables and air pollutants on PM_{10} concentrations over the six provinces. The difference between these two quantiles is found to be significant as shown by the analysis of variance (Table 5).

Table 4: Estimated coefficients of the Quantile Regression model and their correspondents' quantile values for the meteorological variables and air pollutants. τ = 5%,10%, 50%, 75%, and 95%. Only **5%** and **95%** quantile (bold font) are used to investigate the effect of the extreme variables on PM_{10} concentration.

Coefficient	Quantile				
	5%	10%	50%	75%	**95%**
Intercept	**-155.92**	42.73	45.05	9.04	**-327.83**
Maximum Temperature	**0.11**	-0.06	0.33	0.70	**1.08**
Relative Humidity	**-0.25**	-0.31	-0.53	-0.67	**-0.70**

Rainfall	**-0.03**	-0.05	0.03	0.08	**0.04**
Air Pressure	**0.17**	-0.02	-0.02	0.02	**0.35**
Wind Speed	**-0.53**	-0.44	-0.60	-0.89	**-1.03**
Carbon Monoxide (CO)	**10.26**	13.85	35.54	43.04	**48.59**
Ozone (O_3)	**0.34**	0.49	0.65	0.65	**0.90**
Nitrogen Oxides (NO_x)	**0.77**	0.90	1.03	1.27	**1.65**
Sulphur Dioxide (SO_2)	**1.00**	1.04	3.49	5.44	**9.60**

- Degrees of freedom: 3057 total:3047 residuals.

Fig.6 shows the intercept and slopes of the estimated coefficients of quantile regression with their 95% confidence bound as well as the Ordinary Least Square (OLS) estimates and their 95% confidence limits plots too. This figure shows the most interesting meteorological variables and air pollutants, those cross OLS estimates have more effect on the PM_{10} concentrations. Quantile ranges of T_{max} , RH and Press showed significant differences from OLS estimates. While rain and WS showed no differences as they are laying within OLD confidence bound. Also, the quantile ranges of CO, NO_x and SO_2 showed significant differences from OLS, while Ozone showed no difference from OLS estimates. Therefore, only quantiles of the meteorological variables and air pollutants those differ significantly from OLS estimates will have significant effects on PM_{10} concentration predictions. The other variables will have the same impact as the MLR estimates.

Table 5: Quantile Regression Analysis of Deviance. Joint Test of Equality of Slopes: tau in (0.05, 0.95).

Degree of Freedom	Residual degree of Freedom	F value	Pr(>F)

9	6105	102.05	< 2.2e-16 ***

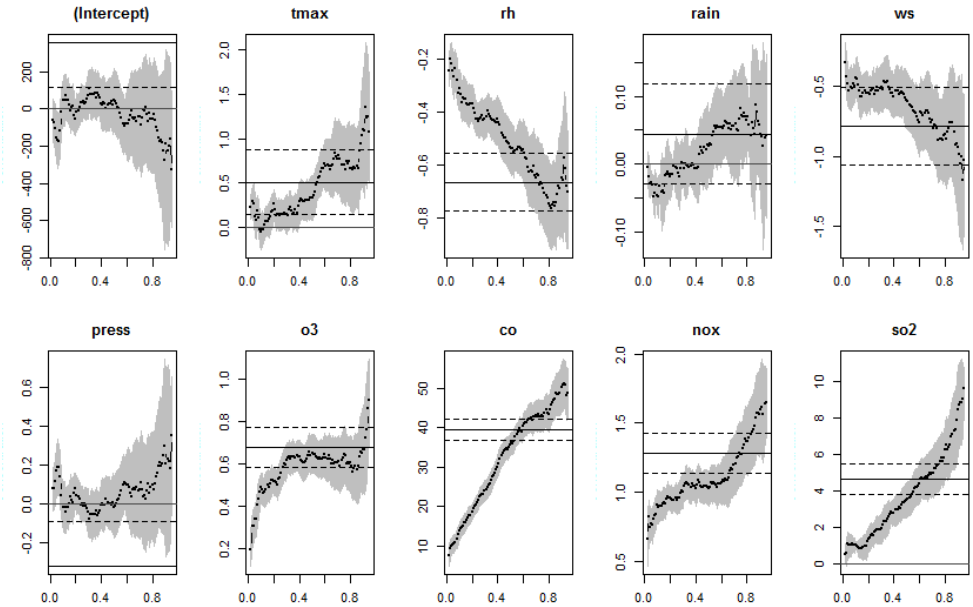

Figure 6: Intercept and slops of the estimated quantile regressions. Quantile regression coefficients (points) are represented with their 95% confidence bound (shaded grey). OLS (solid horizontal lines) are represented with its 95% confidence bounds (horizontal dashed lines).

Figs. 7-10 show QR model predicted PM_{10} concentrations using both 0.05 and 0.95 quantiles, the observed PM_{10} concentrations and Thai 24-hr PM_{10} standard during the period from 2012 to 2015 over the six provinces. It is found that, there are three out of five meteorological variables showed negative coefficients correspondent to 5% quantile (i.e., RH, rain and WS). In contrast, Press and T_{max} showed positive coefficients with 5% quantile. Only RH and WS shows negative coefficients with 95% quantile. All the air pollutants showed positive coefficients correspondent to both 5% and 95% quantiles. CO showed the highest coefficient among the air pollutants and meteorological variables correspondent to both quantiles.

It is obvious that the model exhibited the effect of high and low quantiles of meteorological variables and air pollutants on PM_{10} concentrations in these provinces. Figs. 7-10 show that the model succeeded to predict the

lower (0.05) and higher (0.95) daily PM_{10} concentrations over the analysis period over the six provinces in UNT.

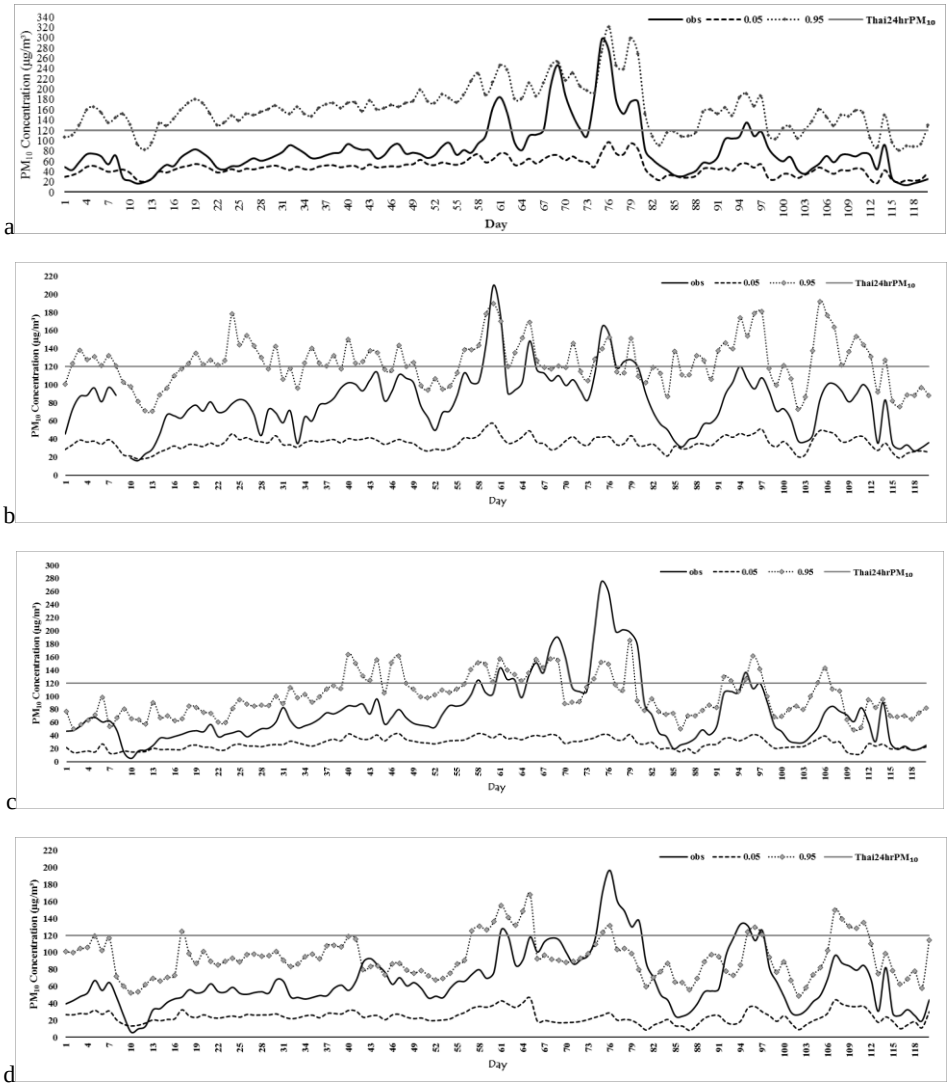

Figure 7: Daily predicted 5% and 95% quantiles (dashed line), observed (solid line), and Thai 24hr PM_{10} standard (gray dashed line) PM_{10} concentrations over: a) Chiang Mai, b) Phrae, c) Phayao, and d) Nan provinces during January - April 2015.

Although, there were some occasions, the model underestimated or overestimated the PM_{10} concentrations over these provinces, especially during the dry season, but it succeeded to capture the general trends throughout the analysis period. Consequently, the effect of the extreme values on PM_{10}

concentrations is clearly depicted by QR model predictions over each province.

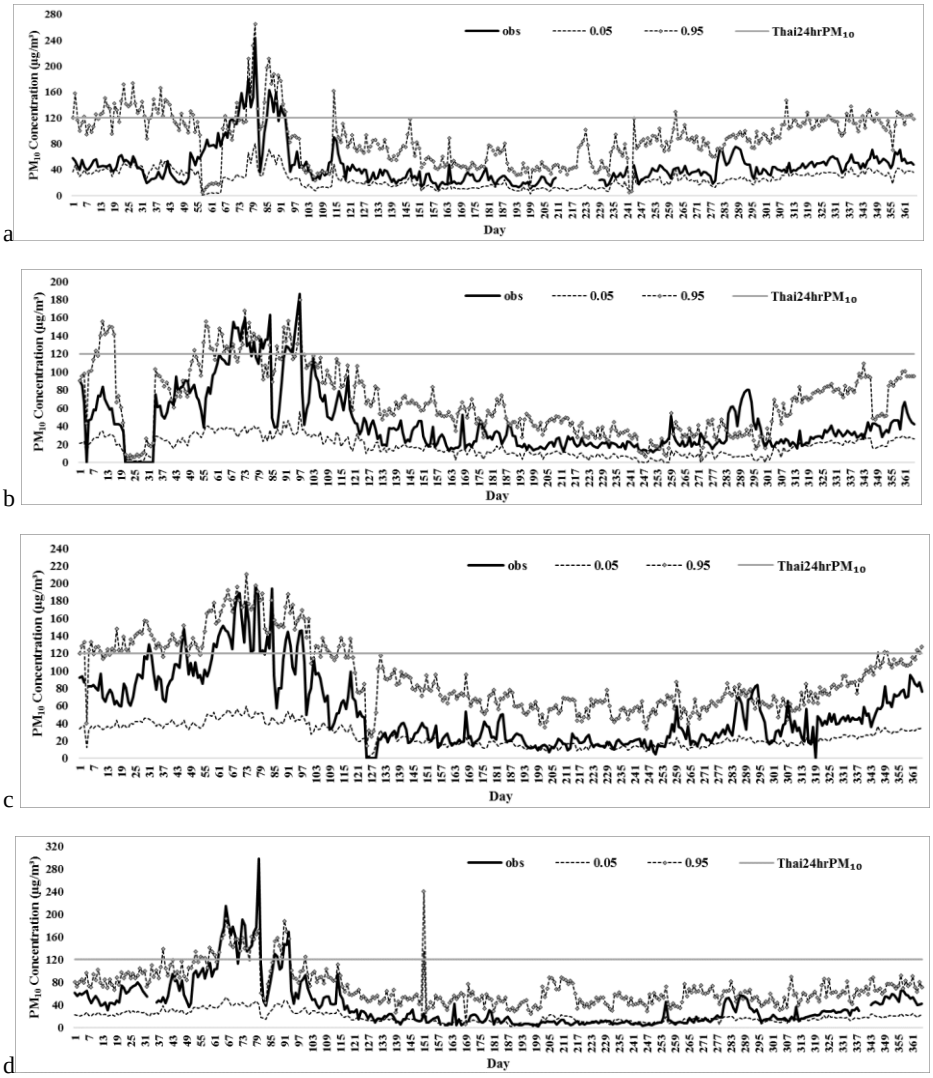

Figure 8: Daily predicted 5% and 95% quantiles (dashed line), observed (solid line), and Thai 24hr $PM_{10\ standard}$ (gray dashed line) PM_{10} concentrations over: a) Chiang Mai, b) Nan, c) Lampang, and d) Phayao provinces during January – December 2014.

The model's behavior is affected mainly by the presence of missing values that inherited in air pollutants data set in addition to the seasonality effects in the meteorological variables time-series. Meteorological data showed almost complete observations with

very few missing values compared with that of air pollutants data, which inherited a lot of missing values as it comprised of hourly observations (Table 2).

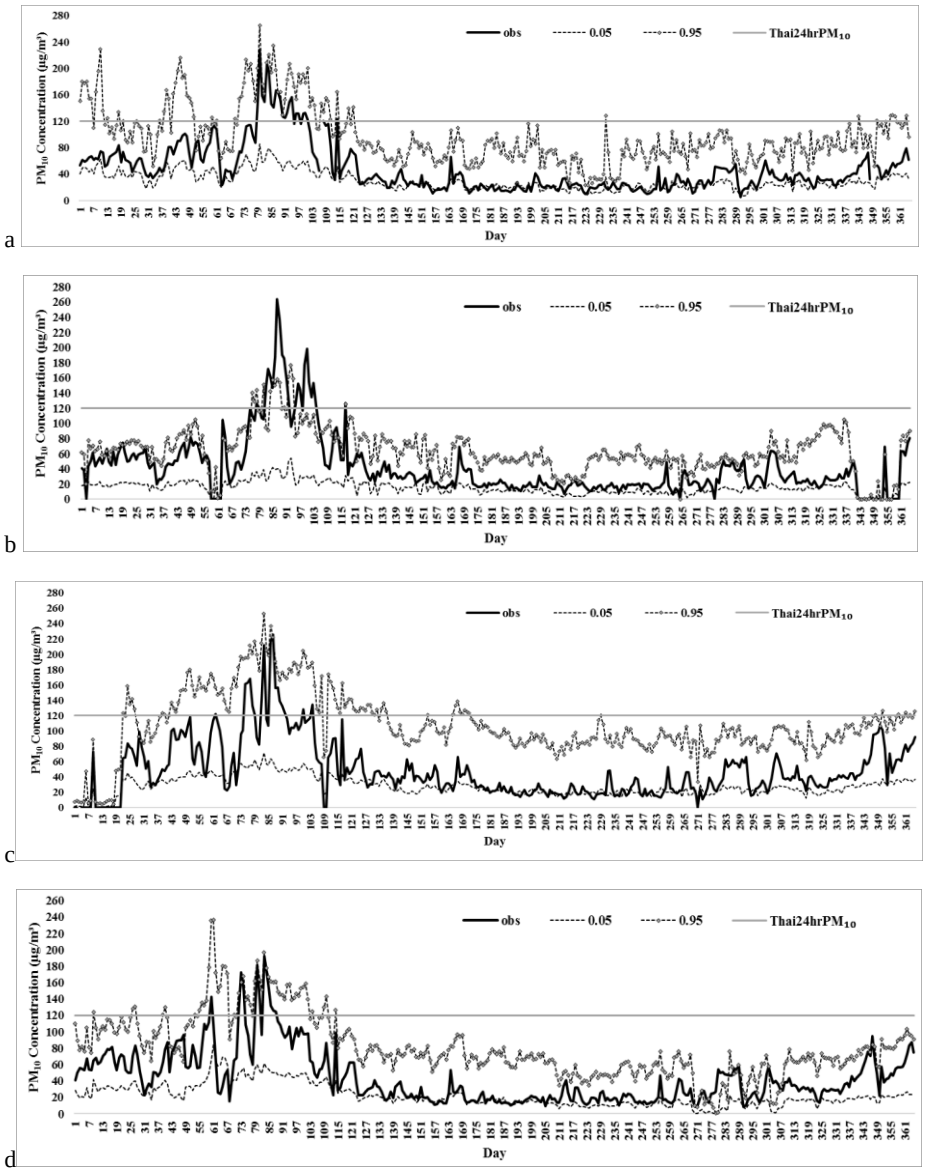

Figure 9: Daily predicted 5% and 95% quantiles (dashed line), observed (solid line), and Thai 24hr PM_{10} standard (gray dashed line) PM_{10} concentrations over: a) Chiang Mai, b) Nan, c) Lampang, and d) Lamphun provinces during January – December 2013

In general, the reduction in air pollutants concentrations is likely to decreases PM_{10} concentrations levels over UNT as depicted by the lower extreme variables (5% quantile). The most important air

pollutant is CO as it showed the highest coefficients (10.26 and 48.59) corresponding to 50% and 95% quantile, respectively. This means that, small increase in CO concentration will cause a significant increase of PM_{10} concentration levels in this region.

a

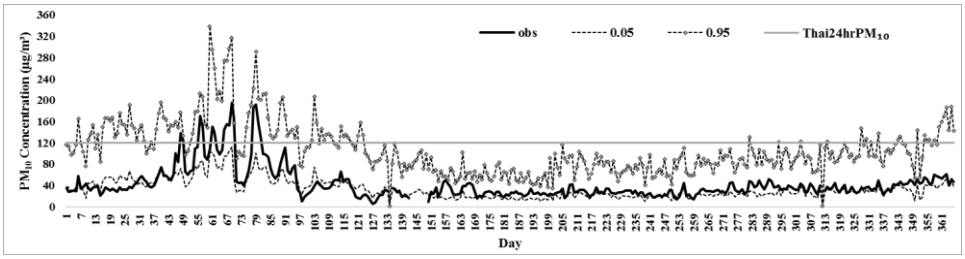

b

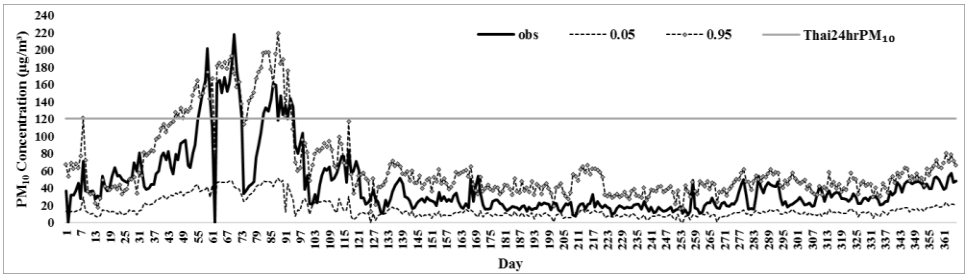

c

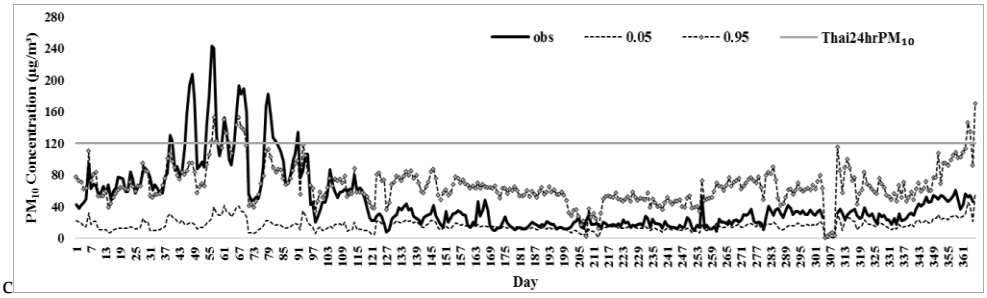

d

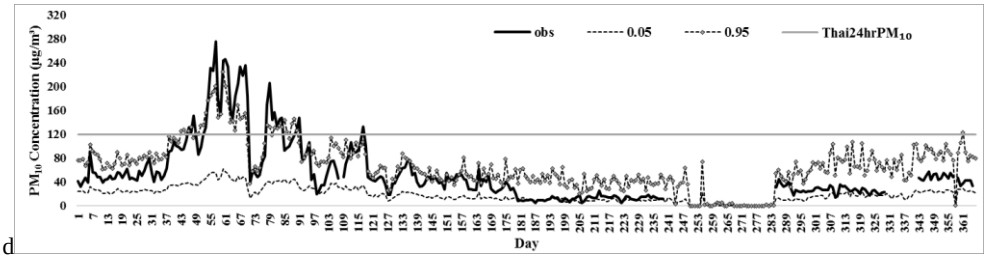

Figure 10: Daily predicted 5% and 95% quantiles (dashed line), observed (solid line), and Thai 24hr PM_{10} standard (gray dashed line) PM_{10} concentrations over: a) Chiang Mai, b) Nan, c) Lamphun, and d) Phayao provinces during January – December 2012.

Thus, it is highly recommended to issue regulations and introduce new

mechanisms to reduce the emission rates from the sources that produce CO, O_3 , NO_x and SO_2 in this region. During the dry season, CO emissions are due to the open biomass burning in this region and neighboring countries.

On the other hand, the effects of meteorological variables on PM_{10} prediction are mixed. The increase in maximum temperature, wind speed, rainfall amounts, relative humidity and decrease in ambient air pressure values will produce favorable conditions for PM_{10} dispersion and settlement. The topography effect is pronounceable in this region which empowers the pollution persistence for long time as they trapped by the inversion layer.

From the results, it is obvious that, producing high concentrations of air pollutants in this region is likely to increase PM_{10} concentration levels which deteriorate air quality and affect human health and the environment adversely. In contrast, controlling the emission sources by reducing their emission rates, especially during the dry season, will result in considerable reduction in PM_{10} concentration levels and will improve the air quality. QR model is succeeded to explain the effect of the extreme meteorological variables and air pollutants on the PM_{10} concentrations over this region. This agrees with the results that obtained by Sayegh et al. (2014) when they employed QR to predict the PM_{10} concentrations.

CONCLUSION

MLR model that was constructed using meteorological variables and air pollutants showed a good explanation power regarding the variations in PM_{10} concentrations in this region compared with the other that applied by Munir et al. (2013), Azid et al. (2015), and Liu et al. (2015). Moreover, it showed a good agreement with the observed PM_{10} concentrations as shown by the statistical performance indicators (RMSE=20.35-40.00, MAE=12.00-30.00, and IOA=65%-93%) from 2012 to 2015 over the six provinces. The observed

discrepancies between the model predictions and the observed concentrations, especially during the dry season (January – April), are mainly due to the missing values and outliers in air pollutants data. Therefore, this model is capable to predict the daily PM_{10} concentrations over this region with good accuracy for air quality management purposes. In addition, this study provided a tool to estimate the missing PM_{10} values over UNT with acceptable level of accuracy.

On the other hand, quantile regression model also succeeded to explain the effects of the extreme meteorological variables and air pollutants on PM_{10} concentrations over UNT during the analysis period. The model successfully predicted lower and higher PM_{10} concentrations than the observed concentrations corresponding to 5% and 95% quantile, respectively. Although, the meteorological variables showed a mixed effect on PM_{10} concentrations as they possessed negative and positive coefficients, they have considerable effect on their persistence and dispersion in this region. In contrast, air pollutants showed positive coefficients corresponding to 5% and 95% quantiles. Carbon monoxide showed the highest coefficients compared with the other air pollutants. Therefore, small increase in CO concentration will cause PM_{10} concentration levels to increase significantly. On the other hand, the reduction of CO and the other air pollutants concentrations will result in a considerable reduction in PM_{10} concentrations and contribute to air quality improvement in this region. These results showed the Appling this knowledge will help in evaluating the PM_{10} levels based on the concentration levels of CO, O_3, NO_x and $SO_2$and over UNT.

The potential applications of these models in this region are to aid in air quality management and policy development, in term of prediction of daily PM_{10} concentrations, estimation of missing values and the evaluation of the effect of extreme values of air pollutants and

meteorological variables on their daily concentration levels. Environmental impact assessment studies can make use of the MLR model to infer the PM_{10} concentration over a specific state or a region. Setting up new limitation of PM_{10} emissions can be supported by the applying QR model results.

ACKNOWLEDGEMENTS

The authors wish to thank Pollution Control Department (PCD) and Thailand Meteorological Department (TMD) for providing air quality and meteorological data. Special thanks extended to Thailand International Cooperation Agency (TICA) for providing the financial support for International Program in Environmental Science fellowship at Chiang Mai University (CMU), Thailand.

REFERENCES

Awang, Norrimi Rosaida, Nor Azam Ramli, Ahmed Shukri Yahaya, and Maher Elbayoumi. 2015. "Multivariate methods to predict ground level ozone during daytime, nighttime, and critical conversion time in urban areas." Atmospheric Pollution Research 726-734. doi:10.5094/APR.2015.081.

Azid, Azman, Hafizan Juahir, Ezureen Ezani, Mohd Ekhwan Toriman, Azizah Endut, Mohd Nordin Abdul Rahman, Kamaruzzaman Yunus, et al. 2015. "Identification Source of Variation on Regional Impact of Air Quality Pattern Using Chemometric." Aerosol and Air Quality Research (Taiwan Association for Aerosol Research) 15: 1545-1558. doi:10.4209/aaqr.2014.04.0073.

Chai, T., and R. R. Draxler. 2014. "Root mean square error (RMSE) or mean absolute error (MAE)? – Arguments against avoiding RMSE in the literature." Geoscientific Model Development (Copernicus Publications on behalf of the European Geosciences Union) 7: 1247-1250. doi:10.5194/gmd-7-1247-2014.

Chantara, Somporn, Sopittaporn Sillapapiromsuk, and Wan Wiriya. 2012. "Atmospheric pollutants in Chiang Mai (Thailand) over a five-year period (2005-2009), their possible sources and relation to air mass movement." Atmospheric Environment (Elsevier) 60: 88-98.

Cook, Benjamin Lê, and Willard G. Manning. 2013. "Thinking beyond the mean: a practical guide for using

quantile regression methods for health services research." Shanghai Archives of Psychiatry 25 (1): 55-59.

Fox, John, and Sanford Weisberg. 2011. An R Companion to Applied Regression. Second. Thaousand Oaks, CA: Stage. http://socserv.socsci.mcmaster.ca/jfox/Books/Companion.

H., Wickham. 2009. ggplot2: Elegant Graphics for Data Analysis. Verlag New York: Springer.

Hamner, Ben. 2012. "Evaluation metrics for machine learning." https://github.com/benhamner/Metrics/tree/master/R.

Kim Oanh, Nguyen Thi, and Ketsiri Leelasakultum. 2011. "Analysis of meteorology and emission in haze episode prevalence over mountain-bounded region for early warning." Science of the Total Environment (Elsevier B.V.) 409: 2261-2271. doi:10.1016/j.scitotenv.2011.02.022.

Liu, Wu, Xiaodong Li, Zuo Chen, Guangming Zeng, Tom'as Le'on, Jie Liang, Guohe Huang, Zhihua Gao, Sheng Jiao, and Xiaoxiao He. 2015. "Land use regression models coupled with meteorology to model spatial and temporal variability of NO2 and PM10 in Changsha, China." Atmospheric Environment 116: 272-280.

Munir, Said, Turki M. Habeebullah, Abdulaziz R. Seroji, and Essam A. Morsy. 2013. "Modeling Particulate Matter Concentrations in Makkah, Applying a Statistical Modeling Approach." Aerosol and Air Quality Research (Taiwan Association for Aerosol Research) 901–910. doi:10.4209/aaqr.2012.11.0314.

PCD, Pollution Control Departmrnt. 2004. "Notification of National Environmental Board No. 24, B.E. 2547 (2004)." http://www.pcd.go.th/info_serv/en_reg_std_airsnd01.html.

Pengchai, Petch, Somporn Chantara, Khajornsak Sopajaree, Sunanta Wangkarn, Urai Tengcharoenkul, and Mongkon Rayanakorn. 2009. "Seasonal variation, risk assessment and source estimation of PM 10 and PM10-bound PAHs in the ambient air of Chiang Mai and Lamphun, Thailand." Environ Monit Assess (Springer Science) 154: 197-218. doi:10.1007/s10661-008-0389-0.

Roger, Koenker. 2015. quantreg: Quantile Regression. R Package. https://CRAN.R-project.org/package=quantreg.

Sayegh, Arwa S., Said Munir, and Turki M. Habeebullah. 2014. "Comparing the Performance of Statistical Models for Predicting PM10 Concentrations." Aerosol and Air Quality Research (Taiwan Association for Aerosol Research) 14: 653-665. doi:10.4209/aaqr.2013.07.0259.

Venables, W. N., and B. D. Ripley. 2002.

Modern Applied Statistics with S. Fourth. New York: Springer. http://www.stats.ox.ac.uk/pub/MASS4.

Willmott, C. J. 1981. "On the validation of models." Physical Geography 2 (2): 184-194.

Wiriya, Wan, Tippawan Prapamontol, and Somporn Chantara. 2013. "PM10-bound polycyclic aromatic hydrocarbons in Chiang Mai (Thailand): Seasonal variations, source identification, health risk assessment and their relationship to air-mass movement." Atmospheric Research (Elsevier) 124: 109-122.

Lignin Separation from Bagasse and Precipitation by Formic acid

Supattra Mataraj[1] and Krisanavej Songthanasak[1]

[1]Department of Agro-industrial, Food and Environmental Technology, Faculty of Applied Science, King Mongkut's University of Technology North Bangkok, Bangkok 10800, Thailand: e-mail: smmunew@gmail.com

ABSTRACT

This research aimed to study the optimum conditions for separating the maximum amount of lignin from bagasse and comparing the precipitation between inorganic and organic acid. The experiments were divided into three procedures. The first procedure was to determine the lignocellulosic compositions in bagasse which were cellulose, hemicellulose, and lignin. Then, the optimum conditions which included temperature, time and the bagasse to solvent ratio in order to extract the lignin from bagasse using sodium hydroxide as solvent was studied. The final procedure was to separate lignin from solution by precipitation using sulfuric and formic acid. The experimental results showed that the bagasse consisted of 43% cellulose, 20% hemicellulose, 21% lignin, and 14% other compounds. The optimum condition for separating lignin was 60 minutes, 120℃, and the ratio was 1 g of bagasse to 10 ml. The lignin was precipitated and their yield were 6.47 and 6.53g/l; 30.8 and 31.1%, respectively. In summary, the formic acid can use for precipitating lignin instead of sulfuric acid and it is also friendly and less toxic chemical for environment more than sulfuric acid.

Keywords: Bagasse; Lignin separation; Lignocellulose

INTRODUCTION

Bagasse, an industrial waste by product left in the sugar manufacturing processes after extraction of sugar juice from crushed sugarcane, can be used as a source of biopolymer and other valuable compounds such as cellulose, hemicellulose, and lignin as lignocellulose biomass [1]. The bagasse generally was incinerated as solid fuel for producing energy and steam in industries and it also is used as a resource for ethanol fuel production by cellulose consisted of bagasse. However, the process of ethanol production is pretreated by eliminating lignin which is an ingredient helps strengthen the plant's strength; a molecule that connects between molecules of cellulose and hemicellulose, and lignin like a wall to protect the enzyme to entering cellulose and hemicellulose [1, 2, 3]. Thus, the lignin removal becomes a waste that will be mixed with waste water and the contaminated lignin is dark and difficult to treat. In industries, the amount of lignin contaminated with water will be evaporated to evaporate the water and the remaining lignin will be burned for energy [3]. The bagasse is another source of lignin. Lignin after separation can be used for applications that have more value than being burned to produce energy. Therefore, this experiment will precipitate lignin using organic solvent instead of inorganic solvent which generally is used for precipitating lignin to be friendly environment when it is discarded.

METHODOLOGY

Bagasse Preparation

Bagasse was collected from sugar industry at Kanchanaburi Province, Thailand, then dried at 60°C, milled and sieved with an approximately size of 0.25-0.5 cm, stored sample at room temperature.

Bagasse Compositions Study

The first procedure was to determine the lignocellulosic compositions in bagasse which were cellulose, hemicellulose, and lignin analyzed by detergent method [4].

The Optimum Condition Studies

A. Lignin Separation

The alkali pretreatment process mainly depends on the solubility performance of lignin in the alkali solution [5]. This experiment used sodium hydroxide as solvent and studied the optimum conditions which included temperature, time and the bagasse to solvent ratio in order to extract the lignin from bagasse. The studied conditions were carried out at 60 and 120℃, times of 30, 60 and 120 minutes and the ratio of bagasse (g) to sodium hydroxide solution (ml) at 1:10, 1:20, and 1:30. Analyst lignin in solution by UV-spectrophotometer at 280 nm [6].

B. Lignin Precipitation

This process was to separate lignin from sodium hydroxide solution by precipitation using sulfuric and formic acid. Lignin precipitation firstly removed the polysaccharide degradation by precipitation at pH 6. Then the pH of solution at pH 5, 4, 3, 2, and 1 were studied to precipitate lignin.

RESULTS AND DISCUSSION

Composition of Lignocellulose Bagasse

The composition of bagasse was analyzed by detergent method. The result of bagasse composition was shown in figure 1. It was found that the bagasse consists of 43% cellulose, 20% hemicellulose, 21% lignin and 16% other contents which the composition of bagasse was mostly consisted of 40-45% cellulose, 25-30% hemicellulose, and 20-25% lignin [7]. The composition of lignin was different because of different type, age, and place.

The optimum condition study for bagasse separation

A. The bagasse to solvent ratio study

This procedure was to study the bagasse to solvent ratio in order to extract the lignin from bagasse using sodium hydroxide as solvent and analyze the lignin with spectrophotometer. The results were shown in figure 2. They found that when the volume of sodium hydroxide solution was increased from 10 to 20 ml., the lignin was

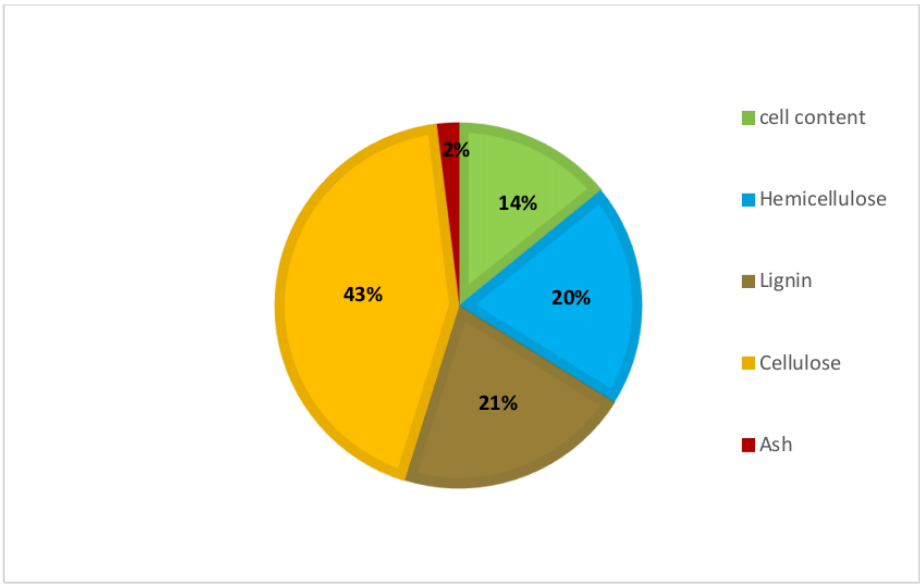

Figure 1 The percentage of bagasse composition.

decreased from 15.59 to 7.14 g/l of lignin solution. The best ratio was dried bagasse 1 g to solvent 10 ml which gave 15.59 g/l of lignin solution or 74% yield of lignin from dried bagasse. The yields of the lignin from solvent 10 ml, 20 ml, and 30 ml were 74%, 53%, and 34% respectively. The reason was that the increased volume of solvent will dilute lignin quantity that can separated from bagasse.

B. Temperature and Time to Bagasse Study

After studying the ratio of bagasse and solvent then chose the best ratio to study the suitable temperature and time for bagasse separation. The results were shown in figure 3. They found that when the time was increased 30 to 120 minutes, the lignin contents was increased in both of studied temperatures (60 and 120°C), however, the lignin contents between 60 and 120 minutes were not different, so the 60 minutes was chosen as the suitable time. The suitable temperature and time of lignin separation was 21.9 g/l at 120°C, 60 minutes.

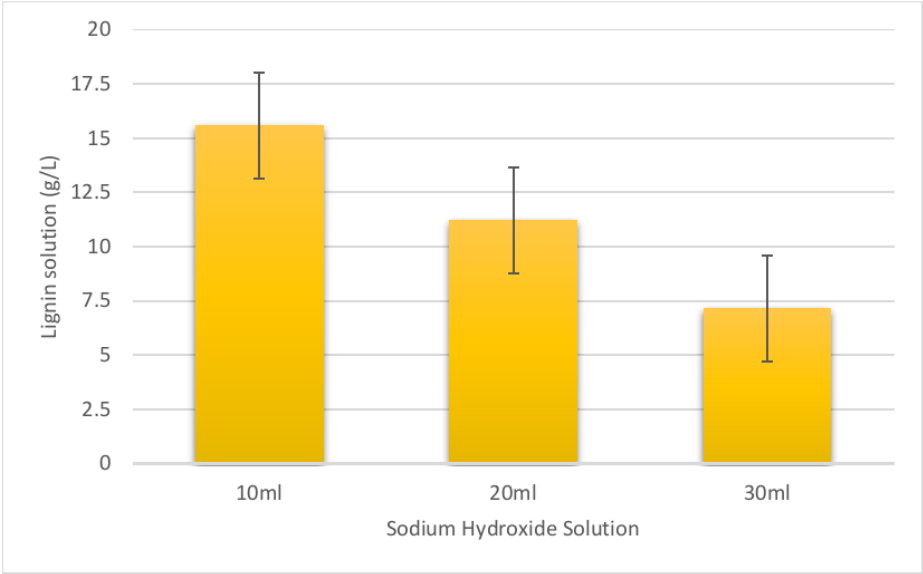

Figure 2 The amount of lignin solution from bagasse to sodium hydroxide solution ratios study.

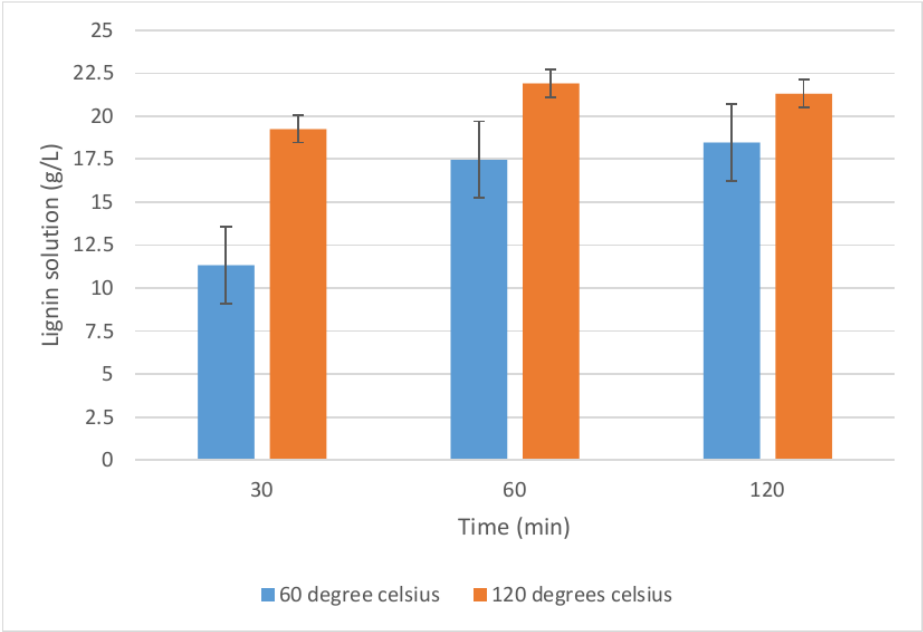

Figure 3 The amount of lignin solution from temperature and time study.

The Optimum Condition for Lignin Precipitation

This procedure studied the pH value to precipitate lignin from the solvent after separating lignin from bagasse with the suitable condition. This study used sulfuric acid for inorganic acid solution comparing with formic acid for organic acid precipitation. The results were shown in the figure 4, they found that pH value from sulfuric acid precipitation decreases from pH5 to pH1, the lignin slightly increased, and the suitable pH value was pH1 and separated lignin was 6.64 g/l. It, close to pH2 and pH3, were 6.52 and 6.47 g/l. The pH value from formic acid precipitation decreases from pH5 to pH3, the lignin slightly increased and when pH value decreased from pH3 to pH1, the lignin decreased. The suitable pH value from formic acid was pH3 and separated lignin was 6.53 g/l. Then, pH3 of sulfuric and formic acid were chosen as suitable pH and the yield of sulfuric and formic acid were 30.8 and 31.1% respectively. The reason that the formic acid could use for precipitating similar to sulfuric acid because carbon-based acids can serve as good precipitating agents and they would not introduce any objectionable elements during the precipitation process, there by producing a greener lignin product [8]. Therefore, it is worth exploring other acids for lignin precipitation that would have much greener consequences on the environment. Moreover, organic acids can be effective alternatives for lignin precipitation and do not release the unfriendly environmental gases [1].

CONCLUSIONS

The best condition of lignin separation was 60 minutes, 120℃, and the ratio was 1 g of bagasse to 10 ml of sodium hydroxide. The lignin was precipitated by sulfuric and formic acid and their yield were 6.47 and 6.53g/l; 30.8 and 31.1%, respectively. The lignin can precipitation by formic acid as well as sulfuric acid, but formic acid is friendly for environment more than sulfuric acid.

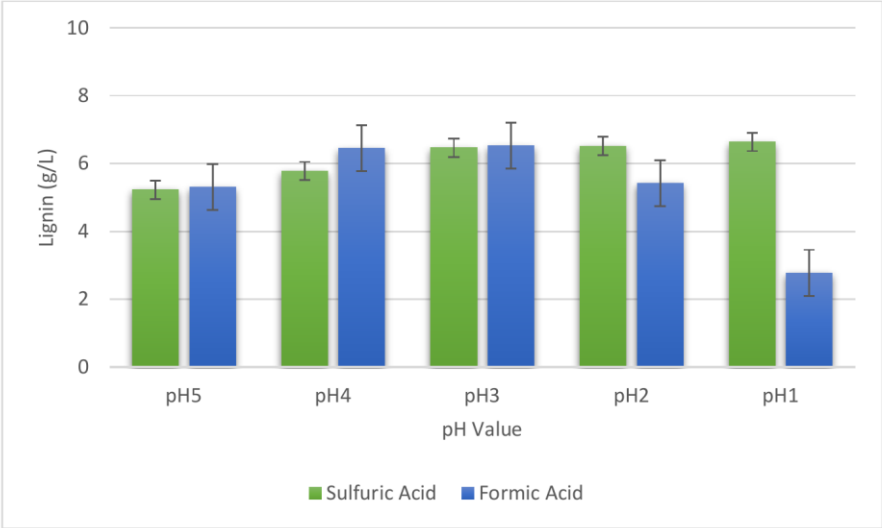

Figure 4 The amount of lignin from acid precipitation study.

ACKNOWLEDGEMENTS

The authors would like to thank Department of Agro-industrial, Food and Environmental Technology, Faculty of Applied Science, King Mongkut's University of Technology North Bangkok.

REFERENCES

[1] Gabove K., Hemming J., and Fardim P. 2017. Sugarcane Bagasse Valorization by Fraction Using a Water-Based Hydrotropic Process. Industrial Crops and Products. 108: 459-504.

[2] Berlin A., Balakshin M. 2014. Analysis, Properties, and Applications: Industrial Lignins. P.315-336.

[3] Dawson L., Boopathy R. 2007. Use of Post-Harvest Sugarcane Residue for Ethanol Production. Bioresource Technology. 98: 1695–1699.

[4] Goering H. K., Van Soest P. J. 1970. Forage Fiber Analyses. P. 387-598.

[5] Polprasert S. 2014. Pretreatment of Lignocellulosic Materials for Ethanol Production. Scholarly Article of Science and Technology. 22(5). 641-649.

[6] Pichainarong W. 2002. Separation of Lignin from Eucalyptus Pulping Liquor. Thesis of Inter-department of Environmental Science. ISBN974-17-2476-4.

[7] Boonruangrod C., Liengprayoon S., Morakul S. 2016. Chemical and Biological Characteristics of Lignin and Energy Efficiency of Acid and Alkali Delignified Bagasse. Naresuan University Journal: Science and

Technology. 24(2). 195-206.

[8] Namane M., Garcia-Mateos F., Sithole B., Ramjugernath D., Rodriguez-Mirasol J., Cordero T. 2016. Characteristics of Lignin Precipitated with Organic Acids as A Source for Valorisation of Carbon Products. Cellulose Chemistry and Technology. 50(3-4). 355-360.

[9] Alexopoulos, C.J., Mims, C.W., Blackwell, M. 1996. Introductory Mycology. 4th Edition. John Wiley, New York. 870 p.

[10] Bharathi, K., Pogaku, R. 2006. Pretreatment Studies of Rice Bran for The Effective Production of Cellulase. Jounal of Environmental Agricultural and Food Chemistry. 5(2):1253-1264.

[11] Caylak, B., and Sukan, F.V. 1998. Comparison of Different Production Processes for Bioethanol. Chemistry. 22: 351-359.

[12] Converti, A., Ami, S., Sato, S., de Carvalho, J.C.M., Aquarone, E. 2003. Simplified Modelling of Fed-Batch Alcohol Fermentation of Sugarcane Blackstrap Molasses. Biotechnology Bioengineering. 84(1): 88-95.

[13] Dawson, L., and Boopathy, R. 2007. Use of Post-Harvest Sugarcane Residue for Ethanol Production. Bioresource Technology. 98: 1695–1699.

Adsorption of Basic Red 29 Using Magnetic Activated Carbon

Panjai Saueprasearsit*, Phimploy Mawan, and Fonthip Mittassa

Faculty of Environment and Resource Studies, Mahasarakham University,
Khamriang Sub-district, Kantarawichai District,
Maha Sarakham, Thailand 44150
E-mail Address: panjai.s@msu.ac.th

ABSTRACT

In this research, the mechanism of the adsorption of Basic Red 29 from aqueous solution using magnetic activated carbon (MAC) prepared by chemical co-precipitation ($FeCl_3.6H_2O$ and $FeSO_4.7H_2O$) was investigated. Adsorption parameters considered in this study included pH, contact time, initial Basic Red 29 concentration and temperature. Adsorption isotherms, kinetics, and thermodynamics were used to determine the maximum adsorption capacity and to explain the adsorption mechanisms.

The optimum conditions for the adsorption of Basic Red 29 color using MAC was pH, 8; contact time, 90 min; initial Basic Red 29 concentration, 200 mg/L; and temperature, 15^{o}C. The maximum adsorption capacity was 256.41 mg of Basic Red 29 /g of MAC. The equilibrium data was fitted well with the Langmuir isotherm, so the adsorption was monolayer and site-specific. The kinetic results corresponded to the Pseudo second order model, indicating chemical sorption as the rate limiting step of adsorption mechanisms. The thermodynamics results revealed the dominant role of an exothermic reaction and a spontaneous reaction. Moreover, MAC had advantages as easy and rapid separation from aqueous solution. All results indicate that MAC is an effective adsorbent for adsorbing Basic Red 29 from aqueous solution.

Keywords: Magnetic Activated Carbon, Adsorption, Basic Red 29

INTRODUCTION

Discharge of industrial dye effluents into the environment has been a serious problem due to their high toxicity and non-biodegradable nature. The dyes used are mainly aromatic compounds with color imparting polar groups. They are usually difficult to degrade due to their complex structures. Conventional bio-treatment methods are not efficient to treat dying effluents (Wang et al., 2004; Aksu and Kabaskal, 2004). However, many techniques such as electrochemical coagulation, reverse osmosis, nano filtration, adsorption using activated materials etc., can be used for the removal of dye from wastewater (Sivakumar and Palanisamy, 2009). Among them, the adsorption technique is based on the transfer of pollutants from the solution to the solid phase. The method is superior to other dye removal techniques in terms of initial cost, simplicity of design, ease of operation, and non-toxicity of the utilized adsorbents compared to other conventional wastewater treatment methods (Kismir and Aroguz, 2011). For this technique, activated carbon (AC) is a widely used adsorbent because it is microporous and high surface area (Iqbal and Ashiq, 2007). In general, powder activated carbon (PAC) is more effective than granular activated carbon (GAC), due to the higher surface area of the PAC. However, the small particle size also makes the separation of PAC from liquids much more difficult than the separation of GAC. In this research, PAC was developed to be magnetic activated carbon (MAC) by using chemical co-precipitation with paramagnetic or ferromagnetic compounds (Mohan et al., 2011) as adsorbents. The spent MAC was rapidly separated from liquids using external magnetic fields. In this research, the adsorption characteristics of dye (Basic Red 29) onto MAC were investigated under varying experimental conditions consisting of pH, contact time, initial

Basic Red 29 concentration, and temperature. The adsorption isotherms, kinetics, and thermodynamics were studied to determine the maximum adsorption capacity and explain the adsorption mechanisms.

MATERIALS AND METHODS

2.1 Chemical and reagents

All chemicals were analytical reagent grade and used without further purification. A Basic Red 29 solution of 1000 mg/L concentration was prepared by dissolving 1 g of Basic Red 29 (DyStar Thai Ltd.) in distilled water (DW) and serially diluted to obtain solutions of desired concentrations.

2.2. Preparation of magnetic activated carbon (Mohan et al., 2011)

Powder activated carbon (PAC, Merck, 50 g) was suspended in mixed solutions of ferric chloride and ferrous sulfate. Ferric chloride solution was freshly prepared by adding 29.96 g of $FeCl_3.6H_2O$ in DW (1300 mL). Ferrous sulfate solution was prepared from 34.2 g of $FeSO_4.7H_2O$ and DW (150 mL). The mixture was slowly stirred at 60–70°C. Then 10 M NaOH (aqueous) was added dropwise into the PAC/Fe^{2+}/Fe^{3+} suspension until the pH reached ~10–11. During NaOH addition, the suspension became dark brown at ~pH6 and then black at ~pH 10. After mixing for 30 min, the suspension was aged at room temperature for 24 h, filtered, and then the filtrate was repeatedly washed with DW followed by ethanol. MAC was vacuum-filtered and dried overnight at 50 °C in a hot air oven. The characteristics of MAC were investigated by using Scanning Electron Microscopy (SEM, HITACHI-S3000N) with Energy Dispersive Analysis (EDS), Fourier Transform Infrared Spectrometer (FT-IR, Perkin Elmer Model Spectrum GX), Vibrating Sample Magnetometer (VSM, LakeShore Model 7404). Figure 1 presents a schematic of the preparation of MAC.

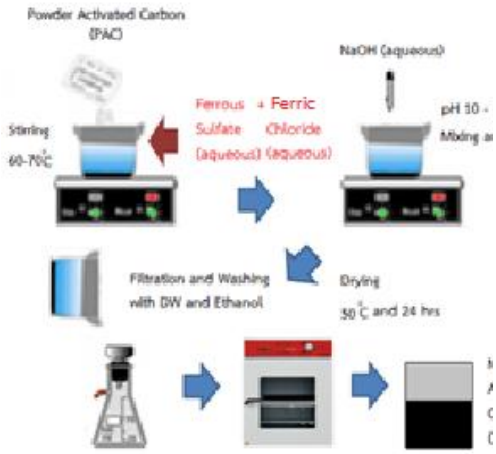

Figure 1 Preparation of MAC
Source: Modified from Mohan et al. (2011)

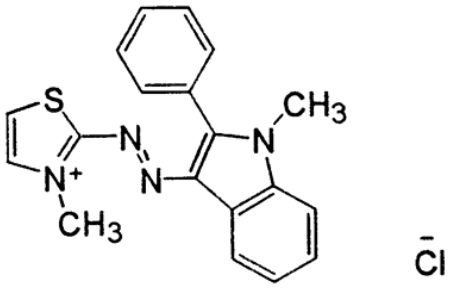

Figure 2 Structure of Basic Red 29
Source: DyStar Thai Ltd. (2019)

2.3 Sorption procedure

2.3.1 Adsorption experiments

Batch experiments were carried out to investigate the effects of pH, contact time, initial Basic Red 29 concentration, and temperature on adsorption onto MAC. 100 mL of different concentrations (100 – 500 mg/L) of Basic Red 29 solutions (C_0) with a range of pH values from 5 to 9 were transferred to a conical flask with 100 mg of MAC. Figure 2 presents the structure of Basic Red 29.

The mixtures were agitated at 150 rpm in an incubated shaker for different times (0 to 180 min) at different temperatures (15, 30 and 60°C). The samples were induced to separate MAC by using a magnet for one minute. The supernatant solutions were analyzed by spectrophotometer (Thermo Scientific, Genesys 20; 510 nm). The removal efficiency (Re) of Basic Red 29 was defined as:

$$Re\ \% = ((C_0 - C_e)/C_0) \times 100 \quad (1)$$

Where C_0 and C_e are the initial and equilibrium Basic Red 29 concentration (mg/L).

In addition, the adsorption capacity at the equilibrium time (q_e) is calculated according to the following equation:

$q_e = ((C_0 - C_e)V)/M$ (2)

Where V is the volume of the solution (L) and M is the mass of MAC (g).

2.3.2 Adsorption Studies

1) Adsorption Isotherms Study

Equilibrium studies that give the capacity of the adsorbent and the equilibrium relationships between adsorbent and adsorbate are described by adsorption isotherms which are usually the ratio between the quantity adsorbed and the remaining in solution at fixed temperature at equilibrium. The earliest and simplest known relationships describing the adsorption equation are the Langmuir and Freundlich isotherms.

1.1) Langmuir isotherm

The Langmuir isotherm is valid for monolayer adsorption onto a surface containing a finite number of identical sites. The isotherm assumes uniform energies of adsorption onto the surface and no transmigration of adsorbate in the plane of the surface (Dada et al., 2012). The Langmuir isotherm (Saha et al., 2010) is commonly expressed as follows:

$C_e/q_e = (1/K_L q_m) + (1/q_m) C_e$ (4)

Where q_m is the maximum adsorption capacity of MAC (mg/g), K_L is the Langmuir isotherm constant relating to the affinity of binding sites and energy of adsorption (L/mg).

1.2) Freundlich isotherm

The Freundlich isotherm applies to adsorption on heterogeneous surfaces with interaction between the adsorbed molecules, and is not restricted to the formation of a monolayer. This isotherm assumes that as the adsorbate concentration increases, the concentration of adsorbate on the adsorbent surface also increases and, correspondingly, the sorption energy exponentially decreases on completion of the sorption centres of the adsorbent (Dada et al., 2012). The well-known expressions for the Freundlich isotherm are given as:

$q_e = K_F C_e^{(1/n)}$ (5)

$\log q_e = \log K_F + (1/n) \log C_e$ (6)

Where K_F is the Freundlich isotherm constant (mg/g) and n is the adsorption intensity.

2) Adsorption Kinetics Study

The study of adsorption kinetics describes the adsorbate uptake rate and evidently, this rate controls the residence time of adsorbate uptake at the solid-solution interface. The kinetics of Basic Red 29 adsorption on MAC was analyzed using pseudo first-order, pseudo second order, and intra particle diffusion models.

2.1) Pseudo first order model

The pseudo first order model assumes that the rate of occupation of sorption sites is proportional to the number of unoccupied sites (Salam, 2013). The pseudo first order equation in linear form is expressed in equation:

$$\log (q_e - q_t) = \log q_e - (k_1/2.303)\, t \quad (7)$$

Where k_1 is the velocity constant of pseudo first order model (1/min).

2.2) Pseudo second order model

The pseudo second order model is based on the assumption that the rate limiting step may be chemical sorption involving valence forces through sharing or exchange of electrons between heavy metal ions and adsorbent (Ho and McKay, 1998).The pseudo second order equation can be given by:

$$t/q_t = (1/k_2 q_e^2) + (1/q_e)\, t \quad (8)$$

Where k_2 is the velocity constant of pseudo second order model ($g.mg^{-1}.min^{-1}$).

2.3) Intra-particle diffusion model

The intra-particle diffusion model is based on the assumption that the adsorption of a solute is controlled by intra-particle diffusion processes. It has been greatly explored in this regard and is represented by the following Cheung et al. (2007) equation.

$$q_t = K_{id} t^{1/2} + a \quad (9)$$

Where K_{id} and a are the intra-particle diffusion model constants.

3) Adsorption thermodynamics study

(Azouaou et al., 2010)

Thermodynamic parameters can be determined using the equilibrium constant K ($1/K_L$) which depends on temperature. Changes in Gibbs free energy (ΔG^0), enthalpy (ΔH^0), and entropy (ΔS^0) associated with the adsorption process were calculated using the following equations:

$$\Delta G^0 = -RT \ln K \quad (10)$$

Where R is the universal gas constant (8.314 $J.mol^{-1}.K^{-1}$) and T is temperature (K).

$$\ln K = (\Delta S^0 /R) - (\Delta H^0 /RT) \quad (11)$$

According to Eq. (11), ΔH^0 and ΔS^0 parameters can be calculated from the slope and intercept of the plot of ln K versus 1/T yields, respectively. The activation energy can be determined from the Arrhenius equation:

$$K = \ln k_0 - (Ea/RT) \quad (12)$$

Where k_0 is the independent temperature factor ($g.mg^{-1}.min^{-1}$).

RESULTS AND DISCUSSION

3.1 Characterization of MAC

Figure 3 (a) and (b) show SEM images of microstructures of PAC and MAC which was synthesized by a chemical process in this study. Figure 3 (b) shows that a number of fine particles which were observed to be dispersed on the surface MAC. The result of EDS spectra for MAC (Figure 4) discovered Fe and O. Moreover, FTIR results (Figure 5) displayed some peaks at 550.10 cm^{-1} which related to Fe – O. In fact, bands of similar frequency were reported before for iron minerals such as maghemite (γ-Fe_2O_3) (Mohan et al., 2011). Table1 shows that the saturation magnetization value of MAC was 13.59 emu/g. All results can indicate that the preparation of MAC was success.

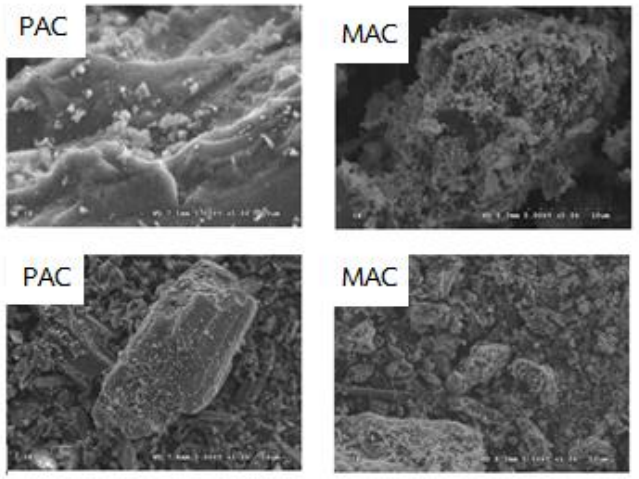

(a) (b)

Figure 3 Scanning electron microscopy images of PAC and MAC at different magnifications

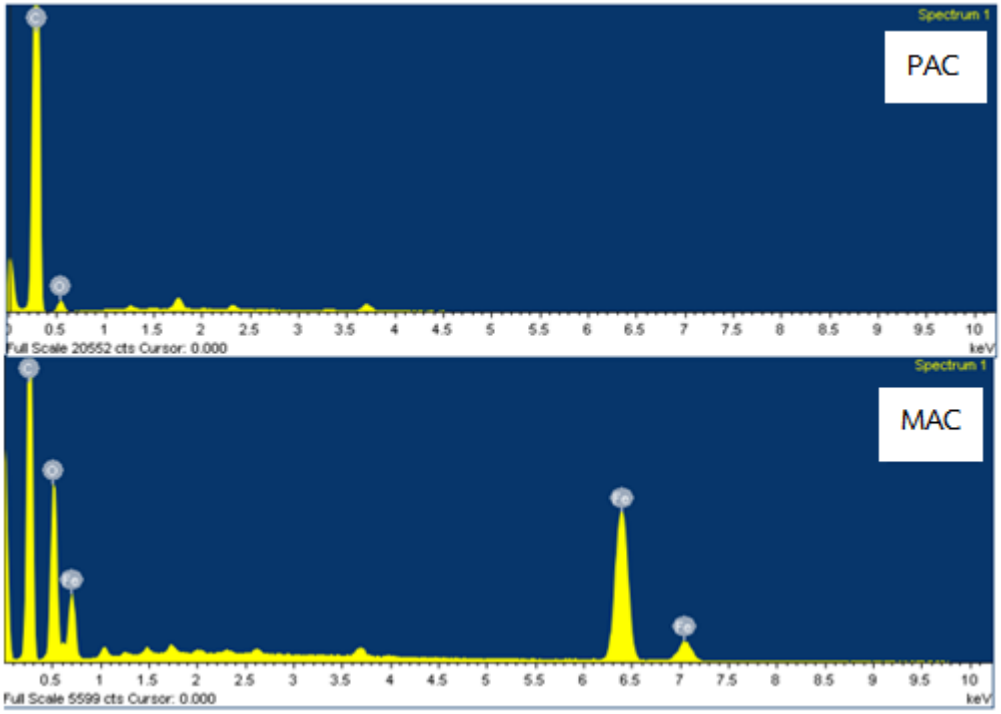

Figure 4 EDS spectra of PAC and MAC

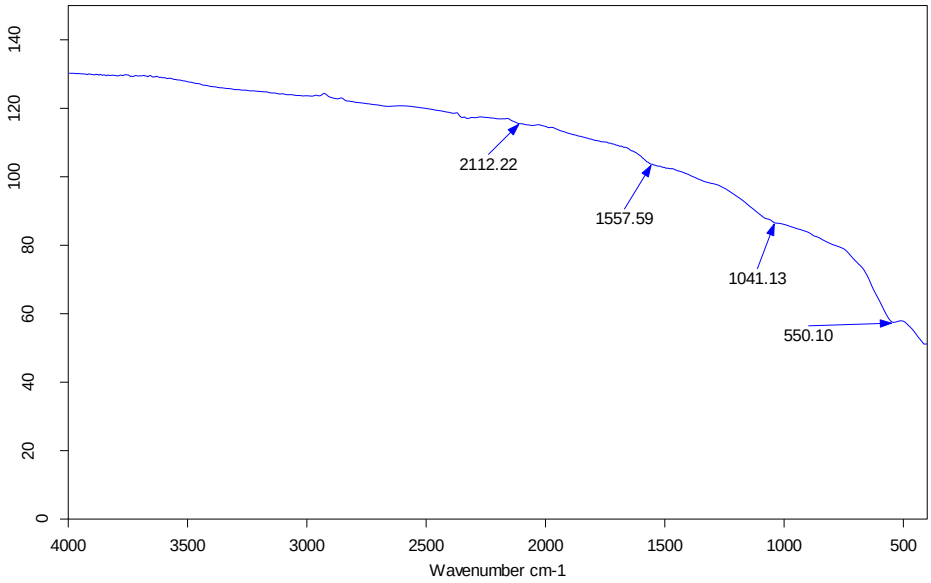

Figure 5 FT-IR spectra of MAC

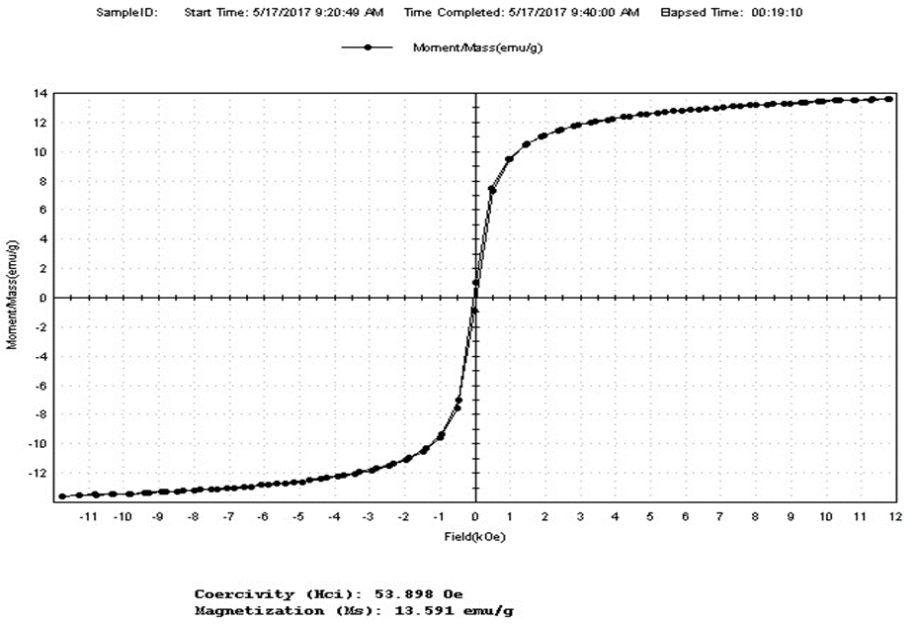

Figure 6 VSM data of MAC

Table 1 Saturation magnetization values of MACs

Researcher	Saturation magnetization value (emu/g)
Zhang J (2011)	2.40
Mohan et al. (2011)	4.47, 6.54
Zhang et al. (2015)	5.61
This research	13.59

3.2 Effect of significant adsorption factors

3.2.1 Effect of solution pH

To characterize the effect of solution pH on Basic Red 29 adsorption using MAC, a set of batch equilibrium adsorption experiments were conducted modifying the pH from 5 to 9. The results obtained are presented in Figure 7. The variation of the initial pH leads to a slight increase of adsorption capacity of Basic Red 29 when the pH value varies from 5 to 8. After this pH, the results show an insignificant decrease of the rate of Basic Red 29 adsorption on MAC. At low pH, it became completion phenomena between Basic Red 29 which has a positive charge and H^+ to adsorb on the surface of MAC. As pH increases, the electrostatic attraction between the negative surface and the cationic dye molecule increases with pH and reaches a saturation at pH 8 (Sivakumar and Palanisamy, 2009).

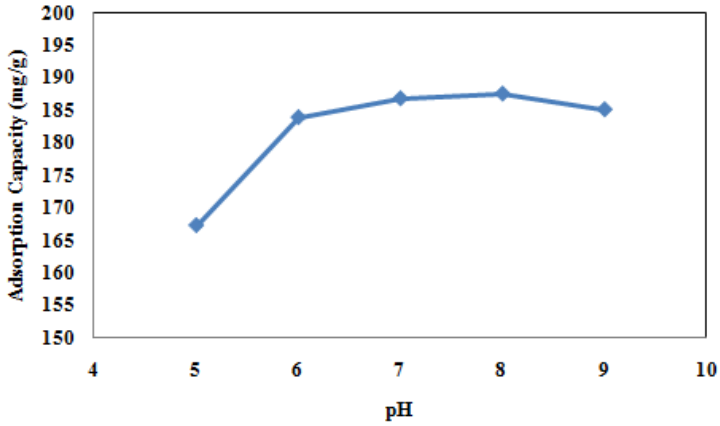

Figure 7 Influence of pH on the Basic Red 29 adsorption onto MAC at 30^0C
(contact time, 30 min; initial Basic Red 29 concentration, 500 mg/L)

3.2.2 Effect of contact time

The effect of contact time was studied for several masses of the adsorbent. The initial Basic Red 29 concentration was fixed at 100 mg/L and 500 mg/L, the agitation velocity at 150 rpm at 30^0C and solution pH at 8. Figure 8 shows a rapid initial uptake rate of Basic Red 29 until 90 min and, thereafter, the adsorption rate become practically constant. The variation in the extent of adsorption may be due to the fact that initially all sites on the surface of the sorbent were vacant and the solute concentration gradient was relatively high. Therefore, the extent of Basic Red 29 uptake decreased with the increase of contact time, which was dependent on the decrease in the number of vacant sites on MAC (Kula et al., 2007). According to the results, the equilibrium time was 90 min. Furthermore, these results (100 mg/L and 500 mg/L) indicate that the initial Basic Red 29 concentration affects to the adsorption rate.

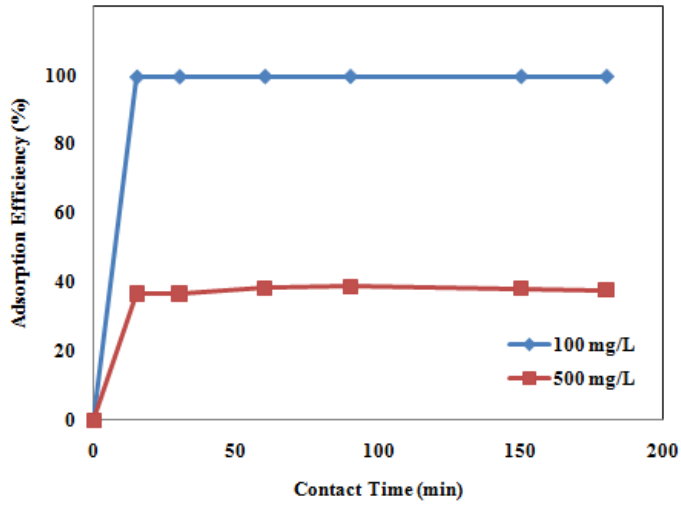

Figure 8 Influence of contact time on the Basic Red 29 adsorption onto MAC at 30^0C
(pH, 8; adsorbent dose, 100 mg)

3.2.3 Effect of initial Basic Red 29 concentration and temperature

The effect of the initial Basic Red 29 concentration on the adsorption capacity was investigated in the range 100 - 500 mg/L. In Figure 9, the results show that the adsorption capacity increases with increasing initial Basic Red 29 concentration. This is due to the increase in the driving force of the concentration gradient produced by the increase in the initial Basic Red 29 concentration (Kumar et al., 2010). Moreover, the effects of temperature (15, 30 and 60 °C) on the adsorption capacity were examined at concentrations of Basic Red 29 (100 - 500 mg/l) and the equilibrium time (90 min). The results are given in Figure 9. The adsorption capacity slightly decreases when increasing temperature from 15 to 60 °C. This may be due to the strengthening of adsorptive forces between the active sites of the adsorbents and adsorbate species and between the adjacent molecules of the adsorbed phase (Kumar et al., 2008).

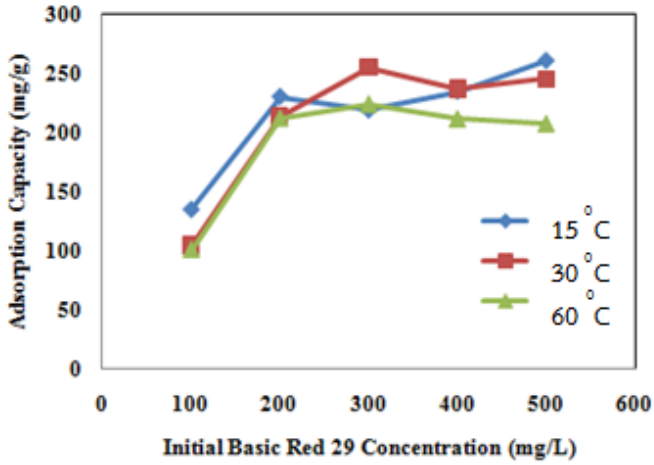

Figure 9 Influence of initial Basic Red 29 concentration and temperature on the Basic Red 29 adsorption onto MAC
(pH, 8; adsorbent dose, 100 mg)

3.3 Adsorption mechanisms

3.3.1 Adsorption isotherms

In order to describe the uptake of Basic Red 29 by MAC, the isotherms data were analyzed using Langmuir and Freundlich isotherms. The various constants of the 2 isotherms were calculated and are represented in Table 2.

Table 2 Isotherm constants for Basic Red 29 adsorption onto MAC

T (^{0}C)	Langmuir Isotherm			Freundlich Isotherm		
	q_{max} (mg/g)	K_L (L/mg)	R^2	K_F (mg/g)	1/n	R^2
15	256.41	0.156	0.9933	152	0.090	0.8201
30	238.10	0.185	0.9965	141	0.092	0.9627
60	208.33	0.521	0.9995	131	0.101	0.7999

By comparing the correlation coefficients (R^2), it can be concluded that the Langmuir isotherm provides a suitable model for the sorption system, which is based on monolayer sorption onto a surface containing a finite number of identical sorption sites (Data et al., 2012). The maximum adsorption capacity decreases with increasing T. The maximum adsorption capacity of MAC is 256.41 mg/g at 15^0C. A comparison of adsorption capacity of MAC with that of various adsorbents is given in Table 3.

Table 3 Maximum adsorption capacities of various adsorbents

Sorbents	**q_{max} (mg/g)**	**References**
Activated Carbon (*Euphorbia Antiquorum L.)*	166.67	Sivakumar and Palanisamy (2009)
Dried Activated Sludge	224.72	Chu et al. (2013)
Magnetic Activated Carbon	256.41	This research

MAC has a high adsorption capacity as compared with that of the other adsorbents. The attractive force between a negative charge of γ-Fe_2O_3 and a positive charge of Basic Red 29 may be a cause of high adsorption capacity of MAC. Therefore, MAC can be used as an alternative material to minimize the concentration of Basic Red 29 in wastewater.

3.3.2 Adsorption Kinetics

In order to define the kinetics of the Basic Red 29 adsorption, the parameters for the adsorption process were studied for contact times ranging between 0 and 180 min for different temperatures (15, 30 and 60 °C), by monitoring the percent removal of Basic Red 29 by adsorbents. The sorption equilibrium was achieved in 90 min. The kinetic data was fitted to the pseudo-first order model, pseudo-second order model, and intra-particle diffusion

model. The kinetic rate constants obtained from the three models are given in Table 4. The results fitted well with the pseudo-second order model (R^2=0.99). Therefore, the rate limiting step may be chemical sorption involving valence forces through sharing or exchange of electrons between heavy metal ions and adsorbent (Ho and McKay, 1998).

Table 4 Kinetic constants for Basic Red 29 adsorption onto MAC

Pseudo-first order model			**Pseudo-second order model**			**Intra-particle diffusion model**		
q_e (mg/g)	**k_1 (min^{-1})**	**R^2**	**q_e (mg/g)**	**k_2 ($g.mg^{-1}.min^{-1}$)**	**R^2**	**K_{id} ($mg.g^{-1}.min^{-0.5}$)**	**a**	**R^2**
3.657	0.001	0.268	204.08	0.003	0.999	36.53	0.232	0.537

3.3.3 Adsorption thermodynamics

Thermodynamic parameters as Gibbs free energy (ΔG°), enthalpy change (ΔH°), and entropy change (ΔS°) were estimated to evaluate the feasibility and the nature of adsorption processes (Table 5). The value of enthalpy change (ΔH°) and entropy change (ΔS°) were found to be -2.21 kJ/mol and 60.58 $J.mol^{-1}.K^{-1}$, respectively. The negative value of ΔH° for Basic Red 29 removal confirms that the adsorption process is exothermic in nature. The positive value of (ΔS°) implies that Basic Red 29 in bulk phase (aqueous solution) is in a much more chaotic distribution compared to the relatively ordered state of solid phase (surface of adsorbent). Similar results have been found in previous works. Moreover, Gibbs free energy change (ΔG°) is between -47.00, -37.92, and -19.74 kJ/mol for temperatures of 288, 303 and 333 K, respectively. The negative ΔG° values indicate that the adsorption was spontaneous thermodynamically (Azouaou et al., 2010).

Table 5 Thermodynamic constants for Basic Red 29 adsorption onto MAC at different temperatures

T(ºC)	T (K)	ΔG° (kJ/mol)	ΔH° (kJ/mol)	ΔS° ($J.mol^{-1}.K^{-1}$)
15	288	- 47.00	-2.21	60.58
30	303	- 37.92		
60	333	- 19.74		

CONCLUSION

The good capacity of MAC to remove Basic Red 29 from aqueous solution was demonstrated in this study, highlighting its potential for effluent treatment processes. The kinetic experiments showed that the adsorption is rapid and maximum adsorption capacities are achieved in 90 min. The effects of several parameters on the removal of Basic Red 29 as pH, contact time, initial Basic Red 29 concentration, and temperature were investigated. The results indicated that the optimal condition for Basic Red 29 adsorption was pH, 8; contact time, 90 min; initial Basic Red 29 concentration, 200 mg/L; and temperature, 15^0C. The maximum adsorption capacity was 256.41 mg of Basic Red 29 /g of MAC. The equilibrium data fitted well with a Langmuir isotherm, so the adsorption was monolayer and site-specific. The adsorption kinetics followed the mechanism of the pseudo-second-order model, confirming chemical sorption as the rate-limiting step of adsorption mechanisms. Moreover, the thermodynamic parameters present that the adsorption was a spontaneous reaction, an exothermic reaction, and an easy reaction.

ACKNOWLEDGEMENTS

Faculty of Environment and Resource Studies, Mahasarakham University financially supports disseminating the results published under this work.

REFERENCES

Azouaou N, Sadaoui Z, Djaafri A, Mokaddem H. Adsorption of cadmium from aqueous solution onto untreated coffee grounds: Equilibrium, kinetics and thermodynamics. Journal of Hazardous Materials 2010; 184(1-3): 126-134.

Aksu Z, Kabaskal E. Batch adsorption of 2,4-dichlorophenoxyacetic acid (2,4-D) from aqueous solution by granular activated carbon. Separation and Purification Technology, 2004; 35, 223-240.

Cheung WH, Szeto YS, McKay G. Intraparticle diffusion processes during acid dye adsorption onto chitosan. Bioresource Technology 2008; 98: 2897-2904.

Chu HC, Lin LH, Liu HS, Chen KM. Utilization of Dried Activated Sludge for the Removal of Basic Dye from Aqueous Solution. Desalination and Water Treatment 2013; 51(37-39): 7074-7080.

Dada AO, Olalekan AP, Olatunya AM, & DADA O. Langmuir, Freundlich, Temkin and Dubinin–Radushkevich Isotherms Studies of Equilibrium Sorption of Zn^{2+} Unto Phosphoric Acid Modified Rice Husk. IOSR Journal of Applied Chemistry (IOSR-JAC) 2012; 3(1): 38-45.

Ho YS, McKay G. Sorption of Dye from Aqueous Solution by Peat. Chemical Engineering Journal 1998; 70: 115-124.

Igwe JC, Abia AA. Adsorption isotherm studies of Cd (II), Pb (II) and Zn (II) ions bioremediation from aqueous solution using unmodified and EDTA-modified maize cob.

Eclética Química 2007; 32(1): 33-42.

Iqbal MJ, Ashiq MN. Adsorption of dyes from aqueous solutions on activated charcoal. Journal of *Hazardous Materials* 2007; 139, 57–66.

Kismir Y, Aroguz AZ. Adsorption characteristics of the hazardous dye brilliant green on

Saklikent mud. Chemical Engineering Journal 2011; 172, 199–206.

Kula I, Uğurlu M, Karaoğlu H, Celik A. Adsorption of Cd(II) ions from aqueous solutions using activated carbon prepared from olive stone by $ZnCl_2$ activation. Bioresource Technology 2007; 99(3): 492-501.

Kumar PA, Chakraborty S, Ray M. Removal and recovery of chromium from wastewater using short chain polyaniline synthesized on jute fiber. Chemical Engineering Journal 2008; 141: 130–140.

Kumar PS, Ramalingam S, Senthamarai C, Niranjanaa M, Vijayalakshmi P, Sivanesan S. Adsorption of dye from aqueous solution by cashew nut shell: studies on equilibrium isotherm, kinetics and thermodynamics of interactions. Desalination 2010; 261: 52-60.

Mohan D, Sarswat A, Singh VK, Alexandre-Franco M, Pittman Jr CU. Development of magnetic activated carbon from almond shells for trinitrophenol removal from water. Chemical Engineering Journal 2011; 172: 1111-1125.

Saha P, Chowdhury S, Gupta S, Kumar I, Kumar R. Assessment on the removal of malachite green using tamarind fruit shell as biosorbent. Clean Soil Air Water 2010; 38 (5–6): 437.

Salam MA. Removal of heavy metal ions from aqueous solutions with multi- walled carbon nanotubes: kinetic and thermodynamic studies. International Journal of Environmental Science and Technology 2013; 10(4):677–688.

Sivakumar P, Palanisamy PN. Adsorption Studies of Basic Red 29 by a Non-conventional activated carbon prepared from Euphorbia Antiquorum L. International Journal of ChemTech Research 2009; 1(3): 502-510.

Wang LK, Hung YT, Lo HH. Yapijakis C. Handbook of industrial and hazardous wastes treatment (2nd ed.). CRC Press; 2004; 10: 141-147.

Weber Jr WJ, Morris JC, Sanit J. Kinetics of adsorption on carbon from solution. Journal of the *Sanitary Engineering Division* ASCE 1963, *89*, 31-38.

Zhang J. Preparation and Characterization of Magnetic Coal-based Activated Carbon in the presence of Fe_3O_4. Advanced Materials Research 2011; 393-395: 1355-1358.

Zhang S, Tao L, Jiang M, Gou G, Zhou Z. Single-step synthesis of magnetic activated carbon from peanut shell. Materials Letter 2015; 157: 281-284.

Photocatalytic degradation of organic pollutants by monoclinic $BiVO_4$ photocatalyst synthesized using cyclic microwave irradiation combined with calcination process

Wimonnat Choklap[1,2], Auttaphon Chachvalvutikul[1,2], Sulawan Kaowphong[2,3,4*]

[1] Graduate School, Chiang Mai University, Chiang Mai 50200, Thailand
[2] Department of Chemistry, Faculty of Science, Chiang Mai University, Chiang Mai 50200, Thailand
[3] Environmental Science Research Center, Faculty of Science, Chiang Mai University, Chiang Mai 50200, Thailand
[4] Center of Excellence for Innovation in Chemistry, Faculty of Science, Chiang Mai University, Chiang Mai 50200, Thailand
Corresponding author: e-mail: sulawank@gmail.com

ABSTRACT

In this work, the m-$BiVO_4$ photocatalyst was successfully synthesized by a cyclic microwave irradiation combined with a calcination process. Effect of microwave radiation powers (300, 450, 600, and 700 W) on physicochemical properties and photocatalytic activity of the synthesized powders were investigated. The synthesized samples were characterized by X-ray powder diffraction spectroscopy (XRD), field emission scanning electron microscopy (FESEM), and UV-vis diffuse reflectance spectroscopy (UV-vis DRS) techniques. XRD spectra of the synthesized powders were indexed as a highly crystalline $BiVO_4$ with a monoclinic crystal structure. FESEM and UV-vis DRS analyses revealed the increase in the particle size and the red-shift of the absorption band edge of the m-$BiVO_4$ particles with the increasing of the microwave power. Photocatalytic activity and selectivity of the photocatalyst

samples for degrading organic dyes, representing organic pollutants, were investigated. The m-$BiVO_4$ photocatalyst synthesized at 700 W exhibited the highest degradation efficiency. In addition, this photocatalyst showed higher photocatalytic selectivity on the cationic dyes (MB and BG) rather than the anionic dye (MO) used.

Keywords: Cyclic microwave synthesis, m-$BiVO_4$, Photocatalytic degradation, Organic pollutants removal

INTRODUCTION

Bismuth vanadate ($BiVO_4$) has been regarded as a promising visible-light driven semiconductor photocatalyst for water splitting [1], O_2 evolution [2], and degrading of organic pollutants in wastewater [3]–[5] due to its narrow band gap energy, high chemical stability against photocorrosion over long-term illumination, excellent optoelectronic properties, and non-toxicity [6], [7]. It is known that there are three polymorphic forms of $BiVO_4$: tetragonal-zircon (t-z), tetragonal-scheelite (t-s), and monoclinic-scheelite (m-s), which depends on different synthesis conditions [8]. Generally, the m-$BiVO_4$ structure with band gap energy of 2.4 eV exhibits a better photocatalytic performance in comparison to the t-$BiVO_4$ structure with band gap energy of 2.9-3.1 eV [9], [10]. The smaller band gap energy of the m-$BiVO_4$ is due to a short transition of photogenerated electron in the additional Bi 6s orbitals in its valence band to the V 3d orbitals in its conduction band, in comparison to the t-$BiVO_4$ which only consists of O 2p orbitals [9]. This phenomena facilitates the better UV-vis absorption properties of the m-$BiVO_4$ [10], promoting the photocatalytic performance of the m-$BiVO_4$. In addition, the energically dislocation of the Bi^{3+} and V^{5+} cations in the m-$BiVO_4$ crystal structure from the centrosymmetric sites along the c axis [11] as well as the smaller effective masses of both

electron and hole generated in the m-$BiVO_4$ can also facilitate the electron-hole pair separation and migration [12]. However, processes of high-temperature synthesis were needed to prepare m-$BiVO_4$ [13].

Many methods for the preparation of m-$BiVO_4$ such as solid-state reaction [14], sol-gel [15], and hydro/solvo -thermal [2]–[4], [6], [16] methods have been reported. However, these methods have some disadvantages, for example, an expensive and complicated equipment or a long reaction time with high energy consumption are required. Therefore, many efforts have been made to develop the synthesis approach which simple, rapid, and economical. Microwave radiation method can be used to overcome these disadvantages as it offers fast chemical reactions, leading to short reaction time, energy saving, and high efficiency for inorganic materials production [17]–[19]. During microwave heating, polar molecules and ions in a solution can orientate with the rapidly changing alternating electric field; thus, heat is generated by the rotation, friction, and collision of molecules, causing a local temperature rise with short reaction time and high reaction rate. This causes the thermal gradients to minimize and reduce the time for particle diffusion; thus, the desired materials can be formed in a shorter time, in comparison to the conventional heating method [20], [21].

In this work, our group reported the synthesis of m-$BiVO_4$ powder by cyclic microwave irradiation, followed by a calcination process. Herein, a domestic microwave oven was applied, instead of an expensive microwave synthesis reactor, aiming to reduce costs of the material production. Typically, a domestic microwave operating with a pulsed irradiation mode usually gives a higher microwave power in the reaction system than the applied power. Consequently, the spontaneous non-controllable exotherms are occurred due to the generation and implosive collapse of a large number of unstable hotspots

in the reaction solution during the microwave irradiation process. To minimize the risk of the uncontrolled overheating, a cyclic-heating route, by providing a more relaxation time, is an alternative and economical way for chemical synthesis. In addition, ethylene glycol was used as a solvent due to its high dielectric loss tangent and high boiling point as well as an ability to prevent a chemical overflowing during the reaction process [22]. The photocatalytic activities of the m-$BiVO_4$ samples synthesized using different microwave powders (300, 450, 600, and 700 W) were examined towards the degradation of methylene blue (MB) under visible light irradiation. Effect of initial MB concentrations on the photocatalytic activity of the m-$BiVO_4$ photocatalyst was also investigated. Moreover, the selectivity for the photodegradation of organic dyes, such as methylene blue (MB), brilliant green (BG) and methyl orange (MO) was also studied.

METHODOLOGY

Synthesis of m-$BiVO_4$

For the synthesis of m-$BiVO_4$, 6.25 mmol of $Bi(NO_3)_3 \cdot 5H_2O$ and 6.25 mmol of NH_4VO_3 were separately dissolved in 25.0 mL of ethylene glycol. The solutions were mixed under vigorously stirring for 30 min. Then, the mixed solution was placed in a domestic microwave oven (2450 MHz-EMS28205, Electrolux). The irradiated microwave powers studied in this experiment were 300, 450, 600, and 700 W. After irradiating for 75 cycles (30 s on and 30 s off), the obtained powder was filtered, washed with deionized water, and dried in an oven. Finally, the dried powder was calcined at 600 °C for 6 h. The synthesized m-$BiVO_4$ powders are denoted as m-$BiVO_4$ (x W), where x represents the microwave radiation powers used in the microwave synthesis process.

Characterizations

An X-ray diffraction spectrometer (XRD, Rigaku Miniflex II) was used to determine crystal structure, purity and crystallinity of the synthesized

powders. A field emission scanning electron microscope (FESEM, JEOL JSM-6335F) was used to determine particle size and morphology of the powders. Energy dispersive X-ray spectroscopy (EDX) was used in conjunction with the FESEM for an elemental analysis. An optical property was also studied by a UV-vis diffuse reflectance spectrometer (UV-vis DRS, UV-1800 Shimadzu), equipped with specular reflectance measurement attachment.

Photocatalytic degradation experiment

Photocatalytic activities of all photocatalysts for the degradation of some organic dyes (methylene blue; MB, brilliant green; BG, and methyl orange; MO) were evaluated. The photocatalyst (100 mg) was dispersed in aqueous solution of organic dyes (200 mL, 10 mgL^{-1}). To reach the adsorption/desorption equilibrium on the surface of photocatalyst, the suspension was kept in dark with constant stirring for 30 min. After that, the suspension was exposed to the 50 W of LED lamp for 270 mins. At every 30 min of irradiation, a 5 mL of suspension was taken from the reaction system and then measured the degradation efficiency at the wavelength of maximum absorption by a UV-vis spectrophotometer. Organic dye photolysis (without catalyst) was also performed under the same experimental conditions. The decolorization efficiency (%DE) was calculated using the following equation; $\%DE = [(C_0 - C)/C_0] \times 100$, where C_0 is the initial dye concentration and C is the dye concentration after the light irradiation.

RESULTS AND DISCUSSION

The XRD patterns of all synthesized powders are shown in Figure 1. No diffraction peak can be observed for the un-calcined m-$BiVO_4$ powder, suggesting that m-$BiVO_4$ has not yet formed even irradiated at 700 W of microwave power. After calcination, the diffraction peaks of all m-$BiVO_4$ samples, corresponding to a monoclinic crystal structure of $BiVO_4$ (JCPDs No. 014-0688), are

observed. In addition, the sharp and narrow diffraction peaks of the m-$BiVO_4$ powders indicate high crystallinity. These results suggest that the synthetic method developed in this study is a simple and rapid route for producing *purified* m-$BiVO_4$ phase with highly crystalline.

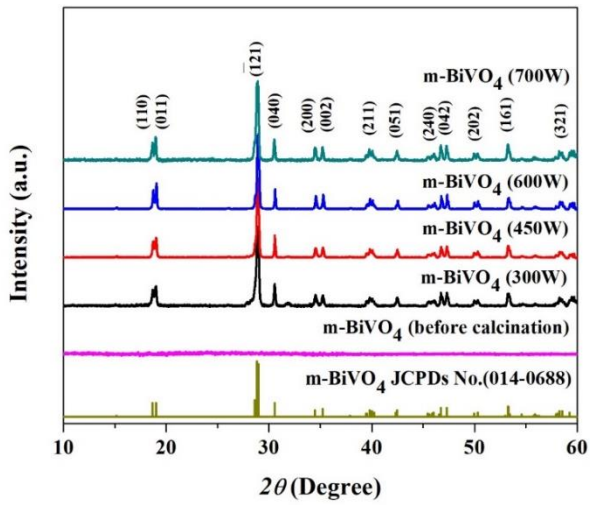

Figure 1 XRD patterns of the un-calcined m-$BiVO_4$ powder and the m-BiVO4 powders synthesized using a combined microwave-calcination process.

The FTIR spectra of the un-calcined and calcined m-$BiVO_4$ (700 W) powders are shown in Figure 2. The FTIR spectrum of the un-calcined powder shows that O–H stretching, O–H bending C–H bending and V–O stretching signals is detected at 3456, 1622, 1384 and 810 cm^{-1}, respectively [19]. In addition, no peak shift or splitting is observed, confirming that the complexation between Bi^{3+} ions and ethylene glycol is not taken place. This suggests that the ethylene glycol molecules are physically adsorbed on the particle's surface as neutral species, which results in the amorphous-liked XRD pattern of the un-calcined powder. For the calcined powder, the absorption peaks of O–H

stretching, O–H bending, and C–H bending are disappeared illustrating that the ethylene glycol molecules are completely removed from the surface of the m-$BiVO_4$ particles by the calcination process.

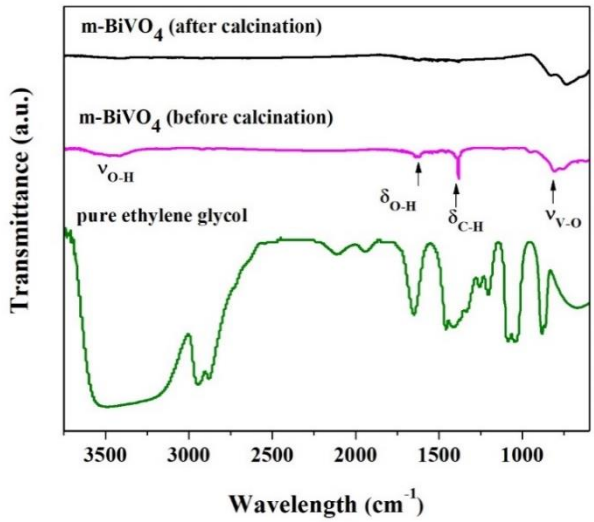

Figure 2. FTIR spectrum of the m-$BiVO_4$ (700 W) powders before and after calcination.

The FESEM images of the m-$BiVO_4$ powders synthesized at different microwave powers are shown in Figure 3. The FESEM images of all m-$BiVO_4$ powders (Figure 3(a-d)) reveals the average particle sizes of 0.57, 0.73, 0.84, and 1.56 μm for the m-$BiVO_4$ particles synthesized at 300, 450, 600, and 700 W, respectively. *Using the higher power of microwave radiation,* the tendency of the m-$BiVO_4$ particle size is larger. This is probably because *the kinetic rates of the conductive species in the reaction system are enhanced when the higher microwave power is supplied [22]. Consequently, the primary particles with smaller size are firstly formed [23]. After that,* the smaller-size particles, having the larger relative surface area and higher surface energy, *tend to agglomerate by physical interactions to reduce their surface energies. Finally, under* the given calcination temperature, the agglomerated

particles are aggregated to form larger particles [24]. EDX spectrum of the m-$BiVO_4$ (700 W) powder (Figure 3(e)) reveals the X-ray energy values of the Bi, V, and O elements. Notably, the additional X-ray signals of C, Au, and Cu elements come from the carbon tape used in the preparation of the sample stub, coated gold, and supporting copper holder, respectively.

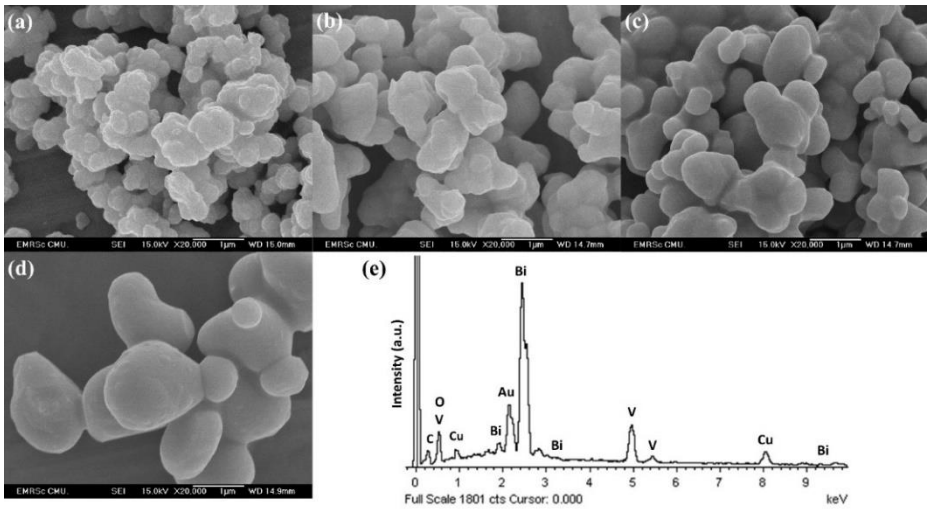

Figure 3. FESEM images of the m-$BiVO_4$ powders synthesized at (a) 300, (b) 450, (c) 600, and (d) 700 W, respectively. (e) EDX spectrum of the m-$BiVO_4$ powder synthesized at 700 W.

Figure 4 shows UV-vis DRS spectra of the m-$BiVO_4$ powders synthesized at different microwave powers. The reflectance spectra were converted to an absorption coefficient *F(R),* according to the Kubelka-Munk (K-M) equation: $F(R) = (1-R)^2/2R$, where R is the proportion of light reflected. The K-M absorption spectra of the m-$BiVO_4$ powders exhibit light absorption in the region of visible light. The absorption band edge exhibits red-shift when the microwave power is increased. In addition, the m-$BiVO_4$ powder synthesized at 700 W shows stronger absorption intensity. The onsets of the absorption band edges of the m-$BiVO_4$ powders synthesized at 300, 450, 600, and 700 W are 535, 540,

546, and 550 nm, respectively, which correspond to 2.32, 2.30, 2.27, and 2.25 eV.

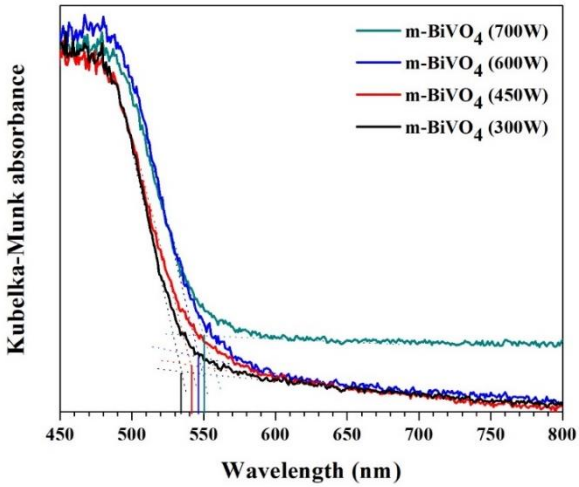

Figure 4. UV-vis DRS spectra of the m-$BiVO_4$ powders synthesized at different microwave powers.

Figure 5(a) shows %DE of MB in the presence of the m-$BiVO_4$ photocatalysts. For the blank experiment, the concentration of MB remains unchanged indicating the stability of MB under visible light irradiation and the photolysis can be ignored. The m-$BiVO_4$ photocatalyst synthesized at 300, 450, 600, and 700 W exhibits higher photocatalytic degradation with %DE of 47.21, 55.57, 78.75, and 99.09%, respectively. The pseudo-first-order kinetic plots of the photodegradation of MB is presented in Figure 5(b). The superior photocatalytic performance of the m-$BiVO_4$ (700 W) photocatalyst in comparison to the other m-$BiVO_4$ photocatalysts is probably due to its optical absorption properties. The m-$BiVO_4$ (700 W) photocatalyst exhibits higher ability to absorb visible light and smaller band gap energy (Figure 4), promoting the photogeneration of electron and hole for the

photocatalytic reaction process. Figure 5(c) shows the photodegradations of BG and MO in the presence of the m-$BiVO_4$ (700 W) photocatalyst, in comparison to MB. The %DE of MB (99.09%) is higher than that of BG (40.64%) and MO (15.78%), respectively. The *k* values for the photodegradation of MB, BG, and MO (Figure 5(d)) are 16.4 x 10^{-3}, 1.9 x 10^{-3}, and 0.8 x 10^{-3} min^{-1}, respectively. These results suggest that the synthesized m-$BiVO_4$ photocatalyst has higher photocatalytic selectivity on the cationic dye (MB and BG) rather than the anionic dye (MO). This is probably because the surface of the m-$BiVO_4$ photocatalyst has a *negative charge* [11], which are more suitable to *adsorb the cationic dyes*.

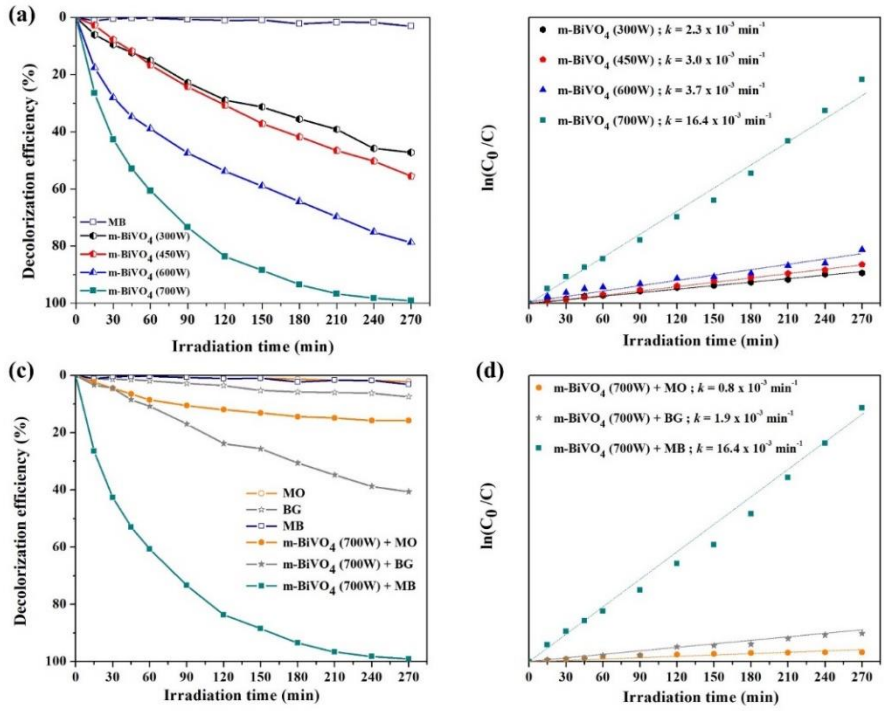

Figure 5. (a) Photocatalytic activities and (b) pseudo-first-order kinetics of the m-$BiVO_4$ photocatalysts for the photodegradation of MB under visible light irradiation. (c) and (d) A comparison of the photodegradation of BG, MO and MB in the presence of the m-$BiVO_4$ (700 W) photocatalyst under visible light irradiation.

Under visible light irradiation, two competitive processes take place simultaneously during the photocatalytic degradations of MB, BG, and MO; *N*-de-alkylation (*N*-de-methylation or *N*-de-ethylation) and destruction of chromophore structure. Considering the UV-vis absorption spectra changes of the photodegradation of MB, BG, and MO shown in Figure 6(a-c), the maximum absorption bands of MB, BG, and MO located at the wavelengths of 664, 625, and 464 nm, respectively, decrease gradually upon increasing irradiation time. In addition, the maximum absorption bands of MB and BG shift to lower wavelength, implying that the photodegradations of MB and BG are due to the *N*-de- alkylation of MB and BG molecules [25], [26]. Thus, under the same photocatalytic degradation pathway of MB and BG, lower photocatalytic activity towards BG than that of MB is probably attributed to a more complicated and larger structure of the BG molecule. For the MO photodegradation process, the maximum absorption bands of MO are not shifted, suggesting the photodegradation with cleavage of the chromophore structure. So, the lowest photocatalytic degradation of MO (anionic dye) in comparison to the other cationic dyes is attributed to the poor adsorption of the anionic MO molecules on the surface of the photocatalyst, which is one of the important steps for the photodegradation process [27].

The effect of initial dye concentrations (10, 20, and 30 ppm) on the photocatalytic activity of the m-$BiVO_4$ (700 W) photocatalyst was also studied. The photocatalyst dosage (100 mg) was kept the same in all these experiments. As illustrated in Figure 7, the %DE of the photocatalyst for degrading 10, 20, and 30 ppm of MB are 99.09, 69.01, and 18.74%, respectively. It was found that the photocatalytic activity of the photocatalyst decreases with increasing the initial MB concentration. This is probably caused by the following two reasons; 1.) at high MB concentration, the

photocatalyst's active sites are completely covered by the MB molecules. Consequently, the generation of reactive species on the photocatalyst surface is decreased, and 2.) the increase in the initial MB concentration limits the path length of photons entering to the MB solution. The generation of reactive species remains constant at a fixed photocatalyst dosage [28].

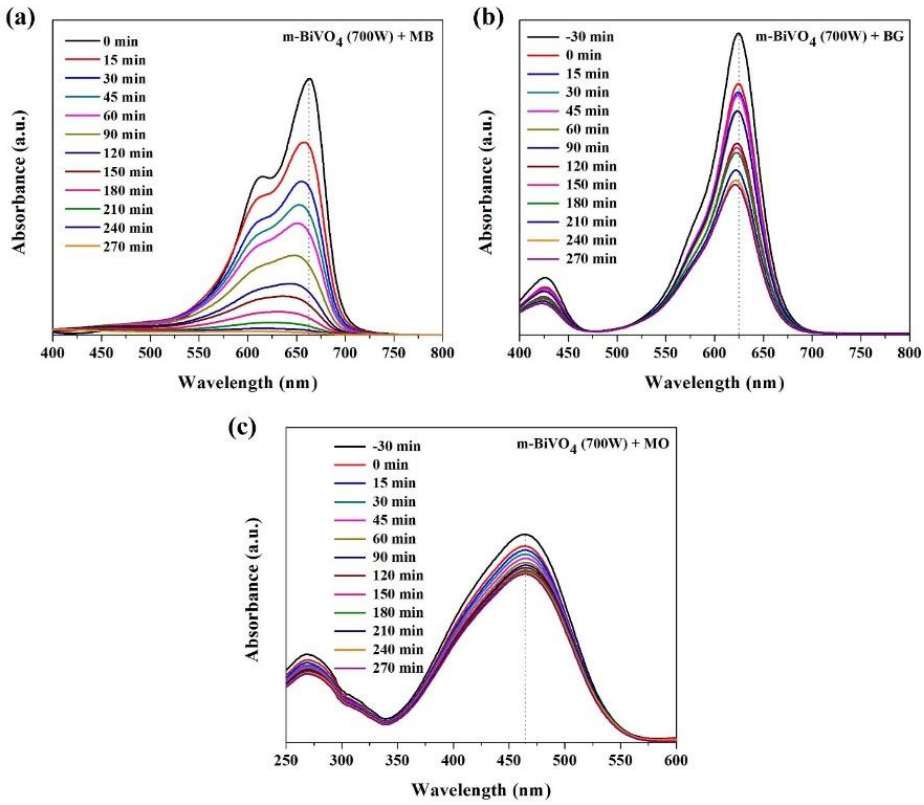

Figure 6. UV-vis absorption spectra changes of (a) MB, (b) BG, and (c) MO aqueous solutions as a function of the reaction time.

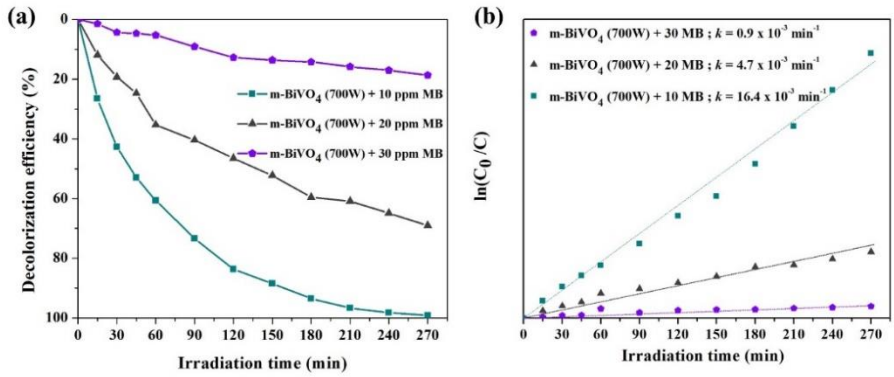

Figure 7. (a) %DE and (b) photocatalytic reaction kinetics of the m-$BiVO_4$ (700 W) photocatalyst for the photodegradation of MB with different initial dye concentrations.

ACKNOWLEDGEMENTS

This research work was supported by the Thailand Research Fund (TRF) and the Office of the Higher Education Commission (Grant number MRG6080270), the Center of Excellence for Innovation in Chemistry (PERCH-CIC), Office of the Higher Education Commission, Ministry of Education (OHEC), and partially supported by Chiang Mai University. W. Choklap and A. Chachvalvutikul would like to thank the Development and Promotion of Science and Technology Talents Project, and Graduate School, Chiang Mai University.

REFERENCES

[1] Wang Q, *et al.* Z-scheme water splitting using particulate semiconductors immobilized onto metal layers for efficient electron relay. Journal of Catalysis 2015; 328: 308–315.

[2] Thalluri SM, *et al.* Elucidation of important parameters of $BiVO_4$ responsible for photo-catalytic O_2 evolution and insights about the rate of the catalytic process. Chemical Engineering Journal 2014; 245: 124–132.

[3] Zhang A, *et al.* Effects of pH on hydrothermal synthesis and characterization of visible-light-driven $BiVO_4$ photocatalyst. Journal of Molecular Catalysis A: Chemical 2009; 304: 28-32.

[4] Chen L, *et al.* Shape-controlled synthesis of novel self-assembled $BiVO_4$ hierarchical structures with

enhanced visible light photocatalytic performances. Materials Letters 2016; 176: 143-146.

[5] Lopes OF, *et al*. Controlled synthesis of $BiVO_4$ photocatalysts: Evidence of the role of heterojunctions in their catalytic performance driven by visible-light. Applied Catalysis B: Environmental 2016; 188: 87-97.

[6] Zhang X, *et al*. Selective synthesis and visible-light photocatalytic activities of $BiVO_4$ with different crystalline phases. Materials Chemistry and Physics 2007; 103: 162-167.

[7] Zhang L, *et al*. Efficient removal of methylene blue over composite-phase $BiVO_4$ fabricated by hydrothermal control synthesis. Materials Chemistry and Physics 2012; 136: 897-902.

[8] Dang S, *et al*. Shape-controlled synthesis of $BiVO_4$ hierarchical structures with unique natural-sunlight-driven photocatalytic activity. Applied Catalysis B: Environmental 2014; 152-153: 413-424.

[9] Samsudin MFR, *et al*. Epigrammatic progress and perspective on the photocatalytic properties of $BiVO_4$-based photocatalyst in photocatalytic water treatment technology: A review. Journal of Molecular Liquids 2018; 268: 438–459.

[10] Tokunaga S, *et al*. Selective preparation of monoclinic and tetragonal $BiVO_4$ with scheelite structure and their photocatalytic properties. Chemistry of Materials 2001; 13: 4624-4628.

[11] Kweon KE, Hwang GS. Hybrid density functional study of the structural, bonding, and electronic properties of bismuth vanadate. Physical review B 2012; 86: 165209.

[12] Park Y, *et al*. Progress in bismuth vanadate photoanodes for use in solar water oxidation. Chemical Society Reviews 2013; 42: 2321-2337.

[13] Li G, *et al*. Difference in valence band top of $BiVO_4$ with different crystal structure. Materials Chemistry and Physics 2012; 136: 930-934.

[14] Gotic´ M, *et al*. Synthesis and characterisation of bismuth(III) vanadate. Journal of Molecular Structure 2005; 744–747: 535–540.

[15] Wang M, *et al*. High performance B doped $BiVO_4$ photocatalyst with visible light response by citric acid complex method. Spectrochemica Acta Part A: Molecular and Biomolecular Spectroscopy 2013; 114: 74-79.

[16] Ou M, *et al*. Graphene-decorated 3D $BiVO_4$ superstructure: Highly reactive (040) facets formation and enhanced visible-light-induced photocatalytic oxidation of NO in gas phase. Applied Catalysis B: Environmental 2016; 193: 160–169.

[17] Zhang Y, *et al*. Monoclinic $BiVO_4$ micro-/nanostructures: Microwave and ultrasonic wave combined synthesis and their visible-light photocatalytic

activities. Journal of Alloys and Compounds 2013; 551: 544–550.

[18] Pingmuang K, *et al*. Phase-controlled microwave synthesis of pure monoclinic $BiVO_4$ nanoparticles for photocatalytic dye degradation. Applied Materials Today 2015; 1: 67–73.

[19] Abraham SD, *et al*. Eco-friendly and green synthesis of $BiVO_4$ nanoparticle using microwave irradiation as photocatalayst for the degradation of Alizarin Red S. Journal of Molecular Structure 2016; 1113: 174-181.

[20] Zhu YJ, Chen F. Microwave-Assisted Preparation of Inorganic Nanostructures in Liquid Phase. Chemical Reviews 2014; 114: 6462−6555.

[21] Gawande MB, *et al.* Microwave-assisted chemistry: Synthetic applications for rapid assembly of nanomaterials and organics. Accounts of Chemical Research 2014; 47: 1338−1348.

[22] Chumha N, *et al.* A single-step method for synthesis of $CuInS_2$ nanostructures using cyclic microwave irradiation. Ceramics International 2016; 42: 15643-15649.

[23] Mousavi-Kamazani M, *et al.* Synthesis and characterization of Cu_2S nanostructures via cyclic microwave radiation. Superlattices and Microstructures 2013; 63: 248–257.

[24] Walterr D. Nanomaterials. Weinheim: Wiley-VCH Verlag GmbH & Co. KGaA 2013: 9-24

[25] Zhang T, *et al.* Photooxidative N-demethylation of methylene blue in aqueous TiO_2 dispersions under UV irradiation. Journal of Photochemistry and Photobiology A: Chemistry 2001; 140: 163–172.

[26] Chen CC, *et al.* Photocatalyzed *N*-de-ethylation and degradation of Brilliant Green in TiO_2 dispersions under UV irradiation. Desalination 2008; 219: 89–100.

[27] Hao R, *et al.* Efficient adsorption and visible-light photocatalytic degradation of tetracycline hydrochloride using mesoporous BiOI microspheres. Journal of Hazardous Materials 2012; 209– 210: 137– 145.

[28] Vignesh K, *et al.* Visible light assisted photocatalytic activity of TiO_2-metal vanadate (M=Sr, Ag and Cd) nanocomposites. Materials Science in Semiconductor Processing 2013; 16: 1521–1530.

People and data: two factors for sustainable development of water quality management in Pak Phanang river basin

Karanrat Thammarak[1*], Chuthamat Rattikansukha[2], Jenjira Kaewrat[2], Rungruang Janta[2], Surasak Sichum[3]

[1*] School of Informatics, Walailak University, Thailand

[2] School of Engineer and Resources, Walailak University, Thailand

[3] School of Science, Walailak University, Thailand.

Corresponding author: e-mail: kanchan.th@mail.wu.ac.th

ABSTRACT

In order to improve the sustainable development of water quality management in Thailand. This paper aims to study in two factors of technology arrangements are data and people. The paper determines the 20 sampling points to assess water quality, applies 10 parameters for WQI assessment and develops a mobile and web application to collect and represent WQI data. In addition, the paper develops open data of water quality assessment that can support both people and machine. overall satisfaction is in a good rank (4.00). In a part of tool usage, a top three responsive are following the WQI in each month (66.7%), Sending a monthly WQI value (53.3%) and calculating and using open data (40%). For the future, this paper focuses on a minimization method for optimizing WQI parameter list and classify parameter list that suitable with each sampling points.

Keywords: Water Quality Assessment, Mobile Application, Open Data, Pak Panang river basin, Sustainable Development

INTRODUCTION

In September 2015, the member states of the United Nations endorsed the Sustainable Development Agenda 2030, which will achieve the goal within 15 years, consisting of 17 sustainable development goals with 169 specific targets and 230 indicators. The SD Agenda aims to apply all SDG to all countries, regions, cities. However, there are many challenges for driving the SDGs to all sector. For example, it lacks focus in linking livelihoods and governance debates to development (Eloise M.Biggs et al., 2015), lacks technological and institutional arrangements which need to adapt to local conditions and a distinction level such as local, regional and global public action. (Mathew Kurian, 2017). In addition, various policy, institutional, and regulatory have been introduced to address the challenges including the data disruption today such as open data, big data, data mining, blockchain and data science were changing personal life, society, and globalization. In Thailand, Sufficiency Economy Philosophy is a development framework that is to achieve sustainable development goals. In addition, Currently, Thailand 4.0 reflects the integration of the sufficiency economy philosophy by focusing on the design of the value-based economic system through new technologies coupled with environmentally friendly.

Focusing on water quality management, there are many SD's targets such as improving water quality by reducing pollution, increasing a water-use efficiency across all sectors and integrating water resources management at all level. In Thailand, The Water Resource Management Strategic Plan 2015 – 2026 was established for supporting the SDG's sixth goal. It has provided an approach in term of water-use efficiency and water resource infrastructure. The challenge in Thailand remains in remote rural areas. For this problem can reduce by using technological arrangement which is an important

opportunity to driven a sustainable development in local condition and a distinct level of public action. The technological arrangement is relevant in various forms and people groups. In term of form, many formats can apply for each level such as mobile application, web application, big data analysis (Caitlin D. Cottrill, 2017) and open data (Nataša Veljković,2015). In term of people, groups are named to a stakeholder who used the technology such as individual, local authorities, government, academic and researcher and others. In order to improve the sustainable development of water quality management in Thailand. This paper aims to study in two factors of technology arrangements are data and people. The initial scope of technology arrangements starts at a quality assessment of surface water. The sample area is Pakphanang river basin. In addition, this paper applied a sustainable livelihood approach (Eloise M. Biggs, 2015) to identify stakeholder requirements. A livelihood comprises the capabilities, assets (stores, resources, claims and access) and activities required for a means of living: (Krantz L,200). SL approach has four basic resources are the natural capital, economic or financial capital, human capital, and social capital. Sarah Parkinson and Ricardo Ramírez applied the sustainable livelihoods framework for assessing the contribution of ICTs to development projects. SL approach can help to broaden their scope in a manageable way and prove more analytically rigorous than other available methods (Sarah Parkinson and Ricardo Ramírez, 2007). The remaining of this paper has organized as follows: Section II describes the methodology. Section III reports the results and discussion. Section IV summarizes the conclusion and future works.

METHODOLOGY

This paper aims to study in two factors of technology arrangement are data and people for supporting SD in water quality management of Pakpanung River Basin. Figure 1 shows the overview of stakeholders,

activities and linkage data to any communities. This project develops a mobile application, web application and open data to supports five activities for water quality management. Mobile Application provides WQI data, alert sign monitoring for local authorities, and General people. In addition, the volunteers can use this mobile application to send WQI data to academic researchers for producing and publishing the final WQI value. Under the Thailand 4.0 policy, the web application provides functions and information for the local authority, government, academic and other in all level such as the monthly report of WQI, Related Research paper, Service API and Open Data.

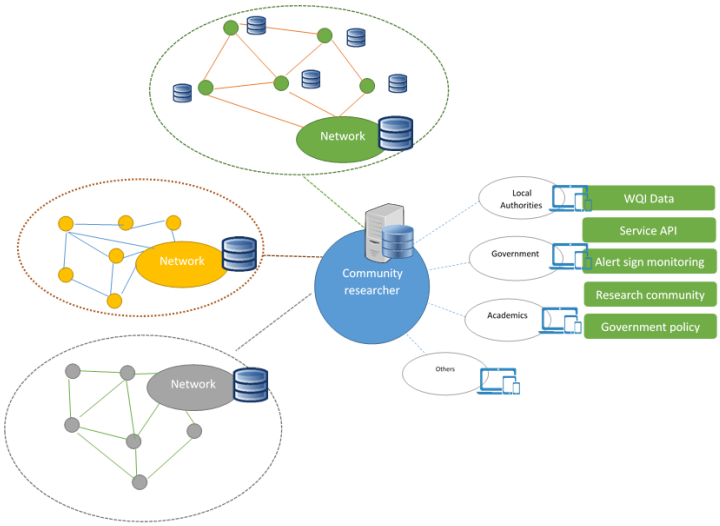

Figure 1 overview of the technology arrangement for supporting people and data linkage.

The population in this research is the Community researcher who lives in the Pakpanang river basin including in local authority, student, government sub-department, volunteer, and academic researcher. In the optional, this paper also pays attention to third parties are living in the outside area which uses any water quality data. This paper uses a random sampling method from the above stakeholders. This research uses questionnaires as a tool to collect data, consisting of 3 main

parts: (1) basic information about respondents such as age, address, and type of using the technology. (2) the satisfaction of using technology, and (3) respondents' behavior using technology and data. The details of collect data method are described in 3 phases are pre-process, on process and post-process phase.

Pre-process phase

The first step is to determine the sampling points to assess water quality. From the data of the pollution control department of Thailand identified The Pakphanang river basin had only 5 water quality assessment station. Each station was updated a lasted-value since July 10, 2018. Therefore, this paper defines a sampling point by a number of communities are living in this area. Figure 2 shows a number of sampling points and the sub-district administration organizations which is a volunteer. The pin sign represents a sampling point and the flag sign represents to the sub-district administration organizations.

The second step is to define the water quality index for assessment. From the study, there are many parameters to use for assessing the surface water that shown in table 1.

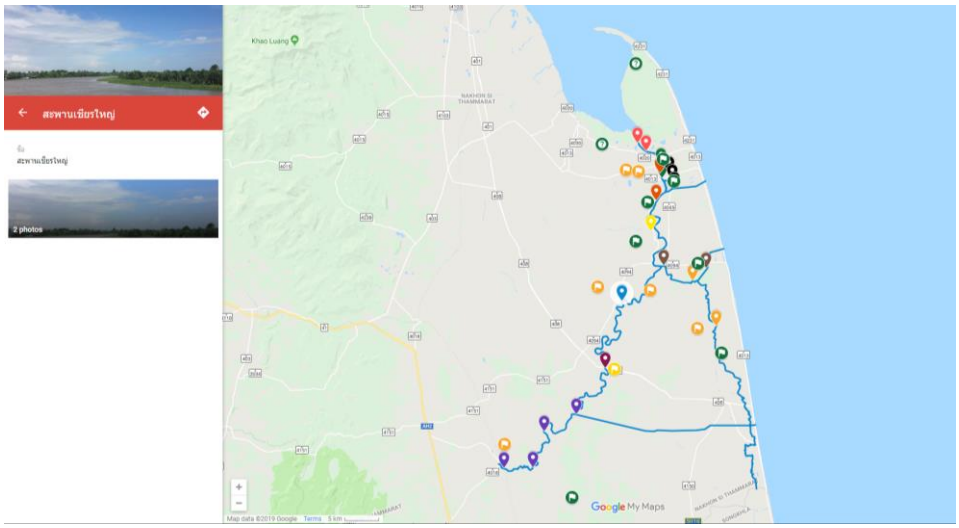

Figure 2 the 20 sampling points and 10 Sub-district Administration

Table 1 A case of surface WQI

Case	WQI Parameters
Goa (India) (Gurdeep Singh,2014)	pH, Total Dissolved Solid (TDS), Total Hardness (TH), Total Suspended Solid (TSS), Calcium, Magnesium, Chloride, Nitrate, Sulphate, Dissolved Oxygen and Biochemical Oxygen Demand (BOD)
Dokan Lake (Abdul Hameed M Jawad Alobaidy, 2010)	pH, Dissolved Oxygen, Turbidity, Conductivity, Hardness, Alkalinity, Sodium, Biochemical Oxygen Demand, Nitrate and Nitrite
Ambazari Lake	pH, electrical conductivity, total dissolved solids, total hardness, alkalinity, calcium, magnesium, sodium, potassium, chloride, sulphate, nitrate, fluorides and iron
Kuwait Bay (P. J. Puri,2014)	pH, turbidity, Total Suspended Solids (TSS), dissolved oxygen, nitrate (NO3), and phosphorus (PO4)

Sampling and collecting method

The pollution control department defined WQI as in 5 parameters are Biochemical Oxygen Demand (BOD), Total Coliform Bacteria (TCB), Fecal Coliform Bacteria (FCB), Total Suspended Solids (TSS) and Dissolved Oxygen (DO). In addition, The Pakphanang river has more geographic diversity including, dam, swamp forest, Watergate, estuary area, etc. In the other hands, focusing on a land use effective, this area has an agriculture zone, consumer zone, industry zone, and fishing industry zone. Therefore, this study is to define an initial WQI in 10 parameters are Biochemical Oxygen Demand (BOD), Total Coliform Bacteria (TCB), Fecal

Coliform Bacteria (FCB), Total Suspended Solids (TSS), Dissolved Oxygen (DO). Chemical Oxygen Demand (COD), Potential of Hydrogen ion (PH), Ammoniacal nitrogen (NH3-N), Total Solid (TS), Salinity (Sal). Some parameters can be measured by a simple test kit such as DO, COD, PH so, every month the community researchers will use the test kit for assessing the water quality and send the result to an academic researcher with a mobile application. Moreover, some parameters need to test by laboratory method so; it is a responsibility of the academic researcher to take their parameters.

On process phase

The fourth step is to develop a mobile application and web application to collect water quality data and represent the result of water quality assessment.

The fifth step is to develop open data of water quality assessment based on Thailand open data framework. The current year have only 7 datasets in Thailand that related to water quality management. Unfortunately, the dataset of Pakphanang river basin is not available. The open data formats are available today consist of xls, xlsx, pdf, CVS, JSON and some non-structure content (image and video). In this paper, define in five format types are xls, xlsx, pdf, and JSON that both people and machine can read it.

The sixth step defines a group of community to build a volunteer and community researcher. This paper starts to set the community researcher at 10 sub-district administration organizations are located in Nakhon Si Thammarat province.

The seventh step is training and meeting the community researchers to prepare knowledge, tool, and skill to measure water quality.

Post process phase

After the seventh step was to finish the post process is to launch the initial operation. The community researchers start to measure and collect a monthly WQI data then, they will send data to academic researchers to interpret and provide final results. After that, the academic

researcher will represent the result to the web, mobile and open data format.

RESULTS AND DISCUSSION

Mobile application and web application

Mobile and web application are developed to support all stakeholders in this works. A mobile application has 6 functions for the community researcher and 1 functions for the general. The community researcher can use for registering, sending a monthly parameter, sending water quality problem, adding and deleting the location, setting notification time and seeing the report and monthly situation of water quality. While the general can see a report and monthly situation of water quality. The web application has a more effective function for supporting any distinctive level of stakeholder. For example, the community researcher can get any report and document are related to water quality in Pakpanang river basin based on his objective and usage type. The local authority can download a period report of water quality to create his budget plan, operation plan, risk plan and etc. The academic researcher and administration can import and export a monthly parameter list to calculate the water quality index. The Governance and others can access WQI result in many formats such as a spreadsheet, pdf, web service, and API. As shown in figure 3.

Open Data: People and Machine Readiness

This study provides an open data architecture to support a global level. The open data were design based on Thailand open data framework that is the both proprietary and nonproprietary format. A spreadsheet, CSV and PDF designed for supporting a people reading and using. While, JSON, CSV, and SOAP designed for the machine. this project provides a monthly WQI dataset. Figure 4 shows the JSON file for the machine. Figure 5 shows the xls file for the people.

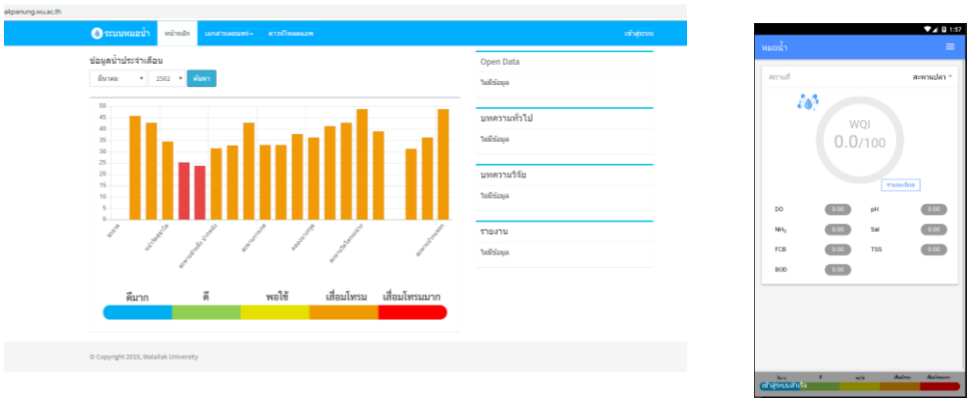

Figure 3 Web and Mobile Application for collect and represent water quality data

Figure 4 JSON file format for describes metadata and dataset for machine reading.

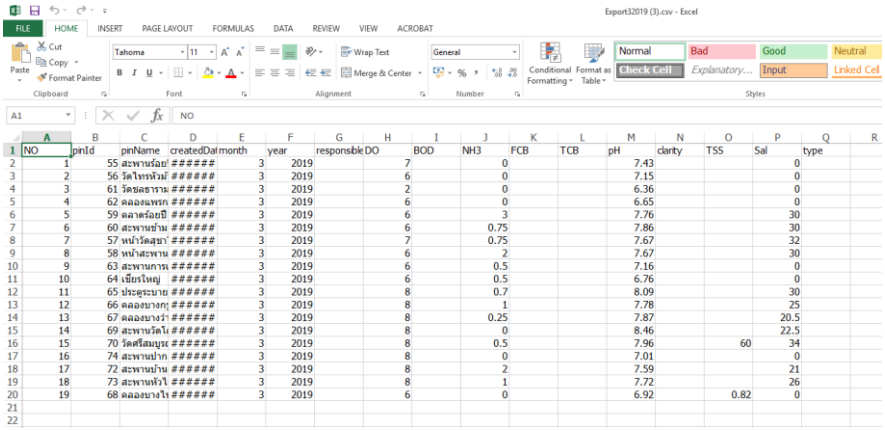

NO	pinId	pinName	createdDat	month	year	responsble	DO	BOD	NH3	FCB	TCB	pH	clarity	TSS	Sal	type
1	55	สะพานร้อยปี	######	3	2019		7		0			7.43			0	
2	56	วัดไทรหัวนี	######	3	2019		6		0			7.15			0	
3	61	วัดชลธาราร	######	3	2019		2		0			6.36			0	
4	62	คลองแพรก	######	3	2019		6		0			6.65			0	
5	59	คลาดร้อยปี	######	3	2019		6		3			7.76			30	
6	60	สะพานข้าม	######	3	2019		6		0.75			7.86			30	
7	57	หน้าวัดสุขา	######	3	2019		7		0.75			7.67			32	
8	58	หน้าสะพาน	######	3	2019		6		2			7.67			30	
9	63	สะพานการ	######	3	2019		6		0.5			7.16			0	
10	64	เขียรใหญ่	######	3	2019		6		0.5			6.76			0	
11	65	ประตูระบาย	######	3	2019		8		0.7			8.09			30	
12	66	คลองบางกุ	######	3	2019		8		1			7.78			25	
13	67	คลองบางว่า	######	3	2019		8		0.25			7.87			20.5	
14	69	สะพานวัดใ	######	3	2019		8		0			8.46			22.5	
15	70	วัดศรีสมบูร	######	3	2019		8		0.5			7.96		60	34	
16	74	สะพานปาก	######	3	2019		8		0			7.01			0	
17	72	สะพานบ้าน	######	3	2019		8		2			7.59			21	
19	73	สะพานหัวไ	######	3	2019		8		1			7.72			26	
20	68	คลองบางใ	######	3	2019		6		0			6.92		0.82	0	

Figure 5 XLSX file format for describes metadata and dataset for people reading.

Water quality assessment

This paper starts the post-process phase since March 2019. The community researchers sent WQI value from a mobile application to the academic researcher then, the academic researcher will calculate and publish complete WQI value on the web and mobile application that shows in figure 6-7.

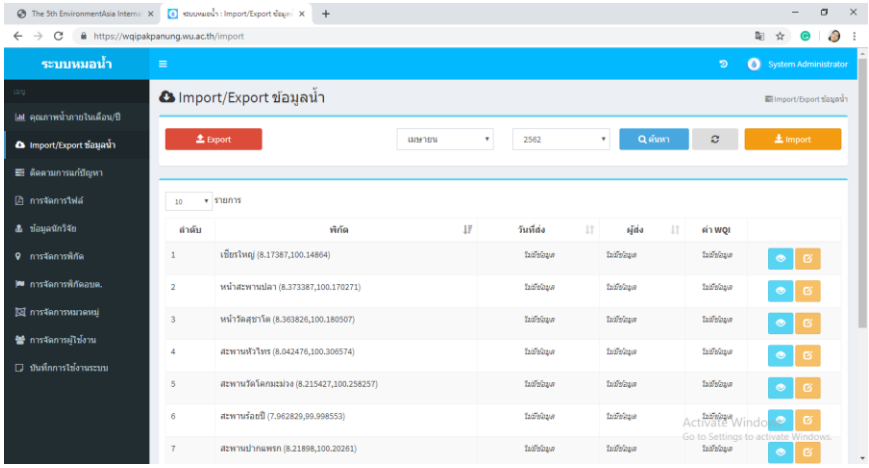

Figure 6 Academic researcher can import and export WQI data for insert laboratory parameter for calculating complete value of WQI

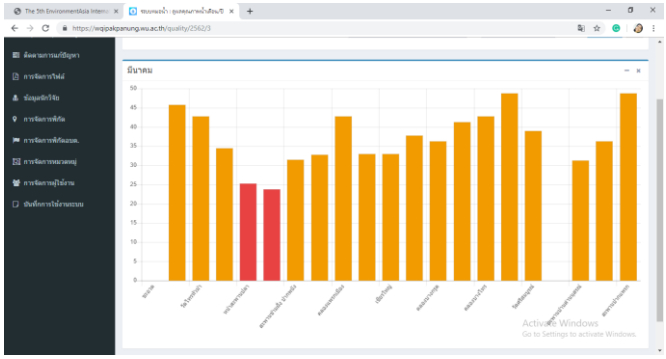

Figure 7 A complete WQI value of each point is represented in bar chart

Evaluation results

This section presents the evaluation results from the questionnaire. The questionnaire has 3 parts are basic information, user satisfaction and user's behaviour in the aspect of useful tool and data. From using random sampling method, this survey has 15 respondents from 4 user types are an academic researcher (26.70%), community researcher (53.3%), local authority(13.3%) and general user (6.7%). The respondents 86.67 % are live in Nakhon Si Thammarat and 13.33% from others area. overall satisfaction is a good rank (4.00). In a part of tool usage, a top three responsive are following the WQI in each month (66.7%), Sending a monthly WQI value (53.3%) and calculating and using open data (40%). As shown in figure 8.

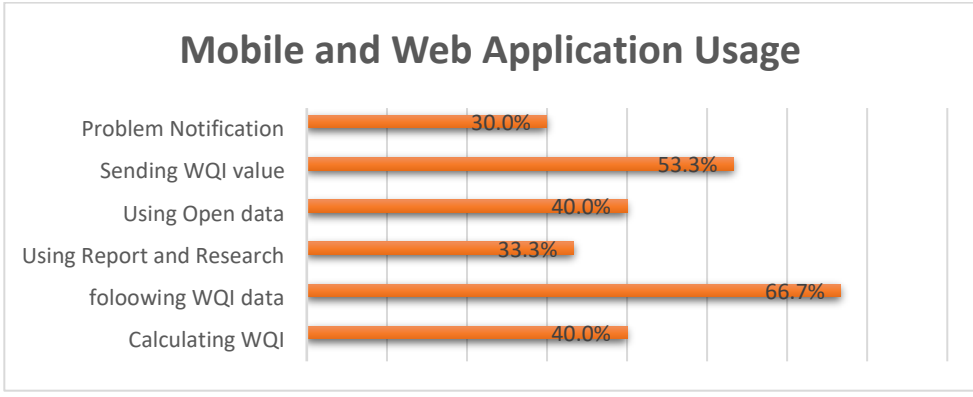

Figure 8 Mobile and Web application usage

CONCLUSIONS

In order to improve the sustainable development of water quality management in Thailand. This paper aims to study in two factors of technology arrangements are data and people. The paper determines the 20 sampling points to assess water quality, applies 10 parameters for WQI assessment and develops a mobile and web application to collect and represent WQI data. In addition, the paper develops open data of water quality assessment based on Thailand open data framework. The open data formats consist of five format types are xls, xlsx, pdf, CVS and json that both people and machine can read it.

Currently, community and academic researchers start to measure and collect monthly WQI data. From using a random sampling method, overall satisfaction is a good rank (4.00). In a part of tool usage, a top three responsive are following the WQI in each month (66.7%), Sending a monthly WQI value (53.3%) and calculating and using open data (40%). For the future, this paper focuses on a minimization method for optimizing WQI parameter list and classify parameter list that suitable with each sampling points.

ACKNOWLEDGEMENTS

I would like to express my deep gratitude to Assistant Professor Sarun Intakosum, my research supervisors, for their patient guidance, enthusiastic encouragement and useful critiques of this research work. I would also like to extend my thanks to the technicians of the laboratory of the software engineering department for their help in offering me the resources in running the program. Finally, I wish to thank my parents for their support and encouragement throughout my study.

REFERENCES

Abdul Hameed M Jawad Alobaidy, Haider S. Abid, Bahram K. Maulood. Kurdistan Region, Iraq Application of Water Quality Index for Assessment of Dokan Lake Ecosystem. Journal of Water Resource and Protection 2010; 792-798.

Al-MUTAIRI, Asma ABAHUSSAIN, and Ali EL-BATTAY A I. Application of Water Quality Index to Assess the Environmental Quality of Kuwait Bay Nawaf. International Conference on Advances in Agricultural, Biological & Environmental Sciences 2014; 1-5.

Caitlin D. Cottrill and Sybil Derrible. Leveraging Big Data for the Development of Transport Sustainability Indicators. Journal of Urban Technology 2017; 45-64.

Eloise M. Biggs , Eleanor Bruce, Bryan Boruff, John M.A. Duncan, Julia Horsley, Natasha Pauli , Kellie McNeill, Andreas Neef, Floris Van Ogtrop, Jayne Curnow, Billy Haworth , Stephanie Duce and Yukihiro Imanari . Sustainable development and the water–energy–food nexus: A perspective on livelihoods. Environmental Science & Policy 2015;(54); 389-397.

Golam Rasul. Managing the food, water, and energy nexus for achieving the Sustainable Development Goals in South Asia. Environmental Development 2016;(18); 14-25.

Gurdeep Singh and Rakesh Kant Kamal. Application of Water Quality Index for Assessment of Surface Water Quality Status in Goa. Current World Environment 2014;(9(3)); 994-1000

Krantz L, The sustainable livelihood approach to poverty reduction, Swedish International Development Cooperation Agency, 2001.

Mathew Kurian. The water-energy-food nexus: Trade-offs, thresholds and transdisciplinary approaches to sustainable development. Environmental Science & Policy 2017; (68); 97-106.

Nataša Veljković, Sanja Bogdanović and Dinić Leonid Stoimenov. Benchmarking open government: An open data perspective. Government Information Quarterly 2014; (2):278-290

P. J. Puri, M.K.N. Yenkie, D.B. Rana and S.U. Meshram Pelagia. Application of water quality index (WQI) for the assessment of surface water quality (Ambazari Lake). Research Library European Journal of Experimental Biology 2014; 5(2):37-52.

Sarah Parkinson and Ricardo Ramirez, Using a Sustainable Livelihoods Approach to Assessing the Impact of ICTs in Development, The Journal of Community Informatics,2006;2(3).

Effects of composting on the production of methane in solid-state anaerobic digestion of corncob

Methit Thammakhet[2,3], Rotsukon Jawana[3], Pruk Aggaransi[3], and Siriwat Jinsiriwanit[1]*

[1]Division of Biotechnology, School of Agro-Industry, Faculty of Agro-Industry, Chiang Mai University, Thailand, 50100
[2]Division of Biotechnology, Graduate School, Chiang Mai University, Thailand, 50200
[3]Energy Research and Development Institute-Nakornping, Chiang Mai University, Thailand, 50100
e-mail: siriwat.jin@cmu.ac.th

ABSTRACT

The solid-state anaerobic digestion (SS-AD) is a simple and efficiency technology for waste management of lignocellulosic residue since it reduces the water footprint and produces higher volumetric methane productivity compared with the liquid anaerobic digestion. The effluent is solid waste which does not require the remediation of the remaining wastewater. The pretreatment is beneficial processes for improving the methane yield of the SS-AD. The composting is one of the pretreatments which is inexpensive and simple to treat lignocellulosic materials. The main goal of this research project was to investigate the effects of composting of corncob on the biogas production from SS-AD by using corncob as raw material. The 30 kg corncob was ground and composted in 200 L composting bin. The effects of composting inoculum, calcium oxide, urea and aeration on the methane yield of SS-AD were investigated. After 60 days of the SS-AD operation, the highest biogas and methane yield were 362.1 and 98.3 mL/gVS respectively which was achieved by adding 1% CaO and 5% composting inoculum. The

methane yield was decreased by the aeration of the compost ($P < 0.05$). The additions of CaO, urea and composting inoculum were not significant to increase the methane yield ($P \geq 0.05$).

Keywords: Pretreatment, Composting, Solid state anaerobic digestion, Methane

INTRODUCTION

The global energy needs are rapidly growing due to the industrial development and economic growth. The dependence of fossil fuel may pose a risk in the energy security. The renewable energy from agricultural residues are used as an alternative energy source to reduce the dependence on fossil fuel because of their availability, low cost and potential sources. The corncob is one of the most abundant organic residues which was left as waste in the agricultural practice resulted in environmental pollution such as burning and rotting. For this reason, the utilization of corncob for biogas production will reduce its environmental impact and reduce the cost of substrate.

The solid state anaerobic digestion (SS-AD) which operates at high total solid contents (more than 15%) is promising for the biogas fermentation of corncob since it produces high volumetric productivity compared with liquid anaerobic digestion (L-AD) (Ge *et al*., 2014; Brown *et al*., 2012), requiring lower water and energy consumption. The zero or nearly zero liquid phase of SS-AD make it easy for the handling of both corncob feed and effluent.

The lignin, crystalline cellulose, acetylated cellulose and hemicellulose in corncob are difficult to be biodegraded and require the pretreatment prior to SS-AD. The chemical pretreatment such as alkali and acidic pretreatment is rapid and efficient to reduce the complex components of corncob in large scale operation. However, the chemical

pretreatment may produce toxic substances which inhibit microorganism in fermentation. Moreover, this process is usually severe, harmful to health and environment and require downstream processes. Comparing with the chemical process, the biological process is mild, low cost and environmentally friendly process (Zheng *et al.*, 2014; Kumar *et al.*, 2009).

The biological process such as the pretreatment by microbial consortium is advantageous for the biodegradation of lignocellulosic residues, because of the synergistic action of microorganisms capable to degrade the complex components of corncob. Furthermore, the raw material does not require the sterilization process to maintain the pure culture condition which make it effective to treat large scale lignocellulosic waste. The consortium is usually obtained from the indigenous microbial community in the substrate or other sources such as compost, food waste, sewage sludge and industrial waste (Zheng *et al.*, 2014).

The combination of microbial consortia with chemical pretreatment improves biodegradation of the lignocellulosic residue. Urea is a nitrogen source to promote the pretreatment of microbial consortia because the C:N ratio of substrate is adjusted for the efficient fermentation of microorganism. The calcium oxide improves the digestion of microorganism by alkali pretreatment and increasing the buffer capacity in anaerobic digestion. Compared with other alkali pretreatment such as NaOH and KOH, the advantage of calcium oxide pretreatment is cheaper, and the calcium ion is easily recovered by reaction with CO_2 (Kumar and Sharma, 2017). Therefore, the main goal in this research project was the investigation of the effects of calcium oxide, inoculum, urea and aeration on pretreatment in the composting of corncob. The corncob compost was subjected to the investigation of biodegradation and biogas product in SS-AD.

METHODOLOGY

1 Raw material and inoculum

Corncob from local maize field in Nakonsawan province, Thailand was collected and air dried. Then, the dried corncob was grinded to 0.5 centimeter particle size approximately. Composting inoculum was the corncob compost obtained from aerobic composting. For SS-AD, the inoculum was obtained from the anaerobic digester treating piggery wastewater of Energy Research and Development Institute - Nakornping, Chiang Mai University. The inoculum was prepared by centrifuging digester's sludge for 6000 rpm at 4 ^{o}C and the centrifuged solid was used as inoculum in SS-AD.

2. Experimental designA 12 run Plackett and Burman design was applied to study the effects of composting on the biogas production from SS-AD by using corncob as raw material. The factors in the experiments consist of CaO, urea, compost inoculum and aeration which were varied at a high (+) and low (−) level as shown in **Table 1** and **2**. 30kg of corncob mixed with each factor (base on dried weight corncob) was composted in 200 L composting bin and incubated at room temperature for 6 days. The initial moisture content of corncob was adjusted to 65%. The aerobic treatment was performed by composting. Every 12 hours, the humidified air was passed through the composting bin for 15 minutes (Fig. 2.1). After the composting, the corncob compost was sampled at the center of fermentation bin and used as the feed of SS-AD.

3. The solid-state anaerobic digestion (SS-AD)

The SS-AD were conducted at 25% total solids (TS). The corncob compost was mixed with SS-AD inoculum at Feed to Inoculum ratios (F/I ratios) of 2 (based on volatile solid (VS)). Each experiment was carried out triplicate in 1 L glass bottle. The bottle content was purged by 99.99% N_2 for 3 minutes and then sealed with the rubber stopper and all experiments were incubated at 35± 2 ^{0}C. The sole inoculum was conducted as the control. The volume

of biogas was continually measured for 60 days

2.4 Analysis

The samples were taken from the SS-AD bottle and measured for pH, TS, and VS according to the Standard Method (APHA, 1998). The total nitrogen was measured by Kjeldahl method (AOAC, 2000). The pH was measured from the supernatant of the suspension of 1 g of sample in 10 ml of water (1:10). The carbon content was calculated by dividing VS content by 1.8 (Adams et al., 1951). The biogas production for each experiment was measured by Micromanometer (Kimo MP112). The biogas content was determined by multichannel portable gas analyzer (GFM406). Statistical analysis data was done using Minitab® software (version 16.1.0)

Table 1 The factors of the experiments

Factor	Symbol	Level	
		-1	+1
Calcium oxide (%)	A	0	1
Urea (%)	B	0	1
Compost (%)	C	0	5
Aeration	D	No aeration	Aeration

Table 2 The experiments in this study

Experiments	Factors
1	Urea +Compost
2	Urea + Compost + Aeration
3	Calcium oxide + Compost
4	Urea + Compost + Aeration
5	Calcium oxide + Urea + Aeration
6	Urea + Calcium oxide + Compost
7	Calcium oxide + Compost +Aeration
8	Compost + Aeration

9	Aeration
10	Urea
11	Calcium oxide
12	No additive

RESULTS AND DISCUSSION

1. The characteristic of corncob compost

The composition of corncob and inoculum was shown in the Table 3. The corncob was suitable material in solid state fermentation, because the corncob was high in the carbon content and volatile solid. However, the microorganisms required the proper moisture contents for metabolisms in fermentation. The fungal contained the high activity enzyme for degradation at 60-70% of the moisture (Delabona *et al*., 2013; Marques *et al*., 2018). Therefore, the corncob compost was conducted at 25% TS.

The result of pH, TS and VS of composting was shown in Table 4. The treatment of urea and calcium oxide in composting increased the pH from 6.65 to 8.55-8.81 since they increase the hydroxide ion in the mixture. Comparing with urea and calcium oxide, the pH of aeration and compost treatment (experiment 8, 9 and 12) was changed from about 6.65 to 6.47-7.27 in composting. The pH, TS and VS were different from pretreatment because there are various types and activities of microorganisms to degrade and grow in fermentation such as, *Nocardia* spp. *Streptomyces* spp. *Thermoactinomyces* spp, *Pseudomonas* spp., *Bacillus* spp., *Enterobacter* spp., *Bacillus* spp., *Penicillium* spp., *Aspergillus* spp, etc (Sánchez *et al*., 2017). However, the TS and VS were adjusted to 25% and 2 (base on F/I ratios) prior to the digestion in SS-AD

Table 3 The characteristic of corncob and inoculum

Factors	Corn cob	Inoculum
C (%)	49.10± 0.12	6.90± 0.01
N (%)	0.28± 0.02	0.53± 0.01
pH	6.65± 0.20	6.54± 0.02
Moisture content (%)	9.8± 0.1	80.9± 0.1
Total solid (%)	90.2± 0.1	19.1± 0.1
Volatile solid (%)	88.4± 0.2	12.4± 0.0
Ash (%)	1.8± 0.2	6.6± 0.1

Table 4 The pH, total solid and volatile solid of corncob after pretreatment

Experiments	Compost pH	Compost TS (%)	Compost VS (%)
1	8.61± 0.08	44.27± 1.45	42.40± 1.32
2	8.81± 0.03	44.98± 1.90	42.68± 2.15
3	8.62± 0.11	38.79± 0.09	37.23± 0.55
4	8.80± 0.02	44.50± 2.02	42.25± 0.00
5	8.79± 0.05	44.98± 1.90	42.68± 2.15
6	8.69± 0.09	48.22± 1.07	45.00± 0.94
7	8.66± 0.02	44.92± 1.62	42.77± 1.57
8	7.08± 0.03	41.82± 2.44	38.81± 2.34
9	6.47± 0.14	53.92± 0.53	52.56± 0.37
10	8.59± 0.14	48.66± 1.59	48.97± 1.65
11	8.55± 0.03	39.44± 0.04	37.21± 0.42
12	7.27± 0.03	40.70± 0.51	39.19± 0.69

2. The effect of composting on methane production in SS-AD

The methane yield of corncob in SS-AD 60 days was shown in Figure 1 respectively. The highest biogas and methane yield were 362.1 ml/gVS and 98.3 ml/gVS respectively in treatment 3. Comparing with no additive (experiment 12), the calcium oxide and compost treatment increased the biogas and methane yield because the effect of calcium oxide and compost increased

degradation and buffering in SS-AD. However, the calcium oxide, composting inoculum and urea didn't show the increase in the methane yield significantly ($P \geq 0.05$). The methane yield was significantly decreased in SS-AD of composting with aeration treatment ($P<0.05$). As reported by Zhou *et al* (2017), the lignocellulosic biomass was pretreated by pre-aeration to reduce lignin content and increase the activity of microorganisms. However, the polysaccharide such as, cellulose and hemicellulose, may be lost in long period of biological pretreatment. In addition, the urea treatment was oxidized and converted to ammonia, nitrite and nitrate accumulated in aerobic fermentation (Sánchez *et al*.,2017; Wang *et al* 2016). These nitrogen compounds exist effect on the methane yield because the nitro-reducing bacteria were competing with methanogens bacteria for substrate in SS-AD (Latham *et al*., 2016). Therefore, the methane yield was decreased in SS-AD.

The characteristics of corncob after 60 days in SS-AD was shown in Table 5 the TS and VS of corncob was decreased due to the organic compounds were degraded and converted into the biogas products such as, CH_4 CO_2 and H_2O. The microorganism produced the enzyme to hydrolyze the corncob into small molecules such as, amino acid, monosaccharide and fatty acid. These small molecules were converted to the organic compound, such as volatile fatty acid, acetic acid, formic acid, propionic acid, and other product, such as H_2, CO_2, H_2S. These organic acids were generated and accumulated. As a result, the pH of compost was decreased (experiment 1-7, 10 and 11). While the optimum pH of the methanogens was 6.5-7.5 in anaerobic digestion (Li *et al*., 2019). For the experiment 8, 9 and 12, the pH was increased due to the organic compound were produced such as, alcohol products and the acetic acid was converted to CH_4 and CO_2 (Budiyono *et al*., 2013; Matheri *et al*., 2016). Theses result showed that the CaO treatment was positively effect on the methane yield by increasing buffering capacity of the SS-AD.

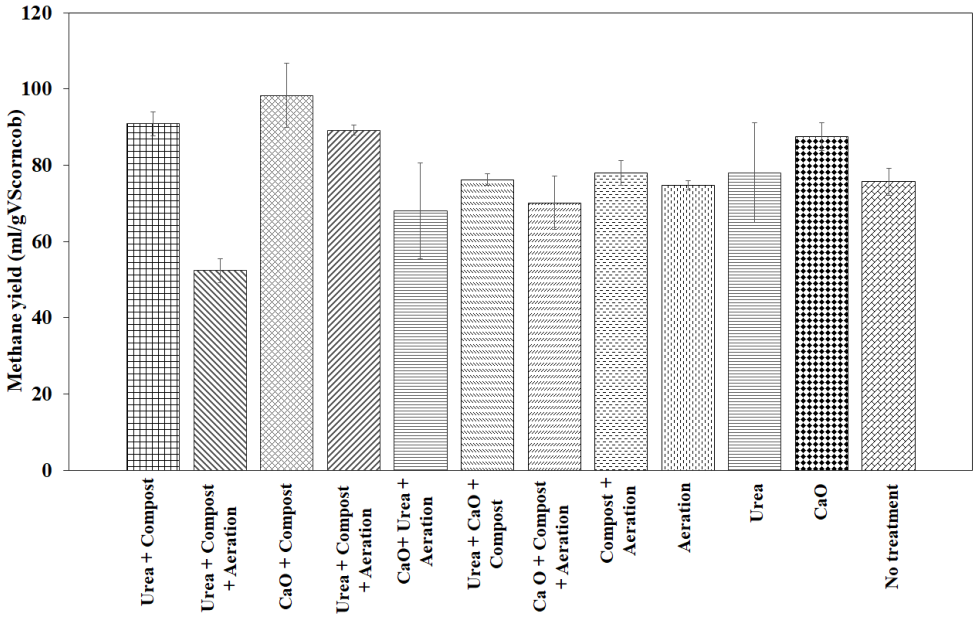

Figure 1 The methane yield accumulation of corncob after SS-AD

Table 5 The pH, total solid and volatile solid of corncob after SS-AD

Experiments	Final pH	Final TS (%)	Final VS (%)	Mass loss (%)
1	7.14± 0.01	21.39± 0.55	16.48± 0.37	16.81± 0.45
2	7.41± 0.02	22.51± 1.58	18.13± 1.36	6.48± 0.35
3	7.23± 0.04	22.16± 2.78	17.48± 2.51	15.32± 0.25
4	7.23± 0.02	21.30± 0.79	15.60± 0.84	7.70± 0.12
5	7.48± 0.04	22.39± 1.46	18.76± 1.63	5.81± 0.06
6	7.50± 0.02	22.23± 0.31	17.83± 0.37	8.13± 0.13
7	7.67± 0.05	22.98± 1.22	18.83± 1.31	7.17± 0.08
8	8.02± 0.01	22.86± 0.38	18.04± 0.48	19.21± 0.25
9	7.46± 0.03	22.41± 1.31	18.53± 0.92	7.88± 0.31
10	7.21± 0.03	22.56± 0.05	18.06± 0.26	8.80± 0.13
11	7.25± 0.02	22.51± 0.00	17.36± 0.16	16.30± 0.36
12	7.97± 0.01	22.12± 0.28	17.72± 0.44	17.13± 0.38

3. The effect of composting time on biogas product

The effect of composting time was investigated for 2, 4, 6, 8, 10 and 12 days in experiment 1. The trend of biogas and methane yield was shown in the Figure 2 and 3. The highest biogas and methane yield were achieved of 363.1 ml/gVS and 104.6 ml/gVS respectively for no pretreatment of corncob. The biogas product of compost was reduced because the microorganism competed in SS-AD, and the polysaccharide were lost to prolong pretreatment. Therefore, the SS-AD of corncob was suggested without pre-aeration process.

The biogas yield was highly accumulated during 15-20 days in SS-AD which was approximately 50% of total biogas yield obtained of 60 days digestion. The long operating time of SS-AD is improper for waste management in the industrial scale because it is not cost effectively (Silva *et al*., 2018).

Table 6 The pH and VS of pretraeted corncob and unpretreated corncob

Composting time (days)	Initial VS (%dry basis)	Composting VS (%)	Final VS (%dry basis)	VS loss (%)
0	98.01± 0.23	-	76.76± 1.26	21.68
2	96.27± 0.25	96.05± 0.27	77.52± 1.71	19.29
4	96.27± 0.25	96.33± 0.98	76.92± 0.66	20.15
6	96.27± 0.25	95.78± 0.65	77.05± 0.58	19.56
8	96.27± 0.25	95.04± 0.18	77.55± 2.12	18.40
10	96.27± 0.25	95.78± 0.51	78.13± 0.54	18.43
12	96.27± 0.25	95.71± 0.23	80.58± 0.04	15.81

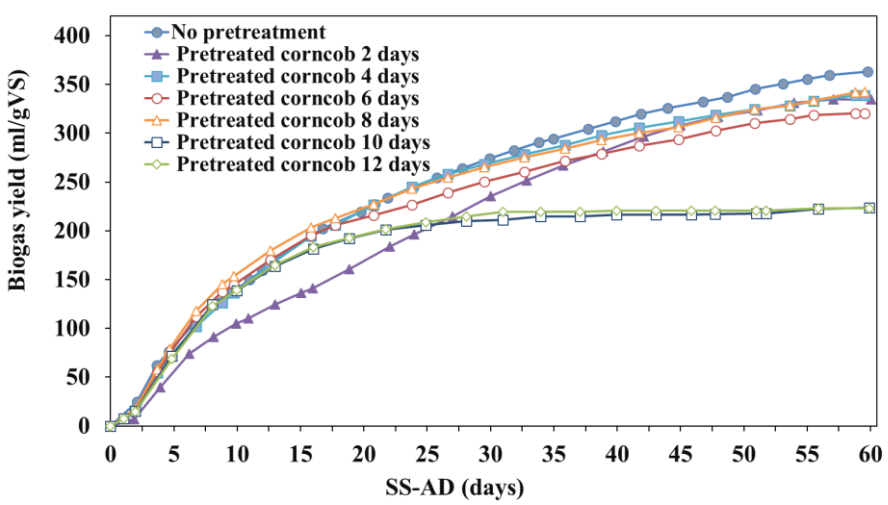

Figure 2 The trend of biogas yield of corncob compost

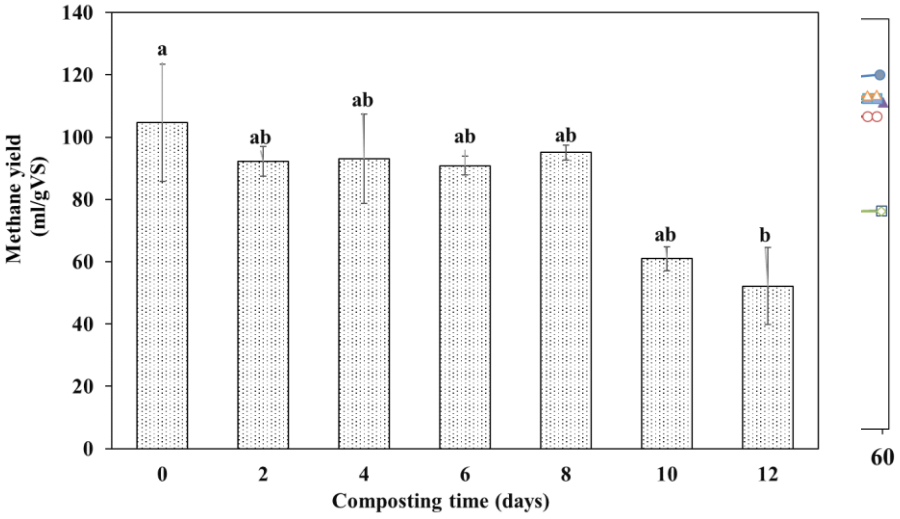

Figure 3. The methane yield of corncob compost

CONCLUSIONS

In conclusion, the addition of CaO, urea and composting inoculum were not significant to increase the methane yield ($P \geq 0.05$). In the other hand the methane yield was decreased by the aeration of the compost ($P<0.05$). However, the addition of CaO increase the methane yield. The unpretreated corncob

showed the highest cumulative methane production. The methane yield was decreased when the corncob was pretreated more than 2 days in aerated composting. This incident suggests corncob was capable of directly used in SS-AD without aerated treatment. In the waste management point of view, the SS-AD system may be the method of choice for treating the lignocellulosic waste SS-AD for its easier handling of feed and effluent and the smaller bioreactor volume. However, the mode of operation and the way to utilize the energy remained in solid effluent has yet to be addressed. Further research should be both focus on the application of the solid effluent such as in agriculture and fuel industry and the investigation on the continuous solid state fermentation to generate biogas.

ACKNOWLEDGEMENTS

The authors would like to thank for the scholarship awarded by Graduate School of Chiang Mai University and Tetra Pak (Thailand) Ltd. This project was also supported by The Energy Research and Development Institute-Nakornping, and Faculty of Agro-Industry Chiang Mai University.

REFERENCES

AOAC. 2000 Official Methods of Analysis. 17th Edition, The Association of Official Analytical Chemists, Gaithersburg, MD, USA.

APHA. 1998. Standard methods for the examination of water and wastewater, 20th edition. American Public Health Association/ American Water Works Association/ Water Environment Federation, Washington DC.

Brown, D., Shi, J., and Li, Y. 2012. Comparison of solid-state to liquid anaerobic digestion of lignocellulosic feedstocks for biogas production. Bioresource Technology, 124, 379–386.

Budiyono. Syaichurrozi, I., and Sumardiono, S. 2013. Biogas production from bioethanol waste: the effect of pH and urea addition to biogas production rate. Waste Tech. Waste Technology, 1(11), 1–5.

Da Silva, C., Astals, S., Peces, M., Campos, J. L., and Guerrero, L. 2018. Biochemical methane potential (BMP) tests: Reducing test time by early

parameter estimation. Waste Management, 71, 19–24.

Delabona, P. da S., Pirota, R. D. P. B., Codima, C. A., Tremacoldi, C. R., Rodrigues, A., and Farinas, C. S. 2013. Effect of initial moisture content on two Amazon rainforest Aspergillus strains cultivated on agro-industrial residues: Biomass-degrading enzymes production and characterization. Industrial Crops and Products, 42(1), 236–242.

Ge, X., Matsumoto, T., Keith, L., and Li, Y. 2014. Biogas energy production from tropical biomass wastes by anaerobic digestion. Bioresource Technology, 169, 38–44.

Kumar, A. K., and Sharma, S. 2017. Recent updates on different methods of pretreatment of lignocellulosic feedstocks: a review. Bioresources and Bioprocessing, 4(1).

Kumar, P., Barrett, D. M., Delwiche, M. J., and Stroeve, P. 2009. Methods for pretreatment of lignocellulosic biomass for efficient hydrolysis and biofuel production. Industrial and Engineering Chemistry Research, 48(8), 3713–3729.

Latham, E. A., Anderson, R. C., Pinchak, W. E., & Nisbet, D. J. (2016). Insights on Alterations to the Rumen Ecosystem by Nitrate and Nitrocompounds. Frontiers in Microbiology, 7, 1–15.

Li, Y., Chen, Y., and Wu, J. 2019. Enhancement of methane production in anaerobic digestion process: A review. Applied Energy, 240, 120–137.

Marques, N. P., de Cassia Pereira, J., Gomes, E., da Silva, R., Araújo, A. R., Ferreira, H., Rodriguese, A., Dussána K. J., Bocchini, D. A. 2018. Cellulases and xylanases production by endophytic fungi by solid state fermentation using lignocellulosic substrates and enzymatic saccharification of pretreated sugarcane bagasse. Industrial Crops and Products, 122, 66–75.

Matheri, A. N., Belaid, M., Seodigeng, T., and Ngila, C. J. 2016. Modelling the kinetic of biogas production from co-digestion of pig waste and grass clippings. Lecture Notes in Engineering and Computer Science, 2224.

Sánchez, Ó. J., Ospina, D. A., and Montoya, S. 2017. Compost supplementation with nutrients and microorganisms in composting process. Waste Management, 69(26), 136–153.

Wang, X., Li, Z., Zhou, X., Wang, Q., Wu, Y., Saino, M., and Bai, X. 2016. Study on the bio-methane yield and microbial community structure in enzyme enhanced anaerobic co-digestion of cow manure and corn straw. Bioresource Technology, 219, 150–157.

Zheng, Y., Zhao, J., Xu, F., and Li, Y. 2014. Pretreatment of lignocellulosic biomass for enhanced biogas production. Progress in Energy and Combustion Science, 42(1), 35–53.

Zhou, Y., Li, C., Nges, I. A., and Liu, J. 2017. The effects of pre-aeration and inoculation on solid-state anaerobic digestion of rice straw. Bioresource Technology, 224, 78–86.

Some Ecological Aspects of Dhole (*Cuon alpinus*) in Huai Kha Khaeng Wildlife Sanctuary, Uthai Thani Province, Thailand

Khwanrutai Charaspet[1], Ronglarp Sukmasuang[1*], Prateep Duangkae[1], Saksit Simchareon[2] and Nucharin Songsasen[3]

[1*] Forest Biology Department, Faculty of Forestry, Kasetsart University, Thailand

[2] Department of National Parks Wildlife and Plant Conservation, Thailand

[3] Smithsonian Institute, USA; Corresponding author: e-mail: fforrls@ku.ac.th

ABSTRACT

The dhole (*Cuon alpinus*) is one of the least studied endangered canid species and many aspects of ecological knowledge are lacking. The objectives of this study were to investigate the spatial movement of dholes, prey abundance, prey selection, and prey overlap with other large carnivorous species in Huai Kha Khaeng Wildlife Sanctuary, Thailand, during November, 2017 and October, 2018. Two adult female dholes were captured and fitted with GPS collars. Twenty camera trap sets were systematically used to survey the area. Scat collection was conducted along forest roads and trails. The home range sizes and activity radii of the two dholes were 3,151.63 ha. and 1,442.84 m., and 33.39 ha. and 331.56 m., respectively. The sambar deer (*Rusa unicolor)* was the most abundant prey species (30.93%). However, dhole fecal analysis showed that they preferred red muntjac (*Muntiacus muntjak*) (57.1%). There was a high degree of prey overlap between dholes and leopards (98%), indicating very high competition. The dholes in this study represent movement patterns in richly abundant prey habitats, but with the presence of other predators that can effect prey selection and movement patterns of the dhole in the area.

Key words: Dhole, GPS-collar, Prey, Huai Kha Khaeng Wildlife Sanctuary

INTRODUCTION

The dhole (*Cuon alpinus*), or Asian wild dog, is one of 37 species in the Canidae family and has been classified as endangered since 2008. (International Union for Conservation of Nature and Natural Resources: IUCN, 2018). Historically, the dholes' distribution was throughout Asia. However, they have disappeared from most of their former ranges and now can only be found in some Asian countries, as a result of habitat reduction and fragmentation, hunting and reduction of their prey populations (Gopi *et al*. 2012). Another important factor is the negative attitude of some people towards dhole, regarding them as pests. In Thailand, some people have suggested elimination of dholes from Thai protected areas (Jenks *et al.*, 2014).

Naturally, the dhole is a predator species that plays an important role in the ecosystem. As on of predator species dhole can have a strong influence not only on their prey but also on one another, with cascading effects on many species and ecosystem processes (Beschta *et al*. 2009). Dholes can kill prey that is as large as that of tigers and leopards. They usually form relatively large packs to efficiently hunt this large prey (Lekagul and McNeely, 1977). In Thailand, the dholes' main prey is medium to large ungulates, ranging between 20-260 kg. However, they will also prey on small animals such as rodents, birds and reptiles (Austin 2002; Slangsingha, 2012; Prayoon, 2014; Charaspet, 2015).

At present, there are few studies on the ecology of dholes. Therefore, in order to better understand their ecology and to assist in conservation efforts, more research is needed for this species (Kamler *et al*., 2012). Specifically, limited knowledge on spatial ecology in association with prey relationships and competiti with other large predators has hampered the ability to establish conservation or management action for the species. This study focused on home range

size, movement patterns, prey species and selection, as well as the overlap of prey species with other large carnivores in the area.

Normally, the knowledge of how animals distribute their activities in space and time is of central importance in an ecological study (Spenser, 2012). Thus, biologists track animals to estimate the sizes and shapes of home ranges, movement patterns within home ranges, home range overlap among individuals, and how home-range boundaries vary over time (e.g. Fieberg and Borger 2012; Fieberg and Kochanny 2005; Powell and Mitchell 2012). The size of a dhole's home range varies with its habitat. Acharya *et al*. (2007) reported that the size of the home range varied from 26-202.8 km^2 in dry deciduous forest, at Pench Tiger Reserve, India. Grassman *et al*. (2005) found that the size of the home range varied from 12-49.5 km^2 in the dry evergreen forest at Phu Khieo Wildlife Sanctuary, Thailand. Austin (2002) studied the size of the area inhabited by dholes using radio signals in Khao Yai National Park, Thailand, and found the size of the area to be 27.6 km^2, and the average daily distance traveled was 1.4 km. Home range formation is, thus, the result of dynamic processes. Both the habitat and internal situation of the animals might change with time, and cause the home range size to vary (Viana *et al*., 2018). Moreover, the home range size may depend on the method of data collection and analysis. Normally, the home range size depends on the quality of the habitat, with higher *habitat quality* allowing them to have *smaller home ranges.* The home range size and dhole movement can be determined using satellite radio signals. Although Huai Kha Khaeng Wildlife Sanctuary (HKK) is one of the most important dhole habitats in Thailand, these aspects have never been studied. The relative abundance of dholes and the characteristics of the prey they consume in the area have also never been investigated. An understanding of home range size, habitat used, and prey characteristics are fundamental for maintaining the dhole population

and habitat management (Rechetelo *et al*., 2016). Advanced research data, including habitat use and prey species, are essential for species conservation, not only in this area but throughout their distributed range.

OBJECTIVES

1. To investigate the spatial movement of dholes using Global Position System (GPS)-collars.
2. To examine the abundance of dholes, their prey and other carnivores using camera traps.
3. To study the prey species of dholes and prey overlap with their competitors.

MATERIALS AND METHODS

Study area

This study was conducted in an area of approximately 200 km^2 between the Klong Phlu Long-term Ecological Research Plot (KP) and the Khao Nang Rum Wildlife Research Station (KNR) in HKK. The sanctuary is located in Banrai and Lansak Districts, Uthai Thani Province and Umpang District, Tak Province. The sanctuary is situated between latitude 15°15' to 15° 45' and longitude 99°5' to 99°25'. Huai Kha Khaeng Stream and Tab Salao Stream are permanent water sources in the area (Faculty of Forestry, Kasetsart University, 1989). The topography in this area includes lowland along the main streams as well as mountainous terrain. The altitude of the sanctuary ranges from 250-1,678 meters above mean sea level (MSL) (Huai Kha Khaeng Wildlife Sanctuary, 2016) (Figure 1).

Field data collection

Dhole trapping and radio collaring

The dhole trapping procedure was conducted from 25th June - 4th July 2018 using soft-catch traps, in the area between the HKK head office and Khao Nang Rum Wildlife Research Station, and from 28th - 31st July 2018 in the area around the Klong Phlu Long-term Ecological Research Plot and Huai Kha Khaeng River. Five to eight soft catch trap stations were employed.

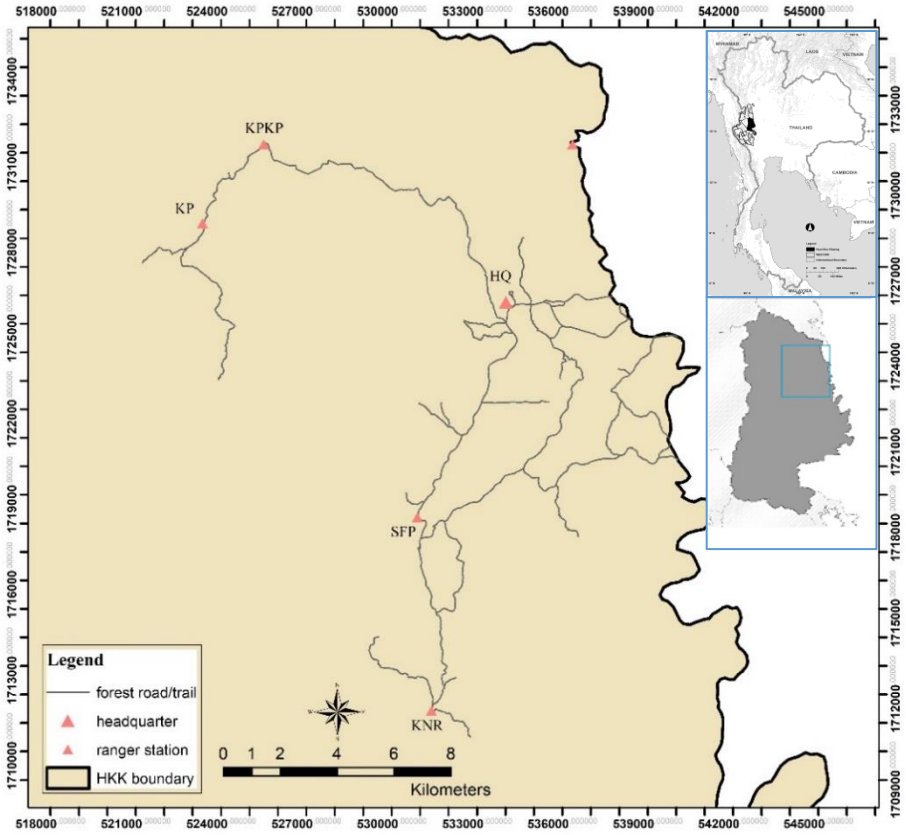

Figure 1 Huai Kha Khaeng Wildlife Sanctuary and the study site location

This method was similar to that used by Jenks *et al*. (2015). The captured dholes were fitted with GPS radio collars and released at the capture site. All of the locations were downloaded via LOTEX website every 4 hours until the signal stopped.

Regular ground checks were performed every month, during the study period, using diurnal VHF system tracking at hilltop sites and forest trails to investigate the habitat characteristics of the collared animals.

Population abundance of dholes and prey

The abundance of dholes, their prey and other large carnivorous mammals were determined by the camera trap method. Twenty camera trap sets

were deployed randomly every month, each within a 1 km^2 grid cell, covering the 200 km^2 study area from November 2017 through June 2018. The cameras were set to take 3 photographs within 10 seconds, after the infrared sensors were triggered (Charaspet, 2015). The camera traps were placed 30 cm above the ground along trails or suitable locations, such as water sources, with higher possibilities of capturing animal images (Moruzzi *et al*., 2002; Charaspet, 2015). The animal photographs were then used for the relative abudance analysis, following the methodologies decribed below.

Prey species

Scats of dholes, tigers and leopards were collected regularly, every month, throughout the study period along forest roads within the study area. Differentiation between dhole's and the two large-felid's scats were determined based on the methods suggested by Petdee (2000); Acharya (2007); Francis (2008); Kawanishi and Sunquist (2008); Simcharoen (2008); Kumaraguru *et al*. (2011) and Simcharoen *et al*. (2018). Found scats were kept in separate plastic bags and labeled. The species, collection date, forest type, scat condition, scat size, scat location, trace, and coordinates were recorded (Charaspet, 2015).

Laboratory procedure

Each animal scat collected in the area was placed in a 1-mm mesh nylon bag, rinsed in water and cleaned again with an ultrasonic cleaner to remove residual dirt (Charaspet, 2015). All the remains in the nylon bag of each scat, such as hair, teeth, feathers, bone and hooves were air dried and stored in paper bags (Ramesh *et al.*, 2012).The remaining hair was prepared following the process recommened by Petdee (2000) and Charaspet (2015). The characteristics such as color, length, cuticle pattern, medullar pattern and cross section pattern were compared with those in our reference collection (Petdee, 2000) to identify prey species.

Data analysis

1. Spatial movement

1.1 Home range size was calculated using minimum convex polygons (MCP). The MCP at 100%, 95%, 75% and 50% were calculated to determine the area covered and core areas using RANGE 9 program.

1.2 Mean activity radii, the distances between centers of home ranges and all of the telemetry locations, were also calculated (Grassman *et al.*, 2005) using the RANGE 9 program.

2. Population abundance

Species identification in each photo was performed for dependent or independent occasions following O'Brien *et al*. (2003). Abundance of dholes and other species gained from camera trap data was calculated all year round and separated by species was calculated from the formula (Kanchanasaka *et al*., 2010):

% relative abundance (%RA) =
(Trap success species i × 100)/
(Total trap days)

where

Trap success is the number of photos of species i

Trap days is the number of camera traps×total days of camera trapping

3. Prey species

3.1 Frequency of occurrence of mammalian prey species in carnivore scats is a commonly used parameter in predator diet studies. Frequency of occurrence (% FO) based on our scat samples and the identification process results were used to calculate %FO using the following formula (Charaspet, 2015; Kamler *et al*., 2012):

% FO = (Number of i × 100)/
(Total scats)

where Number of i is the number of scats of prey species i

3.2. Electivity indices measure the utilization of food types (r) in relation to their abundance or availability in the environment (p) or the indices showing the degree of selection of a particular prey species by the predator being studied. Electivity

index was calculated using the following formula (Jacobs, 1974):

$$\text{Electivity index} = \frac{(r-p)}{(r+p)-2rp}$$

where r is the proportion of the prey category in the predator's diet and p is the proportion of the availability of the prey category in the study area. Dietary electivity index values range from –1 to +1. Index values near +1 indicate that the prey category is selected by the predator in much greater proportion than it is available in the habitat. Conversely, index values near -1 indicate that the prey category is selected much less than its abundance in the study area. Prey with index values near 0 are consumed in proportion to their availability (Kamler *et al*., 2012).

3.3 Investigations of resource utilization by predators, as well as their relationship with their prey and the environment, are important in understanding the mechanisms that influence vertebrate community structure (Vieira and Port, 2007). The three large carnivores' species are reported in HKK. However, resource utilization has never been studied. Overlapping of prey over utilization areas of dholes, leopards, and tigers was calculated using the following Pianka's formula (1974) as the following:

$$\text{Pianka's niche overlap index} = \frac{\sum P_{ij} \times P_{ik}}{\sqrt{(\sum i(P_{ij})^2 \times \sum i(P_{ik})^2)}}$$

where

P_{ij} is the percentage of prey species I of predator j

P_{ik} is the percentage of prey species I of predator k

Pianka's index varies between 0 (total separation) and 1 (total overlap). We used this index to enable comparisons with other studies on the diet similarity of South American foxes that used the same measurement of diet (e.g. Juarez and Marinho-Filho, 2002; Jacomo *et al*., 2004; Zapata *et al*., 2005).

RESULTS AND DISCUSSION

Spatial movement of dhole

Home range size

Two adult female dholes from different packs were captured on the 4th of July 2018 , around Mor Kru Kra area near Sub Fah Pha Forest Ranger

Station (SFP) and on the 31st of July 2018, near Huai Kha Khaeng River, Klong Phlu Long-term Ecological Research Station (KP). For the first dhole, 95 GPS locations were recorded between the 27th July, 2018 and 11th September, 2018. However, for the second dhole, only 31 GPS locations were recorded. The home range sizes at 100%, 95%, 75% and 50% for each dhole are shown in Table 1.

The home range size of the first dhole at 95% core area was 31.5 km^2 which was slightly larger than that of an adult female dhole (26.7 km^2) reported by Austin (2002) using a VHF radio collar in Khao Yai National Park (KY) .This may be due to the latter dhole being solitary, thus using a smaller area than a dhole pack. Jenks *et al.*, (2015) studied dhole using GPS-collars in Khao Ang Rue Nai Wildlife Sanctuary, and reported the home range to be 33 km^2, similar to the size of the first dhole in this study. The author also suggested that the dhole concentrated more around water sources in the dry season. However, the size of the home range of the first dhole was smaller than that reported by Durbin *et al*. (2004), who studied an adult male dhole in India, which had an average home range size of 55.0 km^2. The period of this study was reported to be during the breeding season and the dhole pack were taking care of their pups.

As for the second dhole in this study, data received from the GPS collar was much less than that of the first dhole and the home range was significantly smaller. This may be due to different factors affecting the signal transmission from the collar e.g. the density of the forest, the time schedule for satellite connection or other factors restricting the movement of the dhole. Further continuous monitoring and adding other means, e.g ground radio tracking will be conducted in order to get a better understanding of the home range of the second dhole.

Table 1 Home range size of the collared dholes in Huai Kha Khaeng Wildlife Sanctuary, Thailand, during July and October 2018 using satellite radio collars.

Dhole	The first dhole (Gift)	The second dhole (Klong Phlu)
Number of telemetry locations	95	31
100% core area (ha)	4,474.23	157.71
95% core area (ha)	3,151.63	33.39
75% core area (ha)	214.83	13.24
50% core area (ha)	6.05	3.38

Movement

The movement of the first dhole, based on the 95% core area of the GPS locations, showed an activity radius (average distance from the center of the animal's home) of 1,442.84 m (median = 450.00 m, range 0-8,312.60 m). The second dhole had an activity radius of 331.56 m (median = 209.11 m, range 0-3,476.56 m).

Based on regular ground checks within the animal's home range, concentrated especially in locations with intense activity that had appeared via satellite and radio transmissions, it was found that the home range of the first dhole mostly covered dry dipterocarp, mixed deciduous, and small areas of dry evergreen forests, with proportion in descending order, near Huai Song Thang River. The area of median terrain ranges between 200 - 500 m above mean sea level. The concentrated area found in the dry dipterocarp forest had no forest fires occurring at an elevation of 267 m above mean sea level. A small water source was also found in the area. The second concentrated area identified through ground check was an area 1 km from the forest road, where the animal was captured, 388 meters above mean sea level. This

area is covered with lower dry dipterocarp forest, < 10 m high, at the ridge of the mountain. Stone yards were distributed in this area; the lower area had forest trails used by large ungulates. This area was used by the collared dhole as a resting site. The third area identified was covered with dry evergreen forest near Huai Song Thang River. The carcass of the first collared dhole was found at this location. skeletal examination of the dhole carcass revealed a fractured rib and hip, which may be a result of the dhole's hunting activity. Regular ground checks also found that the first dhole traveled between Khao Nang Rum View Point to the north part of the HKK Head Office with a span of 14,292.29 meters.

On the other hand, the home range area of the second collared dhole mostly covered dry evergreen and mixed deciduous forests, with the proportion in descending order, near Huai Kha Khaeng River. The home range of the animal also covered a hot spring saltlick (Pru Nam Ron) where ungulate species were very abundant, especially sambar deer (*Rusa unicolor*), red muntjac (*Muntiacus muntjak*), gaur (*Bos gaurus*) and smaller wild animals.

The span of the home range was smaller than that of the first collared dhole, with the largest span of 3,920.69 m., but with a higher density of the prey base. The areas utilized by the two dholes in this study were similar to the areas reported by Jenks *et al.*, (2015) within the primary and secondary forest. Supported by the ground check, many animal trails were found, indicating a high density of prey. One of the collared dholes that Grassman (2005) captured was located in a closed forest. He also suggested that two of their prey species, sambar and red muntjac, were solitary and widely dispersed.

Prey abundance

During November 2017 to June 2018, 20 camera traps (a total of 3,172 trap days) were used to survey prey species and their relative

abundance in order to evaluate large predators and their prey's abundance. A total of 4,940 animal occasions were investigated.

The prey species with the highest relative abundance percentage was *Rusa unicolor* (30.93%), followed by birds (e.g. *Pavo muntiacus* and *Gallus Gallus*, 17.02%), *Canis aureus* (15.86%), and *Muntiacus muntjak* (12.96%) (Table 2). These results are similar to those in the Salak Pra Wildlife Sanctuary (SLP), Thailand, where in the same forest complex, *Rusa unicolor* was found to be the most common species (Charaspet, 2015).

During the study period, 30 dhole photographs were recorded with a % RA of 0.95. Among the large predators, the relative abundance of the leopard was the highest, followed by the tiger, and the dhole (Table 3). This result is similar to that of Simcharoen *et al*. (2018), who reported that, in HKK, the density of leopards is more than twice the density of tigers. Dholes had the lowest abundance when compared with tigers and leopards, probably due to the density of those two felids or spatial avoidance (Stainmetz *et al*. 2013; Selvan *et al*., 2013).

The above results show that there were more prey animals than predators. This finding is consistent with the theory of predator and prey interaction (Abrams, 2000). Furthermore, the camera traps detected dhole within the same locations as the two felid species at the area approximately 2 km from the HKK head office heading towards Kra- Pook Kra-Piaeng (KPKP), KP, SFP (Mor Khru Kra) and KNR. These data indicate that the high diversity and abundance of prey is sufficient to support the 3 large predators within the same area. Notably, this study also found domestic dogs in the same area where the three large predators were found. This location is approximately 10 km from the forest edge or the nearest village. This finding was similar to that in Khao Yai National Park. Jenks *et al*. (2011) found a

domestic dog in the central area of the park, 7 km from the park boundary. Domestic dogs may be a threat factor to wild species such as sambar deer, muntjac, civets or dholes. Moreover, domestic dogs may carry diseases harmful to the wild mammal populations (Jenks *et al.*, 2011), such as rabies, canine distemper, etc. (Alexander and Appel, 1994; Sabeta *et al.*, 2018). Strict enforcement of regulations regarding domestic dogs in the area is much needed.

Prey species identification by fecal analysis

Fourteen dholes' scats, 20 leopards' scats and 9 tigers' scats were found and collected during November 2017 to September 2018 along the forest roads in the study area. Fecal analysis results are shown in Figures 3 and

Table 2 Prey species and % relative abundance gained by camera trap technique in Huai Kha Khaeng Wildlife Sanctuary, Thailand, during November 2017 to June 2018, a total of 3,172 trap days.

No.	Scientific name	Common name	# of pictures	%RA
1	*Rusa unicolor*	Sambar deer	981	30.93
2	-	Peafowl and birds	540	17.02
3	*Canis aureus*	Asiatic jackal	503	15.86
4	*Muntiacus muntjak*	Red muntjac	411	12.96
5	*Sus scrofa*	Wild pig	361	11.38
6	*Viverra zibetha*	Large Indian civet	325	10.25
7	*Bos javanicus*	Banteng	303	9.55
8	-	Unknown rodent	284	8.95

Table 2 (Cont')

No.	Scientific name	Common name	# of pictures	%RA
9	*Hystrix brachyura*	Malayan porcupine	269	8.48
10	*Elephas maximus*	Wild elephant	258	8.13
11	*Paradoxurus hermaphroditus*	Common palm civet	231	7.28
12	*Prionailurus bengalensis*	Leopard cat	99	3.12
13	*Lepus peguensis*	Hare	62	1.95
14	*Herpestes urva*	Crab-eating mongoose	40	1.26
15	-	Unknown primate	23	0.73
16	*Ursus thibetanus*	Asiatic black bear	18	0.57
17	-	Unknown mammal	15	0.47
18	*Paguma larvata*	Masked palm civet	13	0.41
19	*Macaca faccicularis*	Long-tail macaque	12	0.38
20	*Viverricula indica*	Small Indian civet	10	0.32
21	*Bos gaurus*	Guar	8	0.25
22	*Tapirus indicus*	Tapir	7	0.22
23	*Macaca nemestrina*	Southern pig-tail macaque	7	0.22
24	*Ursus malayanus*	Sun bear	6	0.19
25	*Martes flavigula*	Yellow-throated marten	5	0.16
26	*Viverra megaspila*	Large-spotted civet	5	0.16
27	*Macaca mulatta*	Rhesus macaque	4	0.13
28	*Manis javanica*	Malayan pangolin	3	0.09
29	*Arctonyx collaris*	Hog badger	2	0.06
30	*Canis familiaris*	Domestic dog	2	0.06

Table 3 Number of dhole pictures and % relative abundance of dholes compared with leopards and tigers in the study area.

No.	Scientific name	Common name	# of pictures	%RA
1	*Cuon alpinus*	Dhole	30	0.95
2	*Panthera pardus*	Leopard	246	7.76
3	*Panthera tigris*	Tiger	103	3.25

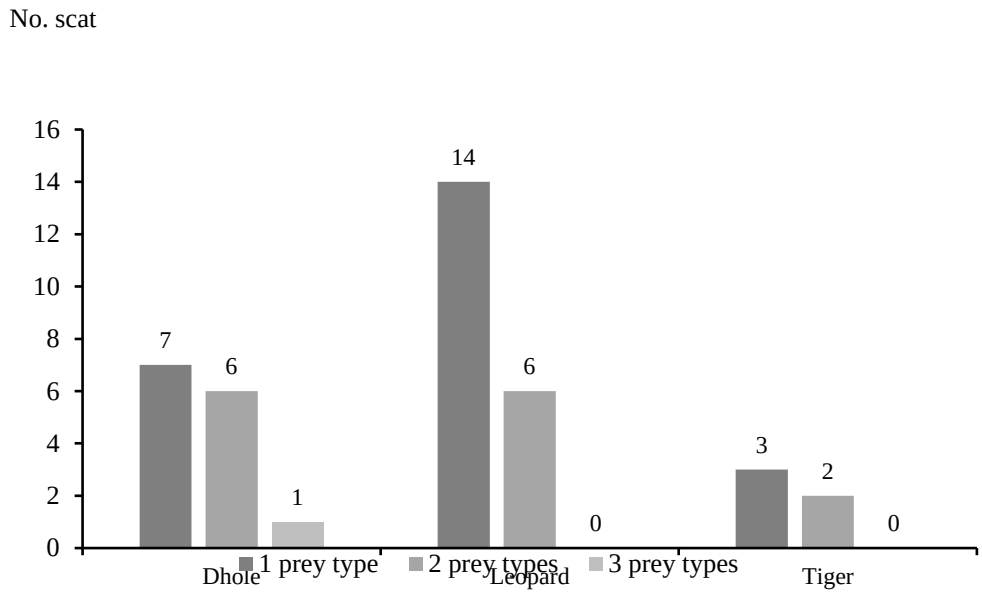

Figure 3 Comparison of the number of prey species found within individual samples of dhole (14), leopard (20) and tiger scats (5) collected from the study site.

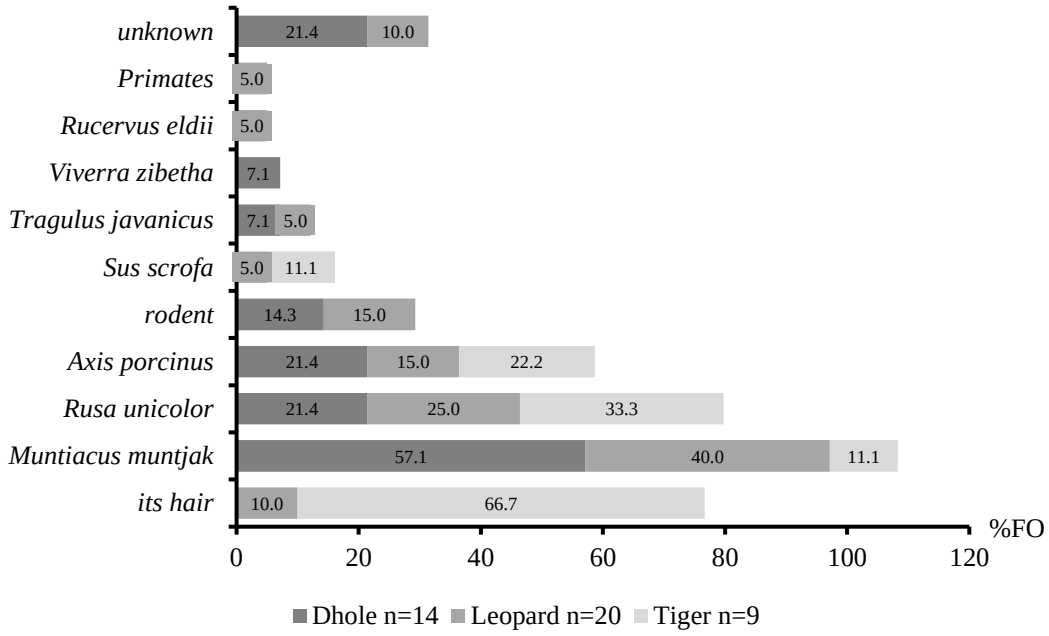

Figure 4 % Frequency of occurrence of dhole prey species in comparison with leopards and tigers within the study site.

Scat analysis revealed that 50% of the dhole scats contained only 1 species of prey, whereas 43% contained 2 prey species and the remaining 7% contained 3 species of prey (Figure 3). At least 6 prey species were confirmed by scat analysis with some hair (21.4%) that could not be identified. The highest frequency of occurrence of prey consumed by dholes was *Muntiacus muntjak* (57.14%), followed by *Rusa unicolor* and *Axis porcinus* (21.43%). This result is similar to two previous studies of dhole diets in Southeast Asia, Nam Et-Phou Louey National Protected Area (NEPL) (Kamler *et al*., 2012) and Phu Khieo Wildlife Sanctuary (PK) (Grassman, 2005), which found that dhole preyed primarily on *Muntiacus muntjak* and *Rusa unicolor* (Grassman, 2005; Kamler *et al*., 2012). These results contrast with those of the studies in Kao Yai National Park, Tap Lan National Park (TL), and SLP, which found that the highest prey selection of

dholes were *Sus scrofa* (Austin, 2002; Prayoon, 2014; Charaspet, 2015). Reasons for the differences in dhole diet in different protected areas may depend on prey diversity and their abundance, the study areas and especially the interaction between dhole and other large carnivores in the area. In the case of HHK, the dholes need to reduce pack size to reduce their competition with leopards and tigers, so smaller prey species were selected. However, in the other protected areas with no large carnivores, larger prey were hunted by a larger pack of dholes. This finding agrees with Karanth and Sunquist (1995), who reported that dhole fed on small bodied prey such as the black-naped hare (*Lepus nigricollis*) and porcupine (*Hystrix indica*), whereas tigers did not, because of the competition between predators and the success of the pack hunting strategy used by wild canids (Aryal *et al.*, 2015).

In this study, the highest % frequency of occurrence in the leopard scat was *Muntiacus muntjak* (40%) and the highest frequency of occurrence from tiger scat analysis was the *Rusa unicolor* (33.33%).

The above results contrast with Simcharoen (2008) who studied leopard scats in the same area and reported 26 prey species, with *Rusa unicolor* having the highest frequency of occurrence (25.96%). Two previous studies of tigers in HKK showed that *Muntiacus muntjak* (42%) and *Bos javanicus* (31.91%) were the most common prey in 1987-1988 and 1996-1998, respectively (Rabinowitz, 1989; Petdee, 2000). In this area, ungulates were the primary prey of the three predators. Prey species changed over time, perhaps because previous studies employed long-term scat-collecting covering many years, as well as because in this period there was a fluctuation in the density of or the population structure of ungulate species, that caused the results to differ.

Electivity index

Based on the Electivity index for measuring preferred prey, dholes mostly preferred smaller prey, *Muntiacus muntjak*, at a rate greater than its availability. Leopards preferred primates and *Muntiacus muntjak* more than their rate of availability. Tigers mostly preferred larger prey (i.e. *Rusa unicolor* and *Sus scrofa*), with the exception of *Muntiacus muntjak* based on their availability. This finding supports the concept of niche overlap with dholes and leopards consuming smaller ungulates and tigers consuming larger ungulates.

Prey overlap

Both interference and exploitation competition have long been recognized as important in shaping the ecological relationships of large carnivores (Kruuk, 1972). Based on Pianka's index used for measuring diet overlap between dholes and leopards, and dholes and tigers, the results showed a very high degree of overlap (0.98) between dholes and leopards, and somewhat high degree of overlap (0.68) between dholes and tigers. This result is similar to the results reported by Ramesh *et al*. (2012) in India, who reported that prey overlap between dholes and leopards was 0.99 and dholes and tigers was 0.62.

This indicates that there are interspecific competition in large predators' guilds (Ramesh *et al*., 2012). From combined data, we found that ungulate species composed of red muntjac, sambar deer, wild boar, and hog deer were the main prey of the three large predator species in HKK .

Results from camera traps in this study showed that the *Rusa unicolor* was the highest in abundance, but the dominant prey of dholes and leopards was small ungulates (*Muntiacus muntjak*). In comparison, tigers tended to consume large ungulates (*Rusa unicolor* and *Sus scrofa*). Perhaps the large body size of the tiger permits the safe capture of large and dangerous prey (Andheria *et al.*, 2007), whereas the leopard's body

size is more than five times smaller than *Rusa unicolor* (Ramesh *et al*., 2012b). Moreover, for efficient coexistence, they have to partition their diet through resources to reduce competition with the tiger (Ramesh *et al*., 2012).

CONCLUSIONS

Spacial distribution studies are of great importance in understanding the ecology of a species and can contribute highly to species management planning for future conservation activities. This study is the first report on the home range and movement of dhole in HKK, one of the richest and most diverse protected areas in Thailand. The distribution and home range of the dholes in this study represent the movement and behavior of the dholes in rich abundance prey habitats, but also overlapping with other predators. The presence of other predators can play an important role in prey selection and movement patterns of the dhole in the area. As shown in this study, the dholes' prey preferences are different from that of dholes reported in other protected areas.

Distribution and home range of the dhole in this study differ due to the difference in the number of points and the time for data collection. Continuous monitoring using various techniques and incresing the number of dholes monitored and the length of the monitoring to cover all seasons will help increase knowledge on the habitat choice, behavior and movement patterns of the dholes in the study area. Furthermore, an increase in the number of dholes monitored within the same pack can improve understanding of the pack dimension, social behavior, movement patterns and pack distribution, knowledge that is still lacking in this species.

ACKNOWLEDGEMENTS

I would like to express my sincere thanks to the Center for Advanced Studies in Tropical Natural Resources (CASTNaR), Kasetsart University, Bangkok, Thailand for

their financial support. I also would like to great thank the Earthwatch Institute USA, for their fellowship of financial support, supplying essential equipment, GPS collars, camera trap sets, and so on, especially the 3 years fund for Dhole research in Thailand. In addition, I am grateful to Mr. Thanee Wongnak, Head of the Huai Kha Khaeng Wildlife Sanctuary, for supporting the research staff and welcoming this research in the sanctuary. I am thankful to Mr. Tarasak Nipanan, Head of Huai Kha Khaeng Wildlife Breeding Center for supporting our team with accommodation every month. Finally, I am most grateful to my parent and my friends for all their motivation and support throughout the period of this research. I also would like to thank Prof. Dr. Robert Orr for editing my manuscript.

REFERENCES

Abrams, P. 2000. The evolution of predator-prey interactions: Theory and evidence. Annual Review of Ecology and Systematics. 31. 79-105. 10.1146/annurev.ecolsys.31.1.79.

Acharya. B. B. 2007. The ecology of the dhole or Asiatic wild dog (*Cuon alpinus*) In Pench Tiger Reserve, Madhya Pradesh. Ph.D Thesis. Saurashtra University, India.

Alexander, K. A. and M. J. G. Appel. 1994. African wild dogs (*Lycaon pictus*) endangered by a canine distemper epizootic among domestic dogs near the Masai Mara National Reserve, Kenya. Journal of Wildlife Diseases 30(4): 481-485.

Andheria, A. P., K. U. Karanth and N. S. Kumar. 2007. Diet and prey profiles of three sympatric large carnivores in Bandipur Tiger Reserve, India. Journal of Zoology 304: Print ISSN 0952-8369.

Aryal, A., S. Panthi, R. K. Barraclough, R. Bencini, B. Adhikari, W. Ji and D. Raubenheimer. 2015. Habitat selection and feeding ecology of dhole (*Cuon alpinus*) in the Himalayas. Journal of Mammalogy 96(1):47-53.

Austin, S. C. 2002. Ecology of Sympatric Carnivores in Khao Yai National Park, Thailand. Ph.D. Thesis, Texas A and M University-Kingsville.

Beschta, R. L., R. J. Ripple. 2009. Large predators and trophic cascades in terrestrial ecosystems of the western United States. Biology Conservation 142: 2401–2414.

Charaspet, K. 2015. Prey Species and Habitat Use of Dhole (*Cuon alpinus*)

in Salakpra Wildlife Sanctuary. M.S. Thesis, Kasetsart University. (in Thai)

Durbin, L.S., A. Venkataraman., S. Hedges and W. Duckworth. 2004. Dhole (*Cuon alpinus*): South Asia–South of the Himalaya (Oriental), pp. 210-219. Cited C. Sillero-Zubiri, M. Hoffmann and D. W. Macdonald, eds. Foxes, wolves, jackal and dogs: an action plan for the conservation of Canids. The wildlife Conservation Research Unit, Oxford, UK.

Faculty of Forestry, Kasetsart University 1989. Huai Kha Khaeng Wildlife Sanctuary Management Master Plan, 1900-1904. Faculty of Forestry, Kasetsart University, Bangkok. (in Thai)

Fieberg J. and L. Borger 2012. Could you please phrase "home range" as a question? Journal of Mammalogy 93 :890–902.

Fieberg J. and C. O. Kochanny. 2005. Quantifying home-range overlap: the importance of the utilization distribution Journal of Wildlife Management 69:1346–1359.

Francis, M. C. 2008. A Field Guide to the Mammals of Thailand and South-East Asia. Asia books, Bangkok.

Gopi, G.V., B. Habib, K.M. Selvan and S. Lyngdoh . 2012. Conservation of the endangered Asiatic wild dog *Cuon alpinus* in Western Arunachal Pradesh: linking ecology, ethnics and economics to foster better coexistence. Dehradun DST Project Completion Report TR-2012. Wildlife Institute of India.

Grassman, Lon I. Jr., N. J. Silvy and K. Kreetiyutanont. 2005. Spatial ecology and diet of the Dhole *Cuon alpinus* (Canidae, Canivora) in north central Thailand. Mammalia 69: 11-19.

Glen, A.S. and C. R. Dickman. 2014. The importance of predators, pp 1-12. In Carnivores of Australia: Past, Present and Future, Chapter: The importance of predators, Publisher: CSIRO Publishing.

Huai Kha Khaeng Wildlife Sanctuary. 2016. Huai Kha Khaeng Wildlife Sanctuary Management Master Plan, 2 016-2019. Huai Kha Khaeng Wildlife Sanctuary, Uthai Thani, Uthai Thani Province. (in Thai).

IUCN. 2018. IUCN Red List of Threatened Species. Available Source: October 15, 2018.

Jacobs, J. 1974. Quantitative measurement of food selection - a modification of the forage ratio and Ivlev's electivity index. Oecologia 14: 413–417.

Jacomo, A. T. A., L. Silveira and J.A.F. Diniz-Filho. 2004. Niche separation between the maned wolf (Crysocyon branchyurus), the crab-eating fox (*Dusicyon thous*) and the hoary fox (*Ducicyon vetulus*) in central Brazil. Journal of Zoology (London) 262, 99-106.

Jenks, K. E., P. Chanteap, K. Damrongchainarong, P. Cutter, P. Cutter, T. Redford, A. J. Lynam, J. Howard and P. Leimgruber. 2011. Using relative abundance indices from camera-trapping to test wildlife conservation hypotheses- an example from Khao Yai National Park, Thailand. Tropical Conservation Science 4(2): 113-131.

N. Songsasen, B. Kanchanasaka, P. Leimgruber and T. K. Fuller. 2014. Local people's attitudes and perceptions of dhole (Cuon alpinus) around protected areas in southeastern Thailand. Tropical Conservation Science 7(4):765-780.

E.O. Aikens, N. Songsasen, J. Calabrese, C. Fleming, N. Bhumpakphan, S.Wanghongsa, B. Kanchanasaka, M. Songer and P. Leimgruber. 2015. Comparative movement analysis for a sympatric dhole and golden jackal in human-dominated landscapes. Raffle's Bulletin of Zoology 63: 546-554.

Juarez, K. M. and Marinho-Filho, J. 2002. Diet, habitat use, and home ranges of sympatric canids in central Brazil. Journal of Mammalogy 83, 925-933.

Kamler, J. F., A. Johnson, C. Vongkhamheng and A. Bousa. 2012. The diet, prey selection, and activity of dholes (*Cuon alpinus*) in northern Laos. Journal of Mammalogy 93, 627-633.

Kanchanasaka, B., S. Tunhikorn, S, Vinitpornsawan, U. Prayoon and K. Faengbubpha. 2010. Status of Large Mammals in Thailand. Wildlife Research Division, DNP, Bangkok. (in Thai)

Karanth KU, Sunquist M.E. 1995. Prey selection by tiger, leopard and dhole in tropical forests. Journal of Animal Ecology 64: 439-450.

Kawanishi, K. and M.E. Sunquist. 2008. Food habits and activity patterns of the Asiatic golden cat (*Catopuma temminckii*) and dhole (*Cuon alpinus*) in a Primary rainforest of Peninsular Malaysia. Mammal Study 33: 73-177.

Kruuk, H. 1972. The spotted hyena. Chicago: A Study of Predation and Social Behavior University of Chicago Press, USA.

Kumaraguru, A., R. Saravanamuthu, K. Brinda and S. Asokan. 2011. Prey preference of large carnivores in Anamalai Tiger Reserve, India. European Journal of Wildlife Research 57: 627-637.

Lekagul, B. and J. A. McNeely. 1977. Mammals of Thailand. Sahakarnbhat, Bangkok Thailand.

Moruzzi, T. L., T. K. Fuller, R. M. De Graaf, R. T. Brooks and W. Li. 2002.Assessing remotely triggered cameras for surveying carnivore distribution. Wildlife Society Bulletin 30(2): 380-386.

O'Brien, T. G., M. F. Kinnaird and H. T. Wibisono. 2003. Crouching tigers, hidden prey: Sumatran tiger and prey populations in a tropical forest landscape. Animal Conservation 6: 131-139.

Petdee, A. 2000. Feeding habits of the tiger (*Pantera tigris* Linnaeus) in Huai Kha Khaeng Wildlife Sanctuary by fecal analysis. M.Sc. Thesis, Kasetsart University, Bangkok. (in Thai).

Pianka, E. R. 1974. Niche overlap and diffuse competition. Proc. Natl. Acad. Sci. 71:2141-2145.

Powell R. A. and M.S. Mitchell. 2012. What is a home range? Journal of Mammalogy 93: 948–958.

Prayoon, U. 2014. Abundance, suitable habitat and main prey of dhole (*Cuon alpinus* (Pallas, 1811)) in Thap Lan National Park. M.S. Thesis, Kasetsart University. (in Thai)

Rabinowitz, A. 1989. The density and behaviour of large cats in a dry tropical forest mosaic in Huai Kha Khaeng Wildlife Sanctuary, Thailand. Nat. Hist. Bull. Siam Soc., 37(2): 235-51.

Ramesh, T, R. Kalle, K. Sankar and Q. Qureshi. 2012. Dietary partitioning in sympatric large carnivores in a tropical forest of western Ghats, India. Mammal study 37: 313-321.

Rechetelo J, A. Grice, A.E. Reside, B.D. Hardesty and J. Moloney. 2016. Movement Patterns, Home Range Size and Habitat Selection of an Endangered Resource Tracking Species, the Black-Throated Finch (*Poephila cinctacincta*). PLoS ONE 11(11):e0167254. doi:10.1371/journal. pone.0167254.

Sabeta, C. T., D. D. J. van Rensburg, B. Phahladira, D. Mohale, R. F. Harrison-White, C. Esterhuyzn and J. H. Williams. 2018. Rabies of canid biotype in wild dog (*Lycaon pictus*) and spotted hyaena (*Crocuta crocuta*) in Madikwe Game Reserve, South Africa in 2014-2015: Diagnosis, possible origins and implications for control. Journal of the South African Veterinary Association ISSN: (Online) 2224-9435.

Selvan, K.M., G.G. Veeraswami, S. Lyngdoh, B. Habib and S.A. Hussain. 2013. Prey selection and food habits of three sympatric large carnivores in a tropical lowland forest of the eastern Himalayan biodiversity Hotspot. Mammalian Biology 78: 296-303.

Slangsingha, N. 2012. Prey Species and Habitat Use of the Dhole (*Cuon alpinus*) in Phu Khieo Wildlife Sanctuary in Chaiyaphum Province. M.S. Thesis, Kasetsart University. (in Thai)

Simcharoen S. 2008. Ecology of the leopards (*Panthera pardus* Linn.) in Huai Kha Khaeng Wildlife Sanctuary. Ph. D. Thesis, Kasetsart University.

Simcharoen, A., S. Simcharoen, S. Duangchantrasiri, J. Bump and J. L. D

Smith. 2018. Tiger and leopard diets in western Thailand: Evidence for overlap and potential consequences. Food web 5: e00085.

Spencer, W. D. 2012. Home ranges and the value of spatial information. *Journal of Mammalogy* 93(4): 929–947.

Stainmetz, R., N. Seuaturien and W. Chutipong. 2013. Tiger, Leopard and Dhole in a half-empty forest: Assessing species interactions in a guild of threatened carnivores. Elsevier 163: 68-78.

Viana, D. S., J. E. Granados, P. Fandos, J. M. Pérez, F. J. Cano-Manuel, D. Burón, G. Fandos, María Ángeles Párraga Aguado, Jordi Figuerola and Ramón C. Soriguer. 2018. Linking seasonal home range size with habitat selection and movement in a mountain ungulate. Movement Ecology 6:1 DOI 10.1186/s40462-017-0119-8

Vieira, E. M.and D. Port. 2006. Niche overlap and resource partitioning between two sympatric fox species in southern Brazil. Journal of Zoology 272: 57-63.

Zapata, S.C., A. Travaini, Delibes, M. and R. Martinez-Peck. 2005. Food habits and resource partitioning between grey and culpeo foxes in southeastern Argentine Patagonia. Stud. Neot. Fauna Environ 40: 97-103.

Traditional Ecological Knowledge of Indonesian Sea Nomads "Orang Suku Laut" on Climate Change Adaptation

Wengki Ariando[1] and Sangchan Limjirakan[2]

[1]International Program of Environment, Development, and Sustainability, Graduate School, Chulalongkorn University, Thailand
[2]Environmental Research Institute, Chulalongkorn University, Thailand
Corresponding author: e-mail: lsangcha@chula.ac.th

ABSTRACT

At the international community, Traditional Ecological Knowledges (TEKs) have been recognized and acknowledged the important roles of indigenous peoples to tackle climate change. The cultural practice, cultural belief and adaptive capacity in managing nature by the *Orang Suku Laut* (OSL), Indonesian indigenous group who are living as nomads in the sea, would be considered as the key drivers to achieve the effectiveness of climate change adaptation. This research aimed to study the TEKs of the OSL on climate change adaptation. The semi-structured questionnaire was developed for a field observation and an in-depth interview the informants by using the purposive sampling method to select the multilevel informants (n= 77). The study found that 80.18% of the OSL have known about climate change and its impacts on their livelihood. The TEKs of the OSL on climate change adaptation include best practice (53.3%), cultural belief (33.3%), and adaptive capacity (13.4%). About 55% of them mentioned that the TEKs would be integrated with any modern technology in adapting to climate change. The study also found that the challenges of the OSL in using their TEKs for climate change adaptation consist of the degradation of their cultural belief and practice. In addition, climate variability, governmental policies, globalization,

and socio-economic situation were observed as principle factors in declining their TEKs. Therefore, the Indonesian action plans on climate change adaptation would take consideration the TEKs regarding their autonomous adaptation. The study would highly recommend the involvement of the OSL through the Free, Prior, and Informed Consent (FPIC) participation in the national strategic plans on climate change adaptation with a clear direction.

Keywords: Traditional Ecological Knowledge (TEK), Indonesian Sea Nomads, Orang Suku Laut (OSL), Climate Change Adaptation

INTRODUCTION

The Indigenous Peoples (IPs) are successor and native of distinctive cultures and ways of thinking with people and the environment whom have treasured social, cultural, economic, and political characteristics that are distinct from those of the assertive societies in which they live (United Nations, 2013). Tauli-Corpuz et al. (2009) also defined the IPs as survivors who are dependent on the land and natural resources from the ecosystems and the forefront of climate change impacts and threats.

Presently, the IPs worldwide stand up to share their experience and joint problems related to their right protections as distinct peoples. The IPs are a vulnerable group on climate change (IPCC, 2014). Climate change would add more complex challenges to be faced by the IPs regarding hazards such as fire and floods, and local environmental management issues in association with invasive species (Bardsley and Wiseman, 2012).

The IPs play a role as the cultural dimension in combating climate change by their TEKs (IPCC, 2014). The knowledge as practices, and cultural belief through direct contact with the environment performs the fundamental framework of the TEKs over many hundreds of years (Berkes, 1993). However, the experiential knowledge of the TEKs

bestow the critical insights for the design of adaptation and mitigation strategies to cope with global environmental change in the present time (Gómez-Baggethun et al., 2013).

The TEKs are the key points in an attempt to successfully translate local knowledge and scientific framings into a concept and its implications in the compelling arena of climate change adaptation (Fernandez-Llamazares et al., 2015). The IPs have the ability to adapt themselves to adjust the timing of activities and employ a variety of techniques in surviving changing conditions for climate change adaptation (Berkes et al., 2000). Regarding the OSL, one the IPs in Indonesia, the group uses their TEKs as an identity to combat climate change through friendly environmental practices. Presently, the OSL is living in the coastal area, small islands in the boat as nomads in the sea.

The integration of the TEKs with scientific knowledge would be a pathway to construct the adaptability on climate change (Negi et al., 2017). The study on the TEKs would be required in providing information and opportunity for climate change policy at local and national level for appropriate implemented climate change adaptation. Susilowardhani (2014) state that the increasing impacts of climate change in Indonesia has raised the need to implement the action plans of climate change adaptation. In this regard, this research aims to study the TEKs of the OSL on climate change adaptation.

Study Area

This research was conducted at the *Orang Suku Laut* communities in the Lingga Regency, Riau Islands Province, Indonesia between November 2018 and January 2019. The Lingga Regency is one of the regencies located on the equator line. There are 30 OSL' communities, 806 households with the population of 3931. Those communities are

shown in Figure 1. The OSL communities of the Lingga Regency are the IPs of Malay Ethnic who are still living under the poverty line. Presently, they are divided into nomadic groups, semi-nomadic group, and sedentary life group.

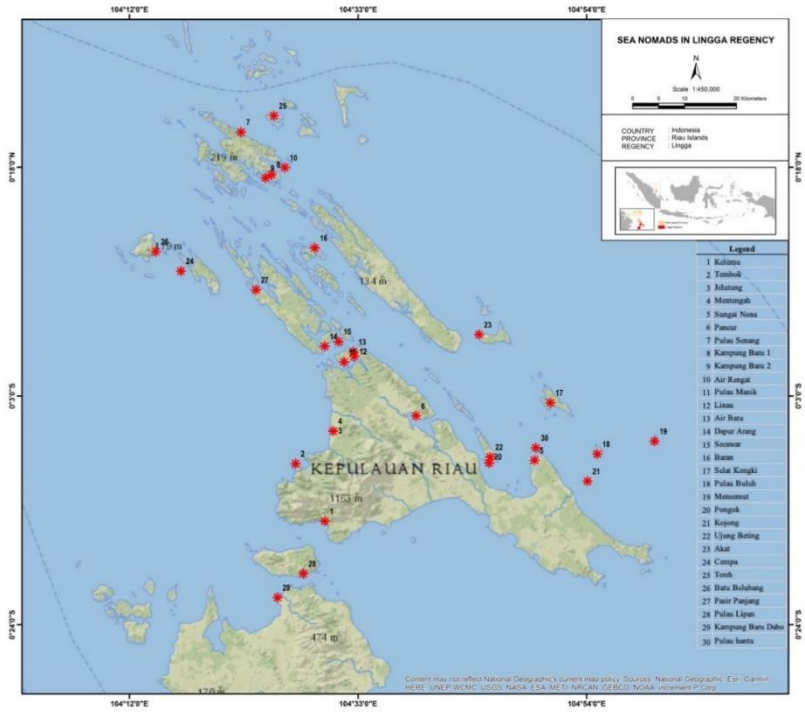

Figure 1 Location of the Orang Suku Laut (OSL) in the Lingga Regenc

METHODOLOGY

A field observation and an in-depth interview of multilevel TEKs' respondents were conducted using semi-structured questionnaire to obtain information on climate change and the TEKs. The respondents were selected using a purposive sampling method, a non-probability form of sampling which aims to sample the cases or participants in a strategic way and relevant to the research questions that are being posed (Bryman, 2012). Those OSL were communities' headmen, elders, women, and youth. Data collected was analyzed using the statistical and descriptive content analysis.

RESULTS AND DISCUSSION

Demographics of Respondents

The respondents consisted of multilevel stakeholders of the communities' headmen (31.03%), elders (27.59%), women (17.24%), and youth (24.14%). 62.07% of the respondents were males and 37.93% were females. The majority ages of the respondents were in the range of 41–50 (24.14%). 93.10% of them were not in school. The occupation of the respondent is a fisherman for males and a housewife for females.

Traditional Ecological Knowledge

The findings of the OSL's TEKs signify the way of thinking of human soul. Their thought respects to natural hazards and environment. The TEKs of the OSL on climate change adaptation have contributed to the understanding of the vulnerabilities, concerns, adaptive capacities, and longer-term aspirations.

Table 1 presents the perception of the OSL on climate change and its impacts. 80.18% of them knew climate change as the environmental changes and natural resources loss. The understanding on current climate is about natural resources degraded, extreme weather events and temperature increased, and fishery productions and incomes declined. 96.88% of respondents mentioned that climate variability impacts on seasonal pattern and their livelihood, such as water and health-related issues

Table 1 Climate Change Perception of the Orang Suku Laut

Category	Climate change (%)	Current climate is changing (%)	Seasonal changes impacted on livelihood (%)
Headmen	100	100	100
Elder	75	75	87.50
Women	60	100	100
Youth	85.71	85.71	100

The study found that TEKs of the OSL on climate change adaptation including cultural practice, cultural belief, and adaptive capacity at the percentage of 53.3, 33.3, and 13.4 as shown in Figure 2. The cultural practices, cultural beliefs and adaptive capacities of the TEKs in climate change adaptation are interconnected practices. The TEKs can help to provide efficient, appropriate, and time-tested ways of responding to climate change for community development projects in a specific place (Pandey et al., 2018). About 55% of the respondents realized that modern technology should be integrated with the TEKs in adapting to climate change.

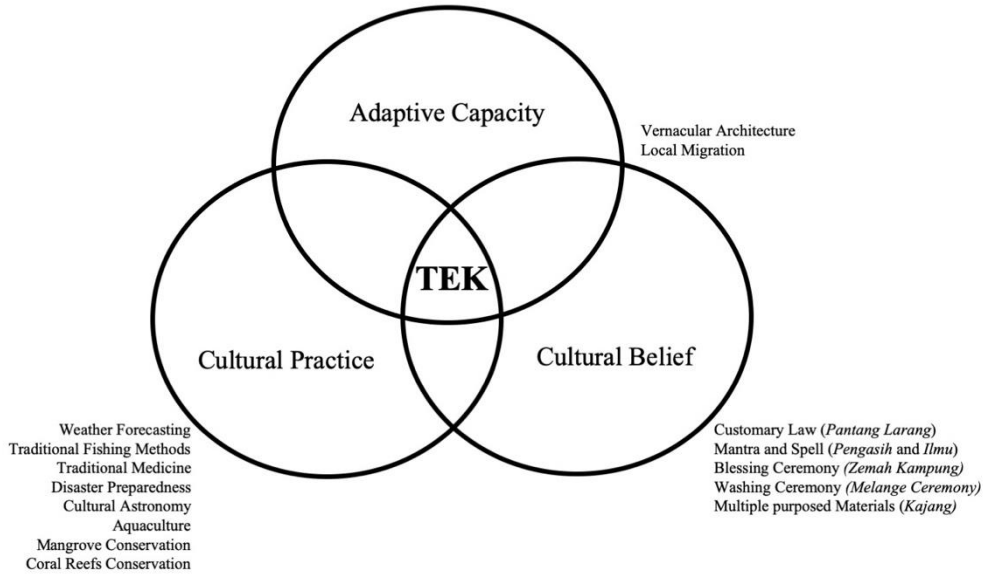

Figure 2 Traditional Ecological Knowledge (TEKs) of the Orang Suku Laut on climate change adaptation

The challenges of the OSL in using their TEKs for climate change adaptation is the degradation of cultural belief and practice. The youth underestimates and abandons the TEKs because of its unreasonable and primitive activities. Nakashima and Roue (2002) reported that severe power relationships among the IPs and society could be the implications of the TEKs reduction.

Cultural Practice

The various practices are the higher expression TEKs of the OSL because they are spontaneously used every day. The TEKs practices on climate change would be a tool to reduce environmental hazards and hydrometeorological threats. The TEKs practices related to climate change are weather forecasting, traditional fishing method, traditional medicine, disaster preparedness, cultural astronomy, aquaculture, mangrove conservation and coral reef conservation.

The TEKs practices of the OSL are influenced by seasonal calendars of the monsoonal season. The northern monsoonal season (December to February) is the highest hydrometeorology hazards. While the eastern monsoonal season (March to May) is the high productivity of fishing. The southern monsoonal season (June to August) is a dry season and the western monsoonal season (September to November) is the rainy season. Currently, the seasonal calendar has changed and become more unpredictable due to climate change that impacts on eco-niches and livelihood of the OSL. Additionally, the OSL have their way to adapt themselves to the drought in the southern monsoonal season. Before the drought season, the OSL will keep much water from various sources using at least a month.

Cultural Belief

Cultural belief is spiritual or religious dimensions (beliefs) that do not make sense to science or fall outside the realm of science (Berkes, 2012). Cultural beliefs of the OSL are dynamic and reflexive which easy to connect with the spirit of the environmental changing such as customary law (*Pantang Larang*), mantra and spell (*Pengasih* and *Ilmu*), blessing ceremony *(Zemah Kampung)*, washing ceremony *(Melange Ceremony)*, and multiple purposed materials (*Kajang)*. The whole practice of cultural beliefs related to the spirituality and taboos of the OSL. For instance, the best practice of the OSL is traditional fishing performed with their cultural

beliefs. Some traditional fishing and aquaculture practices are performed as a ceremony to wish the good things from the sea god and spearfishing (*Zemah Kampung*).

Other cultural beliefs of the OSL are *Pengasih* and *Ilmu*. The *Pengasih* is a cultural belief that studies the personal appeal or group to attract others in protecting nature and living together as a peaceful society. Chou (1997) stated the meaning of *Ilmu* is magic, knowledge, and science of the OSL. According to the headmen and elder respondents of the OSL, their *Ilmu* can reduce the rain intensity, moving the storm, changing weather pattern and weather forecasting.

Adaptive Capacity

Adaptive capacity is the attributes of a system to adjust its characteristics or behavior, to expand its coping range under existing climate variability, or future climate conditions (IPCC, 2014). The study found that the outstanding adaptive capacity of the OSL is a vernacular architecture and local migration. The vernacular buildings are unique interaction between the human mind and experience gathered by observing natural phenomena like climate change (Motealleh et al., 2018). The vernacular architecture as the TEKs of the OSL consists of a stilt house (*Saphaw)* and a rowing boat (*Sampan Kajang).* The *Saphaw* is the stilt house that built in coastal line, in the sea or the small island. The reason why the OSL stays in the *Saphaw* or the *Sampan Kajang* is that they cannot sleep if they do not hear the waves and sea current sound. This stilt house is durable to disaster. The materials used are from wood and leaf that the sunlight can penetrate making the low temperature inside of the house. The *Sampan Kajang* is the rowing boat of the OSL from many generations. The traditional boat is used without harming the environment. The OSL believe that the *Sampan Kajang* is the heritage of their ancestor.

Another adaptive capacity of the OSL is the temporary migration from one

island to another island when the northern monsoonal season is coming. According to Makondo and Thomas (2018), this seasonal or circular migration pattern can be considered as a traditional positive adaptation strategy for seasonal climate variabilities. The traditional climatic knowledge in the high-risk area from the IPs is important to adapt themselves in migrating or relocating to new areas due to droughts, rising tides, floods, pestilence, and political strife (Reedy et al., 2013).

When storm surge is coming, the OSL will migrate to the nearest safety island or go inside the mangrove forest or row into a small river in the big island. The OSL will try to move from the boat to the island. They can predict at least an hour before the storm is coming by investigating the environmental change. The OSL will come back to their settlement or boat when the storm is over.

CONCLUSIONS

The TEKs of the OSL is adequate activities in combating climate change through the interconnection among their cultural practice, cultural belief, and adaptive capacity. The challenges of the OSL in using their TEKs for climate change adaptation consist of the degradation of their cultural belief and practice. Climate variability, governmental policies, globalization, and socio-economic situation were observed as principle factors in declining their TEKs. Therefore, the Indonesian action plans on climate change adaptation would take consideration the TEKs regarding their autonomous adaptation. The study would highly recommend the involvement of the OSL through the Free, Prior, and Informed Consent (FPIC) participation in the national strategic plans on climate change adaptation with a clear direction.

ACKNOWLEDGEMENTS

The author would like to sincerely thank to the support of Dr. Sangchan Limjirakan as an advisor, and the International Program of

Environment, Development, and Sustainability, Graduate School, Chulalongkorn University for a financial support.

REFERENCES

Bardsley, D.K., Wiseman, N.D. Climate change vulnerability and social development for remote indigenous communities of South Australia. Global Environmental Change 2012; 22(3): 713-723.

Berkes, F. Traditional Ecological Knowledge: Concepts and Cases, in: Inglis, J.T. (Ed.), Traditional Ecological Knowledge in Perspective. Canada: International Program on Traditional Ecological Knowledge and International Development Research Centre; 1993.

Berkes, F. Sacred Ecology, 3 ed. New York: Routledge; 2012.

Berkes, F., Colding, J., Folke, C. Rediscovery of Traditional Ecological Knowledge as Adaptive Management. Ecological Applications 2000; 10(5): 1251-1262.

Bryman, A., Social Research Methods. New York: Oxford University Press Inc.; 2012.

Chou, C. (1997) Contesting the tenure of territoriality: the Orang Suku Laut. Bijdragen tot de Taal- Land- en Volkenkunde 1997; 153(4): 605-629.

Fernandez-Llamazares, A., Mendez-Lopez, M.E., Diaz-Reviriego, I., McBride, M.F., Pyhala, A., Rosell-Mele, A., Reyes-Garcia, V. Links between media communication and local perceptions of climate change in an indigenous society. Clim Change (2015); 131(2), 307-320.

Gómez-Baggethun, E., Corbera, E., Reyes-García, V. Traditional Ecological Knowledge and Global Environmental Change: Research findings and policy implications. Ecology and Society 2013; 18(4): 1-8.

IPCC. Summary for Policy Makers, In: Climate Change 2014: Impact, Adaptation, and Vulnerability. Part A: Global and SEctoral Aspects. Contribution of Working Group II to the Fifth Assessment Report of the Intergovernmental Panel on Climate Change, in: Field, C.B., V.R. Barros, D.J. Dokken, K.J. Mach, M.D. Mastrandrea, T.E. Bilir, M. Chatterjee, K.L. Ebi, Y.O. Estrada, R.C. Genova, B. Girma, E.S. Kissel, A.N. Levy, S. MacCracken,, P.R. Mastrandrea, a.L.L.W.e. (Eds.). United Kingdom and New York, NY, USA: Cambridge University Press; 2014. p. 1-32.

Makondo, C.C., Thomas, D.S.G. Climate change adaptation: Linking indigenous knowledge with western science for effective adaptation.

Environmental Science & Policy 2018; 88: 83-91.

Motealleh, P., Zolfaghari, M., Parsaee, M. Investigating climate responsive solutions in vernacular architecture of Bushehr city. HBRC Journal 2018; 14(2): 215-223.

Nakashima, D., Roue, M..Indigenous Knowledge, Peoples and Sustainable Practice, in: Munn, T. (Ed.), Social and economic dimensions of global environmental change. Chichester: John Wiley; 2002. p. 314-324.

Negi, V.S., Maikhuri, R.K., Pharswan, D., Thakur, S., Dhyani, P.P. Climate change impact in the Western Himalaya: people's perception and adaptive strategies. Journal of Mountain Science 2017; 14(2): 403-416.

Pandey, R., Kumar, P., Archie, K.M., Gupta, A.K., Joshi, P.K., Valente, D., Petrosillo, I. Climate change adaptation in the western-Himalayas: Household level perspectives on impacts and barriers. Ecological Indicators 2018; 84: 27-37.

Reedy, D., Savo, V., McClatchey, W. Traditional Climatic Knowledge: Orchardists' perceptions of and adaptation to climate change in the Campania region (Southern Italy). Plant Biosystems - An International Journal Dealing with all Aspects of Plant Biology 2013; 148(4), 699-712.

Susilowardhani, A. The Potential of Strategic Environmental Assessment to Address the Challenges of Climate Change to Reduce the Risks of Disasters: A Case Study from Semarang, Indonesia. Procedia - Social and Behavioral Sciences 2014; 135: 3-9.

Tauli-Corpuz, V., Enkiwe-Abayao, L., Magata, H., Tugendhat, H. Asia Summit on Climate Change and Indigenous Peoples (Ed.) Bali: AMAN; 2009.

United Nations. Indigenous Peoples and the United Nations Human Rights System, in: Nations, U. (Ed.). Geneva, New York: United Nations; 2013

Valuing Benefits of Soil Conservation to Support Payment for Ecosystem Services in Mae Sa Watershed, Chiang Mai Province

Oraphan Pradit[1*], Jirawan Kitchaicharoen[2]

[1*]Agricultural Systems Management Program, Center for Agriculture Resource System Research, Faculty of Agriculture, Chiang Mai University, Chiang Mai, Thailand

[2]Division of Agricultural Economics, Department of Agricultural Economy and Development, Faculty of Agriculture, Chiang Mai University, Chiang Mai, Thailand

Corresponding author: e-mail: mimaggie38@hotmail.com

ABSTRACT

Soil erosion widely affects not only upland farm productivity but also lowland environment through the processes of run-off and sedimentation. Payments for ecosystem services (PES) can be used as a tool to provide incentives for upland farmers to increase their adoption of soil conservation practices. This paper attempts to evaluate these benefits for implementing PES scheme. Soil erosions were assessed using the universal soil loss equation. The cost-benefit analysis was divided into on-site and off-site components. The results found that the economic value of soil conservation of all watershed by bench terrace and contouring, and bench terrace and hillside ditch measure are 5,948,039 and 8,142,588 baht/year which were analyzed from soil erosion rate at 2.56 and 1.02 ton/rai/year. The cost-benefit analysis of soil conservation showed that the costs of soil conservation practice are less than benefit 1.17 and 0.96 times, and the internal rate of return are 9 and 7%.

Keywords: Cost-Benefit Analysis, Soil Erosion, On-Site and Off-Site Cost of Soil Erosion

INTRODUCTION

Land degradation is one of the most important problems in developing countries where the land-based agricultural sector has a strong link with the economic well – being in general, and natural resources and environment in particular as far as an entire watershed ecosystem is concerned. Farmers within their agricultural system context will manage the best their resources; soil, water, money, and labors to produce the most output and/or income. But farming on land with gradients and with negligence from whatever reasons can result in declining soil fertility and nutrients on farm in the long term as well as some negative off-site effects. It thus becomes crucial for farmers in this setting to adopt soil fertility conservation measures such as contour cultivation and terrace construction for protection against agricultural soil quality decay. Without proper conservation measures, soil erosion is foreseeable and its process will disturb the natural balance, impair farmland and output productivity, bring down the financial and economic values of the land, and perhaps eventually bring to farmers the threat of income loss. Moreover, soil erosion destructs the water resources and public assets, and give rise to flooding and silting up of waterways (Telles et al, 2011).

The major problem of soil resources in Thailand is Soil erosion problems with 108.87 million rai, nutrient loss problems in soil with 98.70 million rai and the problem of soil use is not appropriate according to the soil potential with 35.60 million rai, most of which occur on upland areas in the north (National Statistical Office, 2008). These situations can cause economic and environmental damages (Lal, 2001), particularly soil erosion from the cultivation of plants in the upper part of basins which contributes to undesirable off-site sediment deposits.

In Mae Sa watershed, agricultural areas continue to increase under a rapidly expanding economic activities and intensive farming.

Between 2010 and 2015, an additional 2,293 rai of land in Mae Sa watershed was converted to agriculture or an increase of 460 rai per year, approximately. However with recognition of on-going and potential problems about soil erosion and land degradation from farming activities in hilly areas of Northern Thailand including Mae Sa watershed, the government has tried to promote and support the farmers to adopt agricultural conservation practices such as organic farming, soil conservation measures, bench terrace, contouring, hillside ditch and planting Vetiver grass in sloping areas to deal with the problems (Department of Agricultural Extension, 1994). Nowadays, farmers in upstream areas of Mae Sa watershed have been doing soil conservation to prevent soil erosion and improve the ecosystem. Nevertheless, the conservation activities impose additional costs on implementing farmers while generating external benefit to the downstream people in terms of decreased sedimentation. Thus, the latter should pay or support the upstream villagers to undertake such activities and payment for ecosystem services is a mechanism to solve the payment problem.

In this study, the agricultural ecosystem was estimated in terms of soil conservation activity as soil retention (regulating services). There are benefits of soil conservation and costs of soil erosion that occur from agricultural land use. Soil erosion costs can be divided into the on – site and off – site costs. On-site cost is a direct or internal cost of farmers such as nutrient loss, lost yield, drop in land value and biological loss. Off-site cost is indirect or external effects on society, such as sedimentation, flooding, water treatment, electrical power generation, repairing public property, global warming, disasters, and increase of food price (Telles et al, 2011). There are three practices namely terrace and contouring (the recent practice) and bench terrace and hill ditch (full conservation) prevailing in Mae Sa watershed that

were used for assessing and analyzing the costs and benefits of soil conservation.

Thus, our results will benefit those who devise policy regarding soil conservation practices in northern Thailand.

METHODOLOGY

Materials and methods are distinguished into those for data collection by means of questionnaire, for soil erosion assessment using the Universal Soil Loss Equation (USLE) and for economic valuation of soil conservation through cost-benefit analysis. The estimation was divided into short – term (1 year) and long – term (30 years) analysis to show the cost and benefit of soil conservation in 30-year duration. The Universal Soil Loss Equation: USLE was used to analyze soil erosion per year in Mae Sa Watershed. In addition, we used the data of organic matter and nutrient loss from the study of the effect on soil and water conservation in the upland area of Mae Sa Watershed.

Data collection method

Main agricultural areas in Mae Sa watershed are identified as under mixed crops 8,201.25 rai (42.27%); orchards 7,345.69 rai (37.86%), shifting cultivation 1,838.25 rai (9.47%), paddy field 1,491.19 rai (7.69%) and field crops 527.06 rai (2.72%) (Land Development Department, 2017). Planted in mixed crops area are rose, gerbera, chrysanthemum, white cabbage, Chinese cabbage, potato, lettuce, onion, bell pepper, white radish, bean etc. For being predominant, mixed crops were used as representatives of the cultivation in Mae Sa Watershed.

For data collection, the yearly cultivation data such as investment cost, the average of output and price of rose, gerbera, chrysanthemum, white cabbage, Chinese cabbage, potato, lettuce, onion, bell pepper, white radish, bean was divided into 3 degradation practice, bench

management practices: degradation practice, bench terrace and contouring (current practice), and bench terrace and hill ditch (full conservation) with the number of samples of 30, 30 and 10, respectively. The last practice was 10 samples because they hardly to found in Mae Sa watershed.

The total cost of soil erosion was divided into the on-site cost and off-site cost. In this study, the on-site cost was based on loss of N, P, K nutrients and loss of topsoil and the off-site cost was based on increased sedimentation in the calculation (Telles et al, 2012). The private benefits of soil conservation were evaluated by converting the on-site cost of degradation practice into on-site benefits of full conservation. The social benefits were converted from the cost of clearing sedimentation in waterways. This study further considered the private net present value (NPV), the benefit-cost ratio (B/C ratio) and the internal rate of return (IRR) of soil conservation by examining their values per rai for all soil conservation practices in terms of financial and economic benefits (IFRRI, 2008). Soil erosion costs were separated into on-site and off-site. The on-site cost was based on the loss of N, P, K nutrients from the study of "The effect from soil and water conservation in the highland of Mae Sa watershed (Panajumnong, 2008) and the loss of topsoil was calculated from the soil erosion equation. Off-site cost depended on increased sedimentation and soil erosion equation was used to find out sediment volumes. Soil conservation benefits were converted from the cost of soil erosion.

Soil erosion assessment

The Universal Soil Loss Equation (USLE) predicts the average annual rate of soil erosion in sloping fields based on rainfall pattern, soil type, topography, crop system and management practices (Minister of Agriculture, Food and Rural Affairs Ontario, 2016).

$$A = R \times K \times LS \times C \times P \quad (1)$$

Where: A represents the potential average annual soil loss in tons per hectare per year, R is the rainfall and runoff factor by geographic location, K is the soil erodibility factor, LS is the slope length-gradient factor, C is the crop/vegetation and management factor, P is the support practice factor

The economic value of soil conservation

This part was composed of short-term and long-term economic effects. Short-term economic effects were divided into an on-site and off-site cost. Long term economic effects were evaluated by cost-benefit analysis in terms of financial benefits and economic benefits.

1) Short-term economic effects

To define the total cost of soil erosion, the on-site cost (based on the sum of nutrients in the soil and water and loss of soil erosion) and off-site cost (based on sediment yield) were combined together (Telles et al, 2012).

$$C' = C_{on-site} + C_{off-site} \quad (2)$$

Where: C' is the total cost of agricultural soil erosion, $C_{on-site}$ is the cost of resulting from loss of agricultural property, $C_{off-site}$ is the cost resulting from loss of agricultural property which affects society

$$C_{on-site} = \sum_{i=1}^{m}(C_i Q_i) \quad (3)$$

Where: $C_{on-site}$ is the cost of soil erosion on agricultural property, C_i is the price of different types of nutrients (per unit), Q_i is the number of nutrients carried off by soil erosion estimated by USLE, i is the number of nutrients (1-m)

$$C_{off-site} = (\sum_{i=1}^{n} E_i V_i) \quad (4)$$

Where: $C_{off-site}$ is the cost of soil erosion away from agricultural properties, E_i is the value (price) generated by the off-site effects of soil erosion, V_i is the volume (quantity) of off-site effects (sediment volume, estimated using USLE), i is the different off-site effects, from 1 to n (for instance: rivers, waterways, harbors, irrigation channels, etc.)

2) Long-term economic effects

This study further considered the private net present value (NPV), the

benefit-cost ratio (B/C ratio) and the internal rate of return (IRR) of soil conservation by examining the NPV per rai for all soil conservation practices. This part was divided into financial benefits or monetary values, and economic benefits or economic values (IFRRI, 2008).

2.1) Financial benefits

Financial benefits are the benefits in terms of money such as income and profits and a cost-benefit analysis was used to evaluate these benefits of soil conservation in the 30-year duration.

$$NPV = \sum_{t=0}^{T} \frac{(\pi_i^C - \pi_t^D)}{(1+r)^t} \quad (5)$$

$$NPV = \sum_{t=0}^{T} \frac{P_t(Y_t^C - Y_t^D) - [C^C(Y_t^C) - C^D(Y_t^D)] - C_t^C}{(1+r)^t}$$

Where: NPV is net present value of private benefits, π_i^C is the profit from conservation practices, π_t^D is the profit without conservation practice,

$\pi_i^C - \pi_i^D$ is the net benefit obtained from adoption of conservation practices, Y_t^C is the yield in year t from conservation practices, Y_t^D is the yield in year t without conservation practices, $C^C(Y_t^C)$ is the annual cost of production from conservation practice, $C^D(Y_t^D)$ is the annual cost of production without conservation practices, C_t^C is the cost of constructing and maintaining the conservation practices

2.2) Economic benefits

Economic benefits are indirect benefits of farmers such as benefits from decreasing soil erosion and nutrients loss. The cost-benefit analysis was used to evaluate these benefits of soil conservation in the 30- year duration.

$$NPV = \sum_{t=0}^{T} \rho^t(\pi_t^C - \pi_t^D) \quad (7)$$

$$NPV = \sum_{t=0}^{T} \left(\frac{1}{1+r}\right)^t (\pi_t^C - \pi_t^D) = 0$$

Where: T is the farmers' planned cultivation, $\left(\frac{1}{1+r}\right)^t$ farmers' discount factor, where r is the farmers' private discount rate

RESULTS AND DISCUSSION

Soil erosion in Mae Sa watershed

In Thailand, Universal Soil Loss Equation (Wischmerier and Smith, 1965) is still extensively used. Yazidhi (2003) showed that the model can be applied in Thailand situation. To implement the Universal Soil Loss Equation (USLE), the data from the Land Development Department was used to evaluate soil erosion in Mae Sa watershed as follows;

A = R x K x LS x C x P

R – Factor is the factor of soil erosion by rain

R = 38.5 + 0.35P (Merritt, 2002; Merritt et al, 2004)

P = mean annual precipitation Mae Sa District during 1981 – 2015 (mm/year)

R = 38.5 + 0.35(1140.2) = 437.57

R- Factor is 437.57

K – Factor is the soil erodibility factor

K – Factor of sandy loam in Mae Sa watershed is 0.19 (The National Park, Wildlife and Plant Conservation Department, Chiang Mai Office, 2013)

L – Factor is the length of the slope

Slope area more than 21%

L= (λ/22.13)0.7

When λ = 22 m. slope area = 5 – 21%

L – Factor is 0.997

S – Factor is the slope steepness

% slope = 21%

S - Factor = 1.8921 (The National Park, Wildlife and Plant Conservation Department, Chiang Mai Office, 2013)

C – Factor is the plant management

C – Factor of land use type in the North (Land Development Department, 2002)

Mixed crops: c- factor is 0.255

Orchards: c- factor is 0.300

Field crops: c- factor is 0.525

Shifting cultivation: c- factor is 0.250

P – Factor is the soil and water conservation measures

P - Factor of the ratio of soil loss between soil and water conservation measures at the slope area of 17 – 21% (Land Development Department, 2000; Funpang, 2007)

P-Value of without conservation is 1.0

P-Value of contouring is 0.8

P-Value of bench terrace and contouring is 0.4

P-Value of bench terrace and hillside ditch is 0.16

To implement the USLE, the average rainfall in Mae Sa District during 1981 – 2015 (Meteorological Department,

2014) and the data of soil from Land Development Department, 1983 and 2000 were used to evaluate soil erosion in Mae Sa watershed from 3 management practices. It was found that the different of 3 practices was the P – factor. P - Factor is the soil and water conservation measures that the degradation practice had the highest soil erosion. The current practice (bench terrace and contouring) was popular in Mae Sa watershed, implemented by 90% of farmers.

The results revealed that field crops have the highest soil erosion of degradation, bench terrace and contouring, and bench terrace and hillside ditch with 13.17, 5.27 and 2.11 ton/rai/year. Orchards, mixed crops and shifting cultivation have less soil erosion, respectively (Table 1).

Cost of soil erosion

Soil erosion costs were separated into on-site and off-site costs. The on-site cost was based on the loss of N, P, K nutrients from the study of "The effect from soil and water conservation in the highland of Mae Sa watershed (Panajumnong, 2008) and the loss of topsoil was calculated from soil erosion equation. Off-site cost depended on increased sedimentation and soil erosion equation was used to find out sediment volumes. Soil conservation benefits were converted from the cost of soil erosion.

This part consists of 4 issues; loss of topsoil, loss of soil fertility (N, P and K nutrients), loss of water due to the sediments and cost of clearing sediments from the waterways.

1) Loss of topsoil

The price of soil for construction was used to calculate the cost of loss of topsoil. According to Sittichok Company Chiang Mai, the price of soil for construction was 800 baht/truck, meaning that the price of soil was 133.33 baht/cubic meter. The economic value of the loss of topsoil was evaluated by multiplying the amount of soil loss from soil erosion in Mae Sa (Table 2) by price of soil for construction (Sittichok Company, 201

Table 1 Soil erosion in Mae Sa watershed estimated by the USLE

Crop type (ton/rai/year)	Degradation practice	Bench terrace & contouring	Bench terrace & hillside ditch
1. Mixed crops	6.40	2.56	1.02
2. Orchards	7.53	3.01	1.20
3. Shifting cultivation	6.27	2.51	1.00
4. Field crops	13.17	5.27	2.11

Table 2 Economic loss value of top soil loss

Land use type (baht/rai/year)	Degradation practice	Bench terrace & contouring	Bench terrace & hillside ditch
1. Mixed crops	1,280	512	204
2. Orchards	1,506	602	240
3. Shifting cultivation	1,254	502	200
4. Field crops	2,634	1,054	422

1 ton = 1.5 cubic meter

Table 3 Economic value of nutrients loss

Nutrient	Degradation practice	Bench terrace & contouring	Bench terrace & hillside ditch
1) Organic matter	58.85	2.145	Performance of agricultural land with soil loss that is less than 2 tons per rai per year is assumed to be negligible during a period of 25 years (Land Development Department, 2000).
2) Nitrogen (N)	33.25	1.14	
3) Phosphorus (P)	3.14	0.02	
4) Potassium (K)	9.63	0.25	
Sum	104.87	3.55	

1 sack = 50 k

According to conservation practices, the economic loss value from top soil of bench terrace and hillside ditch of all land use types were 200 - 422 baht/cubic meter that less than the degradation practice was 6.2 times.

2) Loss of soil fertility (N, P and K nutrients)

Panajumnong (2008) studied the effects of soil and water conservation measures on upper Mae Sa watershed comparing between bench terrace and no conservation. The results reveal the loss of soil fertility and nutrients differed between the conservation and the non-conservation practices which are the loss of organic matter at the rates of 1.43 and 39.23 kg/rai/year, nitrogen at 0.07 and 2.04 kg/rai/year, phosphorus at 0.001 and 0.131 kg/rai/year, and potassium at 0.012 and 0.131 kg/rai/year, respectively.

For the prices of nutrients, the prices of fertilizers (Department of Internal Trade of Thailand, 2011) were used as their proxies. The price of organic matter thus corresponded to that of manure fertilizer at 75 baht per sack (averagely 1.50 baht/kg). In terms of N, P, K nutrients, they were evaluated from the price of urea fertilizer 46-0-0 at 815 baht per sack (averagely 16.30 baht/kg), phosphorus fertilizer (DAP) 18-46-0 at1,200 baht per sack (averagely 24 baht/kg) and potassium fertilizer (MOP) 0-0-60 at 1,040 baht per sack (averagely 20.80 baht/kg).

The value of economic loss due to the loss of soil nutrients was evaluated by multiplying the loss of nutrients by the prices of fertilizers. As shown in Table 3, the total economic loss value from nutrients loss of bench terrace and contouring practice was 3.55 baht/rai/year while that of no conservation was 104.87 baht/rai/year. However, the value for the bench terrace and hillside ditch could not be evaluated because the loss of soil nutrients was very low (Table 3).

3) Loss of water due to sediments

The water space was replaced by the sediments, leading to a decrease in the availability of water. Thus, the economic loss value of water loss

from sediments was evaluated from the cost of purchased water from other Provincial Waterworks Authority branches and the cost of clearing the sediments from the waterways. To evaluate these costs, the total sediments in Mae Sa watershed were calculated. The total sediments of Mae Sa watershed were evaluated by multiplying the acreage of main cultivation areas by the amount of soil loss per rai. The combined agricultural area in Mae Sa watershed is 19,403.44 rai (22.27%) divided into mixed crops 8,201.25 rai or 42.27%, orchards 7,345.69 rai or 37.86%, shifting cultivation 1,838.25 rai or 9.47% and field crops 527.06 rai or 2.72%. The total sediment volume was evaluated from upstream agricultural areas, being in total 5,187 rai accounting for 27% of agricultural areas in Mae Sa watershed. The total upstream agricultural area comprises mixed crops 2,691 rai or 51.88%, orchards 1,964 rai or 37.86%, shifting cultivation 402 rai or 7.75% and field crops 130 rai or 2.50%.

The economic value of the loss of water from sediments was evaluated by multiplying the total sediments by the price of water. The price of water from other Provincial Waterworks Authority branches was 16.60 baht per cubic meter.

4) Cost of clearing sediments from the waterways

The economic value of clearing the sediments from the waterways was evaluated by multiplying the total sediments by the cost of work to remove the sediments. The reference cost of work to clear the sediments from the waterways was 27.53 baht per cubic meter (Bureau of the Budget, 2012).

The total cost of sediments in the waterways consisted of the cost of purchased water and clearing the waterways. The total cost of degradation practice, bench terrace and contouring, and bench terrace and hillside ditch was respectively 2,399,172, 958,636, and 382,431 baht. From this, it can be concluded that conservation practices can reduce the costs of loss of water from sediments (Table 4).

Short-term economic effects of soil conservation

Short-term economic value is the sum of the on-site and the off-site costs. In this study, the on-site cost was the sum of the economic value of topsoil loss and that of nutrients loss and the off-site cost was the economic value of the loss of water from sediments.

Mixed crops 2,309 rai or 51.88% was used as the representative of total upstream agricultural areas 5,187 rai. The total cost of short-term economic value of the degradation practice, bench terrace and contouring, and bench terrace and hillside ditch was respectively 9,583,167, 3,635,128 and 1,440,579 baht per year. The benefit of soil conservation in terms of making bench terrace and hillside ditch can be calculated from the difference between the cost of soil degradation practice and bench terrace and hillside ditch. Thus, the benefit of soil conservation was 1,570 baht per rai or 8,142,588 baht per year. (Table 5).

Long-term economic effects of soil conservation

This study further considered the net present value and internal rate of return of soil conservation by examining the NPV per rai for all soil conservation practices.

This part was divided into financial benefits or monetary value, and economic benefits or economic value with the interest rate of 7.50% (Bank for Agriculture and Agricultural Cooperatives, 2016).

Financial benefits are the benefits in terms of all farms in Mae Sa watershed. The cost-benefit analysis was used to evaluate these benefits of soil conservation in the 30-year duration. The on-site benefit of soil conservation was used to evaluate the financial benefits of with and without soil conservation.

Economic benefits are direct and indirect benefits of soil conservation practice such as benefits from decreasing the cost of purchased water and clearing sediments from the waterways.

Table 4 Economic value of the loss of water from sediments

Cost	Degradation practice	Bench terrace & contouring	Bench terrace & hillside ditch
1. Purchased water	902,476	360,602	143,856
2. Clearing the waterways	1,496,696	598,034	238,575
Total (baht)	2,399,172	958,636	382,431

Table 5 Total cost of short-term economic value

Economic value	Degradation practice	Bench terrace & contouring	Bench terrace & hillside ditch
1. On-site cost of soil erosion			
1.1 Loss of topsoil	1,280	512	204
1.2 Loss of nutrients	105	4	-
1.3 Total cost/rai	1,385	516	204
1.4 Total cost of watershed	7,183,995	2,676,492	1,058,148
2. Off-site cost of soil erosion			
2.1 Purchased water	902,476	360,602	143,856
2.2 Clearing waterways	1,496,696	598,034	238,575
2.3 Total	2,399,172	958,636	382,431
Total cost of soil erosion (baht/year)	9,583,167	3,635,128	1,440,579
Benefit of soil conservation (baht/rai/year)	-	1,147	1,570
Benefit of soil conservation (baht/year)	-	5,948,039	8,142,588

On-site and off-site benefits were used to evaluate the economic benefits of with and without soil conservation.

Cost of soil conservation consists of the construction cost of terracing, contouring and hillside ditching and cost of soil erosion both on-site and off-site costs. Cost of preparing bench terrace and contouring, and bench terrace and hillside ditch in the first year was calculated at 46,683,000 and 74,692,800 baht per year, respectively. In years of 10th and 20th, cost of preparing bench terrace and contouring, and bench terrace and hillside ditch would be 4,668,300 and 14,004,900 baht per year, respectively. The other year (each year) cost of preparing bench terrace and contouring, and bench terrace and hillside ditch would be 1,556,100 and 3,112,200 baht per year, respectively. The on-site and off-site cost combined of the degradation practice, bench terrace and contouring, and bench terrace and hillside ditch corresponded to 9,583,167, 3,635,128, and 1,440,579 baht per year, respectively.

The benefit of soil conservation is the sum of income, on-site and off-site benefits of soil conservation.

Income was evaluated by multiplying the difference of average yield between degradation and conservation practice, by the average price of mixed crops. The average income of bench terrace and contouring, and bench terrace and hillside ditch practice as different from degradation practice was calculated at 4,848,116 and 6,692,959 baht per year, respectively.

The on-site and off-site benefits of soil conservation in terms of making bench terrace and contouring, and bench terrace and hillside ditch can be calculated from the difference between the cost of soil degradation practice and conservation practice. The benefit of soil conservation of bench terrace and contouring, and bench terrace and hillside ditch is respectively 5,948,039 and 8,142,588 baht per year (Table 6).

Table 6 Cost and benefit of soil conservation of Mae Sa Watershed during 30 years

Cost and Benefit (baht)	Degradation practice	Bench terrace & contouring	Bench terrace & hillside ditch
Costs			
1. 1st year	15,561,000	46,683,000	74,692,800
2. 2nd – 9th year	778,050	1,556,100	3,112,200
3. 10th year	1,556,100	4,668,300	14,004,900
4. 11st – 19th year	778,050	1,556,100	3,112,200
5. 20th year	1,556,100	1,556,100	14,004,900
6. 21st – 30th year	778,050	1,556,100	3,112,200
7. Soil erosion per year	9,583,167	3,635,128	1,440,579
Benefits			
1. Average income difference from degradation per year		4,848,116	6,692,959
2. Benefit of soil conservation per year		5,948,039	8,142,588

Table 7 Long-term economic effects of soil conservation practice

Soil conservation practice	Net present value (baht)	Benefit and cost ratio	Internal Rate of Return
Economic Benefit			
1. Bench Terrace & Contouring	11,298,684	1.17	9%
2. Bench terrace & hillside ditch	-5,273,606	0.96	7%
Financial Benefit			
1. Bench Terrace & Contouring	5,714,602	0.92	7%
2. Bench terrace & hillside ditch	-29,092,096	0.76	6%

However, the analysis of long term economic effect of soil conservation practice has an investment cost in the first year and maintenance cost every year. Thus, the net present value of total economic benefit of bench terrace and contouring, and bench terrace and hillside ditch is respectively 11,298,684 and -5,273,606 baht. The benefit and cost ratio and the internal rate of return of bench terrace and contouring, and bench terrace and hillside ditch are 1.17 vs 0.96 and 9% vs 7%.

The net present value of financial benefits of bench terrace and contouring, and bench terrace and hillside ditch is respectively 5,714,602 and -29,092,096 baht. The benefit and cost ratio and the internal rate of return of bench terrace and contouring, and bench terrace and hillside ditch are 0.92 vs 0.76 and 7% vs 6% (Table 7).

CONCLUSIONS

Soil conservation by terrace and contouring measure was found being practiced by 90 percent of farmers in Mae Sa watershed. These practices

generate social cost from loss of water availability due to sediments and cost for clearing the waterways. Thus, the best conservation practice is bench terrace and hillside ditch that made more benefits which were analyzed from soil erosion rate at 1.02 ton/rai/year that assumed to be negligible during a period of 25 years.

However, the results of cost-benefit analysis of soil conservation showed that the net present value, the benefit cost ratio and the internal rate of return of bench terrace and hillside ditch are not worth for investment. Hence the government organizations or the Sub-district Administrative Organization especially Mae Ram should pay and support the upstream farmers in order to change terrace and contouring into terrace and hillside ditch practices.

Thus, soil conservation is important for agricultural land use, especially in upstream areas. Moreover, off-site benefits or social benefits could be accounted for in the ecosystem conservation project that has an effect on all stakeholders. It is reasonable to conclude that the middle and downstream households, the government organizations should pay or support the farmers in the upstream area to do soil conservation practice.

ACKNOWLEDGEMENTS

The authors would like to thank National Research Council of Thailand for the financial support and Integrated Community-based Forest and Catchment Management through an Ecosystem Service Approach (CBFCM project) for the permission to attend the conservation activities in Mae Sa watershed.

REFERENCES

Department for Environment, Food and Rural Affairs. 2013. “Payment for Environmental Services.” Environment International. 67: 27-42.

IFRRI. 2008. “On-Site and Off-Site Long-Term Economic Impacts of Soil Fertility Management Practices.” The Case of Maize-Based Cropping Systems in Kenya. Environment and Production Technology Division.

Land Development Department. 2005. "Academic documents of the master plan for land use planning to prevent soil deterioration and increase the potential economic crops as well as soil and water conservation" Ministry of Agriculture and Cooperatives, Land Development Department.

Land Development Department. 2017. Available at http://www.ldd.go.th/ldd_en/, accessed October 2017.

Lal, R. 2001. Soil Degradation by Erosion. Land Degradation and Development. 12: 519 – 539.

Minister of Agriculture, Food and Rural Affairs Ontario. 2016. "Growing Ontario's agri-food sector and supporting rural communities, helping to create a stronger economy for the province". Available at http://www.omafra.gov.on.ca/english/about/about.html. assessed May 2017.

National Statistical Office. 2008. "National Statistical Office of Thailand". Available at: http://web.nso.go.th/en/survey/env/data_env/560920_env12_LandsAndSoil.pdf, accessed October 2017.

Panajumnong. Chaiyan. 2008. "Effects of highland soil and water conservation measures on upper Mae Sa Catchment Quality". M.S. Thesis in Soil Science. Graduate School, Chiang Mai University.

129 – 148.

Telles, T. S., S. C. F. Dechen., L. G. Antonio., Maria. D. F.G., 2012. "Valuation and assessment of soil erosion costs." Sci. Agric. 70(3): 209-216.

Wischmeier, W.H., and D.D. Smith. 1965. "Predicting rainfall-erosion losses from cropland east of the Rocky Mountains: Guide for selection of practices for soil and water conservation". U.S. Dep. Agrie, Agrie. Handbook. No. 282.

Wunder, S. 2007. "The Efficiency of Payments for Environmental Services in Tropical Conservation." Conservation Biology 2(1): 48 – 5.

Yazidhi Bamutaze. 2003. "A Comparative study of soil erosion modelling in Lom Kao-Phetchanun, Thailand". International institute for geo-information science and earth observation enschede, theNetherlands. [Online]. Available: https://webapps.itc.utwente.nl/librarwww/papers_2003/msc/ereg/bamutaze_yazidi.pdf. [13 September 2016].

Economic Return of Crop Rotation and Reduction of Open-air Rice Straw Burning in Rice-based Cropping System in Upper Northern Thailand

Thambitaks K.[1]*, Kitchaicharoen J.[2], Sangchyoswat C.[3] and Jakrawatana N.[4]

[1*]Ph.D. student of Agricultural Resource Management, Graduate Program, Faculty of Agriculture, Chiang Mai University, Chiang Mai 50200, Thailand
[2] Department of Agricultural Economy and Development, Faculty of Agriculture, Chiang Mai University, Chiang Mai 50200, Thailand
[3] Center for Agricultural Resources System Research, Faculty of Agriculture, Chiang Mai University, Chiang Mai 50200, Thailand
[4] Department of Environmental Engineering, Faculty of Engineering, Chiang Mai University, Chiang Mai 50200, Thailand ;
*Corresponding author ;Email: thorn97@yahoo.com

ABSTRACT

Open-air burning of crop residues (OBRS) has been widely practiced after the harvesting while seriously affecting the human health and the environmental quality. The benefits of crop's residue management in terms of economic evaluation are useful guidelines to the post-harvesting time. This study shows the economic return of three crop rotation and the reduction of OBRS in the upper Northern Thailand. The external costs were evaluated based on the environmental impacts of the greenhouse gases and the human health damage with climate change and the particulate matter (PM), to estimate the value of disability-adjusted life year (DALY). The results show that the farmers lose the day of good health 153-295 day per hectare that it is the external cost of 5,560 million baht for the total burning area. However, after rice harvesting, the incorporation of the rice straw into the soil returns most of the nutrients.

It shows the benefits of this are 3,521 baht per hectare. For the crop rotation, legume is the crop with most value of nutrients (6,644 baht per hectare followed by *Crotalaria juncea* (6,094 baht per ha) and maize (2,639 baht per ha).

Keywords: Economic valuation, Open-air rice straw burning, value of DALY, value of social benefits

Introduction

In Asian countries, the estimation of biomass burning was 730 million tons in a typical year that consisted of forest burning at 45%, the burning of crop residues at 34% and the burning of grassland and savanna at 20% in which the total included China 25%, India 18%, Indonesia 13% and Myanmar 8% (Streets et al., 2003). The slash-and-burn and open field burning are widely practiced after the harvesting in several countries in Asia, especially, open-field burning of rice straw (OBRS). Although OBRS effectively removed biomass within a short time at farmer's low

cost for preparing the next crop, it reduced soil organic matter and macro-nutrients, especially nitrogen (Singh *et al*., 2001; Dobermann *et al*., 2002; Adam, 2013). It found that the reduction of OBRS and ploughing increased rice yield from about 5,394 to 5,688 kg per ha (DOA, 2012), and a crop rotation would drop the cycle of open-field burning and enriched macronutrients in soil (DOAE, 2005; Supapong *et al*., 2007; LDD, 2011).

It was indicated that OBRS has emitted greenhouse gases (GHGs) and degraded air quality of surround areas (Streets *et al*., 2003; Danutawat *et al*.,2007; Gadde *et al*., 2009; Chiuet *et al*., 2011). GHGs have had an effect on climate change as resulted in global warming and consequently impacted the environment. The particular matters, ozone, nitogen dioxide of GHGs were mainly caused respiratory diseases and carcinogens which have effected human health damage (WHO, 2003; Torigoe *et al*., 2000).

Life cycle assessment (LCA) can be used to estimate the effect of GHGs on environment (midpoint) and human health damage (endpoint) (McMichael *et al*., 2003; Rosalie *et al*., 2008; Mark *et al*., 2012). Although the previous studies have expressed the benefit of straw incorporating into soil, crop rotation and the negative impact of OBRS, but the explanation was showed in term of environmental impacts, not in money of economic evaluation.

This paper shows the economic return of the reduction of OBRS and the applying of crop rotation that increases nutrients in soil. Additionally, the human health benefit from the reduction of external cost of disability of adjust life years (DALYs) is also integrated.

Materials and Methods

Data collection

Chiang Rai and Phayao provinces were selected as the study areas as more than a half of rice production in Upper Northern Thailand has been growing in these two provinces. They had produced about 54% of 2.16 million tons of rice in 2014/2015 (OAE, 2015). The number of rice growing households in these two provinces were collected in the crop-year 2015/16, coming to 413 total. The sample area (739 ha[1]) of the total area (140,523 ha) included the sample burning area 243 ha (33%) and the estimation of total burning area was roundly 44,905 ha. After rice harvesting, some farmers used the land for growing other crops in order to improve soil structure and fertility with a crop rotation area of about 32 ha (4% of sample area).

Evaluation of the benefit of macronutrients

The plowing crop residues into the soil (the macronutrients: NPK) were estimated by the nutrient contents as shown in Table 1. The amounts of N, P_2O_5, K_2O were converted into the major fertilizers including Urea (46-0-0) for N, Diammonium Phosphate (DAP 18-46-0) for P and Potassium Chloride (0-0-60) for K and

[1] Hectare

multiplied by the average prices to get the economic value of macronutrients as shown in Table 2 and 3.

Assessment of external cost from OBRS

The external costs were GHGs that were emitted from OBRS evaluated based on the environmental impacts and human health damage. The economic valuation methods were used to evaluate the impacts via a monetary unit.

In order to quantify the gases emission from OBRS, the initial step was to estimate the quantity of rice straw burning that was based on the quantity of rough rice product (yield) as shown in equation (1) and (2) (Gadde *et al*., 2009).

$$Q_{SSFB} = PRR \times SGR \times Q_{sFB} - -(1)$$

Where Q_{SSFB} was quantity of rice straw subject to open burning in kg/ha; PRR was rough rice production in kg/ha; SGR was a straw to grain ratio (0.75); Q_SFB was proportion of rice straw subject to open field burning (%). In this study, all rice straw was burned 100% then GHGs emission of OBRS was estimated using the following equation.

$$E_a = Q_{SSFB} \times EF_a \times f_{Co} - - - (2)$$

Ea was emission of ***a*** (type of greenhouse gas) in kg/ha; EF_a was the emission factor of ***a*** in g/kg of dry straw; f_{Co} was the combustion factor of 0.8. In this study, the emission factors (g/kg of dry straw) of CO_2, NO_x, SO_2, PM_{10} were 1,460, 3.1, 2.0, and 3.7 respectively (Gadde *et al*., 2009). Following the climate change and PM_{10} in 1993, WHO assessed the human health damage with DALY which measured as years of life lost for mortality and morbidity (WHO, 2013, 2015). The correlation of GHGs and DALYs showed the problems in malnutrition, diarrhea, cardiovascular diseases, coastal and inland flooding and vector borne diseases in the characterization factors (CFs) (Mc Michael, 2003; Mark, 2012; Rosalie, 2003) as following 1.19×10^{-6} DALYs of CO_2, 5.7×10^{-5} DALYs of NO_x, 5.1×10^{-5} DALYs of SO_2 and 0.00026 DALYs

of PM_{10}. To assess DALYs from OBRS, CFs (years lost per kg emission) were multiplied by the quantity of gases being emitted (kg).

To assess the value of DALY, WHO (2001) had developed an acceptance threshold budget for the government of developing countries to invest for the healthcare promotion each year. The effective cost to reduce 1 unit of DALY would be less than 3 times the gross domestic product per head (GDP per capita), which it was estimated for the costs of illness, accident, diseases and violence (WHO, 2001, 2002; John *et al*., 2008; David, 2008; Dalal *et al*., 2015). In this study, to calculate the costs of DALY from OBRS, were multiplied by one time of GDP per capita. (WHO, 2001, 2002; John *et al*., 2008). The conceptual framework for the assessment of the benefits of macronutrients and the external cost of OBRS was shown in Figure 1. If the rice straw burning is able to reduce or avoid, the external cost from OBRS is able to consider as the benefit of OBRS reduction

Table 1. Nutrient contents of crop residues incorporation into soil

Crop residue types	Quantity of residue (kg/ha)	Quantity of nutrients (kg/ha)		
		N	P_2O_5	K_2O
Rice	3,937.5	21.6	3.5	94.1
Maize	3,062.5	16.2	4.6	67.6
Legumes	3,625	67.7	22.1	106.6
Crotalaria juncea[*]	4,062.5	97.5	8.9	97.5

Source : LDD, 2011 ; [*]Supapong et al., 2007

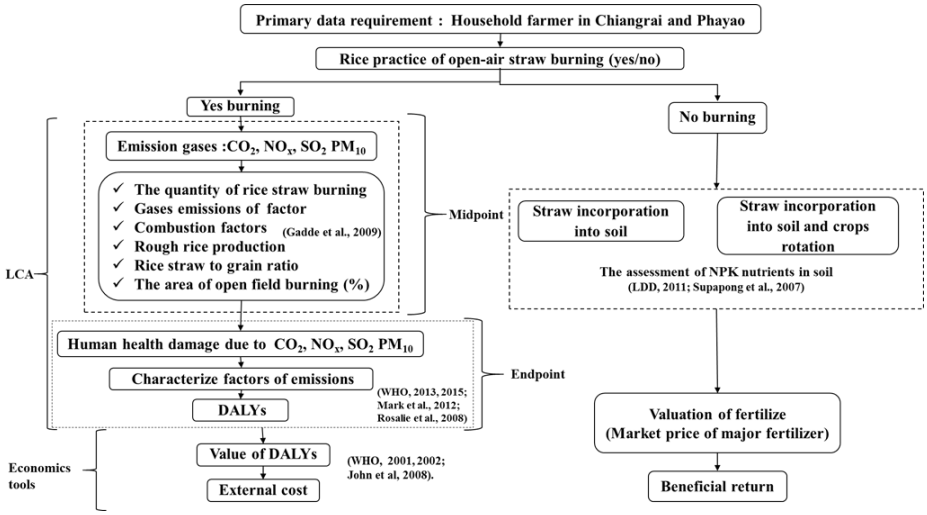

Figure 1: Conceptual framework of the study

RESULTS AND DISCUSSION

The economic benefit of macronutrients from non-OBRS and crop rotation

According to sample areas from the survey, 67% of 739 ha have been reported applying non-OBRS. Based on the value of 3,521 baht per ha from the nutrients of 1 ha of rice straw being incorporating into the soil, the total value of non-burning rice was calculated at about 1.74 million baht as shown in Table 2. If the sample farmers stop burning rice straw after harvesting, the rice straw from 33% (243 ha) turn into nutrients which will be valued at 855,683 baht as shown in Table 2.

From the macronutrients of crop rotation in Table 3, it showed the sample area of crop rotation as 32 ha. The total NPK nutrient incorporated into soil was calculated at 1,622 kg of N, 263 kg of P_2O_5 and 2,605 kg of K_2O. Total value of macronutrient was about 134,918 baht, of which legume was the crop with the most value of nutrients (6,644 baht per ha) followed by *Crotalaria juncea* (6,095 baht per ha) and maize (2,639 baht per ha) as shown in Table 3.

To calculate the benefits of crop rotation, the returns of crop rotation from its yield was also calculated and integrated into the total benefit of crop rotation. The rotated crop that

had the highest average profit per ha was maize (37,669 baht) followed by legumes (24,219 baht) and *Crotalaria juncea* (5,481 baht) as shown in Table 4.

In addition, the opinions of 268 farm households for the alternative use of rice straw included leaving straw in fields at 37%, ploughing at 25%, fodder at 11%, selling at 9%, gardening at 5%, using for mushroom farm at 5%, composting at 5% and the others 3%.

For estimation, the external cost of OBRS, the total external cost was calculated from the total area. Whereas, in case of non-OBRS, the benefit of macronutrients also was calculated from the total area of rice. These calculations determined that 3,521 baht per ha of rice straw, 2,639 baht per ha of maize residue. The profit of yield comed to 37,669 baht per ha for maize and the total was 43,829 baht per ha. That was scaled up to evaluate the benefits of macronutrients from the rice production of total burning area, which was about 44,905 ha.

Table 2. The value of N P_2O_5 K_2O of nutrients 3,521 baht/ha from the straw incorporation in soil

Study area (district)	**Practice**	**Farmer** person	**Sample area(**ha)	**%**	**Total nutri. of rice straw** (kg)			**Value** Baht
					N	**P_2O_5**	**K_2O**	
Mueang Chiang Rai	Burn	50	79.84	**45.1**				
	Non-burn	53	97.04	54.9	2,098.5	339.6	9,127.8	341,688.3
	If Stop-burn	103	176.88	100	3,825	619.1	16,637.8	622,813.5
Phan	Burn	26	51.04	30.7				
	Non-burn	55	114.96	69.3	2,486	402.4	10,813.4	404,786.6
	If Stop-burn	81	166	100	3,589.8	581	15,614.4	584,503.9
Thong	Burn	28	45.08	44.7				
	Non-burn	40	55.72	55.3	1,205	195	5,241.2	196,196.1
	If Stop-burn	68	100.8	100	2,179.8	352.8	9,481.5	354,840.1
Mueang Phayao	Burn	11	22.44	27.2				
	Non-burn	51	60.08	72.8	1,299.2	210.3	5,651.3	211,548.2
	If Stop-burn	62	82.52	100	1,784.5	288.8	7,762	290,561.8
Dok Khamtai	Burn	14	19.92	15.5				
	Non-burn	47	108.84	84.5	2,353.7	380.9	10,237.8	383,237.4
	If Stop-burn	61	128.76	100	2,784.4	450.7	12,111.5	453,377.8

	Burn	16	24.72	29.4				
Chun	Non-burn	22	59.4	70.6	1,284.5	207.9	5,587.3	209,153.8
	If Stop-burn	38	84.12	100	1,819.1	294.4	7,912.5	296,195.6
	Burn	145	243	**33**				
Total	Non-burn	268	496	67	10,726.9	1,736.1	46,658.8	1,746,610.3
	If Stop-burn	413	739	100	15,982.6	2,586.8	69,519.7	2,602,292.8
								855,683*

Note: * Supposed to stop 100 % of OBRS, the benefit up top**;** The average price of major fertilizers (baht per kg) are 13.56, 20.16 and 17.41

Table 3. The value of N, P_2O_5 and K_2O from the residues of crop rotation

Study area	**Crop**	**Farmer**	**Sample**	**Total nutri. of residues (kg)**			**Value**	**Value/area**
(district)	**Type**	**person**	**area**(ha)	**N**	**P_2O_5**	**K_2O**	baht	baht/ha
Mueang Chiang Rai	Maize	2	8.8	142.5	40.2	595.1	23,226.6	2,639
Thong	Maize	6	5.44	88.1	24.8	367.9	14,358.2	2,639
	Legumes	1	0.48	42.1	10.6	51.2	3,189	6,644
Mueang Phayao	Maize	5	2.16	35	9.9	146.1	5,701.1	2,639
	Legumes	1	0.16	14	3.5	17.1	1,063	6,644
	Crotalaria juncea	5	3.6	351	32.2	351	21,937.5	6,095
Dok Khamtai	Legumes	1	2.88	252.5	63.5	306.9	19,134	6,644
	Crotalaria juncea	1	1.6	156	14.3	156	9,750	6,095
Chun	Maize	1	1.12	18.1	5.1	75.7	2,956.1	2,639
	Legumes	2	0.8	70.2	17.7	85.3	5,315	6,644
	Crotalaria juncea	3	4.64	452.4	41.5	452.4	28,275.57	6,095
Total		28	32(4%)[1]	1,622	263	2,605	134,918[2]	

Note:[1] % of sample area (739 ha); [2] The price of major fertilizers (baht per kg) are 13.56, 20.16 and 17.41

Table 4. The return of crop rotation product

Crop type	**Farmer** (case)	**Sample** area(ha)	**Product**[1] (kg/ha)	**Cost**[1] (baht/ha)	**Sell-price** (baht/kg)	**Profit**[1] (baht/ha)
Maize	14	17.5	6,454.94	10,219.69	6.93	37,669
Crotalaria juncea	9	9.8	3,750[2]	0[4]	19	5,481
Legumes	5	4.3	1,231.25[3]	5,087.5	25.75	24,219

Note: [1]average value, [2]only 2.08 ha, [3] only 3.68 ha, [4] the project contribution of seed and buying product

3.2 The external costs of OBRS due to emission

From the field survey, there were 243 ha of sample burning area, which generated 77,809 tons of CO_2, 165 tons of NO_x, 107 tons of SO_2, and 197 tons of PM_{10}.Those amounts of emission were converted into DALYs. According to the calculated DALY, the gas that had the highest impact on human health was CO_2 with the average of 0.38 DALY per ha, followed by PM10 with the average of 0.2 DALY per ha. The results showed that one hectare of OBRS had an effect on life year's loss in the range of 0.42 to 0.8 DALY. As one DALY unit was a life year lost, then this meaned that a farmer would lose his quality of life within the range of about 153 to 295 days from OBRS one ha as shown in Table 5.

The evaluation of DALY per ha was in the range of 80,257 to 155,193 baht, depending on the study area. For, the technique estimated the total value of impacts from OBRS, this study assumed 145 farms did OBRS of 739 ha during the same period. By doing that, the total external cost derived from health loss would be about 30.45 million baht for the sample burning area. To extend the calculation of the external cost to cover the total burning areas by using the percentage of burning area would result in 44,905 ha and the total external cost would be as high as 5,560 million baht, as shown in Table 6

Table5. The quantity of gases and DALY from OBRS

Study area	Area	Burn	Total gases (ton)				Average gases kg / ha				[1]DALY/ha from				Total	[2]DALY
(district)	Burn (ha)	(%)	CO_2	NOx	SO_2	PM_{10}	CO_2	NOx	SO_2	PM_{10}	CO_2	NOx	SO_2	PM_{10}	DALY/ha	Day/ha
Mueang Chiang Rai	79.8	45.1	31,655.8	67.2	43.4	80.2	396,491	841.9	543	1004.8	0.47	0.048	0.03	0.26	0.81	295
Phan	51	30.7	12,674.6	26.9	17.4	32.1	248,327	527.3	340	629.3	0.3	0.03	0.02	0.16	0.51	185
Thong	45.1	44.7	14,608.9	31	20	37	324,066	688.1	444	821.3	0.39	0.039	0.02	0.21	0.66	241
Mueang Phayao	22.4	27.2	5,163.3	11	7.1	13.1	230,094	488.6	315	583.1	0.27	0.028	0.02	0.15	0.47	171
Dok Khamtai	19.9	15.5	4,084.4	8.7	5.6	10.4	205,042	435.4	281	519.6	0.24	0.025	0.01	0.14	0.42	153
Chun	24.7	29.4	9,621.9	20.4	13.2	24.4	389,235	826.5	533	986.4	0.46	0.047	0.03	0.26	0.79	290
Burn same day[3]	243	32.9	77,809	165.2	107	197.2	320,149	679.8	439	811.3	0.38	0.039	0.02	0.21	0.65	238

Note: [1]Gases emission (Kg/ha) multiphied CF of gas emission (years lost per kg emission); [2] DALY multiphied 365 day; [3]supposing burn at same period

Table 6. The value of DALY from OBRS

Study area (district)	Total area (ha)	Total Burning area(ha)	Sample area(ha)	Sample Burning area(ha)	Burning area (%)	Total DALYs /ha	[1]GDP per capita	Value of DALY (baht/ha)	Total value of DALY (Million baht)	
									Sample burning	Total burning
Mueang Chiang Rai	25,776	11,625	176.9	79.8	45.1	0.81	191,890	155,193	12.39	1,804
Phan	28,244	8,684	166	51	30.7	0.51	191,890	97,200	4.96	844
Thong	22,727	10,164	100.8	45.1	44.7	0.66	191,890	126,845	5.71	1,289
Mueang Phayao	15,090	4,105	82.5	22.4	27.2	0.47	191,890	90,063	2.02	369
Dok Khamtai	28,680	4,445	128.8	19.9	15.5	0.42	191,890	80,257	1.59	356
Chun	20,005	5,882	84.1	24.7	29.4	0.79	191,890	152,353	3.76	896
Total	140,523	44,905[2]	739.1	243	33	0.65			30.45[3]	5,560[3]

Note: [1] GDP per capita 5,814.86 dollars in 2015 and 1 dollars is 33 baht; [2]estimation from % burning area of total area; [3] to suppose, burning at same period

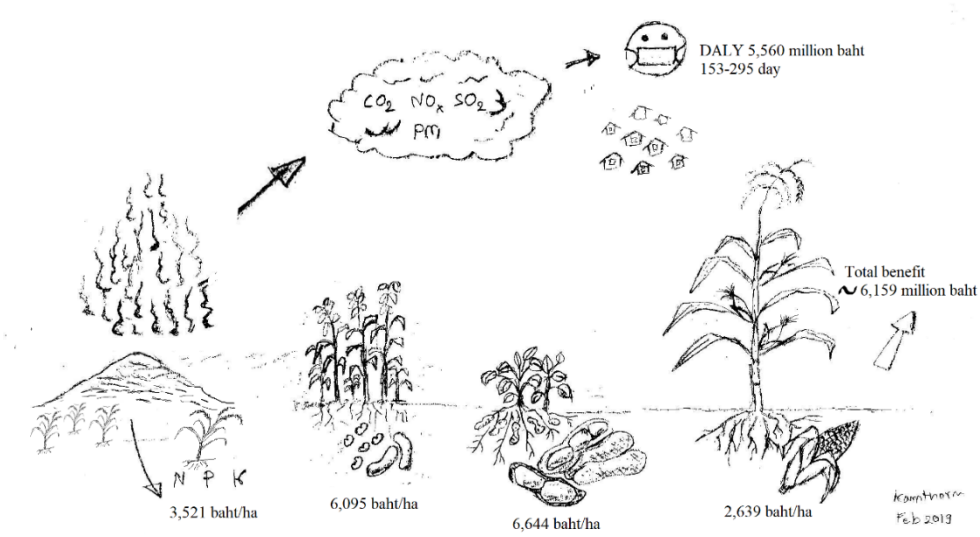

Figure 2: Conclusion drawn

Discussion This study shows non-OBRS and rice straw incorporating into the soil would give economic benefits to the farmers, totalling about 3,521baht per ha or 494 million baht for the total area. To incorporate rice straw into the soil, farmers apply the dry shallow tillage about 5 to 10 cm depths and it can mitigate the increasing methane from anaerobic decomposition, which should be done 2 to 3 week after harvesting. This method would return most of the nutrients and reserves to them in the long-term

(Doberman *et al*., 2002; Ruensuk *et al*., 2010). However, the disadvantages of the incorporation rice straw into soil from surveyed farmer's opinions are the difficulty of mixing straw into soil, the need for appropriate equipment, and that the straws obstructed in the rotary tiller during the second ploughing of tillage. Therefore, the ban on the rice straw burning needs more information to compare against the other options.

For the crop rotation, the water sufficiency for processing is an important factor to consider. Maize is a high return crop when the water is not a problem, and the farmers understand production, trading and the risk of price fluctuation in maize market. Lequmes (mung bean) is a

durable crop for water deficiency area which is short time (60-70 days) and high return (35-40 baht per kg). However, the farmers need more knowledge in the production and more understanding of the market system. *Crotalaria juncea* consumes less water and the harvest time is 120-130 days, but the flowering stage (45 days) is the most suitable period of ploughing for the highest nutrients of green manure in organic rice production. However, the disadvantage of farmers have limited access to the market of seeds and selling products (LDD, 2011, 2017; Supapong *et al*., 2007).

The incorporation of rice straw into the soil can change the external cost of DALY (5,560 million baht for the total burning area) to gain the benefit about 43,829 baht per ha from their macronutrient (3,521 baht per ha), and the crop rotation residue and yield (2,639 and 37,669 baht per ha for maize). Furthermore, the monetary benefit in the total burning area (44,905 ha) should be 1,968 million baht. The total economic benefit of the crop rotation and the reduction of OBRS in the total area (140,523 ha) of rice production would be 6,159 million baht, as shown in Figure 2.

Thus, the government should provide finances, the knowledge and the equipment to the participating farmers who do not burn their straw. In the long term, the development of effective crop residue management is important in order to change the farmer s' vision.

Acknowledgement

Authors would like to thank for the 5th EnvironmentAsia International Conference (EnvironmentAsia 2019) at Chiang Mai, Thailand and Dr. Chirabhorn Sri Brahma for valuable comments, farm households for providing the useful information. Finally, I would like to thank the generosity from University of Phayao and companion staffs to allow for the further study at Chiangmai University.

References

Adam J. Alternatives to open-field burning on paddy farms. Option 18 2013;

Available from: http://www.siani.se/sites/clients.codepositive.com /files/profile/key_papers/alternatives_to_open_field_burning_on_paddy_farms.pdf

Chiu JC, Shen YH, Li Hsing W, Chang Shun S, Wang Lin C and Chang-Chien Guo P.Effect of biomass open burning on particulate matter and polycyclic aromatic hydrocarbon concentration levels and PAH dry deposition in ambient air. Journal of Environmental Science and Health 2011; Part A. 46(2): 188-97. DOI:10.1080/10934529.2011.532438

Danutawat T and Nguyen TKO. Effects from open rice straw burning emission on air quality in the Bangkok metropolitan region. Science Asia 2007; 33:339-345. DOI: 10.2306/scienceasia1513-1874.2007.33.339

David WB. Economic value of disability-adjusted life years lost to violence: estimates for WHO member states. Revista Panamericana de Salud Publica 2008; 24/3: 203-09.

Dalal K and Svanström L. Economic burden of disability adjusted life years (DALYs) of injuries. Health. 2015; 7: 487-494. DOI: 10.4236/health.2015.74058

DOA. Decomposition of rice straw by microorganisms. New letter Pri Bai (in Thai) Department of Agriculture (DAO). 2012; Available from: http://www.doa.go.th/pibai/pibai/n17/v_8-sep/korkui.html

DOAE. The instruction of organic fertilizer for academic (in Thai) Department of Agricultural Extension (DOAE). 2005; Available from: http://www.servicelink.doae.go.th/webpage/ book%20PDF/soil/s004.pdf

DOAE. The plantation of maize after rice harvesting (in Thai) Department of Agricultural Extension (DOAE). 2016; Available from: http://esc.agritech.doae.go.th/ebooks/download-pdf/maize.pdf

Dobermann A and Farihurst TH. Rice straw management. Better Crops International 2002; 16:7-11. Available from: https://www.researchgate.net/profile/Thomas_Fairhurst/publication/228850474_Rice_straw_management/links/54c9dece0cf2f0b56c24d3e8.pdf

Gadde B, Bonnet S, Menke C and Savitri G. Air pollutant emissions from rice straw open field burning in India, Thailand and the Philippines. Environmental Pollution 2009; 157/5: 1554-58. DOI: http://dx.doi.org/10.1016/j.envpol.2009.01.004

John RM and Ross H. Economic value of disability-adjusted life years lost to cancers. Journal of Clinical Oncology 2008; 28/15: 1561-1561. DOI: 10.1200/jco.2010.28.15_suppl.1561

LDD. The sustainable soil management from ploughing stubble (in Thai). Land Development Department 2011; Available from: http://r07.ldd.go.th/WEB_R07_Version2/07_KM/DATA/Km2.pdf

LDD. Planting green manure for storing seeds (in Thai). Office of Technology Transfer and to Supervise Land Development (OTASLD) in Land Development Department 2011; Available from: http://www.ldd.go.th/menu_Dataonline /G1/G1_27.pdf

LDD. Green manure project under the integrated rice production and marketing plan (in Thai). Land Department Department 2017; Available from: http://www.ldd.go.th/www/lek_web/web.jsp?id=18474

Mark G, Reinout H, Mark H, An De S, Jaap S and Rosalie VZ. A life cycle impact assessment method which comprises harmonized category indicators at the midpoint and the endpoint level.Ruimteen Milieu Ministerie Van Valkshuisvesting, Ruimtelijke Ordeningen Milieubeheer 2012.

McMichael AJ, Campbell-Lendrum DH, Corvalan CF, Ebi KL, Githeko A, Scheraga JD, Woodward A. Climate change and human health. Risk and responses. Geneva: Word Health Organization; 2003, 322p.

Nguyen TKO, Ly BT, Tipayarom D, Manandhar BR, Prpat P, Simpson CD and Sally LLJ. Characterization of particulate matter emission from open burning of rice straw. Atmospheric Environment 2011; 45(2): 493-502. DOI:http://dx.doi.org/10.1016/j.atmosenv.2010.09.023

OAE. The upper northern of rice production year 2014/15 (in Thai). Office of Agricultural Economics 2015; Available from: http://www.oae.go.th/download/prcai/DryCrop/amphoe/majorrice-amphoe56.pdf

Rosalie vZ, Mark AJ Huijbregts, Henri A den Hollander, Hans A van Jaarsveld, Ferd J Sauter, Jaap Struijs, Harm J van, Wijnen dik van de Meent. European characterization factors for human health damage of PM10 and ozone in life cycle impact assessment. Atmospheric Environment 2008; 42/3: 441-53. DOI:http://dx.doi.org/10.1016/j.atmosenv.2007.09.072

Ruensuk N, Mongkonbunjong P and Inthaleang W. Effect of rate of straw incorporation into the soils on rice growth and yield In Proceedings of the 19th World Congress of Soil Science, Soil Solutions for a Changing World 2010 Aug (pp. 140-142). Available from: http://www.iuss.org/19th%20WCSS/Symposium/pdf/1437.pdf

Singh Yand Bijay S. Efficient management of primary nutrients in the rice-wheat system. Journal of Crop Production

2001; 4(1): 23-85. DOI:10.1300/J144v04n01_02

Streets DG, Yarber KF, Woo JH and Carmichael GR. Biomass burning in Asia: annual and seasonal estimates and atmospheric emissions. Global Biogeochemical Cycles 2003; 17/4. DOI:10.1029/2003gb002040

Supapong C, Saelime S, Ratanakaew T, WattanWangJunsuk C and Prasukri N. Green manure soil improvement and sustainable economy (in Thai). Land Development Department 2007; Available from: http://www.servicelink.doae.go.th/webpage/Academic%20articles/Manure.pdf

Torigoe K and Hasegawa S. Influence of emission from rice straw burning on bronchial asthma in children. Pediatrics International 2000; 42(2): 143-150. DOI:10.1046/j.1442-200x.2000.01196.x

WHO.Commission on macroeconomics and health macroeconomics and health, investing in health for economic development. World Health Organization 2001; Available from: http://apps.who.int/bookorders/anglais/detart1.jsp?sesslan=1&codlan=1&codcol=1511&codcch=491

WHO. The world health report 2002 - reducing risks, promoting healthy life. World Health Organization 2002; Available from: http://www.who.int/whr/2002/en/

WHO. Health aspects of air pollution with particulate matter, ozone and nitrogen dioxide, report on a WHO working group; Bonn, Germany 13-15 January 2003. Available from: http://www.euro.who.int/__data/assets/pdf_file/0005/112199/E79097.pdf

WHO. Methods and data sources for global burden of disease estimates 2000-2011. Department of Health Statistics and Information Systems WHO, Geneva, 2013; Available from: http://www.who.int/healthinfo/statistics/GlobalDALYmethods_2000_2011.pdf?ua=1

WHO. Health statistics and information systems, Global burden of disease (GBD). 2015; Available from: http://www.who.int/healthinfo/global_burden_disease/gbd/e

The Development of A Liveable Agricultural Community Through Community-Based Natural Resource Management: A Case Study of Salaengphan Sub-District, Lamplaimat District, Burirum Province, Thailand

Imporn Ardbutra[1]

[1]Faculty of Environment and Natural Resource Studies, Mahidol University, Thailand *E-mail: imp.ardbutra@gmail.com

ABSTRACT

The objective of this research was to analyse the guidelines for community-based natural resource management (CBNRM) for the agricultural sector in Salaengphan community. The quantitative and qualitative data were collected from representatives of government and the private sector, community leaders and consumers. A total of 146 farmers were randomly selected from four villages of Salaengphan sub-district. Data were collected using questionnaires, in-depth interviews, and focus group discussions. Rice and vegetables are the main agricultural crops in this community. Some farmers have been certified by Good Agricultural Practices (GAP) but most are still using chemicals in their agricultural practice. They normally grow, harvest and sell to middlemen although some of the vegetables are delivered to a local supermarket as part of a CSR programme. In the past, before the pilot groundwater project was implemented, the community suffered from severe water shortages. Farmers are currently facing problems of plant disease and insects as well as the lack of sufficient income to purchase seeds and machinery. To achieve a liveable agricultural community, the community members have set the vision "Farmers will work together in order to cultivate organic vegetables". CBNRM guidelines have been developed through the focus group discussion as follows: to implement zoning for organic agriculture; to create and strengthen

the farmer leaders in organic agriculture; to support farmers in capacity building in the organic agricultural sector; to cultivate medicinal plants and to raise awareness of organic agriculture.

Keywords: Community-based natural resource management (CBNRM), liveable agricultural community

INTRODUCTION

The rapid growth of urban areas has had an immense impact on the world's population structure, especially in less developed countries. Currently, 54 percent of the world's population lives in urban areas; this is expected to increase to 66 percent by 2050 (United Nations, 2014). The rapid growth of urban areas is strongly interrelated with an increase in the world's population (McMichael, 2000). Currently estimated at approximately seven billion, it is expected to increase to nine billion by 2050 (United Nations, 2015). By extension, this increase brings with it several consequences. Where natural resources were once seen as raw materials that could be traded as commodities for the purpose of driving economic growth, nowadays countries across the globe struggle to balance economic prosperity with measures that promote resource conservation and protect the environment.

This research is a case study that focuses on Salaengphan sub-district of Burirum province in Thailand. It provides an overview of the community's agricultural activities and the challenges it faces in terms of drought and water scarcity. Similar to other communities in the Northeastern region, this community cultivates rice, vegetables and fruits. Based on the Agricultural Development Plan of this community, it can be concluded that the residents are highly dependent on natural resources and the resultant productivity.

In 1998, the members of Salaengphan community adopted strategies based

on the principles of the sufficiency economy and self-reliance. The combination of both concepts has helped them cope with the numerous challenges they have been facing. The Royal Development Learning Centre was set up by a woman who strongly believes in the self-reliance concept and has a vision that the community should enjoy a better livelihood. The aim of the learning centre is to distribute knowledge based on the sufficiency economy principle in order to improve the livelihood of the community and to develop better management of water, soil, waste, and energy resources for the agriculture sector, which is in line with the concept of community-based natural resource management (CBNRM).

This research therefore aims to analyse guidelines for CBNRM especially in the agricultural sector. Another goal is to help activate all stakeholders and assist them in a proper analysis of the target area, as well as develop guidelines for an agricultural development plan that will lead to a liveable agricultural community and sustainable livelihoods.

Sustainable livelihood assets consist of: 1) Human Capital: H includes skills, education and ability to work and adapt with good health in order to achieve the livelihood strategies and objectives. Farmers should have direct access to cash incomes. 2) Social Capital: S aims to achieve the livelihood outcomes and consists of network and associations such as community enterprises and cooperatives. Cultural and traditional capital can be listed under social capital as well. 3) Natural Capital: N represents the common environmental resources such as land, trees and wildlife. It is important for the farmers who derive everything from resource-based activities. 4) Physical Capital: P comprises the basic infrastructure such as adequate water supply and sanitation plus clean and affordable energy which can facilitate livelihood activities. 5) Financial Capital: F comprises saving and a revolving fund within the community

such as income, village fund and cooperative fund. This means the community members have accessibility to the mentioned funds.

All parts of a sustainable livelihood framework aim to help eliminate poverty. The framework is considered as a tool to improve the understanding of livelihoods especially at the community level (DFID, 1999).

Agricultural product systems are linked with natural resources, namely land, water, biodiversity, forest, pasture and wildlife. Farm activities can have such impacts as pollution and soil erosion on natural resources. It is crucial that farmers adopt more sustainable methodologies for the farm system in order to improve livelihoods. Normally, decision-making on natural resource management takes place at several levels such as international, national and sub-national and sometimes at the household level (World Bank, 2006).

The CBNRM concept has been introduced over the last two decades as a centralised form of management predicated on stage control resources. This alternative approach involves the management of wildlife, forests, fisheries, water resources and coastal resources (Armitage, 2005). Natural resources sustainability is a major problem in cases from Africa and Asia. However, the concept of CBNRM is well-known in African countries. CBNRM is considered as an approach to natural resource management by local communities with the objectives of improving livelihoods and security of the local people, empowering them and enhancing environmental conservation (Adhikari, 2001). CBNRM can also empower the rural communities with knowledge, skills and authority (United States Agency for International Development; USAID, 2013).

The main objectives of the CBNRM concept are to conserve natural resources and to increase livelihoods. The benefits of CBNRM include

environment, social aspects and community economics. It is more likely to efficiently allocate funds and achieve environmental goals whilst strengthening community confidence, cohesion and building social capital (Smith, 2012).

The component of CBNRM can be analysed based on scale, time, complexity, implementation plan, land tenure, partnership, traditional leadership and ecological status of the natural resources. Targets of CBNRM include improving the livelihood of the community, managing natural resources effectively, increasing community participation and supporting the local authorities. CBNRM can help build a good relationship and trust between the local people and the government sector, create effective communication among the local networks, promote better decision-making and make known the main interest of the community area (Hutacharoen, 2013).

METHODOLOGY

Study Area

The research area is located in Salaengphan sub- district, Lamplaimat district, Burirum, which is one of the north- eastern provinces of Thailand. Salaengphan sub-district has 17 villages altogether and 91% of this sub- district is considered paddy field. Most of the community members are farmers and depend on the eco- system and the groundwater. The research focuses on four villages: Ban Nongsuang (Moo 3) , Ban Bukantong (Moo 12) , Ban Salaengphan Pattana (Moo 14), and Ban Bukantong Pattana (Moo 16) where members of the community enterprise and cooperatives reside. These areas are suitable for cultivating rice, vegetables and fruits such as cantaloupe. Furthermore, the areas were selected to be part of the pilot area for the development of groundwater project. Most of the farmers in this area are involved with the community agricultural supply chain and the value chain. Due to the scarcity of water, the community leaders and members have to manage natural resources effectively for a

sustainable livelihood and liveable agricultural community.

Target Population

The target population selection of this research is specific to the Salaengphan sub- district and is occupied with natural resource management in the agricultural sector and with an emphasis on farmers. The research is applied using the purposive sampling technique. The data are collected from questionnaires, in- depth interviews and focus group discussion. Secondary data from relevant governmental organisations are analysed. The sample size of the questionnaire was determined based on Krejcie and Morgan's sample size calculation. The total number of the agricultural households in villages (Moo) 3, 12, 14, 16 is 266. The sample size representative of the agricultural community members among these four villages was determined to be 157 households.

Data Collection

1) Primary data were collected from the field work. Questionnaires, in-depth interviews and focus group discussion were conducted with the key stakeholders or community representatives. 2) Secondary data were analysed from the document study, related literature, thesis dissertation and journals including online articles that led to the questionnaires and in- depth interviews.

Data analysis

1) Quantitative data analysis: After collecting the data from the questionnaire, especially on the livelihood assets, the obtained data was analysed using descriptive statistics, frequency distribution, and cross tabulation in order to understand the nature of the farmers. Descriptive statistics were applied to summarise the socio-economic characteristics of the farmers in the Salaengphan community. Frequency was used in order to understand the value which occurs most frequently in each data set. 2) Qualitative data analysis**:** The researcher applied

content analysis for the questionnaires, in-depth interviews and focus group discussion. The CBNRM issues were analysed from the focus group discussion which leads to the liveable agricultural community. The analysis focused on holistic understanding and finding the truth from the key informants.

RESULTS AND DISCUSSION

The result is summarized and categorised as follows:

Demographic profile of the respondents in Salaengphan community

The questionnaire data were collected. While 160 respondents contributed to these data, only 146 questionnaires were actually completed. The questionnaire revealed a gender composition of the respondents of 43% male and 57% female. 35% of the respondents were over 60 years old and the average age was 54. The average farming experience was 26 years and the majority of farmers in this category were 50 years old and had been cultivating since they were young. However, according to the head of the community enterprise, the new generation was encouraged to choose other career paths.

The majority of respondents have been residing in this sub-district since they were born (76%) and 24% of respondents relocated to this sub-district after marriage or for work reasons. With respect to educational background, 71 of respondents completed primary school but did not pursue secondary education as they were required to support their parents in agricultural activities. In addition, it was found that 48% of respondents earned less than 3,000 THB per month per person and some households had only one breadwinner. Only 5% of respondents earned more than 15,000 THB per month. The National Statistic Office of Thailand gives annual income per capita in 2011 as 39,761 THB, which is higher than the average amount in the Salaengphan community. Moreover, 70% of respondents had no additional jobs other than farming (Table 1).

Table 1 Demographic profile of respondents of Salaengphan community

General Information	**Amount**	**Percentage**
Gender		
- Male	63	43
- Female	83	57
Age		
- Less than 20 years old	4	3
- 20 – 29 years old	44	30
- 30 – 39 years old	39	27
- 40 – 49 years old	7	5
- 50 – 59 years old	1	1
- Older than 60 years old	51	35
Duration of life in Salaengphan Sub-district		
- Have been living here since they were born	111	76
- Moved to Salaengphan later on	35	24
Educational Level		
- None	7	5
- Primary Education	104	71
- Vocational Education/ High school	30	21
- Diploma/ Higher vocational education	3	2
- Undergraduate studies	2	1
- Graduate studies and Higher	0	0
Income (Monthly)		
- Less than 3,000 THB	70	48
- 3,001-6,000 THB	38	26

General Information	Amount	Percentage
- 6,001-8,000 THB	17	12
- 8,0001-10,000 THB	6	4
- 10,001-15,000 THB	8	5
- More than 15,000 THB	7	5
Other income generation activity		
- No	102	70
- Member of SAO	2	1
- Assistant to Head of Village	1	1
- Mill business	1	1
- Commerce	10	7
- Beauty Salon	1	1
- Employee (Labour Work)	23	16
- Livestock	6	4

Sustainable livelihood assets

Salaengphan community is considered to have several capitals that benefit the livelihoods of its residents. The social capital can be strengthened since there are existing networks and groups within the community. However, the question is how to make those groups active and sustainable. Basic infrastructure is provided. The government sector eventually decided to pave the new concrete road in August. Water is one the most prominent issues and is heavily consumed in the community. Groundwater is the solution for vegetable cultivation but not rice cultivation. The community must consider that groundwater resources will run out in the future and find a way to use it more sustainably. Similar to other communities in the Northeastern region, people still live in poverty. Respondents mostly have lower-than-average incomes.

The Salaengphan community focuses on the management of water, soil, waste and energy resources. Local

authorities play important roles in supporting the development of agriculture in the community. The private sector and civil society hardly take part in the community's development in terms of natural resource management. The ability to maintain a balance between supply and demand in the agricultural supply chain is dependent on natural resources, such as crops and fresh water. In general, resource scarcity is either a local or global phenomenon that impacts the logistics in a supply chain. There is therefore a need for environmental and natural resource management.

The supply chain means the intermediary plays an important role in the movement from producers to consumers. The agricultural supply chain of Salaengphan community encompasses upstream, midstream and downstream and involves farmers, collectors, middlemen and consumers. Farmers are the key players and are integrated in all streams. The supply chain is mixed between rice, fruits and such vegetables as onion flower stem, kaffir lime leaf, great morinda, peppermint, red morning glory, cherry tomato, sea holly, hairy basil, chaiya plants, young tamarind leaves, butterfly pea, sesban, white popinac, Colubrina Asiatica, turkey berry, white eggplant and eggplant. The farmers have been cultivating rice for more than 50 years but have been growing vegetables for only 19 years. The farmers allow middlemen to collect the vegetables on their land by themselves. Labour costs are therefore deducted and this further decreases the benefits. It is important to develop a processing and branding plan since the problems occur mostly during the collection period. So-called "grade C" vegetables should be processed and turned into other products while "grade A" vegetables should be delivered to the supermarket and "grade B" sold in the community markets.

The Salaengphan community has several stakeholders that are managing the natural resources such as the government sector, private

sector and civil society. The content in this section comes from in-depth interviews, questionnaires, observations and the focus group discussion. The community focuses mainly on water resources, waste, land use and soil and energy management.

The agriculture product system is linked with natural resources. The importance of natural resources and the environment is directly related to human- beings. People need the environment to survive and use soil to grow their food. The abundance of the environment is the main factor in supporting human settlement. Moreover, the environment will determine the occupation and culture in each area (Sakmanee, 2003).

Community- based natural resource management (CBNRM) for a liveable agricultural community

CBNRM aims to improve the local livelihood and enhance environmental conservation at the same time (Adhikari, 2001). The process of CBNRM in Salaengphan Community involves both the sub-national and household levels. The approach of CBNRM refers to the local communities who are given the rights to manage the natural resources. (Milupi et al 2017). Environmental and natural resource management requires engagement from all stakeholders – government sector, private sector, civil society and the community that also makes use of the environmental resources.

An effective CBNRM in the agricultural sector can be beneficial to farmers. They can take part in the decision- making process. CBNRM will promote participatory rural development and empowerment of the farmer population. Importantly, it can help with financial capital if farmers decide to switch to organic agriculture, which will lead to the liveable agricultural community. In Vietnam, shifting from the traditional cultivation method has taken many years and required financial and technical support from international donors, especially for the cost of the Participatory Guarantee System (PGS) Certification from IFOAM,

which is equal to 2,000 USD or 64,000 THB when the farmer can earn around 200 USD or 6,400 THB per month (Dung, 2012). Such a complete change requires the paradigm shift mentioned earlier and will take time and effort.

During the focus group discussion, the participants were asked to discuss " What is the definition of Salaengphan Liveable Agricultural Community?" Participants were provided with cards to give their definition individually. They were active and expressed their opinions in the written communications. Some participants would like to see harmony within the community. Farmers could work together effectively and cultivate organic produce, consider the soil and water conservation and adopt the Sufficiency Economics Philosophy (SEP). Other participants would like to develop the community for eco-tourism. Moreover, there should be capacity building for all farmers to develop the agricultural products. Afterwards, the facilitator used the clustering method and prioritised the cards according to the consensus of the participants. The prioritisation covered 1) Organic vegetables; 2) Cultural conservation; 3) Environmental Protection; 4) Capacity Building for farmers; and 5) Working together- Forming a group of farmers. Afterwards, the farmers were asked to vote on which topic provided the most suitable definition of a liveable city. Two topics received an equal number of votes: Working together and organic vegetables. This can be taken as meaning "Farmers will work together in order to cultivate organic vegetables".

The CBNRM guidelines are developed to solve the issues in the agricultural supply chain and to achieve the vision of the community. During the focus group discussion, participants were asked to brainstorm on the guidelines and discuss who should implement them and who should support them within the community. The results are listed in the table below:

Table 2 Guideline for the Liveable Agricultural Community

Guideline	Responsible Agencies	Supporting Agencies
1) To implement zoning for organic agriculture	- Farmers	- Land development department
2) To create and strengthen the farmer leaders in organic agriculture	- Head of Villages - Village committee - Farmers	- BAAC - Community Development - Lamplaimat Agriculture Office
3) To support farmers on capacity building in organic agricultural sector	- SAO	- Learning centre
4) To cultivate medicinal plants	- Farmers	- Markets
5) To raise awareness on organic agriculture	- Community leaders - Scholars - Role model - Schools	- Salaengphan Health Promoting Hospital - Burirum College of Agriculture and Technology

During the last session of the focus group discussions, they listed these guidelines and discussed how to achieve them. They can use the existing group and networks such as the community enterprise and the learning centre to extend the membership and convince more farmers to grow organic vegetables. The bigger the number they can convince, the easier it will be to start zoning. With the support of the Land Development Department, they can start land use planning. Once the zoning is in place, they can start cultivating as

role models or leaders. If the role models are successful, other farmers will tend to follow. The participants have selected to focus on vegetables and especially medicinal plants, as there is a demand for the plants and the Salaengphan Health Promoting Hospital has started cultivation. Importantly, the way of thinking needs to change. Conventional farming might not be the answer for a liveable city in the long run. A paradigm shift will take time as it involves changing thinking and habits. Salaengphan Sub- District Administrative Organization (SAO) has offered support in capacity building on how to develop a proposal to apply for training. The government sector has allocated a small budget for the agricultural sector in each municipality. Overall, the participants brainstormed and wrote actively during all the sessions.

CONCLUSIONS

In terms of liveable agricultural community, Salaengphan is leaning towards an organic agricultural community that can be followed using the aforementioned guidelines. Within the five capitals of livelihood assets, there are many governmental agencies and private sectors that have been supporting the community. These include the Groundwater Resources Region 5 (Nakhon Ratchasima), Lamplaimat District Agriculture Officer, Salaengphan Sub-District Administrative Organization (SAO) while the private sector includes the local supermarket. The livelihoods assets are also linked with the agricultural supply chain. To ascertain the CBNRM in Salaengphan community, all the resources were examined through in-depth interviews, questionnaires and focus group discussion. Managing the natural resources sustainably is challenging. The users from different stakeholders have to be motivated to manage their resources. Based on the focus group discussion, the community

has a vision of farmers working together in order to cultivate organic vegetables, which will lead to a liveable agricultural community. The guidelines for achieving this vision have been developed but require effort and support from every stakeholder if a sustainable livelihood is to be achieved.

ACKNOWLEDGEMENTS

First and foremost, I would like to express my sincere gratitude to my advisor, Dr. Wipawan Tinnungwattana for the continuous support throughout my thesis with her patience and immense knowledge whilst allowing me the room to work in my own way. It is an honour for me to working with her. One simply could not wish for a better or friendlier advisor.

In addition, I would like to thank the co-advisors, Dr. Sittipong Dilokwanich for his constructive recommendations and encouragement. Without his input, the questionnaires could not have been successfully achieved.

Finally, I would like to thank my parents, my fellow student colleagues from Mahidol University, my colleagues from German International Cooperation (GIZ) and my friends, especially Mr. Krai Noi-Sewok, all of whom have supported me in every possible way to see the completion of this thesis.

REFERENCES

Adhikari JR. Community Based Natural Resource Management in Nepal with Reference to Community Forestry: A Gender Perspective. A Journal of the Environment 2001; Vol. 6, No. 7; 9.

Armitage D. Adaptive Capacity and Community-Based Natural Resource Management. Environmental Management 2005; Vol. 35, No. 6, pp. 703–715. DOI: 10.1007/s00267-004-0076-z.

Department for International Development (DFID). Sustainable livelihoods guidance sheets. [Internet]. 1999 [cited on 3 Dec 2017] Available from: http:// www. livelihoodscentre.org/documents/20720/100145/Sustainable+livelihoods+ guidance+sheets/8f35b59f-8207-43fc-8b99-df75d3000e86.

Dung T T. Organic Vegetable Supply Chain in Vietnam: Marketing and Finance Perspectives. The Vietnamese Initiative for Food and Agricultural Policy; 2012.

Hutacharoen R. Environmental and Natural Resource Management Based on Appropriated Technology and Community Participatory. 2nd ed. Nakornpathom: Faculty of Environment and Resource Studies: Mahidol University; 2013.

McMichael A. J. The urban environment and health in a world of increasing globalization: issues for developing countries. Bulletin of the World Health Organization [Internet]. 2000 [cited on 1 May 2017]. Available from: http://www.who.int/bulletin/archives/78(9)1117.pdf.

Milupi ID, Somers MJ, Ferguson W. A Review of Community-Based Natural Resource Management. Applied Ecology and Environmental Research 2017; 1121-1143.

Sakmanee B. Community Environmental Management. Bangkok: Chulalongkorn University; 2003.

Smith A. The Benefits of Community-Based Resource Management. [Internet]. 2012 [cited on 2 June 2017]. Available from: https://www.sustainablebusinessto olkit. com/benefits-community-based-resource-management/

The World Bank. Agriculture Investment Sourcebook. Washington D.C.; 2006.

United Nations. World's population increasingly urban with more than half living in urban areas [Internet]. 2014 [cited on 1 May 2017]. Available from: http:// www.un.org/en/development/desa /news/population/world-urbanization-prospects-2014.html.

United Nations. World population projected to reach 9.7 billion by 2050 [Internet]. 2015 [cited on 1 May 2017]. Available from:http://www.un.org/en/ development/desa/news/population/2015-report.html.

USAID. A Global Assessment of Community Based Natural Resource: Management: Addressing the Critical Challenges of the Rural Sector: 2013.

Assessing of Water Balance Components in Dry Dipterocarp-Forested Watershed in Phayao, Thailand

Phenruedee Khamsorn[1], Montri Sanwangsri[1,2], Chatkaew Chailuecha[1], Pimsiri Suwannapat[1,2*]

[1*]School of Energy and Environment, University of Phayao, Phayao 56000, Thailand
[2*]Atmospheric Pollution and Climate Change Research Unit,
School of Energy and Environment, University of Phayao, Phayao, Thailand
; Corresponding author: e-mail:
Pimsiri.su@up.ac.th

ABSTRACT

Dry dipterocarp-forested (DDF) watershed is an important water source of Phayao lake and upper Ing River. Changes in water balance in watershed forested impact on ecosystem service. Accurate estimation of water balance components is needed for good decision-making in water management in Phayao province. This study aims to understand the variations of water balance components in DDF watershed including rainfall (P), evapotranspiration (ET), runoff (Q) and soil water storage change (ΔS) between 2014 - 2017. P and ΔS were measured by micro-meteorological equipment, while ET was estimated by eddy covariance technique. The 4-year average annual of P, ET, Q and ΔS were 985±52.2, 854±59.6, 131±35.4 and 0.1±0.3 mm, respectively. Noteworthy, the seasonal P and Q in wet season 2015 significantly declined 23% and 57% compared with 4-year average. In addition, ET decrease 5% and 20% in wet 2015 and dry season 2015/2016, respectively. Dynamic of water components in wet and dry season was consistent with the El Niño event in 2015/2016. However, a distributed Q for

5 months per year according to post-rainfall event exhibited the considerable impact of DDF for water conservation.

Keywords: Dry dipterocarp forest, Eddy covariance, Water balance components, Forested watershed

INTRODUCTION

Dry dipterocarp forests are prominent in tropical Southeast Asia Countries that found as a watershed forest only in Vietnam, Laos, Cambodia, Thailand, Myanmar, India, and south China (Bunyavejchewin et al., 2011). This forest is located in the tropical climates, where wet and dry seasons are clearly different. Although the dipterocarp forests normally appear a lot of big rocks, soil shallow depth, less soil nutrient and low water storage (Bunyavejchewin, 1983; Rundel and Boonpragob, 1995), they have a rapid turnover of nutrients and energy when there is enough moisture in the soil, (Thaiutsa and Puangchit, 2004) an important forest-ecosystem service, a water level and carbon storage control (Bunyavejchewin, et al., 2011; Rundel and Boonpragob, 1995). Dry dipterocarp forest will be shedding leaves in the dry season for reduce water loss in trunk and spring their leaves in the rainy season. It has a clear physical appearance in response to seasonal changes. If the weather conditions are variable, the process of deciduous forest may still be adaptable and helps maintain the water balance of water in ecosystem. The study of water balance in ecosystem is a strategy to predict the impact and ecosystem response.

Dry dipterocarp forests in Phayao, Thailand is a watershed forest area of Phayao Lake, which play a part in the largest reservoir of Ing River and the important international wetland of northern Thailand. Water in Phayao Lake is supported from 12 lines of the upstream flows to nourish local communities along Ing River and finally run into Mekong River. It is also the tap water supply and

aquaculture of freshwater fish, the most important in the northern Thailand. Water management has been implemented using local wisdom. However, lack of information and understanding of water balance in watershed forest lead to ineffectively water management.

The study of water balance in forest ecosystems needs to estimate amount of water input into the ecosystem as P and water loss by Q, ET and ΔS. The hydrological studies in Southeast Asia are limited, Southeast Asia has a sophisticated ET control system due to its diverse ecosystem and climate (Li et al., 2010). Especially those of dry environments, ET is the largest part of water balance, accounting for at least 90% of the P (Zhang et al., 2001). Most of hydrological studies conducted in the Amazon region, revealing ET range between 50% to 90% compare with P (Jipp et al., 1998; Malhi et al., 2002). Therefore, correction of ET measurement is important for reliably water balance assessment. The various methods have been developed, for example soil water balance (Reddy, 1983), sap flow (Smith and Allen, 1996), catchment water balance (Bosch and Hewlett, 1982) and eddy covariance technique (Yaseef et al., 2009). A soil water balance is method for total water loss from the soil. Advantage of this technique is that it can provide insight on the relative contribution of various rooting depths to the total transpiration source. However, ET estimates from this method do not account for canopy interception. The measurements are representative of only a small area, and high spatial variability of soil water content results in sampling difficulties (Dunin, 1991). Sap flow measurements provide mechanistic details environmental controls of transpiration and able to measure in complex terrain and spatial heterogeneity. However, radial gradients of sap flow in the sapwood can result in errors (Clearwater et al., 1999). This technique uses for only measures transpiration and additional restrictions when the overall water budget is required (Wilson et al.,

2001). The catchment water balance is assessment of annual ET for an area of fixed dimensions. This method could not provide the in temporal scales (Luxmoore and Huff, 1989). The estimated ET at high resolution by eddy covariance technique can be linked between hydrology processes. This technique is sometimes difficult to interpret during weakly turbulent periods, usually at night (Baldocchi et al., 2000). All the above methods, the eddy covariance technique is a scientific method to collect accurate ET data in water management (Baldocchi, 2003; Foken and Wichura, 1996), and can study the ET in real-time (Da Rocha et al., 2009). This study aims to understand variations of water balance components in DDF watershed including P, ET, Q and ΔS. P and ΔS were measured by micro-meteorological equipment, while ET was estimated by eddy covariance technique.

METHODOLOGY

Site description

The study site is Dry dipterocarp forest Phayao, Thailand (DPT), located at 19°02' 14.38" N, 99°54' 10.96" E, at an elevation of 512 m, where is the forested watershed of Phayao Lake. Dominant species growing on complex terrain were *Shorea obtuse* Wall., *Shorea siamensis* Miq., *Dipterocarpus tuberculatus* Roxb. and *Dipterocarpus obtusifolius Teijsm*. ex Miq. Standing trees were mainly found in the forest, with relatively fewer saplings (1,821 and 600 $treeha^{-1,}$ respectively). Main texture of top soil was sandy loam (0-10 cm depth) and sandy clay loam in lower layer (Intanil et al., 2018). The site has a tropical monsoon climate, the onset of wet season in May to October and dry season in November to April (Tanaka et al., 2008).

Meteorological measurements

Meteorological variables measured and collect data on tower at 36 m included P, air temperature and relative humidity (WXT520 weather transmitter; Campbell Scientific Inc., USA), net radiation (NR01 net

radiometer sensor; Campbell Scientific Inc., USA) and calculate vapor pressure deficit by Allen et al. (1998). Soil temperature and SWC measurements at dept 5 cm by soil thermocouple probe and soil water content reflectometer (CS616; Campbell Scientific Inc., USA). Data were recorded at 10-min to data logger (CR1000; Campbell Scientific Inc., USA)

Measurement and data analysis to estimate ET by eddy covariance technique

Eddy covariance systems was installed at 42 m to measure water vapor flux and net CO_2 flux by a 3D-sonic anemometer (CSAT3, Campbell Scientific Inc.) and EC150 open-path CO_2/H_2O analyzer (Campbell Scientific Inc.) Flux data was collected in high-frequency (10 Hz). The measured data was analyzed latent heat (LE) values with EddyPro express software (open source version 6.2.1, LI-COR Bioscience 2017). Data analysis by EddyPro was adjusted wind direction according to the theory by rotating the wind direction 2 times (double rotation) and despikes were removed by statistical tests embed in the software (Vickers and Mahrt, 1997; Vickers, 2009) and density corrections were applied during post-processing to the half-hourly averaged data (Webb et al., 1980). Then average LE half-hourly was remove data in during calm conditions were ejection data based on low friction velocity ($u^*<0.05$ m/s) and during it rains. In this study, LE lost was 39%, 19%, 40% and 43% in 2014 - 2017 respectively. Which missing data will be gap filling by applying appropriate corrections for site-specific parameter and gaps were filled using the mean diurnal variation (MDV) and nonlinear regression method, respectively (Falge et al., 2002). In case the data is slightly lost (2-3 hours), gap filling by average diurnal. But in case the data is than week lost, gap filling by use average previous 7 day in daytime and 14 days in nighttime (Wolf et al., 2011). Finally, estimate ET by the constant value of LE that causes 1 kg of water to evaporate in 1 day, approximately

2.45 MJ kg^{-1} to evaporate water at 20°C (Novák, 2012)

Water balance calculation

In this study, Q was estimated using water balance equation as follows;

$$Q = P - ET \pm \Delta S \quad (2)$$

where P is rainfall, ET is evapotranspiration and $\pm\Delta S$ is the soil water storage change. The unit of all components are mm. ΔS are calculated by considering gains or losses of SWC between subsequent days.

RESULTS AND DISCUSSION

Meteorological data

Meteorological data was measured from January 2014 to December 2017. Amount of P was range between 957.4 to 1,067.0 mm $year^{-1}$, most of the P occurs in May to October and dry season during November to April. Thailand P distribution has an influenced form southwest and southeast monsoon. It can be divided into two period as wet season (November-April) and dry season (May-October) (Tanaka et al., 2008). 4-year average P was 985 mm and mean air temperature (Ta) and soil temperature (Ts) was 25.0 and 24.8 °C respectively. While average soil water content (SWC) was 14.4 %VWC (measured in 2014-2017 at DPT station). The P values show a significant drop 23% and 36% in wet season 2015 and dry seasons 2015/2016, respectively. This trend is similar with SWC which decease 14.3 and 10.7 %VWC in wet and dry seasons in this year (Table 1). This low P value affect to RH and VPD in atmosphere. The lowest Rn value, 82.9±10.5 Wm^{-2}, was also observed in dry season 2015/2016. In this study, Ta and Ts insignificantly change. The above incident was consistent with the El Niño phenomenon during 2015 to 2016, from the study of Kaewthongrach et al. (2018), they found SWC decreases below 5 %VWC in dry season

Table 1. Microclimate variables in dipterocarp forest including P, SWC, VPD, RH, Rn, Ta and Ts during 2014-2017.

season	Year	P	SWC	VPD	RH	Rn	Ta	Ts
Wet	2014	861.7	15.0±2.4	0.9±0.2	75.1±5.0	131.7±5.1	25.6±1.1	25.7±0.8
Wet	2015	626.9	14.3±1.9	1.1±0.3	71.1±5.4	132.2±14.3	26.0±1.1	25.4±0.5
Wet	2016	846.4	16.4±2.4	1.0±0.5	72.3±8.0	132.5±9.6	25.8±1.5	26.3±1.2
Wet	2017	913.7	22.7±1.8	0.9±0.2	76.4±4.0	134.4±9.0	25.2±0.9	25.5±1.2
Dry	2014*	58.9	10.2±0.3	1.8±0.5	51.0±8.6	83.6±13.2	25.3±3.5	24.5±3.0
Dry	2014/2015	254.8	11.9±1.5	1.4±0.5	57.4±9.7	90.8±19.2	24.0±2.8	23.6±2.2
Dry	2015/2016	131.2	10.7±2.0	1.8±0.8	52.3±12.9	82.9±10.5	25.1±3.9	24.5±4.4
Dry	2016/2017	233.2	13.2±2.5	1.3±0.5	60.1±10.7	100.9±17.3	24.1±2.3	24.2±2.5
AVG	**Wet**	**812.2**	**17.1±4.1**	**1.0±0.3**	**73.7±6.3**	**132.7±10.3**	**25.7±1.1**	**25.7±1.0**
	Dry	**169.5**	**11.5±2.2**	**1.6±0.7**	**55.2±11.6**	**89.5±17.2**	**24.6±3.3**	**24.2±3.2**
	annual	**984.6**	**14.5±2.0**	**1.2±0.1**	**65.3±2.3**	**111.2±3.3**	**25.0±0.3**	**24.8±0.4**

Note: * Incomplete season data.

Annual totals of components of water balance

Table 2 show annual water balance of 2014-2017. Average P of 4 years-study was 984.6 mm. ET, ΔS and Q were 87%, 0.01% and 13% of P, respectively. ET in each year were 87, 90, 81 and 89% of P. For Q was 13, 10, 19 and 11% of P, respectively. For ΔS found negligible change (lower than 1%). The minimum ET, it showed in March 2016 and maximum in May 2014 at 26.5, 105.7 mm, respectively. The daily pattern of ET, we found that it started to decrease in November and lowest value in March (Fig 2), because P was suspended and SWC gradually decreased to lowest in April which found the lowest SWC in April 2016 at 7.8 %VWC. In addition, VPD was gradually increased and maximum in April (maximum VPD in April 2016 at 3.2 kPa), it inverses with relative humidity. However, SWC in March 2016 had similar value with April 2016 which is consistent with the lowest ET in March (1.1 mm day^{-1}). Generally, during the period April to early May Thailand usually influenced by tropical monsoon. It affects to get the rain before rainy

season. In this reason ET in April to increase rapidly.

For ET during a day would be increase about 8 am and peaked around mid-day to 1pm (Fig 4). The average daily ET of 4 years-study was between 0.3-7.0 mm day^{-1} or average ET was 2.3 mm day^{-1}. Additionally, we notice that ET in 2014 and 2015 were decreased 3% when compared with average ET of 4 years-study. It consistent with P in 2014 and 2015, it also decreased (3 and 6%, respectively). P in 2016 had nearby with the average P of 4 years-study. In contrast, ET decreased to 6% from the average ET. Because the cumulative P in previous years (2015) less than other year. While in 2017, P increased 8% from the average P. It affected to ET also increased at 12% from the average. When viewed from the ratio of P/ET in each year, we found that 2015 was P lower than other years (1.15, 1.13, 1.17 and 1.15 in 2014 to 2017, respectively). In the other hand, ET was high. In these results, it affected to assessment Q from equation 1 in 2014s 2015s, 2017s to decreased 2, 28 and 14% from the average. However, Q from this study is still preliminary estimated data. we suggest that validation of Q value is needing to more explain accuracy of the estimation method. Q value comply with ET also decrease lower than other years in 2015-2016 and in this year occurred the severe El Nino from 1950 (L'Heureux et al., 2017). We found that the dry dipterocarp forest in study lose the water through ET more than 80% of P, it so higher than other forest types such as mixed deciduous forest (65%) (Witthawat chutikul, 2011), evergreen forest at 54% (Tanaka, et al., 2003) and 50% (Chunkao et al., 1982). Tropical rain forest at 78% (Li et al., 2010), dry evergreen forest at 65% (Tatsuhiko et al., 2007), tropical monsoon valley tall forest at 64% (Kuricheva et al., 2015). While ET of the dry dipterocarp forest at Ratchaburi province was 95% (Sanwangsri et al., 2017a). which this forest is secondary dry dipterocarp forest, the results in this study was lower than because there are different proportions of

young and large wood. However, the difference of ET depends on precipitation distribution and topography and forest canopy interception capacity associated tree species and leaf area. The study of Chunkao et al, (1971) found that dry dipterocarp forest efficient to intercept the water to 60% of P, the water was evaporated to atmosphere in finally. From Q study in other ecosystems found that Q of mixed deciduous forest was 29% of P (Witthawatchutikul, 2011), hill evergreen forest was 50% (Chunkao et al., 1982), tropical monsoon valley tall forest was 39% (Kuricheva et al., 2015) and dry dipterocarp forest was 0.6% of P (Chankao et al., 1985). When compared Q with other forests, the dry dipterocarp forest was lower than due to it has soil shallow depth, the most water enter to the ET process rapidly. Therefore, Q in dry dipterocarp forest will provide when soil water-saturated. And Q will flow continuously until raining stop, Q will stop immediately (Phapan et al., 2011). Q assessment in this study, we found that the deciduous forest in the study area has 5 months for Q, it flows between April until October every year. Consistent with the Q study of watershed stream of Phapan et al, (2011), they found that monthly Q of the deciduous forest was about 5 months (July-November) by 120°C V-notch weir. However, the difference of Q will depend on precipitation, altitude and slope of area, soil depth and forest type (Witthawatchutikul, 2011).

Seasonal variations in the components of water balance. Seasonal of water balance shown in Table 2. P and ET during 46.8 to 303.6 mm and 0 to 171.2 mm, respectively. While seasonal ET was significant differences, range of ET in wet season was during 9.6 to 105.6 mm and 14.7 to 72.8 mm in dry season.

Table 2 The average annual values of the components of the water balance for the DPT site in 2014-2107.

Year	P	ET	ΔS	Q
	(mm)			
2014	957±82.7	829±21.1	-0.30±0.8	128±68.0
2015	927±71.5	832±20.7	0.12±1.0	94±64.1
2016	987±75.1	799±26.7	0.06±1.5	154±57.2
2017	1067±99.5	954±19.7	0.52±1.8	112±89.3
AVG	985±52.2	854±59.6	0.10±0.3	131±35.4

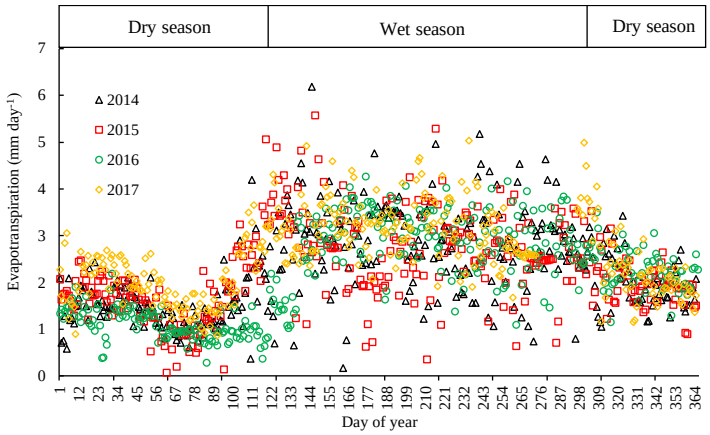

Figure 2 The daily patterns of mean ET from 2014 - 2017.

The 4-year study found ET in wet season higher than dry season around 25%, because dry dipterocarp forest in dry season reduce water loss by shedding their leaves, causing the solar to reach the ground directly and resulting to different ET changes. The dry dipterocarp forest has a short growing season. Most ET will occur during the wet season, when there is enough moisture in the soil (Thaiutsa and Puangchit, 2004). In addition, during the wet season, there is also a quantity of interception canopy to be involved. Because some trees have large leaves such as *Dipterocarpus tuberculatus* Roxb. The trees in the deciduous forest have thick bark. Some leaves are hair, causing a lot of dew on the leaves (Chunkao et al.,

1971). And Shi et al. (2008) reported that the rain during the monsoon caused the leaves to expand fully, combined with the proper air temperature for growth and transpiration of the trees. Therefore, evaporation and transpiration are likely to be a factor that results in ET in the wet season higher than the dry season. Daily ET in wet season and dry season were 2.9 ± 0.9 and 1.7 ± 0.9 mm day^{-1}, respectively which is similar to ET in seasonal results of Sanwangsri et al. (2017) in dry dipterocarp forest in Ratchaburi province, they found that the wet and dry season were 3.6±0.4 and 1.2±1.2 mm day^{-1}. And from the seasonal ET study of Sanwangsri et al, (2017), found that in accordance with ET dry dipterocarp forest in the study area, ET in the wet season was clearly higher than the dry season. However, ET in dry dipterocarp forest Ratchaburi province found a slightly higher value. Because density of tree at Ratchaburi are more than the deciduous forest in this study. This study there are young trees and large tree at 600 and 1,821 trees ha^{-1} (Intanil et al, 2018) and 2,586 and 1,724 trees ha^{-1}, respectively (Hanpattanakit et al., 2015). In addition, the study of Yaseef et al. (2009) also found the weight / light and size of the raindrops also affect the amount of ET. The smaller rain can more interception on the canopy and when passing through the canopy layer to soil, most water will accumulate in the top soil. Because the dry deciduous forest has shallow soil layers. Therefore, most of the rain may enter the ET process quickly. In contrast, the evergreen forest has deep soil layers, there are thick heap biomass on top soil. Additionally, the evergreen forest has the canopy covered throughout the year so it can keep more water in the soil than the dry dipterocarp forest. From the Q assessment, found that the dry dipterocarp forest has only Q during the wet season was 117.5 to 335.0 mm, due to increasing P and SWC. While in the dry season, most water is used in the ET process, so it may result in a negative Q assessment, means that there is no Q. It is possible that the water in the

ecosystem in the dry season will be used in other processes (García-Leoz et al., 2018). From the relationship test, it was found ET during the dry season was positively correlated with SWC significantly. With the correlation coefficient (r) was 0.99 ($p < 0.05$). On the other hand, ET is inversely proportional to the VPD. The wet season, ET has not clear relation with P. Li and Fu (2004) said that ET during the dry season is an important driver in changing seasons from dry season to wet season. Therefore, in the dry season, can see the response of ET to environmental factors clearly (Li and Fu, 2004; Fu and Li, 2004). The ET of the dry dipterocarp forest has an average of more than 80% of P throughout the study 4-year period. Therefore, in this study, soil moisture and P are important factors that play a role in ET in the dry deciduous forest ecosystem.

Table 2 Seasonal of water balance components during 2013 to 2017 in DPT site (Wet season start at November to April and Dry season at May to October).

Year	Season	P	ET	ΔS	Q
		(mm)			
2014	Dry	*	*	*	*
2014	Wet	861.7	526.7	0.1	335.0
2014/2015	Dry	254.8	322.2	0.3	-67.7
2015	Wet	626.9	509.8	-0.4	117.5
2015/2016	Dry	131.2	254.5	-0.2	-123.0
2016	Wet	846.4	527.0	0.6	318.9
2016/2017	Dry	233.2	381.1	-0.5	-147.5
2017	Wet	913.7	578.1	-0.1	335.6
AVG	**Dry**	**169.5±66.0**	**284.9±63.3**	**0.4±1.7**	**-115.7±40.3**
	Wet	**812.2±126.8**	**535.4±29.6**	**0.3±2.3**	**276.5±105.1**

* Incomplete season data.

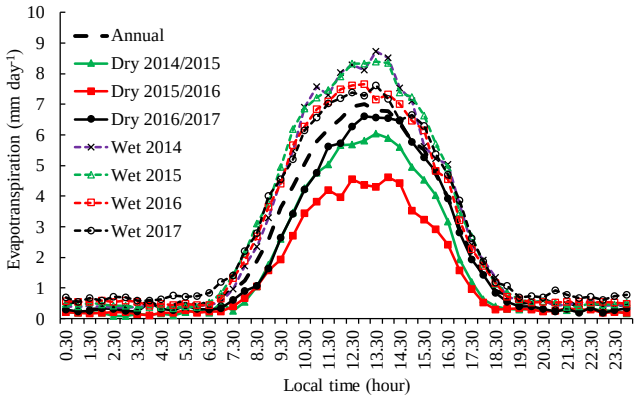

Figure 4 Diurnal of ET in dry and wet seasons during 2013-2017 in dry dipterocarp forest.

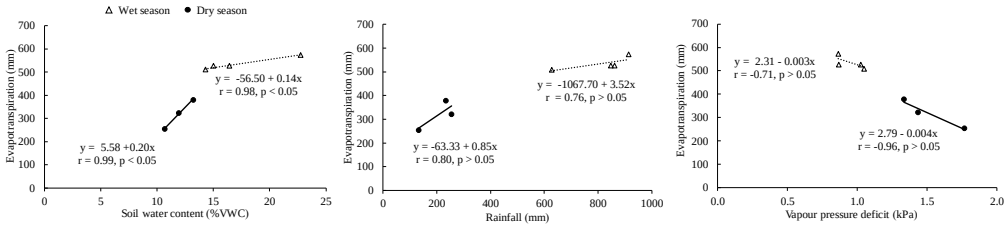

Figure 5 Relationship between monthly ET of wet (triangle) and dry season (circles) with (a) soil water content (b) rainfall and (c) vapor pressure deficit.

According to the study of seasonal water balance, we found anomaly of ET in during wet season in 2014-2016, ET decrease of approximately 2%, 5% and 2%, respectively, compared to the average wet season. ET, the wet season in 2015 the largest decrease, corresponding with P found the lowest (626.9 mm) or decrease around 23% from average in wet season. Making the SWC the lowest compared to other wet seasons was 14.3 %VWC or decrease from average wet season around 17%. While VPD found the highest value, on the other hand, RH was found lower than other years during the wet season. Resulting in the evaluation of Q in the wet season 2015 lowest or decrease from average in wet season around 57%. While the dry season of 2015/2016 was found to be consistent with wet season 2015, because P and SWC were less than other years in during dry season. Which decreased from the average in the dry season

about 36% and 20% respectively. The SWC found the lowest was 10.7% VWC or decreased from an average of 7% in the dry season. Which is consistent with the study of Kaewthongrach et al. (2018) in dry dipterocarp forest in Ratchaburi province, they found abnormalities of P and SWC decreased significantly in 2015/2016. Which found that the period was consistent with the El Niño phenomenon in Thailand (NOAA, 2017).

The ET change, found that is clearly in seasonal, is likely to controlled by the pattern of P and SWC However, the dry deciduous forest has adapted to reduce water loss by shedding leaves in dry season. This may be that in the future, if extreme climate changes, the dry deciduous forest may be adapted to maintain the water balance in ecosystem and ecosystem service, especially water.

CONCLUSIONS

Water balance components were assessed under dry dipterocarp-forested watershed during 2014 to 2017. Four-year average annual P, ET, ΔS and Q were 985, 854, 0.1 and 131 mm, respectively. Most of P was use for ET process more than 87% of P, storage in soil water change was 0.01% and out of ecosystem from Q around 13% of P. The Q will be between 4-5 months per year. In addition, the drought event during study period were affected from decreasing precipitation around 23% in wet season 2015. From this event results that Q in 2015 declined about 57% from average wet season or decrease 28% from average annual. These responses may be related with El Niño year which occurred in Thailand. The environmental factors affected to Q was P and SWC respectively. The result of this study can be used to support decision-making on water resources management in the watershed. However, we should be measure actual Q to compare data with estimate. And there should be study ET components in the future to improve our understanding water loss process in ecosystem.

ACKNOWLEDGEMENTS

This study was supported by grants from the University of Phayao. The authors would like to thanks to Atmospheric Pollution and Climate Change Research Center (APCC), members of Micrometeorology Laboratory (MiLab) and School of Energy and Environment, University of Phayao, Phayao, Thailand for their strong support throughout this project.

REFERENCES

Allen RG, Pereira LS, Raes D. Smith M. Crop Evapotranspiration-Guidelines for computing crop water requirements-FAO Irrigation and drainage paper 56. FAO. Rome 1998; 300(9): D05109.

Baldocchi D. Assessing the eddy covariance technique for evaluating carbon dioxide exchange rates of ecosystems: past, present and future. Global change biology 2003;9(4):479-92.

Baldocchi D, Finnigan J, Wilson K, Falge E. On measuring net ecosystem carbon exchange over tall vegetation on complex terrain. Boundary-Layer Meteorology. 2000; 96(1-2):257-91.

Bosch JM, Hewlett JD. A review of catchment experiments to determine the effect of vegetation changes on water yield and evapotranspiration. Journal of Hydrology. 1982; 55: 2-23.

Bunyavejchewin S. Canopy structure of the dry dipterocarp forest of Thailand. Thai Forest Bulletin 1983; 14: 1–132.

Bunyavejchewin S, Baker PJ, Davies SJ. Seasonally dry tropical forests in continental Southeast Asia: structure, compositon and dynamics. In McShea WJ, Davies SJ, Bhumpakphan N, editors, The Ecology and Conservation of Seasonally Dry Forests in Asia. 1 ed. United States: Smithsonian Institution Scholarly Press 2011; 9 - 35.

Chunkao K, Tangtham N, Boonywat S, Niyom W, Suwannarat. Watershed management research on mountainous land: Water balance in the hill evergreen forest, Doi-Pui, Chiangmai. Research reports, Kasetsart University 1982; 125.

Chunkao K, Thangtham N, Angkulpuldeekul S. Measurements of rainfall in carly wet season under hill- and dry-evergreen, natural teak and dry dipterocarp forests of Thailand. Kog-Ma watershed Research 10 1971. Kasetsart University, Bangkok

Cunkao K, Niyom W, Tantannasarit S, Boonyawat S. Water balance of various land use patterns at Sakaerat Environment Research Station (SERS). Kasetsart university 1985.

Clearwater MJ, Meinzer FC, Andrade JL, Goldstein G, Holbrook NM. Potential errors in measurement of nonuniform

sap flow using heat dissipation probes. Tree physiology. 1999;19(10):681-7.

Dunin, F. Extrapolation of 'point'measurements of evaporation: some issues of scale. Vegetatio 1991; 91(1-2): 39-47.

Da Rocha HR, Manzi AO, Cabral OM, Miller SD, Goulden ML, Saleska SR, et al. Patterns of water and heat flux across a biome gradient from tropical forest to savanna in Brazil. Journal of Geophysical Research: Biogeosciences. 2009;114(G1).

Dunin F. Extrapolation of 'point'measurements of evaporation: some issues of scale. Vegetatio. 1991;91(1-2):39-47.

Falge E, Baldocchi D, Tenhunen J, Aubinet M, Bakwin P, Berbigier P, et al. Seasonality of ecosystem respiration and gross primary production as derived from FLUXNET measurements. Agricultural and Forest Meteorology. 2002;113(1):53-74.

Foken T, Wichura B. Tools for quality assessment of surface-based flux measurements. Agricultural and forest meteorology 1996;78(1-2):83-105.

Fu R, Li W. The influence of the land surface on the transition from dry to wet season in Amazonia. Theoretical and applied climatology 2004; 78(1-3): 97-110.

García-Leoz V, Villegas JC, Suescún D, Flórez CP, Merino-Martín L, Betancur T, León JD. Land cover effects on water balance partitioning in the Colombian Andes: improved water availability in early stages of natural vegetation recovery. Regional Environmental Change 2018; 18(4): 1117-1129.

Göckede M, Foken T, Aubinet M, Aurela M, Banza J, Bernhofer C, Bonnefond J-M, Brunet Y, Carrara A, Clement R, … Yakir D. Quality control of CarboEurope flux data. Part 1: coupling footprint analyses with flux data quality assessment to evaluate sites in forest ecosystems. Biogeosciences 2008; 5: 433–450.

Hanpattanakit, P., Leclerc, M.Y., Mcmil-lan, A.M.S., Limtong, P., Maeght, J., Panuthai, S., Inubushi, K., Chidthaisong, A. Multiple timescale variations and con-trols of soil respiration in a tropical dry dipterocarp forest, western Thailand. Plant Soil 2015; 390(1), 167-181

Intanil P, Sanwangsri M, Boonpoke A, Hanpattanakit P. Contribution of Root Respiration to Soil Respiration during Rainy Season in Dry Dipterocarp Forest, Northern Thailand. Applied Environmental Research 2018; 40(3):19-7.

Jipp PH, Nepstad DC, Cassel DK, Carvalho CR. Deep soiศ moisture storage and transpiration in forests and pastures of seasonallydry Amazonia. Climatic Change 1998; 39: 395–412.

Kaewthongrach, R. Kieu DP, Chidthaisong A, Suepa T, Sanwangsri M, Hanpattanakit P, and Arnkovida P, Detecting the EL NIÑO'S induced changes in phenology of a secondary dry dipterocarp forest by using remote sensing. Sirindhorn

Conference on Geoinformatics 2018, Chonburi.

Kuricheva OA, Avilov VC, Dinh DB, Kurbatova JA. Water cycle of a seasonally dry tropical forest (Southern Vietnam). Izvestiya Atmospheric and Oceanic Physics 2015; 51(7): 693-711.

L'Heureux ML, Takahashi K, Watkins AB, Barnston AG, Becker EJ, Liberto TED, Gamble F, Gottschalck J, Halpert MS, Huang B, Mosquera-Vásquez K, Wittenberg AT. Observing and Predicting the 2015/16 El Niño. Bulletin of the American Meteorological Society 2017; 98(7): 1363-1382.

Li W, Fu R. Transition of the large-scale atmospheric and land surface conditions from the dry to the wet season over Amazonia as diagnosed by the ECMWF re-analysis. Journal of Climate 2004; 17(13): 2637-2651.

Li Z, Zhang Y, Wang S, Yuan G, Yang Y, Cao M. Evapotranspiration of a tropical rain forest in Xishuangbanna, southwest China. Hydrological processes 2010; 24(17): 2405-2416.

Luxmoore RJ, Huff DD. Water. In: Johnson DW, Van Hook RI (Eds.). Analysis of Biogeochemical Cycling Processes in Walker Branch Watershed. Springer. New York; 1989. p. 164–196.

Malhi Y, Pegoraro E, Nobre AD, Pereira MGP, Grace J, Culf AD, Clement R. Energy and water dynamics of a central Amazonian rain forest. Journal of Geophysical Research 2002; 107(D20): 8061.

Novák V. Evapotranspiration in the Soil-plant-atmosphere System: Springer Science & Business Media; 2012.

Phapan S, Thitirojanawat T, Wittawatchutikul P. Runoff coefficient polygons of forested watershed. Watershed research, Department of national parks wildlife and plant conservation 2011.

Reddy SJ. A simple method of estimating the soil water balance. Agricultural Meteorology. 1983;28(1):1-17.

Rundel PW, Boonpragob K. Dry forest ecosystems of Thailand. In: Bullock SII, Mooney HA, Mcdina E (eds) Seasonally Dry Tropical Forests. Cambridge University Press, Cambridge, UK; 1995.

Sanwangsri M, Hanpattanakit P, Chidthaisong A. Estimating Evapotranspiration and understanding its variations in a Seasonal Dry Dipterocarp Forest, Western Thailand. Journal of Chemistry Environment 2017a; 21(9).

Shuttleworth WJ. Evaporation from Amazonian rainforest. Proceedings of the Royal Society of London, Series B: Biological Sciences 1988; 233: 321-346.

Smith DM, Allen SJ. Measurement of sap flow in plant stems. Journal of Experimental Botany 1996; 47: 1877-1844.

Tanaka K, Takizawa H, Tanaka N, Kosaka I, Yoshifuji N, Tantasirin C, Piman S, Suzuki M, Tangtham N. Transpiration peak over a hill evergreen forest in northern Thailand in the late dry season:

Assessing the seasonal changes in evapotranspiration using a multilayer model. Journal of Geophysical Research: Atmospheres 2003; 108(D17).

Tanaka N, Kume T, Yoshifuji N, Tanaka K, Takizawa H, Shiraki K, Tantasirin C, Tangtham N, Suzuki M. A review of evapotranspiration estimates from tropical forests in Thailand and adjacent regions. Agricultural and Forest Meteorology 2008; 148(5): 807-819.

Tatsuhiko N, Akira S, Naoki K, Yoshio T, Tayoko K, Toshio A, Makoto A, Koji Tamai, Sophal C, Nang K. Year-Round Observation of Evapotranspiration in an Evergreen Broadleaf Forest in Cambodia. Springer 2007; 1(5).

Thaiutsa B, Puangchit L. Management of Integrated Tropical Forest Ecosystems: experience from MaeKlong Watershed Research Station. National Research Council of Thailand. Bangkok; 2004.

Vickers D, Mahrt L. Quality control and flux sampling problems for tower and aircraft data. Journal of Atmospheric and Oceanic Technology 1997;14(3):512-26.

Vickers D, Thomas C, Law BE. Random and systematic CO2 flux sampling errors for tower measurements over forests in the convective boundary layer. agricultural and forest meteorology 2009;149(1):73-83.

Webb EK, Pearman GI, Leuning R. Correction of flux measurements for density effects due to heat and water vapour transfer. Quarterly Journal of the Royal Meteorological Society. 1980;106(447):85-100.

Wolf S, Eugster W, Potvin C,Buchmann N. Strong seasonal variations in net ecosystem CO2 exchange of a tropical pasture and afforestation in Panama. Agricultural and Forest Meteorology 2011; 151(8): 1139-1151.

Witthawatchutikul P. Water supply of Forested Watershed. Watershed conservation and management office. Department of national parks, Wildlife and plant conservation 2011. Bangkok.

Wilson KB, Hanson PJ, Mulholland PJ, Baldocchi DD, Wullschleger SD. A comparison of methods for determining forest evapotranspiration and its components: sap-flow, soil water budget, eddy covariance and catchment water balance. Agricultural and forest Meteorology 2001;106(2):153-68.

Yaseef NR, Yakir D, Rotenberg E, Schiller G, Cohen S. Ecohydrology of a semi-arid forest: partitioning among water balance components and its implications for predicted precipitation changes. Ecohydrol. 2009; 3: 143-154.

Zhang L, Dawes WR, Walker GR. Response of mean annual evapotranspiration to vegetation changes at catment scale. Water Resources Research 2001; 37(3): 701-708.

Satellite Remote Sensing for Agricultural Mapping at Nang Lae Sub-district, Mueang Chiang Rai District, Chiang Rai Province

Krittawit Suk-ueng[1], Kittichai Chantima[1*],and Tippawan Prasertsin[2]

[1*] Energy and Environment Program, Faculty of Science and Technology, Chiang Rai Rajabhat University, Chiang Rai, Thailand; Corresponding author: e-mail: kittichai.cha@crru.ac.th

[2] Biological Science Program, Faculty of Science and Technology, Chiang Rai Rajabhat University, Chiang Rai, Thailand

ABSTRACT

Agricultural areas in Nang Lae Sub-district have changed dramatically over the past 10 years (2006-2016). Sustainable land-use planning is therefore required. Satellite remote sensing has been used for agricultural management. Nang Lae sub-district, Mueang Chiang Rai district, Chiang Rai province, is considered in this study because of its importance for economic agricultural production from paddy fields, other field crops (e.g. pineapple) and orchards (e.g. lychee, longan and pomelo). Systematic stratified sampling was applied to the study site, for ground-truth observations. Three plots in each agricultural area were surveyed and identified. Thaichote satellite imageries were used to digitally classify the agricultural area into three agricultural classes, namely paddy fields, field crops (pineapple) and orchards (lychee / longan / lemon / pomelo). Both underestimation (omission errors) and overestimation (commission errors) occurred due to mixed reflectance of field crop and orchard trees which led to less classification accuracy. Using high spatial resolution images with environmental information may help improve agricultural mapping. However the result suggested that there is an immediate

need to monitor current land use across reserve forest areas to assist with implementing municipal and government policies concerning agriculture and forestry.

Keywords: Remote sensing, Thaichote satellite, Agricultural land classification, Chiang Rai province, Landuse

INTRODUCTION

Landuse mapping is very important for local and nation plans to address issues of declining environmental quality and loss of forest in agricultural areas. Satellite image processing has contributed much to mapping agriculture at both small and large agricultural scales (Adegoke and Carleton, 2002; Al-Ahmadi and Hames, 2009; Usha et al., 2012; Rujoiu-Mare and Mihai, 2016; Mohammed et al., 2018).

Satellite remote sensing is an advanced tool for agricultural inventory and also for agricultural planning at both local and regional scales (Patil et al., 2012; Tezera et al., 2016). Multispectral imageries such as very high spatial resolution (e.g. Worldview and Quickbird), high spatial resolution (e.g. RapidEye), medium spatial resolution (e.g. Landsat, SPOT and ASTER) are used as basemap for agricultural classification. Open source software with various digital image classification algorithms have several advantages to design agricultural mapping for developing countries. QGIS has an open-source license, under the GNU General Public License, to automatically identify agricultural classes in a given area (Girouard et al., 2004; Huth et al., 2012; Usha et al., 2012; Jung, 2013; Tommasini et al., 2019).

Nang Lae Sub-district, Mueang District, Chiang Rai Province is an important source of economic crops in Chiang Rai, including paddy field (8,954 rai) and field crops and gardens (6,228 rai), especially Phu Lae pineapple (4,755 rai) and mixed

orchards (2,803 rai). The 3-year development plan (2016-2018) of Nang Lae Municipality, Strategy No.6 focuses on the development and promotion of management, conservation, rehabilitation and utilization of natural resources and the environment (Nang Lae Municipality, 2019a; Nang Lae Municipality, 2019b). This research was therefore conducted to provide an up-to-date of agricultural areas in 2018 using Thaichote satellite image processing. The software version, used in this research was QGIS 3.6.0 with the plugin, "Semi-automatic classification" (Congedo, 2016). The plugin can provide guidance for agricultural sustainability of farmers and Nang Lae municipality.

METHODOLOGY

1. Study area and field survey

Nang Lae sub-district, Mueang district, Chiang Rai province, was chosen as the study site (Figure 1). The approximate area is 5,500 ha, located at 19°53′40″ to 20°07′10″ N and 99°45′51″ to 99°57′24″ E. Visual surveys on foot were carried out from November 2018. Agricultural areas were selected based on a land use map dated 2016 (Land Development Station Chiang Rai, 2016), a satellite image from the Geo-Informatics and Space Technology Development Agency (GISTDA) and survey results of the study site. Systematic stratified sampling was applied on the study site for ground truthing (Mas et al., 2017). Three plots of each agricultural type were surveyed and identified as paddy field or field crop or mixed orchard (lychee / longan / lemon / pomelo).

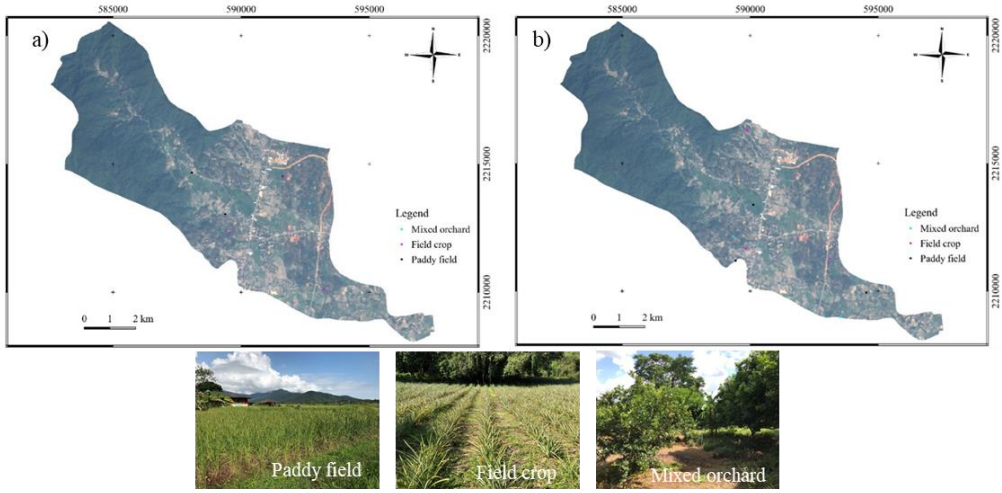

Figure 1 9 pixels of training samples (a) and 9 pixels of testing samples (b).

2. Thaichote imagery and geoinformatics software

Thaichote imagery (4 multispectral bands, band 1 (blue), band 2 (green), band 3 (red) and band 4 (near-infrared)) covering the study area, on cloud-free days were provided by Geo-Informatics and Space Technology Development Agency (GISTDA). GISTDA also operated the image with radiometrically corrected and geocoded. The imagery was acquired on 9 February 2017. The satellite images were captured for the study site (Figure 1) before further image processing. Quantum GIS version 3.6.0, semi-automatic classification plugin (Figure 2), was used for image processing (QGIS Development Team, 2019).

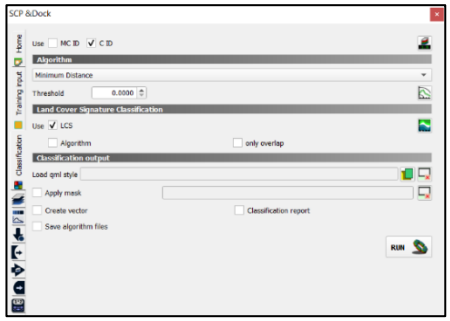

Figure 2 Semi-automatic classification plugin.

3. Thaichote satellite image processing

Thaichote image was transformed by using Normalized Difference Vegetation Index (NDVI), derived from a ratio of original band 3 and 4 ((band 4–band 3)/(band 4+band 3)). Then, agricultural classification results following semi-automatic classification plugin were verified against testing samples (9 pixels) from the field survey. The Kappa was used for accuracy assessment of satellite image classifications, for evaluating the quality of the maps (Lillesand et al., 2004). The values of Kappa ranged from -1 to 1. Ranges of Kappa were categorized into strong (>0.8), moderate (0.4-0.8) and poor (<0.4) agreements (Landis and Koch, 1977). (Figure 3).

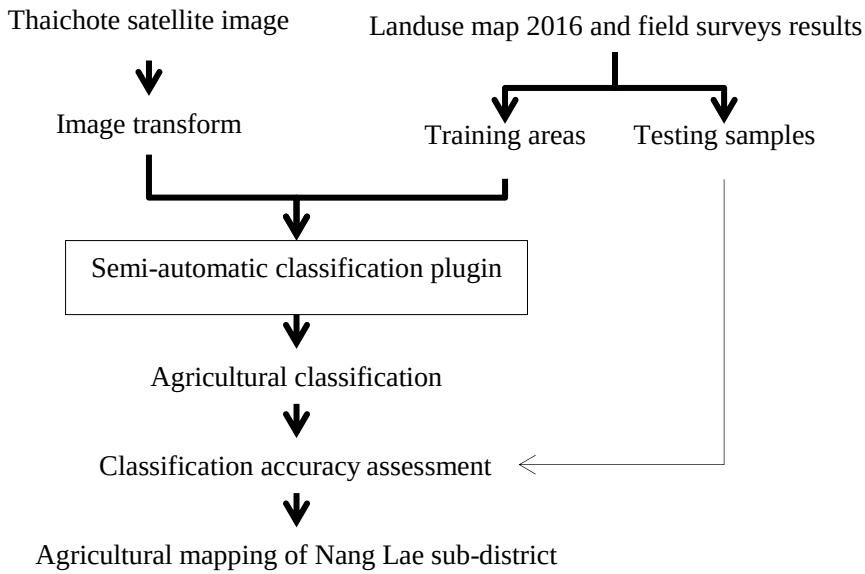

Figure 3 Use of field data combined with semi-automatic classification plugin for guidance for agricultural sustainability

RESULTS AND DISCUSSION

1. Image transformation and agricultural classification

Image transformation using the Normalized Difference Vegetation Index (NDVI) equation (NIR-Red) / (NIR + Red) to highlight land use data helped to visually interpret

image. Plants derived from NDVI had the highest DN values (green), followed by open areas (gray) and water sources (pink i.e. a negative DN) respectively (Figure 4).

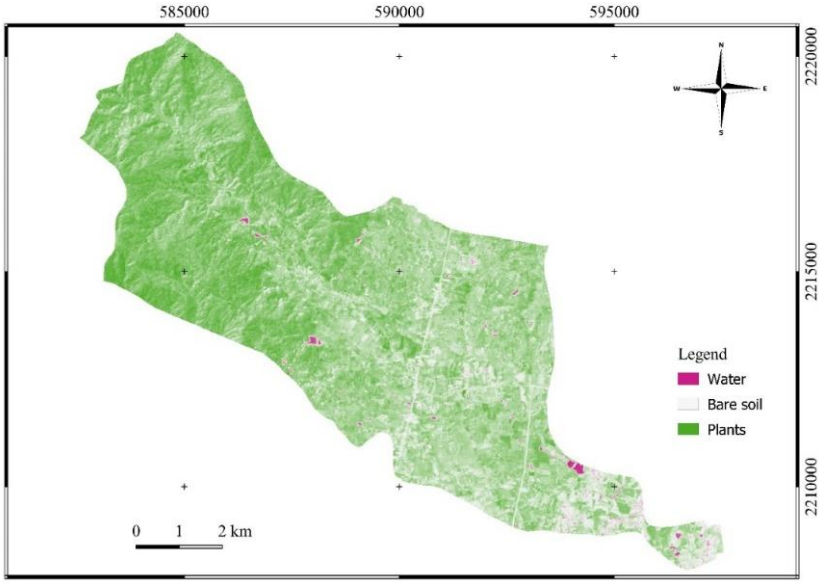

Figure 4 Transformed image, based on Thaichote image, derived from NDVI

Agricultural mapping using maximum likelihood classifier showed that "the following signature has not a covariance matrix and is excluded". However, minimum distance (MD) and spectral angle mapping (SAM) (Figure 5) were presented in the plugin.

2. Classification accuracy assessment

Based on error matrix, field crop and mixed orchard were identified with high accuracy of the image. Due to the dominance of paddy field and mixed orchard in the study area, MD and SAM (Figure 5) classifiers shown that total accuracy of supervised classification was 22.22% with kappa statistic of -0.15, which indicated poor agreement.

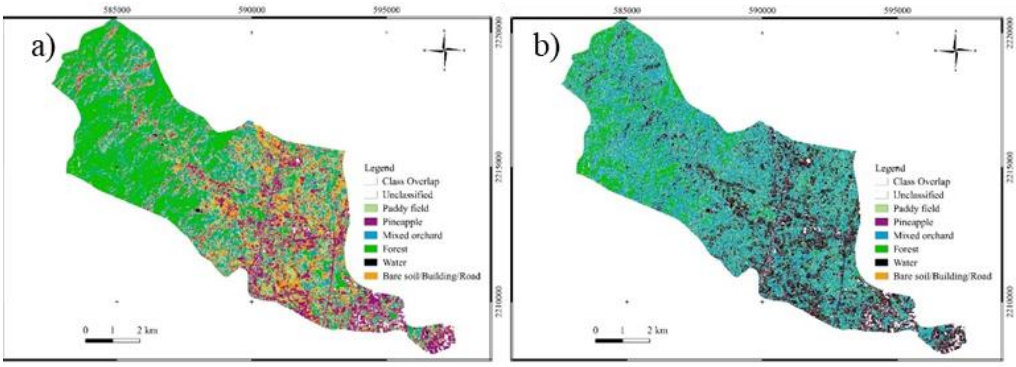

Figure 5 Agricultural classification techniques; a) Minimum distance classifier (Threshold = 90); b) Spectral angle mapping (Threshold = 90)

From the error matrix shown in Table 1, producer's accuracies of paddy field and mixed orchard were 33.33% and 33.33%, respectively, and user's accuracy of paddy field and mixed orchard was 33.33% and 20%, respectively. The highest values (100%) of omission and commission errors occurred for field crop (Table 1) because of the mixed-pixel problem.

The satellite imagery in this study was acquired before study period. It is different in case of change in the agricultural areas (Mas et al., 2017). Su and Noguchi (2013) suggested that the image acquisition should be involved with study period. In addition, Thaichote sensor specification might not be appropriate for agricultural classification. Low Kappa of supervised classifications and high error of omission and commission in ground truth data were described following Lunetta et al. (1991) and Foody (2002). The very low accuracy of agricultural classification was due to the mix of mixed orchard and field crop plantation in the same pixel. The method in this paper enabled us to produce, in a reasonably short period of time, these training and testing samples are inadequate random sampling for remote sensing techniques (Mas et al., 2017). Achieving higher overall accuracy needs a study site with more training samples. Further studies are required

to focus on algorithms with high accuracy for a more accurate agricultural classification. In addition, using hyperspectral band (e.g. EO-1) and high spatial resolution with multispectral bands (e.g. IKONOS and WorldView-2) combined with strong plant-environment relationship should be tested for agricultural mapping However, the results suggested that there is an immediate need to monitor current land use across the reserved forest area (Doi Nang Lae, Doi Yao and Doi Prabhat reserve forest) to assist with implementing municipal and government policies concerning agriculture and forestry (Eckert and Kneubhuler, 2004; Shah and Sharma, 2015; Yousefi et al., 2015).

CONCLUSIONS

The two classifiers used to classify agricultural land for mapping of Nang Lae sub-district (minimum distance and spectral angle mapping) resulted in total accuracy of supervised classifications of only 22.22% with K statistic of -0.15. This low accuracy was due to the dominance of paddy field and mixed orchard.

ACKNOWLEDGEMENTS

We are grateful to thank Chiang Rai Rajabhat University for supporting the research fund (fund#ABC020, ABC021 and ABC022). We would like to express our thanks to the Geo-Informatics and Space Technology Development Agency (GISTDA) for their kind support in providing satellite images. Our thanks are also presented to my students of Energy and Environment Program, Faculty of Science and Technology, Chiang Rai Rajabhat University for field survey and data collection.

Table 1 Land use data using minimum distance and spectral angle mapper in error matrix

Classifiers	Landuse types	Paddy field	Field crop	Mixed orchard	Total	Commission error (%)	User's accuracy (%)
Minimum distance (Threshold = 90)	Paddy field	1	0	2	3	2/3*100= 66.67%	1/3*100= 33.33%
	Field crop	1	0	0	1	1/1*100= 100%	0%
	Mixed orchard	1	3	1	5	4/5*100= 80%	1/5*100= 20%
	Total	3	3	3	9		
	Omission error (%)	2/3*100= 66.67%	3/3*100 =100%	2/3*100 =66.67%			
	Producer's accuracy (%)	1/3*100= 33.33%	0%	1/3*100 =33.33%			
Spectral angle mapper (Threshold = 90)	Paddy field	1	0	2	3	2/3*100= 66.67%	1/3*100= 33.33%
	Field crop	1	0	0	1	1/1*100= 100%	0%
	Mixed orchard	1	3	1	5	4/5*100= 80%	1/5*100= 20%
	Total	3	3	3	9		
	Omission error (%)	2/3*100= 66.67%	3/3*100 =100%	2/3*100 =66.67%			
	Producer's accuracy (%)	1/3*100= 33.33%	0%	1/3*100 =33.33%			

REFERENCES

Adegoke JO, Carleton AM. Relations between soil moisture and satellite vegetation indices in the U.S. corn belt. Journal of Hydrometeorology 2002; 3(4): 395-405.

Al-Ahmadi FS, Hames AS. Comparison of four classification methods to extract land use land cover from raw satellite images for some remote arid areas, Kingdom of Saudi Arabia. Journal of King Abdulaziz University; Earth Sciences 2009; 20(1): 167-191.

Congedo L. Semi-automatic classification plugin user manual, release 5.0.0.1. http://dx.doi.org/10.13140/RG.2.1.1219.3524; 2016.

Eckert S, Kneubhuler M. 2004. Application of HYPERION data to agricultural land classification and vegetation properties estimation in Switzerland. In XXth ISPRS

Congress (pp. 866-872). Istanbul, Turkey.

Foody GM. Status of land cover classification accuracy assessment. Remote Sensing of Environment 2002; 80: 185-201.

Girouard G, Bannari A, Harti A, Desrochers A. Validated spectral angle mapper algorithm for geological mapping: Comparative study between quickbird and landsat-tm. In: The 20th International Society for Photogrammetry and Remote Sensing Congress, Istanbul, Turkey; 2004. pp. 599–605.

Huth J, Kuenzer C, Wehrmann T, Gebbhadt S, Tuan VQ, Dech S. Land cover and land use classification with TWOPAC: towards automated processing for pixel-and object-based image classification. Remote Sensing 2012; 4: 2530-2553.

Jung M. LecoS - A python plugin for automated landscape ecology analysis. Ecological Informatics 2016; 31: 18-21.

Landis J, Koch G. The measurement of observer agreement for categorical data. Biometrics 1977; 33: 159-174.

Lillesand TM, Kiefer RW, Chipman JW. Remote sensing and image interpretation. (5th ed.). United States of America: John Wiley & Sons; 2004.

Lunetta RS, Congalton RG, Fenstermaker LK, Jensen JR, McGwire KC, Tinney LR. Remote sensing and geographic information system data integration: Error sources and research issues. Photogrammetric Engineering & Remote Sensing 1991; 57(6): 677-687.

Mas J-F, Lemoine-Rodríguez R, González-López R, López-Sánchez J, Piña-Garduño A, Herrera-Flores E. Land use/land cover change detection combining automatic processing and visual interpretation. European Journal of Remote Sensing 2017; 50(1): 626-635.

Mohammed EA, Hani ZY, Kadhim GQ. Assessing land cover/use changes in Karbala city (Iraq) using GIS techniques and remote sensing data. Journal of Physics: Conference Series 2018; 1032: 1-7.

Nang Lae Municipality. 2019a. The 3-year development plan (2016-2018) of Nang Lae Municipality. Retrieved from http://www.nanglae.go.th/index. php/2552-2554.

Nang Lae Municipality. (2019b). Community development project. Chiang Rai: Nang Lae Municipality.

Patil MB, Desai CG, Umrikar BN. Image classification tool for land use/land cover analysis: A comparative study of maximum likelihood and minimum distance method.

International Journal of Geology, Earth and Environmental Sciences 2012; 2(3): 189-196.

QGIS Development Team. QGIS Geographic Information System. Open Source Geospatial Foundation Project; 2019.

Rujoiu-Mare M-R, Mihai B-A. Mapping land cover using remote sensing data and GIS techniques: A case study of Prahova Subcarpathians. Procedia Environmental Science 2016; 32: 244-255.

Shah S, Sharma DP. Land use change detection in Solan Forest Division, Himachal Pradesh, India. Forest Ecosystems 2015; 2(26): 1-12.

Su B, Noguchi N. Discimination of land use patterns in remote sensing image data using minimum distance algorithm and watershed algorithm. Engineering in Agriculture, Environment and Food 2013; 6(2): 8-53.

Tezera A, Chanie T, Feyisa T, Jemal A. Impact assessment of land use/land cover change on soil erosion and rural livelihood in Andit Tid watershed, North Shewa, Ethiopia. Archives of Current Research International 2016; 3(1): 1-10.

Tommasini M, Bacciottini A, Gherardelli M. A QGIS tool for automatically identifying asbestos roofing. International Journal of Geo-Information 2019; 8(131): 1-13.

Usha M, Anitha K, Iyappan L. Landuse change detection through image processing and remote sensing approach: A case study of Palladam Taluk, Tamil Nadu. International Journal of Engineering Research and Applications 2012; 2(4): 289-294.

Yousefi S, Mirzaee S, Tazeh M, Pourghasemi H, Karimi H. Comparison of different algorithms for land use mapping in dry climate using satellite images: A case study of the Central regions of Iran. Desert 2015; 20-1: 1-10.

Water footprint of superabsorbent polymer

Amonwan Choodonwai[1*]

[1*]Soontaree Khuntong
Namon8133@gmail.com

ABSTRACT

The water footprint (WF) is an indicator of water consumption both direct and indirect water use in manufacturing. WF concept can be applied to companies to evaluate the sustainability of product and production process. This paper aims to evaluate the existing water footprint of superabsorbent polymer (SAP) process per ton of SAP following the global water footprint standard. The evaluation scope is agreed with cradle-to-gate covering both supply chain and production process. Blue and gray water were focused in this evaluation excepted green water due to its has not been consumed in process. SAP has been developed for over 20 years in the world. These polymers have the ability to absorb and retain a large volume of liquid without water soluble. They are made from partially neutralized, lightly cross-linked polyacrylic acid that is low solids levels, and are dried and milled into white granular solids. SAP is extremely swelled to a soft gel in water that in some cases can be up to 99wt% water. The major of SAP consumption is for hygiene application, e.g. baby diapers, adult incontinence, and napkin. Calculation data was based on annually consumption. Simplified flow diagram was calculated, raw material which is small consumption values are grouped and evaluated. According to the limitation of emission factor, the equivalent factors were implemented for calculation. The results showed total WF of SAP process requires 176.71 m^3 H_2O per ton, which 99.96% and 0.04% of blue and gray water, respectively. WF was divided into 5 sectors which supply chain 82.95%, material 16.79%,

the manufacturing process 0.20%, packing and transferring 0.03% and disposal 0.03%.

Keywords: Water footprint, Sustainability, Superabsorbent polymer, Life cycle assessment

INTRODUCTION

The world's population is expected between 9.4 to 10.2 billion in 2050 (United Nations, 2017). The results of rapid population growth, urbanization and industrialization that increased resources consumption as well as water usages, water pollution and others environmental effected. Freshwater is the most important resource for all mankind, it is one of the essential resources that used in economic activities such as materials supply, manufacturing process and transportation. To achieve water security the water management in sustainable way must be considered in all global sectors. For industry, these issues threaten the long-term viability of business, serious financial and operational risks that rely on amount of water for process, service and raw material. In the same time companies are seeking the actions to prevent their business from these issues that related to water resource availability. (ERM, 2018). Operation cost and consumption are key focus of saving activities in widely manufacturing, cost minimization and resources consumable efficiency are often approached to saving actions. Water footprint (WF) is the one methodology for assessing both direct and indirect of water consumption associated with materials, manufacturing process, transportation, services or other activities chain.

Refer to population growth and consumers behavior the disposable baby diapers market growth continuously. EDANA who is the international association

serving the nonwovens and related industrials reported in the sustainability report 2015 according to the compositions of an open baby diaper in 2013 were SAP 33%, fluff pulp 24%, nonwovens 21%, elastic and adhesive tape 13%, polyethylene film 5%, adhesive 3% and other 1% (EDANA, 2015). As consequence SAP was the majority consumption for a piece of baby diaper hence their manufacturing process was studied in this paper.

Superabsorbent polymer (SAP) materials are hydrophilic networks that can absorb and retain huge amounts of liquid. Their application is widely implemented in baby diapers and others disposable hygienic. SAP can be divided into 2 classes which synthetic and natural. Synthetic SAP are produced from petrochemical based, acrylic acid that frequency implemented. However, the synthetics SAP was focused in this studied excepted natural class. Generally, the synthetics SAP consumed acrylic acid around 52.60% meanwhile the remaining 47.4% are initiator chemicals and cross-linking excepted soft water that implemented for dilution. The mixture solution goes into a reactor with strong UV radiation that drives polymerization and cross-linking reactions. Polymer gels which contain 60-70% of water are output of reactions. Dried polymers are screened for proper particle size as customers require. WF of business was implemented for SAP manufacturing process in this studied, the total amount of WF that consists of quantity of water consumption in production process (direct), the volume of water used to produce raw materials (indirect) and water volume that consumed for services. The WF evaluated results showed the existing situation and efficiency of water management in business however the studied results could be implemented for future improvement guideline accord to water management in each sectors of the manufacturing.

METHODOLOGY

This approach followed similar steps as a global water footprint standard (Arjen Y. Hoekstra, 2011) to evaluate the WF of the existing SAP manufacturing process using within the framework. The evaluation steps can be divided into boundary definition, inventory analysis and water footprint accounting. That they were explained in the following section.

Boundary definition

The studied boundary process showed as Figure.1 that covered the general process associated with raw material acquisition, water/energy consumption, transportation, manufacturing processing, wastewater and solid waste disposal. The calculation considered the amount of raw material, energy and utility requires that were supplied for 1 ton of superabsorbent polymer.

Raw materials which evaluated were mainly component and high consumption, they were acrylic acid, sodium hydroxide, soft water for dilution and liquid nitrogen that used in de-oxygen process. Others additive chemical also considered by grouping.

Supply chain was considered about raw materials transportation form vender's locations to manufacturing, allocation methodology was applied for raw materials which multi-supplied sources. This paper considered supply chain of acrylic acid, sodium hydroxide, liquid nitrogen, wastewater and solid waste transportation. Others additive chemical were excluded in this studied because of there were very low consumption per ton SAP

Due to Acrylic acid which the mainly raw material was transported form oversea by road. The distance around 1,700 kilometers from supplier to factory. Sodium hydroxide which the second requires material also evaluated. There were two suppliers who supplied sodium hydroxide, the actual consumption was allocated for calculation,

transportation distances from supplier A and supplier B's manufacturing around 46 and 47 kilometers. Liquid nitrogen that used for production process are transferred to manufacturing by tank truck with distance 41kilometers. For utilities such as electricity, water and natural gas are supplied via pipe lines by Industrial estate that excluded evaluation in this part. Waste transportation from factory to disposal company was considered in this part which roll-off truck with distance 16 kilometers and tank truck for wastewater with 119 kilometers

Manufacturing process was evaluated as one process due to inventory data in each sub- process were not available, energy and utility supplied were considered in this sector. Electricity for production, natural gas consumption for drying and boiler also water for cooling, production activity such as cleaning were evaluated. Packing and internal transferring by LPG forklift were separated from manufacturing process nevertheless it was considered to packing and transferring sector.

Wastewater and solid waste which generated from process due to cleaning activity or production troubleshooting. The current management both were transported to the authorizes disposal parties. Disposal incinerator was applied for wastewater and landfilled disposal was implemented for solid waste. However, waste transportation was calculated under supply chain

Manufacturing process was evaluated as one process due to inventory data in each sub- process were not available, energy and utility supplied were considered in this sector. Electricity for production, natural gas consumption for drying and boiler also water for cooling, production activity such as cleaning were evaluated. Packing and internal transferring by LPG forklift were separated from manufacturing

process nevertheless it was considered to packing and transferring sector.

Wastewater and solid waste which generated from process due to cleaning activity or production troubleshooting. The current

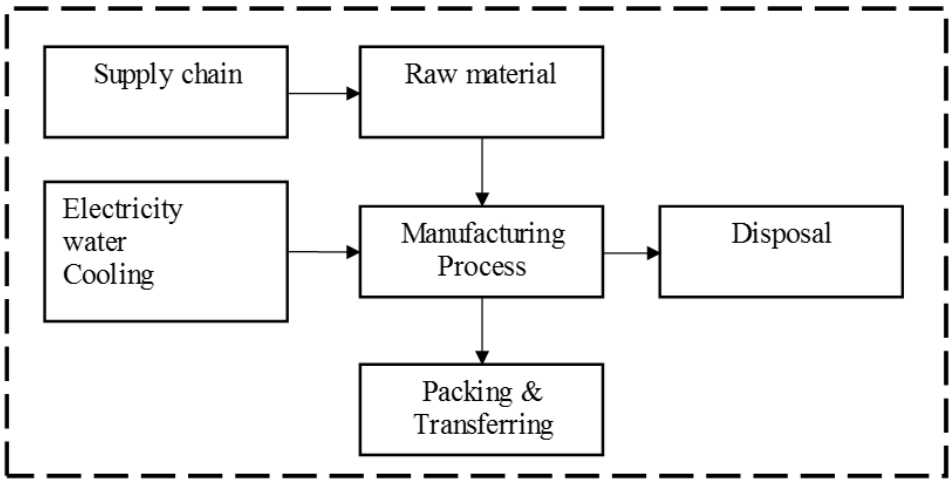

Figure 1 Boundary Definition.

management both were transported to the authorizes disposal parties. Disposal incinerator was applied for wastewater and landfilled disposal was implemented for solid waste. However, waste transportation was calculated under supply chain sectors that together with raw material acquisition.

Water footprint method

The water footprint of this study is defined as the total amount of freshwater that is used directly and indirectly to operate and support the SAP manufacturing process. There were two main components which operational

WF (or direct) was the amount of water that consumed or polluted due to the manufacturing and supply chain WF (or indirect) which volume consumed or polluted to produce the SAP and services that from the inputs of production. The overview concept for water footprint of SAP showed in Figure.2

The WF of SAP was calculated following the water footprint assessment manual (Arjen Y. Hoekstra, 2011) which cradle-to-gate boundary. The WF of products generally covered green WF, blue WF and gray WF. It should be noted that the green WF is not considered in this work since green WF is associated mainly with evapotranspiration losses in agriculture. Therefore, this WF calculation contains the demand for blue water in manufacturing process and production supply chain of SAP that covered direct and indirect portions of WF. Data obtained for investigation were both primary and secondary sources that corresponded to the WF due to electricity consumption, raw materials used in production and operational process. Unless the additive chemical and others which was very small consumption were grouped and calculated under others component does not factor significantly in this evaluation. The

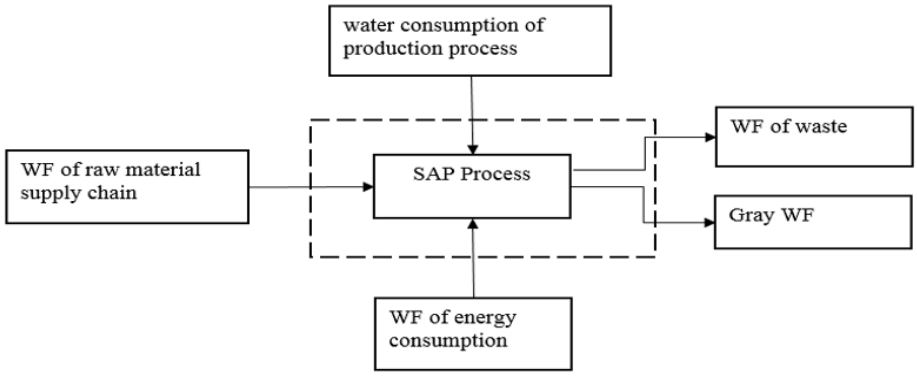

Figure 2 Water footprint of SAP.

$$WF_{product} = WF_{manufacturing} + WF_{supply\ chain} \quad (1)$$

$$WF_{product} = WF_{supply\ chain} + WF_{raw\ material} + WF_{process} + WF_{packing} + WF_{disposal} \quad (2)$$

$$WF_{supply\ chain} = (WF_i \times D_i \times EF_i)_{supply} + (WF_i \times D_i \times EF_i)_{return} / \text{truck capacity} \quad (3)$$

When W_i = Loading weight (ton)

D_i = Distance (kilometer)

EF_i = WF of truck

item. The required components for 1 ton of SAP were multiplied by emission factors. The general calculation equation for WF of SAP as presented in equation (1) however in this studied WF was calculated which five sectors that were defined as supply chain, raw material, process, packing and transferring and disposal. The consumptive of all five sectors that covered the manufacturing WF and its supply chain WF shows as equation (2). Due to supply chain water footprint was considered the raw materials and waste transportation from originates to SAP factory. Evaluated equation for each material shows as equation (3). Their WFs that presented in water footprint of biofuel-based transport (Gerbens-Leenes & Hoekstra, 2011). were multiplied with the distances. However, the transportation WFs were mentioned in rage valves hence this evaluation was applied the maximum value for 100% loading and minimum valve was multiplied with 0% loading

The raw material WF per unit was the consumptive of the various input materials that calculated by the consumption that required for ton of SAP multiply by their WF. The overall materials which supplied by difference sources, their WF from each supplier should be applied but in this studied which sodium hydroxide was supplied by two suppliers, the same WF value that mentioned in literature(Corporation, 2013). was applied for both sources instead of WF from each originate suppliers. Calculation method presented in equation (4)

Water footprint of process associated with energy and utility that consumed to produce the SAP product.

WF components consisted of WF that can be directly associated with the production and overhead

$$WF_{material} = (WF_{material\ 1} + WF_{material\ 2} + WF_{material\ i} + \ldots) \quad (4)$$

$$WF_{process} = WF_{energy\ and\ utility\ input} + WF_{overhead} \quad (5)$$

WF. The process WF was the consumptive electricity, natural gas and water for cooling consumption that associated with process. The overhead water used in process also considered excepted water used in administration activities. WF process was evaluated as equation (5).

Water footprint of packing and transferring was considered the material that consumed for packing activities which bag, pallet plastics. Product transferring from production areas to storage areas within manufacturing boundary was included by considered LPG fuel consumption that used for forklift. Calculation equation same as mentioned (4). Water footprint of disposal was calculated for wastewater and solid waste that generated during production process. The volume of waste generated was multiplied by their available WF same as equation (4)

Water footprint factor

Emission factor (EF) or water used coefficient was applied for calculation in the studied, they were referenced from the available literatures. Table 1 presented the EF values of blue and green water of each materials and services in m^3 H_2O per unit which applied for this evaluation. Nonetheless the limitation of EF, indirect calculation was modified for water footprint of acrylic acid and liquid nitrogen

The dataset of liquid acrylic acid which referred from ecoinvent database 2007 (Primas, 2007) was implemented for EF calculation. The calculation methodology was similar water footprint method which the

$$\text{Require material, energy, waste} = \frac{\text{Actual annually data (unit)}}{\text{Total SAP output (Ton)}} \quad (6)$$

quantity of raw materials and energy required for 1 kilogram of liquid acrylic production were multiplied by their available WF. Emission factor of liquid nitrogen also implemented with the same concept. Finally, the EF of acrylic acid and liquid nitrogen of 0.032 and 0.158 m^3 H_2O per kilogram, respectively, were applied for the studied. Moreover, EF of others material and services the available emission factors in concerning literatures were applied. Table 1 shows the EF which implemented for evaluation in this paper.

Inventory data

In order to evaluations, the actual annually consumption and output in 2018 were applied, they were referred from financial report, invoices and operation recorded, However, the detail of inventory data was not shown in the paper. The total quantity of materials, electricity, water and others were consumed to produce SAP in 2018 were divided by total SAP output as presented in equation (6). Wastewater and waste which generated from process also applied with the same concept.

Table 1 Emission factor

Item (unit)	Factor (m^3 H_2O/Unit)		Reference
	Blue	Gray	
Acrylic Acid (kg)	0.032	0	Hischier,2013
Sodium Hydroxide (Ton)	2.86	0	IFC,2013
Soft water (m^3)	1.311	0.0216	ecoinvent,2.2
Other chemical(kg)	0.0078	0	ecoinvent,2.2
Liquid Nitrogen(kg)	0.158	0	Pimas,2007
Water(m^3)	1.3	0	ecoinvent,2.2
Natural Gas(MJ)	2.54E-05	0	Nim-O,2019
Electicity(kWh)	0.26	0	Kamalaporn,2019
Land fill(Ton)	3.2	2.3	PCD,2005
LPG(kg)	0.0084	0	SimaPro
Wastewater(Ton)	0.173	0	Malakahmad,2017
Plastic(Ton)	2.8	2.2	PCD,2005
Lorry with 100% Load(tkm)	1.03E-01	0	Gerbens-Leenes & Hoekstra, 2011
Lorry with 0% Load(tkm)	1.75E-01	0	

RESULTS AND DISCUSSION

The analysis water footprint of superabsorbent polymer in cubic metre (m^3) per ton SAP showed the total WF 176.71 m^3 H_2O which 176.64 and 0.07 m^3 H_2O for blue and gray water, respectively. The highest WF was supply chain sector that contributed 146.58 m^3 H_2O for blue water excepted gray water that was 82.95% of total water required for SAP manufacturing process . Mainly WF's supply chain was generated from acrylic acid that presented 94.98% which transferred from other countries. The WF of Sodium hydroxide, liquid nitrogen, waste supply chains were 2.14%, 0.13% and 2.76%, respectively.

To reduce WF of this part, the transportation routes management, modes of transportation such as rail-way due to WF-blue of rail way is 3-6 litre per 1,000 kilogram of freight per kilometer while WF of truck is 103-175 litre per 1,000 kilogram of freight per kilometer, trailer truck and cargo ship that are alternatives for company too. Moreover, the future study might be combined the difference transportation modes because of one transportation modes cannot achieved material supply to manufacturing. Local suppliers are also WF reduction possibility

The second sector was materials that had WF 29.67 m^3 H_2O that was 16.79% of total WF of SAP, which 29.64 and 0.03 m^3 H_2O for blue and gray water, respectively. There were 79.04% of acrylic acid, 5.97% of sodium hydroxide, 8.36% of liquid nitrogen, 5.56% of soft water that used for dilution and 1.08% of other chemicals. This sector was considered the amount consumption of raw material. Whatever process optimization, consumption tracking and analysis, production improvement programs and waste reduction program that are the options to decrease WF of materials. Due to manufacturing process required 0.35 m^3 H_2O or 0.20% of total WF of SAP which blue water. Electricity, natural gas, water for production activities and

cooling were considered in this sector. The results showed 0.04%, 3.27%, 44.33% and 52.36% of electricity, natural gas, water for production and cooling respectively. However, the amount of WF of process was very less when compared with other sectors but these direct to affects the manufacturing Process reliability, equipment and machines effectiveness which the options to reduce WF in process. Modern technology with low energy supply and high efficiency could be considered too. For the existing machines the separate electricity meter of critical machines that is useful for inventory data that used for WF reduction programs implemented. Manufacturing reliability program also help to reduce WF for process due to le energy loss from system. The WF of packing and transferring result within manufacturing areas was 0.05 m^3 H_2O it was 0.03% of total WF which packaging material and plastic pallets were 99.40% and LPG for forklift was 0.6%. Blue water for this sector was 0.03 m^3 H_2O and gray water was 0.02 m^3 H_2O. Lay-out management could be applied to decrease WF of forklift and waste reduction program that the option for packaging. Disposal (solid waste and wastewater) generated form the process that the last sector was evaluated. There was WF of 0.06 m^3 H_2O which blue and gray were 66.67% and 33.33%, respectively. The percentage of waste disposal was 0.03% of total WF of SAP. Although waste reduction, reuse and recycle programs in manufacturing that the possibility to reduce WF in this sector. The WF results of each sector were presented in Table 2 and the percentage showed in Table.3

A Life cycle inventory of baby diapers in Canada was

Table 2 Water footprint of each sector

Sector	WF (m^3 H_2O/Ton)		
	Blue	Gray	Total
Supply chain	146.58	0.00	146.58
Material	29.64	0.03	29.67
Process	0.35	0.00	0.35
Packing & Transferring	0.03	0.02	0.05
Disposal	0.04	0.02	0.06
Total	176.64	0.07	176.71

Table 3 Percentage of Water footprint

Sector	%WF		
	Blue	Gray	Total
Supply chain	82.95	0.00	82.95
Material	16.77	0.02	16.79
Process	0.20	0.00	0.20
Packing & Transferring	0.02	0.01	0.03
Disposal	0.02	0.01	0.03
Total	99.96	0.04	100.00

evaluate(Vizcarra_et_al, 1994) mentioned absorbent gelling material that used for baby diapers was 0.07 kg per baby week (38 pieces of diapers) and water consumption of absorbent gelling material was 0.012 m^3 per baby-week, therefore water consumption for 1,000 kilograms of SAP should be 171.43 m^3. However, the analysis results presented the total WF of SAP process was 176.71 m^3 that was slightly higher due to inventory evaluation was included transportation, energy consumption and waste disposal.

The calculated of WF of SAP might be affected by emission factors of both acrylic acid and liquid nitrogen which applied in this study. According to indirect calculated concept, the statistical consumption for both production processes were implemented instead of actual

inventories. Materials requisition might be excluded in statistical consumption.

CONCLUSIONS

The consumptive WF of SAP expressed as the total volume of water consumption over the supply chain, material, energy for production process, packing and disposal. The finding indicated that the consumptive WF of supply chain was higher than those in process sector due to the distances of transportation. Other finding which WF material contributed as the second. Both were indirect WF that might be difficult for company to consider WF reduction. However, the analysis data could be implemented for water management guideline for business in part of process

ACKNOWLEDGEMENTS

The author acknowledge the financial support and operation team to explained and provided data.

REFERENCES

Alex Pimas, (2007). Dataset information; air separation, cryogenic, ecoinvent ,version 2.0

Arjen Y. Hoekstra, e. a. (2011). The Water Footprint Assessment Manual. In.

International Finance Corporation, IFC (2013). *NaOH factor WFN_2013.Tata_Industrial_Water_Footprint_Assessment*.

Ecoinvent 2.2 (2013)

EDANA. (2015). sustainability-report_4th edition 2015.

ERM. (2018). ERM Sustainability-report.

Gerbens-Leenes, W., & Hoekstra, A. Y. (2011). The water footprint of biofuel-based transport. *Energy & Environmental Science, 4*(8). doi:10.1039/c1ee01187a

Phumpradab, K., Gheewala, S. H., & Sagisaka, M. (2009). Life cycle assessment of natural gas power plants in Thailand. *The International Journal of Life Cycle Assessment, 14*(4), 354-363. doi:10.1007/s11367-009-0082-

Roland Hischier, Dataset information; Acrylic acid production, ecoinvent ,version 3.01(2013)

SimaPro,LCA Food DK

United Nations, Department of Economic and Socail Affairs, Population Devision. (2017). *World Population Prospects The 2017 Revision Key Finding and Advance Tables*. Retrieved from

Vizcarra_et_al. (1994). A Life cycle inventory of baby diapers subject to Canadian condition

Water quality management division, Pollution control Department PCD,2005. Industry and residential wastewater factor Water quality management division.

Identifying and locating trees of framework species using photography from an unmanned aerial vehicle (UAV)

Krishna Bahadur Rai[1] and Stephen Elliott[2]

[1]Masters Degree Program in Environmental Science, Environmental Science Research Center (ESRC), Faculty of Science, Chiang Mai University, Chiang Mai, 50200, Thailand

[2]Forest Restoration Research Unit (FORRU), Biology Department, Faculty of Science, Chiang Mai University, Chiang Mai, 50200, Thailand

Corresponding author email: kr7320@gmail.com

ABSTRACT

The need to locate and identify potential seed trees has become crucial, if we are to meet ambitious global reforestation targets of UN New York Declaration on Forests, 2014, which aims to restore forest in 350 million ha of degraded land by the year 2030. The possibility of viewing trees from above, using remote sensing platforms and imaging technologies such as hyperspectral imagery and LiDAR, are being investigated. However, such technologies are very expensive and not readily accessible. In contrast, Unmanned Aerial Vehicle (UAV's), with high-resolution cameras, have become a lot more affordable in recent years. Therefore, the research presented here determined if an off-the-shelf UAV could be used to easily identify 9 target tree species in dense regenerating forest at Ban Mae Sa Mai (BMSM), Doi Suthep-Pui National Park, Northern Thailand. Digital aerial photographs were used to develop dichotomous and tree species identification keys, based on crown and leaf characteristics and image filtering. The keys were then tested for reliability in another similarly aged validation plot, using

independent volunteer observers. Identification accuracy exceeded 50% for seven of nine target species and over 70% for four of these species. The approach developed in this research will make the process to locate trees of framework tree species more efficient, especially for seed collection which is essential in forest restoration projects.

Keywords: Tree species identification keys, Dichotomous keys, Digital aerial photographs from UAV

INTRODUCTION

In most countries, tree seed collection from remnant forest remains essential for forest restoration projects, but current methods of seed collection are primitive, inefficient, unpredictable and expensive. The possibility of approaching trees from above, using remote sensing platforms, is therefore an attractive alternative (Sutton, 2001). Remote sensing techniques, particularly hyperspectral and high-resolution satellite imaging offer potential alternatives for mapping species distributions (Pouliot *et al.*, 2002; Leckie *et al.*, 2003; Gergel *et al.*, 2007). However, only few studies have successfully used satellite images to map tree species distributions in tropical forests (Clark *et al.*, 2005; Asner *et al.*, 2008). Even when hyperspectral and high-resolution satellite images are used, it is difficult to identify tree species (Read *et al.*, 2003; Clark *et al.*, 2004) and such techniques are very expensive. A potential simple and inexpensive alternative is high resolution digital aerial photographs (Vooren & Offermans, 1985; Herwitz *et al.*, 2000; Trichon & Julien, 2006; Gonzalez-Orozco *et al.*, 2010; Morgan *et al.*, 2010). Studies on the potential use of aerial photographs for tropical tree identification started in the early 1970's. Sayn-Wittgenstein *et al.* (1978) found that species could be

identified with a reasonable degree of success in Surinam. Subsequently, Myers (1982a) explored means of describing upper canopy tree crowns in Northern Queensland rain forests in Australia. Since the 1990's, significant advances in aerial photo survey techniques have been made through use of aerial photographs (Brandtberg & Walter, 1998; Culvernor, 2002; Fenshman *et al.*, 2002; Chubey *et al.*, 2006). Trichon (2001) drew up a list of 12 Guianese trees, likely to be identifiable using aerial photographs. Each tree SGS (Species or Group of species) was described using criteria adapted from similar past studies by Sayn-Wittgenstien *et al.* (1978) and Myers(1982a). Trichon & Julien (2006) tested the accuracy of Trichon's (2001) method and found an overall identification success of 87% in French Guiana. Gonzalez-Orozco *et al.* (2010) in Ecuador identified tree species at overall identification accuracy of 50% to 70%. Garzon-Lopez *et al.* (2012) evaluated the potential to use canopy tree crown maps, derived from high resolution aerial digital photographs to measure large-scale tree distributions at Barro Colorado Island, Panama. Most researchers in the past used photographs taken from customized cameras, mounted on hot-air airships, helicopters and small planes (Trichon *et al.*, 2006; Morgan *et al.* 2010; Dandois *et al.*, 2013). However, with recent technological advances now allow the use of lightweight unmanned aerial vehicles, flying close to forest canopies, as an alternative to more costly satellite or airborne based imaging systems (Koh & Wich, 2012; Anderson & Gaston, 2013; Getzin *et al.*, 2012). Several studies have demonstrated that high-resolution imagery acquired from UAV can be used to map of invasive species (Michez *et al.*, 2016), to monitor tropical forest recovery (Zahawi *et al.*, 2015) and biodiversity (Paneque-Gálvez *et al.*, 2014), to identify tree species for analysis of the state of vegetation for implementation of community based conservation and restoration in the area (Baena *et al.*, 2017; Onishi &

Ise, 2018). Therefore, objectives of this study were to develop taxonomic keys to identify trees of framework species from digital aerial photographs based on crown morphology (type, shape, texture), leaf characteristics (shape, arrangement), phenology (leaf fall/flush, flowering, fruiting, etc.), image filtering (hue, saturation, brightness) using Image-J and then, to test the reliability and efficacy of keys to locate tree species in another similarly aged validation plot.

METHODOLOGY

Study area

The study area was located at Ban Mae Sa Mai (BMSM) (18°51′29.38″N 98°50′53.60″E), Doi Suthep-Pui National park in Northern Thailand (1,360 m above sea level), which is about 30 km away from Chiang Mai city. The research was carried out in two restored forest plots namely; 98.2 (Training plot) and 98.3 (Validation plot) each with a total area of 0.64 ha. The forest in both of these plots had been restored by Forest Restoration Research Unit, Chiang Mai University (FORRU-CMU), in collaboration with local communities using the framework species method (Goosem & Tucker, 1995) in the year 1998. The framework species method of forest restoration was developed by Goosem & Tucker (1995) in Australia. The framework species method is the least intensive of the tree planting options, as it exploits natural seed dispersal mechanisms to bring about biodiversity recovery. It involves planting the fewest trees necessary to shade out weeds (i.e. site "re-capture") and attract seed-dispersing animals. The framework tree species have characteristics of high survival rate, rapid growth, dense crowns to shade out herbaceous weeds, high resilience to wild fires, flowering and fruiting at young age to attract seed-dispersing wildlife.

Mapping and ground truthing of selected species

Digital aerial photographs were obtained over the training plot (98.2) using a DJI Phantom 4 Pro at an altitude of 100 m above ground in June 2018. The aerial photographs were taken at 50-70 % overlap, which was adjusted manually while photographs were taken. All visible crowns on digital photographs were marked and numbered using a freehand marker in the Preview App (MacOS). Ground truthing was then carried out, to locate and match tree crowns at ground with those in the images. The tree species were identified by locating identification tags attached to the trees by a previous FORRU-CMU study. For trees without such tags, leaf voucher specimens were collected and compared with named specimens in the Chiang Mai University (CMU), Herbarium. Nine (9) framework tree species (*Artocarpus gomezianus, Castanopsis calathiformis, Castanopsis tribuloides, Choerospondias axillaris, Ficus altissima, Magnolia garrettii, Pinus kesiya, Prunus cerasoides* and *Toona ciliata*) were selected for the study. A total of 48 tree crowns of nine tree species were identified and used to develop keys in the training plot.

Digital aerial photographs

Aerial digital photographs were acquired from DJI Phantom 4 Pro digital camera at an altitude of 50 meters above ground, over all individual target tree species, once every month for eight months (June 2018 to January 2019). In order to maintain uniformity of the quality of photographs for all months, the ISO camera setting for DJI Phantom Pro 4 was set to automatic. In automatic settings, the ISO range (100-3200), Mechanical shutter speed (8-1/2000s) and Electronic shutter speed (8-1/8000s). The GPS coordinates of all the target trees were recorded on the ground with a handheld GPS receiver and then used to program flight plans in the LITCHI application. Photography along the fixed flight plans was repeated monthly from June 2018 to January 2019, using the DJI Phantom 4 Pro,

flown 50 m above the ground using the Litchi flight planning software. The resolution of the photographs was 5472 x 3078 pixels.

Development of dichotomous and monthly tree species identification keys

The digital aerial photographs were analyzed to develop dichotomous and monthly tree species identification keys based on crown and leaf characteristics, phenology and image filtering (Image J). Koelmeyer (1959), Trichon and Julien (2006) & Gonzalez-Orozco's (2010) crown criteria were modified and adapted to match the crown types of the tree species selected for this study. Seven crown properties were used to develop dichotomous keys. Image filtering keys, based on quantifiable filtering of image hue, saturation and brightness (HSB) were developed. Since, the UAV was flown close to the tree crowns (<30 m) and was equipped with a high-resolution camera, leaf characteristics, hitherto unobservable from conventional remote sensing platforms, could be recorded. Accordingly, leaf properties and descriptors were modified and adapted from Gardner *et al*. (2007). Four most distinctive leaf properties were used to develop the leaf key.

Validation of keys

Validation of keys was carried out by adapting and modifying the methods of Trichon & Julien (2006) and Gonzalez-Orozco *et al.* (2010). Eleven (11) volunteer 'photo-interpreters' participated in validation process. Image J software and a folder consisting of one target crown key and two unidentified photographs for each species were preinstalled in the computers used for the validation process. The photographs for seven months (July 2018 to January 2019) were used for validation activity. The folder provided to each photo-interpreter comprised of photographs of nine species and all seven months, which was randomly mixed. Crowns of all the target tree species in each unidentified photograph were

counted prior to validation. In order to identify tree species, photo-interpreters were directed to open the unidentified photographs in Microsoft Paint software. The photo-interpreters then drew a circle around each tree they recognized as one of the 9 target species, using paint brush and then save it in same folder. All folders were collected and then results were analyzed using data analysis adapted from Gonzalez-Orozco et. al. (2010)

RESULTS & DISCUSSION

Tree species with identification accuracy of 100%

Pinus kesiya was the most correctly identified, at 100% identification accuracy and no errors of omission and commission (Fig. 1). The high identification accuracy for *Pinus kesiya* was because it had the most distinctive and largest crowns, compared to the other species. The whorls of needle leaves were very easily to be distinguished from the broad leaves of all the other species. Similar results were reported by Gonzalez-Orozco *et al.* (2010) and Garzon-Lopez *et al.* (2012) for palms trees, which looked very distinct compared to other tree families.

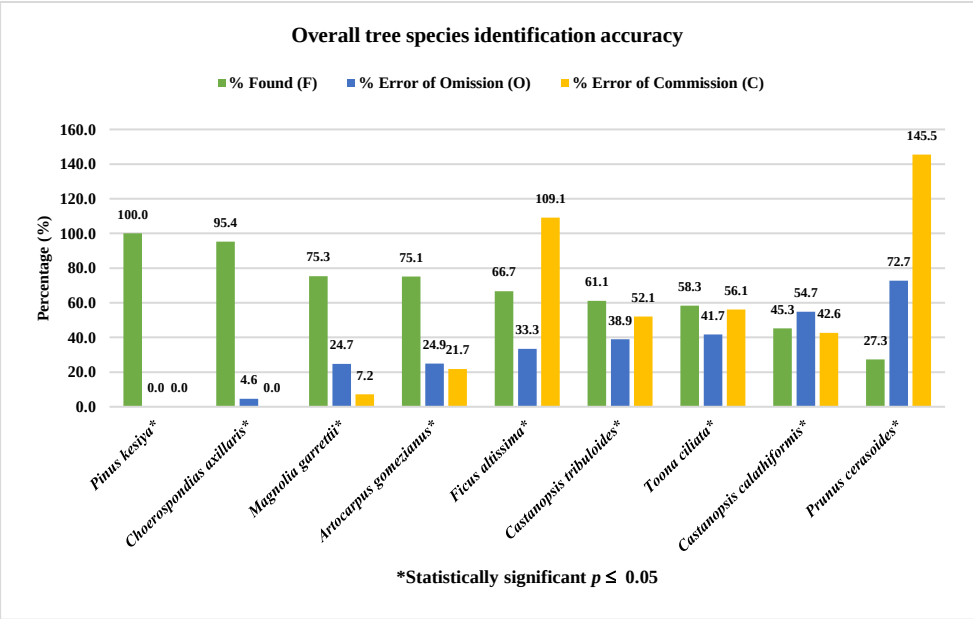

Fig. 1 Overall tree species identification accuracy

*Chi-square test was carried out for tree species and identification accuracy data where; it was found that, the identification accuracy was significant to tree species.

Tree species with identification accuracy of 75% to 95%

Choerospondias axillaris was identified with an accuracy of 95%. The error of omission was only 5% with no error of commission (Fig. 1). *Magnolia garrettii* and *Artocarpus gomezianus* were both identified with an accuracy of 75% and error of omission was at 25%. The % error of ommission for *Magnolia garrettii* was 7% and 22% for *Artocarpus gomezianus* (Fig. 1). *Choerospondias axillaris*, *Magnolia garrettii* and *Artocarpus gomezianus* had high identification accuracy because they were the most abundant species in the research plots. Similar results were also reported by Gonzalez-Orozco *et al.* (2010) and Garzon-Lopez *et al.* (2012) in their studies. *Magnolia garrettii* and *Artocarpus gomezianus* had larger leaves than those of other species, which might also have

contributed to higher identification accuracy for these species (Fig.1).

Tree species with identification accuracy of 50% to 70%

Ficus altissima was identified with an accuracy of 67%, followed by *Castanopsis tribuloides* and *Toona ciliata*. The highest error of commission was committed for *Ficus altissima* at 109% followed by *Toona ciliata* and *Castanopsis tribuloides*. The error of omission was highest for *Toona ciliata* at 42%, followed by *Castanopsis tribuloides* and *Ficus altissima* (Fig.1). A very high error of commission in case of *Toona ciliata* was because most of the photo-interpreters misidentified it to be *Choerospondias axillaris*, as it looked very similar on photographs due to similar leaf type and arrangement. One of the reasons for low identification accuracy of *Toona ciliata* was because it was less abundant species and similar findings were also reported by Gonzalez-Orozco *et al.* (2010) and Garzon-Lopez *et al.* (2012).

Tree species with identification accuracy of 50% and below

Castanopsis calathiformis was identified at an accuracy of 45% followed by *Prunus cerasoides* at 27%. The error of omission was at 73% for *Prunus cerasoides* and 55% for *Castanopsis calathiformis*. The error of commission was 146% for *Prunus cerasoides* and 43% for *Castanopsis calathiformis* (Fig. 1). One of the reasons for a very low identification accuracy and a very high % error of commission for *Prunus cerasoides* was because it was the rarest species in validation plot. In addition, most of photo- interpreters committed high % error of commission for *Castanopsis calathiformis* as *Castanopsis tribuloides*. One of the reasons for this was because both of these species had similar looking crowns and leaf characteristics.

Phenology and identification accuracy

It was found that, the identification accuracy was highest for tree species

at phenophases as presented in Table 1. Our results were consistent to findings of Trichon & Julien (2006) and Garzon-Lopez *et al.* (2012) where they also reported that, tree species were easier to be identified at particular phenophases when it was most visually striking.

Table 1 Phenophases and identification accuracy

SN	species	month/year	phenophase	identification accuracy (%)
1	*Castanopsis calathiformis*	July 2018	Flowering	100%
2	*Choerospondias axillaris*	January 2019	Leaf fall	100%
3	*Prunus cerasoides*	January 2019	Flowering	100%
4	*Toona ciliata*	August 2018	Leaf flushing	83%

Limitation and challenges

Our approach to identify tree species works well only for species with tall trees, as the identification keys were developed based on visible upper layer of crowns. In addition, our approach is more suited for identification of abundant species (Trichon *et al.*, 2006). Certain inconsistencies in quality of digital aerial photographs were observed, which might have some influence in identification accuracy. These inconsistencies might have been because of inherent flaws in DJI Phantom Pro 4 camera and LITCHI app. Weather, light conditions and light reflectance (Gonzalez-Orozco *et al.*, 2010) also contributed for such inconsistencies. Image geometric distortion (Gonzalez-Orozco *et al.*, 2010) made more difficult to identify the edge of the crowns, which affects the visual judgement of the crowns that are located at the edge of photographs. Topographic variation in landscape (Gonzalez-Orozco *et al.*, 2010) also complicated the aerial

identification of tree crowns. The shape of tree crowns varies between different species and within same species. The crown shapes also vary widely depending on strata and age of tree (Richards, 1996; Brunig, 1974). Photo-interpreter's familiarity (Gonzalez-Orozco *et al.*, 2010) with the keys and Image J software might also have contributed to errors in identification accuracy

CONCLUSION

The combined use of dichotomous and monthly tree species identification keys (crown, leaf and image J) developed using digital aerial photographs from unmanned aerial vehicle (UAV) makes our research original. In this research, we got an overall tree species identification accuracy of 67%, while error of omission was 33% and error of commission was 48%. The overall species-wise identification accuracy for seven of nine species exceeded 50% of which, for four species (*Pinus kesiya*, *Choerospondias axillaris*, *Magnolia garrettii*, *Artocarpus gomezianus*), it was above 70%. Our approach has great potential to be applied to look for trees of framework species especially for seed collection (Elliott *et al.*, 2003) and to monitor forest recovery in restoration projects (Trichon & Julien, 2006; Gonzalez-Orozco *et al.* 2010). In future, studies need to explore ways to link our keys to the automatic species identification approaches (Asner *et al.* 2007, 2008; Holmgren *et al.*, 2008; Lucas *et al.*, 2008; Baena *et al.*, 2017), object-oriented technologies (Gonzalez-Orozco *et al.*, 2010) and deep learning (Onishi & Ise, 2018).

ACKNOWLEDGEMENTS

I would like to acknowledge and thank the Royal Government of Bhutan (RGOB) and Thailand International Cooperation Agency (TICA) for awarding scholarship to purse post graduate studies at Chiang Mai University, Thailand.

In addition, I would also like to thank Forest Restoration Research Unit, Chiang Mai University (FORRU-CMU) for a small project research grant. I express my heartfelt gratitude to my thesis advisor Dr. Stephen Elliott, FORRU-CMU for his continued and relentless support during the course of my study. Special thanks to FORRU-CMU's staff for their kind support at the field and CMU Herbarium for their support. I also thank the University Studies Abroad Consortium (USAC), CMU students for assisting me to validate my thesis results.

REFERENCES

Anderson, K. & Gaston, K. 2013. Lightweight unmanned aerial vehicles will revolutionize spatial ecology. Frontiers in Ecology and the Environment. 11. 138-146. 10.2307/23470549.

Asner, G.P., Knapp, D.E., Kennedy-Bowdoin, Ty., Jones, M.O., Martin, R.E., Boardman, J. & Field, C.B. 2007. Carnegie airborne observatory: inflight fusion of hyperspectral imaging and waveform light detection and ranging (LiDAR) for three-dimensional studies of ecosystems. Journal of Applied Remote Sensing 1: 1–20.

Asner, G.P., Knapp, D.E., Kennedy-Bowdoin, Ty., Jones, M.O., Martin, R.E., Boardman, J. & Hughes, F. 2008. Invasive species detection in a Hawaiian rainforest using airborne imaging spectroscopy and LiDAR. Remote Sensing of Environment 112: 1942– 1955.

Baena, S., Moat J., Whaley O. & Boyd D.S. 2017. Identifying species from air: UAVs and the very high-resolution challenge for plant conservation. PLoS ONE 12(11): e0188714.

Brandtberg, T. & Walter, F. 1998. Automated delineation of individual tree crowns in high spatial resolution aerial images by multiple-scale analysis. Machine Vision and Applications 11: 64–73.

Brunig, E. F. (1974) Ecological studies in the kerangas forests of Sarawak and Brunei. Kuching, Malaysia: Borneo Literature Bureau for Sarawak Forest Department.

Chubey, M., Franklin, S.E. & Wulder, M.A. 2006. Object-based analysis

of Ikonos-2 imagery for extraction of forest inventory parameters. Photogrammetric Engineering of Remote Sensing 72: 383–394.

Clark, D.B., Read, J.M., Clark, M.L., Cruz, A.M., Dotti, M.F. & Clark, D.A., 2004. Application of 1-m and 4-m resolution satellite data to ecological studies of tropical rain forests. Ecol. Appl. 14, 61–74.

Clark, M., D. Roberts & D. Clark. 2005. Hyperspectral discrimination of tropical rain forest tree species at leaf to crown scales. remote sens. environ. 96: 375–398.

Culvernor, D.S. 2002. TIDA: an algorithm for the delineation of tree crowns in high spatial resolution remotely sensed imagery. Computers Geoscience 28: 33–44.

Dandois, J. & Ellis, E.C., 2013. High spatial resolution three-dimensional mapping of vegetation spectral dynamics using computer vision. Remote Sens. Environ. 136, 259.

Elliot, S., Blakesley, J. F. Maxwell, S. Doust, & S. Suwanarattana. 2003. Selecting Framework tree species for restoring seasonally dry tropical forests in northern Thailand based on field performance. Forest Ecology and Management 184; 177–191

Fenshman, R.J., Fairfax, R.J., Holman, J.E. & White-head, P.J. 2002. Quantitative assessment of vegetation structural attributes from aerial photographs. International Journal of Remote Sensing 2311: 2293–2311.

Gardner, S., Sidisunthorn P. & Anusarnsunthorn V., 2007, Field Guide to Forest Trees of Northern Thailand, Kobfai Publishing Project, Bangkok, ISBN 978-974-8367-29-3

Gergel, S. E., Y. Stange, N. C. Coops, K. Johansen & K. R. Kirby. 2007. What is the value of a good map? An example using high Spatial resolution imagery to aid riparian restoration. Ecosystems 10: 688–702.

Getzin, S., K. Weigand, I. & Schöning. 2012. Assessing biodiversity in forests using very high-resolution Images and unmanned aerial vehicles. Meth. Ecol. Evol. 3: 397–404.

Gonzalez-Orozco, C. E., M. Mulligan, V. Trichon & A. Jarvis. 2010. Taxonomic Identification of Amazonian tree crowns from aerial photography. Appl. Veg. Sci. 13: 510–519.

Goosem, S.P. & Tucker, N.I.J., 1995. Repairing the Rainforest—Theory

and Practice of rainforest Re-establishment in North Queensland's Wet Tropics. Wet Tropics Management Authority, Cairns. 80 pp.

Herwitz, S., Slye, R. & Turton, S., 1998. Redefining the ecological niche of a tropical rain forest canopy tree species using airborne imagery: long-term crown dynamics of Toona ciliata. J. Trop. Ecol. 14, 683–703.

Herwitz, S. R., R. E. Syle & S. M. Turton. 2000. Long-term survivorship and crown area dynamics of tropical rain forest canopy trees. Ecology 81: 585–597.

Holmgren, J., Persson, A. & Soderman, U. 2008. Species identification of individual trees by combining high resolution LiDAR data and multi-spectral images. International Journal of Remote Sensing 29: 1537–1552.

Leckie, D.G., Gougeon, F.A., Walsworth, D. & Paradine, D. 2003. Stand delineation and composition estimation using semi-automated individual tree crown analysis. Remote Sensing of Environment 85: 355–369.

Lucas, R.M., Bunting, P., Paterson, M. & Chisholm, L. 2008. Classification of Australian forest communities using aerial photography, CASI and HyMap data. Remote Sensing of Environment 112: 2088–2103.

Koelmeyer, K.O., 1959. The periodicity of leaf change and flowering in the principal forest communities of Ceylon. Ceylon for., 4:157-189.

Koh, L. & Wich, S. 2012. Dawn of drone ecology: low-cost autonomous aerial vehicles for conservation. Tropical Conservation Science. 5. 121-132. 10.5167/uzh-72781.

Morgan, J.L., S. E. Gergel & N. C. Coops. 2010. aerial photography: A rapidly evolving tool for Ecological Management. Bioscience 60: 47–59.

Michez, A., Piégay, H., Jonathan, L., Claessens, H. & Lejeune, P., 2016. Mapping of riparian invasive species with supervised classification of Unmanned Aerial System (UAS) imagery. Int. J. Appl. Earth Obs. Geoinf. 44, 88–94

Myers, B.J. & Benson, M.L., 1981. Rainforest species on large-scale colour photos. Photogramm. Eng. Remote Sensing 41, 505–513.

Myers, B.J., 1982. Guide to the identification of some tropical rainforest species from large-scale

color aerial photographs. Aust. Forester 45 (1), 28–41.

Myers, B.J. 1982a. Large-Scale color aerial photographs: a useful tool for tropical biologist. Biotropica 14: 156– 157.

Myers, B.J. 1982b. Guide to the identification of some tropical rain forest species from large-scale colour aerial photographs. Australian Forestry 45: 28–41.

Myers, N., Mittermeier, R.A., Mittermeier, C.G., da Fonseca, G.A.B. & Kent, J., 2000. Biodiversity hotspots for conservation priorities. Nature 403, 853– 858.

Onishi M. & Ise T., 2018, Automatic classification of trees using a UAV onboard camera and deep learning, arXiv preprint arXiv:1804.10390

Paneque-Gálvez, J., McCall, M.K., Napoletano, B.M., Wich, S.A. & Koh, L.P., 2014. Small drones for community-based forest monitoring: An assessment of their feasibility and potential in tropical areas. Forests 5 (6), 1481–1507.

Pouliot, D.A., King, D.J., Bell, F.W. & Pitt, D.G. 2002. Automated tree crown detection and delineation in high-resolution digital camera imagery of coniferous forest regeneration. Remote Sensing of Environment 82: 322–334.

Read, J.M., Clark, D.B., Venticinque, E.M. & Moreiras, M.P., 2003. Application of merged1-m and 4-m resolution satellite data to research and management in tropical forests. J. Appl. Ecol. 40, 592–600.

Richards, P.W., 1996. The tropical rain forest: An ecological study, second edition. Cambridge University Press, Cambridge, UK. xxiii + 575 pages. ISBN 0-521-42194-2.

Sayn-Wittgenstein, L., De Milde, R. & Inglis, C.J. 1978. Identification of tropical trees on aerial photographs FMR-X-113. Forest Management Institute, Canada.

Sayn-Wittgenstein, L. 1978. New developments in tropical forest inventories. Proceedings of the 12th International Symposium on Remote Sensing of Environment. pp. 1187–98. Ottawa, Ontario, CA.

Sutton, S.L., 2001. Alice grows up: canopy science in transition from Wonder-land to Reality. Plant Ecol. 153, 13–21.

Trichon, V., 2001. Crown typology and the identification of rain forest trees on large-scale aerial

photographs. Plant Ecol. 153, 301–312.

Trichon, V. & Julien, M.P. 2006. Tree species identification on large-scale aerial photographs in a tropical rain forest, French Guiana-application for management and conservation. Forest Ecology and Management 225: 51–61.

Vooren, A.P. & Offermans, D.M.J., 1985. An ultra-light aircraft for low-cost, large-scale stereoscopic aerial photographs. Biotropica 17 (1), 84–88.

Zahawi, R.A., Dandois, J.P., Holl, K.D., Nadwodny, D., Reid, J.L. & Ellis, E.C., 2015. Using lightweight unmanned aerial vehicles to monitor tropical forest recovery. Biol. Conserv. 186, 287–295.

Relationship between topographic wetness index and soil thickness in Nam Hia creek catchment, Phetchabun, Thailand

Rugkiet Chansorn[1], Pawee Klongvessa[4], and Srilert Chotpantarat[1,2,3*]

[1*]Department of Geology, Faculty of Science, Chulalongkorn University, Bangkok, Thailand.

[2] Research Program on Controls of Hazardous Contaminants in Raw Water Resources for Water Scarcity Resilience, Center of Excellence on Hazardous Substance Management (HSM), Chulalongkorn University, Bangkok, Thailand.

[3]Research Unit Control of Emerging Micropollutants in Environment, Chulalongkorn University, Bangkok, Thailand.

[4]Department of Environmental Technology and Management, Faculty of Environment, Kasetsart University, Bangkok, Thailand.

Corresponding author e-mail: csrilert@gmail.com or Srilert.C@Chula.ac.th

ABSTRACT

Soil thickness is an important data to evaluate an occurrence probability of landslide. However, the soil thickness can be observed directly at only few points in the area which are not enough for soil thickness mapping. With this reason, a comparison between the topographic wetness index (TWI) and sampled soil thickness is an interesting method for the mapping. This study aimed to determine the relationship between TWI and soil thickness in the Nam Hia creek catchment. First, the value of the TWI was generated from digital elevation model (DEM). Then, the TWI was compared with observed soil thickness at each sampling point. Finally, a linear relationship between TWI and soil thickness was generated. The results show that the soil thickness (meters) in the area can be estimated as 0.1 of TWI. It varies between 0 and 1.66 m with the lower value on the ridge and higher value in the valley. The relationship found in this study is similar to those in Taiwan which were found in previous studies. The similar climate between Thailand and Taiwan which lead to similar erosion and weathering rates are the possible reason to describe these similar relationships.

Keywords: Topographic wetness index, Soil thickness, Landslide, Nam Hia creek catchment

INTRODUCTION

Landslide is a natural disaster that causes a lot of damages and casualties. Information for evaluation of the landslide occurrence is important for the warning and finding an appropriate mitigation. The information includes slope, soil thickness, physical characteristics of soils and rocks, flooding, heavy rainfall, earthquake, and etc. (Highland and Bobrowsky, 2008). The soil thickness, which this study focused on, affects an occurrence probability of landslide because the thicker soil has more movable mass which leads to more driving force than the thinner soil. The soil over the high slope area often collapses when it is saturated with water (Akiyama et al., 2009). One of problems in gathering the soil thickness data is that direct observations at many points requires time and expense due to the characteristics of the area which cause difficulty in getting access. With this reason, the estimation of the soil thickness at the unobserved points by the topographic wetness index (TWI), a steady state wetness index that generated by the topography, also known as the compound topographic index (CTI), is an interesting method for the soil thickness mapping.

The TWI is used in the hydrological process but would inferior in the vast flat area. The linear relationship between TWI and soil thickness have been found in Lee et al. (2009) and Ho et al (2011). Lee et al. (2009) studied the occurrence of landslide in Taiwan by the hydrological models (Lee et al., 2009) while Ho et al. (2011) studied the occurrence of shallow landslide.

This study aimed to determine the relationship between TWI and soil thickness in the Nam Hia creek catchment, a small catchment in Phetchabun province, Thailand. The location of the study area is shown in figure 1. There have

been a lot of landslides in this area (Tatong, 2008).

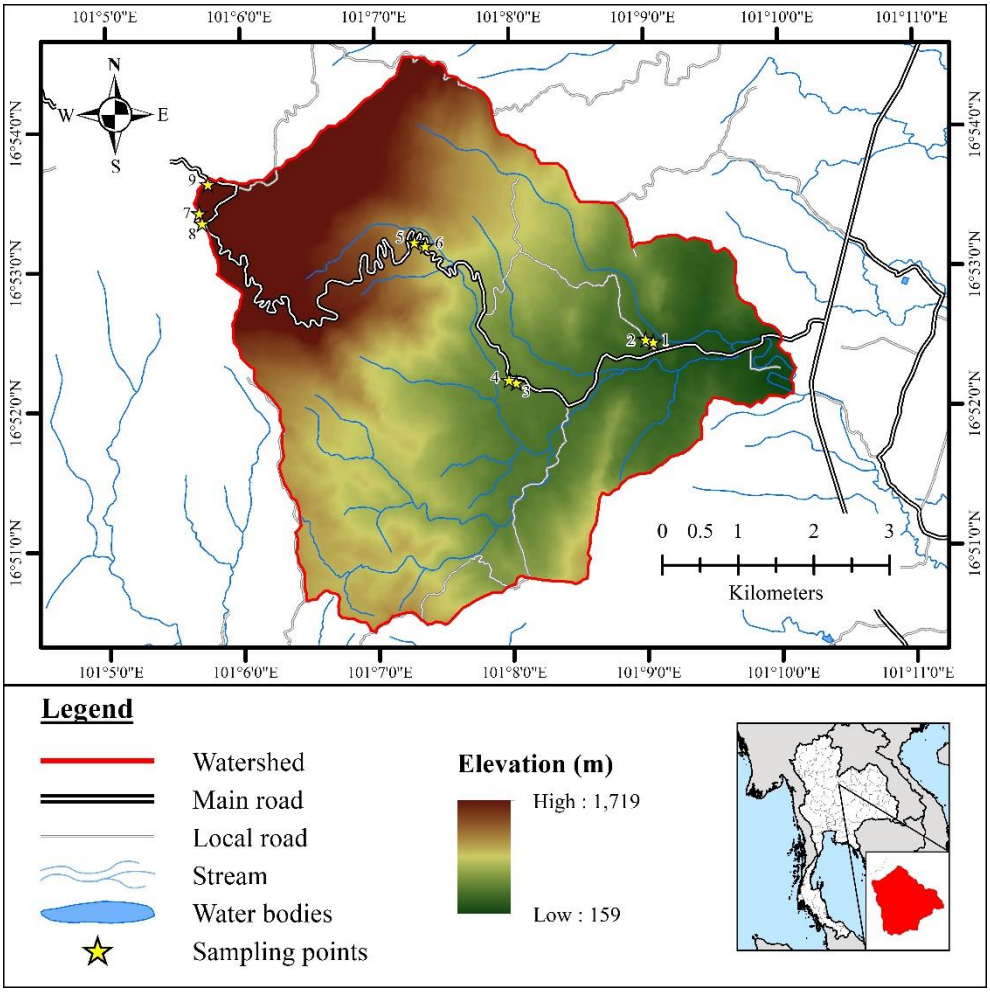

Figure 1 Location of the sampling points in Nam Hia creek catchment.

METHODOLOGY

Generating the topographic wetness index

The TWI was generated form the slope of the terrain by equation 1.

$$\mathrm{TWI} = \ln\left(\frac{\alpha}{\tan\beta}\right) \quad (1)$$

where α is the contributing area per unit contour length and β is the local slope in radian (Sørensen et al., 2006). The data used to calculate TWI was the digital elevation model (DEM) provided by The National Aeronautics and Space

Administration (NASA) with the resolution of 12.5 m.

Comparison between the topographic wetness index and observed soil thickness

After the value of the TWI was generated, the observed soil thicknesses collected in February 2019 at 9 points where outcrops are found in the study area (see figure 1) were plotted against the TWI associated with their locations. The area near the valley has a large value of soil thickness (> 1 m) and it is difficult to reach the base rock from the surface. Therefore, the data used in this study was only that measured in the ridge area.

Finally, the linear relationship between the value of the TWI and observed soil thickness was determined and the soil thickness map was generated from that relationship.

RESULTS AND DISCUSSION

Topographic wetness index of the study area

The TWI map of the study area is shown in figure 2. The value of the TWI is higher near the valley and lower near the ridge. The maximum value is 16.56 and the minimum value is 0. These values are consistent with those in the previous studies (Lee et al., 2009; Ho et al., 2011). In addition, the finding of Sørensen et al. (2006) that the higher soil moisture is associated with the higher value of TWI in the valley and the lower moisture is associated with the lower value of TWI on the ridge also support our generated TWI.

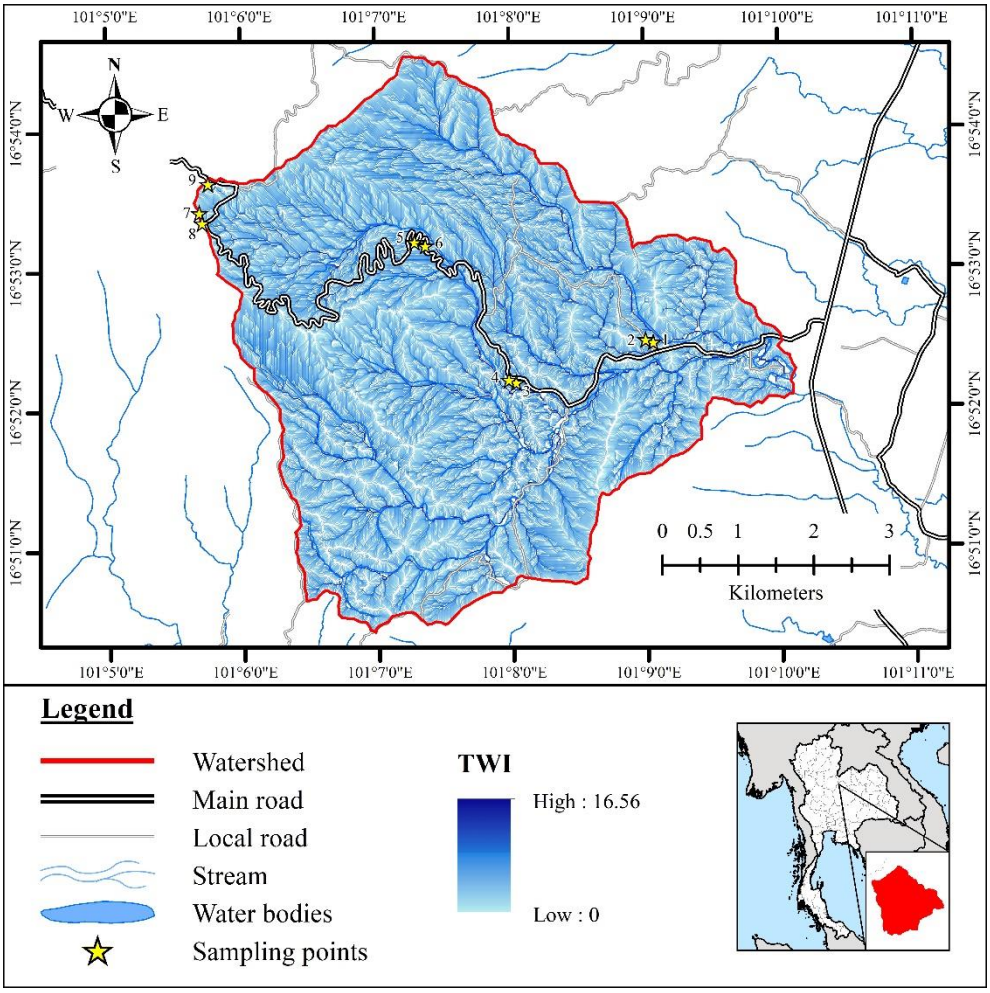

Figure 2 Topographic wetness index map of Nam Hia creek catchment.

Linear relationship between the topographic wetness index and observed soil thickness

The data collected from field study is showed in table 1 which includes geographic coordinates, value of the TWI, and observed soil thickness, and the linear relationship between TWI and the observed soil thickness is showed in figure 3. The soil thickness (m) can be estimated as 0.1 of TWI. The value of R^2 which is 0.34 suggests that the fitting is not very good. It is because of too small sample size. However, the relationship found in this study is similar to those in the previous studies in Taiwan (Lee et al., 2009; Ho et al., 2011). The similar climate between Thailand and Taiwan, which

leads to similar erosion and reason to describe these similar weathering rates, is the possible relationships.

Table 1 TWI and observed soil thickness in Nam Hia creek catchment.

Sampling point	Longitude	Latitude	TWI	Soil thickness (m)
1	101° 09' 03.2" E	16° 52' 28.1" N	4.05	0.30
2	101° 08' 59.8" E	16° 52' 29.2" N	1.61	0.25
3	101° 08' 01.9" E	16° 52' 11.2" N	2.87	0.30
4	101° 07' 58.6" E	16° 52' 12.4" N	2.9	0.30
5	101° 07' 17.1" E	16° 53' 12.0" N	2.63	0.25
6	101° 07' 21.9" E	16° 53' 10.4" N	2.15	0.25
7	101° 05' 41.2" E	16° 53' 25.3" N	1.83	0.20
8	101° 05' 42.4" E	16° 53' 21.0" N	1.16	0.20
9	101° 05' 45.2" E	16° 53' 37.8" N	3.66	0.50

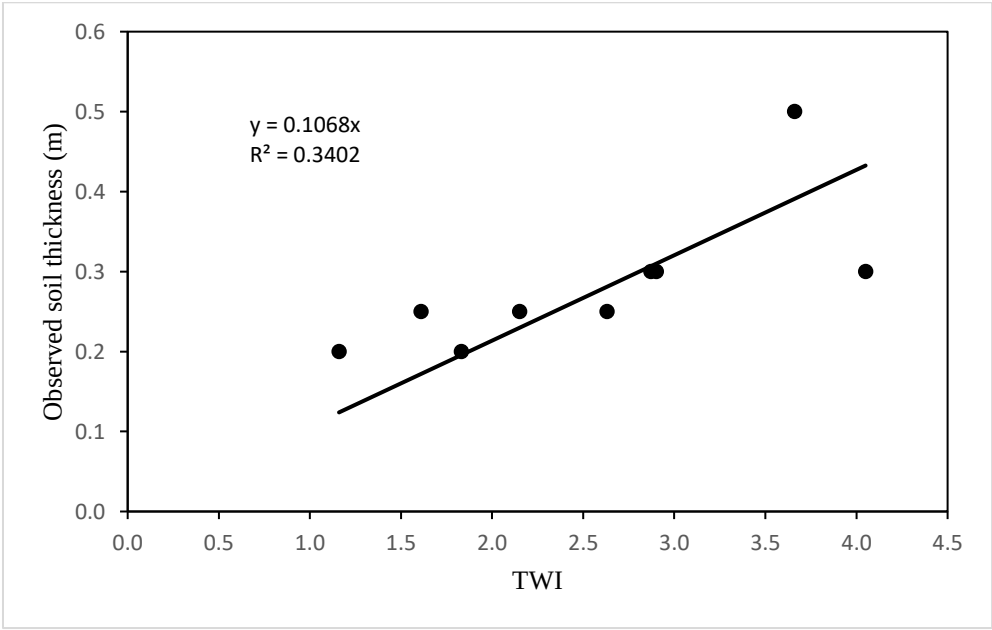

Figure 3 Linear relationship between TWI and soil thickness in Nam Hia creek catchment.

Soil thickness map in Nam Hia creek catchment

The soil thickness data generated by the TWI map and linear relationship between TWI and soil thickness is shown in figure 4. The soil thickness is higher in the valley with the maximum value of 1.66 m and is lower on the ridge with the minimum value of 0 m. The thicker soil in the valley and thinner soil on the ridge are caused by the movement of the eroded sediment from the ridge to the valley by gravity (Romeo et al., 2015).

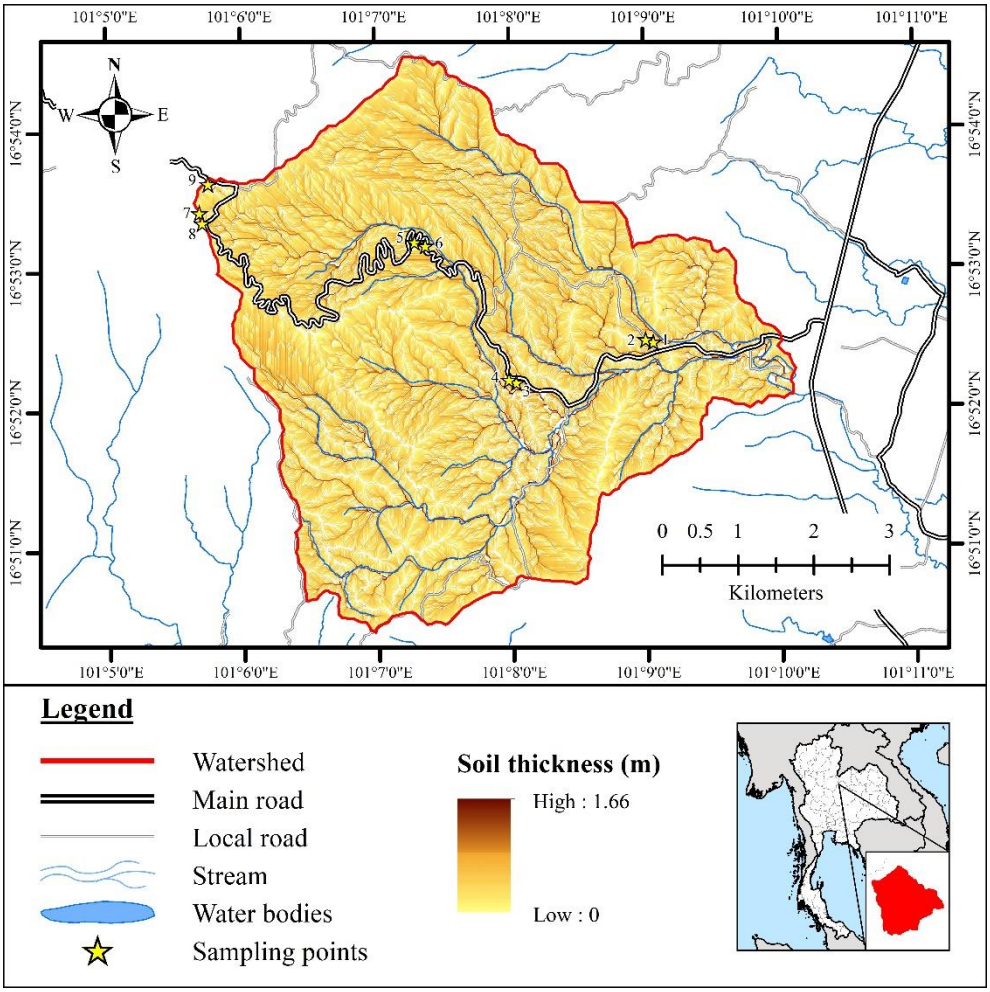

Figure 4 Soil thickness map of Nam Hia creek catchment.

CONCLUSIONS

Soil thickness is an important data to evaluate the occurrence probability of landslides. However, it is difficult to get the soil thickness data at many points. With this reason, the relationship between the value of TWI and observed soil thickness has been used to calculate soil thickness at unobserved points and generate a soil thickness map.

This study determined the linear relationship between TWI and soil thickness and generate the soil thickness map in the Nam Hia creek catchment, Thailand. The results of this study show that the soil thickness is higher in the valley with the maximum value of 1.66 m and is lower on the ridge with the minimum value of 0 m.

However, the linear relationship used to fit the TWI and soil thickness is of the low R^2 because the number of observed soil thickness data used in this study was too small and the resolution of TWI map was too low. The low resolution caused large grid size which led to several thicknesses in each grid. Gathering more soil thickness data and generating the TWI map with higher resolution can lead to more reliable results.

ACKNOWLEDGEMENTS

This research was funded by the Ratchadaphisek Sompoch Endowment Fund (2019), Chulalongkorn University (762003-CC). The authors are also thankful for assistance in the field studies from Mr. Apiwat Intiyakoset.

REFERENCES

Akiyama K., Uchida T., Mori N., Tamura K., and Yamakoshi T. The role of soil thickness on shallow landslide initiation. Geophysical Research Abstracts 2009; 11: EGU2009-7905.

Highland L. and Bobrowsky P. The landslide handbook-a guide to understanding landslides: a landmark publication for landslide education and preparedness. U.S. Geological Survey 2008: 129 p.

Ho J.-Y., Lee K.T., Chang T.-C., Wang Z.-Y., and Liao Y.-H. Influences of

spatial distribution of soil thickness on shallow landslide prediction. Engineering Geology 2011; 124: 38-46.

Lee K.T., and Ho J.-Y. Prediction of landslide occurrence based on slope-instability analysis and hydrological model simulation. Journal of Hydrology 2009; 375: 489-497.

Romeo R., Vita A., Manuelli S., Zanini E., Freppaz M., and Stanchi S. Understanding Mountain Soils: A contribution from mountain areas to the International Year of Soils 2015. Food and Agriculture Organization of the United Nations 2015: 158 p.

Sørensen R., Zinko U., and Seibert J. On the calculation of the topographic wetness index: evaluation of different methods based on field observations. Hydrology and Earth System Sciences 2006; 10: 101-112.

Tatong T. Study of landslides and floods for surveillance and warning. Thailand Department of Mineral Resources 2008: 45 p. (in Thai)

Soil and water quality assessments for agricultural uses in Nang Lae sub-district, Mueang district, Chiang Rai province

Krittawit Suk-ueng[1], Kittichai Chantima[1], and Tippawan Prasertsin[2 *]

[1]Energy and Environment Program, Faculty of Science and Technology, Chiang Rai Rajabhat University, Chiang Rai, Thailand
[2*]Biological Science Program, Faculty of Science and Technology, Chiang Rai Rajabhat University, Chiang Rai, Thailand; Corresponding author: e-mail: tippawan_pra@hotmail.com

ABSTRACT

Assessments of soil and water quality are valuable for agricultural production, which were used for appropriate decision making regarding sustainable agricultural land uses. Therefore, this study was conducted to assess soil and water quality of different agricultural land use in Nang Lae sub-district, Mueang district, Chiang Rai province. Nine soil samples were collected from 3 land use types of agricultural area (paddy field crop, field crop and orchard). The water quality based on certain physico-chemical parameters was also determined at 10 sampling sites located along the watercourse of this area. Results of this study revealed that the soil sample of different agricultural land use was slightly acid to moderately acid (pH 5.93-6.93). Organic matter content of these soils was relative low (0.13-2.07%). These soils had relative low total nitrogen (1,200-2,800 mg/Kg). The available phosphorus and potassium were also very low to low ranged from 1.86-5.94 mg/Kg and 0-78.00 mg/Kg, respectively. These soils have low soil fertility status which possesses physical and chemical properties unsuitable for crop cultivation. Moreover, in this study we found that soil samples from paddy fields and orchard fields were contaminated with high arsenic content (4.50-6.32

mg/Kg), which was higher than the standard of National Environment Board of Thailand. In addition, the assessment of water quality based on the trophic status indicated that water bodies were classified as oligo-mesotrophic to mesotrophic status. The water was also classified as class II-III that can be used for consumption but general killing of microorganisms was required and also can be used for fisheries and agricultural.

Keywords: Soil quality, Water quality, Nang Lae sub-district, Assessment, Land use

INTRODUCTION

Soil and water quality are two of the three components of environmental quality, besides air quality. Water quality is defined by their degree of pollution that impacts directly on ecosystems. Meanwhile, soil quality is commonly defined more broadly as the capacity of a soil to function within ecosystem and land use boundaries to maintain environmental quality and promote plant and animal health (Bünemann et al., 2018). Many researchers have suggested that soil quality is simply related to the quantity of crops produced. Dynamic soil quality is the result of human use and management on soil function (Seybold et al., 1998). As Rosa and Sobral (2008) state the results of exploiting land use systems without consideration of the consequences on soil quality have been environmental degradation. Agricultural use and management systems have been generally adopted without recognizing consequences on soil conservation and environmental quality, and therefore decline in agricultural soil quality. Furthermore, the land used classification system does not provide an interpretation of the agricultural suitability of land for the production of specific crops or the potential productivity of those crops (Road and Bay, 2016). Likewise, unsuitable land use and improper application of chemicals and soil management in agriculture also have

affected the water quality. Therefore, the assessments of soil and water quality are valuable for agricultural production, which were used for appropriate decision making regarding sustainable agricultural land uses.

Nang Lae is the one of sub-district of Mueang Chiang Rai district, Chiang Rai province, Thailand which is the main agricultural area of Mueang Chiang Rai district. In 2014, it had a total population 10,312 people and has 16 villages (Nang Lae Municipality, 2014). Nang Lae sub-district is located in the lower part of Kok river basin which is the catchment area of many small rivers supplying the water that supports the livelihood of the people in this area. Nang Lae sub-district covers an area of 5,500 ha of Mueang Chiang Rai district and has agricultural area of 1,814.4 ha (Department of Mineral Resources, 2013). Land use of Nang Lae sub-district comprises mainly rice production (806.88 ha), orchard (330.4 ha) and field crop (677.12 ha) (Nang Lae Municipality, 2014). This area is considered as study site due to source of important economic plants, especially field crop i.e., Phulae and Nanglae pineapple. Phulae and Nanglae pineapple (*Ananas comosus* L. Merr) are important geographical indications of Chiang Rai Province. Phulae pineapple refers to the queen pineapple variety (Kongsuwan et al., 2009). Recently, both pineapple cultivars are becoming popular not only for local consumption, but also for export market. Therefore, the aim of this study was to assess and evaluate soil and water quality of different agricultural land use in Nang Lae sub-district, Mueang district, Chiang Rai province.

METHODOLOGY

Study area

The study was conducted in Nang Lae sub-district, Mueang district, Chiang Rai province, which is located from latitude 19°53'40" N to 20°07'10"N and longitude 99°45'51"E to 99°57'24"E. The elevation is 415-580 m above sea level, with a territory of approximately 55 km^2. The annual

precipitation and temperature in the region add up to approximately 1,7 6 4 . 7 mm and 24.4°C, respectively. This area is an important source of economic plants in Chiang Rai, i.e., rice and pineapple, which is the main agricultural area of Mueang Chiang Rai district.

Soil sampling and analysis

Soil samples were taken from 9 stations located inside agricultural area of Nang Lae sub-district, which were collected on October 2018 from 3 land use types of agricultural area, including paddy field crop, field crop and orchard). The sampling stations and geographical positions were recorded and shown in Table 1. At each sampling station, soil sample was composed by mixing 15 sub-samples which were collected at 0-15 cm depth. The soil samples were gently mixed, and the visible roots, plant residues and stones were removed. Method of drilling and collecting soil samples were performed according to Land Development Department protocols (Land Development Department, 2010).

All sample was air-dried, and then prepared to be analyzed for six soil indicators, which were measured per sample using the corresponding standard laboratory analytical methods. Soil pH was determined using 1:1 soil to water ratio and then analyzed by digital pH meter (Peech, 1965). Soil organic matter was measured using the Walkley-Black method (Walkley and Black, 1947). Total nitrogen was determined by the Kjeldahl method, and the available potassium was analyzed by flame photometer after extraction using 1 M ammonium acetate at pH 7 (Jackson, 1958), and the available phosphorus was extraction using Bray II (Bray and Kurtz, 1945). Furthermore, the inductively coupled plasma mass spectrometry (ICP-MS) was used to determine the content of arsenic in soil samples. For the assessment of soil fertility for crop production was evaluated using some parameter, including soil organic matter, available potassium and phosphorus described by Division of Soil

Resources Survey and Research (1980) and Kheoruenromne (2005).

Table 1 List of soil sampling station and their detail of land use type.

Code	Land use type	Coordinate	Remark
A1-1	Paddy field crop	20.011803N, 99.857939E	Paddy field
A1-2	Paddy field crop	20.026511N, 99.845574E	Paddy field
A1-3	Paddy field crop	20.024949N, 99.879477E	Paddy field
A2-1	Field crop	20.005423N, 99.859588E	Pineapple field crop
A2-2	Field crop	20.024709N, 99.879500E	Pineapple field crop
A2-3	Field crop	19.985269N, 99.894693E	Pineapple field crop
A4-1	Orchard	20.034340N, 99.836674E	Lychee orchard
A4-2	Orchard	20.027942N, 99.863820E	Longan orchard
A4-3	Orchard	20.015516 N, 99.889455E	Mixed orchard

Water sampling and analysis

The water quality based on certain physical and chemical parameters was also determined at 10 sampling stations located along the watercourse of agricultural area on October 2018. The details of sampling station were shown in Table 2. The water temperature (Temp), conductivity (Con), total dissolved solid (TDS) and pH were directly measured at each sampling station using the multi-probe water quality meters (EUTECH CyberScan PCD650), and dissolved oxygen (DO) was measured using the azide modification method (Greenberg et al., 2005). Water samples were then collected at a depth of 30 cm from the surface of each sampling station using polyethylene bottles. The water samples were kept at 5-7°C in a cool box until their analyses in the laboratory of biochemical oxygen demand (BOD), nitrate nitrogen (NO_3^-), ammonium nitrogen (NH_4^+), soluble reactive phosphorus (PO_4^{3-}) and turbidity (Tur). The analyses were done using the azide modification method for BOD, and NO_3^-, NH_4^+ and PO_4^{3-}, was assessed using the cadmium reduction method, nesslerization method and ascorbic method, respectively according to the protocol of Greenberg et al. (2005).

Water turbidity was measured using a turbidity meter.

The trophic status of the water was classified according to the Applied Algal Research Laboratory Physical and Chemical Score (AARL-PC Score) method described by Peerapornpisal et al. (2004), which were used the main parameters including conductivity, DO, BOD, NO_3^-, NH_4^+ and PO_4^{3-}. Moreover, the water quality was also classified according to surface water standard of Thailand (National Environmental Board, 1994).

Table 2 The detailed of water sampling station and geographical positions.

Code	Sampling station	Coordinates
B1-1	Nang Lae waterfall	20.0444432N, 99.8294290E
B2-1	Irrigation canal	20.0115103N, 99.8580770E
B2-2	Irrigation canal	20.0266894N, 99.8452859E
B2-3	Irrigation canal	20.0292123N, 99.8630951E
B2-4	Irrigation canal	20.0259961N, 99.8712095E
B2-5	Irrigation canal	19.9889680N, 99.9043860E
B2-6	Irrigation canal	19.9774710N, 99.8970022E
B3-1	Stream	20.0104029N, 99.8688977E
B4-1	Reservoir	20.0372004N, 99.8323751E
B4-2	Reservoir	19.9876658N, 99.9036350E

RESULTS AND DISCUSSION

Soil quality assessment

Soil samples gathered through borehole drilling from 9 sampling stations, and some physical and chemical properties and arsenic content were analyzed according to standard methods followed by assessment of the soil fertility status. The analysis results of soil sample from different agricultural land use were presented in Table 3. These soils were slightly acid to moderately acid (pH 5.33-6.93). Soil pH is essential for agricultural production which is the one of the most important soil parameters. Most agricultural crops develop best in soil with a pH from 5.5 to 6.5 (Havlin et al., 1999). The soil pH recorded in

most sampling stations during the study appears therefore to be favorable to crop production. Organic matter content of all these soils was relative low (0 . 1 3 -2.07%) corresponding to the standard of Division of Soil Resources Survey and Research (1980) and Kheoruenromne (2005). The organic matter content was noted that sampling station A2-2 (pineapple field crop) displaying very lower value (0.13%) when compared to other stations. Soil organic matter is one of the key attributes of soil quality that is vital to many of these soil functions. Thus, the conservation agricultural systems often lead to high surface soil organic matter, and therefore, high soil quality. According to Franzluebbers (2008) who suggested that more intensive cropping increases the quantity of residues produced, which can lead to higher soil organic matter. Furthermore, perennial pastures often reduce water runoff volume and soil loss even further than with conservation-tillage cropland due to greater accumulation of surface soil organic matter (Franzluebbers and Stuedemann, 2002; 2008).

Total nitrogen is the main nutrient used for vegetation growth and is also used as a key soil quality assessment (Ren et al., 2014). The total nitrogen amount in these soils varies from 1,200 mg/Kg to 2,800 mg/Kg, with the quality of total nitrogen in agricultural land to low level group according to the standard of Division of Soil Resources Survey and Research (1980), which is suggested for Thailand soil. The available phosphorus and potassium contents are also vital soil properties that considerably affected due to in change of vegetation cover, total biomass production, microbial decomposition of organic residues and nutrient cycling (Turrion et al., 2000; Solomon et al., 2002; Kheoruenromne, 2005). The available phosphorus of soils in this study was found that low to low ranged from 1.86-15.94 mg/Kg. Interestingly, most of these soil samples were not found the available potassium, particularly the soil sample from pineapple field crop

(A2-1, A2-2, A2-3), paddy fields (A1-1, A1-2), and Longan orchard (A4-2), while A1-3 (paddy field), A4-1 (lychee orchard) and A4-3 (mixed orchard) were found the available potassium of these soils in the low ranges (55.00-78.00 mg/Kg). For the assessment of soil fertility for crop production was evaluated using some parameter described by Division of Soil Resources Survey and Research (1980) and Kheoruenromne (2005). The results show that these soils have low soil fertility status which possesses physical and chemical properties unsuitable for crop productions. Therefore, agricultural uses of soils in this area need careful selection of production options and must implement combined application of organic and chemical fertilizers along with nutrient management. However, proper soil and water conservation management practices are also needed to maintain healthy environment for land use sustainability.

In addition, in this study we found that soil samples were contaminated with high arsenic (As) content in paddy fields and orchard fields. Evidently, soil existed with the higher As at paddy fields (A1-1, A1-2) and orchard fields (A4-1, A4-2) with a range from 4.56-5.17 mg/Kg and 4.50-6.32 mg/Kg, respectively, which were higher than the maximum concentration level of soils used for living and agriculture specified by the office of the National Environment Board of Thailand as 3.90 mg/kg of soil for agriculture (National Environment Board, 1992). Arsenic is one of the most toxic substances found in the environment. Arsenic contamination in soils indicated the potential risk to human health. Exposure to sufficiently high concentrations of As in the natural environment has proven to be harmful to human health and the ecosystem (Tiankaoa and Chotpantarat, 2018). Consequently, this hotspot should be intensively paid attention for preventing and remediation measures

Table 3 Nutrient status and arsenic content of the soil and fertility level of the study soils.

Parameter	Sampling station								
	A1-1	**A1-2**	**A1-3**	**A2-1**	**A2-2**	**A2-3**	**A4-1**	**A4-2**	**A4-3**
pH	6.70	6.90	6.77	6.00	5.33	6.03	6.93	6.90	6.70
TN (mg/Kg)	1,500	1,700	2,400	1,200	1,800	2,600	1,700	2,800	2,400
OM (%)	1.32	1.11	1.96	1.66	0.13	1.58	1.32	1.04	2.07
OM Score	1	1	1	1	1	1	1	1	1
Avail. P (mg/Kg)	11.11	6.81	14.57	12.62	3.52	4.19	10.36	15.94	1.86
Avail. P Score	2	1	2	2	1	1	2	2	1
Avail. K (mg/Kg)	0.00	0.00	55.00	0.00	0.00	0.00	78.00	0.00	54.00
Avail. K Score	1	1	1	1	1	1	2	1	1
Total Scores	**4**	**3**	**4**	**4**	**3**	**3**	**5**	**4**	**3**
Fertility level	**Low**	**Low**	**Low**	**Low**	**Low**	**Low**	**Low**	**Low**	**Low**

Note: TN = total nitrogen, OM = organic matter, Avail. P = available phosphorus, Avail. K = available potassium. Fertility status of the soil was used to numbers in the table scores. Total is 7 or less is considered low soil fertility. Total score 8-12 is considered soil fertility is medium. Total score is 13 or more is considered high soil fertility.

Water quality assessment

There was variation in the recorded physico-chemical parameters of water among the sampling stations. The details of the physico-chemical parameters of the water quality in agricultural area of Nang Lae sub-district are shown in Table 4. There was a variation in water temperature across sampling stations, with values ranging from 24.2°C to 30.4°C. The TDS varied widely in different sampling station, range from 0.72 mg/L to 4.52 mg/L, and the water turbidity was also showed varied widely (4.85-56.4 NTU). The overall conductivity was found to be between 19.7-113.7 μS/cm with the highest value at irrigation canal (B2-2), which all sampling stations were normal for general water resources, meaning that the water was livable for living organisms and suitable for human consumption as it did not exceed the quality standard (<300 μS/cm) of surface water (National

Environmental Board, 1994). The value of DO was between 1.91 and 8.00 mg/L. Oxygen was one of the most important factors for water quality and the associated aquatic life. The oxygen content of natural waters varies with temperature, salinity, turbulence, the photosynthetic activity of algae and plant and atmospheric pressure. The solubility of oxygen was decrease when the temperature and salinity were increase. The results of some sampling stations showed that did not exceed the standard of surface water (National Environmental Board, 1994). The BOD was an approximate measure of the amount of biochemically degradable organic matter present in water sample. It was defined by the amount of oxygen required for the aerobic micro-organisms in the sample to oxidize the organic matter to a stable inorganic form. The ranges of BOD in this study was varied from 0.68-3.90 mg/L, which were classified to class II-III of water quality that can be used for consumption but general killing of microorganisms was required and also can be used for fisheries and agricultural (Pollution Control Department, 2019). The ranges of NO_3^- at each sampling station varied from 0.1–1.1 mg/L with the highest value at irrigation canal (B2-4) and reservoir (B4-2) which all station showed that not exceed the values of Thailand's prescribed surface water quality standards (<5 mg/L) (National Environmental Board, 1994). The NH_4^+ ranging from 0.14-0.47 mg/L which all station also not exceed the values of Thailand's prescribed surface water quality standards (<0.5 mg/L) (National Environmental Board, 1994). While, the PO_4^{3-} values were noted that sampling station B4-1 (reservoir) displaying higher values when compared to other stations.

Table 4 The physical and chemical parameters of water in each sampling station.

Parameter	Sampling station									
	B1-1	**B2-1**	**B2-2**	**B2-3**	**B2-4**	**B2-5**	**B2-6**	**B3-1**	**B4-1**	**B4-2**
Temp (°C)	24.2	24.4	28.1	25.9	26.1	26.6	27.6	25.2	27.4	30.4
pH	6.6	6.4	6.7	6.7	6.6	5.3	6.5	6.9	6.9	6.6
TDS (mg/L)	2.24	2.04	4.52	2.25	2.03	0.88	3.66	2.83	2.69	0.72
Tur (NTU)	4.92	56.4	41.2	45.6	40.0	4.85	41.3	24.3	6.07	15.2
Con (µS/cm)*	57.20	53.60	113.70	57.70	53.10	20.80	94.50	72.60	66.70	19.70
DO (mg/L) *	8.00	6.50	4.60	5.64	6.08	1.91	3.19	7.63	4.37	5.20
BOD (mg/L) *	1.00	0.85	3.90	1.34	0.68	0.71	3.20	1.83	1.37	3.70
NO_3^- (mg/L) *	1.10	0.20	0.10	0.70	1.10	0.70	0.70	0.70	0.40	1.10
NH_4^+ (mg/L) *	0.27	0.47	0.41	0.40	0.29	0.14	0.37	0.18	0.21	0.19
PO_4^{3-} (mg/L) *	1.11	0.81	0.52	0.96	0.27	0.27	0.66	0.74	2.31	0.17
AARL-PC Score	2.8	2.5	2.7	2.6	2.5	2.0	2.8	2.7	3.3	2.7
Trophic status	M	M	M	M	M	OM	M	M	M	M

Note: * = Parameters used to evaluate the trophic status of water; M = Mesotrophic; OM = Oligo-mesotrophic

The trophic status of the water was evaluated from the main parameters, which were: conductivity, DO, BOD, NH_4^+, NO_3^- and PO_4^{3-} by the AARL-PC Score method (Peerapornpisal et al., 2004). The results indicated that water bodies were classified as oligo-mesotrophic to mesotrophic status. Most of the sampling stations were found to be mesotrophic status. This is due to the fact that different activities were taking place along the water bodies. The sampling stations with oligo-mesotrophic status were surrounded by deciduous forests, so there was less contamination in the water bodies, whereas most sampling stations with mesotrophic status were contaminated by the waste from communities, fish ponds, and agricultural activities. Furthermore, the water quality was also classified as class II-III according to surface freshwater standard of Thailand (National Environmental Board, 1994). The water can be used for consumption

but general killing of microorganisms was required and also can be used for fisheries and agricultural.

CONCLUSIONS

The findings of this study revealed that soil fertility status in all land use types of Nang Lae sub-district belong to the level low which possesses physical and chemical properties unsuitable for crop productions. Furthermore, contamination of arsenic in soils higher than the maximum concentration level of soils used for living and agriculture, which were found in paddy fields and orchard fields. Further studies of As distribution and transportation phenomena are of very interesting in this area. Meanwhile, the assessment of water quality indicated that water bodies were classified as oligo-mesotrophic to mesotrophic status, and also classified as class II-III that can be used for consumption but general killing of microorganisms was required and also can be used for fisheries and agricultural.

ACKNOWLEDGEMENTS

The author gratefully acknowledges the financial support by Chiang Rai Rajabhat University through the Research and Development Institute (Grand no. ABC020, ABC021, ABC022), and field work supported by Biological Science Program and Energy and Environment Program, Faculty of Science and Technology, Chiang Rai Rajabhat University. The author also highly appreciates the cooperation of the farmers during the field works.

REFERENCES

Bray RH, Kurtz LT. Determination of total, organic and available forms of phosphorus in soils. Soil Science 1945; 59: 39-45.

Bünemann EK, Bongiorno G, Bai Z, Creamer RE, Deyn GD, Goede RD, et al. Soil quality-A critical review. Soil Biology and Biochemistry 2018; 120: 105-125.

Department of Mineral Resources. Land slide database project of Nang Lae

Dub-district, Mueang Chiang Rai District, Chiang Rai Province. 2013. Department of mineral resources, Ministry of Natural Resources and Environment, Bangkok, Thailand. (In Thai).

Division of Soil Resources Survey and Research. Soil suitability classification guide for economic crops. 1980. Land Development Department, Ministry of Agriculture and Cooperatives. Bangkok, Thailand. (In Thai)

Franzluebbers AJ. Linking soil and water quality in conservation agricultural systems. Electronic Journal of Integrative Biosciences 2008; 6(1): 15-29.

Franzluebbers AJ, Stuedemann J.A. Particulate and non-particulate fractions of soil organic carbon under pastures in the Southern Piedmont USA. Environmental Pollution 2002; 116: S53-S62.

Franzluebbers AJ, Stuedemann JA. Soil-profile organic carbon and total nitrogen during 12 years of pasture management in the Southern Piedmont USA. Agriculture, Ecosystem and Environment 2008; (doi:10.1016/j.agee.2008.06.013).

Greenberg AE, Clescerri LS, Eaton AD. Standard Methods for the Examination of Water and Wastewater. American Public Health Association (APHA) 2005. Washington DC, USA.

Havlin JL, Beaton JD, Tisdale SL, Nelson WL. Soil fertility and fertilizers: An introduction to nutrient management. 1999. USA: Prentice-Hall Inc.

Jackson ML. Soil chemical analysis. 1958. Prentice-Hall Inc., Englewood Cliffs, New Jersey, USA.

Kheoruenromne I. Soil survey (2nd ed.). 2005. Kasetsart University, Bangkok, Thailand.

Kongsuwanm A, Suthiluk P, Theppakorn T, Srilaong V, Setha S. Bioactive compounds and antioxidant capacities of Phulae and Nanglae pineapple. Asian Journal of Food and Agro-Industry 2009; Special Issue: S44-S50.

Land Development Department. Guide book for soil chemical analysis. 2010. Land Development Department, Ministry of Agriculture and Cooperatives. Bangkok, Thailand. (In Thai)

Nang Lae Municipality. The three years development plan of Nang Lae Municipality (2014-2016). 2014. Nang Lae Municipality, Chiang Rai, Thailand. (In Thai)

Notification of the National Environmental Board No.8, B.E.2537 (1994), Issued Under The Enhancement And Conservation Of National Environmental Quality Act

B.E.2535 (1992): The Surface Water Standard.

Peech M. Soil pH by glass electrode pH meter. Methods of Soil Analysis. American Society of Agronomy 1965; 60: 914-925.

Peerapornpisal Y, Chaiubol C, Kraibut H, Chorum M, Wannathong P, Ngernpat N, et al. The monitoring of water quality in Ang Kaew reservior of Chiang Mai University by using phytoplankton as bioindicator from 1995-2002. Chiang Mai Journal of Science 2004; 31: 85-94.

Pollution Control Department. 2019. Surface water quality standard of Thailand. Retrieved from http://www.wepa-db.net/policies/law/thailand/std_surface_water.htm. Notification of the National Environmental Board, No. 8, B.E. 2537 (1994), issued under the Enhancement and Conservation of National Environmental Quality Act B.E.2535 (1992) , published in the Royal Government Gazette, Vol. 111, Part 16, dated February 24, B.E.2537 (1994).

Ren T, Wang J, Chen Q, Zhang F, Lu S. The effects of manure and nitrogen fertilizer applications on soil organic carbon and nitrogen in a high-input cropping system. PLoS One 2014; 9(5).

Road HC, Bay G. Soil and agricultural capability and suitability assessment district lots 7045, 7046 and 8653, Columbia Shuswap District. 2016. VAST Resource Solutions Inc. Cranbrook, British Columbia.

Rosa DDL, Sobral R. Soil quality and methods for its assessment. In: Land use and soil resources. Ademola K, Braimoh PL, Vlek G. (eds). 2008. Springer, Dordrecht, Netherlands, 167-200.

Seybold C, Mausbach M, Karlen D, Rogers H. Quantification of soil quality, In: Soil processes and the carbon cycle, Lal R. (ed). 1998. Boca Raton, FL: CRC Press, pp. 387-404.

Solomon D, Fritzsche F, Tekalign M, Lehmann J, Zech W. Soil organic matter dynamics in the subhumid Ethiopian highlands: Evidence from natural 13C abundance and particle-size fractionation. Soil Science Society of America Journal 2002; 66: 969-978.

Tiankaoa W, Chotpantarat S. Risk assessment of arsenic from contaminated soils to shallow groundwater in Ong Phra Sub-District, Suphan Buri Province, Thailand. Journal of Hydrology: Regional Studies 2018; 19: 80-96.

Turrion MB, Glaser B, Solomon D, Ni A, Zech W. Effects of deforestation on phosphorus pools in mountain soils of the Allay range, Khyrgyzia. Biology and Fertility of Soils 2000; 31: 134-142.

Walkley A, Black IA. Chromic acid titration method for determination of soil organic matter. Soil Science Society of America Proceedings 1947; 63: 257.

Potential alternative to conventional fungicides to control fungal phytopathogen by biosurfactant-producing *Bacillus licheniformis* F2.2

Sirita Siammai, Jiraporn Thaniyavarn, Panan Rerngsamran*

Department of Microbiology, Faculty of Science, Chulalongkorn University, Bangkok, Thailand *Corresponding author: panan.r@chula.ac.th

ABSTRACT

Successive usage of chemical fungicides to control fungal phytopathogen has several drawbacks. Thus, the search for a potential alternative method is still needed. One of the possible methods is to use antagonistic bacteria that are able to produce biosurfactant. *Bacillus licheniformis* F2.2 was previously isolated from fermented food in Thailand. In this work, the ability of this strain to inhibit the growth of fungal phytopathogen, as well as its ability to produce biosurfactant were determined. The results revealed that *B. licheniformis* F2.2 had broad spectrum against fungi consisting of *Acremonium furcatum*, *Colletotrichum gloeosporioides*, *Fusarium moniliforme*, *Fusarium proliferatum*, *Fusarium solani*, *Pyricularia oryzae*, and *Phytophthora palmivora* which are the causal agents of diseases in several economic plants. The percentage of inhibition were ranging from 34.79-44.51%. Based on techniques such as drop collapse, oil displacement, emulsification and hemolytic tests, indicated that *B. licheniformis* F2.2 was capable of producing biosurfactant. It was found that both antifungal activity and emulsification index of the culture filtrate from *B. licheniformis* F2.2 were maintained at a wide range of temperature and pH. These results revealed that *B. licheniformis* F2.2 have potential to be used as biocontrol agent to control phytopathogen alternative to the usage of conventional chemical fungicides.

Keywords: *Bacillus licheniformis*, Biosurfactant, Antifungal compound, Biological control

INTRODUCTION

Over thousands years, plant disease has been a major factor affect to food production (He et al., 2016). One of the most important causal agents for plant disease is fungi, which cause serious damage and decrease the quality to agricultural products (Bach et al., 2016; Mihalache et al., 2018). The control of the diseases is mainly based on chemical treatments. However, the widespread use of chemicals causes harmful effects on the environment, and nontarget organisms, as well as the issues of health risks (Jeong et al., 2017; Zouari et al., 2016). Attention was concerned to find alternative methods, which are eco-friendly, for controlling of plant diseases (Zhao et al, 2016; Zheng et al., 2013). Several biological controls have been developed in recent years to manage plant diseases. These included the use of antagonistic microorganisms that is safe to human health and ecosystem, and sustainable (Jiang et al., 2017; Leelasuphakul et al., 2008). Among antagonistic microorganisms that commonly used as plant biological control, bacterial antagonists have much received attention because of their ability to control different types of plant pathogens through a various modes of action, and the possibility to combined use with other control methods (Vitullo et al., 2012).

Bacillus species are widely distributed in soils, could produce spores that are resistant to various physical and chemical treatments. It is known that they are considered safe for the environment, with ability to colonize the plant, thereby eliminating pathogen infection and stimulating for plant protection (Torres et al., 2016; Wang et al.,

2014), and have interesting property of producing variety of secondary metabolites and very diverse structures (Tao et al., 2011), for example, biosurfactants, antibiotics, lipopeptides, cell wall-degrading enzymes, and volatile compounds (Leelasuphakul et al., 2008). Several strains of *Bacillus* have received much attention as biocontrol agents (Dimkić et al., 2013), and widely used for agricultural biocontrol, industrial enzyme production, and antibiotic production (Torres et al., 2016). Gond et al. (2015) reported that *Bacillus subtilis* SG JW.03 isolated from Indian popcorn showed strong inhibition of *Fusarium moniliforme*. Jeong et al. (2017) reported that *Bacillus licheniformis* MH48 from rhizosphere soil demonstrated strong antifungal activity against various fungi including *Rhizoctonia solani*, *Colletotrichum gloeosporioides*, and *Phytophthora capsici*. Yánez-Mendizábal et al. (2012) showed that *B. subtilis* CPA-8 cell-free supernatant had strong ability to control *Monilinia laxa* and *Monilinia fructicola* in peaches. Subsequently, biosurfactants including fengycin, iturin and surfactin lipopeptides were identified as major factors that effect in the antifungal activity. Several reports described that both temperature and pH stability could influence the metabolite production by *Bacillus* spp. that subsequently affect the biological control of plant pathogen. For example, Zhang et al. (2017) reported that bioactive substances in culture filtrate of *B. subtilis* Z-14 was stable against *Gaeumannomyces graminis* var. *tritici (Gg*t) after heated at 100°C for 30 min, and at pH ranging from 3 to 8, the antifungal activity remained almost unchanged (>95%).

It was found from previous study that *Bacillus licheniformis* F2.2 isolated from fermented food in Thailand could produce biosurfactants (Thaniyavarn, et al., 2003). However, the biosurfactant from this bacterium has not been explored in the aspect of

plant biological control. Therefore, in this study, the ability to produce biosurfactant was reconfirmed using several techniques including drop collapse test, oil displacement test, emulsion test, and hemolytic activity test (Cooper and Goldenberg, 1987; Mouafi et al., 2016; Sarwar et al., 2018). In addition, effect of physical factors on antifungal activity of biosurfactant such as temperature and pH were investigated. The cells of, or the biosurfactants obtained from, *B. licheniformis* F2.2 will be a potential alternative to conventional fungicides to control fungal phytopathogen for sustained agriculture.

METHODOLOGY

Antifungal activity test

Fungal phytopathogen used in this research were obtained from the culture collection of Department of Microbiology, Faculty of Science, Chulalongkorn University. For dual culture test, agar plugs of *Acremonium furcatum*, *Colletotrichum gloeosporioides*, *Fusarium moniliforme*, *Fusarium proliferatum*, *Fusarium solani*, and *Pyricularia oryzae* were placed on potato dextrose agar (PDA), whereas the plugs of *Phytophthora palmivora* were placed on V8 agar medium; then *B. licheniformis* F2.2 was inoculated on the plates approximately 2 cm from the fungal plugs. The plates were incubated at 30°C for 3-5 days at which the percentage of inhibition was measured comparing to control plate contained the corresponding fungus using the formula of Nielsen et al. (1998) as followed:

$$\% \text{ inhibition} = [1-(\frac{E}{C})]\times 100$$

E = the average diameter of the treatment

C = the average diameter of the control plate

Ability to produce biosurfactant

B. licheniformis F2.2 was cultured in Luria-Bertani (LB) at 200 rpm 37°C for 18 h, after that the culture was

centrifuged at 8,000 rpm for 10 min. The supernatant was collected and passed through 0.45 μm filter to obtained cell-free supernatant. Biosurfactant in the supernatant was determined by several methods as followed.

Drop collapse test

Twenty microliters of xylene oil were drop into each circle on the lid of 96 wells plate and left for 1 h at room temperature for the oil to cover the circle area. Five microliters of bacterial supernatant were drop onto each area that covered with xylene oil. Sodium dodecyl sulfate (SDS) (10 mg/ml) and broth medium were used as positive and negative controls, respectively. The collapse of supernatant indicated the present of biosurfactant in the culture supernatant.

Oil displacement test

Ten milliliters of deionized water were placed into a Petri dish (60x15 mm). Five microliters of crude oil were slowly drop at the center of the plate over the water surface at which the oil was spread to cover the surface of water. Five microliters of bacterial supernatant were slowly drop to the center of crude oil film. SDS (10 mg/ml) and broth medium were used as positive and negative controls, respectively. The displacement of oil film was the indication of the present of biosurfactant.

Emulsion test

Four hundred microliters of xylene oil were placed in a clear SepCap glass vial (8x40 mm). Then, 400 μl of bacterial supernatant were added and mixed for 2 min using vortex mixer. The vial was stand at room temperature for 24 h for phase separation. Emulsification index at 24 h (E_{24}) was calculated according to the formula of Cooper et al. (1987) as followed:

$$E_{24} = \frac{\text{Height of emulsion phase}}{\text{Total height of the liquid}} \times 100$$

Hemolytic activity test

B. licheniformis F2.2 was inoculated on blood agar (5% v/v). The plate was incubated at 30°C for 24 h. Clear zone around the bacterial colony represented hemolytic activity of red blood cells due to the presence of biosurfactant.

Effect of physical factors on antifungal activity of biosurfactant

Temperature

The culture filtrate was separately exposed to various temperatures (20°C, 37°C, 60°C, 80°C, 100°C and 121°C) for 15 min. When temperature was equal to room temperature, the antifungal activity by mixing the culture filtrate with melted broth medium, and emulsion tests were evaluated.

Acidity and alkalinity

The culture filtrate was separately adjusted to pH 6, 8, 10, and 12 for 30 min at 37°C. After readjusted back to pH 8, the antifungal activity and emulsion tests were performed.

For all experiments, three individual tests were repeated. The mean values and standard derivation values were determined.

RESULTS AND DISCUSSION

Antifungal activity by B. licheniformis F2.2

Antifungal activity against several phytopathogenic fungi by *B. licheniformis* F2.2 is shown in figure 1. The result revealed that *B. licheniformis* F2.2 had broad spectrum over seven fungal plant pathogens tested with 34.79-44.51 % inhibition.

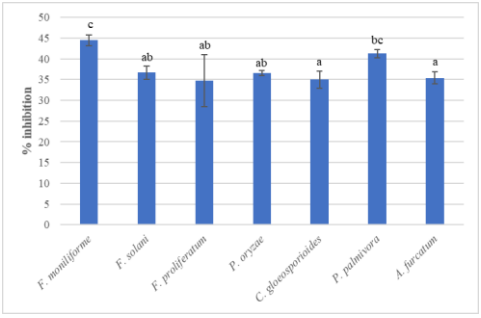

Figure 1 Percentage of inhibition by *B. licheniformis* F2.2 against fungal phytopathogen

Ability to produce biosurfactant by B. licheniformis F2.2

Drop collapse test

As seen in figure 2, the collapse of the culture filtrate drops on the surface of microtiter plate's lid covered with xylene oil were observed compared to the negative control (broth medium).

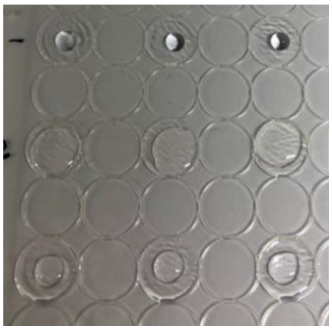

Figure 2 Drop collapse test of broth medium (negative control), 10 mg/ml SDS (positive control), and culture filtrate of *B. licheniformis* F2.2

Oil displacement test

The displacement of crude oil film by culture filtrate of *B. licheniformis* F2.2 was observed as shown in figure 3 compared to the negative control (broth medium).

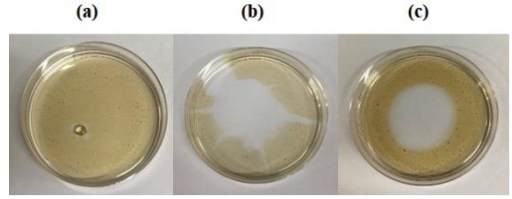

Figure 3 Oil displacement test (a) negative control (broth medium), (b) positive control (10 mg/ml SDS), and (c) culture filtrate from *B. licheniformis* F2.2

Emulsification index (E_{24})

Emulsion (Fig. 4) obtained from *B. licheniformis* F2.2 culture filtrate was comparable to that from SDS. The E_{24} was 62.5% and 65.97%, respectively.

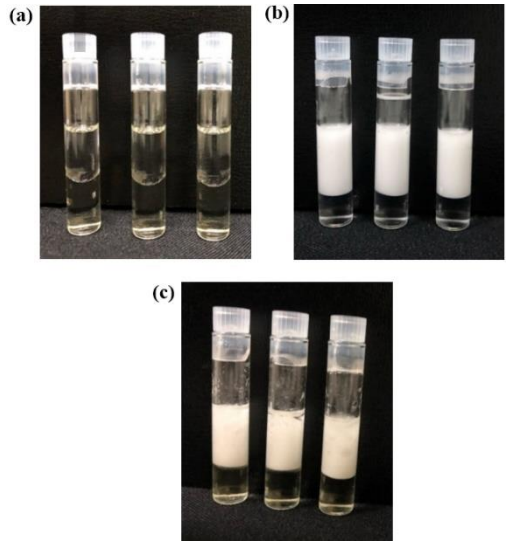

Figure 4 Emulsification of (a) negative control (broth medium), (b) positive control (10 mg/ml SDS), and (c) culture filtrate from *B. licheniformis* F2.2

Hemolytic activity test

By culturing *B. licheniformis* F2.2 on blood agar, clear zone around bacterial colony due to the lysis of red blood cells was observed as seen in figure 5.

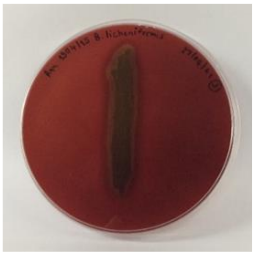

Figure 5 Ability to lyse red blood cell of *B. licheniformis* F2.2 on blood agar

Effects of physical factors on antifungal activity and emulsification index of B. licheniformis F2.2

Effect of temperature

The culture filtrate of *B. licheniformis* F2.2 containing biosurfactant with antifungal activity was incubated at various temperatures, and then left at room temperature before testing for antifungal activity and E_{24}. The results in figure 6a showed that the antifungal activity against all fungi tested still remained even treated at 121°C. The inhibition against *P. oryzae*, the causal agent of rice disease, was strongest, followed by *C. gloeosporioides*, the causal agent of anthracnose disease in several economic plants. The result in figure 6b also revealed that biosurfactant as determined using E_{24} index was significantly different ($P < 0.05$), and were stable at all temperature (20-121°C). The E_{24} still remained around 56.52-63.19% comparable to SDS positive control.

(a)

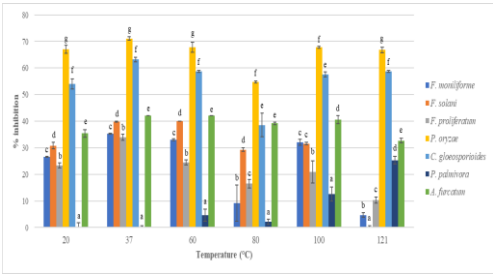

(b)

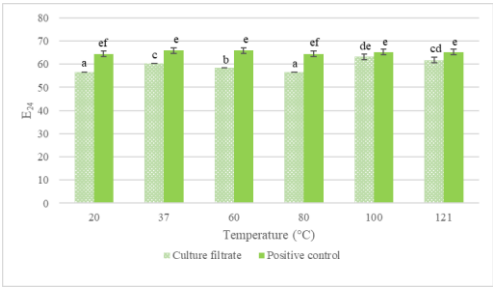

Figure 6 Effect of temperature on (a) antifungal activity and (b) Emulsification index (E) at 24 h (E_{24}) of *B. licheniformis* F2.2. Bars represent the standard deviations of three replicates; bars with different letters differ significantly according to the Duncan's test ($P < 0.05$).

Effect of pH

The results showed in figures 7a demonstrated that the antifungal activity was somewhat stable between pH 6-10, and slightly decrease at pH12. Interestingly, emulsification index were stable at all pH tested (pH 6-12).

(a)

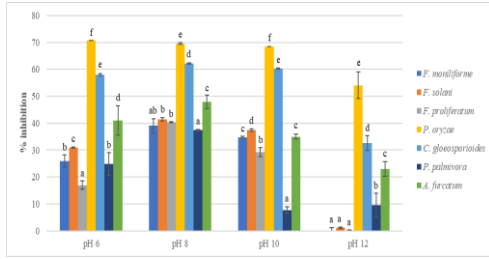

(b)

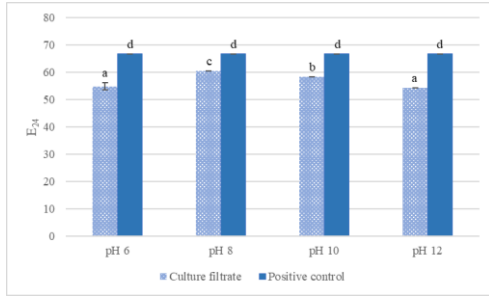

Figure 7 Effect of pH on (a) antifungal activity and (b) Emulsification index at 24 h (E_{24}) of *B. licheniformis* F2.2. Bars represent the standard deviations of three replicates; bars with different letters differ significantly according to the Duncan's test ($P < 0.05$).

CONCLUSIONS

In this study, drop collapse, oil displacement, emulsion tests, and

hemolytic activity could be used to verify the biosurfactants production by using only small volume of the sample. The results of all assays indicated that *B. licheniformis* F2.2 had ability to produced biosurfactant. Among these tests, emulsification assay was more qualitative method, since it refers to the amount of biosurfactant in sample supernatant which correlated with the E_{24} index. In this research, E_{24} from supernatant culture for 18 h of *B. licheniformis* F2.2 was 62.5%. El-Sheshtawy, et al. (2015) obtained E_{24} at 62% by supernatant from *B. licheniformis* that was cultured for 12 h. They also found that by increasing cultivation time to 72 h, the E_{24} was increased to 96%. Thus, in case of *B. licheniformis* F2.2, variation of cultivation time is worth to perform in order to obtain higher amount of biosurfactant. Effect of temperature and pH on antifungal substances in culture filtrate of *B. licheniformis* F2.2 indicated that antifungal activity could be maintained at a wide range of both temperature (20-121 °C) and pH (6-12). Nawaz, et al. (2018) reported that *B. licheniformis* OE-04 metabolites exhibited significant antagonistic activity against *Colletotrichum gossypii*, with stability at high temperature from 28°C to 100 °C and was stable at pH 5 to 9. These stability tests revealed that the antifungal substances and biosurfactants were not sensitive to high temperature, even after exposed to 121ºC for 15 min or at pH 10 for 30 min. The activity and stability of biosurfactant at extreme condition of temperature and pH were reported to be suitable for oil recovery enhancement (Sharma, et al., 2018), which may also be true for the agricultural application. Further studies such as production and purification of biosurfactant from *B. licheniformis* F2.2 will be performed. The antifungal activity of the purified biosurfactant will be analyzed. *B. licheniformis* F2.2 is a potent antagonistic bacterium that can be used to control fungal plant

pathogen alternative to the usage of conventional chemical fungicide.

ACKNOWLEDGEMENTS

The Scholarship from the Graduate School, Chulalongkorn University to commemorate the ๑๒ nd anniversary of his Majesty King Bhumibala Aduladeja is gratefully acknowledged.

REFERENCES

Bach, E., dos Santos Seger, G.D., de Carvalho Fernandes, G., Lisboa, B.B. and Passaglia, L.M.P. Evaluation of biological control and rhizosphere competence of plant growth promoting bacteria. Applied Soil Ecology 2016; 99:141-149.

Cooper, D.G. and Goldenberg, B.G. Surface-active agents from two *Bacillus* species. Applied and Environmental Microbiology 1987; 53(2):224-229.

Dimkić, I., Živković, S., Berić, T., Ivanović, Ž., Gavrilović, V., Stanković, S. and Fira, D. Characterization and evaluation of two *Bacillus* strains, SS-12.6 and SS-13.1, as potential agents for the control of phytopathogenic bacteria and fungi. Biological Control 2013; 65(3):312-321.

El-Sheshtawy, H.S., Aiad, I., Osman, M.E., Abo-ELnasr, A.A. and Kobisy, A.S. Production of biosurfactant from *Bacillus licheniformis* for microbial enhanced oil recovery and inhibition the growth of sulfate reducing bacteria. Egyptian Journal of Petroleum 2015; 24:155–162.

Gond, S.K., Bergen, M.S., Torres, M.S. and White, J.F., Jr. Endophytic *Bacillus* spp. produce antifungal lipopeptides and induce host defence gene expression in maize. Microbiological Research 2015; 172:79-87.

He, D.C., Zhan, J.S. and Xie, L.H. Problems, challenges and future of plant disease management: from an ecological point of view. Journal of Integrative Agriculture 2016; 15(4):705-715.

Jeong, M.-H., Lee, Y.-S., Cho, J.-Y., Ahn, Y.-S., Moon, J.-H., Hyun, H.-N., Cha, G.-S. and Kim, K.-Y. Isolation and characterization of metabolites from *Bacillus licheniformis* MH48 with antifungal activity against plant pathogens. Microbial Pathogenesis 2017; 110:645-653.

Jiang, C., Song, J., Zhang, J. and Yang, Q. Identification and characterization of the major antifungal substance against *Fusarium sporotrichioides* from *Chaetomium globosum*. World Journal of Microbiology and Biotechnology 2017; 33(6):108.

Leelasuphakul, W., Hemmanee, P. and Chuenchitt, S. Growth inhibitory properties of *Bacillus subtilis* strains and their metabolites against the green mold pathogen (*Penicillium digitatum* Sacc.) of citrus fruit. Postharvest Biology and Technology 2008; 48(1):113-121.

Mihalache, G., Balaes, T., Gostin, I., Stefan, M., Coutte, F. and Krier, F. Lipopeptides produced by *Bacillus subtilis* as new biocontrol products against fusariosis in ornamental plants. Environmental Science and Pollution Research International 2018; 25(30):29784-29793.

Mouafi, F.E., Abo Elsoud, M.M. and Moharam, M.E. Optimization of biosurfactant production by *Bacillus brevis* using response surface methodology. Biotechnology Reports 2016; 9:31-37.

Nawaz, H.H., Nelly Rajaofera, M.J., He, Q., Anam, U., Lin, C. and Miao, W. Evaluation of antifungal metabolites activity from *bacillus licheniformis* OE-04 against *Colletotrichum gossypii*. Pestic Biochem Physiol 2018; 146:33-42.

Nielsen, M.N., Sorensen, J., Fels, J. and Pedersen, H.C. Secondary metabolite- and endochitinase-dependent antagonism toward plant-pathogenic microfungi of *Pseudomonas fluorescens* isolates from sugar beet rhizosphere. Applied and environmental microbiology 1998; 64(10):3563-3569.

Sarwar, A., Brader, G., Corretto, E., Aleti, G., Ullah, M.A., Sessitsch, A. and Hafeez, F.Y. Qualitative analysis of biosurfactants from *Bacillus* species exhibiting antifungal activity. PLoS One 2018; 13(6):e0198107.

Sharma, R., Singh, J. and Verma, N. Production, characterization and environmental applications of biosurfactants from *Bacillus amyloliquefaciens* and *Bacillus subtilis*. Biocatalysis and Agricultural Biotechnology 2018; 16:132-139.

Tao, Y., Bie, X.M., Lv, F.X., Zhao, H.Z. and Lu, Z.X. Antifungal activity and mechanism of fengycin in the presence and absence of commercial surfactin against *Rhizopus stolonifer*. Journal of Microbiology 2011; 49(1):146-150.

Thaniyavarn, J., Roongsawang, N., Kameyama, T., Haruki, M., Imanaka, T., Morikawa, M. and Kanaya, S. Production and characterization of biosurfactants from *Bacillus licheniformis* F2.2. Bioscience, Biotechnology, and Biochemistry 2003; 67(6):1239-1244.

Torres, M.J., Brandan, C.P., Petroselli, G., Erra-Balsells, R. and Audisio, M.C. Antagonistic effects of *Bacillus subtilis* subsp. subtilis and *B. amyloliquefaciens* against *Macrophomina phaseolina*: SEM study of fungal changes and UV-

MALDI-TOF MS analysis of their bioactive compounds. Microbiological Research 2016; 182:31-39.

Vitullo, D., Pietro, A.D., Romano, A., Lanzotti, V. and Lima, G. Role of new bacterial surfactins in the antifungal interaction between *Bacillus amyloliquefaciens* and *Fusarium oxysporum*. Plant Pathology 2012; 61(4):689-699.

Wang, Z., Wang, Y., Zheng, L., Yang, X., Liu, H. and Guo, J. Isolation and characterization of an antifungal protein from *Bacillus licheniformis* HS10. Biochemical and Biophysical Research Communications 2014; 454(1):48-52.

Yánez-Mendizábal, V., Zeriouh, H., Viñas, I., Torres, R., Usall, J., de Vicente, A., Pérez-García, A. and Teixidó, N. Biological control of peach brown rot (Monilinia spp.) by Bacillus subtilis CPA-8 is based on production of fengycin-like lipopeptides. European Journal of Plant Pathology 2012; 132(4):609-619.

Zhang, D., Gao, T., Li, H., Lei, B. and Zhu, B. Identification of antifungal substances secreted by *Bacillus subtilis* Z-14 that suppress *Gaeumannomyces graminis* var. *tritici*. Biocontrol Science and Technology 2017; 27(2):237-251.

Zhao, Q., Mei, X. and Xu, Y. Isolation and identification of antifungal compounds produced by *Bacillus* Y-IVI for suppressing *Fusarium* wilt of muskmelon. Plant Protection Science 2016; 52(3):167-175.

Zheng, M., Shi, J., Shi, J., Wang, Q. and Li, Y. Antimicrobial effects of volatiles produced by two antagonistic *Bacillus* strains on the anthracnose pathogen in postharvest mangos. Biological Control 2013; 65(2):200-206.

Zouari, I., Jlaiel, L., Tounsi, S. and Trigui, M. Biocontrol activity of the endophytic *Bacillus amyloliquefaciens* strain CEIZ-11 against *Pythium aphanidermatum* and purification of its bioactive compounds. Biological Control 2016; 100:54-62.

Physical and Chemical Properties of Groundwater and Surface Water for Water Resource Management in Wiang Pa Pao Basin, Chiang Rai Province

Chirapa Tanya[1], Schradh Saenton[2], Somporn Chantara[3], Chitchol Phalaraksh[4*]

[1]Master's Degree Program in Environmental Science, Environmental Science Research Center, Faculty of Science, Chiang Mai University, Chiang Mai, 50200, Thailand

[2]Department of Geological Sciences, Faculty of Science, Chiang Mai University, Chiang Mai, 50200, Thailand

[3]Department of Chemistry, Faculty of Science, Chiang Mai University, Chiang Mai, 50200, Thailand

[4]Department of Biology, Faculty of Science, Chiang Mai University, Chiang Mai, 50200, Thailand

*Corresponding Author's E-mail: chitcholp@gmail.com

ABSTRACT

Wiang Pa Pao basin in Chiang Rai Province has been facing variety of anthropogenic activities and experiences drought and flood problems annually. This study was aimed to investigate and compare physical and chemical properties of groundwater, surface water and hot spring in Wiang Pa Pao basin. Water samples were collected from 28 study sites including shallow groundwater (10-50 meter), deep groundwater (50-150 meter), surface water and hot spring in February 2019. The results indicated that Physico-chemical parameters of hot spring were different from groundwater and surface water. However, the quality of both groundwater and surface water were classified in moderate level according to the water quality standard of Thailand.

Moreover, hydrochemical facies can be classified on Piper–trilinear diagram. All of water samples were similar that presented into bicarbonate regions. Hydrochemical facies of surface water and shallow groundwater were Ca^{2+}-Mg^{2+}-HCO_3^- and Na^+-K^+- HCO_3^-. While, the deep groundwater and hot springs were Na^+-K^+- HCO_3^-.

As the result, physical and chemical properties of water resource were not significantly different. Thus, this study can infer that water resource in the basin was recharged by same source. In conclusion, water resource management in the basin should consider both groundwater and surface water.

Keywords: water quality, physic-chemical parameter, hydrochemical facies

INTRODUCTION

Water Resources, refer to surface water and groundwater, are important for humans, living organisms and ecosystems. Presently, using of water resources increase that lead to face both quality and quantity problems. These problems bring to more serious in the future (Hydro and Agro Informatics Institute, 2012). Therefore, management of water resource is important for preventing and resolving the problems.

The study of physical and chemical properties of water resource can use to assess the source of water and evaluate the interaction between the groundwater and surface water for water management (Kwansirikula et al, 2005; Zhao et al., 2018; Singh and Kumar, 2005).

Thus, this study was conducted to investigate and compare physical and chemical properties of groundwater, surface water and hot spring in Wiang Pa Pao basin and assess the interaction between the groundwater and surface water.

Hydrology at Study area

Wiang Pa Pao basin, located in Wiang Pa Pao District in Chiang Rai Province, has a variety of anthropogenic activities using plenty of water resource and can affect quality and quantity of water resource.

Hydrometeorology in the basin was studied from Meteorological Survey Station located in Chiang Rai Province. Average annual precipitation in Chiang Rai Province is 1,698.1 millimeters per year and the lowest precipitation is on February. Moreover, Average annual evaporation was 1,312 millimeters per year (Hydro and Agro Informatics Institute, 2012).

The Basin has Mae Lao River flowing through the area and locates in Mae Lao sub-watershed. Average annual volume of Mae Lao River is 27.30-79.92 Mm^3 with the lowest volumes is in February (Hydro and Agro Informatics Institute, 2012).

Moreover, Wiang Pa Pao groundwater basin covers 2,800 square kilometers of hills and plains. The basin consists of two major aquifer systems (Table1) which are (1) Young Terrace unconsolidated sediments aquifer (Qyt) or shallow groundwater and (2) Old Terrace unconsolidated sediments aquifer (Qot) or deep groundwater (Department of Groundwater Resources, 2010).

Furthermore, the basement rocks at Wiang Pa Pao basin are Triassic *Igneous* Rocks, which include Biotite granite, Tourmarine granite, Granodirorite, and Carboniferous-Permian Sedimentary rocks, which include Sandstone, Limestone, and Chert. (Department of Mineral Resources, 2007).

Consequently, the basin in dry season is low precipitation, high evaporation, and has less volume of surface water. The basin risks a drought in dry season. Therefore, water resource management is important in this area.

Table 1 Hydrogeological characteristic and groundwater quality of major aquifer in Wiang Pa Pao basin (Department of Groundwater Resources, 2010).

Aquifer	Description	Lithology	Average Depth (m)	Yield (m^3/hr)	flow direction
Qyt	Terrace deposits	coarse fluvialtile sediments that fill gravel beds, sand, silt, and clay	10 - 50	10 - 20	south to north
Qot	Un-consolidated and semi-consolidated sediment	fluvialtile sediments that fill gravel beds, sand, silt, and clay	20 - 60	10 - 20	west to east

METHODOLOGY

Water samples collection

Water samples were collected from 28 study sites including shallow groundwater (10-50 meter), deep groundwater (50-150 meter), surface water and hot spring in February 2019 or dry season (Figure 1). On site study, 8 samples of surface water (SW) were collected along Mae Lao river from upstream at Khun Chae National Park, located south of the basin, to downstream at San Sali Sub-District located North of the basin. Thirteen samples of shallow groundwater (with Young Terrace unconsolidated sediments aquifer (Qyt) and the groundwater well depth about 10-60 m.) and 5 samples of deep groundwater (with Old Terrace unconsolidated sediments aquifer (Qot) the groundwater well depth about 60-150 m.) were collected from existing groundwater wells. Finally, 2 samples of hot springs (HS) were collected at Mae Kha Chan and Pong Ta Wee hot spring. Surface water and

hot spring samples were collected at about 10-15 cm. depth under surface of water, whereas groundwater samples were pumped out or some groundwater well were collected by water sampler. All of the water samples were contained in tightly closing bottles.

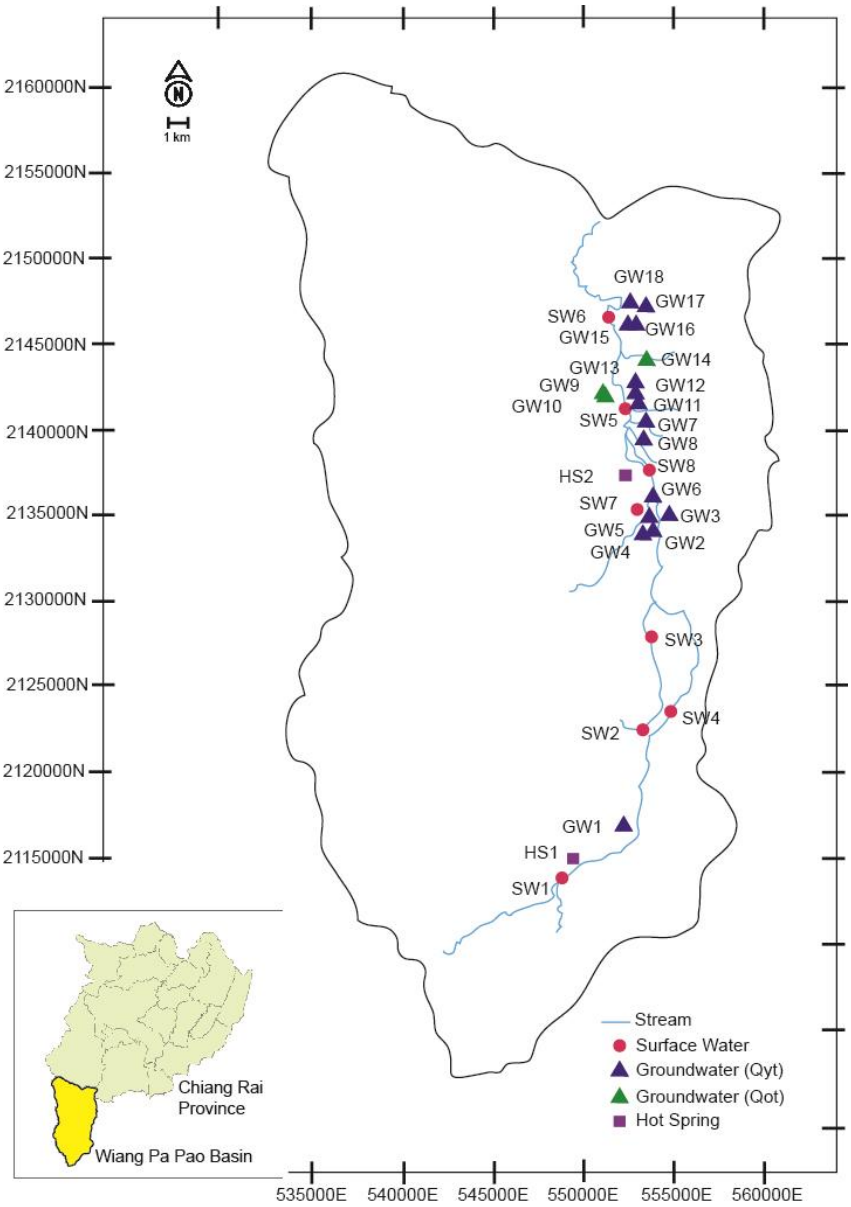

Figure 1 Location of water sampling sites in Wiang Pa Pao Basin, Chiang Rai Province.

On site data measurement

The physico-chemical parameters were measured in field study because some physico-chemical parameters can change in stored sample or between sampling and analyses in laboratory such as temperature, alkalinity, and dissolved oxygen (DO) (Mazor, 1997). The physico-chemical parameters including electrical conductivity (EC), total dissolved solid (TDS), pH and dissolved oxygen (DO) were measured by multi-parameter analyzer (Horiba U-50 Series multi-parameter water quality meters) for analysis water quality.

Ion Chromatograph

The Major ions of water samples were delineated by Dionex Ion chromatograph DX-300 at Chemistry Department, Chiang Mai University to analyze cations and anions of water for determination of chemical properties. Furethermore, hydrochemical properties can be classified on the basis of the major ions by the Piper trilinear diagram as hydrochemical facies.

RESULTS AND DISCUSSION

Physico-chemical parameters

The physico-chemical parameters from on-site data measurement of all water samples are shown in Table 2. From the average pH value, surface water, shallow groundwater and deep groundwater were acidic water. Furthermore, the DO values of surface water were higher than the other water types, which range between 3.05 to 8.36 mg/l due to the air-water exchangeable. Moreover, the average EC and TDS of hot spring were high values, which were 454.50 µS/cm and 295.50 mg/l, respectively. Therefore, it was the cause of high values of EC and TDS in surface water approaching to the hot spring. However, EC and TDS of surface water, shallow groundwater and deep groundwater were not significantly different ($p<0.05$) due to the similar source.

As the result, the physico-chemical parameters of hot springs were difference when compare with surface water and both types of the groundwater. However, water quality of both groundwater and surface water were classified as moderate clean level according to the water quality standard of Thailand (Pollution Control Department, 2000).

Chemical Composition

Major ions of water samples were shown in Table 3. Hydrochemical facies can be classified on Piper–trilinear diagram (Figure 2). All of water samples from the different water type were similar in their hydrochemical facies that fell into Bicarbonate regions. Hydrochemical facies of Surface water (SW) and Shallow Groundwater (Qyt) were Calcium-Magnesium Bicarbonate (Ca^{2+}- Mg^{2+}-HCO_3^-) and Sodium-Potassium Bicarbonate (Na^+-K^+-HCO_3^-). While, Deep Groundwater (Qot) and Hot springs (HS) were Sodium-Potassium Bicarbonate (Na^+-K^+- HCO_3^-).

The chemical compositions of surface water may reach from precipitation and/or shallow Groundwater. While, the different aquifer had difference in hydrochemical facies in some study sites due to water-rock interaction during flow (Ghadimi et al., 2012). The difference in chemical properties may occur from the infiltration of water which flow through the soil into aquifer. The sodium, potassium and magnesium in groundwater may obtain from igneous rock (granite) and sedimentary rocks (conglomerate rock and sandstone) in west of basin containing mica group, plagioclase-feldspar and clay minerals, while calcium may derive from carbonate rock. And, bicarbonate may come either from the carbonate rocks or from carbon dioxide in atmosphere (Kwansirikul et al., 2005).

Table 2 The average of Physico-chemical parameters of water in the Wiang Pa Pao basin.

Groups	Statistical Parameters	TDS (mg/L)	EC (µS/cm)	pH	DO (mg/L)
SW	Average	100.08	154.21	6.36	6.33
	Maximum	185.00	284.00	6.80	8.36
	Minimum	42.33	65.33	6.07	3.05
Qyt	Average	149.54	221.85	5.75	1.59
	Maximum	365.00	570.00	6.85	2.67
	Minimum	28.00	43.00	5.11	0.79
Qot	Average	75.00	116.33	5.17	1.89
	Maximum	135.00	208.00	5.66	3.31
	Minimum	15.00	23.00	4.56	0.85
HS	Average	295.50	454.50	7.60	1.36
	Maximum	318.00	489.00	7.63	1.58
	Minimum	273.00	420.00	7.57	1.14

Table 3 Chemical compositions of water in Wiang Pa Pao basin.

Groups	Sample No.	TDS (mg/L)	Ca^{2+} (mg/L)	Mg^{2+} (mg/L)	$Na^{+} + K^{+}$ (mg/L)	NH_4^{+} (mg/L)	Cl^{-} (mg/L)	SO_4^{2-} (mg/L)	HCO_3^{-} (mg/L)	NO_3^{-} (mg/L)	PO_4^{2-} (mg/L)
SW	SW1	42.33	6.54	2.65	5.66	0.08	1.20	1.54	113.87	0.46	3.05
	SW2	49.00	12.46	6.49	18.38	0.17	1.58	1.51	147.42	0.35	0.00
	SW3	74.00	11.29	4.48	11.07	0.21	1.01	4.51	142.33	0.00	0.00
	SW4	61.00	10.29	3.57	9.20	0.11	4.36	3.36	127.08	0.97	0.62
	SW5	185.00	16.98	6.69	38.55	1.39	57.78	13.16	177.92	3.97	0.00
	SW6	180.00	16.95	6.48	37.07	0.26	54.03	10.25	172.83	3.32	0.00
	SW7	75.00	13.45	4.78	11.13	0.29	3.29	3.13	284.67	0.99	0.00
	SW8	134.33	14.84	5.65	27.17	1.01	34.27	7.37	132.17	2.42	0.00
Qyt	GW1	285.00	41.40	8.86	23.55	0.67	8.87	0.58	294.83	0.00	3.28
	GW2	107.00	6.93	3.49	21.23	0.55	3.35	0.20	101.67	0.00	0.00
	GW3	59.67	4.54	2.32	13.04	0.18	0.52	0.14	86.42	0.00	0.00
	GW4	140.00	9.19	6.26	10.80	0.41	10.48	0.29	142.33	0.00	0.00
	GW5	365.00	99.99	20.46	22.67	1.12	17.98	20.32	274.50	2.48	2.02
	GW8	102.00	11.14	3.87	13.74	0.45	22.97	8.93	101.67	0.41	0.46

Table 3 *Cont'd*

Groups	Sample No.	TDS (mg/L)	Ca^{2+} (mg/L)	Mg^{2+} (mg/L)	$Na^{+} + K^{+}$ (mg/L)	NH_4^{+} (mg/L)	Cl^{-} (mg/L)	SO_4^{2-} (mg/L)	HCO_3^{-} (mg/L)	NO_3^{-} (mg/L)	PO_4^{2-} (mg/L)
Qyt	GW11	291.00	12.05	1.67	105.89	1.59	20.21	1.75	284.67	0.50	0.00
	GW12	130.00	8.40	4.05	44.65	0.14	1.79	1.30	167.75	0.00	0.00
	GW13	161.00	11.79	5.21	43.74	0.33	3.87	0.86	177.92	0.00	0.00
	GW15	95.00	0.58	0.00	3.70	0.16	2.10	0.31	66.08	0.18	0.00
	GW16	28.00	2.18	1.15	3.00	0.09	0.74	0.16	66.08	0.18	0.00
	GW17	119.33	12.84	4.62	7.77	0.35	5.57	0.42	127.08	0.12	0.00
	GW18	61.00	12.32	3.11	4.19	0.17	2.94	8.14	127.08	4.36	0.00
	GW11	291.00	12.05	1.67	105.89	1.59	20.21	1.75	284.67	0.50	0.00
HS	HS1	273.00	9.53	1.30	99.73	0.43	5.15	28.13	279.58	0.00	0.00
	HS2	318.00	9.97	1.27	117.11	0.46	9.03	31.50	355.83	0.00	0.00

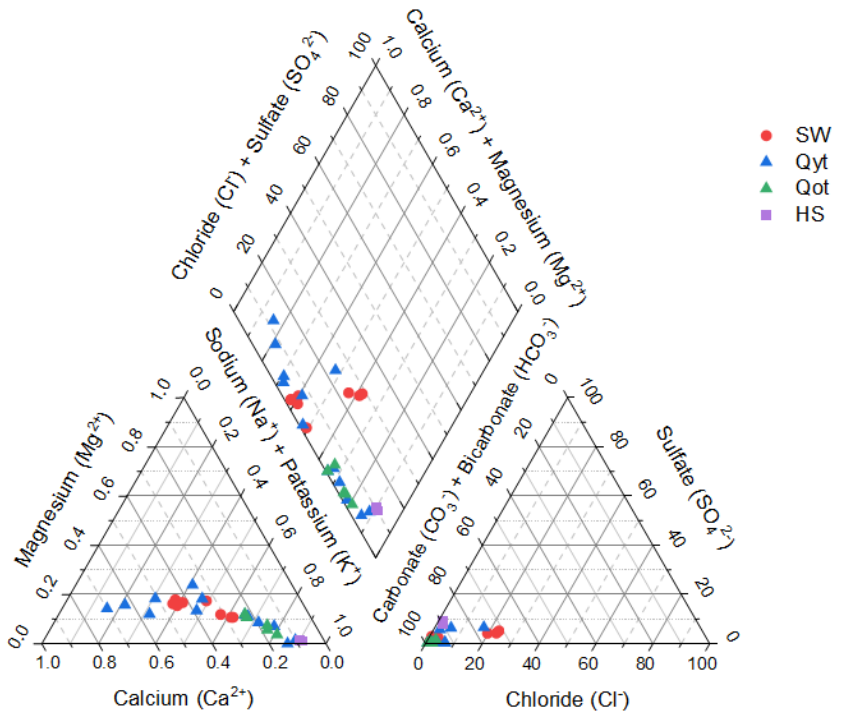

Figure 2 Hydrochemical facies of water sample. Red dot, blue triangle, green triangle and purple square symbols represent surface water, shallow groundwater, deep groundwater, and hot spring samples, respectively.

CONCLUSIONS

In this study, physical and chemical properties were reported as same as the hydrochemical facies of surface water, groundwater and hot springs in the Wiang Pa Pao Basin. The water quality of ground and surface water were classified in moderate clean level which can be used for consumption purposes. Additionally, the hydrochemical facies of water were similar. The major cations and anions were sodium, calcium, magmesium, potassium and bicarbonate. The main hydrochemical facies were Calcium-Magnesium Bicarbonate (Ca^{2+}-Mg^{2+}-HCO_3^-) and Sodium-Potassium Bicarbonate (Na^+-K^+- HCO_3^-).

As a result, physical and Chemical Properties of water resource did not differ in physic-chemical parameters and hydrochemical facies,

demonstrating that all of the water resource in the Wiang Pa Pao basin had been similar source. Accordingly, water resource management in the basin should be considered both about groundwater and surface water in planning, preventing, and resolving issues of water resource.

ACKNOWLEDGEMENTS

Authors would sincerely like to thank the Development and Promotion of Science and Technology Talents Project (DPST) for financial support. Thanks also to the local government organizations in Wiang Pa Pao District for field facilities. We also thank the Environmental Science Research Center and the Freshwater Biomonitor Research Laboratory (FBRL), Faculty of Science, Chiang Mai University for providing help on laboratory analysis.

REFERENCES

Department of Groundwater Resources. (2010). *Groundwater potential assessment of the Kok river plain (In Thai)*. Thailand: Ministry of Natural Resources and Environment.

Department of Mineral Resources. (2007). *Geologic Map of Chiang Rai*. Retrieved August 16, 2018, from Department of Mineral Resources Website: http://www.dmr.go.th/main.php.

Ghadimi, F., Mirzaei, M., Ghomi, M., and Mina, M. (2012). Hydrochemical Properties of the Thermal Waters of Mahalat Abgarm, Iran. *Geothermal Resources Council (GRC), 36*, 1355-1358.

Hydro and Agro Informatics Institute. (2012). *Kok river plain*. Thailand: Ministry of Natural Resources and Environment.

Kwansirikula, K., Singharajwarapanb, F. S., Kitac, I., & Takashimac, I. (2005). Hydrochemical and Isotopic Characteristics of Groundwater in the Lampang Basin, Northern Thailand. *science asia*, 31,77-84.

Mazor, E. (1997). *Chemical and Isotopic Groundwater Hydrology*. Marcel Dekker, Inc.

Pollution Control Department, 2000. Retrieved April 16, 2019, from Pollution Control Department Website: http://www.pcd.go.th/info_serv/reg_std_water01.html.

Singh, B. P., & Kumar, B. (2005). *Isotopes in hydrology, hydrogeology and water resources*. Alpha Science Int'l Ltd.

Zhao, D., Wang, G., Liao, F., Yang, N., Jiang, W., Guo, L., & Shi, Z. (2018). Groundwater- surface water interactions derived by hydrochemical and isotopic (222Rn, deuterium, oxygen-18) tracers in the Nomhon area, Qaidam Basin, NW China. *Journal of Hydrology*, *565*, 650-661.

Biosurfactant from *Bacillus velezensis* B49 as an alternative to chemical fungicide to inhibit the growth of fungal plant pathogen

Siraphop Pumiputikul[1], Kwantida Popitool[1], Rapeewan Sowanpreecha[2], Chompoonik Kanchanabanca[1], and Panan Rerngsamran[1*]

[1]*Department of Microbiology, Faculty of Science, Chulalongkorn University, Bangkok, Thailand*
[2]*Department of Agricultural Science and Technology, Faculty of Science and Industrial Technology, Prince of Songkla University, Surat Thani Campus, Surat Thani, Thailand*
[*]Corresponding author: panan.r@chula.ac.th

ABSTRACT

Phytopathogenic fungi destroy agricultural products worldwide. Biological control is an alternative way to reduce the usage of chemical fungicides. In this study, the ability to antagonize several plant pathogenic fungi by *Bacillus velezensis* B49 was evaluated. The results revealed that bacterial cells were able to inhibit all fungi including *Acrimonium furcatum*, *Colletotrichum gloeosporioides*, *Fusarium moniliforme*, *Fusarium proliferatum*, *Fusarium solani*, *Pyricularia oryzae*, and *Phytophthora palmivora*. Percentages of inhibition using cell-free supernatant were 17.26%, 18.74%, 33.03%, 33.90%, 59.23%, and 68.50% for *F. moniliforme*, *F. proliferatum*, *F. solani*, *A. furcatum*, *C. gloeosporioides*, and *P. oryzae*, respectively. No inhibition was found against *P. palmivora*. These results indicated that *B. velezensis* B49 was able to produce several types of secreted antifungal substances. Some of the substances, especially the one with anti-*Phytophthora* were heat labile. We are interested in the biosurfactant class of antifungal substances. Four methods for detecting biosurfactant including drop collapse, oil displacement, emulsion, and hemolytic activity tests were performed. The results revealed that *B. velezensis* B49 gave positive results for all tested confirming its ability to produce biosurfactant. Taken together, *B. velezensis* B49 can be used to control phytopathogenic fungi as an alternative to chemical fungicide for sustained agriculture.

Keywords: *Bacillus velezensis*; Biocontrol; Biosurfactant; Fungal plant pathogen

INTRODUCTION

Phytopathogenic fungi was the main pathogen that destroy agricultural products all over the world (Thilagam, et al., 2018). The fungi that were frequently reported to reduce the yield of several economic crops in Thailand were *A. furcatum, C. gloeosporioides, F. moniliforme, F. proliferatum, F. solani, P. palmivora* and *P. oryzae* (Jantasorn, et al., 2016; Ko Ko, et al., 2011). The target crops of these fungi, among several plants, include rice, tomato, chili, mango, rubber tree, and siam tulip (Chee, 1969; Noble and Coventry, 2005; Terry and Joyce, 2004; Than, et al., 2008; Thongwai and Kunopakarn, 2007). The fungi can cause various symptoms such as wilt, blight, rot, and necrosis (Terry and Joyce, 2004). In addition, the phytopathogenic fungi can produce mycotoxin that has impact on human and animal health (Fink-Grernmels, 1999). Mycotoxin, fumonisin B_1 from plant pathogenic fungi were reported to promote tumors in the liver of rats (Wang, et al., 1991), as well as to be toxic and carcinogenic to horses and pigs (Ross, et al., 1990).

The farmers normally control and prevent the fungal diseases by using chemical fungicides due to the rapid action and the ability to destroy several types of plant pathogens (Chandrashekara, et al., 2012). However, these fungicides are toxic to humans. For example, it has been reported that mancozeb, metalaxyl, and tebuconazole which frequently used in agriculture could inhibit luteal steroid synthesis in women leading to hazardous effect on female reproductive system (Atmaca, et al., 2018). Apart from the toxicity issue, the usage of chemical fungicides brought about additional cost to the growers (Aguilar-Barragan, et al., 2014). Therefore, the researcher must find an alternative way to reduce the use of chemical fungicides, and one of this is biocontrol method. This method is chosen because it is less toxic and more environmental

friendly (Chandrashekara, et al., 2012). Biocontrol uses several living organisms such as bacteria, fungi, algae or virus to control other detrimental organisms (Sigee, et al., 1999). Bacteria such as *Pseudomonas* sp., *Lactobacillus* sp., and *Bacillus* sp. is one of the most popular living organisms that were used as biocontrol agent (Santoyo, et al., 2012). The biocontrol agent can be used in the form of either bacterial cells or their metabolites (Ulloa-Ogaz, et al., 2015). Several studies used *Bacillus* sp. as biocontrol agent. *Bacillus* spp. were reported to inhibit the growth of *Podosphaera fusca*, the causal agent of cucurbit powdery mildew (Romero, et al., 2004). Cell-free supernatant produced by *Bacillus velezensis* strain AR1 inhibited the growth of *Glomerella cingulate* that caused anthracnose and fruit rotting diseases in many crops (Regassa, et al., 2018). Moreover, *Bacillus* spp. were found to produce several antifungal bioactive substances such as protease, chitinase, volatile organic compounds and biosurfactants (Asari, et al., 2016; Gond, et al., 2015). In this work, we are interested in the biosurfactant class of bioactive substances that can inhibit the growth of fungi. Biosurfactants can be classified as glycolipids, rhamnolipids, trehaloselipids, sophorolipids, lipopeptides, fatty acids, phospholipids and polymeric biosurfactants (Rahman and Gakpe, 2008). It was stated that biosurfactants from *B. velezensis* RC 218 were able to inhibit the growth of *Fusarium graminearum*, the causal agent of Fusarium head blight in wheat (Palazzini, et al., 2016). We thus used *B. velezensis* B49 that, from our previous basic screening, found to inhibit some fungi (Popitool, 2017). In this research we tested *B. velezensis* B49's ability to inhibit 6 true fungi and one water mold that caused diseases in various economic plants in Thailand, and its ability to produce biosurfactant was investigated. The objective of this research was to gain basic knowledge related to antifungal

activity and biosurfactant production by *B. velezensis* B49, with the aim to use the biosurfactant as the alternative to chemical fungicides to control plant diseases that caused by fungi.

METHODOLOGY

Microorganisms and growth conditions

B. velezensis B49 was grown on Luria-Bertani (LB) agar at 37°C for 24 hours. Phytopathogenic fungi were obtained from Plant Protection Research and Development Office, Department of Agriculture, Ministry of Agriculture and Cooperatives. *A. furcatum*, *C. gloeosporioides*, *F. moniliforme*, *F. proliferatum*, *F. solani* and *P. oryzae* were grown on potato dextrose agar (PDA) incubate at 25 °C for 3-5 days, and *P. palmivora* was grown on V8 agar at 25°C for 3-5 days.

Antifungal activity

Dual-culture assay

Agar plugs of each phytopathogenic fungi were cut using 6 mm diameter cork borer, and then placed on the surface of PDA or V8 plates at about 2 cm from the edge of the plate. *B. velezensis* B49 was streaked on PDA or V8 plates at 2 cm from the agar plug. The plates were incubated at 25°C for 3-5 days. The inhibition of the fungal growth was determined after 3 days (Susilowati, et al., 2011), and percentage of inhibition was calculated according to the following equation:

$$\% \text{ inhibition} = \frac{C - T}{C} \times 100$$

where C is the average diameter of three replicates of the control, and T is the average diameter of three replicates of the test plate (Sowanpreecha and Rerngsamran, 2018).

Mixed supernatant assay

B. velezensis B49 was grown in LB broth until the optical density (OD) at 600 nm reached about 0.5. The culture (1% inoculum) was inoculated into fresh LB broth and incubated at 37°C for 18 hours with shaking at 200 rpm. Supernatant

was obtained by centrifugation at 4°C, 8,000 rpm for 20 min. The supernatant was passed through 0.45 µm sterile filter to obtain cell-free supernatant. The cell-free supernatant was mixed with warm PDA or V8 medium at 1:10 ratio of supernatant to medium. The agar plug of fungal mycelium was cut using 0.6 mm cork borer, and then placed at the center of PDA or V8 plates. The plates were incubated at 25°C for 3-5 days. The inhibition of the fungal growth was determined compared to the control plate contained the same fungus growing on the same media without the cell-free supernatant using the method previously described (Sowanpreecha and Rerngsamran, 2018).

Determination of biosurfactant production ability

Blood agar test

B. velezensis B49 was streaked on blood agar containing 5% v/v sheep blood, and the plate was incubated at 37°C for 24 hours. Haemolytic activity of red blood cells due to the presence of biosurfactant was investigated (Vigneshwaran, et al., 2018).

Drop collapse test

The drop collapse assay was carried out on the lid of 96 wells plate. The lid contains marks that correspond to the wells of the 96 wells plate. Xylene oil, 20 µl, were dropped to the marks on the lid, and let stand for 1 hour at room temperature for the formation of thin film. Cell-free supernatant of *B. velezensis* B49, 10 µl, was dropped onto the xylene oil film, and after 1 min, the collapsed of the supernatant drops due to the presence of biosurfactant were observed (Ibrahim, 2016). Sodium dodecyl sulfate (SDS) (0.1%) was used as a positive control, whereas LB medium was used as a negative control.

Oil displacement test

Oil displacement experiment was performed by adding 20 ml of deionized water into 15x60 mm Petri dish. Ten microliters of crude

petroleum oil were slowly added onto the water to form a thin film over the water surface. A drop of cell-free supernatant of *B. velezensis* B49, 10 µl, was carefully added on the oil film, and the displacement of oil film due to the presence of biosurfactant was observed (Ibrahim, 2016).

Emulsification index

The emulsification index was determined by the addition of 400 µl xylene oil into clear snap cap vial, and 400 µl of the cell-free supernatant of *B. velezensis* B49 was added. The mixture was mixed using vortex mixer for 5 min to obtain emulsion. The tube was stand at room temperature for 24 hours for phases separation. The emulsification index at 24 hours (E_{24}) was determined according to the following equation (Suganthi, et al., 2018):

$$E_{24} = \frac{\text{Height of emulsion layer}}{\text{Height of total solution}} \times 100$$

RESULTS AND DISCUSSION

Antifungal activity

Dual culture assay revealed that *B. velezensis* B49 showed antagonistic effect against all fungi tested (Fig. 1). As seen in figure 2, mixed supernatant assay demonstrated a semi-quantitative inhibition by *B. velezensis* B49 against all fungi. The percentages of inhibition were 17.26% for *F. moniliforme*, 18.74% for *F. proliferatum*, 33.03% for *F. solani*, 33.90% for *A. furcatum*, 59.23% for *C. gloeosporioides*, and 68.50% for *P. oryzae*. By using mixed supernatant technique, the result also showed that the growth

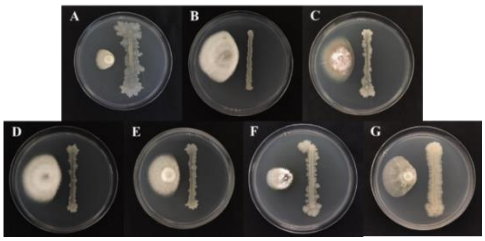

Figure 1. Dual-culture assay of *B. velezensis* B49 against different fungi including A) *A. furcatum*, B) *C. gloeosporioides*, C) *F. moniliforme*, D) *F. proliferatum*, E) *F. solani*, F) *P. oryzae*, and G) *P. palmivora*

of *P. palmivora* was almost similar to control. This result indicated that *B. velezensis* B49 produces several bioactive compounds, and the ones that active against *P. palmivora* was heat labile when they were exposed to warm media (about 50°C). It was reported that *Bacillus* spp. were able to produce various secondary metabolites and/or proteinaceous antimicrobial, and some of which were sensitive to high temperature (Ali, et al., 2016). In addition, the remained bioactive substances caused some morphology change to *P. palmivora* in termed of mycelial growth and zoosporangial production (figure 2G) as has been found by Budi et al. (1999).

Determination of biosurfactant production ability

This research was interested in the antifungal bioactive compounds that belong to biosurfactant class, therefore several techniques were performed in order to investigate the properties related to the biosurfactant production. These techniques included drop collapse test, oil displacement test, emulsion test, and hemolytic activity test as described (Anjum, et al., 2016; Carrillo, et al., 1996; Youssef, et al., 2004). It was observed that *B. velezensis* B49 gave positive result on blood agar showing the lysis of red blood cells around the bacterial colony (Fig. 3A). This is one of the primary screening methods for biosurfactant production recommended by various researchers (Płaza, et al., 2006; Satpute, et al., 2008; Vigneshwaran, et al., 2018). Cell-free supernatant of *B. velezensis* B49 also showed positive results for drop collapse and oil displacement tests as seen in figures 3B and 3C, respectively.

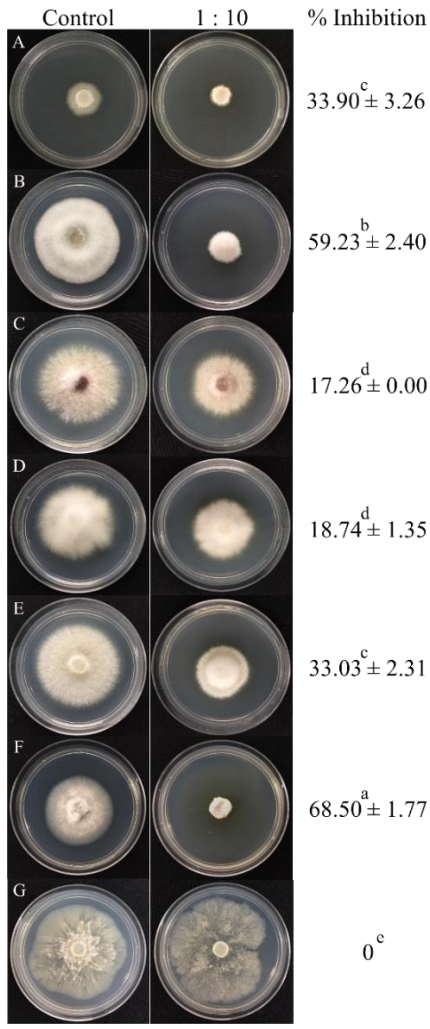

Figure 2. Mixed supernatant assay for metabolites from *B. velezensis* B49 against several fungi at 1:10 ratio compared to control without bacterial supernatant. A-G refer to fungi as shown in figure 1. Different superscript letters indicates significant differences ($p < 0.05$) in one-way ANOVA and Duncan's Multiple Comparison Test.

The E_{24} was 62.5% as shown in figure 3D. It was reported by Liu et al (2010) that biosurfactant production by *B. valezensis* H3 was time and temperature dependent. Therefore, the variation of time and temperature will be performed in order to obtain higher amount of the first evidences that *B. velezensis* B49 has ability to produce biosurfactant.

biosurfactant by *B. velezensis* B49.

Taken together, these results were

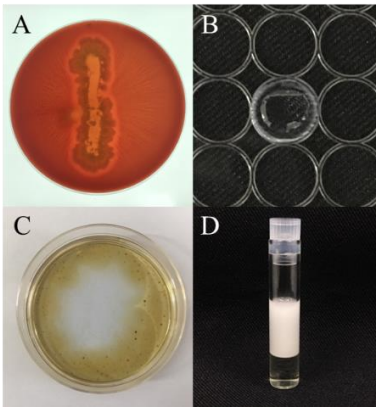

Figure 3. Detection of biosurfactant production A) Blood agar test, B) Drop collapse test, C) Oil displacement test, D) Emulsification index

Bacillus spp. are well-known as biocontrol agents, and their commercialized produce have been available in several countries worldwide (Radhakrishnan, et al., 2017). Several reports have stated that *Bacillus* spp. can produce several substances as bioactive compounds such as antibiotics, cell-wall degrading enzymes, volatile organic compounds, lipopeptides and/or biosurfactants (Jamalizadeh, et al., 2011; Rahman and Gakpe, 2008; Santoyo, et al., 2012).

Most antifungal biosurfactants were known to have mechanism which disrupt fungal cell membranes, form pores, cause lysis of the fungal cells, and subsequently cause cell death (Ines and Dhouha, 2015).

In summary, this study showed the antagonistic ability of *B. velezensis* B49 against *A. furcatum*, *C. gloeosporioides*, *F. moniliforme*, *F. proliferatum*, *F. solani*, *P. oryzae*, and *P. palmivora* which are pathogen of several economic plants in Thailand. The antifungal

compounds were secreted out of the bacterial cells, and showed antifungal activity against all fungi. Some of the substances were heat labile. *B. velezensis* B49 revealed the ability to produce biosurfactant substances. Therefore, the property of its biosurfactant will be further determined using techniques previously described, for example, silica gel column chromatography, thin-layer chromatography or high-performance liquid chromatography of the compound (Morikawa, et al., 1993; Singh, 2012; Sivapathasekaran, et al., 2009) The ability of the purified biosurfactant to inhibit the growth of fungi (Sarwar, et al., 2018) will be examined, and the identification of the biosurfactant will be performed using LC-MS or equivalent methods (Satpute, et al., 2010).

REFERENCES

Aguilar-Barragan, A, García-Torres, AE, Odriozola-Casas, O, Macedo-Raygoza, G, Ogura, T, Manzo-Sánchez, G, James, AC, Islas-Flores, I and Beltrán-García, MJ. Chemical management in fungicide sensivity of *Mycosphaerella fijiensis* collected from banana fields in México. Brazilian Journal of Microbiology 2014; 45(1): 359-364.

Ali, GS, El-Sayed, AS, Patel, JS, Green, KB, Ali, M, Brennan, M and Norman, D. *Ex vivo* application of secreted metabolites produced by soil-inhabiting *Bacillus* spp. efficiently controls foliar diseases caused by *Alternaria* spp. Applied and Environmental Microbiology 2016; 82(2): 478-490.

Anjum, F, Gautam, G, Edgard, G and Negi, S. Biosurfactant production through *Bacillus* sp. MTCC 5877 and its multifarious applications in food industry. Bioresource Technology 2016; 213: 262-269.

Asari, S, Matzén, S, Petersen, MA, Bejai, S and Meijer, J. Multiple effects of *Bacillus amyloliquefaciens* volatile

compounds: plant growth promotion and growth inhibition of phytopathogens. FEMS Microbiology Ecology 2016; 92(6): fiw070.

Atmaca, N, Arikan, S, Essiz, D, Kalender, H, Simsek, O, Bilmen, FS and Kabakci, R. Effects of mancozeb, metalaxyl and tebuconazole on steroid production by bovine luteal cells *in vitro*. Environmental Toxicology and Pharmacology 2018; 59: 114-118.

Budi, Sv, Van Tuinen, D, Martinotti, G and Gianinazzi, S. Isolation from the *Sorghum bicolor* mycorrhizosphere of a bacterium compatible with arbuscular mycorrhiza development and antagonistic towards soilborne fungal pathogens. Applied and Environmental Microbiology 1999; 65(11): 5148-5150.

Carrillo, P, Mardaraz, C, Pitta-Alvarez, S and Giulietti, A. Isolation and selection of biosurfactant-producing bacteria. World Journal of Microbiology and Biotechnology 1996; 12(1): 82-84.

Chandrashekara, KN, Chandrashekara, C, Chakravathi, M and Manivannan, S. Biological control of plant disease. In: Singh, VK, Singh, Y and Singh, AS, editors, Ecofriendly innovative approaches in plant disease management. Dehradun: International Book Distributors; 2012. p. 147-166.

Chee, K. Variability of *Phytophthora* species from *Hevea brasiliensis*. Transactions of the British Mycological Society 1969; 52(3): 425-436.

Fink Grernmels, J. Mycotoxins: their implications for human and animal health. Veterinary Quarterly 1999; 21(4): 115-120.

Gond, SK, Bergen, MS, Torres, MS and White Jr, JF. Endophytic *Bacillus* spp. produce antifungal lipopeptides and induce host defence gene expression in maize. Microbiological Research 2015; 172: 79-87.

Ibrahim, HM. Characterization of biosurfactants produced by novel strains of *Ochrobactrum anthropi* HM-1 and *Citrobacter freundii* HM-2 from used engine oil-

contaminated soil. Egyptian Journal of Petroleum 2016; 27: 21-29.

Ines, M and Dhouha, G. Lipopeptide surfactants: production, recovery and pore forming capacity. Peptides 2015; 71: 100-112.

Jamalizadeh, M, Etebarian, H, Aminian, H and Alizadeh, A. A review of mechanisms of action of biological control organisms against post-harvest fruit spoilage. EPPO Bulletin 2011; 41(1): 65-71.

Jantasorn, A, Moungsrimuangdee, B and Dethoup, T. *In vitro* antifungal activity evaluation of five plant extracts against five plant pathogenic fungi causing rice and economic crop diseases. Journal of Biopesticides 2016; 9(1): 1.

Ko Ko, TW, McKenzie, EHC, Bahkali, AH, To-Anun, C, Chukeatirote, E, Promputtha, I, Abd-Elsalam, KA, Soytong, K, Wulandari, NF and Sanoamuang, N. The need for re-inventory of Thai phytopathogens. Chiang Mai Journal of Science 2011; 38(4): 625-637.

Liu, X, Ren, B, Chen, M, Wang, H, Kokare, CR, Zhou, X, Wang, J, Dai, H, Song, F, Liu, M, Wang, J, Wang, S and Zhang, L. Production and characterization of a group of bioemulsifiers from the marine Bacillus velezensis strain H3. Applied Microbiology and Biotechnology 2010; 87(5): 1881-1893.

Morikawa, M, Daido, H, Takao, T, Murata, S, Shimonishi, Y and Imanaka, T. A new lipopeptide biosurfactant produced by *Arthrobacter* sp. strain MIS38. Journal of Bacteriology 1993; 175(20): 6459-6466.

Noble, R and Coventry, E. Suppression of soil-borne plant diseases with composts: a review. Biocontrol Science and Technology 2005; 15(1): 3-20.

Palazzini, JM, Dunlap, CA, Bowman, MJ and Chulze, SN. *Bacillus velezensis* RC 218 as a biocontrol agent to reduce *Fusarium* head blight and deoxynivalenol accumulation: genome sequencing and secondary metabolite cluster profiles.

Microbiological Research 2016; 192: 30-36.

Płaza, GA, Zjawiony, I and Banat, IM. Use of different methods for detection of thermophilic biosurfactant-producing bacteria from hydrocarbon-contaminated and bioremediated soils. Journal of Petroleum Science and Engineering 2006; 50(1): 71-77.

Popitool, K. Screening of microorganisms and biosurfactant production for inhibition of plant fungal pathogen. Report. Bachelor Degree, Department of Microbiology, Faculty of Science, Chulalongkorn University 2017. 125p. (written in Thai).

Radhakrishnan, R, Hashem, A and Abd_Allah, EF. *Bacillus*: a biological tool for crop improvement through bio-molecular changes in adverse environments. Frontiers in Physiology 2017; 8: doi: 10.3389/fphys.2017.00667.

Rahman, PK and Gakpe, E. Production, characterisation and applications of biosurfactants-Review. Biotechnology 2008; 7(2): 360-370.

Regassa, AB, Taegyu, C and Lee, YS. Supplementing biocontrol efficacy of *Bacillus velezensis* against *Glomerella cingulata*. Physiological and Molecular Plant Pathology 2018; 102: 173-179.

Romero, D, Pérez-García, A, Rivera, M, Cazorla, F and De Vicente, A. Isolation and evaluation of antagonistic bacteria towards the cucurbit powdery mildew fungus *Podosphaera fusca*. Applied Microbiology and Biotechnology 2004; 64(2): 263-269.

Ross, P, Nelson, P, Richard, J, Osweiler, G, Rice, L, Plattner, R and Wilson, T. Production of fumonisins by *Fusarium moniliforme* and *Fusarium proliferatum* isolates associated with equine leukoencephalomalacia and a pulmonary edema syndrome in swine. Applied and Environmental Microbiology 1990; 56(10): 3225-3226.

Santoyo, G, Orozco-Mosqueda, MdC and Govindappa, M. Mechanisms

of biocontrol and plant growth-promoting activity in soil bacterial species of *Bacillus* and *Pseudomonas*: a review. Biocontrol Science and Technology 2012; 22(8): 855-872.

Sarwar, A, Brader, G, Corretto, E, Aleti, G, Abaidullah, M, Sessitsch, A and Hafeez, FY. Qualitative analysis of biosurfactants from *Bacillus* species exhibiting antifungal activity. PloS One 2018; 13(6): e0198107.

Satpute, S, Banpurkar, A, Dhakephalkar, P, Banat, I and Chopade, B. Methods for investigating biosurfactants and bioemulsifiers: a review. Critical Reviews in Biotechnology 2010; 30(2): 127-144.

Satpute, S, Bhawsar, B, Dhakephalkar, P and Chopade, B. Assessment of different screening methods for selecting biosurfactant producing marine bacteria. Indian Journal of Marine Sciences 2008; 37(3): 243-250.

Sigee, D, Glenn, R, Andrews, M, Bellinger, E, Butler, R, Epton, H and Hendry, R. Biological control of cyanobacteria: principles and possibilities. Hydrobiologia 1999; 395/396: 161-172.

Singh, V. Biosurfactant–isolation, production, purification & significance. International Journal of Scientific and Research Publications 2012; 2(7): 1-4.

Sivapathasekaran, C, Mukherjee, S, Samanta, R and Sen, R. High-performance liquid chromatography purification of biosurfactant isoforms produced by a marine bacterium. Analytical and Bioanalytical Chemistry 2009; 395(3): 845-854.

Sowanpreecha, R and Rerngsamran, P. Biocontrol of orchid-pathogenic mold, *Phytophthora palmivora*, by antifungal proteins from *Pseudomonas aeruginosa* RS1. Mycobiology 2018; 46(2): 129-137.

Suganthi, SH, Murshid, S, Sriram, S and Ramani, K. Enhanced

biodegradation of hydrocarbons in petroleum tank bottom oil sludge and characterization of biocatalysts and biosurfactants. Journal of Environmental Management 2018; 220: 87-95.

Susilowati, A, Wahyudi, AT, Lestari, Y, Suwanto, A and Wiyono, S. Potential *Pseudomonas* isolated from soybean rhizosphere as biocontrol against soilborne phytopathogenic fungi. HAYATI Journal of Biosciences 2011; 18(2): 51-56.

Terry, LA and Joyce, DC. Elicitors of induced disease resistance in postharvest horticultural crops: a brief review. Postharvest Biology and Technology 2004; 32(1): 1-13.

Than, P, Jeewon, R, Hyde, K, Pongsupasamit, S, Mongkolporn, O and Taylor, P. Characterization and pathogenicity of *Colletotrichum* species associated with anthracnose on chilli (*Capsicum* spp.) in Thailand. Plant Pathology 2008; 57(3): 562-572.

Thilagam, R, Kalaivani, G and Hemalatha, N. Isolation and identification of phytopathogenic fungi from infected plant parts. International Journal of Current Pharmaceutical Research 2018; 10(1): 26-28.

Thongwai, N and Kunopakarn, J. Growth inhibition of *Ralstonia solanacearum* PT1J by antagonistic bacteria isolated from soils in the northern part of Thailand. Chiang Mai Journal of Science 2007; 34: 345-354.

Ulloa-Ogaz, A, Muñoz-Castellanos, L and Nevárez-Moorillón, G. Biocontrol of phytopathogens: antibiotic production as mechanism of control. In: A., M-V, editor, The battle against microbial pathogens: basic science, technological advances and educational programes. Spain: Formatex; 2015. p. 305-309.

Vigneshwaran, C, Sivasubramanian, V, Vasantharaj, K, Krishnanand, N and Jerold, M. Potential of *Brevibacillus* sp. AVN 13 isolated from crude oil contaminated soil for biosurfactant production and its optimization studies. Journal of

Environmental Chemical Engineering 2018; 6: 4347-4356.

Wang, E, Norred, W, Bacon, C, Riley, R and Merrill, AH. Inhibition of sphingolipid biosynthesis by fumonisins. Implications for diseases associated with *Fusarium moniliforme*. Journal of Biological Chemistry 1991; 266(22): 14486-14490.

Youssef, NH, Duncan, KE, Nagle, DP, Savage, KN, Knapp, RM and McInerney, MJ. Comparison of methods to detect biosurfactant production by diverse microorganisms. Journal of Microbiological Methods 2004; 56(3): 339-347.

Quality and production cost of some framework tree species seedlings grown with different root pruning techniques.

Preeyaphat Chaiklang[1*], Sutthathorn Chairuangsri[2,3], Pimonrat Tiansawat[2,3]
[1]Master Degree Program in Environmental Science, Environmental Science Research Center, Faculty of Science, Chiang Mai University, Chiang Mai, 50200, Thailand
[2]Environmental Science Research Center, Faculty of Science, Chiang Mai University, Chiang Mai, 50200
[3]Department of Biology, Faculty of Science, Chiang Mai University Chiang Mai, 50200
* Corresponding author: e-mail: preeyaphat.ch@gmail.com

ABSTRACT

About half of the cost for forest restoration with Framework Species Method is seedling production cost. Root pruning is a seedling care practice which promotes better tree seedlings, but it is time consuming and labor intensive. This study aims to find a suitable nursery practice to reduce seedling production cost and to yield good quality seedlings. The study was conducted in Forest Restoration Research Unit tree nursery in Khlong Thom district, Krabi province, Southern of Thailand. Five framework tree species including *Saraca indica*, *Sandoricum koetjape*, *Cleistocalyx operculatus*, *Lepisanthes rubiginosa* and *Garcinia speciosa* were propagated with three different production practices; First, put seedlings on the ground without crates (control), Second, use plastic crates placed on shelves (air-pruning + crate) Third, put seedlings in plastic crates and placed on the ground (crate). The seedlings from different species response to treatments differently. Seedling biomass of *L.rubiginosa* and *G.speciosa* were significantly higher in the crate

treatment in comparison to the control treatment. However, the biomass of *S. indica*, *S. koetjape*, and *C. operculatus* in three treatments were not significantly different (p-values>0.05). Across species, the cost of production in crate, air pruning + crate, and the control treatment were 19.08, 20.64 and 20.15 baht per seedling respectively.

Keywords: Air-pruning, Seedling production, Framework species method, Cost effectiveness, Krabi province

INTRODUCTION

Tropical rainforest is the important carbon sink, it can absorb up to 30 percent of all greenhouse gas emissions. Nevertheless, over the last 25 years (1990 – 2015) the world forest areas decrease continuously. In Thailand, deforestation is also primarily a concern. From 1973 to 2014, the annual deforestation rate was estimated at 0.6% or 140,000 hectares per year (FAO, 2015). Tree plantation is a common tool to restore ecosystem and increase forest areas. The framework species method is forest restoration that promote biodiversity recovery by exploits natural seed dispersal mechanisms (FORRU, 2006). It involves planting 20-30 native tree species 3,125 seedlings per ha. About half of forest restoration with this method is seedling production. High quality seedlings are essential for success of forest restoration project. Various traits of plants such as growth rate, crown development, flowering, and fruiting are related to the quality of tree seedlings (Davis and Jacobs, 2005). Root pruning is a technique which commonly applied to commercial tree seedling in the nursery to facilitate transplanting and induced branching of the root (Andersen *et al.*, 2000). Previous studies showed that root pruning could increase the entire surface area of the pruned seedling in *Quercus robur* (L.) up to 245,000cm² compared with only 122,000cm² in unpruned root (Watson *et al.*, 1987). The study of Mitre *et al.* (2012)

found that root pruning also increased the yield of the apple trees. However, root pruning consumes a lot of time and labor. Air root pruning is an alternative method for seedling care. In this method, the seedlings will be lifted from the ground to allow air to flow under the container. When roots are exposed to air, they will dried out and died.The study of Walker (2005) and Marler *et al.* (1996) shown that air pruning can promote lateral root branching, and keeps the root systems compact and increase yield of trees. In contrast, unpruned roots may grow around the container in a constricted pattern; may spiral, twist, kink or become strangled. Loppe *et al*. (1992) also revealed air pruned plants had more secondary root and suffered less transplant shock.

Many root pruning and air pruning research studies have been focus on the commercial species, there are only a few information about the effect of root pruning on forest tree production especially framework species and absent of information of the economic viability of seedling production processes. This study aimed to find a suitable nursery practice to reduce seedling production cost and to yield a good quality seedling.

METHODOLOGY

Study site

The experiment was established at Forest restoration research unit (FORRU) tree nursery (18° 48' N, 98° 55' E at 100 m above sea level) in Khlong Thom district, Krabi province, Southern of Thailand. The site formerly supported lowland tropical rain forest. Meteorological Department of Thailand reported the average annual precipitation is 2,183.5 millimeter per year. The average annual temperature is 28ºC and the average humidity is 80 percent, which peaks in October by a rainy season.

Seed germination

Five native tree species, which used as framework tree species for southern Thailand, were selected for this research according to seed availability. The five species were

Saraca indica L. (Fabaceae), *Sandoricum koetjape (Burm. f.)* Merr. (Meliaceae), *Cleistocalyx operculatus* (Roxb.) (Myrtaceae), *Lepisanthesrubiginosa (Roxb.)* Leenh. (Sapindaceae) and *Garcinia speciosa* Wall. (Guttiferae). The seeds were collected from the mother trees, cleaned, and air-dried before germination. After germination, seedlings with true leaves and grow up to 10 centimeter height was potted in a plastic bag which contained forest soil mixed with coconut husk and rice husk before moving to the experimental plots.

Seedling Growth

The experiment was divided into three treatments including First, Control: standard nursery practices, put seedling containers on a plastic sheet on the ground. Second, Air-pruning + crate: seedling containers were put in twelve cavity plastic crates and arranged on 2 x 2.5 m. wire bench, sixty centimeter height above ground. Third, Crate: seedling containers were put in twelve cavity plastic crates and arranged on a plastic sheet on the ground.

Forty-eight seedlings from each tree species were randomly selected for each replicate. There were three replicates from each treatment (432 seedlings per species). The experiments were arranged in a randomized complete block design with three replicates. The seedlings were taken care of by standard nursery practices. After sixth months, nine seedlings per replication were harvested for biomass determination. The seedlings were dried at 70ºC for 72 hours and biomass dry weight was determined (Peìrez *et al*., 2013).

Seedling Production Cost

The cost for different seedling production processes was separated into establishment cost (purchase of equipment, soil and compound preparation, potting, etc.) and maintenance cost (labor, transports, nursery care, etc.). The cost was calculation base on six months of seedling production and assume that the material for the establishment will last in five years. The total cost will

be compared to evaluate economically feasible of each production process.

Data analysis

Analyses of variance ANOVA in the R Programming language, version 3.4.1 (R Core Team, 2018) was used to compare the seedling growth among treatment.

RESULTS AND DISCUSSION

1. Seedling Growth and Biomass

A seedling from different species response to the treatments differently Figures 1 show the increasing of seedling height within six months. The species that have higher height were *C. operculatus* and *S.koetjape.*

The crate treatment and air pruning+crate significantly increase the height of *C.operculatus*, *L.rubiginosa* when compared with control treatment. The biomass of all five species also shown that each species response to treatments differently. Crate treatment and air pruning+crate treatment tended to increase seedling biomass. However, there were only two species that the crate treatment could significantly increase biomass (Figure 2) including *L. rubiginosa* and *G. speciosa*. The dry weight of *L.rubiginosa* seedling in crate treatment was 1.63 ± 0.20 g. per seedling follow by air-pruning + crate treatment (1.06 ± 0.44 g. per seedling) and the lowest weight was recorded in control treatment (0.72 ± 0.21 g. per seedling). In *G. speciosa*, dry weight of seedling in crate treatment was 2**.** 02 ± 0**.** 31 g. per seedling, while that of air pruning+crate and control were 1.40±0.29 and 1.16 ± 0**.** 23 g. per seedling respectively**.** (Table 1)

These may due to the effect of air pruning which also occurred in crate treatment. Although in crate treatment, the crates were put on the ground but there was a small gap between seedling containers and ground when the root grows out of the containers, the root growth was limited by dry air in the gap and air-pruning process could occur. This could promote better root system and

hence increased in biomass of seedlings that agreed with the work of Van Sambeek *et al.* (2013) and Loppe *et al.* (1992). They reported that the air root pruning had potential to produce seedlings with larger fibrous root systems and faster height, diameter, and biomass growth than conventional root pruning method.

In the air pruning+crate treatment although seedlings growth were promoted by air pruning but the seedling in this treatment were subjected to low moisture and high nutrient leaching from the container. Therefore, to promote seedling growth in this treatment, more watering may be needed. Moreover, the height of the wire bench at 60 cm. above ground in air pruning treatment provided a more convenient working position for the nursery staff. In control treatment, coil or spiral roots were found in some seedlings. Seedlings were compresses due to a un-regulate arrangement on the ground. Roots of some seedling grew out from the container and reached to the soil. The roots could be damaged during seedling transport and may cause a seedling shock when planting out in the field.

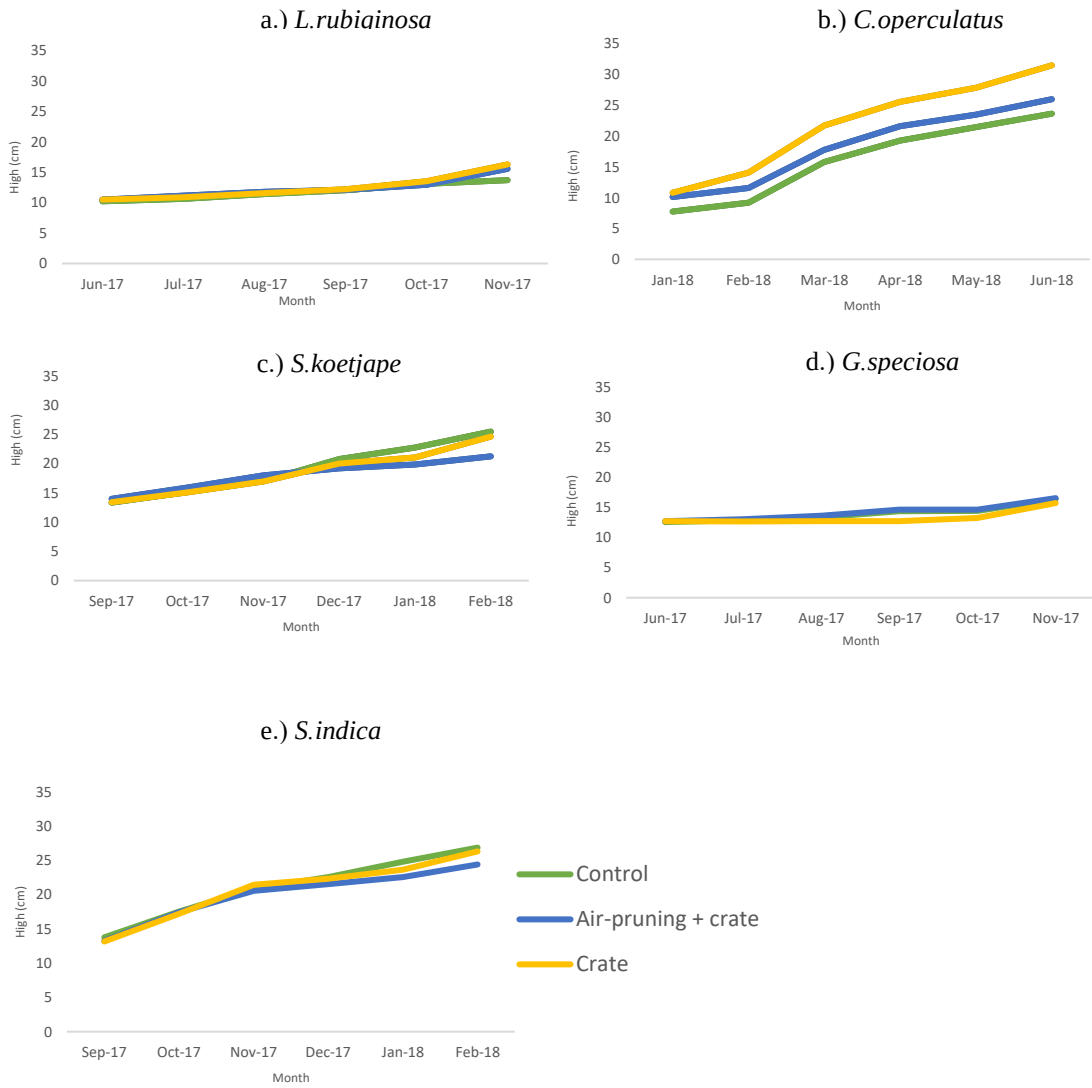

Figure 1. Seedling height in each species among three different production practice.

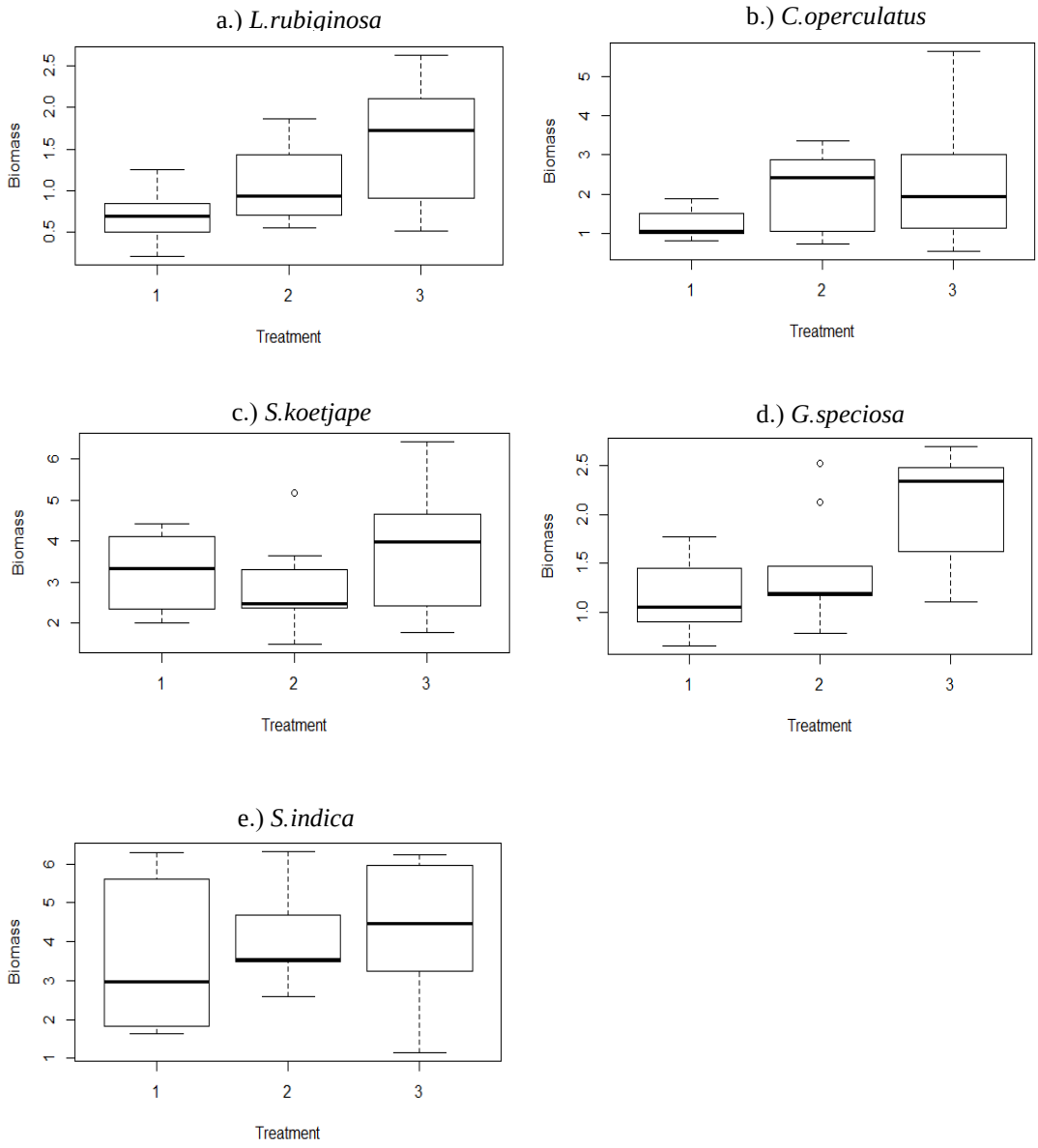

Figure 2. Seedling biomass of five selected species treated with three different production practices.

Table 1. Average seedling biomass and standard deviations for among three treatment of five species at the nursery trees.

Species	Treatment	Biomass (g/seedling)	*P*-value[a]
L.rubiginosa	Control	0.72a ±0.21	0.0086*
	Air pruning+ crate	1.06a ±0.44	
	Crate	1.63b ±0.20	
C.operculatus	Control	1.24 ±0.35	0.1644
	Air pruning+ crate	1.99 ±0.58	
	Crate	2.26 ±1.48	
S.koetjape	Control	3.22 ±1.05	0.3171
	Air pruning+ crate	2.82 ±0.55	
	Crate	3.71 ±1.45	
G.speciosa	Control	1.16a ±0.23	0.0071*
	Air pruning+ crate	1.40a ±0.29	
	Crate	2.02b ±0.31	
S.indica	Control	3.64 ±1.43	0.6687
	Air pruning+ crate	4.10 ±0.84	
	Crate	4.35 ±0.66	

Different letter in same species indicate the significant different between treatment with in species.

[a] *P*- value are based on ANOVA and Multiple Comparison test (Tukey's HSD)* were used at the 0.05 probability level.

2. Cost

The seedling production cost was calculated based on 2,160 seedling, which culture in the nursery for 6 months. The total cost of seedling production was highest in Air pruning + crate treatment, about 44,586.80 baht. For control treatment and crate treatment the cost were 43,526.16 baht and 41,208.00 baht respectively (Table 2). The highest proportion was labor cost which represented 85-95 percent of total cost. The seedling production with air pruning+crate and crate could reduce the labor cost two days per month. That was the time needed to do a conventional root pruning by hand. However, the air pruning + crate was the most expensive method for seedling production at 20.64 baht per seedling because this treatment included material cost to set up shelf and crate for the first time. However, in long term, this method could reduce labor cost and therefore reduce the total production cost. The cheapest treatment was the crate method, which put seedling in a crate on the ground; the cost was about 19. 08 baht per seedling (Table2). This method also promote growth of some species. Thus, crate method is particularly recommended as a cost effective and efficient method for tree seedlings production for forest restoration in the long term.

Table 2 Establishment and maintenance costs for 2,160 seedling production of five species for the six months of study and assume that material for experiment set up will last for five years.

Order	Prices (baht)		
	Control	Air pruning+ crate	Crate
Crate	-	1,500.00	1,500.00
Material[a]	-	3,378.80	-
Soil	518.40	518.4	518.4
Plastic bag	518.40	518.4	518.4
Coconut husk	345.60	345.60	345.60
Rice husk	144.00	144.00	144.00
Labor cost[b] (1person)	41,999.76	38,181.6	38,181.6
Total costs	**43,526.16**	**44,586.8**	**41,208**
Cost per seedling	**20.15**	**20.64**	**19.08**

[a]Material cost include material for setup such as iron tubes, wire bench.

[b] Labor cost calculated by averaged of control treatment 22 working days per month differs from air pruning and crate treatment 20 working days per month.

CONCLUSIONS

The crate treatment were successfully promote the growth of *G. speciosa* and *L. rubuginosa* in the nursery. The seedling biomass were significantly higher in comparison to the control treatment. The method could provide air pruning effect and at the same time it could maintain moisture and nutrient for seedling. This technique requires less time and labor. Therefore, the total cost for

seedling production will be reduced in the long term. Finally, seedling in crate could be move and transport easier. However, each tree species may response to the treatment differently. Therefore, further study on the response of seedling to air pruning are necessary.

ACKNOWLEDGEMENTS

The authors would like to thank the staff of Forest Restoration Research Unit Krabi for helping with seed collection and seedling care. This study was supported by the Center of Excellence on Biodiversity. In addition, we are grateful to Environmental Science Research Center, Faculty of Science, Chiang Mai University.

REFERENCES

Andersen, L., Rasmussen, H. N., & Brander, P. E. (2000). Regrowth and dry matter allocation in Quercus robur (L.) seedlings root pruned prior to transplanting. New Forests, 19(2) , 205-214.

Davis, A. S. , & Jacobs, D. F. (2005) . Quantifying root system quality of nursery seedlings and relationship to outplanting performance. New Forests, 30(2-3), 295-311.

Food and Agriculture Organization of the United Nations. (2015). Global Forest Resources Assessment 2015: How are the World's Forests Changing. Food and Agriculture Organization of the United Nations.

FORRU. 2006. Planting trees. In: Elliott, S., Blakesley, D., Maxwell, J.F., Doust and Suwannaratana. S. How to plant a forest: the principles and practices of restoring tropical forests. Biology Department, Science Faculty, Chiang Mai University, Chiang Mai p. 103–132.

Louppe. D.. and OuaUara, N'klo. 1992. Growth of Faidherbfa albfda in nurseries: standard production techniques or air pruning? Pages 141143ill Faidherbia albidfl in the West African semi~arid tropics: proceedings of a workshop, 22-26 Apr 1991, Nlamey, Niger (Vandenbeldt, R.J.,ed.), Patnncheru, A,P. 502 324, India: International Crops Research 1nstltute for the Semi- Arid Tropics; Ilnd Nairobi, Kenya: Jnternallonal Centre for Research in Agroforestry.

Mitre, V., Mitre, I., Sestras, A. F., & Sestras, R. E. (2012). Effect of Roots Pruning upon the Growth and Fruiting of Apple Trees in High Density Orchards. Bulletin of the University of Agricultural Sciences & Veterinary

Medicine Cluj-Napoca. Horticulture, 69(1).

Marler, T. E., & Willis, D. (1996). Chemical or air root-pruning containers improve carambola, longan, and mango seedling root morphology and initial root growth after transplanting. Journal of environmental horticulture, 14(2), 47-49.

Pérez-Harguindeguy N., Díaz S., Garnier E., Lavorel S., Poorter H., Jaureguiberry P., Bret-Harte M. S., Cornwell W. K., Craine J. M., Gurvich D. E., Urcelay C., Veneklaas E. J., Reich P. B., Poorter L., Wright I. J., Ray P., Enrico L., Pausas J. G., de Vos A. C., Buchmann N., Funes G., Quétier F., Hodgson J. G., Thompson K., Morgan H. D., ter Steege H., van der Heijden M. G. A., Sack L., Blonder B., Poschlod P., Vaieretti M. V., Conti G., Staver A. C., Aquino S. and Cornelissen J. H. C.. (2013). New handbook for standardised measurement of plant functional traits worldwide. Australian Journal of Botany, 61, 167-234.

R Core Team (2018). R: A language and environment for statistical computing. R Foundation for Statistical Computing, Vienna, Austria. URL https://www.R-project.org/.

Van Sambeek, J. W., Godsey, L. D., Walter, W. D., Garrett, H. E., & Dwyer, J. P. (2016). Field Performance of Quercus bicolor Established as Repeatedly Air-Root-Pruned Container and Bareroot Planting Stock. Open Journal of Forestry, 6, 163-176.

Watson, G. W., & Sydnor, T. D. (1987). The effect of root pruning on the root system of nursery trees. Journal of arboriculture (USA).

Walker, J. (2005). Development and construction of an air-pruning propagation bench, and its proper use. Guidebook for Native Plant Propagation. ESRM 412 – Native PlantProduction,http://depts.washington.edu/propplnt/Chapters/air-pruning.htm#_edn9

The Effect of the Solid Retention Time on Simultaneous COD, TKN, and TP Removal from Slaughterhouse Wastewater Using Sequencing Batch Reactor

Siriluck Pinvattanachai[1,2] Withida Patthanaissaranukool[1,2] and Chaowalit Warodomrungsimun[1,2*]

[1]Department of Environmental Health Sciences, Faculty of Public Health, Mahidol University, Thailand
[2]Center of Excellence on Environmental Health and Toxicology (EHT), Thailand
Corresponding author: email: chaowalit.war@mahidol.ac.th

ABSTRACT

This study investigated the effect of short sludge retention time (short SRT) compare with a prolonged sludge retention time (prolonged SRT) on the performance of Sequencing Batch Reactor (SBR) system for chemical oxygen demand (COD), total kjeldahl nitrogen (TKN), and total phosphorus (TP) removals from the slaughterhouse wastewater treatment. In addition, the phosphorus accumulation in sludge was investigated. The operation of the SBR was controlled by sludge ages as short SRT at 20 and 25 days and prolonged SRT at 60 days with anaerobic/anoxic I/oxic I/anoxic II/oxic II sequencing batch reactor (AnA^2/O^2 SBR) operated a cycle time of 12 hours. This system performed under anaerobic static fill (0.5 hours), reaction time (8 hours), settling time (0.5 hours), draw time (0.25 hour), and idle time (2.75 hours). The results showed that in all SRT had the removal efficiencies of COD and TKN more than 95%. However, SRT 60 days had removal efficiencies of COD, TKN, and TP was 95.9, 95.9, and 56.4%, respectively, which it was the lowest performance when compared with SRT 20 and 25

days. This result indicated increasing sludge age or SRT effect to decreasing TP removal in wastewater.

Keywords: Sludge Retention Time (SRT), P-content, Sequencing Batch Reactor (SBR), Nutrient Removal, Slaughterhouse wastewater

INTRODUCTION

The capacity of the food industry was increased with the increase of human needs. The picture was shown in the current situation as the food industries in Thailand gets to top exporter in the world (Ministry of Industry, 2017). This increase result in increasing the growth of the meat processing industry. In addition, this industry has generated high-strength organic wastewater during slaughtering and cleaning operation.

The characteristics of slaughterhouse wastewater (SHWW) have consisted of high organic matters and nutrients (nitrogen and phosphorus). The constituents of concern in SHWW are urine, blood, fat, and tissues, etc. Thus, SHWW has to treatment before discharge into the environment. Effect of high organic matter and nutrients to a natural water source may result in oxygen levels in the water decreased, leading to the death of aquatic animal life. From the study of wastewater characteristics of swine slaughterhouse, the parameters are as follows: COD (1250 - 15,900 mg/L), TN (50 – 841 mg/L), and TP (25 - 200 mg/L) (Lecompte et al., 2017). Nitrogen and phosphorus are essential for the growth of the plant so, they make to the rapid growth of aquatic plants such as the algae bloom or eutrophication.

Phosphorus is an essential element for plants. At the present, found nature phosphorus had a trend to decrease (Faculty of Science, Mahidol University, 2015) and Phosphorus is an element that occurs naturally very slowly. Or, it may bis

an element cannot occur naturally (Rambo PW, 2014). Therefore, phosphorus recovery for further use is important.

Sequencing Batch Reactor (SBR) is a biological wastewater treatment that organic substance in wastewater can be removed by microorganism in the SBR system. The SBR system has been successfully used to treat both municipal and industrial. Equalization, aeration, biological treatment, and clarification can all be achieved using a single tank using a timed control sequence.

The biological wastewater treatment for SHWW in this research using the Sequencing Batch Reactor (AnA^2/O^2 SBR) system. This system is processes used for simultaneous COD, N and P removal by alternating working conditions of anoxic and oxic in one cycle (Buayoungyuen et al., 2016).

The system was controlled by sludge retention time (SRT) or sludge age. Phosphorus removal from this system will be leading to phosphorus accumulation in sludge.

Thus, this research aims to investigate the removal efficiency of COD, TKN, TP, and phosphorus accumulation in sludge which is controlled by different SRT.

MATERIALS AND METHODS

Experimental Setup and Research Design

The reactor consisted of a 4-liter acrylic cylinder with a diameter at 13 cm, a length of 37 cm, with both ends of the cylinder sealed. Aeration and agitation were provided by using an air pump/air diffusers and stirrer as linking with a slowly rotating motor (30 rpm). The schematic diagram of AnA^2/O^2 SBR was presented in Figure 1. The reactor of experimental was set up and operated at the laboratory of Environmental Health Sciences Department, Faculty of Public Health, Mahidol University.

Sludge biomass was collected from activated sludge line of Din Daeng wastewater treatment plant (BMA). Slaughterhouse wastewater used in this study was collected from

swine slaughterhouse industry at Nakhon Pathom, Thailand. The slaughterhouse wastewater characteristics are illustrated in Table 1. Sludge biomass was acclimatized in three reactors (initial MLSS concentration at 1,500 mg/L in each reactor) by Influent feeding step by step, starting from 10%, 20%, 50%, 75% and 100% of the total working volume. Until the system reaches to steady state.

The slaughterhouse wastewater was treated by an AnA^2/O^2 which the system was operated with varying the solid retention times (SRTs) (20, 25 and 60 days) at cycle time of 12 hours; anaerobic static fill (0.5 hours), anoxicI/oxicI/anoxicII/oxicII (1.5/2.5/2.5/1.5 hours), settle time (0.5 hours), draw time (0.25 hour) and idle time (2.75 hours). This system was controlled by COD loading (800-1,500 mg/L), the oxic period has dissolved oxygen (DO) (2-4 mg/L) and pH (6.5-8.5).

The analyzed of COD, TKN, and TP from Influent and effluent of the SBR system were used to describing the system performance and removal efficiencies. The parameter was COD, TKN, TP, and MLSS also followed the standard method (APHA, 2012) as shown in Table 2.

The SRTs will be maintained constantly by wasting the sludge and can be calculated following the Equation (3.1) and (3.2).

$$SRT\,(d) = \frac{MLSS \times V_W}{MLSS_W \times MLSS_V} \quad \ldots(3.2)$$

Assuming completely mixed, so $MLSS \approx MLSS_W$

$$MLSS_V\,(L/d) = \frac{V_W}{SRT\,(d)} \quad \ldots(3.3)$$

By

MLSS is Mixed Liquor Suspended Solids (mg/L)

$MLSS_V$ is wasted MLSS volume (L/d)

$MLSS_W$ is wasted MLSS (mg/L)

V_W is working volume of reactor (L)

Table 1 characteristics of slaughterhouse wastewater

Parameter		Range	Average
pH		6.8 - 7.3	7.0 ± 0.2
BOD	(mg/L)	758.7 - 2,820.0	1,754.3 ± 758.7
COD	(mg/L)	978.7 - 4,884.0	2,452.6 ± 913.8
TKN	(mg/L)	98.0 - 170.8	135.8 ± 27.4
NH_3-N	(mg/L)	34.2 - 77.8	56.4 ± 17.8
TP	(mg/L)	31.4 - 37.3	35.2 ± 2.7
TSS	(mg/L)	438.0 - 580.0	509.0 ± 71.0

Data of average are given as mean ± SD and range are given as min-max

Table 2 Analytical methods

Parameter	**Method**	**Standard Code**
COD	Close Reflux, Titrimetric Method	5220 C
TKN	Macro-Kjeldahl Method	4500-N_{org} B
TP and P-content	Sulfuric-Nitric Acid Digestion and Colorimetric Method (Vanadomolybdophosphoric Acid)	4500-P C
MLSS	Gravimetric Method	2540 D

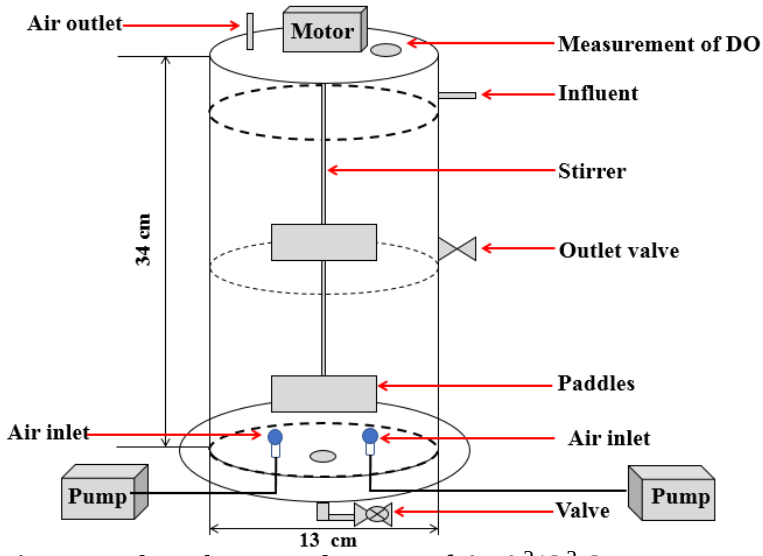

Figure 1 The schematic diagram of AnA^2/O^2 SB

RESULTS AND DISCUSSION

System performance

The system performance of AnA^2/O^2 SBR system treating slaughterhouse wastewater was shown in the form of COD, TKN, and TP removal.

The slaughterhouse waste-water (SHWW) has an average influent characteristics as follows: COD (1,151.0 ± 228.4 mg/L), TKN (65.5 ± 23.5 mg/L) and TP (29.1 ± 14.4 mg/L). The removal efficiencies of COD, TKN, and TP was shown in Table 3.

Furthermore, the concentrations of COD, TKN, and TP in effluent were lower the limitation of the effluent discharge standard or met the standard requirement (PCD, 2017).

Effect of SRT to COD

From the study of COD removal in SHWW found SRT 25 days was highest in COD removal efficiency (Table 3). The statistical analysis found in each SRT wasn't significantly differed ($p>0.05$) for the efficiency of COD removal. This result indicated that this system could remove COD in a high rate similar in each SRT which in Slaughterhouse wastewater contains organic substances (BOD ~ 80% of COD). Organic substances in wastewater will be degraded by microorganisms in the system. This processes occurred in nitrogen and phosphorus removal which operated according to the alternating system state of anoxic and oxic phase.

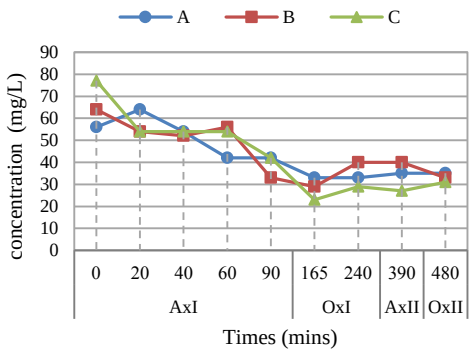

Figure 2 Cyclic profile of COD removal. (A) SRT 20 days; (B) SRT 25 days; (C) SRT 60 days. Ax is Anoxic condition, Ox is Oxic Conditio

The pattern of COD removal shown in the cyclic profile (Figure 2). COD was degraded rapidly during the first anoxic I in all SRT, indicating that

the sludge age does not affect the COD removal efficiency.

Table 3 System performance of SRT 20, 25 and 60 days

Parameter	SRT 20 days		SRT 25 days		SRT 60 days	
	Effluent (mg/L)	Removal (%)	Effluent (mg/L)	Removal (%)	Effluent (mg/L)	Removal (%)
COD	55.2	94.9[a]	40.0	96.3[a]	45.0	95.9[a]
TKN	2.1	96.7[a]	1.9	96.9[a]	2.2	95.9[a]
TP	3.9	85.7[a]	1.2	95.9[b]	11.8	56.4[c]

Data of effluent are given as an average value

Different superscript letters ([a, b, c]) are significant differences ($p < 0.05$)

Effect of SRT to TKN

From the study of TKN removal in SHWW found that at SRT 25 days had the highest TKN removal efficiency was 96.9%. When statistical analysis found that in each SRT wasn't a statistical difference for TKN removal efficiency. This result similarly with the study of Buayoungyuen et al., (2016) and Saikomon et al, (2017). In addition, the result found that the average value of carbon to nitrogen (C: N) ratio of influent wastewater was 15:1. In accordance with the research of Dhiriti et al., (2010) suggested that the optimum carbon to nitrogen (C: N) ratio of 10:1 for successful removal of nitrogen from the wastewater. The SBR operated with a C: N ratio of 10:1 can be removed more than 90% of nitrogen. The ratio of C: N is not less than 12.5: 1 that could be the process of denitrification

is complete (Panswad, 2002). However, the increase in SRT didn't increase nitrogen removal.

Effect of SRT to TP

From the study of TP removal in SHWW found that at SRT 25 days had the highest of TP removal efficiency. When statistical analysis found that TP removal efficiency in each SRT was significantly different ($p < 0.05$). However, the result has shown that at low SRT (20 and 25 days) had TP removal efficiency more than 85%, but when increasing sludge age was SRT 60 days found that reduced phosphorus removal. This result agreeable with (Chuang et al., 1977) reported that lower SRT values are generally recommended to achieve the low effluent TP concentrations. And higher phosphorus removals would be found when SRT was operated for less than 25 days. The biological treatment system is operated with a high sludge age requires a higher ratio of COD: P than a low sludge age. The wastewater will have the same low phosphorus concentrations (Panswad, 2002).

Phosphorus accumulation in sludge

In the process of biological wastewater treatment, phosphorus was removed from the wastewater by microorganisms (Polyphosphate accumulating organism, PAO). The major process of Bio-P removal was accumulated in sludge biomass. The percentage of phosphorus content in sludge biomass was shown in Figure 3. From the results, it was found that P-content slightly decreased when increasing the SRT. However, when the statistical testing found P-content in each SRT wasn't significantly differ ($p>0.05$). Increasing SRT of the system means the potential of P removal by sludge wasting is reduced as the biomass production decreases (Zhu et al., 2018). The phosphorus uptake into the cell depends on the amount of phosphorus released by PAO which if the sludge age is increased, the system will have a lower phosphorus release rate (Panswad, 2002). The phosphate uptake rate of microbial in aerobic conditions depending on the

concentration of PHA in biomass, which is based on organic matters and phosphorus in wastewater. Moreover, if the system had more phosphorus dissolve outside the microbial cell, the phosphorus uptake rate will increase. (Amornwit, 1999).

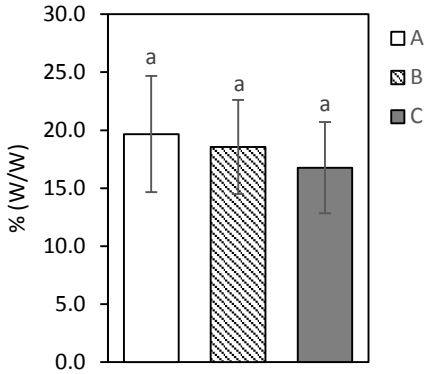

Figure 3 Phosphorus accumulation in sludge. SRT 20 days (A); SRT 25 days (B); SRT 60 days (C). Different superscript letters (a) are significant differences ($p < 0.05$)

CONCLUSIONS

The optimal operation was obtained at SRT 25 days with average COD, TKN and TP removal efficiencies of 96.3%, 96.9%, and 95.9%, respectively. However, the P-content of each SRT did not significantly differ ($p > 0.05$). The phosphorus was accumulated in biomass that an important for the process of phosphorus recovery, that will be the further use, such as fertilizer.

ACKNOWLEDGEMENT

This research work was supported by a grant from the Center of Excellence on Environmental Health and Toxicology (EHT).

REFERENCES

Amornwit B. Response of an EBPR/SBR process to the partial addition of orthophosphate at the aerobic stage. 1999. Available from:http://cuir.car.chula.ac.th/handle/123456789/10988.

APHA. Standard methods for the examination of water and wastewater. 22nd ed. American Public Health Association: Washington DC, USA. 2012.

Buayoungyuen S, Warodomrungsimun C, Feungpean M, Fongsatitkul P. Anaerobic Sequencing Batch Reactor (AnA^2/O^2 SBR) under Short Cycle Time and SRTs in Treating Slaughterhouse Wastewater. Asia J Public Health 2016; 7: 4-11.

Chuang SH, Ouyang CF, Yuang HC, You SJ. Effects of SRT and do on nutrient removal in a combined as-biofilm process. Water Science and Technology 1997; 36: 19-27.

Dhiriti R, Komi H, Raj B. Effect of carbon to nitrogen (C: N) ratio on nitrogen removal from shrimp production wastewater using sequencing batch reactor. J Ind Microbiol Biotechnol 2010; 37:1105–1110.

Faculty of Science; Mahidol University. Phosphorus Crisis – World Crisis. 2015. Available from: http://www.sc.mahidol.ac. th/usr/?p=461.

Lecompte CB, Mehrvar M, Bolaños EQ. Slaughterhouse Wastewater Characterization and Treatment: An Economic and Public Health Necessity of the Meat Processing Industry in Ontario, Canada. Journal of Geoscience and Environment Protection 2016; 4: 175-86.

Ministry of industry. Trend of Thailand industrial food in 2017. Available from: http://www.industry.go.th/industry/index.php/th/knowledge/item/39443-020525601645.

Panswad T. Biological nitrogen and phosphorus removal. 2nd ed. Bangkok: Environmental Engineering Association of Thailand; 2002.

PCD. Effluent standard. 2560. Available from: http://www.pcd.go.th/info_serv/ reg_std_water04.html.

PCD. Pollution problem complaint statistics. 2560. Available from: http://www.pcd.go.th/info_serv/pol2_stat2560.html.

Rambo PW. Soil fertility and plant nutrition. 2014. Available from: https://ag2.kku.ac.th/eLearning/132351/Doc/132351%20Lec7%20NutrTransport-57.pdf.

Saikomon S, Fongsatitkul P, Elefsiniotis P. Treatment of a Slaughterhouse Wastewater using Sequencing Batch Reactors at a Shortened Operating Cycle. Environment Asia 2017; 10: 9-16.

US EPA. The Problem Nutrient Pollution. 2017. Available from: https://www.epa.gov/nutrientpollution/problem.

Zhu Z, Chen W, Tao T, Li Y. A novel AAO-SBSPR process based on phosphorus mass balance for nutrient removal and phosphorus recovery from municipal wastewater. Water Research 2018; 144: 763-773.

Start-up of aerobic granulation in sequencing batch reactors treating acetate synthetic wastewater

Saengjan Boonket[1*] and Saroch Boonyakitsombut[2]

[1]Graduate student, Department of Environmental Engineering, Faculty of Engineering, King Mongkut's University of Technology Thonburi, Bangkok 10140, Thailand

[2]Assistant Professor, Department of Environmental Engineering, Faculty of Engineering, King Mongkut's University of Technology Thonburi, Bangkok 10140, Thailand

Corresponding author: email: saengjan.b@mail.kmutt.ac.th

ABSTRACT

Aerobic granules are large biological aggregates with compact interiors that can be used in efficient wastewater treatment. The main objective and minor objective of this work were to study aerobic granulation during start-up period and to compare efficiency of SBRs between with and without calcium carbonate addition. In this work aerobic granulation was investigated in two laboratory scale sequencing batch reactors (SBRs). Both reactors were fed with acetate synthetic wastewater and operated under similar conditions during the experiment. Reactor SBR1 was augmented with $CaCl_2$ solution, while $CaCO_3$ powder was added into the reactor SBR2. The influent COD and NH_4^+-N concentrations to the SBRs were kept at 1000 $mgL^{-1}$and 60 mgL^{-1}, respectively. The organic loading rate of 2 kg COD $m^{-3}day^{-1}$ with hydraulic retention time of 12 hours was controlled. The reactors were operated under room temperature (28±2°C). The results showed that, after operation of 128 days, aerobic granules were observed in both reactors. The nitrification were

occurred in both reactors. The reactor SBR2 had a slightly higher treatment efficiency than reactor SBR1. The COD, BOD and TKN removal efficiencies of both reactors were higher than 95%, 97% and 80%, respectively. The Ratio of the mixed liquor volatile suspended solids to mixed liquor suspended solids (MLVSS/MLSS ratio) of reactor SBR1 and SBR2 were 0.65 and 0.60, respectively.

Keywords: Aerobic granules, Granulation, Start-up, SBRs, $CaCO_3$

INTRODUCTION

Aerobic granulation technology has become attractive in wastewater treatment, which is a novel biotechnology and promising approach to overcome the principal weaknesses of the activated sludge process. Aerobic granules have strong and compact microbial structure, excellent settle ability, high biomass retention, resistance to shock load and toxicity of pollutants in wastewater. (Adav et al., 2008; Lee et al., 2010) Aerobic granulation has been applied in a wide range, both municipal and industrial wastewater. However, reluctance to accept this technology is mainly from long start-up time and high difficulty of granulation. (Pijuan et al., 2011)

Recently, various efforts have been developed to shorten the start-up time of aerobic granulation, such as optimization of operation conditions, augmentation process and introduction of nucleus were quite effective for the acceleration of aerobic granulation. (Liu et al., 2008; Liu et al., 2014; Zhou et al., 2015) Calcium carbonate ($CaCO_3$) was accumulated at core of aerobic granules. The calcium accumulated granules have high structure strength. (Ren et al., 2008) Calcium precipitate formed at core can serve as nuclei for subsequent cell attachment and granule growth. (Wan et al., 2015) The purpose of this study was to investigate the effects of calcium carbonate on aerobic granulation during start-up period and reactor performance by using acetate synthetic wastewater.

METHODOLOGY

Experimental set-up and SBR operation

Two identical aerobic sequencing batch reactors (100 cm in height and 12 cm in diameter with a working volume of 10 L in each reactor) were used in this study. Air was introduced through a diffuser at the reactor bottom by air pump. The dissolved oxygen (DO) concentration was 0.5-3 mgL^{-1} during aeration. The experiments were conducted at a room temperature of 28±2ºC. The first reactor SBR1 was augmented with $CaCl_2$ solution at 50 mgL^{-1} Ca^{2+}, while $CaCO_3$ powder at 50 mgL^{-1} Ca^{2+} was added into the reactor SBR2. Both reactors were operated under the same condition. The schematic diagram of experiment set-up was shown in Fig. 1.

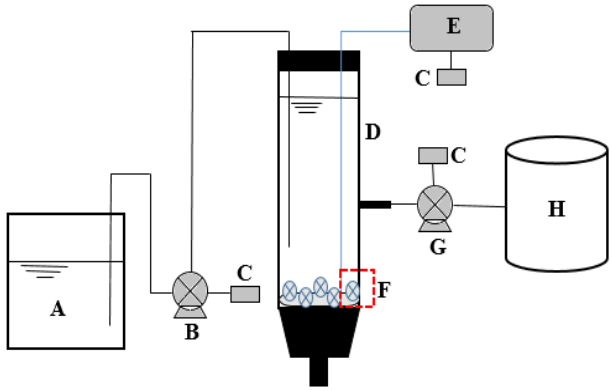

Figure 1 experiment set-up: (A) Influent tank; (B) Influent pump; (C) Timer; (D) Reactor; (E) Air pump; (F) Air diffuser; (G) Effluent pump; (H) Effluent tank

The reactor was operated sequentially with a cycle time of 6 hours, which included 10 min of influent filling, 275-305 min of aeration, 30-60 min of settling and 15 min of effluent discharging from the middle port of the reactor with a volumetric exchange ratio of 50%. The cycle configuration was modified during the operation and shown in detail in Table 1. This operation resulted in 12 hours hydraulic retention time (HRT). The organic loading rate was 2 kg COD $m^{-3}d^{-1}$.

Table 1 Operation of the SBRs cycle

Stage	Period 1	Period 2
Filling (min)	10	10
Aeration (min)	275	305
Settling (min)	60	30
Discharging (min)	15	15
Total cycle duration (min)	360	360

Influent and inoculum

Synthetic wastewater was used in this experiment with sodium acetate as organic source. The composition of synthetic wastewater was follows (in mgL^{-1}): Sodium acetate, 2273; NH_4Cl (N source), 200; K_2HPO^4 (P source), 60; $CaCl_2$, 80; $MgSO_4$, 30; $FeSO_4$, 20 (Liu et al., 2016). The influent pH was adjusted to 7.0 by adding 2 M HCl solution. In addition, 1.0 mL of trace element solution was added into 20 L influent which contained (in mgL^{-1}): H_3BO_3, 50; $ZnCl_2$, 50; $CuCl_2$, 30; $MnSO_4$, 50; $(NH_4)_2Mo_7O_{24}$, 50; $AlCl_3$, 50; $CoCl_2.6H_20$, 50 and $NiCl_2$, 50 (Ren et al., 2008). The COD concentration was about 1000 mgL^{-1}, NH_4^+-N about 60 mgL^{-1} and Phosphorus about 10 mgL^{-1}.

Activated sludge taken from sludge recycling tank in Thung-khru wastewater treatment plant was used as Seed sludge for the reactors at a respective initial sludge concentration of 6000 mgL^{-1} in mixed liquor suspended solids (MLSS) and mixed liquor volatile suspended solids (MLVSS) of 3300 mgL^{-1} in two reactors. The ratio value of MLVSS/MLSS was about 55%. The seed sludge was dark brown in color and had a sludge volume index (SVI) was about 92 mLg^{-1}.

Analytical methods

To evaluate the treatment system efficiency, pH, COD, BOD, TKN, NO_2^-, NO_3^-, phosphorus, mixed liquor suspended solids (MLSS), mixed liquor volatile suspended solids (MLVSS), sludge volume index (SVI), dissolved oxygen

(DO) and temperature were monitored. The samples were periodically collected and analyzed according to APHA standard. The samples were filtered passed through a 0.47 µm pore size filter (GF/C diameter 47 mm, Whatman). The pH and DO concentrations were measured with a pH meter (SevenGo, Mettler toledo) and DO meter (HQ40d, Hach), respectively. The morphology of microbial aggregates were visualized using a light microscope (BH2, Olympus).

RESULTS AND DISCUSSION

Morphology variation of aerobic granules

Through microscopy observation, (Fig. 2 A) the initial seed sludge was typical floc with a fluffy, irregular and loose morphology. In the process of aerobic granulation, after 30 days of operation, biomass increased and most microbes of both reactors were dark brown and mainly in floc form (Fig. 2 B and C). During the operation, floc in both reactors were broken and discharged out with the effluent discharge. To fix this problem, therefore, the aerated rate was reduced and the settling- time was increased from 30 to 60 min. After 100 days, small sludge particles appeared in both reactors, shown in Fig. 2 D and E. Over the next 128 days, the flocs gradually changed to granular sludge with time. The aerobic granulation continuously developed in both reactors. (Fig. 2 F and G)

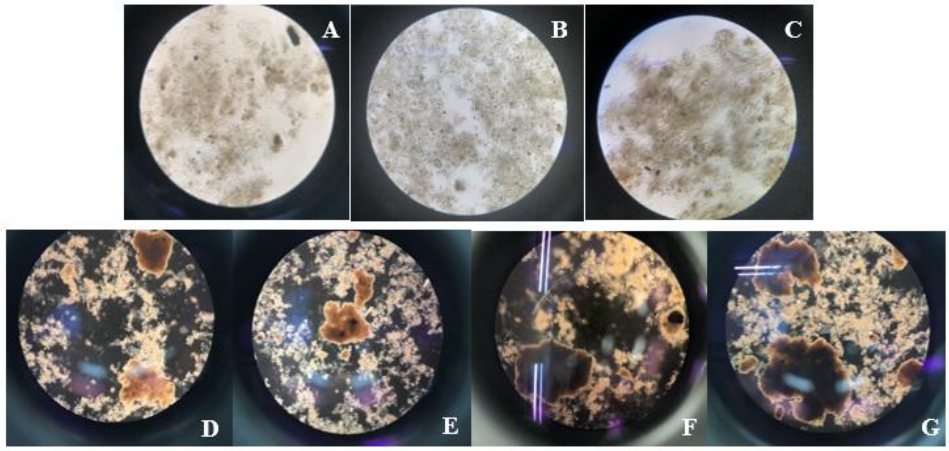

Figure 2 The morphological variation of microbes (Magnification = 40×):
(A) initial seed sludge, (B) the sludge after 30 days in SBR1 and (C) SBR2, (D) the sludge after 100 days in SBR1 and (E) SBR2, (F) the sludge after 128 days in SBR1 and (G) SBR

Biomass profile and settling property

MLSS and SVI values were used to evaluate the performance of aerobic granules. The variation of both MLSS and SVI in both reactor SBR1 and SBR2 was compared within 128 days of operation, as indicated in Fig. 3 and 4. MLSS values in reactor SBR1 and SBR2 decreased from 6000 mgL^{-1} on day 1 to 5312 mgL^{-1} and 5300 mgL^{-1} on day 128, respectively. However, the MLSS value slightly decreased after day 30, probably due to the loss of biomass in the effluent. The sludge observed the early stage showed poor settling property, as indicated by a high SVI value of 125.8 mLg^{-1} and 120.3 mLg^{-1} in reactor SBR1 and SBR2 on day 30, respectively. Filamentous bacteria occurred in both reactors, then increased SVI value to 280.7 mLg^{-1} in SBR1 and 290 mLg^{-1} in SBR2 on day 95. As the sludge flocs were gradually transformed into granular sludge, the SVI value decreased to 84.1 mLg^{-1} in reactor SBR1 and 83.8 mLg^{-1} in reactor SBR2 on day 128.

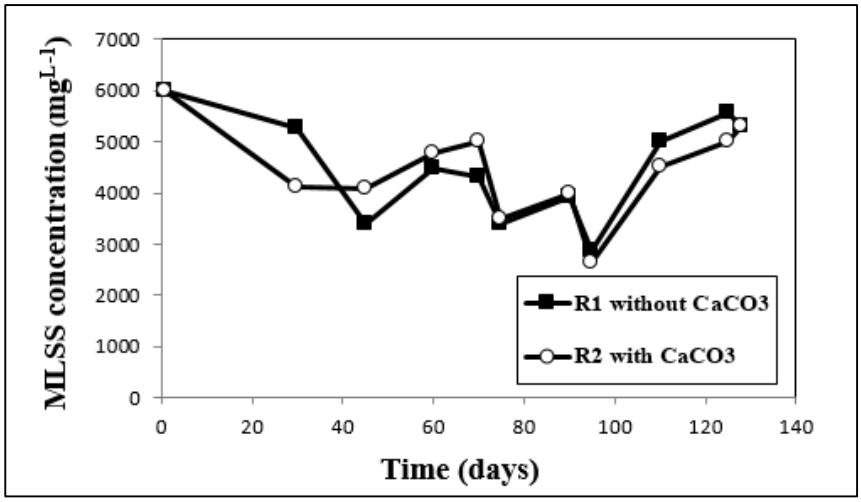

Figure 3 Variation of MLSS in SBR1 and SBR2 during 128 days of operation

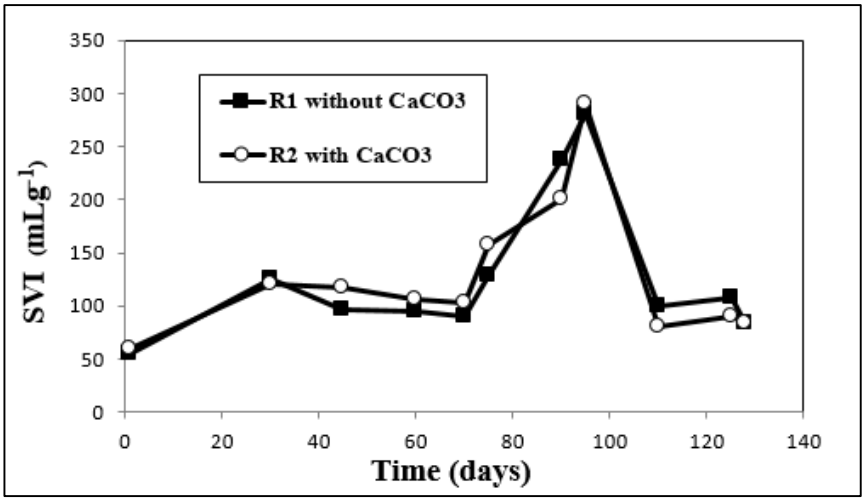

Figure 4 Variation of SVI in SBR1 and SBR2 during 128 days of operation.

The MLVSS/MLSS ratios of reactor SBR2 with $CaCO_3$ powder augmentation was about 0.60 and reactor SBR1 without $CaCO_3$ augmentation was about 0.65. The MLVSS/MLSS ratio was similar in the two reactors. (Fig. 5).

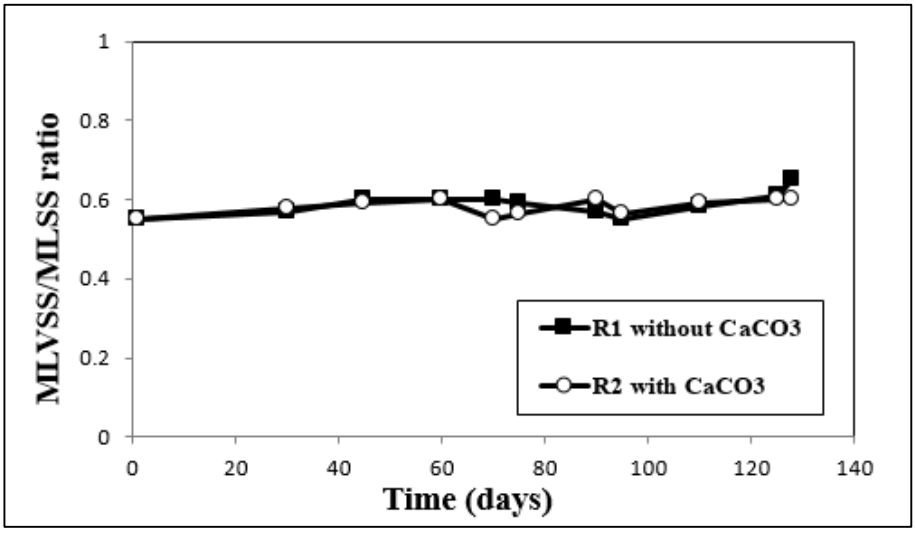

Figure 5 MLVSS/MLSS ratios in SBR1 and SBR2 during 128 days of operation.

Reactor performance and effluent quality

In this experiment, influent COD and BOD concentrations were 1000 mgL^{-1} and 750 mgL^{-1}, respectively. Average effluent COD and BOD concentrations of both reactors were 28.7 mgL^{-1},12.2 mgL^{-1} in reactor SBR1 and 20.2 mgL^{-1}, 8.21 mgL^{-1} in reactor SBR2, respectively. (Fig. 6 and 7). With influent TKN concentration of 60 mgL^{-1}, average effluent TKN concentration was 6.58 mgL^{-1} in reactor SBR1 and 5.74 mgL^{-1} in reactor SBR2 (Fig. 8). Compared to the industrial effluent standard of Thailand (Ministry of industry, 1996) (COD and BOD concentrations must be less than 120 mgL^{-1} and 20 mgL^{-1}, respectively), effluent quality passed the standards. The nitrification were also occurred in both reactors as shown in Fig. 9.

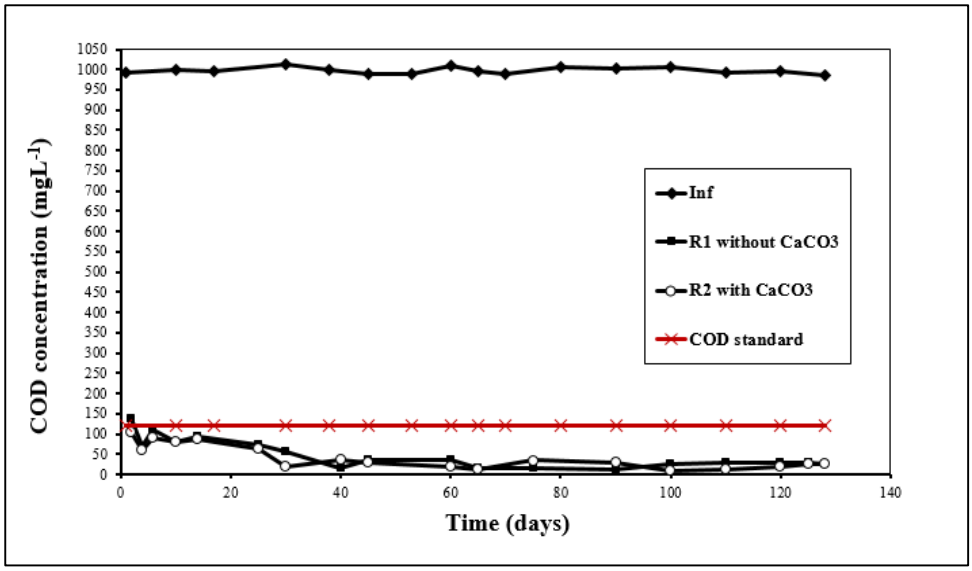

Figure 6 Influent and effluent concentration of COD in SBR1 and SBR2.

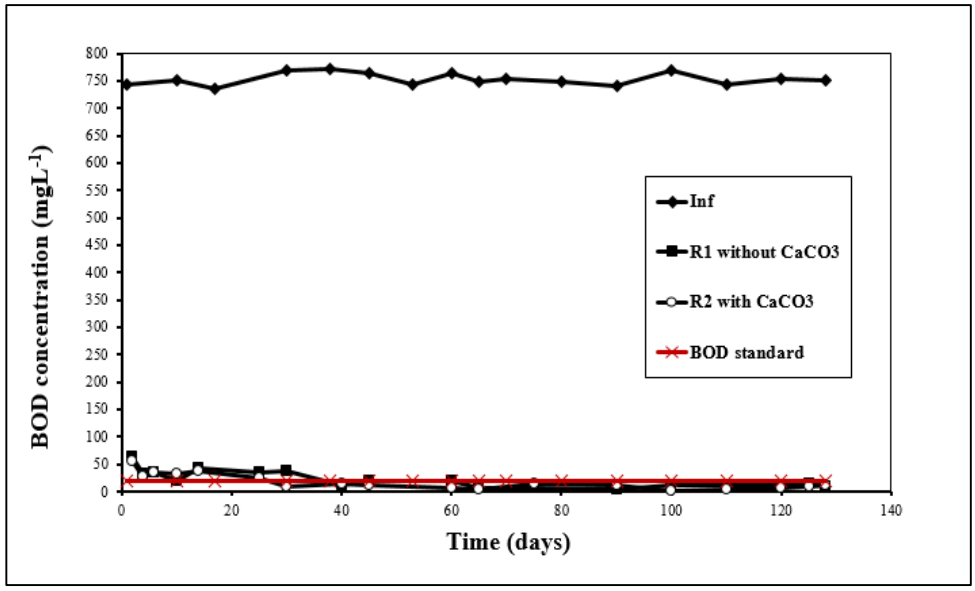

Figure 7 Influent and effluent concentration of BOD in SBR1 and SBR2.

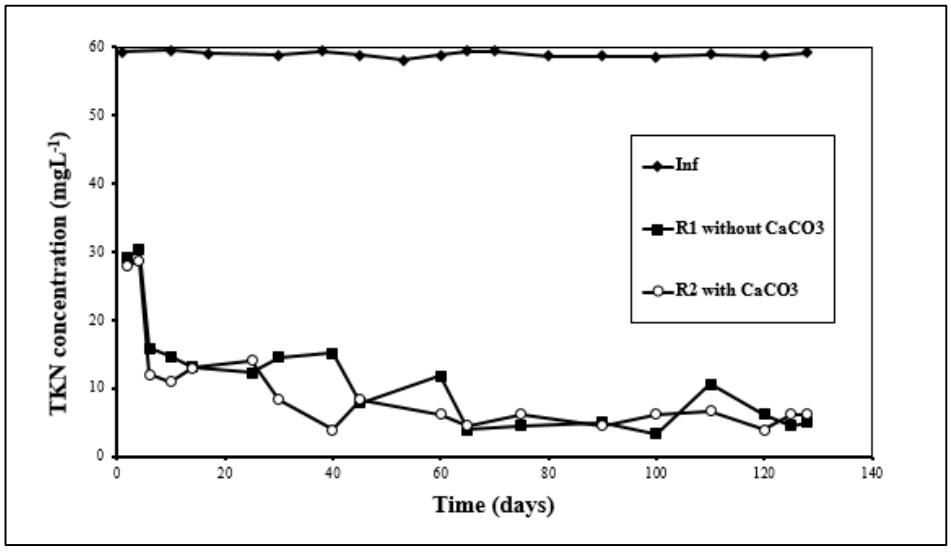

Figure 8 Influent and effluent concentration of TKN in SBR1 and SBR2.

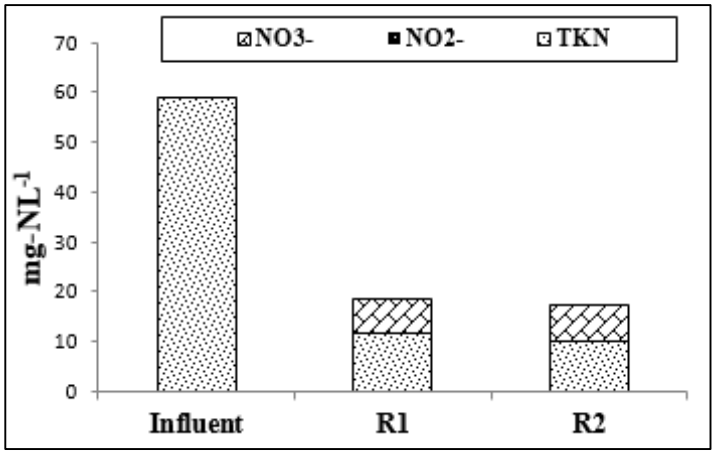

Figure 9 TKN effluent, NO_2^- and NO_3^- in SBR1 and SBR2.

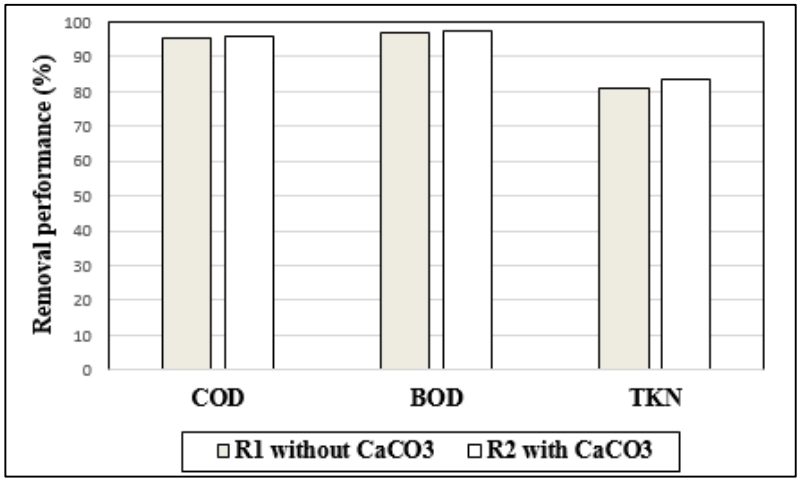

Figure 10 Overall of removal performance in reactor SBR1 and SBR.

Fig. 10 demonstrates the overall removal performance of reactor SBR1 and SBR2, the COD, BOD and TKN removal efficiencies of both reactors were higher than 95%, 97% and 80%, respectively. The COD efficiency of reactors SBR1 and SBR2 were 95.5% and 95.8%, respectively. The BOD efficiencies of reactors SBR1 and SBR2 were 97.1% and 97.6%, respectively. The TKN efficiencies of reactors SBR1 and SBR2 were 80.8% and 83.5%, respectively.

CONCLUSIONS

During start-up period, aerobic granules were observed in both SBRs. In comparison, the reactor performance of both reactors were similar, the COD,

BOD and TKN removal efficiencies were higher than 95%, 97% and 80%, respectively. Average effluent COD and BOD concentrations of both reactors were less than 120 mgL^{-1} and 20 mgL^{-1}, respectively.

ACKNOWLEDGEMENTS

The authors are grateful to the Thung-khru wastewater treatment plant for supports with seed sludge and department of Environmental Engineering, Faculty of Engineering, King Mongkut's University of Technology Thonburi, Bangkok, Thailand.

REFERENCES

Adav SS, Lee DJ, Show KY and Tay JH, Aerobic granular sludge: Recent advances, Biotechnol 2008; 26: 411-423.

Lee DJ, Chen YY, Show KY, Whiteley CG and Tay JH, Advances in aerobic granule formation and granule stability in the course of storage and reactor operation, Biotechnol 2010; 28: 919-934.

Pijuan M, Werner U and Yuan Z, Reducing the start-up time of aerobic granular sludge reactors through seeding fluccular sludge with crushed aerobic granules, Water Res 2011; 45: 5075-5083.

Liu YQ and Tay JH, Influence of starvation time on formation and stability of aerobic granules in sequencing batch reactor, Bioresour 2008; Technol. 99: 980-985.

Liu Z, Liu YJ, Zhang AN, Zhang C and Wang XC, Study on the process of aerobic granule sludge rapid formation by using the poly aluminum chloride (PAC), Chem Eng 2014; 250: 319-325.

Zhou JH, Zhou H, Hu M, Yu HT, Xu XY, Vidonish J, Alvares PJJ and Zhu L, Granular activated carbon as nucleating agent for aerobic sludge granulation: Effect of GAC size on velocity field differences (GAC versus flocs) and aggregation behavior, Bioresour Technol 2015; 198: 358-363.

Ren TT, Liu L, Sheng GP, Liu XW, Yu HQ, Zhang MC and Zhu JR, Calcium spatial distribution in aerobic granules and its effects on granule structure, strength and bioactivity, Water Res 2008; 42: 3343-3352.

Wan C and Lee DJ, Calcium precipitate induced aerobic granulation, Bioresour Technol 2015; 176: 32-37.

Liu YQ, Lan GH and Zeng P, Size-dependent calcium carbonate precipitation induced microbiologically in aerobic granules, Chem Eng 2016; 285: 341-348.

Notification of ministry of Industry, Issued under Factory Act. 1992, The Royal Government Gazett 1996; Vol.113: part 52D

Optimization of Factors Affecting the Biosynthesis of Silver Nanoparticles Using Orange Peel Extract

Cathleen Ariella Simatupang[1*], Vinod K. Jindal[2], Ranjna Jindal[1]

[1]Department of Civil and Environmental Engineering, Mahidol University, Thailand [2]Department of Chemical Engineering, Mahidol University, Thailand

Corresponding author: email: cathleen.ariella@gmail.com

ABSTRACT

Interest in the biosynthesis of silver nanoparticles (AgNPs) has been steadily increasing over the past years in view of their numerous applications in various fields primarily due to low-cost, use of non-toxic environmentally friendly materials and ease of operation. This study investigated the influence of the experimental factors on the absorbance spectra and particle size in biosynthesis of AgNPs using orange peel extract as the reducing agent. A central composite design in response surface methodology was used with orange peel extract concentration, pH and silver nitrate concentration as independent variables. The biosynthesized AgNPs were characterized by UV-Vis spectroscopy in 350-550 nm wavelength range for monitoring absorbance spectra and dynamic light scattering to determine the particle size. The developed models accounted for the effects of peel extract concentration, pH and $AgNO_3$ concentration on peak absorbance and a characteristic shift in wavelengths, and particle size. Results showed that pH had the maximum influence on the formation of AgNPs compared to orange peel extract and silver nitrate concentrations. An increase in pH led to an increase in the peak absorbance values, and a corresponding decrease in AgNPs size and surface plasmon resonance wavelength.

Keywords: Green synthesis, Silver nanoparticles, Response surface methodology, UV-vis spectrophotometer, DLS

INTRODUCTION

Nanotechnology has attracted great interest due to the wide range of potential applications such as biological products development, drug delivery system, antimicrobial activity and in water purification (Krishnaraj *et al.*, 2012). The nanotechnology appears to possess relatively good performance in comparison to other existing techniques due to extremely small size of nanoparticles and very high surface/volume ratio (Pandey and Mishra, 2016). Silver, gold, copper and platinum are some of the most commonly used materials in nanotechnology. Among these nanomaterials, silver nanoparticles (AgNPs) have gained considerable attention due to their good antibacterial and optoelectronic properties. AgNPs are extensively used in health industry, food production, textile coating, and several environmental applications (Babu *et al.*, 2015).

The commonly employed techniques for the synthesis of nanoparticles include physical, chemical and biological methods. Biological methods have been shown to be very effective for the synthesis of nanomaterials. These have also been proposed in the literature as an alternative to physical and chemical methods due to their being very simple, low cost and eco-friendly (Patil *et al.*, 2012). Biosynthesis of nanoparticles is inspired by the observations from nature and is an environment-friendly approach tha

employs unicellular and multicellular biological entities such as plants, bacteria, fungus, yeast, and viruses (Rauwel *et al.*, 2015; Iravani S, 2014; Salahuddin K and Husen A, 2016; Merzlyak A and Lee S, 2006). Lately, researchers have focused on using plant-based materials such as roots, leaves, flower broth, fruits, bark and peel extract to produce nanoparticles (Bhakya *et al.*, 2015; Jassal *et al*., 2016; Padalia *et al.*, 2015; Heydari and Rashidipour, 2015; Shetty *et al.*, 2014; Ibrahim 2015; Awad et al. 2014). Plant extract can reduce metal ions in a metal salt solution (Panigrahi *et al.*, 2004) due to the presence of components such as polyphenols reducing sugars, nitrogenous bases and amino acids (Haverkamp *et al.*, 2009; Shankar *et al.*, 2004; Ahmad *et al.*, 2010).

Biosynthesis of silver nanoparticles using orange peel is bottom up approach involving reduction of silver ions (Gada R and Unnati P, 2018). By nature orange peel extract is a light yellow in colour, which contains citric acid as main source. It can act as reducing agent for synthesis of metal oxides (MgO, TiO2, ZnO etc.) (Ana *et al.*, 2016). The mechanism involving reduction of Ag+ ions to Ag nanoparticles has been explained as follows (Sajid *et al.*, 2016):

$$4Ag^{+} + C_6H_8O_7 \text{ (citric acid)} + 2\,H_2O \rightarrow 4Ag^{0} + C_6H_8O_7 + 4\,H^{+} + O_2 \quad (1)$$

The use of orange peel in biosynthesis of silver nanoparticles also serves as a stabilizing agent to restrict the agglomeration of reduced Ag atoms, thus limiting the aggregation and the size of Ag nanoparticles (Saion E *et al.*, 2013).

Biosynthesis of AgNPs is an emerging technology currently under investigation by a large number of researchers. However, it is important to mention that a wide variation in the size and shape of AgNPs may result in different plasmon resonance bands. For example, the synthesis of triangular AgNPs has been discussed by Mansouri *et al.* (2009). Besides that, a lot of efforts have been

directed towards the optimization of the process parameters in AgNPs synthesis, and in particular improving the stability of the product and increasing the yield, especially in bulk production (Balavandy *et al.*, 2014).

In general, one-factor-at-a-time (OFAT) approach is commonly employed by most researchers to determine the optimum process conditions. However, the method based on the design of experiments (DOE) offers distinct advantages over the conventional OFAT method. For example, a central composite design (CCD) in response surface methodology (RSM) can be effectively used as a potent tool for determining the main and interaction effects of the independent variables, and the resulting process optimization with minimum number of experiments (Saat *et al.*, 2012).

The main purpose of this study was to investigate the biosynthesis of AgNPs using orange peel extract as a reducing agent and to determine the optimum process conditions for the production of AgNPs and the resulting particle size. The DOE approach was based on a CCD in RSM with orange peel extract concentration, pH and silver nitrate concentration as independent variables. The biosynthesized AgNPs were then characterized for their size by dynamic light scattering (DLS) and surface plasmon resonance (SPR) wavelength by UV-vis analysis as response variables.

METHODOLOGY

Plant Extract Preparation

Fresh orange peels were washed with distilled water and cut into small pieces, and then oven dried at 93°C for 60 minutes. The dried peels were ground using a blender to obtain a fine powder. A sample of dried orange peel powder weighing 5 g was mixed with 100 ml of distilled water at 60 ^{o}C using a magnetic stirrer for 10 minutes. The peel extract solution was cooled, filtered and stored at 4 °C until its use for the biosynthesis of AgNPs (Caroling *et al.*, 2013, Aysha *et al.*, 2014).

Biosynthesis of AgNPs and Characterization

The synthesis of AgNPs was carried out using silver nitrate in aqueous solution and orange peel extract as reducing agent. The reaction was complete within minutes. The resulting AgNPs were characterized using DLS for particles size and UV-vis spectrophotometer for detecting plasmonic resonance peaks. Subsequently, optimum process conditions were determined based on the developed statistical models.

In general, 20 ml of AgNPs suspension was produced in each experiment based on pre-selected levels of orange peel concentration, pH and $AgNO_3$ concentration in CCD. A 10 mM stock solution of $AgNO_3$ in deionized water was diluted as needed. Likewise, orange peel extract with 0.05 g/ml concentration was used in varying amounts. At first, the pH in peel extract was adjusted using 1 mM KOH solution, and followed by the addition of $AgNO_3$ solution and DI water to make up the 20 ml volume. All experiments were carried out at room temperature under bright day light conditions.

2.3 Experimental Design

In biosynthesis of AgNPs using orange peel extract, the effects of three independent variables (orange peel concentration, $AgNO_3$ concentration and pH) on the nanoparticles size, peak absorbance and SPR wavelength were investigated. A five-level-three-factor central composite design (CCD) was used. The independent variables and their levels both in coded and actual units are shown in Table 1. The selected range of this study were from the previous work

Table 1. Coded and actual values of independent variables in CCD for biosynthesis of AgNPs.

Variables	CCD coded levels				
	-1.682	-1	0	1	1.682
Peel extract conc. (X_1) (g/ml)	0.0008	0.0025	0.005	0.0075	0.0092
pH (X_2)	5.64	7	9	11	12.4
AgNO3 conc. (X_3) (mM)	0.16	0.5	1	1.5	1.84

2.4 Statistical Analysis

The experimental data obtained from the biosynthesis of AgNPs were fitted the following second-order polynomial model (Equation 1) using regression analysis in MS Excel.

$$Y = \beta_0 + \sum_{i=1}^{3} \beta_i . X_i + \sum_{i=1}^{3} \beta_{ii} . X_i^2 + \sum_{i=1}^{2} \sum_{j=i+1}^{3} \beta_{ij} X_i . X_j \quad (2)$$

Where Y is the response (dependent variable); βo is constant, βi, βii, and βij are coefficients; Xi, Xj are the independent variables. Equation 1 was used for developing models based on CCD. Subsequently, optimal conditions for the biosynthesis of AgNPs were determined by the Excel solver function using the developed models.

RESULTS AND DISCUSSION

3.1 Biosynthesis of AgNPs

The results from a typical experiment for the biosynthesis of AgNPs using 1.5 mM $AgNO_3$ solution, orange peel concentration of 0.0075 g/ml, and pH of 11 are presented in Figures 1 and 2. The formation of nanoparticles was evident from the change of the color of solution from yellowish to light brown (Figure 1) within 15 to 30 minutes. A plot of absorbance vs. wavelength in 350-550 nm range from a UV-vis Spectrophotometer clearly indicated the presence of a characteristic surface plasmon resonance (SPR) peak for AgNPs around 410 nm wavelength in Figure 2. Subsequently, DLS was used to determine the size distribution of AgNPs in suspension. However, the wavelength corresponding to peak absorbance and the width of SPR are greatly influenced by the size and

shape of the nanoparticles (Evanoff and Chumanov, 2005).

Figure 1. Orange peel extract (left) and biosynthesized AgNPs suspension (right).

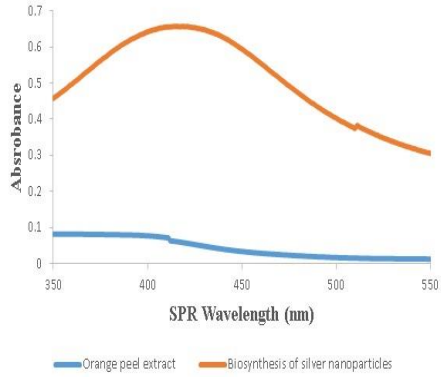

Figure 2 Absorption spectrum of AgNPs in solution**.**

3.2 Models Based on CCD

A CCD was used to determine the effects of orange peel extract concentration, pH and silver nitrate concentration on the formation of AgNPs. The CCD had eight factorial, six axial and six center point experiments resulting in a total of 20 experimental runs for the biosynthesis of AgNPs shown in Table 2 for both coded and actual conditions as given in Table 1. Regression analysis was used to develop the models and analyze the results to evaluate the effects of individual factors and their interactions. The developed models were subsequently used to determine the optimum conditions using Solver function in Excel.

Equations 2 to 4 present the models developed for three response variables including peak absorbance, SPR wavelength (nm) and average AgNPs size (nm), respectively. The predictor variables include the orange peel extract concentration (X_1,g/ml), pH (X_2), and silver nitrate concentration (X_3, mM). The coefficients of determination (R^2) for the developed models ranged from 0.735 to 0.923. The coefficients of various terms in the models indicated their contributions to the estimation of a given response variable.

Table 2 Experimental and predicted values of response variables in biosynthesis of AgNPs based on the CCD.

Run No	Coded variables			Absorbance		SPR Wavelength (nm)		AgNPs size based on number (nm)	
	X_1	X_2	X_3	Expt.	Pred.	Expt.	Pred.	Expt.	Pred.
1	-1	-1	-1	0.32	0.24	430	436	50.80	45.45
2	1	-1	-1	0.34	0.33	414	422	46.19	46.71
3	-1	1	-1	0.49	0.44	408	416	14.04	13.71
4	1	1	-1	0.57	0.52	402	404	25.32	13.20
5	-1	-1	1	0.33	0.33	428	434	48.43	60.81
6	1	-1	1	0.53	0.52	424	424	38.93	39.52
7	-1	1	1	0.66	0.61	418	418	36.21	35.95
8	1	1	1	0.77	0.79	406	408	7.28	12.89
9	-1.68	0	0	0.24	0.32	434	426	57.01	53.31
10	1.68	0	0	0.55	0.55	410	407	31.64	34.98
11	0	-1.68	0	0.34	0.37	440	432	59.78	55.07
12	0	1.68	0	0.72	0.76	405	402	1.64	5.98
13	0	0	-1.68	0.19	0.27	438	427	48.95	19.33
14	0	0	1.68	0.57	0.57	430	429	42.76	31.99
15	0	0	0	0.48	0.43	422	425	28.75	32.03
16	0	0	0	0.46	0.43	415	425	33.26	32.03
17	0	0	0	0.39	0.43	431	425	32.41	32.03
18	0	0	0	0.43	0.43	425	425	29.44	32.03
19	0	0	0	0.42	0.43	425	425	35.95	32.03
20	0	0	0	0.44	0.43	429	425	32.30	32.03

$$Y_1 = 0.432 + 0.067\ X_1 + 0.1178\ X_2 + 0.088\ X_3 - 0.0264\ X_1X_2 + 0.0246\ X_1X_3 + 0.0197\ X_2X_3 - 0.00057\ X_1^2 + 0.0461\ X_2^2 - 0.0064\ X_3^2 \quad (R^2 = 0.923) \quad (2)$$

$$Y_2 = 424.822 - 5.737\ X_1 - 8.849X_2 + 0.625X_3 + 0.25X_1X_2 + 0.75\ X_1X_3 + 0.75X_2X_3 - 2.996\ X_1^2 - 2.819X_2^2 + 1.2448\ X_3^2 \ (R^2 = 0.735) \quad (3)$$

$$Y_3 = 32.0328 - 5.449\ X_1 - 14.59\ X_2 + 3.762\ X_3 - 0.444\ X_1X_2 - 5.637\ X_1X_3 + 1.720\ X_2X_3 + 4.282\ X_1^2 - 0.531\ X_2^2 - 2.249\ X_3^2 \ (R^2 = 0.859) \quad (4)$$

Where Y_1 = peak absorbance, Y_2 = SPR wavelength (nm), Y_3 = nanoparticle size (nm), X_1 = orange peel concentration (g/ml), X_2 = pH, and X_3 = silver nitrate conc. (mM).

3.3 Model Evaluation and Optimization

The developed models (Equations 2-4) indicated that the pH had the maximum effect on the biosynthesis of AgNPs among the three predictor variables. The influence of the change in each independent variable on the normalized absorbance spectra of AgNPs solution was evaluated by keeping the other two independent variables at their mean values. Thus, in case of the orange peel concentration, sample no. 9, 10 and 15 were considered. As shown in Figure 3, an increase in the orange peel extract concentration resulted in a distinct shift in the SPR wavelength indicating the formation of smaller AgNPs. In comparison, the resulting change in peak absorbance was relatively small. The influence of pH of the solution on the biosynthesis of AgNPs based on sample nos. 11, 12 and 15 is presented in Figure 4. It was obvious that nanoparticles of large size were produced at low pH of about 5.68. In comparison, smaller size nanoparticles were produced at high pH as indicated by the shift in the wavelength corresponding to the peak absorbance (Figure 4). A possible reason could be the ability of pH to affect the biomolecules present in the reducing agent (Vanaja *et al.*, 2013). The effect of silver nitrate concentration was evaluated using sample nos. 13, 14 and 15. Interestingly, an increase in the concentration of silver nitrate resulted in a decrease of SPR wavelength from 438 to 430 nm and an increase in absorbance from 0.187 to 0.572 indicating the formation of smaller AgNPs (Fig. 5). The experimental data in Table 2 along with the overall trends presented in Figures 3-5 clearly indicate that an increase in the values of process variables resulted in an increase in the peak absorbance, and a decrease both in SPR wavelength and nanoparticles size.

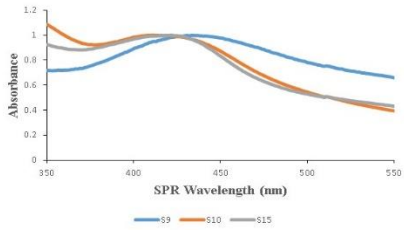

Figure 3. Effect of orange peel concentration on absorbance spectra of biosynthesized AgNPs.

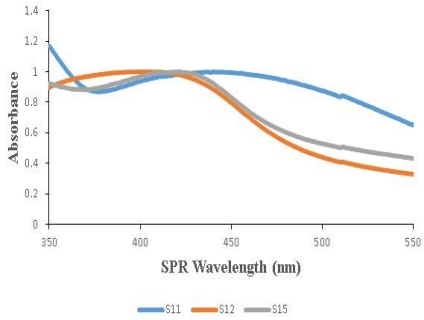

Figure 4. Effect of pH on absorbance spectra of biosynthesized AgNPs.

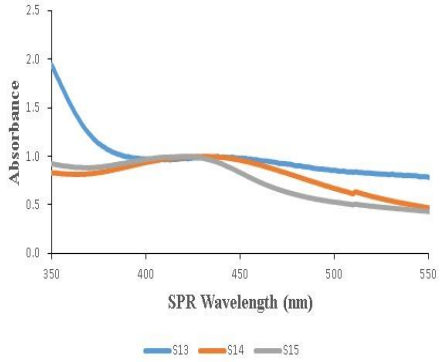

Figure 5. Effect of AgNO3 concentration on absorbance spectra of biosynthesized AgNPs.

The optimum conditions for the biosynthesis of AgNPs are shown in Table 3 based on the models developed using CCD for peak absorbance, SPR wavelength and average nanoparticles size. Thus, the orange peel extract concentration, pH and silver nitrate concentration could be selected in the respective ranges of 0.0075 g/ml, 11 and 1.5 mM in general for the biosynthesis of AgNPs. The smaller size of AgNPs is most effective for dye degradation since the increased surface area improves the reaction capability (Kankeu E *et al.*, 2013).

Table 3. Optimum conditions for biosynthesis of AgNPs using orange peel extract**.**

Response variable	Coded and actual values of independent variables			Optimum value
	X_1	X_2	X_3	
Absorbance	1 (0.0075)	1 (11)	1 (1.5)	0.79
SPR wavelength (nm)	1 (0.0075)	1 (11)	-0.854 (0.427)	403.8
Mean particle size (nm)	1 (0.0075)	1 (11)	1 (1.5)	12.89

Note: X_1=orange peel extract concentration (g/ml), X_2=pH, X_3=AgNO3 concentration (mM). Actual values are shown in parentheses

3.4 Surface Plots for Particle Size and Peak Absorbance for Biosynthesis of AgNPs

The surface and contour plots are very useful in visualizing the interrelationships between the response and input variables. The top plot in Figure 6 shows the absorbance as a function of orange peel concentration and pH with silver nitrate concentration held constant at mean value for biosynthesis of AgNPs. It is obvious that an increase in both orange peel concentrations and pH resulted in an increase in the absorbance value of the AgNPs solution within the respective ranges of experimental variables. Similar trends were observed in the middle and bottom plots for the effect of silver nitrate concentration and pH, and concentrations of both silver nitrate and orange peel extract on peak absorbance

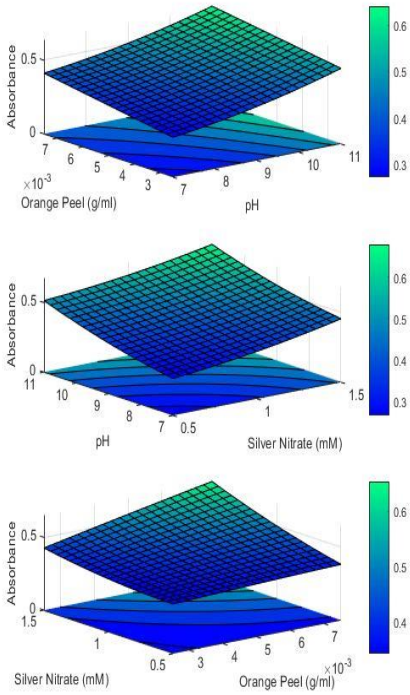

Figure 6. Surface plots showing absorbance as a function of orange peel conentration and pH (top), $AgNO_3$ concentration and pH (middle), and orange peel extract concentration and $AgNO_3$ concentration (bottom).

Figure 7 presents the effects of process variables in biosynthesis of AgNPs on the average size of nanoparticles. Nanoparticles with smallest size were produced at higher pH in combination with lower concentrations of orange peel extract

or silver nitrate (top and middle plots in Figure 7). However, lower concentration of silver nitrate and higher concentration of orange peel extract appeared to result in lower nanoparticle size as shown in bottom plot in Figure 7. The plots in Figures 6 and 7 clearly indicated that the process variables resulting in maximum absorbance and minimum nanoparticle size followed the identical trends.

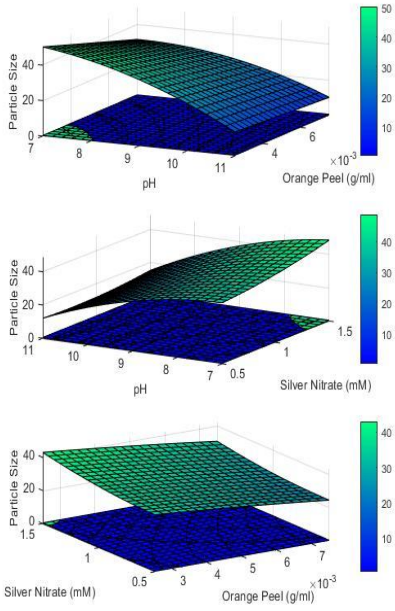

Figure 7. Surface plots showing AgNPs size as a function of orange peel conentration and pH (top), AgNO3 concentration and pH (middle), and orange peel extract concentration and AgNO3 concentration (bottom).

3.5 Relationship between SPR Wavelength, Peak Absorbance and AgNPs Size

The estimation of particle size from spectrophotometric measurements in the biosynthesis of AgNPs is of practical significance as an alternative to DLS measurements. The influence of the size and shape of the nanoparticles on peak absorbance and SPR wavelength has been studied in the past. Figures 8 and 9 present nanoparticles size as a function of SPR wavelength and peak absorbance, respectively. It is well known that an increase in particle size results in an increase in the peak SPR wavelength and a decrease in peak absorbance values. Thus, the trends exhibited in Figures 8 and 9 are in line with the information available in literature showing an increase in SPR wavelength and a decrease in absorbance with an increase in the size of the nanoparticles. Therefore, the shifting of SPR wavelength clearly indicated the change in the size of

nanoparticles. The results of these experiments indicate that the absorbance increased with decreasing particle size in the experimental range. However, general trend has been discussed on gold nanoparticles by Haiss Wolfgang (2007). Nevertheless, the relationships in Figures 8 and 9 need to be further refined for any practical application.

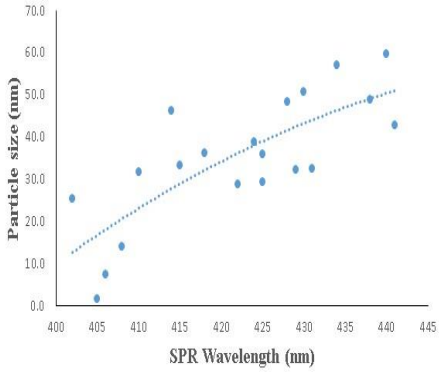

Figure 8. Relationship between the size of AgNPs and wavelength corresponding to peak surface plasmon resonance in UV-vis spectra.

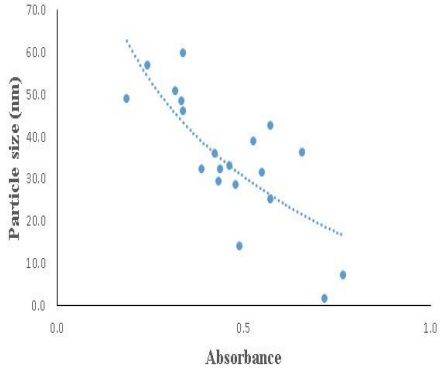

Figure 9. Relationship between the size of AgNPs and peak absorbance in UV-vis spectra.

CONCLUSIONS

The biosynthesis of AgNPs using orange peel extract as a reducing agent was found to be an inexpensive and eco-friendly method without requiring toxic chemicals. A CCD in RSM was used to develop models to identify the effects of orange peel extract concentration, pH and silver nitrate concentration on the biosynthesis of AgNPs with peak absorbance, SPR wavelength and particle size as response variables. The pH had the maximum influence on AgNPs formation compared to orange peel extract and silver nitrate concentration. The higher values of pH led to an increase in the values of peak absorbance and a decrease in

AgNPs size. The optimum conditions were determined to be orange peel extract concentration of 0.0075 g/ml, pH equal to 11 and $AgNO_3$ concentration of 1.5.mM resulting in a particle size of 12.89 nm. The peaks in absorbance spectra of AgNPs in solution corresponded to the SPR wavelengths in 402-440 nm range. The minimum AgNPs size of 12.89 also corresponded to the lower SPR wavelength of 403.8 nm.

ACKNOWLEDGEMENT

The authors would like to express their sincere appreciation to the Department of Civil and Environmental Engineering, Faculty of Engineering, Mahidol University, Salaya campus for making available the laboratory facilities.

REFERENCES

Ahmad N, Sharma S, Alam MK, Singh VN, Shamsi, S F, Mehta BR, Fatma. A Rapid Synthesis of Silver Nanoparticles Using Dried Medicinal Plant of Basil. Colloids Surf., B: Biointerfaces , 2010, 81,81−86.

Ana María Torrado, Sandra Cortés, José Manuel Salgado, Belén Max, Noelia Rodríguez, Belinda P. Bibbins, Attilio Converti and José Manuel Domínguez, Citric Acid Production From Orange Peel Wastes By Solid-State Fermentation, Brazilian Journal of Microbiology, 42, 394 2011

Aysha, OS, and Nisha, NS. 2014. Biosynthesis of silver nanoparticles using *Citrus limon* (LINN) Burm. F. peel extract and its antibacterial property against selected urinary tract pathogens. Journal of Biological & Scienific Opinion. 2(3):248-252.

Awad MA, Hendi AA, Ortashi KM, Elradi DF, Eisa NE, Al- lahieb LA, Shorog. MAl, Nada M, Abdelelah AG. Silver nanoparticles biogenic synthesized using an orange peel extract and their use as an anti-bacterial agent. Int J Phys Sci. 9:34–40.

Babu S, Michelle OC, Kesete Ghebreyessus. Rapid synthesis of highly stable silver nanoparticles and its application for colourimetric sensing of cysteine, Journal of Experimental Nanoscience, 10:16, 1242-1255, DOI:10.1080/17458080.2014.994680

Balavandy SK, Kamyar S, Dayang R, Zurina ZA. Stirring time effect of silver nanoparticles prepared in glutathione mediated by green method. Chemistry Central Journal, 2014. 8(1): p. 11.

Bhakya S, Muthukrishnan S, Sukumaran M, Muthukumar M. Biogenic synthesis of silver nanoparticles and their antioxidant and antibacterial activity. Appl Nanosci. 6:755–766.

Caroling, G., Tiwari, SK., Mercy Ranjitham A., and Suja, R. Biosynthesis of silver nanoparticles using aqueous broccoli extract- characterization and study of antimicrobial, cytotoxic effects. Asian Journal of Pharmaceutical and Clinical Research. 6(4):165-172.

Evanoff DD, Chumano G. Synthesis and optical properties of silver nanoparticles and arrays. Chem. Phys. Chem. 6(2005) 1221.

Fosso-Kankeu, E, Waanders, F., & Geldenhuys, M. Impact of nanoparticles shape and dye property on the photocatalytic degradation activity of TiO2. *International Journal of Science and Research*, *5*(11), 528-535.

Haiss, W., Thanh, N. T., Aveyard, J., & Fernig, D. G. Determination of size and concentration of gold nanoparticles from UV− Vis spectra. *Analytical chemistry*, *79*(11), 4215-4221.

Haverkamp R, Marshall A. The Mechanism of Metal Nanoparticle Formation in Plants: Limits on Accumulation. J. Nanoparticle Res. 2009, 11, 1453−1464.

Heydari R and Rashidipour M. Green synthesis of silver nanoparticles using extract of oak fruit hull (Jaft): synthesis and in vitro cytotoxic effect on MCF-7 cells. Int J Breast Cancer. 2015. doi:10.1155/2015/ 846743.

Ibrahim HM. Green synthesis and characterization of silver nanoparticles using banana peel extract and their antimicrobial activity against representative microorganisms. J Radiat Res Appl Sci. 8:265–275.

Iravani S. Bacteria in Nanoparticle Synthesis: Current Status and Future Prospects.Int. Sch. Res. Notices 2014 (2014)

Jassal V, Shanker U, Kaith BS. Aegle marmelos mediated green synthesis of different nanostructured metal hexacyanoferrates: activity gainst photodegradation of harmful organic dyes. Scientifica 2016. doi:10.1155/2016/2715026.

Krishnaraj C, Ramachandran R, Mohan K, Kalaichelvan PT. Optimization for rapid synthesis of silver nanoparticles and its effect on

phytopathogenic fungi. Spectrochim Acta A Mol Biomol Spectrosc. Jul;93:95-9. doi: 10.1016/j.saa.2012.03.002. Epub 2012 Mar 13.

Mansouri, S.S. and S. Ghader. Experimental study on effect of different parameters on size and shape of triangular silver nanoparticles prepared by a simple and rapid method in aqueous solution.Arabian Journal of Chemistry, 2009. 2(1): p. 47-53.

Merzlyak A, Lee SW, Curr. Phage as templates for hybrid materials and mediators for nanomaterial synthesis. Curr Opin Chem Biol. 2006 Jun;10(3):246-52

Padalia H, Moteriya P, Chanda S. Green synthesis of silver nanoparticles from marigold flower and its synergistic antimicrobial potential. Arab J Chem. 8:732–741.

Panigrahi, S, Kundu S, Ghosh S, Nath, S, Pal T. General Method of Synthesis for Metal Nanoparticles. J. Nanoparticle Res. 2004, 6, 411−416.

Pandey S, Mishra SB. Au nanocomposite based chemiresistive ammonia sensor for health monitoring. Am Chem Soc. 2016;1(1):55–62.doi:10.1021/ acssensors.5b00013.

Patil R S, M. R. Kokate, and S. S. Kolekar. Bioinspired synthesis of highly stabilized silver nanoparticles using *Ocimum tenuiflorum* leaf extract and their antibacterial activity, *Spectrochimica Acta A*, vol. 91, pp. 234–238, 2012.

Rauwel P, Kuunal S, Ferdov S, Rauwel E. A Review on the Green Synthesis of Silver Nanoparticles and Their Morphologies Studied via TEM. Advances in Materials Science and Engineering Vol. 2015, Article ID 682749, http://dx.doi.org/10.1155/2015/682749

Saat MN, Mohammad Sufan MA, Zazali Alias, Baki Bin Akbar. Effects And Optimization Of Selected Operating Variables On Laccase Production From Pycnoporus Sanguineus In Stirred Tank Reactor. International Journal of Chemical Reactor Engineering, 2012. 10(1).

Saion, E., Gharibshahi, E., & Naghavi, K. (2013). Size-controlled and optical properties of monodispersed silver nanoparticles synthesized by the radiolytic reduction method. *International journal of molecular sciences*, *14*(4), 7880-7896.

Sajid, P. A., Chetty, S. S., Praneetha, S., Murugan, A. V., Kumar, Y., & Periyasamy, L. (2016). One-pot microwave-assisted in situ reduction of Ag+ and Au 3+ ions by Citrus limon extract and their carbon-dots based nanohybrids: a potential nano-bioprobe for cancer cellular imaging.

RSC Advances, *6*(105), 103482-103490.

Salahuddin Siddiqi K, Husen A. Fabrication of Metal Nanoparticles from Fungi and MetalSalts:ScopeandApplicationNanoscaleRes.Lett. 11 (2016) 98.

Salihu A, Zahangir Alam, M. Ismail AbdulKarim, Hamzah M. Salleh. Optimization of lipase production by Candida cylindracea in palm oil mill effluent based medium using statistical experimental design. Journal of Molecular Catalysis B: Enzymatic, 2011. 69(1): p. 66-73.

Shetty P, Supraja N, Garud M, Prasad T. Synthesis, characterization and antimicrobial activity of Alstonia scholaris bark-extract-mediated silver nanoparticles. J Nanostruct Chem. 4:161–170.

Shankar S. S, Rai A, Ahmad A, Sastry M. Rapid Synthesis of Au, Ag, and Bimetallic Au Core-Ag Shell Nanoparticles Using Neem (Azadirachta indica) Leaf Broth. J. Colloid Interface Sci. 2004, 275, 496−502.

Vanaja M, Rajeshkumar S, Paulkumar K, Gnanajobitha G, Malarkodi C, Annadurai. G. Kinetic study on green synthesis of silver nanoparticles using Coleus aromaticus leaf extractAdvances in Applied Science Research, 4 (3) (2013), pp. 50-5

Inactivation of tetracycline-resistant bacteria by a combination of chlorine and UV irradiation

Narissara Chareewan[1] and Songkeart Phattarapattamawong[1*, 2]

[1]Department of Environmental engineering, Faculty of engineering, King Mongkut's University of Technology Thonburi (KMUTT)
[2]Center of Excellence on Hazardous Substance Management (HSM)
Corresponding author: email: songkeart.pha@kmutt.ac.th

ABSTRACT

Antibiotic Resistant Bacteria (ARB) are one of the biggest threats to global health issues. Contamination of ARB to environment has increased since the use of antibiotics is unplanned. Chlorination and UV irradiation are conventional treatment processes for inactivating pathogen. A combination of chlorine and UV irradiation (chlorine/UV) is proposed to enhance the inactivation. The study aims to investigate the inactivation kinetic of ARB by chlorination, UV irradiation and chlorine/UV processes. Tetracycline-resistant bacteria (TRB) are used for representing ARB because tetracycline is widely used antibiotic in Thailand. For chlorination, the inactivations for chlorine doses of 0.5, 1.0 and 2.0 mg/L were 5.55 ± 0.06 log, 6.27 ± 1.27 log and 8.11± 0.33 log, respectively. The kinetic constants were 1.68 ± 0.06, 1.92 ± 0.14 and 2.13 ± 0.25 min^{-1} for chlorine doses of 0.5, 1.0 and 2.0 mg/L, respectively. The UV irradiation inactivated TRB by 4.56 ± 0.42 log, 5.18 ± 0.29 log and 7.37 ± 0.61 log for the UV intensities of 3.59 (1 lamp), 6.22 (2 lamp) and 9.03 (3 lamp) mW/cm^2, respectively. The kinetic constants were 0.42 ± 0.03, 0.63 ± 0.01 and 1.12 ± 0.01 min^{-1} for intensities of 3.59, 6.22 and 9.03 mW/cm^2, respectively. The chlorine/UV process (1.0 mg/L of chlorine and light intensity of 6.22 mW/cm^2) resulted in the kinetic constant equivalent to 2.01 ± 0.31 min^{-1} and the inactivation of 7.60 ± 0.23 log.

Keywords: Advances Oxidation Process, Antibiotic Resistant Bacteria, Chlorination, Kinetic, UV irradiation

INTRODUCTION

Antibiotics have been extensively used for patient treatment. Because of drug absorption of human body is incomplete, the antibiotics and their metabolites contaminate in wastewater. Although the wastewater is treated by a wastewater treatment plant, an increase in antibiotic residuals in environment has been annually observed (Dodd, 2012). This contamination induces a development of microorganisms to survive and resist to the drugs. The developed bacteria is called as Antibiotic Resistant Bacteria (ARB). Prolongation of ARB can cause an increase in human mortality due to an infected patient cannot be treated. In 2010, an estimated number of dead from ARB in Thailand is 38,481 per annum. Thus, Thai National Strategic Plan has set the goal to reduce 50% of antimicrobial resistance morbidity: 20% in human use and 30% in animals (Sutthiruk et al., 2018). The prevalence of ARB in environmental becomes the major risk of human because more than 700,000 people are annually killed by ARB and the number will increase to 10,000,000 persons in 2050 (Na et al., 2018)

Tetracycline has been widely used to against infectious diseases in human, animals and plant. In 1953, the first resistant microbial to tetracycline is *S.dysenteriae* (Hartman et al., 2003). In the present, tetracycline is one of the most used antibiotics in Thailand (Thamlikitkul, 1998). Clendennen et al. (1992) found that *N. gonorrhoeae* isolated in Thailand were resistant to penicillin and tetracyclineChlorination and UV irradiation are commonly used in a water treatment plant for disinfection because they are low cost and easy for implementation. Chlorination utilizes a chlorinating agent to inactivate pathogens. UV irradiation destroys deoxyribonucleic acid (DNA) in bacteria cell. However, these traditional disinfection

processes may not be sufficient to sufficient to eliminate ARB. Therefore, a combination between chlorine and UV irradiation (chlorine/UV) that has been considered as a novel advanced oxidation process (AOP) is proposed in this study. The UV irradiation can activate the free chlorine to produce stronger oxidants (e.g., •OH, •Cl). These free radicals are high reactive to organic substances, resulting in the greater oxidation.

The objective of the study is to enhance the ARB inactivation by the chlorine/UV process. The ARB disinfection by chlorination, UV irradiation and the chlorine/UV process were compared. Finally, a removal kinetic of three disinfection processes was investigated and compared. Tetracycline-resistant bacteria were used for representing ARB because tetracycline is widely used antibiotic in Thailand.

METHODOLOGY

Tetracycline resistant bacteria preparation

Escherichia coli (E.coli) was used as a representative of pathogens. E. coli in wastewater taken from a swine farm was isolated in an Eosin Methylene Blue agar spiked with tetracycline (16 μg/ml). The survive E.coli was collected and called as tetracycline-resistant bacteria (TRB). The selected colony was cultured in a Luria-Bertani broth at 37℃ for 6 hours. The culture solution was rinsed with a phosphate buffer saline (PBS) before the experiment.

Chlorination

The chlorination was performed in a batch reactor. TRB were transferred to a glass bottle contained PBS. The sample was mixed by a magnetic stirrer. Sodium hypochlorite (NaOCl) was diluted to achieve 0.5, 1.0 and 2.0 mg/L of chlorine dose. The sample was collected at the contact time of 0, 1, 2, 5, 10, 20 and 40 min. The dechlorination was conducted by addition of sodium thiosulfate solution. The free chlorine concentration was determined by a N, N diethyl-p-phenylenediamine (DPD) method. The test was carried

out at room temperature (25-27℃) and pH at 7-7.4

UV irradiation

For UV irradiation, the batch reactor was equipped with a low-pressure UV-C lamp (16W, 254 nm) inserted in a quartz sleeve. Intensity of UV-C lamp was determined by the iodide/iodate actinometer (Rahn et al., 2006). The UV intensities for one, two and three lamps were 3.59, 6.22 and 9.03 mW/cm2, respectively. The UV lamps were warmed for 20 min before starting the experiment. The test was carried out at room temperature (25-27℃) and pH 7-7.4

Chlorine/UV process

For the chlorine/UV process, the chlorine dose was controlled at 1.0 mg/L, and the UV intensity was 6.22 mW/cm2. The UV lamp was warmed for 20 min before chlorine addition. The test was carried out at room temperature (25-27℃) and pH 7-7.4

Microbial analysis

A plate count method was used for determining the inactivation of TRB. The dilution technique was used for sample preparation. The sample was inoculated on a plate count agar with 16 μg/ml of tetracycline. The samples were incubated at 37℃ for 18 hours.

Disinfection theory

To elaborate the factors influencing the inactivation, the data were fitted with the Chick-Watson's equation (Equation 1, 2).

$$\ln(N/N0) = -kt = -k'Cnt \quad (1)$$

$$\ln C = - 1/n \ln t + 1/n\ln[1/k \ (-\ln N/N\_0)] \quad (2)$$

where N0 and N are a number of viable cells initial and time t, t is reaction time, k is an inactivation rate constant, k' is a die-off constant, n is a coefficient of dilution, and C is disinfectant concentration. The n value higher than one indicates the disinfectant concentration is more important than time. On the other hand, time is more important than the concentration when the n value below one. If the n value equals to one, both

the concentration and time are important (Tilley, 1939).

RESULTS AND DISCUSSION

TRB inactivation by chlorination

The inactivation of TRB by chlorination is shown in Figure 1. The TRB inactivations for the chlorine dose at 0.5, 1.0 and 2.0 mg/L were 5.55 ± 0.06 log, 6.27 ± 1.27 log at 40 min and 8.11 ± 0.33 log at 20 min, respectively. The number of TRB for the chlorine dose at 2.0 mg/L was below the detection limit (30 colonies) when the contact time was extended to 20 min. Similarly, Huang et al. (2013) found that the TRB inactivation by chlorination was 5-log for 10 min-contact time with 1.0 mg/L of chlorine dose. Furukawa et al. (2017) reported that three chlorinating conditions (40 min-contact time with 0.5 mg Cl2/L, 20 min-contact time with 1.0 mg Cl2/L, and 3 min-contact time with 3.0 mg Cl2/L) achieved more than 7-log inactivation of vancomycin-resistant enterococci. The reaction occurred quickly at the initial contact time (0 – 5 min). Then, the inactivation was gradually increased, resulted from rapid decreases in chlorine residuals (Figure 2). Although the chlorine residuals still remained for chlorination at 1.0 mg/L, the inactivation was slightly increased after 5 min-contact time. A previous study revealed that viable cells could agglutinate with the dead cells, resulting in lower efficiency of disinfection (Templeton et al., 2009). The reaction rate was fitted with the pseudo-first order kinetic (Table 1). The inactivation rate constant (k) increased, depending on the chlorine dose. The k values for 0.5, 1.0 and 2.0 mg/L were 1.68 ± 0.06, 1.92 ± 0.14 and 2.13 ± 0.25 min-1, respectively. The n value for 4 log inactivation was 0.17, indicating that the contact time was more important than the chlorine dose

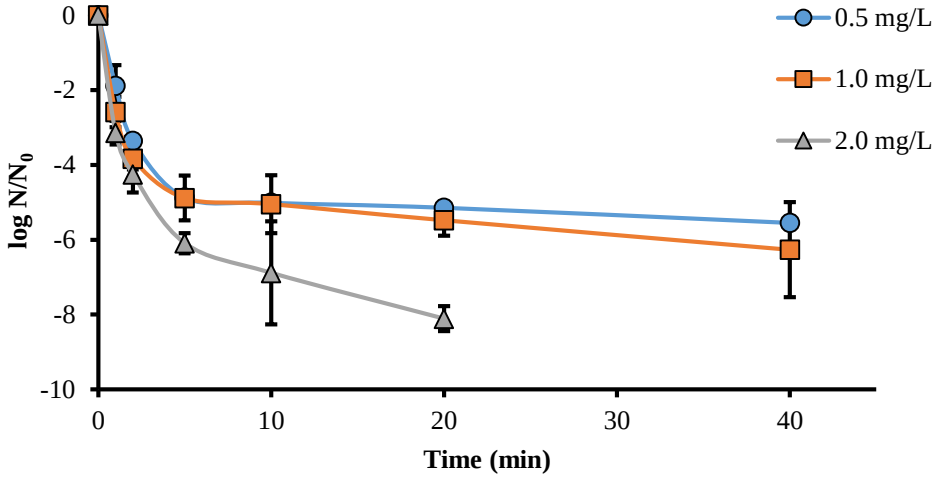

Figure 1 TRB inactivation by chlorination (n = 3)

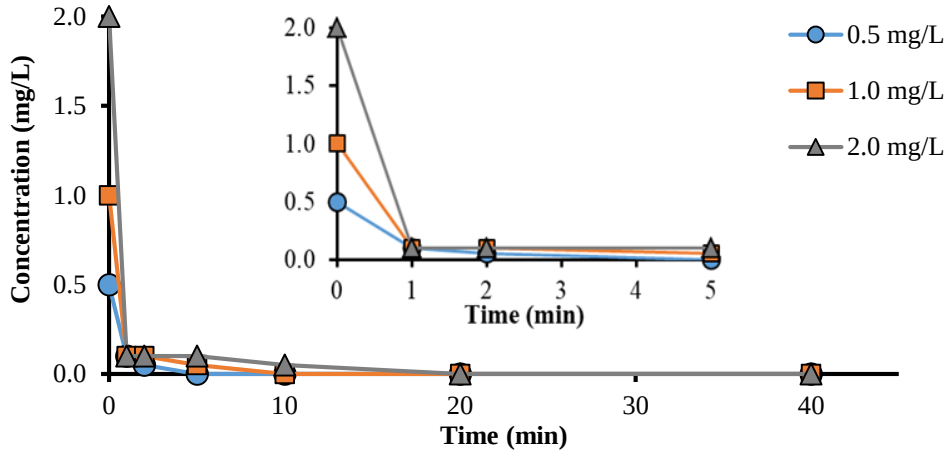

Figure 2 Concentration of chlorine

Table 1 The pseudo-first order kinetic (k) by chlorination

Chlorine dose (mg/L)	*k* (min^{-1})	R^2
0.5	1.68 ± 0.06	0.9951
1.0	1.92 ± 0.14	0.9613
2.0	2.13 ± 0.25	0.9297

TRB inactivation by UV irradiation

The TRB inactivations by the UV irradiation at the intensities of 3.59, 6.22 and 9.03 mW/cm^2 were 4.56 ± 0.42 log, 5.18 ± 0.29 log and 7.37 ± 0.61 log, respectively (Figure 3) at 40 min. Rizzo et al. (2013) reported that only 2.3 log of ARB inactivation was observed for 60 min-contact time at 0–2.5 × 10^4 μWs/cm^2. The bacteria inactivation rate was divided into 2 sections. Firstly (0 – 5 min), the reaction took place quickly because the UV emission directly contacted to viable cells. When the non-viable cells increased and accumulated, the tailing phenomena (dead cells shading the viable cells) occurred. Thus, the reaction rate decreased, causing the inactivation gradually increased after 5 min. This similar trend was found in Zhang et al., (2017). The *k* value, determined by using the initial rate method, was tabulated in Table 2. Increase in UV intensities enhanced the inactivation rates. The *k* values were 0.42 ± 0.03, 0.63 ± 0.01, 1.12 ± 0.01 min^{-1}, respectively for the UV irradiation at the intensities of 3.59, 6.22 and 9.03 mJ/cm^2. For the 4 log inactivation by the UV irradiation, the n value was 1.13. Thus, the inactivation by the UV irradiation preferred to depend on the light intensity than the contact time.

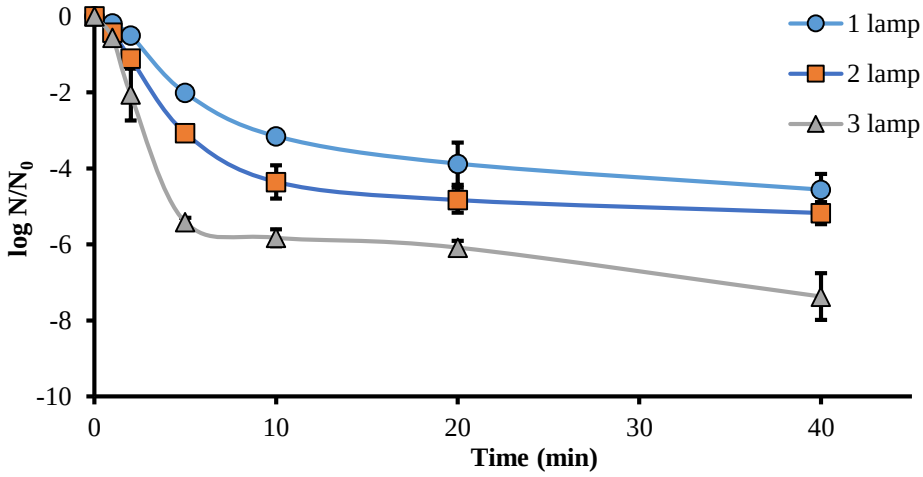

Figure 3 TRB inactivation by UV irradiation (n = 3)

Table 2 The pseudo-first order kinetic (k) by UV irradiation

UV intensity (mW/cm^2)	*k* (min^{-1})	R^2
3.59	0.42 ± 0.03	0.9727
6.22	0.63 ± 0.01	0.9959
9.03	1.12 ± 0.01	0.9907

TRB inactivation by the chlorine/UV process

The combined process of chlorine/UV (chlorine dose, 1 mg/L; UV intensity, 6.22 mW/cm^2) effectively inactivated the TRB. The 7.60 ± 0.23 log inactivation was obtained with the contact time of 10 min (Figure 4). The free radicals (e.g., •OH, •Cl) generated in the chlorine/UV process could be a reason for enhancement of the inactivation. The *k* value (2.01 ± 0.31 min^{-1}) for the chlorine/UV process was three-fold higher than that for the standalone UV irradiation (Table 3). Although the *k* value for the chlorine/UV process was comparable to the chlorination at the same dose (1 mg/L), the chlorine/UV process completely inactivated the TRB within 10 min. Extending the reaction

time resulted in the counted cells lower than the acceptable level (30 colonies). The chlorine residual decreased to 0.1 mg/L for 2 min-contact time. Then, it was completely consumed at 10 min-contact time.

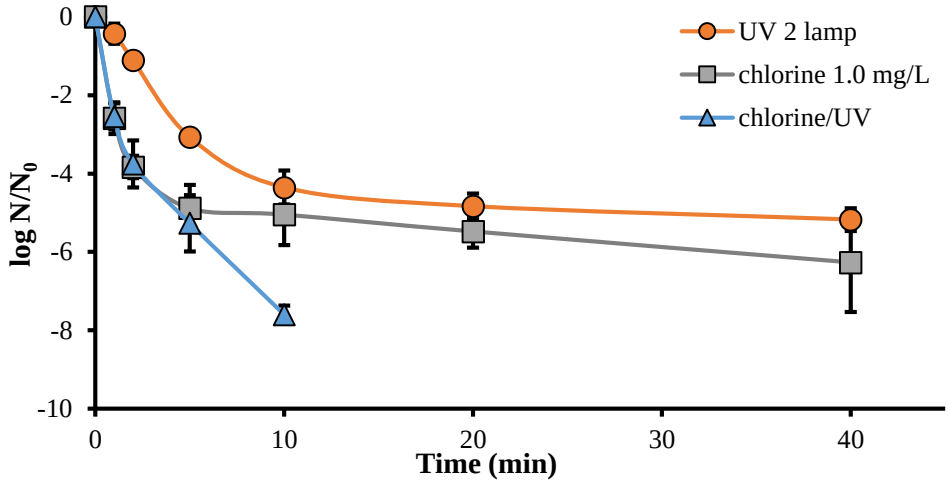

Figure 4 TRB inactivation by chlorination, UV irradiation and chlorine/UV process (n = 3)

Table 3 The kinetic inactivation rate for the chlorine/UV process

Process	***k* (min^{-1})**	**R^2**
Chlorination (1.0 mg/L)	1.92 ± 0.14	0.9613
UV irradiation (6.22 mW/cm^2)	0.63 ± 0.01	0.9959
Chlorine/UV process (1.0 mg/L + 6.22 mW/cm^2)	2.01 ± 0.31	0.9519

CONCLUSIONS

Chlorination was more effective for disinfection than the UV irradiation. The inactivations of tetracycline-resistant bacteria (TRB) by the chlorine dose at 0.5, 1.0 and 2.0 mg/L were 5.55 ± 0.06 log, 6.27 ± 1.27 log and 8.11 ± 0.33 log, respectively. The TRB inactivations by the UV irradiation at the intensities of 3.59, 6.22 and 9.03 mJ/cm^2 were 4.56 ± 0.42 log, 5.18 ± 0.29 log and 7.37 ± 0.61 log, respectively. The inactivation by chlorination was

depended on the contact time than the chlorine dose, while the inactivation by the UV irradiation highly relied on the light intensity. The inactivation by the chlorine/UV process reached to 7.60 ± 0.23 log within 10 min-contact time. The inactivation rate constant for the chlorine/UV process (k = 2.01 ± 0.31 min^{-1}) was three-fold higher than that for the standalone UV irradiation (k = 0.63 ± 0.01 min^{-1}), and it was comparable to the standalone chlorination (k = 1.92 ± 0.14 min^{-1}).

ACKNOWLEDGEMENTS

The study was funded by the Office of the Higher Education Commission and the Thailand Research Fund (MRG6180274).

REFERENCES

Clendennen TE, Echeverri P, Saengeur S, Kees ES, Boslego JW and Wignall FS, Antibiotic Susceptibility Survey of *Neisseria gonorrhoeae* in Thailand, Antimicrobial Agents and Chemotherapy 1992; 36(8): 1682-1687.

Dodd M, Potential impacts of disinfection processes on elimination and deactivation of antibiotic resistance genes during water and wastewater treatment, Journal of Environmental Monitoring 2012; 14(7): 1754-1771.

Furukawa T, Jikumaru A, Ueno T and Sei K, Inactivation Effect of Antibiotic-Resistant Gene Using Chlorine Disinfection, Water 2017; 9(7): 547.

Hartman AB, Essiet II, Isenbarger DW and Lindler LE, Epidemiology of Tetracycline Resistance Determinants in *Shigella* spp. and Enteroinvasive *Escherichia coli*: Characterization and Dissemination of *tet*(A)-1, Journal of Clinical Microbiology 2003; 41(3): 1023-1032.

Huang J, Hu H, Wu Y, Wei B and Lu Y, Effect of chlorination and ultraviolet disinfection on tetA-mediated tetracycline resistance of Escherichia coli, Chemosphere 2013; 90: 2247-2253.

Na G, Lu Z, Gao H, Zhang L., Li Q, Li R, Yang F, Huo C and Yao Z, The effect of environmental factors and migration dynamics on the prevalence of antibiotic-resistant *Escherichia coli* in estuary environments, Scientifics Reports 2018; 8(1): 1663.

Rahn RO, Bolton J and Stefan MI, The Iodide/Iodate Actinometer in UV disinfection: Determination of the Fluence Rate Distribution in UV

reactor, Photochemistry and Photobiology 2006; 82: 611-615.

Sutthiruk N, Cosidine J, Hutchinson A, Driscoll A, Malathum K and Botti M, Thai clinicians' attitudes toward antimicrobial stewardship programs. American Journal of infection control 2018; 46(4): 425-430.

Rizzo L, Fiorentino A and Anselmo A, Advanced treatment of urban wastewater by UV radiation: Effect on antibiotics and antibiotic-resistant E. coli strains, Chemosphere 2013; 92; 171-176.

Templeton MR, Oddy F, Leung W-K and Rogers M, Chlorine and UV disinfection of ampicillin-resistant and trimethoprim-resistant *Escherichia coli.*, Journal of Environmental Engineering and Science 2009; 36(5): 889-894.

Thamlikitkul V, Antibiotic Dispensing by Drug Store Personnel in Bangkok, Thailand, Journal of Antimicrobial Chemotherapy 1998; 21(1): 125-131.

Tilley FW, An Experimental Study of The Relation between Concentration of Disinfectants and Time Required for Disinfection, Journal of Bacteriology 1939; 38(5): 499-510.

Zhang CM, Xu LM, Wang XC, Zhuang K and Liu QQ, Effects of ultraviolet disinfection on antibiotic-resistant *Escherichia coli.* from wastewater: inactivation, antibiotic resistant profiles and antibiotic-resistant genes, Journal of Applied Microbiology 2017; 123: 295-306.

The effect of bentonite on the properties of landfill liner from clay mixed with industrial wastes

Woottipong Prakongwittaya[1], Rungroj Piyaphanuwat[2], Suwimol Asavapisit[3*]

[1]Graduate student, Environmental Technology, School of Energy, Environmental and Materials, King Mongkut's University of Technology Thonburi, Pracha U-thit Road, Bangmod, Thung-kru, Bangkok 10140, Thailand

[2]Assistant Professor, Ratchaburi Learning Park, King Mongkut's University of Technology Thonburi, Rang Bua, Chom Bueng, Ratchaburi 70150, Thailand

[3]Associate Professor, Environmental Technology, School of Energy, Environmental and Materials, King Mongkut's University of Technology Thonburi, Pracha U-thit Road, Bangmod, Thung-kru, Bangkok 10140, Thailand

Corresponding author: email: suwimol.asa@kmutt.ac.th

ABSTRACT

This research studied the engineering properties of landfill liner produced from clay mixed with industrial wastes. The water treatment (WTR) and calcium carbine (CCR) residues were generated from water treatment plant and acetylene gas production, respectively. The landfill liner was made from WTR, CCR and clay at the ratio of 40:40:20 and bentonite was added at 1, 3, 6, 9, and 12 wt.%. The unconfined compressive strength (UCS), hydraulic conductivity, and durability of the liner were investigated. Experimental results showed that addition of bentonite at the amount that does not exceed 3 wt.% gave the composite landfill liner with the hydraulic conductivity values within the standard limit of compacted clay liner for secure landfill which is defined at 1.0×10^{-7} cm/s. For durability results, the maximum slake durability

index was found from the composite landfill liner with 1 wt.% of bentonite. SEM images showed that addition of bentonite induced a denser microstructure of the composite landfill liner. This could be caused by the filling effect of bentonite in the air void and pores which also lead to an increase in the UCS, slake durability index and a reduction in hydraulic conductivity.

Keywords: Composite landfill liner, Water Treatment Residue, Calcium carbine residue, Hydraulic conductivity, Compressive strength

INTRODUCTION

Secured Landfill is normally designed and constructed for the storage and disposal of hazardous wastes. Inappropriate disposal of hazardous waste may cause the release of hazardous components especially from the bottom of the landfill to the surrounding soil and groundwater. To prevent the transport of contaminants through the bottom of the landfill, a compacted clay liner is needed to minimize the negative effects on the human health and the environment. According to the Ministry of Industry, a compacted clay liner for the secure landfill with a minimum thickness of 60 cm and hydraulic conductivity of 1.0×10^{-7} cm/s are required [1]. Apart from the role as a barrier to leachate migration, the compacted clay liner also provides strength to prevent settlement during waste placement.

Compacted clay liner is typically used in both the sanitary and secure landfills. However, the fractures in the liner which were caused by desiccation or unequal settlement decrease the engineering and hydraulic conductivity properties of the liner. Several research works reported the use of general industrial wastes or residues to improve the properties of the clay liner including coal fly ash, spilitic mining wastes, and foundry sand [2-5]. The present research study, calcium carbide residue (CCR) and water treatment residue (WTR) were used in

combination with clay at the ratio of 40: 40: 20 and a small amount of bentonite (1, 3, 6, 9, and 12 wt.%) to produce composite liner. It is expected that bentonite which is expanded in the presence of water could act as pore sealant and as a result the hydraulic conductivity of the liner is lower to the desirable level.

METHODOLOGY

1.1 Materials

This research used soft clay, calcium carbide residue and water treatment residue as raw materials. Soft clay was collected from the construction of KLK PRODUCTS COMPANY LIMITED, Chachoengsao province, Thailand at the depth of 6-8 meters. The calcium carbide residue (CCR) was a light gray solid and was brought from a M. THAIINDUSTRIAL co., Ltd. in Samutsakhon province. The water treatment residue (WTR) was from Metropolitan Water works Bang Khen, Bangkok. Bentonite from Bentonil Co.,Ltd. is sodium bentonite and API Grade.

The three materials were open-air dried and grounded to reduce particle size using the Los Angeles Abrasion machine. The ground materials were passed through sieve no.40 and stored in a tight-lid container. The chemical compositions of these materials were determined by X-ray fluorescence (XRF) and is shown in Table I.

1.2 Mixing proportions

Clay, CCR and WTR were mixed using the proportion equals to 40: 40: 20 wt. % . The Optimum Moisture Content (OMC) of each mixture was determined by Standard Proctor Compaction test according to ASTM D698 - 12e1. The moisture content at 1. 2 OMC was used to prepare the sample for unconfined compressive strength and water permeability test.

Table 1. Chemical properties of clay, WTR and CCR

Chemical composition	Clay	WTR	CCR
SiO_2 (%wt.)	62.29	59.59	7.15
Al_2O_3 (%wt.)	20.27	26.51	4.76
CaO (%wt.)	1.78	1.29	85.9
Fe_2O_3 (%wt.)	7.37	7.36	0.46
SO_3 (%wt.)	3.78	0.79	0.54
MgO (%wt.)	0.19	1.12	1.09
Na_2O (%wt.)	1.46	0.34	0.08
Specific gravity	2.66	2.40	2.52

1.3 Method for testing

The composite clay liner was prepared using Clay: WTR: CCR equals to 40:40:20 containing 0, 1, 2, 3, 6, 9 and 12 wt.% of bentonite. Mixing water was used at 1.2 times of the optimum moisture content (OMC) value. The mixture was compacted in a cylindrical mold, 5 cm in diameter and 10 cm in height, using the same modified proctor compaction energy. The unconfined compressive strength (UCS) at 3, 7, 14 and 28 days was tested following ASTM D2166. Water permeability was conducted at constant head test at 0.7 kg/ cm^2 at the age of 7 days following ASTM D 508 whereas the durability test was done according to ASTM D4644 – 16.

RESULTS AND DISCUSSION

Effect of Bentonite on Unconfined compressive strength development of composite clay liner

Unconfined compressive strength development of compacted clay combined with WTR and CCR at the ratio of 40:40:20 containing 0, 1, 2, 3, 6, 9 and 12 wt.% bentonite were shown in Fig. 1. The UCS of compacted samples containing bentonite at all levels was lower than the control (sample without bentonite) at all curing duration observed. At 14 days, compacted sample with 1 wt.% of bentonite gave

UCS of 0.922 MPa and increase to 1.64 and 2.79 MPa at 28 and 56 days. The increase UCS of the compacted samples was due to the hydration reaction between $Ca(OH)_2$ from CCR reacted with SiO_2 and Al_2O_3 from clay and WTR and transformed to CSH and CAH that contributing to UCS of compacted samples [5-8]. When the level of bentonite increased to 2, 3, 6 and 9 wt.%, UCS of compacted clay WTR and CCR also increased. The highest UCS was obtained from the compacted samples with 9 wt.% of bentonite at the age of 28 and 56 days which gained 2.33 and 3.51 MPa, respectively. This positive effect was resulted not only from the hydration reaction between CCR and clay minerals but also from the expansion of bentonite in the presence of water thus filling the air voids and pores existing in the compacted samples [9,10]. However, results showed that UCS of the compacted samples with 12 wt.% of bentonite reduced. This could be caused by the water in OMC was absorbed by bentonite during sample compaction and desiccated when the samples were curing which leads to the shrinking of bentonite particle thus leaving an empty space around the bentonite particle and this has brought to a reduction in the UCS [11].

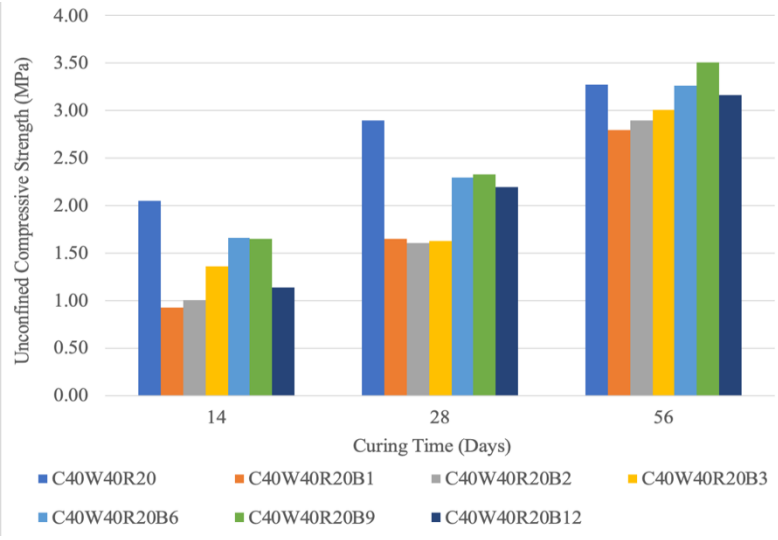

Figure 1 UCS development of composite clay liner containing various amounts of bentonite

Effect of bentonite on coefficient of permeability of composite clay liner

Coefficient of permeability of composite clay liner in the presence of various amounts of bentonite is shown in Figure 2. The coefficient of permeability of the control sample without bentonite was 1.42×10^{-7} cm/s which was higher than the standard limit of compacted clay liner for secure landfill (1×10^{-7} cm/s). Results showed that presence of 1, 2 and 3 wt.% of bentonite reduced the coefficient of permeability of the compacted samples to 0.321, 0.533 and 0.812×10^{-7} cm/s, respectively as compared to the control and meets the requirement of the compacted clay liner for secure landfill. It is observed that the coefficient of permeability did not meet the standard limit of 1×10^{-7} cm/s when 6, 9 and 12 wt.% of bentonite was added.

At 1 to 3 wt.% of bentonite in compacted samples made a little increase coefficient of permeability from 0.3 to 0.85×10^{-7} cm/s while addition of bentonite 3 to 12 wt.% rapidly increase coefficient of permeability. It can be explained in polynomial equation $y = 0.0361x^2 + 0.4678x - 0.5533$ and $R^2 = 0.9706$. The increase of coefficient of permeability of compacted samples with increasing levels of bentonite could be caused by an increase amounts of absorbed water on the surface of increasing bentonite. As a result, the absorbed water on the surface of bentonite was desorbed and evaporated during the curation of the sample; leaving some spaces surrounded the bentonite particles. These spaces act as channeling for water to flow through and are the cause of an increase coefficient of permeability value [9-13] .

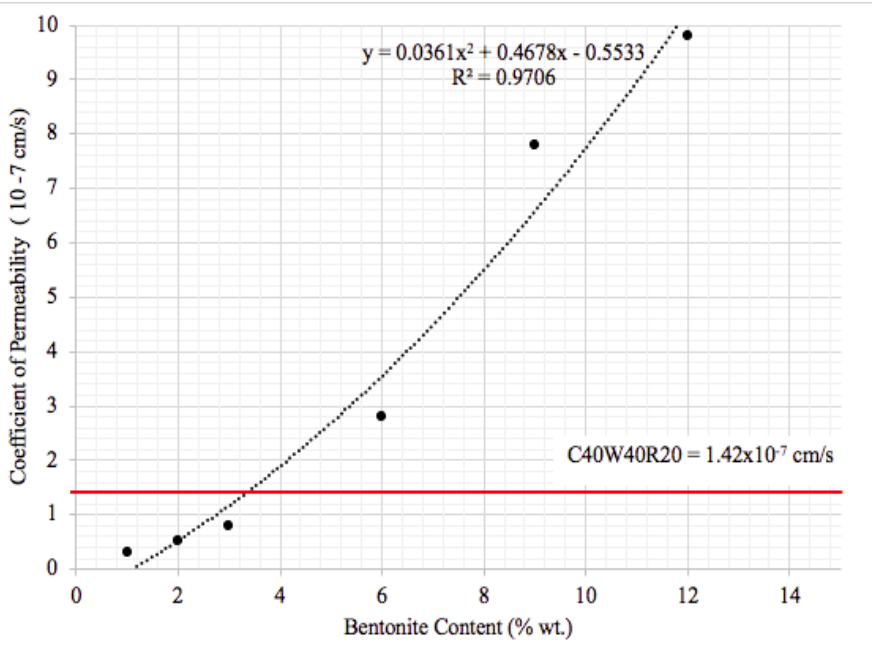

Figure 2 Coefficient of permeability of compacted clay and wastes.

Effect of bentonite on durability of composite clay liner

Durability property of composite clay liner was reported as slake durability index (SDI) following ASTM D4644- 16 and is shown in Figure 3. All samples were tested in duplicate and the percentage of weight loss was reported in the term of SDI. Experimental results showed that SDI increased with increasing cycle of the test. SDI after cycle No. 2 for control sample without bentonite was 75.97 % and decreased to 46.25% when 3 wt.% of bentonites was added. This is due to the added bentonite when contacted with water, expanded and filled in the pores of compacted samples. As a consequence, the pores are closed by the expanded bentonite and the water cannot flow through the sample or flow through at a reduced rate thus leaving the sample with less disturbance [9-11]. For the samples containing 6, 9 and 12 wt. % of bentonite, an increase SDI was observed. At 12 wt. % of bentonite, the compacted sample has

SDI of 65.23% which was lower than the control sample. This resulted from high volume of water in OMC which was absorbed by bentonite evaporates and leads to increase the space around bentonite particles [11, 12]. The optimum dosage of bentonite in composite clay liner from this work was 3 wt.% (Figure 4).

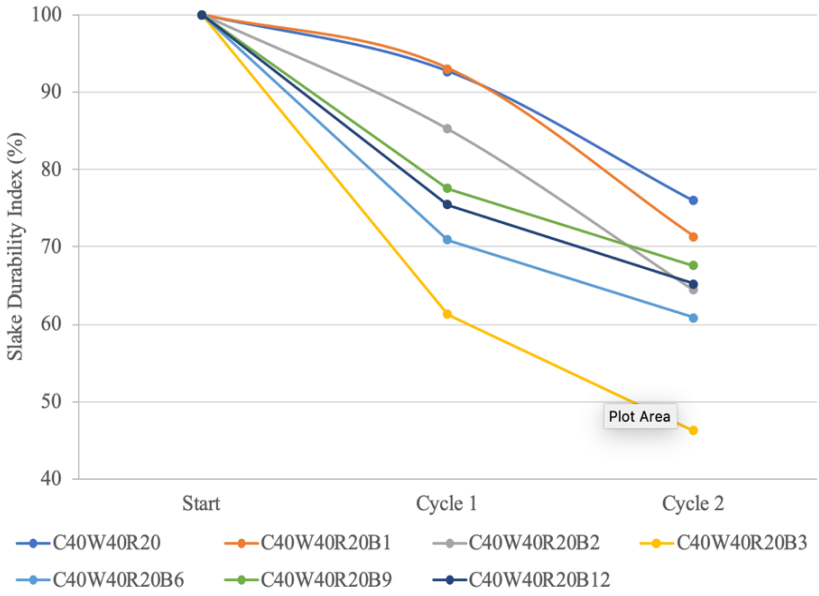

Figure 3 Slake durability index of composite clay liner containing various amounts of bentonite

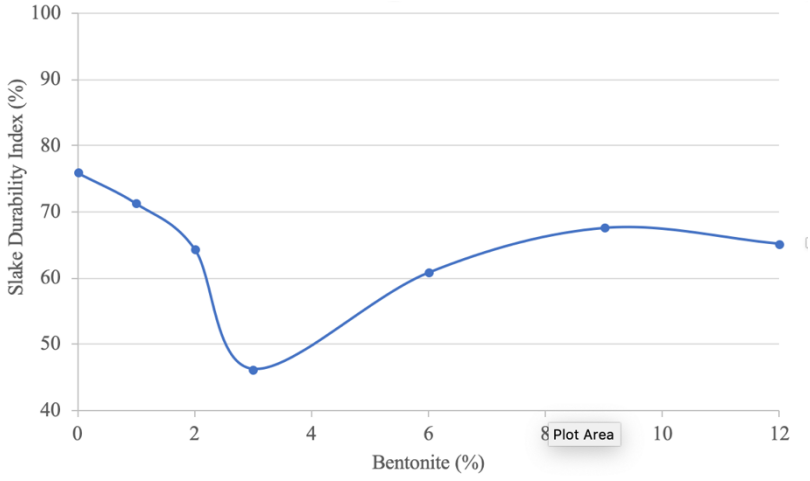

Figure 4 Relationship between slake durability index and bentonite dosage of composite clay liner

Microstructure of composite clay liner

Figure 5a reveals the microstructure image of composite clay liner without bentonite. A uniform and dense microstructure was present as a result of hydration products obtained from the reaction between CCR and SiO_2 or Al_2O_3 from clay and WTR. These hydration products sit in the existing pore space of the compacted clay liner. When bentonite was added at 3 wt.% to the compacted samples, a dense microstructure compared to the control sample was observed (Figure 5b). Air voids and pores are hardly visible. The swollen particles of bentonite were distributed throughout the image. This is in consistent with the results of coefficient of permeability and SDI.

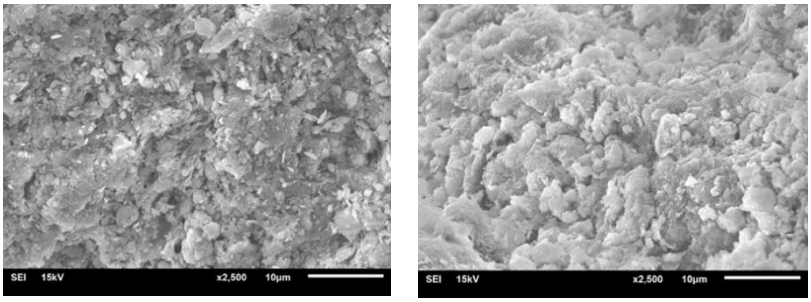

0 wt.% bentonite b) 3 wt.% bentonite

Figure 5 Microstructure of compacted Clay:WTR:CCR at 40:40:20 a) 0 wt.% bentonite and b) 3 wt.% bentonit

CONCLUSION

This research studied the effect of bentonite dosage on UCS, coefficient of permeability, SDI and microstructure of compacted clay, WTR and CCR. When bentonite dosage increased, the UCS and coefficient of permeability increased. The SDI of compacted samples with bentonite decrease when bentonite

was added about 1-3% wt. and vice versa when bentonite dosage was higher than 3% wt. Coefficient of permeability and SDI results are consistence with microstructure in

that bentonite absorbs water and swell thus it acts as sealant for the porous matrix. However, the UCS of the composite clay liner does not benefit from these positive effects. This is because the bentonite absorbs water and swell but does not harden so it cannot contribute to strength. The optimum bentonite dosage from this research work for composite clay liner consisting of clay:WTR:CCR at 40:40:20 was 3 wt.%

REFERENCES

Standard of secure landfill, Ministry of Industry, 1988.

Guney, Y., Cetin, B., Aydilek, A. H., Tanyu, B. F. and Koparal, S., "Utili-zation of sepiolite materials as a bottom liner material in Solid waste landfills," Waste Management, vol. 34, no. 2014, pp. 112-124, 2013.

Herrmann, I., Svensson, M., Ecke, H., Kumpiene, J., Maurice, C., Andreas, L., Lagerkvist, A., 2009, "Hydraulic conductivity of fly ash–sewage sludge mixes for use in landfill cover liners", Water Research, Vol. 43(14), pp. 3541-3547.

Maritsa, L., Tsakiridis, P. E. Katsiotis, N. S. Tsiavos, H., Velissariou, D., Xenidis, A., Beazi- Katsioti, M., 2016, "Utilization of spilitic mining wastes in the construction of landfill bottom liners", J. Environmental Chemical Enginreeing, Vol. 4(2), pp. 1818-1825.

Prakongwittaya, W., Asavapisit, S., Piyapanuwat, R., Muhummud, T., 2017, " Effect of Seasons and Sources of Raw Water on the Properties of Water Treatment Residue Compacted Clay", International Journal of Environmental Science and Development, Vol. 8, No. 5, pp. 337-341.

Takachart, P., Piyaphanuwat, R., Asavapisit, S., Effect of Water Treatment Residue on Properties of Compacted Clay Liner, International Conference on Science and Technology 2015, 4-6 November 2015, Rajamangala University of Technology Thanyaburi, pp. 48-52

Vichana, S., Rachana, R., Horpibulsuk, S., 2013, "Strength and microstructure development in Bangkok clay stabilized with calcium carbide

residue and biomass ash" , ScienceAsia, Vol. 39, pp. 186–193.

Vichana, S., Rachana, R., 2013, "Chemical stabilization of soft Bangkok clay using the blend of calcium carbide residue and biomass ash", Soils and Foundations, Vol. 53, No. 2, pp. 272-281.

Xu, H., Shu, S., Wang, S., Zhou, A., Jing, P., Zhu, W., Fan, X., Chen, L. ,2019, " Studies on the chemical compatibility of soil-bentonite cut-off walls for landfills", Journal of Environmental Management, Vol. 237, pp.155-162.

Norris, A., Emidio, G.D., Malusis, M. A., Replogle, M. , 2018, " Modified bentonites for soil-bentonite cutoff wall applications with hard mix water" Applied Clay Science, Vol. 158, pp. 226-235.

Morandini, T. L. C. , Leite, A. L. , 2015, " Characterization and hydraulic conductivity of tropical soils and bentonite mixture s for CCL purposes", Engineering Geology, Vol. 196, pp. 251-267.

Zhou, L., Monreal, C. M., Xu, S., Shu, McLaughlin, N.B.,Zhang, H., Hao, G., Liu, J., 2019, " Effect of bentonite- humic acid application on the improvement of soil structure and maize yield in a sandy soil of a semi-arid region", Geoderma, Vol.338, pp.269-280.

Wang, Y., Chen, Y., Xie, H., Zhang, C., Zhan, L. , " Lead adsorption and transport in loess- amended soil-bentonite cut- off wall" , Engineering Geology, Vol. 215, pp. 69-80.

Utilization of Bagasse Ash in Interlocking Block Production

Rungroj Piyaphanuwat[1*], Suwimol Asavapisit[2]

[1]Ratchaburi Learning Park, King Mongkut's University of Technology Thonburi, Rang Bua, Chom Bueng, Ratchaburi 70150, Thailand
[2]Environmental Technology, School of Energy, Environmental and Materials, King Mongkut's University of Technology Thonburi, Pracha U-thit Road, Bangmod, Thung-kru, Bangkok 10140, Thailand
Corresponding author: email: rungroj.piy@kmutt.ac.th

ABSTRACT

In the present work, the interlocking blocks was modified by partial substitution of lateritic soil (LS) with bagasse ash (BA). The effect of ordinary Portland cement (OPC) to LS ratio of 1:3 1:5 1:7, 1:9 and 10, 15 and 20 wt.% of BA content on the engineering properties of interlocking blocks was investigated. The chemical and physical properties of LS and BA were determined by X-ray fluorescence spectrometer, sieve analyzer, and scanning electron microscope. The engineering properties of modified interlocking blocks were compared with interlocking blocks without replacement of BA. The results shows that BA was a porous material with high water adsorption. The adding BA to interlocking blocks decreased compressive strength, dry density values and lead to high void within interlocking blocks structure. The interlocking blocks at OPC:LS ratio of 1:5 with 15 wt.% of BA were perfectly suitable for inside and outside building construction (Community product Standard for interlocking blocks).

Keywords: Lateritic soil, Bagasse ash, Interlocking blocks, compressive strength

INTRODUCTION

Sugarcane, as raw material for sugar production, is an important agricultural economics in Thailand. It is particularly in Kanchanaburi and Ratchaburi provinces having approximately 8- 10 factories with each factory producing sugar more than 10,000 tons per year. A large amount of sugarcane waste known as bagasse is mostly used as fuel for steam generator (boiler) in the sugar industry, resulting in a lot of bagasse ash (BA). At present, BA is dumped in landfill, or agriculturist may bring BA to adjustment of agricultural land. BA dust has an air pollution and human health in factory and surrounding communities. Nevertheless, the chemical compositions of BA consist of 60- 70 wt. % of SiO_2 + Al_2O_3 + Fe_2O_3, leading to using BA as partial substitution for ordinary portland cement (OPC) in concrete manufacturing [1].

Interlocking blocks are an interesting cementitious and construction materials. They are continuously developed thanks to easy production process, production cost reduction and use of local raw materials, for example, fine lateritic soil, crushed dust and sand . Interlocking blocks were use to build wall, water tank and decorate garden, in addition it easy produce and using nature materials. The OPC, lateritic soil (LS) and small gravel were main composition materials for producing interlocking blocks. The LS occur weathering of laterite rock that is as fine aggregate in interlocking block [2, 3].

The lateritic soil (LS) is major composition in interlocking blocks production. Interlocking blocks can be generally varied OPC: LS ratio from 1: 1 to 1: 12 in order to reduce OPC content and production cost. In this work, we have focused on utilization of BA for producing interlocking blocks. The effects of OPC: LS ratio and BA content on interlocking blocks properties were studied. The compressive strength, dry density and water adsorption of modified interlocking blocks were compared to original ones.

METHODOLOGY

Raw materials

Portland cement type I (OPC) was purchased from Elephant brand of SCG Cement – Building Materials Company Limited. LS was provided from Ratchaburi Block Din Cement Factory, Ratchaburi province, Thailand. BA, as sugarcane waste from sugar manufacturing process, was gained from Ratchaburi Sugar Company Limited, Ratchaburi province, Thailand. LS and BA were sun-dried and ground by Los Angeles abrasion machine until the particle size was less than 0.85 mm (Sieve No. 40). LS and BA were analyzed with a X-ray fluorescence spectrometer (XRF). The particle size distribution was determined by sieve analyzer according to ASTM C136M-14 [4].

Production of interlocking blocks

OPC and LS were thorough mixed in several proportions of 1:3, 1:5, 1:7, and 1:9 and then slowly added water. The optimal water content was estimated by standard compaction test following ASTM 1557-12 [5]. After that, the mixtures were formed by compression molding machine at 1 time. The obtained interlocking blocks with 10 cm height, 25 cm length and 12.5 cm wide were represented as the original interlocking blocks. These interlocking blocks were covered on wet curing for 7 days and further wrapped with plastic film for 14 and 28 days. The interlocking blocks could be modified by partial substituting BA for LS. BA was added in the interlocking blocks at 10, 15 and 20 wt.% based on the LS weight. Preparation and production of the modified interlocking blocks were performed as the original ones. All proportion of interlocking blocks shown in Table 1

Table 1` Proportion of original and modified interlocking blocks

Sample	Mix proportion (wt.% for 1000g)		
	OPC	LS	BA
1:3	250	750	-
1:3 + 10 wt.% BA	250	675	75
1:3 + 15 wt.% BA	250	638	113
1:3 + 20 wt.% BA	250	600	150
1:5	167	833	-
1:5 + 10 wt.% BA	167	750	83
1:5 + 15 wt.% BA	167	708	125
1:5 + 20 wt.% BA	167	666	167
1:7	125	875	-
1:7 + 10 wt.% BA	125	787	88
1:7 + 15 wt.% BA	125	744	131
1:7 + 20wt.% BA	125	700	175
1:9	100	900	-
1:9 + 10 wt.% BA	100	810	90
1:9 + 15 wt.% BA	100	765	135
1:9 + 20 wt.% BA	100	720	180

Characterization of raw materials

The chemical compositions of LS and BA were analyzed with a XRF equipped with Cu Kα radiation. The particle size distribution was determined by sieve analyzer according to ASTM C136M-14 [4]. Basic soil properties, including liquid limit and plastic limit, were measured by Atterberg test device.

Characterization of interlocking blocks

The compressive strength of interlocking blocks was carried out using a universal testing machine (UTM) and calculated on the following ASTM C31-15[6]. The water adsorption was tested by using three replications of each interlocking block. All samples were dried at temperature of 110 ºC for 24 h and then weighed. Next the samples were soaked with water for 24 h and weighed again. Calculation of water adsorption value accorded with ASTM C642-13[7].

RESULTS AND DISCUSSION

Characterization of raw materials

The chemical compositions of LS and BA are shown in Table 2. LS and BA had high content of SiO2 (90.49 and 68.60 wt.%, respectively). SiO2 and Al2O3 were the main components of BA. Other phases, such as Al2O3, Fe2O3, K2O, MgO and CaO, wwere presented as impurities in both raw materials. Table 3 shows physical properties of LS and BA. At sieve number of 100 and 200, the retained percentage values of LS and BA were relatively high, resulting from the large particle size in these raw materials. The particle sizes of LS and BA were in range of 0.15-0.425 mm and 0.075-0.15 mm, respectively. However, the uniformity coefficients of both starting materials was 2 that indicated that were uniform soil. For curvature coefficient of both materials was 1 that shown the good distribution of materials. The atterberg limit of LA was 14.08 and 12.36 wt.% water content for liquid limit and plastic limit. LS had low plasticity index expressing as slightly sticky soil. Furthermore, LS (2.78) was higher specific gravity than BA(1.56). These results corresponded to the microstructures of LS (Figure 1 (A)) and BA (Figure 1 (B)): LS was larger particle size than BA

Table 2 Chemical compositions of LS and BA

Compound	Chemical compositions (wt.%)	
	LS	**BA**
SiO_2	90.49	68.60
Na_2O	0.03	1.07
K_2O	0.44	3.92
Al_2O_3	6.22	3.97
CaO	0.11	7.85
Fe_2O_3	1.25	3.16
Cl	-	0.95
P_2O_5	0.03	1.71
MgO	0.20	1.69
TiO_2	-	0.27
MnO	-	0.14
SO_3	0.04	1.44

Table 3 Physical properties of LS and BA

	LS	**BA**
Retained percentage (wt.%)		
No.4 (4.75 mm)	0	0
No.10 (2 mm)	2.09	0
No.40 (0.425 mm)	13.81	10.23
No.100 (0.15 mm)	74.48	20.11
No.200 (0.075 mm)	6.02	68.22
Pan	3.60	1.44
Coefficient of uniformity, C_u	2	2
Coefficient of curvature, C_c	1	1
Liquid limit, LL (%)	14.08	-
Plastic limit, PL (%)	12.36	-
Specific gravity (g/m^3)	2.78	1.56

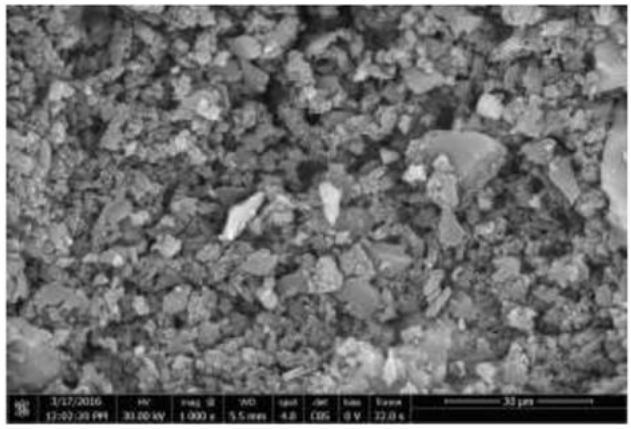

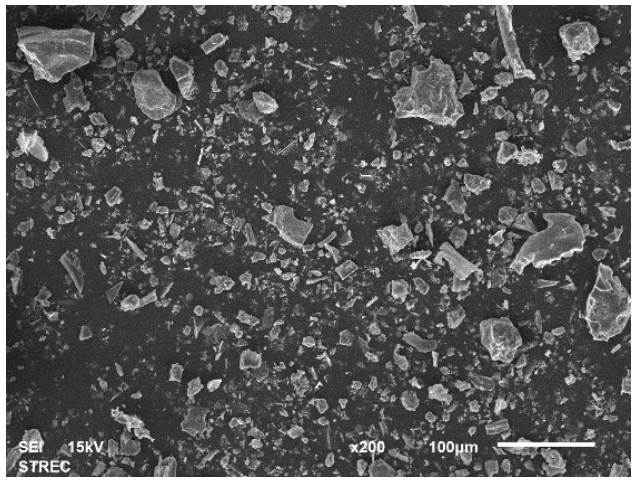

B)

Figure 1 SEM images of (A) LS and (B) BA.

Characterization of interlocking blocks

The original interlocking blocks were prepared from mixing various OPC and LS mixtures with water . With reference to Table 4, color of interlocking blocks at OPC: LS ratio of 1: 3 was red, following on the LS color. Their surfaces depended on the particle size of LS. Other ratios (1: 5, 1: 7, 1: 9 and 1: 11) were similar to above results. The interlocking blocks with partial replacing LS with 10 wt. % BA were red brown to dark brown color and smooth surface, relating to small particle size of BA. Although the adding BA to interlocking blocks increased more

than 10 wt.%, the interlocking blocks turned black color and easy cracking. It might be due to partial OPC and water drained away from the mixture during compression molding process. The high BA content in interlocking blocks cannot make completely molded because it was low cement binder [ ].

Table 4 Textural properties of original and modified interlocking blocks at OPC:LS ratio of 1: 3

BA content (%)	Top view	Side view
0	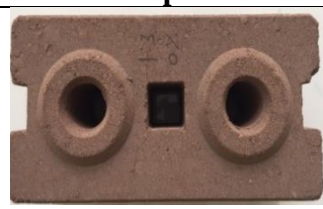	
10 wt.%BA		
15 wt.%BA		
20 wt.%BA	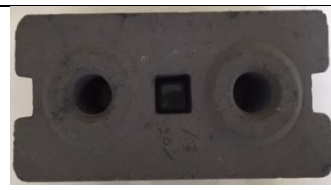	

Compressive strength

Compressive strength of original interlocking blocks at various OPC:LS ratios is illustrated in Figure 2. The compressive strength of all interlocking blocks was rapidly raised in the first 7 days and then slightly increased. It was due to the cement hydration producing calcium silicate hydrate and calcium aluminate hydrate compounds having adhesive property [1]. At the curing

time of 28 days, the compressive strength value of interlocking blocks with the increased OPC:LS ratio from 1:3 to 1:9 was continuously changed from 4.29 to 1.56 MPa. The reduction of compressive strength resulted from increase of BA that resulted in reduction of cement binder[8] . Figure 3 shows compressive strength of modified interlocking blocks at curing time of 28 days. An increasing of BA content in interlocking blocks significantly decreased the compressive strength value because the specific gravity of BA was lower than that of LS: the 20 wt.% BA was equal to 40 w/v% one. Therefore, the OPC component did not thoroughly dispersed in interlocking blocks, total volume of all modified interlocking block mixtures was raised. It was especially OPC:LS ratio of 1:9. According to Thai Community Product Standard (TCPS 602/ 2547) for interlocking blocks (Minor strusture type) [9], the compressive strength value must be at least 2.5 MPa. Thus, the suitable conditions for interlocking blocks production following the TCPS 602/2547 were using OPC:LS ratio of 1:3 + 0-20 wt.% of BA, 1:5 + 0-15 wt.% of BA and 1:7 + 0-10 wt.% of BA.

Dry density

Figure 4 demonstrates dry density of original and modified interlocking blocks at various OPC:LS ratios. The raising of OPC:LS ratio from 1:3 to 1: 9 gradually decreased the dry density value of interlocking blocks from 1. 73 to 1. 43 g/ m3 (approximately 20 %), resulting from the specific gravity value of OPC as 3.15 g/m3 which was higher than that of LS. The weight of interlocking blocks became lighter than the usual.

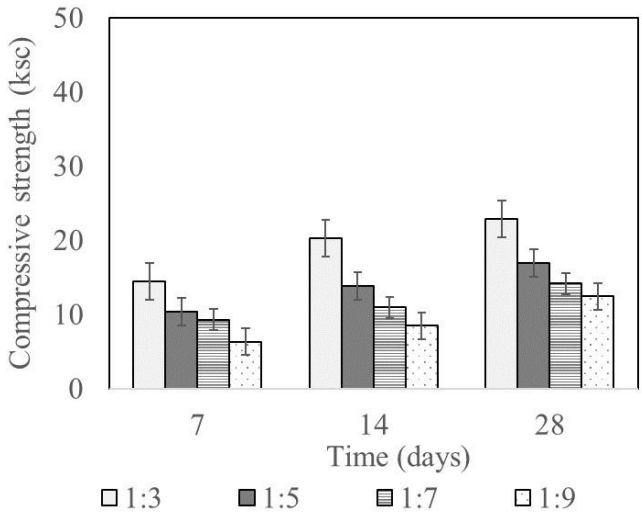

Figure 2 Compressive strength of original interlocking blocks

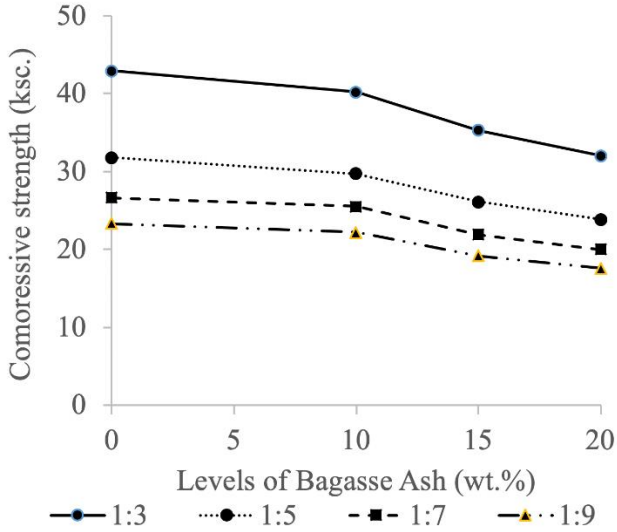

Figure 3 Compressive strength of modified interlocking blocks.

Using the 10 wt. % BA as a replacement to LS reduced dry density value by 2-6 % and further lessened to 20-25 % with increased BA content to 20-30 wt. %. The reduction of dry density made increase porevolume that leaded to low compressive strength [10].

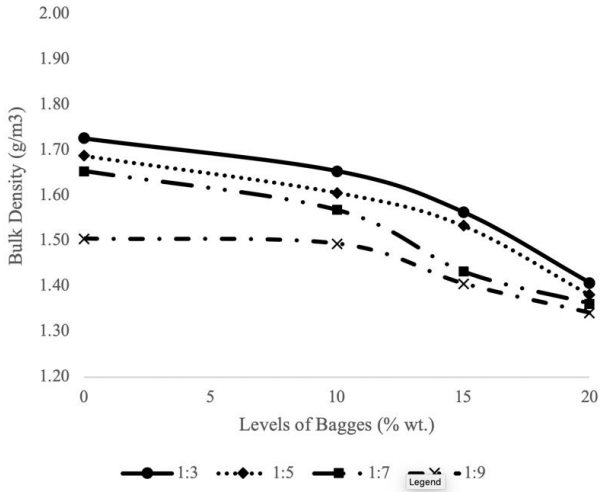

Figure 4 Bulk density of modified interlocking blocks.

Water adsorption

Figure 5 illustrates water adsorption of original and modified interlocking blocks at various OPC:LS ratios. The water adsorption value of interlocking blocks raised from 181 to 246 kg/m3 (approximately 35 %) when increased OPC: LS ratio from 1: 3 to 1: 9. The water adsorption of LS was better than that of OPC since the hydration between OPC and water created adhesive compounds having low water adsorption capacity. The partial replacement of LS by BA improved the water adsorption efficiency of interlocking blocks. From the SEM results of starting materials (Figure 1), the LS structure composed plenty of soil beads aggregation causing interparticle void within its structure, but structure of BA was the porosity on surface. It was suggested that the porosity of BA was more than LS. The increased water adsorption of interlocking blocks associated with decreasing of dry density. The water adsorption value complied with TCPS 602/2547 for minor structure interlocking blocks, which was between 130 and 270 kg/m3, was optimum using OPC: LS ratio of 1: 3 + 0-15 wt.% of BA, 1:5 0-15 wt.% of BA and 1:7 0-10 wt.% of BA.

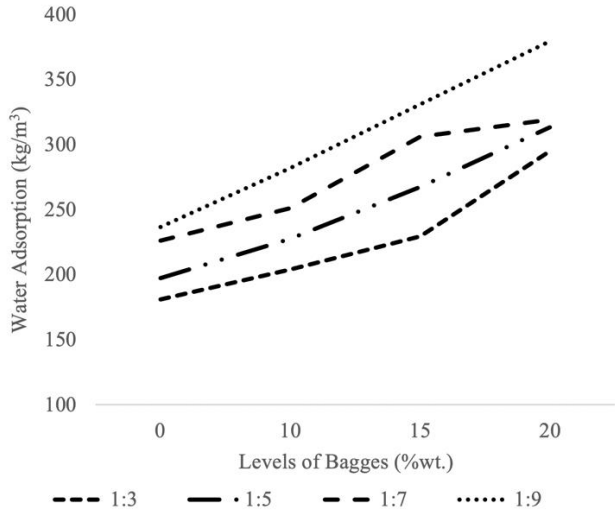

Figure 5 Water adsorption of original interlocking blocks.

CONCLUSIONS

Engineering properties of interlocking blocks depended on OPC: LS ratio and BA content. The interlocking blocks with increased OPC: LS ratio and BA content slightly decreased compressive strength and dry density values. The water adsorption was raised, especially when using BA replaced to LS because OPC binder cannot perfectly dispersed in interlocking blocks. The interlocking blocks were molded and joined by only compressive force. BA had a lot of porosity and good water adsorption, leading to void within interlocking blocks structure. The maximum BA content and engineering properties of inter interlocking blocks passing TCPS 602/ 2547 (minor structure type) was found in 1:5 0-15 wt.% of BA that was the most suitable in creation of interlocking blocks for indoor and outdoor construction.

ACKNOWLEDGEMENTS

The authors would like to give special thanks to the Thailand Research Fund, for their financial support. The authors also appreciate the King Mongkut's University of Technology Thonburi (Ratchaburi) for providing access to their laboratories.

REFERENCES

Loh, Y. R., Sujan, D., Rahman, M. E., Das, C. A., 2013, Sugarcane bagasse—The future composite material: A literature review, Resources, Conservation and Recycling, Vol.75, pp. 14-22

Ali, M., Gultom, R.J., Chouw, N., 2012, " Capacity of innovative interlocking blocks under monotonic loading", Construction and Building Materials, Vol. 37, pp.812-821

Carlesso, M., Giacomellia, R., Krause, T., Molotnikov, A., Koch, D., Kroll, S., Tushtev, K., Estrin, Y., Rezwan, K., 2013, " Improvement of sound absorption and flexural compliance of porous alumina-mullite ceramics by engineering the micro-structure and segmentation into topologically interlocked blocks", Journal of the European Ceramic Society, Vol.33(13-14), pp. 2549-2558.

American Society for Testing and Materials (2014), Standard Test Method for Sieve Analysis of Fine and Coarse Aggregates, (ASTM Standard C136 / C136M - 14). USA: ASTM International

American Society for Testing and Materials (2012), Standard Test Methods for Laboratory Compaction Characteristics of Soil Using Modified Effort (56,000 ft-lbf/ft3 (2,700 kN- m/ m3)) 1 (ASTM Standard 1557-12). USA: ASTM International.

American Society for Testing and Materials (2015). Standard Practice for Making and Curing Concrete Test Specimens in the Field (ASTM Standard C31-15). USA: ASTM International

American Society for Testing and Materials (2013). Standard Test Method for Density, Absorption, and Voids in Hardened Concrete (ASTM Standard C642-13). USA: ASTM International.

Uygunoğlu, T., Topcu, I.B., Gencel, O., Brostow, W., 2012, "The effect of fly ash content and types of aggregates on the properties of pre-fabricated concrete interlocking blocks (PCIBs)", Construction and Building Materials, Vol. 30, pp. 180-187.

Thai Community Product Standard (2004). Interlocking Block (TCPS Standard 602- 2547). Thailand: Thai Industrial Standards Institute (TISI)

Zareei, S.A., Ameri, F., Bahrami, N., 2018, " Microstructure, strength, and durability of eco-friendly concretes containing sugarcane bagasse ash", Construction and Building Materials, Vol. 184, pp. 258-268.

The study on the effects of chemical coagulation and cost estimates throughout the water supply treatment cycle of Phichit provincial waterworks authority

Somsamai Khamching[1], Pajaree Thongsanit[2]

[1]Master student of civil engineering department, faculty of engineering, Naresuan University, Phitsanulok, Thailand 65000
[2]Assistant Professor Doctor of civil engineering department, faculty of engineering, Naresuan University, Phitsanulok, Thailand 65000 ;
Corresponding author: email: somsamaik59@email.nu.ac.th, Dek_oo@hotmail.com

ABSTRACT

This research studied the effect of pH on chemical coagulation processes in a water supply using the jar test method. It focused on the water production process at the Phichit provincial waterworks authority during the rainy season from mid-May to mid-October in 2018. The raw water was sampled from the Nan River water production process at the Phichit site. The range of turbidity and pH of raw water were 90.5 NTU to 364 NTU and 7.50 to 7.96 respectively. Adjustment raw water pH using NaOH was studied. The result found that the best flocculation conditions occurred when the raw water pH was 8.5. At this pH, the optimum dose of Poly Aluminum Chloride (PACL) during the turbidity test was 4 to 50 ppm. The obtained values of two water parameters: turbidity and color, decreased at pH 8.5. The efficiency of turbidity removal was 30 % to 64% and color removal was 43% to 75%. The data obtained on nine water parameters; pH, temperature, conductivity, alkalinity, total hardness, calcium, chloride, iron (Fe) and manganese (Mn) did not differ with pH adjustment. The chemical cost of PACL and NaOH at pH 8.5 was 0.64 to

1.31 Baht per m^3 of water supply. The equation for the turbidity of raw water (X) and the optimum dose of PACL (Y) was $Y = 0.0003X^2 + 0.0396X + 0.98$.

Keywords: chemical coagulation processes, cost estimates, water supply, Phichit provincial waterworks authority, jar test

INTRODUCTION

Phichit provincial waterworks authority is located in the lower northern part of Thailand. This water supply plant has used raw water only from the Nan River for water production. In the rainy season with heavy rain, the water has caused erosion and resulting sediment from the Nan riverbank. Data from ASDECON CORPORATION CO., LTD, in February 2012 indicated that bank erosion of the Nan River Basin downstream from Sirikit Dam was more severe than that from the Nan Northern Basin, causing soil erosion and landslide to occur generally. Problem areas in Nan Province included Pua, Thung Chang, Bo Kluea and Tha Wang Pha districts, and Wiang Sa Santisuk city. Problem areas in Uttaradit Province included Phichai and Tron districts. Problem areas in Phichit Province included Mueang, Sak Lek, Bang Mun Nak and Taphan Hin districts. Problem areas in Phitsanulok Province included Mueang, Phrom Phiram, Bang Krathum and Nakhon Thai districts.

The occurrence of bank erosion affected water resources. Heavy rain eroded sediment along the riverbank in the watershed area, causing the physical characteristics of the basin to change. Turbidity, suspended solids and sediment concentration increased, which interfered with the passage of light passing through the water, thus causing the dissolved oxygen (DO) content of the water in the basin to decrease. Also, color of water change from nature.

Although the production process was strictly monitored and controlled, variations in water quality affected the

operation of the Phichit Provincial Waterworks Authority in controlling the water supply production process, including difficulty in removing turbidity by the chemical coagulation process, and receiving complaints about water quality from customers regarding turbid and yellow or brown coloured water.

However, even though there were no complaints during the summer and winter seasons, there were variations in raw water quality. For example, the winter season, low turbidity waters are usually hard to coagulate because of its floc formation of particles which demand optimum coagulant dosage. Small particles or colloids generally had lower removal efficiencies in the solid and liquid separation process following flocculation, since smaller particles generally settled down more slowly than larger particles of similar density [1]. Therefore, over the winter season these processes impacted control of the production process and water supply quality. This researcher was also interested in studying the effects of a chemical coagulationprocess in water supply using a jar test in order so the results could be used as guidelines in improving the water production process in each season and reducing customer complaints.

Coagulation is a widely applied unit process to remove particles and organic matter present in water treatment works (WTW) [2].

One property that may have a significant impact at water treatment works is characteristics of flocs, which cause a critical effect on solid/liquid separation process [2].

In this study, the major objectives were to find optimum coagulant dosage and to study the physical and chemical properties of water samples from the chemical coagulation process after adjustment of raw water pH, especially the coagulation mechanism at various coagulant dosages and pH values of raw water [3]. The results can be used to evaluate the chemical costs for water production plant at the Phichit site.

Coagulation is the most important step before sedimentation. [4]. Factors such as the nature of the water, the coagulation pH and concentration of coagulant affect the range of species formed and hence the treatment performance [4].

METHODOLOGY

Materials and methods

1. The Raw water

Raw water sampling was conducted from the Nan River at the water production plant on the Phichit site from mid-May to mid-October in 2018. In the study, eleven water quality parameters were analyzed, which are shown in Table 1

2. Coagulant chemical

The water production plant at the Phichit site used Poly Aluminum Chloride (PACL) as the main coagulant chemical.

Table 1 Water quality parameters of the raw water

Parameters	Range (Minimum–Maximum)
1.Turbidity (NTU)	90.5 – 364
2.pH	7.50 – 7.96
3.Color (Pt-Co)	1125 – 5570
4.Temperature (°C)	28.9 – 29.8
5.Conductivity(Us/cm)	81.1 – 182.4
6.Alkalinity (mg/L)	56 – 74
7.Total Hardness (mg/L)	56 – 75
8.Calcium (mg/L)	15 – 23
9.Chloride (mg/L)	5 - 12
10.Iron (mg/L)	1.13 – 4.05
11.Manganese (mg/L)	0.479 – 1.31

PACL has generally been reported to perform better than ALUM in terms of turbidity reduction, dead organic content removal and color removal [5]. For this research, a PACL stock solution at a

concentration of 1 % was prepared using PACL 1 g in 100 mL of distilled water before each set of experiments. This PACL coagulant was added to water samples in each jar which to be optimum dose and to compare dose of PACL coagulant before and after the adjustment of pH.

3. pH adjustment

H_2SO_4 solution at 0.1 N concentration and NaOH solution at 1 N concentration were used to adjust raw water pH in beakers to 6.0, 6.5, 7.0, 7.5, 8.0 and 8.5. The different pH values affected floc formation and removal efficiency. The pH at which coagulation occurred was the most important parameter for proper coagulation performance as it affected the surface charge of colloids [6].

4. Jar test

A jar test used in water production plant at the Phichit site consisting of six paddles. The jar test was used to estimate the optimum dose of PACL. One litre of raw water was added to each of six beakers and Phichit site condition for coagulation in water treatment plant, followed by rapid mixing at 100 rpm for 30 seconds. Slow mixing was then used in 3 stages at 75 rpm for 5 min, 49 rpm for 5 min and 39 rpm for 5 min followed by settling for 6 min. The water samples after settling were collected for analysis of water parameters as shown in Table 1

5. Analytical Equipment

The raw water samples and water obtained from experiment were analyzed for turbidity using a portable HACH 2100 Q turbidity meter. Values of pH were obtained using a Thermo scientific orion 3 star pH meter. Conductivity and temperature were measured using a portable HACH HQ14d. Color was determined using a HACH DR 2800 portable spectrophotometer. Total alkalinity, total hardness, calcium and chloride were measured by a titration method following the *Standard Methods* for the Examination of Water and Wastewater *22nd edition* (2012), iron content was measured using the FerroVer method, and Manganese was measured using a 1-(2-Pyridylazo)-2-Naphthol (PAN) with a HACH DR 2800 portable spectrophotometer.

RESULTS AND DISCUSSION

The experimental work was executed at provincial waterworks authority laboratory at the Phichit lab cluster site.

1. Optimum pH

Analysis of the water production process at the Phichit site from mid-May to mid-October in 2018 showed the following results. The range of raw water turbidity was 90.5 to 364 NTU, which was in the high turbidity range, and made control of production at the plant difficult. Many previous studies have identified that coagulation pH is an important factor in affecting enhanced coagulation and a few researchers have also studied the properties of flocs formed under different coagulation pH values [7]. Therefore, this experiment used pH adjustment in the raw water at pH values of 6.0, 6.5, 7.0, 7.5, 8.0 and 8.5.The results showed that adjustment of pH in raw water was more effective than not adjusting pH, and the best flocculation conditions were provided in a raw water pH of 8.5. The adjustment of pH at 8.5 could reduce the required dose of PACL and residual turbidity, and decrease color.

From Figure 1, the jar test with the raw water with no pH adjustment, residual turbidity was in the range of 2.24 to 5.01 NTU. Under experimental conditions with pH adjusted to 8.5, the raw water dose of PACL decreased and residual turbidity was in the range of 1.55 to 3.41 NTU. The efficiency of turbidity removal was therefore from 30 % to 64%

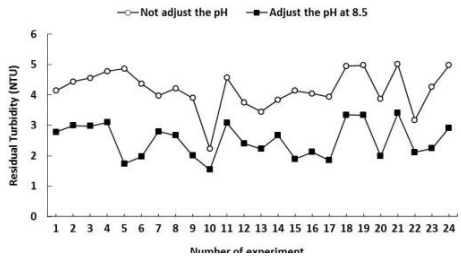

Figure 1 Effect of removal the turbidity of raw water at adjustment the pH at 8.5

Similarly in Figure 2, when the raw water was not adjusted for pH, the result showed that residual color was in the range of 6 to 12 Pt – Co, while after adjusting the pH of the raw water to 8.5, the residual color was in the range of 2 to 5 Pt – Co. The efficiency of color removal was therefore from 43 % to 75 %.

2. Optimum PACL dosage

In this experiment, when the raw water pH was not adjusted, and the Jar test was performed for optimum PACL dose, it was found that the dose of PACL used for coagulation of turbidity concentration was 7 to 55 ppm. When the pH of the water was adjusted to pH 8.5, it was found that the dose of PACL was reduced to 4 to 50 ppm as shown in Figure 3. In addition, the cost reduction of reduced coagulants also resulted in increased removal efficiency.

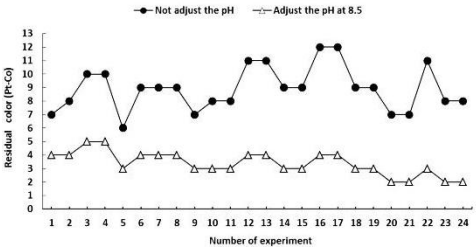

Figure 2 Effect of removal the color of raw water at adjustment the pH at 8.5

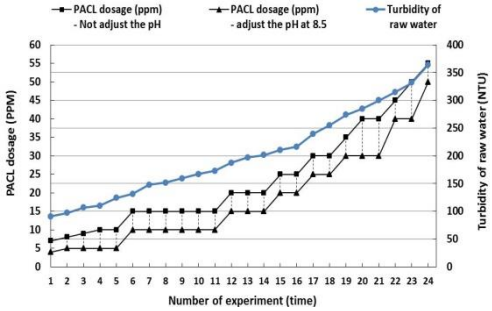

Figure 3 Optimum PACL dosage from jar test at varying raw water turbidity

In addition, the experimental result provided an equation to estimate the optimum PACL dosage as follows: $Y = 0.0003X^2 + 0.0396X + 0.98$, where turbidity of raw water was X and optimum dose of PACL was Y, as shown in Figure 4.

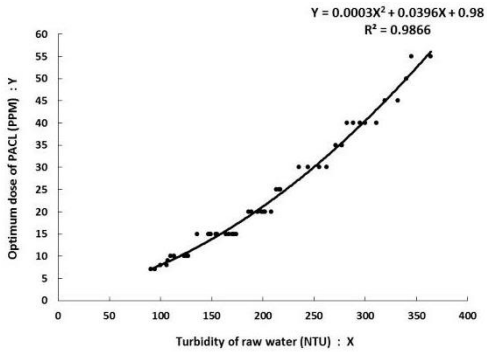

Figure 4 The relationship between turbidity of raw water (X) and optimum dose of PACL (Y)

3. Physical - chemical water quality

This study compared the physical and chemical water quality between the water samples after the chemical coagulation process with no pH adjustment and with pH adjustment by comparing chemical sedimentation efficiency according to the following eleven water quality parameters: turbidity (NTU), pH, color (Pt-co), temperature (°C), conductivity (Us/cm), alkalinity (mg/L), total hardness (mg/L), calcium (mg/L), chloride (mg/L), iron (mg/L) and manganese (mg/L), where the pH of raw water was adjusted to 8.5 and the use of the appropriate PACL dose was used to increase the removal of turbidity and color efficiency. Meanwhile, the effects of pH, conductivity, temperature, alkalinity, total hardness, calcium, chloride, iron and manganese between pH adjustment and non-adjustment were not found difference. The results of water quality from coagulation process are shown in Table 2

Table 2 Water quality before and after coagulation process by jar test

Results of water quality before coagulation process by jar test

Samples of experimental	Turbidity (NTU)	Color (Pt-Co)	pH	Temperature (°C)	Conductivity (us/cm)	Alkalinity (mg/L)	Total Hardness (mg/L)	Calcium (mg/L)	Chloride (mg/L)	Iron (mg/L)	Manganese (mg/L)
Raw water	90.5 - 364	1125 - 5570	7.50 - 7.96	28.9 - 29.8	81.1 - 182.4	56 - 74	56 - 75	15 - 23	5 - 12	1.13 - 4.05	0.479 - 1.315

Results of water quality after coagulation process by jar test

Samples of experimental	Residual turbidity (NTU)	Residual color (Pt-Co)	pH	Temperature (°C)	Conductivity (us/cm)	Alkalinity (mg/L)	Total Hardness (mg/L)	Calcium (mg/L)	Chloride (mg/L)	Residual iron (mg/L)	Residual manganese (mg/L)
Water samples after experiment from not adjustment of pH	2.24 - 5.01	6 - 12	7.25 - 8.09	29.1 - 30.0	85.6 - 186.3	52 - 71	55 - 73	16 - 21	11 - 22	0.014 - 0.14	0.019 - 0.036
Water samples after experiment from adjustment of pH at 8.5	1.55 - 3.41	2 - 5	7.70 - 8.20	29.0 - 30.0	105.4 - 220	51 - 78	56 - 75	17 - 22	10 - 19	0.010 - 0.11	0.012 - 0.028

However, the results obtained from the experiment indicated that iron and manganese were significant. Although the pH adjustment of raw water did not affect differently to the iron and manganese removal efficiency when comparing to the non-adjustment of pH, when considering from the iron

and manganese conditions before and after the experiment, chemical coagulation would remove almost 100 % of iron and manganese. The efficiency of iron removal in raw water was as high as 96.54 % to 98.76 % as shown in Figure 5

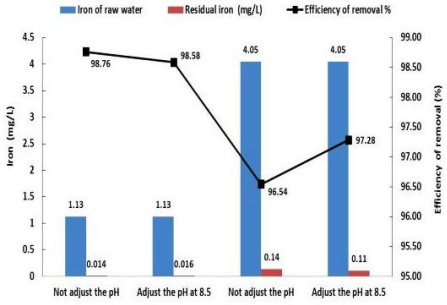

Figure 5 Effect of removal of iron from raw water

And the efficiency of manganese removal in raw water was 96.03 % to 97.87 % as shown in Figure 6.

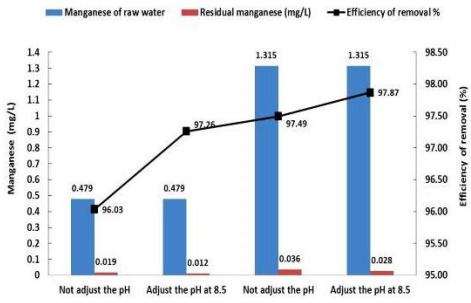

Figure 6 Effect of removal of manganese from raw water

4. Chemical cost of coagulation process

In the experiment to determine the optimum PACL dose for removing turbidity of raw water in the range of 90.5 to 364 NTU, it was found that raw water that was not pH adjusted and used PACL as only coagulant in sedimentation process, the concentration of PACL was used at 7 to 55 ppm, which is considered as chemical cost at 0.10 to 0.79 Bath/m3. While raw water with pH adjustment used concentration of PACL at 4 to 50 ppm which considered as chemical cost at 0.64 to 1.31 Baht/m3 as shown in Figure 7.

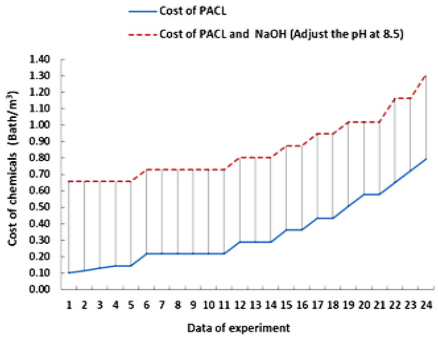

Figure 7 Cost of chemicals for coagulation process

CONCLUSIONS

This study focused on the effect of chemical coagulation by jar test with PACL as coagulant. Experimental

results shown that using PACL is effective in removing turbidity and the color from raw water, and adjusting the pH provided a higher removal efficiency and used a lower concentration of PACL at the optimum pH value for the coagulation process of 8.5. Before adjusting the pH of raw water the optimum dosage concentration of PACL for the coagulation process was 7 to 55 ppm, resulting in a cost of PACL from 0.10 to 0.79 Baht per m^3 but after adjusting the pH of raw water to 8.5, the concentration of PACL was reduced to 4 to 50 ppm and after the experiment on turbidity removal efficiency, it was increased from 30 to 64%, and the color removal efficiency was 43 % to 75 %. The cost of PACL and NaOH chemicals was 0.64 to 1.31 Baht per m^3, which increased from 0.52 to 0.54 Baht per m^3. In addition, the result of optimum PACL dosage from the experiment provided an equation for estimation of the usage dose of PACL as follows: $Y = 0.0003X^2 + 0.0396X + 0.98$, where turbidity of raw water is X and the optimum dose of PACL is Y

However, the Phichit Provincial Waterworks Authority should study the use of other chemicals in order to increase the chemical coagulation efficiency and lower chemical costs for the coagulation process, and identify other factors that may affect the formation and sedimentation of flocs, such as rapid mixing, slow mixing and the time of mixing for the water production process at the Phichit site.

REFERENCES

[1] Boller, M. Blaser, S. (1998), Particles under stress, Water Sci. Technol. 37,9-29.

[2] Z. Ma, J. J. Qin, C. X. Liou, "Effects of coagulation pH and Mixing Condition on Characteristic of Flocs in Surface Water Treatment,"ACEM. J. (2012) 26-30.

[3] N. Wei, Z. Zhang, D. Liu, Y. Wu, J. Wang, and Q. Wang, "Coagulation behavior of polyaluminum chloride: Effect of pH and coagulant dosage," Chin. J. Chem. Eng. 23 (2015) 1041-1046.

[4] T. Jowa, and L. L. Mguni, "Treatment of Low Turbidity Wateer Using Poly-Aluminium Chloride (PAC) and Recycled Sludge: Case study Chinhoyi," Zim. J. Sci. Technol. 10 (2015) 101-108.

[5] Zouboulis A., & Traskas G., (2005). Comparable evaluation of various of commercial availiable alumina-based coagulants for the post-treatment of urban wastewater. Journal of Chemical Technology and Biotechnology 80;1136-1147

[6] Yan, M., Wang, D., Yu, J., Ni, J., Edwards, M., Qu, J. (2008) "Enhanced coagulation with polyaluminum chlorides: Role of pH/Alkalinity and speciation" Chemosphere 71 1665-1673

[7] C. baichuan, G. BaoYu, X. ChunHua, F. Ying, and L. Xin, "Effects of pH on coagulation behavior and floc properties in Yellow River water treatment using ferric based coagulants," Chinses Sci Bull May (2010) vol.55 No. 15.

A. Baghvand, A. D. Zand, N. Mehrdadi, and A. Karbassi, "Opimizing Coagulation Process for Low to High Turbidity Waters Using Aluminum and Iron Salts,"Am. J. Environ. Sci., 6(5): 442-448, 2010.

A. F. Ashery, K. Radwan, and M. I. G. Al-Alm Rashe, "THE EFFECT OF PH CONTROL ON TURBIDITY AND OM REMOVAl IN CONVENTIONAL WATER TREATMENT,".Journal IWTJ (2011) vol.1 – Issue 2.

C. baichuan, G. BaoYu, X. ChunHua, F. Ying, and L. Xin, "Effects of pH on coagulation behavior and floc properties in Yellow River water treatment using ferric based coagulants," Chinses Sci Bull May (2010) vol.55 No. 15.

J. Feria-Diaz, J. P. Rodino-Arguello, and G. E. Guierrez-Ribon, "Behavior of turbidity, pH, alkalinity and color I Sinu River raw water treament by natural coagulants," Univers de Antioquia, No 78 (2016) 119-128.

M. R. Kemunto, "Optimisation of Cost Effectiveness of Water Treatment Works: Coagulation Process," F16 (2011).

PM10 and dust fall concentrations from mobile sources in the Sukhothai Municipality

Nattaphong Moomuangsong[1], Pajaree Thongsanit[2]*

[1]Master's degree student, civil engineering department, Faculty of Engineering, Naresuan University, Phitsanulok, Thailand 65000
[2]Assistant Professor, civil engineering department, Faculty of Engineering, Naresuan University, Phitsanulok, Thailand 65000
Jumbo.big.9@gmail.com@hotmail.co.th

ABSTRACT

This research produced a particulate matter inventory report from mobile sources in the Sukhothai municipality. Forty-eight samples of PM_{10} were collected using high volume air samplers for 24 hours at a flow rate of 1.7 cubic meters per minute. In addition, 48 samples of dust fall were collected using a gravimetric technique modified from the Department of Pollution Control (PCD). The dust fall containers were set from August 2017 to July 2018 at four sample stations. There were also two points of traffic survey by Closed Circuit Television (CCTV) cameras and the results were combined with an emission factor method to quantify emissions. The highest PM_{10} data was 108 micrograms per cubic meter at the police fort site in April, 2018. The highest dust fall data was 247 milligram per square meter per day at the police station site in April, 2018. The lowest dust fall data was 70 milligram per square meter per day at the Trirat community station in June, 2018. The major mobile source of PM_{10} emissions in the Sukhothai Municipality was motorcycles and tricycles.

Keywords: particulate matter, inventory, Sukhothai

INTRODUCTION

In the past, the area in the Sukhothai municipality developed economically and divided into the current 12 community areas. The population and number of buildings are increasing in the area. Air pollution problems in the Sukhothai municipality are from various sources, including traffic and agricultural open burning outside the Sukhothai municipality during the harvesting season.

The expansions on the population and constructions have been increasing. So, air pollution was a problem in the Sukhothai municipality that has been becoming severe air pollutants.The vehicles have come on the area were much, tourists, transport, and etc. That is causing a release more particulates matter smaller than 10 (PM10) which is a cause on effect to health that is a respiratory tract as mentioned above. it is causing the air pollution problems in the Sukhothai municipality.

This reason has sawed the importance of accounting on air pollution emissions in the Sukhothai municipality. The results may be guidelines for control and supervision measures for relevant agencies in the Sukhothai municipality**.**

The main objective of this study was to create a dust inventory in the area of the Sukhothai Municipality and compare the ratio of sources of dust emissions in the Sukhothai Municipality and other cities.

Figure 1 Sukhothai Municipality map, showing collection points

METHODOLOGY

In this research, samples of dust accumulation were collected from four sampling points in the Sukhothai

Municipality area, namely the Khlong Ta Phet community area, the entrance to Soi Sirisamarang (Trirat community), the police fort, and the Wichian Chamnong community.

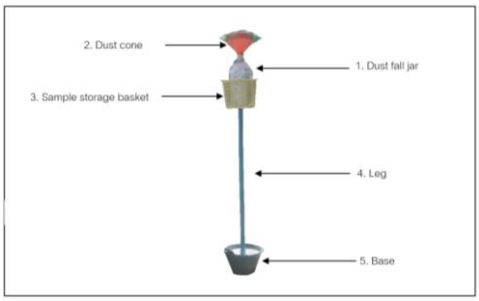

Figure 2 Dust collection tools and equipment

Samples of dust fall were collected using the dust fall Jar method. One sample was collected at each point per month for 12 months, producing a total of 48 samples, which were then analyzed to establish the amount of dust falling each month. The equipment used for collecting dust samples consisted of a sample bottle, a dust cone, a sample storage basket, a sampling basket stand made of PVC pipe. These were placed at the point where the sample is to be collected. The bottles were then analyzed in a laboratory to find the concentration of falling dust in mg per m^2 per day. Also, collection of small dust particle samples of less than 10 microns (PM_{10}) was performed using a High Volume Air Sampler to continuously collect samples over 24 hours at an air flow rate of 1.1 - 1.7 m^3 per minute and using one 8 x 10 inch glass fiber filler for each sample. One sample per month over 12 months was collected from each collection point, providing a total of 48 samples.

The samples were analyzed and the data provided a report of the dust falls in mg/m^2/day and PM10 in microgram/m^3/day.

Mobile sources of PM10 emissions consisted of pollution from gasoline vehicles, small diesel cars, large diesel trucks and motorcycles and tricycles. Calculation of traffic volume used an enumeration method from CCTV from two directions, according to the types of vehicles on the roads. Traffic volume counting was conducted for 12 hours per day (07.00 - 19.00 hrs.) over 3 days between Monday to Friday and on also on Saturday and Sunday. The

calculation of the amount of air pollution from vehicles used equation is;

$$E = N \; x \; EF \; x \; D$$

E = emissions (gram/day)

N = Average daily traffic volume (car/day) (**Table 1.**)

EF= emissions factor (gram/kilometer/day) (**Table 2.**)

D = Distance (kilometer) = 1 kilometer.

Figure 3 High Volume Air Sampler

RESULTS AND DISCUSSION

The results of the study of dust measurements in the Sukhothai municipality were calculated by the dust fall method. Each jar was collected every 30 days from August 2017 to July 2018, thus covering the rainy, winter and summer seasons. The highest dust fall occurred during April. There was a high volume at the police fort sampling, where the maximum amount of accumulated fall throughout the sampling period was 246.56 mg / square meter / day. The dust was mostly caused by traffic raising dust from the road surface. There were heavy traffic conditions in April, which continued over consecutive holidays. Most people travel back to their homes during the holiday festival and the sample

matchine and Hygroscopic cabinet standards, with a value of 1 3 3 milligrams per square meter per day, it was found that 40 samples from the total of 48 samples were above the Malaysian standard. The minimum amount of accumulated dust was measured during the rainy season in October 2017 at 69.49 mg / sq.m / day.

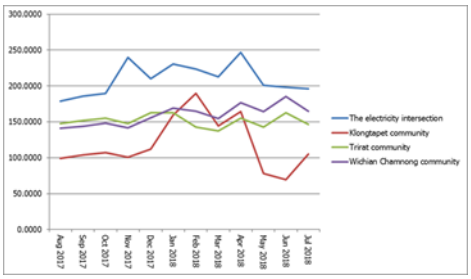

Figure 1 The amount of dust accumulation in the municipality of Sukhothai (The Y axis represents PM10 concentration and the X axis represents the months of measuement)

1. From a review of the formation of accumulation of dust in the municipality of Sukhothai During the month of April 2018, it was found that the accumulation of dust in the area had spread around the area of the 4 sampling points, due to dust blowing from the periphery of the Sukhothai municipality into the city center

2. Quantity of small dust particles (PM_{10}) . From collection of dust samples of not more than 10 microns (PM_{10}) using high volume air samplers, it was found that the area with the maximum (PM10) level was at the police fort intersection (Electric intersection) in April with a reading of 108 µg / Cu.m., while the lowest was at Trirat community station (entrance to Soi Sirisamarang) during August with a reading of 24 µg / Cu.m. None of the measurement results obtained exceeded the PCD standard set at 120 µg / Cu.m.

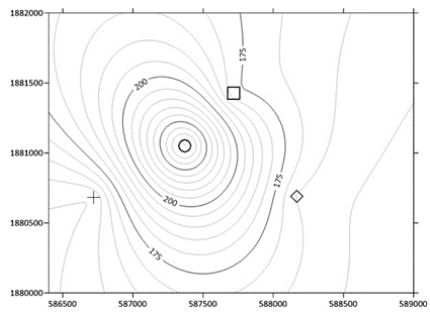

Figure 2 shows the level of dust concentration in the Sukhothai municipality area (The Y axis represents longitude and the X axis represents latitude)

From the PM $_{10}$ dust contour line during April 2018, it was found that the high level of PM $_{10}$ dust was distributed at the point 1 and point 4 due to traffic from people visiting from outside the area in cars and also due to emissions from diesel truck engines.

Figure 3 shows the level of small dust concentration (PM10) (The Y axis represents PM10 concentration and the X axis represents the months of measuement)

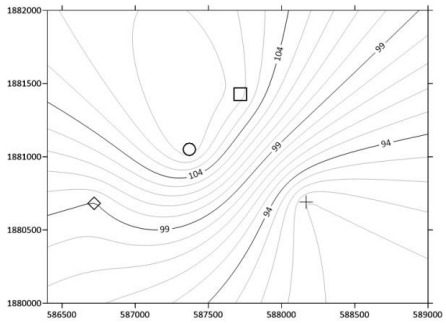

Figure 4 shows the level of dust concentration in the Sukhothai municipality area. (The Y axis represents longitude and the X axis represents latitude)

From the PM1 0 dust contour line during April 2 0 1 8 , it was found that(14%). These results are shown in figure 5.

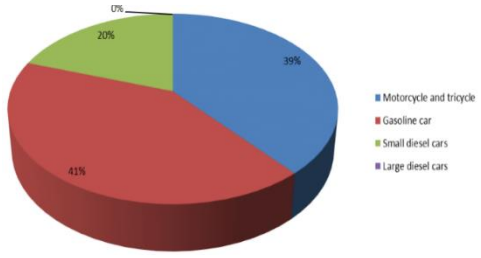

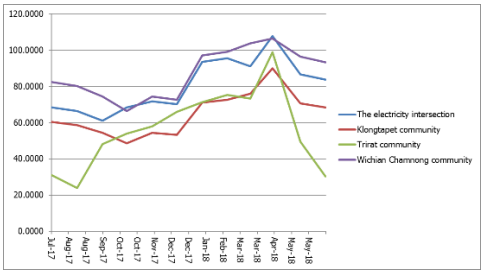

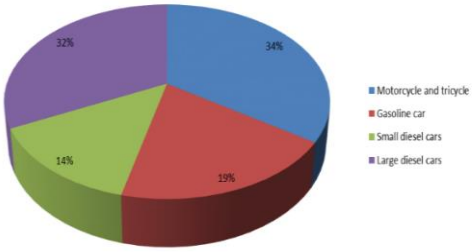

Figure 5 Proportion of dust emissions (PM_{10}) at the police fort site

List of sources of mobile pollution emissions. From the collection of traffic data in the Sukhothai municipality by way of a CCTV operating in 2 directions at the police fort intersection, the highest source of PM_{10} was from motorcycles and tricycles (47%), followed by diesel engine trucks (32%), gasoline engine cars (19%), and small diesel cars

Figure 6. Proportion of dust emissions ($PM_{1\ 0}$) at Wichian Chamnong community site

From CCTV observations of the Wichian Chamnong community site, the highest level of PM_{10} emissions was from gasoline cars (47%), followed by motorcycles and tricycles (39%), and small diesel cars

(20%).

This community was a business district with many pedestrians and where the road width was limited, so large diesel trucks could not enter and no data was recorded for them.

Table 1 Average daily traffic volume at each counting point

Traffic volume counter	Average daily traffic volume (cars / day)			
	Motorcycle/Tricycle	Gasoline car	Small diesel cars	Large diesel cars
1. The police fort electricity intersection	1,244	590	1,032	87
2. Wichian Chamnong community	950	861	987	-

Table 2 Vehicle emission factors used in the study

Car Type	**EF (Gram / km / car)**
	PM
Motorcycle/Tricycle	0.086
Gasoline car	0.101
Small diesel cars	0.042
Large diesel cars	1.150

Note From Pollution Control Department 2008)

CONCLUSIONS

The highest PM_{10} emissions data was 108 micrograms per cubic meter at the police fort site in April, 2018. The highest dust fall data was 247 milligram per square meter per day at the police fort site in April, 2018. The lowest dust fall data was 70

milligram per square meter per day at the Trirat community station in June, 2018. The major mobile source of PM10 emissions in the Sukhothai Municipality was motorcycles and tricycles.

ACKNOWLEDGEMENTS

The researchers wish to thank the Department of Environmental Engineering, Department of Civil Engineering, Faculty of Engineering, Naresuan University who kindly supported this project with all equipment and research funding.

REFERENCES

Karar, K., Gupta, A. K., Kumar, A. and Biswas, A. K. (2006). Characterization and identification of the sources of chromium, zinc, lead cadmium, nickel, manganese and iron in $PM_{10}$and iron in PM_{10} particulates at the two sites of Kolkata, India. Environmental Monitoring and Assessment, 120, 347–360.

Omar.A.Al-Khashman.(2004). Heavy metal distribution in dust and soils from the work place in Karak Industrial Estate,Jordan. Chemistry Department, Mutah University, Jordan

Vassilakos, Ch., Veros, D., Michopoulos, J., Maggos, th. and O' Connor,C. M. (2007). Estimation of selected heavy metals and arsenic in PM_{10} aerosols in the ambient air of the Greater Athens Area, Greece. Journal of Hazardous Materials. 140, 389-398.

Yunchao, H., Zhigang, G., Zuosheng, Y., Ming, F. and Jialiang, F. (2007). Seasonal variations and sources of various elements in the atmospheric aerosols in Qingdao, China. Atmospheric Research. 85, 27-37.

Zemba, S.G., Ames, M.A., and Alvarado, M.J. (2002), Risk Assessment for the Evaluation of Kiln Stack Emissions and RCRA Fugitive Emissions from the Lone Star Alternate Fuels Facility, Greencastle, Indiana.

Pollution Control Department. 2008; Air Pollution Database Project, Samut Prakan Provice.

Chemical oxygen demand and heavy metal content of dry deposited particles on bituminous road shoulders in Tak Province, Thailand

Parinya Prasertsang, Pajaree Thongsanit*

[1]Master's degree student, civil engineering department, Faculty of Engineering, Naresuan University, Phitsanulok, Thailand 65000

[2]Assistant Professor, civil engineering department, Faculty of Engineering, Naresuan University, Phitsanulok, Thailand 65000

*E-mail: pajareet@nu.ac.th

ABSTRACT

Dust accumulated on a road surface is an environmental problem, especially as it contains dirt and pollutants from natural water sources, public canals and watercourses, and motor vehicles. The objectives of this research were to study Chemical Oxygen Demand (COD) and heavy metals in the dust on the road pavement at Wang Chao District, Tak Province. Samples were collected using an artificial skin sheet of the same material as the paved road surface, with size 30 x 50 x 0.05 centimeters, placed on the roadside shoulder. These were paced at three points about 1 km distant from each other, on Highway 1, a 4-lane major road running through Tak Province, at about the 493 Km marker.

Samples were collected between November 2018 and January 2019, sampled on day 1, day 7, day 15, day 30, and day 60. The COD concentrations found in the Day-1 samples varied from 56 to 120 mg/l. The other COD concentrations found were, day-7, 108 to 164 mg/l, day-15, 93.1 to 194mg/l, day-30 days, 937-1598 mg/l and day-60 day, 242-1209 mg/l The dust

samples were analysed for eight types of heavy metal. Manganese (0.040 mg/l), Iron (1.205 mg/l), and Copper (0.100 mg/l.) were found, but Lead, Arsenic, Cadmium, Mercury and Chromium were not present.

Keywords: Chemical Oxygen Demand, COD, heavy metals, bituminous road surface, road surface pollutants, roof service residues

INTRODUCTION

Wang Chao Municipality is an important economic area of Tak province in Thailand, with an area of 328 square kilometers and a population of 29,810 people. On Highway 1, a major arterial road running from Bangkok to Chiag Mai, through Wang Chao Municipality, experiences constant heavy traffic that is a source of air pollution; a potentially serious public health problem. Our research studied the effects of accumulations of dry dust on the road shoulder road of Highway 1 in Wang Chao Tak province during November 2018 to January 2019. The road surface dust is a major air pollution source. (Marisa,1999 and Pajaree, 2009) It was reported that the high volume of traffic was a significant source of pollution by spreading surface dust on the road, which originated from various

sources, including rain water, canal water and other sources of dirty water, as well as mechanical friction and wear of coated parts, brake pads, etc. in motor vehicles, and soluble from vehicles such as fuel, brake fluid, grease. These are sources of heavy metals such as lead, zinc, chromium, copper and nickel. (Mongkhon et al, 2007, Kwanruthai, 2010 and Chitcharoen Sornkwan, 2007)

We analyzed the amount of COD and heavy metals found in the compaction of the slurry surface. We also identified the types of equipment and vehicles that these metals were likely to derive.

MATERIALS AND METHODS

Location of the Study

This research was conducted National Highway 1 in Wang Chao District, Tak Province (see Figure 1 for map).

Figure 1: Map of Wang Chao District, Tak Province

Sample Collection

The sampling period was from November 2018 to January 2019. Samples were collected on days 1, 7, 15, 30 and 60, taken during the rush hours of 7 AM - 9 AM and 4:00 PM - 6:00 PM to ensure maximum sediment settling. These "rush hours" were simply established by counting the volume of vehicular traffic over the day.

Sampling Method

We laid an artificial "skin" or road surface across the width of the road, at three separate locations in the highway, about 1 kilometer apart. Figure 2 shows the "artificial skins" laid at the side of the road.

Sampling Method

We laid an artificial "skin" or road surface across the width of the road, at three separate locations in the highway, about 1 kilometer apart. Figure 2 shows the "artificial skins" laid at the side of the road.

The collected samples washed out of the artificial skin pads with Reverse Osmosis (RO) filtered water (Figures 3).

Figure 2: Washing the dust sample from the artificial skin collection pad.

Each sample analyzed to find COD and heavy metal values using equipment shown in Figures 3 & 4.

Figure 3: Equipment used for evaluating COD

Figure 5: Atomic Absorption Spectrophotometer (AAS)

The heavy metal content of the dust samples analyzed using an Atomic Absorption Spectrophotometer (AAS) (Figure 5)

The relationship between vehicular volume, metal, chemical, and heavy metals volumes in the dust sample calculated using the vehicle counts and the mean of the values found in the samples, taken at the various peak times.

RESULTS AND DISCUSSION

COD values and heavy metal values of dry dust on the bituminous surface of road analyzed in samples collected at 3 points along the road. The analysis results shown in Figure 6.

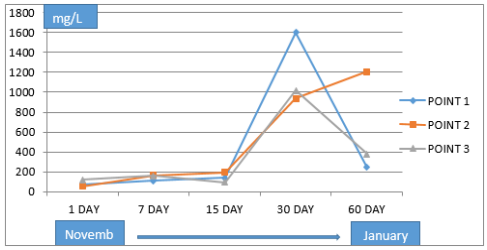

Figure 6: Amount of COD in the dry dust samples at 3 collection points

This graph shows the continuous increase in the volume of accumulated dust over the 8-week time period.

Heavy Meta Content

The value of heavy metals obtained from the collected samples is shown in Table 1.

Table 1: Heavy Metal Values from the dust samples

heavy metal	Before dry to collect dust	taken to collect dry dust samples at 1 day
Mn	0. 050 mg/L	0. 040 mg/L
Cu	not found	0. 100 mg/L
Fe	0. 250 mg/L	1. 205 mg/L
Cd	not found	not found
As	not found	not found
Cr	not found	not found
Pb	not found	not found
Hg	not found	not found

The concentrations of manganese. (Mn), Cupper (Cu) and iron (Fe) in samples these taken to collect dry dust samples at 1 day were 0.040 0.100 and 1.205 mg/l

Traffic Volume Counting

Traffic volume and vehicle types were identified during peak hours between 7 am - 9 am and evening at 4 pm - 6 pm, twice a week during the study period. This was done to gain an understanding of the main "polluters" responsible for spraying polluted rainwater onto the verges of the road.

The types of vehicles were categorized according to the guidelines of the Traffic Engineering Division, Department of Highways (Department of Rural Roads, 2010) were:

Motorcycle and Motor Tricycle: C2.
Passenger Car and Taxi: C & T
Light Bus: LB
Passenger vehicles from 6 wheels or more (Heavy Bus: HB)
Light Truck: LT
Medium Truck: MT
10-wheel trucks and trailers (Heavy Truck: HT)
Bicycle and Tricycle: B & T

The results are shown as the average per two hours per week for the study period November to January (Table 2). Made from asphalt, concrete, asphalt, cement or asphalt, and when the artificial surface was dried for 1 day and the sample is found to have 1 heavy metal Including copper (Cu) of copper (Cu) are found in the production of container and metal furniture industry. Used as a mixture

of metal production, electrical wire and electronic circuits can be used to produce chemical dyes, etc. It can be seen that copper (Cu) that is found should be derived from car parts that have run through on the road itself.

CONCLUSION

Table 2: Traffic volumes categorised by vehicle type

November → January

Type of car	Week 1	Week 2	Week 3	Week 4	Week 5	Week 6	Week 7	Week 8
MC	20	44	55	20	37	31	12	32
C & T	143	143	165	123	83	198	67	87
LB	1	1	1	1	1	1	2	0
HB	3	3	1	2	2	1	2	2
LT	224	224	203	192	155	232	105	120
MT	45	45	39	46	30	18	17	26
HT	103	103	71	74	45	27	28	51
B & T	0	0	1	2	2	1	1	3

Dust samples were collected from three separate points along Highway 1 in Wang Chao District in Tak Province. This is a major national highway, and that District is a center of industry and has a large volume of traffic in and around, and passing through. The samples of dust collected and tested for COD values and heavy metal values. We found that the COD values tended to increase over the sampling period of 2 months with a fall in readings at the end probably due to rain washing away the dust. The heavy metals manganese (Mn) and iron (Fe) were in found in measurable quantities but the other metas and chemicals, CD, AS, CR PB and Hg were not found.

ACKNOWLEDGEMENTS

Thank you, Wichaya Imkrajang, a scientist. Environmental Engineering Laboratory Department of Engineering Naresuan University and would like to thank the Department of Engineering for supporting research tools and equipment.

REFERENCES

Chitcharoen Sornkwan, Study of lead and iron concentrations in particulate matter in Atmosphere Rajabhat Institute Phetchaburi Wittayakon, under the royal patronage, Valaya Alongkorn Rajabhat University, Samut Prakan, Environment. Environmental Engineering Association of Thailand. Page 2007; 2, 1, 2-32,

Kwanruthai Thongbunrit. The concentration of heavy metals in dust falls from the source in the province, 2010 Naresuan University master thesis

Marisa Phensutphupinyokun. Traffic dust: mechanism for the impact on health, Environmental health situation: 1999; Year 4, Issue 6, BE 2542, searched on 15 July 2012

Mongkhon Raya Nakorn Somporn Chantara, Sunanta Wangkan, Urai Tengcharoenkun, Phisansakit Sawangpaiboon, Pornchai Chantha, Ing-Arun Chaisri, Valaya Saengchan and Duang Duen Saengboon. Analysis project for finding air pollution in dust particles in Chiang Mai and Lamphun provinces. Under the support of the Thailand Research Fund. (TRF). 2007.

Pajaree Thongsanit, Particle, Naresuan university Engineering Journal, 2009, 3, 1, 1-4

Composition of dry deposition from roads construction and management Nakhon Sawan Province, Thailand

Thanadet Yiangyong [1], Pajaree Thongsanit[2]

[1]Master's degree student, civil engineering department, Faculty of Engineering, Naresuan University, Phitsanulok, Thailand 65000
[2]Assistant Professor, civil engineering department, Faculty of Engineering, NaresuanUniversity, Phitsanulok, Thailand 65000
thanadettor58@gmail.com

ABSTRACT

This research studied the composition and management of dry fall from road construction in the area of Phaholyothin Road (Nong Ben- Khao Khat), Nakhon Sawan Province. Samples were collected by vacuum at 5 roadside locations on Phaholyothin Road, namely, the PT petrol station, Wat Sawan, Nong Rong Temple, the Tawana Resort and the Chintana Phabai site. The dust fall jar method, adapted from the Pollution Control Department (PCD), was used in this study. The dust fall samples were collected in December 2018 and January 2019. The result of dust fall measurement at the PT petrol station was 94 and 78 milligrams of dust per square meter per day in December and January respectively. The data at other sites did not exceed the national standard, except at Nong Rong Temple where the dust fall concentrations were 136 and 147 milligrams per square meter per day. The samples were analyzed for dust size using the Sieve Analysis Test with sizing of: > 600 µm, 450- 600µm, 300- 450µm, 150- 300µm, 75- 150µm, and < 75 µm and weighing of the dust in each size range. The highest weight was in the dust size of greater than 600 µm.

Keywords: Dust fall, dry deposition, construction road, silt

INTRODUCTION

Nakhon Sawan Province set in the lower northern region of Thailand with an area of approximately 9,597 square kilometers. This province has been important in the history of Thailand. (Nakhon Sawan Tourist Office, 2011) The surrounding provinces include Phichit and Kamphaeng Phet in the north, Phetchabun and Lop Buri in the east, Sing Buri, Chainat and Uthai Thani in the south, and Tak province in the west. Road transport in Nakhon Sawan province uses major highways, including National Highway No. 1 or Phaholyothin Road to connect to the lower central and northern regions of Thailand. National Highway No. 117 connects to Phichit Province and Phitsanulok Province, National Highway No. 11 connects to Sing Buri Province, Pichit province and Phitsanulok Province. Highway No. 225 connects to Phetchabun and Chaiyaphum-Province (Department of Hightways., 2011

Air quality data for particle smaller size than 10 micron (PM10) of Pak Nam Pho Sub- district, Muang District, Nakhon Sawan Province from 9 to 15 September 2018, showed values in the range of 29 to 47 micrograms per cubic meter, which is from good to moderate quality levels. Dust in the air came from many sources. The sources of air pollution were vehicles and open burning, industry, road construction, and pavement construction. (Pajaree, 2009) Road construction consisted of two main steps: the design of the road and road construction. Road design uses calculations from many methods including finding of land boundaries. Road shape design uses both vertical and horizontal levels. The road design calculates the drainage direction of the area. The road blocked an original waterway. The construction of the road, started with digging or filling the soil to achieve a level similar to the design. The research objectives were to study dry dust composition and concentration caused by road construction in the road area and to

study guidelines for reducing dust caused by road construction and dust management caused by construction.

METHODOLOGY

The dust fall sampling equipment complied with PCD methods and included a water sampling cylindrical bottle with a diameter of about 13 cm and height of 20 cm. A plastic cone funnel with 8 inch diameter was used to collect dust fall and rain into the bottle. Plastic screening protected the sample. The dust sampling equipment was mounted vertically on a 1.5 m pipe. A bucket was used for the bottle samples. **(Fig. 1a.)**. (Phatthakorn, 2010).

Silt samples were collected from the roadside using an Electrolux vacuum cleaner **Fig. 1c**., with silt samples stored in 7x11" heat- resistant bags **(Fig. 1d.)** Two samples were taken from each site over a period of 2 months. Sample collection bottles were analyzed in a laboratory to determine the weight of dust falling in mg. using electric scales **(Fig. 1b.)**. Silt samples results in weight was units per area of the container per storage period (milligrams per square meter per day). The equation of the dust fall concentration showed below

$$DF(mg/m^2/day) = \frac{(W_2(g) - W_1(g)) \times 10^3}{A \times T}$$

DF = The concentration of dust fall (milligrams per square meter per day)

W1 = Pre weight of the dust sample (milligrams)

W2 = Post weight of the dust sample (milligrams)

A = Area of cone surface (square meter)

T = Time (Day)

10^3 = Gram to milligrams

The dust samples collected from the area of the road by vacuum cleaner were analyzed to determine the amount of silt in a laboratory. The Sieve test method was in accordance with the ASTM C-136 standard method. The silt volume in laboratory was the amount of dust that passes through 200 grains, which was as small as 75 microns, and collects sample slides on the road. The dust samples collected from the area of the

road where collected by vacuum cleaners.The silt analyzed in the civil engineering laboratory. The samples took to determine the size of the dust using the Sieve Analysis Test on sizing > 600 µm and 450- 600µm, 300- 450µm, 150- 300µm, 75- 150 µm, and < 75 µm and weighing the dust. The most of weight was in the sizing of dust more than 600 µm. The silt samples weighted and analyzed.

RESULTS AND DISCUSSION

The dust fall samples

The dust fall samples were collected from the 5 stations in December 2018 and January 2019. The 5 stations **(see Fig. 2)**, were: on the roadside at the PT petrol station (station A), on the roadside in front of Wat Sawan Temple (station B), on the roadside in front of Tawana Resort (station C), on the roadside in front of Nong Rong Temple (station D), and on the edge of the Chintana Phabai Site (station E), which were all on Phaholyothin Road (Nong Ben- Khao Khat) in Nakhon Sawan Province

In December 2018 **(Fig.3)**, station A had a dust intensity of 93. 77 mg/ m^2/ day, station B (Wat Sawan Temple) had a dust intensity of 97.55 mg/ m^2/ day, station C had a dust intensity of 61.33 mg/m^2/day, station D had the highest dust intensity of 136 mg/ m^2/ day, which exceeded the standard of 133 mg/ m^2/ day and station E had a dust intensity of 71.84 mg/m^2/day.

In January 2019 **(Fig.3)**, at station A had a dust intensity of 77. 89 mg/ m^2/ day, station B had a dust intensity of 110. 75 mg/ m^2/ day, station C had a dust intensity of 61.33 mg/m^2/day, station D had the highest dust intensity of 147 mg/ m^2/ day, which exceeded the standard of 133 mg/ m^2/ day and station E had a dust intensity of 85. 24 mg/ m^2/ day. The results showed that the sources of dust fall were vehicles and road work machines and road silt. The health effect on the people who live in the areas of highest dust concentrations should be studied in the future.

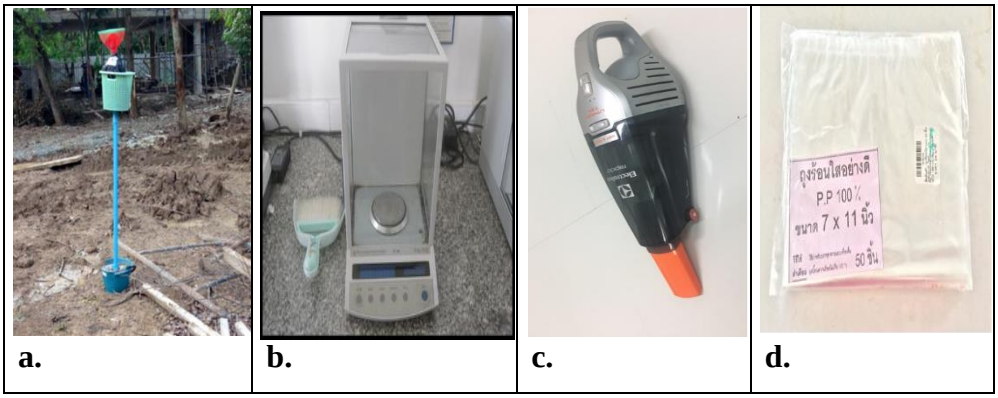

a. **b.** **c.** **d.**

Figure 1. Dust sample equipment

a. Dust fall jar

b. Four decimal point electrical scales

c. Electrolux vacuum cleaner model ZB6106WD, voltage: 220-240V 50 / 60Hz

d. Heat-resistant bag size 7x11 inches

in the area of Phaholyothin Road (Nong Ben-Khao Khat), Nakhon Sawan Province

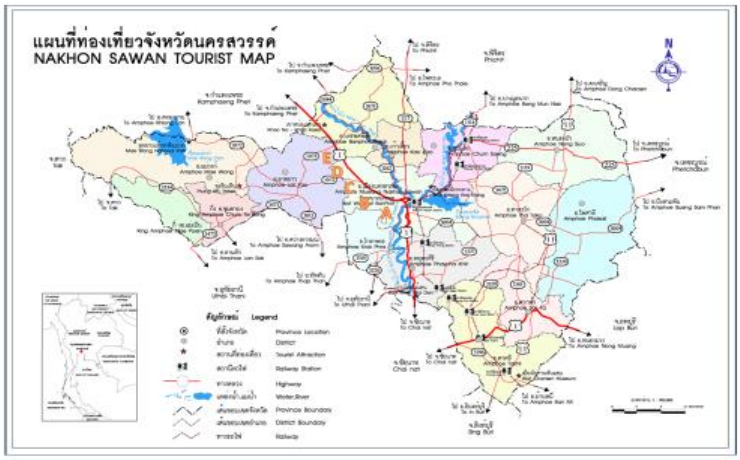

Figure 5

Figure 2. Map of the 5 stations

station A (at the PT petrol station)

station B (Wat Sawan Temple)

station C (Tawana Resort)

station D (Nong Rong Temple)

station E (Chintana Phabai site)

Dust Fall Jar Container	DEC.-2018 (mg/m2/day)	JAN.-2019 (mg/m2/day)
PT petrol stations	93.77	77.89
Wat Sawan Temple	97.55	110.75
Tawana Resort	61.33	61.33
Nong Rong Temple	136	147
Chintana Phabai site	71.84	85.24

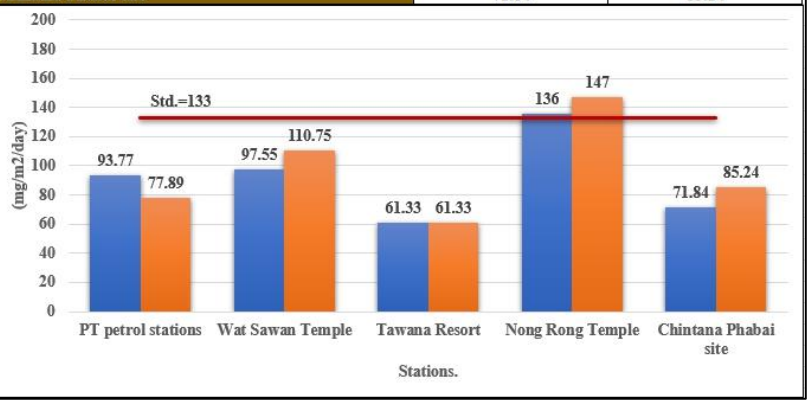

Figure 3. Dust fall results at the 5 stations

The amount of silt

The amount of silt was studied on Phaholyothin Road (Nong Ben-Khao Khat) , Muang District, Nakhon Sawan Province using a vacuuming technique. The samples were collected from the road by a vacuum sweeping machine (see fig 1c) and separated according to the size of the dust using Sieve Analysis in December 2018.

In December 2018 the results of dust analysis were as follows: **(Fig.4)**,
at station A the aggregate dust sizes were as follows: dust size > 600 at 203.18gms, dust size 450 - 600 μm at 104. 13 gms, dust size 300 - 450 μm at 18.19 gms, dust size150-300 μm at 16. 78 gms, dust size 75 - 150 μm at 18. 69 gms and dust size <75 μm at 5.13 gms,

at station B the aggregate dust sizes were as follows: dust size > 600 at 178. 16 gms, dust size 450 - 600 μm at 115. 34 gms, dust size 300 - 450 μm at 16. 57 gms, dust size150- 300 μm at 14. 79 gms, s. dust size 75 - 150 μm at 8.75 gms and dust size <75 μm at 8.51 gms,

at station C the aggregate dust sizes were as follows: dust size > 600 at 121. 13 gms, dust size 450 - 600 μm at 20.13 gms, dust size 300 - 450 μm at 0 gms, dust size150- 300 μm at 8. 75 gms, dust size 75 - 150 μm at 9. 73 gms and dust size <75 μm at 9.25 gms,

at station D the aggregate dust sizes were as follows: dust size > 600 at 105.05.. gms, dust size 450 - 600 μm at 14.34 gms, dust size 300 - 450 μm at 5. 17 gms, dust size150- 300 μm at 6. 79 gms, dust size 75 - 150 μm at 12. 73 gms and dust size <75 μm at 3.68 gms,

at station E the aggregate dust sizes were as follows: dust size > 600 at 126. 35 gms, dust size 450 - 600 μm at 24.34 gms, dust size 300 - 450 μm at. 6. 18 gms, dust size150- 300 μm at 5. 78 gms, dust size 75 - 150 μm at. 9. 21 gms and dust size <75 μm at 8.83 gms.

All of the dust was sourced from the construction.

Hand Sweeping an upswept Street Area	DEC.-2018	
	Dust size	(gram)
PT petrol stations	Dust size > 600 µm	203.18
	Dust size 450 - 600 µm	104.13
	Dust size 300 - 450 µm	18.19
	Dust size 150-300 µm	16.78
	Dust size 75 - 150 µm	18.69
	Dust size < 75 µm	5.13
Wat Sawan Temple	Dust size > 600 µm	178.16
	Dust size 450 - 600 µm	115.34
	Dust size 300 - 450 µm	16.57
	Dust size 150-300 µm	14.79
	Dust size 75 - 150 µm	8.75
	Dust size < 75 µm	8.51
Tawana Resort	Dust size > 600 µm	121.13
	Dust size 450 - 600 µm	20.13
	Dust size 300 - 450 µm	0
	Dust size 150-300 µm	8.75
	Dust size 75 - 150 µm	9.73
	Dust size < 75 µm	9.25
Nong Rong Temple	Dust size > 600 µm	105.05
	Dust size 450 - 600 µm	14.34
	Dust size 300 - 450 µm	5.17
	Dust size 150-300 µm	6.79
	Dust size 75 - 150 µm	12.73
	Dust size < 75 µm	3.68
Chintana Phabai site	Dust size > 600 µm	126.35
	Dust size 450 - 600 µm	24.34
	Dust size 300 - 450 µm	6.18
	Dust size 150-300 µm	5.78
	Dust size 75 - 150 µm	9.21
	Dust size < 75 µm	8.83

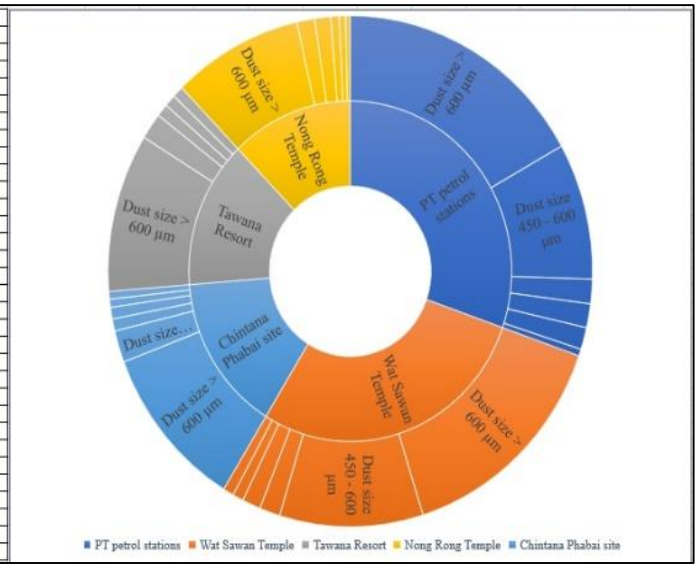

Figure 4. Dust aggregate size and amounts at the 5 stations

Figure 5. Sieve test

CONCLUSION

The dust fall sample were collected in December 2018 and January 2019. Dust fall results showed that at the maximum readings at the PT petrol station were 94 and 78 milligrams of dust per square meter per day in December and January, respectively. The data at other sites did not exceed the national standard except at Nong Rong Temple where the dust fall concentrations were 136 and 147 milligrams per square meter per day in December and January, respectively. The study of the silt on Phaholyothin Road (construction road) used vacuuming for collection of samples from 5 stations in December and January 2018. The samples were taken to determine the size of the dust using the Sieve Analysis Test for sizing as: > 600 μm and 450 - 600 μm, 300 - 450 μm, 150-300 μm, 75 - 150 μm, and < 75 μm. Most of the silt was in the sizing of dust more than 600 μm.. Most of the dust in the roadside area within Nakhon Sawan province was caused by construction and transportation.

ACKNOWLEDGMENTS

Thank you, Asst. Prof. Dr. Pajaree Thongsanit, Advisors and Wichaya Imkrajang, a scientist. Environmental Engineering Laboratory Department of Engineering Naresuan University and would like to thank the Faculty of Engineering for supporting research tools and equipment.

REFERENCES

Department of Highways, Map showing traffic volume on Nakhon Sawan province. Retrieved on 19, 2011 from http://bhs.doh.go.th/download/map

Nakhon Sawan Tourist Office, Ministry of Tourism and Sports, Map of Nakhon Sawan Province Department of Highways. , 2011

Pajaree Thongsanit, Particle, Naresuan University Engineering Journal 2009; 3:1,1-4.

Phatthakorn kasun and Panupan Lumkao The deposition of dust fall in area and vicinity of Naresuan University, Bachelor thesis 2010

The effect of Na_2O/SiO_2 and SiO_2/Al_2O_3 ratios on engineering properties of alumino-silicious materials solidified plating sludge

Parichat Muensita[1], Suwimol Asavapisit[2*], Rungroj Piyaphanuwat[3]

[1]Graduate student, Environmental Technology, School of Energy, Environmental and Materials, King Mongkut's University of Technology Thonburi, Bangmod, Thung-kru, Bangkok 10140, Thailand

[2]Associate Professor, Environmental Technology, School of Energy, Environmental and Materials, King Mongkut's University of Technology Thonburi, Bangmod, Thung-kru, Bangkok 10140, Thailand

[3]Assistant Professor, Ratchaburi Learning Park, King Mongkut's University of Technology Thonburi, Rang Bua, Chom Bueng, Ratchaburi 70150, Thailand; *Corresponding author: e-mail: suwimol.asa@kmutt.ac.th

ABSTRACT

This research studied the performance of geopolymer synthesized from the water treatment residue (WTR), bituminous fly ash (BFA) and Si waste (SWA) as solidification binder and NaOH as alkali-activator. The ratio of SiO_2/Al_2O_3 of 1:1, 2:1, 3:1 and Na_2O/SiO_2 at 0.25, 0.20, and 0.30 are conditions for study in this research. The result showed that optimum compressive strength was found in ratios of Na_2O/SiO_2 at 0.25, 0.20 and 0.30 for WTR, BFA and SWA geopolymer. When SiO_2/Al_2O_3 in geopolymer was adjusted using Si waste and aluminium hydroxide that led to increase compressive strength with an increase of the molar ratios of SiO_2/Al_2O_3. At 28 days, the compressive strength of WTR, BFA and SWA geopolymer at SiO_2/Al_2O_3 ratio of 3:1 have 8.15, 9.65 and 1.66 MPa, respectively. When 30 wt.%PS was added in WTR, BFA and SWA geopolymer, the compressive

strength at 28 days decreased to 2.22, 2.57 and 1.14 MPa for WTR BFA and SWA geopolymer, respectively. It was caused an interfering effect of heavy metal in plating sludge that may be dissolved from solid to liquid and may blockade reaction of geopolymer binder. But compressive strength at 28 days of all geopolymer binder solidified 30 wt.%PS were higher than the minimum requirement for dumped in landfill disposal) 0.345 MPa. In addition, XRD result shows that a crystalline phase, sodium aluminum silicate hydrate (NASH) and heavy metal (Zn, Cr, and Fe) while SEM result shows the heavy metals precipitated on the surface of the geopolymer. It was a cause of reduction of compressive strength of geopolymer solidified plating sludge.

Keywords: Geopolymer, Water Treatment Residue, Bituminous Fly Ash, Si Waste, Plating Sludge

INTRODUCTION

Geopolymer is inorganic materials caused by the reaction of an alkali and/or an alkali silicate solution with alumino-silicious materials. The silica (Si) and alumina (Al) are major chemical compositions of materials. Most of silica and alumina materiales are pozzolanoic materials such as fly ash, rice husk ash, kaolinite, water treatment redidue, blast furnace slag, silica waste etc. Sodium hydroxide, potassium hydroxide, sodium silicate and other alkali substant were used as alkali activators. When Si and Al containing materials were mixed with alkali solution, they will change from amorphous phase to semi-crystalline threedimensional aluminosilicate network [1,2,3,4]. The ratio of Si/Al, Si/Na, alkaline activator dosage, curing time and temperature has been acknowledged as having significant impacts on geopolymerization [4,6,7].

In environmental works, heavy metal, radioactive waste, toxic sludge

and sludge can treated using stabilization and solidification process. The wastes can fix in cement matrix. The cement manufacturing industry releases the large volumes of CO_2 emitted. Actually, this industrial sector is thought to create 5–7% of the total CO_2 anthropogenic emissions. Concern over the impact of anthropogenic carbon emissions on the global climate has increased in recent years due to growth in global warming awareness. There are several research[1,2,9,10,11] used the pozzolanic materials replaced some parts of cement binder or used other green materials such as lime-pozzolanic, alkali-activated sludge, geopolymer etc. The geopolymers are green materials that were synthesised from waste containing aluminosilicates. It was used as solidified binder in stabilization and solidification process. The heavy metal, radioactive waste, toxic sludge and sludge can fix in geopolymer matrix and reduces dissolution of waste to the environment before dumping in secure landfill. So, this research studied the performance of geopolymer from water treatment residue (WTR), bituminous fly ash (BFA) and Si waste (SWA) as binder to solidify plating sludge.

METHODOLOGY

1. Materials

Water treatment residue, bituminous fly ash and Si waste were used as solidified binders. The water treatment residue (WTR) is wastes from a water treatment plant at Bangkaen in Bangkok Province, Thailand. It was pretreated by calcining the residue at temperatures of 800 °C for 1 h.[3,8]. Bituminous Fly Ash (BFA) is wastes from BLCP power station in Rayong province. Si waste (SWA) is wastes from AGC Automotive (Thailand) Co., Ltd., in Chonburi Province. WTR and SWA were ground to particle size of which was retained on sieve No. 325 (45 mm) using Los Angeles abrasion machine. In addition, Al source was prepared from analytical grade

aluminium hydroxide that used adjusted SiO_2/Al_2O_3 of binder. The alkali solution were prepared from analytical grade sodium hydroxide (NaOH) that is alkali activator. The chemical composition of three binder were analyzed by X-ray fluorescence (XRF) that were shown in Table 1.

Plating sludge (PS) is sludge from the wastewater treatment plant in an electroplating industry located in Bangkok, Thailand. The PS was dried by air-oven at 105 °C and reduced to 50 mm using Los Angeles abrasion machine. The PS was digested by microwave digestion and determined the concentration of heavy metals in the PS by atomic absorption spectrophotometry. The PS has Zn, Fe and Cr at the concentration of 690, 164, and 37.5 g/kg dry wt., respectively.

2. Sample Preparation

First, studying the optimum of Na_2O/SiO_2 ratio of three solidified binder. Second, selecting the optimum of Na_2O/SiO_2 ratio in each materials, then adjusting SiO_2/Al_2O_3 ratio to be 1:1 2:1 and 3:1 by using aluminium hydroxide. The water content used for mixing was determined by applying the normal consistency method of cement pastes. All samples were used to solidify 30 wt.% PS that is shown in Table 2. After mixing the solid binder with water and alkali solution, it was transferred to PVC cylindrical molds (diameter =35 mm, height =70 mm). After that, all samples were

Table 1 Chemical compositions of materials

oxide content (%)	Materials		
	WTR	**BFA**	**Si waste**
SiO_2	60.6	60.10	68.1
Al_2O_3	25.7	28.70	4.85
Na_2O	0.345	0.38	11.6
CaO	0.919	1.45	9.53
MgO	1.12	0.47	3.98
Fe_2O_3	7.00	4.70	0.958
K_2O	2.20	1.25	0.552
SiO_2/Al_2O_3	2.36	2.09	14.04

wrapped using cling film and cured at an ambient temperature (30±2°C). At 7, 28 and 60 days, all samples were removed from mold in order to determine the strength development and the characteristics of the microstructure.

3. Method for testing

Strength development of the geopolymer was determined by compaction machine after curing for 7, 28 and 60 days following ASTM D1633-17 test method. The compressive strength results of 6 samples were averaged before showing in graph. The crystalline phases of the geopolymer with and without PS were studied using X-ray diffraction (XRD). A Bruker AXS series D8 Discover with Cu K radiation with an average wavelength of 1.54184° was used. The powder sample was scanned at a rate of 0.02° per step. The morphology was characterized with scanning electron microscopy (SEM). A JEOL series JSM-6400 operated at 15 kV, all geopolymer samples prepared for SEM were coated with gold.

Table 2 Mix proportions of geopolymer

Sample	Alumino-silicious materials (%)						Sample	Alumino-silicious materials (%)					
	WTR	BFA	Si	Al	PS	Total		WTR	BFA	Si	Al	PS	Total
WTR1:1	61	-	-	39	-	100	WHM1:1	42	-	-	28	30	100
WTR2:1	94	-	-	6	-	100	WHM2:1	66	-	-	4	30	100
WTR3:1	76	-	24	-	-	100	WHM3:1	54	-	16	-	30	100
BFA1:1	-	63	-	37	-	100	BHM1:1	-	44	-	26	30	100
BFA2:1	-	98	-	2	-	100	BHM2:1	-	68	-	2	30	100
BFA3:1	-	67	33	-	-	100	BHM3:1	-	47	23	-	30	100
SWA1:1	-	-	46	54	-	100	SHM1:1	-	-	32	38	30	100
SWA2:1	-	-	66	34	-	100	SHM2:1	-	-	46	24	30	100
SWA3:1	-	-	75	25	-	100	SHM3:1	-	-	53	17	30	100

RESULTS AND DISCUSSION

1. The effect of Na_2O/SiO_2 molar ratios on strength development of geopolymer binders

Figure 1 shows 28 days compressive strength with SiO_2/Al_2O_3 molar ratio of geopolymer from WTR, BFA and SWA. 28 days compressive strength of geopolymer from WTR at Na_2O/SiO_2 ratio of 0.20, 0.25 and 0.30 equal to 7.75, 8.63 and 4.90 MPa., respectively. At Na_2O/SiO_2 ratio of 0.20 in geopolymer from WTR made low compressive strength because low level of NaOH dissolved a little silicon (Si) and aluminum (Al) from binders which will reduce the degree of polymerization that leaded to the reduction of compressive strength. The geopolymer from WTR at Na_2O/SiO_2 of 0.25 had higher compressive strength than Na_2O/SiO_2 of 0.20 because of high level of dissolved Si and Al more that leaded to highest compressive strength. The geopolymer from WTR at Na_2O/SiO_2 of 0.30 have lower compressive strength than Na_2O/SiO_2 of 0.20 and 0.25 because of high alkalinity made high level of dissolved Si and more than enough to react and precipitated on surface of WTR. It was cause of inhibition geopolymerization reaction that leaded to reduction of compressive strength.

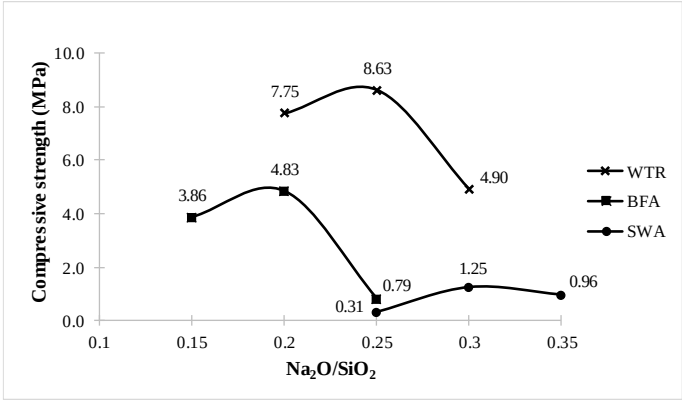

Figure 1 Strength of geopolymer at various Na_2O/SiO_2

The 28 days of compressive strength of geopolymer from BFA at Na_2O/SiO_2 ratio of 0.15, 0.20 and 0.25 were 3.86, 4.83 and 0.79 MPa, respectively. While geopolymer from SWA had compressive strength were 0.31, 1.25 and 0.96 MPa for Na_2O/SiO_2 ratio of 0.25, 0.30 and 0.35. The maximum strength was found at Na_2O/SiO_2 ratio of 0.20 and 0.30 for geopolymer from BFA and SWA. These proportion was optimum alkalinity for dissolution of Si and Al and leaded to generating of aluminosilicate structure[3,6]. When the Na_2O/SiO_2 ratio of the WTR BFA and SWA geopolymer increased from optimum ratio, the compressive strength decreased because high alkalinity from activator can dissolve a lot of aluminum Si and Al from raw materials and precipitate on surface of binder. This would be the cause of inhabitation of geopolymerization reaction between binder which reduce the compressive strength [4,5,7].

2. The effect of SiO_2/Al_2O_3 molar ratios on strength development of geopolymer binders

Figure 2 shows 28 days compressive strength development of geopolymer from WTR BFA and SWA with SiO_2/Al_2O_3 molar ratio of 1:1 2:1 and 3:1. Increase of SiO_2/Al_2O_3 molar ratio of three geopolymer increased compressive strength at 28 days. At SiO_2/Al_2O_3 molar ratio of 1:1, the compressive strength at 28 days of geopolymer from WTR BFA and SWA were 0.43 0.59 and 0.39 MPa, respectively. The compressive strength increased to 8.16 9.66 and 1.66 MPa. when SiO_2/Al_2O_3 molar ratio increased to 3:1. Previously research reported that increased the Si/Al ratio, the structure will change from poly (sialate;-Si-O-Al-O-), to poly (sialate-siloxo;- Si-O-Al-O-Si-O-), to poly (sialate-disiloxo;-Si-O-Al-O-Si-O-Si-O-). These form can produce the materials for structures that was call "geopolymer backbone". It had strong bonding between substance that resulted in

high compressive strength[12]. So, this research added 30 wt% of plating sludge with geopolymer from WTR BFA and SWA at SiO_2/Al_2O_3 molar ratio of 3:1 and studied engineering properties.

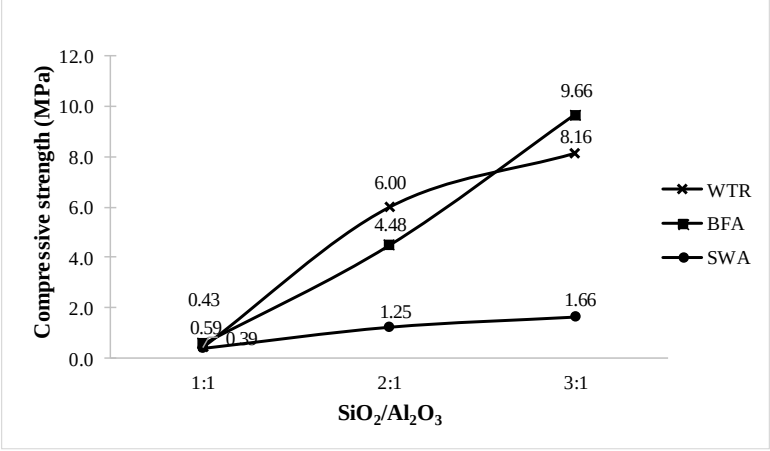

Figure 2 Strength of geopolymer at SiO_2/Al_2O_3 = 1:1 2:1 and 3:1

3. Strength development of solidified geopolymer binders

Additioin of 30 wt.%PS was added in the geopolymer from WTR BFA and SWA (Na_2O/SiO_2 ratio of 0.25, 0.20 and 0.30) with SiO_2/Al_2O_3 ratio of 3:1 resulted in reduction of compressive strength that were shown in Figure 3. At 28 days, all geopolymer samples containing 30 wt. %PS had compressive strength great than standard of landfill disposal requirements (0.345 MPa). When comparison of strength of geopolymer with and without 30 wt. %PS, the compressive strength decreased from 8.16 to 2.23, 9.66 to 2.57 and 1.66 to 1.44 MPa, for geopolymer from WTR BFA and SWA, respectively. The reduction of compressive strength of geopolymer solidified plating sludge (PS) was caused from reduction of geopolymer binders. In addition, heavy metals (Cr, Fe and Zn) from plating sludge may dissolve and react with Si, Al,

OH in environment and inhibited or reduced geopolymerization reaction that was cause of reduction of compressive strength of geopolymer matrix[10,11]. It related with several reserch[3,4,5,7,11], that report both synthesized metal hydroxides ($Zn(OH)_2$, $Cr(OH)_3$ and $Fe(OH)_3$) and plating sludges had interfered to geopolymerization reaction and leaded to reduce compressive strength.

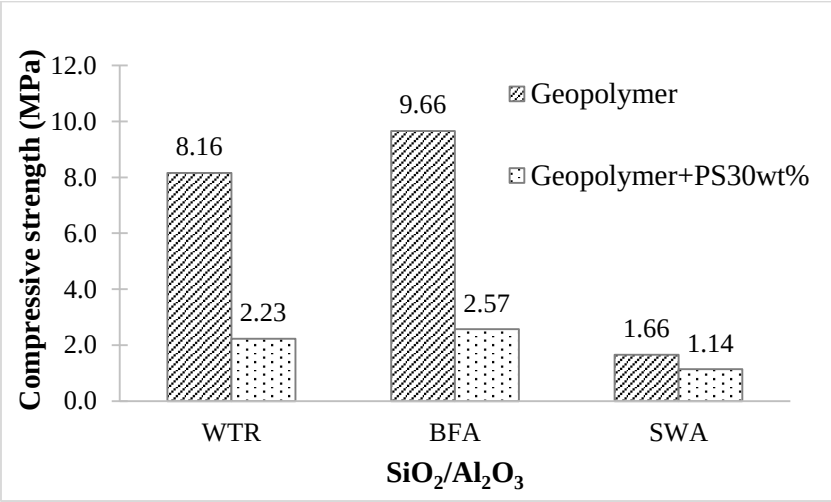

Figure 3 Strength of geopolymer with/without 30 wt.%PS, SiO_2/Al_2O_3 = 3:1 at 28 days

4. Effect of plating sludge on crystalline phase of geopolymer

The XRD patterns of geopolymer from WTR BFA and SWA (SiO_2/Al_2O_3 = 3:1) without plating sludge were showed in Figure 4. Quartz(SiO_2), Muscovite and Sodium aluminum silicate hydrate (NASH) were found in geopolymer from WTR. Both Quartz(SiO_2), Muscovite are major phase in raw materials (calcined WTR) while NASH was produced from almimo silicate and silicon reacted sodium hydroxide solution. This would help increase the strength development[3]. XRD

pattern of geopolymer from BFA shows Quartz, Mullite and NASH phase while XRD pattern of geopolymer from SWA shows Quartz Mullite Muscovite and NASH. The SiO_2 and Al_2O_3 from raw materials (WTR BFA and SWA) reacted with NaOH solution and generated NASH. Consequently, help increase the compressive strength of geopolymer from WTR BFA and SWA.

The peaks of Zinc Iron Oxide ($ZnFe_2O_4$), Aluminium Iron Oxide ($FeAlO_3$), Maghemite (Fe_2O_3), Zinc Silicate ($ZnSiO_4$), and Chromium Oxide (CrO), Quartz (SiO), Muscovite, Mullite, NASH were found in the XRD pattern of geopolymer from WTR BFA and SWA geopolymer with 30 wt.% PS (Fig. 5). The most of heavy metals (Cr, Fe and Zn) in plating sludge precipitated on the surface of alumino-silicious materials and generated the metal silicate or aluminate or oxide that reduced the degree of geopolymerization [3,8,10].

The previous research reported that heavy metals from sludge can precipitated on surface of raw materials and new products and interfered reaction. It was cause of reduction of compressive strength of geopolymer and cement hydration [9,10,11].

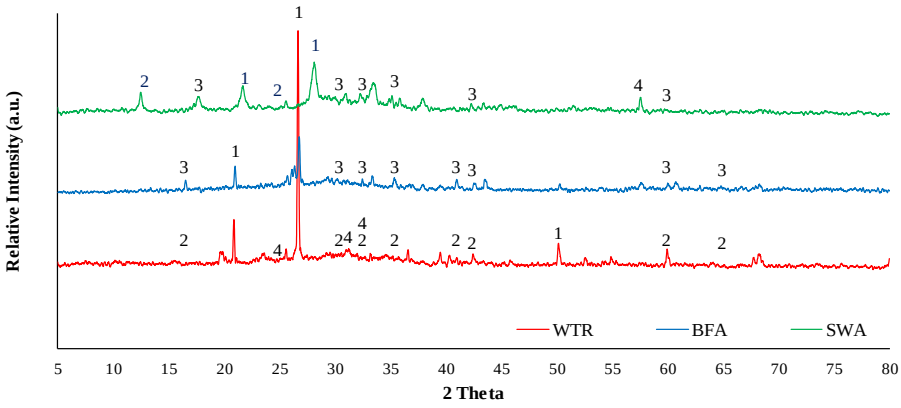

Figure 4 XRD of geopolymer at SiO_2/Al_2O_3 ratio of 3:1

1=Quartz(SiO_2), 2=Muscovite, 3=Mullite, 4=NASH-Sodium aluminum silicate hydrate.

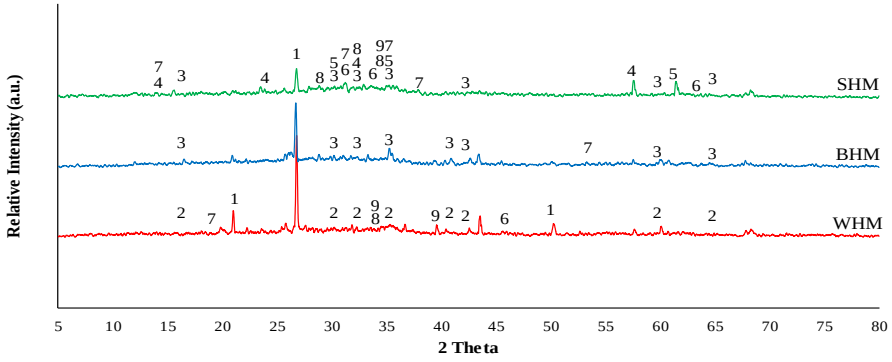

Figure 5 XRD of geopolymer with 30 wt.%PS,

at SiO_2/Al_2O_3 ratio of 3:1

1=Quartz(SiO), 2=Muscovite, 3=Mullite, 4=NASH-Sodium aluminum silicate hydrate, 5= Zinc Iron Oxide ($ZnFe_2O$), 6= Aluminium Iron Oxide ($FeAlO_3$), 7= Maghemite (Fe_2O_3), 8= Zinc Silicate ($ZnSiO_4$), 9= Chromium Oxide (CrO)

5. Effect of plating sludge on microstructure of geopolymer

SEM images of 28 days of geopolymer from WTR BFA and SWA with and without 30 wt.%PS were showed in Figure 6. (6a, 6b and 6c) showed precipitated gel-like geopolymer product (NASH) on the surface. It related with XRD pattern that found crystalline phase of NASH. When 30 wt.%PS was added in geopolymer from WTR BFA and SWA, the some hydroxides of heavy metals (Zn, Fe and Cr) are precipitated (White spots) on surface of raw materials (6d, 6e and 6f).

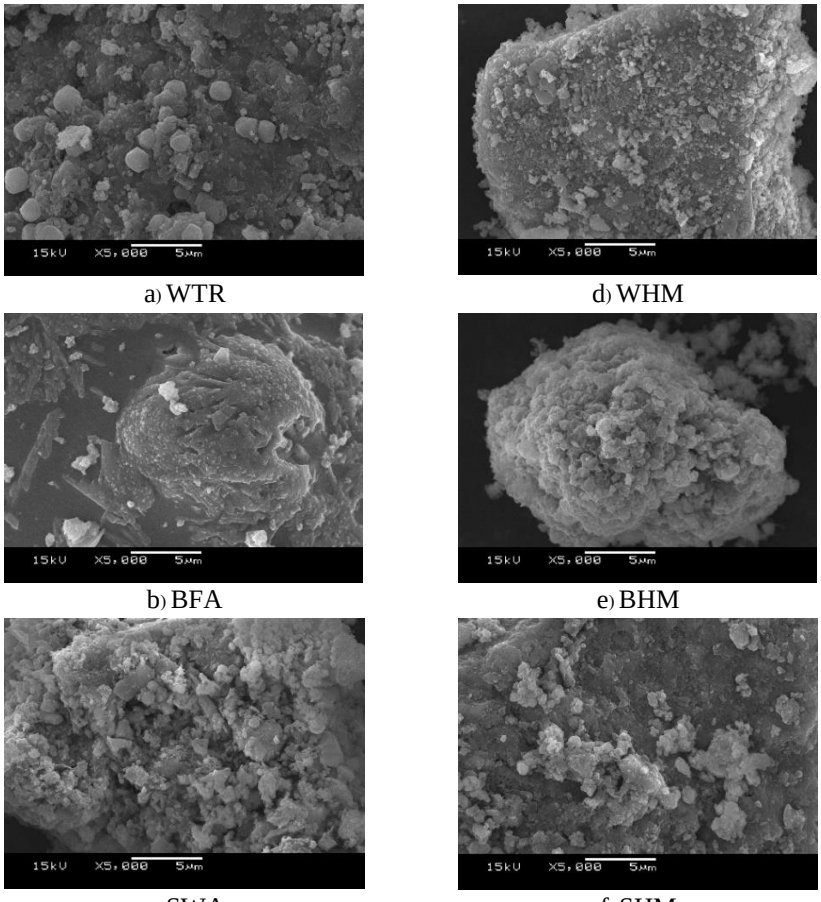

a) WTR d) WHM

b) BFA e) BHM

c) SWA f) SHM

Figure 6 SEM–EDS images of of geopolymer with and without 30 wt.% PS at SiO_2/Al_2O_3 ratio of 3:1

Some part of heavy metal can react with Si, Al and OH in matrix and generate new product that was shown in XRD pattern[8,9,10,11]. It is possible that addition of heavy metals hydroxide may leaded to reduction of mechanical strength of these geopolymers[3,8].

CONCLUSIONS

This experiment results indicated that the optimum ratio was found in synthesis WTR BFA and SWA geopolymer at Na_2O/SiO_2 molar ratio of 0.25, 0.20 and 0.30, respectively, and SiO_2/Al_2O_3 molar ratio 3:1. Addition of 30 wt.%PS in geopolymer binder resulted in reduction of strength but at 28 days compressive strength of all the samples were higher than the minimum requirement of the standard criteria regulated by the ministry of industry B.E. 2548, Thailand. The XRD pattern indicated the alumino-silicious materials and NASH while, SEM images shows a geopolymer gel product (NASH) . Furthermore, XRD and SEM results were found metal hydroxides, metal silicate and other precipitate on surface of raw materials that inhibited reaction. It was cause of reduction of compressive strength.

ACKNOWLEDGEMENTS

This thesis is partially supported by a research scholarship funded by the national research council of Thailand. The Environmental technology Laboratory, School of Energy, Environmental and Materials, KMUTT, deserved appreciation for providing access to their laboratories.

REFERENCES

[1] Davidovits, J. 2008. Geopolymer Chemistry & Applications, Institute Géopolymère, France.

[2] Provis, J.L., van Deventer, J.S.J. 2009. Geopolymer: Structure, processing, propoties and industrial applications, Woodland Publishing Limited, UK.

[3] Waijarean, N, Asavapisit, S. , Sombatsompop, K., 2014. Strength and microstructure of water treatment

[4] Duxson, P., Fernández-Jiménez, A., Provis, J. L., Lukey, G. C., Palomo, A., van Deventer, J. S. J. 2007, Geopolymer Technology: The Current State of the Art, Journal of master Sci. 42: 2917-2933.

[5] Muensita, P., Asavapisit, S., Piyaphanuwat, R., 2018. Performance of Synthesis Geopolymer from Si Waste Solidified Plating Sludge. The 7th International Conference on Environmental Engineering, Science and Management. 24-25 May, Udon Thani, Thailand.

[6] Zhang B, MacKenzie KJD, Brown IWM. 2009. Crystalline phase formation in metakaolinite geopolymers activated with NaOH and sodium silicate. Journal of Mater Science 44:4668–76.

[7] Zheng, L., Wang, W., Shi, Y. 2010. The effects of alkaline dosage and Si/ Al ratio on the immobilization of heavy metals in municipal solid waste incineration fly ash based geopolymer. Journal of Chemosphere 79: 665–671.

[8] Waijarean, N., MacKenzie, K. J. D., Asavapisit, S., Piyaphanuwat, R., and Jameson, G. N. L., 2017, Synthesis and properties of geopolymers based on water treatment residue and their immobilization of some heavy metals", J Mater Sci (2017), Vol 52, pp. 7345–7359.

[9] Piyapanuwat, R., Asavapisit, S., 2011. Performance of lime-BHA solidified plating sludge in the presence of Na_2SiO_3.Journal of Environmental Management 92: 2222-2228.

[10] Asavapisit, S., Macphee, D. E. 2007. Immobilization of metal-containing waste in alkali-activated lime–RHA cementitious matrices. Cement and Concrete Research 37:776–780.

[11] Asavapisit, S., Ruengrit, N. 2005. The role of RHA-blended cement in stabilizing metal-containing wastes, Cem. Concr. Compos. 27:782–787.

[12] Davisa, G., Montesa, C., Sven Eklundb, S.,2017. Preparation of Lunar Regolith Based Geopolymer Cement Under Heat and Vacuum. Advances in Space Research 59(7):1872-1885

Comparing the opinions of people towards the implementation of participation in environmental management from case of Bangpakong Combined Cycle Power Plant number 5 and case of crude oil leak crisis Samed Island, Rayong Province

Danai Bawornkiattikul [1]

[1] Environmental Health Department, Faculty of Public Health, Burapha University, Thailand
E-mail: danai@go.buu.ac.th

ABSTRACT

This study was conducted from research data related to people participation in environmental task from 2 case studies: Bangpakong Combined Cycle Power Plant No 5 (2012) and compensation on the environmental impact of tourism place after crude oil leak crisis at Samed island (2015) with the purpose to compare the implementation of people participation from different case studies. This has been based on 5 forms of people participation by International association for public participation (2012). Determined the level of people participation from the opinions by using classification interaction as 5 levels, took data from people opinion for participation implementation to analyze statistics by using the average score ($\bar{x}$) to compare. The result found that inform and consult to opinions, average score ($\bar{x}$) of the Bangpakong power plant project was at the moderate level ($\bar{x}$ = 2.64, 2.56) as same as compensation for the crude oil leak crisis in Samed island case ($\bar{x}$ = 3.38, 3.21). For involve and collaborate, the average score of the Bangpakong power plant project is at low level ($\bar{x}$ = 2.47, 2.34), which is

different from the compensation for the crude oil leak crisis in Samed island case that was still in moderate level ($\bar{x}$ = 3.27, 3.38). As a form of empower, the average score of Bangpakong power plant project was in the lowest level ($\bar{x}$ = 2.20), it is different from the compensation for the crude oil leak crisis in Samed island which was still in moderate participation level ($\bar{x}$ = 3.35). Meanwhile in situation of environmental crisis and quality of life of people and not environmental management system of developing project, there would be efficient and covering people participation implementation. It is also consist that the prevention and solving of environmental impacts from the developing project in normal situation with the total average score is in low level ($\bar{x}$ =2.05) that is different from the crude oil leak crisis situation at Samed island at a moderate level ($\bar{x}$ =3.33).

Keywords: People participation; Environmental management

INTRODUCTION

Implementation of people participation in environmental work of development projects that changes and impacts of the environment is considered as important for the quality of the environment and the quality of life of people living in that environment and also effect the smoothness or obstructions in the implementation of that developing project as well. In addition, in different environmental situation by crisis or environmental impact caused by developing project. People participation is even more important for solving problems and crisis.

By academic work in the past, there has been various study of people participation in environmental work of developing projects in different forms and areas conducting study in the normal situation of the environment in those developing project. Also, there were studies of the people participation in environmental impact situations.

Especially, in critical situations or environmental disasters from direct development projects. The results of each study of developing project and environmental area are usually different and there may be some factors that cause differences in the people participation in this different situation.

The researcher studied the participation of people in two different situations. One was the normal environment situation of Bangpakong Combined Cycle Power Plant Project No. 5, Chachoengsao Province, in 2012 A.D. by studying of people participation in general environmental management such as pollution prevention, project impact monitoring . Other was crisis environment situation from crude oil leaks in Samed Island in 2015 A.D. by studying people participation in solving and compensation for the environmental impact from crude oil leaks. However, both 2 studies have enough similarities in forms, methods and statistical data to compare to statistical and academic work to consider factors different situations that give the result in different implementation. It leads to suggestions for supporting the people participation in the environmental work for more effective implementation of developing projects in all situations.

METHODOLOGY

1) To take raw data about people opinion on the participation implementation of developing projects from research "Evaluating status of People Participatory in Environmental Impact Monitoring Model for Developing Projects" (2012 A.D.) and from research "Developing of People Participation in Environmental Impact Compensation in Tourism place from case study of Crude oil liege Samed island, Rayong Province" (2015 A.D.)

2) To define 5 levels of people participation by rating range, according to the interactions

classification method Nawarat Trairak (2006) as follows:

2.1 Average score 4.21 - 5.00 with most participation.

2.2 Average score 3.41 - 4.20 with much participation.

2.3 Average score 2.61 - 3.40 with moderate participation

2.4 Average score 1.81 - 2.60 with less participation

2.5 Average score 1.00 - 1.80 with minimal participation

3) To provide the principle of people participation implementations by form and activities of people participation that principles of International association for public participation (2014) was defined as follows

3.1 Inform by print media, announcement labels, television, radio and internet.

3.2 Consult by meeting, public stage.

3.3 Involve by the representatives from the public to attend in the event.

3.4 Collaborate by representatives from the public to consider.

3.5 Empower by committee from the public to determine measures.

4) To process and analyze raw data from 2 researches by the statistical program Excel 2016, use the average score ($\bar{x}$) and standard deviation score (S.D.) as an indicator of participation level, to compare 2 statistical data by mentioned principles of people participation implementation, discussing details and differences in the implementation of people participation and provide suggestions for improvement of people participation.

RESULTS AND DISCUSSION

Taking raw data from questionnaires of 210 samples concerning people opinion of participation implementation of developing projects from research "Evaluating status of People Participatory in Environmental Impact Monitoring Model for Developing Projects" (2012) by using case of Bangpakong Combined Cycle Power Plant No. 5, Chachoengsao Province, reprocessing by statistical program Excel 2016 to measure the level of

people participation as shown in the table 1.

From Table 1, it was found that the Average score ($\bar{x}$) of public opinions on the people participation implementation in environmental management of Bangpakong Combined Cycle Power No. 5 was during 2.20 - 2.64 which was at less to moderate participation level, Standard Deviation (S.D.) was during 1.02 - 1.08 and most participation activities are checking monitoring and collaboration when environmental impact from the project occurs.

Result subtitle 2

Taking raw data from questionnaires of 240 samples concerning people opinion of participation implementation of developing projects from research "Developing of People Participation in Environmental Impact Compensation in Tourism place from case study of Crude oil liege Samed island, Rayong Province" (2016), reprocessing by statistical program Excel 2016 to index the level of people participation as shown in the table 2. From Table 2, it was found that the average of public opinions on the people participation implementation in environmental impact compensation of Samed Island, Rayong Province was during 3.21 - 3.38 which was at moderate participation level in high amount (Average score 2.61 - 3.40 with moderate participation) Standard deviation was during 0.883 - 0.916 and participation activities are to Involve Collaborate and Empower to provide and conduct the pursuit compensation for impact of environment occurring from crude oil leak.

Result subtitle 3

Comparison of statistical data from the questionnaire on public opinion on the participation in environmental management of developing project from 2 research projects. It is able to be statistically processed by the Excel 2016 program to index the level of people participation as shown in the table 3.

CONCLUSIONS

According to case study of people participation in environmental management in 2 cases in case of Bangpakong power plant, it was the participation of people of the communities living and career around the radius of 5 kilometers from the power plant project for prevention, solving and monitoring of environmental impacts caused by the operation of the power plant. This is in accordance with the content and requirements in the EIA document in normal situation and conducting in regular event in the annual routine and there is no any phenomena such as natural disasters, environmental degradation and resources as well as damage to life quality and economy of around people.

Table 1 Show the Average score ($\bar{x}$) and Standard deviation (S.D.) of opinions on the people participation in environmental management in Bangpakong Combined Cycle Power Plant number 5, Chachoengsao Province

Form and activities of people participation		**Level score of participation implementation**					**Average**	**S.D.**
		1	**2**	**3**	**4**	**5**		
1. Inform by publish, poster, television, radio and internet	No.	29	70	63	44	4	*2.64*	1.02
	Percentage	13.81	33.33	30.00	20.95	1.90		
	Score	29	140	189	176	20		
2. Consult by meeting, public stage.	No.	38	62	68	38	4	*2.56*	1.04
	Percentage	18.10	29.52	32.38	18.10	1.90		
	Score	38	124	204	152	20		
3. Involve by the representatives from the public to attend in the event.	No.	42	72	55	37	4	*2.47*	1.06
	Percentage	20.00	34.29	26.19	17.62	1.90		
	Score	42	144	165	148	20		
4. Collaborate by representatives from the public to consider.	No.	56	65	53	33	3	*2.34*	1.08
	Percentage	26.67	30.95	25.24	15.71	1.43		
	Score	56	130	159	132	15		
5. Empower by committee from the public to determine measures.	No.	63	70	49	27	1	*2.20*	1.06
	Percentage	30.00	33.33	23.33	12.86	0.48		
	Score	63	140	147	108	5		

Table 2 Show the Average score ($\bar{x}$) and Standard deviation (S.D.) of opinions on the people participation in compensation of environmental impact in tourism place Samed Island, Rayong Province.

Form and activities of people participation		Level score of participation implementation					Average	S.D.
		1	2	3	4	5		
1. Inform by publish, poster, television, radio and internet	No.	11	22	88	102	17	*3.38*	0.916
	Percentage	4.58	9.17	36.67	42.50	7.08		
	Score	11	44	264	408	85		
2. Consult by meeting, public stage.	No.	9	35	105	79	12	*3.21*	0.886
	Percentage	3.75	14.58	43.75	32.92	5.00		
	Score	38	124	204	152	20		
3. Involve by the representatives from the public to attend in the event.	No.	10	25	106	89	10	*3.27*	0.860
	Percentage	4.17	10.42	44.17	37.08	4.17		
	Score	10	50	318	356	50		
4. Collaborate by representatives from the public to consider.	No.	7	28	89	100	16	*3.38*	0.883
	Percentage	2.92	11.67	37.08	41.67	6.67		
	Score	7	56	267	400	80		
5. Empower by committee from the public to determine measures.	No.	12	24	85	106	13	*3.35*	0.916
	Percentage	5.00	10.00	35.42	44.17	5.42		
	Score	12	48	255	424	65		

to stimulate or accelerate the participation of people. Therefore, the average of people participation in 5 forms is in low to moderate level (2.20 - 2.64).

In crude oil leak crisis at Samed Island, it was provided as an unusual crisis situation and occurred in important tourist place that need normal environment and ecology greatly. The implementation to solve impact both during and after the crisis must be conducted in a strong, fast and efficient manner. Additionally, the participation of people who live and career in the area after the disaster is also important especially compensation for damage to life quality, economy and society of people in the crisis area. Therefore, the developing project that impacted and related sectors have taken strong people participation in order to achieve satisfaction and acceptance

of compensation for the environmental impacts that occur. Statically speaking, value of standard deviation of Bangpakong power plant case is higher than Samed Island case in all form of people participation

Table 3 Comparison of total Average score and Standard deviation (S.D.) of public opinions on the level of people participation in 2 cases study.

Form and activities of people participation		Bangpakong Combined Cycle Power Plant		Impact with Tourism Place Samed Island	
		Level of participation		Level of participation	
1. Inform by publish, poster, television, radio and internet	Average	2.64	moderate	3.38	moderate
	S.D.	1.02		0.916	
2. Consult by meeting, public stage.	Average	2.56	less	3.21	moderate
	S.D.	1.04		0.886	
3. Involve by the representatives from the public to attend in the event.	Average	2.47	less	3.27	moderate
	S.D.	1.06		0.860	
4. Collaborate by representatives from the public to consider.	Average	2.34	less	3.38	moderate
	S.D.	1.08		0.883	
5. Empower by committee from the public to determine measures.	Average	2.20	less	3.35	moderate
	S.D.	1.06		0.916	

It showed that most of raw score of Bangpakong power plant case are more distributed especially in minimal to moderate than Samed Island case that most raw score clustered in much and most interval score. These proved that crisis is one factor that is more influence than normal situation for people participation implementation.

While considering with Nawarat Trirat (2005), it was found that the sample group participated in the conservation of natural resources and the environment at a low level. The most participation aspect was benefit sharing process. Followed by collaboration in monitoring and evaluation process which is consistent with the results of the study in case of BangPakong power plant project. Because it is an implementation that no benefits for public or a stakeholder. Since there is no environmental impact problem unlike case of crude oil leak crisis

that people are truly stakeholders. The participation of the people is therefore strong and effective.

When we compare with Bo-sin Tang, Siu-wai Wong, Milton Chi-hong Lau a (2008) by discussing the assessment Mitigation as well as the participation of the community in urban development and compare with the practice in western society and summed up the fuzzy expectations for the Social Impact Assessment (SIA) people participation in development planning due to environmental laws that are not yet seriously implemented. Roles of government and society including the concept of socialism in China that is not yet conducive to public participation.

Suggestions from studies to improve public participation

1)The implementation of people participation in environmental work, especially about developing projects, it needs to communicate and explain the benefits that will be concrete and public. It will help people interested and intend to participate in the operation

2) Promotion of people participation in environmental work necessary to start from the people and surrounding communities to understand and recognize their role that is important to the environment and local resources that they live in.

3) There should be a scenario of large-scale impact or disaster from the environmental and community developing project, then provide process for people participation in mitigation as well as compensation for environmental impacts and the quality of life of people that must be carried out in order to effectively correct the environmental impact and public participation and be ready to accommodate various situations.

ACKNOWLEDGEMENTS

These 2 researches in this paper were finance sponsored by Faculty of Public Health Burapha University.

REFERENCES

Danai Bawornkiattikul, Deachit Nommeechai. 2013. Evaluating

status of People Participatory in Environmental Impact Monitoring Model for Developing Projects. Faculty of Public Health Burapha University.

Danai Bawornkiattikul, Deachit Nommeechai.2016. Developing of People Participation in Environmental Impact Compensation in Tourism place from case study of Crude oil leak Samed island, Rayong Province Faculty of Public Health Burapha University.

Bo-sin Tang, Siu-wai Wong, Milton Chi-hong Lau a 2008. Social impact assessment and public participation requisition in Guangzhou: Environmental Impact Assessment Review 28: 57–72

International association for public participation. 2014. "Spectrum of Public Participation" [online]. Available:http://www.iap2.org/4September2012 [Accessed on 17 April 2019].

Nawarat Trirak. 2006. Participation in natural resources and environment of people in Donhualo Sub district Muang district Chonburi province. Independent study Master of Public in Public Policy Administration Program Graduate school of Public Administration Burapha University.

Walkability Indexes of Current Pedestrian Facilities nearby Universiti Putra Malaysia, Serdang Campus

Kelrindra Pengabang[1], Nazatul Syadia Zainordin[1*], Farah Aini Omar[1],

Annabel Jukinol[1], Nurul Nabiha Hazman[1]

[1]Department of Environmental Management, Faculty of Environmental Studies, Universiti Putra Malaysia, 43400 UPM Serdang, Selangor, Malaysia
Corresponding author: e-mail: nazatulsyadia@upm.edu.my

ABSTRACT

Pedestrians' safety and comfortability is one of the important factors in road traffic system as they are the most vulnerable road user. Institutional area is an area which is expected to have high density of pedestrians as well as high traffic volume. Several cases have been recorded on the conflict between both road users, however, the impact is more severe to the pedestrians. In order to reduce the number of fatalities and injuries among pedestrians, well-designed pedestrian crossing and other facilities should be built. The objective of this study was to assess the walkability indexes of three selected areas, which specifically evaluate in term of safety and comfortable elements of the current pedestrian facilities nearby Universiti Putra Malaysia, Serdang Campus. A set of evaluation form has been used to assess both elements and the evaluation was conducted based on justification of nine parameters by referring to road cross-section of the areas together with on-site visualization. Walkability indexes of all selected sites were produced based on the parameters scoring. From the evaluation, the results showed that, for overall, 4 out of 9 parameters were following the standard and best guidelines at all selected areas, which were in terms of vertical clearance from any obstructions, safety gap between footpath and driveway, provided street lightings and traffic calming. As for the walkability, two areas recorded high indexes, which can be considered as well-built of pedestrian facilities. The highest walkability index was recorded at

CP2, where 8 out of 9 parameters were following the best standards and guidelines. Meanwhile, CP3 recorded the lowest walkability, which was only 5. This showed that, in this area, some of the pedestrian facilities were under-designed. Therefore, attention should be given in terms of providing properly built of pedestrian facilities in order to have safe and comfortable walking experiences while reducing the conflict between pedestrians and vehicles on road.

Keywords: Pedestrian crossing, pedestrian behavior, traffic vehicles, comfortability level, safety level

INTRODUCTION

Walking is one of the modes of transportation in a transportation system. In this system, walking can be categorized as green transportation because it is an active environmentally friendly mode. World Health Organization (WHO) (2013) stated that pedestrian is someone who travels or moves to one place to another on foot, whether walking or running without the use of any motor vehicle. Besides that, they also explained that pedestrians, cyclists or a group of road users that are not related to any vehicle mode are defined as Vulnerable Road Users (VRU).

Pedestrian are the most exposed to conflict with the road vehicles. Thus, as a VRU, their life is in jeopardy (Koh et al., 2014). WHO (2018) reported that pedestrians represent 26% of all deaths globally. They also reported that there are more than one-fifth of people killed on the world's road and most of them are pedestrians in 2013. Pedestrian facilities have been built to reduce and prevent this number of pedestrians' fatalities from increasing. Unfortunately, some of the built facilities are not in a good condition and impossible to attract people to fully utilize it. This leads to

the presence of jaywalkers on the road.

This paper reports the assessment of the current condition of pedestrian facilities according to the standard and best guidelines of geometric design specifically on pedestrian facilities by Public Works Department Malaysia (JKR) and Ministry of Works Malaysia (MOW). Walkability of the area can be measured when it takes into consideration the quality of the pedestrian facilities, the condition of the roadway, land use patterns, community support, security and comfort for walking (Ariffin & Zahari, 2013).

METHODOLOGY

Background of Study Area

This study focuses mainly at educational area since this type of area recorded high pedestrian density and activities nearby roadway. The study area where this research was conducted is in Universiti Putra Malaysia (UPM). UPM has two campuses which are Serdang Campus and Bintulu Campus. Serdang Campus is located at province of Serdang in Selangor state, meanwhile, Bintulu Campus is located in Bintulu, Sarawak.

After doing site investigation by including the factor of traffic volume, three checkpoints were selected as shown in Figure 1 and the details are shown in Table 1. In high population and traffic volume area, high pedestrians are expected to use the pedestrian facilities near the area (Rastogi et al., 2013).

Figure 1 Location of the study area

These three checkpoints were selected as the location situated nearby the main entrances, which links the main campus and students resident colleges.

Table 1: Details of the checkpoints

Checkpoints	Checkpoints ID	Coordinate	Landmarks
Checkpoint 1	CP1	N3.000047º E101.7145°	Faculty of Modern Language and Communication, UPM
Checkpoint 2	CP2	N2.998875° E101.7097°	Gate 15, UPM
Checkpoint 3	CP3	N2.998622° E101.707°	Post Office, UPM

Standards and Guidelines of Geometric Design for Pedestrian Facilities

Extension of pedestrian built environment should not only focus on footpath design but also include other elements of safety and connectivity of the facilities, which are pedestrian crossings and traffic calming. Footpath should be built by following the dimension requirement, which provides safety and comfortability way for pedestrians including the users with

Table 2: Standards and guidelines of geometric design of footpath and the basic elements (JKR, 1986; JKR, 1997; MOW, 2002)

Parameters	**Standards and guidelines**
Footpath width	Adequate width of footpath: 0.9m – 2.4m or wider
Vertical clearance	Height clearance ≥ 2.0m
Horizontal clearance	Footpath should not be obstructed by all street furniture, business activity and parked vehicles.
Safety gap between traffic lane and footpath	Clearance ≥ 1.0m between traffic lanes and footpath
Kerb height	Kerbs ≤ 0.15m
Footpath surface	Footpath surface should be firm, even, smooth and skid resistance especially in wet condition.
Street lightings	When there is significant night-time use by pedestrians, street lighting to an approved standard should be provided.
Crosswalk	Pedestrian crossings width = 1.8m – 3.6m (based on volume of pedestrians and vehicles) At signalized crosswalk, 3m desirable space should be provided for motorcycles between pedestrian crosswalk and vehicle stop line. Where overhead pedestrian crossings are provided, side barriers must be installed at both sides of the location of the crossing to prevent jaywalking. Distance of barriers = 75m. Minimum spacing between crossings = 400m.
Traffic calming	Installation of traffic calming • Speed bump (width: < 1m) • Speed hump (width: 3.5m – 4.0m) • Transverse bar (width: 300mm, spaced c/c: 2.75m, distance: 50m from crosswalk or speed hump) • Textured pavement (no specific dimension)

mobility impairments. Standards and guidelines of geometric design for pedestrian facilities and other basic elements that taken into consideration to construct a well-built footpath are summarized in Table 2. A checklist to evaluate the pedestrian facilities was referred to this table.

Rolling measure was used to measure dimension of several footpath and roadway components such as footpath width, crosswalk width, road width, road shoulder and traffic calming (speed bump, speed hump, transverse bar and textured pavement). Meanwhile, measuring tape was used to measure two footpath components, which are height of kerbs and vertical clearance of sidewalk for vertical obstruction on footpath. Other footpath components which are horizontal clearance, footpath surface and street lighting were evaluated by on-site visualization. Footpath was evaluated

on its clearance from obstructions (parked vehicles, street furniture, etc). Surface of footpath was evaluated whether it is firm, even, smooth and skid resistant. Meanwhile, availability of street lightings was evaluated when there is significant night-time use by pedestrian. Data samplings collected from all the measurements were gathered to create the cross-section of every checkpoint in order to have better visualization and understanding of the current pedestrian facilities available on the location.

Evaluation of the Pedestrian Facilities

Evaluation of pedestrian facilities at checkpoints are assessed based on two aspects which are via cross-section and on-site visualization (Kelly et al., 2007). Scores were given for every parameter in each elements of pedestrian facilities i.e. footpath, pedestrian crossing and traffic calming. The scores which represent the condition of the pedestrian facilities are shown in Table 3.

In order to evaluate the condition of pedestrian facilities nearby selected areas, several points were picked in a distance of 100m from the center of the checkpoints. Scores of every parameter were computed to find the score percentage. If the total percentage is equal or more than 75%, the parameter will be considered to comply with the Malaysian standards and guidelines. This is because the data are considered adequate to represent the total data (Raleigh Central Office QAP, 2012.

Table 3 Description of score given for the condition of pedestrian facilities

Score	Description of score
0	Unavailability of specific pedestrian facilities parameter
1	Specific pedestrian facilities parameter is available but under designed or improperly designed
2	Specific pedestrian facilities parameter is available and well-designed and accessible

Development of Walkability Index

Walkability index will be used as an overall evaluation method for the pedestrian facilities provided nearby selected areas whether it is accessible, safe and comfortable to use by pedestrian. Walkability measures are not "one size fit all" but vary by trip purpose and socioeconomic characteristics of residents (Manaugh and El-Geneidy, 2011). A significant walkability index was produced by following some of the parameters from Global Walkability Index (GWI) created by Krambeck (2006) with additional of other parameters.

Walkability index will be gained as a result of total number of score for overall parameters of pedestrian facilities as mentioned in the evaluation method section. Higher number of total score can be an indicative that checkpoint has a high walkability index where most of the pedestrian facilities elements were provided and well-built, thus they were accessible, safe and comfortable to use by pedestrians. Inversely, a lower number of total score, indicates a lower walkability index where most of the pedestrian facilities elements are not provided or improperly designed nearby the area even though the pedestrian density is expected to be high which eventually can lead to reduction of attractiveness for the people to use the facilities.

RESULTS AND DISCUSSION

Pedestrian Facilities Parameters Evaluation

Data gathered from all checkpoints by scoring are shown in Table 4. Parameter number one until nine showed the scoring for the main element of pedestrian facilities.

Referring to Table 4, both CP1 and CP2 were properly provided with adequate footpath width between 0.9 to 2.4m. Meanwhile, CP3 did not comply with the guidelines, due either to the under-designed or not continuously provided. Lack of adequate footpath at nearby area with high pedestrians density can caused them to share pavement with

motorized vehicles.

In terms of obstructions on footpaths, all checkpoints complied with the acceptable height clearance by the Malaysian guidelines.

Table 4: Compliances of pedestrian facilities nearby checkpoints by parameters

Parameters	CP1	CP2	CP3
Footpath width	✓	✓	×
Vertical clearance	✓	✓	✓
Horizontal clearance	✓	✓	×
Safety gap	✓	✓	✓
Height of kerbs	×	✓	✓
Footpath surface	✓	✓	×
Street lightings	✓	✓	✓
Crosswalk	×	×	×
Traffic calming	✓	✓	✓
TOTAL	**7**	**8**	**5**

Meanwhile, only CP3 has observed to have horizontal obstruction on footpath due to presence of trees and street furniture. Obstructions whether vertically or horizontally will decrease the attractiveness of using the pedestrian facilities in the area. Obstructions on footpath tend to divert pedestrians to walk on roadway which can increase probability of conflict between vehicles and pedestrians.

Clearance of at least 1.0m should be provided between footpath and roadway. From the cross-sections, this parameter complies with the Malaysian guidelines for all checkpoints. When there are high traffic volume and or high speed vehicles, it can increase probability of conflict between pedestrian and vehicle. Higher clearance may also reduce the annoyance due to splash from vehicles especially during wet condition.

Kerbs are common roadside feature

which define the edge delineation of the footpaths and improve aesthetics of the roadway (Karim, 2012). The presence of raised kerbs along the roadway tend to caused vehicles to drive away, and thus increase safety walk of the pedestrians. In this study, kerbs were found not uniformly built along the roadway in CP1. Difficulty for pedestrian to step up and down to the roadway level at intersection has become a major issue especially for disabled people. Whenever the situation is encountered, footpath should have ramped that meet the level of the roadway.

Most of the surfaces of footpaths at all the checkpoints except for CP3 were found to be even and smooth along the way. Condition of the footpath surface is also important to attract pedestrians to use the facilities. Footpath should be firm, even, smooth and skid resistant to avoid injury from the tripping over the walkway especially during wet weather.

Street lighting will produce comfortable and clear visibility to the pedestrians and drivers on the road. From the on-site visualization, many of the students were recorded to use the facilities even at night due to classes and other activities. Due to this, all of the checkpoints have uniformity of lightings along the footpaths. The need of street lighting is essential to ensure safety and comfort whenever they stay by the roadway.

During on-site visualization on pedestrian crosswalks, all checkpoints were not complied with the guidelines due to inappropriate width of pedestrian crossing which was too small for the students to cross especially during peak period. At CP3, there is overhead crossing provided between the students' resident colleges and the main campus. However, the facility was not fully utilized as the location is not located at the area where the high density of pedestrians was found. Side barriers were also not installed at both sides of the location as

suggested in the guidelines. Thus, possibility of jaywalking by the students is high. In Movahed et al. (2012) studies, crosswalk should be located at a suitable area by also considering the pedestrians' safety. Approaching drivers should have fine view of incoming pedestrians at both sides of the road. Thus, appropriate width of pedestrian crossing and its location should be expediently planning.

Based on the Table 4, all checkpoints are installed with traffic calmings. From the on-site visualization, the typical traffic calmings that are often found nearby the area are transverse bar, speed hump, speed bump and textured pavement. Installation of this parameter is crucial at high pedestrian area. Some drivers ignore or not realize they are entering the area with probability of presence of pedestrian.

Walkability Indexes of the Study Area

Figure 2 shows the walkability index of the current pedestrian facilities at three selected checkpoints.

Walkability index is a scoring value that can be used to understand the condition of selected sites whether the pedestrian facilities are well-designed or under-designed (Zainordin & Ramli, 2014). Higher walkability index define the pedestrian facilities provided nearby the area is well-built and inversely to the lower walkability index which represent improperly-designed facilities provided nearby the area.

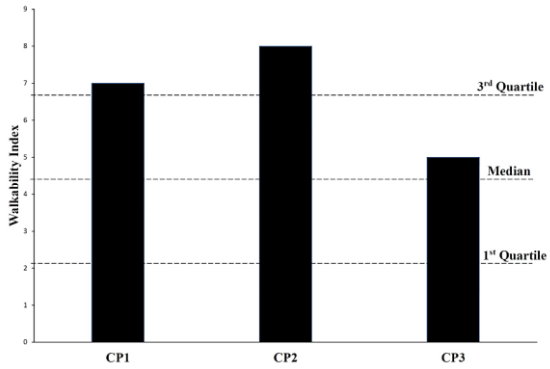

Figure 2 Walkability index of the pedestrian facilities at checkpoints

The highest number of walkability index that is considered to be well-designed pedestrian facilities is 9. Based on these three checkpoints, CP2 scored the highest walkability index which was 8 while the lowest walkability index was scored by CP3 which scored 5 out of the total of 9. The mean of the walkability index for all selected checkpoints was 6.67.

Based on classification of higher and lower walkability index suggested by Leslie et al. (2005), CP1 and CP2 can be considered as high walkability index where most of the important pedestrian facilities elements are well-designed which are continuous, accessible, comfortable and safe to use. Meanwhile, CP3 can be considered slightly under-designed due to lower walkability index which was lower than the third quartile of the total walkability score.

Interest should be given around the educational area in terms of providing properly built of pedestrian facilities in order to have safe and comfortable walking experiences while reducing the conflict between pedestrians and vehicles on road.

CONCLUSIONS

This study assessed the availability and condition of current pedestrian facilities according to standards and best guidelines of proper geometric design of pedestrian facilities. Walkability index give the indicator of whether pedestrian facilities nearby selected schools were well-built or poorly-built. Based on the walkability indexes for all three checkpoints, CP2 recorded the highest index while CP3 recorded the lowest. Much attention should be given in terms of geometric designs of pedestrian facilities especially at educational area due to high traffic volume and high density of pedestrians. Lack of pedestrian facilities provided at these areas may discourage them to use the facilities provided which lead to the jaywalking activities, which will be a hazard and lead to the direct conflict

between the pedestrians and incoming vehicles.

ACKNOWLEDGEMENTS

The authors would like to thank Universiti Putra Malaysia for the financial support under IPM Grant (GP-IPM/2018/9662500).

REFERENCES

Ariffin, R. N. R., & Zahari, R. K. (2013). Perceptions of the urban walking environments. Procedia- Social and Behavioral Sciences, 105, 589-597.

Jabatan Kerja Raya (JKR), Malaysia (1986). ArahanTeknik (Jalan) 8/86 - A Guide on Geometric Design of Roads. JKR Malaysia

Jabatan Kerja Raya (JKR), Malaysia (1997). Nota Teknik Jalan 18/ 97 - Basic Guidelines on Pedestrian Facilities.JKR, Malaysia.

Karim, S. N. A. (2012). Road Infrastructure Design Made Simple. UiTM Press, Malaysia.

Koh, P. P., Wong, Y. D., & Chandrasekar, P. (2014). Safety evaluation of pedestrian behaviour and violations at signalised pedestrian crossings. Safety science, 70, 143-152.

Kelly, C. E., Tight, M. R., & Hodgson, F. C. (2007). Techniques for assessing the walkability of the pedestrian environment. Institute for Transport Studies, University of Leeds, Leeds, LS2 9JT, UK.

Krambeck, H. V. (2006). The Global Walkability Index. [PDF File]. Massachusetts Institute of Technology Master in City Planning and Master of Science in Transportation

Leslie, E., Saelens, B., Frank, L., Owen, N., Bauman, A., Coffee, N., & Hugo, G. (2005). Residents' perceptions of walkability attributes in objectively different neighbourhoods: a pilot study. Health & Place, 11(3), 227-236.

Manaugh, K., & El-Geneidy, A. (2011). Validating walkability indices: How do different households respond to the walkability of their neighborhood?. Transportation Research Part D: Transport and Environment, 16(4), 309-315.

Ministry of Works (MOW), Malaysia (2002). Traffic Calming Guidelines. Malaysian Centre for Transport Study (MaCTRANS) and Ministry of Works, Malaysia.

Movahed, S., Azad, S. P. & Zakeri, H. (2012). A safe pedestrian walkway; creation a safe public space based on pedestrian safety. Procedia – Social and Behavioral Sciences 32, 572-583.

Raleigh Central Office QAP, USA (2012). Data Review & Validation QA Plan for Continuous Gaseous & Non- Speciated Particulate Monitors Section IV Raleigh Central Office Responsibilities. Retrieved September 2018, from: http://daq.state.nc.us/monitor/QAPlans/2_41_RCO_Procedures_for_Continuous_Monitors.pdf

Rastogi, R., Ilango, T. & Chandra, S. (2013). Pedestrian flow characteristics for different pedestrian facilities and situations. European Transport - Trasporti Europei 53, 1-21.

World Health Organization. (2013). Pedestrian Safety: A road safety manual for decision- makers and practitioners [PDF file]. Geneva, Switzerland: WHO Library Cataloguing- in- Publication Data. Retrieved from http://apps.who.int/iris/bitstream/10665/79753/1/9789241505352_eng.pdf?ua=1

World Health Organization. (2018). Global Status Report on Road Safety [PDF file]. Villars- sous- Yens, Switzerland: WHO Library Cataloguing- in- Publication Data. . Retrieved from https://www.who.int/violence_injury_prevention/road_safety_status/2018/en/

Zainordin, N. S., & Ramli, N. A. (2014). Assessment Of The Current Condition Of Pedestrian Facilities At Tanah Rata , Cameron Highlands For Probability In Reducing Ozone Concentrations, 242–248.

Potential of *Sphingobium yanoikuyae* to eliminate H_2S in biogas

Saowaluck Haosagul[1,3], Nipon Pisutpaisal[2,3]*

[1]The Joint Graduate School for Energy and Environment (JGSEE), King Mongkut's University of Technology Thonburi, Bangkok, 10140, Thailand

[2]Department of Agro-Industrial, Food and Environment Technology, Faculty of Applied Science, King Mongkut's University of Technology North Bangkok, Bangkok, 10800, Thailand

[3]Biosensor and Bioelectronics Technology Centre, King Mongkut's University of Technology North Bangkok, Bangkok, 10800, Thailand

*E-mail: nipon.p@sci.kmutnb.ac.th, h_saowaluck@hotmail.com

ABSTRACT

Corrosion of hydrogen sulfide (H_2S) is a major problem for biogas use. Sulfur oxidizing bacteria (SOB) is widely used in the treatment of hydrogen sulfide in biological systems. *Sphingobium yanoikuyae* strain TRE1, isolated a full-scale H_2S removal biotrickling in an ethanol plant was used to develop an H_2S removal biotrickling inoculated with a single bacterial strain. Inlet H_2S in synthetic biogas in the range of 0-2,000 ppm was fed in the biotrickling filter with immobilizing *S. yanoikuyae* on packing media. The gas upflow rate was controlled at 0.5 LPM (120 s EBRT) and counter flow with water spraying at the top of the biotrickling filter. Liquid samples were collected every 24 h to analyzed growth rate and sulfate concentration to follow the activity of *S. yanoikuyae*. At the 1,000 ppm inlet concentration, *S. yanoikuyae* can eliminate H_2S from the gas stream 53.5%. A little amount of sulfate accumulated about 4.6 mg L^{-1}, with pH value decreased from 7 to 6.8. Results showed that *S. yanoikuyae* could oxidize H_2S in the biogas but higher removal efficiency is needed.

Keywords: Hydrogen sulfide, *Sphingobium yanoikuyae,* Biotrickling filters, Ethanol industry, Sulfur oxidizing bacteria

INTRODUCTION

Hydrogen sulfide (H_2S) is extremely toxic gas, corrosive, and odorous, it can be produced in biogas fermentation with concentrations ranging from 0.1 to 3 % (1,000-30,000 ppm) (Schieder et al., 2003; Montebello et al., 2012; Fortuny et al., 2008) that cause toxic to bacteria in anaerobic digestion, especially the methanogens (Hulshoff et al., 1998) resulting the amount of methane gas used is reduced. The removal H_2S in biogas can be done in a biological

process by sulfur oxidizing bacteria (SOB) to degrade H_2S and others inorganic sulfur compound into elemental sulfur or sulfate with addition of air/oxygen (Mamun and Torii, 2015).

Omri et al. (2013) studied performance of biofilter developed to treat inlet H_2S concentrations of 200-1300 mg H_2S/m^3 from municipal wastewater treatment plant (WWTP), the results showed 99% removal efficiency at an empty bed retention time (EBRT) of 60 s. by heterotrophic sulfur oxidizing bacteria. Zhou et al. (2015) examined activated sludge to remove H_2S in biogas in biotrickling filter using polypropylene carrier as packing material, H_2S concentrations ranging from 2,065±234 to 7,818±131 ppmv H_2S was completely achieved. The elemental sulfur about 80% was produced when inlet H_2S concentration was increased. CH_4 content in biogas increased after H_2S removal, which was beneficial for the further utilization of biogas. Potivichayanon et al. (2005) examined H_2S removal efficiency from fixed-film bioscrubber by two new strains SOB are *Acinetobacter* sp. MU1_03 and *Alcaligenes faecalis* MU2_03. They found that H_2S removal efficiency by two species (98%) higher than using a single species (91%), sulfate accumulation increased when H_2S was oxidized.

However, no previous research has been able to isolate and use the *Sphingobium yanoikuyae* species to solve problems related to H_2S contamination in the biogas system. Therefore, this research aims to study the potential of *Sphingobium yanoikuyae* strain TRE1 which isolated from a full-scale H_2S removal in the ethanol industry to eliminate H_2S in biogas.

METHODOLOGY

Isolation and identification of Sphingobium yanoikuyae

Microbial sludge was collected from a full-scale H_2S removal biotrickling reactor treating H_2S from biogas in

the ethanol manufacture plant. The full scale biotrickling reactor is operated under the following operating conditions: inlet H_2S of 12,000 ppm (flow rate 350 m^3 h^{-1}), the water spray with flow rate of 7 m^3 h^{-1}, empty bed residence times (EBRT) of 15 min and the removal efficiency is up to 99%. Firstly, one gram of bacteria was mixed thoroughly with 1 ml of distilling water. The culture was streaking onto the surface of TMM agar plates and incubated at 30°C for 24 h. The ingredients of TMM agar are described as followed (g/L): 10 $Na_2S_2O_3 \cdot 5H_2O$, 4 KH_2PO_4, 4 K_2HPO_4, 0.4 NH_4Cl, 0.2 $MgCl_2 \cdot 6H_2O$, 0.01 $FeSO_4 \cdot 7H_2O$ and 16 nutrient agar. The isolated colonies with different morphology (size, shape, color) were observed. Further individual pure colonies were then streaked in fresh TMM agar plate, and incubated at 30°C for 24 h. Then, DNA templates for PCR amplification were extracted from isolated colonies using Genomic DNA mini kit (Geneaid Biotech Ltd., Taiwan). The universal primer 27F, 518F, 800R and 1492R were used for amplified double strands 16S rDNA sequencing. Finally, the nucleotide sequence was assembled using cap contig assembly program and the sequences similarity was calculated by a global alignment algorithm (Myer and Miller, 1988). One pure colony which could grow on TMM agar plates was named as *Sphingobium yanoikuyae* (accession no. MH045947) that available on the GenBank database. *S. yanoikuyae* was cultivated in 50 mL TMM broth and incubated at 30°C, 125 rpm for 48 hours. Liquid samples were collected every 6 hours for optical density measurement (OD_{600}) and colony forming unit (CFU mL^{-1}).

Immobilized S. yanoikuyae in a biotrickling filter

A biotrickling filter is made of transparent glass tube with a diameter and height of 475 mm and 720 mm, respectively (Vikromvarasiri, 2015). Sterilized packing media weight 150 g. (1 L working volume) is contained within the biotrickling filter for *S.*

yanoikuyae to form a biofilm on the surface. 200 ml of *S. yanoikuyae* in TMM broth (5.33×10^7 CFU/ml) was mixed into 1,800 ml of sterilized TMM broth which is spraying on packing media. The liquid sample was collected every 24 hours to monitoring the *S. yanoikuyae* growth, sulfate accumulation, the changing pH value and including observing the biofilm formation. The theoretical yield of sulfate per gram of thiosulfate can be calculated by using the formula (Eq. 1).

$$S_2O_3^{2-} + H_2O + 2O_2 \rightarrow 2SO_4^{2-} + 2H^+ \quad (1)$$

H_2S oxidation by *S. yanoikuyae*

TMM broth without *S. yanoikuyae* in the total volume of 2 L was prepared to recirculate liquid through the glass tube. Thiosulfate 10 g/L in the formula will be instead by hydrogen sulfide to observing *S. yanoikuyae* oxidized sulfides instead of inorganic sulfate. Synthetic biogas consists of hydrogen sulfide 5,000 ppm, methane 60% and balanced by carbon dioxide was used as inlet gas of biotrickling filter. In this experiment, there was a variation of the H_2S concentration of 500, 1,000, 1,500, 2,000 ppm, respectively. Adjusted H_2S was mixed with a constant air 1.5%, which has a total gas flow rate fixed as 0.5 LPM (120 s EBRT) and liquid recirculation rate was 3.6 L/h. Gas and liquid samples were collected every 24 h to analyzed inlet and outlet H_2S, pH, biomass yield, cell dry weight and sulfate concentration to follow the activity of *S. yanoikuyae* in a biotrickling filter.

Analytical techniques

Gas composition (H_2S, CH_4, O_2 and CO_2) were measured by hand-held portable gas analyser (GFM416, England). Sulfate content was analyzed by a turbidimetric method (OD_{420}) using a spectrophotometer. pH measured by a potentiometric method and cell dry weight (TS) were determined according to the standard methods (Adams, 2017). Colony forming unit (CFU mL^{-1}) to estimate the number of viable bacteria by drop plate method. The Gompertz equation (Eq.2) was used to fit the data of the optical density (OD_{600})

versus time for describing the biomass concentration (y), the specific growth rate (μ_m) and lag time (λ) in the period growth of bacteria (Wang et al, 2004; Gu, 2016). Where, y is the biomass concentration at the time (t) of incubation, A is the maximum biomass yield (OD_{600}), μ_m is the maximum specific growth rate (h^{-1}), λ is a lag phase time (h) and e is equal to 2.71828.

$$y = A \times \exp\left\{-\exp\left[\frac{\mu_m e}{A}(\lambda - t) + 1\right]\right\} \quad (2)$$

RESULTS AND DISCUSSION

S. yanoikuyae from ethanol industry

Double strands 16S rDNA sequencing was successfully to identify a new SOB species as *Sphingobium yanoikuyae* (MH045947*)* with 99.6% similarity. Colonies of *S. yanoikuyae* strain TRE1 are small circular, yellowish white, convex, smooth. When picking up colonies to TMM broth and incubation for 48 h, the growth of the isolated *S. yanoikuyae* was shown the high ability to oxidize thiosulfate as sulfate of 607 mg L^{-1}, the average of suspended cells in the recirculating broth was 2.33×10^8 CFU/ml. The maximum biomass yield of *S. yanoikuyae* has similar S-shape and fitted to the Gompertz equation with $R^2 > 0.95$ as provides a strong correlation. Interestingly, *S. yanoikuyae* was apparently short lag time ~2 h and then rapidly growth at 18-24 h incubation with the maximum biomass yield 0.075 (Fig 1). *S. yanoikuyae* is chemotrophic sulfur oxidizing bacteria belong to the class Alphaproteobacteria with there are sulfur oxidation enzyme (*soxABXYZ*) that oxidized thiosulfate to sulfate without free intermediate of sulfur globule formation (Eq.3) consistent with studies on specific genes in the SOB community (Meyer et al., 2007; Berben et al., 2019).

$$S_2O_3^{2-} + 5\,H_2O \rightarrow 2\,SO_4^{2-} + 8e^- + 10\,H^+ \quad (3)$$

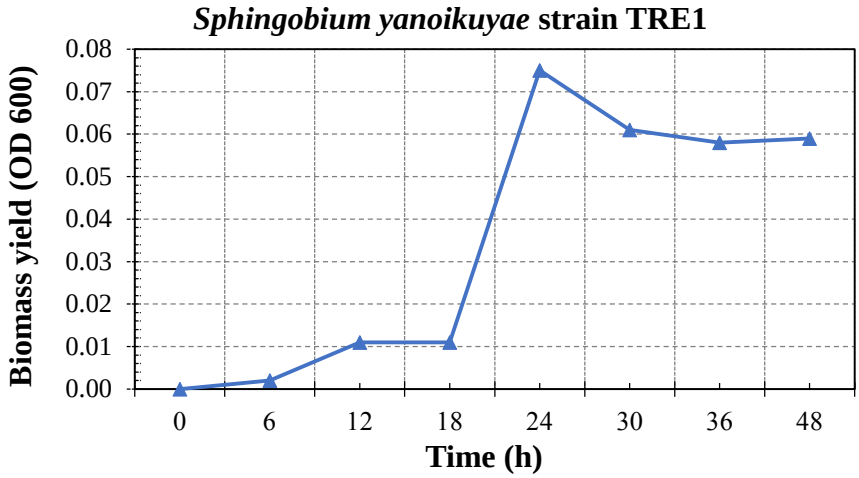

Figure 1. Growth curve of *Sphingobium yanoikuyae* in TMM broth.

Immobilizing *S. yanoikuyae* on packing media

The rectangular bars shows the amount of sulfate increased until 4 days and then decreased at day 5 while the pH started to continuously decrease corresponded with sulfate accumulation throughout the 5 days of immobilizing *S. yanoikuyae* on packing media (Fig 2). Log CFU/ml of suspended cells was gradually increased to 10.71 on the day 3 and quickly decreased to 5.88 in day 5 because the suspended cells of *S. yanoikuyae* are well attached on packing media, resulting in decrease cell in a recirculating broth. When observed on the media, it was found that the white mucilage of the *S. yanoikuyae* increased. After that, the recirculating broth was prepared without thiosulfate and tested *S. yanoikuyae* to eliminate H_2S in the concentration range of 500-2,000 ppm, respectively.

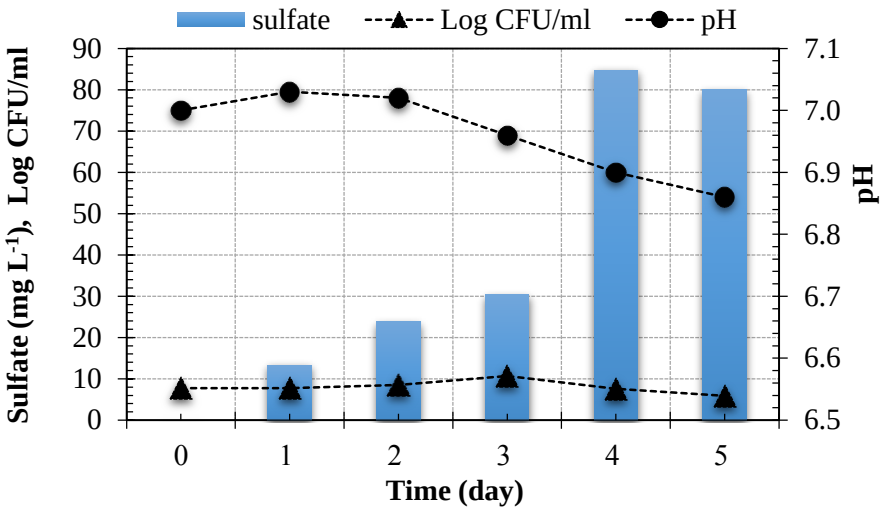

Figure 2 Sulfate content, Log CFU/ml and pH in immobilize process

Effects of H_2S concentration on *S. yanoikuyae*

At the inlet H_2S concentration about 500-1,000 ppm, the remove efficiency at 120 s EBRT in the range of 53.3-53.5% (Fig 3A), whereas the removal efficiency decreased when increasing the inlet H_2S concentration at 1,500 ppm and 2,000 ppm were 41.6 and 22.3%, respectively. Furthermore, the percentage of oxygen being used was decreased as the inlet H_2S concentration was increased, this result indicated that the oxygen was not limited. Carbon dioxide content in all case is dereased due to the consumtion by *S. yanoikuyae*. While methane gas has a constant value after hydrogen sulfide treatment. In the recirculating broth (Fig 3B), suspended cells of *S. yanoikuyae* in water have a similar value in the range Log CFU/ml of 5.26-5.34 (inlet H_2S 500-1,500 ppm), which is less than 0 ppm (the beginning of the process) that indicates *S. yanoikuyae* is well immobilized on packing media by not falling off with recirculating broth. In contrast, *S. yanoikuyae* cells that grow on the packing media (11.378 g dry weight) after that fall into TMM broth (Log CFU/ml of 5.9) when the concentration is increased to 2,000 ppm resulting in reduced H_2S

removal efficiency. The trend of sulfate accumulation is similar to the trend of H_2S removal efficiency in the concentration range 0-2,000 ppm. Results showed that *S. yanoikuyae* oxidized H_2S in the synthetic biogas through *soxABXYZ* enzyme under aerobic condition, which can be described as the following reactions (Eqs. 4-6) (Friedrich et al, 2001; Tang et al, 2009; Barton et al. 2014; Pokorna and Zabranska, 2015).

$$H_2S+0.5O_2 \rightarrow S^0+H_2O;\ \Delta G^0 = -209.4kJ/reaction \quad (4)$$

$$S^0+1.5O_2+H_2O \rightarrow SO_4^{2-}+2H^+;\ \Delta G^0 = -587.41kJ/reaction \quad (5)$$

$$H_2S+2O_2 \rightarrow SO_4^{2-}+2H+;\ \Delta G^0 = -798.2kJ/reaction \quad (6)$$

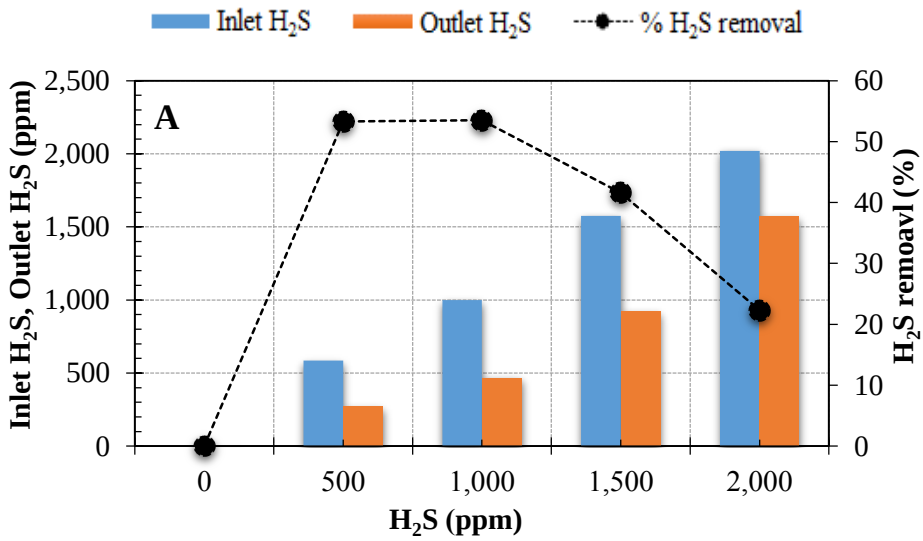

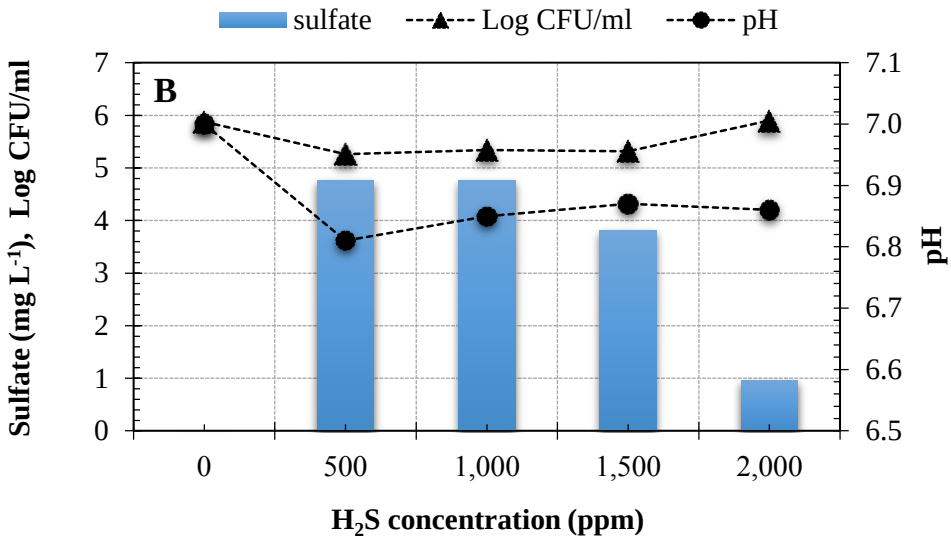

Figure 3. (A) showed relationship between the removal efficiency and H_2S concentration varying, **(B)** the trend of sulfate accumulation and suspended cells of *S. yanoikuyae.*

CONCLUSIONS

Pure SOB strain isolated from a full-scale H_2S removal in the ethanol industry was *Sphingobium yanoikuyae* (MH045947). The performance of *S. yanoikuyae* to eliminate H_2S in synthetic biogas was 500-1,000 ppm, with up to 53% removal efficiency. The future work, we will be studied by using more than one species to increase hydrogen sulfide removal efficiency.

ACKNOWLEDGEMENTS

The authors would like to thank the financial support from Research and Researchers for Industries (Grant No. PHD60I0028) and the financial support (Grant No. JGSEE 739) from the Joint Graduate School of Energy and Environment, King Mongkut's University of Technology Thonbur.

REFERENCES

Adams VD. (2017). Water and wastewater examination manual. Routledge.

Al Mamun MR, Torii S. Removal of hydrogen sulfide (H2S) from biogas using zero-valent iron. Journal of Clean Energy

Technologies 2015; 3(6): 428-432.

Barton LL, Fardeau ML, Fauque GD. Hydrogen sulfide: a toxic gas produced by dissimilatory sulfate and sulfur reduction and consumed by microbial oxidation. In: The Metal-Driven Biogeochemistry of Gaseous Compounds in the Environment. Springer, Dordrecht 2014; pp. 237-277.

Berben T, Overmars L, Sorokin DY, Muyzer G. Diversity and distribution of sulfur oxidation-related genes in thioalkalivibrio, a genus of chemolithoautotrophic and haloalkaliphilic sulfur-oxidizing bacteria. Frontiers in microbiology 2019; 10: 1-15.

Fortuny M, Baeza JA, Gamisans X, Casas C, Lafuente J, Deshusses MA, Gabriel D. Biological sweetening of energy gases mimics in biotrickling filters Chemosphere 2008; 71: 10-17.

Friedrich CG, Rother D, Bardischewsky F, Quentmeier A, Fischer J. Oxidation of reduced inorganic sulfur compounds by bacteria: emergence of a common mechanism? Appl. Environ. Microbiol 2001; 67: 2873-2882.

Gu JD. More than simply microbial growth curves. Applied Environmental Biotechnology 2016; 1: 63- 65.

Hulshoff PLW, Lens PNL, Stams AJM, Lettinga G. Anaerobic treatment of sulphate-rich wastewaters. Biodegradation 1998; 3: 213–22.

Meyer B, Imhoff JF, Kuever J. Molecular analysis of the distribution and phylogeny of the soxB gene among sulfur-oxidizing bacteria–evolution of the Sox sulfur oxidation enzyme system. Environmental Microbiology 2007; 9: 2957-2977.

Montebello AM, Fernández M, Almenglo F, Ramírez M, Cantero D, Baeza M, Gabriel D. Simultaneous methylmercaptan and hydrogen sulfide removal in the desulfurization of biogas in aerobic and anoxic biotrickling filters. Chemical Engineering Journal 2012; 237: 200–202.

Myers EW, Miller W. Optimal alignments in linear space. Bioinformatics 1988; 4: 11-17.

Nunthaphan Vikromvarasiri. (2015) Development of biotrickling filter for hydrogen sulfide removal

in biogas by autotrophic bacteria. King Mongkut's University of Technology Thonburi/Bangkok.

Omri I, Aouidi F, Bouallagui H, Godon JJ, Hamdi M. Performance study of biofilter developed to treat H2S from wastewater odour Saudi. Journal of Biological Sciences 2013; 20: 169–176.

Pokorna D, Zabranska J. Sulfur-oxidizing bacteria in environmental technology. Biotechnology Advances 2015; 33: 1246-1259.

Potivichayanon S. 2005. Removal of hydrogen sulfide by fixed- film bioscrubber. Ph.D. Thesis. Faculty of Science, Mahidol University, Bangkok, Thailand, 230 pp., ISBN 974-04-5955-2.

Qiying Zhou, Hong Liang, Senlin Yang, Xia Jiang. The Removal of Hydrogen Sulfide from Biogas in a Microaerobic Biotrickling Filter Using Polypropylene Carrier as Packing Material. Appl Biochem Biotechnol 2015; 175: 3763–3777.

Schieder D, Quicker P, Schneider R, Winter H, Prechtl S, Faullstich M. Microbiological removal of hydrogen sulfide from biogas by means of a separate biofilter system: experience with technical operation. Water Science and Technology 2003; 48: 209–212.

Wang Y, Qian P, Gu JD. Effects of UV, H2O2 and Fe3+ on the growth of four environmental isolates of Aeromonas and Vibrio species from a mangrove environment. Microbes and environments 2004; 19: 163-171.

Performance of pitaya production by using life cycle methods: a case study in Sepang, Selangor

Amir Hamzah Sharaai[1,2] and Mohd Hafizuddin Shamsudin[1]

[1*]Faculty of Environmental Studies, Universiti Putra Malaysia, 43400 UPM Serdang, Malaysia

[2]Institute of Plantation Studies, Universiti Putra Malaysia, 43400 UPM Serdang, Malaysia

Corresponding author: e-mail: amirsharaai@upm.edu.my

ABSTRACT

The demand for pitaya *Hylocereus polyrhizus* (dragon fruit) is increasing on the export market which leads to the increasing number of planted areas all over the year in Malaysia especially in Selangor. Selangor is known as the third largest producer of pitaya in Malaysia, therefore Sepang is selected due to the existence of the pitaya farm almost 16 years ago. Most of the farms definitely need to come out with their total production in handling and managing the pitaya plantation. At the same time, they need to consider the environmental costs that will be contributed during the production. Thus, the purpose of this study is to analyze the performance of the pitaya production by calculating the total production cost of pitaya production and estimating the total environmental cost incurred in the system. To achieve this purpose, three methods were implemented, which are; 1) life cycle assessment (LCA), 2) environmental life cycle costing (ELCC), and 3) life cycle costing (LCC). The LCA's result shows that there are several potential impacts from pitaya production which are the ozone layer, at about 6.06 kg CFC-11 equivalent, summer smog or respiratory inorganic, estimated at 3.81 kg C_2H_4 equivalent, climate change at 3.4 kg CO_2 equivalent, carcinogens or human eco-toxicity at 1.21 kg Benzo(a)pyrene equivalent, radiation at 1.1 kg bq C-14 equivalent, fossil fuels at 0.856 kg CO_2 equivalent, eco-toxicity at 0.659 kg Cu equivalent, mineral depletion at 0.077 kg Mj Surplus equivalent, and acidification at 0.028 kg SOx equivalent. The total environmental cost for pitaya production was estimated to be EUR5,400.39. After the environmental cost is included in the variable cost, the NPV is EUR10,608.21, IRR is 14%, payback period is 5.46 years and the breakeven point is 39437.25. To sum up, ELCC will help to estimate the cost incurred for pitaya farm where the environmental cost is actually capable to be borne by the owner without incurring any losses. Besides, this study will help the producers and suppliers of pitaya to come out

with the eco-friendly practices and to consider some allocations to protect the environment.

Keywords: pitaya production performance; ELCC; LCA; LCC

INTRODUCTION

Nowadays, the demand of pitaya is increasing and fetching premium prices in the export market. Pitaya production is not only important to the economic but social as well. The network of people related to pitaya is not only the suppliers, but also the consumers, traders and sellers which resulting in the impact on the lives and well-being of millions of people across the world.

In Malaysia, although the production of pitaya was decreasing since 2015, the planted area is increasing every year since 2014 according to Department of Agriculture (2016) (**Table 1**). The planted area is expected to grow because of the existence of the Economic Transformation Programme (ETP) and the National Key Economic Areas (NKEA), where one of their goals is to increase the productivity and income of small farmers. In 2016, the Department of Agriculture reported Selangor as the third largest production of pitaya among the 14 states in Malaysia (**Table 2**). The total production of pitaya in Selangor that year was estimated about 794.6 Mt with the area involved was around 70.1 Ha. This was supported by the value of production which was about EUR533,892.24 during that year. This is the reason why pitaya was also included as a major crop in Selangor.

Since the production of pitaya is expected to increase, the producer needs to be concern about the environmental cost being included in its production. This is because when the production cost tends to rise, the environmental cost through the impacts of pitaya production also

increases. Therefore, the purpose of this study is to analyze the performance of the pitaya production by estimating the production and environmental cost of the whole process involved in the pitaya production system.

Table 1: National Pitaya Planted Area and Production

Year	Planted Area (Ha)	Production (Mt)
2010	1,526.7	10,192
2011	962.8	7,943
2012	812.5	6,252
2013	451.8	8,577
2014	613	8,589
2015	688.1	5,474.6
2016	693.5	4,401

Table 2: Area, Production and Value of Production of Pitaya by State in Malaysia, 2016.

State	Hectare (Ha)	Harvested Area (Ha)	Production (Mt)	Value of Production (EUR')
Johor	159.3	166.6	1,280.3	860.11
Kedah	7.3	7.3	81.1	54.46
Kelantan	1.5	1.0	1.9	1.24
Melaka	227.2	150.8	1,506.8	1,012.34
Negeri Sembilan	60.0	52.0	436.1	292.98
Pahang	1.7	1.7	7.6	5.07
Perak	0.4	0.4	1.9	1.26
Selangor	70.1	65.2	794.6	533.89
Terengganu	7.0	6.0	8.6	5.72
Sabah	70.0	53.8	262.9	176.63
Sarawak	54.4	5.9	20.0	13.44
Penang, Labuan, & Perlis	-	-	-	-

(Source: Department of Agriculture, Malaysia, 2016)

METHODOLOGY

In this section, the detailed explanation on the method in conducting this study will be discussed in depth based on the research framework (**Figure 1**).

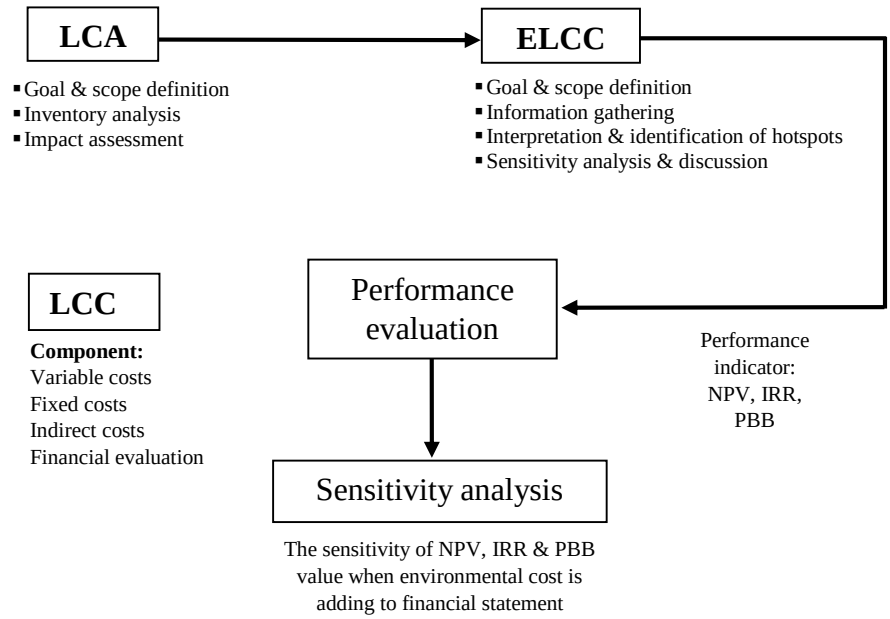

Figure 1 The research study framework

a) Life Cycle Assessment (LCA)

LCA is a standardized procedure, which is reliable and transparent. The standards are provided by the International Organization for Standardization (ISO) in ISO 14040 and 14044 2006, and it defines the four main phases of an LCA:

1. Goal and scope,
2. Inventory analysis,
3. Impact assessment, and
4. Interpretation.

For this purpose of study, there were only three phases of LCA conducted in the environmental life cycle costing (ELCC) methodology which are goal and scope, inventory analysis and impact assessment. As for the interpretation phase, it was quite similar with the ELCC under phase 3 and 4 which will be explained later in the ELCC subtopic.

The goal and scope definition will guarantee the LCA is being done consistently where this LCA model is a product, service, or system life

cycle that interpret for a complex reality and represent the reality in some way but still, there is challenger in develop the model.

The best way to deal with the problem is to carefully define the goal and scope of the LCA study such as the reason for executing the LCA, a precise definition of the product and its life cycle, and a description of the system boundaries. For this study, the main goal is to measure and identify the potential impact towards environment from the pitaya production. The scope of this study is defined within a system boundary including: 1) Provision of lands and areas, 2) Planting, 3) Weed Control, 4) Fertilization, 5) Flowering Induction, 6) Harvesting, and 7) Distribution. The scope of this study is shown in **Figure 2**. The functional unit has to be the same as in the underlying LCA because it is built on the same product system providing the same function. The functional unit for this study is 1000kg of pitaya.

For life cycle inventory (LCI) phase, a field visit was conducted at the Multi Rich Pitaya Dragon Fruit Farm, Sepang, Selangor. The primary data obtained from the activity was the distribution of the pitaya fruit. Another data that is needed to implement this study was obtained from the Department of Agriculture such as the value of pitaya production in Malaysia and Selangor. In this phase, it is important to produce a flow model for the process. The outputs and inputs must be identified clearly. **Figure 3** shows the framework for conducting the LCI Analysis. The SimaPro software was used in analyzing the inventory data in order to analyze the impact of environment based on the data gained from the study. Besides, the on-site data or known as the foreground data, the background data, was gained from the Eco invent databases. The life cycle inventory phase included two stages, namely: 1) the data collection from field visit on-fields data for practices in production of pitaya such as environmental costs,

research & development (R&D) costs and pitaya's cultivation process that being supported by the data from the Department of Agriculture through interview and follow up communication such as the data of pitaya's plantation areas and harvested area and also including the background process (petrol fuel production and water production) and, 2) calculation of amount of resource use (input) and emission of the pollutant (output).

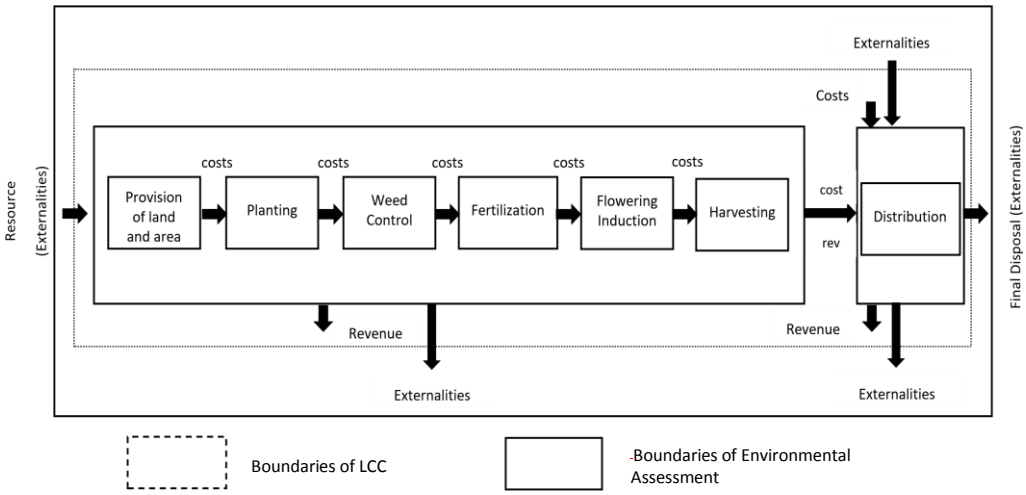

Figure 2 System boundary of pitaya production

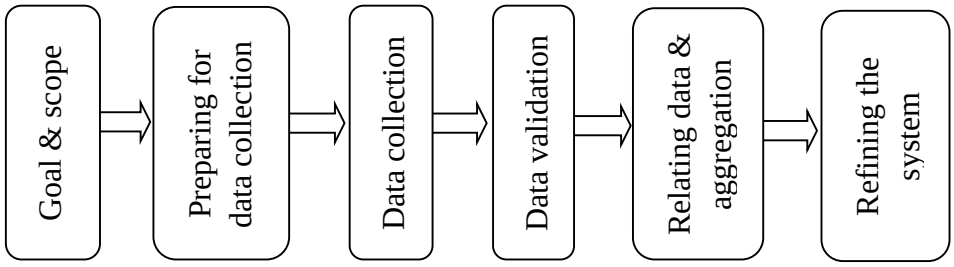

Figure 3. A framework for conducting the LCI analysis

The next phase is Life Cycle Impact Assessment (LCIA). LCIA provides further interpretation of the LCI data. The inventory data was multiplied by the characterization factors in order to give an indicator for the environmental categories.

S = Inventory data × Characterization factors (**Equation 1**)

Where;
S = Indicator for the environmental categories

This phase transforms the LCI results into environmental impacts. The impact assessment method for this study was performed by using the method implemented in Eco invent CML 2001. In terms of characterization, the concept of "problem-oriented approach" was used in this study. Because of that, the baseline indicators were at the "mid-point level".

b) Life Cycle Costing (LCC)

In this LCC methodology, all the relevant costs during the production of pitaya were gathered including the fixed and variable costs. The depreciation of the fixed cost was also calculated. Then, an income statement of the company being studied was created. The total profit or revenue, net present value (NPV), IRR, payback period, and breakeven point were estimated.

NPV:	**Difference between the present value of the future cash flows from an investment and the amount of investment.**
IRR:	The interest rate at which the net present value of all cash flows from the company.
Payback period:	The length of time required to recover the cost of an investment.
Breakeven point:	The revenues needed to cover a company's total amount of fixed and variable expenses during a specific period of time.

c) Environmental Life Cycle Costing (ELCC)

The Environmental Life Cycle Costing (ELCC) is an enhancement from the Conventional Life Cycle Costing (CLCC) which involved the integration of LCA of the product to be internalized for decision relevant to future cost. The ELCC involve four specific steps in general framework:

a) Goal and scope definition,
b) Information gathering,
c) Interpretation and identification of hotspots, and
d) Sensitivity analysis and discussion

The first component in an ELCC is the definition of goal and scope. It needs to be explained clearly. For this study, the main goal is to measure and calculate the total costs involving all the stakeholders related to the pitaya production in Selangor and the significant costs of impacts toward environment. The next phase is the information gathering. In this phase, all the data for conducting LCA and LCC is important to make sure the ELCC methodology for pitaya production is successful. The data must cover the production system fully, which includes the amount of input or output and also the total cost incurred for pitaya production. The next stage is the interpretation and identification of the hotspots. The identification of the hotspots is an important element in conducting ELCC. It is the core results analysis which is important if a sensitivity analysis is carried out. In this stage, there are two assignments need to be done by the researchers which are the assignment of the production cost and the assignment of the environmental cost. The production cost will be calculated based on the primary and secondary data. In order to get the production cost, all the costs involved in every stage of the pitaya production need to be calculated. For the second assignment which is the assignment of the environmental cost, the Eco-cost 2012 LCA database must be used (**Figure 4**). The Eco-cost database (**Table 3**)

needs to be converted by using the currency converter from Euro (EUR) currency to Malaysian Ringgit (RM) as to reflect the current rate in Malaysia. It is an important step before the assignment of cost was conducted using the ABC method. The formula used in ABC method is shown in (**Equation 2**). After that, the aggregation of the environmental cost was done by summing up the environmental cost with the LCI within the same group according to the Eco-cost 2017 LCA database for the whole stage in pitaya production system.

$$\sum n \sum \text{m } (\mu\text{m } x \sum p \sum q \text{ amount } q \text{ x costs } p) \quad \textbf{(Equation 2)}$$

Where,

m = process specific variable
p = cost category – specific variable
q = process flow – specific variable
μ = process scaling factor related to the product system
n = life cycle phase

Table 3: Data for emission of toxic substances in the Eco-cost 2017 system

Category	Multiplier (marginal prevention costs)
eco-costs of acidification	8.83 €/kg SOx equivalent
eco-costs of eutrophication	4.17 €/kg phosphate equivalent
eco-costs of Eco toxicity	55.0 €/kg Cu equivalent
eco-costs of human toxicity	3754 €/kg Benzo(a)pyrene equivalent
eco-costs of summer smog)	10.38 €/kg C_2H_4 equivalent
eco-costs of fine dust	34.0 €/kg fine dust PM2.5

(Source: The Model of the Eco-costs / Value Ratio (EVR)

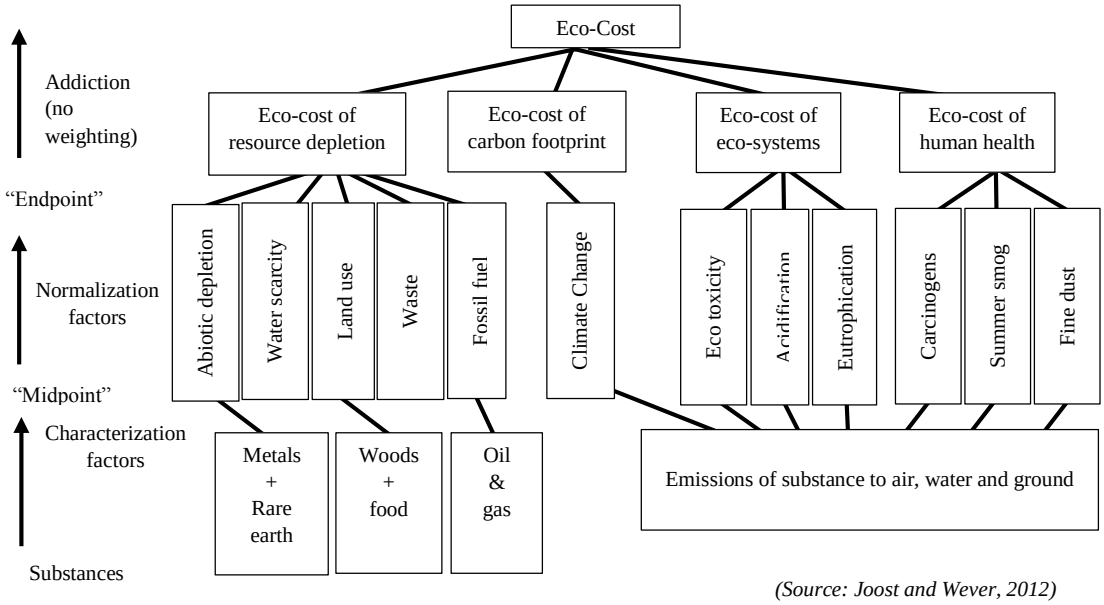

(Source: Joost and Wever, 2012)

Figure 4 Calculation structure of the system of Eco-costs 2012 result

Next, is the sensitivity analysis phase. In this stage, the environmental costs obtained were include in the variable cost and the financial statement to be evaluated through NPV, IRR, payback period and breakeven point. Then, it was compared with the financial evaluation of pitaya production that does not include the environmental cost in their expenses as part of the performance evaluation of the life cycle of pitaya production.

RESULTS AND DISCUSSION

In this section, the result and discussion are divided in four parts:

a) Potential Environmental Impact of Pitaya Production,
b) Cost of Production,
c) Environmental Cost for Life Cycle of Pitaya Production, and
d) Sensitivity Analysis.

a) Potential Environmental Impact of Pitaya Production

From the inventory analysis, the potential impacts toward

environment were identified (**Table 4**). The characterization result clearly shows that; the production of pitaya will bring a lot of impact in regard to the depletion of ozone layer which is about 6.06 kg CFC^{-11} equivalent/year. The second highest impact is summer smog or also called respiratory organic which is about 3.81 kg C_2H_4 equivalent/year. Next, there are significant impact toward the climate change and carcinogens which were estimated about 3.4 kg CO_2/year and 1.2 kg Benzo(a)pyrene equivalent/year. The impact toward fine dust or also interchangeably identified as respiratory inorganic and radiation were estimated about 1.05 kg fine dust PM2.5 equivalent/year and 1.1 kg bq C^{-14} equivalent/year. Other impacts being identified were fossil fuels (0.856 kg CO_2 equivalent/year), Eco-toxicity (0.659 kg Cu equivalent/year) and mineral depletion (0.077 kg Mj Surplus equivalent/year). The lowest impact from the production of pitaya was acidification, estimated at about 0.028 kg So_x equivalent/year.

The result obtained through SimaPro also can be divided into four damage categories (**Table 5**). The damage category is recognized as an end-point of the result and the impact categories within that end-point is called as the mid-point impact category. Acidification and eco-toxicity were the mid-point impact under the damage category of eco-system. The mid-point impact for the damage category of human-health were carcinogens, summer smog, fine dust, ozone layer and radiation. For damage category of resource depletion, the mid-points were mineral depletion and fossil fuels. Climate change was the only mid-point under the global warming damage category

Table 4: The Damage Category

Damage Category	Impact Category
1) Eco-system	a) Acidification
	b) Eco-toxicity

2) Human Health	a) Carcinogens
	b) Summer smog
	c) Fine dust
	d) Ozone layer
	e) Radiation
3) Resource Depletion	a) Mineral depletion
	b) Fossil fuels
4) Global Warming	a) Climate change

Table 5: The Characterization Result of Pitaya

Impact Category	Total
Carcinogens	1.21 kg Benzo(a)pyrene eq
Summer smog	3.81 kg C_2H_4 eq
Fine dust	1.05 kg fine dust PM2.5 eq
Climate Change	3.4 kg CO_2 eq
Radiation	1.1 kg bq C^{-14} eq
Ozone layer	6.06 kg CFC^{-11} eq
Eco-toxicity	0.659 kg Cu eq
Acidification	0.028 kg So_x eq
Minerals Depletion	0.077 kg Mj Surplus
Fossil fuels	0.856 kg CO_2 eq

b) Cost of Production

The total revenue from the sales of pitaya was about EUR39,011.37 per year where the average of pitaya production within a year was estimated about 15,000 tons. The price for 1 kg of pitaya in market was about EUR2.60. The total cost for pitaya production at Multi-Rich Pitaya Dragon Fruit Farm, Sepang, Selangor was about EUR265,347.15 and it can be divided into two categories which are fixed costs and variable costs. The total fixed cost of pitaya production is EUR177,374.10 including the equipment at the farm such as lorry, building, gloves, spade trowel, pickaxe mattock, peatland wheelbarrow, fork, sprayer bearing, buckets, safety helmet, safety mask,

apron, garden scissor, seed, concrete pillars and rubber boots. The total variable cost is about EUR87,613.05. The variable costs included the agriculture lime (Humibox), CIRP (Australia), organic fertilizer (Harvester), NPK fertilizer (Nitrophaska), folia fertilizer (Booster), mould poison (Typhoon), insecticides (Decis), fruit wrap, raffia rope, the supervisors' salary, permanent workers' salary and water bills.

c) Environmental Cost for Life Cycle of Pitaya Production

From the results obtained in **Table 6**, the most identified hotspots for environmental cost of impacts is carcinogens, at EUR4,646.41/kg Benzo(a)pyrene equivalent and 86.03% of the total cost incurred for environmental protection. Carcinogens can be defined as any substances which has a potential to cause cancer in living tissue and it is related to human health (Ndlovu, 2015). For pitaya production, the large number of carcinogens is due to the ethane substances coming from the weed control stage. Other than that, the large number of magnesium oxide that is an important element in lime formation will influence the huge potential impact of carcinogens.

The second highest environmental cost is for ozone layer which is about EUR619.89/kg CFC^{-12} and 11.50% of the total eco-cost in pitaya production. The ozone layer known as the concentration of molecules is available at the stratosphere, situated along 65 km above the surface of the earth (Mogensen, 2018). The depletion occurred due to the process of neutralization of the soil for plantation where the owner tends to use a large amount of lime. Magnesium oxide and calcium nitrate influence the impact toward the ozone layer.

The environmental cost of summer smog or respiratory organics is about EUR40.43/kg C_2H_4 equivalent which is 0.75%. Summer smog is one of the indicators in human health's damage category from the accumulation of the

greenhouse gases and pollutants, which reduces the visibility and impairs the respiratory functions. It comes from the fertilization stage, where a lot of fertilizers were used in order to increase the production of pitaya. The use of nitrogen, phosphate, and potassium in the fertilization stage will give an impact toward the environment in terms of summer smog. One of the main things lead to the summer smog is due to the use of nitrogen oxide from the fertilizer (Bienkowski, 2018).

For eco-toxicity, the environmental cost is EUR37.07/kg Cu equivalent or 0.67%. This impact occurred due to the manganese element in the fertilization stages. Eco-toxicity is an indicator in the eco-system's damage category. The agricultural practice uses three main chains which are nitrogen, potassium and phosphorus. However, when the nitrogen is converted to become ammonia, nitrite and nitrate it becomes toxic to the environment. Phosphorus is usually related to the agricultural drainage as it is being mixed with the fertilizer and pollutes the water supply (Jeremy, 2010).

Other than that, other impact also influence the cost for environmental protection in a pitaya production, but it is not significant or brings a large impact as mentioned above. Those are fine dust (EUR36.52/kg fine dust PM2.5 equivalent), fossil fuels (EUR19.39/kg CO_2 equivalent), global warming (EUR0.41/kg CO_2 equivalent) and the least significant impact is acidification (EUR0.25/kg So_x equivalent). Cleaning activities at the farm could lead to soil exposure due to the lack in vegetation cover, and at the same time, resulted in soil disturbance caused by the agricultural activities. Finally, it resulted in high number of wind erosion and dust emission (Sivakumar, 2009). Fine dust reduces the photosynthetic activity that leads to delay in plant development and reduces the productivity of plants (Jeremy, 2010). The fossil fuels come directly from the nitrogen fertilizer produced by a

huge amount of natural gas and coal, which also bring an effect in the pitaya plantations (Anand, 2014). Usually, fossil fuels come from two activities in the farm, namely, the fertilizers and the power or electricity (Anand, 2014). Coal and diesel were used for the electricity generation in the farms, and fertilizers for the production of plant.

Table 6: Total Environmental Cost of Pitaya

Damage category	**Impact category**	**(MPC/£)**	**(MPC/EUR)**	**LCI**	**Total environmental costs (EUR) (MPC x LCI)**
Eco-system	Acidification	8.83	9.03	0.028	0.25
	Eco-toxicity (/kg Cu equivalent)	55	56.26	0.659	37.07
	Carcinogen (/kg Benzo(a)pyrene equivalent)	3 754	3840.01	1.21	4,646.41
Human health	Summer smog (/kg C2H4 equivalent)	10.38	10.62	3.81	40.45
	Fine dust (/kg fine dust PM2.5)	34	34.78	1.05	36.52
	Ozone layer (/kg CFC^{-12} equivalent)	100	102.27	6.06	619.89
Resource depletion	Fossil fuels (/kg CO_2 equivalent)	22.14€	22.65	0.856	19.39
Climate change	Global warming (/kg CO_2 equivalent (GWP 100)	0.116€	0.12	3.4	0.41
Total Cost Incurred in Environmental Protection					**5,400.39**

d) Sensitivity Analysis

The sensitivity analysis for this study discussed about the expectation of the environmental

cost to be included during the production stage and the effect on the

financial evaluation of the study area. To perform this part, the total environmental cost had been calculated, reaching EUR5,400.39 and was added to the expenses of the company, distributed within a year. The financial statement produced by including the environmental cost was compared and evaluated with the financial statement that did not include the environmental cost (**Table 7**). The NPV, internal rate of return (IRR), payback period and breakeven point were the several indicators being compared and analyzed.

NPV for Multi-Rich Pitaya Dragon Fruit Farm, Sepang, Selangor, including the environmental protection cost for pitaya production is EUR10,608.21. The amount obtained decreases about 73% of the NPV value without the environmental cost.

IRR for Multi-Rich Pitaya Dragon Fruit Farm, Sepang, Selangor, including the environmental cost as part of the variable cost is about 14%. It shows that, the IRR value is lower compared to the cost without the environmental cost.

After including the environmental cost of pitaya production, the payback period was about 5.46 years. It is quite long as to be compared to the financial statement without the environmental cost, which is about 3.69 years to recover the initial investment for Multi-Rich Pitaya Dragon Fruit Farm, Sepang, Selangor.

By adding the environmental cost in pitaya production, the BEP for Multi-Rich Pitaya Dragon Fruit Farm, Sepang, Selangor is EUR8,547.23 and EUR6,245.25 without the environmental cost.

Table 7: Financial Evaluation

Without Environmental Cost	**With Environmental Cost**

NPV	EUR 39,334.31	NPV	EUR 10,608.21
IRR	24%	IRR	14%
B/C	EUR 0.36	B/C	EUR 0.25
Payback Period	3.69 year	Payback Period	5.46 years
Breakeven Point	EUR 6,245.25	Breakeven Point	EUR 8,547.23

CONCLUSION

The modelling of ELCC for pitaya production demands a complex task involving a large number of the agricultural process. It also requires a multi-disciplinary research methodology to be conducted like LCA and LCC and an integration of the findings from different investigations.

There are several potential environmental impacts according to every kilogram of pitaya production, which have been identified through the implementation of LCA. The biggest impact of pitaya production is toward the ozone layer, which is about 6.06 kg CFC^{-11} equivalent. Another impact is toward the summer smog or respiratory inorganic which is estimated at 3.81 kg C_2H_4 equivalent, climate change 3.4 kg CO_2 equivalent and carcinogens or human eco-toxicity 1.21 kg Benzo(a)pyrene equivalent. The production of pitaya also has a potential impact toward radiation (1.1 kg bq C^{-14} equivalent), fine dust or respiratory organic (1.05 kg fine dust PM2.5), and fossil fuels (0.856 kg CO_2 equivalent). Another potential impact is less significance compared to the impacts mentioned earlier, but still appears in the production stage of pitaya such as eco-toxicity (0.659 kg Cu equivalent), mineral depletion (0.077 kg Mj Surplus equivalent) and acidification (0.028 kg So_x equivalent). The presence of these potential impacts is due to the substances used in the pitaya production system especially in fertilization and weed control stage.

The financial evaluation was done as it is important to conduct the LCC. The total fixed cost and variable cost were counted which amounted to EUR38,520.28 and EUR18,988.36 for the production of 15,000 kg pitaya per year. The total environmental cost for pitaya production was estimated at EUR5,400.39 where the cost to protect the environment for carcinogens was identified as the highest contribution for the total environmental cost which is estimated at EUR4,646.41/kg Benzo(a)pyrene equivalent.

In order to reduce the potential impacts during the production process, the company may reduce the usage of the inorganic fertilizers which does a lot of damage toward the environment especially for carcinogens impacts which is one of the indicators in human health's damage category. This is due to the presence of a large amount of nitrogen, potassium and phosphate, which are the main elements in fertilizers. For that purpose, the owner of the company should increase the usage of organic fertilizers, which is more eco-friendly compared to inorganic fertilizers. Other than that, the government may also charge a high tax on the inorganic fertilizers and pesticides, at the same time provide subsidies for organic fertilizers to the farmers in order to increase the usage of it, and give an incentive to the companies that implement the eco-friendly practices, like reducing their income tax percentage. This element is important to make sure that the production of pitaya or any other crops does a minimum impacts to the environment.

Because of the limitations that occurred especially during the data collection process, all the companies and organizations should always record their expenditure and other important things regarding their business. Government and also non-government organization (NGO) should organize a program to encourage the owners of any business organization to manage their

companies properly and systematically.

The most important thing in protecting the environment is the responsibility from the institutional organization especially the educational organization where a study needs to be done focusing on the ELCC either by students or lecturers. This will not only bring the benefit to the owners of the companies but also to others in learning what ELCC methodology is, and where it could be applied in the future since there are limited studies on its methodology in Malaysia and worldwide.

ACKNOWLEDGEMENT

This research was fully supported by Putra Grant UPM (GP/2018/9592300).

REFERENCES

Abdul Azis Ariffin, Jamilah Bakar, Chin Ping Tan, Russly Abdul Rahman, Roselina Karim, and Chia Chun Loi. 2008. Essential fatty acids of pitaya (dragon fruit) seed oil. Food Chemistry, 114 (2): 561–564

Anand, M. (2014). Direct and Indirect use of Fossil Fuels in Farming: Cost of Feul Price Rise for Indian Agricultural. National Institute of Public Finance and Policy New Delhi.

Andersson, K., T. Ohlsson, et al. (1994). Life cycle assessment (LCA) of food products and production systems. Trends in Food Science & Technology 5(5): 134-138.

Bienkowski, B. (2018, February 1). Fertilizer is fouling the air in California: Study. Retrieved from Environmental Health New: http://www.ehn.org/ california-fertilizer-nitrogen-air-pollution-2530258544.html

Fruit crops statistic Malaysia (2016). Department of Agriculture. Retrieved from http://www.doa. gov.my/

Islam, M. T. Khan, M. M. Hoque, and M. M. Rahman (2012). Studies on the processing and preservation of dragon fruit (hylocereus undatus) jelly. The Agriculturists, 10 (2): 29-35

Ingwersen WW, Stevenson MJ (2012) Can we compare the environmental performance of this product to that one? An update on the development of product category rules and future challenges toward alignment. J Clean Prod 24:102–108.

Jeremy Woods, A. W. (2010). Energy and the food system. US National Library of Medicine National Institute of Health

Mogensen, J. F. (2018, January 31). Researchers Just Found a Hidden Cause of California's Smog Problem. Retrieved from Mother Jones : https://www.mother jones.com/environment/2018/01/researchers-just-found-a-hidden-cause-of-californias-smog-problem/

Ndlovu, S. G. (2015, September 5). Tree Planting lessen ozone layer damage. Retrieved from Chronicle: http://www.chronicle. co.zw/tree-planting-lessens-ozone-layer-damage/

Nobel, P. S. and de la Berrera, E. (2002). Stem water relations and wet C02 uptake for hemi epiphytic cactus during short term drought. Environment and Experimental Botany, 48: 129-137.

Nerd, A. Tel-Zur, N. and Mizrahi, Y. 2002. Chapter 10: Cactus Pear Fruit Production In: Nobel, P.S. (ed.) Cacti: biology and uses. University of California Press, Berkeley, 163 p.

Ruviaro CF, Gianezini M, Brandão FS, Winck CA, Dewes H (2012) Life cycle assessment in Brazilian agriculture facing worldwide trends. J Clean Prod 28:9–24

Roy Rajkumar, Partha Datta, Fransisco Javier Romero Rojo and John Ahmet Erkoyoncu (2009). Cost of industrial product-service systems. Keynote Paper Proceedings of the 16th CIRP on International Conference on Life Cycle Engineering (LCE), 4-6th May 2009, Cairo, Egypt.

Stephen S. Hecht (1991), Tobacco smoke carcinogens and lung cancers. JNCI: Journal of the National Cancer Institute, Volume 91, Issue 14, 21 July 1999, Pages 1194–1210, https://doi.org/10.1093/jnci/91.14.1194

Sivakumar, R. S. (2009). Impacts of sand and dust storms on agriculture and potential agricultural applications of a SDSWS. IOP Conference Series: Earth and Environmental Science.

Weitz A. Keith and Aarti Sharma (1998) Practical life cycle assessment through streamlining. Volume 7, Issue 4 Summer 1998 Pages 81–87.

Length and Weight Relationship and Fish Condition of Non-Native Fish Species in Selected Recreational Lakes, Kuala Lumpur, Malaysia

Rohasliney Hashim*, Noor Farahanizan Zulkifli, Nur Hidayah Bujang, Muhammad Faris Zulkiffly, Ong Jing Yi

Faculty of Environmental Studies, Department of Environmental Management, Universiti Putra Malaysia, 43400 UPM Serdang, Selangor, Malaysia.

*E-mail: *rohasliney@upm.edu.my*

ABSTRACT

This study aimed to determine the Length-Weight Relationship (LWR) and fish condition of non-native fish species found in four selected recreational lakes in Kuala Lumpur, Malaysia (i.e., Recreational Park Bukit Jalil, Metropolitan Kepong, Metropolitan Batu, and Permaisuri lakes). Fishes were caught by using gill nets with different mesh sizes, cast nets and fishing rods. Sampling was carried out from December 2017 to March 2018. The *b* value for *Oreochromis mossambicus* found at the Metropolitan Kepong, Metropolitan Batu and Permaisuri lakes was, 2.71, 2.66, and 2.46, while the average condition factor (K) was 2.19, 1.88 and 3.02, respectively. Meanwhile the *b* value for *Clarias macrocephalus* and *Clarias gariepinus* in Recreational Park Bukit Jalil Lake was 2.47 and 2.11, while average K was 1.63, and 1.31, respectively. The *b* value for *Cichla ocellaris* and *Clarias gariepinus* found in the Permaisuri Lake was 2.73 and 3.09, while K value was 1.23 and 0.60 respectively. Native fish species such as *Channa striatus, Clarias batrachus*, *Barbonymus schwanenfeldii*, and *Barbonymus gonionotus* were caught at Recreational Bukit Jalil and Metropolitan Batu lakes and were found not

severely impacted by the non-native fishes. In conclusion, the growth of non-native fish species in four selected recreational lakes was moderate to good, with *b* values ranging from 2.11 to 3.09 showing a negative allometric growth. As for fish condition, all non-natives collected during the study were mostly in good condition (1.00 <K<1.40).

Keywords: Non-native, inland fish, length-weight relationship, condition factor, recreational lake

INTRODUCTION

Most recreational parks in Malaysia feature lakes as a recreational facility (National Hydraulic Research Institute of Malaysia, 2016). Non-native fish species have been intentionally or accidently introduced into these recreational lakes. Mostly intentionally whether by the local people and from the authorities. Non-native alien fish were brought to Malaysia by fish hobbyists. These fish are considered to be ornamental aquarium fish that are kept for aesthetic purposes. For example, Flowerhorn cichlids (*Cichlasom* sp.), Spotted gar (*Lepisosteus oculatus*), Arapaima (*Arapaima gigas*), to name a few. However, the maintenance of these ornamental fishes is expensive. The hobbyists who cannot afford to maintain these fish release them into a lake (The Malay Mail, 2018). Some of them release these ornamental fish pets just because they grow bored with the fish and buy new fish species. Hence, recreational lakes have become one large dumpsite for ornamental fishes. In addition to that, recreational fishing contributes to the second major introduction and establishment of non-native fish species. Peacock bass (*Cichla ocellaris*) was released into the lake for sport fishing (Khairul Adha et al. 2013). Recreational lakes in Kuala Lumpur are normally venues for fishing competitions and tournaments held by the local authorities. Some anglers, usually ignorant of biological processes, assume that adding more fish to a

lake is somehow helping nature. Certain freshwater fish species used for recreational angling are released into lakes without an environmental impact assessment or monitoring for the sole purpose of providing enjoyment for anglers. This practice has become so widespread that people often think that some of the invasive species are actually native ones.

The Malay Mail (2018) reported the discovery of two new foreign predatory fish known as the Earth eater cichlids (*Geophagus steindachneri*) and the Black ghost knife (*Apteronotus albifrons*). The Earth eater cichlids was caught from Timah Tasoh Dam, Perlis, while the Black ghost knife was found by anglers at several rivers of Kedah, Perak and Selangor (Rosli & Hanneeyzah, 2019). Jaguar cichlids (*Parachromis managuensis*) can be found mostly in an ex-mining pool of Selangor. There are also reports that African catfish (*Clarius gariepinus*) have been released for the purpose of certain religious activities such as paying vows (Ilah, 2017). Those who released the fish were not subject to legal action as no specific clause mentions the matter in any state law. Meanwhile, Rosli (2017) reported in the New Strait Times that peacock bass and several species of cichlids were initially released in to lakes by anglers for sport fishing, but the fishes escaped into nearby rivers during floods.

This evidence obviously shows that recreational lakes currently support a high density of non-native fish. The fish community and size structure in recreational lakes have shifted to only non-native fish compositions. Apparently, in favorable environmental conditions such as recreational lakes, non-native fish species should demonstrate faster growth rates, greater reproductive potential, and higher survival rates (Pope & Kruse, 2007). Therefore, this study addressed the length-weight relationships and fish condition of non-native fish species in selected recreational lakes of Kuala Lumpur and Selangor.

METHODOLOGY

Description of sampling sites

Sampling was conducted at four recreational lakes around Kuala Lumpur and Selangor, Malaysia (Figure 1). Four sampling points were randomly selected from each lake except for Metropolitan Batu Lake. The area of Metropolitan Batu Lake is 54.7 hectare (ha) (coordinate 3.213821, 101.679599). Metropolitan Kepong Lake was an ex-mining pool with the depth of 40 meters and area of 45.7 ha (coordinate 3.224424, 101.645744). All four lakes are surrounded with residential, commercial and recreational townships. The lakes provide various facilities such as a jogging track, children's playground, walking trails, exercise stations and others. These lakes are in public parks managed by the Landscape and Recreational Department of Kuala Lumpur City Hall, Kuala Lumpur (DBKL). Metropolitan Kepong and Permaisuri lakes are occasionally used for a routine fishing tournament. The coordinate of Permaisuri Lake is 3.098765, 101.720095). In contrast, fishing activities are banned at Recreational Bukit Jalil Lakes, all year around (coordinate 3.03080, 101.40319).

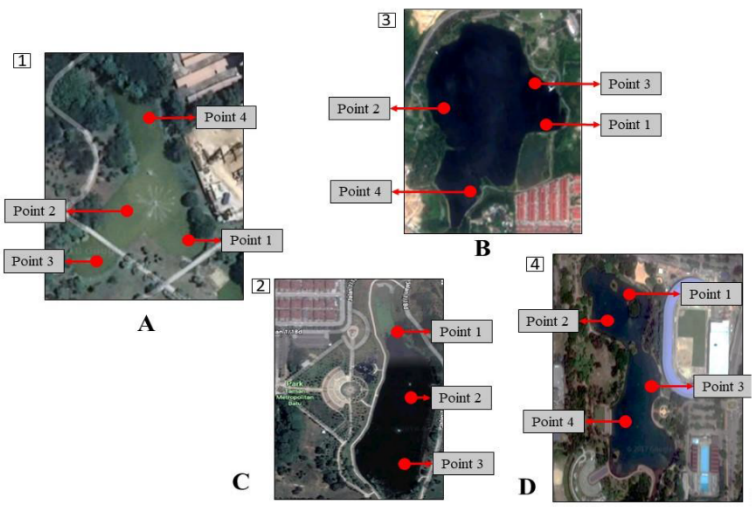

Figure 1 Four selected recreational lakes showing sampling points (**A**: Recreational Park Bukit Jalil Lake; **B**: Metropolitan Kepong Lake; **C**: Metropolitan Batu Lake; **D**: Permaisuri Lake)

Fish sampling

Fish sampling was conducted from December 2017 to March 2018. Experimental gill nets (measuring 30 m length, 1.5 m depth with stretch mesh size of 1, 2, 3 and 4 inches) were randomly set at each sampling station of the four selected recreational lakes. Gill nets were set in the morning, and each net was inspected every one to two hours. Sampling was conducted for 8 hours during the day. Meanwhile, in Permaisuri Lake, sampling was conducted in the evening until late at night. A cast net was used whenever possible to maximize the fish catch. A scoop net with a mesh size of 2.5 was also used in the littoral zone areas where the depth of the water is wadeable.

All fishes caught were released after measurement. Fish sampling strictly followed the Rapid Bioassessment Protocols for Use in Streams and Wadeable Rivers: Periphyton, Benthic Macroinvertebrates, and Fish - Second Edition (Barbour et al. 1999). Fishes were individually measured (total length (mm), weighed (g)) and enumerated (collectively by species) (Mohsin & Ambak, 1983; Ambak et al. 2010).

Data analysis

Fish length-weight (log-transformed) was plotted on a scatter diagram and the relationships were determined by using linear regression analysis. The length- weight relationships (LWR) equation (Le Cren, 1951) is stated below:

$$W = aL^b$$

W = weight (g); L = total length (cm)
a and *b* are coefficient and exponent, respectively. $b < 3.0$ represents fish that become less rotund as length increases, while $b > 3.0$ represents fish that become more rotund as length increases. The *b* value in LWR may vary due to a combination of one or more factors such as area/season effect, habitat, age, gonadal maturity, fish condition and fish health.

Meanwhile, fish condition was determined using the Fulton condition index. Condition indices were used to assess several aspects of fish condition, including the general health of fish stock and physiological condition (Pope & Kruse, 2007). Changes in condition can provide information about trophic conditions in a system, e.g., prey availability. Condition factor was calculated by using the formula below (Froese, 2006):

$$K = 100WL^3$$

K = Condition factor; W = weight (g); L = length (cm)

Fulton's K assumes that the weight of the fish is simply proportional to L = 3 and in the equation the b exponent is a constant.

Further statistical analysis was performed (i.e. One-Way ANOVA repeated measure) to compare LWR and fish condition among sampling points. Logarithmic transformations were performed when necessary to address requirements of normal distributions for parametric statistics (Zar, 1974). Statistical analysis was conducted with Statistical Package for Social Science (SPSS) software. Significant differences were further investigated using the non-parametric least significant difference (LSD) multiple range test. An alpha level of 0.05 was used for accepting or rejecting hypotheses. Only fish species with 50 individuals and above were used for calculating LWR and fish condition.

RESULTS AND DISCUSSION

Abundances and composition

A total of 259 fish individuals were captured at Recreational Bukit Jalil Lake during this study, which represented two families and five species. Two species (*Clarias gariepinus* and *C. macrocephalus*) were considered to be non-native alien species. Meanwhile, two species, Tinfoil barb (*Barbonymus schwanenfeldii*) and Silver barb (*B. gonionotus*) were native fish species of most river ecosystems in Peninsular Malaysia. High dominance of Clariidae was observed from Recreational Bukit Jalil Park

Lake (Table 1). Surprisingly, no cichlids such as Mozambique tilapia were caught from this lake.

Metropolitan Kepong Lake was dominated by Mozambique tilapia (*Oreochromis mossambicus*) (N = 55) (Table 1). Although it was reported by the DBKL that several fish species were released during a fishing tournament, the fishes were not caught during the sampling period. This might be due to a low number of these fishes in the lake, or probably most were caught during the fishing tournament. Fishes released for the fishing tournament were Indonesian snakehead (*Channa micropeltes*), Asian catfish (*Clarias batrachus*), Climbing perch (*Anabas testudineus*), Striped catfish (*Pangasianodon hypophthalmus*), and Amazon sailfin catfish (*Pterygoplichthys pardalis*).

Fifty-six fish individuals were caught at the Tasik Metropolitan Batu Lake, which comprised of two families with four species (Table 1). This lake was dominated by the cichlids with a higher percentage from Mozambique tilapia (93%), followed by Red hybrid tilapia (3.4%), Mozambique hybrid tilapia (1.8%) and Striped snakehead (1.8%).

A total of 165 individual fish were caught during this sampling period at the Permaisuri Lake. This lake was dominated by three fish species, namely Mozambique tilapia (32%), African catfish (32%) and Peacock bass (32%). Silver barb was also caught, which made up 4% of the total catch there (Table 1). Overall, this study indicated that non-native fish species dominated all four recreational lakes. The major fish groups for non-native fish species were either carnivores or omnivores. These fishes are dependent on small fishes, insects, mollusks, plants and zooplankton. The manifestation of high numbers of omnivorous and carnivorous fishes in the lakes reflect a degraded lake environment (Rohasliney, 2005). Omnivorous fishes are less sensitive to environmental stress, primarily due to their ability to vary their diet

(Rohasliney & Jackson, 2009). Excellent adaptation of non-native fishes in these lakes causes the niche for native species to decrease and the reproduction of native species becomes depressed (Jan et. al, 2015). Potential pests such as Mozambique tilapia and Peacock bass may limit the abundance of native fish species. Nevertheless, the top predator of native species such as Striped snakehead and Asian catfish will survive and continue competing for food sources. It was reported that the presence of Asian catfish in Malaysia is currently deteriorating (Argungu et al., 2013) and the presence of African catfish is contributing to the decreasing number of Asian catfish (Ahmad et al., 2012) in the river ecosystem. Apart from that, native omnivorous fish species such as Tinfoil barb and Silver barb are struggling to survive among the top predators at Recreational Park Bukit Jalil and Permaisuri lakes. This is probably due to the presence of plankton (phytoplankton and zooplankton), zoobenthos, and detritus, which contributed to food availability for these cyprinids. Tinfoil barb also can be considered to be a tolerant native fish species, because Tinfoil barb was reported to withstand a changing habitat (Muzzalifah et al. 2015). Mohamad Radhi et al. (2017) also reported that Kelantan River can still support the higher abundance of Tinfoil barb despite changing habitat caused by human activities which contributed to habitat destruction and water turbidity (i.e., sand mining).

The statistical analysis showed that the *b* values were similar among the four recreational lakes ($P > 0.05$).

Table 1 Total number of fishes captured from four selected recreational lakes using gill nets, cast nets and scoop nets. Sampling was carried out from December 2017 to March 2018. Fish status were confirmed from Fishbase.org (2017) (A: Recreational Park Bukit Jalil Lake; B: Metropolitan Kepong Lake; C: Metropolitan Batu Lake; D: Permaisuri Lake)

Family	Species	Status	Sampling sites			
			A	B	C	D
Channidae	Striped snakehead *Channa striatus*	Native			+	
Clariidae	Walking catfish *Clarias macrocephalus*	Non-native	+++			
	Asian catfish *Clarias batrachus*	Native	+++			
	African catfish *Clarias gariepinus*	Non- native	++++			+++
Cichlidae	Mozambique tilapia *Oreochromis mossambicus*	Non- native		+++	+++	+++
	Mozambique hybrid tilapia *Oreochromis mossambicus* x *O. urolepis hornorum*	Non- native			+	
					+	
						+++
	Red hybrid tilapia *O. mossambicus*×*O. niloticus*	Non- native				
	Peacock bass *Cichla ocellaris*	Non- native				
Cyprinidae	Tinfoil barb *Barbonymus schwanenfeldii*	Native	+++			
	Silver barb Barbonymus gonionotus	Native	++			+

+ 1 – 20 individual, ++ 21 – 41 individuals, +++ 42 – 62 individuals, ++++ 63 – 83 individuals

Length-weight relationships of non-native fishes

The total length of three clariids at Recreational Bukit Jalil Park Lake ranged from 13.7 to 55.4 cm. Meanwhile clariids' total length at the Permaisuri Lake was between 26.4 cm to 35.3 cm. The weight for all three clariids caught from Recreational Bukit Jalil Lake ranged from 120 to 2080 g, while the weight of clariids from Permaisuri Lake ranged from 100.0 to 258.5 g.

The total length for Mozambique tilapia at the Metropolitan Kepong Lake ranged between 12.1 to 20.1 cm, with the weight ranging from 30.1 to 161.2 g. The total length of this species at the Metropolitan Batu Lake was between 10.5 to 25.4 cm with the weight ranging from 35. 6 to 310.3 g. At the Permaisuri Lake, the total length of Mozambique tilapia was from 12.9 to 39.0 cm and the weight ranged from 71.4 to 1423.2 g.

The LWR parameters of Mozambique tilapia (*O. mossambicus*) are presented in Table 2. The *b* value is the most important for LWR analysis because *b* value indicates different types of fish growth; $b < 3$ (negative allometric growth), $b = 3$ (isometric growth) and $b > 3$ (positive allometric growth) (Froese, 2006). Isa et al. (2010) reported that as the *b* value of freshwater fishes increases, the fish size should increase as fishes usually grow proportionately in all directions. LWR for Mozambique tilapia at three recreational lakes indicated that their growth is below the normal range ($b < 3$) which indicated that this fish was less rotund, meaning the fish grow more in length than in weight or width. The result for this study concurred with the study by Iskandar et al. (2017). Froese (2006), which stated that if the *b* value for most fishes falls from 2.5 to 3.5 they are usually still considered to grow in a good shape. Although, there is a probability of unsuitable environmental conditions at these lakes, such as seasons, water temperature, salinity, food (quantity, quality and size), sex and stage of maturity that influence the condition

of fish species when the fish species show a negative allometric growth pattern (Atama et al. 2013). This study concurred with the findings in Anambra River, Nigeria, where all six cichlids species were found to be less rotund as they grew in length, especially Nile tilapia (*O. niloticus*) (Atama et al. 2013).

The relative condition factor for Mozambique tilapia showed variation in all three recreational lakes (Table 2). Pope and Kruss (2007) proposed that if the K value is 1.00, the condition of the fish is poor, long and thin. A K value of 1.20 indicates that the fish is in moderate condition and acceptable. Fish that have a good health condition, are in a suitable environmental condition with variety of food, possess a K value of 1.4. Achakzai et al. (2013) reported that the fish condition for Mozambique tilapia from Manchar Lake (District Jamshoro), Pakistan, ranged between 0.86 to 1.03 for males and 1.02 to 1.4 for females, respectively. Mozambique tilapia caught from this study showed higher fish condition compared to other studies. This may be due to less competition with other species especially for food and space. In addition to that, as omnivores, Mozambique tilapia are able to adapt to a varying diet.

Table 3 represented LWR and condition for African catfish (*Clarias gariepinus*). The *b* value for Recreational Park Bukit Jalil Lake was lower than from Permaisuri Lake. This result demonstrated that fish length is actually greater than the changes in its weight. This may be due to three dominant clariids found in the former lake. Therefore, competition for food and space are crucial for this species. It was observed from this study that the *b* value for African catfish at the Permaisuri Lake was positive allometric ($b > 3$), but with low fish condition value (Table 3). Although it was reported that fish species with elongated thin bodies will tend to have a lower *b* value ($b < 3$), catfish caught in this lake showed a slightly plump body. This was in contrast

with African catfish caught from Recreational Park Bukit Jalil Park (Table 3). The K value for African catfish at the Recreational Park Bukit Jalil Lake was acceptable and showed they were in a moderate condition. Fishbase.org (2014) showed that the K value of African catfish from several countries ranged from 0.03 to 0.5 when the total length ranged from 67 cm to 360 cm. Competition with Peacock bass probably influences the healthiness of this species. Adult African catfish normally occur mainly in quiet waters, lakes and pools and prefer rather shallow and swampy areas with a soft muddy substrate and calmer water. This also might influence the acceptable habitat for the species.

Two clariids from Recreational Park Bukit Jalil Lake were Walking catfish (*Clarias macrocephalus*) and Asian catfish (*Clarias batrachus*). Both clariids showed similar *b* and K values which indicated that both had negative allometric growth ($b < 3$) and were considered to be in good health (Table 4). Although Asian catfish is a native fish, the population was not threatened by the non-native catfishes (Table 4).

Peacock bass (*Cichla ocellaris*) caught at Permaisuri Lake showed a less rotund shape ($b = 2.73$). The condition value indicates that this fish is in a moderate condition and is acceptable (K= 1.23). Peacock bass had a good growth rate because it is likely that Peacock bass are considered more tolerable of variation and fluctuation in water parameters, food and space, thus enabling them to survive and grow better. Furthermore, Peacock bass are important piscivores and, when introduced into other tropical waters, can impact other non-native and native fishes directly and indirectly and impact ecosystem structure (Jepsen et al. 1999).

For Table 2,3 and 4, *a* value for all fishes ranged from 0.05 to 2.37. In some report, a value is used to determine the shape of the fish. If *b* value is 3 then *a* is a form-factor with a = 0.001 which gives a fish an eel-

like shape, a = 0.01, fish with fusiform shape (i.e., cod, tunas), and a = 0.1, fish with spherical shape (i.e., puffers, boxfish). However, in this study, the fish shape cannot be determined by using *a* value as most of the fishes gave *a* value more than 0.1 including the catfishes. The result concurred with the study of mudskippers collected from the mangrove areas of the Selangor coast where *a* value of mudskippers ranged between 1.56 to 8.99 (Khaironizam & Norma-Rashid, 2002). In addition to that, it was also reported that if the *b* value is isometric ($b > 3$), then *a* value can be a condition factor. However, according to Khaironizam and Norma-Rashid (2002), if the *b* value is allometric, *a* value as condition factor is questionable.

Statistical analysis showed that LWR was differed significantly among the four recreational lakes ($P < 0.05$) where Permaisuri Lake had the highest LWR as compared to others. Meanwhile K condition also showed a significant difference among the lakes ($P < 0.05$). Permaisuri Lake had the highest K condition as compared to other lakes and Mozambique tilapia demonstrated to be in a very excellent health among other fishes ($P < 0.05$).

From this study, the fish composition of all four recreational lakes was dominated by non-native fish species. It was uncertain whether these lakes were once dominated by any endemic fish species. There were no prior data of fish structure and composition from these lakes. Therefore, whether these non-native species had caused the loss of endemic species were indeterminate. However, this study had showed that tolerant native fish species caught from the Recreational Park Bukit Jalil Lake (i.e., Tinfoil barb, K = 3.03 and Silver barb, K = 3.76) can co-exist with non-native species although these two species showed an allometric growth with *b* value of 1.46 ($R^2 = 0.93$) and 1.45 ($R^2 = 0.88$), respectively.

Table 2 Length and weight relationships and fish condition (K) for *Oreochromis mossambicus* captured from three recreational lakes using gill nets, cast nets and scoop nets. Sampling was carried out from December 2017 to March 2018. (B: Metropolitan Kepong Lake; C: Metropolitan Batu Lake; D: Permaisuri Lake)

Lakes	*b* value	$W = aL^b$	R^2	K
B	2.71	$W = 0.05L^{2.71}$	0.60	2.19
C	2.66	$W = 0.26L^{2.66}$	0.91	1.88
D	2.46	$W = 0.87L^{2.46}$	0.85	3.02

Table 3 Length and weight relationships and fish condition (K) for *Clarias gariepinus* captured from two recreational lakes using gill nets, cast nets and scoop nets. Sampling was carried out from December 2017 to March 2018. (A: Recreational Park Bukit Jalil Lake; D: Permaisuri Lake)

Lakes	*b* value	$W = aL^b$	R^2	K
A	2.11	$W = 0.64L^{2.11}$	0.96	1.31
D	3.09	$W = 2.37L^{3.09}$	0.94	0.60

Table 4 Length and weight relationships and fish condition (K) for catfishes captured from Recreational Park Bukit Jalil Lake using gill nets, cast nets and scoop nets. Sampling was carried out from December 2017 to March 2018.

Fish	*b* value	$W = aL^b$	R^2	K
Clarias batrachus	2.18	$W = 0.61L^{2.18}$	0.96	1.91
C. macrocephalus	2.47	$W = 0.38L^{2.47}$	0.90	1.63

CONCLUSION

In conclusion, the growth of non-native fish species in four selected recreational lakes was moderate to good with *b* values ranging from 2.11 to 3.09 showing mostly an allometric growth pattern. The *b* value is generally different among species and can be sensitive to biotic and abiotic influences, leading to different values of *b* between sexes or localities, even within the same species. Striped snakehead, Asian catfish, Tinfoil barb, Silver barb can be considered as tolerant native species showed a moderate condition

co-existing with non-native fish species. The analysis of fish condition from these non-native fish showed that robustness of an individual varied depending on the space and food variability in each lake. Predator-prey interaction also plays an important role in determining the well-being of the individual fish, whether it reflected a heathier physiological state of a fish or otherwise. This study demonstrated that understanding the growth of non-native species as well as its condition in small waterbodies are very important in order to prioritize control and coordinate fisheries management options for invasive species.

ACKNOWLEDGEMENTS

The authors would like to thank Kuala Lumpur City Mall (DBKL) for granting approval for us to conduct the study in these public recreational lakes. Extended thanks to Mr Norisyam Md Nor and Mr Amirul Ashraf for assistance in the field. Our gratitude also goes to En Sulkifly Ibrahim and Ms Dalina Jaafar for their assistance in the Aquatic Laboratory, Department of Environmental Management, Faculty of Environmental Studies, UPM. This study was independently funded.

REFERENCES

Achakzai WM, Saddozai S, Baloch WA, Memon N. Length-Weight Relationships and Condition Factor of *Oreochromis mossambicus* (Peters, 1852) from Manchar Lake Distt. Jamshoro, Sindh, Pakistan. Sindh Univ. Res. Jour. (Sci. Ser.) 2013; 45(2): 201-206.

Ahmad R, Pandey RB, Arif SH, Nabi N, Jabeen M, & Hasnain A. Plymorphic A and Y lens crystallins demonstrate latitudinal distribution of threatened Walking catfish Clarias Batrachus (Linn.), Population in North-western India. Jounal of Biological Sciences 2012; 12: 98-104.

Ambak MA, Mansor MI, Mohd Zaidi Z, Mazlan AG. Fishes of Malaysia. Kuala Terengganu: Universiti Malaysia Terengganu; 2010.

Argungu LA, Christianus A, Amin SN, Daud SK, Siraj SS, Aminur Rahman M. Asian catfish *Clarias batrachus* (Linnaaeus, 1758) getting critically endangered. Asian Journal of

Animal and Veterinary Advances 2013; 8(2): 168-176.

Atama C, Ekeh F, Ezenwaji N, Onah I, Ivoke N, Onaja U, Eyo J. Length-weight relationships and condition factor of six cichlid (Cichlidae Perciformes) species of Anambra River, Nigeria. Journal of Fisheries and Aquacutlure 2013; 4(2): 82-86.

Barbour MT, Gerritsen J, Snyder BD, Stribling JB. Rapid Bioassessment Protocols for Use in Streams and Wadeable Rivers: Periphyton, Benthic Macroinvertebrates and Fish, Second Edition. EPA 841-B-99-002. Washington, D.C: U.S. Environmental Protection Agency, Office of Water; 1999.

FishBase. List of Freshwater Fishes reported from Malaysia. Retrieved February 4, 2019, from FishBase.org: https://www.fishbase.de/Country/CountryChecklist.php?c_code=458&vhabitat=fresh&csub_code=&cpresence=present; 2017, June 2).

Fishbase.org. Fishbase. Retrieved April 26, 2019, from Growth parameters for Clarias gariepinus: https://www.fishbase.se/popdyn/LWRelationshipList.php?ID=1934&GenusName=Clarias&SpeciesName=gariepinus&fc=139; 2014.

Froese R. Cube law, Condition factor and weight-length relationships: history, meta-anaylisis and recomendations. Journal of Applied Ichthyology 2006;, 22: 241-253.

Ilah AH. Keli Afrika ancaman ekosistem sungai tempatan. Berita Harian; 2017.

Isa MM, Che Salmah MR, Rosla R, Anuar S, & Shah M. Length-weight relationships of freshwater fish species in Kerian River Basin and Pedu Lake. Research Journal of Fisheries and Hydrobiology 2010; 5: 1-8.

Iskandar N, Nyanti L, Yee L, Grinang J. Comparison of length-weight relationship and condition factor of three fish species between regulated and nutarl rivers. Transactions on Science and Technology 2017; 4(2): 118-122.

Jan C, Hana S, Zdenek J, Petr P. Competition among Native and Invasive Impatiens Species: The Roles of Environmental Factors, Population density and Lifestage species. AoB Plants 2015; 1-12.

Jepsen DB, Winemiller KO, Taphorn DC, Rodriguez OD. Age structure and growth of peacock cichlids from rivers and reservoirs of Venezuela. Journal of Fish Biology 1999; 55: 433–450.

Khaironizam MZ, Norma-Rashid Y. Length-weight Relationship of Mudskippers (Gobiidae: Oxudercinae) in the Coastal Areas of Selangor, Malaysia.

Bayan Lepas: WorldFish Center; 2002.

Khairul Adha AR, Yuzine E, Aziz A. The Influence of Alien Fish Species on Native Fish Community. Kuroshio Science 2013; 7(1): 81-93.

Le Cren ED. The length-weight relationships and seasonal cycle in gonad weight and condition in the perch (Perca fluviatilis). Journal of Animal Ecology 1951; 20: 201-219.

Mohamad Radhi A, Rohasliney H, Zarul Hazrin H. Fish composition and diversity in Perak, Galas and Kelantan rivers (Malaysia) after the major flood of 2014. Transylvanian Review of Systematical and Ecological 2017; 19(3): 41-56.

Mohsin AM, Ambak MA. Freshwater fishes of Peninsular Malaysia. Serdang, Selangor: Universiti Putra Malaysia; 1983.

Muzzalifah A, Mashhor M, Siti Azizah M. Length-weight relationships and condition factor of fish populations in Temenggor Reservoir: Indication of environmental health. Sains Malaysiana 2015; 44(1): 61-66.

National Hydraulic Research Institute of Malaysia. Blueprint for lake and reservoir resesarch and develeopment (R&D) in Malaysia. Seri Kembangan: NAHRIM; 2016.

Pope KL, Kruse CG. Condition. In C. S. Guy, & M. L. Brown (Eds.), Analysis and Interpretation of Freshwater Fisheries Data (pp. 423-467). Maryland: American Fisheries Society; 2007.

Rohasliney H. Lignite mining influences on stream ecosystem dynamics along the Natchez Trace Parkway. Unpublished doctoral dissertation. Starkville: Mississippi State University; 2005.

Rohasliney H, Jackson DC. Fish assemblages in streams subject to anthropogenic disturbances along the Natchez Trace Parkway, Mississippi, USA. Tropical Life Sciences Research 2009; 20(2): 29-47.

Rosli, Z. Biosecurity knowledge needed to tackle invasive alien species. New Straits Times; 2017.

Rosli, Z., & Hanneeyzah, B. B. Ancaman Hantu Hitam. My Metro; 2019.

The Malay Mail. Beware of alien species in our environment — Sahabat Alam Malaysia. MalayMail; 2018.

Zar H. Biostatistical analysis. New Jersey: Prentice-Hall, Inc.; 1974.

Assessment of the municipal solid waste management system in Carmona, Cavite: a 'Wasteaware' benchmark indicator approach customized to Philippine setting

Remsce Pasahol[1], Gladys Gopez[2], Leoneil John Francisco[1], Marilyn Ramos[2], Djoana Eve Rivera[1], and Edwin Ventigan[2]*

[1]MA Urban and Regional Planning Student, University of the Philippines
[2] Diploma in Urban and Regional Planning Student, University of the Philippines;
Corresponding author e-mail: remscepasahol@gmail.com

ABSTRACT

This case study aims to look at how local government units (LGUs) in the Philippines can evaluate their solid waste management (SWM) System with the aim of generating baseline information and actionable insights that can be considered on in reinforcing its efficiency and sustainability. In doing such, the 'Wasteaware' framework, an international benchmark indicators set deemed encompassing all aspects of solid waste management, was adopted and customized to the Philippine local governance landscape. The developed performance evaluation tool based on this framework was initially applied to Carmona, Cavite, a multi-awarded local government for its exemplary SWM practices. Other than pilot-testing the evaluation tool, its initial application also caused the recording of good practices worthy of replication by other local governments. It reveals that the provision of free waste collection service to all households and the recognition of the informal recycling sector in the SWM System can be a reality even in a municipality located in a lower middle income country like the Philippines. While the local government of Carmona can be considered to be in the right direction, there are still points that it needs

to strengthen to further bolster the sustainability of its SWM System. Foremost of which are on leveraging resources from households and commercial establishments, and on engaging in inter-LGU initiatives. The results of this case study provide inputs for policy-making and new research direction relative to monitoring and evaluation of performance of local SWM Systems in the Philippines

Keywords: Wasteaware' benchmark indicators set, solid waste management

INTRODUCTION

In the Philippines, monitoring and evaluation tools are primarily input-oriented, focusing on mere presence of mandated basic structures, plans, policies, services and activities which lay the foundation for an effective solid waste management system in local government units. While these tools resulted to increasing trend of LGUs' compliance with the basic services and institutional mechanisms required of the country's Ecological Solid Waste Management Act, the question on whether all the constituents feel the benefits of these provisions still remain. Also, the perspective and the actions of other SWM actors such as the informal recycling sector and private service providers are often overlooked. When it comes to self-evaluation undertaken by LGUs, their performance indicators are primarily focused on fund utilization and project completion. Hence, there is a need to develop a tool which is more outcome-driven and encompassing both the physical and governance aspects of the SWM system.

There are various comprehensive assessment tools for evaluating SWM system aimed toward informed-decision making. However, full utilization of these tools remained to be realized in low- and middle-income countries like the Philippines (Zurbrügg et. al., 2014). One of these tools is the 'Wasteaware' benchmark indicators set (Wilson et al., 2014)

which assesses the sustainability of a municipal/city SWM system by looking into the physical attributes and governance elements of the system. Chanhthamixay et al (2016) affirmed that this indicator set, when properly used, can provide an overview of a city's solid waste management performance revealing those aspects that are performing well and not so well.

Other than its comprehensibility, having a clear means of results interpretation is also a laudable feature of the indicator set. It has successfully operationalized its assessment criteria not just on how variables will be measured but also on how the results will be analyzed. The presence of scales in analyzing results and the color-coding system for visualization of results are deemed helpful in assessing the level of performance of a municipality/city in terms of waste management.

In the Philippines, the predecessor version of 'Wasteaware' had been applied in Quezon City, a highly urbanized city located at the National Capital Region (Wilson et al., 2012). The updated version is yet to be applied in the country particularly in a low-waste generating municipality. This current study aims to address the gap in practice and in research by tailor-fitting the 'Wasteaware' benchmark indicators set to the local situation, to allow a municipal government to assess its own performance in terms of delivering a more sustainable and equitable solid waste management services to its citizenry.

METHODOLOGY

Locale of the Study

The performance evaluation tool was pilot-tested in Carmona, Cavite. It is a first class municipality with a total land area of 3,092 hectares which represents 2.17% of the total land area of the Province of Cavite. It is comprised of eight urban and six rural barangays.

Based on the 2014 Community-Based Monitoring System, its population is 88,096 with an average annual growth rate of 7%. The

tremendous rise in economic activities and population growth of the municipality lead to challenges on increasing volume of waste generation. In spite of these challenges, the municipality remains to be multi-awarded LGU for its remarkable solid waste management practices.

Scope and Limitation

The SWM system was primarily assessed based on the 2017 data from the Municipal Environment and Natural Resources Office (MENRO). However, data pertaining to indicators requiring site inspection and stakeholder consultation reflect the situation during the current year (2018) when this study was conducted.

In terms of waste composition, this study considered only the municipal solid wastes –wastes coming from households and commercial establishments (Scheinberg et al., 2010; Wilson et al., 2014).Industrial wastes were not considered as industrial or technology parks located in the municipality manage their own wastes.

Theoretical Framework

The parameters employed in this study were based on the framework of the 'Wasteaware' benchmark indicators set (Wilson et al., 2014). In the framework, the waste-related data refers to the municipality's waste per capita and waste composition. For the background information, these data will be gathered—municipality's population and total municipal solid waste generation for the assessed year. These waste-related data and background information will be considered in assessment of the SWM system using the benchmark indicator set.

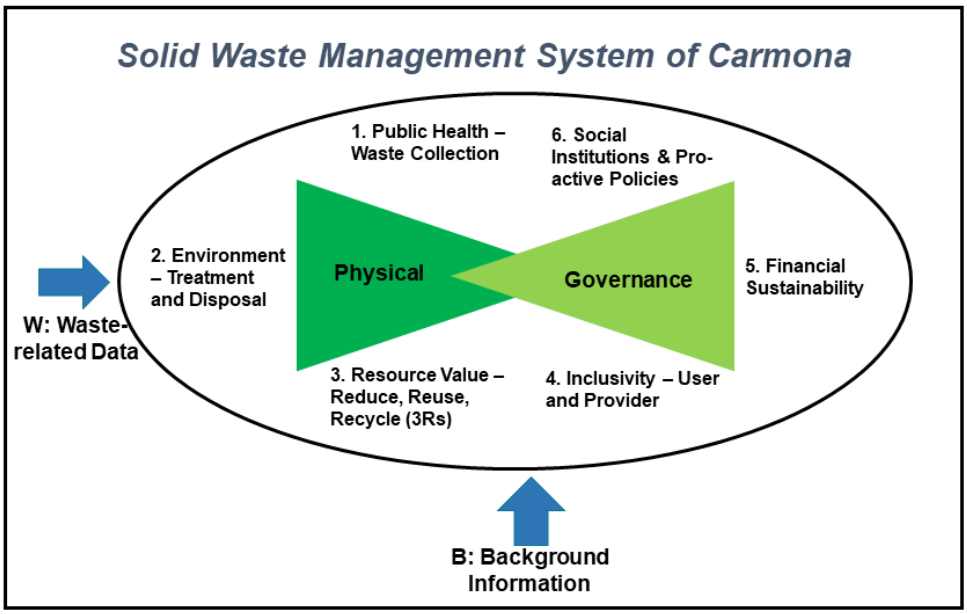

Figure 1. Theoretical Framework of the Study

At the center of the framework are the components of the ISWM system which are primarily grouped into two main sub-parts: the physical elements and the governance aspects. In assessing the physical elements of the system, the following parameters were considered in each specific component under it (Wilson et al., 2014):

1. Public health- the maintenance of healthy conditions in the municipality while good waste collection service is being provided;
2. Environment Protection- the presence of environment-friendly processes throughout the waste chain, particularly during treatment and disposal; and
3. Resource Management- the institution of interventions that advance high waste prevention/diversion, organics recovery, reuse and recycling rates.

On the other hand, for the governance aspects of the ISWM system, the assessment were focused on the following parameters (Wilson et al., 2014):

1. Inclusivity- the creation of enabling environment where stakeholders can freely contribute in the ISWM system as users, providers and/or enablers;
2. Financial sustainability- the cost-effectiveness and affordability of the ISWM services; and
3. Social Institutions and Proactive Policies- presence of institutional mechanisms instituted to ensure a well-coordinated implementation of the ISWM services.

To contribute in the continuous improvement of the 'Wasteaware' Benchmark Indicator Set, this study also consider the feedback of the user who used the performance evaluation tool developed in this study. This is done to generate comments and suggestions that can be considered to further reinforce the usability and applicability of the indicator set in the Philippines.

Data Gathering

While the "Wasteaware' Benchmark Indicator Set is meant to use existing data and not to carry out actual survey work, this study employed validation mechanisms to verify the information provided by the local authority.

The primary methodology for the collection of data is the administration of a self-administered questionnaire (SAQ) which was accomplished by the MENRO. Supporting documents were also provided to substantiate their answers. The second methodology was through stakeholder consultation in the form of an interviewer-assisted questionnaire for households and key informant interviews with CSO representative in the Municipal SWM Board. The third methodology was site inspection in the municipality's Carmona Ecology Center, materials recovery facility, municipal hall,

public market, major roads (Governor's Drive and JM Loyola Street), and park. Scores based on the responses of the MENRO were lowered whenever inconsistency occurs between the information provided and the data gathered through the stakeholder consultation and/or site inspection.

For household survey, household survey, the top three barangays (i.e., Milagrosa, Mabuhay and Lantic) that produce the bulk of municipal wastes were purposively selected. In selecting the households for the survey within these barangays, the Maximum Variation/Heterogeneous Purposive Sampling was employed. Different types of households were purposively selected through the help of the key people in the community (e.g., barangay official). This is to provide as much insight as possible with regard to the phenomenon being studied. Thus, high-, mid-, and low-end residences were represented. Also, those engaged with commercial ativities (e.g., carinderia/eatery) were also represented. For the purpose of this study, households in exclusive and gated subdivisions were considered as high-end residences. Seven (23.33%) respondents were included in this group. Nine (30%) households who are earning at most National Statistical Coordination Board threshold of Php 9,061 per month constitute the low-income group. The remaining 14 (46.67%) who earns Php 9,062 to Php 100,000 per month constitute the middle income group.

Data Analysis

While there is an available Excel User Form for data analysis devised by the 'Wasteaware' proponents, this current study opted to develop its own results matrix as some of its original indicators were not included in assessing the performance of the municipality's SWM system. Similar to the proponent's user form, this study's excel user form also accommodates the normalization of scores and the generation of averages which are vital in getting the overall

rating for each variables composed of multiple indicators.

Using the rating scale provided in the user manual developed by Wilson et al. (2014) as guide, the score for each indicator was determined based on the data from the MENRO, consultation with stakeholders, and site inspection.

For composite indicator (e.g., local institutional coherence) where multiple sub-indicators were considered in scoring, a composite score (presented in percentage) was computed. It is calculated through this formula (Chanhthamixay et al., 2016):

$$N = \frac{\sum_{i=1}^{n} Ci}{20n} x100$$

where: C= score for the sub-indicator; n= number of sub-indicators; 20= perfect score for each sub-indicator.

The scores for each indicator were then interpreted using the scale provided in the 'Wasteaware' User Manual. The interpretation of scores for qualitative indicators is shown in Table 1 while Table 2 shows the interpretation for quantitative indicators.

Table 1. Interpretation of numerical ratings for qualitative indicators

Rating	Interpretation	Color Code
0-20%	Low	
21-40%	Low/Medium	
41-60%	Medium	
61-80%	Medium/High	
81-100%	High	

This current study aims to generate a single index that will encapsulate the solid waste management landscape in the LGU. Hence, a normalized score for each variable were derived by translating the interpretation of the

indicator score, into a numerical rating following this conversion rule: low=1, low/medium=2, medium=3, medium/high=4, and high=5. The average of all normalized indicator scores will constitute the variable score for the variable.

Table 2. Interpretation of numerical ratings for quantitative indicators

Indicator Name and Definition	Interpretation				
	LOW	LOW/ MEDIUM	MEDIUM	MEDIUM/ HIGH	HIGH
Waste Collection Coverage	0-49%	50-69%	70-89%	90-98%	99-100%
Waste Captured by the solid waste management and recycling system	0-49%	50-69%	70-89%	90-98%	99-100%
Controlled treatment or disposal	0-49%	50-74%	75-84%	85-94%	95-100%
Recycling rate	0-9%	10-24%	25-44%	45-64%	65% and over

Finally, to get the final index, the formula below was used:

$$I = \frac{\sum_{i=1}^{n} VS_i}{5n} x\ 100$$

where: I= final index; VS= variable score; n=number of variables (6); 5=perfect score for each variable

The absence of bases for determining the weights of each component prompted the researchers to resort to getting the average and the percentage, indicating equal contribution of each components in the final index. Table 5 was used in interpreting the final index.

RESULTS AND DISCUSSION

Although it perceived the performance evaluation tool to be a bit difficult to use, the MENRO

considered answering it to be a very helpful exercise for them to learn and understand how they are progressing in ISWM.

Overall performance of the Municipality of Carmona is at 90.57%. Rating is classified as high which suggests exemplary performance of ISWM system with ome rooms for improvements. Justifications for the rating for each variable were provided.

Table 3. Summary of Results

Variable		Benchmark Indicator	Rating and Interpretation	Color Code		Normalized Score	Component Score
Physical Components							
1	Public health – Waste collection	1.1 Waste collection coverage	100% (HIGH)			**5**	**4.67**
		1.2 Waste captured by the system	96% (MEDIUM /HIGH)			**4**	
1C		Quality of waste collection service	88% (HIGH)			**5**	
2	Environmental control – waste treatment and disposal	Controlled treatment and disposal	100% (HIGH)			**5**	**4.5**
2E		Quality of environmental protection of waste treatment and disposal	MEDIUM/ HIGH (80%)			**4**	
3	Resource Value – 3Rs: Reduce, Reuse, Recycle	Recycling rate	59% (MEDIUM /HIGH)			**4**	**4**
3R		Quality of 3Rs – Reduce, reuse, recycle - provision	MEDIUM/ HIGH (79%)			**4**	
Governance Factors							

Variable		Benchmark Indicator	Rating and Interpretation	Color Code		Normalized Score	Component Score
4U	Inclusivity	User inclusivity	92% (HIGH)			**5**	**5**
4P		Provider inclusivity	100% (HIGH)			**5**	
5F	Financial sustainability	Financial sustainability	80% (MEDIUM/HIGH)			**4**	**4**
6L	Sound institutions, proactive policies	Local institutional coherence	92% (HIGH)			**5**	**5**

Physical Components

All the households, regardless of income, receive regular waste collection service at least twice a week. There were separate schedule for biodegradable and non-biodegradable wastes. There were garbage bins were wastes are picked up by the collectors. There were also 22 Materials Recovery Facility/Storage where residents can place their recyclable wastes. No accumulated wastes around these collection points/containers were observed one day before and after collection schedule. Absence of litter and overflowing litter bins in the municipality's main streets and key public spaces was also noticeable.

For an efficient waste transport, smaller dump trucks were used to pick up wastes from the households. The residual wastes were then transferred to a larger dump truck in the transfer station. Once the dump truck was completely filled, the wastes were immediately transported to the landfill to avoid accumulation in the station. However, it was observed that the smaller dump trucks coming from distant barangays lack top cover during its travel after collecting wastes.

In terms of service planning, the

collection scheme was well planned through the Solid Waste Management Board to ensure complete coverage. The LGU also maintain a report on waste collection which is updated daily.

Currently, the LGU utilizes two facilities for controlled treatment and disposal of solid wastes—the privately managed state-of-the-art engineered sanitary landfill and the local government-run Carmona Ecology Center for biodegradable wastes. The former was found to be compliant to the Environmental Compliance Certificate by the DENR and was classified as a Category 4 SLF, indicating a high degree of control. Meanwhile, the latter was recognized by the DENR and the Department of Science and Technology (DOST) for its biological treatment. Two 500-kg bioreactors serve as main composting equipment while four two-ton capacity rotary drum composters and two shredders function as relievers. The end-product of this biological treatment was a soil conditioner. To indicate the presence of the two facilities, a medium/high rating was given—the midway between the ratings for its controlled recycling facility for biodegradable wastes and the state-of-the art SLF for residual wastes.

Of the total volume (2,707.21MT) of dry recyclables collected, only 1,482.24MT (55%) was sold to junkshop or turned into usable product. In terms of biodegradable wastes, only 1,959.72MT (62%) of the 3,173.97MT was turned into soil conditioner through the biological treatment process conducted in the Ecology Center. These two recycling rates fall under the medium/high level (45%-64%). These rates are also higher than the average waste diversion rates in the National Capital Region (48%) and in local governments outside the capital (46%).

Segregation at source was very much evident among low- and mid-end residences. It is interesting to note that the interviewed household heads living in exclusive subdivisions do

not segregate their wastes at home. However, this does not come as big deal considering that their homeowner's association management provides for the consolidation and the segregation of wastes prior to the collection of LGU waste collectors. While quality control practices in the processing of organic wastes were in place, it cannot be denied that the non-segregation of wastes in some households may affect the quality of the soil conditioner being produced.

When it comes to occupational health and safety measures from collection to disposal/treatment, it was observed that while safety equipment and attires (boots, gloves and face masks) were provided to LGU personnel engaged in waste management activities, not all of them are using them regularly based on the interview with the residents and actual observation of the researchers.

Governance Factors

User inclusivity is very much evident in the ISWM system. Local users were not just mere beneficiaries but also active participants in the different phases of ISWM implementation. Women's group (Samahan ng Nagkakaisang Kababaihan sa Carmona) and youth sector (Sangguniang Kabataan Chairperson) are represented in the Solid Waste Management Board which is regularly conved for purposes of planning, coordinating and monitoring the implementation of the LGU'S solid waste management plan. Carmona Task Force Kalikasan and Carmona Tanggol Kalikasan were also organized for the implementation and/or monitoring of solid waste management initiatives particularly on proper waste segregation and actions against illegal dumping. Public consultations were also conducted before the passage of any policy.

Feedback mechanisms were made available and accessible to the communities. Among the 30 respondents, they have enumerated the following mechanisms: drop-in in

the MENRO office, telephone thru the LGU's hotline and the national government's 888-hotline, and internet thru sending email to LGU's email address.

Public education and awareness initiatives are also in place. Ako Basurero Campaign, serves as a flagship initiative on this matter. It features "BNOY, ang Basurerong Pinoy, a mascot; and Mag-3R Tayo," the official jingle of the campaign which were showcased during community meetings and school programs relating to proper waste management.

LGU's effort to integrate the informal recycling sector (IRS) in the ISWM system was admirable. IRS has access to working capital and were provided with inputs (e.g., push carts and safety equipment). They were tapped by the LGU in monitoring the volume of recyclable wastes generated in the municipality. This was made possible through the provision of seed money to these IRS coming from the monetary award it gets from the DILG after passing the SGLG assessment.

Private sectors were also given the chance to help the LGU in realizing its waste management mandate. The local government forge partnership with the private sector for the provision of solid waste management services that it cannot provide.

Compliance to bidding process as one of the indicators in the provider inclusivity, showed that the LGU of Carmona upholds transparency and accountability. This is based on its positive opinion from the Commission on Audit and the LGU's consistent compliance with the Full Disclosure Policy based on DILG's assessment.

In terms of financial sustainability, the LGU allocated PhP12.193M for operating cost, PhP 1.823M for maintenance cost, PhP 2M for necessary improvements, and PhP 2.50M for cost of capital (to cater unserved areas, replace existing vehicles and equipment). This only shows that ISWM is taken seriously by the LGU.

On local institutional coherence, the LGU has designated a department, the Municipal Environment and Natural Resources Office, for the delivery of SWM services. This is in spite the fact that MENRO is only an optional office in a municipal government pursuant to the Local Government Code. The LGU also has a ten-year Solid Waste Management Plan (CY 2015-2025) duly approved by the NSWMC. Other than the involvement of its mayor in the Provincial Solid Waste Management Board, the LGU has no other inter-LGU cooperation engagement for SWM.

CONCLUSIONS

The municipal government's fund allocations for SWM services only show that solid waste management is an integral part of its development thrusts. As a result, the SWM system of Carmona recorded remarkable performance in several aspects particularly on waste collection coverage, user and provider inclusivity and local institutional coherence. For other aspects, some recommendations are hereby provided.

Limited observance of occupation health and safety measures, non-separation of wastes at source among high-end households, and waste transportation lapses are the primary areas for improvement in the physical component of the SWM system. The first two concerns will require information and education campaign and strict monitoring of concerned stakeholders' observance on set standards. For the last concern, it is highly recommended that cover be placed on top of the small dump trucks on its travel from distant barangays to the transfer station to avoid windblown litter.

On the other hand, financial sustainability remains a key issue for the municipal SWM system's governance component. The municipal government could explore financing opportunities through collecting garbage fee. It could benchmark from Marikina City which imposes garbage fee by

including it in the real property tax or business permit renewal fees. They could also tap other financing opportunities such as funding from the national government and international organizations. It can also consider selling the soil conditioner it produces from biological treatment. To improve the market viability of this product, an accreditation from a certification body like the Department of Agriculture will be helpful.

In terms of using the performance evaluation tool, it is highly recommended that LGUs will facilitate the complete documentation of SWM activities and their outputs/impacts to ensure accurate application of its assessment criteria.

For future work, researchers may consider further testing the performance evaluation tool in other LGUs of different attributes (e.g., income classification, volume of wastes). The tool can also be customized for other levels of local governments (i.e., provinces, cities, barangays) who have different mandated SWM functions by virtue of the administrative power hierarchy principle in Philippine's local governance. Agencies with oversight functions relative to monitoring of local SWM system should also consider the results of this study as they transition from compliance monitoring toward performance evaluation for a more relevant assessment.

ACKNOWLEDGEMENTS

The researchers would like to extend their sincerest appreciation to the Municipal Government of Carmona, particularly its MENRO for being their active partner in conducting this study, and to Dr. Jose M. Regunay of UP School of Urban and Regional Planning for guiding the researchers throughout the duration of this study.

REFERENCES

Chanhthamixay, B., Vassanadumrongdee, S. & Kittipongvises, S. (2016). Assessing the Sustainability Level of Municipal Solid Waste Management in Bangkok, Thailand by Wasteaware

Benchmarking Indicators. *Applied Environmental Research, 39* (3), 49-61.

DENR Administrative Order No. 2001 – 34. December 20, 2001. Implementing Rules and Regulations of Republic Act 9003.

Municipality of Carmona, Cavite-Solid Waste Management Plan 2015-2024. Date Retrieved: October 15, 2018

Municipality of Carmona, Cavite-Volume 1: Comprehensive Land Use Plan (2011-2022)

Municipality of Carmona, Cavite-Volume 2: Zoning Ordinance (2011-2022)

Municipality of Carmona, Cavite- Waste Analysis and Characterization Study/ Survey (2017)

Republic Act 9003. January 6, 2001. An Act Providing for an Ecological Solid Waste Management Program, Creating the Necessary Institutional Mechanisms And Incentives, Declaring Certain Acts Prohibited and Providing Penalties, Appropriating Funds Therefore, and for Other Purposes.

Republic Act 7160. October 10, 1991. The Local Government Code of 1991.

Scheinberg, A., Wilson, D.C. and Rodic, L. (2010). *Solid Waste Management in the World's Cities*. Third edition in UN-Habitat's Statte of Water and Sanitation in the World's Cities Series. Published by Earthscan for UN-Habitat, March 2010.

Wilson, D. C., Rodic, L., Cowing, M. J., Velis, C. A., Whiteman, A. D., Scheinberg, A., . . . Oelz, B. (2014). 'Wasteaware' benchmark indicators for integrated sustainable waste management in cities. *Waste Management,35*, 329-342.

Wilson, D. C., Rodic, L., Scheinberg, A., Velis, C. A., & Alabaster, G. (2012). Comparative analysis of solid waste management in 20 cities. *Waste Management & Research, 30*(3), 237-254.

Zurbrügg, C., Caniato, M., & Vaccari, M. (2014). How Assessment Methods Can Support Solid Waste Management in Developing Countries—A Critical Review. *Sustainability,6*(2), 545-570.

An investigation and Assessment of the Material and Pollutant Pathway from Dismantling of Refrigerator

Thidapon Ketthong[1*], Nattharika Rittippant [1], Noramon Intranont [2], Premrudee Kanchanapiya [2] Pawadee Methacanon [2], and Alice Sharp [3,4]

[1]Sirindorn International Institute (SIIT), 99 Moo 18, Khlong Luang, Pathum Thani 12120, Thailand; Corresponding author: e-mail: k.thidapon@gmail.com

[2]National Science and Technology Development Agency, 111 Thailand Science Park (TSP), Phahonyothin Road, Khlong Nueng, Khlong Luang, Pathum Thani 12120, Thailand

[3]Department of Biology, Faculty of Science, Chiang Mai University, 239 Huay Kaew Road, Muang District, Chiang Mai, Thailand, 50200, Thailand

[4]Environmental Science Research Center, Faculty of Science, Chiang Mai University, 239 Huay Kaew Road, Muang District, Chiang Mai, Thailand, 50200, Thailand

ABSTRACT

This study aims to estimate 1) the amount of materials, 2) to study the materials pathway and 3) to assess the environmental impacts of refrigerator dismantling to suggest the potentially refrigerator waste policy. The results were conducted from plant visiting and interviewing 26 of informal dismantling stores located in each region of Thailand. 1) In 2019, the amount of recyclable materials from the refrigerator waste were mainly found such as 34,207 tons of steel, 8,783 tons of polystyrene, 6,520 tons of polypropylene, 6,274 tons of acrylonitrile butadiene styrene, 2,069 of copper, 315,646 litters of lubricating oil and so on. 2) For the valuable materials pathways, the materials would be roughly separated by dismantling stores and sold to recycling stores. The stores act as a middle man and sale the materials to processing factories so as to recycling. 3) The environmental impacts from non-valuable materials using emission factors from SimaPro, the results

indicated that the impacts came from the releasing of refrigerants to environment which was approximately 175,489,810 kg CO_2 eq. of GWP in 2019. This is due to the vapour of refrigerants would be emitted to environment directly during dismantling processes. In order to avoid the impacts, following the draft of Thailand WEEE Act, the refrigerator wastes should be dismantled by formal sectors, however, this may affect the informal sectors' income. Thai government has to compromise, give out incentives and find ways to solve these problems.

Keywords: Refrigerator dismantling, refrigerator waste, environmental impacts

INTRODUCTION

In Thailand, electronic wastes (e-waste) tend to increase every day. The statistics from the Pollution Control Department of Thailand (PCD) indicated that the amount of the e-wastes reached 384,233 tons in 2015 (Wittayaanumas 2017; The pollution control department (PCD) 2013). Refrigerator is e-waste which contains some substances realized as Ozone Depletion Substances (ODSs) and high Global Warming Potential (GWP) such as refrigerant and foam blowing agents. In 2015 the amount of refrigerator wastes which ranked the third tier of all e-wastes are approximately 17% (65,765 tons) (Wittayaanumas 2017). Up to date, there are no specific rules for controlling the e-wastes in Thailand, whereas, there is only the draft of Waste from Electrical and Electronic Equipments Act (WEEE) by PCD (The Ministry of digital economy and society 2018). This law was approved by the National Legislative Assembly Coordinating Committee on 27 August 2018. The regulation controls 6 types of e-waste including computer, telephone, air conditioner, television, refrigerator and other types of e-waste as prescribed in the ministerial regulations. Following the

draft, discarding the e-waste combining with the municipal solid waste (MSW) was prohibited and permitted only formal sectors could dismantle the e-waste. The old refrigerators or other types of e-waste would be collected by a product return center that was established and registered according to the announcement of the PCD. The draft also imposed the responsibility of a producer. The producers have to control their e-waste after used and dispose in an appropriate way. Furthermore, none of the dismantling stores can appropriately dismantle the refrigerators (Hai 2014) and there is no comprehensive electronic waste recycling system in Thailand (Vassanadumrongdee 2012). As a results, the discarded refrigerators in Thailand are dismantled by informal sectors.

In the domestic refrigerator, there are many parts that made from different materials. Some of them contain heavy metals or hazardous substances. The compressor is the heart of the refrigerator, which contain refrigerant and lubricating oil affecting the environment (Belman-Flores et al. 2015). There was a research on the additives of lubricating oil which is Zinc dialkyldithiophosphates (ZDTPs) acting as antioxidants, antiwear agents and corrosion inhibitors. If these substances were emitted to water, it could be accumulated in freshwater organism or in the food chain resulting human health damage as mutagenic substances (Cisson, Rausina, and Stonebraker 1996). For the refrigerants, chlorofluorocarbon substances or CFCs were introduced in 1930 and used as refrigerant for a period of time. They were replaced by R-134a in 1980 because CFCs were realized as ODSs, and were banned (Tuomas 2006). However, they still have the global warming potential (GWP) so they must be appropriately managed at disposal phase.

To understand the actual refrigerator waste management situation in

Thailand, this research aims to study the materials and pollution pathways from dismantling refrigerator in Thailand by identifying the materials in refrigerators and the environmental effects from refrigerator dismantling processes.

METHODOLOGY

The material pathways for valuable materials

The material pathways of the valuable materials from refrigerator waste were collected from stakeholders. The stakeholders who were interviewed include dismantling stores which are responsible for dismantling the discarded refrigerators. The next stakeholder was recycling stores which are responsible for buying the valuable materials from dismantling stores. Another stakeholder was processing factories which are responsible for buying the valuable materials from recycling stores and then feed them into the recovering or recycling processes to produce the raw materials or finish goods from scraps The data on the materials pathway was collected by phone interview, field visit and from the environmental impacts assessment (EIA) reports (from the Division of Environmental Impact Assessment Development's website). The valuable materials include steel (outer wall), aluminum (evaporators), copper (condenser tubes, capillary tube, and wires) acrylonitrile butadiene styrene (ABS plastic inner wall), polypropylene (PP plastic standing) and polystyrene (PS plastic shelves).

The amounts of valuable material scraps from discarded refrigerators at a present year were estimated by interviewing the refrigerators manufacturers in Thailand. The weight of each part of the refrigerator was collected. The average life expectancy for property maintained refrigerator is imposed at 14 years (The pollution control department (PCD) 2007; Leibniz 2018). Under the assumption, the refrigerator would be sent to dismantling stores to

be dismantled. The number of refrigerators production and sales data in Thailand at 14 years ago was referred to the industrial statistic of Thailand. To estimate the material mass flow at a present year, the equation (1) and (2) were used;

$$\boldsymbol{W_A = \sum W_i X_i \ldots (1)}$$

where $\boldsymbol{W_A}$ is an average weight of each material, $\boldsymbol{W_i}$ is the weight of each material from the refrigerator in each size. (kg) and $\boldsymbol{X_i}$ is proportional to refrigerator sales data in each size. (%).

$$\boldsymbol{M_m = W_A \cdot N_i \ldots (2)}$$

where M_m is mass of each material (kg), W_A is an average weight of each material in different size of refrigerators and N_i is a number of refrigerators that was produced and sold in Thailand in 2004.

The environmental impacts assessment from non-valuable materials by using the database from SimaPro

The non-valuable materials and waste scenarios from discarded refrigerators were defined by collecting data from dismantling stores. To analyze the environmental impacts of non-valuable materials, emission factors of the waste from SimaPro were used. Methods midpoint the capital (H) or Hierarchist recipe were selected which based on the most common policy principles, regarding to time-frame and other issues. The medium time frame of a 100-year timeframe for global warming represent as GWP100.

After analysis of the emission factors of the wastes obtained from SimaPro, the environmental impacts of waste from refrigerators were estimated. To calculate the environmental impacts of non-valuable parts from refrigerators, the weight of each part multiplied by the number of refrigerators that were sold 14 years ago in Thailand and the emission factors from SimaPro. The equation is shown below;

$$\boldsymbol{X_n = W_A \cdot N_i \cdot E_i \ldots (3)}$$

where X_n is environmental impacts of non-valuable materials, W_A is an average weight of each material in

different size of refrigerators and N_i is a number of refrigerators that was produced and sold in Thailand in 2004 and E_i is emission factors of each type of waste obtained from SimaPro.

RESULTS AND DISCUSSION

The material pathways for valuable materials

Twenty six of dismantling stores were interviewed in order to collect the pathways of valuable materials. The refrigerator would be dismantled at dismantling stores which are the informal sectors. The materials roughly separated and sold to recycling stores. The stores act as a middleman and sell the materials to recycling factories so as to recycling. Twelve of recycling stores were interviewed. At recycling stores, the metals would be pressed in cubic sharp for more convenient to transportation and the plastics would be separated by their type and color before they would be crushed into small pieces. After that, the crushed plastics and the cubic metals would be sold to processing factories or recycling factories for recycling and finish goods production from the scraps. The data on the finish goods and processes were collected from 50 of recycling factories. At recycling factories, the metals would be re-melted by using a combination of metal types in different proportion to obtain the finish goods depending on requirements. In the end, the scraps from refrigerator dismantling could be recovered to make new raw materials or finish goods. Plastic will be recycled to form plastic pellet used as raw materials to make plastic recycling. Steel scraps from refrigerators can be recycled to round bar steel, deformed bar steel, equal angle steel, channels steel, structural steel or raw materials such as steel billet. Aluminum scraps can be processed to become raw materials as aluminum ingots. Copper scraps can be recycled to become level wound coil (inner grooved tube), level wound coil (plain tube) and other strength tubes depending on the scrap composition that is added into

production processes. The lubricating oil will be recycled and used as fuel oils. The data collecting from stakeholders were shown in Table 1

The weight of each material in the refrigerator was collected from 2 of refrigerator production manufactures as shown in Table 2. The data on the proportional of refrigerator sales data in each size (X_i) was collected from the 4 of refrigerator manufacturers include Sharp, Hitachi, Haier and Mitsubishi which equaled 60% of number of refrigerator manufacturers in Thailand as shown in Table 3. These data were used to calculate the average weight of each material from refrigerators (W_A) in equation (1).

From the calculation using equation (2) and data collected from stakeholders, the materials pathways could be defined and the weight of craps from dismantling refrigerator at a present year could be estimated that are shown in Figure 1.

Table 1 The stakeholder's data that were collected on the pathway of materials

Stakeholders	Numbers	Details
Dismantling stores	28	28 stores dealing with all types of electronic equipment.
Recycling stores	12	2 stores dealing with steel, copper, aluminum and plastics
		6 stores dealing with steel, copper, aluminum
		4 stores dealing with steel, copper, aluminum, paper
Recycling factories	50	10 stores dealing with aluminum smelting and recycling
		5 stores dealing with copper smelting and recycling
		23 stores were steelmaking
		4 stores were plastic pellet making

		1 store was plastic pellet trading
		6 was lubricating oil recycling
		1 was Printed Circuit Board recycling factory
Refrigerator manufacturers	4	Sharp, Hitachi, Haier and Mitsubishi
Summary		54

Table 2 The weight of material in different size in refrigerators

Materials	**Weight (kg)**			
	Size 0-200 L	Size 200-350 L	Size 350-500L	Size > 500 L
1. Steel	24.24	27.70	30.62	44.40
2. Aluminum	0.80	1.00	1.50	2.00
3. Copper	1.37	1.61	1.91	3.38
4. ABS plastic	3.00	5.00	8.00	12.50
5. PP plastic	6.00	4.00	5.00	6.00
6. PS plastic	5.00	7.00	10.00	15.00
7. PU foam	4.35	7.15	9.90	12.95
8. PVC	1.20	1.50	2.00	2.80
9. Lubricating oil	0.28	0.22	0.24	0.27
10. Refrigerant	0.07	0.09	0.13	0.15
11. Lightbulb	0.0061	0.0069	0.0071	0.0075

Table 3 The data on the proportional of refrigerator sale data in each size (X_i)

Production year	**The proportional of refrigerator sale data in each size (%)**			
	0-200 L	200-350 L	350-500 L	> 500 L
2016	46	29	16	8
2015	47	30	16	8
2014	50	26	17	7
2013	52	24	16	8
average	49	27	16	8

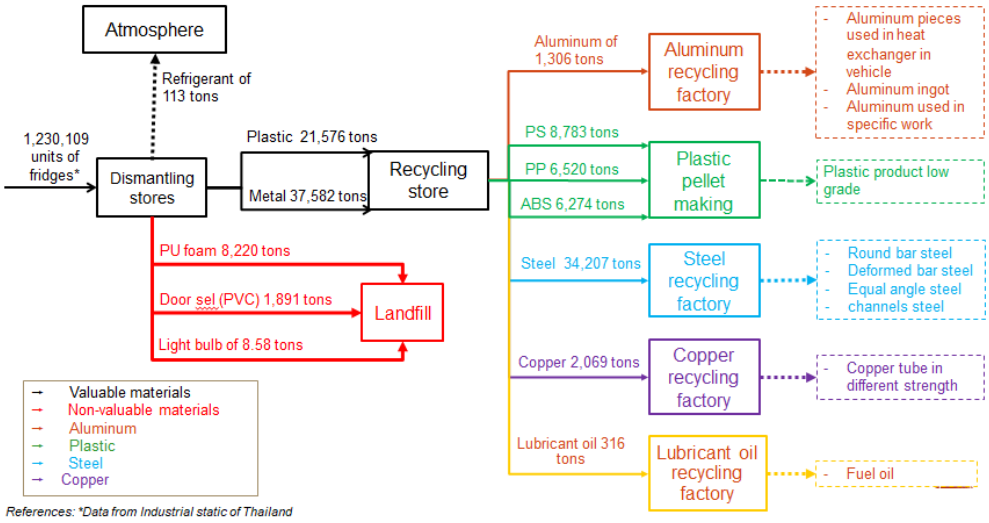

Figure 1 The pathway of material represents weight of scraps during dismantling of refrigerators waste in 2019.

The environmental impacts assessment from non-valuable materials by using the database from SimaPro

In dismantling refrigerator processes, non-valuable materials include polyurethane (PU), polyvinyl chloride (PVC), refrigerant and lightbulb. These materials would be disposed and mixed with municipal solid waste (MSW) which ended up in a landfill. The refrigerants would be emitted directly to the atmosphere. After the emission factors of waste from the SimaPro program (table 4) were added into the equation (3), the environmental impacts of non-valuable materials from dismantling refrigerator waste in 2019 could be estimated as shown in Figure 2. The highest impact of the GWP was the releasing of refrigerants (R-134a) estimated as 175,489,810 kg CO_2 eq. The highest impact of human non-carcinogenic toxicity was the disposal of polyvinyl chloride (PVC) which is equaled to 1,065,748 kg 1,4-DCB. For the human carcinogenic toxicity, the highest impact came from the releasing of refrigerant which estimated as 7,654 kg 1,4-DCB. Another one was the terrestrial ecotoxicity which came from the disposal of PU waste estimated as 104,730 kg 1,4-DCB. From the interview of dismantling stores, it

was indicated that only 7.7% of dismantling stores (2 stores from 26 stores) who collected and sale the PVC to other stakeholders while 92.3% of dismantling stores (24 stores from 26 stores) dispose the PVC combining with MSW.

Table 4 The emission factor from SimaPro (E_i)

No.	Impact category	Unit	Refrigerant (R-134a)	PU Foam	PVC
1	Global warming	kg CO2 eq	1550	0.005423	0.083378
2	Stratospheric ozone depletion	kg CFC11 eq	0	3.78E-09	7.19E-09
3	Ionizing radiation	kBq Co-60 eq	0	0.000165	0.000415
4	Ozone formation, Human health	kg NOx eq	0	4.52E-05	8.02E-05
5	Fine particulate matter formation	kg PM2.5 eq	0	1.37E-05	2.71E-05
6	Ozone formation, Terrestrial ecosystems	kg NOx eq	0	4.62E-05	8.18E-05
7	Terrestrial acidification	kg SO2 eq	0	3.04E-05	5.73E-05
8	Freshwater eutrophication	kg P eq	0	6.25E-07	1.82E-06
9	Marine eutrophication	kg N eq	0	5.14E-08	0.000106
10	Terrestrial ecotoxicity	kg 1,4-DCB	0	0.012742	0.025566
11	Freshwater ecotoxicity	kg 1,4-DCB	0	5.42E-05	0.034729
12	Marine ecotoxicity	kg 1,4-DCB	0	8.43E-05	0.047397
13	Human carcinogenic toxicity	kg 1,4-DCB	0.0676	0.000141	0.002491
14	Human non-carcinogenic toxicity	kg 1,4-DCB	0.0826	0.001711	0.563686
15	Land use	m2a crop eq	0	0.000949	0.003052
16	Mineral resource scarcity	kg Cu eq	0	1.01E-05	3.47E-05
17	Fossil resource scarcity	kg oil eq	0	0.003481	0.00582
18	Water consumption	m3	0	0.000171	0.000282

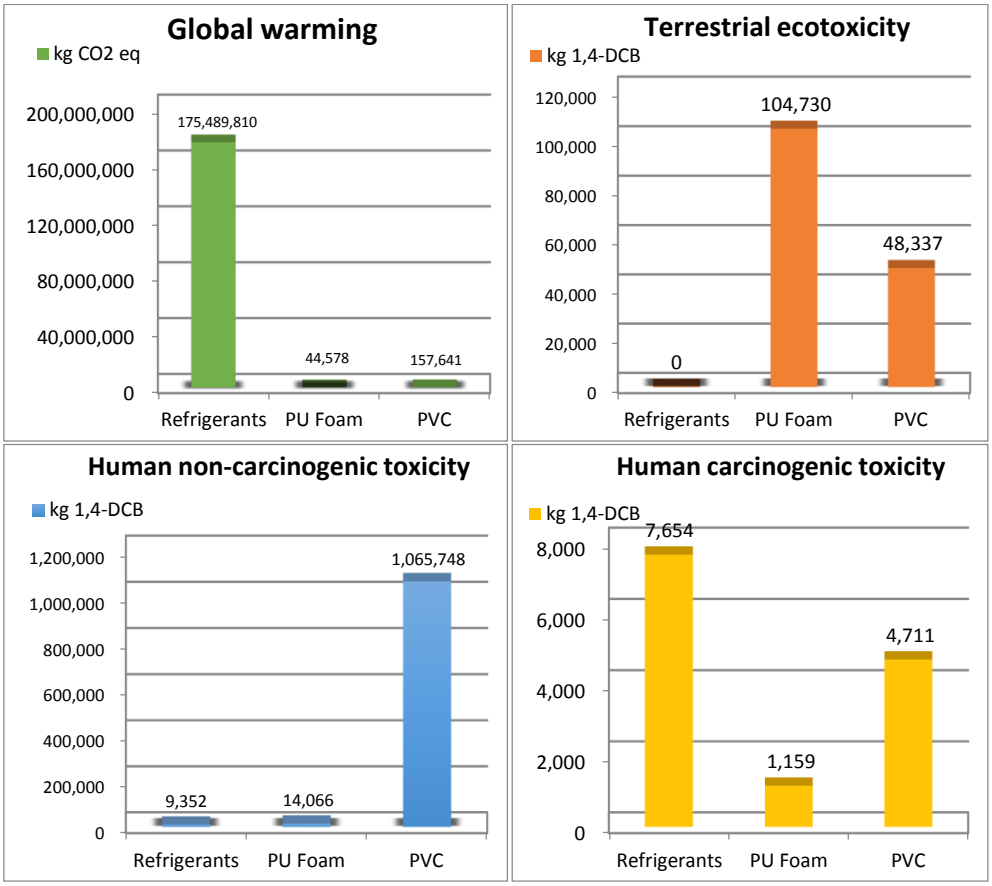

Figure 2 The environmental impacts of non-valuable materials from dismantling refrigerator waste

CONCLUSIONS

The recyclable materials from the refrigerator waste can be classified as metal such as aluminum, steel, and copper, and plastics (i.e. ABS, PP and PS). For environmental impacts from non-valuable materials, the highest GWP impact was of refrigerant (R-134a) emission. The reason is that the refrigerator dismantling processes are conducted by informal sectors. The refrigerant was also emitted to environmental directly during the compressor dismantling process. Moreover, labors that dismantle compressors do not have any protective equipment to protect themselves from the vapors of refrigerants. For the environmental impacts from dismantling refrigerators, the result showed that the impacts of releasing refrigerant included both human non-carcinogenic toxicity and

carcinogenic toxicity which reached to 9,352 and 7,654 kg 1,4-DCB respectively. Not only GWP but also human health effects from refrigerant vapour exposure should be aware of. The treatment of refrigerants and understanding of labors, therefore, are needed in order to reduce the environmental effects of dismantling refrigerators. For lubricating oil, there are 4 stores from 26 dismantling stores who release the oil to the environment without collection for recycling. Discarding lightbulb was mostly mixed with MSW. Unfortunately, SimaPro has no database on lightbulb, resulting no impacts can be quantified. Thus, these can cause environmental impacts too. Following the list of hazardous waste attached to the announcement of the Ministry of Industry (The Ministry of Industry 2013), the lubricating oil was classified as the hazardous waste, categorized in chemical waste. The used lubricating oil which had amount more than 20 litters was classified as hazardous waste in the 1st order of the list of hazardous waste. Therefore, the collection, transportation and disposal of the used lubricating oil need to be controlled and reported to follow the announcement of the Ministry of Industry on "the disposal of waste or unused materials" (The Ministry of Industry 2005). According to the draft of WEEE Act, this law was approved by the National Legislative Assembly Coordinating Committee on 27 August 2018. In case of the WEEE act is implemented, the informal sectors would be prohibited to dismantle the refrigerators and other e-waste. This may be the most effective way to control e-waste in Thailand. However, the informal sectors would be directly affected. The Thai government should give out incentives for the informal sectors by providing information and time for adaptation. Moreover, the government should give an opportunity to the informal sectors to improve or register to become formal sectors before the WEEE Act become enforcement.

ACKNOWLEDGEMENTS

This research was financially supported by National of Metal and Materials Technology Center (MTEC), National Science and Technology Development Agency (NSTDA), Thailand and Thai Health Promotion Foundation, Project No. P1850443 and Sirindhorn International Institute of technology (SIIT), Thammasat university.

REFERENCES

Belman-Flores, JM Barroso-Maldonado, AP Rodríguez-Muñoz, and G Camacho-Vázquez. Enhancements in domestic refrigeration, approaching a sustainable refrigerator–a review', Renewable and Sustainable Energy Reviews 2015, 51: 955-68.

Hai, Huynh Trung. 2014. "Electric and Electronic Waste Recycling in Vietnam." In 4th INTERNATIONAL E-WASTE MANAGEMENT NETWORK. Hanoi, Vietman.

Leibniz. 2018. '23rd Annual Portrait of The U.S. Appliance Industry Saturation, share-of-market, and life expectancy figures are given along with a comprehensive listing of Who's Who in the Appliance Industry', Leibniz information centre for science and technology university library. https://www.tib.eu/en/search/id/BLSE%3ARN084175500/23rd-Annual-Portrait-of-The-U-S-Appliance-Industry/#documentinfo.

Michael Cisson, C, Gary A Rausina, and Peter M Stonebraker. 'Human health and environmental hazard characterisation of lubricating oil additives', Lubrication Science 1996, 8: 145-77.

The Ministry of digital economy and society. 2018. 'the draft of Waste from Electrical and Electronic Equipments Act (WEEE)', Accessed January 12. http://www.lawamendment.go.th/attachments/article/717/%E0%B8%A3%E0%B9%88%E0%B8%B2%E0%B8%87%20WEEE%20610831.pdf.

The Ministry of Industry. 2005. "the announcement of the Ministry of Industry on “the disposal of waste or unused materials”.

The Ministry of Industry. 2013. "the announcement of the Ministry of Industry.".

The pollution control department (PCD). 2007. "WEEE strategy.".

The pollution control department (PCD). 2013. "Thailand State of Pollution Report 2012." In, 74-75.

Tuomas, Roger. 2006. 'Properties of oil and refrigerant mixtures: lubrication of ball bearings in refrigeration compressors', Luleå tekniska universitet.

Vassanadumrongdee, Sujitra and Manomaiwiboon, Panate. 2012. Electronic waste management. In, 1-7.

Wittayaanumas, Jirakorn Yingpaiboonyong, Tippawan Kaewmeesri and Wattana Karnjananit. 2017. "Electronic waste management in Thailand." In *TDRI Report*.

Infectious Waste Management Among Health Personnel in Sub-district Health Promoting Hospital in Sukhothai Province

Sane Saengngoen[1]*, Tavorn Maton[2]

[1,2]Faculty of Public Health, Ramkhamhaeng University, Sukhothai, 64120

*E-mail: drsane2513@gmail.com, sane.s@ru.ac.th

ABSTRACT

This descriptive research aimed to examine infectious waste management among health personnel in sub-district health promoting hospital in Sukhothai Province and to investigate factors influencing appropriate infectious waste management among health personnel in sub-district health promoting hospital in Sukhothai Province .The samples were 190 health personnel recruited with multistage random sampling .Data collection was performed between January 1st and 30th, 2019 using a questionnaire .Data were analyzed with frequency, percentage, mean, standard deviation, minimum, maximum and Pearson's product moment correlation coefficient .

The results showed that most of the participants were female) 79.4(% with mean age of 39.74 years .A large proportion of them were married)63.4(% and held a Bachelor's degree)65.5 .(%Regarding occupation, 45.9% were nurses with 17.34 years of work experience. Additionally, the participants had high levels of knowledge of infectious waste management)66.5(%, attitude of infectious waste management)14.9(%, motivation of infectious waste management)20.1(%, support from administrator for infectious waste management)6.7(%, management of infectious waste sorting)13.4(%, management of infectious waste collection)12.9(%, and overall infectious waste management)12.3 .(%Results also indicated that knowledge, attitude, motivation and support from administrator were significantly influencing appropriate infectious waste management)r =0.208, p=0.004; r=0.256, p<0.001; r=0.213, p=0.003; r=0.345, p<0.001 respectively .(However, age and work experience were not influencing appropriate infectious waste management)r =0.015, p=0.840; r-=0.065, p=0.370 .(

Therefore, the responsible organizations should improve knowledge of infectious waste management among health personnel in sub-district health promoting hospitals, as well as motivate and support the right method of sorting and collecting infectious waste management in sub-district health promoting hospitals.

Keywords: infectious waste management, health personnel

INTRODUCTION

Today, Thailand has more than 37,000 nursing and health care institutes in forms of hospitals, public health service centers, health stations, public and private clinics .Those institutes produce a huge amount of infectious waste from providing nursing care, diagnosis, immunization programs, and research studies conducted in humans and animals .Infectious wastes can spread diseases .Other wastes include radioactive waste, deteriorated drugs, hazardous chemicals, and sharp objects)Pollution Control Department, 2017 :online .(Most nursing and health institutes do not collect, store or dispose of wastes properly .Some parts of infectious wastes are disposed outside and mixed with municipal wastes, increasing risks of disease transmission that deteriorates people's health and hygiene)Kaweekorn et al., 2017) (Bureau of Environmental Health, 2014.(

In 2016, the quantity of infectious wastes was 55, 646 tons increasing from 2015 by 1,778 tons or 3.3 .% This amount included 56.79% of infectious wastes generated by public hospitals, 17.05% by private hospitals, 19.21% by clinics, 6.37% by sub-district health promoting hospitals, 0.58% by veterinary nursing institutes, and 0.01% by hazardous disease laboratories)Manager, 2018 :online .(Health problems caused by infectious wastes are hepatitis B and C, tetanus, skin inflammation from needle injection or cuts with sharp instruments, allergy, dermatitis, eye irritation,

asthma and shortness of breath from inhaling disinfectant, antiseptic, medicines or chemicals used in a laboratory, cancer, respiratory tract disease, and hazard from poisonous chemicals caused by infection waste incinerators such as dioxins)Chantanakul, 2018 :online.(

From the mentioned reasons, the study on infectious waste management among health personnel in sub-district health promoting hospitals in Sukhothai Province serves as a guideline to solve the problem of improper management of infectious waste disposal, prevent hazard from infectious wastes, prevent disease transmission, reduce expenses for infectious waste disposal, and increase income for agencies responsible for recycling waste management, as well as to instill a conscience of health personnel in environment conservation.

OBJECTIVES

1.To study infectious waste management of health personnel in sub-district health promoting hospitals in Sukhothai Province .

2.To study factors influencing appropriate infectious waste management of health personnel in sub-district health promoting hospitals in Sukhothai Province.

METHODOLOGY

This study was a descriptive research using quantitative research method .Data collection period was during January 1st-30th, .2019

Population in the research was 360 health personnel working in sub-district health promoting hospitals in Sukhothai Province who were directly exposed to patients.

1 (Krejcie and Mogran's)1970 (sample size table was used to determine sample size with 95 % reliability .The sample size included 186 persons .To prevent sample loss or incomplete data, the sample size was increased by 10 .%Therefore, the total sample size comprised 190 persons.

2 (Multistage random sampling was used for simple random sampling from districts and sub-districts .Stratified sampling method

was used to partition groups of sample by checking a name list of health personnel working in sub-district health promoting hospitals in Sukhothai Province .Next, random sampling was performed from population of each sub-group with the same proportion based on the following inclusion criteria :1 (being public health personnel, 2 (working at sub-district health promoting hospitals that involved providing treatment to patients, 3 (voluntarily participating in the study and living in the area of study during the research process.

Research instruments

For data collection, the researcher used a developed interview form comprising 5 parts:

Part 1 :6 items of demographic data consisting of gender, age, marital status, highest educational level, position, and duration of working time .

Part 2 :15 items of knowledge about infectious waste management with a 3-point rating scale of Yes/No/Uncertain .

Part3 :15 items of attitude towards infectious waste management with 3-point rating scale of strongly agree / moderately agree /slightly agree .

Part 4 :15 items of motivation in infectious waste management with 3-point rating scale of strongly agree / moderately agree /slightly agree .

Part 5 :10 items of support from executives in managing infectious wastes with 3-point rating scale of strongly agree /moderately agree / slightly agree .

Part 6 :10 items of infectious waste management practice with 3-point rating scale of strongly agree / moderately agree /slightly agree.

Scoring criteria and interpretation of results

1.The scoring criteria of knowledge about infectious waste management are Yes =1 point, No = 0 point, Uncertain =0 point .The criteria of interpretation are divided into 3 levels; high, moderate, low based on Bloom's)1971 (taxonomy interpretation .The total scores of all points in each item are gathered and levels of knowledge are divided by

the following scores :

The highest level includes the scores that are higher or equal to 80%)8-10 points .(The moderate level includes the scores that are between 60 –79) %6-7 points .(The low level includes the scores that are lower than 60) %0-5 points .(

2 .Attitude and motivation, support from executives in managing infectious wastes are based on the following scoring criteria :

	Positive message	Negative message
Agree/high practice.	3	1
Agree/moderate practice.	2	2
Agree/low practice	1	3

Interpretation of results are divided into 3 levels :high, moderate, and low obtained from the highest point minus the lowest point and divided by the required measuring levels based on Best's concept)Best, 1977 (as follows :

The highest level =the average scores 2.34 –3.00 .

The moderate level =the average scores 1.67 –2.33 .

The low score =the average scores 1.00 –1.66.

Content validity of questionnaires was checked by three experts and improved before testing with 30 public health personnel working in sub-district health promoting hospitals in Srisamrong District, Sukhothai Province, who were not the sample .Reliability was analyzed using Cronbach's alpha coefficient, yielding 0.87.

Data collection :The researcher and the assistants questioned the sample using questionnaires and this process took approximately 20 minutes.

Computer program for data analysis was used and statistical significance level was determined at 0.05 .

1 (Descriptive statistics used in data analysis were percentage, mean, and standard deviation.

2 (Inferential statistics were measured using Pearson's correlation coefficient statistics .

A threshold level of the correlation coefficient, r, was divided by the threshold of Elifson)1990 (which

may range from -1 to +1 according to the following:

r =± 1 indicates perfect relationship

r =± 0.71 to ± 0.99 indicates strong relationship

r =± 0.31 to ± 0.70 indicates moderate relationship

r =± 0.01 to ± 0.30 indicates weak relationship

ETHICAL CONSIDERATION

This research was granted approval from the Ethics Review Committee for Human Research of Sukhothai Provincial Health Office)IRB number 1/2019 (for the protection of rights of the sample and participants in the research .The researcher met the sample and made self-introduction, described objectives of the study to all participants, asked for collaboration for collecting data, and informed the rights to accept or refuse participation in this study .The researcher presented a big picture and the application of data for this study only .During question and answer sessions, if the participants were uncomfortable or preferred not to answer questions, they could withdraw participation from the research without the need to inform any reasons.

RESULTS

The demographic data showed that 79.4%of the sample were females, aged 39.74 years on average .They were married)63.4 (% and graduated with a bachelor's degree)65.5 .(%They were registered nurses)45.9 (%and had worked for 17.34 years on average.

With regard to knowledge about infectious waste management, 10.3%of them had a low level of knowledge, 24.2%had a moderate level of knowledge, and 65.5% had a high level of knowledge .

For attitude towards infectious waste management, 19.9%of them had a low attitude level, 55.2%had a moderate attitude level, and 14.9% had a high attitude level .

For motivation in infectious waste management, 18.4%of them had a low, level of motivation, 61.5% had a

moderate level of motivation, and 20.1%had a high level of motivation .

For support from executives in managing infectious wastes, 57.8% of them had a low level of support, 35.5%had a moderate level of support, and 6.7% had a high level of support .

Infectious waste management practice indicated that 25.1%of them had a low level of infectious waste management, 62.6%had a moderate level of infectious waste management, and 12.3%had a high level of infectious waste management) Table 1(.

The analysis of relationship between selected factors and overall infectious waste management

revealed that knowledge had a low level of positive relationship with infectious waste management with statistical significance ($r = 0.208$, $p = 0.004$); attitude had a low level of positive relationship with behavior in infectious waste management with statistical significance ($r = 0.256$, $p < 0.001$); motivation had a low level of positive relationship with behavior in infectious waste management with statistical significance ($r = 0.213$, $p = x\ 0.003$(, and support from executives had a moderate level of positive relationship with behavior in infectious waste management with statistical significance)r =0.354, $p<$ 0.001 ((Table 2).

Table 1 :Number and percentage of levels of knowledge, attitude, motivation, support from executives and infectious waste management (n =190).

Factors	Interpretation					
	High		Moderate		Low	
	Number	%	Number	%	Number	%

Knowledge about infectious waste management	124	(65.5)	46	(24.2)	20	(10.3)
Attitude towards infectious waste management	29	(14.9)	105	(55.2)	56	(19.9)
Motivation in managing infectious wastes	38	(20.1)	117	(61.5)	35	(18.4)
Support from executives in managing infectious wastes	13	(6.7)	67	(35.5)	110	(57.8)
Infectious waste management	23	(12.3)	119	(62.6)	48	(25.1)

Table 2 shows relationship between selected factors and infectious waste management)n =190 (

Selected factors	Infectious waste management	
	r	p-value
Age	0.015	0 .0.840
Duration of working time	-0.065	0.370
Knowledge about infectious waste management	0.208	0.004
Attitude towards infectious waste management	0.256	<0.001
Motivation in managing infectious wastes	0.213	0.003
Support from executives in managing infectious wastes	0.345	<0.001

DISCUSSION

The study results showed that 65.5%of the sample had a high level of knowledge about infectious waste management .This was probably because most of them graduated with a bachelor's degree, and received news and information related to infectious waste management from documents distributed by public health agencies .This was consistent with a study conducted by Natheewatana)2012 (which showed that 89.4% of the sample had knowledge about infectious waste management in public nursing and health care institutes. It was also in harmony with a study conducted by Rabiebdee)2018(which indicated a high level of knowledge about infectious waste management (70.3%). In contrast, a study conducted by Chaisoonthorn (2013) reported that knowledge about infectious waste management of personnel in nursing care institutes was at a low level (32.7%).

The study results revealed that 57.8%of the sample had a low level of support from executives in infectious waste management .This is probably caused by the fact that the

sample did not receive academic support and adequate equipment for infectious waste management .It was congruent with a study conducted by Poltamtim)2010 (who found the lack of supportive budget and policy for infectious waste management and no personnel was authorized to manage infectious wastes .However, this result was different from that of the study by Chaisoonthorn)2013 (in which owners of nursing and health care institutes reportedly provided a high level support for equipment in managing infectious wastes) $\overline{X}$ = 3.73).

The findings from the study also showed that 62.6% of the sample had a moderate level of infectious waste management .It was probably because the samples were in need of awareness and motivation in managing infectious wastes .This was consistent with a study conducted by Kamchom)2013 (who found a moderate level of infectious waste management of personnel in sub-district health promoting hospitals. Similarly, the study by Natheewatana)2012 (who found that 64.4%of the samples had correct practice of infectious waste management.

Moreover, the study results indicated that support from executives in managing infectious wastes had a moderate level of positive relationship with infectious waste management with statistical significance)r =0.354, $p < 0.001$.(This probably resulted from the fact that support in body of knowledge, materials and equipment in managing infectious wastes was necessary and allowed health personnel to have proper infectious waste management accordingly .Likewise, a study by Charasri)2015 (reported a positive relationship between the perception scores of policy and scores of practices in accordance with the standard precautions for infection prevention with statistical significance)r =0.51, $p < 0.001$(. However, this contradicted the study by Rabiebdee)2018 (which showed that support from executives and leading team in infectious waste

management had no relationship with infectious management of personnel in Kantang Hospital with statistical significance)r =0.194, p =0.23 .(

CONCLUSIONS

1. It was found that 25.1%of the samples had a low level of infectious waste management practice; 62.6%had a moderate level of infectious waste management practice, and 12.3%had a high level of infectious waste management practice .

2. Knowledge, attitude, motivation, and support from executives were related to infectious waste management with statistical significance)$p < 0.05$.(

3. Age and duration of working time had no relationship with infectious waste management.

SUGGESTIONS

Suggestions and implications

1 .Based on the study results, 20.1%of the samples had a low level of knowledge about infectious waste management while 25.1%had a low level of infectious waste management .Therefore, knowledge and revision of infectious waste management practice should be provided continually .

2 .From the study results, 18.4%had a low level of motivation in managing infectious wastes . Therefore, executives should build motivation by awarding and honoring health personnel who have efficient infectious waste management .

3 .From the study results, 57.8% had a low level of support from executives in managing infectious wastes .Thus, executives should formulate an outstanding policy and practical guideline for infectious waste management.

Suggestions for future research

1 .A study should be conducted on a model to manage infectious wastes produced by nursing care activities in communities .

2 .A study should be conducted on measures to reduce risks from infectious wastes in sub-district health promotion hospitals .

3 .A study should be conducted on

cost-effectiveness of infectious waste management to make a comparison between the implementation by sub-district health promotion hospitals and community networking hospitals.

ACKNOWLEDGEMENTS

The research team would like to express gratitude to the professors of the Faculty of Public Health, Ramkhamhaeng University who provided useful opinion until this research could be completely finished. The research team would like to thank all research participants who provided good collaboration and devoted their precious time to give information to the research team.

REFERENCES

Bureau of Environmental Health .2014 .A training manual for infectious waste practitioners, the course of prevention and suppression disease transmission or hazard from infectious wastes . Bangkok :Sam Charoen Panich)Bangkok (Co.,Ltd .

Jomjan Natheewatana .Knowledge and Behavior in Managing Infectious Waste in Public Nursing and Health Care Institutes :Journal for Public Health Research. 2012; 5)3 (47-56 .

Krejcie, R .V .& Morgan, D .W .1970 . Determining Sample Size for Research Activities .Educational and Psychological Measurement, 30)3 :(607-610.

Kitti Poltabtim .2010 .Situation of infectious waste management in health stations, Promburi district, Singburi province . Independent study-Master of Public Health Program, Major -Environmental Health and Occupational Health Management .Thammasat University .

Manager .2018 :online .1 year “Infectious wastes ”increased more than 1,700 tons .Retrieved on 1 February 2019 from https//:mgronline.com/qol/detail/9600000128764 .

Pollution Control Departmebt .2017:onlin .(Action Plan”Thailand Zero Waste ”in accordance with “Pracharat ”Scheme for 1 year)2016 –2017 .(Retrieved on 1 February 2019, from www.dla.go.th .

Prachumporn Kaweekorn et al .Model Development of Waste Management in Yasothon Province. Community Health Development Journal .2017; 5)4 :(703-728.

Suthinan Chantanakul .2018 :online . Infectious wastes .Retrieved on 1 February 2019 from https//:www.ayo.moph.go.th

Teepaka Chaisoonthorn .2013 .Study on

Infectious Waste Management :Case Study of Private Nursing and Health Care Institutes providing overnight stay for patients in Pattaya City Municipality, Chonburi province . Thermatic Paper-Master of Science in Building Technology Management . Dhurakij Pundit University .

Teerawat Kamchom .2013 .Model Development of Infectious Waste Management in Sub-District Health Promotion Hospitals in Phetchabun Province .Dissertation-Doctor of Philosophy in Environmental Study, Mahasarakham University .

Ubon Charasri, Pipat Laksameejarankul, Dusit Sujirarat, and Nara Kulwannawijit .Policy perception and Practice in accordance with the Standard Precautions for Infection Prevention of Personnel in Provincial Hospital .Public Health Journal .)Special Issue .(2015 : 3-17 .

Warunee Rabiebdee . 2018 . Factors associated with infectious waste management of personnel in Kantang Hospital, Kantang district, Trang province .Independent study-Master of Public Health Program in Public Health Administration, Ramkhamhaeng University.

Life Cycle Assessment of Nang Lae Pineapple Productio

Phanuphat Oonkasem[1], Bhanupong Phrommarat[1*], and Dirakrit Buawech[1]

[1] Department of Environmental Science, Faculty of Science, Silpakorn University Sanamchandra Campus, Nakhon Pathom 73000;
Corresponding author email: b.phrommarat@gmail.com

ABSTRACT

Pineapple is a fruit of economic importance in Thailand. Pineapple products contributed national income over 28,000 million baht/year from their export value during 2014-2018. In the northern region of Thailand, Nang Lae pineapple is considered to be a famous variety which is mainly cultivated locally in Nang Lae Subdistrict, Muang District, Chiang Rai province. Apart from its economic value, pineapple production, like other agricultural activities, is normally associated with different environmental impacts arising from agricultural inputs and the use of natural resources. Therefore, this study aimed to focus on assessing environmental impacts from different stages of Nang Lae pineapple production using life cycle assessment (LCA). The objective of the study was to assess the environmental impacts of growing Nang Lae pineapple throughout its life cycle considering from raw material extraction to harvesting (cradle-to-farm-gate). The results indicated that the use of nitrogen fertilizer or urea fertilizer in Nang Lae pineapple cultivation caused the greatest impact on all categories. It contributed to the overall results ranging from 40% to 70%. In terms of endpoint indicators, the damage on resources was found to be highest (2.37E-12 pt) as a result of fossil fuels utilization in nitrogen fertilizer production.

Keywords: Life cycle assessment, Nang Lae pineapple, Environmental impact

INTRODUCTION

Pineapple is a fruit of economic importance in Thailand. Various products from pineapple are exported every year such as fresh pineapple, dried pineapple, canned pineapple and pineapple juice. Pineapple products contributed national income over 28,000 million baht/year from their export value during 2014-2018 (OAE, 2018). In the northern region of Thailand, Nang Lae pineapple is considered to be a famous variety which is mainly cultivated locally in Nang Lae Subdistrict, Muang District, Chiang Rai province and has been registered to be geographical indication with good taste and specific identity for local plant to make it to be favorite fruits and on need of both domestic and international markets. (Kamhangwong and Auttarapong, 2012). The total area of pineapple cultivation in Chiang Rai province in 2016 was 2,474.08 ha covering 9 districts (OAE, 2016).

However, pineapple growers in Chiang Rai province encounter problems in various aspects such as low yield and low quality of pineapple, lack of knowledge in farm planning, low selling prices, high production costs and farmers' debts. In addition to social and economic problems, pineapple cultivation also brings a variety of environmental problems such as greenhouse gas emissions, ecotoxicity, acidification and eutrophication. Pineapple production, like other agricultural activities, is normally associated with different environmental impacts arising from agricultural inputs such as chemicals, pesticides, fertilizers and fuels, and the use of natural resources including water and soil. These factors lead to direct and indirect impacts on the environment. Therefore, identifying causes and environmental impacts from production activities and factors is important for finding ways to improve the production process in order to reduce environmental impacts. Moreover, reducing the

impact on the environment will also result in a reduction of production costs due to the decrease of unnecessary resources and lessening the impact on society in terms of the public health from avoiding the use of substances that cause toxicity to humans. One of the environmental management tools that can assess the overall environmental impacts in different stages of a product is “Life Cycle Assessment (LCA)”. LCA involves tracing out the major stages and processes involved over lifecycle of a product or process covering raw materials extraction, manufacturing, product use, recycling and final disposal, by identifying and quantifying relevant environmental impacts on each stage. In addition, it aims to facilitate a systematic view in product and process evaluation (Joshi, 2000) and can be considered as one of the major approaches in the field of industrial ecology (Udo De Haes, 2002).

There are some previous studies focusing on assessing environmental impact assessment of fresh pineapples using life cycle assessment. A farm-to-shelf study conducted in Costa Rica found that the environmental impacts of fresh pineapple resulted mainly from the cultivation process caused by the production of fertilizers and the use of nitrogen fertilizer as well as the use of diesel and the use of pesticides in pineapple cultivation (Ingwersen, 2012). It is consistent with a study in Ghana that assessed of greenhouse gas emissions by using life cycle assessment and identified that the cultivation process had the highest greenhouse gas emissions from the production and use of fertilizer (WAFF, 2011). In the Philippines, a cradle-to-gate study was conducted in order to assess the impact of pineapple production and also indicated that nitrogen fertilizer accounted for the largest contribution (45%) of carbon emissions (De Ramos et al., 2018). In addition to fresh pineapple, an LCA study on processed pineapple product namely, concentrated pineapple juice and

canned pineapple, was also executed. The results showed that the emission of carbon dioxide per kilogram of the product from the production of concentrate pineapple juice (1,235 $kgCO_2$ eq.) is higher than that from the production of canned pineapple (1,089 $kgCO_2$eq.) (Paisoontornsuk, 2010). A comparative study of pineapple juice and orange juice in Thailand revealed that orange juice had higher impact than pineapple juice, and a small container, 200 ml, had a higher impact per liter than a bigger container, 1,000 ml due to the use of raw materials and energy consumption to produce bigger containers (Tanaparisutti, 2010).

According to literature review, it found that the case studies on LCA of fresh pineapple in Thailand are relatively scarce compared to other agricultural products such as rice, cassava, and sugarcane. Therefore, the main objective of this study was to assess the impacts of growing Nang Lae pineapple on the environment throughout its life cycle in order to improve environmental performance of pineapple production as well as to find an opportunity to reduce the cost of cultivation.

METHODOLOGY

Goal and scope definition

In this study, environmental hotspots of Nang Lae pineapple cultivation throughout its life cycle under a "cradle-to-farm-gate" system boundary, considering from land preparation to harvesting process, were identified. The framework of LCA was designed in accordance with ISO14040 standard series. The product system consisting of three main stages are displayed in Figure 1. The intended audience of this study was pineapple farmers that can use the results to improve the production process and lower environmental impacts. The selected functional unit was one kilogram of fresh Nang Lae pineapple harvested at the farm.

The study was undertaken in the cultivation year of 2018. Primary data related to production processes

such as use of fertilizers, agrochemicals, fuels, and the total amount of production, etc., were obtained by questionnaires. These were derived from three major pineapple producers in Nang Lae sub-district, Mueang District, Chiang Rai, a northern province of Thailand. The total land owned by the three producers and used for Nang Lae pineapple cultivation covered 4.8 ha with an average Nang Lae pineapple yield of 2,145 kg/ha. Secondary data such as fertilizers production, diesel production and pesticide production or other data under background systems was drawn from literature along with the LCI database, Ecoinvent version 3.3. The database was used to connect the system flows and process flows to the product system in order to calculate the life cycle impact assessment (LCIA) results based on the local data (Chandra et al., 2018)

Life cycle inventory

As mentioned before, the considered product system comprised three main phases, namely, land preparation, pineapple cultivation, and harvesting. All relevant parameters in each process are illustrated in Table 1. Acquisition of data and assumptions used in the analysis for each life cycle stage are described as follows:

1. Land preparation

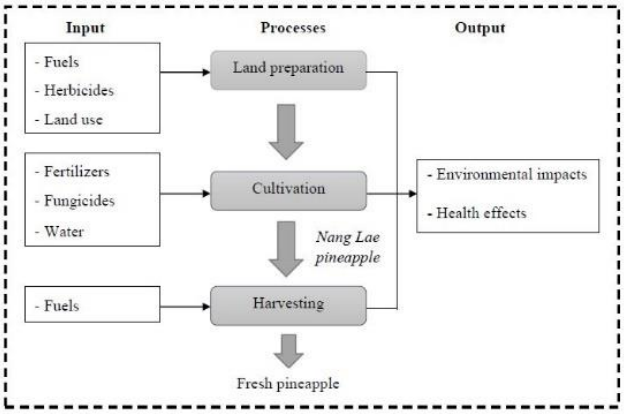

Inputs in this stage were diesel used in agricultural machinery for tillageby a walk-behind power tiller and mowing by a backpack lawn

Figure 1 System boundary of Nang Lae pineapple production.

mower. After tillage, an herbicide, glyphosate, was applied to control weeds such as Kunai grass, Coco grass and Giant sensitive. Emissions in this stage included air emissions caused by the combustion of diesel in agricultural machinery and soil emissions from herbicide use.

2. Cultivation

The principal source of water used on the farm was from rain. Therefore, the amount of water use in this stage was excluded. The considered inputs in this stage included chemical fertilizers and fungicide during planting and maintaining. The chemical fertilizers used were 46-0-0 and 16-20-0 formula fertilizers to provide essential nutrients for the crops. The fungicide used by the farmers was fosetyl-aluminum to prevent rot. As for the output side, emissions associated with the production and use of chemical fertilizers and fungicides were taken into account.

3. Harvesting

Human labor was employed to harvest ripe fruits; therefore, it was assumed that there was no environmental impact occurring in this phase. Nonetheless, after harvesting, the products were transported to local buyers by a small-sized truck or pick-up truck. A distance was assumed to be 10 km. Environmental emissions in this stage was mainly caused by the combustion of diesel in the transportation.

Life cycle impact assessment

Inventory analysis and impact assessment of the product system were modelled by OpenLCA software version 1.6.3, developed by GreenDelta (GreenDelta, 2018), along with the LCI database, Ecoinvent version 3.3. The environmental impact method adopted in the analysis was ReCiPe (Goedkoop el al., 2009); the most recent indicator approach integrated the CML and Eco-Indicator ’99 methods. The method classifies indicators at two levels: 17 midpoint indicators and three endpoint damage categories.

Table 1 Summary of pineapple farm data

Stage	Item	Unit	Data range	Average
Land preparation	Agricultural machinery			
	- Tillage	ha	0.16	0.16
	- Mowing	ha	0.16	0.16
	Glyphosate	g	192	192
Cultivation	Fertilizers			
	- N	kg	31-70	49
	- P	kg	10	3.33
	- K	kg	0	0
	Fosetyl-Al	g	80	80
Harvesting	Transportation	km	10	10
	Fresh pineapple	kg	2,050-2,215	2,145

RESULTS AND DISCUSSION

The life cycle impacts of 1 kg of Nang Lae pineapple from land preparation to harvesting was assessed by ReCiPe Endpoint (Hierarchist; H) method normalized and weighted based on an average world environmental impact for the year 2000 (World ReCiPe H/H, 2000). The results of impact assessment was divided into two levels: results of characterization under damage assessment groups (midpoint), and results of the weight indicators (endpoint).

Characterized indicator results

There were 17 categories assessed as the midpoint indicators, namely; climate change (CC), freshwater

ecotoxicity (FET), freshwater eutrophication (FE), marine ecotoxicity (MET), terrestrial acidification (TA), terrestrial ecotoxicity (TET), agricultural land occupation (ALO), natural land transformation (NLT), urban land occupation (ULO) , human toxicity (HT), ionizing radiation (IR), ozone depletion (OD), particulate matter formation (PMF), photochemical oxidant formation (POF), fossil depletion (FD), and metal depletion (MD). Impact assessment results of characterization indicators were listed in Table 2. The impact on climate change showed the highest score in human health damage categories while the impact on fossil depletion was the most dominated impact in the resources damage category. It is consistent with the previous research conducted by WAFF (2011) pointing out that the cultivation process had the highest greenhouse gas emissions from the production. The contribution of the various processes to the midpoint indicators were illustrated in Figure 2. It was found that the use of N-fertilizer in the cultivation was the key contributor showing the highest impact on all midpoint indicators. It contributed to the overall results ranging from 40% to 70% due to the production and use of nitrogen fertilizer or urea fertilizer in Nang Lae pineapple cultivation causing environmental emissions to soil, water and air. The production of nitrogen fertilizer was an energy and material intensive process. In addition, an excess of nitrogen is ingested into the environment in reactive forms such as nitrate (NO_3), ammonia (NH_3), and nitrogen oxides (NO_x and N_2O) and subsequently effluents into the environment causing an impact on eutrophication, acidification of soils, air quality degradation, enhancement of global climate change, and impairing human and environmental health (Bashir et al., 2013). Apart from N-fertilizer, transportation and machinery operation in tillage were likely to play important roles in causing the overall impact results. The

environmental impacts from transportation and tillage were directly associated with the combustion of diesel that releases various types of air pollutants found in diesel exhaust such as carbon monoxide (CO), nitrogen oxides (NO_x), sulfur dioxides (SO_2), hydrocarbon (HC) and particulate matter (PM).

Table 2 Impact assessment results of characterization indicators

Climate Change	**DALY**	**Human health**	**1.12E-07**
Human toxicity	DALY	Human health	2.77E-08
Ionizing radiation	DALY	Human health	1.21E-10
Ozone depletion	DALY	Human health	2.59E-11
Particulate matter formation	DALY	Human health	8.42E-08
Photochemical oxidant formation	DALY	Human health	2.16E-11
Fossil depletion	USD	Resources	4.26E-03
Metal depletion	USD	Resources	4.85E-04

Nitrous oxides, in particular, are the primary pollutants that can create low-level ozone leading to photochemical smog, acid rain and nitrate particulates. Nitrous oxides also have effects on human health, for example, aggravating heart and lung problems and increasing the susceptibility to respiratory infection (DES, 2014). Particulates from the combustion adversely affect plant growth and damage soil structure and property. Moreover, black carbon particulates can act as greenhouse agent as it absorbs heat wave leading to atmospheric warming. Short term exposure of particulates aggravates heart and lung problems while long-term exposure can lead to the development of heart and lung diseases (DES, 2014).

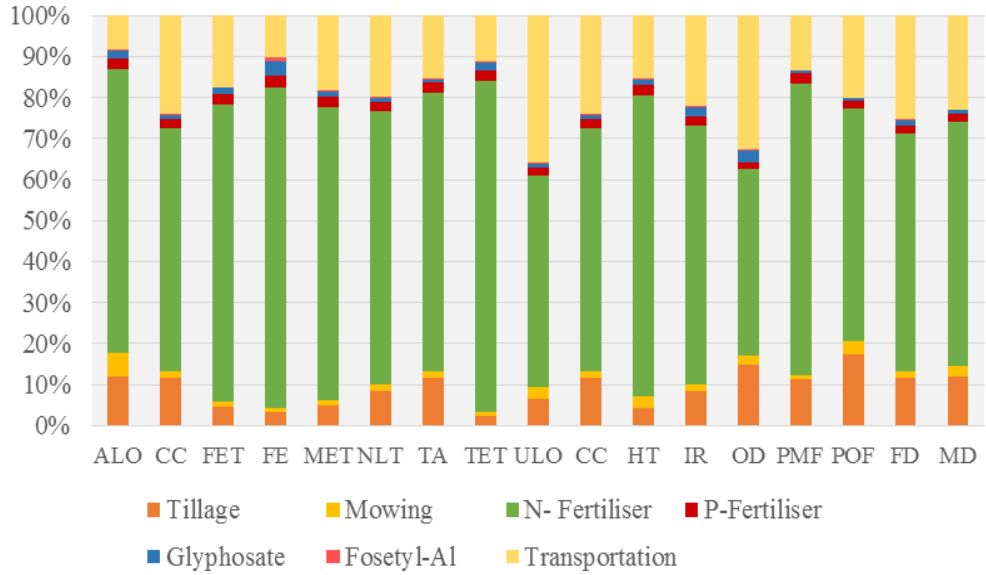

Figure 2 Impact assessment result of midpoint characterization indicators.

Impact category	Unit	Damage category	Amount
Agricultural land occupation	species.yr	Ecosystems	4.77E-11
Climate Change	species.yr	Ecosystems	6.32E-10
Freshwater ecotoxicity	species.yr	Ecosystems	9.25E-13
Freshwater eutrophication	species.yr	Ecosystems	1.73E-12
Marine ecotoxicity	species.yr	Ecosystems	1.81E-13
Natural land transformation	species.yr	Ecosystems	8.01E-11
Terrestrial acidification	species.yr	Ecosystems	3.14E-12
Terrestrial ecotoxicity	species.yr	Ecosystems	3.45E-12
Urban land occupation	species.yr	Ecosystems	3.45E-11

Table 3 Weighted results of the damage categories.

Damage category	Unit	Amount
Ecosystems	pt	6.58E-14

Human health	pt	7.26E-13
Resources	pt	2.37E-12
Total	**pt**	**3.17E-12**

Weighted indicator results

In the endpoint assessment, the midpoint results were normalized and weighted into three main damage categories including ecosystems, human health, and resources. The total impact from all those were also weighted and determined in terms of single score impact or point (pt). The weighted results of the damage categories were shown in Table 3. The total damage score was 3.17E-12 pt. Most of the total score originated from the damage on resources that was 2.37E-12 pt as a result of the use fossil fuels, including coal, oil and natural gas, utilization in nitrogen fertilizer production as well as from diesel used in transportation and agricultural machinery. As for ecosystems and human health damages, the impact of climate change was the dominant indicator in both damages as a consequence of greenhouse gas emissions from fossil fuels combustion.

CONCLUSIONS

The environmental impacts of Nang Lae pineapple determined under the life cycle approach revealed that the use of nitrogen fertilizer in the cultivation process was the key environmental hotspot. The results seemed to be consistent with the previous studies (Ingwersen, 2012) indicating that N-fertilizer plays a significant role in causing environmental effects in the pineapple production. However, the absolute values of environmental impact can be varied according to different influencing factors such as production factors, crop yield and mean of transportation. This study is an initial stage of pineapple LCA study in Thailand and can be beneficial to fulfill the information of the life cycle environmental impacts of pineapple, improve environmental performance of pineapple production and reduce the cost of cultivation.

Further suggestions can be made based on the result to reduce environmental impacts on cultivation stage such as using the optimal amount of nitrogen fertilizers by analyzing soil nutrients before applying and considering organic fertilizer to substitute chemical fertilizer at an optimal quantity.

ACKNOWLEDGEMENTS

Authors would like to thank Department of Environmental Science, Faculty of Science, Silpakorn University for facilitating research materials and financial support and Nang Lae pineapple farmers who provided some useful data used in this study.

REFERENCES

Bashir MT, Ali SB, Ghauri B, Adris A, Haroon R. Impact of Excessive Nitrogen Fertilizers on the Environmental and Associated Mitigation Strategies. Asian Journal of Microbiology, Biotechnology and Environmental Sciences 2013; 15(2):213-221.

Basosi R, Spinelli D, Fierro A, Jez S. Mineral Nitrogen Fertilizers: Environmental Impact of Production and Use. 1st ed. Publisher: NOVA Science Publishers; 2014.

Chandra VV, Hemstock SL, Mwabonge ON, Ramon N'Yeurt AD, Woods J. Life Cycle Assessment of Sugarcane Growing Process in Fiji. Sugar Tech 2018;20(6):692–699.

De Ramos RMQ, Taboada EB. Cradle-to-Gate Life Cycle Assessment of Fresh and Processed Pineapple in the Philippines. Nature Environment and Pollution Technology 2018;17(3):783-790.

Department of Environment Services (DES). Diesel Vehicles and Equipment: Environmental and Public Health Impacts. Environmental Fact Sheet. Concord, New Hampshire; 2014.

Goedkoop M, Heijungs R, Huijbregts M, Schryver AD, Struijs J, van Zelm R. ReCiPe 2008: A Life Cycle Impact Assessment Method which Comprises Harmonized Category Indicators at the Mid-point and the Endpoint Level. 1st ed. Netherlands: National Institute for Public Health and the Environment; 2013.

GreenDelta. Software: Tools for supporting your work [Internet]. 2018 [cited 3 Sep 2018]. Available form: https://www.greendelta.com/software/.

Ingwersen, WW. Life cycle assessment of fresh pineapple from Costa Rica. Journal of Cleaner Production 2012;35:152-163.

Joshi S. Product Environmental Life Cycle Assessment Using Input Output Techniques. Journal of Industrial Ecology 2000;3(2−3):95−120.

Kamhangwong D, Auttarapong D. Affected Cognitive consumer of Phulae and Nanglae pineapple identities on packaging design for retailing. Naresuan Phayao Journal 2012;5(3):269-301.

Office of Agricultural Economics (OAE). Annual Pineapple Production Report in 2016. Bangkok: Office of Agricultural Economics (of Thailand); 2018.

Office of Agricultural Economics (OAE). Export Statistics Report in 2015-2018. Bangkok: Office of Agricultural Economics (of Thailand); 2018.

Paisoontornsuk P. Environmental Evaluation of Canned Pineapple and Concentrate Pineapple Juice. Master of Engineering (Energy and Environmental Technology Management, Thammasat University); 2010

Tanaparisutti P. Life Cycle Assessment of Pineapple and Orange Juice in Thailand. Master of Science (Environmental Technology and Management, Kasetsart University); 2010.

Udo De Haes, H.A. Industrial ecology and life cycle assessment, in R.U. Ayres and L.W. Ayres (eds.). Handbook of Industrial Ecology. Cheltenham, United Kingdom: Edward Elgar; 2002.

West Africa Fair Fruit (WAFF). Summary of Studies on Environmental Performance of Fresh Pineapple Produced in Ghana for Export to Europe [Internet]. 2011 [cited 18 May 2018]. Available form: http://www.twinn.com.au/pdf/C-footprint-of-pineapple-production-and-transport-WAFF.pdf.

Identification sources of PM2.5 in Thepha, Songkhla Province, Southern Thailand

Muanfun Inerb[1], Worradorn Phairuang [1,2*], Racha Dejchanchaiwong [2,3]
Perapong Tekasakul[2,4], and Surajit Tekasakul[5]

[1]Faculty of Environmental Management, Prince of Songkla University, Hat Yai, Songkhla, 90112, Thailand
[2] Air Pollution and Health Effect Research Center, Prince of Songkla University, Hat Yai, Songkhla, 90112, Thailand
[3] Department of Chemical Engineering, Faculty of Engineering, Prince of Songkla University, Hat Yai, Songkhla, 90112, Thailand
[4]Department of Mechanical Engineering, Faculty of Engineering, Prince of Songkla University, Hat Yai, Songkhla, 90112, Thailand
[5] Department of Chemistry, Faculty of Science, Prince of Songkla University, Hat Yai, Songkhla, 90112, Thailand
*Corresponding author: e-mail: worradorn.p@psu.ac.th

ABSTRACT

Particulate Matters diameter less than 2.5 microns ($PM_{2.5}$) were collected seven samples (July-October 2018) in every 7 days by using DustDETEC sampler and operated with 7 liters/minute of flow rate. The results showed two locations (four stations) in Thepha city, Songkhla, Thailand. The highest monthly data in July from community areas (15.17 ± 7.65 µg/m^3) that higher than non-community areas (14.21 ± 9.82 µg/m^3). Emission sources of $PM_{2.5}$ were identified by water-soluble ionic species (K^+, Na^+, Mg^{2+}, Ca^{2+}, NH_4^+, SO_4^{2-}, NO_3^- , and Cl^-) as well as heavy metals (Cr, Co, Pb, Cd, Ni, Mn, and As) using Principle Component Analysis (PCA).

Factor loading is rotated into four sources in non-community areas including mixed source of soil dust (SD) and secondary aerosols (SA), industrial emissions (IE), mixed source of biomass burning (BB) and Sea salt (SS) and

mixed source of vehicular emissions (VE) and BB. While community areas related to five sources including SD+VE, BB+SA, IE, IE+SA and SS.

We were reporting the mass concentration data through an online monitoring system relied on the website in order to rapid report to the community. Moreover, this study can be used to lead guidelines in the best practices of air pollution policy in Thailand.

Keywords: Emission sources, Songkhla, PM 2.5, Online Monitoring

INTRODUCTION

Air pollution is one of the serious environmental problems in Thailand. The composition of particulate matters (PM) depends on their sources, atmospheric chemical process as well as meteorological conditions (Jain et al., 2018). However, they are generally chemical complexity and dynamic mixtures of solid and liquid particles. (Browne et al., 1999) The composition of PM including organic carbon (OC), elemental carbon (EC), ammonium, nitrates, sulfates, mineral dust, and other trace elements, which can be produced by natural or anthropogenic activities (Jain et al 2017). Particulate Matters diameter less than 2.5 microns (PM2.5) that can be contaminated with non-toxic and toxic elements are directly linked to inhalation who spend a long time in outdoor activities and can deeply penetrate into the lungs and can remain there for a substantial time. (Santoso et al., 2008).

The Southern Thailand experiences smoke and haze problems which are caused by many emission sources. However, Thepha area, Songkhla Province, Southern Thailand has not so far been studied about the air quality. The motivation of this study is to investigate the physical and chemical characteristic of PM2.5. The mass concentration was investigated for hourly, daily and monthly data by DustDETEC sampler in Thepha, Songkhla Province and vicinities. In order to

identify their sources, the water-soluble ionic species: WSI (K^+, Na^+, Mg^{2+}, Ca^{2+}, NH_4^+, SO_4^{2-}, NO_3^- and Cl^-) and heavy metals: HM (Cr, Co, Pb, Cd, Ni, Mn, and As) were categorized by Principle Component Analysis (PCA). This study will help to lead guidelines in the best practices of air pollution policy in southern Thailand.

METHODOLOGY

Sampling sites

All sampling sites are located in rural areas (the site far from cities, low buildings, and the population density is less than 10,000 people and mainly have farming or agricultural areas). The stations can divide into four stations into two areas. The sampling sites were shown in figure1, station 01 Thepha beach (TPB) (6°51.714'N, 100° 59.163'E) and station 03 Wangyai (WY) (6°43.076' N, 100°51.347'E) are located in non-community areas. Instead, station 02 Songkhla Community College (SKCC) (6°49.543'N, 100°58.022'E), and station 04 Pattani (PN) (6°52.891'N, 101°14.208'E) are located in community areas.

PM2.5 sampling

The samples were collected seven samples (July-October 2018) in every seven days with quartz filter (Pallflex Products Corp, 2500 QAT-UP) and stored in a refrigerator at -4 ^{0}C after sampling. All filters were pre-baked (350 ^{0}C for 1 hour), before and after weight by an analytical microbalance (Sartorius BT25S) and stabilizing control under temperature (25 ^{0}C) and humidity (40%).

PM2.5 were sampling using by DustDETEC sampler using electrostatic charge measurement of particle**.** PM is passed through the PM2.5 impactor and to remove PM outside (the measurement range particles with diameter larger than 2.5 μm), the flow system controlled with 7 liters/minute. PM2.5 directly introduced into particle charger to the attachment of ions produced by the corona discharge, the ions are transported by an electric field and measured electrically in a Faraday

cup electrometer. Then the developed sensor can also be controlled and sampled by a personal computer through a USB port cable. The software was developed based on Visual Basic programming and able to display both size distribution and mass concentration. (Intra et al., 2013) All data is through an online monitoring system relied on the website in order to rapid report to the community.

Chemical analysis

The sample filters and blank filters were used to analyze for WSI and HM. Half of each filter was determined WSI-cation (K^+, Na^+, Mg^{2+}, Ca^{2+}) and heavy metals (Cr, Co, Pb, Cd, Ni, Mn, As) by Inductively Coupled Plasma Optical Emission Spectrometer (ICP-OES) (PerkinElmer, AVIO 500) at central equipment division, faculty of science, Prince of Songkla University (PSU). The extracted 2 mL 65% $HNO_3^-$for 1 hour, 0.5 mL 30% H_2O_2 for 30 min and digested in a water bath at 95°C and diluted 10 ml.

One-fourth of each filter was determined NH_4^+ and WSI-anion (SO_4^{2-}, NO_3^- , and Cl^-), extracted 25 mL with ultrapure water, inside the with vial bottles using membrane Filter, 0.45 µm pore size 47 mm diameter. Extracted sample 5 ml prepare to determine NH_4^+ using Ammonium Test-kit (Merck) by Photometric method at central equipment division, faculty of science, PSU. After that, the extracted samples 20 ml for WSI-anion (SO_4^{2-}, NO_3^- and Cl^-) were determined by Ion Chromatograph (DIONEX, DX-500,) under in house method CSE-SIS-WI-WA-12 Base on Standard method for the examination of water and wastewater, APHA, AWWA, WEF 22nd Edition 2012, part 4110 B at The Center of Scientific and Technological equipment, Walailuk University.

Source identification using PCA

Principle Component Analysis (PCA) is a statistical technique that identify pattern in all data (Jain et al,

2017), the correlation between chemical composite of PM and factors (sources) by Linear Combination (Hirunkam.2013). A total of seven samples and fifteen species was performed by OriginPro 8.6 to identify their sources of PM2.5.

RESULTS AND DISCUSSION

Physical characteristic: Mass concentration of PM2.5

The monthly averaged data, daily data, and hourly data at two locations (four stations) are listed in Figure 2. The results showed the comparison between community areas (15.17 ± 7.65 µg/m³) that higher than non-community areas (14.21 ± 9.82 µg/m3) in Figure 2a. The highest monthly data found in July from TPB (16.15 ± 10.98 µg/m³) and WY (10.98 ± 8.65 µg/m³). In community areas, SKCC found the highest monthly data in July (15.53 ± 6.89) and PN had the highest monthly data in September (18.48 ± 8.01) in Figure 2b. All averages of daily data are lower than Thailand NAAQS (PM2.5 concentration below 50 µg/m³ for 24 hours), but the average concentration in WY (day 13 to 15 and 27) and PN (day 7). The concentrations of PM2.5 were 30.02, 36.76, 30.00 25.79 and 30.09, µg/m^3, respectively, which higher than WHO standard (25 µg/m³ per 24 hours) in Figure 2c.

Hourly data in non-community, especially TPB ranged during 11:00-13:00 am from household activities. On the other hand, WY and community areas as SKCC and PN during 7:00-9:00 am and 18:00-20:00 pm from community activities and traffic prime time in Figure 2c.

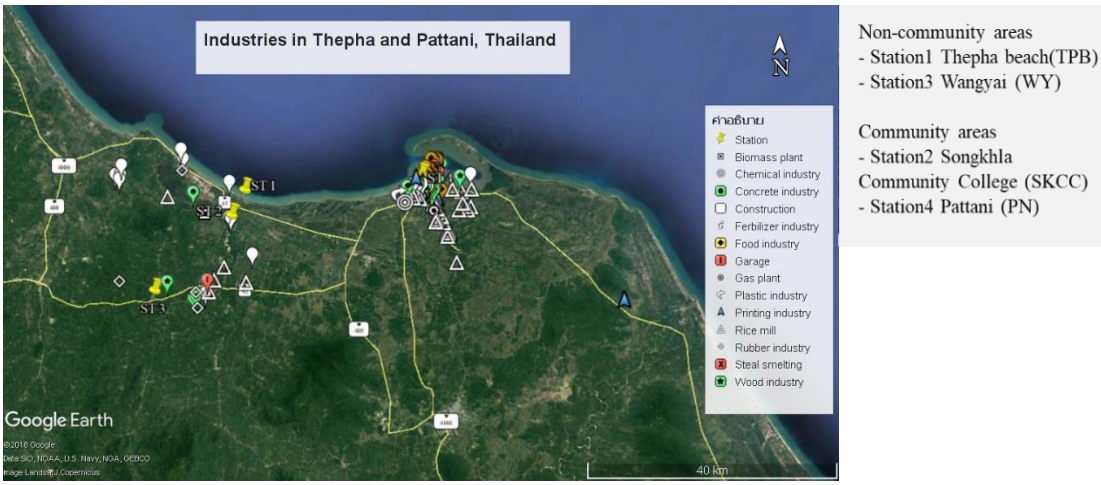

Figure 1 Industrial factories and sampling site 4 stations into 2 locations.

Chemical characteristic: WSI and heavy metals

In this study, WSI and heavy metals are shown in Table1 and **Figure 3** the highest fractions of chemical composites and WSI are SO_4^{2-}. The concentrations in TPB, WY, SKCC, and PSU were 1413.39 ± 688.20 (43%), 986.50 ± 1166.70 (49%), 1128.42 ± 1106.67 (31%) and 1252.47 ± 1000.80 (46%) ng/m^3, respectively. SO_4^{2-}, NH_4^{+}, and Ca^{2+}. SO_4^{2-} , NH_4^{+}, and Ca^{2+} are dominated chemical composite in all areas because SO_4^{2-} , NH_4^{+} were secondary pollutants formed many compounds in the atmosphere involved by a photochemical process. Ca^{2+} was higher at SKCC (938.14 ± 517.99 ng/m^3) that community areas from soil dust were dominated contributor of Ca^{2+} in the atmosphere (Chen et al.,2019).

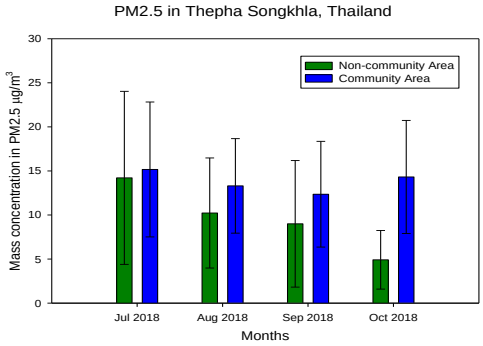

(a.) Comparison of PM2.5 in two locations

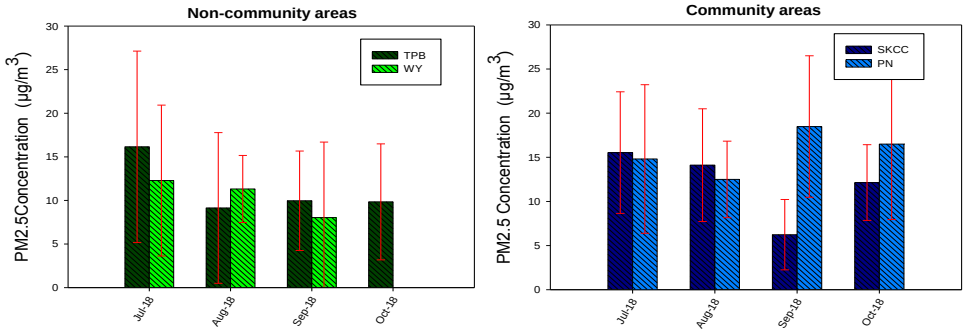

(b). Monthly Averaged data

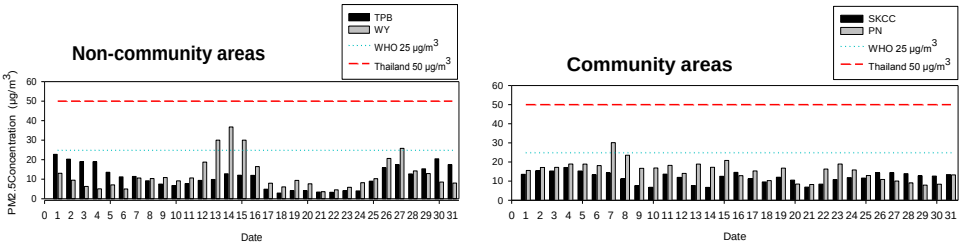

(b.) Daily Averaged data

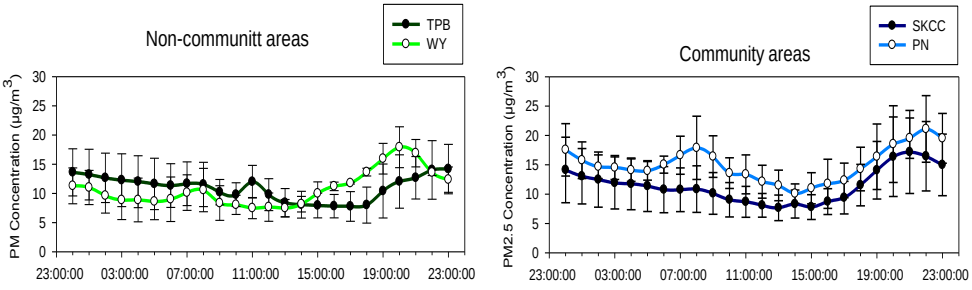

Hourly Averaged data

Figure 2 The monthly daily and hourly averaged data in 2 locations

Table 1 Chemical composite of PM2.5 in July-October 2018

Chemical composite		Non-community areas				Community areas			
		TPB		WY		SKCC		PN	
		Average	SD	Average	SD	Average	SD	Average	SD
Heavy metals (ng/m^3)	As	0.78	0	0.20	0.39	1.17	0	0.59	0.83
	Cd	LD	LD	0.16	0.35	LD	LD	LD	LD
	Co	0.78	0	0.39	0.65	0.78	0	0.52	0.45
	Cr	4.43	4.18	0.78	1.21	1.56	0	LD	LD
	Mn	5.08	6.53	4.69	6.03	7.35	5.01	8.60	9.97
	Ni	7.43	9.59	0.94	1.89	2.54	3.04	19.75	26.64
	Pb	LD	LD	1.37	2.74	LD	LD	0.98	1.38
WSI (ng/m^3)	K^+	70.40	48.50	18.62	29.97	63.36	51.35	92.99	88.56
	Ca^{2+}	526.47	671.52	222.23	373.31	938.14	517.99	377.37	482.12
	Mg^{2+}	202.80	265.23	86.90	151.61	296.09	172.92	138.93	206.14
	Na^+	133.77	203.43	95.72	153.96	319.79	225.98	172.38	216.21
	NH^{4+}	530.83	227.07	433.04	513.02	564.35	394.13	511.27	324.59
	Cl^-	262.71	194.94	179.92	354.41	145.00	53.17	147.23	158.69
	NO_3^-	163.72	433.16	LD	LD	143.60	379.94	LD	LD
	SO_4^{2-}	1413.39	688.20	986.50	1166.70	1128.42	1106.67	1252.47	1000.80

LD = Lower than Limits Detection

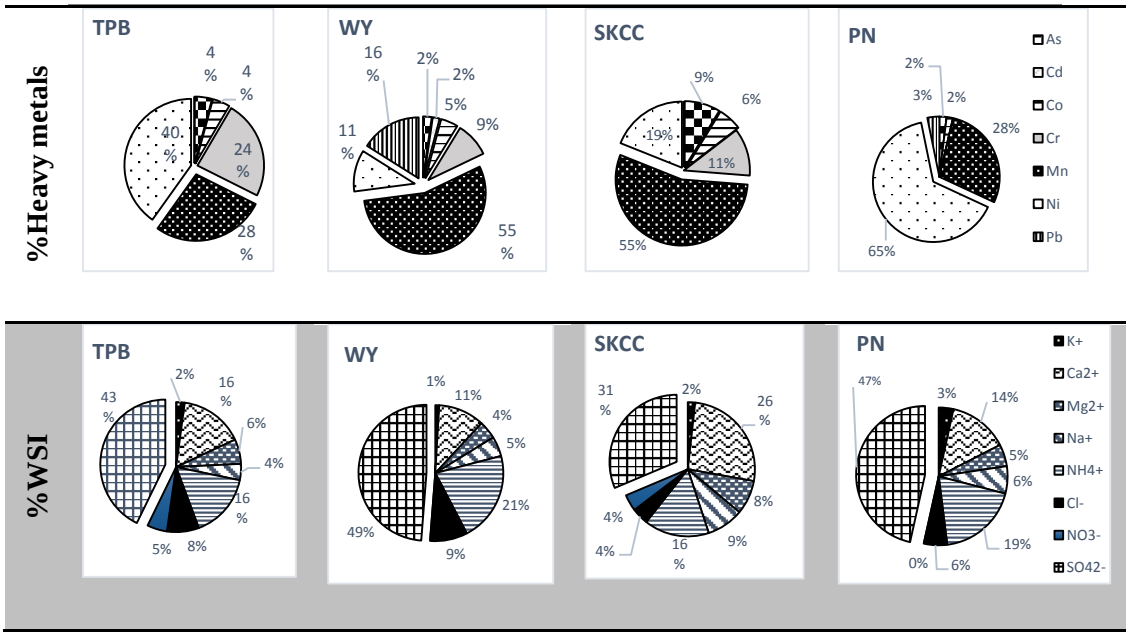

Figure 3 Ratio of chemical composite in PM2.5 from four stations.

The fraction of heavy metals in TPB dominates in Ni, Mn, Cr, and Co that it is similar to SKCC site. While WY station dominates Ni, Mn, Pb, Ni, and Cr that it is similar to PN station. The main source of air pollution in Thepha areas mainly originate from human sources including construction, paint and melting metal nearby the station. Pb levels at suburban locations tend to be lower than at urban or industrial sites, but it can still be substantial. Pb concentration mainly in fine particles, implying that emissions from combustion and other industrial processes are probably the most important sources of ambient air (Li et al., 2010).

Table 2 Source identification of PM2.5 into two locations (four stations)**.**

Chemical composite	Non-community areas							Community areas					
	ST.1 TPB				ST.3 WY			ST.2 SKCC			ST.4 PN		
	PC1	**PC2**	**PC3**	**PC4**	**PC1**	**PC2**	**PC3**	**PC1**	**PC2**	**PC3**	**PC1**	**PC2**	**PC3**
As	-0.03	-0.39	**0.49**	0.31	0.04	0.1	**0.69**	0.06	0.27	**0.48**	0.09	**0.54**	-0.02
Cd	0.00	0.00	0.00	0.00	**0.31**	-0.17	-0.18	0.00	0.00	0.00	0.00	0.00	0.00
Co	0.27	**-0.32**	**0.31**	0.25	0.19	0.01	**0.58**	0.25	-0.17	**0.60**	**0.33**	0.25	-0.08
Cr	-0.01	**0.56**	**0.35**	-0.02	0.13	**0.48**	-0.30	0.00	0.00	0.00	0.00	0.00	0.00
Mn	**0.37**	-0.03	0.16	0.13	**0.32**	0.08	0.12	**0.42**	0.01	0.17	0.26	**0.37**	-0.13
Ni	0.03	**0.57**	**0.32**	0.00	**0.31**	-0.16	-0.12	**0.37**	-0.23	0.03	0.15	**0.50**	-0.01
Pb	0.00	0.00	0.00	0.00	**0.31**	-0.17	-0.18	0.00	0.00	0.00	**0.33**	-0.23	-0.09
K^+	0.16	-0.20	0.00	**-0.81**	**0.32**	-0.13	0.07	0.11	**0.48**	-0.04	**0.35**	0.07	-0.16
Ca^{2+}	**0.38**	0.01	-0.07	0.02	**0.33**	-0.09	0.04	**0.35**	0.21	-0.28	**0.32**	-0.25	0.17
Mg^{2+}	**0.38**	0.00	-0.07	0.02	**0.33**	-0.1	-0.01	**0.38**	0.14	-0.26	**0.33**	-0.24	0.08
Na^+	**0.37**	0.07	-0.11	0.07	**0.32**	-0.11	-0.05	**0.34**	0.24	-0.29	**0.33**	-0.19	0.25
NH^{4+}	0.24	0.19	0.13	-0.02	0.27	**0.35**	-0.04	0.05	**0.38**	0.18	**0.34**	-0.04	0.09
Cl^-	-0.04	0.13	**-0.58**	**0.41**	0.01	**0.60**	0.01	-0.31	**0.30**	-0.14	-0.04	0.21	**0.91**
NO_3^-	**0.38**	-0.02	-0.09	0.02	0.00	0.00	0.00	**0.37**	-0.23	-0.04	0.00	0.00	0.00
SO_4^{2-}	**0.36**	0.14	-0.18	-0.01	0.26	**0.38**	0.00	0.00	**0.45**	0.29	**0.36**	0.00	-0.03
%Cov	**51.40 %**	**18.51 %**	**15.54 %**	**8.20 %**	**65.38 %**	**19.90 %**	**14.37 %**	**46.02 %**	**33.50 %**	**12.07 %**	**60.84 %**	**26.40 %**	**8.40%**
*** Source identification**	**SD+ SA**	**IE**	**IE**	**BB+ SS**	**VE+ BB**	**IE**	**IE**	**SD+ VE**	**BB+ SA**	**IE**	**IE+ BB**	**IE**	**SS**

***Source identification : Secondary aerosols)SA(, Industrial emissions)IE(,Vehicle emissions)VE(, Biomass , Burning)BB(, Soil dust)SD(, Sea Salt)SS(**

Source identification

The higher correlation of WSI and HM represents the same emission source, whereas the lower correlation of WSI and HM means the different emission source. Tabachnick and Fidell (2007) use more cut-offs going from 0.32 (poor), 0.45 (fair), 0.55 (good), 0.63 (very good) or 0.71 (excellent) correlation.

Factor loading is rotated into four sources in non-community areas including mixed source of soil dust (SD) and secondary aerosols (SA), industrial emissions (IE), mixed source of biomass burning (BB) and Sea salt (SS) and mixed source of vehicular emissions (VE) and BB. While community areas related to five sources including SD+VE, BB+SA, IE, IE+SA and SS.

A mixture of secondary aerosol as well as biomass burning, construction dust besides dust dominated contributor of Mn, Ca^{2+}, Na^{+} and Mg^{2+} into the atmosphere (Amil et al.,2015; Zhou et al.,2016; Saxane et al., 2017; Jain et al.2017; Chen et al.2019). Industrial emission was one of the important sources of Cr, Pb, As, K^{+}, Ca^{2+},Cl^{-}, SO_4^{2-}, NO_3^{-}, and NH_4^{+} (Amil et al., 2015; Zhou et al., 2016; Saxane et al., 2017; Jain et al., 2017; Zou et al., 2017; Chen et al., 2019). In general, K^{+}, Cl^{-}, Ca^{2+}, Na^{+}, Mg^{2+} were suggested as the main tracers of biomass burning (Amil et al,.2015; Saxane et al., 2017; Chen et al.2019). Almost stations in non-community areas and community areas showed the first factor could mean, soil dust that represents the major source because soil dust made from many activities in residual areas such as construction.

There is also a correlation of Cd, Ni, Mn and Pb that major composition of motor vehicle emission and K^{+}, Na^{+}, Mg^{2+}, Ca^{2+} that major composition of biomass burning in WY station in non-community area. Furthermore, various factors i.e. meteorological parameter or emissions from combustion and other industrial processes are probably the most

important sources of ambient in figure 1.

CONCLUSIONS

In this study, both locations (community and non-community) have the various chemical composition of PM2.5. The community areas that have industrial area and vehicle emissions can cause emission heavy metal more than non-community areas. Almost source from soil dust, secondary aerosol and anthropogenic particles (vehicle emissions). Additionally, non-community get vehicle emissions in fine particulate matter (PM2.5) depend on various factor such as meteorological parameter, emission, physical and chemical mechanism model. This is preliminary because the mixed factor limited to the sample, these results should be continued with the future investigation.

ACKNOWLEDGEMENTS

The authors are grateful to thank the faculty of Environmental Management, Air Pollution and Health Effect Research Center, Prince of Songkla University, Hat Yai, Songkhla, Thailand.

REFERENCES

Amil, N., Latif, M. T., Khan, M. F., & Mohamad, M. Meteorological-gaseous influences on seasonal PM 2.5 variability in the Klang Valley urban-industrial environment. Atmospheric Chemistry & Physics 2015; 15(19).

Browne, D. R., Husni, A., & Risk, M. J. Airborne lead and particulate levels in Semarang, Indonesia and potential health impacts. Science of the total environment 1999; 227(2-3), 145-154.

Chen, Y., Xie, S. D., Luo, B., & Zhai, C. Characteristics and Sources of Water-Soluble Ions in PM2. 5 in the Sichuan Basin, China. Atmosphere 2019; 10(2), 78.

Intra, P., Yawootti, A., & Tippayawong, N. An electrostatic sensor for the continuous monitoring of particulate air pollution. Korean Journal of Chemical Engineering 2013; 30(12), 2205-2212.

Jain, S., Sharma, S. K., Mandal, T. K., & Saxena, M. Source apportionment of PM10 in Delhi, India using PCA/APCS, UNMIX and PMF. Particuology 2018; 37, 107-118.

Li, C., Wen, T., Li, Z., Dickerson, R. R., Yang, Y., Zhao, Y.,Wang & Tsay, S. C. Concentrations and origins of atmospheric lead and other trace species at a rural site in northern China. Journal of Geophysical Research: Atmospheres 2010; 115(D7).

Santoso, M., Hopke, P. K., & Hidayat, A. Sources identification of the atmospheric aerosol at urban and suburban sites in Indonesia by positive matrix factorization. Science of the total environment 2008; 397(1-3), 229-237.

Saxena, M., Sharma, A., Sen, A., Saxena, P., Mandal, T. K., Sharma, S. K., & Sharma, C. Water soluble inorganic species of PM10 and PM2. 5 at an urban site of Delhi, India: seasonal variability and sources. Atmospheric Research 2017; 184, 112-125.

Tabachnick, B. G., Fidell, L. S., & Ullman, J. B. Using multivariate statistics 2007;(5). Boston, MA: Pearson.

Titiphat Hirunkam. Heavy metal concentration and classification analysis of dust in Nakhon Ratchasima. 2013; Degree of Master of Engineering in Environmental Engineering Suranaree University of Technology.

Zhou, J., Xing, Z., Deng, J., & Du, K. Characterizing and sourcing ambient PM2. 5 over key emission regions in China I: Water-soluble ions and carbonaceous fractions. Atmospheric environment 2016; 135, 20-30.

Zou, B. B., Huang, X. F., Zhang, B., Dai, J., Zeng, L. W., Feng, N., & He, L. Y. Source apportionment of PM2. 5 pollution in an industrial city in southern China. Atmospheric Pollution Research 2017; 8(6), 1193-1202.

Environmental evaluation on rigid polyurethane foam disposal from refrigerator waste in Thailand

Soraya Suwannafon[1*], Nattharika Rittippant[1], Alice Sharp[2,3], Shigeo Nishikizawa[4], Pawadee Methacanon[5], Noramon Intaranont[5], Premrudee Kanchanapiya[5]

[1*]Sirindhon International Institute of Technology, 99 Moo 18, Paholyothin Rd., Khlong Luang, Pathum Thani, Thailand.
[2]Department of Biology, Faculty of Science, Chiang Mai University, 239 Huay Kaew Road, Muang District, Chiang Mai, Thailand.
[3]Environmnetal Science Research Center, Faculty of Science, Chiang Mai University, 239 Huay Kaew Road, Muang District, Chiang Mai, Thailand.
[4]Tokyo Institute of Technology Suzukakedai Campus, 4259 Nagatsutacho, Midori Ward, Yokohama, Kanagawa Prefecture 226-8503, Japan.
[5]National Metal and Materials Technology Center, 114 Thailand Science Park (TSP), Paholyothin Rd., Khlong Luang, Pathum Thani, Thailand.
Corresponding author: e-mail: Suwannafon.soraya@gmail.com

ABSTRACT

Rigid polyurethane foam (RPUF) is used as thermal insulation, especially in a refrigerator. After the refrigerator was discarded, it was dismantled by the dismantler. Most of the time, RPUF waste was found illegally disposed or openly burned, causing environmental problems and human health issues, owing to reckless management. Therefore, RPUF waste is one of the most concerning waste disposal, leading to this study. This study investigates on RPUF waste started from the beginning of the cycle, which was the chemical production, to the end of the cycle, followed by the dismantling site. The result revealed that the blowing agent, for example, HCFC-141b, HFCs, and cyclopentane, was added in a foam production process for refrigerator, an amine group was added as a catalyst and a flame retardant was not added in

the RPUF used in the refrigerator. The study was collected survey from the dismantling sites in 5 regions of Thailand (19 dismantling sites). These indicated that the disposal options of the RPUF wastes were landfill (47.83%), open burning (21.74%), sanitary landfill (13.04%) incineration (13.04%) and refuse-derived fuel or RDF (4.35%), respectively. Landfill presents the main disposal method for RPUF waste in Thailand. For environmental aspect, in 2018-2031, the landfill disposal will affect the environment in terms of global warming 22,175.36-39,290.65 kg CO2 eq/yr, ozone depletion 0.015-0.027 kg CFC11 eq/yr and terrestrial ecotoxicity 52,098.17-92,308.34 kg 1,4-DCB/yr.

Keywords: Rigid polyurethane foam waste, Disposal, Environmental impact.

INTRODUCTION

The rigid polyurethane foams (RPUFs) are vastly used as insulation in an appliance, building, refrigerated-truck, and automotive. Its structure of highly crossed-link and closed cell made RPUF high thermal resistance and appropriate for insulated applications (Szycher, 2013; Sharmin and Zafar, 2012).

RPUF is mainly reacted by polyols and isocyanates. The chemicals added in the production process are a catalyst, blowing agent, flame retardant, and other additives such a surfactant (Kaneyoshi and Kadzuo, 1995; Singh, 2016). The crossed-linked structure of RPUF leads to difficult degradation and occupy landfill spaces. Besides, the blowing agent added; e.g.CFC-11, HCFCs, for foam formation to provide the high efficiency in thermal insulation also causes environmental problems (Kaneyoshi, 2007). Although the CFC-11 was banned and phased out under the Montreal Protocol since 1989 and 1996 for a developed country (Singh, 2002), in Thailand (a developing country in Article 5(1)) CFCs had been freeze in 1999 and was phased out in 2010 (The

Department of Industrial Works, 1995).

With the encouragement of the Polyurethane Industry (PUI) in Thailand, information on chemicals usage for polyurethane production was examined in 2017. Approximately 75,000 tons of chemicals are used for 9 applications a year. The chemicals are used in refrigerator, ice box, panel, commercial fridge, spray, pipe, truck & boat, box foam, and rigid headlining for automotive — the number of chemicals are used for each application as shown in Figure 1.

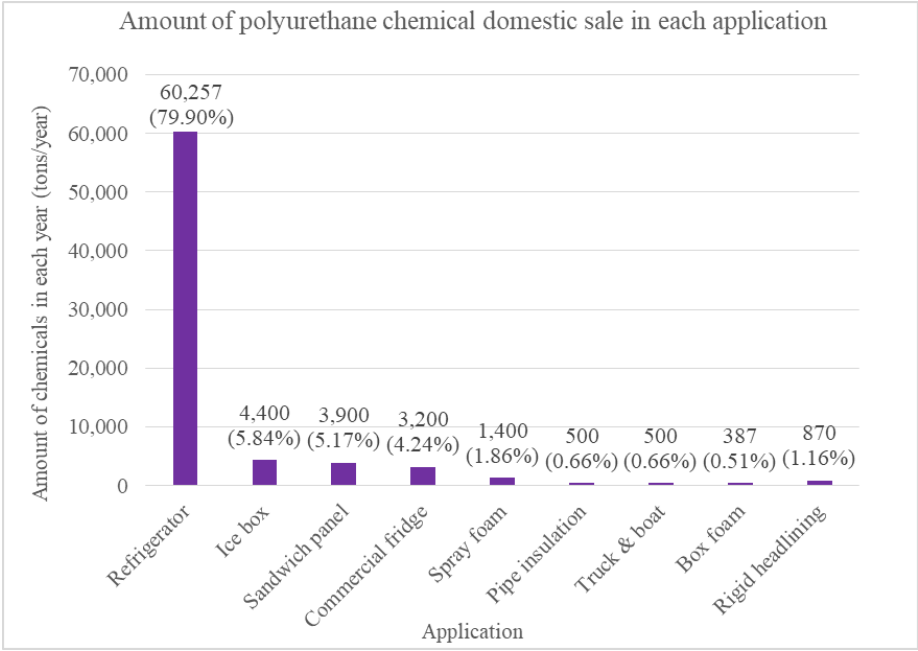

Figure 1 Amount of chemicals domestic sale in each application

The highest amount of polyurethane usage goes to a refrigerator, approximately 80% of chemical usage. Thus, this study will focus on the RPUF wastes from the refrigerator. According to the Office of Industrial Economics (OIE), the statistic of refrigerator domestic sale

in 2000-2018 was around 1-2 million units/year. The expected lifespan of a refrigerator in Thailand is 14 years (The Pollution Control Department, 2007). During the freeze period, it is possible that CFC-11 blowing agent was being added to RPUF in the refrigerator. There is a possibility that CFC gas releases into the environment during the refrigerator lifespan (Kjeldsen and Jensen, 2001).

Flame retardant is another substance from the refrigerators that is concerned in the study. Due to its the effect to animal and human health which can cause bioaccumulation in blood, breast milk and umbilical cord blood (Ike and Jacob, 2012; Beard and Angeler, 2010). Overall, this research aims to investigate the RPUF waste disposal in Thailand, especially on blowing agent and flame retardant, which can be used as the baseline data for further development of management planning and policy. The information on foam wastes disposal would be used for an assessment of environmental pollutants and suggest alternative disposal or recycling options for the refrigerator foam wastes.

METHODOLOGY

Data collection

Regarding the study of RPUF waste baseline management and environmental impact, the scope of stakeholders was set from the chemical manufacturers to the end of the life products. Stakeholders were classified into three groups in which the respondents were interviewed through phone and field visit.

(1) A chemical producer refers to the producer of polyurethane where the chemicals would be imported or produced. Information on chemical; i.e., a blowing agent and a flame retardant, used for rigid polyurethane foam, were given from 5 respondents out of 15 polyurethanes industry memberships.

(2) A refrigerator producer refers to a refrigerator manufacturer that may

give information on the refrigerator chemical usage and the disposal or recycle of PU foam wastes from the production process. The information was obtained from 4 respondents out of 10 most prominent companies which accessed from the database of the Department of Business Development.

All respondents come from large and well-known companies; thus, the obtained information can represent the chemical used in the refrigerator and also the disposal or recycling process.

(3) Dismantling site refers to a store or a shop or people who disassemble a used refrigerator. The required information from the dismantling sites was a focus on current foam wastes management, transportation, disposal fee, and trouble of foam wastes management, which was shown in Table 1.

The survey information was obtained from 28 respondents from 5 regions which comprised of 19 dismantling sites, 8 recycling sites, and 1 industrial waste recycling plant. The difference location presents either the similarity route or the different route for foam wastes disposal in each region.

Table 1 The data collection from dismantling sites each region

Topic	Total respondent	Required information
Central (Bangkok, Nakhon Pathom) North (Chiang Mai, Lampoon)	5 9	1) The used refrigerator disassembling process 2) The disposal option or recycling process for RPUWs

East (Sa Kaeo) North-east (Kalasin) South (Nakhon Si Thammarat, Phuket)	6 3 5	3) Transportation & disposal fee 4) The problem of RPUWs management

Environmental impact assessment

The environmental impacts from the main disposal option of RPUF waste were evaluated by using an emission factor from the SimaPro software. The world ReCiPe midpoint impact assessment method was selected to estimate the environmental impacts of this study.

The environmental impact of polyurethane foam waste disposal in this study would assess by the following equation.

Environmental impact = EF x (NFx Di)

Where EF is an emission factor

NF is the amount of RPUF generated from refrigerator wastes in each year (tons/year)

Di is the percentage of the largest disposal method (%)

The lifespan of the refrigerator was estimated to be an average of 14 years (The Pollution Control Department, 2007). RPUF waste generated would be calculated from domestic sale of the refrigerator in the past 14 years and the amount of RPUF used in the refrigerator (average 7 kg/refrigerator) which obtained from the refrigerator production interviewed. With the assumption that those refrigerators would

become waste in the next 14 years; i.e., from 2018 to 2031, the disposal of RPUF wastes would definitely affect the environment.

RESULTS AND DISCUSSION

The chemical used for rigid polyurethane foam

The chemical concern in this study is blowing agents and flame retardants. According to the interview, the chemical used for foam formation consists of blowing agent; i.e. HCFC-141b (20-30 %phr of polyol), HFC-245fa (10-15%phr of polyol), HFC-134a, HFC-365, Cyclopentane (12-15 %phr of polyol), isocyanate and water. All refrigerator producers reported that cyclopentane has been using as the blowing agent for more than 10 years, which conform to the phased out period of CFC-11 in Thailand (The Department of Industrial Works, 1995).

However, flame retardant was not found as an additive in a refrigerator RPUF (appliance application). Whereas, flame retardant in RPUF was found in building application and transportation such panel, spray, pipe ,and refrigerated truck since those applications are required for fire safety issue (Edward and Sergei, 2004). Brominated flame retardant was widely used to reduce the flammability of products in the past. Due to the Stockholm Convention on Persistent Organic Pollutants, the brominated flame retardants were added on the list in 2009 which induced to an alternative flame retardant use such as organophosphorus flame retardants (OPFR) (Haffner and Schecter, 2014).

The producers also reviewed that rigid polyurethane foam wastes from production process were transported to the cement plant by authorized agent and used as a replacement fuel. However, the recycling process of RPUF wastes such as mechanical recycling or chemical recycling was not found from both chemical and refrigerator producer, but waste to energy option was chosen by the transporting foam waste to a cement

plant.

Disposed of rigid polyurethane foam wastes

The information of RPUW from the dismantling sites in 5 regions of Thailand showed that the used refrigerators were compiled from either household or hotel/industry by recycling collector or recycling store. The fridge would be disassembled into 2 parts at the dismantling site (1) valuable materials; i.e., steel and copper, and (2) non-valuable materials. RPUWs were mostly classified as non-valuable materials.

According to the management of RPUW in central of Thailand interviewed, from both Bangkok and Nakhon Pathom with registered population of 5,682,415 and 911,492 in 2017 respectively (Announcement of the Bureau of Registration Administration, 2017), stated that RPUWs were gathered up till approximately 1 ton to transport using a pick-up truck to a disposal site in 1-2 times/month. As a result, all dismantling sites (5 sites) revealed that their foam wastes are disposed at a landfill or a municipality disposal site for domestic waste. The disposal fee is required to pay. Transportation of foam wastes to the disposal site is the main problem for the foam wastes management, due to its high volume and may not be economically worthwhile.

In the northern part of Thailand (Chiang Mai and Lampoon with registered population of 1,746,840 and 405,918 in 2017 respectively (Announcement of the Bureau of Registration Administration, 2017)). The amount and the managed procedure of RPUWs of the north are similar to the central one, which is dumped to the designated area for domestic waste or sanitary landfill. Besides, open burning is one of the foam waste management options in the north. The results (from 5 dismantling sites) showed that 20% of dismantling sites disposed to landfill, 20% of them conduct open burning and 60% of them transported

foam waste to the sanitary landfill. Regarding the waste disposal fee and foam waste problem, they are similar to the central one.

Sa Kaeo province, had the population of 560,531 in 2017 (Announcement of the Bureau of Registration Administration, 2017), was chosen in the study as the Thailand-Cambodia bordered where electronic wastes may be imported into the country. According to the interview, there is only one dismantling site out of six respondents which presents the most significant source of foam waste in the eastern region. As a part of refrigerators, such the partitions and the doors which contained a large amount of RPUF, was dismantled. The foam wastes were piled up and transported to the industrial waste management area where the foam wastes were shredded and mixed with others wastes to produce refuse-derived fuel (RDF) product. RDF is a fuel produced from various type of waste which has adequate heating value to replace fossil fuel. The disposal fee is required if the industrial waste management take care of the foam wastes. On the other hand, if the dismantler is carrying foam waste by themselves, the disposal fee is not necessary.

Kalasin province, the northeastern region of Thailand, with a population of 986,005 in 2017 (Announcement of the Bureau of Registration Administration, 2017), is one of the most significant places for dismantling electronics waste, including refrigerator, non-valuable materials were dump to landfill where it becomes e-waste's landfill at present. The results revealed that all of the dismantlers transported the foam wastes to the disposal site near dismantling sites by a pick-up truck. After the wastes were ended up in landfill, it was burnt in order to get valuable-materials remaining attached beside the foam; i.e., copper. The interview showed that the disposal option for foam wastes was 50% disposed to landfill and open burning 50%. Moreover, there is no

policy on the disposal fee at present; thus the payment is not required.

In the southern part of Thailand, Nakhon Si Thammarat and Phuket were chosen to collect information because Nakhon Si Thammarat has the highest population of 1,557,482 in 2017 (Announcement of the Bureau of Registration Administration, 2017) and Phuket is the largest island in Thailand, with a population of 402,017 in 2017 (Announcement of the Bureau of Registration Administration, 2017). The foam waste management demonstrated differently from other regions. There are 3 options to dispose RPUF waste in southern; i.e., landfill, open burning, and incineration. The landfill (33.33%) and open burning (16.67%) options were found in Nakhon Si Thammarat, while, the incineration option (50%) was found in Phuket. Regarding the topography, Phuket is an island where the disposal option is quite attractive compared to other provinces. This is due to the used refrigerator from both household and hotel would be sent to the dismantling site. As a result, all of the dismantling sites transported foam wastes to the incineration plant belong to Phuket's municipality. The foam waste would be combusted together with municipal solid waste. The disposal fee also required, and the main problem of the foam waste from the dismantler point of view is also the transportation.

Consequently, the disposal method is related to the location of the dismantling and disposal site. For example, if the dismantling site located close to a landfill, the foam wastes will go to the landfill site. Whereas, dismantler will burn the wastes if there is no disposal site nearby. The summary of RPUW management options from the dismantling sites in 5 regions showed in Figure 2.

The overall disposal options from 19 dismantling sites in Thailand implied that the main disposal for the foam wastes is the landfill

method (47.83%) followed by open burning (21.74%), sanitary landfill (13.04%), incineration (13.04%) and RDF plant (4.35%). Figure 3 illustrated the route of RPUF wastes disposal in Thailand.

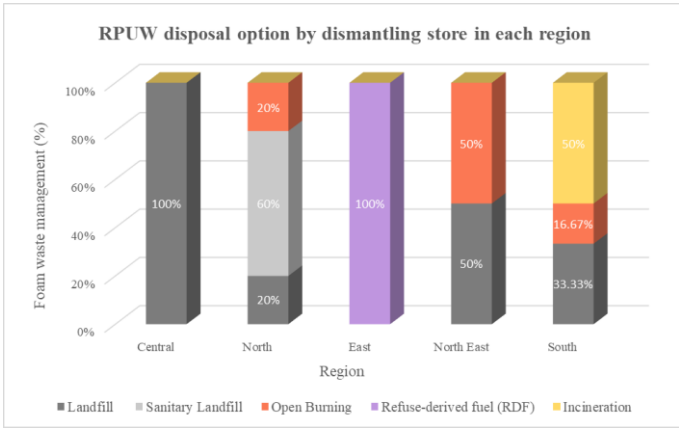

Figure 2 The rigid polyurethane foam wastes management in each region

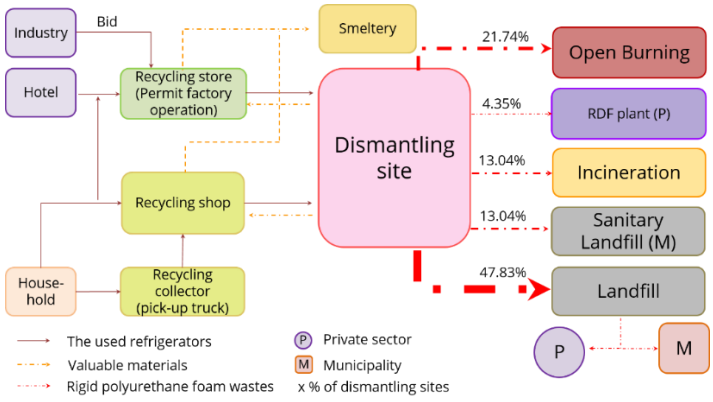

Figure 3 Route of rigid polyurethane foam wastes disposal in Thailand

Environmental impacts assessment

This study would focus on an environmental impact from the majority of the disposal method. As mentioned, almost 50 percent of RPUW method is landfill. Moreover, the information from the chemical production and the refrigerator production shows that HCFCs and cyclopentane are used as blowing agent and non-use of flame retardant. Thus, the flame retardant effect would not be evaluated. The SimaPro database for 1 kg of RPUF waste

disposed to a landfill was selected with the most common impact categories from polyurethane foam waste comprise of global warming and stratospheric ozone depletion. Besides, this study also concerns about toxicity; thus, the terrestrial ecotoxicity was selected because it shows the highest emission factor among other toxicities (Marine, freshwater, human carcinogenic, and non-carcinogenic toxicity). The emission factors are 0.0054 $kgCO_2eq$ for global warming, $3.78x10^{-9}$ kgCFC11eq for stratospheric ozone depletion and 0.0127 kg1,4-DCB for terrestrial ecotoxicity.

The prediction of an environmental impact from RPUW disposed to the landfill was calculated from both the SimaPro database and the estimated foam waste, shown in Figure 4. As a result, the used refrigerator disposal in the past 14 years would affect the environment at present (2018) and the next 14 years in term of the global warming about 22,175.36 – 39,290.65 $kgCO_2eq/yr$, and affect the stratospheric ozone depletion about 0.015-0.027 kgCFC11eq/yr. These impacts mainly come from the blowing agent, using in RPUF. When compare the greenhouse gas (GHG) emission from RPUF in landfill with total GHG emission from the waste sector in Thailand which was $11,830x10^6$ $kgCO_2eq/yr$ in 2013 (Ministry of Natural Resources and Environment, 2017), the RPUF in landfill emission is so small. To compare the impact on the stratospheric ozone depletion with a total emission of ozone-depleting substances, which was about $32x10^{10}$ kg CFC11 eq/yr in 2014 (Hegglin et al., 2014), bury of RPUW shows a small emission. An assessment on terrestrial ecotoxicity result that about 52,098.17 – 92,308.34 kg 1,4-DCB/yr would be affected due to the emission of silicon and barium, which are the components of RPUW. Generally, silicon is added as a surfactant for rigid polyurethane foam while barium sulfate (barytes) is used as filler for both flexible foam and semi-rigid foam, especially for

noise absorption application. Moreover, Yadav and Samadder (2017) assessed an environmental impact of municipal solid waste (MSW) landfilled, which was the main existing option in India. It indicated that landfill of 1 kg MSW affected the environment and had global warming potential 9.42 $kgCO_2eq$, ozone depletion potential 7.60×10^{-10} kgCFC11eq, and terrestrial ecotoxicity 7.87×10^{-6} kg 1,4-DCB (Yadav and Samadder, 2017). It can imply that 1 kg RPUW landfilled has more considerable terrestrial ecotoxicity impact than MSW, less global warming potential, and slightly high for ozone-depleting potential.

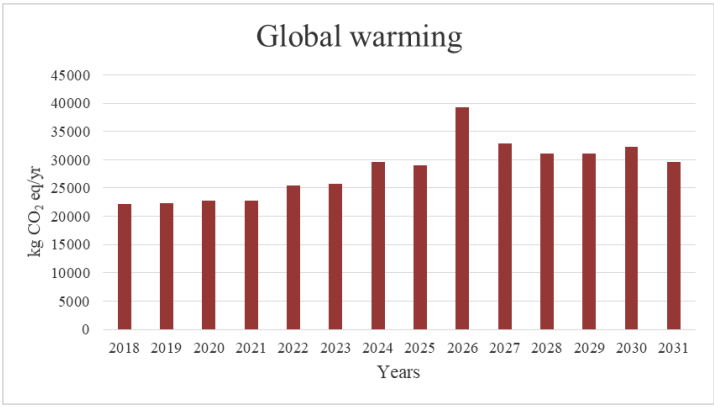

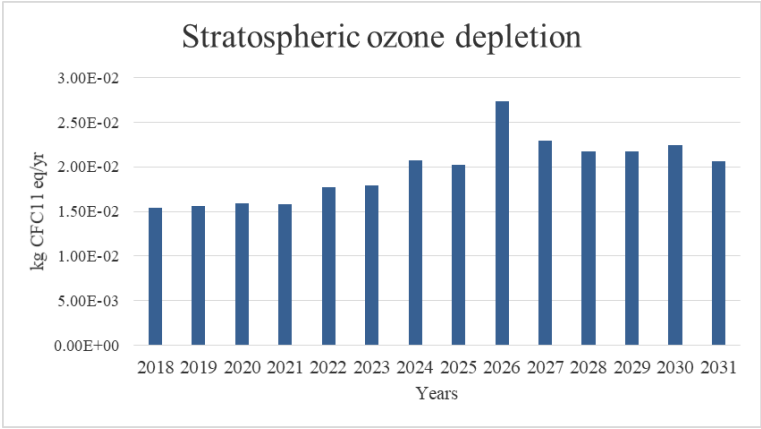

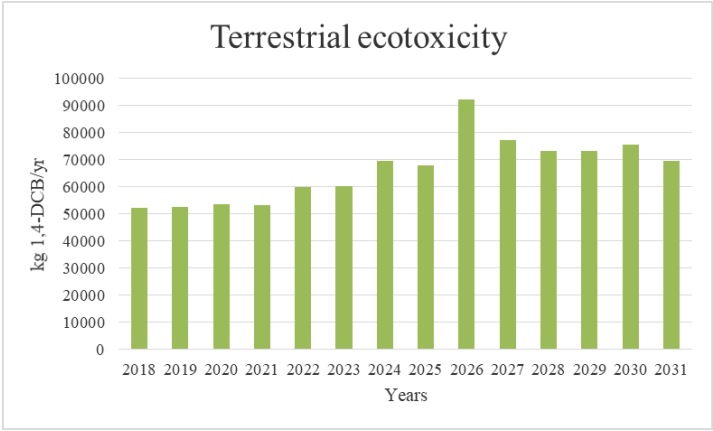

Figure 4 The prediction of environmental impacts; i.e., global warming, stratospheric ozone depletion, and terrestrial ecotoxicity, from landfill method for rigid polyurethane foam waste

From the calculations, the highest impacts show in 2026 because the great flooding occurred in Thailand (2011) and the domestic refrigerator sale was increased by 35% in the following year. The amount of foam wastes, therefore, would be increased in 2026. The highest environmental impacts also demonstrated in the same year.

However, this assessment predicted from the used refrigerator when CFC11, blowing agent, may be added during the foam production. As mentioned, CFC11 was phased out in 2010, and it could signify that the refrigerator produced during that time would affect the environment. Under the Montreal Protocol, an environmental impact, especially ozone depletion and global warming should decrease. Since an alternative blowing agent; i.e., HCFCs, HFCs, and cyclopentane, was proposed as it presents low ozone depletion, and global warming potential compares to CFC11 (The United Nations Environment Programme, 1994).

CONCLUSIONS

This research aims to obtain the current situation of rigid polyurethane foam wastes disposal in Thailand and evaluate environmental impacts from the wastes disposal

options. An exploration from the cradle to the grave found that RPUF wastes from their production process were sent as fuel to a cement plant while the foam wastes from the refrigerator dismantlers were mainly transported to a landfill site. Not only reduce the landfill area but RPUW also affect climate and ozone depletion because of blowing agent added. Besides, silicon and barium used in foam production would affect the terrestrial ecotoxicity. Those impacts would be long term effect due to the structure of polyurethane is challenging to degrade; thus, this research would suggest waste to energy option for foam wastes management. These waste to energy options; i.e., incineration and RDF, would be possible because some dismantling sites and refrigerator producers are using. However, both options should be installed the control equipment in order to reduce and control the pollutant emission to meet the air quality standard.

ACKNOWLEDGEMENTS

This research was supported by National Metal and Materials Technology Center, Sirindhon International Institute of Technology and the estimation of polyurethane foam waste in Thailand, Research fund No. P1850443. The authors would like to thank the chemical producer, refrigerator producer and especially dismantler at Ratchada 36, Bangkok and Dontum district, Nakhon Pathom, Chiang Mai and Lampoon, Sa Kaeo, Kalasin, Nakhon Si Thammarat, and Phuket for gave us information with generous support.

REFERENCES

Beard A, Angeler D. Flame retardants: chemistry, applications, and environmental impacts. In: Lackner M, Winter F, Agarwal KA, editors. Handbook of combustion vol.1: fundamentals and safety. Weinheim, WILEY-VCH Verlag GmbH & Co. KGaA; 2010. p. 415-439.

Edward DW, Sergei VL. Commercial flame retardancy of polyurethanes. Journal of Fire Sciences 2004; 22(3): 183-210.

Haffner D, Schecter A. Persistent Organic Pollutants (POPs): A primer for

practicing clinicians. Current Environmental Health Reports 2014; 1: 123-131.

Hegglin MI, Fahey DW, McFarland M, Montzka SA, Nash ER. Twenty questions and answers about the ozone layer: 2014 update. Ennis CA, editor. Scientific Assessment of Ozone Depletion: 2014. World Meteorological Organization (WMO); 2014. p. 1-84.

Ike van der V, Jacob de B. Phosphorus flame retardants: Properties, production, environmental occurrence, toxicity and analysis. Journal of Chemosphere 2012; 88: 1119-1153.

Kaneyoshi A. Polyurethane and related foams: chemistry and technology. Boca Raton: Taylor & Francis Group; 2007.

Kaneyoshi A, Kadzuo I. Thermosetting foams. In: Arthur HL, editor. Handbook of plastic foams. William Andrew; 1995. p. 11-220.

Kjeldsen P, Jeansen MH. Release of CFC-11 from disposal of polyurethane foam waste.

Ministry of Natural Resources and Environment. Second biennial update report of Thailand 2017.

Sharmin E, Zafar F. Polyurethane: an Introduction. In: Zafar F, Sharmin E, editors. Polyurethane. Intechopen; 2012. p. 3-16.

Singh H. Rigid polyurethane foam: A versatile energy efficient material. Key Engineering Materials 2016; 678: 88-98.

Singh SN. Blowing agents for polyurethane foams. United Kingdom: Rapra Technology Limited; 2002.

Szycher M. Szycher's handbook of polyurethanes. 2nd edition. New York; 2013.

The Bureau of Registration Administration. Announcement of the Bureau of Registration Administration 2017.

The Department of Industrial Works. The Montreal Protocol on substances that deplete the ozone layer 1995.

The Pollution Control Department. Waste from electrical and electronic equipment strategy. Bangkok; 2007.

The United Nations Environment Programme. Cyclopentane: a blowing agent for polyurethane foams for insulation in domestic refrigerator-freezers 1994.

Yadav P, Samadder SR. Environmental impact assessment of municipal solid waste management options using life cycle assessment: a case study. Environmental Science and Pollution Research 2018; 25(1): 838-854.

Education as a Key Social System for the Global Environmental Protection Deduced from a Biosystematic View of Civilization

Kunio Kawamura [1]

[1] Department of Human Environmental Studies, Hiroshima Shudo University, 1-1-1, Ozuka-higashi, Asaminami-ku, Hiroshima 731-3195, Japan.

ABSTRACT

A systematic view on the basis of comparative analysis of life-like systems at different hierarchical levels is a useful approach for analyzing and organizing knowledge about the biosystems. Here, we will discuss the importance of education for the development and innovation concerning science and technology for the global environmental protection on the basis of a biosystematic view of civilizations (BVC). Prior to discuss the characteristics of civilizations on the basis of the BVC, the Ecological View of History (EVH) proposed by T. Umesao in 1957, which is not still popular in Western scholars, will be briefly introduced as a successful theory for description of the parallel behaviors of the Western Europe and Japan. Both the EVH and BVC theories involve the principle of systematic views for analyzing the civilizations. Our analysis of civilizations based on the BVC suggested that civilization possesses inherent controlling machinery for information, which characterizes the nature of civilization. Furthermore, civilization possesses inherent machinery for incorporating energy, materials, and information from outside, of which the information for assignment of these functions is stored in the civilization. From this viewpoint, civilization resembles the cell type organisms. Based on this fact, we deduced the importance of education, and

the development of science and technology. Base on the BVC, a potential approach will be proposed for the global environmental protection.

Keywords: education, comparative biosystematic view of civilizations, global environmental protection, ecological view of history, key technology, carbon waste

INTRODUCTION

1.A Principle Determining Civilizations Deduced from a Biosystematic View

The effectiveness of whole human's efforts for the global environmental protection innovations seems to be weak although people seem to attempt for fitting their behaviors to global environmental protection (Kawamura, 2014; 2015a, 2015b). For instance, the total energy consumption of the world is indeed increasing during the last few decades after the time peoples notified the importance of global environmental protection. The increase in energy supply is the greatest issue regarding global environmental protection. In other words, the reduction of energy consumption of worldwide must be focused on global environmental protection. The gap between the actions of people and the direction of the societies seems to become larger even after the main international agreement regarding global environmental protection. It is roughly said that the total human's actions are not effective for the actual environmental protection. I described briefly this reason and why our efforts do not lead us effectively to the goal of environmental protection. We have continuously carried out the comparative analysis of biosystems and its application to the behavior of civilization. The results support the idea that civilization is a biosystem, and the individual humans are regarded as the building blocks in civilization. Besides, civilization involves a special characteristic,

which resembles the nature of cell-type organisms.

Biosystems are classified from the fact whether the two specific functions named as CCSI and CMIO are involved in the biosystems. CCSI is the central controlling system for information and CMIO is the central controlling machinery for inflow and outflow of energy, material, and information. Naturally, the cell-type organisms possess the inherent machinery for both CCSI and CMIO inside of the organisms. The assignment between genotype and phenotype is involved in the CCSI of the cell-type organisms. The ecosystem is also regarded as a biosystem since including organisms. However, there is no inherent machinery for the CCSI and CMIO within the ecosystem at the higher hierarchical level of individual organisms as building blocks. CCSI directs the information regarding CMIO. And, the energy, material, and information from and to outside CCSI are supplied by CMIO. The connection between CCSI and CMIO is essential, for instance, in cell-type organisms and civilizations. We proposed a hypothesis that the presence of CCSI and CMIO and the linkage between CCSI and CMIO is the special characteristics to determine that the system behaves as alive. We concluded that civilization possesses inherent machinery for the CCSI and CMIO. Thus, we propose an idea that humans need to know the characteristics of civilization and all the policies should be consistent with the property of CCSI and CMIO.

2. The Relationship between the Civilization and Humans

2.1 The Ecological View of History

Although Umesao Tadao proposed the ecological View of history (EVH) for the first time in 1957, it is not widely known in the western community in social science; the translated version in English was published at 2003 (Umesao, 1957; 1967; 2003). The principle was deduced from the observation of parallels regarding historical transitions between Western Europe

and Japan from ancient to modern, in which the ecological view was based on the principle of ecological succession. The EVH demonstrated the reason that Western Europe and Japan were modernized in parallel, where the ecological and geological location of these areas resemble at the west and east edges of the Eurasian continent (Fig. 1).

This situation has resulted in the consecutive change of societies in these areas, which have not been damaged by the societies in the arid region of the Eurasia continent. Actually, the parallels of historical change from an ancient kingdom, feudalism, absolute monarchy, and the people's revolution occurred. The changes of societies enhanced the accumulation of capital and bourgeois and led the society to the Industrial Revolution until the end of the 19th century. However, there are parallel historical phenomena among other societies of the Eurasia continent, such as China, India, Arabia, and Russia. The extensive incorporation of technologies into the societies in the Eurasia continent has happened in recent years in these areas as compared to Western Europe and Japan.

We realize that the EVH involves a systematic view, where the civilizations can be analyzed from the viewpoint of the framework of natural science. The success of understanding the parallels between Western Europe and Japan by EVH supports strongly the fact that human history can be analyzed by the approaches based on natural science.

2.2 The Biosystematic View of Civilization

We have investigated the analogies of biosystems at different hierarchical levels, such as eukaryotes, prokaryotes, social insects, ecosystems, species, civilizations, viruses, and viroids (Kawamura, 2007). The approach analyzing the civilizations from the viewpoint of biosystems was originally attempted to clarify how life-like systems

emerged on the primitive Earth. This was succeeded for analyzing the characteristics of the cell-type organisms resulting in the insight into the mechanisms for the emergence of life on the Earth (Kawamura, 2016). Then, we noted that the biosystematic view would be useful for analyzing the behaviors of civilizations, named as the biosystematic view of civilization (BVC) (Kawamura, 2015c). Civilization is classified as a style of human's society, and the solution for the global protection must be obtained from the deep considerations on properties of civilization since the relationship between human societies and the environments can be regarded as the relationship between civilization and the environments nowadays.

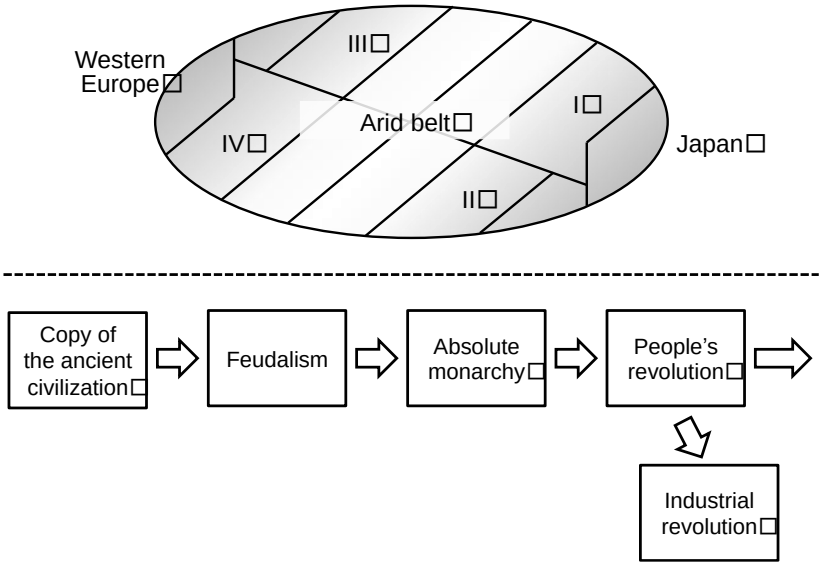

Figure 1. The view of EVH, top) the locations of Western Europe and Japan, bottom) the spontaneous transformation of the social system of Western Europe and Japan.

As mentioned above, civilization possesses its inherent machinery of CCSI and CMIO at the hierarchical level beyond the individual humans. We applied the principle of BVC to the behaviors of West Europe, Japan,

and North America, which was excluded in the EVH as mentioned in the Umesao's first publication about EVH. It was succeeded that the behavior of civilizations in North America is understood by the BVC. This result indicates the fact that the BVC is useful to analyze the behaviors of civilizations from the different aspect of human societies. The relationship between civilization and the environments from the viewpoint of the BVC was briefly demonstrated in our previous publications (Kawamura, 2007; 2015a; 2015b; 2015c).

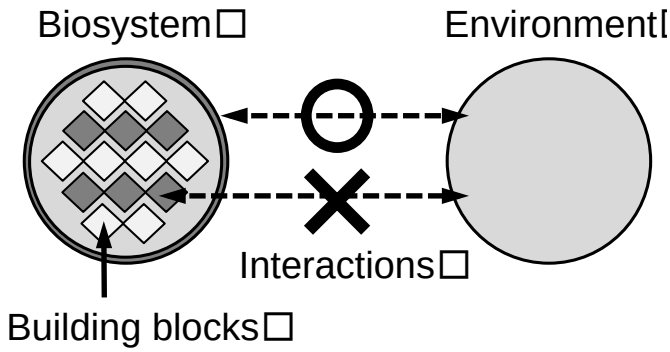

Figure 2. The relationship between biosystems and environment.

According to the BVC, the analysis of the analogies of biosystems at different hierarchical levels deduced an assumption that individual humans are regarded as the building blocks for constructing the civilizations (Fig. 2). This figure indicates the roles of a biosystem and its building blocks for the environment. There is a trend that building blocks, such as humans in a civilization and cells in a multicellular organism, do not directly interact with the environment. This is consistent with our perceptive view about the relationship between humans and societies. In modern civilizations, there is a strong trend that the individual humans do not directly interact with the environments while civilization always mediates for the interaction between the environments and the individual humans. This

situation is analogical to that multicellular organism as a higher hierarchical level of cells mediates for the interaction between the environments and the individual cell. Individual humans living in a modern city, for instance, cannot easily obtain any food and other materials unless the system of civilization.

In addition, the combination of CCSI and CMIO in civilization is a major system to control the relationship between the societies and the environments, that is, the behavior of civilization (Fig. 3). In this figure, the relationship between CMIO and CCSI, and their linkage are illustrated as the key elements for determining the nature of biosystems. CMIO and CCSI involve inherent mechanisms at the hierarchical level of the system. The strong interaction between CCSI and CMIO of the cell-type organisms so called as the central dogma. Besides, there is a strong connection between CCSI and CMIO in civilization. From this viewpoint, it is regarded that civilization is analogical to the cell-type organisms. According to our analysis of the history of civilizations, it seems that the connection between CCSI and CMIO has become stronger continuously from the ancient civilizations to the modern civilizations. The large scale irrigated agriculture established the ancient civilizations and the modern civilizations have experienced the Industrial Revolution. This trend becomes strong with the development of civilizations, where the role of humans as the building blocks for the civilizations become strong. These facts would be useful for our strategies for global environmental protection.

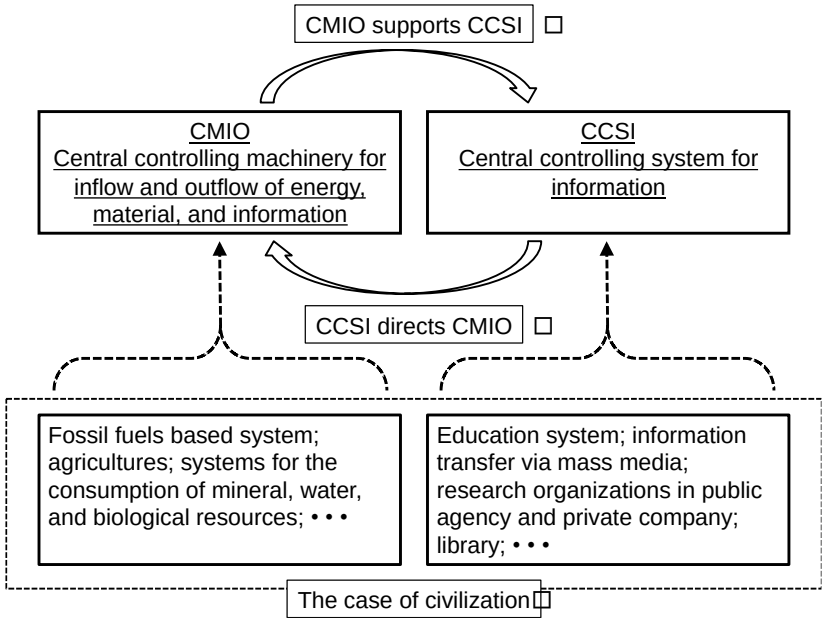

Figure 3. The relationship between CMIO and CCSI.

2.3. Roles of Education and Innovation in the Civilizations

In our previous publications, we demonstrated what is the actual machinery corresponding to the CCSI and CMIO in civilization. The CCSI of civilization probably includes the wide meaning of education and innovation systems of the societies. The wide meaning of education can be regarded as the information transfer, so this includes the educations in schools, the information transfer through mass media, the communications among humans, etc. Besides, the wide meaning of innovation includes the incorporation of new information into the civilization, so this simply involves the technological innovations based on scientific facts, the innovations in other fields, such as economics, politics etc. These innovations in different fields are nowadays systematically created in public and private research organizations. The newly created technologies from mainly the developed countries easily transfer to other places. The civilizations possess systematic organizations, such as the library, for preserving

information into the civilizations. The modifications of information happen by the systematic developments in the research organizations and are obtained through the information transfer.

The information in the cell-type organisms is efficiently and accurately reproduced by replication of DNA sequences, of which the base substitution error reaches typically 10^{-7} to 10^{-8} (Kunkel, 2004). For instance, the duplicate of eukaryotes or single-celled prokaryotes amplifies the total amount of information by increasing the population. Although mutations and horizontal gene transfer from other organisms also occur (Smith et al., 1993; Maria et al. 1999), the fidelity of copy of the cell-type organisms is high. Although for multicellular organisms the amplification of the information by the increase of individual organisms involves somewhat complicated methods, the accuracy of the information amplification caused by the amplification of organisms is also high. However, the information in civilization is not so accurately reproduced by the machinery of CCSI, such as education systems. That is to say, the difference of accuracy of the information reproduction through the CCSI systems between cell-type organisms and civilization would be a useful index for analysis of the behavior of civilizations (Fig. 4). A shown in Fig. 4., the accuracy of reproduction of information between the cell-type organisms, for instance eukaryote) and civilization is different. Although the reproduction of information in the cell-type organisms is normally very accurate, that in civilization, of which education is a major system, is readily collapsed.

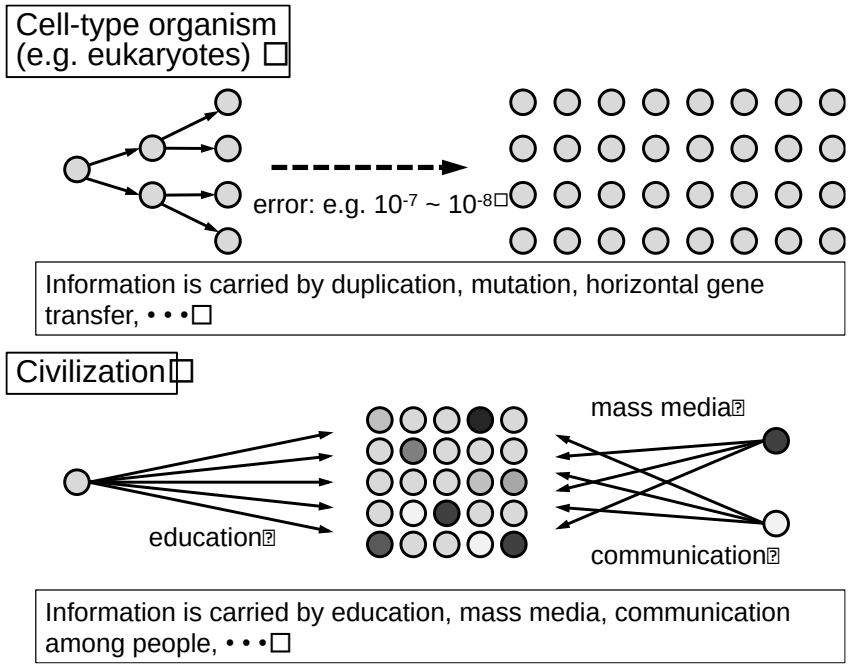

Figure 4. Accuracy of information reproduction in biosystems, top) cell-type organisms, bottom) civilization.

On the other hand, the CMIO in civilization can be regarded as energy, material, and information transfer from and to the environments, where the information about these functions are preserved in civilization. The energy supply from the environments after the Industrial Revolution mainly comes from fossil fuels while that before the Industrial Revolution comes from agriculture, etc. The energy, materials, and information to cell-type organisms are frequently supplied as chemical forms. The CMIO in biosystems should be controlled fluently so the lack of even a single path among the network of the CMIO would decrease the efficiency of CMIO.

3. The Environmental Protection from the BVC

3.1. Weakest Elementary Technology is the Key for Green Technology

As mentioned, there is no sign of decrease of energy consumption even after the major international

agreements regarding the global environmental protection although people behave to fit their lifestyle for such international agreement (United Nations, 1997; BP 2018). This implies that the behavior of people does not readily affect the behaviors of civilization even in the presence of great financial supports (United Nations, 2016). This paradox can be understood from the presence of the CCSI and CMIO of civilization. For example, our present technological networks are primarily dependent on the energy supply from fossil fuels. The system of civilization is fitted with the energy flow through the CMIO, of which the information for maintaining the CMIO is preserved in the CCSI of civilization. It is reasonable that CCSI and CMIO control the stability of the biosystems. Thus, this means that the present CCSI and CMIO strongly support the stability of present civilizations. The change of characteristics of present civilizations would be difficult unless the characteristics of the CCSI and CMIO of the civilizations will be changed.

The improvement of civilizations, for example, from a civilization based on agriculture to a civilization based on fossil fuels, has been achieved by consecutive development of important technologies, such as the success of power supply and production by machines. For example, the ammonia production established at the beginning of the 20th century is supported by several elementary technologies (Smil, 1997; 2004; Frink et al. 1999). For instance, the formation of hydrogen was succeeded by the steam reforming of coal, the high-pressure process of ammonia production from hydrogen and nitrogen, and catalysts, etc. If one of these technologies was not present, the total technology was not succeeded.

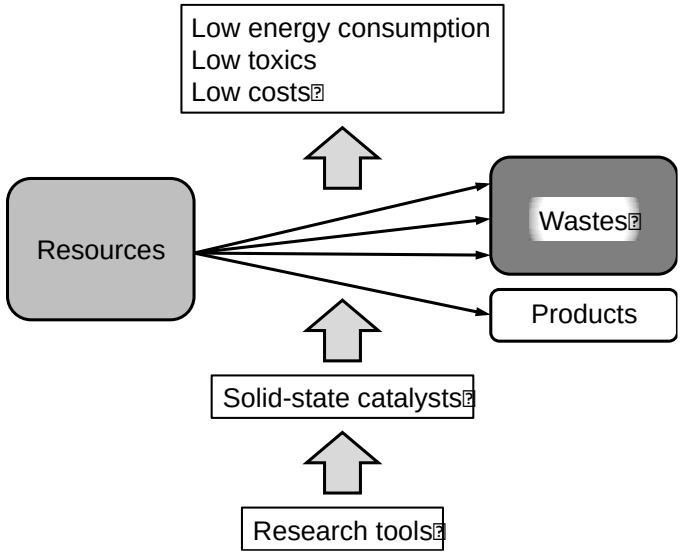

Figure 5. Development of solid-state catalysts as the key technology for chemical processes.

This fact indicates that low efficient technologies, which may be called as key technologies, determine the total efficiency of the whole technology (Yotsuyanagi, 1999). This example is consistent with the principle that the inferior technology or process must be targeted to improve is a strategy for the establishment of an efficient total technology network (Yotsuyanagi & Ishiyama, 2011).

In our case, we have focused on a research tool for solid-phase catalysts since a number of the chemical processes remain still very low efficiency (Fig. 5). The improvement of low efficient chemical processes would reduce energy consumption, the toxics, and even the costs. Solid-state catalysts are expected to promote the improvement of these processes, but there were no suitable research tools. Thus, the improvement of research tools for the development of the solid-state catalyst finally results in the goal of reduction of energy consumption, etc. So, the development of solid-state catalysts is a key technology for improvement of the efficiency of such chemical processes. However, there was not a suitable research tool

for the development of solid-state catalysts. This was partly solved by our in situ monitoring system for chemical reactions in liquid phases at high temperature and pressure in the presence of solid-state catalysts (Kawamura, et al., 2016; 2017). Recently, we are attempting a chemical recycling system for the cotton waste by focusing the key technology among the complete system of recycling system of cotton. (Kawamura et al., 2014; 2015) (Fig. 6). The great amounts of resources including water, labor power, land, and fertilizers, so on are supplied to the cotton productions, but a small part of the wastes is reused and recycled. Although the chemical processes to produce 5'-hydroxymethylfurfural have been developed, the recovering process as a key technology is not succeeded.

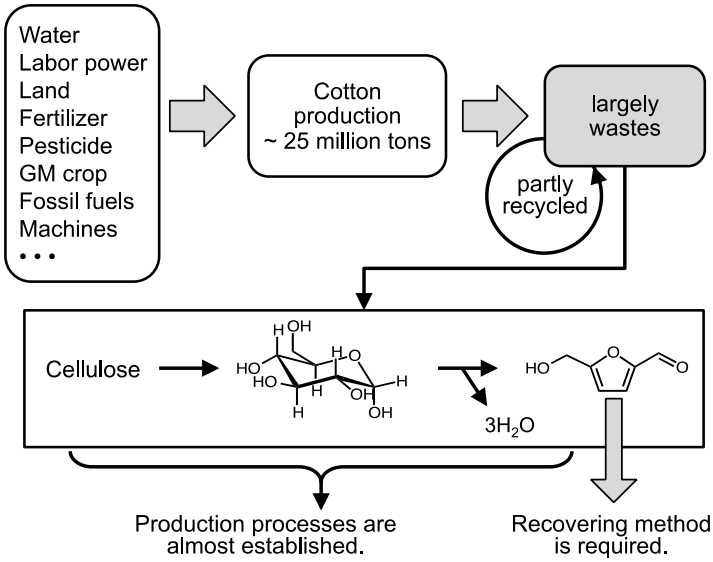

Figure 6. Improvement of cotton waste recycling.

The information that assigns the technologies is also incorporated in the CCSI of civilization. Unfortunately, the effort by the researchers would finally contribute to enhancing the strength of CCSI and CMIO leading the strength of civilization. This implies that the development of technologies and also science as fundamental studies regarding even the environmental protection would hardly contribute to the actual environmental protection as long as the researchers also behave as building blocks of the civilization. Even our development of the in situ monitoring method of chemical reactions may not be used for the global environment protection but may be used for enhancement of the strength of the technological networks of the civilizations.

3.2. Alternative Network of Technologies Independent from the Conventional CCSI and CMIO

Although the civilization is considered as a unit of societies including CCSI and CMIO at the beginning of the discussion for BVC, there is room for discussion whether the minimum unit of society including CCSI and CMIO is civilization or smaller societies. For example, it is assumed that the country as the minimum unit of society possessing both the CCSI and CMIO would be suitable; the countries normally link with other societies and the definition of the country is not established. The analysis of the unit of societies will be carried out as a future subject. The discussion would deduce that the size of societies, which possess inherent CCSI and CMIO, would affect the behavior of the societies. The appearance of anti-globalism against globalism would reflect that globalism is going to result in the strong connection of CCSI and CMIO to make strong the trend that humans act as the building blocks of civilization. There is a trend that the innovation, which is regarded as the machinery of CCSI, is maintained effectively by the LS-CcsiCmio, and the efficiency is altered by

supplement of energy, materials, and information from outside. It is reasonable that the larger scale of innovation would be effective as compared to the smaller scale one. Then, the researchers working in the CCSI machinery hardly work independently from the policy of the society. Thus, the feedback of innovations affects the society, but it would be true that the feedback hardly affects local communities since the influence appears indirect.

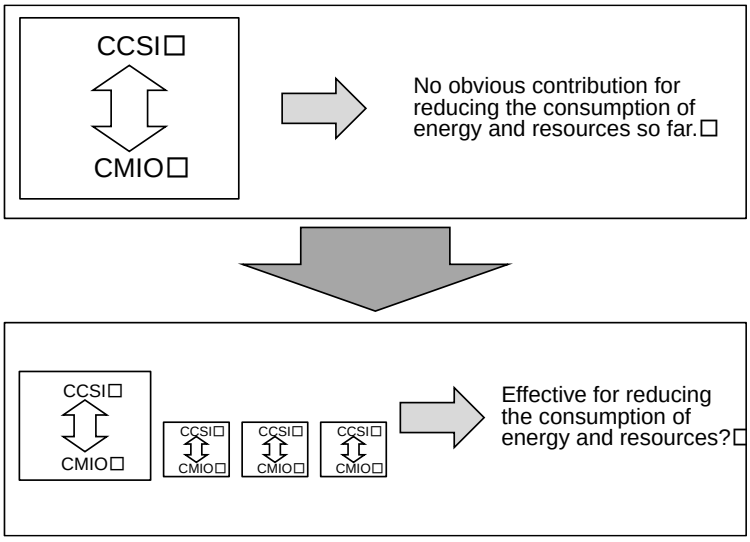

Figure 7. Alternative combination of CCSI and CMIO.

The proposed analysis suggested that our effort for global environmental protection is not effective unless the roles of CCSI and CMIO in civilization are dramatically changed. Also, the improvement and development of technologies may not be useful for global environmental protection. To solve this situation, we proposed a possible solution in our previous paper (Kawamura, 2015a; 2015b). Here, we deduce possible methods to reduce or stop the strong connection of CCSI and CMIO in the present civilizations. One is the reduction of the size of CCSI and CMIO (Kawamura, 2015a; 2015b). Another one is the reduction of the

strong connection between CCSI and CMIO. These are probably consistent with the framework of anti-globalism. As we proposed in our previous paper, the method that the migration of organizations for innovation to the local and/or small societies would be effective. These methods directly or indirectly act to reduce the robustness of the system consisting of CCSI and CMIO. This is named as the change from the large-system of CCSI and CMIO (LS-CcsiCmio) to the small-system of CCSI and CMIO (SS-CcsiCmio) (Fig. 7). The connection of CCSI and CMIO is normally very strong. This causes ineffective contribution of both actions from individual humans and politics. Division and reduction of the connection between CCSI and CMIO would reduce the ineffectiveness of the present situation. The divided small CCSI in SS-CcsiCmio should be directed directly by individual humans so the suitable size of societies consisting of SS-CcsiCmio will be determined from this viewpoint.

3.3. Education Supported by Independent Energy as a Key

The reproduction (or amplification) in CCSI is an important factor for determining the behavior of the biosystems. The reproduction of information in cell-type organisms is formed by replication; the reproduction of information of multicellular organisms is not simply amplified by replication. However, the accuracy level of reproduction in the CCSI of civilizations is much lower than that of organisms. The education system is the main machinery of CCSI in our societies, but this is affected by other types of machinery of CCSI, such as the mass media, for the reproduction of information in our societies (Fig. 3, 4). This is a notable characteristic of civilization as a biosystem, which is notably different from the cell-type organisms. This fact supports that education is key for determining the fate of the civilizations, and this is consistent with our general perceptive view regarding education.

Although education has become popular continuously in human history, there are problems, such as deflection, inequality, efficiency, and inaccuracy regarding education. The condition for education is determined by the fact of what and how education is provided to individual humans in civilization. In the present paper, we do not focus on how these problems will be solved, but we believe that the division of education system as an element of CCSI is useful as a first step for the reform from the civilization consisting of LS-CcsiCmio to SS-CcsiCmio. Then, an independent energy and material supply would be necessary to establish SS-CcsiCmio to make a linkage between CCSI and CMIO in a small unit of society since the CMIO directed by CCSI is essential for civilization. Naturally, the absolute independence of such a small society from the other societies may be hardly achieved, but even partial independence will be useful to reduce the robustness of the present system or act as an alternative system to support human societies.

CONCLUSION

We showed the importance of education as s social system for global environmental protection from the BVC. The direction of the existing civilizations has not been changed even after the international agreements and treaties. Thus, dividing and reducing the connection of existing CCSI and CMIO would be a useful strategy to add an alternative path for our societies. Although the efficiency of SS-CcsiCmio to the global environmental protection is not yet analyzed, the formation of SS-CcsiCmio would reduce the strong connection of existing CCSI and CMIO. This method would reduce the total energy consumption.

ACKNOWLEDGEMENTS

This study was supported by JFE 21st Century Foundation and Hiroshima Shudo University.

REFERENCES

BP. Statistical Review of World Energy 2018. https://www.bp.com

Frink CR, Waggoner PE, Ausubel JH. Nitrogen fertilizer: retrospect and prospect. Proc. Natl. Acad. Sci. USA 1999; 96: 1175-1180.

Kawamura K. Civilization as a biosystem examined by the comparative analysis of biosystems. BioSystems 2007; 90 (1): 139-150.

Kawamura K. Global Environmental protection on the basis of a biosystem view of civilization, the role of education and invention. Journal of Human Environmental Studies 2014; 12: 65-83.

Kawamura K. Global Environmental protection on the basis of a biosystem view of civilization: implication on inflow and outflow of energy, material, and information. Journal of Human Environmental Studies 2015a; 13: 53-69.

Kawamura K. Global Environmental protection on the basis of the biosystematic view of civilization – importance of information flow, and roles of energy and material flow –, Proceedings of The 3rd EnvironmentAsia International Conference on "Towards International Collaboration for an Environmentally Sustainable World", pp. 385-395, Thai Society of Higher Education Institutes on Environment, June 17-19, 2015b, Montien Riverside Hotel, Bangkok, Thailand.

Kawamura K. A biosystematic view of civilizations: Western Europe and Japan: before and after the industrial revolution. Comparative Civilizations Review 2015c; 73: 77-100.

Kawamura K. A hypothesis: life initiated from two genes, as deduced from the RNA world hypothesis and the characteristics of life-like systems. Life 2016; 6(3): 29.

Kawamura K, Ogata T, Sako K, Tanabe K. Japan Patent 2014; Patent Application 2014-048918 (opened).

Kawamura K, Ogata T, Sako K, Tanabe K. Japan Patent 2015; Patent Application 2015-064031 (opened).

Kawamura K, Yasuda T, Hatanaka T, Hamahiga K, Matsuda N, Ueshima M, Nakai K, Oxidation of aliphatic alcohols and benzyl alcohol by H_2O_2 under the hydrothermal conditions in the presence of solid-state catalysts using batch and flow reactors, Chemical Engineering Journal 2016; 285: 49-56.

Kawamura K, Yasuda T, Hatanaka T, Hamahiga K, Matsuda N, Ueshima M, Nakai K, In situ UV-VIS spectrophotometry within the second time scale as a research tool for solid-state catalyst and liquid-phase reactions at high temperatures: Its

application to the formation of HMF from glucose and cellulose, Chemical Engineering Journal 2017; 307: 1066-1075.

Kunkel TA. DNA replication fidelity. J. Biol. Chem. 2004; 279(17): 16895-16898.

Jain R, Rivera MC, Lake JA. Horizontal gene transfer among genomes: The complexity hypothesis. Proc. Natl. Acad. Sci. USA 1999; 96: 3801-3806.

Smith JM, Smith NH, O'rourke M, Spratt BG. How clonal are bacteria? Proc. Natl. Acad. Sci. USA 1993; 90: 4384-4388.

Umesao T. An ecological view of history. Chuou Kouron 1957; 72: 32-49.

Umesao T. An ecological view of history. Tokyo: Chuou Kouron Sha; 1967.

Umesao T. 2003. An ecological view of history: Japanese civilization in the world context. Melbourne: Trans Pacific Press; 2003.

United Nations. COP3 - Reports, Report of the conference of the parties on its third session, held at Kyoto from 1 to 11 December 1997. United Nations Report 1998.

United Nations. Annual Reports 2016. https://www.unenvironment.org/annualreport/2016/

Smil V. Global population and the nitrogen cycle. Sci. Am. 1997; 277(1): 76-81.

Smil V. Enriching the Earth: Fritz Haber, Carl Bosch, and the transformation of world food production. Cambridge: MIT Press; 2004.

Yotsuyanagi T. Chemical analysis and measurement as a key technology for human survival in 21th. Century. Bunseki Kagaku 1999; 48(12): 1037-1041.

Yotsuyanagi T, Ishiyama J. Prospect for education of engineering talent by chemical experiments. Kougaku Kyouiku (J. of JSEE) 2011; 59(1): 24-30.

.

Adsorption of Nickel and Chromium from synthetic wastewater by activated carbon derived from waste rubber tires

Ketkanok Saeuang[1], Siraporn Potivichayanon[2*], and Panarat Rattanaphanee[3]

[1]Environmental Pollution and Safety Program
[1,2*]School of Environmental Health,
Institute of Public Health, Suranaree University of Technology,
Nakhon Ratchasima, Thailand
[3]School of Chemical Engineering, Institute of Engineering,
Suranaree University of Technology, Nakhon Ratchasima, Thailand;
Corresponding author: e-mail: siraporn@sut.ac.th

ABSTRACT

The objectives of this research were to investigate physicochemical properties of activated carbon derived from waste rubber tires or carbon black and the optimum conditions of nickel and chromium adsorption. The physicochemical properties were structure morphology, texture, and adsorption capacity. The structure morphology and compositional analysis were observed by a field emission scanning electron microscope with energy dispersive X-ray fluorescence spectrometer. The results showed the porous structure of activated carbon was changed and increased when compared with carbon black. The energy dispersive X-ray fluorescence spectrum showed carbon more than 80%. Brunauer Emmett Teller has characterized the textural property of activated carbon. It was found that surface area and total pore volume were improved to 149.74 m^2/g and 1.05 cm^3/g, respectively. This total pore volume was in mesoporous. The adsorption capacity can be studied by iodine number and density appears. Iodine number results showed activated

carbon absorbed iodine solution up to 1,506 mg/g and density appears results revealed at $0.73\ g/cm^3$. After that, the optimum conditions were studied with mixed aqueous solution containing 10 mg/l of nickel and 10 mg/l of chromium, pH 5, 30 min of contact time and 3 g of adsorbent dosage. Nickel and chromium were absorbed more than 50% and 99.99% of efficiency, respectively, In addition, this adsorption process could be proved by Langmuir model with correlation coefficient of nickel and chromium at 0.94 and 0.99, respectively.

Keywords: Carbon black, Activated carbon, Adsorption, Waste rubber tires, Heavy metals

INTRODUCTION

The rapid development of Thailand industry has led to problems of water pollution because water is important for process productions. Industrial wastewater plating is one of the key factors due to it has heavy metals contamination. The important toxic metals are Ni, Cr, Cd, Pb and Zn, etc. Nickel and chromium are the best to use for electroplating industry which are toxic to human's health and the environment (Gonsalvesh et al., 2016). Heavy metal toxicity affects the nervous system, lungs, kidney and liver (Lata et al., 2014). Different methods were used to wastewater treatment. However, adsorption method is considered as an efficient and universal method of wastewater treatment with the guidelines of WHO and EPA. This is because of its cost effectiveness and easy to manage (Fu and Wang, 2011).

Waste rubber tires have been a major disposal problem. Some of tires were took up to landfill spaces and pyrolysis process in industry (Williams, 2013; Saleh and Gupta, 2014). Recently, waste rubber tire from pyrolysis process is an alternative that it was used as an absorbent because waste rubber tires are low costs and high amount of carbon which were called activated

carbon (Williams, 2013; Hadi et al., 2016; Saleh and Gupta, 2014) after either physical or chemical activation methods.

Consequently, the waste rubber tire is an interesting source of raw materials for the preparation of activated carbon (Gupta et al., 2013) which it has been applied to wastewater treatment in the adsorption of heavy metals (Gupta et al., 2013; Karunarathne and Amarasinghe, 2013; Saleh et al., 2013; Acosta et al., 2016).

The objectives of the present study were to investigate the physicochemical property of activated carbon. The physical properties were included morphology and texture. The chemical property were included iodine number and density appears and optimum condition of nickel and chromium adsorption.

METHODOLOGY

1 Preparation of adsorbent

Activated carbon was prepared from waste rubber tires via pyrolysis of petroleum tire industry. It was called carbon black. Carbon black was treated with 6% of hydrogen peroxide solution to oxidize organic at 60^0C for 24 hrs. Then, it was washed with deionized water and dried at 105^0C for 4 hrs. The dried material was activated at 900^0C for 2 hrs by heating in muffle furnace (CARBOLITE/Control 201), cooled in desiccator and stored in desiccator. The material was treated with 1 M of hydrochloric solution to remove the ash content and washed with deionized water and dried at 105^0C and then cooled in desiccator. The final product was called activated carbon (Gupta et al., 2012).

2 Physicochemical properties

2.1 Physical properties

Morphology

The morphology of adsorbent was studied by a field emission scanning electron microscope (FE-SEM, Carl Zeiss, AURIGA) with energy

dispersive X-ray spectroscopy (EDX) for compositional analysis. It was analyzed the composition presented in carbon black and activated carbon (Gupta et al., 2012).

Texture

The surface area and pore volume of the adsorbents were determined by N_2 gas adsorption isotherm at -196 ^{0}C (77 K). The adsorption and desorption isotherms were studied with Brunauer Emmett Teller (BET, Bel sorp mini 11, Bel-Japan, Japan). The carbon black and activated carbon were degassed for 6 hrs at 300 ^{0}C (Gonsalvesh et al., 2016) and analyzed for 24 hrs.

2.2 Chemical properties

Adsorption capacity:

Iodine number

The activated carbon was dried at 105^{0}C for 1 hr and weighed 0.5 g in each Erlenmeyer flask. Then, 10 ml of 5% HCl solution was added and boiled for 30 sec. The sample flasks were added with 100 ml of 0.1 N iodine solution and shaken for 30 sec. All samples were filtered with filter paper No. 42. After that, 50 ml of the sampler was taken in a flask and titrated with 0.1 N sodium thiosulfate solution, added a few drop of the starch indicator solution and continued the titration with 0.1 N sodium thiosulfate solution. Record the volume of sodium thiosulfate used (ASTM, 1986). The experiment was done in triplicate.

Density appears

The carbon black and activated carbon were placed in each cylinder, tapped several times until constant volume at 1 cm^3 and then weighed. These was calculated as the ratio of the weight sample to its volume and expressed in g/cm^3 (Baccar et al., 2009).

3 Optimum conditions

The Erlenmeyer flasks containing 3, 5 and 10 g of activated carbon were added to 100 ml of mixed aqueous solutions containing 10 mg/l of nickel and 10 mg/l of chromium and the pH was adjust to 2, 4 and 5 with 1 M NaOH and 1 M H_2SO_4 solution and shaken for 30, 60, 90, 120 and 150 min at 150 rpm. All experiments were conducted at room temperature.

The final was analyzed by atomic absorption spectroscopy (AAS, analytik jena, nova AA).

The removal efficiency of nickel and chromium were calculated by Eq. (1) (Mousavi et al., 2010)

$$\%Removal = ((C_i-C_e)/C_i)\times 100) \quad (1)$$

Where C_i and C_e are the initial and equilibrium concentrations in mg/l, respectively. The nickel and chromium adsorption capacity Q_e (mg/g) was calculated by Eq. (2) (Gonsalvesh et al., 2016; Karunarathne and Amarasinghe, 2013).

$$Q_e = ((C_i-C_e)/W)\times V) \quad (2)$$

Where V is the volume of solution in L. W is the weight of adsorbent in g.

4 Adsorption isotherm

The adsorption isotherm was performed with different concentrations at 5, 10, 30, 50, 100, 200 and 250 mg/l of mixed aqueous solutions under the optimum conditions from the previous experiments. These studies were controlled at room temperature. Batch isotherm experiments using 100 ml of mixed aqueous solutions were done in Erlenmeyer flask and shaken at 150 rpm for 30 min of a contact time. All samples were analyzed for concentration of nickel and chromium by AAS to study Langmuir and Freundlich isotherm.

Langmuir isotherm was calculated by Eq. (3) (Mousavi et al., 2010; Karmacharya et al., 2016).

$$C_e/Q = (1/(Q_0\times b)) + (C_e/Q_0) \quad (3)$$

Where C_e is the equilibrium concentration (mg/l), Q is the amount of heavy metals sorbed, b is the sorption constant which is related to the affinity of the sorbate to the sorbent (l/mg), Q_0 is the maximum sorption capacity (mg/g)**.**

Freundlich isotherm was calculated by Eq. (4,5 or 6) (Mousavi et al., 2010; Karmacharya et al., 2016).

$$q_e = x/m = K_f C_e^{1/n} \quad (4)$$

$$Q_e = K_f C_e^{1/n} \quad (5)$$

$$\text{or} \quad \log q_e = \log K_f + 1/n \log C_e \quad (6)$$

Where K_f and n are the Freundlich constants related to the adsorption

capacity and adsorption intensity, respectively. The intercept and the slope of the linear plot of $\ln q_e$ versus $\ln C_e$ at given experimental conditions provide the values of K_f and 1/n, respectively.

5. Chemicals

All chemicals used (HNO_3, $Ni(NO_3)_2$, $Cr(NO_3)_3$, H_2O_2, HCl, H_2SO_4, NaOH, I_2, $Na_2S_2O_3$, $H_6N_2O_4S$ and $C_6H_{12}N_6$) were analytical grade. Solutions were prepared by dissolving the corresponding reagent in distilled water. All experiments were done in triplicate.

RESULTS AND DISCUSSION

1 Physical properties

Morphology

The FE-SEM was employed to visualize carbon black and activated carbons morphology and porous structure (Gupta et al., 2012, 2013). The image exhibits two distinct morphologies. One of the carbon black are large porous structure and unregulated, as presented in Figure 1 that there are organic substances on the surface which effect to adsorption (Williams, 2013) and activated carbons are small porous structure when compared with carbon black (Figure 2). This may be due to the activated carbons developed by heating from the preparation that made the pore structural changes in the adsorbent. Consequently, the porous structure of activated carbon was increased after the activation which was related with the property of adsorbent. In addition, an EDX analysis was used to analyze component of the carbon black and activated carbon as shown in Table 1. It was presented the main components of carbon, oxygen, sulfur whereas there was not nickel and chromium (Figure 3). These results also showed more than 80% of dominant carbon that corresponds to the properties of the raw materials for activated carbon production (Gupta et al., 2012; Williams, 2013) which generally activated carbon from waste rubber tires have in the range of 70-90% of carbon components (Gupta et al., 2012, 2013; Saleh and Danmaliki, 2016)

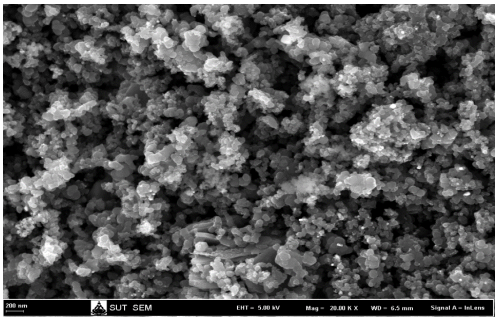

Figure 1 FE-SEM image of Carbon black 20000 kx

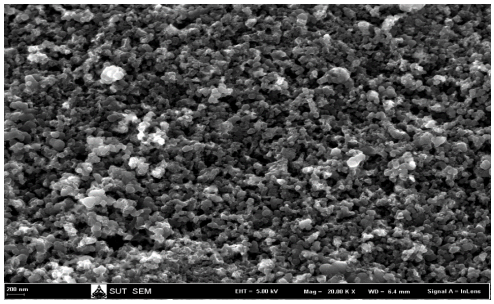

Figure 2 FE-SEM image of Activated carbon 20000 kx

Table 1 Energy dispersive X-ray analysis (EDX) quantitative microanalysis of carbon black and activated carbon

Absorbents	Weight%		
	C	O	S
Carbon black	84.01	2.54	3.38
Activated carbon	83.51	4.68	3.07

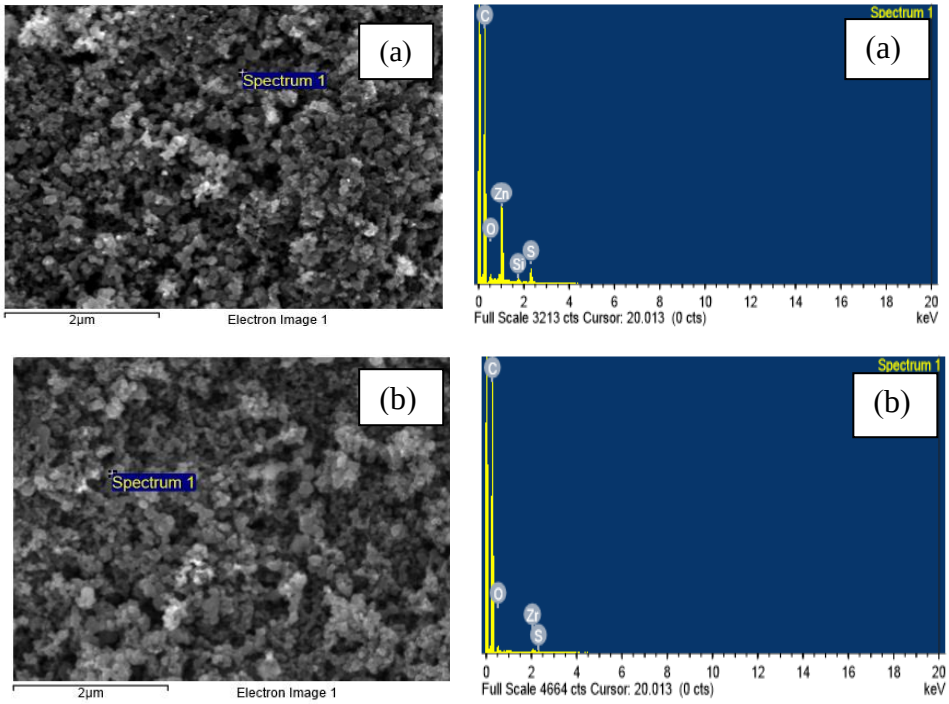

Figure 3 Example of EDX image, carbon black (a) and activated carbon (b)

Texture

The carbon black and activated carbon were analyzed by BET. The parameters of BET were summarized in Table 2. The results were presented about increasing surface area and total pore volume of activated carbon after activation when compare with carbon black and then refer to the adsorption was increased when the surface area and total pore volume were also increased (Saleh and Danmaliki, 2016; Williams, 2013) . The mean pore diameter of activated carbon was called mesoporous because the value is in the range of 20-50 nm which is suitable for adsorption liquid phase (Bansal et al., 2005).

Table 2 Physical properties of the adsorbent

Adsorbents	Surface area (m^2/g)	Total pore volume (cm^3/g)	Pore diameter (nm)
Carbon black	58.37	0.54	37.30
Activated carbon	149.74	1.05	27.99

2 Chemical properties

Adsorption capacity

Iodine number

The iodine number of carbon black and activated carbon were summarized in Table 3. It revealed that the activated carbon was in the standard values which presented more than 600 mg/g (Ministry of industry, Thai industrial standards institute, 2004) . Consequently, the activated carbon has many small porous (Baccar et al., 2009) and adsorption tends to increase (Printhorn, 2008) because the atomic structure of activated carbon was destroyed by heating that it was causing space or porous (Hadi et al., 2016).

Density appears

The density appears is one of the properties in the standard values. The density appears of activated carbon showed the decreasing value as shown in Table 3 because the atomic structure was destroyed by heating (Hadi et al., 2016; Williams, 2013). Furthermore, the adsorption will increase with the density appears decrease (Chuachan, 2013). When compared with the standard values in the range of 0.2-0.75 g / cm^3, it was also found that the activated carbon was in Thailand's standard (Ministry of industry, Thai industrial standards institute, 2004). In addition, the general commercial activated carbon has a range density appears of 0.38-0.74 g/cm^3. Consequently, the activated carbon from waste rubber

tires also has density appears similar to commercial activated carbon. Therefore, this activated carbon can be produced as an adsorbent for treatment dye, organic matter and heavy metals in wastewater (Saleh and Gupta, 2014; Acosta et al., 2016).

Table 3 Adsorption capacity

Absorbents	Iodine number (mg/g)	Density appears (g/cm^3)
Carbon black	371.84	0.80
Activated carbon	1,506.13	0.73

3 Optimum conditions

Effect of pH

The pH is one of the important factors for adsorption process. These experiments were carried out at pH 2, 4 and 5 in mixed aqueous solution containing 10 mg/l of Ni and 10 mg/l of Cr. The optimum pH for adsorption was 5 because Ni and Cr can be adsorbed on the surface of activated carbon which some of the efficiency was more than 50% and 99.99%, respectively (Table 4). It may be due to the proton of solution (H^+ or H_3O^+) which increase with decreasing of pH (Langmuir, 1997) and also is high as compared with ions of nickel (Ni^{2+})(Gupta et al., 2013) and chromium (Cr^{3+}, $Cr(OH)^{2+}$ or $Cr(OH)_2^+$)(Gonsalvesh et al., 2016)at pH 2 and 4. It competed in binding during adsorption with ions of metals for surface active sites of the adsorbent which has negative charge (Bansal et al., 2005; Gonsalvesh et al., 2016; Saleh et al., 2013; Gupta et al., 2013; Langmuir, 1997)

Table 4 Adsorption of nickel and chromium

Heavy metals	pH	Final concentration after adsorption (mg/l)	Removal efficiency (%)
Ni	2	7.84±0.09	19.36±0.89
	4	6.17±0.01	36.50±0.07
	5	4.84±0.26	50.17±2.64
Cr	2	5.15±0.99	43.92±1.08
	4	N.D.	100±0.00
	5	N.D.	100±0.00

N.D. is heavy metal concentration are lower than detection limit (<0.01 mg/l)

Effect of contact time

The effect of contact time were studied at 30, 60, 90, 120 and 150 min. The activated carbon at 3g could effectively adsorb Ni and Cr within the first 30 min with more than 50% and 99.99% of efficiency, respectively. This rapid uptake can be explained by the creation of more active sites on the surface of the activated carbon by the activation process during preparation of activated carbon from waste rubber tires. After 30 min, the removal efficiency was stable which the activated carbon could not adsorb nickel and chromium. Furthermore, the optimum contact time might depend on the adsorbent dosage and also the concentration of heavy metals in solution (Karmacharya et al., 2016; Gupta et al., 2013).

Effect of adsorbent dosage

The removal efficiency of nickel was increased when the adsorbent dosage increased from 3 to 5 g (Figure 4) due to the resulting in more surface area to adsorb (Cecen et al., 2012; Bansal et al., 2005) and stable when the activated carbon was increased from 5 to 10 g because the adsorption into the equilibrium state. The removal efficiency of Cr was very high that presented more than 99.99% in all experiments and showed the removal

efficiency was not different because 3 g of activated carbon may be almost adsorb Cr due to having more surface area. The activated carbon could adsorb Cr better than Ni at 3, 5 and 10 g. However, the optimum of adsorbent dosage at 3 g was used for further experiment for isotherm study to reduce the use of activated carbon.

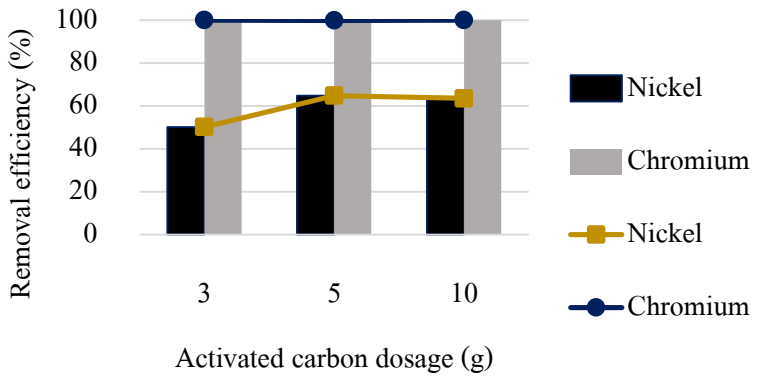

Figure 4 Effect of adsorbent dosage on the amount of Ni, Cr adsorbed on the activated carbon, (conditions: contact time = 30 min, and Ni and Cr concentration = 10 mg/l)

4 Adsorption isotherm

The equilibrium adsorption isotherms of Ni and Cr onto the activated carbon adsorbent were investigated with the different concentrations at 5, 10, 30, 50, 100, 200 and 250 mg/l in mixed aqueous solution under the optimum condition at pH 5 in presence of 3 g of adsorbent and 30 min of contact time. The important reason of the analysis of adsorption system was explanation with Langmuir and Freundlich adsorption models (Gonsalvesh et al., 2016). The results of their linear regressions as presented in Table 5. The correlation coefficients (R^2) obtained from the plots of Langmuir ($1/q_e$ vs $1/C_e$) as show in Fig. 5 and 6. These revealed that the adsorption was the best fit in Langmuir adsorption model with R^2. Therefore,

Ni and Cr was adsorbed onto the activated carbon surface by homogeneous. The Langmuir isotherm can be explained in four assumptions which include 1 adsorption occurs at a definite site on the surface, 2 one site can bind only one molecule of solution, 3 the energy of adsorption all site is the same and 4 it have no forces of interaction (Cecen et al., 2012; Bansal et al., 2005; Langmuir, 1997).

Table 5 The values of correlation coefficient in various isotherm

Heavy metals	Langmuir isotherm			Freundlich isotherm		
	Q_0 (mg/g)	b (l/mg)	R^2	K_f (g/mg)	1/n	R^2
Nickel	4.3956	0.0508	0.9414	0.3902	0.4845	0.7713
Chromium	4.1000	1.3897	0.9938	0.4793	0.5058	0.7416

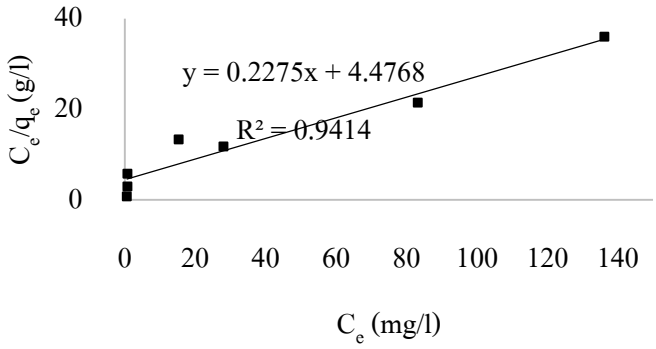

Figure 5 Langmuir adsorption isotherm of Ni

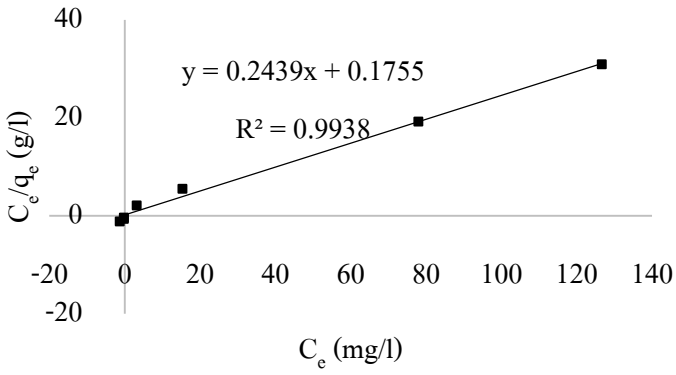

Figure 6 Langmuir adsorption isotherm of Cr

CONCLUSIONS

The activated carbon prepared from waste rubber tires were developed for nickel and chromium adsorption in synthetic wastewater to study the physicochemical properties and the optimum conditions. The activated carbon has properties according to the standard. The optimum parameters revealed at pH 5, 30 min of contact time and 3 g of activated carbon dosage. The adsorption isotherm was Langmuir isotherm. In addition, the removal efficiencies of nickel and Chromium were more than 50% and 99.99%, respectively under the optimum conditions.

ACKNOWLEDGEMENTS

This research was supported and funded by petroleum tire industry, national science and technology development agency (NSTDA) and Suranaree University of Technology, Nahkon Ratchasima, Thailand.

REFERENCES

American Society for Testing and, Materials. 1986. “Standard test method for determination of iodine number of activated carbon”, Philadelphia, PA: ASTM Committee on Standards.

Acosta. R., Fierro. V., Martinez de Yuso, A., Nabarlatz, D., and Celzard, A., 2016. “Tetracycline adsorption onto activated carbons produced by KOH activation of tyre pyrolysis char”, Chemosphere 149 168-176.

Bansal, R. C., and Goyal, M., 2005. Activated carbon adsorption. Boca Raton: Taylor & Francis.

Baccar, R., Bouzid, J., Feki, M., and Montiel, A., 2009. "Preparation of activated carbon from Tunisian olive-waste cakes and its application for adsorption of heavy metal ions", Journal of hazardous materials 162 1522-1529.

Cecen, F., and Aktas, O., 2012. Activated carbon for water and wastewater treatment. Weinheim, Germany: Wiley-VCH Verlag & Co. KGaA, Boschstr.

Chuachan K., 2013. Effect of carbonization temperature on the properties of charcoal and activated carbon from coconut shell. A thesis for the degree of Master of Chemical Engineering. Suranaree University of Technology.

Fu, F., and Wang, Q., 2011. "adsorption efficiency of heavy metal ions from wastewaters: A review", Journal of Environmental Management 92 407-418.

Gupta, V. K., Ganjali, M.R., Nayak, A., Bhushan, B., and Agarwal, S., 2012. "Enhanced heavy metals removal and recovery by mesoporous adsorbent prepared from waste rubber tire", Chemical Engineering Journal 197 330-342.

Gupta, V. K., Ali, I., Saleh, T. A., Siddiqui, M. N., and Agarwa, S. 2013. "Chromium removal from water by activated carbon developed from waste rubber tires", Environmental Science Pollution 20:1261-1268.

Gonsalvesh, L., Marinov, S. P., G. Gryglewicz, R. Carleer, and J. Yperman., 2016. "Preparation characterization and application of polystyrene based activated carbon for Ni (II) removal from aqueous solution", Fuel Processing Technology 149 75-85.

Hadi, P., Yeung, K. Y., Guo, J., Wang, H., and McKay, G., 2016. "Sustainable development of tyre char-based activated carbons with different textural properties for value-added applications", Journal of Environmental Management 170 1-7.

Karunarathne, H.D.S.S., and Amarasinghe, B.M.W.P.K., 2013. "Fixed bed adsorption column studies for the removal of aqueous phenol from activated carbon prepared from sugarcane bagasse", Energy Procedia 34 83-90.

Karmacharya M.S., Gupta, V. K., Tyagi I., Agarwal, S., and Jha, V. K., 2016. "Removal of As (III) and As (V) using rubber tire derived activated carbon modified with alumina composite", Journal of molecular liqids 216 836-844.

Langmuir, D., 1997. Agueous Environmental Geochemistry. New Jersey: Prentice-H all.

Lata, S., Singh, P.K., and Samadder, S.R., 2014. "Regeneration of adsorbents and

recovery of heavy metals: a review", J. Environ. Sci. Technol., pp. 1461-1478.

Lenia, G., Stefan P. M., Grazyna G., Robert C. and Jan Y. 2016. Preparation, characterization and application of polystyrene based activated carbons for NiII) removal from aqueous solution. Fuel Processing Technology. 149 75-85

Ministry of industry, 2004. "Office of Industrial Product Standards", Standard of Industrial Activated Carbon Product TIS 900-2004.

Mousavi, H. Z., Housseynifar, A., Jahed, V., and Dehghani, S. A. M., 2010. "Removal of Lead from aqueous solution using waste tire rubber ash as an adsorbent", Brazilian Journal of Chemical Engineering (79-87).

Printhorn T., 2008. Preparation and analysis of specific characteristics of activated carbon from bamboo tong and bamboo dog. Master of Science Thesis (Chemistry). Kasetsart University.

Saleh, T. A., Gupta, V. K., and Al-Saadi, A. A., 2013. "Adsorption of lead ions from aqueous solution using porous carbon derived from rubber tires: Experimental and computational study", Journal of Colloid and Interface Science 396 264-269.

Saleh, T. A., and Gupta, V. K., 2014. "Processing methods characteristics and adsorption behavior of tire derived carbons: A review", Advances in Colloid and Interface Science 211 93-101.

Saleh, T. A., and, Gaddafi I. Danmaliki, 2016. "Influence of acidic and basic treatments of activated carbon derived from waste rubber tires on adsorptive desulfurization of thiophenes", Journal of Taiwan institute Chemical engineers 60 460-468.

Williams, T., 2013. "Pyrolysis of waste tyres: A review", Waste Management 33 1714–1728.

Effects of Organophosphate Insecticides on Acetylcholinesterase Activity in Earthworms and Dragonfly Nymph from Highland Rose Cultivation Area in Chiang Mai Province

Nout Kanyaphim[1], Supap Saenphet [2], Chitchol Phalaraksh[2]*

[1] Master's Degree Program in Environmental Science, Environmental Science Research Center, Faculty of Science, Chiang Mai University, Chiang Mai, 50200, Thailand.

[2] Department of Biology Faculty of Science, Chiang Mai University, Chiang Mai, 50200, Thailand;

Corresponding author: e-mail: chitcholp@gmail.com

ABSTRACT

The study aimed to investigate the effect of organophosphates insecticides on acetylcholinesterase (AChE) activity in earthworms and dragonfly nymphs from highland rose cultivation area. The field study was designed in two seasons, dry season and rainy season. The study was carried out in the private rose cultivation farms at Baan Buak Toey Village, Pong Yeang Sub-district and the headwater area along Mae Rim River, Mae Rim District, Chiang Mai Province, Thailand. The samples of earthworms and dragonfly nymphs were collected once a month in February, April and July 2018. The effects of insecticides were evaluated by measuring the biomarker activities of AChE. Head of earthworm and dragonfly nymph samples were dissected and analyzed for AChE activity using Ellman's procedure. The results showed that some AChE activity in earthworm on treatment sites were significant difference (p<0.05) as compare to the reference site in February and April. In February, the activity in treatment site was $0.01x10^{-5}$, while the reference site

was $0.12x10^{-5}$. In April, those values in treatment were $0.01x10^{-5}$, $0.01x10^{-5}$, $0.03x10^{-5}$ and reference site was $0.07x10^{-5}$. However, a different activity was observed in treatment of July it was found that $0.09x10^{-5}$, and one site was $0.03x10^{-5}$. The unit of AChE activity is mole substrate hydrolyzed/min/g tissue. A significant inhibition of AChE activity in earthworms varied in different months owing to use of insecticides by rose farmer in their field and also possibly have been influenced by use of biochar in some part of rose cultivation area. For the dragonfly nymphs, the significant difference of AChE activities for months of February and April could not be observed. By contrast, in July one treatment site was significantly different ($p<0.05$) compared to the reference site, the results showed $0.03x10^{-5}$ and one treatment site was $0.11x10^{-5}$. AChE activity in the dragonfly nymphs were not significantly different between February and April which possibly due to changing in temperature and dissolve oxygen in case that normal temperature and low dissolve oxygen in water causes of AChE activity increased for a short duration after that AChE activity slightly decreased and also depending on season since during rainy season the intensive rainfall cause surface runoff and subsurface flow and increases the transport of pesticides.

Keywords: organophosphate insecticides, acetylcholinesterase activity, earthworm, dragonfly nymph

INTRODUCTION

Highland agriculture is now much more diverse with intensive production of vegetables, fruits and flowers in fixed fields becoming the dominant type of land use, especially in those areas where infrastructure and markets are both well-developed (Jiang et al., 2007). The intensification and commercialization of highland agriculture has brought economic benefits to previously marginalized communities in mountainous parts of Southeast Asia, but has also raised concerns about sustainability, notably the intensive use of agrochemicals and especially that of synthetic pesticides (Midmore and Poudel, 1996; Poudel et al., 1998; Praneetvatakul et al., 2001; Mazlan and Mumford, 2005; Kunstadter, 2007; Chalermphol and Shivakoti, 2009). The more intensive use of pesticides in highland systems needs to be seen in the context of Thailand's crop protection policy, which, compared to most developed countries, is rather supportive of pesticide use. It builds on the widely shared assumption among policy makers that synthetic pesticides are essential for maintaining and increasing the country's agricultural production (Kunstadter, 2007). Almost all agricultural pesticides used in Thailand are imported, but pesticides used in agriculture are exempted from import duties, business and municipal taxes (Poramacom, 2001). Pesticides, in spite of having various beneficial effect to agriculture, constitute some persistent problems in causing pollution in the environment. Agricultural pesticide application represents a serious hazard to wildlife and ecosystem resources, which has led to a growing concern worldwide over the indiscriminate use of such chemicals (Venkateswara Rao, 2006; Sparling and Fellers, 2007; Kathuria, 2007). Although the pesticide even when present in small quantities, their variety, toxicity and persistence have an adverse effect on ecological system. Especially, Organophosphate and carbamate insecticides are increasingly used in agriculture has

resulted in their widespread distribution in the environment. Due to high efficiency and lower persistence in the environment. Both operate through inhibiting the enzyme acetylcholinesterase, allowing acetylcholine to transfer nerve impulses indefinitely and causing a variety of symptoms such as weakness or paralysis. Moreover, organophosphate negatively affect to aquatic invertebrate as biomarker on acetylcholinesterase activity due to the effects of pesticide runoff in an agricultural area. The ecotoxicological risk of benthic communities, estimated through the assay of biochemical markers, can be used as an early warning signal for environment alterations. In addition, the use of pesticides is generally toxic to non-target soil organisms and as a consequence may hamper proper functioning of the soil. Ecologically concern, earthworms pay an important role in the soil ecosystem and a key role in modifying the physical structure of soils by producing new aggregates and pores, which improves soil tilth, aeration, infiltration, and drainage. Earthworms produce binding agents responsible for the formation of water-stable macro-aggregates. They improve soil porosity by burrowing and mixing soil and feeding activities stimulate microbial proliferation and trigger changes in microbial communities change in temperature and soil moisture would affect microbial processes and other potential producer of soil extracellular enzymes such as earthworms. Moreover, the addition of modifying such as biochar could be an environmentally friendly solution to help in the stabilization of extracellular enzymes in the soil.

Acetylcholinesterase (AChE) activity is inhibited mainly from the toxicity of organophosphate pesticides. AChE is responsible for the hydrolytic degradation of acetylcholine, which is the primary neurotransmitter in the sensory and neuromuscular systems in most animal species. This enzyme plays a key role in regulation of cholinergic nervous transmission. AChE inhibition leads to overstimulation of

the central and peripheral nervous system, resulting in deleterious effects for the organism, and ultimately death. Therefore, since the 1970s, inhibition of AChE is proposed as a specific biomarker for pesticide exposures (Payne et al., 1996; Fulton and Key, 2001).

METHODOLOGY

Study area

The study was conducted in Mae Ja Noi, Mae Ja Loung stream and headwater of Mae Sa river which cover the area of Konghae village and Queen Sirikit Botanic Garden at Pong Yeang Sub-district and Mae Rim River. The lower Mae Sa River and Mae Ja stream. This area is highland agricultural area which intensively use of pesticides, especially in rose cultivation which cover rather large area on the hill. The research was carried out in the private rose cultivation area which located in Baan Buak Toey, Pongyeang Sub-district and the headwater area along Mae Sa River Mae Rim district, Chiang Mai Province Thailand, 45 km north of Chiang Mai city. Field study was designed for both dry and wet seasons. Earthworms were sampled from two rose cultivation gardens, with two sampling sites for each area (total of four treatments). One site in Baan Konghae with no agricultural area representative as reference site. The coordination of earthworms and dragonfly nymphs sites namely site 1 MJN1 (18°53'29" N 98°47'33" E) and site 2 MJL1 (18°52'56" N 98°47'9" E) are located in private rose cultivation area, where the farmers used insecticides extensively, site 3 MS1 (18°51’43” N 98°48'26" E) is the reference site was located in Baan Konghae, which was uncultivated and fallow land, free from any insecticides, site 4 MJN2 (18°52'51" N 98°48'23" E) located in Mea ja Noi stream, Pong Yaeng village, site 5 MJL2 (18°52'42" N 98°47'25" E) and site 6 MJL3 (18°52'50" N 98°48'44" E) located in Mea Ja Loung stream, Pong Yaeng village as well as site 7 MS2 (1°53'25" N 98°52'3" E) located in Mea Sa River, in front of Queen Sirikit Botanic Garden.

Earthworms collection

Adult earthworms were collected from rose cultivation area and reference station, once a month in February, March and May 2018. Random sampling method was used for this process; where, trowel and shovel were used to dig up earthworms from both rose crop and the reference site. A total ten earthworms were collected from each site locations. These specimens were stored in plastic bag and kept in ice bottles and brought back to laboratory for AChE activity analysis and comparison of results.

Dragonfly nymph collection

The dragonfly nymphs (Odonata) were collected from 7 study sites by using pond nets by kick method. The specimens were stored in plastic bag and preserved in ice bottles. The samples were safely stored in laboratory.

Acetylcholinesterase activity assay

Ellman's procedure (Ellman et al., 1961) was used for determination of cholinesterase activity and the monitoring of enzymatic hydrolysis of acetylcholine (ACh) by acetylcholinesterase (AChE). The heads of earthworm samples and dragonfly nymph samples were dissected on ice and placed in a pre-weighted Eppendorf tube before measurement of the head weight and used for analysis of AChE concentration. Assay of ChE activity were performed using 96-well plates. Each head was then homogenized by using a glass homogenizer in 1ml of 0.1 M (pH 8.0) phosphate buffer saline (PBS). The homogenates were transferred into 1 ml Eppendorf tubes and centrifuged at 3,500 revolutions per minute (rpm) at 4°C for 10 minutes. 1 ml of supernatant was removed to an Eppendorf tubes and kept on ice for AChE analysis. In the assay was added of 0.2 mM 5,5'-dithiobis - (2- nitrobenzoic acid) 1300 µL and 130 µL of the supernatants were added. 62.5 µL of 0.75 mM acetylthiocholine iodide was added and the solution was well

mixed, and then measurements were done. Blanks were used as PBS buffer instead of supernatants. The AChE enzyme activity was detected using an ELISA reader, Tecan Austria GmbH 5082 Grogig, Austria, for cycles 2 min at 5 times at a wavelength of 405 nm. Absorption kinetics were calculated in the rate absorbance, then converted to optical density per minute. The enzymatic activity was expressed as mole of acetylcholine hydrolyzed min^{-1} g^{-1} of tissue.

Statistical analysis

All results of earthworms and dragonfly nymph are expressed as the mean ± standard deviation of AChE activity. The treatment sites were compared with the reference sites. The comparisons between sites were evaluated by analysis of variance one-way (ANOVA) in SPSS version 22.0 and were performed using Duncan test to determine the significance *p*-level was set at 0.05. The probability level for statistical significance was $p<0.05$.

RESULTS AND DISCUSSION

AChE activity in earthworms

The AChE activities were measured once a month in February, April and July 2018. The results (Figure 1) showed that some AChE activity in earthworm on treatment sites were significant difference ($p<0.05$) as compare to the reference site in February and April. In February, the AChE activity in treatment site (MJN1) was $0.01x10^{-5}$ reference site was $0.12x10^{-5}$. In April, those values in treatment were $0.01x10^{-5}$ (MJN1), $0.01x10^{-5}$ (MJN1 Bio), $0.03x10^{-5}$ (MJL1) and reference site was $0.07x10^{-5}$. However, in July treatment sites no significant between reference site were observed ($p>0.05$) but, the treatment site MJL1 Bio which used biochar was showed $0.09x10^{-5}$ significantly different as compare to the MJL1 in crop was $0.03x10^{-5}$. Organophosphate cause inhibition of AChE activity, in this study AChE activity were measured to indicate toxic effect resulting the

farmer exposure to insecticides on their rose filed. For this study, the samples were collected on February, April and July. For February and April all treatment sites were inhibited by organophosphate insecticides. A significant inhibition of AChE activity in earthworms varied in different months owing to use of insecticides by rose farmer in their field. For the month of May also it had been influenced by use of biochar in some part of rose cultivation area. In previous studies earthworm perionyx exposed to sublethal doses (0.03 and 0.3mg kg-1) of dimethoate the percentage inhibition of AChE was 34.6%, 69.2% (Somanka Sayal et al., 2017). In addition, exposure to pirimiphos-methyl caused significant inhibition of AChE activity in *Eisenia foetida* (Mirna Velki et al., 2014). Similar results regarding acute toxicity of chlorpyrifos was examined *E. foetida* inhibition at 12, 24, 36, and 48 hours, respectively (Hackenberger et al., 2008). However, the rainy season in July, we detected high AChE activity possibly because the insecticides got diluted by rain and also due to less use of insecticides by farmer. Moreover, in dry season (February and April). This was mainly because of extensive use of insecticides to increase the rose production to fulfil the market demand. July (wet season) is a low rose flower harvest time, so the farmers do not use much insecticides. Therefore, we found a higher AChE activity in earthworms as compared to the dry season. MJN1 bio site which used biochar had higher AChE activity, which showed that AChE activity was influenced by use of biochar in some part of rose cultivation area. Li *et al*., (2011) carried out an oxidative stress assay in earthworm *Eisenia foetida* to assess the potential toxicity of the soil impregnated with biochar. They reported that, the earthworm's avoidance of soil was not due to the presence of toxic compounds in a biochar exposed soil. This is mainly because biochar can carry out soil remediation by reducing the bioavailability of organic and inorganic pollutants Janus *et al*., (2015). For organophosphorus

contaminated soils, treatment with addition of biochar and NH_4NO_3 result showed reduction of 31.90% pesticide concentrations, as a result of reduced level of pesticides, microorganism activities increased which helps to improve soil fertility (Meinan Zhen *et al*., 2018)

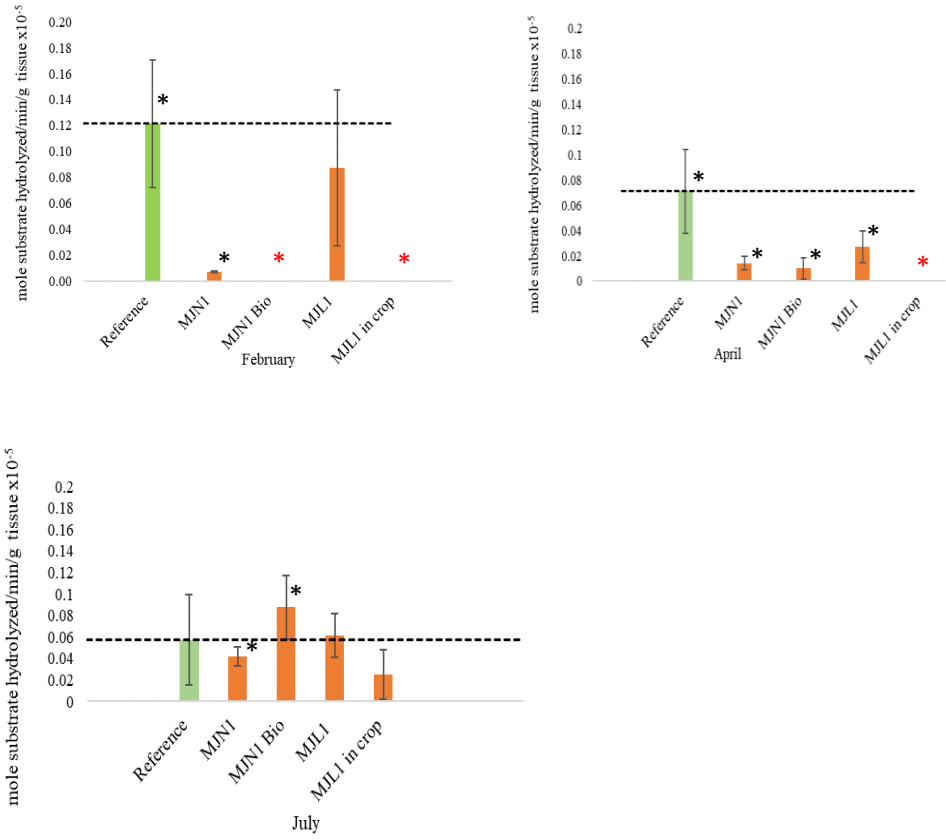

Figure 1 AChE activity measured in earthworms a month in February, April and July 2018

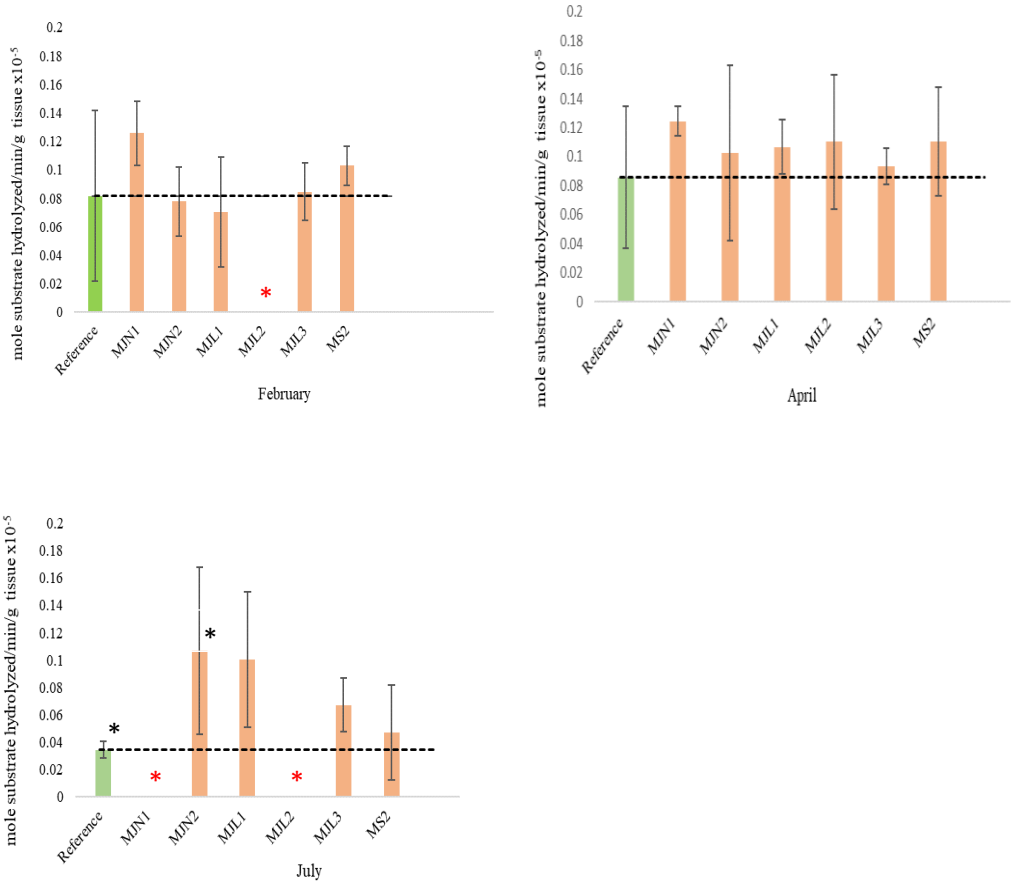

Figure 2 AChE activity measured in dragonfly nymph a month in February, April and July 2018.

*significant difference ($p<0.05$) between reference and treatment sites

*The samples were not collected

CONCLUSIONS

AChE activity detected in earthworms and dragonfly nymphs in the private rose cultivation farms at Baan Buak Toey Village, Pong Yeang Sub-district and the headwater area along Mae Ra River, Mae Rim District, Chiang Mai Province, Thailand. The earthworms have been found to serve as a good bioindicator for AChE biomarker. Since, the use of insecticides are directly toxic to non-target soil organisms and as a consequence may hamper proper

functioning of the soil as well as amount of insecticides consider to be toxic in the soil depends on the farmer usage on their crop. AChE biomarkers in dragonfly nymphs did not present a clear picture in our observation.

ACKNOWLEDEMENTS

The authors are grateful to Thailand International Cooperation Agency (TICA) for scholarship and financial and facilitated supports from Chiang Mai University and the Environmental Science Research Center, Faculty of Science, Chiang Mai University. We thank Medicinal Plant and Reproductive Research Unit and Freshwater Biomonitoring Research Laboratory (FBRL), Faculty of Science, Chiang Mai University for providing assistance to carry out field works and also laboratory works.

REFERENCES

Baer, K. N., Olivier, K., & Pope, C. N. (2002). Influence of temperature and dissolved oxygen on the acute toxicity of profenofos to fathead minnows (Pimephales promelas). *Drug and chemical toxicology*, *25*(3), 231-245.

Brewer, S. K., & Atchison, G. J. (1999). The effects of chlorpyrifos on cholinesterase activity and foraging behavior in the dragonfly, Anax junius (Odonata). *Hydrobiologia*, 394, 201-208.

Daam, M. A., & Van den Brink, P. J. (2010). Implications of differences between temperate and tropical freshwater ecosystems for the ecological risk assessment of pesticides. *Ecotoxicology*, 19(1), 24–37.

Ellman, G. L., Courtney, K. D., Andres Jr, V., & Featherstone, R. M. (1961). A new and rapid colorimetric determination of acetylcholinesterase activity. *Biochemical pharmacology*, 7(2), 88-95.

Hackenberger, B. K., Jarić-Perkušić, D., & Stepić, S. (2008). Effect of temephos on cholinesterase activity in the earthworm Eisenia fetida (Oligochaeta, Lumbricidae). Ecotoxicology and environmental safety, 71(2), 583-589.

Janus, A., Pelfrêne, A., Heymans, S., Deboffe, C., Douay, F., & Waterlot, C. (2015). Elaboration, characteristics and advantages of biochars for the management of contaminated soils with a specific overview on Miscanthus biochars.

Journal of environmental management, 162, 275-289.

Kahl, G., Ingwersen, J., Nutniyom, P., Totrakool, S., Pansombat, K., Thavornyutikarn, P., & Streck, T. (2008). Loss of pesticides from a litchi orchard to an adjacent stream in northern Thailand. *European Journal of Soil Science*, 59(1), 71–81.

Kunstadter, P. (2007). Pesticides in Southeast Asia: environmental, biomedical, and economic uses and effects. *Silkworm Books*, Ms Trasvin. pp. 326.

Li, D., Hockaday, W. C., Masiello, C. A., & Alvarez, P. J. (2011). Earthworm avoidance of biochar can be mitigated by wetting. *Soil Biology and Biochemistry*, 43(8), 1732-1737.

Mazlan, N., Mumford, J., (2005). Insecticide use in cabbage pest management in the Cameron Highlands, Malaysia. Crop Prot. 24, 31-39.

Midmore, D.J., Poudel, D.D., (1996). Asian vegetable production systems for the future. *Agricultural Systems* 50, 51-64.

Poramacom, N., (2001). Pesticide markets and related situations in Thailand. *Kasetsart Journal of Social Science* 22, 205-211.

Poudel, D.D., Midmore, D.J., Hargrove, W.L., (1998). An analysis of commercial vegetable farms in relation to sustainability in the uplands of Southeast Asia. *Agricultural Systems* 58, 107-128.

Praneetvatakul, S., Janekarnkij, P., Potchanasin, C., Prayoonwong, K., (2001). Assessing the sustainability of agriculture: a case of Mae Chaem Catchment, northern Thailand. *Environment International* 27, 103-109.

Sanyal, S., Kaviraj, A., & Chakravorty, P. P. (2017). Response of enzyme biomarker and life-history parameters of *epigeic* earthworm *Perionyx excavatus* exposed to organophosphate pesticide. *Journal of Entomology and Zoology Studies*. 5 (3), 774-778.

Velki, M., Hackenberger, B. K., Lončarić, Ž., & Hackenberger, D. K. (2014). Application of microcosmic system for assessment of insecticide effects on biomarker responses in ecologically different earthworm species. *Ecotoxicology and environmental safety*, 104, 110-119.

Zhen, M., Song, B., Liu, X., Chandankere, R., & Tang, J. (2018). Biochar-mediated regulation of greenhouse gas emission and toxicity reduction in bioremediation of organophosphorus pesticide-contaminated soils. *Chinese Journal of Chemical Engineering.* 9, 10-39.

Noise exposure among flower garland sellers who work at the red light intersection of Warinchamrap to Ubon Ratchathani bypass road, Ubon Ratchathani Province

Laksanee Boonkhao[1*], Nittaya Chakhamrun[2], Prapatsorn Nasok[3]

[1,2,3]College of Medicine and Public Health, Ubon Ratchathani University;

Coresponding author: e-mail: lasans76@yahoo.com

ABSTRACT

This descriptive research aims to study the noise exposure among flower garland sellers at the red light intersection of Warinchamrap to Ubonratchathani by-pass road, Ubonratchathani Province. The study area was at 6 different intersections including Lukhamhan, Nongtaphon, Kham Nam Saep, Dong Uphueng, Wanarom and Nonhongthong. The study was conducted by having flower garland sellers use a noise dose meter monitor while working and then comparing it to the national standard noise levels. There were 2 representatives per each intersection. The study showed that the average noise dosimeter level throughout an 8 hour working period (TWA8) was between 58.7-78.9 dBA. The highest level collected was 78.9 dBA (or 21.57 %Dose) from the flower garland seller who works at the Dong Uphueng intersection and the lowest level was 58.7 dBA (or 1.30 %Dose) from the flower garland seller who works at the Nonhongthong intersection. While comparing the noise dosimeter with the national standard, it was found that the noise level that was monitored from all sellers were consistent with the standard (TWA □90 dBA). However, when the flower garland sellers are exposed to the noise for a long time, with the increase of traffic conditions, they may have chances of health risks, particularly with their hearing functions. Therefore, to prevent and solve

the noise exposure problem from this type of work, the sellers should use noise protection devices such as ear plugs, complete an annual hearing test, and agencies should further help train and inform the sellers on the proper ways to handle noise protection while working.

Keyword: noise dosimeter, flower garland sellers, intersections, Ubon Ratchathani

INTRODUCTION

Selling flower garlands along red light intersections is a way that sellers can earn money. However, it also makes them vulnerable to various health problems as they are standing and walking around a lot during their working hours. In addition, sellers are also faced with smoke problems caused from car exhausts, the sun, rain, the risk of accidents, and noise exposure caused by road traffic. According to the survey of the Statistics Transportation Group, Transport Planning Division within the study of Neatchanok Rattanarin, 2015 [1], it is shown that the number of vehicles in Bangkok continuously increase annually. Based on vehicle statistics from the Department of Transport, in 2011 and 2012, there were 36,763 and 43,236 new registered vehicles, respectively. These addition of vehicles may cause a lot of noise pollution. Therefore, being exposed to noise pollution for a long, consecutive amount of time may cause health hazards both mentally and generally. Mental health hazards can include: disruption of sleep, interference with work efficiency, a loss of work accuracy, communication interference, and lack of identifying various signals of danger through hearing. Even more so, general health issues can include the following: changes in physiology, physical and mental exhaustion, nausea, irritability, high blood pressure, gastritis, tension and muscle pain [2]. The noises from road

traffic in each area can be caused by many reasons, such as exhaust, road surface, and the density of traffic which sometimes can cause noise pollution exceeding 90 dB(A). As the study of Puttapong Charoynuch and et al., (2012) [3] shown, road traffic noise may be the cause of many health problems. According to the law on noise pollution and vibration in Thailand, there is a general noise level standard set for national environmental quality at a maximum of 115 dB(A), and the average noise level for 24 hours, not higher than 70 dB(A). Based on the data from the Pollution Control Department in 2010 and 2011[4], it was found that 5 out of 6 roadside areas of districts in Bangkok had accumulated noise exceeding the national 24 hour noise standard. According to the noise monitors at the areas placed along the road, the minimum average of noise levels ((Leq)24 hrs) in 2014 and 2015 were 52.5 dB(A) at Mueang Songkhla Municipality and 46.5 at Mueang Hat Yai Municipality, respectively. The maximum average of noise levels ((Leq)24 hrs) in 2014 and 2015 were 83.3 dB(A) at Mueang Khon Kaen District and 84.0 at Mueang Phuket District, respectively [5]. Within the studies on the effects of noise and vibration pollution towards health, it was found that the noise levels among Bangkok sweeper communities along the Chinatown road and Saphan Khwai Community were 72.7 - 92.7, 71.4 - 83.0 and 78.5 - 83.4 dB(A), respectively[6].

As opposed to the above information found, there was no data presented on the noise level monitors in Ubon Ratchathani Province. However, there are many flower garland sellers working at the red light intersection roads, especially on the bypass road of Warinchamrap District to Mueang District. There was a total of 6 intersections consisting of Lukhamhan, Nong Ta Phon, Kham Nam Saep, Dong U Phueng, Wanarom and Non Hong Thong which many of the health risks that the flower garland sellers were exposed to were caused by road

traffic. The researchers were interested in studying the noise dosimeter level among flower garland sellers who work at the red light intersection of Warinchamrap District to Mueang District, Ubon Ratchathani bypass road, Ubon Ratchathani Province. The results were useful for concern agencies to further plan for the preventive actions on reducing and solving health risks of noise pollution among flower garland sellers.

MATERIALS AND METHODS

Studied sites

This descriptive study was taken place at the red light intersection of Warinchamrap District to Mueang District, Ubon Ratchathani bypass road during August 2017 to May 2018.

Subjects & Sampling strategy

The population in this study were flower garland sellers who work at the red light intersection of Warinchamrap District to Mueang District, Ubon Ratchathani bypass road totaling 56 persons. The sellers with the highest noise exposure were recruited at each intersection (for the worst case scenario where monitors presented duplicate information, 2 participants were selected versus 1 at each intersection). The participants were selected with a 3 step criteria: firstly, the sellers who worked for the longest hours a day were selected. Secondly, if the working times of sellers were equal, the period of time the worker has been a seller is considered. Thirdly, the sellers who were open to be a part of the study were selected. The demographic of the selected participants are shown in Table 1:

Table 1 Demographic of participants (n=12 persons)

No.	Demographics	Number (person)	Percentage
1	Gender - Male - Female	 8 4	 66.7 33.3
2	Age (year) Mean 28.0 (SD= 7.04), Maximum = 39, Minimum= 21		
3	Work period (year) Mean 5.1 (SD= 2.2), Maximum = 10, Minimum= 3		
4	Working hour /day (hrs.) Mean 7.6 (SD= 0.9), Maximum = 9, Minimum= 6		
5	Annual hearing examination - No	 12	 100.0
6	Noise effect training - No	 12	 100.0

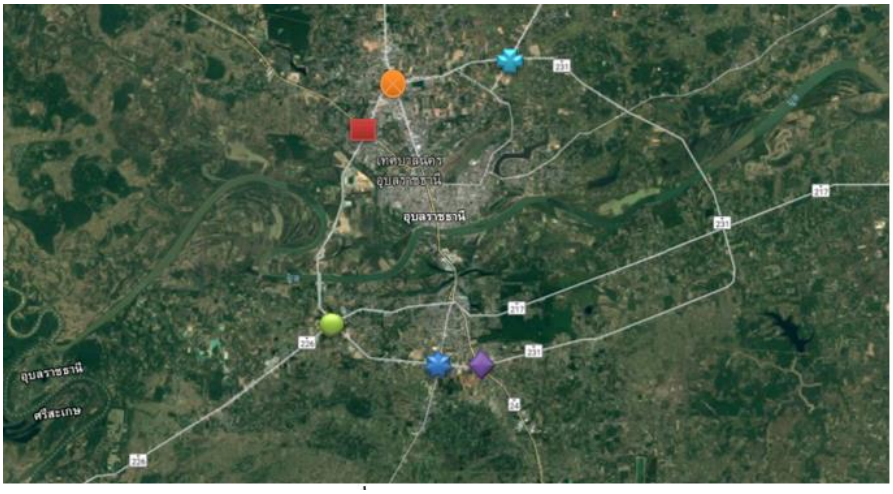

Figure 1 the area for noise monitoring

Remark

- Lukhamhan Intersection
- Nong Ta Phon Intersection
- Kham Nam Saep Intersection
- Dong Uphueng Intersection
- Wanarom Intersection
- Non Hong Thong Intersection

The area for noise monitoring within each red light intersection is shown in figure 1

Tools

1. Noise dosimeters that undergo rigorous testing protocols to ensure that the electronic components were in good working order. These periodic calibrations occur annually and are done before the monitor is used as a noise calibrator.
2. Noise record format paper
3. The environmental survey form: general conditions of red light intersection.

Data collection

1. Noise dosimeters and instruments preparation.
2. Monitoring the noise level by personal noise dosimeters which were worn on the bodies of sellers with a microphone mounted on the top- middle of the person' s most exposed shoulder who work at 6 red light intersections including 1) Lukhamhan Intersection, 2) Nong Ta Phon Intersection, 3) Kham Nam Saep Intersection, 4) Dong Uphueng Intersection, 5) Wanarom Intersection and 6) Non Hong Thong Intersection. Information collected was then used to calculate the noise dosimeters within time weighted average for 8 hours per day.
3. Environmental survey at each intersection.
4. Data analysis.

The researchers calculated the noise dosimeter during working hours and compared the result with the noise standard of the Ministerial regulations prescribing standards for the management of occupational safety, health and working environment regarding heat, light and noise, 2016, which set the TWA of noise less than 90 dBA.

To calculate the noise dosimeter to percentage of exposure (D) at the stable noise level (L) though working hours (T) the following formula was used [7]:

$$D = 100 \times (C / T)$$

When

C = Working hour per day

T = Reference time

To calculate the Time Weighted Average (TWA) for 8 hours of noise

dosimeter level, the following formula was used:

$$TWA\ 8\ hours = 16.61 \log_{10}(D/100) + 90$$

RESULTS

In regard to the general environment at each red light intersection, there were no high buildings nearby each intersection. The surrounding areas were open except at Dong Uphueng Intersection which was surrounded by a small forest. (Table 2)

While comparing the noise level in each intersection with the standard of the Ministerial regulations prescribing standards for the management of occupational safety, health and working environment regarding heat, light and noise, 2016, which set the TWA of noise less than 90 dBA, it was found that the noise dosimeter at each red light intersection did not exceed the standard. Additionally, when comparing the noise dosimeter for seller exposure within percentage Dose unit (%Dose) which that the level must less than 100 the result showed normal level at 1.30-21.57%Dose. Details as shown in Table 3

Table 2 General environmental conditions at each red light intersection

No	Intersection name	General detail
1	Lukhamhan Intersection	This intersection is next to the Charoensri Market. The intersection split the way between Warinchamrap district and Det Udom district which passes Ubon Ratchathani University. The green light shows for 30 seconds and the red light shows for 90 seconds.
2	Nong Ta Phon Intersection	This intersection splits the way to go to Warinchamrap District which leads to Lotus Warinchamrap Superstore and the way to go to Kantaralak district which leads to go to Big C Warinchamrap Superstore. The green light shows for 30 seconds and the red light shows for 110 seconds.
3	Kham Nam Saep Intersection	This intersection splits the way to go to Warinchamrap district which leads to Warinchamrap hospital and the way to go to Sisaket Province. The green light shows for 30-45 seconds and the red light shows for 135 seconds.
4	Dong Uphueng Intersection	This intersection has a lot of traffic as it splits the way to go to Prasrimahaphothi Hospital, Rajabhat Ubon Ratchathani University and Yasothon Province. The green light shows for 50 seconds and the red light shows for 118 second. There is a small forest around this intersection.
5	Wanarom Intersection	This intersection splits the way to go to Amnatcharoen Province and Mueang Ubon Ratchathani District. The green light shows for 37 seconds and the red light shows for 137 seconds.
6	Non Hong Thong Intersection	This intersection splits the way to go to Trakan Phuet Phon District and Phibun Mangsahan District. The green light shows for 30 seconds and the red light shows for 90 seconds.

Table 3 The noise dosimeter among flower garland sellers at the intersection of Warinchamrap to Ubonratchathani by-pass road.

Area	sampling no.	Time range for measurement	%Dose	TWA (dBA)	Std.Comparative results
Lukhamhan Intersection	1	07.59-15.59	2.03	61.9	Pass
	2	12.58-20.58	3.56	65.9	Pass
Nong Ta Phon Intersection	1	08.10-16.10	2.76	64.1	Pass
	2	13.14-17.14	1.58	60.0	Pass
Kham Nam Saep Intersection	1	07.50-15.50	3.02	64.7	Pass
	2	12.56-16.56	7.28	71.1	Pass
Dong Uphueng Intersection	1	07.59-16.59	21.57	78.9	Pass
	2	12.50-20.50	8.59	73.5	Pass
Wanarom Intersection	1	07.53-15.53	17.26	77.3	Pass
	2	13.02-21.02	7.08	72.3	Pass
Non Hong Thong Intersection	1	08.15-16.15	1.31	58.8	Pass
	2	13.00-17.00	1.30	58.7	Pass

Remarks:

- %Dose = the noise dosimeter among sellers within the unit of %Dose which must be less than 100
- The national standard of noise 90 dBA

DISCUSSION AND CONCLUSION

Discussion

According to the study of noise exposure among flower garland sellers at the red light intersection, Warinchamrap District to Mueang District, Ubon Ratchathani bypass road was an area with heavy traffic. The researchers distributed the noise dosimeter to the representative population by selecting 2 persons per red light intersection. The persons selected have had long time noise exposure. The data was then collected and compared with the national standard. The results showed that the Time Weighted Average (TWA) of noise dosimeter among flower garland sellers was between 58.7-78.9 dBA. The highest of average noise level was at Dong

Uphueng Intersection which was 78.9 dBA or 21.57%Dose. The lowest of average noise level was at Non Hong Thong Intersection which was 58.7 dBA or 1.30 %Dose. All intersections' average noise level were consistent with the standard of the Ministerial regulations prescribing standards for the management of occupational safety, health and working environment regarding heat, light and noise, 2016[8]. Although there was heavy traffic on such bypass roads, the surrounding areas were open space. Furthermore, there were no high buildings which is a reflection of the traffic noise that will affect flower garland sellers who work at the intersection areas. However, the Dong UPhueng intersection had an average noise dosimeter level higher than other intersections. This may be due to the fact that the Dong UPhueng intersection is apart from the connection between Warin Chamrap District and Ubon Ratchathani Province. This intersection also connects the high way from Yasothon Province which means it is possible that many more vehicles are present as opposed to other intersections causing the noise exposure among flower garland sellers to be higher. Even though the measurement results did not exceed the standard, this study was not consistent with the study of Praworada Pochanajun and et al., 2009[9]. They found that workers in Bangkok, had been affected by traffic noise pollution exceeding the standard (> 90 dBA) due to the amount of vehicles and the density of traffic in Bangkok which was higher than in rural provinces such as Ubon Ratchathani Province [10]. However, this study's sample size may have been too small to make big generalizations. Further studies should be conducted to have more accurate findings, to calculate the amount of vehicles that pass through each intersection, and to evaluate the density of traffic. Furthermore, the impact of the noise to the people who live around each intersection should be analyzed. By analyzing this, the

findings can help create more health and safety guidelines that can help the people who live around these areas.

Conclusion

The average of noise dosimeter levels throughout an 8 hour working period (TWA8) among flower garland sellers was between 58.7-78.9 dB(A). The highest level was 78.9 dB(A) (or 21.57 %Dose) among the sellers who work at the Dong Uphueng intersection. The lowest level was 58.7 dB(A) (or 1.30 %Dose) among the sellers who work at the Nonhongthong intersection. All noise levels that were exposed to all sellers at each intersection were consistent with the standard (TWA ≤90 dBA).

Recommendation from the study

This study showed that all flower garland sellers were exposed to the noise level that were consistent with the standard (TWA ≤ 90 dBA) . However, the sellers who are exposed to the noise for a long time with the continuous increase of traffic conditions nowadays may have a higher chance of health risks, particularly hearing risks. Therefore, sellers should use noise protection devices such as ear plugs, complete an annual hearing test, and concerned agencies should further help train and inform the sellers on the proper ways of noise protection while working.

ACKNOWLEDGMENTS

The authors extend a thanks to all of the flower garland sellers who work at the red light intersection of Ubon Ratchathani bypass road and Ubon Ratchathani University to support the work until the project was completed.

REFERENCES

[1] Neatchanok Rattanarin . A Study of The Effect of Agricultural Price Change on The Number of Isuzu Pickup (Out of Warranty) in Isuzu Standard Service Center in The Southern Area of Thailand. Business Economics, Department of Economics. Independent Study, Kasetsart University;2015.

[2] Bureau of Technical Advisors. Noise pollution.

http://advisor.anamai.moph.go.th/main. php?filename= env2 0 3 . Accessed 20 September 2018.

[3] Puttapong Charoynuch and et al., The impact of road traffic noise among motorcyclists Bangkok: 2012. ; http://www.dms.eng.su.ac.th/filebox/FileData/ WPS018. Accessed 20 September 2018.

[4] Thammasart University . Traffic Noise pollution control. Bangkok: 2010. http://digi.library.tu.ac.th/thesis/la/1577/ 03CHAPTER2. pdf. Accessed 17 September 2018.

[5] Air and Noise Quality Management Division. Pollution Control Department. Noise level data in Thailand 2014-2015.http://noisemonitor.net/web/download.php. Accessed 27 may 2019.

[6] Bureau of Technical Advisors. The situation and trends of environmental health problems. http://advisor.anamai.moph.go.th/main. php?filename= env203. Accessed 27 may 2019.

[7] Department of Labour Protection and Welfare. Guidelines for compliance with Ministerial Regulations prescribing standards for the management of occupational safety, health and working environment concerning heat, light and sound, 2006-Noise Measurement. Bangkok: 2006. http://hm.measure1.co.th/Knowledge/practice_noise; Accessed 20 September 2018.

[8] Department of Labour Protection and Welfare. Ministerial Regulations for Heat, Light and Sound. Bangkok; 2017. http://www.oshthai.org/index.php?option=com_phocadownload&view=category&id=57%3A-m---m-s&Itemid=186 ; Accessed 28 May 2018.

[9] Praworada Pochanajun and et al., Noise pollution and hearing performance of people and workers affected by noise pollution along the traffic area in Bangkok. Faculty of Science and Technology Suan Dusit Rajabhat University: Bangkok; 2009.

[10] . Department of Land Transport, Ministry of Transport. The statistics of The province with the highest number of registered cars, 10 orders, 2009 – 2011. http://service.nso.go.th/nso/nsopublish/ TopTen/ 14/ T1401/ th/ th. htm. Accessed 22 May 2019.

The inhalation exposure and health effect of PM10 of population in faculty of engineering, Naresuan University and particle management

Theerapon Suksamran[1], Pajaree thongsanit[2]

[1]Master's degree student, civil engineering department, Faculty of Engineering, Naresuan University, Phitsanulok, Thailand 65000
[2]Assistant Professor, civil engineering department, Faculty of Engineering, NaresuanUniversity, Phitsanulok, Thailand 65000;
Coresponding author: e-mail: theerapons61@email.nu.ac.th

ABSTRACT

Research conducted from 2010 to 2017 by the Faculty of Engineering, Naresuan University revealed a dust problem. Accordingly, this latest research studied inhalation exposure and health effects of particulate matter with an aerodynamic diameter equal to a nominal 10 µm. (PM10). The PM10 samples were collected from the environments of volunteers using low volume air samplers with a flow rate of 1.7 L/min. The volunteers, from six occupational groups (lecturers, administrative staff, students, gardeners, security officers, and housemaids), were asked to carry the air samplers for 1 working day (8 hours). Fifty samples were collected from January 2019 to March 2019. The lowest level of the inhalation exposure was collected from the lecturers at $0.75x10^{-4}$ mg/kg/day, while the highest level was from the security officers at $2.1x10^{-4}$ mg/kg/day. When the data was divided into 3 groups (skilled workers, students and, unskilled workers), the skilled workers, with a Hazard Quotient (HQ) of $8.12x10^{-3}$, were exposed to less PM10 than the unskilled workers and the students, with a HQ of $7.86x10^{-3}$, were exposed to less PM10 less than the unskilled workers, while both the skilled workers and students

had a coefficient of determination of 59.70%. This meant there was a very low effect on health. It suggested the volunteers from occupations who worked outside the building were exposed to more PM10 than those who worked or spent most of their time within the building. However, the results did not suggest a high risk for all of the six occupational groups.

Keywords: Inhalation exposure, Health effect, PM10, Naresuan University

INTRODUCTION

Naresuan University has a population of 24,801 people within an area of 2.08 square kilometers [1]. With a density of 11,924 people per square kilometers, it can be interpreted as a moderate density. The Faculty of Engineering has 9.1 percent of the total population of the university. There have been many construction sites around the area. The Faculty of Agriculture, which is close to the Faculty of Engineering, has been undergoing construction from 27 September 2018 to 21 December 2019. This construction has been one of many factors giving rise to particulate matter smaller than 10 microns (μm.). In addition, there has been a lot of dust from rock drilling, cigarette smoking, cooking, vehicles and harvesting, etc.

From research conducted from 2010 to 2017, the Faculty of Engineering encountered dust exceeding the Pollution Control Department (PCD) standard of 120 $\mu g/m^3$ throughout 2017. Primrudi studied the amount of accumulated dust on the main road surface in the Naresuan University area, which measured 75 μg. The greatest amount accumulated between October and January [2]. In 2017, Supakit studied dust collection in the building in the Faculty of Engineering, the Faculty of Medicine, the Faculty of Agriculture, Natural Resources and Environment, and the Faculty of Medical Science. The amount of dust falling outside these faculties was 217, 238, 233 and 234 milligrams per square meter per day ($mg./m^2/day$), respectively, which exceeded the PCD standard of 133 $mg./m^2/day$ [3]. Phatthanan

conducted a study of PM10 at the Faculty of Engineering library, where there was 64.63 micrograms per cubic meter ($\mu g/m^3$). The female bathrooms had the highest level at 133.22 $\mu g/m^3$, which exceeded the 120 $\mu g/m^3$ PCD PM10 standard. These results may have been caused by the indoor air circulation system or the students and staff taking dust into the building [4].

Objective

This research aimed to study indoor and outdoor PM10 concentrations **(Fig. 1).** It also studied the health effects of PM10 inhalation exposure on all six occupations and PM10 management at the Faculty of Engineering, Naresuan University.

METHODOLOGY

Sampling

Samples taken from inside the multi-story buildings were collected from 80% of the total floor area in places with a lot of people, or areas which contained sources of important problems, such as near the smoking area or the photocopying room etc. [5]

The samples collected from outside the building were collected randomly from outdoor air sampling station number 5, as shown in **Fig. 1**, for comparison with those taken from inside the building.

Criteria for choosing volunteers

Volunteers were members of the Faculty of Engineering aged from 17 to 59 years of age. During the study, volunteers who did not wish to continue participating in the program could cancel immediately without any impact on the other volunteers. **(Table 1)**. The volunteers from six occupational groups (lecturers, administrative staff, students, gardeners, security officers, and housemaids) were asked to carry the air samplers for 1 working day (8 hours). Fifty samples were collected between January 2019 and March 2019.

Questionnaire

The questionnaire content was designed to be consistent with the activities in the area of Faculty of Engineering. There were 3 parts as follows:

Part1: General information such as gender, age, body weight, occupation, number of years working in the area,

congenital diseases as diagnosed by doctors, smoking behavior of family members in their house, residential characteristics and sources of dust that the volunteers received.

Part2: Health impacts from air pollution, smoking behavior, acute symptoms after exposure to air pollutants, awareness of the volunteers' illness, and self-protective behavior.

Part3: Activities within the Faculty of Engineering for 1 working day (8 hours).

License to use the questionnaire

This questionnaire was reviewed and approved by the Human Research Committee of Naresuan University, License Number: No. 062/2562.

Equipment

The sampling was performed using Low Volume Air Samplers with a flow rate of 1.7 L/min. PM10 collection equipment consisted of a personal air sampler encased in a shoulder bag. It had a hose from the device connected to a 37 mm diameter, glass fiber PM10 cassette filter. The equipment had an air intake situated about 30 cm from the volunteer's nose and mouth. **(Fig.2)**

Analysis

Calculation of PM10 concentration [6]

The glass fiber filters were collected and then analyzed in a laboratory to determine the PM10 concentration by Gravimetric Analysis. The weight of the results was measured in micrograms per cubic meter per 8 hours ($\mu g/m^2$/8 hours)

$$\textbf{Conc. of PM10} = \frac{[W2 - W1] \times 10\text{^}6}{V}$$

W_2 = the weight of the fiber filter after collection (grams)

W_1 = the weight of the fiber filter before collection (grams)

V = the volume of the air (cubic meters per min)

The amount of pollutant intake in the body through the respiratory system [7]

After measuring the PM10 concentration (CA), the samples were analyzed for air pollution exposure per day, using an average inhalation (IR) of 0.83, as set by the Agency for Toxic Substances and Disease Registry (ATSDR), the exposure time

(ET) of 8 hours/day, a frequency of exposure (EF) of 127 days/year (based on average yearly working days from 2014 to 2018), the average number of years the volunteers had worked in the area (ED), the weight (BW) and the age (AT).

$$\mathbf{CDI} = \frac{(\mathbf{CA} \times \mathbf{IR} \times \mathbf{ET} \times \mathbf{EF} \times \mathbf{ED})}{(\mathbf{BW} \times \mathbf{AT})}$$

CDI = Chronic Daily Intake
(micrograms per kilogram per day)
CA = Chemical Concentration in Air
(micrograms per cubic meter)
IR = Inhalation Rate
(cubic meter per hour)
ET = Exposure Time (hour per day)
EF = Exposure Frequency
(day per year)
ED = Exposure Duration (year)
BW = Body Weight (kilogram)
AT = Average Time (day)

Dose – Response Assessment. [8]
From the obtained CDI values, the health risk was calculated using a reference concentration (RfC) of 0.011 mg/kg/day (EU legislation)**.**
The risk characteristics of the pollutants were shown as a Hazard Quotient (HQ) which was determined as follows:

$$\mathbf{HQ} = \frac{\mathbf{Exposure:\ CDI\ (mg/kg/day)}}{\mathbf{RfC\ (mg/kg/day)}}$$

A HQ ≥ 1 meant that the number of pollutants that the volunteer had received may have caused health effects or health risks.
A HQ < 1 meant that the number of pollutants that the volunteer had received was within acceptable criteria.

Analyzing the occupational group for inhalation exposure
This analysis was done using the SPSS program to find which of the occupational groups had PM10 inhalation exposure higher than the others, using ANOVA analyisis [9]. In addition, the occupational groups which had the highest PM10 exposure could be predicted using Regression Analysis from the HQ value.

RESULTS AND DISCUSSION

The volume of PM10

1. **Measurement of PM10 in ambient air**

At station number 5 (**Fig.1**), the air was measured at least 2 times per week by High Volume Air Sampler, from February 2019 to March 2019. Over this period the PM10 was mostly higher than 80 µg / m^3, especially in March. The PM10 levels on 14 and 15 March 2019 were 139.73 µg/m^3/day and 125.77 µg/m^3/day, respectively. This amount exceeded the PCD standard of 120 µg/m^3/day **(Fig.3).**

From December 2018 to March 2019, sugar cane harvesting occurred close to Naresuan University **(Fig.4)**. From sugar cane production data, the amount of sugar cane harvested by burning was very high **(Table 2.)**. In addition, the wind blew in the direction of the university. This may have had an influence on increments in particulate matter in Naresuan University **(Fig.4)**, thus causing detrimental health effects.

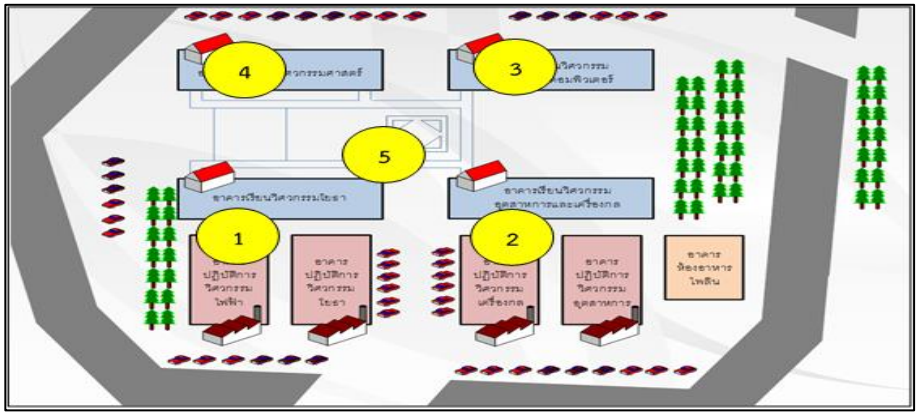

Figure 1 The area of the Faculty of Engineering, Naresuan University;
1 = Civil Engineering, 2 = Industrial and Mechanical Engineering,
3 = Electrical and Computer Engineering, 4 = Engineering Lecture Building and 5 = Ambient air sampler

Table 1 Sampling selection

Occupations	Group	The building of Faculty of Engineering, Naresuan University			
		CE	IE	EE	EN
Lecturers	Skilled workers	2	2	2	0
Administrative staff		2	2	2	1
Students	Students	4	4	4	4
Security officers	Unskilled workers	2	2	2	2
Housemaids		2	1	2	2
Gardeners		2	1	2	1
Total		50			

Note: CE = Civil Engineering, IE = Industrial and Mechanical Engineering, EE = Electrical and Computer Engineering, EN = Engineering Lecture Building

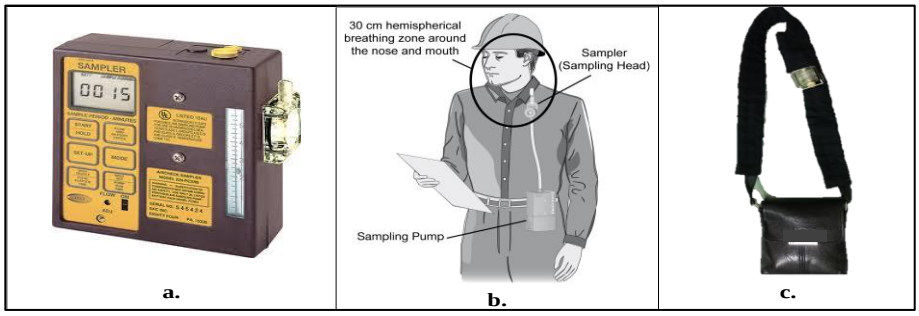

Figure 2 The configuration of equipment
a. Personal Air Sampler.
b. The distance between the nose and to the device about 30 cm.
(Jeremy Evans SKC Sales Development Manager)
c. Modified shoulder bag contains Personal Air Sampling

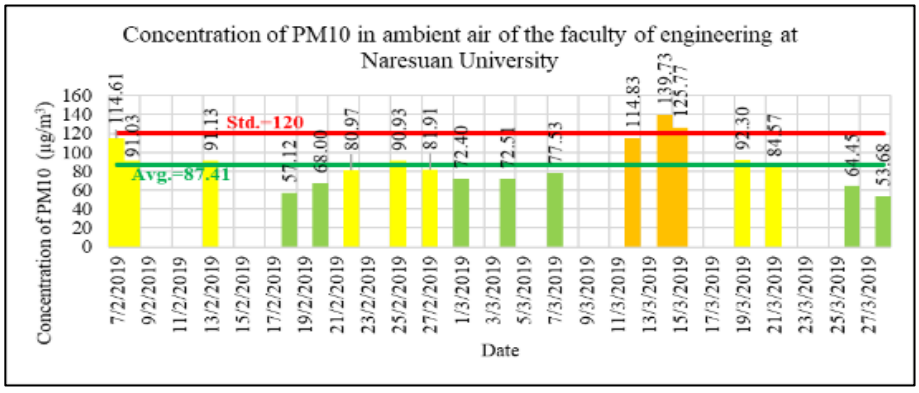

PM10 (µg/m³)	0-50	51-80	81-120	121-180	181 up
Index Color	Excellent	Satisfactory	Moderate	Unhealthy	Very Unhealthy

Figure 3 The PM10 ambient air concentration

Table 2 Sugar factory production in 2561/2562 [10]

Factory	Date		Burned sugar cane (TON)	Increase (TON)
Phitsanulok	1/12/61	8/3/62	1,674,257.870	N/A
	1/12/61	9/3/62	1,695,006.460	20,748.590
	1/12/61	10/3/62	1,717,102.430	22,095.970
	1/12/61	11/3/62	1,738,071.850	20,969.420
	1/12/61	12/3/62	1,758,383.160	20,311.310
	1/12/61	15/3/62	1,817,376.140	58,992.980
	1/12/61	16/3/62	1,836,665.990	19,289.850
	1/12/61	17/3/62	1,857,445.010	20,779.020

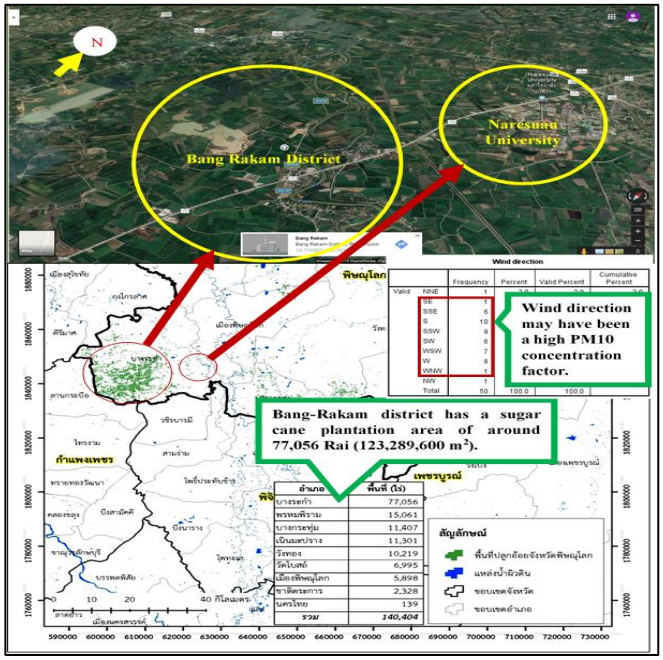

Figure 4 Sugar cane plantation area. [11]

2. <u>The measurement of PM10 in the six occupational groups</u>

The six occupational groups **(Fig.5)** (lecturers, administrative staff, students, gardeners, security officers, and housemaids), had varying activities both inside and outside the building. At station numbers 1 to 4 (**Fig.1**), the air was measured daily by Personal Air Sampler, from January 2019 to March 2019.

The concentration of PM1 0 in each occupational group was different, depending on the activities, which were inside or outside the building. If the volunteers stayed close to the source of PM1 0 **(Fig.6)**, which was outside the building, they were likely to have been

exposed to higher PM10 levels than the others. Most of the PM10 amounts detected inside the building were lower than the Bureau of Environmental Health (BEH) standard of 50 μg/m^3/8 hours. The concentrations of PM10 in each occupational group is shown as follows:

-Lecturers. The highest PM10 level was 26.47 μg/m^3 in February 2019, while the lowest was 7.84 μg/m^3 in March 2019. This did not exceed the BEH standard.

-Administrative staff. The highest PM10 level was 25.49 μg/m^3 in early March 2019 while the lowest was 11.76 μg/m^3 in late March 2019. This did not exceed the BEH standard.

-The students. It was found that PM10 had the highest amount of 33.33 μg/m^3 in the end of January 2019 while the lowest was 9.80 μg/m^3 in mid-January 2019. Nevertheless, it did not exceed the BEH standard.

-The security officers, The highest PM10 level was 66.67 μg/m^3 in the middle of January 2019, which exceeded the standard, while the lowest was 37.25 μg/m^3 in late February 2019.

-The housemaids. The highest PM10 level was 41.18 μg/m^3, both in the middle of January and the end of February 2019, while the lowest was 31.37 μg/m^3, both in mid-January and early March 2019. Accordingly, it almost exceeded the standard.

-The gardeners. The highest PM10 level was 37.25 μg/m^3 and the lowest amount was detected at 19.61 μg/m^3 in mid-March 2019. As a result, it almost exceeded the standard.

In each occupation group, the amount of PM10 exposure was different. The security officers had the highest concentration of PM10 at 66.67 μg/m^3 /8 hours, which was higher than the BEH standard of 50 μg/m^3/8 hours. The lecturers had the lowest concentration of PM10 7.84 μg/m^3 /8 hours. Therefore, the occupation groups who worked outside the

building received a higher amount of PM10 than the others, who spent most of the time working inside the building.

Apart from sugar cane ash, there were some other factors affecting the amount of PM10 exposure. There are many construction sites close to the Faculty of Engineering. **(Fig.6)**, which may have influenced increments in PM10 levels.

The amount of pollutant intake in the body through the respiratory system (CDI) per occupational group are shown in **Table 3.** It was found that the security officers were exposed to PM10 at $2.1x10^{-4}$ mg/kg/day, while the lecturers exposure to PM10 was lowest at $0.75x10^{-4}$ mg/kg/day.

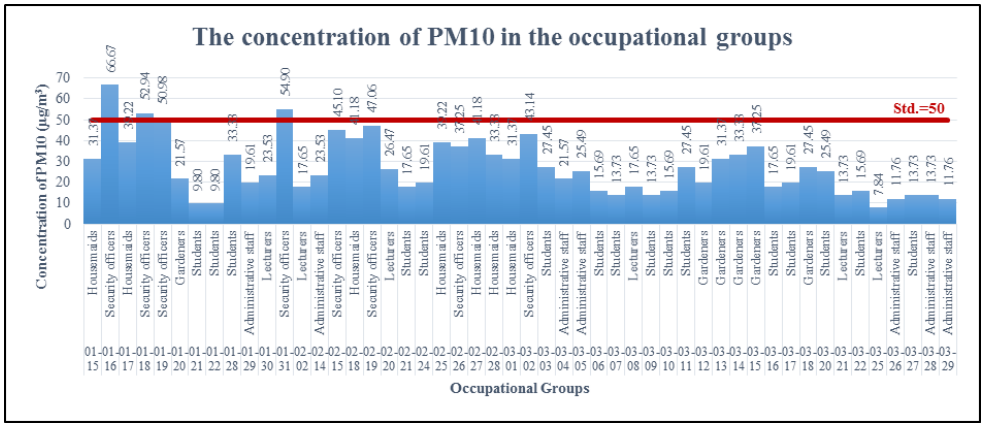

Figure 5 The concentration of PM10 for six occupational groups

Table 3 Occupational group average concentrations of PM10-Inhalation (mg/kg/day)

Occupational groups	Average of the PM10-Inhalation (mg/kg/day) $x10^{-4}$
Lecturers	0.75
Administrative staff	0.77
Students	0.78
Security officers	2.10
Housemaids	1.55
Gardeners	1.20

Figure 6 Building construction between 27 September 2018 and 21 December 2019 around the Faculty of Engineering

3. <u>Health effects assessment</u>

The analysis of effects on health the volunteers was shown as the Hazard Quotient (HQ**) (Fig.7)** for exposure to PM10. The security officers had the highest HQ value of 0.019, while lecturers had the lowest HQ value at 0.0068, **(Table 4)**, due to their location outside or inside the building, respectively. HQ values were consistent with the amount of PM10 in the ambient air, i.e. when the PM10 in the ambient air increased to unhealthy levels, the HQ also increased. However, the HQ value for all occupations did not exceed "1". As a result, the amount of PM10 that they received did not exceed the US EPA safety standard and was not harmful to their health. Therefore, it is suggested that the people, who need specialized health care, should reduce outdoor activities or use self-protection equipment when the ambient air PM10 levels air exceed the PCD standard of 120 µg/m^3/24 hours. [12]

Analysis of correlations using Regression Analysis by Enter method resulted in a coefficient of determination (R^2) of 59.7% **(Table 5).**

When comparing HQ values between 3 groups (skilled workers, students, and unskilled workers) with ANOVA analysis, it was found that the correlation could predict the comparison with statistical significance at 0.00 **(Table 6.).** When comparing 3 groups using the group of unskilled workers with highest HQ as a comparison, it was found that

skilled workers, with HQ $8.12x10^{-3}$, were exposed to less PM10 than unskilled workers. Students, with HQ $7.86x10^{-3}$, were exposed to less PM10 than unskilled workers **(Table 7)**

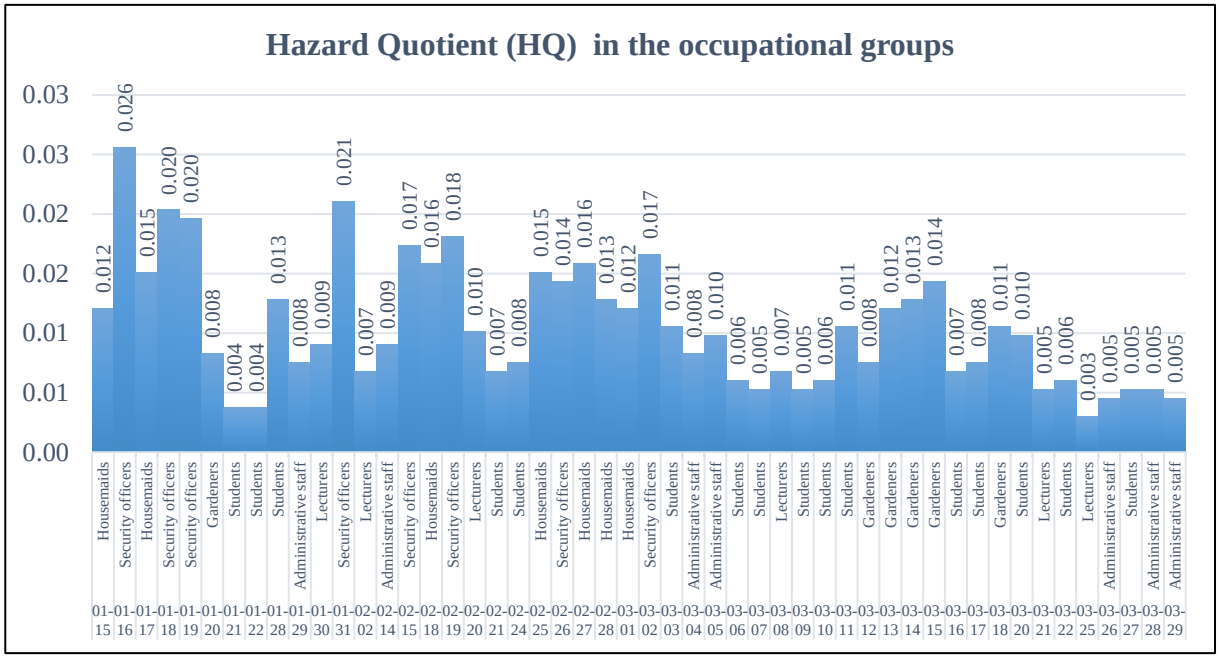

Figure 7 The graph shown the Hazard Quotient (HQ) of PM10 in six occupational groups

Table 4 The Hazard Quotient (HQ) for exposure the PM10 of the Occupational groups

Occupational groups	**Groups**	**HQ**	**Average**
Lecturers	Skilled workers	$6.84395x10^{-3}$	$6.92019\ x10^{-3}$
Administrative staff		$6.99643\ x10^{-3}$	
Students	Students	$7.1108\ x10^{-3}$	$7.110798\ x10^{-3}$
Security officers	Unskilled workers	$19.1191\ x10^{-3}$	$14.71494\ x10^{-3}$
Housemaids		$14.1005\ x10^{-3}$	
Gardeners		$10.9252\ x10^{-3}$	

Table 5 Regression for predicted the coefficient

Variables Entered/Removed[a]			
Model	Variables Entered	Variables Removed	Method
1	skilled workers[b] , students		Enter
a. Dependent Variable: $HQx10^{-3}$			
b. All requested variables entered.			

Model	R	R^2	Adjusted R^2	SEE.
1	.773[a]	.597	.580	3.33609
a. Predictors: (Constant), students, skilled workers				

Table 6 ANOVA[a] analysis for correlation between occupational groups when comparing HQ

Model		Sum of Squares	df	Mean Square	F	Sig.
1	Regression	774.225	2	387.113	34.783	.000[b]
	Residual	523.086	47	11.129		
	Total	1297.311	49			
a. Dependent Variable: $HQx10^{-3}$						
b. Predictors: (Constant), students, skilled workers						

Table 7 Coefficients[a], for the HQ between the occupational groups

Model		Un-Std. Coefficients		Std. Coefficients	t	Sig.
		B	Std. Error	Beta		
1	(Constant)	14.905	.728		20.475	.000
	skilled workers	-8.121	1.207	-.681	-6.727	.000
	student	-7.864	1.088	-.731	-7.225	.000
a. Dependent Variable: $HQx10^{-3}$						

CONCLUSIONS

The amount of exposure to PM10 in all six occupational groups in the Faculty of Engineering, Naresuan University did not exceed the standard. The security officers had the highest exposure at 2.10×10^{-4} mg/kg/day,

while the lecturers had the lowest exposure at $0.75x10^{-4}$ mg/kg/day.

The health effects for all six occupational groups was shown as the Hazard Quotient (HQ) for exposure of the PM10. All the HQ values were less than "1". This indicated that there was no health impact. From comparison of the 3 groups, it was found that skilled workers, with HQ $8.12x10^{-3}$, were exposed to less PM10 than unskilled workers. Students, with HQ $7.86x10^{-3}$, were exposed to less PM10 than unskilled workers.

This suggested the people from occupations who worked outside the building were exposed to more PM10 than those who worked or spent most of their time within the building. However, the results did not suggest a high risk for all of the six occupational groups.

ACKNOWLEDGEMENTS

The researchers would like to express our gratitude to our advisor, Asst. Prof. Dr. Pajaree Thongsanit, and Asst. Prof. Dr. Ponpisut Worrajiran, who sacrificed time and provided advice on performing this research. This research was funded by the Faculty of Engineering, Naresuan University Fiscal year 2019.

REFERENCES

[1] Education Service Division, Naresuan University. tatistics (REG: R70-01-84). 2018.

[2] Primrudi. The concentration of PM-10 inside private dormitories around Naresuan University. 2017.

[3] Supakit B. Studies the dust collection in the building. 2017.

[4] Phatthanan T, Kanokporn S. Particulate matter smaller than 10 microns (PM10) in Engineering Buildings, Naresuan University. 2010.

[5] Department of Health in Thailand. The guidelines monitor the air pollution in risk areas. 2015.

[6] Environmental and Industrial Sciences Division. Standard Operating Procedure for Particulate Matter (PM) Gravimetric Analysis.(July 2008)

[7] U.S. Environmental Protection Agency. Exposure Assessment Tools by Routes – Inhalation Calculations.From:www.epa.gov/expobox/exposure-assessment-tools-routes-inhalation

[8] U.S. Environmental Protection Agency. Risk Assessment for

Other Effects from www.epa.gov/fera/risk-assessment-other-effects

[9] Faculty of Education, Taksin University. Analysis of variance analysis of variance: ANOVA. (2004).

[10] The Office of Cane and Sugar Board (OCSB), Thailand. The sugar production report of the sugar factories. (2018-2019).

[11] The Office of Cane and Sugar Board (OCSB), Thailand. The sugar production report of the sugar factories. (2017-2018).

[12] World Health Organization. (May 2018). Ambient (outdoor) air quality and health retrieved from https://www.who.int/news-room/fact-sheets/detail/ambient-(outdoor)-air-quality-and-health

Microplastic contamination in Din Daeng wastewater treatment plant

Katekanya Tadsuwan[1*], Sandhya Babel[1]

School of Bio-chemical Engineering and Technology, Sirindhorn International Institute of Technology, Thammasat University, Thailand

Corresponding author: e-mail: katekanya.t@gmail.com

ABSTRACT

Plastic waste has become global environmental concern due to large amount of consumption. It can be broken down by environmental degradation into smaller size range, so called microplastic, which easily spread and is ubiquitous in marine environment. One of the land-based sources of microplastics is wastewater effluent. Therefore, this study aims to investigate the amount of microplastic pollution present in urban wastewater treatment system in Thailand. Microplastic samples were collected mainly from the influent and effluent of selected WWTP and examined in order to find the types and sources. Wastewater was filtered through a set of sieves of sizes 5 mm, 1 mm, 500 µm, and 53 µm. Microplastic samples were processed using wet peroxide oxidation method and characterized into size, color, and shape categories under stereomicroscope. FTIR was used to confirm the type of microplastics. Number of microplastics found was 28.75 particles per liter in the influent and 3.45 particles per liter in the effluent. When treatment capacity of 350,000 m^3 is taken into account, 1.24×10^8 microplastic particle is daily released to freshwater environment . The majority of microplastics found in both influent and effluent was fiber, and transparent microplastics were abundantly inspected. Results from FT-IR analysis showed that major types of microplastic contaminated in the influent were polyethylene, polyester, and polyurethane. While, polyethylene and polyester were found in the effluent.

This finding indicates that conventional wastewater treatment plant may act as a pathway for microplastic in the environment.

Keywords: Microplastic, wastewater treatment plant, removal, morphology, FTIR

INTRODUCTION

Plastic waste has become global environmental concern due to large amount of consumption. Plastic materials are produced from fossil-derived monomers which are non-biodegradable, such as ethylene and propylene (Geyer, Jambeck, & Law, 2017). Thus, due to its high stability and durability, plastic litter is extremely persistent, it tends to accumulate in wide range of natural habitats and ends up in the ocean. Microplastic is commonly defined as plastic particle with diameter less than 5 mm. It can be categorized into primary and secondary microplastic. Primary microplastics are manufactured in small size for industrial and domestic applications such as virgin resin pellets, microbeads in personal care products, industrial scrubbers, and plastic powders, whereas secondary microplastics are the result of fragmentation of bigger size plastic (Talvitie, Mikola, Koistinen, & Setälä, 2017). Concerns have been raised regarding potential impacts of microplastics on the environment, wildlife, and human health. Recent studies have focused on the source of microplastic in aquatic and marine environment. One of the land-based sources of microplastics besides surface runoff is wastewater effluent. As microplastics have been detected in wastewater effluent, many studies suggested that wastewater treatment plant (WWTP) is a pathway for microplastics. However, there is a gap of knowledge of the fate of microplastics and their transport behavior in wastewater treatment plant (Talvitie et al., 2015). Due to small size of microplastic, the efficiency of wastewater treatment process in every step until the

discharge of final effluent needs to be focused on. Therefore, this study aims to investigate characteristics and types of microplastics found in wastewater treatment system which could be used to trace back the source/origin of microplastics. It is also necessary to quantify the amount of each type of microplastics in order to estimate pollution levels of microplastic entering the ocean.

METHODOLOGY

Study site

Microplastic samples were collected from Din Daeng wastewater treatment plant which is the largest WWTP in Bangkok with treatment capacity of 350,000 m^3/day. Din Daeng WWTP is responsible for serving 8 districts in Bangkok where the population is approximately 1 million. Figure 1 shows the flow chart of this WWTP. Treatment technology used in this WWTP is biological activated sludge process with nutrient removal. Sludge after treatment from this WWTP will be sent to sludge treatment facility in Nong Khaem WWTP.

Sampling of microplastic from liquid fraction

A set of Tyler sieve was also used as a sampling device in order to acquire different size fraction of microplastic in WWTP. Mesh size of sieves include 5 mm, 1 mm, 500 µm, and 53 µm. In order to avoid contamination, equipment's were rinsed with DI water before use.

Samples were collected in dry season in January. Samples were collected at different stages of WWTP; influent, after primary sedimentation, after secondary sedimentation, and final effluent by grab sample. 40 L of wastewater sample was filtered through a set of sieves. Each sieve was rinsed with DI water, and microplastic samples on the sieve were stored in a separate laboratory jars. Microplastic samples were stored in a refrigerator prior to the analysis.

Sample preparation

Samples were dried over night at 70ºC before digestion. The digestion solution used in this analysis is called

Fenton's reagent. It is the mixture of hydrogen peroxide (H_2O_2) with iron catalyst ($FeSO_4.7H_2O$). It was proven as the solution with highest removal efficiency compared to H_2O_2 and other alkaline solution such as NaOH and KOH. Digestion solution was added to the sample and heated on a hot plate at 70ºC until the boiling was observed. More of the solution was added to the samples if there was a trace of organic matters observed by naked eyes. Digested samples were rinsed with DI water and dried over night at 90ºC.

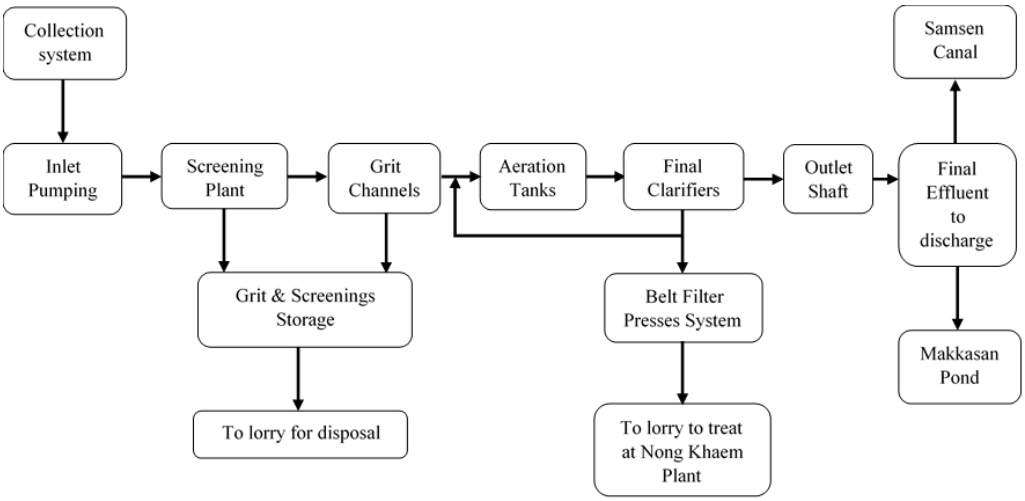

Figure 1 Flow chart of Din Daeng wastewater treatment plant

Samples from domestic wastewater might contain some inorganic particles such as sand and gravels which are drained through the sewage. Density separation is an approach which make these non-plastic particles sink to the bottom because of their higher density. Generally, saturated salt solution is used in density separation. $ZnCl_2$ was prepared in a density of 1.7 g/cm^3. $ZnCl_2$ was added into each beaker and stirred continuously. They were left on a lab bench for 10 minutes to allow sediments to settle. Microplastic which has lower

specific gravity than salt solution will float on the surface due to supernatant property, and it could be easily removed. After each size fractions were grouped into polymer type, microplastic samples will be vacuum-filtered on sterile cellulose nitrate membrane filter with pore size 45 µm.

Visual Identification

Samples were inspected under stereomicroscope with magnification ×4 and ×10. Microplastic samples were counted and grouped into colors and shape categories; fiber, fragment, film, and bead. Organic materials or natural polymers were sorted out using forceps. Some shapes and colors were used to distinguish microplastics from organic materials. However, microplastic particles must be later confirmed the type using FT-IR.

FT-IR analysis

Suspected particles were analyzed using spectroscopic technique. FTIR in attenuated total reflectance (ATR) mode with diamond microtip was used in the identification of polymer types of larger particles which can be handled with forceps. The appropriate infrared radiation was from 600 to 4000 cm^{-1}, and the resolution for analysis was 8 cm^{-1}. The identification by FT-IR results in fingerprint spectrum which can be compared to reference spectra library to obtain polymer type in OMNIC software.

RESULTS AND DISCUSSION

Sorting

Water volume filtered through a set of sieves by grab sample was 20 L at the influent, after grit removal, and the final clarifier. Microplastic samples were rinsed of the sieves and stored in glass bottles. They were categorized into 3 groups regarding to size; 1 mm, 500 µm, and 53 µm. For each size, the number of microplastics found in the influent were 0.75, 10.6, and 17.4 per liter, respectively. No microplastic bigger than 1 mm was found in water sample after grit removal and the effluent. The number of 500 µm, and 53 µm

groups found in the effluent were 0.25 and 3.2 microplastic per liter. Therefore, the total number of microplastics contaminated in the influent, after grit removal, and the effluent were 28.75, 10.05, and 3.45, respectively.

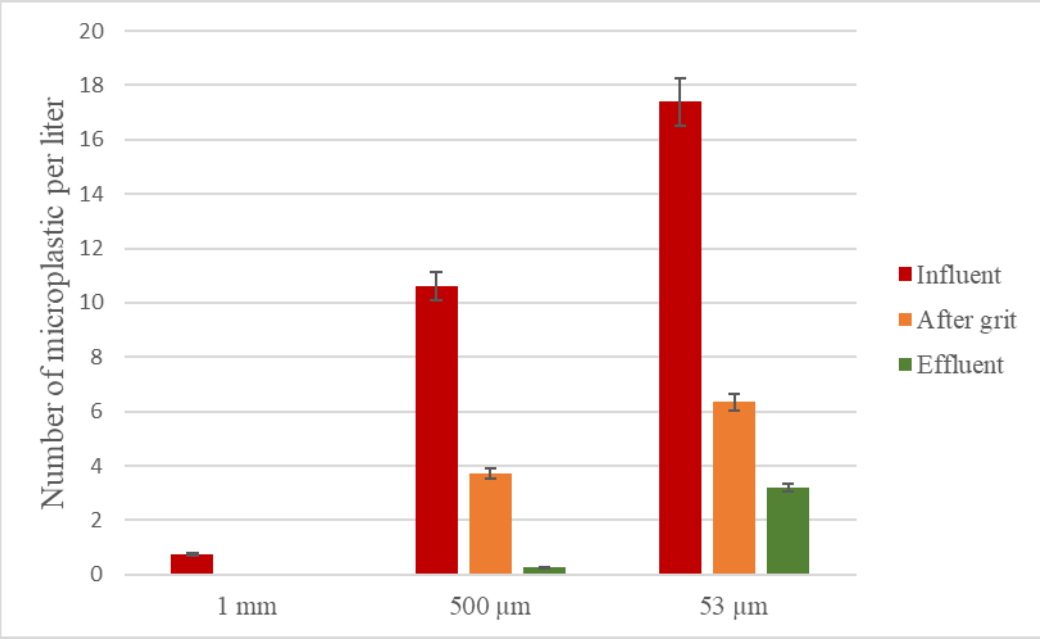

Figure 2 Number of microplastic found in each stage of WWTP

Microplastic characterization

The majority of microplastics in the effluent, after grit removal, and effluent was fiber which was accounted for 79% of total microplastics found (Figure 2). The largest group of microplastic was transparent which was accounted for 78% of total microplastics detected in all size groups (Figure 3).

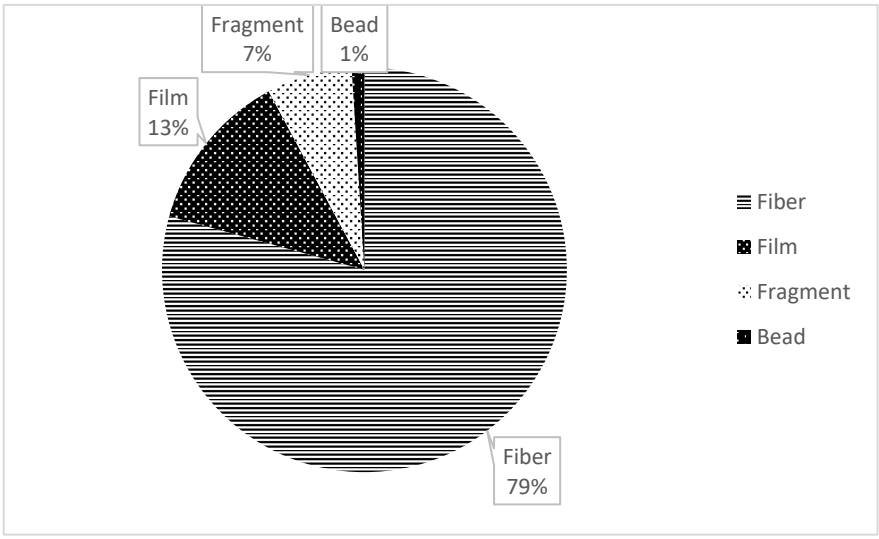

Figure 3 Pie chart of different shapes of MPs sample found in Din Daeng WWTP shown in percentage distribution

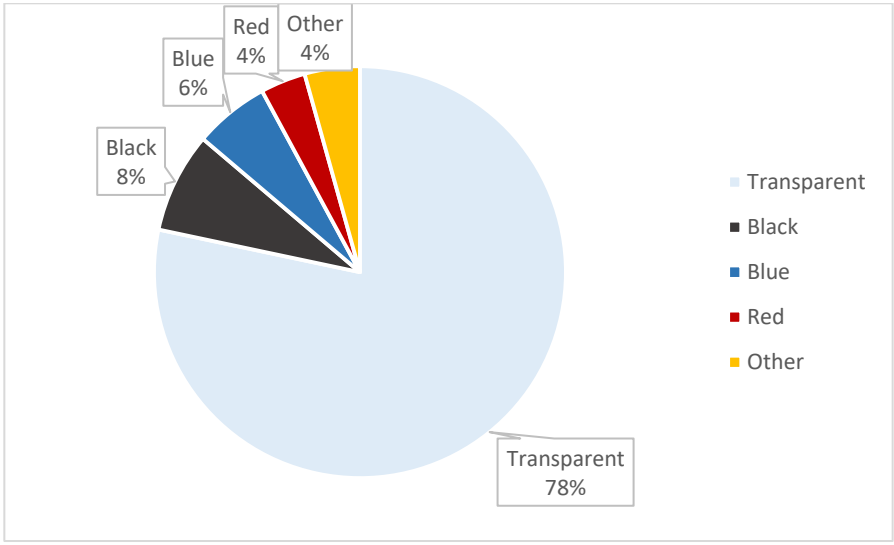

Figure 4 Pie chart of different colors of MPs sample found in Din Daeng WWTP shown in percentage distribution

FT-IR analysis

Microplastic samples, which were large enough to be handled with tweezers, were chosen for chemical characterization using FT-IR. Some examples of microplastic found in the

influent were polyethylene, polyester, and polyeurethane. Microplastics after grit removal consisted of polyeurethane. While polyethylene and polyester were found in the effluent. However, some of microplastic particles could not be analyzed using FT-IR due to their minute size.

Discussion

Particles larger than 1 mm were successfully removed in the system of WWTP by screening processes. While particles smaller than 1 mm were partially removed by screening processes, grit removal, and activated sludge. This study shows that there were 28.75 microplastics in the influent and 3.45 in the effluent indicating 88% removal of microplastics. When treatment capacity is taken into account, approximately 1.24×10^8 particles are released daily. Most of the contaminated plastics were textile fibers which are light-weighted. They can be an airborne contamination in the sedimentation tanks. Moreover, the morphological characterization of microplastics has some limitations. Transparent plastics were less visible under microscope. Thus, staining of microplastics particles should be performed in order to obtain more accurate identification. Yellow-pigmented plastics had to be distinguished from the yellowing of plastic from oxidation.

In order to find out types of microplastics and confirm the suspected particles, spectroscopic method was performed. However, small size particles could not be analyzed with FT-IR because they could not be handled with tweezers. Therefore, advance infrared spectroscopy, called micro-FT-IR should be employed in order to confirm the type of smaller size plastics. Knowing types of polymers are important for further management strategies.

CONCLUSIONS

Number of microplastics found was 28.75 particles per liter in the influent and 3.45 particles per liter in the effluent. When treatment capacity of 350,000 m^3 is taken into account,

1.24×10^8 microplastic particles are daily released to freshwater environment . The majority of microplastics found in both influent and effluent were fiber, and transparent microplastics were abundantly inspected.

ACKNOWLEDGEMENTS

This study is financially supported by Sirindhorn International Institute of Technology, Thammasat University.

REFERENCES

Geyer, R., Jambeck, J. R., & Law, K. L. (2017). Production, use, and fate of all plastics ever made. *3*(7). doi:10.1126/sciadv.1700782 %J Science Advances

Talvitie, J., Heinonen, M., Pääkkönen, J.-P., Vahtera, E., Mikola, A., Setälä, O., & Vahala, R. (2015). Do wastewater treatment plants act as a potential point source of microplastics? Preliminary study in the coastal Gulf of Finland, Baltic Sea. *Water Science and Technology, 72*(9), 1495-1504. doi:10.2166/wst.2015.360

Talvitie, J., Mikola, A., Koistinen, A., & Setälä, O. (2017). Solutions to microplastic pollution – Removal of microplastics from wastewater effluent with advanced wastewater treatment technologies. *Water Research, 123*, 401-407. doi:https://doi.org/10.1016/j.watres.2017.07.005

Carbon footprint of finishing process in Weatherstrip manufacturing

Methaporn Somsookcharoen[1], Soontree Khuntong[2*]

[1]Master of Engineering Program in Safety Engineering and Environmental Management, Faculty of Engineering at Sriracha, Kasetsart University, Chonburi, Thailand
[2*]Faculty of Science at Sriracha, Kasetsart University, Chonburi, Thailand;
Coresponding author: e-mail: srcstk@ku.ac.th
methapornssc@gmail.com

ABSTRACT

Rubber parts are one of the importance for automotive industries particularly weatherstrip for protection of leakage of liquid phase and temperature controlling in the cabin. The raw materials of weatherstrip are polyvinyl chloride (PVC) and thermoplastic polyolefin (TPO) that consume the enormous energy and raw material as well as large quantities of rubber waste. Waste and energy minimization are the company policies based on carbon footprint concept. The weatherstrip production is comprised of two main processes including extrusion and finishing. In this study, the assessment of carbon footprint is focused on finishing process because the rubber waste is mostly generated from this process. The more rubber waste is generated, the higher carbon dioxide is emitted. The functional unit was initiated from raw material (PVC, TPO and chemicals) supply until finished products (cradle-to-gate). The finishing processes include rubber blending, cutting, and inspection. Due to semiautomatic system, the major carbon dioxide is originated from the electrical consumption. The data collection have made from electrical meter using each instrument and scrap quantities (rubber

waste) for one year (2018). The observed carbon footprints were calculated in ton CO_2 equivalent from multiplied products of corrected qualities and emission factors. The recycle scrap was normalized the actual scrap waste prior calculation. The carbon footprint reached the highest for cutting process (11,232 ton CO_2 eq) followed by blending (7,851 ton CO_2 eq) and inspection (1,795 ton CO_2 eq). The results may be used as guideline for decreasing carbon footprint by remodeling machine in finishing process and investigating clean technology. The improvement will came scrap reduction and increase manufacturing process also.

Keywords: Carbon footprint, Weatherstrip, Finishing process

INTRODUCTION

As a result of many activities, global emissions are at an all-time high. In the last four years Arctic temperatures have risen by 3°C. (United Nations, 2019). These affects all ecosystems. One major problem, the carbon dioxide (CO_2) data in 2018 was as much as 37,100 million tons. Many industries and burning fossil fuels released dirty pollutions from 1.8 to 3.7 percent caused of these carbons (Le Quéré et al. 2018). Private organization and government agencies are enthusiastic to reduce carbon dioxide for manufacturing process in general industries, and they used the clean technology to upgrade old machines efficiently for reducing the minimum waste.

Automotive industries such as engine, motor, and chassis have the upward trend in Thailand. Weatherstrip is a rubber part which can protect the liquid leakage in the cabin. Two raw materials of weatherstrip are polyvinyl chloride (PVC) and thermoplastic polyolefin (TPO) mixed with chemicals then go through the extrusion process. The first procedure, the products are formed by heat and cooling system for the second step. After the extrusion process, these products compose of three processes: rubber

blending, cutting, and inspection which cause a large number of scraps.

So, this study focused on the finishing processes about decrease the carbon dioxide in automotive industries and research the new technology for protecting the environment.

METHODOLOGY

Data and scope

This area study is in Automotive Industries at Amata City, Chonburi province. (Figure 1)

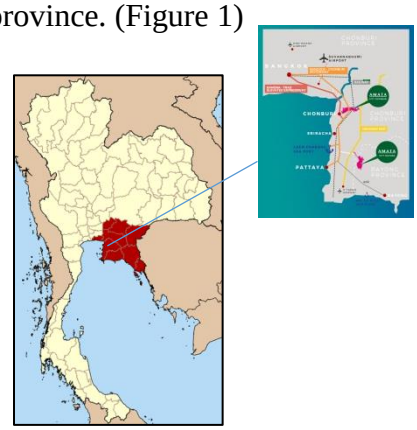

Figure 1 The study area is located at Amata City, Chonburi province

The main processes cause of the carbon footprint are made of the rubber waste in production from the weatherstrip manufacture in 2018 (January – December). The data were collected the electrical consumption in main processes, raw materials (polyvinyl chloride (PVC) and thermoplastic polyolefin (TPO)) and scrap quantities (rubber waste). In this study, choosing particularly weatherstrip (automotive industries) by cradle-to-gate method.

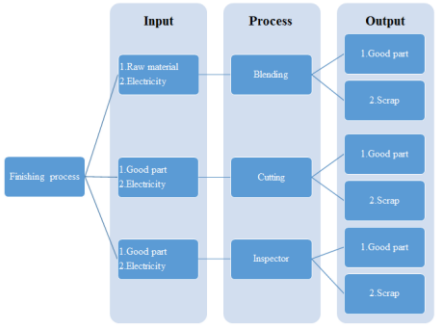

Figure 2 Finishing processes

Correct emission factor

The carbon footprint assessment of weatherstrip used the table of emission factors (Effective date : 1 February 2019) from Thailand Greenhouse Gas Management Organization.

Emission factors of carbon footprint.

Table 1 Emission factors of raw material and electrical consumption used data from Thai National LCI Database/MTEC (with TGO Electricity 2014)

No.	Name	EF ($kgCO_2eq/Unit$)
1.	PVC	2.1415
2.	TPO	2.16
3.	Electrical	0.5821

Assessment of carbon footprint

The carbon footprint is calculated by using below formulas.

1. Raw material of PVC parts

CO_2 emissions in pounds =Total weight 1 unit of PVC part × PVC emissions factor × Total amount of PVC parts of months

2. Raw material of TPO parts

CO_2 emissions in pounds =Total weight 1 unit of TPO part × TPO emissions factor × Total amount of PVC parts of months

3. Electrical meter from each instrument CO_2 emissions in pounds =

(average amount of electric bill per month ÷ price per kwh) × electricity emissions factor × workdays in a year

4. Quantities of scrap (rubber waste) CO_2 emissions in pounds = (Total weight of PVC scrap each process × PVC emissions factor) + (Total weight of TPO scrap each process × TPO emissions factor)

RESULTS AND DISCUSSION

The data are between January – December in 2018 shows the amount of carbon footprint from calculation. These are divided into 3 processes including usage the raw materials (PVC,TPO), electrical meter from each instrument and quantities of scraps.

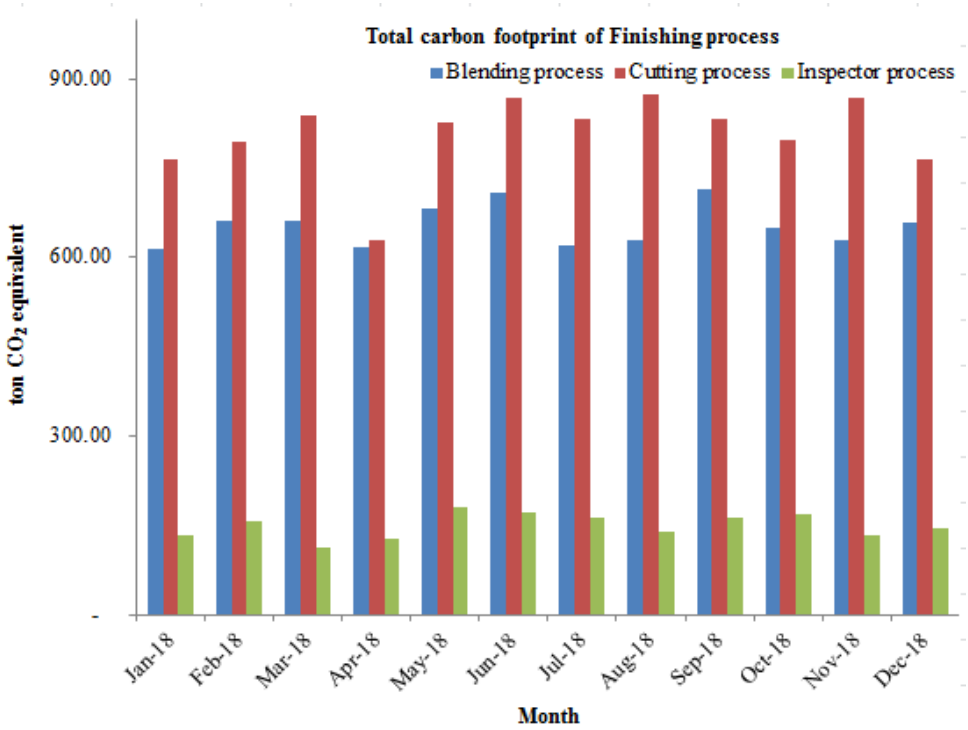

Figure 3 Carbon footprint of Blending, cutting and inspector process.

Figure 3 This figure showed reached highest for cutting process (11,232 ton CO_2 eq) followed by blending (7,851 ton CO_2 eq) and inspection (1,795 ton CO_2 eq).

Therefore, researching new technologies for reduce quantities of carbon footprint in all process. Now, this automotive industries add new machines were clean technology replace some machine for studied function and modify processes to reduce carbon footprint.

REFERENCES

Suwat P, Natworapol R, Prin B, Saharat W.2013.Carbon Footprint from the production of plastic cup polypropylene white size 22 oz printed. A case study of plastic packaging industry.

Phantip T. 2014. Carbon Footprint Assessment of Rubber Smoked Sheet : A Case Study Coopaerative Rubber Sheet Factories (CRSFs) od Songkhla Province, Songkhla University.

Thailand Greenhouse Gas Management Organization. Emission factor of carbon footprint, 1 February 2019, http:// thaicarbonlabel.tgo.or.th

United Nations. 2019, https://www.un.org/en/climatechange

Le Quéré et al. (2018) Global Carbon Budget 2018. Earth System Science Data Discussions. https://doi.org/10.5194/essd-10-1-2018.

Andreozzi R, Caprio V, Insola A, Marotta R. 1994. Advanced oxidation processes (AOP) for water purification and recovery. Catalysis Today 53: 51-59.

Eisenberg, G. Colorimetric determination of hydrogen peroxide. Industrial and Engineering Chemistry, Analytical Edition 1943; 15(5): 327-328

Hassaan MA, Nemr AE. Health and Environmental Impacts of Dyes: Mini Review. American Journal of Environmental Science and Engineering 2017; 1(3): 64-67.

Phase of transport process during loading from certification oil tank to storage tank

Kittiya Klaharn[1], Soontree Khuntong[2*]

[1]Master of Engineering Program in Safety Engineering and Environment,
Faculty of Engineering at Si Racha, Kasetsart University,
Chonburi, Thailand
[2]Faculty of Science at Si Racha, Kasetsart University, Chonburi, Thailand;
Coresponding author: e-mail: kittiharn@hotmail.com

ABSTRACT

The phase of transport process during loading from certified oil truck to storage tank was investigated. An incident was studied in case of accidence occurring from abnormal conditions including tank leakage and did not tightly hose. The leakage of naphtha may cause explosion following by potentially domino effect of toxic fume, thermal radiation and fire spreading. ALOHA (Ariel Location of Hazardous Atmosphere) program was applied for evaluation of explosion from highly volatile solvent (naphtha) within specified areas. The study process was focused on loading from certified oil truck to storage tank. Moreover, meteorological conditions including wind direction and speed, temperature and humidity provided additionally critical impact to domino effect. The explosion will cause domino effect with fire, toxic fume and thermal radiation from fire ball. Due to BLEVE (Boiling Liquid Expanding Vapor Explosion) resulted from 150 scenarios simulation using ALOHA model, the large leakage hole (7-inch) caused highest critical impact followed by 3-inch leakage and puddle type leakage respectively. The uncontrolled factors including relative humidity, temperature as well as wind direction and speed affected domino effect. Within relatively high humidity

and low wind speed might create vapor toxic cloud in low dispersant condition. Moreover, the oil tank structure damaged in each situation causing puddle type leakage. Furthermore, the explosion may produce a large fire ball with thermal radiation exceeding 10 kW/m^2 in all situations. In conclusion, the assessment results could be applied and implemented for emergency response plan related to safety work procedures and lowering human and environmental risk for workers and neighboring communities.

Keywords: ALOHA, BLEVE, Domino effect, Explosion, Naphtha

INTRODUCTION

The lubricant means a substance, such as oil or grease, used for minimizing friction, especially in an engine or component. Application of lubricants; lubricants are primarily used to reduce friction stress between surfaces. Some specific uses of certain variants of lubricants are synthetic lubricants used in turbines, vacuum pumps, and semiconductor devices. Lubricants are also used as cutting fluids in many industries. Oil, water, and oil emulsion are used as cutting fluids. These liquids are used to cool as well as to lubricate surfaces.

For Naphtha as solvent is main ingredient for produce solvent product and indisposing oil. The physical and chemical of naphtha solvent has flash point as > 41°C (106°F), flammable limits (Approximate volume % in air) as LEL: 0.8 and UEL: 7.0 , and vapors pressure as 0.2 kPa. (1.5 mm Hg) at 20 °C , 0.7 kPa (5.25 mm Hg) at 38°C and 1.3 kPa (9.75 mm Hg) at 50°C.

These are Aromatic Hydrocarbon chemical group that was produced lubricant from solvent naphtha transfer process. The leakage could be occurred that may impact danger during transfer.

When liquid and flammable vapor are burned, the incomplete combustion from smoke and vapor can make fatality impact if being swallowed

and passed through the respiratory system. The impact symptom effects to dizziness and respiratory irritation for employee. Also, the fume or fog was created that the substance or this substance group could be released in fire burning case. The ALOHA (Area Location of Hazardous Atmospheres) and Marplot program were applied for substance which came from those combustions in order to predict specific distribution, boundary, including toxic smoke concentration as each distance. The data compliance and signification was checked with ALOHA and Marplot program application for those impact assessments. The objectives of this work are (i) to apply the ALOHA program for assessing the severity, leakage of chemicals that occurred while transferring, (ii) to apply the Google earth information system with the forecasting of ALOHA and Marplot programs in order to know the area or radius that is affected in the incident of an explosion, and (iii) to find out the safety distance employee in the factory staff to leave the incident as soon as possible and to find out the safety distance between factories and adjacent areas.

ALOHA is a modeling program that estimates threat zones associated with hazardous chemical releases, including toxic gas clouds, fires, and explosions. A threat zone is an area where a hazard (such as toxicity) has exceeded a user-specified Level of Concern (LOC). ALOHA is part of the CAMEO® software suite of products for emergency responders and planners.[1]

The simulation model was jointly developed by organizations including the United States Environmental Protection Agency (USEPA). The Chemical Emergency Preparedness and Prevention Office (CEPPO), and National Oceanic and Atmospheric Administration Office of Response and Restoration (NOAA). In recent years, the ALOHA model has evolved into a PC assistive management software intended for rapid deployment by emergency responders. The ALOHA model of dispersion is a free application provided by NOAA (National Oceanic and Atmospheric

Administration) of the United States and EPA (Environmental Protection Agency) and it is the tool for the assessment of toxic gas cloud threat zones recommended by the USEPA. The model is capable of simulating the dispersion model for over 900 chemicals and is primarily used in the simulation of accidental release of hazardous substances and the dispersion of chemical vapor. [1]

ALOHA models have many release scenarios: toxic gas clouds, BLEVEs Boiling Liquid Expanding Vapor Explosions), jet fires, vapor cloud explosions, pool fires, and flammable areas. Theevaluates different types of hazard (depending on the release scenario): toxicity, flammability, thermal radiation, and overpressure [1].

METHODOLOGY

2.1 Study Area.

The factory is lubricant factory was located within the Amata City Rayong Industrial Estate, Pluak Daeng District, Rayong Province.

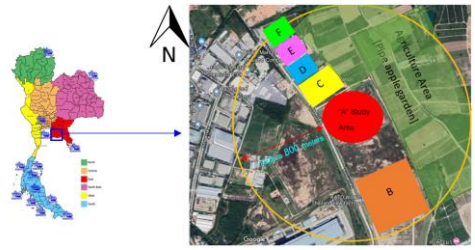

Figure 1 Factory location [2]

The lubricating oil production plant has a factory adjacent area in a radius of 80 0 meters, covering the whole industrial area including agricultural areas. There are 5 adjacent factories (A, B, C, D, E and F factory) and agriculture area that there are areas affected as a lot of number of factories in the radius studied. The - factory "A" means lubricant oil plant manufacturing, "B" means mobile crane production and retailer, "C" means the other machine production for general usage, "D" means manufacturing automotive parts and equipment, "E" means copper production, and "F" means assembly or device for every appliance production, retailer, and export.

Fig. 2 Layout of factory [3]

That composed of office building and production building that the warehouse area was set up at the middle of that. In emergency case,

the shutter door between the warehouse and the production area will be slid down to close immediately in order to protect the smoke from entering into any areas.

2.2 Data Collection

Table 1 The height of level above sea level [4]

Industrial estate	The height of level above middle sea level	
	Minimum	Maximum
Hemaraj Chonburi Industrial Estate	+126	+134
Eastern Seaboard Rayong Industrial Estate	***+65***	***+90***
Hemaraj Eastern Seaboard Industrial Estate	+73	+111
Hemaraj Rayong Industrial Estate	+44	+75

Due to study area where the lubricant oil production plant is located in the Amata City Rayong Industrial Estate which this estate has an area close to the area of the Eastern Seaboard Industrial Estate Rayong than other industrial areas; Therefore, using the height from the sea level of the Eastern Seaboard Industrial Estate to be referenced in the ALOHA program.

Table 2 The parameters using in a ALOHA program

Parameter	[1]Wind	
	Direction	Speed
1.[2]Wind		
Summer	SSW	0-5
	W	0-6
	NW	0-10
	NNW	0-10
Winter	N	0-4
	NNE	0-7
	NE	0-12
	W	0-9
Rainy	W	0- 10
	NNE	0-7
2.Surface condition of area	Factory area (urban or forest)	
3.The stability of atmosphere	[6]Phase (D) ,(E) for daytime [working day]	
4. [3]Chemical container condition	Cylinder-shape tank, horizontal type with 2-metre diameter, 9-meter length, 26000-litre volume	
5. [4]Chemical status	Flammable liquid	
6. [5]Leakage cause	Leaking from the ISO Tank while loading chemicals into the storage tank	

[1]*Wind Speed; Max-Min*

[2]Atmosphere means the value including the data in ALOHA program.

[3]Container condition means ISO tank have been certificate oil truck and have condition as diameter, length and capacity of quantity.

[4]Chemical status means type of chemical as a flammable liquid and toxic using in factory.

[5]Leakage cause means during loading raw material as naphtha solvent from the certificate oil truck into the storage tank. The chemical leakage during transferring to storage tank.

[6]The phase D and, E mean the stability of the atmosphere, such as the weather is sunny, the temperature of the air above the surface is high which causing air currents above the surface of the ground to make the air stable, normal (Study only during daylight hours because most educational factories work only during the hours (08:00 - 17:00)

Table 3 Temperature and relative humidity of the study areas during Feb 2017 – Oct 2018 [5]

Temperature /Humidity (°C/%)	Winter (Oct'17 – Jan'18)	Summer (Feb-May'18)	Wet (Jun-Sep'18)
Avg. Min	19.1/34.87	21.5/46	23.57/51.5
Avg. Max	34.07/96.06	33.92/97.5	33.95/97

The environment variables such as weather, relative humidity, average maximum temperature of each season, wind speed and wind direction blowing through the factory, which is a control factor in education, were determined

2.3 Program Simulation

The data being used with the ALOHA program was the chemical used in the factory group that is frequently used with health hazards and easy to get burning. Because such areas are at risk of causing leakage, flammability or explosion; therefore, when that happens, it will affect the employees working in the area including the effects that occur on Amata City Industrial Estate, Rayong, and the other variables related to the simulation.

Table 4 Program Simulation

Source				
Leak hole size	**Seasons**	**Wind /Speed**	**Scenario**	**Result from Program**
1.Puddle 2.Leak hole size 3-inch 3.Leak hole size 7-inch	Dry	SSW/5	BLEVE	Thermal radiation from a fireball and/or pool fire
			Flammable Area (where a Flash Fire might occur)	Flammability
			Pool Fire	Thermal radiation
			Toxic Vapor Cloud	Toxicity
			Vapor Cloud Explosion	Overpressure

The simulate programs was started from determining the wind direction that influences the study area. Also, the events may occurred (puddle, 3-inch leaks and 7-inch leaks) in 1 direction of wind which will run all 3 seasons (winter, Dry, and Wet) which must be simulated to complete the specified event. And all wind direction according to table 2.

RESULTS AND DISCUSSION

From the simulated program, Aloha case study of the phase of transport process during loading from certified oil truck to storage tank as total of 150 cases, with floor-based leaks the hole size was considered as 3-inch, 7-inch and puddle type that the wind direction blowing through Rayong Province area as all 9 directions and simulation as 3 seasons (Winter, Dry and Wet) according to table 2 Furthermore, for velocity size and weather condition of those wind direction, the Meteorological Department defined the maximum wind speed are different. The condition controlled temperature parameters according to table 3.

Table 5 the effect of the affected areas.

Seasons	[1]Scenario	Result (from Program)	Evidence
Winter	NNE-LP	Threat Modeled: Thermal radiation from pool fire Red : 16 meters --- (10.0 kW/(sq m) = potentially lethal within 60 sec) Orange: 21 meters --- (5.0 kW/(sq m) = 2nd degree burns within 60 sec) Yellow: 29 meters --- (2.0 kW/(sq m) = pain within 60 sec)	
	NNE-L3 NNE-L7	Threat Modeled: Thermal radiation from fireball Red : 350 meters --- (10.0 kW/(sq m) = potentially lethal within 60 sec) Orange: 496 meters --- (5.0 kW/(sq m) = 2nd degree burns within 60 sec) Yellow: 774 meters --- (2.0 kW/(sq m) = pain within 60 sec)	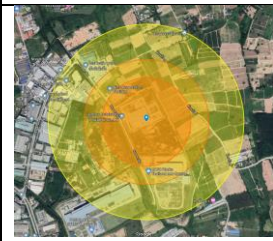
	N-L7	Model Run: Gaussian Red : no recommended LOC value --- (N/A = AEGL-3 [60 min]) Orange: 62 meters --- (360 ppm = AEGL-2 [60 min]) Yellow: 101 meters --- (140 ppm = AEGL-1 [60 min]) Maximum diameter of the puddle: 75 meters	
Dry	NNW-L3, NNW-L-7	Threat Modeled: Thermal radiation from fireball Red : 270 meters --- (10.0 kW/(sq m) = potentially lethal within 60 sec) Orange: 381 meters --- (5.0 kW/(sq m) = 2nd degree burns within 60 sec) Yellow: 595 meters --- (2.0 kW/(sq m) = pain within 60 sec)	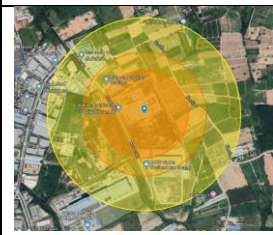
Wet	NNW-L3, NNW-L7	Threat Modeled: Thermal radiation from fireball Red : 270 meters --- (10.0 kW/(sq m) = potentially lethal within 60 sec) Orange: 381 meters --- (5.0 kW/(sq m) = 2nd degree burns within 60 sec) Yellow: 595 meters --- (2.0 kW/(sq m) = pain within 60 sec)	

[1] NL ; Wind Direction is N, NNE and so onLeak hole size is Leak from Puddle, 3-inch, 7-inch

The result of simulate from 3 seasons (Winter, Dry and Wet) the effects of the leakage and explosion of solvent (Naphtha) at an average wind speed of o knots. The ALOHA program cannot convert data due to the limitations of the program. For winter time, the wind direction that affects the leakage of chemical in the ground (puddle) and cause flammability poor fire is NNE and NE. The leakage of 3 - inch and 7 - inch holes. The spread of toxic fog that dose not catch fire (Toxic Area of the Vapor Cloud) have low value, but will accumulate in areas near the leak point in the N direction. The BLEVE explosion wind direction that affects to N, NNE, NE and W. For summer time, wind direction affecting chemical leakage and cause a BLEVE explosion. The wind direction affects to SSW, W, NW and NNW. For rainy season, the wind direction affected chemical leakage and cause a BLEVE explosion. The wind direction affects W and NNW.

From table 5, it was found that the BLEVE explosion would produce the most damage from a large fireball in every 3 inch and 7 inch leak hole, by considering the total wind direction, wind speed, Daytime weather, Average temperature and relative humidity for each season.

For the other situations, this was not mentioned because the amount of chemicals does not affect the area of the incident or nearby areas

Discussion

Areas affected by flammability and explosions can be divided into 2 types: poor fire and BLEVE, effects of the explosion of Solvent Naphtha, the area of chemical spread and concentration. Each season is no different. And the wind direction does not affect the occurrence of simulated events. The wind direction that causes the explosion of BLEVE comes from the direction N, NNE, NE, W, SSW, NNW, with the hole size of 3 inches and 7 inches by Solvent Naphtha explosion using quantitative risk assessment. When the explosion occurs in both the poor fire and BLEVE models at the

highest intensity, the heat is worth more than 10 kilowatts per square meter. For the poor file covering the study plant area. For the BLEVE explosion, will cover a radius of 800 meters near the study area according to Fig. 1. The flammability results in an incident that continues to spread to other areas nearby which matches the popular word "Domino Effect".

The advantage of ALOHA is that there is information on the terrain of the place of birth. Because the database has Latitude and Longitude, resulting in more accurate data

For this research study, the researcher will expand the results by comparing and analysing chemical spill events using the ALOHA program compared to Marplot.

CONCLUSIONS

The factors that affect the leakage of the substance, except the airflow, wind speed, humidity and the size of the leak hole. Found that the size of the leak hole is 3 inches and 7 inches when there is a non-combustible leak and the spread of highly toxic gas At the distance from the leakage point of 60 meters at 140 PPM concentrations at AEGL, equal to 60 minutes, the area that touches the radiant gas less than 10 meters.

And the leak also exploded Will cause damage in the distance of 774 meters, with a distance of 336 meters if in the area of 60 seconds.

For the effects of the explosion Using quantitative risk assessment When BLEVE explosion occurs at the highest intensity level Effects of heat radiation Greater than or equal to 10 kW / sq m at the distance from the leakage point which will result in immediate death in 60 seconds, covering 3 areas (Solvent Room, Tank farm and warehouse). Flammability results in an incident that continues to spread to nearby areas which is a domino effect which creates an impact on the factory, nearby the plant, most agricultural and community areas.

The analysis of leaks, naphtha compounds analyze according to the local wind direction. If at any one time the wind changes direction, this will need to simulate again.

From analysis, this can be used to determine the area of the gathering point establishing an emergency plan to receive assistance from outside agencies while preventing the occurrence of winter events should arrange the loading time in the morning due to the fact that the air humidity is drier than the other seasons.

ACKNOWLEDGEMENTS

From my success in this literature review, I would like to thank you my academic supervisors: Soontree Khuntong; Faculty of Science, who is the significant advisor in the specific definition of literature review. This literature review cannot be finished without consultation from this person. I would like to thank to my friends, and relatives for their encouragement. Finally, I would like to thank my parents in which give me a life, a chance of university studies, and everything.

REFERENCES

[1]ALOHA/AlohaHelp/aloha_help.htm

[2]Google earth

[3]Layout factory of study area

[4]www.hemaraj.com/e_newsletters/Oct_11/Announcement-Flood_Report_4_pd_th.sp

[5]Huai Pong Agricultural Weather Group Rayong Meteorological Station 2017 Meteorological data report Huai Pong Station, Rayong Province, Nov 2017 - Oct. 2018

J.M. TSENGa, T.S. Sua, C.Y. KUOb 2012. Consequence evaluation of toxic chemical releases by ALOHA

SHAO Hui, DUAN Guoning 2012. Risk quantitative calculation and ALOHA simulation on the leakage accident of natural gas power plant.

Chantima Khampanya. 2008 Assessment of the effects of leaks and bursts of rectangular shaped fuel tanks. Sittayanaphon Ph.D., Kasetsart Universit

Ministry of Industry. Hazardous substances list announcement, 2013, 28 August 2013.

Department of Industrial Works 2000, Department of Industrial Works records on criteria for hazard identification risk assessment And the preparation of the risk management plan, 2000

The public health Journal of Burapha University. 2515 Development of Information Management System for chemical Incident Preparedness and /response Application on ALOHA, Marplot, Google Earth and Microsoft Excel Vol.10 No.1 January – June 2515

Emission Estimates during Landing/Take-off Activities from the Commercial Aircrafts at Large International Airports in Thailand

Weerapong Thanjangreed[1], Nares Chuersuwan[2]*

[1]Graduate Program in Environmental Pollution and Safety, Institute of Public Health, Suranaree University of Technology, Nakhon Ratchasima, Thailand

[2]School of Environmental Health, Institute of Public Health, Suranaree University of Technology, Nakhon Ratchasima, Thailand

Corresponding author: e-mail: nares@sut.ac.th

ABSTRACT

This study aims to estimate the annual emissions of carbon monoxide (CO), nitrogen oxide (NO_x), and hydrocarbon (HC) from the commercial aircrafts at Suvarnabhumi and Don Mueang airports, the two largest international airports in Thailand. The emissions were calculated based on landing/take-off cycle (LTO) which included the activities of the aircraft during taxi, take-off, landing, initial-climb, climb-out, and approach modes. Emission factors and actual flight data were used, based on the year 2015 data. More than three hundred thousand flights data were collected at Suvarnabhumi airport and two hundred thousand flights data occurred at and Don Mueang airport. The route maps were created within 1 km x 1 km resolution for each flight using spatial coordinate data. The annual emissions at each coordinate along the route maps were spatially analyzed with the satellite image of the airports to provide the spatial emissions. The annual emissions during LTO cycle at Suvarnabhumi airport were about 1.47 Mtons for CO, 4.96 Mtons for NO_x, and 0.25 Mtons. Don Mueang airport accounted about 0.77 Mtons of CO, 1.27 Mtons of NO_x, and 0.18 Mtons of HC. The spatial emissions of CO and HC at Suvarnabhumi

airport were high at the end of the runway on the eastern side. High spatial emissions of NO_x were observed at the center of the runway. Don Mueang airport had high CO emissions at the end of the runway, while the spatial emissions of HC were high at the end and center of the runway. High emissions of NO_x were observed at the center of the runway as well.

Keywords: Commercial aircraft emission, LTO cycle, Suvarnabhumi, Don Mueang, Thailand

INTRODUCTION

Air traffic has increased in recent years, including in the Asia-Pacific region. In 2017 this region had the highest number of passengers, 1.5 billion passengers overall or 36% market share (IATA, 2018). The two largest airports of Thailand, Suvarnabhumi and Don Mueang airports have the important role in handling the air traffic. Suvarnabhumi airport is the biggest and busiest airport in Thailand, one of the most crowded airports in the world (ACI, 2012). Don Mueang is also a major airport serving both domestic and international routes. Air transportation data in 2015 showed that the commercial aircraft movement increased by 9.50% for Suvarnabhumi and 29.76% for Don Mueang from 2014 (AOT, 2015) . High numbers of the air traffic mean high emissions. Emissions from the commercial aviation relate to the aircraft activities (Belgian Science Policy, 2007). Landing/Take-off (LTO) is the aircraft activities which has an effect on released emissions. Flying cycle, especially LTO cycle, was defined by the International Civil Aviation Organization (ICAO) that the flying cycle were operated at the altitude under 1,000 meters (Graver

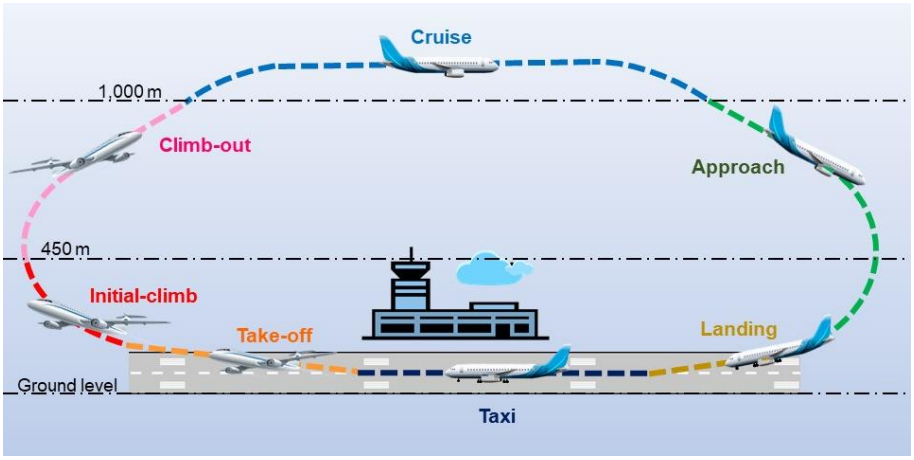

Figure 1 Flying cycle (Adopt from ICAO, 2016 and IPCC, 2000)

and Frey, 2009). The LTO cycle includes aircraft taxi, take-off, initial-climb, climb-out, approach and landing modes (Figure 1). Aircraft taxi, take-off and landing modes occur at the ground level in the runway's area, while initial-climb and climb-out modes are operated at the altitude between 0 to 450 and 450 to 1,000 meters, respectively and the approach mode is controlled at 0 to 1,000 meters (Watterson et al., 2004). The LTO cycle was used to estimate the emissions from the commercial aircraft in this study. In addition, cruise is one mode of the flying cycle that autonomically operated at the high altitude over 1,000 meters (IPCC, 2000). Cruise mode was not performed in this study due to emissions at the altitude above 1,000 meters do not interfere the pollution at the altitude below 1,000 meters (Wayson and Fleming, 2000). Fuel used in aircraft engines is an important factor which has effect on the emissions from the aircraft (Winther and Rypdal, 2014). Kerosene is distilled by middle distillation of crude oil and used as aviation fuel for almost aircraft (Masiol and Harrison, 2014). Emissions from fuel combustion in aircraft's engine are found both complete and incomplete combustion. Carbon monoxide (CO), nitrogen oxide (NO_x), and hydrocarbon (HC) are the pollution emitted from incomplete combustion in actual condition (Weubbles et al.

2007; Norton, 2014). These pollutants were emitted less than 1% of all pollution that released from aircraft, about 84% of NO_x, 11.8% of CO, 4% of HC and 0.2% other (Lewis et al., 1999; Masiol and Harrison, 2014). A study at Raleigh-Durham International Airport indicated the HC, CO, and NO_x emissions of the commercial aircrafts were 60.2, 514, and 492 tons per year, respectively, in 2006 (Graver and Frey, 2009)

This study estimated the annual emissions of CO, NO_x, and HC based on the LTO cycle and estimates the spatial emissions at Suvarnabhumi and Don Muang airports.

METHODOLOGY

Data collection

Numbers of aircraft flight and flight number of each flight were collected from the official website of the Airport Authority of Thailand (Airport of Thailand Co., Ltd.). Numbers of aircraft flight were summed for the same flight number and used in calculation of the annual emissions.

Flight route coordinate data (latitude and longitude data) were gathered from the website "Flight Aware" (https://flightaware.com/). Flight number was also used to determine the aircraft engine's type and its number. These data were used as inputs and prepared for emission calculations and spatial analysis.

Emission calculation

Annual emissions from the commercial aircraft were estimated with the actual numbers of flight data and available emission factors through equation (Watterson et al., 2004).

$$E_{LTOa,m,p,s} = N_s \times T_{a,m,s} \times F_{a,s}(t_{a,m,s}) \times I_{a,p,s}(t_{a,m,s})$$

Where $E_{LTOa,\,m,\,p,\,s}$ is the emissions in mode *m* of pollutant *p* for a specific aircraft type *s* at airport type *a*, *a* is the airport type, *m* is the flying mode, *p* is the type of pollutant, *s* is the specific aircraft type, N_s is the number of engines on aircraft type *s*, $T_{a,\,m,\,s}$ is time in mode *m* for a specific aircraft type *s* at airport type *a* (s), $F_{a,}$

$_s$ is weighted average fuel flow for an engine on aircraft type *s* at airport type a for thrust t (kg s^{-1}), $I_{a,\ p,\ s}$ is weighted average emission factor of pollutant *p* for an engine on aircraft type *s* at airport type a for thrust t (kg/kg fuel), and $T_{a,\ m,\ s}$ is engine thrust setting during mode m for aircraft type *s* at airport type *a* (%).

The time in mode ($T_{a,\ m}$) for taxi mode could be calculated from the equation (Watterson et al., 2004).

$$T_{a,\ m} = 0.1 \times R_a$$

Where $T_{a,\ m}$ is the time in mode *m* (Taxi-in or Taxi-out) at airport *a* (s), *a* is the airport, m is the mode (Taxi-in or Taxi-out), and R_a is the length of the longest runway at airport *a* (m).

Each mode in the LTO had the default thrust setting values. These values were used for calculating the annual emissions during LTO cycle.

Table 1 Default thrust setting in LTO cycle (Watterson et al., 2004)

Mode	Default thrust setting (%)
Taxi	7
Take-off	100
Initial-climb	100
Climb-out	85
Approach	30
Landing	7

Spatial analysis

The XY coordinate data of each flight were used for creating route maps through a GIS program. Route maps consisted of the aircraft's movement points. Then, the annual emission data were added to each point as attribute table of emission data of the route maps.

Each point of emission data in the route maps were spatially analyzed and interpolated to provide the spatial distribution of emissions on the maps.

RESULTS AND DISCUSSION

The movement of the commercial aircraft

The commercial aircraft movement during taxi mode at Suvarnabhumi airport occurred at the end of the runways on both sides, while take-off and landing were found at the center of the runways. Initial-climb, climb-out and approach were observed both sides at the area 10 kilometers away from the runways as showed in Figure 2. Each dot represented the locations of the aircrafts' movement.

(a) (b)

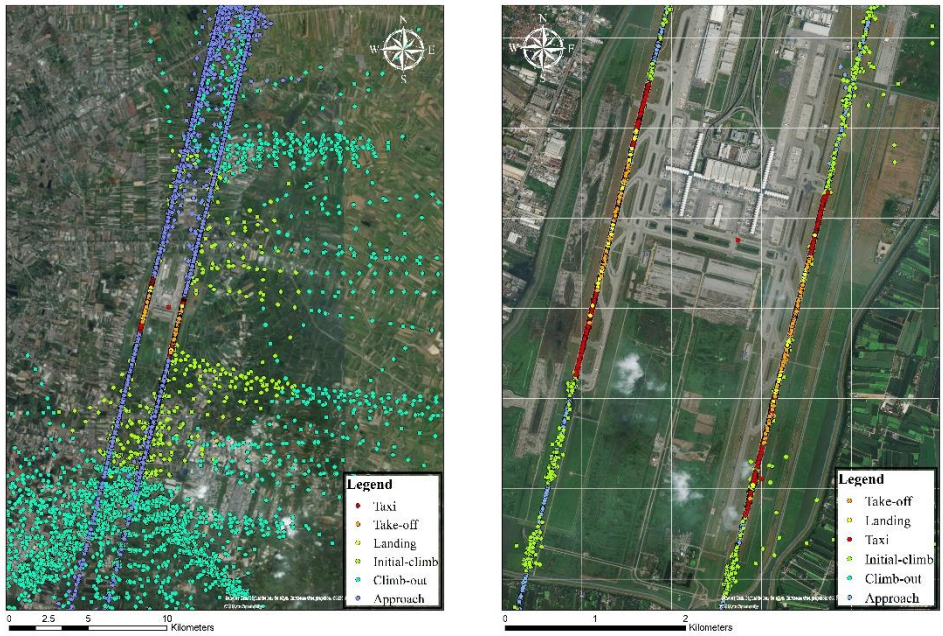

Figure 2 The commercial aircraft movement at Suvarnabhumi airport (a) and map in scale enlargement (b)

(a) (b)

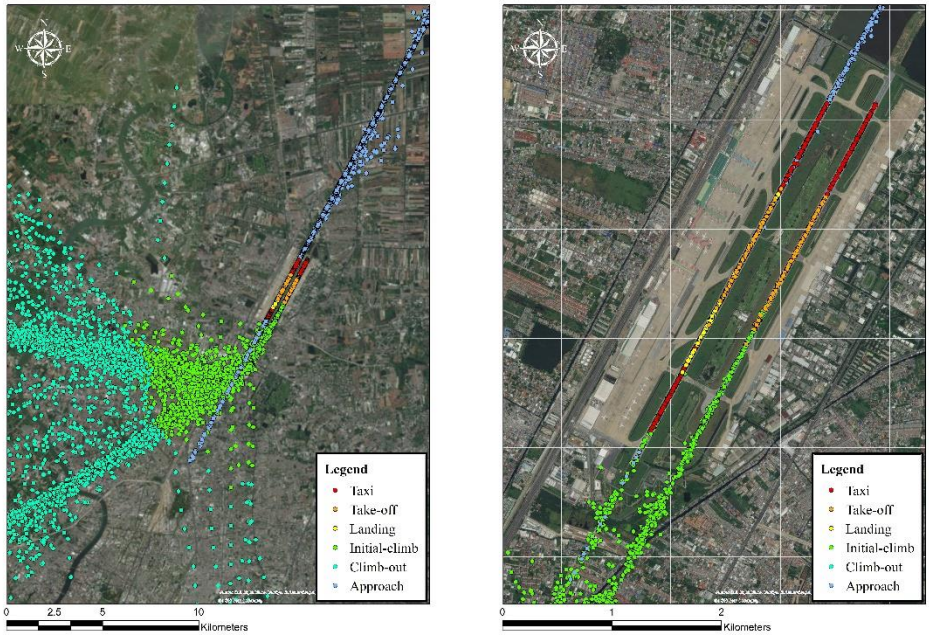

Figure 3 The commercial aircraft movement at Don Mueang airport (a) and map in scale enlargement (b)

At Don Mueang airport (Figure 3), the aircraft taxi mode occurred at the end of the left runway on both sides, while the right runway was found only one side at the end in the northeast direction. Initial-climb and climb-out were operated at the area away the runways in the southwest direction, while the approaching was observed at both sides of the runways.

Annual emission of the commercial aircraft

Annual emissions from the calculations with actual flight data and emission factors were showed in Table 2. Suvarnabhumi airport, during taxi mode accounted about 1,124 ktons of CO, 225 ktons of NO_x, and 188 ktons of HC, annually. Take-off emitted about 24 ktons of CO, 2,200 ktons of NO_x, and 6 ktons of HC, annually. The annual emission of CO through the initial-climb was 12 ktons, 990 ktons of NO_x, and 3 ktons

Table 2 Annual emissions throughout LTO cycle

Modes	Emissions (ktons)					
	Suvarnabhumi			Don Mueang		
	CO	NO_x	HC	CO	NO_x	HC
Taxi	1,124	225	188	537	81	112
Take-off	24	2,200	6	17	532	30
Initial-climb	12	990	3	8	236	2
Climb-out	17	926	3	14	247	3
Approach	200	600	34	148	159	26
Landing	94	20	14	44	11	9
Total	1,471	4,961	248	768	1,266	182

of HC. During the climb-out mode, the annual emissions were 17, 926, and 3 ktons for CO, NO_x, and HC, respectively. The approach mode released about 200, 600, and 34 ktons for CO, NO_x, and HC, annually. The annual emissions of the landing mode accounted about 94, 20, and 14 ktons of CO, NO_x, and HC, respectively.

The annual emissions during taxi mode at Don Mueang were 537 ktons for CO, 81 ktons for NO_x, 112 ktons for HC, respectively. The annual emissions during take-off mode were accounted about 17, 532, and 30 ktons for CO, NO_x, and HC, respectively. Initial-climb emitted about 8 ktons for CO, 236 ktons for NO_x, and 2 ktons for HC, annually. The annual emissions during climb-out mode accounted about 14, 247, and 3 ktons of CO, NO_x, and HC, respectively. The approach mode emitted about 148, 159, and 26 ktons for CO, NO_x, and HC, annually. The annual emission of CO through landing was 44 ktons, 11 ktons of NO_x, and 9 ktons of HC, respectively.

Spatial emission of the commercial aircraft

The spatial emissions were obtained from interpolating the emissions at each point through the GIS program. Figure 4 is the annual spatial

emissions at Suvarnabhumi airport and Figure 5 is for Don Mueang airport.

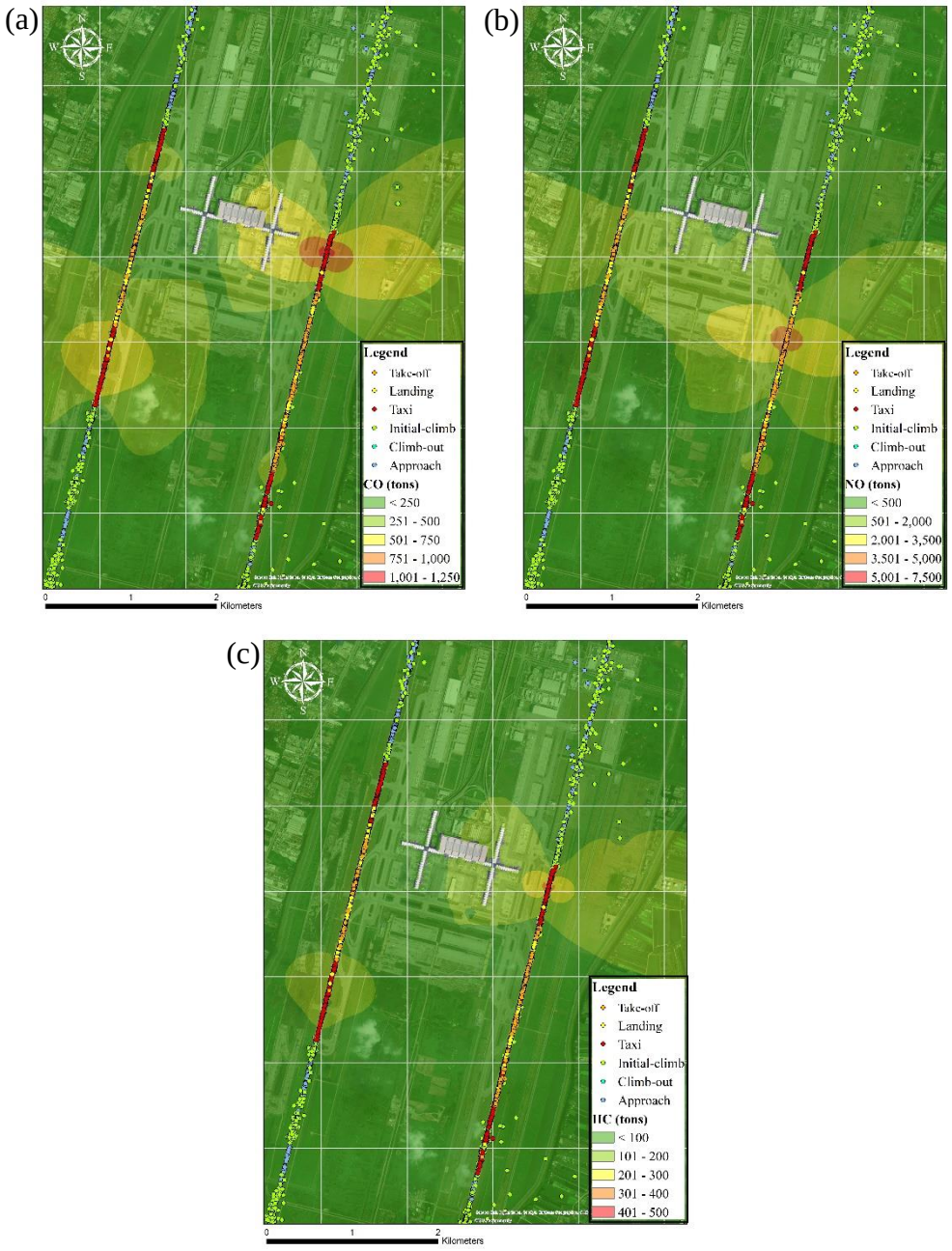

Figure 4 Spatial emissions during LTO cycle at Suvarnabhumi airport

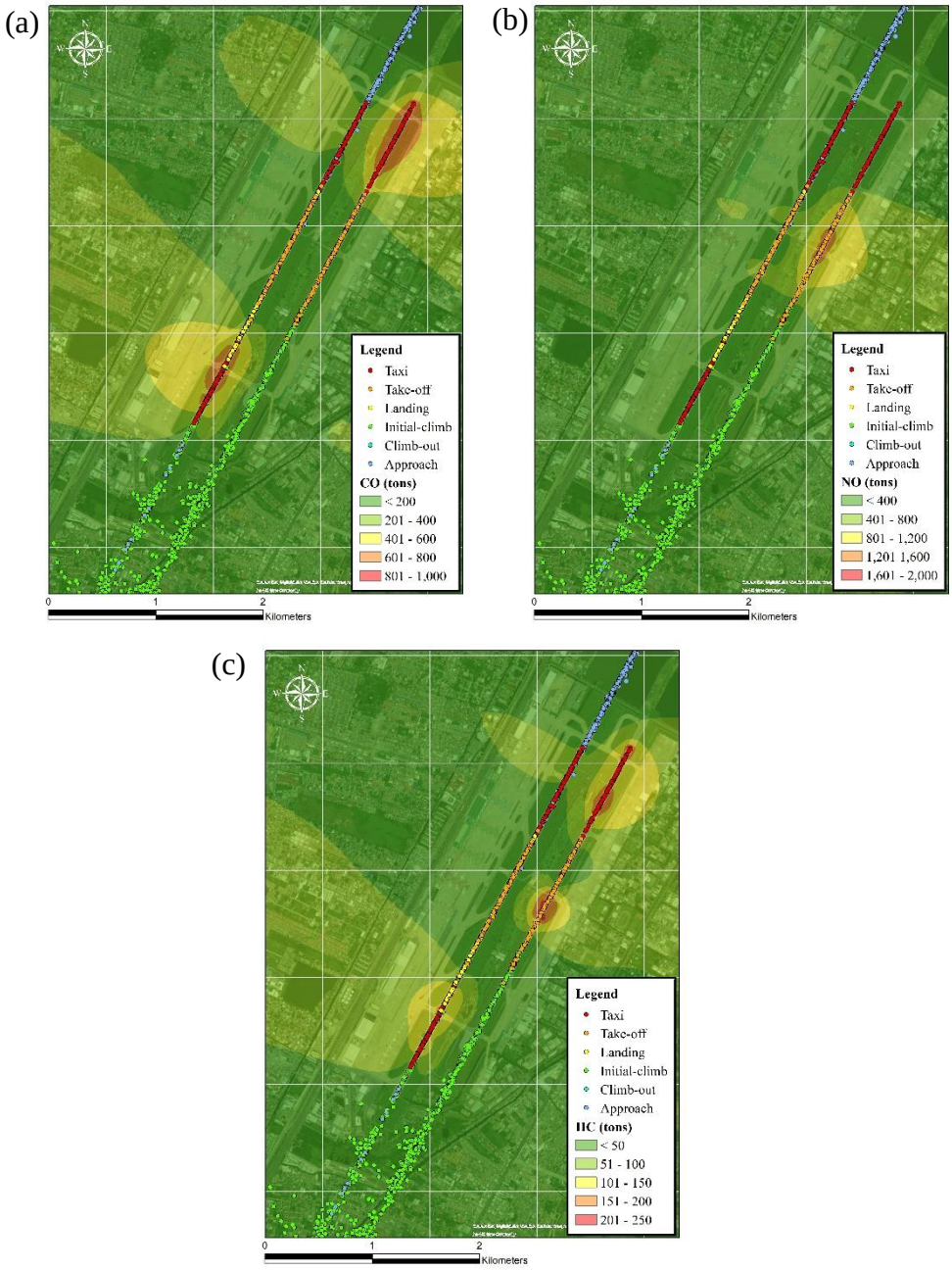

Figure 5 Spatial emissions during LTO cycle at Don Mueang airport

Annual spatial emission of CO at Suvarnabhumi airport was the highest, about 1,000 to 1,250 tons, at the end of the right runway in the northeast direction and the nearby area, aircraft parking areas next to the terminal building and taxi way. The highest spatial emission of NO_x

ranged from 5,000 to 7,500 tons, high at the center of the right runway, while the spatial emission of HC was 400 to 500 tons, high at the areas similar to CO.

CO emission at Don Mueang airport accounted about 800 to 1,000 tons and the highest emission was observed at the end of the left runway in the southwest direction and at the end of the right runway in the northeast direction. In addition, high emission of CO also was found at aircraft parking areas near the terminal building. Emission of NO_x ranged from 1,600 to 2,000 tons and the highest spatial emission was found at the center of the right runway. The highest emission of HC, 200 to 250 tons, occurred at the end and at center of the right runway and the end of left runway in the southwest direction.

High emissions of CO and HC were found during aircraft taxi mode due to incomplete combustion (Jacobson, 2012), at the condition of low oxygen while fuel is burned in the engine chamber. The emission of NO_x was high during aircraft take-off, further away from the runway. NO_x is released when the combustion condition is at high temperature (1,300 Celsius) and with excess air condition (US. EPA., 1999), during take-off mode.

CONCLUSIONS

This research had shown that aircraft emissions could be estimated using actual flight data along with emission factors. The emissions should separate into LTO cycle and the spatial distribution required actual flight tracking data. The annual emissions of the commercial aircrafts in 2015 at Suvarnabhumi airport were about 1,471 ktons for CO, 4,961 ktons for NO_x, and 248 ktons for HC. The annual emissions at Don Mueang airport were 768 ktons for CO, 1,266 ktons for NO_x, and 182 ktons for HC. Emissions of CO and HC were high during taxi mode as the result of incomplete combustion, while the emission of NO_x was highest when compared to CO and HC during take-off mode due to excess air and high temperature condition. The spatial emissions of CO and HC were

observed at the end of the runway where aircraft taxi mode occurred as well as the area near terminal building and aircraft parking stand. The high spatial emission of NO_x was found at the center of the runway both Suvarnabhumi and Don Mueang airport.

ACKNOWLEDGEMENTS

The authors express the grateful to Suranaree University of Technology, Nakhon Ratchasima, Thailand for the grant and Institute of Public Health for the support and facilitation through this study.

REFERENCES

ACI. 2012. Preliminary 2012 World Airport Traffic and Rankings. Montreal, Canada: Airport Council International.

AOT. 2015 Traffic Report. Airport of Thailand Public Company Limited: Air Transport Information and Slot Coordination Division; 2015.

Belgian Science Policy. Aircraft emissions. Brussels Belgium: ABC Impacts Aviation and the Belgian Climate Policy; 2007.

Graver B.M. and Frey H.C. 2009. Estimation of Air Carrier Emissions at Raleigh-Durham International Airport. Proceedings, 102nd Annual Conference and Exhibition, Air and Waste Management Association 2009; Paper 2009-A-486-AWMA.

IATA. 2018. 62nd World Air Transport Statistics (WATS). International Air Transport Association.

ICAO. 2016. Continuing traffic growth and record airline profits highlight 2015 air transport results. International Civil Aviation Organization.

IPCC. 2000. Good Practice Guidance and Uncertainty Management in National Greenhouse Gas Inventories. Intergovernmental Panel on Climate Chang.

Jacobson MZ. Air pollution and global warming: history, science, and regulation. 2nd ed. United Kingdom: Cambridge University Press; 2012.

Masiol M and Harrison RM. Aircraft engine exhaust emissions and other airport-related contributions to ambient air pollution: A review. Atmospheric Environment 2014; 95 (2014) 409e455.

Norton TM. 2014. Aircraft Greenhouse Gas Emissions during the Landing and Take-off Cycle at Bay Area Airports. Master's Projects. United States: University of San Francisco.

Watterson J, Walker C and Eggleston S. Revision to the method of estimating emissions from aircraft in the UK Greenhouse Gas Inventory. United Kingdom: Report to Global Atmosphere Division, DEFRA 2004; netcen/ED47052.

Winther M, and Rypdal K. EMEP/EEA emission inventory guidebook 2013 (update July 2014). Copenhagen, Denmark: European Environment Agency; 2014.

Roger L. Wayson and Gregg G. Fleming. 2000. Consideration of Air Quality Impacts by Airplane Operations at or Above 3000 feet AGL. Federal Aviation Administration; U.S. Government Printing Office: Washington, DC, United States.

US.EPA. Nitrogen Oxides (NO_x), Why and How They Are Controlled., Research Triangle Park, North Carolina, United States: U.S. Environmental Protection Agency; 1999.

PM10 and dust fall concentrations from mobile sources in the Kamphaeng Phet Municipality

Sekpinya Suban[1], Pajaree thongsanit[2]

[1]Master's degree student, civil engineering department, Faculty of Engineering, Naresuan University, Phitsanulok, Thailand 65000
[2]Assistant Professor, civil engineering department, Faculty of Engineering, Naresuan University, Phitsanulok, Thailand 65000;
Coresponding author: e-mail: p-w-a@hotmail.co.th

ABSTRACT

This research developed a particulate matter inventory report from mobile sources in the Kamphaeng Phet municipality. Sixty PM10 samples were collected using a high-volume air sampler over 24 hours at a flow rate of 1.7 cubic meters per minute. The 60 samples of dust fall were collected using a gravimetric technique which was modified from the Department of Pollution Control (PCD) dust collection guidelines. Dust fall containers were set between June 2017 and May 2018 at 5 sample stations. Also, three points of motor vehicle traffic were surveyed using Closed Circuit Television (CCTV) cameras. This study used the emission factor method to quantify emissions. Two samples from 60 PM10 samples exceeded the ambient Thai standard of 120 micrograms per cubic meter. The highest PM10 data was 130.72 micrograms per cubic meter at the Chula-Kanchanaphisek fort site in January 17, 2018. The highest dust fall data was 336.41 milligram per square meter per day at the Chula-Kanchanaphisek fort in February 2018. The major mobile source in Kamphaeng Phet Municipality was heavy diesel vehicles.

Keywords: Particulate matter, PM10, Dust fall, Kamphaeng Phet municipality

INTRODUCTION

The Kamphaeng Phet municipality has an area of 14.9 square kilometers with a population density of 1,960 people per square kilometer. In the past, the Kamphaeng Phet municipality has had a lot of economic and social development in eighteen community areas. Over a ten year period, the number of communities expanded to twenty seven and population and building areas also increased. [1]. At present, the traffic in Kamphaeng Phet municipality is crowded. The various vehicles in Kamphaeng Phet city include motorcycles, private cars, buses and trucks. These vehicles emit particulate matter smaller than 10 micron (PM10) into the ambient air, thus affecting the respiratory systems and health of the population. Other air pollution sources are the burning of agricultural waste in the open areas of Kamphaeng Phet municipality during the harvesting season and construction activities in the Kamphaeng Phet area. This research aimed to study PM10 concentrations and dust fall from mobile sources on a road in the Kampaeng Peth municipality.

MATERIALS AND METHODS

In this research, two sets of samples were collected from each of five sampling stations. These were PM10 and dust fall samples and the five sampling stations in the Kamphaeng Phet municipality were the Clock Tower, the Ton Pho (Pho tree) Roundabout, the Bang Temple, the Chula-Kanchanaphisek fort, the Muang Kamphaeng Phet Traffic Center Police Station and a station on Route 112. Dust fall sampling using the dust fall jar technique was conducted, where one dust fall sample per month was collected from each of the same 5 stations for 12 months from June 2017 to May 2018, resulting in 60 samples in total. Subsequent quantitative analysis used gravimetric and sedimentation methods. Dust sample collection equipment consisted of a sample collection jar and a storage dust cone in a basket set on a 1.5 meter high PVC pipe. The

surrounding sampling area had no walls or any other obstructions for at least 10 meters. The samples were collected and analyzed in a laboratory to determine dust fall concentration. This analysis consisted of weighing the samples and determining weight per unit of area of the container per storage period. This provided data in units of milligrams per square meter per day. PM10 sampling used high-volume air samplers for 24 hours at an air flow rate of 1.7 cubic meters per minute [2]. The high volume air sampler calibrated the air flow rate every month and used an 8 x 10 inch glass fiber filter, at one filter per sample. Similarly to dust fall sample collection, PM10 samples were collected once per month over the same period, resulting in 60 samples conducted for 12 hours per day (07.00 - 19.00 hrs.) over 3 days between Monday to Friday and on also on Saturday and Sunday. The calculation of the amount of air pollution from vehicles used equation is;

$$\boldsymbol{E = N\ x\ EF\ x\ D}$$

PM10 was reported in micrograms per cubic meter.

The resulting sample collection data was used to form an inventory report of particulate matter emissions from mobile sources including gasoline vehicles, light diesel cars, heavy diesel cars and motorcycles.

The traffic volume survey method in this study was based on methods from academic documents from a traffic volume survey by the department of rural roads [3]. The traffic volume used an enumeration method from CCTV, from both directions, according to the types of vehicles on the roads. The three traffic counting points were the Chula-Kanchanaphisek fort, Bang Temple and the Muang Kamphaeng Phet Traffic Center Police Station. Traffic volume counting was

E = emissions (gram/day)

N = Average daily traffic volume (car/day) (**Table 1.**)

EF = emissions factor (gram/kilometer/day) (**Table 2.**)

D = Distance (kilometer) = 1 kilometer [4].

RESULTS AND DISCUSSION

Dust fall concentration: The study of dust emissions in the Kamphaeng Phet municipality from 5 points used the dust fall method, with samples taken once per month from June 2017 to May 2018. The sampling time covered the rainy, winter and summer seasons. The accumulation of dust from January 2018 to March 2018 was at high concentrations from the sampling point at the Muang Kamphaeng Phet Traffic Center Police Station. The sampling point at Chula-Kanchanaphisek fort reported the highest dust reading at 336.41 milligrams per square meter per day in February 2018. At the Muang Kamphaeng Phet Traffic Center Police Station, the dust fall concentration was lowest in February 2018 at a concentration of 327.52 milligrams per square meter per day. The main dust sources were road dust, traffic, sugarcane burning and construction. When compared with the air quality dust fall standards from Malaysia which specify a value of 133 milligrams per square meter per day, it was found that 47 samples from the total of 60 samples were higher than the Malaysian standard. The Malaysian standard was used as no standard exists in Thailand. The minimum value of dust fall was measured during the rainy season in October 2017, at 51.17 milligrams per square meter per day

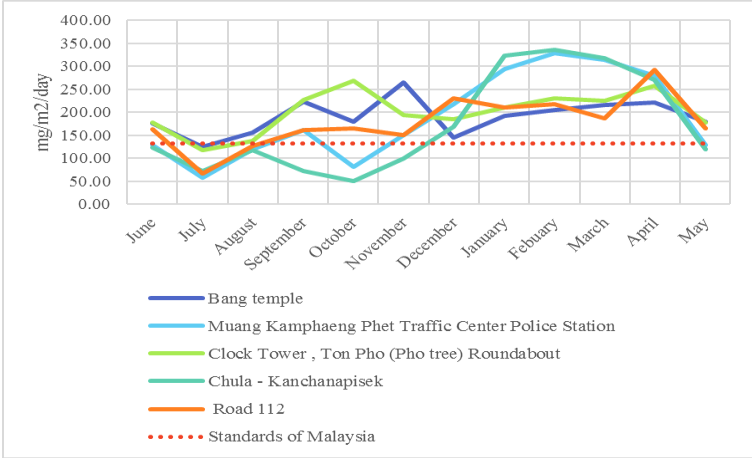

Figure 1 The concentration of dust fall in Kamphaeng Phet municipality

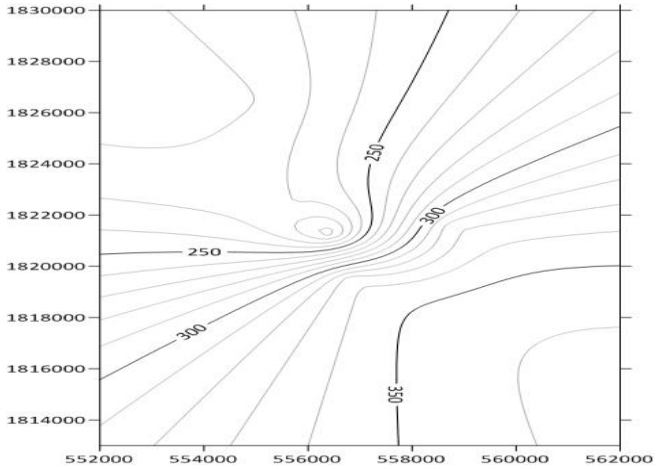

Figure 2 Dust fall concentration levels in the Kamphaeng Phet

Municipality area (longitude is shown on the y axis and latitude is shown on the x axis).

The level of dust fall in Kamphaeng Phet Municipality during the month of February year 2018 from the 5 sampling points was influenced by fly ash from sugarcane burning in areas outside the city area into the municipality. The other sources of dust were transportation and construction activities. 2. The concentration of dust particles smaller than 10 micron (PM10) exceeded the Thai standard of 120 micrograms per cubic meter at 2 sampling points during the January 2018. The two sampling stations

were Muang Kamphaeng Phet Traffic Center Police Station where the concentration was 126.63 micrograms per cubic meter on 3 January and at Chula-Kanchanaphisek fort where the concentration was 130.72 micrograms per cubic meter on 17 January 2018. The high concentrations where due to agricultural traffic and road construction. The lowest PM10 data was at 24.51 micrograms per cubic meter on August 14, 2017 at the Chula-Kanchanaphisek fort ampling point.

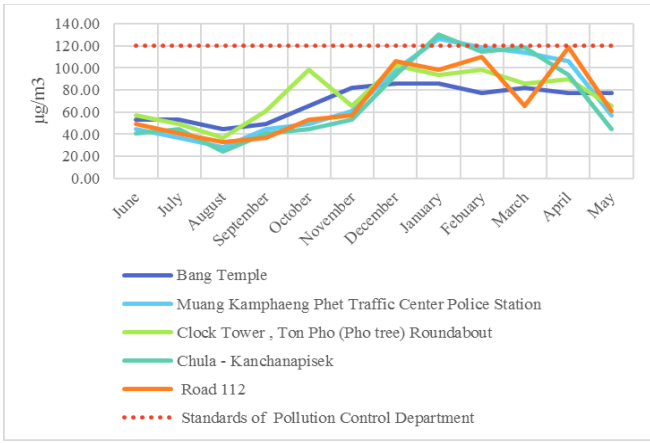

Figure 3 The concentration of PM10 in the Kamphaeng Phet Municipality area. (longitude is shown on the y axis and latitude is shown on the x axis)

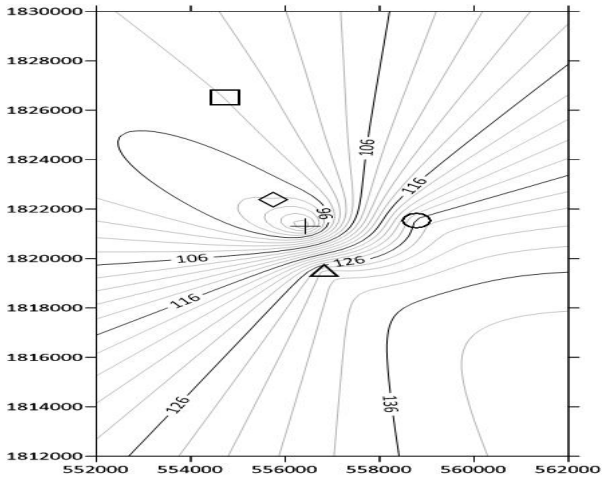

Figure 4 PM10 concentrations in Kamphaeng Phet Municipality area

Figure 4 shows PM10 concentration levels in the Kamphaeng Phet municipality area. Many areas in city were above the Thai standard of 120 microgram per cubic meter. The main source of PM 10 in the city was from combustion processes such as truck traffic.

3. Traffic volume of Kamphaeng Phet Municipality

The traffic volume was measured according to the type of vehicle using CCTV from two directions. The three counting points were Chula-Kanchanaphisek fort, Bang Temple station and Muang Kamphaeng Phet Traffic Center Police Station. Traffic volume counting was conducted for 12 hours per day (07.00 - 19.00 hrs.) over 3 days between Monday to Friday and on also on Saturday and Sunday. The data is shown in Table 1.

Table 1 Traffic volume in Kamphaeng Phet Municipality

Traffic volume check point		Average daily traffic volume (cars / day)			
		Motorcycle / Tricycle	Gasoline cars	Light diesel cars	Heavy diesel vehicles
1.	Chula Kanchana phisek Station.	1,844	744	958	962
2.	Bang Temple Station.	1,840	950	711	-
3.	Muang Kamphaeng Phet Traffic Center Police Station	1,935	821	1,250	1,547

Remark "-" signifies no vehicles were present

The traffic volume data in table 1 was analysed for PM10 loading in the city. The researcher used traffic volume data in table 1 and the dust emission factors (EF) in table 2. The PM10 loading was calculated using traffic volume data combined with the related dust emission factors.

Table 2 The emission factor (EF) of the PM10 concentration using of this data [4]

	EF (Grams / Kilometer / Cars)
	PM
Motorcycle / Tricycle	0.086
Gasoline cars	0.101
Light diesel cars	0.042
heavy diesel cars	1.150

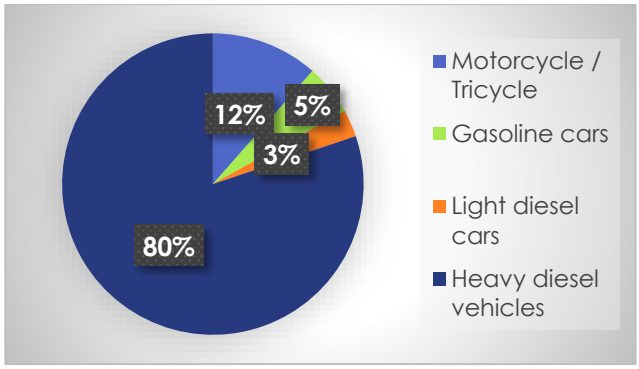

Figure 5 The ratio sources of PM10 loading at Chula-Kanchanaphisek fort

Data from the figure 5 that were calculated from equation;

$$\boldsymbol{E = N\ x\ EF\ x\ D}$$

It found that the ratio of PM10 dust emission of vehicles at the Chula-Kanchanaphisek was from heavy diesel vehicles (80%), motorcycles (12%), gasoline cars (5%) and light diesel cars (3%).

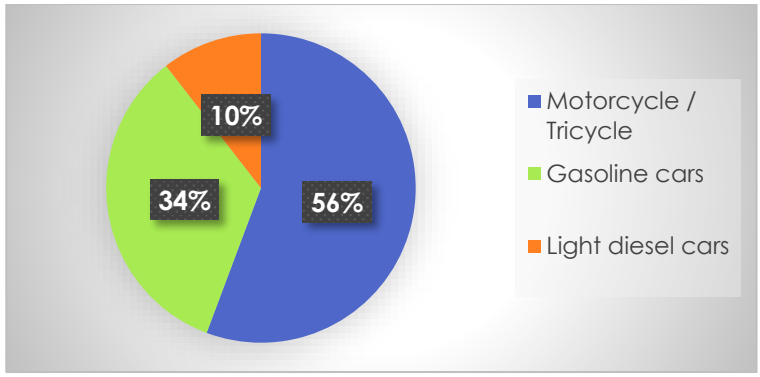

Figure 6 Ratio of sources of PM10 emissions at Bang Temple

The PM10 dust emission of vehicles in the temple area, was 56% of motorcycles (56%), 34% of gasoline cars (34%) and light diesel cars (10%). Due to the narrow roads in this area, heavy diesel trucks could not reach the road.

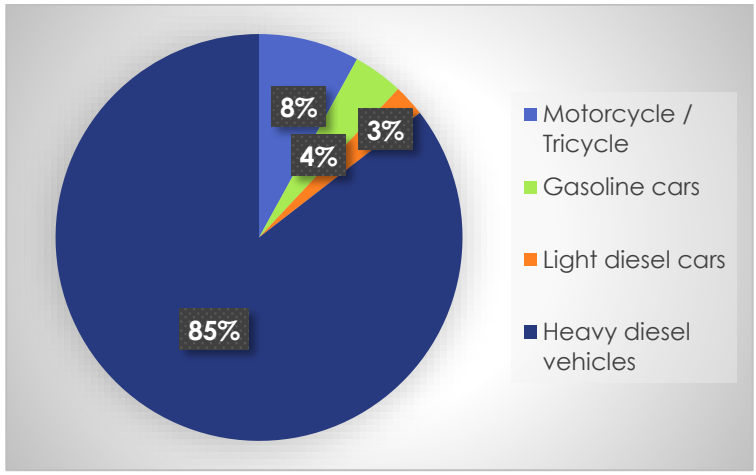

Figure 7 Ratio of sources of PM10 emissions at Muang Kamphaeng Phet Traffic Center Police Station

The PM10 dust emissions at the traffic center of Muang Kamphaeng Phet Traffic Center Police Station found where from heavy diesel vehicles (85%), motorcycles (8%), gasoline cars (4%) and light diesel

cars (3)

CONCLUSION

It was found that the concentration of dust accumulation from January to March was highest at the Muang Kamphaeng Phet Traffic Center Police Station sampling point. The up by traffic. Dust from sugarcane burning outside the municipality and dust from construction contributed small dust particles (PM10) exceeding the standard of 120 micrograms per cubic meter during the month of January 2018 at the sampling point area at the Muang Kamphaeng Phet Traffic Center Police Station, where measured value was 126.63 micrograms per cubic meter. The sampling point at the Chula-Kanchanaphisek fort measured 130.72 micrograms per cubic meter in January.

It was found that from January 2018 until March 2018, both samples of high PM10 were due to the harvest season of agricultural products. As for the PM10 dust emission rate from vehicles in Kamphaeng Phet sampling point of Chula-Kanchanaphisek Fort, had the lowest concentration in October 2017, although it conversely had the highest concentration in February 2018. The dust mainly arose from dust on the road surface being picked

Municipality, it was found that the Chula-Kanchanaphisek Fort area had the highest PM10 emission ratio, originating from large diesel vehicles (80%). The highest source of PM10 at Bang Temple (56%) was from motorcycles. At the Muang Kamphaeng Phet Traffic Center Police Station, the highest source of PM10 emissions was from large diesel vehicles (85%).

ACKNOWLEDGMENT The researchers wish to thank the Department of Environmental Engineering, Department of Civil Engineering, Faculty of Engineering, Naresuan University who kindly supported this project with all equipment and research funding.

REFERENCES

[1] Community development welfare division Kamphaeng Phet municipality, 2015) Retrieved March 20,2017 Website: http://www.kppmu.go.th

[2] Chuchai Lawnimitdee. 2006; The study on source apportionment of Polycyclic of aromatic hydrocarbons (PAH_S) in fine particulate matter (PM10) of the roadside air environment in phitsanulok. Thesis of Master Engineering.Naresuan University,Phisanulok.

[3] Departmemt of Rural roads. 2010; Average Annual Daily Traffic on Hight ways 2009, Changwat: Nakhon Ratchasima.

[4] Pollution Control Department. 2008; Air Pollution Database Project, Samut Prakan Provice.

[5] Sarid Kotula. 2010; Emission Inventory of Air Pollution Nakhon Ratchasima Municipality Area. Thesis of Master Engineering. Suranaree University of Technology, Nakhon Ratchasima.

Using PRTR database to assess human toxicity and eco-toxicity: a case study on emission sources in Rayong province, Thailand

Krisda Chidsanit[1, 2], Piyapat Saenpao[1, 2], Vasita Tunlathorntham[1, 2], Kanisorn Jindamanee[1, 2], and Sarawut Thepanondh[1, 2]*

[1]Department of Sanitary Engineering, Faculty of Public Health, Mahidol University, Bangkok 10400, Thailand
[2]Center of Excellence on Environmental Health and Toxicology (EHT), Bangkok 10400, Thailand;
Corresponding author: e-mail: sarawut.the@mahidol.ac.th

ABSTRACT

Thailand's Eastern Seaboard has emerged as the country's industrial hub. Rayong Province is the largest home of the petroleum and petrochemical productions as well as other heavy industries which leads to potential environmental threats. This study aims to apply the USEtox Model for evaluating human and ecological toxicity based on the data achieved from the Pollutant Release and Transfer Registers (PRTR) database of the study area. The database used in this analysis consisted of 107 chemical compounds covering from pesticides, heavy metals, inorganic and organic compounds. Results from the analysis by USEtox indicated that acrylonitrile has the highest potential health impact (1.5E+0 CTUh) followed by paraquat dichloride (1.46E+0 CTUh) and chlorpyrifos (1.17E+0 CTUh). As for environmental toxicity, ametryn is evaluated as the most toxic substance (2.02E+08 CTUe) followed by chlorpyrifos (1.66E+08 CTUe) and paraquat dichloride (2.48E+07 CTUe). It was found that these harmful substances are mainly emitted from agriculture activities except for acrylonitrile which is mainly emitted from the industrial sources. This study reveals the necessity to

develop the emission data and further evaluate them for potential health and environmental impacts for future sustainable management of the area.

Keywords: Maptaphut / Rayong / PRTR / USEtox model / Toxicity

INTRODUCTION

Thailand's Eastern Seaboard has emerged as the country's industrial hub. Rayong Province is the largest industrial area, where petrochemical and related productions are key industries. The area has been facing several severe environmental problems which impose serious impacts on the health and quality of life of the local people. One of the most important pollution in Rayong's industrial area is air pollution in which the major types of concerns are VOCs, SO_2, and NO_x. The government agencies have been trying to solve the problems through several measures mainly under the Rayong's Pollution Reduction and Mitigation Action Plan. However, the problems still exist. Concentrations of several air pollutants still exceed the national ambient air quality standards.

There are several studies have been attempted to monitor and evaluate the environmental impacts in this area. For example Poboon (2012) and Chusai (2010) studies and examined the management of air pollution situation in this industrial zone and suggest mitigation scenarios for improvement of air pollution management in the area. Moreover, Chusai et al (2012) determined the distribution of nitrogen dioxide (NO_2) in the ambient air over the area using an air dispersion model. The results were also interpreted for the cost of NO*x* emission reduction in Map Ta Phut industrial area. Vadakan (2012) studied exposure to volatile organic compounds and health risks. The results revealed that those who lived longer than 5 years in an exposure area had an increased risk for dyspnea and wheezing. Older adults (> 40 years) were more affected by chronic respiratory problems, lower respiratory symptoms, and eye irritation. Result of the study also reported that women had a higher risk of acute and chronic

respiratory symptoms than men. Similar finding was also reported by Kongtip (2013).

Due to its home to the industrial activities in Thailand, Rayong province was selected to implement the Pollutant Release and Transfer Registration (PRTR) in Thailand. The PRTR is an environmental database or inventory of potentially harmful releases to air, water and soil as well as wastes transported to treatment and disposal sites. Facilities releasing one or more of the substances report periodically as to what was released, how much, and to which environmental media. Data are then made available to interested parties. In addition to reports from stationary sources, some PRTR versions include diffuse releases such as transport and agricultural releases which are estimated based on specific data and statistics. (OECD, 1997)

USEtox is an environmental model for characterization of human and ecotoxicological impacts in Life Cycle Impact Assessment (LCIA) and Comparative Risk Assessment (CRA). It has been developed by a team of researchers from the Task Force on Toxic Impacts under the UNEP-SETAC Life Cycle Initiative. The USEtox model was developed to implement in Microsoft Excel that is designed to describe the fate, exposure and effects of chemicals. The UNEP-SETAC Initiative supports the development, evaluation, application, and dissemination of USEtox to improve understanding and management of chemicals in the global environment. (USEtoxTeam, 2017)

The aim of the study is to use the PRTR database in assessing the potential human toxicity and eco-toxicity in their releasing area. The chemical substances in the PRTR database will be ranked for their contribution to the human toxicity and eco-toxicity through the evaluation by the USEtox model. Results obtained from this study will be very much useful in an effort to prioritize and set up the appropriate mitigation and measures in managing of release and transfer of chemicals by considering their potential threats to the environment.

METHODOLOGY

Study area

Rayong province was chosen as the study area. The study domain covered an area of 100 x 100 km^2 of the provincial area.

Pollutant Information

Pollutant Information analyzed from secondary data in Pollutant Release and Transfer Register (PRTR) (http://prtr.pcd.go.th/ , 2013). PRTR database is developed under 'Right to know in public' policy. Therefore, these data can be used without collecting new data. Under PRTR system, entrepreneurs will evaluate and report the amount of released pollutant to any types of environment (soil water and air). It also includes transferring the amount of pollutant outside of the area to treatment and waste management. The reports are in form of annual report in each factory. This information will be reported to the PRTR designated government agency. Their duties are collecting PRTR report from every potential source to evaluate the amount of release and transfer polluted substances apart from industry waste (i.e., vehicles, agriculture, households, etc.). All information will be reported to elucidate the status of pollutant discharge especially the main source and trend of changing the amount of pollutant emitted in each area. This information collected by the government will be presented to the public which depended on the rights to know in public by presenting in various forms such as annual report or internet network.

The chemicals or pollutants under the PRTR system consists of 107 substances, based on hazard or toxic data, consumption information along with the levels of chemicals detected in the environment.

- Toxic data are considered by the list of chemicals or pollutants that are prescribed under Thai law and relevant international obligations in other countries and chemicals with U.S.EPA hazard information.

- The level of chemicals detected in the environment that is likely to get into the body (exposure).

USEtox Model

USEtox Model is the environmental model for determine the characteristic of Toxicology and the effect to ecosystem and human by evaluate the cycle of life. It is used to calculate the factor of toxic in human and the toxic in ecosystem by applying the concept of life cycle impact assessment for the calculation.

Life cycle impact assessment

Life cycle impact assessment has purpose in reviewing the importance of emissions in each product or any services in life. In the USEtox, average weight in releasing pollution substances in product system were used along with other factors for the calculation of impact score (IS) as followed:

$$IS = \sum_{i} \sum_{x} CF_{x,i} \times m_{x,i}$$

Where:

IS is Impact score e.g. toxic rate in human

$CF_{x,i}$ are factors that determines substances x's character which is released from i

$m_{x,i}$ is substance x's mass to i (kg)

(In case of USEtox are in human's toxin or ecology's toxin)

For human toxicity, USEtox model will calculate the factors that determine the impact from carcinogen, non-carcinogen or both (They are calculated by finding the average of carcinogen and non-carcinogen or at the end of the point). The factors affected the toxicity in freshwater ecology may affect some species (PAF) at midpoint. Moreover, there are some loss in some species (PDF) at endpoint in freshwater (m^3) and a day (d.) per emitting PAF a kilo (PAF.m^3.d / kg) at midpoint and kilo (PAF.m^3.d / kg) at endpoint. The factor in specific USEtox's character and human's toxin are in average and the number of DALY at endpoint per emitting PAF a kilo (at midpoint) and DALY/ kg at endpoint. Therefore, the specific USEtox's character can be concluded as the comparison between CTU at midpoint and CDU at endpoint are for

emphasis the factor's characteristic's comparison.

Human toxicity

In USEtox's model, substance that have potential to increase the rate of human's illness in case of human's toxin are from 3 factors; fate factors (FF) human exposure factors (XF) and human toxicological effect factors (EF)

$$CF = EF\ XF\ FF$$

The effect from fate factor matrix (FF) and human exposure factors (XF) in matrix:

$$iF = XF\ FF$$

In USEtox, respiratory and ingestion pathways will be considered in iF as the fate factor matrix (FF) with the emitting amout to ecology and mass of substance (or intensity) as in case of ecology's toxin and hunman's toxin. Aprt from the risk factors, the effect factors (EF) in human reflects the change in probability in age due to the change in consuming pollution in life time (case/kilogram) USEtox separates carcinogen, non-carcinogen and also the information in impact of respiratory and digestion pathways to reach acceptable endpoint. The factor of midpoint in human's toxin is multiplied by the factor of violence (DALY / case). This calculation is seperated from non-cancer disease.

Eco toxicity

In USEtox, there are three factor that affect ecology; fate factors (FF), freshwater ecosystem exposure factors (XF), and freshwater aquatic ecosystem toxicity effect factors (EF)

$$CF = EF\ XF\ FF$$

Multimedia fate models is used to forcast fate factors (FF) and freshwater ecosystem exposure factors (XF) for concerned substances. In this form, the study area is shown as the mixed zone. In each zone, they show the specific part in different ecology (e.g. atmosphere, water, soil) substance's fate factors (FF) can be calculated with the

mass's equation to explain in each process, for example, decomposition and transfer between gap. fate factors (FF) means the increase of chemical mass in the environment. (for toxicity of fresh water ecology). Information of the release of substances in the specific room can be interpreted as the result of the discharge that reaches fresh water (no dimension) as present in fresh water. Exposure factors (XF) is the ability to use the substance, for example, the dissolved chemical in fresh water. The most important processes for certain compounds, depending on the physical and chemical properties of the compounds. Also, the environment (temperature, rainfall, etc.) affects the predictions of the form.

Moreover, fate factors (FF) and Freshwater ecosystems exposure factors (XF) need to calculate the factor of characteristics in ecosystem. Ecotoxicological effect factor reflects the change in species' PAF at midpoint level. And, the change in the loss of PDF at the endpoint because the change in intensity of released substances to the freshwater (m^3), PAF. m^3/kg. (midpoint level) and PDF. m^3/kg. (endpoint level). The factor in characteristics of ecological freshwater's toxin has report for emitting greenhouse gas in the house, air in the building in the town, air on land, freshwater, ocean and soil. At the highest level, the best point of factor in freshwater ecosystem's toxin will multiply the factor of violence.

RESULTS AND DISCUSSION

Human Toxicity

Characteristics factor of each substance are multiplied with the amount of release of each substance obtained from the Pollutant Release and Transfer Register database.

Twenty substances having the highest impact on toxicity to human's health are listed in Table 1. It was found that acrylonitrile had the highest impact score (1.5E + 00), followed by paraquat dichloride (1.46E + 00) and chlorpyrifos (1.17E + 00), respectively. In addition, substances that are routinely monitored by the

Pollution Control Department and related agencies in the area, such as vinyl chloride, toluene, styrene, benzene, 1,3-butadiene were also listed in this top-twenty posing high impact on human health, significantly.

Table 1 Impact score of the top 20 substances (human)

Chemical	CAS NO.	Impact score
Acrylonitrile	107-13-1	1.50E+00
Paraquat Dichloride	1910-42-5	1.46E+00
Chlorpyrifos	5598-13-0	1.17E+00
Xylenes	1330-20-7	2.41E-01
Formaldehyde	50-00-00	1.38E-01
Vinyl Chloride	75-01-4	1.35E-01
N-Hexane	110-54-3	1.24E-01
Toluene	108-88-3	8.91E-02
Acrylic Acid	79-10-7	6.76E-02
Naphthalene	91-20-3	6.53E-02
Styrene	100-42-5	5.86E-02
1,2-Dichloroethane	107-06-2	4.97E-02
Propylene Oxide	75-56-9	3.80E-02
Acetaldehyde	75-07-0	3.38E-02
1,4-Dichlorobenzene	106-46-7	3.12E-02
Benzene	71-43-2	3.08E-02
Methyl Methacrylate	80-62-6	2.61E-02
1,3-Butadiene	106-99-0	1.53E-02
Acrylamide	79-06-1	1.30E-02
Methylene Chloride	75-09-2	8.56E-03

Eco - Toxicity

As for an effect of toxicity to the ecosystem, list of top-20 substances having the highest impact score is presented in Table 2. It was found that ametryn had the highest impact score (1.61E+06) which is a very high value, followed by phenol and butachlor at 6.78E+05 and 5.90E+05, respectively. It should be noted that mostly of the top 20 substances are chemicals used in agriculture.

Table 2 Impact score of the top 20 substances (ecology)

Chemical	CAS NO.	Impact score
Ametryn	834-12-8	2.02E+08
Chlorpyrifos	5598-13-0	1.66E+08
Captain	133-06-2	4.03E+07
Paraquat Dichloride	1910-42-5	2.48E+07
Glyphosate-isopropylammonium	38641-94-0	1.38E+07
Propanil	709-98-8	9.48E+06
Bisphenol A	80-5-7	1.61E+06
Phenol	108-95-2	6.78E+05
Butachlor	2318-66-9	5.90E+05
1,4-Dichlorobenzene	106-46-7	3.30E+05
Formaldehyde	50-00-00	8.63E+04
Acrylonitrile	107-13-1	7.92E+04
Methyl Acetate	70-20-9	7.04E+04
Hydroquinone	123-31-9	6.06E+04
Methanol	67-56-1	2.96E+04
Naphthalene	91-20-3	1.80E+04
Acetone	67-64-1	1.77E+04
Xylenes	1330-20-7	1.19E+04
1,2-Dichloroethane	107-06-2	1.18E+04

Chemical	CAS NO.	Impact score
Toluene	108-88-3	1.10E+04

Table 3 The relationship between toxicity and emission release

Chemical	Toxicity CTU/kg	Emission release (kg/y)	Impact score
Acrylonitrile	6.51E-05	23089.5	1.50E+00
Paraquat Dichloride	7.78E-06	187750	1.46E+00
Chlorpyrifos	3.74E-05	31176	1.17E+00
Xylenes	2.17E-07	1109798.318	2.41E-01
Formaldehyde	2.55E-05	5429.2985	1.38E-01
Vinyl Chloride	6.68E-06	20213	1.35E-01
N-Hexane	2.41E-07	514209.1357	1.24E-01
Toluene	9.45E-08	943206.1382	8.91E-02
Acrylic Acid	9.42E-05	718.1	6.76E-02
Naphthalene	3.40E-06	19198.4957	6.53E-02
Styrene	1.21E-06	48400.6282	5.86E-02
1,2-Dichloroethane	5.14E-07	96683.91	4.97E-02
Propylene Oxide	7.25E-06	5237.397	3.80E-02
Acetaldehyde	1.11E-06	30491.8479	3.38E-02
1,4-Dichlorobenzene	3.53E-07	88516.03	3.12E-02
Benzene	5.49E-07	56170.7859	3.08E-02
Methyl Methacrylate	1.86E-06	14010.6002	2.61E-02
1,3-Butadiene	2.81E-06	5458.71	1.53E-02
Acrylamide	1.58E-04	82.394	1.30E-02
Methylene Chloride	9.97E-07	8582.01	8.56E-03

When considering the relationship between the values of characteristic factor (impact sores) that shows the toxicity of the substance together with the amount of emission release (for example, human toxicity). The results revealed that acrylonitrile even with a small amount of release as compared with some substances such as xylenes can have a very high toxicity value. Thus, the impact score calculated was calculated for this substance as shown in Table 3.

CONCLUSIONS

PRTR database system is one of tool used for environmental management involved three major stakeholders (government, private sector and publics). The PRTR database is developed under the policy 'The rights to know in public'. It has three main objectives, including promoting public rights to know, monitoring of environmental policy, and promoting voluntary reductions of emissions and risk. In this study, PRTR data were analyzed using the USEtox model by mean of characterization of human toxicological and ecotoxicological life cycle impacts.

From the analysis, it can be concluded that acrylonitrile had the highest impact score (1.5E + 00) among 107 chemicals reported in the PRTR database. However, it should be noted that the completeness of data used in this analysis is the major factor limited to this analysis. For example, there were only 89 factories among 844 industrial facilities (about 10.54%) which reported their emissions to the PRTR database. About 22.48% of the factories located within the industrial estate reported their emissions in the PRTR (118 among 525 factories). Therefore, for accuracy in the assessment of toxicity a concern should be given to update the data as much as possible. Temporal comparison of amount of emission and release of the pollutant in the same area will be very much useful information to evaluate the voluntary reduction of emission particularly from those industrial sources. Results from this analysis clearly revealed that it is much necessity to consider not only amount of release but also the toxic and

characteristic of substances for prioritization and management of chemicals in each area. Analysis of the potential source contribution of those prioritized substances will be very useful as it can identify the major emission sources which should be given a priority in managing and controlling the amount of emissions and releases in order to support the area-based management of pollution.

ACKNOWLEDGEMENTS

The authors would like to thank all staff of the Department Sanitary Engineering, Faculty of Public Health, Mahidol University for their helpful support encouragement, the Pollution Control Department and the Meteorological Department in providing emission data and meteorological used in this study. The National Research Council of Thailand (NRCT) under the graduated research scholarship supports this research in 2019.

REFERENCES

Bungsri A. (2011). Performance Evaluation of AERMOD Air Quality Dispersion Model with Map Ta Phut Industrail Estate Area, Rayong, Field Datasets.

Department, P. c. (2010). Pollutant Release and Transfer Registration.

Elorri Igos R. M., Benetto E., Biwer A., Guiton M., Dieumegard P. (2014). Development of USEtox characterisation factors for dishwasher detergents using data made available under REACH. Chemosphere, 160 - 166.

Vázquez-Rowe I., Lucía Cáceres A., Larrea-Gallegos G., QuispeI., Kahhat R. (2017). Assessing the magnitude of potential environmental impacts related to water and toxicity in the Peruvian hyper-arid coast: A case study for the cultivation of grapes for pisco production. Science of The Total Environment, 532 - 542.

Caneghem J., Vandecasteele C.. (2010). Assessment of the impact on human health of industrial emissions to air: Does the result depend on the applied method Journal of Hazardous Materials, 788 - 797.

JICA-PRTR Team , Department of Industrial Works, Industrial Estate Authority of Thailand. (2015). Pollutant Release and Transfer Register data (2013) Rayong province. 4 - 7.

Rasanen K., Porvari P., Kurppa S., Tiilikkala K. (2015). Estimating the development of ecotoxicological pressure on water systems from pesticides in Finland 2000e2011. Journal of Cleaner Production, 65 - 77.

Sörme L., Finnveden G. (2016). Using E-PRTR data on point source emissions to air and water-First steps towards a national chemical footprint. Environmental Impact Assessment Review, 102 - 112.

Nordborg M., Cederberg C. , Woodhouse A. (2017). Freshwater ecotoxicity impacts from pesticide use in animal and vegetable foods produced in Sweden. Science of The Total Environment, 448 - 459.

OECD. (1997). Pollutant release and transfer registers (PRTRs): A Tool for Environmental Management and Sustainable Development. (PRTR Workshop for the America's San Juan del Rio, Mexico).

Alberto Moraisa S., Gabarrell X. (2013). Accounting for the dissociating properties of organic chemicals in LCIA: An uncertainty analysis applied to micropollutants in the assessmentof freshwater ecotoxicity. Journal of Hazardous Materials, 461 - 468.

Sukkasem P. (2015). Industrial air quality management using air quality models with clean technology approach.

USEtox Team (2017). USEtox® 2.0 Documentation.

Thepanondh S. (2013). PRTR: A Tool for Managing and Controlling the Pollution Problem. Journal of Environmental Management, Volume 9 73 - 83.

Ambient $PM_{2.5}$ and its ion composition in Chiang Mai Provinces during open burning season 2018

Patcharee Saejiw[1, 2], Wan Wiriya[2, 3], Somporn Chantara[2, 3*]

[1]Master's Degree Program in Environmental Science, Environmental Science Research Center, Faculty of Science, Chiang Mai University, 50200, Thailand
[2] Environmental Chemistry Research Laboratory, Department of Chemistry, Faculty of Science, Chiang Mai University, Chiang Mai, 50200, Thailand
[3] Environmental Science Research Center, Faculty of Science, Chiang Mai University, Chiang Mai, 50200, Thailand;
Coresponding author: e-mail: somporn.chantara@cmu.ac.th.

ABSTRACT

Chiang Mai Province experiences an annual air pollution during dry season due to intensive open burning in Southeast Asian region. This study aims to analyse ion composition of ambient particulate matters with aerodynamic diameter less than or equal to 2.5 µm ($PM_{2.5}$) during open burning season (13 February – 30 April 2018) for source identification. Daily $PM_{2.5}$ samples (24-hour sampling) were collected by using a mini-volume air sampler with a flow rate of 5 L min^{-1}. A sampling station is located in sub-urban area of Chiang Mai surrounded by agricultural field. $PM_{2.5}$ samples (n=71) were extracted in deionized water and analysed for their ion composition by ion chromatography. An average 24-hour $PM_{2.5}$ concentration was 45.5 ± 25.7 µg m^{-3} (min – max = 7.0 – 185 µg m^{-3}). About 31 % (22 days) of the sampling showed that the 24-hour average $PM_{2.5}$ concentration was higher than National Ambient Air Quality Standards (NAAQSs) in Thailand (50 µg m^{-3}). Dominant ion species of $PM_{2.5}$ were sulphate (6.75 ± 3.05 µg m^{-3}), ammonium (2.06 ± 1.10 µg m^{-3}) and nitrate (2.04 ± 0.67 µg m^{-3}). Potassium ion, which is generally used as biomass burning tracer, was also found (0.91 ± 0.42 µg m^{-}

^{3}). $PM_{2.5}$ mass concentration was well correlated with nitrate and potassium (r~ 0.7) indicating that they were mainly generated from biomass burning. Sulphate and ammonium were also well correlated (r~0.7) showing influence of photochemical reactions. Principal Component Analysis (PCA) of ions and their correlations revealed various forms of major compounds (i.e. $(NH_4)_2SO_4$ and KNO_3) and various sources of $PM_{2.5}$ in this area including biomass burning, traffic emission, agricultural activity and soil dust.

Keywords: Air pollution, Biomass Burning, $PM_{2.5}$, Ion content, Source identification

INTRODUCTION

Chiang Mai Province and other provinces in upper northern Thailand, have been annually facing air pollution during almost every dry season (February–April). Air pollution has been recorded as a serious problem for well over 10 years. Most of cities in upper northern Thailand are located in a flat plain basin and are surrounded by mountain ranges. This geographical feature of mountains valley limits the dispersion of air pollution. Moreover, it also depends on both meteorological conditions (i.e. temperature inversion, wind velocity and precipitation) and emission source intensity (Chantara et al., 2012). Which is produced large amount of $PM_{2.5}$ emissions (Wiriya et al., 2016). Emissions of $PM_{2.5}$ are increasing rapidly in Southeast Asia (SEA) (Shi et al., 2018). Sillapapiromsuk et al. (2013) reported that burned areas detected from agricultural land and forest in Chiang Mai, Thailand in 2010 (3,510 km^2) was much higher than in 2011 (866 km^2) due to low burning activity due to unusually high precipitation in 2011. PM_{10} emission rates were 2,794 and 560 tons in 2010 and 2011, respectively. Moreover, a wide range of biomass burning activities over the region, particularly in the dry season deteriorates the air quality of the city and coincides with the peak of the annual haze episode. This region is also tempered by a low latitude and moderate elevation, which

makes the atmospheric boundary layer (ABL) more complex (Wang et al., 2015). Therefore, to estimate the contribution of different sources to a given ambient particulate sample, a characteristic compound in each of the potential source materials is considered. Chemical analysis of $PM_{2.5}$ and $PM_{2.5-10}$ during forest fires showed that potassium (K^+) and ammonium (NH_4^+) are the dominant cations and sulphate (SO_4^{2-}) is the most important anion (Pio et al., 2008). Similar study on PM_{10}-bound ions was also conducted in Chiang Mai with SO_4^{2-}, NH_4^+, NO_3^- and K^+ as the top four ions of ambient PM_{10} (Chantara et al., 2009). The purpose of this study is to collect $PM_{2.5}$ during open burning season for analysis of ion composition in order to identify and confirm sources of the $PM_{2.5}$ in Chiang Mai.

METHODOLOGY

$PM_{2.5}$ sampling

The sampling was carried out during dry season for about two and half months (13 February – 30 April 2018) at Mae Hia Air Quality Monitoring Station (AQM), which is located at the north eastern part of Chiang Mai city (18°45'39.84"N 98°55'54.33"E) and has on altitude about 310 m above mean sea level (Figure 1a). Chiang Mai is the largest metropolitan area in northern Thailand. It is the second largest city in Thailand with a population of 1.73 million in a total area of 20,107 km^2. $PM_{2.5}$ samples were collected daily (24-hour) using a mini volume air sampler (Air metric, USA) at a flow rate of 5 L min^{-1} (Figure 1b). The samples were collected on quartz fiber filters (Whatman's, China, Ø 47 mm). Total sample number is 71.

Prior to sampling, all filters were stored in a desiccator for 24 hours to remove moisture and were then pre-weighed 3 times using a microbalance (microgram unit) (Mettler Toledo, Switzerland) in a control room under controlled temperature (25 ± 2 ˚C) and relative humidity (41 ± 5%). After sample collection, the filters were stored individually in plastic boxe wrapped with aluminum foil to avoid photodegradation until transfer to a desiccator for 24-hour, after which they

were re-weighed. The filter boxes were stored in sealed plastic bags and kept refrigerated until analysis (Duangduean et al., 2019).

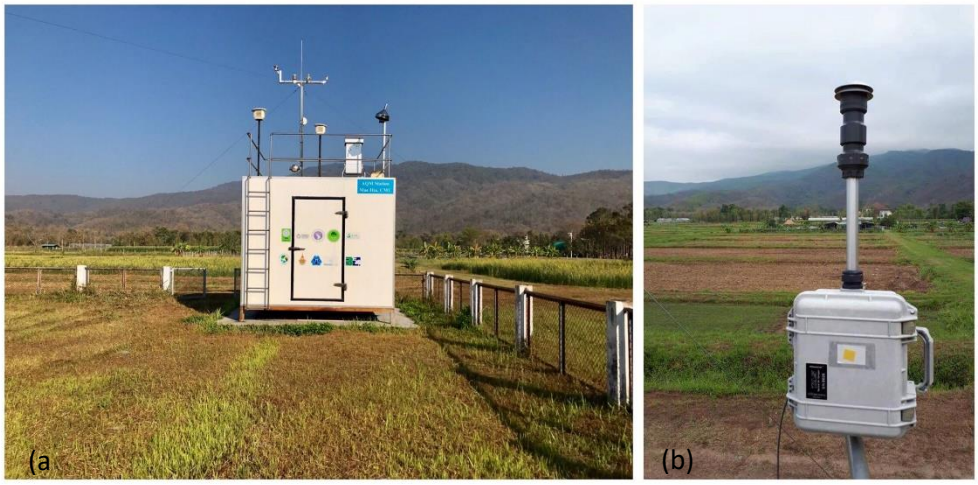

Figure 1 Sampling site (a) Mae Hia AQM station and (b) mini volume air sampler.

Sampling extraction and analysis

After the sampling, a sampling filter was cut into halves by a stainless-steel paper cutter. Half of the filter was placed into a 50 mL centrifuge tube and added by 15 mL deionized water. The tube was covered by a cap and extracted by using an ultrasonicator (Elma, Germany) at 35˚C for 30 minutes. The extraction solution was filtered by cellulose acetate membrane (pore size 0.45 µm, diameter 13 mm) and analyzed for cations (Na^+, NH_4^+, K^+, Ca^{2+} and Mg^{2+}) and anions (Cl^-, NO_3^- and SO_4^{2-}) by Ion Chromatograph (882 Compact IC plus, Metrohm, Switzerland). The analytical columns for anion and cation were Metrosep A Supp5 250/4.0 mm and Metrosep C4-100/4.0 mm, respectively. The eluent for anion analysis was 3.2 mM Na_2CO_3/1.0 mM $NaHCO_3$ buffer at the flow rate of 0.7 mL min^{-1}, while the regenerant for the suppressor consisted of 100 mM H_2SO_4. The cation analysis was a non-suppressed system. The mobile phase was a mixture of 1.7 mM HNO_3/0.7 mM dipicolinic acid buffer and the flow rate was recorded at 0.9 mL min^{-1}. Five blank samples of $PM_{2.5}$ were

also extracted and analyzed for ion content by IC using the same method as samples (Sillapapiromsuk et al., 2013). Concentration of total cations is a sum of five cation species, while that of total anions is a sum of three anion species. Total ions concentration is a sum between concentrations of total cations and total anions.

Quality control of ion analysis

The instrument detection limit (IDL) of Ion Chromatograph (IC) for individual ion was obtained by multiplying the standard deviation (SD) of the seven sample injections by three of the lowest ion concentrations used for the construction of the calibration curve (Taylor, 1987). The IDLs of Cl^-, NO_3^- and SO_4^{2-} were 0.30, 0.53 and 0.99 mg L^{-1}, respectively, while those of Na^+, NH_4^+, K^+, Ca^{2+} and Mg^{2+} were 0.17, 0.20, 0.10, 0.15 and 0.05 mg L^{-1}, respectively. Accuracy of the method was tested by triplicated injection of artificial rain samples (reference materials), with known ion concentrations. Percentages of difference of almost all ions were very good (3.24 – 30.61%) with the exception of K^+ (30.61%).

Data Analysis

A log-transform (log (x+1)) approach was employed for data transformation to obtain a normal distribution. Pearson's correlation was used to determine relationships between ions species and $PM_{2.5}$ concentrations. Principal component analysis (PCA) was used to identify possible sources of pollutants detected (Khamkaew et al., 2016).

RESULTS AND DISCUSSION

Trend of $PM_{2.5}$

Figure 2 shows daily variation of $PM_{2.5}$ concentration (µg m^{-3}) collected from Mae Hia AQM station together with data from Pollution Control Department (PCD) station at Chiang Mai Government Center (station code: 35t), which is located about 10 km south of the sampling site. They were plotted with amount of rain (mm) data obtained from the meteorological station in Chiang Mai province and fire hotspot data from

nine provinces detected by NASA's MODIS (National Aeronautics and Space of Administration Moderate Resolution Imaging Spectroradiometer). An average $PM_{2.5}$ concentration (n = 71) was 45.5 ± 25.7 μg m^{-3}. It was found that 31% (22 samples) of the samples has higher concentration of $PM_{2.5}$ than the National Ambient Air Quality Standards (NAAQSs) in Thailand (50 μg m^{-3}). The highest $PM_{2.5}$ concentration (24-hour average) at Mae Hia AQM station was found on 15 April 2018 (185 μg m^{-3}), which is noticeably higher than that of the PCD station on the same day (90.4 μg m^{-3}). This might be caused by local activity such as open burning at or nearby the sampling site. The lowest concentration was observed on 28 April 2018 (7 μg m^{-3}) due to large amount of rain (15.4 mm) on the day before (figure 2a). $PM_{2.5}$ concentration decreased with the increase of rain amount. In addition, the single command for zero-burning policy (no open burning for about 60 days during February to April) was implemented by the government in nine provinces of Northern Thailand. In some provinces (Tak and Lampang), it ended on 10 April, resulting in an upsurge in open burning activities (figure 2b). It was found that $PM_{2.5}$ concentration abruptly increased during this period. The pattern was spotted again after 21 April when burning ban in Chiang Mai ended.

$PM_{2.5}$ and its ion composition

Table 1 shows concentration of $PM_{2.5}$ and its ion composition. The average concentration of total anions and cations were 9.17 ± 3.56 μg m^{-3} and 4.08 ± 1.62 μg m^{-3}, respectively. Mean total ions concentration was 13.25 ± 4.92 μg m^{-3}, accounted for about 27% of $PM_{2.5}$ mass concentration. Ion concentrations in descending order were SO_4^{2-}, NH_4^+, NO_3^-, K^+ and Na^+. Ions such as SO_4^{2-}, NH_4^+ and NO_3^- are secondary inorganic aerosol (SIA). They are products of precursor gases (NO_x, SO_2 and NH_3), which are generated from various anthropogenic sources (Yao et al., 2016; Kalabokas et al., 1999). K^+ is extensively emitted during biomass burning

(Sillapapiromsuk et al., 2013), while Na^+ is from crustal origin which may come from soil dust or soil combustion during biomass burning (Jimenez et al., 2006).

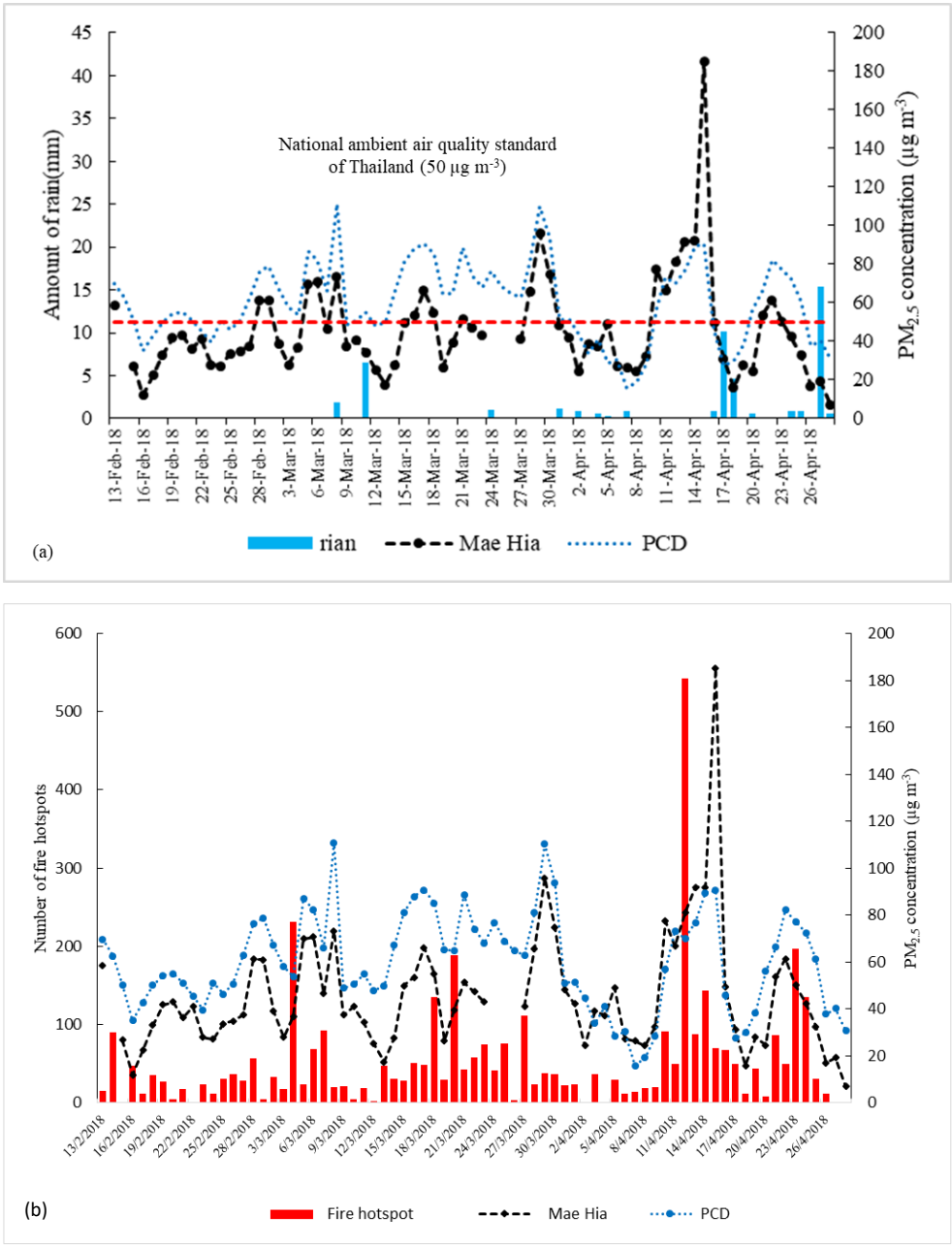

Figure 2 Daily variation of $PM_{2.5}$ concentrations collected from Mae Hia AQM station comparing with measuring data from PCD station (Chiang Mai

Government Center, 35t) plotting with (a) rain amount and (b) number of fire hotspots of nine provinces

Table 1. Concentration of $PM_{2.5}$ and its ion composition from Mae Hia AQM station, Chiang Mai Province.

Parameter	Concentrations (μg m^{-3})			
	Mean	SD	Min	Max
$PM_{2.5}$	45.48	25.70	6.97	185.30
Cl^-	0.38	0.45	ND	2.41
NO_3^-	2.04	0.67	0.48	4.72
SO_4^{2-}	6.75	3.05	1.48	16.19
Total Anions	9.17	3.56	1.96	19.92
Na^+	0.76	0.51	ND	2.45
NH_4^+	2.06	1.10	0.18	5.64
K^+	0.91	0.42	0.04	2.12
Ca^{2+}	0.35	0.24	ND	1.16
Mg^{2+}	0.01	0.01	ND	0.04
Total Cations	4.08	1.62	1.05	8.97
Total ions	13.25	4.92	3.01	27.64

ND: Not Detected (IDL values of ions are provided in Quality Control Topic).

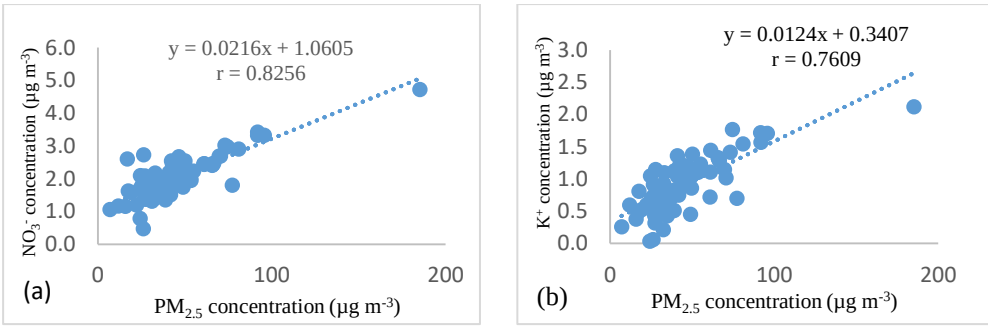

Figure 3 Correlations between $PM_{2.5}$ and NO_3^- (a) and $PM_{2.5}$ and K^+ (b).

The major anion constituents in Cl^-, while cations were NH_4^+ > K^+ descending order were SO_4^{2-} > NO_3^- > >Na^+. The pattern was similar with the

previous study conducted in Chiang Mai (Chantara et al., 2009). The correlations between concentrations of $PM_{2.5}$ and NO_3^-, K^+, NH_4^+ and SO_4^{2-} were relatively strong ($r > 0.7$), particularly $PM_{2.5}$ & NO_3^- and $PM_{2.5}$ & K^+ (Figure 3). NO_3^- is a secondary pollutant generated from NO_x from combustion process and K^+ is often used as a tracer for biomass burning (Chantara et al., 2012).

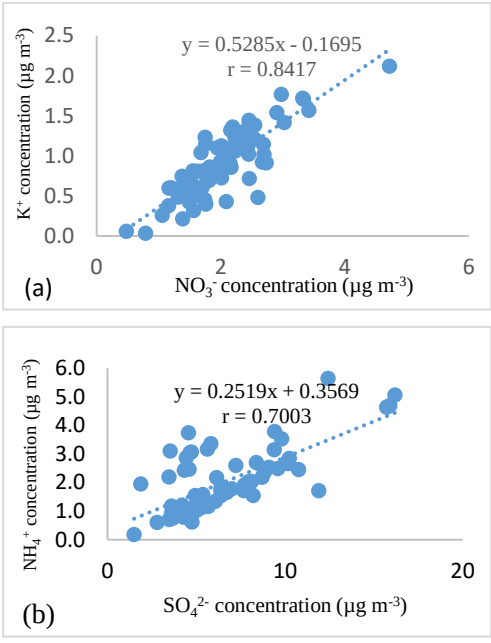

Figure 4 Correlations between concentrations of K^+ & NO_3^- (a) and NH_4^+ & SO_4^{2-} (b).

Correlations between ions revealed various forms of major compounds (Figure 4). K^+ and NO_3^- were strongly correlated ($r = 0.84$) indicating the present of KNO_3 in the atmosphere, which most likely came from biomass burning (Li et al., 2003). Strong correlation was also found between SO_4^{2-} and NH_4^+ ($r = 0.70$), which is similar to the results of Thepnuan et al. (2019). Both ions are secondary inorganic aerosol and were found relative abundant in the atmospheric particle in the form of $(NH_4)_2SO_4$ (Yao et al., 2016).

Possible sources of $PM_{2.5}$ in Chiang Mai

The principal component analysis (PCA) was performed resulting in three components with 72.7% cumulative variance (Table2). Component 1 (38% of total variance), was associated with ions from SIA (SO_4^{2-}, NO_3^-, NH_4^+) and also with K^+ from biomass burning indicating mixed sources. However, due to low variance in component 1, biomass burning contribution to air pollution might be low in 2018. Using K^+ as biomass burning tracer, when there is low contribution from biomass burning, might be ambiguous (Zhang et al. 2010), thus explaining why K^+

was in the same component as SIA. SO_4^{2-} is a source associated with the formation of secondary SO_4^{2-} from combustion sources (Tao et al., 2013; Huang et al., 2014). K^+, NO_3^- and NH_4^+ are generated from agricultural activity (Sillapapiromsuk et al., 2013). Na^+ and Ca^{2+} most likely came from marine source and soil characteristics and Cl^- represented the contribution of the sea salt (Chantara et al., 2012). Component 2, explaining 18% of total variance, was identified as sea salts with high contribution of Na^{2+} and Cl^-. Component 3, explaining 17% of total variance, had high contribution of Ca^{2+} and Mg^{2+} indicated crustal origin most likely from soil dust and road dust particle.

Table 2. Principal components analysis of ion concentrations.

Ions	Component		
	1	2	3
Cl^-	0.283	**0.666**	-0.385
NO_3^-	**0.891**	-0.005	0.117
SO_4^{2-}	**0.818**	0.085	0.016
Na^+	0.083	**0.911**	0.075
NH_4^+	**0.804**	0.284	-0.178
K^+	**0.907**	0.151	0.039
Ca^{2+}	0.031	0.111	**0.840**
Mg^{2+}	0.025	-0.213	**0.670**
% of Variance	37.75	18.02	16.95
% Cumulative	37.75	55.76	72.71

Bold numbers represent significant correlation (r>0.5).

CONCLUSIONS

$PM_{2.5}$ and their ion composition in Chiang Mai atmosphere during open burning season 2018 were analyzed. An average concentration of 24-hour $PM_{2.5}$ was 45.5 ± 25.7 μg m^{-3}. Dominant ions were SO_4^{2-}, NH_4^+ and NO_3^- . The main source of SO_4^{2-} emission is the combustion process including traffic emission, while NH_4^+ and NO_3^- are from the agricultural activity and combustion, respectively. K^+ and NO_3^- were strongly correlated with $PM_{2.5}$. K^+ and NO_3^- as well as NH_4^+ and SO_4^{2-} were also well correlated indicating the present of KNO_3 and $(NH_4)_2SO_4$ in the atmosphere. PCA analysis indicated mixed sources for ambient $PM_{2.5}$ with ion contribution from SO_4^{2-}, NH_4^+, NO_3^- and K^+.

ACKNOWLEDGEMENTS

Financial supports from Haze Free Thailand Project supported by National Research Council of Thailand (NRCT) and the Graduate School of Chiang Mai University are gratefully acknowledged.

REFERENCES

Chantara, S., Wangkarn, S., Tengjaroenkul, U., Sangchan,W. and Rayanakorn, M. Chemical analysis of airborne particulates for air pollutants in Chiang Mai and Lamphun Provinces, Thailand. Chiang Mai Journal of Science 2009, 36: 123–135.

Chantara, S., Sillapapiromsuk, S. and Wiriya, W. Atmospheric pollutants in Chiang Mai (Thailand) over a five-year period (2005–2009), their possible sources and relation to air mass movement. Atmospheric Environment 2012, 60: 88–98.

Huang, X.H.H., Bian, Q., Ng, W.M., Louie, P.K.K. and Yu, J.Z. Characterization of PM2.5 major components and source investigation in suburban Hong Kong: A one year monitoring study. Aerosol Air Quality Research 2014, 14: 237–250.

Jimenez, J., Wu, C.F., Claiborn, C., Gould, T., Simpson, C.D.,Larson, T. and Liu, L.J.S. Agricultural burning smoke in eastern Washington-part I: atmospheric characterization. Atmospheric Environment 2006, 40: 639–650.

Kalabokas, P.D., Viras, L.G., Repapis, C.C. Analysis of the 11-year record (1987–1997) of air pollutionmeasurements in Athens, Greece. Part I: primary air pollutions.GlobalNEST International Journal 1999, 1: 157–167.

Khamkaew, C., Chantara, S., Janta, R., Pani, S.K., Prapamontol, T., Kawichai, S., Wiriya, W. and Lin, N.H. Investigation of biomass burning chemical components over northern Southeast Asia during 7-SEAS/BASELInE 2014 campaign. Aerosol Air Quality Research 2016, 16: 2655–2670.

Kim Oanh, N.T. and Leelasakultum, K. Analysis of meteorology and emission in haze episode prevalence over mountain-bounded region for early warning. Science of the Total Environment 2011, 409: 2261–2271.

Li,J. Posfai,M. Hobbs,P.V. and Buseck,P. Individual aerosol particles from biomass burning in southern Africa: 2, Compositions and aging of inprganic particles. Journal of Geophysical Research: Atmospheres 2003, 108(D13): 8484.

Pio, C.A., Legrand, M., Alves, C.A., Oliveira, T., Afonso, J., Caseiro, A., Puxbaum, H., SanchezOchoa, A., Gelencsér, A. Chemical composition of atmospheric aerosols during the 2003 summer intense forest fire period. Atmospheric Environment 2008, 42: 7530–7543.

Shi, Y., Matsunaga, T., Yamaguchi, Y., Li, Z., Gu, X. and Chen, X. Long-term trends and spatial patterns of satellite-retrieved $PM_{2.5}$ concentrations in South and Southeast Asia from 1999 to 2014. Science of the Total Environment 2018; 615: 177–186.

Sillapapiromsuk, S., Chantara, S., Tengjaroenkul, U., Prasitwattanaseree, S.and Prapamontol, T. Determination of PM_{10} and its ion composition emitted from biomass burning in the chamber for estimation of open burning emissions. Chemosphere 2013; 93: 1912–1919.

Tao, J., Zhang, L., Engling, G., Zhang, R., Yang, Y., Cao,J., Zhu, C., Wang, Q. and Luo, L. Chemical composition of $PM_{2.5}$ in an urban environment in Chengdu, China: Importance of springtime dust storms and biomass burning. Atmospheric Environment.2013; 122: 270–283.

Taylor, J.K. Quality Assurance of Chemical Measurements. Lewis Publishers,Chelsea, MI. 1987.

Thepnuan,D., Chantara, S.Lee,C.T.,Lin,N.H. and Tsai,Y.I. Molecular markers for biomass burning associated with the characterization of $PM_{2.5}$ and component sources during dry season haze episodes in Upper South East Asia. Aerosol Air Quality Research 2019; 658: 708–722.

Wang, S.H., Welton, E.J., Holben, B.N., Tsay, S.C., Lin,N.H., Giles, D., Stewart, S.A., Janjai, S., Nguyen, X.A.,Hsiao, T.C., Chen, W.N., Lin, T.H., Buntoung, S.,Chantara, S. and Wiriya, W. Vertical distribution and columnar optical properties of springtime biomass burning aerosols over Northern Indochina during 2014 7-SEAS Campaign. Aerosol Air Quality Research.2015; 15: 2037–2050.

Wiriya, W., Chantara, S., Sillapapiromsuk, S. and Lin, N.H., 2016. Emission profiles of PM_{10}- bound polycyclic aromatic hydrocarbons from biomass burning determined in chamber for assessment of air pollutants from open burning. Aerosol Air Quality Research.2016; 16: 2716–2727.

Yao, L., Yang, L., Yuan, Q., Yan, C., Dong, C., Meng, C., Sui, X., Yang, F., Lu, Y. and Wang,W., 2016.Sources apportionment of $PM_{2.5}$ in a background site in the North China Plain. Aerosol Air Quality Research, 541: 590–598.

Zhang, X., Hecobian, A., Zheng, M., Frank, N.H. and Weber, R.J. Biomass burning impact on $PM_{2.5}$ over the southeastern US during 2007: integrating chemically speciated FRM filter measurements, MODIS fire counts and PMF analysis. Atmospheric Chemistry and Physics. 2010, 10: 6839-6853.

Levels of Saxitoxins Toxicity in Relation to Body Size of Green Mussel *(Perna viridis)*

Phatchada Nochit[1*] and Wutthikrai Kulsawat[1]

[1] *Thailand Institute of Nuclear Technology (Public Organization),
Head Office 9/9 Moo7 Ongkharak, Nakhon-Nayok
Corresponding author: e-mail: phatchada@tint.or.th

ABSTRACT

Paralytic Shellfish Poisoning (PSP) is a public health concern worldwide caused by the consumption of bivalves contaminated with Saxitoxins (STXs). In this study, levels of STXs in 270 mussels *(Perna viridis)* collected from upper and central Gulf of Thailand during 2014-2016 were determined using Receptor Binding Assay of tritiated saxitoxin [^{3}H-STX]. Parameters including total tissues wet weight and dry weight, maximum length, and the physiological performance of mussels using Condition Index were carried out. A two-way ANOVA was performed and statistical differences was accepted at $p<0.05$. Analysis of STXs toxicity in mussel (per individual) revealed the lower levels in smaller sized mussels (2.0-2.5 cm) and the higher in the larger sized group (6.5-7.0 cm). However, the levels of STX toxicity in μg STXeq. 100 g^{-1} flesh differed insignificantly according to size group. No apparent relationship was observed between the length of Green mussel *(Perna viridis)* and the detection of STXs in this study *($p>0.05$).* As the US regulatory limit is 80 μg STXeq. 100 g^{-1} of shellfish. Toxin levels found were 2.34 – 6.15 μg STXeq. 100 g^{-1} in flesh, indicating that mussels in the study areas were safe for consumption.

Keywords: Paralytic Shellfish Poisoning, Gulf of Thailand, Receptor binding assay

INTRODUCTION

Harmful algal blooms (HABs) are proliferations of certain algal species that have expanded greatly in recent decades and pose a severe threat to humans, wildlife, and ecosystems through the production of toxins or by causing physico–chemical stress. Marine biotoxins are affect human illnesses mainly through foodborne intoxications, i.e. consumption of contaminated seafood directly or through food chain and occasionally through direct exposure to seawater aerosols (James et al. 2010; Berdalet et al. 2016). In fact, zooplankton, filter-feeding shellfish, and herbivorous fishes can ingest these algae and act as vectors to humans either directly or through further food web transfer to higher trophic levels (Cho et al. 2016; Manfrin et al. 2012). Widespread syndrome caused by contaminated bivalve molluscs is the Paralytic Shellfish Poisoning (PSP). Saxitoxin and its analogues (STXs) are main causative substances of PSP Although seasonal micro-algal blooms are considered as a natural phenomenon, their frequency of which globally indicated as Paralytic Shellfish Toxins (PSTs). STXs naturally produced by marine phytoplankton species of the dinoflagellate genera, *Alexandrium*. PSP accumulates in bivalves which feed on toxic microalgae. Those vulnerable filter feeding bivalves are mussels, oysters, scallops and clams. Initial symptoms include tingling or numbness of the tongue and lips that spreads to the face, neck, arms, fingers, legs and toes. Headache, nausea, vomiting, diarrhea, hypersalivation, fever, and diaphoresis may also occur. Subsequent symptoms are a feeling of dizziness or “floating,” owing to distortion of sensation and proprioception, paraesthesia arm and leg, and ataxia. Rapid development of paralysis and respiratory failure may occur within 24 hours in severe cases. In fact, almost 2,000 PSP cases are reported per year in human, with occasional fatal consequences. (Cao et al. 2018; Grattan et al. 2016; Michalski. 2007). occurrences appears to have increased in the recent years. The expansion in marine biotoxins

contamination and increased in intoxication frequencies of marine organisms have been found continuously all over the world, and are considered to be related with changes in marine environments caused by eutrophication and human disturbance and their resulted frequent incident of HABs (Cao et al. 2018). Unfortunately, algal toxins are not detectable by sight or smell and contaminated seafood appears normal and they are heat resistible and thereby unaffected by cooking. The feasible prevention methods for PSP are to avoid the consumption of

The present study aims to evaluate the Saxitoxins levels in relation to body size of green mussel *(Perna viridis)* collected in the upper and central Gulf of Thailand (GOT) during 2014-2016. The Receptor Binding Assay (RBA) technique using microplate format; an AOAC method for PSP (AOAC, 2012) was applied in this study.

METHODOLOGY

Study area

The Gulf of Thailand is located in the western region of the South China Sea (Fig. 1). (Department of Marine and Coastal Resources 2015) It is a shallow inlet and considered to be a marginal water body of the Pacific Ocean. The Gulf of Thailand is bordered by Vietnam, Cambodia, and Thailand. . It occupies a seabed area of 304,000 km^2 from 6° N to 13°30' N latitude and 99°E to 104° E longitude. Its maximum depth is 279 feet and its average depth is 190 feet. The northern tip of the gulf is the Bay of Bangkok at the mouth of the Chao Phraya River. The southern boundary of the gulf is defined by a line from Cape Bai Bung in southern Vietnam (just south of the mouth of the Mekong River) to the city of Kota Bharu on the Malaysian coast. The Gulf is a two layered shallow water estuary. The upper layer has low salinity due to rain and freshwater runoff from rivers. The deeper layer has high salinity due to cool water flowing into the Gulf from the South China Sea (Department of Marine and Coastal Resources 2015; Wattayakorn G. 2006).

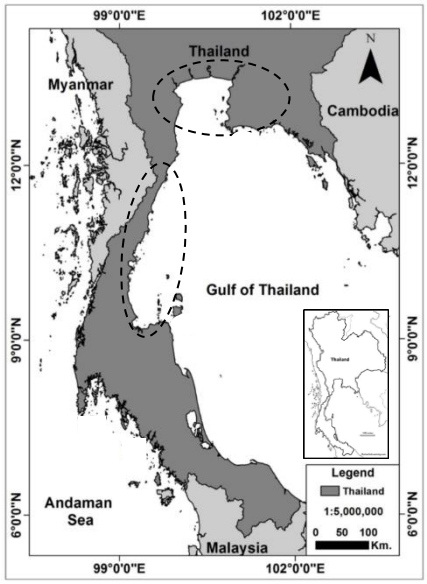

Figure 1 Sampling locations in the upper and central Gulf of Thailand

The sampling locations included Samut Songkram (Don Hoi Lord), Chachoengsao (Bang Pakong), Chonburi (Bang Saen and Ang Sila), Phetchaburi (Bang Taboon), Prachub Kirikhan (Pachub Kirikhan Bay), Chumbhorn (Tung Ka Sawee Bay) and Suratthani (Pak Nam Kadae Bay and Phum Reang Bay).

Sample collection and preparation

Green mussels (*Perna viridis*) were collected from the rock surface at random during low-tide in the upper and central GOT. Green mussel of totally 170 samples were collected from the upper gulf and another 100 samples from the central gulf during 2014-2016. For the purpose of the study on body size variation of STX contents, mussels were selected according to size and separated into size groups: 2.0-2.5 cm, 3.5-4.0 cm, 5.0-5.5 cm and 6.5-7.0 cm. Number of mussel in each group was counted and recorded. The soft tissues were separated from the valves, pooled, homogenized, and aliquots used for subsequent STX analysis.

The allometric effect was studied based on mussel Condition Index (CI) which was determined according to Crosby and Gale (1990).

Tissue extraction method

Weigh 5.0 g tissue homogenate into a tared 15 mL conical tube. Add 5.0 mL of 0.1 M HCl, vortex, and check pH. If necessary, adjust pH to 3.0–4.0 as determined by a pH meter or pH paper. To lower pH, add 1 M HCl dropwise with mixing; to raise pH, add 0.1 M NaOH dropwise with well mixing to prevent local alkalization and consequent destruction of toxin. Place the tube in a water bath for 5 min with the caps loosened. Remove and cool to room temperature. Check pH and adjust cooled mixture to pH 3.0–4.0 as described above. Transfer entire contents to graduated centrifuge tube and dilute volumetrically to 10 mL. Gently stir contents to homogeneity and centrifuge at 3000 × g for 10 min. Retain clarified supernatant and transfer to a clean vial. Store extracts at –40°C until tested in receptor binding assay.

Receptor Binding Assay

A receptor binding assay was performed following the AOAC Official Method of Analysis (AOAC, 2012). Briefly, a known amount of radio-labelled saxitoxin ([^{3}H] STX) competes with unlabeled molecules for the sodium channel sites in a porcine-crude membrane. When the binding equilibrium is reached, free [3H] STX is removed by filtration and the collected receptor-bound [3H] STX is quantified by liquid scintillation counting. The reduction in [3H] STX binding is directly proportional to the amount of unlabeled toxin present.

For toxin quantification: Three separated dilutions of the unknown sample were prepared in distilled water. The assay was performed as the above while preparing the Standard Curve. The quantity of STX equivalent was obtained by solving the regression equation for X from the standard plot.

Statistical Analysis

GraphPad Prism V.8 (GraphPad Software, Inc., La Jolla, California, USA) was used to generate curves and to perform data analysis. Two-way ANOVA was used to test for

difference among size groups and seasonal variations. The normality and homogeneity of the data were tested using Kolmogorov-Smirnov and Levene tests, respectively. Statistical significance was designed as being at the level of $p < 0.05$ (Quinn GP and Keough MJ 2002; Zar JH 1999).

Condition Index

Each sample group was separated by individual shell length, whole body, soft tissue, and shell were weighed and plot was made of soft tissue weight and shell length. It was found that individual soft tissues weight increased as a power function of the shell length variable (Fig. 2).

RESULTS AND DISCUSSION

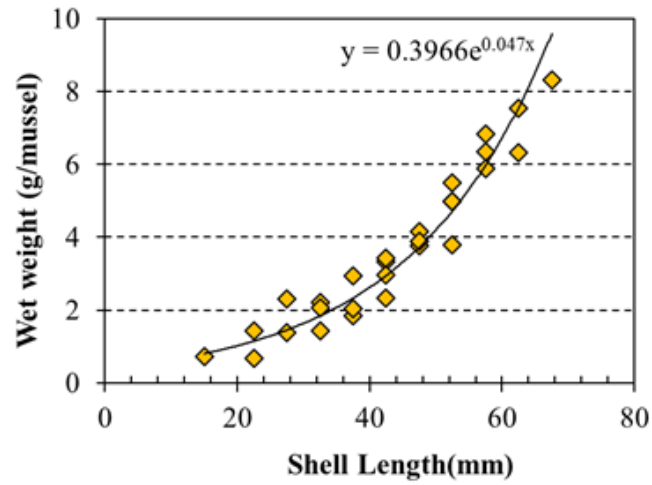

Figure 2. Mussel growth as a function of the shell length

The regression equation of

$$Wet\ weight = 0.397e^{0.047 shell\ length}$$

describes an allometric effect absolutely based on size. The curve of weight changes as a function of mussel maximum shell length increments may be designated by annual growth cycle (Calvaho et al., 2010).

Saxitoxins Analysis

Detection limits of the assay was 2.18 μg STXeq. 100 g^{-1} tissue. The variations of STXs levels among size

groups of mussel samples were observed in the upper and central GOT. It revealed the same pattern in both sampling sites that higher values of body burden STXs (μg STXeq/mussel) were found in the bigger body size or longer shell length. This means that the STXs body burden slightly increased with increasing age. However, STXs body burden did not change significantly over the seasons of the year *($p > 0.05$).*

The STXs toxicity levels of each body sizes were compared by two-way ANOVA ($p<0.05$). The relationship of STXs levels in the bivalves expressed as μg STXeq. 100 g^{-1} tissue and body size was not found neither in the upper GOT nor in the central gulf *($p>0.05$).* STXs by the different body sizes of this green mussel species *(Perna viridis)* were insignificantly higher at a longer body sizes or shell length *($p>0.05$).* No apparent relationship was observed between the length of Green mussel *(Perna viridis)* and the detection of STXs in this study. The positive STXs found in this investigation existed more often in the upper than in the central gulf although mussels were collected during the same period. As growth of phytoplankton was enhanced under physico-chemical conditions i.e., seawater temperature, salinity, dissolved inorganic nitrogen, and dissolved inorganic phosphorus. The effect of these conditions was significantly to the phytoplankton bloom in the upper gulf than in the central and lower gulf. These variations between the upper and lower were due to the influence of freshwater discharge from the Bang Pakong River to the upper GOT (Somsap, N. et al. 2015).

STXs toxicity in 270 green mussel samples were in the range of $\leq$ 2.18 to 6.15 μg STXeq. 100 g^{-1} tissue which were considerably lower than the 80 μg STXeq. 100 g^{-1} tissue considered unfit for human consumption (NSSP, 1997). Therefore, based on the international maximum permissible limit, the obtained STXs levels of mussels in

the 9 sampling sites of this studied area were considered safe for human intake.

CONCLUSIONS

HABs represent a serious and emerging issue for human health. STXs is one of the most biotoxins causing paralytic shellfish poisoning in human by the consumption of bivalves either raw or cooked. Therefore, considerable researches on STXs have been carried out. Comparatively, limited data were available on the relationship between STXs toxicity and body size of bivalves.

This study observed the higher STXs toxicity per individual in the larger body size. However, the levels of STX toxicity in μg STXeq. 100 g^{-1} shellfish differed insignificantly according to size group *(p>0.05).* No apparent relationship was observed between the length of green mussel *(Perna viridis)* and the detection of STXs in this study. The STXs body burden slightly increased with increasing age. However, STXs body burden (μg STXeq/mussel) did not change significantly over the seasons of the year *(p > 0.05)*.

Based on the US regulatory limit of 80 μg STXeq. 100 g^{-1} of shellfish, green mussels of the upper and central GOT in this study were safe for human consumption. Further investigations based on large amount of samples, different species including physical properties of seawater were suggestion.

ACKNOWLEDGEMENTS

This research was financially supported by the National Research Council of Thailand. The authors would like to thank anonymous reviewers for their invaluable comments and the editorial staff of the EnvironAsia2019 for assistance in the revision and production of this manuscript.

REFERENCES

AOAC International, AOAC Official Method 2011.27. Paralytic shellfish toxins (PSTs) in shellfish, receptor binding assay, in: Official Methods of Analysis of AOAC International,

eighteenth ed., AOAC International, Gaitherburg, MD, 2011. Section 49.10.06.

Berdalet E, Fleming LE, Gowen R, Davidson K, Hess P, Backer LC, Moore SK. 2016. Marine harmful algal blooms, human health and wellbeing: challenges and opportunities in the 21st century. Journal of the Marine Biological Association of the United Kingdom, 96: 61–91.

Cao R, Wang D, Wei Q, Wang Q, Yang D, Liu H, Dong Z, Zhang X, Zhang Q, Zhao J. 2018. Integrative biomarker assessment of the influence of saxitoxin on marine bivalves: A comparative study of the two bivalve species oysters, crassostrea gigas, and scallops, Chlamys farreri. Frontiers of Physiology.
doi : 10.3389/fphys.2018.01173

Carvalho FP, Oliveira JM, Alberto, G, Batlle, JVI. 2010. Allometric relationships of ^{210}Po and ^{210}Pb in mussels and their application to environmental monitoring. Mar. Pollut. Bull. 60: 1734-1742.

Cho Y, Tsuchiya S, Yoshioka R, Omura T, Konoki K, Oshima Y, Yotsu-Yamashita M. 2016. Column switching combined with hydrophilic interaction chromato- graphy-tandem mass spectrometry for the analysis of saxitoxin analogues, and their biosynthetic intermediates in dino flagellates. J of Chromatography A. 1474: 109-120.

Crosby MP, Gale LD. 1990. A review and evaluation of bivalve condition index methodologies with a suggested standard method, J. of Shellfish Research. 9 (1): 233-237.

Department of Marine and Coastal Resources (http: marinegiscenter dmcr go th)

Grattan LM, Holobaugh S, Morris JG Jr. 2016. Harmful algal blooms and public health Review. Harmful Algae. 57: 2-8

James KJ, Carey B, O'Halloran J, van Pelt F, ŠKrabÁKovÁ Z. 2010. Shellfish toxicity: human health implications of marine algal toxins. Epidemiol. Infect. 138: 927-940.

Manfrin C, De Moro G, Torboli V, Venier P, Pallavicini A, Gerdol M. 2012. Physiological and molecular responses of bivalves to toxic dinoflagellates. Review. Invertibrate Survival Journal. 9: 184-199.

Michalski M. 2007. Paralytic shellfish poisoning as a health risk. Med Water. 63: 1530-1533.National Shellfish Sanitation Program Manual of Operations, Part 1 and 2, 1997 Revision. US Department of Health and Human Services, Food and drug administration, Washington. DC.

Quinn GP and Keough MJ. Experimental Design and Data Analysis for Biologist. Cambridge University Press. 2002: 542p.

Somsap, N, Gajaseni, N, Piumsomboon, A. Physico-Chemical Factors Influencing Blooms of Chaetoceros spp. and Ceratium furca in the Inner Gulf of Thailand, Kasetsart J. (Nat. Sci.), 2015; 49: 200 – 210.

Wattayakorn, G. Environmental issues in the Gulf of Thailand. In E. Wolanski (ed.) The Environment in Asia Pacific Harbours 2006: 249-259. Netherlands: Springer.

Zar JH. Biostatistical Analysis. 4th ed. Prentice Hall, Upper Saddle River, NJ. 1999: 662 p.

Determination of elemental composition of ambient PM_{10} and $PM_{2.5}$ during open burning season in Chiang Mai, Thailand

Tantaraporn Charoenporn[1], Wan Wiriya[2, 3], Somporn Chantara[2,3*]

[1]Master's Degree Program in Environmental Science, Environmental Science Research Center, Faculty of Science, Chiang Mai University, Chiang Mai, 50200, Thailand

[2]Environmental Science Research Center, Faculty of Science, Chiang Mai University, Chiang Mai 50200, Thailand

[3]Environmental Chemistry Research Laboratory, Chemistry Department, Faculty of Science, Chiang Mai 50200, Thailand

Coresponding author: e-mail: somporn.chantara@gmail.com

ABSTRACT

Air pollution due to open burning, occurs almost every dry season in Southeast Asia including northern Thailand. This study aims to determine and compare PM_{10} and $PM_{2.5}$ concentrations and their elemental composition during open burning season. Ambient particulate matters ($PM_{2.5}$ and PM_{10}) were collected by mini volume air samplers during 3 March to 7 April 2016 at a rooftop of a nine story building in Chiang Mai University. The samples were extracted by aqua regia (HCl + HNO_3; 3:1 v/v) and analyzed for elemental composition using Inductively Coupled Plasma-Optical Emission Spectroscopy (ICP-OES). Average PM_{10} and $PM_{2.5}$ concentrations were 84.10 ± 19.56 µg/m^3 (n=36) and 69.86 ± 15.24 µg/m^3 (n=36), respectively. Average $PM_{2.5}$ concentration accounted for 83% of PM_{10} meaning that fine particulate matters are a major part of ambient aerosols during the burning season. Moreover, daily average $PM_{2.5}$ concentration obtained from this study was about 1.5 higher than Thailand ambient air quality standard (50 µg/m^3) and 3

times higher than WHO guideline (25 μg/m^3). Major elements found in the samples were Fe (1.93 and 0.09 μg/m^3), Mg (1.77 and 1.20 μg/m^3), K (0.76 and 0.84 μg/m^3) and Al (0.10 and 0.18 μg/m^3) for PM_{10} and $PM_{2.5}$, respectively. Mg, K and Al were not significantly different comparing between PM_{10} and $PM_{2.5}$ samples ($p > 0.05$), while Fe in PM_{10} was significantly higher than in $PM_{2.5}$ samples. In PM_{10} fraction, Fe was the most enriched element, while Mg was the dominant species of $PM_{2.5}$. Sources of Fe and Mg could be from soil dust resuspension. High concentration of K (biomass burning tracer) was also found, particularly in $PM_{2.5}$ samples, revealed the biomass burning source during the sampling period. Some toxic metals such as As and Pb were found (0.005 and 0.012 μg/m^3, respectively) in $PM_{2.5}$, Which could leak to health impact in a long team expose.

Keywords: Air pollution, Elemental composition, Metals, Biomass burning

INTRODUCTION

Air pollution is one of the important environmental problems. Air pollutants are harmful to human and ecosystems. The pollutant has particulate matter (PM), the particles with a diameter less than 10 μm and 2.5 μm (PM_{10}, $PM_{2.5}$). They can pass through and accumulate in respiratory tract and cause a significant threat to human health. Element and toxic metals are found in atmospheric contaminates from human activities and can causeserious problem worldwide. Zn, Cu, Cr and Ni at are normally used in industry for brass wares and electroplating, toxic metals i.e. Pb and Cd can be found at traffic and commercial sites. Oil combustion emits Ni and V. Re-suspended soil can be composed of Ca, Fe, Al and Si. Traffic source could generate Pb, Br and Se. (Dinis M.D.L. and Fiúza A., 2010; Pal R. et al., 2014; Khodeir M. et al., 2012).

Northern Thailand is suffering from air pollution during dry season almost every year. The geographical features as a basin surrounded by

high mountain, together with low air-flow and inversion temperatures causing high accumulation of air pollutants. Major sources of air pollution in this area is open burning including forest fires and agriculture residue burning (Wiriya et al., 2013). PM_{10} collected from urban area of Chiang Mai Province in 2005-2006 found high concentration of elements and toxic metals (Pb, Cd, Hg and As) in dry season (Chantara et al., 2009). Toxic metals found in PM composition could lead to heath impact as the metals are transported into the lung and accumulate in body (Das R. et al., 2015). Previous studies also showed that major elements such as K, Mg, Al, Fe and Zn were found in $PM_{2.5}$ collected in both suburban and mountain areas of Chiang Mai during burning season (Khamkaew et al., 2016a,b). Moreover, PM and soil metals such as Al may originate from transportation. However, metal pollutants including Cr, Cu, Fe and Zn are common vehicular pollutants, which are produced from both exhaust and non-exhaust actions of engines such as in fuel combustion, lubricant oil combustion, tire wear, crash barriers corrosion and brake lining wear. Therefore, particles in the air and their elemental composition could result in enormous deteriorating impacts on human health, climate changes and ecosystem (Janta R. and Chatara S., 2017). The purposes of this study are to determine and compare PM_{10} and $PM_{2.5}$ concentration and elemental composition collected from high building during burning season.

METHODOLOGY

Sampling site and Sample Collection

Daily (24 hours) PM_{10} and $PM_{2.5}$ samples were collected at the roof top of the nine storey building (SCB1), Faculty of science, Chiang Mai University during open beaning season (3 March-7April 2016). The samples were collected for 24 hours on quartz fiber filters (Whatman's, UK, Ø 47 mm.) using two mini volume air samplers (Air metric, USA) with a flow rate of 5 L/min. The filters were stored in desiccators before and after the sampling for at

least 24 hours prior to being weighed using a microbalance (Mettler Toledo, Switzerland) in a controlled room (temperature 25 ± 2 ºC and relative humidity 41 ± 5%) and kept in a freezer until extraction. Samples concentration were compared with values obtained from an automatic active sampler (Taper Element Oscillation Microbalance; TEOM) at the air quality monitoring station (AQM) belonging to the Pollution Control Department (PCD, 35t).

Analysis of Elemental Composition

The sampling filters were extracted with 4 mL of aqua regia (HCl + HNO_3; 3:1 V/V) in double layer Teflon digestion bombs at a temperature of 140 ºC for 4 hours. After extraction, the solution was cooled down and then adjusted with 2% HNO_3 to 10 mL in a volumetric flask. Extracted solutions were filtered with 0.45 µm nylon membrane and stored at 4 ºC prior to analysis. Sixteen element (Al, As, Cr, Cu, Fe, K, Mg, Mn, Ni, Pb, Sb, Se, Si, Sn, V, and Zn) were analyzed by using Inductive Coupled Plasma-Optical Emission Spectrometer (ICP-OES; Optima 3000, Perkin Elmer, Germany). The sample solutions were measured in triplicates, while quality control of the ICP performance was done by use of a mixed standard solution (0.1 and 1 ppm) for peak area comparison at every 10 sample injections. A median value was used for background subtraction from each sample (Khamkaew et al., 2016a; Janta R. and Chatara S., 2017).

Data Quality Control

Accuracy of the elemental analysis and extraction condition was checked by using pond sediment (National Institute for Environmental studies; NIES) as Certified Reference material (CRM). Seven sets of 100 mg pond sediment were extracted and analyzed using the same method as the samples. High recoveries (66–139%) of elements (Al, Cr, Cu, Fe, K, Mg, Mn, Ni, Pb, V and Zn) were obtained. Other elements, which are not found in the CRM, including As, Sb, Se, Si and Sn were spiked with known concentration into filters.

They were extracted using the same condition described above and high recoveries (87-118%) were obtained.

RESULTS AND DISCUSSION

PM_{10} and $PM_{2.5}$ Concentrations

Number of samples collected were 36 for both PM_{10} and $PM_{2.5}$ samples. Average PM_{10} and $PM_{2.5}$ concentrations were 84.10 ± 19.56 μg/m^3 and 69.86 ± 15.24 μg/m^3, respectively. The concentration ratio of $PM_{2.5}/PM_{10}$ accounted for 83% meaning that fine particulate matters are major part of ambient aerosols. The highest PM_{10} and $PM_{2.5}$ concentrations were observed on 25 Mach 2016 (160.85 and 138.29 μg/m^3 , respectively).The trend of daily PM concentrations obtained from mini volume air samplers and Taper Element Oscillation Microbalance (TEOM) were similar (Figure 1). The average 24 hour PM_{10} concentration was higher than WHO guideline (50 μg/m^3), but lower than Thailand's National Ambient Air Quality Standard (NAAQS) (120 μg/m^3). The average $PM_{2.5}$ concentration obtained from this study was about 1.5 times higher than NAAQS (50 μg/m^3) and 3 times higher than WHO guideline (25 μg/m^3).

Concentrations of PM_{10} and $PM_{2.5}$ Bound Elements

Elemental composition of PM_{10} and $PM_{2.5}$ samples were analyzed and 16 elements were found as shown in Table 1. Average concentrations of total elements were 16.18 ± 6.03 and 6.34 ± 4.01 μg/m^3 for PM_{10} and $PM_{2.5}$, respective. Elements found in all PM_{10} samples were Fe, Mg, K, Cr, Ni, Cu and Mn while those found in all $PM_{2.5}$ samples were Mg, K and Cr. Al, Pb, Sn and Zn were only found in some samples. Trace elements like As, Sb, Se and V were only found in few samples. Some elements (Sb, Se, Si and V) were not detected because their concentrations were lower than the instrument detection limit values (0.001-0.300 μg/m^3). Toxic metals such as Cr, Ni, and Zn were found in both PM_{10} and $PM_{2.5}$ for almost all samples. Highly toxic metals such as As and Pb were found only in some samples.

Relative percentages of dominant elements found in PM_{10} samples were Fe (32%) > Mg (30%) > K (13%), while those found in $PM_{2.5}$ samples were Mg (45%) > K (31%) > Al (7%) (Figure 2). Average elemental concentration of Mg, K and Al in PM_{10} and $PM_{2.5}$ samples were not significantly different ($p > 0.05$). Fe found in PM_{10} samples was significantly higher ($p < 0.05$) than that of $PM_{2.5}$ samples. This is because Fe is the most enriched element found in larger particles sizes i.e. 7 µm and 2.0-3.3 µm (Gioda A. et al., 2007). Major elements found in this study were similar to the study conducted in Chiang Mai reported by Khamkaew et al. (2016a).

Regarding the sources of elements, K is mainly generated from biomass combustion and is used as a tracer for biomass burning (Reche C. et al. 2012; Zhao P., 2013). In this study, K was found both in PM_{10} and $PM_{2.5}$ samples, revealed that there was an influence of biomass burning during the sampling period. Al, Fe, and Mg might come from soil resuspension. Mg was found highest in $PM_{2.5}$ and likely came from soil combustion during biomass burning (Hailin W. et al., 2008). Some toxic metals i.e. As, Cr and Pb were also found in this study, comparing to the previous studies, which also conducted in Chiang Mai (Chantara et al., 2009 and Khamkaew et al., 2016a).

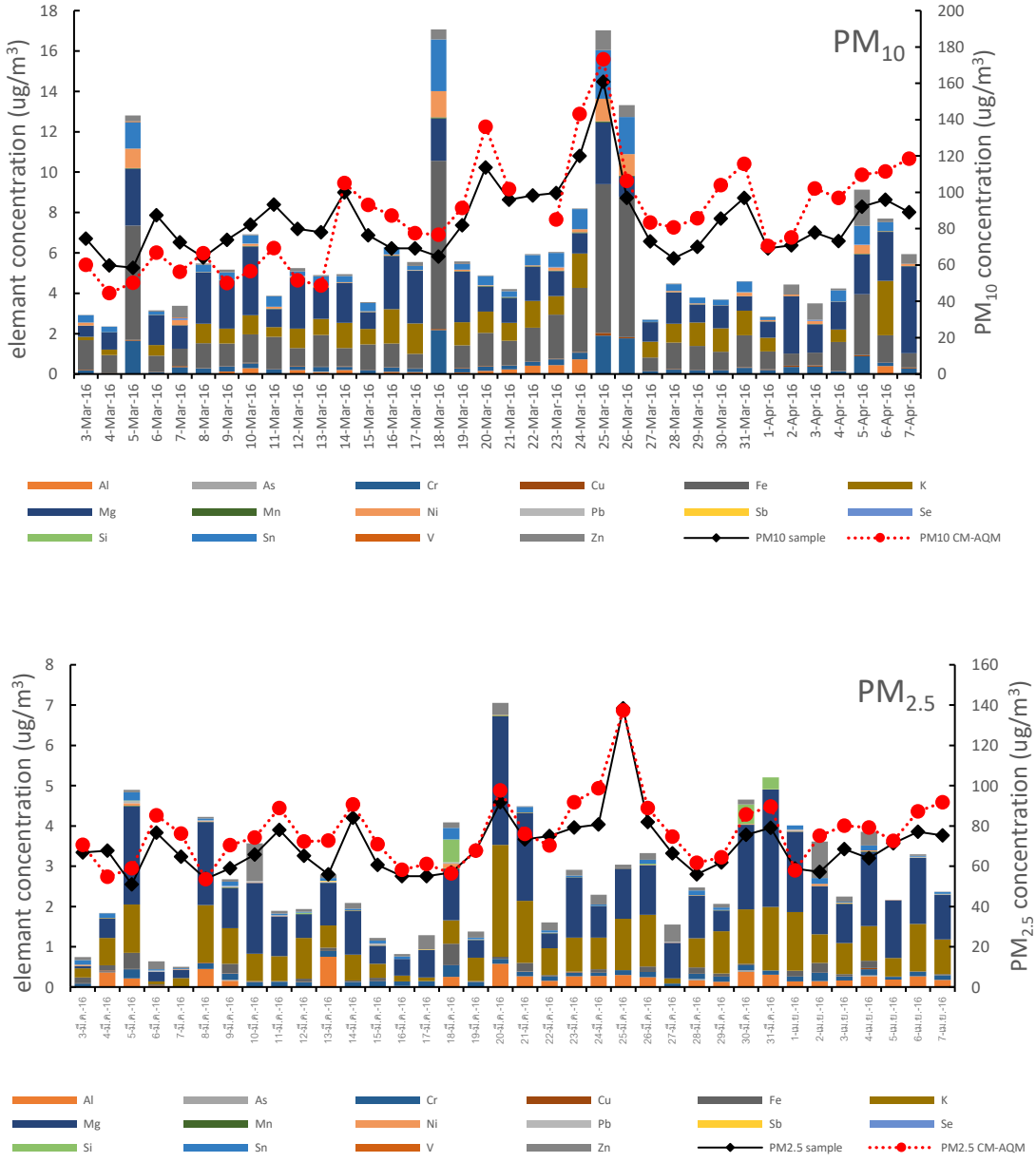

Figure 1 Variation of daily PM_{10} and $PM_{2.5}$ concentrations and their elemental composition during dry season 2016.

Table 1 Average concentration of elements (μg/m^3) of PM_{10} and $PM_{2.5}$ Bound Elements

Elements	DL (μg/m^3)	PM_{10} (N=36)				$PM_{2.5}$ (N=36)			
		No. of samples detected (%)	Mean ± SD	Min	Max	No. of samples detected (%)	Mean ± SD	Min	Max
Al	0.090	14(39)	0.099±0.167[a]	ND	0.729	24(67)	0.184±0.175[a]	ND	0.751
As*	0.002	2(6)	0.001±0.004	ND	0.023	6(17)	0.005±0.012	ND	0.048
Cr**	0.013	36(100)	0.421±0.533	0.034	2.171	36(100)	0.121±0.051	0.02	0.298
Cu	0.012	36(100)	0.033±0.023	0.013	0.135	20(56)	0.004±0.006	ND	0.030
Fe	0.005	36(100)	1.926±1930	0.604	8.330	29(81)	0.090±0.114	ND	0.523
K	0.034	36(100)	0.759±0.612[a]	0.167	2.695	36(100)	0.839±0.534[a]	0.073	2.778
Mg	0.012	36(100)	1.766±0.882[a]	0.537	4.313	36(100)	1.203±0.752[a]	0.055	3.190
Mn	0.001	36(100)	0.023±0.012	0.003	0.055	27(75)	0.007±0.006	ND	0.026
Ni**	0.003	36(100)	0.194±0.339	0.003	1.307	25(69)	0.013±0.021	ND	0.113
Pb*	0.009	7(19)	0.003±0.007	ND	0.034	15(42)	0.012±0.016	ND	0.052
Sb	0.015	0(0)	ND			5(14)	0.002±0.004	ND	0.016
Se	0.020	4(11)	0.006±0.020	ND	0.099	0(0)	ND		
Si	0.049	0(0)	ND			7(19)	0.040±0.128	ND	0.568
Sn	0.007	32(89)	0.536±0.595	ND	2.558	27(75)	0.063±0.062	ND	0.286
V	0.009	3(8)	0.002±0.009	ND	0.042	0(0)	ND		
Zn**	0.004	34(94)	0.225±0.359	ND	1.797	33(92)	0.161±0.210	ND	0.924
Total			**16.18±6.03**				**6.34±4.01**		

ND = Not detected, * heavy toxic metals, ** toxic metals

[a] not significantly different ($\rho > 0.05$)

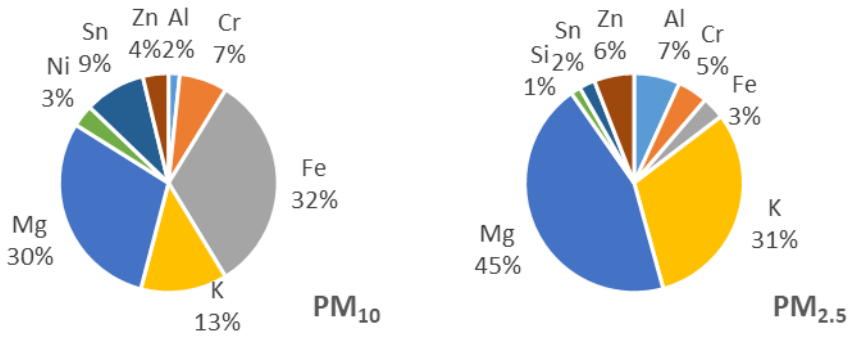

Figure 2 Percentages of elemental composition of PM_{10} and $PM_{2.5}$ samples collected during open burning season.

CONCLUSIONS

PM_{10} and $PM_{2.5}$ concentrations were found to be higher than Thailand's NAAQS for 2 and 36 days, respectively. The average $PM_{2.5}$ concentration accounted for 83% of PM_{10} meaning that fine particulate matters are major part of ambient aerosols in this area. K is generally used as biomass burning tracer and it was found to be a major element bound in both PM sizes, confirming major biomass burning influences in the area. Fe concentration in PM_{10} was significantly higher than that of $PM_{2.5}$ as Fe were caused by mechanical force such as soil dust particle generated from construction activities rather than from combustion. Some toxic metals such as As, Cr, Ni, Pb and Zn were found in the samples which could affect human heath under prolonged exposure.

ACKNOWLEDGEMENTS

Financial support from Faculty of Science and the Graduate School of Chiang Mai University are gratefully acknowledged.

REFERENCES

Chantara S., Wangkaarn S.,tengcharoenkul U.,Sangchan W.and Rayanakorn M.Chemical Analysis of Airborne Particulates for Air Pollutants in Chiang Mai and Lamphun Provinces, Thailand. Chiang Mai Journal of Science 2009; 36(2):123-135.

Das R., Khezri B., Srivastava B., Datta S.,Sikdar K. P.,Webster D. R. and Wang X. Trace element composition of $PM_{2.5}$ and PM_{10} from Kolkata - a heavily polluted Indian metropolis. Atmospheric Pollution Research 2015; 6: 742-750.

Dinis M.D.L. and Fiúza A. Exposure Assessment to Heavy Metals in the Environment: Measures to Eliminate or Reduce the Exposure to Critical Receptors. Environmental Heavy Metal Pollution and Effects on Child Mental Development: Risk Assessment and Prevention Strategies 2010; 27-50.

Hailin W., Yahui Z.,Ying W., Yele S.,Hui Y., Guoshun Z. and Zhengping H.Long-term monitoring and source apportionment of $PM_{2.5}/PM_{10}$ in Beijing, China.

Journal of Environmental Sciences 2008; 20: 1323–1327.

Gioda A., Peréz U., Rosa Z. and Jimenez-Velez D. B. Particulate Matter (PM_{10} and $PM_{2.5}$) from Different areas of Puerto Rico. Fresenius Environmental Bulletin 2007; 16(8).

Janta R. and Chantara S. Tree bark as bioindicator of metal accumulation from road traffic and air quality map: A case study of Chiang Mai, Thailand. Atmospheric Pollution Research 2017; 8: 956-967.

Khamkaew C., Chantara S., Janta R., Kumar Pani S., Prapamontol T., Kawichai S., Wiriya W., Neng-Huei Lin. Investigation of Biomass Burning Chemical Components over Northern Southeast Asia during 7-SEAS/BASELInE 2014 Campaign. Aerosol and Air Quality Research 2016; 16: 2655–2670.

Khamkaew C., Chantara S. and Wiriya W. Atmospheric $PM_{2.5}$ and Its Elemental Composition from near Source and Receptor Sites during Open Burning Season in Chiang Mai, Thailand. International Journal of Environmental Science and Development 2016; 7(6): 436-440.

Khodeir M., Shamy M., Alghamdi M., Zhong M., Sun H., Costa M., Chen L. and Maciejczyk P. Source apportionment and elemental composition of $PM_{2.5}$ and PM_{10} in Jeddah City, Saudi Arabia. Atmospheric Pollution Research 2012; 3: 331-340.

Pal R.,Kumar A.,Gupta A.,Tripathi M.and Tripathi A. Source Identification and Distribution of Toxic Trace Metals in Respirable Dust (PM_{10}) in Brasscity of India. Global Journal of HUMAN-SOCIAL SCIENCE: B Geography, Geo-Sciences, Environmental Disaster Management 2014; 14(5): 1-12.

Reche C., Viana M., Amato F., Alastuey A., Moreno T., Hillamo R., Teinila K., Saarnio K., Seco R., Penuelas J., Mohr C., Prevot A.S.H. and Querol X. Biomass burning contributions to urban aerosols in a coastal Mediterranean City. Science of the Total Environment 2012 428–428: 175–190.

Wiriya W., Prapamontol T. and Chantara S. PM_{10}-bound polycyclic aromatic hydrocarbons in Chiang Mai (Thailand): Seasonal variations, source identification, health risk assessment and their relationship to air-mass movement. Atmospheric Research 2013; 124: 109–122.

Zhao P.S., Dong F., He D., Zhao X.J., Zhang X.L., Zhang W.Z., Yao Q. and Liu H.Y. Characteristics of concentrations and chemical compositions for $PM_{2.5}$ in the region of Beijing, Tianjin, and Hebei, China. Atmospheric Chemistry and Physics 2013; 13: 4631–4644.

Identification of micro-plastics in different brands of bottled water in Thailand

Dinuka Kankanige[1*] and Sandhya Babel[1]

[1]School of Bio-Chemical Engineering & Technology, Sirindhorn International Institute of Technology, Thammasat University-Rangsit Center, Pathumthani 12120, Thailand.

[*]kdmalshani@gmail.com

ABSTRACT

Micro-plastic contamination of drinking water is of high concern in the current field of micro-plastic research. This work focuses on quantitative and qualitative analysis of micro-plastics in different brands of PET-bottled water, purchased from Thailand. Two sample sets were processed in equal volumes, to analyse in two ways: 1) optical microscopic sorting (≥50 μm) and 2) fluorescent tagging (6.5-20 μm and ≥20 μm). ATR-FTIR spectroscopy detected the polymer composition in both instances. Under optical microscopic sorting, an average of 36.6 ± 5.8 p/L was found for ≥50 μm particles. Fluorescence microscopic detection revealed a total average of 222.5 ± 20.4 p/L (≥6.5μm), where 152.2 ± 18.6 p/L and 70.3 ± 8.3 p/L were found in the size range of 6.5-20 μm and ≥20 μm, respectively, with fibers dominating in both. Fluorescent tagging seemed to be a more effective technique for micro-plastic sorting than optical microscopy. FT-IR spectra indicated the presence of PET and PE mainly, which could be released from the package. The quantity of micro-fibres increases with the decreasing particle size. Smaller sized-plastic fibres cause a potential threat to human health as they can easily penetrate the cells.

Keywords: Microplastics, PET-bottled water, Optical microscopy, Fluorescence microscopy, FT-IR spectroscopy

INTRODUCTION

Plastic contamination of drinking water is the topic of interest in current microplastic research field. A global study of 259 mineral water bottles from 11 international brands, finds an average microplastic content of 325 particles/L in 6.5-100 μm range and 10.4 particles/L with size above 100 μm (Mason et al., 2018). As per Oßmann et al. (2018), single-use PET-bottled water contains a mean particle concentration of 2649±2857 p/L, analyzed by micro-Raman spectroscopy. When considering the polymer composition, PET, PP, PE and PS have been commonly found in them (Oßmann et al., 2018). Drinking water contaminated by microplastics expose humans directly to anthropogenic particles. Few recent investigations imply that its toxicity increases with decreasing particle size (Wu et al., 2019). Microplastics lesser than 10 μm potentially damage human intestinal cells (Wu et al., 2019). However, related health assessments are limited due to the lack of details on quantity and characteristics of microplastics in drinking water. This work is aimed at quantitative and qualitative analysis of microplastics detected in 5 popular brands of bottled-mineral water in Thailand. Totally 22.88 L of mineral water was processed while the analysis was conducted in two ways: 1) visual sorting with optical microscope 2) fluorescence microscopic detection, both followed by FT-IR spectroscopy.

METHODOLOGY

Sample collection

PET-bottled water was collected from 5 brands available in Thailand grocery stores. Samples from each brand were purchased from the same batch. A total sample volume of 22.88 L was filtered during the entire

analysis: 1) 11.44 L was directly filtered for optical microscopic observation 2) 11.44 L was stained with Nile Red and filtered for fluorescence microscopic analysis. Each sample set contained 8 bottles of 330 mL from Singha (A), 4 of 600 mL from Crystal (B), 4 of 500 mL from Mont Fleur (C), 4 of 600 mL from Chang (D), and 4 of 500 mL from Evian (E). Results were averaged across these corresponding replicates for each brand. **Error! Reference source not found.** consists of the total filtered volume from each brand, for the two analytical procedures separately.

Table 1 Filtered sample volumes

Brand	Batch No.	Volume (L): case 1	Volume (L): case 2
Singha (A)	885099900-2675	2.64	2.64
Crystal (B)	885195235-0161	2.40	2.40
Mont Fleur (C)	885153011-1009	2.00	2.00
Chang (D)	885199333-8012	2.40	2.40
Evian (E)	306832005-5008	2.00	2.00
Total filtered volume		**11.44**	**11.44**

Filtration and size fractionation

A strict cleaning procedure was followed during sample manipulation to avoid the external contamination. Glassware were rinsed with Ethanol 50% (v/v, deionized water/ Ethanol absolute, RCI Labscan limited, > 99.8%) and deionized water. Lab-blanks of de-ionized water were analyzed in parallel to real samples for confirming any additional contamination that could occur during sample processing. These blanks were treated same as the real samples.

11.44 L of PET bottled water from the 5 brands was vacuum filtered through cellulose nitrate membrane

filters (47 mm diameter, 0.45μm pore size, Sartorius Stedim Biotech GmbH, Germany), for visual sorting by optical microscope (Olympus CX41, Philippines, 4×-100× objective, 10× eyepiece). Based on the analytical limits of the microscope, particles to be sorted by this technique were fractionated into ≥50 μm size class. Another 11.44 L from the same brands was transferred to glass beakers sample-wise, and injected with Nile Red dye (Nile Blue A Oxazone, Sigma Aldrich, GmbH, Germany). Nile Red stock solution was prepared in Methanol (PGII, Ajax Finechem, ThermoFisher Scientific, NZ) in 1 mg/mL concentration, added to the sample to gain a working concentration of 10 μg/L, and samples were incubated at 30^0C for 30 minutes (Maes et al., 2017). After incubation, they were vacuum filtered through cellulose filters (45 mm diameter, 20 μm pore size Whatman, GE Healthcare Life Sciences, Germany) and cellulose nitrate membrane filters (47 mm diameter, 0.45 μm pore size, Sartorius Stedim Biotech GmbH, Germany), subsequently. Considering the pixel size that could be observed and imaged under 4× objective of the fluorescence microscope (GE Healthcare, Deltavision Elite, USA), combined with SoftWoRx 6.5.2 (GE Healthcare, USA) image analysis software, two size classes were set as ≥20 μm and 6.5-20 μm. Filters were allowed to dry at 30^0C for 24 hours before analysis.

Particle sorting followed by FT-IR analysis

For case 1, filters of ≥50 μm size class were observed through optical microscope. For case 2, initially, 2 stained filters were scanned with DAPI filter (excitation-318/390 nm, emission-435/448 nm) and TRITC filter (excitation-527/542 nm, emission-545/597 nm). DAPI filter provided minimal disturbance from background staining under applied staining conditions. Hence, DAPI was selected over TRITC for the analysis. 4 square-shaped segments (12×12 mm), were cut off each filter

so that one segment would represent one quadrant of the circular filter. One segment, was scanned at a time. Nile Red is absorbed by polymers that could be either synthetic or natural, and they fluoresce under specific excitation and emission wavelengths, making it easy to distinguish between polymer and non-polymer particles (Maes et al., 2017). Blue-fluoresced particles were counted and average count on 4 segments were totaled for the whole filtered area. In both cases particles were sorted based on morphology: fibers and fragments. From each case, 2 filters per each brand were selected for FT-IR confirmation (totally 10 filters). 3 particles that were barely visible to the naked-eye, were picked from each filter (totally 30 specimen) and analyzed by ATR-FT-IR spectroscopy (Nicolet iS50, Thermo Fisher Scientific, USA) to identify the polymer composition. 5 lab-blanks, each representing the 5 brands were also selected for FT-IR analysis. 1-2 specimen from each filter were analyzed in the same procedure.

RESULTS AND DISCUSSION

Particle sorting by optical microscope

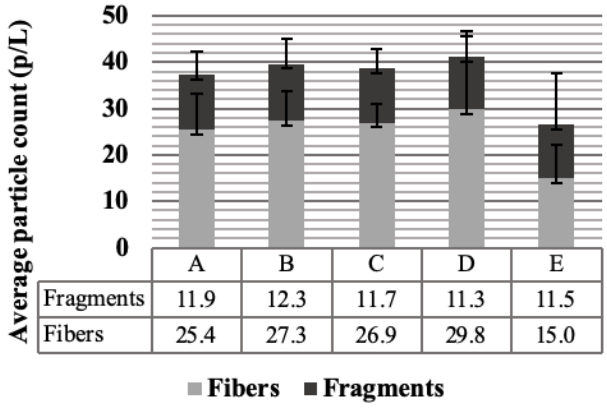

Figure 1 Average particle count for ≥50 μm (Optical microscopy)

Figure 1 shows the average particle count obtained for ≥50 μm size class in each brand. Here, the possibility of external contamination of samples was taken into consideration. Accordingly, the average number of particles observed on the filters of blank de-ionized water samples was deducted from the corresponding real sample-count. That count, in average, was found to be 5.0±1.2 p/L. The total average particle count for all the brands is 36.6±5.8 p/L. Mason et al. (2018) who quantified particles by combining fluorescence microscopy with Galaxy-count software, obtained 10.4 of ≥100 μm plastics in 1 L of bottled water. Obviously, it should be lesser than the current finding (36.6±5.8 p/L) as it does not take 50-100 μm range into account.

The microscopic views of the particle (Figure 2) confirm that fibers are the foremost morphology-type observed.

However, some of the particles were observed as films and pellets, but since rarely found, and due to the subjectivity of observation they too were classified as fragments. Average count of fibers and fragments were found to be 24.9±5.7 p/L and 11.7±0.4 p/L respectively (Figure 1), while fibers contributed to almost 68.0% of the particle count. In contrast, Mason et al. (2018) depicts that, of ≥100 μm particles, fragments represent 65% while fibers account to 13%. The reasons for this difference are, that those results do not consider 50-100 μm range and fiber fraction could have increased for the range below 100 μm.

.

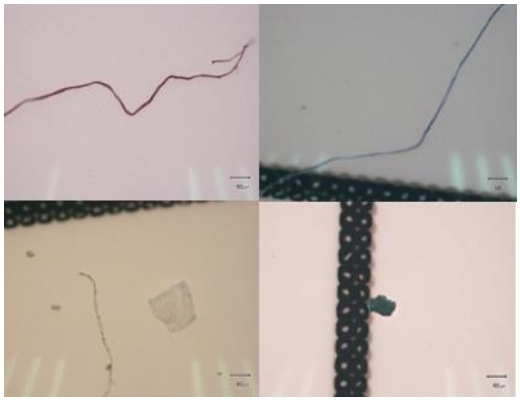

Figure 2 Microscopic views of particles (Olympus CX41, 100× total magnification)

However, the main disadvantage of this method is the inability to confirm whether the observed particles are exactly polymers. Therefore, the above counts may include both polymers and non-polymers. Also, white and transparent ones could be missed leading to underestimation. These circumstances were avoided in particle enumeration by fluorescent tagging.

Quantification by fluorescence microscope

Photos of some red- (excitation: 542/27 nm, emission: 587/45 nm, TRITC filter) and blue- (excitation: 390/18 nm, emission: 435/48 nm, DAPI filter) fluoresced particles under fluorescence microscope are shown in Figure 3. Red fluorescence prevented clear identification of particles due to the background staining. But, blue-fluoresced particles were visualized more clearly.

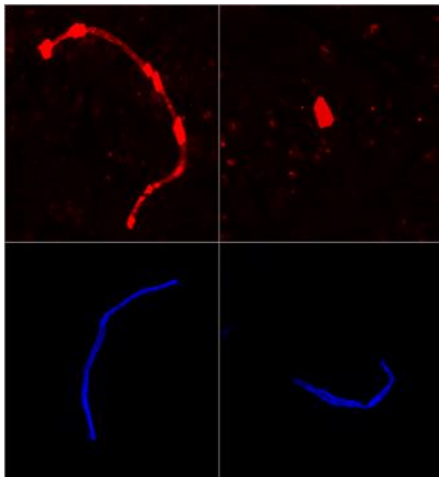

Figure 3 Fluoresced particles found in bottled water samples

Identification and enumeration of fluoresced particles by image analysis were more convenient and likely to be more accurate than optical microscopic method. Particle-shape was clearly visualized, unlike in instances where microscopic views could not distinguish between fragments, films and spherical-shaped particles. Particles that seemed to be pellets under optical microscope were identified as fragments by this image analysis. The average particle count for ≥20 μm range is given in Figure 4.

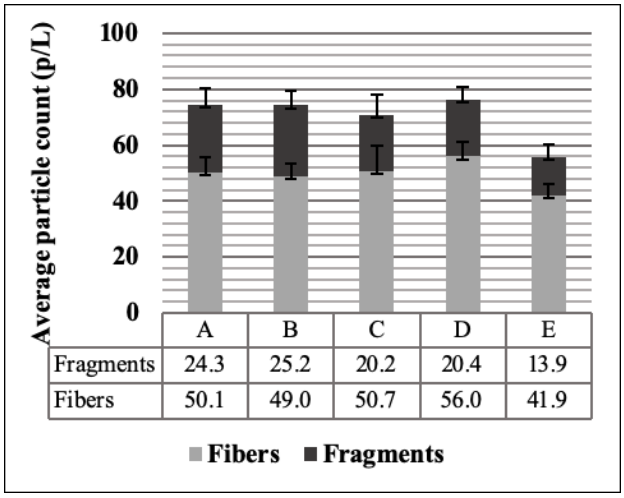

Figure 4 Average particle count for ≥20 μm (Fluorescent tagging)

The above chart shows the corrected particle count, obtained by reducing the particles in lab-blanks (11.5±1.9 p/L in average) from the direct count. When considering the two mean particle concentrations: 70.3±8.4 p/L for ≥20 μm (case 1), and 43.7±3.5 p/L for ≥50 μm (case 2), a significant difference exists between the two due to 1) exclusion of 20-50 μm range in optical microscopic sorting and 2) under-estimation of particles in case 1. Mason et al. (2018) who also analyzed microplastics in bottled water using Nile Red, finds 325 p/L for 6.5-100 μm and 10.4 p/L for ≥100 μm particles. But, they cannot be directly compared with those of the current study due to size range-variations. However, according to Mason et al. (2018), ≥100 μm microplastic abundance is approximately 30 times lesser than that of ≤100 μm. By correlating this fact, it can be concluded that the current finding of 70.3±8.4 p/L of ≥20 μm category, contains a majority of microplastics in 20-100 μm range while the minority would be of ≥100 μm. Micro-Raman spectroscopic counts obtained by Oßmann et al. (2018) indicate that, in reusable PET-bottled water, out of total average (4889±5432 p/L), >10 μm particles comprise 1.7% (83.1±92.3 p/L). This value is compatible with 70.3±8.4 p/L for ≥20 μm found in this study.

When considering the morphology-fractions, fibers (49.5±5.1 p/L) dominate all the brands covering 70.4% of the count, while the minor composition relates to fragments (29.6%). These conditions are in contrast to those of Mason et al. (2018) who finds only 13% of ≥100 μm particles as microfibers and 65% as fragments. The size class-variation is the reason for this contradiction. If they considered <100 μm particles too, the fiber fraction would have been largely increased.

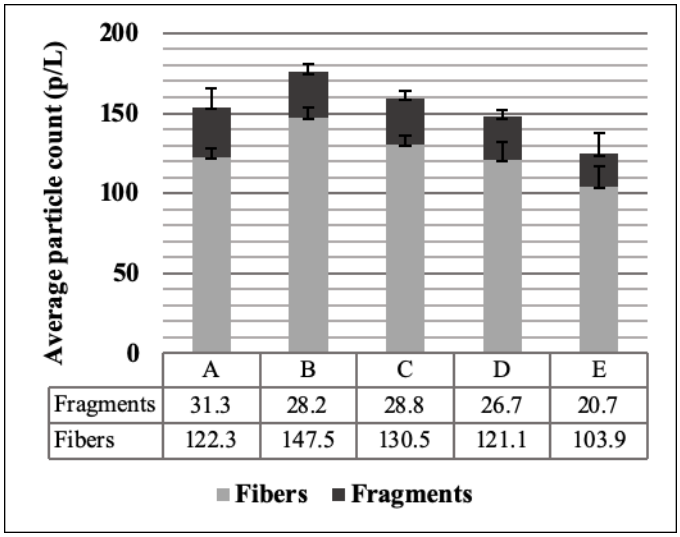

Figure 5 Average particle count for 6.5-20 μm (Fluorescent tagging)

Particle content found in the least size class (6.5-20 μm) is indicated in Figure 5. Direct count was corrected for possible contamination as done in previous instances. The average of 6.5-20 μm range (152.2±18.6 p/L) is significantly higher (approximately 2 times) than that of ≥20 μm range. As usual, fibers dominate over fragments comprising almost 82.2%. It implies that fiber fraction largely increases for smaller size classes. Out of all morphologies, fibers have more structural features that enable them a less-disturbed escape from and entry into a system. Moreover, microplastics exhibit size-dependent toxicity (Wu et al., 2019). Study by Wu et al. (2019) reveals that the cellular uptake of 0.1 μm PS-MPs by human intestinal cells is higher than that of 5 μm PS-MPs, which implies that the smaller the particle size, the higher the health risk is. Thus, prevalence of a large quantity of smaller-sized fibers in drinking water is a potential threat to human health.

Focusing on the total mean particle concentration (≥6.5 μm) determined by fluorescent tagging (222.5±20.4 p/L), it is lesser than that found by Mason et al (325 p/L) for 6.5-100 μm particles. A possible reason for this discrepancy is that, in their study, the

Galaxy Count software effectively detects the fluoresced particles, whereas in this study, slightly fluoresced particles were ignored.

Microplastics found in drinking water are suspected to release mainly from the packaging itself (Mason et al., 2018 & Schymanski et al., 2018). Fragments and highly abundant fibers in drinking water could possibly be a consequence of the plastics decomposed from the packaging due to physical abrasion and thermal impacts.

When comparing between the brands, Evian reports the least particle count at every instance, in terms of all size categories. A possible reason could be that the packaging material of Evian was particularly thicker than that of others, resulting in a comparatively high resistance to particle release.

FTIR confirmation

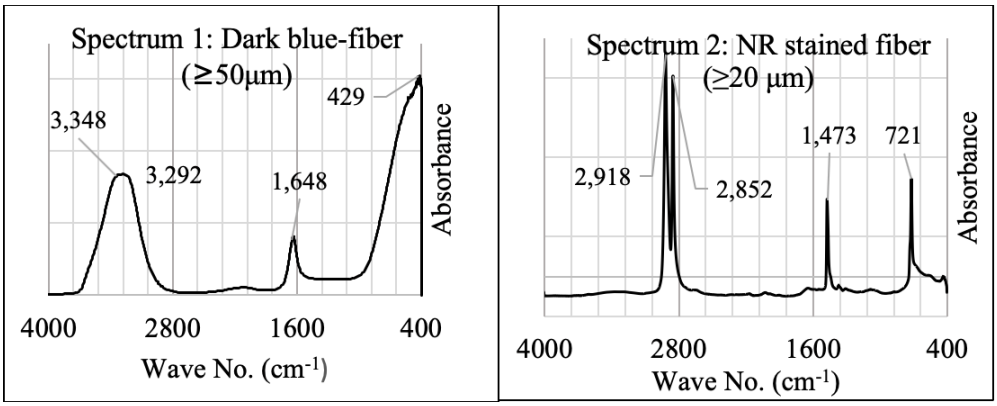

Figure 6: ATR-FT-MIR spectra of 2 fibers detected as PE

Figure 6 shows two of the ATR-FT-MIR spectra (Spectrum 1 and 2) that were identified as PE with respect to the reference peaks of LDPE/LLDPE adopted from Jung et al. (2018). Spectrum 1, obtained for a ≥50 µm light blue-fiber picked from a Singha filter, does not straightly seem to be relating to PE. The characteristic bands around 3000 cm^{-1} (3348, 3392 cm^{-1}) are of lesser intensity and not figured out as in reference. The two individual peaks at 1648 and 429 cm^{-1} relate to the two bands of reference

PE spectrum between 1500 and 600 cm^{-1} representing CH_2 bend (1467/1462 cm^{-1}) and CH_2 rock (730 cm^{-1}) (Jung et al., 2018) respectively, but not sharply pointed as in reference. These unimproved spectra qualities are possibly due to the atmospheric water vapor that interferes with characterization (Wilson & Wison, 2017). Spectrum 2 was obtained for a fiber from Nile Red-stained ≥20 μm samples belonging to Mont Fleur brand. The characteristic vibrational bands at 2918 and 2852 cm^{-1} and the individual finger print between 1473 and 721 cm^{-1} are more or less similar to the absorption peaks of the reference: 2915 and 2845 cm^{-1} for C-H stretch, 1467/1462 cm^{-1} for CH_2 bend, 730/717 cm^{-1} for CH_2 rock (Jung et al., 2018).

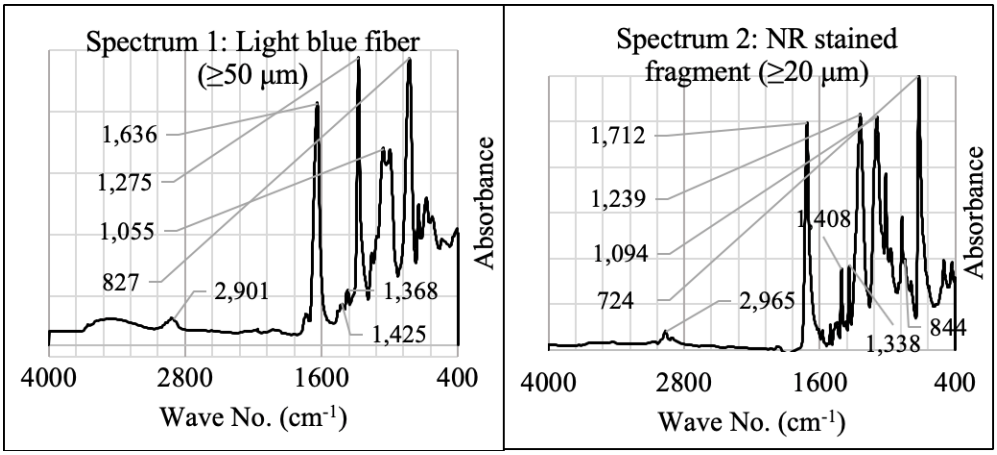

Figure 7: ATR-FT-MIR spectra of a fiber and fragment detected as PET

Figure 7 shows two of the ATR-FT-MIR spectra (Spectrum 1 and 2) identified as PET by comparing against the reference peaks of PET spectrum adopted from Jung et al. (2018). In spectrum 1 (≥50 μm, light blue fiber, Crystal brand), although not completely identical to the reference, its absorption peaks at 1636, 1275, 1055 and 827 cm^{-1} are representative of the critical absorption peaks used for identification: 1713 (C=O stretch), 1241 (C–O stretch), 1094 (C–O

stretch) and 720 cm^{-1} (aromatic CH out of plane bend) (Jung et al., 2018), respectively. When further compared with the PET-characteristic bands given in Wilson and Wison (2017), it is found that peaks at 2901, 1425 and 1368 (less intense) cm^{-1} approach the reference absorption peaks of 2908 (C-H symmetrical stretching), 1410 and 1342 cm^{-1} (C-O deformation stretch of O-H group) (Wilson & Wison, 2017), respectively. Spectrum 2 (≥20 μm, Nile Red-stained fragment, Crystal brand) is more promising than spectrum 1. It depicts the critical peaks with same intensity as mentioned by Jung et al. (2018), as well as majority of the vibrational characteristics of reference peaks with similar intensity given by Wilson & Wison (2017). The observed critical peaks are 724 (720: Aromatic CH out of plane bend), 1094 (1096: CH stretch), 1239 (1241: C–O stretch), and 1712 (1713: C–O stretch) (Jung et al., 2018). The other representative bands are 1338 and 1408 (1342 and 1410: C–O stretch and O–H deformation), 844 (848: aromatic rings 1,2,4,5), 2965 cm^{-1} (2969: C–H symmetrical stretch) (Wilson & Wison, 2017). They exhibit better spectra qualities making spectrum 2 an effective representative of PET.

Out of the 60 specimen tested for FT-IR analysis, PET and PE were commonly found in every brand while 2 specimens from Crystal and 1 from each Chang and Evian, showed PP identity. Additionally, some specimen provided spectra similar to Nylon. Components including Cellophane, Rutile, and Polytetrafluoroethylene (PTFE) which were identified by database matches (library: HR Hummel Polymer and Additives), with low match factors (>0.20). Accordingly, out of all 60 specimens analyzed, PET, PE and PP represented 40.0%, 30.0% and 6.7% respectively, with Nylon contributing to 8.3% and other components collectively forming 15.0%. Regarding, PET, PE and PP found in this study, it can be assured that PET definitely arises from packaging material while PE and PP

from bottle caps. These suggestions are further supported by Mason et al. (2018) and Schymanski et al. (2018), who also convince that PEST (PET+PES), PE and PP originate from bottle-material. However, most of the particles analyzed from lab-blanks showed Nylon identity proving the rapid contamination of Nylon from atmospheric particles. Therefore, the presence of Nylon in bottled water is doubtful since it is more likely to be a result of air-borne contamination during sample processing and/or analysis. Mason et al. (2018) finds Nylon fibers as the 2nd most (16%) abundant by their FT-IR confirmation of NR-tagged particles, but does not confirm the possible source of origin. On the other hand, it is also possible to contaminate drinking water through air during the production process in plants. When considering, the specimens that indicate other chemical compositions, it cannot be assured exactly that bottled water was already contaminated by them. For instance, Cellophane is a filter paper component, so that the tested specimen could have been contaminated with a filter paper particle. In a latest research, PTFE has been found in treated water from conventional drinking water treatment plants (Pivokonsky et al., 2018). Oßmann et al. (2018), in their study, detects pigments (Rutile, PB15, PV23 etc.) contaminated in PET-bottled water, by micro-Raman spectroscopy. Thus, among those additional components detected by library matches, there is a high possibility for Rutile (TiO_2) to be a contaminant in bottled water, as it is a pigment used to color bottle caps.

However, analyzing only 3 particles from each filter (≥50 μm, ≥20 μm) by ATR-FTIR spectroscopy, and excluding 6.5-20 μm from FT-IR confirmation, limit the identification of a wide range of polymers. Therefore, it is a critical need to analyze more particles by micro-FT-IR or micro-Raman spectroscopy which will aid in identifying more polymer types along with plastic additives.

CONCLUSIONS

In the 5 brands of PET-bottled water analyzed, the average count of ≥50 μm particles sorted by optical microscope is 36.6±5.8 p/L. Fluorescence microscopic analysis of Nile Red-stained samples indicates 43.7±3.5 p/L in ≥20 μm range. 6.5-20 μm particle density (152.2±18.6 p/L) is nearly 3.5 times higher than ≥20 μm particle average, implying that microplastics are highly abundant in lower size fractions. When comparing between brands, Evian has the least particle count of every size and fibers dominate fragments for all brands. FTIR analysis finds PET and PE to be abundant, while few specimens show PP identity. These results suggest that they are released to water by the packaging and bottle caps. Due to Nylon detected in lab-blank filters, this work suspects Nylon to contaminate the samples externally processing and/or analysis. But, there is also the possibility of adding it during manufacturing. Signs of other components, especially Rutile, suggest that pigments could leach packaging and contaminate drinking water.

Fluorescent-tagging eliminates the overestimation and underestimation of particles, enabling an analysis down to 6.5 μm. Thus, fluorescence microscopy is more promising for microplastic sorting than optical microscopy. The current findings can be improved by increasing the processing sample volume and the filter area of analysis. It is important to conduct further research on this matter, as smaller-sized microplastics are found to be a threat to human health in terms of cell damage and chemical toxicity.

REFERENCES

Jung MR, Horgen FD, Orski FV, Rodriguez V, Beers KI, Balazs GH, Jones TT, Work TM, Brignac KC, Royer S-J, Hyrenbach KD, Jensen BA, Lynch JM. Validation of ATR FT-IR to identify polymers of plastic marine debris, including those ingested by marine organisms. Marine Pollution Bulletin 2018; 127: 704-716.

Maes T, Jessop R, Wellner N, Haupt K, Mayes A. G. A rapid-screening approach to detect and quantify microplastics based on fluorescent tagging with Nile Red. Scientific Reports 2017; 7(44501): doi:10.1038/srep44501

Mason SA, Welch VG, Neratko J. Synthetic Polymer Contamination in Bottled Water. Frontiers in Chemistry 2018; 6(407).

Oßmann BE, Sarau G, Holtmannspötter H, Pischetsrieder M, Christiansen SH, Dicke W. Small-sized microplastics and pigmented particles in bottled mineral water. Water Research 2018; 141: 307-316.

Pivokonsky M. Cermakova L, Novotna K, Peer P, Cajthaml T, Janda V. Occurrence of microplastics in raw and treated drinking water. Science of the Total Environment 2018; 643: 1644-1651.

Schymanski D, Goldbeck C, Humpf H-U, Fürst P. Analysis of microplastics in water by micro-Raman spectroscopy: Release of plastic particles from different packaging into mineral water. Water Research 2018; 129: 154-162.

Wilson & Wison. Comprehensive Analytical Chemistry: Charaterization and Analysis of Microplastics. In: Rocha-Sanos TAP, Duarte AC, editors. Morphological and Physiacl Characteristics of Microplastics. 1st ed. 1000 AE Amsterdam, Netherlands: Elsevier; 2017. 49-62.

Wu B, Wu X, Liu S, Wang Z, Chen L. Size-dependent effects of polystyrene microplastics on cytotoxicity and efflux pump inhibition in human Caco-2 cells. Chemosphere 2019; 221: 333-341.

Author Index

Author Index

Author Index

LIST OF REVIEWERS

Dr. Alice Sharp
Chiang Mai University, Thailand
Email: alice.sharp@cmu.ac.th

Dr. Chanida Puangpila
Chiang Mai University, Thailand
Email: taytayuv@hotmail.com

Dr. Chanyud Kritsunankul
Naresuan University, Thailand
Email: chanyud@gmail.com

Asst. Prof. Dr. Chidhathai Petchuay
Ubon Ratchathani University, Thailand
Email: chidhathai.p@ubu.ac.th

Asst. Prof. Dr. Chitchol Phalaraksh
Chiang Mai University, Thailand
Email: chitcholp@gmail.com

Dr. Chuthamat Rattikansukha
Walailak University, Thailand
Email: crattikansukha@yahoo.com

Prof. Dae-Woon Jeon
Changwon National University, Republic of Korea
Email: dwjeong@changwon.ac.kr

Asst. Prof. Dr. Decha Tapunya
Chiang Mai University, Thailand
Email: thapanya2@hotmail.com

Assoc. Prof. Dr. Jaroon Jakmunee
Chiang Mai University, Thailand
Email: jakmunee@gmail.com

Asst. Prof. Dr. Jeeraporn Pekkoh
Chiang Mai University, Thailand
Email: jeeraporn.p@cmu.ac.th

Dr. Kiattikhun Manokruang
Chiang Mai University, Thailand
Email: kiattikhun.m@cmu.ac.th

Asst. Prof. Lt.Col. Dr. Kittiphop Promdee
Chulachomklao Royal Military Academy, Thailand
Email: nuumensci@gmail.com

Asst. Prof. Dr. Kontad Ounnunkad
Chiang Mai University, Thailand
Email: suriyacmu@gmail.com

Dr. Kullapa Chanawanno
Chiang Mai University, Thailand
Email: kullapa.c@gmail.com

Asst. Prof. Dr. La-ongnuan Srisombat
Chiang Mai University, Thailand
Email: slaongnuan@yahoo.com

Dr. Natapol Thongplew
Ubon Ratchathani University, Thailand
Email: natapol.t@ubu.ac.th

Asst. Prof. Dr. Nuta Supakata
Chulalongkorn University, Thailand
Email: nuta.s@chula.ac.th

Asst. Prof. Dr. Orawan Tue-Ngeun
Naresuan University, Thailand
Email: orawant@nu.ac.th

Asst. Prof. Dr. Pajaree Thongsanit
Naresuan University, Thailand
Email: pajareet@nu.ac.th

Asst. Prof. Dr. Pantana Tor-ngern
Chulalongkorn University, Thailand
Email: Pantana.T@chula.ac.th

Asst. Prof. Dr. Panwadee Suwattiga
King Mongkut's University of Technology North Bangkok, Thailand
Email: panwadee.s@sci.kmutnb.ac.th

Assoc. Prof. Dr. Patana Anurakpongsatorn
Kasetsart University, Thailand
Email: fscipna@ku.ac.th

Asst. Prof. Peerapong Pornwongthong
King Mongkut's University of Technology North Bangkok, Thailand
Email: peerapong.p@sci.kmutnb.ac.th

Asst. Prof. Dr. Pitchaya Mungkornasawakul
Chiang Mai University, Thailand
Email: pitchaya16@gmail.com

Dr. Pokkate Wongsasuluk
Chulalongkorn University, Thailand
Email: pokkate_wong@hotmail.com

Assoc. Prof. Pongsak Noophan
Kasetsart University, Thailand
Email: fengpsn@ku.ac.th

Assoc. Prof. Dr. Prasak Thavornyutikarn
Chiang Mai University, Thailand
Email: prasakth@hotmail.com

Asst. Prof. Dr. Prasit Wangpakapattanawong
Chiang Mai University, Thailand
Email: prasitwang@yahoo.com

Dr. Pumis Thuptimdang
Chiang Mai University, Thailand
Email: pumis.th@gmail.com

Assist. Prof. Dr. Ratcha Chaichana
Kasetsart University, Thailand
Email: fscircc@ku.ac.th

Asst. Prof. Dr. Roongkan Nuisin
Chulalongkorn University, Thailand
Email: roongkan.n@chula.ac.th

Asst. Prof. Dr. Sangrawee Sriwichai
Chiang Mai University, Thailand
Email: saengrawee.s@cmu.ac.th

LIST OF REVIEWERS

ORGANISING COMMITTEE

Secretary Committee

Asst. Prof. Dr. Somporn Chantara
Faculty of Science, Chiang Mai University
Asst. Prof. Dr. Sutthathorn Chairuangsri
Faculty of Science, Chiang Mai University
Asst. Prof. Dr. Siranee Sreesai
Faculty of Public Health, Mahidol University
Asst. Prof. Dr. Uma Langkulsen
Faculty of Public Health, Thammasat University
Asst. Prof. Dr. Ratcha Chaichana
Faculty of Environment, Kasetsart University

Registration Committee

Asst. Prof. Dr. Jeeraporn Pekkoh
Faculty of Science, Chiang Mai University
Dr. Dia Panitnard Shannon
Faculty of Science, Chiang Mai University
Asst. Prof. Dr. Nadchanok Rodrussamee
Faculty of Science, Chiang Mai University
Assoc. Prof. Dr. Patana Anurakpongsatorn
Faculty of Science, Kasetsart University
Assoc. Prof. Dr. Soontree Khuntong
Faculty of Science at Sriracha, Kasetsart University Sriracha Campus
Asst. Prof. Dr. Pajaree Thongsanit
Faculty of Engineering, Naresuan University

Venue and Audio-visual Equipment Committee

Asst. Prof. Dr. Deacha Tapunya
Faculty of Science, Chiang Mai University
Dr. Wittaya Pheera
Faculty of Science, Chiang Mai University
Dr. Pumis Thuptimdang
Faculty of Science, Chiang Mai University
Asst. Prof. Dr. Thipsuree Kornboonraksa
Faculty of Engineering, Burapha University
Asst. Prof. Dr. Vorapot Kanokkantapong
Faculty of Science, Chulalongkorn University

Venue and Audio-visual Equipment Committee

Dr. Teerawit Poopa
Faculty of Public and Environmental Health, Huachiew Chalermprakiet University

Public Relations Committee

Asst. Prof. Dr. Pitchaya Mungkornasawakul
Faculty of Science, Chiang Mai University
Asst. Prof. Dr. Saengrawee Sriwichai
Faculty of Science, Chiang Mai University
Asst. Prof. Dr. Deacha Tapunya
Faculty of Science, Chiang Mai University
Asst. Prof. Dr. Runglawan Somsunan
Faculty of Science, Chiang Mai University
Dr. Kullapa Chanawanno
Faculty of Science, Chiang Mai University
Dr. Warapong Tungittiplakorn
Faculty of Applied Science, King Mongkut's University of Technology North Bangkok
Asst. Prof. Turenjai Doolgindachbaporn
Faculty of Science, Khon Kaen University
Dr. Chidsanuphong Chart-asa
Faculty of Science, Chulalongkorn University
Dr. Varinthorn Boonyaroj
Faculty of Science and Technology, Rajamangala University of Technology Phra Nakhon
Asst. Prof. Dr. Parnjai Seuprasertsith
Faculty of Environment and Resource Studies, Mahasarakham University

Academic Committee

Professor Dr. Wanida Jinsart
Faculty of Science, Chulalongkorn University
Asst. Prof. Dr. Jaranai Panichkun
Faculty of Science, Kasetsart University
Assoc. Prof. Dr. Naiyanan Ariyakanon *Faculty of Science, Chulalongkorn University*
Asst. Prof. Dr. Roongkan Nuisin
Faculty of Science, Chulalongkorn University

Academic Committee

Dr. Supawin Watcharamul
Faculty of Science, Chulalongkorn University
Dr. Sermpong Sairiam
Faculty of Science, Chulalongkorn University
Asst. Prof. Dr. Sarawut Srithongouthai
Faculty of Science, Chulalongkorn University
Asst. Prof. Dr. Tassanee Prueksasit
Faculty of Science, Chulalongkorn University
Asst. Prof. Dr. Nuta Supakata
Faculty of Science, Chulalongkorn University
Asst. Prof. Dr. Pantana Tor-ngern
Faculty of Science, Chulalongkorn University
Assoc. Prof. Dr. Jaroon Jakmunee
Faculty of Science, Chiang Mai University
Dr. Alice Sharp
Faculty of Science, Chiang Mai University
Asst. Prof. Dr. Prasit Wangpakapattanawong
Faculty of Science, Chiang Mai University
Asst. Prof. Dr. Somporn Chantara
Faculty of Science, Chiang Mai University
Asst. Prof. Dr. Chitchol Phalaraksh
Faculty of Science, Chiang Mai University
Asst. Prof. Dr. Schradh Saenton
Faculty of Science, Chiang Mai University
Asst. Prof. Dr. Tinakorn Kanyanee
Faculty of Science, Chiang Mai University
Dr. Pumis Thuptimdang
Faculty of Science, Chiang Mai University
Asst. Prof. Dr. Peerapong Pornwongthong
Faculty of Applied Science, King Mongkut's University of Technology North Bangkok
Asst. Prof. Dr. Panwadee Suwattiga
Faculty of Applied Science, King Mongkut's University of Technology North Bangkok
Asst. Prof. Dr. Pajaree thongsanit
Faculty of Engineering, Naresuan University
Assoc. Prof. Dr. Pongsak Noophan
Faculty of Engineering, Kasetsart University

Academic Committee

Asst. Prof. Lt.Col. Dr. Kittiphop Promdee
Department of Environmental Science, Chulachomklao Royal Military Academy
Assoc. Prof. Dr. Patana Anurakpongsatorn
Faculty of environment, Kasetsart University
Asst. Prof. Turenjai Doolgindachbaporn
Faculty of Science, Khon Kaen University
Assoc. Prof. Dr. Soontree Khuntong
Faculty of Science at Sriracha, Kasetsart University Sriracha Campus
Asst. Prof. Dr. Siranee Sreesai
Faculty of Public Health, Mahidol University
Asst. Prof. Dr. Chidhathai Petchuay
Faculty of Science, Ubon Ratchathani University
Dr. Chuthamat Rattikansukha
School of Engineering and Technology, Walailak University
Dr. Natapol Thongplew
Faculty of Science, Ubon Ratchathani University
Asst. Prof. Dr. Ratcha Chaichana
Faculty of Environmental, Kasetsart University
Dr. Aranpak Pitakpong
School of Medicine, University of Phayao
Dr. Varinthorn Boonyaroj
Faculty of Science and Technology, Rajamangala University of Technology Phra Nakhon

Evaluation Committee

Asst. Prof. Dr. Jeeraporn Pekkoh
Faculty of Science, Chiang Mai University
Asst. Prof. Dr. Chayakorn Pumas
Faculty of Science, Chiang Mai University
Dr. Preprame Pattanamahakul
Faculty of Science, Chulalongkorn University
Asst. Prof. Dr. Chidhathai Petchuay
Faculty of Science, Ubon Ratchathani University

Finance and Accounting Subcommittee

Asst. Prof. Dr. Siranee Sreesai
Faculty of Public Health, Mahidol University

Finance and Accounting Subcommittee

Asst. Prof. Dr. Sutthathorn Chairuangsri
Faculty of Science, Chiang Mai University

Asst. Prof. Dr. Itthayakorn Promputtha
Faculty of Science, Chiang Mai University

Asst. Prof. Dr. Thipsuree Kornboonraksa
Faculty of Engineering, Burapha University

Fund Raising Committee

Asst. Prof. Lt.Col. Dr. Kittiphop Promdee
Department of Environmental Science, Chulachomklao Royal Military Academy

Asst. Prof. Dr. Prasit Wangpakapattanawong
Faculty of Science, Chiang Mai University

Asst. Prof. Dr. Somchai Lapanantnoppakhun
Faculty of Science, Chiang Mai University

Asst. Prof. Dr. Sitthichok Puangthongtub
Faculty of Science, Chulalongkorn University

Asst. Prof. Dr. Rattapon Onchang
Faculty of Science, Silpakorn University

Ceremonial Committee

Dr. Wan Wiriya
Faculty of Science, Chiang Mai University

Asst. Prof. Dr. Nuttee Suree
Faculty of Science, Chiang Mai University

Asst. Prof. Dr. Pimonrat Tiansawat
Faculty of Science, Chiang Mai University

Lt. Col. Pongsakorn Kaewkornmuang
Department of Environmental Science, Chulachomklao Royal Military Academy

Asst. Prof. Dr. Pasicha Chaikaew
Faculty of Science, Chulalongkorn University

SUBCOMMITTEE

Chiang Mai University

Steering Subcommittee

Head of Environmental Science Research Center
Associate Dean for Research and International Relations
Assoc. Prof. Dr. Jaroon Jakmunee
Asst. Prof. Dr. Sutthathorn Chairuangsri
Asst. Prof. Dr. Jeeraporn Pekkoh
Asst. Prof. Dr. Pitchaya Mungkornasawakul
Dr. Wan Wiriya
Ms. Prusanee Sriponvaree
Mr. Suttipat Junjunejerm

Registration and Evaluation Subcommittee

Asst. Prof. Dr. Jeeraporn Pekkoh
Asst. Prof. Dr. Chayakorn Pumas
Lect. Dr. Dia Panitnard Shannon
Asst. Prof. Dr. Nadchanok Rodrussamee
Lect. Dr. Alice Sharp
Lect. Dr. Pumis Thuptimdang
Mr. Aekapon Kumsan

Exhibition, Venue and Audio-visual Equipment Subcommittee

Asst. Prof. Dr. Deacha Tapunya
Lect. Dr. Wittaya Pheera
Lect. Dr. Pumis Thuptimdang
Mr. Mongkon Supa
Mr. Suthat Pota
Mr. Suphod Pota
Mr. Yuttapong Janploy
Mr. Werapan Suwanta
Mr. Dusit Saiprom
Mr. Arnon Chaikham
Mr. Tairat Jirato
Mr. Aekapon Kumsan
Mr. Nopparat Monsi
Mr. Kamron Inmasom
Mr. Prajak Poonyawatpornkul
Mr. Wutthiphong Anonthayee
Mr. Whalunchai Prantuntanadid

Public Relations Subcommittee

Asst. Prof. Dr. Pitchaya Mungkornasawakul
Asst. Prof. Dr. Saengrawee Sriwichai
Asst. Prof. Dr. Deacha Tapunya

Public Relations Subcommittee

Asst. Prof. Dr. Runglawan Somsunan
Lect. Dr. Kullapa Chanawanno
Ms. Sainatee Jaihom
Ms. Jutakan kantalue

Academic Subcommittee

Assoc. Prof. Dr. Jaroon Jakmunee
Assoc. Prof. Dr. Alice Sharp
Asst. Prof. Dr. Prasit Wangpakapattanawong
Asst. Prof. Dr. Somporn Chantara
Asst. Prof. Dr. Chitchol Phalaraksh
Asst. Prof. Dr. Schradh Saenton
Asst. Prof. Dr. Tinakorn Kanyanee
Asst. Prof. Dr. Sila Kittiwachana
Lect. Dr. Pumis Thuptimdang

Finance and Accounting Subcommittee

Asst. Prof. Dr. Sutthathorn Chairuangsri
Asst. Prof. Dr. Itthayakorn Promputtha
Head of Accounts, Finance and Commodities Section
Mrs.Ratree Jaisat

Fund Raising Subcommittee

Asst. Prof. Dr. Prasit Wangpakapattanawong
Asst. Prof. Dr. Somchai Lapanantnoppakhun
Faculty Secretary
Head of Accounts, Finance and Commodities Section
Head of Research Administration, Academic Services and International Relations Section
Mr. Phichai Nakpathom
Ms. Pornnapat Pota

Ceremonial and Reception Subcommittee

Lect. Dr. Wan Wiriya
Asst. Prof. Dr. Nuttee Suree
Lect. Dr. Pimonrat Tiansawat
Lect. Dr. Chanida Puangpila
Ms. Prusanee Sriponvaree
Mr. Suttipat Junjunejerm
Lect. Dr. Aussara Panya
Lect. Dr. Jomkwhan Meerak
Asst. Prof. Dr. Terd Disayathanoowat

ORGANISOR, CO-ORGANISORS AND COLLABORATORS

ORGANISORS

CO-ORGANISORS

COLLABORATORS

SPONSORS


TCEB
THAILAND CONVENTION
& EXHIBITION BUREAU


PerkinElmer
For the Better


Metrohm
Siam Ltd.


MERCK


SITHIPORN
associates


บริษัท ซายน์เทค จำกัด
SCIENCE TECH CO.,LTD.
www.sciencetech.th.com
ISO 9001:2015


NETbay